MINUTES
CHINO BASIN WATERMASTER
WATERMASTER BOARD – SPECIAL MEETING
May 22, 2020

The Watermaster Board special meeting was held via GoToMeeting (conference call and web meeting) only on May 22, 2020.

WATERMASTER BOARD MEMBERS PRESENT ON CALL

Jeff Pierson, Chair	Agricultural Pool – Crops
James Curatalo, Vice-Chair	Fontana Union Water Company
Bob Kuhn, Secretary/Treasurer	Three Valleys Municipal Water District
Bob Bowcock	CalMat Co.
Steve Elie	Inland Empire Utilities Agency
Don Galleano	Western Municipal Water District
Paul Hofer	Agricultural Pool – Crops
Victor Preciado	City of Pomona
Peter Rogers	City of Chino Hills

WATERMASTER STAFF PRESENT AT WATERMASTER

Peter Kavounas	General Manager
Janine Wilson	Senior Accountant
Vanessa Aldaz	Administrative Assistant

WATERMASTER STAFF PRESENT ON CALL

Joseph Joswiak	Chief Financial Officer
Edgar Tellez Foster	Water Resources Mgmt. and Planning Dir.
Anna Nelson	Executive Services Director/Board Clerk
Justin Nakano	Water Resources Technical Manager

WATERMASTER CONSULTANTS PRESENT ON CALL

Scott Slater	Brownstein Hyatt Farber Schreck, LLP
Brad Herrema	Brownstein Hyatt Farber Schreck, LLP
Mark Wildermuth	Wildermuth Environmental, Inc.
Andy Malone	Wildermuth Environmental, Inc.

OTHERS PRESENT ON CALL

Ron Craig	City of Chino Hills
Chris Berch	Jurupa Community Services District
David De Jesus	Three Valleys Municipal Water District
Gino Filippi	Agricultural Pool – Crops
Sylvie Lee	Inland Empire Utilities Agency
Pete Hall	Agricultural Pool – State of CA – CIM/CDCR
Shivaji Deshmukh	Inland Empire Utilities Agency
Brian Geye	California Speedway Corporation
Katie Gienger	City of Ontario
John Schatz	John J. Schatz, Attorney at Law
Eduardo Espinoza	Cucamonga Valley Water District
Bob Feenstra	Agricultural Pool – Dairy
Ben Lewis	Golden State Water Company
Brian Lee	San Antonio Water Company
John Bosler	Cucamonga Valley Water District
Tracy Egoscue	Egoscue Law Group, Inc.
Carol Boyd	State of California – CIM
Courtney Jones	City of Ontario
Richard Rees	Wood plc

Andrew Gagen	Kidman Gagen Law, LLP
Scott Burton	City of Ontario
Ryan Shaw	Western Municipal Water District
Eunice Ulloa	City of Chino
Justin Scott-Coe	Monte Vista Water District

CALL TO ORDER
Chair Pierson called the Watermaster Board meeting to order at 10:32 a.m.

(0:02:08) Ms. Nelson conducted the roll call and announced that all Board members were present.

PUBLIC COMMENTS
None

AGENDA - ADDITIONS/REORDER
None

I. BUSINESS ITEMS

A. 2020 SAFE YIELD RESET

Adopt Resolution 2020-03 related to the 2020 Safe Yield Reset.

(0:04:11) Messrs. Kavounas and Wildermuth gave a presentation. A discussion ensued.

(0:40:12) Mr. Galleano introduced a motion to approve Business Item I.A. Mr. Rogers seconded the motion. Additional discussion ensued.

(0:45:38) Vote taken
Motion by Mr. Don Galleano, seconded by Mr. Peter Rogers, and by majority roll call vote as attached to these minutes

Moved to Adopt Resolution 2020-03 related to the 2020 Safe Yield Reset as presented.

Mr. Hofer and Chair Pierson voted against the motion.

ADJOURNMENT
Chair Pierson adjourned the Watermaster Board special meeting at 11:20 a.m.

Secretary: _____

Approved: June 25, 2020

Attachments:
1. Resolution 2020-03 (2020 Safe Yield Reset)
2. 20200522 Watermaster Board Roll Call Vote Outcome for Business Item II.A.

RESOLUTION 2020-03
OF THE
CHINO BASIN WATERMASTER
REGARDING THE 2020 SAFE YIELD RESET

1. **WHEREAS**, the Chino Basin Watermaster ("Watermaster") was appointed pursuant to the Judgment in Chino Basin Municipal Water District v. City of Chino (San Bernardino Superior Court Case No. RCV RS51010) to administer and enforce the provisions of the Judgment and any subsequent instructions and orders of the Court;

2. **WHEREAS,** the Judgment was entered in 1978 and set the initial Safe Yield of the Chino Basin at 140,000 acre-feet per year ("AFY"), but reserved continuing jurisdiction to the Court to amend the Judgment, inter alia, to redetermine the Safe Yield after the first ten years of operation of the Physical Solution established under the Judgment;

3. **WHEREAS**, on April 28, 2017, the Court entered its Orders for Watermaster's Motion Regarding 2015 Safe Yield Reset Agreement, Amendment of Restated Judgment, Paragraph 6 ("April 28, 2017 Order"), which, among other things: (1) reset the Safe Yield of the Chino Basin to 135,000 AFY; (2) directed Watermaster to initiate a process to evaluate and reset the Safe Yield by July 1, 2020 to establish the Safe Yield of the Chino Basin for the time period commencing on July 1, 2020 and ending on June 30, 2030; and, (3) directed Watermaster to conduct the 2020 Safe Yield reset evaluation pursuant to the methodology described in the Reset Technical Memorandum, and while relying upon long-term hydrology and data from 1921 to the date of the reset evaluation in order to account for short-term climatic variation.

4. **WHEREAS**, the Court confirmed its direction to reset the Safe Yield provided in the April 28, 2017 Order in subsequent rulings in its March 15, 2019 Findings and Order Regarding Amendments to Restated Judgment, Peace Agreement, Peace II Agreement, and Re-Operation Schedule.

5. **WHEREAS,** the Reset Technical Memorandum provides the following methodology adopted by the April 28, 2017 Order to reset the Safe Yield:

> 1. Use . . . newly collected data . . . in the re-calibration process for the Watermaster's groundwater-flow model.
>
> 2. Use a long-term historical precipitation falling on current and projected future land uses to estimate the long-term average net recharge to the Basin.
>
> 3. Describe the current and projected future cultural conditions, including, but not limited to the plans for pumping, stormwater recharge and supplemental-water recharge.
>
> 4. With the information generated in [1] through [3] above, use the groundwater-flow model to redetermine the net recharge to the Chino Basin taking into account the then existing current and projected future cultural conditions.
>
> 5. Qualitatively evaluate whether the groundwater production at the net recharge rate estimated in [4] above will cause or threaten to cause "undesirable results" or "Material Physical Injury". If groundwater production at net recharge rate estimated in [4] above will cause or threaten to cause "undesirable results" or "Material Physical Injury" then Watermaster will identify and implement prudent measures necessary to mitigate "undesirable results" or "Material Physical Injury", set the value of Safe Yield to ensure there is no "undesirable results" or "Material Physical Injury", or implement a combination of mitigation measures and a changed Safe Yield.

6. **WHEREAS**, Watermaster commenced the process to reset the Safe Yield pursuant to the April 28, 2017 Order in 2019. In compliance with the April 28, 2017 Order, Watermaster, with the assistance of Wildermuth Environmental, Inc., Watermaster's engineer, compiled current and projected water demand and water supply planning data, updated and recalibrated the Chino Basin groundwater model, and estimated the Safe Yield of the Basin based upon current and projected cultural conditions. Watermaster's engineer documented this work and its findings in its 2020 Safe Yield Recalculation Report ("Safe Yield Report"), which is attached hereto as **Exhibit A** and incorporated herein by reference.

7. **WHEREAS,** Watermaster convened workshops in July 2019 and January 2020 to allow stakeholders to review data, review calibration results, and review proposed model projections.

8. **WHEREAS**, in March 2020, Watermaster invited Luhdorff & Scalmanini Consulting Engineers ("LSCE"), an independent groundwater expert consulting firm, to perform a peer review of the methodology used in evaluating the Safe Yield. LSCE was provided a draft of the Safe Yield Report, as well as access to Watermaster's files and documents, and attended a meeting with Watermaster's consultant, along with technical experts associated with the Appropriative Pool and parties in the Overlying (Agricultural) Pool, to discuss the Safe Yield analysis, methodology, modeling, and its application. After completing its evaluation, LSCE concluded that the model employed to develop the Safe Yield Report meets and/or exceeds generally accepted industry standards, and that application of the model and the Safe Yield Report is consistent with prevailing professional standards.

9. **WHEREAS**, a draft of the Safe Yield Report was released to the Watermaster parties on April 2, 2020, and considered by the Pool Committees and the Advisory Committee at their regularly scheduled meetings in April 2020.

10. **WHEREAS**, based upon requests made by the Overlying (Agricultural) Pool, the Appropriative Pool and the Advisory Committees, Watermaster convened a stakeholder workshop on April 29, 2020 to present the Safe Yield Report and receive and respond to comments thereon.

11. **WHEREAS**, the final version of the Safe Yield Report was released to the Watermaster parties on May 14, 2020. The final version includes certain editorial changes and written responses to comments received from the parties. However, the conclusions and findings in the Safe Yield report remained unchanged.

12. **WHEREAS**, the Safe Yield Report concludes that: "Watermaster should recommend that the Court set the Safe Yield at 131,000 AFY for the 2021 through 2030 period. No MPI or undesirable results are projected to occur if the Safe Yield were to be set at this value."

13. **WHEREAS**, the Safe Yield Report further concludes that a reduction in net recharge to the Basin could occur if the State implements certain water conservation measures as required by Water Code, § 10609, et seq. Accordingly, when the State adopts such water conservation measures, "Watermaster should evaluate the significance of any resulting change in cultural conditions, and, if cultural conditions are judged to have changed such that the Safe Yield would be changed by more than 2.5%, Watermaster should move the Court to reset the Safe Yield accordingly."

NOW, THEREFORE, BE IT RESOLVED, on the basis of the staff reports, expert opinions and substantial evidence presented, finds that:

1. The Safe Yield Report's evaluation of the Safe Yield of the Basin for the for period of July 1, 2020 through June 30, 2030 was conducted in accordance with the Court's April 28, 2017 Order and the Reset Technical Memorandum, and accurately considers the current and projected conditions of the Chino Basin.

2. The Court should amend Paragraph 6 of the Restated Judgment, setting the Safe Yield of the Chino Basin for the period July 1, 2020 to June 30, 2030 at 131,000 AFY, and no undesirable results or Material Physical Injury will result if the Safe Yield is reset in this manner.

3. If the State develops water conservation measures that reduce net recharge to the Chino Basin (i.e., reduced Evapotranspiration Adjustment Factors), as required by Water Code, § 10609, et seq., Watermaster should evaluate the significance of any resulting change in cultural conditions, and, if cultural conditions are judged to have changed such that the Safe Yield would be changed by more than 2.5%, Watermaster should move the Court to reset the Safe Yield accordingly.

4. Watermaster legal counsel is directed to prepare and file a motion with the Court to reset the Safe Yield in accordance with this Resolution and the Court's April 28, 2017 Order.

ADOPTED by the Watermaster Board on this 22nd day of May 2020.

By: _____
Chairman, Watermaster Board

ATTEST:

_____
Board Secretary
Chino Basin Watermaster

STATE OF CALIFORNIA)
) ss
COUNTY OF SAN BERNARDINO)

I, Bob Kuhn, Secretary of the Chino Basin Watermaster, DO HEREBY CERTIFY that the foregoing Resolution being No. 2020-03, was adopted at the special meeting of the Chino Basin Watermaster Board by the following vote:

AYES: 7

NOES: 2

ABSENT: 0

ABSTAIN: 0

CHINO BASIN WATERMASTER

Board Secretary

Date: May 22, 2020

LIST OF EXHIBITS

Exhibit A: 2020 Safe Yield Recalculation Final Report

2020 Safe Yield Recalculation
Final Report

May 15, 2020

Prepared for:

Chino Basin Watermaster
Partners in Basin Management

Prepared by:

WEI
Wildermuth Environmental, Inc.

This Page Intentionally Blank

WILDERMUTH ENVIRONMENTAL, INC.

May 15, 2020

Chino Basin Watermaster
Attention: Peter Kavounas
9641 San Bernardino Road
Rancho Cucamonga, CA 91730

Subject: ***Transmittal of 2020 Safe Yield Recalculation Final Report***

Dear Mr. Kavounas:

Transmitted herewith is the 2020 Safe Yield Calculation report pursuant to our task order with the Watermaster. Wildermuth Environmental, Inc. prepared this report pursuant the Court's April 28, 2017 order using the Court-ordered Safe Yield recalculation methodology. Our recommendations regarding resetting the Safe Yield can be found in Section 7.6 of this report.

We appreciate the opportunity to serve the Watermaster on this significant work. We are appreciative of the support of the Parties and their consultants in supplying information critical our work and their thoughtful participation and comments at: two colleague/peer review meetings that occurred on July 23, 2019 and January 27, 2020; the independent expert review process that occurred in late March 2020; and the April 29, 2020 workshop. Their input was extremely valuable in the completion of the work.

Please contact me if you need further assistance.

Wildermuth Environmental, Inc.

Mark J. Wildermuth, PE
President and Principal Engineer

This Page Intentionally Blank

Table of Contents

List of Tables

List of Figures

List of Figures

List of Figures

List of Figures

Acronyms, Abbreviations, and Initialisms

af	acre-feet
afy	acre-feet per year
AP	Ayala Park
Arrowhead	Arrowhead Mountain Spring Water Company
ASCE	American Society of Civil Engineers
BLUE	best linear unbiased estimation
CDA	Chino Desalter Authority
CDFM	cumulative departure from mean
Chino	City of Chino
Chino Hills	City of Chino Hills
CIMIS	California Irrigation Management Information System
CVM	2020 Chino Valley Model (also referred to as the "2020 CVM")
CVWD	Cucamonga Valley Water District
DIPAW	deep infiltration of precipitation and applied water
DWR	California Department of Water Resources
DYYP	Dry Year Yield Program
ET	evapotranspiration
ETAF	ET adjustment factor
ft/day	feet per day
ft-bgs	feet below ground surface
FWC	Fontana Water Company
GSWC	Golden State Water Company
HCMP	Hydraulic Control Monitoring Program
HSAs	hydrologic sub areas
HSCS	hydrostratigraphic cross-sections
HTD	historical temperature detrended
IEUA	Inland Empire Utilities Agency
InSAR	Interferometric Synthetic Aperture Radar
JCSD	Jurupa Community Services District
LACFCD	Los Angeles County Flood Control District
M&I	municipal and industrial
MAR	managed artificial recharge
MGal	Milligals
MPI	Material Physical Injury

Acronyms, Abbreviations, and Initialisms

MVWD	Monte Vista Water District
MWD	Metropolitan Water District of Southern California
MWELO	Model Water Efficient Landscape Ordinance
MZ1	Management Zone 1
MZ2	Management Zone 2
MZ3	Management Zone 3
Niagara	Niagara Bottling, LLC
NOAA	National Oceanic and Atmospheric Administration
Norco	City of Norco
NRCS	Natural Resources Conservation Service
NSE	Nash-Sutcliffe efficiency
OBMP	Optimum Basin Management Plan
OCWD	Orange County Water District
Ontario	City of Ontario
OSWDS	onsite waste disposal system
PEST	Parameter ESTimation
Pomona	City of Pomona
RWQCB	Regional Water Quality Control Board
SARWC	Santa Ana River Water Company
SAWCo	San Antonio Water Company
SBCFCD	San Bernardino County Flood Control District
SCS	Soil Conservation Service
SFI	Storage Framework Investigation
SGMA	Sustainable Groundwater Management Act
SMP	Storage Management Plan
TDS	total dissolved solids
Upland	City of Upland
USACE	US Army Corps of Engineers
USDA	United States Department of Agriculture
USGS	United States Geological Survey
UWMPs	Urban Water Management Plans
VIC	variable infiltration capacity
Watermaster	Chino Basin Watermaster
WEI	Wildermuth Environmental, Inc.

Acronyms, Abbreviations, and Initialisms

WMWD	Western Municipal Water District
WRCWRA	Western Riverside County Regional Wastewater Authority
WVWD	West Valley Water District

1.1 Background

The Chino Basin covers about 230 square miles of the upper Santa Ana River Watershed. Figure 1-1 shows the location of the Chino Basin. The basin is bounded by the Cucamonga Basin and the San Gabriel Mountains to the north; the Rialto-Colton Basin to the northeast; the chain of Jurupa, Pedley, and La Sierra Hills to the southeast and south; the Temescal Basin to the south; the Chino and Puente Hills to the southwest; the Spadra Basin, San Jose Hills and the Six Basins to the northwest. The Chino Basin lies within the Counties of Los Angeles, Riverside and San Bernardino and it includes the Cities of Chino, Chino Hills, East Vale, Fontana, Montclair, Ontario, Pomona Rancho Cucamonga and Upland.

The Chino Basin is an integral part of the regional and statewide water supply system. One of the largest groundwater basins in Southern California, the Chino Basin contains several million acre-feet (af) of water and has an unused storage capacity exceeding 1,000,000 af. Cities, water districts, water companies, and industries pump groundwater to supply all or part of their demands. Agricultural users also pump groundwater from the basin to irrigate crops and to supply water to dairies. Several pumpers in the basin have access to multiple water sources and conjunctively manage their sources making use of storage space in the basin.

The boundary of the Chino Basin is defined in the Stipulated Judgment (Judgment) entered in 1978 (Chino Basin Municipal Water District vs. the City of Chino et al. [SBSC Case No. RCV 51010]). Figure 1-1 shows the adjudicated of the basin. Since that time, the basin has been operated, as described in the Judgment, under the direction of a Court-appointed Watermaster. The Judgment included a Safe Yield of 140,000 acre-feet/year (afy), an allocation of pumping rights among the Parties to the Judgment, and a physical solution that, among other things, requires Watermaster to offset pumping that occurs in excess of pumping rights.

In 2000, the Watermaster developed its Optimum Basin Management Program (OBMP), and the Parties to the Judgment developed the Peace Agreement to implement it. The Peace Agreement contains the OBMP Implementation Plan. The OBMP Implementation Plan requires Watermaster to recalculate the Safe Yield of the basin in 2011 and every ten years thereafter.

In 2012, Watermaster began conducting an investigation to recalculate the Safe Yield pursuant to the Peace Agreement. This work was completed 2015. The investigation developed a methodology for calculating Safe Yield and concluded, based on that methodology, that the Safe Yield for the period 2011 through 2020 was 135,000 afy. On April 28, 2017, the Court approved the methodology and ordered that the Safe Yield be set to 135,000 afy for the period 2015 through 2020. The Court also ordered the Watermaster to start the process of recalculating the Safe Yield in January 2019 for the 2021 through 2030 period using the Court-ordered methodology

This report documents the investigation to recalculate the Safe Yield for the period of 2021 through 2030 pursuant to the Peace Agreement and the Court-approved Safe Yield recalculation methodology.

1.2 Definition and Theory of Net Recharge and Safe Yield

Net recharge, as used herein, is the exploitable inflow to a groundwater basin over a specified period, either under historical conditions or in a future projection under prescribed operating conditions, and it is a result of the hydrology, cultural conditions, and water management practices of the time period.

The most common definition of safe yield is attributed to (Todd, 1959):

> "[T]he rate at which groundwater can be withdrawn perennially under specified operating conditions without producing an undesirable result."

Most modern groundwater adjudications use some form of this definition. The Stipulated Agreement for the Chino Basin defines safe yield as:

> "[T]he long-term average annual quantity of groundwater (excluding replenishment or stored water but including return flow to the basin from the use of replenishment or stored water) which can be produced from the Basin under cultural conditions of a particular year without causing an undesirable result."[1]

This definition ties the safe yield to the cultural conditions of a specific year, presumably a near current or representative year if cultural conditions are changing. The 1978 Judgment declared the Chino Basin Safe Yield to be 140,000 af.[2]

Undesirable results listed in the Sustainable Groundwater Management Act (SGMA) include[3]:

(1) Chronic lowering of groundwater levels indicating a significant and unreasonable depletion of supply if continued over the planning and implementation horizon. Overdraft during a period of drought is not sufficient to establish a chronic lowering of groundwater levels if extractions and groundwater recharge are managed as necessary to ensure that reductions in groundwater levels or storage during a period of drought are offset by increases in groundwater levels or storage during other periods.
(2) Significant and unreasonable reduction of groundwater storage.
(3) Significant and unreasonable seawater intrusion.
(4) Significant and unreasonable degraded water quality, including the migration of contaminant plumes that impair water supplies.
(5) Significant and unreasonable land subsidence that substantially interferes with surface land uses.
(6) Depletions of interconnected surface water that have significant and unreasonable adverse impacts on beneficial uses of the surface water.

Chronic lowering of groundwater levels and unreasonable reductions of groundwater storage were the primary undesirable results that the Chino Basin Judgment sought to protect against. The physical solution provided in the Judgment and the groundwater management plan in the OBMP limit the undesirable results listed above through the implementation of localized management programs. The Judgment requires Watermaster to offset pumping in excess of the Safe Yield by acquiring an amount of water equal to the pumping in excess of the Safe Yield recharge it into the basin to ensure no uncontrolled depletion of storage. Watermaster assesses the Parties that pump groundwater in excess of their Safe Yield allocation to fund the purchase of replenishment water. The OBMP requires that Watermaster use its discretion when recharging supplemental water to balance recharge and discharge in every area and subarea of the basin to manage against chronic lowering of groundwater levels.

[1] Judgment, Section I Introduction, Paragraph 4 Definitions.
[2] Judgment, Section II Declaration of Rights, Part A Hydrology, Paragraph 6 Safe Yield.
[3] See the following link for the definition of "undesirable result":
http://leginfo.legislature.ca.gov/faces/codes_displayText.xhtml?lawCode=WAT&division=6.&title=&part=2.74.&chapter=2.&article=

Common engineering practice is to estimate net recharge and safe yield based on hydrologic principles. The following discussion describes the basic methodology used to estimate net recharge and safe yield from hydrologic principles.

Net recharge is estimated as the average net inflow to the basin, excluding the direct recharge of supplemental water. Supplemental water, as used herein, refers to water not tributary to the basin and includes imported and recycled waters. Returns from agricultural uses and on-site wastewater disposal systems (e.g. septic tanks, cesspools, etc.) that overlie the basin are included in net recharge. There are two ways to compute net recharge under this concept, both of which can be derived from the continuity equation. The continuity equation is:

$$\text{Change in Storage } (\Delta S) = [\text{Inflow } (I) - \text{Outflow } (O)] * \Delta t \quad (1)$$

Where:

S^t is the storage at time t,

ΔS is the change in storage calculated as S^{t+1} minus S^t,

I is the total inflow to the basin over the period *t* to *t+1* and is equal to the sum of Streambed Recharge (I_{sr}) + Deep Infiltration of Precipitation (I_p) + Subsurface Inflow (I_{ssi}) + Artificial Recharge of Supplemental Water (I_{ar}) + Deep Infiltration of Irrigation Return Flows ($I_{rf.}$),

O is the total outflow from the basin over the period *t* to *t+1* and is equal to the sum of Groundwater Pumping (O_p) + Subsurface Outflow (O_{ss}) + Groundwater Discharge to Surface Water (Q_{rw}) + Evapotranspiration (Q_{et}), and

Δt is the length of the time period used to compute the balance.

The inflow and outflow terms listed above have dimensions of L^3/T.[4] If expanded using the hydrologic terms listed above, the continuity equation becomes:

$$\Delta S = [I_{sr} + I_p + I_{ssi} + I_{ar} + I_{rf.} - O_p - O_{ss} - O_{rw} - O_{et}] * \Delta t \quad (2)$$

The net recharge (net inflow) to a basin for a single year is:

$$\text{Net recharge} = I_{sr} + I_p + I_{ssi} + I_{rf.} - O_{ss} - O_{rw} - O_{et} = S^{t+1} - S^t + O_p - I_{ar} \quad (3)$$

The net recharge over a multiple-year period can be estimated from:

$$\text{Net recharge} = [\,\Sigma I_{sr} + \Sigma I_p + \Sigma I_{ssi} + \Sigma I_{rf.} - \Sigma O_{ss} - \Sigma O_{rw} - \Sigma O_{et}] \,/\, \Delta t \quad (4)$$

$$= [\,\Delta S + \Sigma O_p - \Sigma I_{ar}]/\Delta t$$

The summation symbol (Σ) in equation 4 for each term aggregates the contiguous time series over multiple years that comprise a base period or period of interest.

In modern practice, the most pragmatic way to estimate net recharge is to rigorously apply numerical models and evaluate equation (4):

[4] L means length, and T means time.

$$\text{Net recharge} = \Delta S/\Delta t + O_p - I_{ar} \quad (5)$$

Where O_p and I_{ar} are the average groundwater pumping and average supplemental water recharge over the base period, respectively.

1.3 Safe Yield Criteria

The net recharge to a groundwater basin, estimated using equations 4 or 5 above, corresponds to the net inflow to a groundwater basin over a specified period of time. If the period includes representative long-term hydrology and meets other safe yield related criteria *described below*, the net recharge for that period can be assumed to be the safe yield.

1.3.1 Base Period

In safe yield determinations, it is common engineering practice to select a base period from precipitation records that span a reasonably long period of time, containing wet periods and dry periods, and for which the annual average precipitation equals the long-term average annual precipitation. The availability of data for estimating the inflow, outflow, and storage terms can also factor into the base period selection.

The land use, water management, and drainage conditions that are tributary to and overlie a basin at a specific time are herein referred to collectively as the cultural conditions of a basin. The types of land uses that overlie a groundwater basin have a profound impact on recharge; this is demonstrated in Sections 6 and 7. The land use transition from natural conditions to agricultural uses and subsequently to urban uses changes the amount of recharge to a basin. Furthermore, irrigation practices change over time in response to agricultural economics (e.g. demand for various agricultural products, commodity prices, production costs, etc.), the availability of water, regulatory requirements, technology, and the cost of water. Urbanization increases the amount of imperviousness, decreasing the irrigable and pervious areas, which allow irrigation return flows and precipitation to infiltrate through the soil, and conversely increases the amount of stormwater produced on the land surface. Drainage improvements associated with the transition from natural and agricultural uses to urban uses reduce the recharge of stormwater; stream channels are hydraulically improved, including concrete-lining, to move stormwater efficiently through the watershed overlying the groundwater basin.

Changes in land use, water management, and drainage over time produce groundwater recharge and discharge time histories that are not stationary: the relationship of the inflow and outflow terms to precipitation and other hydrologic and water management practices change over time. Thus, the selection of a representative historical base period that satisfies the traditional criteria for a determination of safe yield that is representative of current and near-future cultural conditions is not possible using the actual historical record.

1.3.2 Storage

The availability of water in groundwater storage at the beginning of the base period and the availability of operational storage space during the base period must be such that pumping at the estimated safe yield can be sustained. There must be enough storage space to provide the head to get groundwater to

flow into wells and operational storage[5] space available to store recharge in excess of the safe yield during wet years so that it can be available when recharge is less than the safe yield during dry years.

1.3.3 Basin Area

The safe yield is determined for a geographically defined groundwater basin. Recharge and discharge to the basin occur over or on the boundaries of the basin. The Chino Basin has two boundaries: the adjudicated boundary, as defined in the 1978 Judgment, and the hydrologic boundary, which more accurately reflects the locations of physical barriers to groundwater movement and basin recharge. Figure 1-1 shows the locations of these boundaries. The primary differences in these boundaries can be observed in the northern part of the basin and its boundary with the Cucamonga Basin. The net recharge computed in this investigation is based on the hydrologic boundary; the net recharge applies to the adjudicated boundary.

1.3.4 Cultural Conditions

Cultural conditions, as used herein, refers to land use and associated soil, crop and water management practices. With few exceptions, as land is converted from natural undeveloped conditions to human uses, it becomes more impervious and produces more stormwater runoff. Historically, when land use has converted from natural and agricultural uses to urban uses, imperviousness has increased from near zero to between 60 and almost 100 percent, depending on the specific land use. In an undeveloped state, most of the precipitation that fell on the watershed tributary to and over the Chino Basin was intercepted by vegetation or absorbed into the soils overlying the Basin. This water would have either been consumed by native vegetation or lost to evaporation. The overlying soils would become wet during the winter and completely dry before the next winter. Infrequent large storms produced significant runoff, some of which recharged the underlying groundwater basin through streambed infiltration.

Most of the precipitation that falls on paved areas and roofs becomes runoff. In the urban landscape, pervious areas are covered with vegetation that is irrigated and cultivated or left unplanted and not irrigated. The soil underlying irrigated vegetation is maintained in a moist state and never completely dries out—the significance being that when soil is continuously moist, some of the irrigation water and precipitation can infiltrate beyond the root zone and recharge the underlying groundwater basin.

Agricultural irrigation is never 100-percent efficient. Flood and furrow irrigation practices have irrigation efficiencies typically ranging from 40 to 60 percent and sprinkler irrigation from 70 to 80 percent. Irrigation return flows were a major source of recharge to the basin when irrigated agriculture dominated the land use.

Drainage improvements that were incorporated into the agricultural and urban landscapes were designed to convey stormwater rapidly, safely, and efficiently from the land surface, and discharge it away from agricultural and urban areas. Until the late 1990s there was little or no thought as to the value of the stormwater that discharged out of the Chino Basin.

1.4 Court Direction to Reset the Safe Yield

On April 28, 2017, the Court issued an order to reset the Safe Yield and provided related direction to Watermaster regarding subsequent Safe Yield resets. Paragraphs 4.2 through 4.7 of that order, listed

[5] Operational storage space is the volume of storage required to regulate the variable recharge over time to ensure that the safe yield can be pumped.

below, provide context to the Safe Yield recalculation efforts described herein and to the Watermaster's process to reset the Safe Yield.

> "4.2 Scheduled Reset. Watermaster will initiate a process to evaluate and reset the Safe Yield by July 1, 2020 as further provided in this order. Subject to the provisions of Paragraph 4.3 below, the Safe Yield, as it is reset effective July 1, 2020 will continue until June 30, 2030. Watermaster will initiate the reset process no later than January 1, 2019, in order to ensure that the Safe Yield, as reset, may be approved by the court no later than June 30, 2020. Consistent with the provisions of the OBMP Implementation Plan, thereafter Watermaster will conduct a Safe Yield evaluation and reset process no less frequently than every ten years. This Paragraph is deemed to satisfy Watermaster's obligation, under Paragraph 3.(b) of Exhibit "I" to the Restated Judgment, to provide notice of a potential change in Operating Safe Yield.
>
> 4.3 Interim Correction. In addition to the scheduled reset set forth in Paragraph 4.2 above, the Safe Yield may be reset in the event that, with the recommendation and advice of the Pools and Advisory Committee and in the exercise of prudent management discretion described in Paragraph 4.5(c), below, Watermaster recommends to the court that the Safe Yield must be changed by an amount greater (more or less) than 2.5% of the then-effective Safe Yield.
>
> 4.4 Safe Yield Reset Methodology. The Safe Yield has been reset effective July 1, 2010 and shall be subsequently evaluated pursuant to the methodology set forth in the Reset Technical Memorandum. The reset will rely upon long-term hydrology and will include data from 1921 to the date of the reset evaluation. The long-term hydrology will be continuously expanded to account for new data from each year, through July 2030, as it becomes available. This methodology will thereby account for short term climatic variations, wet and dry. Based on the best information practicably available to Watermaster, the Reset Technical Memorandum sets forth a prudent and reasonable professional methodology to evaluate the then prevailing Safe Yield in a manner consistent with the Judgment, the Peace Agreements, and the OBMP Implementation Plan. In furtherance of the goal of maximizing the beneficial use of the waters of the Chino Basin, Watermaster, with the recommendation and advice of the Pools and Advisory Committee, may supplement the Reset Technical Memorandum's methodology to incorporate future advances in best management practices and hydrologic science as they evolve over the term of this order.
>
> 4.5 Annual Data Collection and Evaluation. In support of its obligations to undertake the reset in accordance with the Reset Technical Memorandum and this order, Watermaster shall annually undertake the following actions:
>
> > (a) Ensure that, unless a Party to the Judgment is excluded from reporting, all production by all Parties to the Judgment is metered, reported, and reflected in Watermaster's approved Assessment Packages;
> >
> > (b) Collect data concerning cultural conditions annually with cultural conditions including, but not limited to, land use, water use practices, production, and facilities for the production, generation, storage, recharge, treatment, or transmission of water;
> >
> > (c) Evaluate the potential need for prudent management discretion to avoid or mitigate undesirable results including, but not limited to, subsidence, water

quality degradation, and unreasonable pump lifts. Where the evaluation of available data suggests that there has been or will be a material change from existing and projected conditions or threatened undesirable results, then a more significant evaluation, including modeling, as described in the Reset Technical Memorandum, will be undertaken; and,

(d) As part of its regular budgeting process, develop a budget for the annual data collection, data evaluation, and any scheduled modeling efforts, including the methodology for the allocation of expenses among the Parties to the Judgment. Such budget development shall be consistent with section 5.4(a) of the Peace Agreement.

4.6 Modeling. Watermaster shall cause the Basin Model to be updated and a model evaluation of Safe Yield, in a manner consistent with the Reset Technical Memorandum, to be initiated no later than January 1, 2024, in order to ensure that the same may be completed by June 30, 2025.

4.7 Peer Review. The Pools shall be provided with reasonable opportunity, no less frequently than annually, for peer review of the collection of data and the application of the data collected in regard to the activities described in Paragraphs 4.4, 4.5, and 4.6 above."

1.5 Court-Approved Methodology to Calculate Safe Yield

The Safe Yield calculation methodology used in the 2020 Safe Yield calculation is documented in a technical memorandum dated August 15, 2015 and was subsequently approved by the Court on April 28, 2017. The methodology is described below.

"The methodology to redetermine the Safe Yield for 2010/11 and the recommended methodology for future Safe Yield evaluations is listed below. This methodology is consistent with professional custom, standard and practice, and the definition of Safe Yield in the Judgment and the Physical Solution.

1. Use the data collected during 2000/01 to 2009/10 (and in the case of subsequent resets newly collected data) in the re-calibration process for the Watermaster's groundwater-flow model.
2. Use a long-term historical record of precipitation falling on current and projected future land uses to estimate the long-term average net recharge to the Basin.
3. Describe the current and projected future cultural conditions, including, but not limited to the plans for pumping, stormwater recharge and supplemental-water recharge.
4. With the information generated in [1] through [3] above, use the groundwater-flow model to redetermine the net recharge to the Chino Basin taking into account the then existing current and projected future cultural conditions.
5. Qualitatively evaluate whether the groundwater production at the net recharge rate estimated in [4] above will cause or threaten to cause "undesirable results" or "Material Physical Injury". If groundwater production at net recharge rate estimated in [4] above will cause or threaten to cause "undesirable results" or "Material Physical Injury" then Watermaster will identify and implement prudent measures necessary to mitigate "undesirable results" or "Material Physical Injury", set the value of Safe Yield

> to ensure there is no "undesirable results" or "Material Physical Injury", or implement a combination of mitigation measures and a changed Safe Yield."

1.6 Scope of Work

The scope of work required to recalculate the Safe Yield includes updating and recalibrating Watermaster's existing Chino Basin model, updating future water demands and water supply plans, and using the updated model to project the net recharge, basin response and Safe Yield. The scope of work to recalculate the safe Yield included:

- Task 1 Project Management and Meetings
- Task 2 Update Hydrogeologic Conceptual Model
- Task 3 Recalibrate Groundwater Model
- Task 4 Update Planning Projections
- Task 5 Conduct Planning Simulations to Update Projections of Net Recharge and Safe Yield
- Task 6 Prepare 2020 Safe Yield Recalculation Report

1.7 Scope of the Model Update

The model used in the previous Safe Yield recalculation was developed in 2012, described in detail in *2013 Chino Basin Groundwater Model Update and Recalculation of the Safe Yield Pursuant to the Peace Agreement* (WEI, 2015), and is referred to herein as the 2013 Model. The model domain of the 2013 Model is bounded by bedrock and adjacent groundwater basins, all of which contribute inflow to the Chino Basin. The Temescal Basin is included in the 2013 Model because there is no known barrier separating it from the Chino Basin and pumping in the Temescal Basin affects inflow to the Chino Basin and surface water discharge in the Santa Ana River. The aquifer system is represented by a thick vadose zone and three saturated layers. Surface and ground water interaction was included for the Santa Ana River and its tributaries

For the 2020 Safe Yield recalculation, the model domain was extended to include the Cucamonga, Six, and Spadra Basins. This was done by combining existing Cucamonga and Six Basins models with the 2013 Model and extending the 2013 Model domain to incorporate the Spadra Basin. This model expansion was done to improve estimates of recharge to the Chino Basin and to ensure consistency in groundwater management planning among the Parties that pump groundwater in Chino and these other basins. Most of the pumpers in the Six Basins and all the pumpers in the Cucamonga Basin are Parties to the Chino Basin Judgment. This expanded model is referred to herein as the Chino Valley Model, CVM or 2020 CVM. At the request of Cucamonga Basin water agencies, the water budgets and basin response for the Cucamonga Basin will not be reported herein. The same courtesy was extended to the water agencies in the Six, Spadra and Temescal Basins. The 2020 CVM-estimated subsurface outflow from these basins to the Chino Basin is included in the Chino Basin water budget

The aquifer system in the Chino Basin was updated to include five layers for improved groundwater flow simulation to enable future simulation of land subsidence and improved water quality simulation. Layers 1, 3 and 5 are courser-grain aquifers that are exploited by pumping wells, Layers 2 and 4 are aquitards that separate the courser grain aquifers. Section 2 describes the updated hydrogeologic conceptual model for the 2020 CVM.

1.8 Scope of the Planning Projection Update

Pursuant to the court-approved Safe Yield recalculation methodology, the Safe Yield was estimated to be the average net recharge for the period of 2021 through 2030. The net recharge was estimated with

the calibrated 2020 CVM and the-projected future water demands and water supply plans provided by the Parties and others.

Watermaster and the Parties updated their projected future water demands and water supply plans for the recently completed *2018 Storage Framework Investigation* (WEI, 2018) and refined them again in 2019 for the *2020 Storage Management Plan* (WEI, 2019). This updated planning data is used in the 2020 Safe Yield recalculation. The planning projection update also includes estimates of the impacts of climate change on recharge, based on an approach developed by the California Department of Water Resources (DWR). The updated planning projections and the incorporation of climate change are described in Section 7.

1.9 Stakeholder and Technical Reviews

Documentation of the technical work to recalculate the Safe Yield and its periodic review occurred as listed below:

- July 23, 2019 Colleague/Peer Review Workshop. This workshop was attended by the Parties and their invited technical consultants to discuss the updated conceptual model of the 2020 CVM and the calibration approach. Questions and comments from the workshop participants were addressed at the workshop and the more significant questions and comments were recorded and subsequently responded to in writing.
- January 27, 2020 Colleague/Peer Review Workshop. This workshop was attended by the Parties and their invited technical consultants to discuss the Court Ordered Safe Yield methodology, calibration of the 2020 CVM and the technical approach to estimating Safe Yield with the 2020 CVM. Questions and comments from the workshop participants were addressed at the workshop and the more significant questions and comments were recorded and subsequently responded to in writing.
- Submittal of Administrative (internal review) Draft Report to Watermaster Staff – March 23, 2020
- Expert Technical Review. Mr. Will Halligan of Luhdorff & Scalmanini Consulting Engineers, was invited by Watermaster staff to perform a peer review of the Watermaster Engineer's methodology in evaluating the Safe Yield, including the construction and utilization of the 2020 CVM. Two meetings occurred that that involved several hours of discussion between Mr. Halligan, WEI staff and technical consultants to the State of California and Appropriative Pool. After completing his evaluation, Mr. Halligan reached the conclusions that: (i) the model meets and/or exceeds generally accepted industry standards, and (ii) that the application of the model and the Safe Yield evaluation has been consistent with prevailing professional standards.
- Submittal of the Draft Final Report to Watermaster – April 2, 2020
- April 29, 2020 Stakeholder Workshop. This workshop was attended by the Parties and their invited technical consultants to discuss the application of the Court Ordered Safe Yield methodology to estimate Safe Yield. Questions and comments from the workshop participants were addressed at the workshop and the more significant questions and comments were recorded and subsequently responded to in writing.
- Submittal of the Final 2020 Safe Yield Recalculation Report – May 15, 2020.

1.10 Report Organization

The remaining sections of this report are described below.

Section 2 – Hydrogeologic Setting: Section 2 describes the hydrogeologic conditions of the Chino Basin, including the geologic setting, hydrostratigraphy, the occurrence and movement of groundwater, aquifer

properties, groundwater levels, and groundwater quality. These data were used to construct a hydrogeologic conceptual model of the Chino Basin for input to the groundwater-flow model.

Section 3 – Hydrologic Setting: Section 3 describes the hydrologic conditions and data used to develop the 2020 CVM.

Section 4 – Computer Codes: Section 4 describes the computer codes used in the 2020 CVM.

Section 5 – Model Construction: Section 5 describes how the hydrogeologic conceptual model was translated into a numerical model. The model domain, initial conditions, boundary conditions, and hydraulic conditions are defined in this section.

Section 6 – Model Calibration: Section 6 discusses the model calibration process and results for fiscal years 1978 through 2018.

Section 7 – 2020 Safe *Yield Calculation:* Section 7 describes projected water demands and water supply plans, net recharge, and projected basin response and assessment of undesirable results and recommended Safe Yield.

Section 8 – References

Technical Appendices

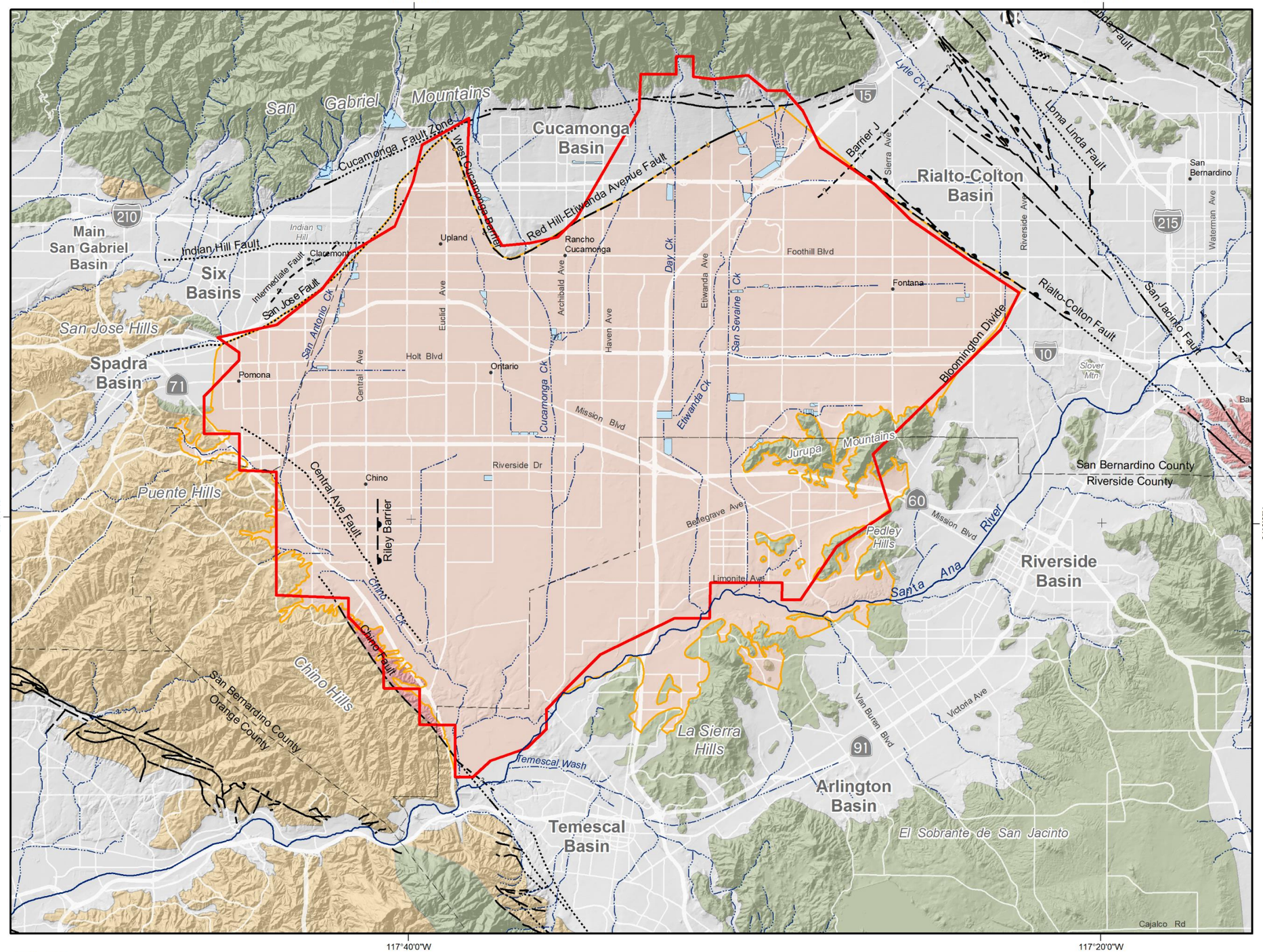

Chino Basin Hydrologic Boundary

Chino Basin Adjudicated Boundary

Streams & Flood Control Channels

Flood Control & Conservation Basins

Geology

Water-Bearing Sediments

Quaternary Alluvium

Consolidated Bedrock

Plio-Pleistocene Sedimentary Rocks

Cretaceous to Miocene Sedimentary Rocks

Pre-Tertiary Igneous and Metamorphic Rocks

Fault (solid where accurately located; dashed where approximately located or inferred; dotted where concealed)

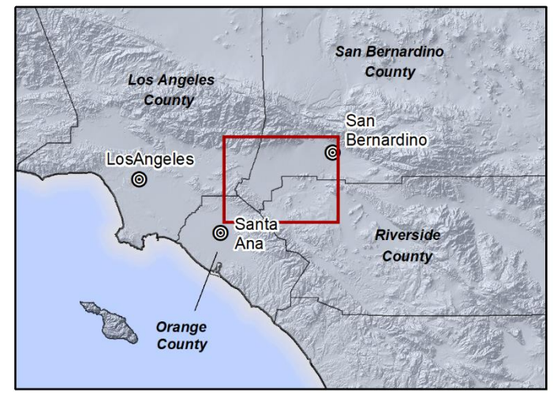

Produced by:

WEI
WILDERMUTH ENVIRONMENTAL, INC.

Author: MJC

Date: 3/23/2020

Document Name: Figure_1-1_20200323_Intro

0 1 2 3 4 5 Miles

0 2 4 6 8 KM

Prepared for:

2020 Safe Yield Recalculation

CHINO BASIN WATERMASTER
Partners in Basin Management

Hydrologic and Adjudicated Boundaries of the Chino Basin

Figure 1-1

This section describes the geologic and hydrogeologic settings for the Chino, Cucamonga, and Six Basins, based on the most current information available. As mentioned in Section 1, these basins are referred to herein as the Chino Valley Basins. Specifically, below, geologic settings and stratigraphy, the occurrence and movement of groundwater, hydrostratigraphy, and aquifer properties are discussed.

2.1 Geologic Setting

The basins that comprise the Chino Valley (Chino, Cucamonga, Six, Spadra, and Temescal Basins) are part of a large and broad alluvial-filled plain situated between the San Gabriel Mountains to the north (Transverse Ranges) and the elevated Perris Block to the south (Peninsular Ranges). The surrounding mountains and hills were uplifted by tectonic compression and faulting during the Quaternary Period[6] and sediments were eroded and washed-out of the mountains by streams and deposited in the low-lying depressions on the Perris Block. The Chino Valley can be characterized as a broad smooth plain that slopes from the San Gabriel Mountains to the Santa Ana River. Towards the northern part of the Chino Valley, major faults and groundwater barriers define the Chino, Cucamonga, and Six Basins boundaries. Figure 2-1 is a generalized geologic map illustrating the major geologic rock formations, faults, and groundwater barriers surrounding the Chino Valley Basins.

The major faults shown in Figure 2-1—the Cucamonga Fault Zone, the Rialto-Colton Fault, the Red Hill-Etiwanda Avenue Fault, the San Jose Fault, Central Ave Fault, and the Chino Fault—are at least partly responsible for the uplift of the surrounding mountains and the depression of the basins. These faults are significant in that they are known barriers to groundwater flow within the aquifer-system(s) and define some of the external boundaries of the basins by influencing the magnitude and direction of groundwater flow. These faults, their effects on groundwater movement, as well as the geology and hydrogeology of the Chino Valley Basins areas have been documented by various entities and authors. These entities and authors are documented in *Section 8 – References* and are cited accordingly throughout this report.

2.2 Stratigraphy

For the purposes of this report, the stratigraphy of the Chino Valley Basins area is comprised of two natural divisions: (1) permeable formations that comprise the primary groundwater reservoirs, termed "water-bearing sediments," and (2) less permeable formations that enclose the groundwater reservoirs, termed "consolidated bedrock." Water-bearing sediments overlie consolidated bedrock. Consolidated bedrock is exposed at the surface in the surrounding hills and mountains. These geologic formations are described below in stratigraphic order, starting with the oldest formations.

The terms used in this report to describe the bedrock formations—such as "consolidated," "non-water-bearing," and "impermeable"—are used in a relative sense. In fact, the water content and permeability of these bedrock formations is not zero. Pervious strata or fracture zones in bedrock formations may yield water to wells locally; however, the storage and transmissive properties are typically inadequate for sustained production. The primary point is that the permeability of the geologic formations in the areas flanking the basins is much less than that of the aquifers in the basins.

.

[6] Approximately 2 million years ago to the present.

2.2.1 Consolidated Bedrock

The consolidated bedrock formations that flank and underlie the Chino Valley Basins area are comprised of a wide variety of pre-Tertiary age igneous and metamorphic rocks that are overlain by a thick sequence of Tertiary age volcanic and sedimentary rocks consisting of consolidated marine and continental deposits. The upper part of the sedimentary rock sequence consists of semi-consolidated sedimentary rock deposits. Figure 2-1 shows the surface outcrops of the consolidated bedrock formations that surround the basins. Note that the consolidated bedrock comprised of pre-Tertiary igneous and metamorphic rocks flanks the Cucamonga and Six Basins to the north and the Chino Basin to the southeast and that the consolidated bedrock comprised of Tertiary age sedimentary rocks flanks the Chino and Six Basins to the west.

2.2.1.1 Basement Complex

The basement complex consists of igneous deformed and recrystallized metamorphic rocks that have been invaded in places by masses of granitic and related igneous rocks. The intrusive granitic rocks, which make up most of the Basement Complex, were emplaced about 110 million years ago in the late Middle Cretaceous (Larsen, et al., 1958). These rocks were subsequently uplifted and exposed by erosion, as presently seen in the San Gabriel Mountains and in the uplands of the Perris Block (Jurupa Mountains and La Sierra Hills). Weathering and erosion of the Basement Complex in the San Gabriel Mountains have been the major source of detritus to the overlying sedimentary deposits and, in particular, the water-bearing sediments of the Chino Valley Basins.

2.2.1.2 Consolidated and Semi-Consolidated Sedimentary and Volcanic Rocks

Undifferentiated pre-Pliocene age rocks comprised of consolidated sedimentary and volcanic rocks unconformably overlie the Basement Complex within the Chino Valley Basins area. The consolidated sedimentary and volcanic rocks are exposed as outcrops in the Chino Hills and Puente Hills along the western margin of the Chino and Six Basins. The deposits consist of well-stratified marine sandstones, conglomerates, shales, and interlayered lava flows that range in age from late Cretaceous to Miocene. Durham reported that this sequence reaches a total stratigraphic thickness of more than 24,000 feet in the Puente Hills and is down-warped more than 8,000 feet below sea level in the Prado Dam area (Durham, et al., 1964).

Plio-Pleistocene age sediments comprised as a thick series of semi-consolidated clays, sands, and gravels of marine and non-marine origin overlie the consolidated sedimentary rocks. These deposits are exposed in the Chino, Puente, and San Jose Hills. For this report, these deposits are considered consolidated bedrock, and they are likely the first bedrock penetrated in the southwestern portion of the Chino Basin. The upper portion of the semi-consolidated sedimentary rock deposits are more permeable than the lower portion, thus representing a gradual transition from water-bearing sediments to non-water-bearing consolidated rocks. The semi-consolidated, water-bearing sediments are similar in texture and composition to the overlying water-bearing alluvium, which makes the distinction between the formations difficult to identify in borehole data.

2.2.2 Water-Bearing Sediments

Beginning in the Pleistocene and continuing to the present, an intense episode of faulting depressed the Chino Valley Basins and uplifted the surrounding mountains and hills. Detritus eroded from the mountains and hills were transported and deposited in the basins atop the consolidated bedrock formations as interbedded, discontinuous layers of gravel, sand, silt, and clay to form the water-bearing sediments.

In general, the water-bearing sediments deposited within the Chino Valley Basins are over 1,000 feet thick in the deeper portions of the basins but thin towards the San Gabriel Mountains to the north and towards the east across the Chino Basin. Eckis (1934) speculated that the contact between consolidated bedrock and water-bearing sediments in the Chino Basin is unconformable, as indicated by an ever-present weathered zone in the consolidated bedrock directly underlying the contact with the water-bearing sediments. Because of this, the semi-consolidated sedimentary bedrock formations can have a similar texture and composition to the overlying water-bearing sediments. Downhole borehole geophysical data collected from each of the basins have aided in identifying the contact between consolidated bedrock and water-bearing sediments as well as the contact between Older and Younger Alluvium.

For this report, the water-bearing sediments are differentiated into Pleistocene -age Older Alluvium and Holocene -age Younger Alluvium. The general character of these formations is known from driller's logs, borehole geophysical data, and surface outcrops.

2.2.2.1 Older Alluvium

The Older Alluvium typically consists of reddish-brown, moderately to well consolidated, dissected alluvial fan deposits of Early Pleistocene age. These deposits are comprised of silt, sand, gravel, and conglomerates. The Older Alluvium is commonly distinguished in surface outcrop from Younger Alluvium by its red-brown or red-brick color and is more weathered than the overlying Younger Alluvium.

In the Chino Basin, the Older Alluvium varies in thickness from about 200 feet near the southwestern end of the Chino Basin to over 1,100 feet southwest of Fontana. The pumping capacities of wells completed in the Older Alluvium generally range between 500 and 1,500 gallons per minute (gpm). Capacities exceeding 1,000 gpm are common, and some modern production wells test-pumped at over 4,000 gpm (e.g. Ontario Wells 30 and 31 in southeastern Ontario). In the southern part of the basin, where water-bearding sediments tend to be more clay rich, wells generally yield less than 1,000 gpm.

The Older Alluvium in the Cucamonga Basin is exposed as surface outcrops along the southern margin of the basin and just north of the Red Hill-Etiwanda Avenue Fault. These deposits are generally compromised of silt, sand, gravel, and conglomerates. Cobbles and boulders become more abundant in driller's logs closer to the San Gabriel Mountains. The Older Alluvium is about 700 to 800 feet thick and is the main water-bearing formation within the Cucamonga Basin.

In the Six Basins, the Older Alluvium is exposed at Indian Hill. Across the Six Basins, the Older Alluvium is typically thicker than the overlying Younger Alluvium in the central and deeper portions of the basin and is the main source of groundwater for production wells in the area. Near the southeastern edge of Six Basins, the Older Alluvium is composed of thick sediment sequences that contain layers of clay-rich, fine-grained sediments that are interfingered with coarser-grained sediments. These fine-grained layers have low permeabilities and can cause confining conditions within the aquifer-system and artesian conditions at wells that penetrate the fine-grained layers.

2.2.2.2 Younger Alluvium

The Younger Alluvium occupies streambeds, washes, alluvial fan deposits that flank the mountain and hill fronts, and other areas of recent sedimentation. Oxidized particles tend to be flushed out of the sediments during transport, and the Younger Alluvium is commonly light yellow, brown, or gray. It consists of rounded fragments derived from the erosion of bedrock, reworked Older Alluvium, and the mechanical breakdown of larger fragments within the Younger Alluvium itself.

Across the Chino Basin, the Younger Alluvium varies in thickness from over 100 feet near the mountains to a just few feet south of Interstate 10 and generally covers most of the northern half of the basin. The Younger Alluvium is not saturated and, thus, does not yield water directly to wells. Water percolates readily in the Younger Alluvium, and most of the large flood control and conservation basins in the Chino Basin are located in the Younger Alluvium.

The Younger Alluvium in the Cucamonga Basin is less than approximately 250 feet thick, and although the sediments that comprise the unit are highly permeable, the Younger Alluvium is not considered to be water bearing—groundwater levels are typically below the bottom of this unit.

Across the Six Basins, the Younger Alluvium is absent in places and is thin (less than about 150 feet) compared to the Older Alluvium. Where present, the unit is generally unsaturated and not considered to be water-bearing—groundwater levels are typically below the bottom of this unit.

2.3 Effective Base of the Freshwater Aquifer

The consolidated bedrock formations occur at depth underlying the water-bearing sediments of the Chino Valley Basins act as the effective base of the freshwater aquifer or bottom of the aquifer. Figure 2-2 is a map of the current interpretation of the effective base of the freshwater aquifer across the Chino Valley Basins. The map shows contours of equal elevation of the effective base of the freshwater aquifer or, in other words, the approximate elevation to the buried contact between the water-bearing sediments and the consolidated bedrock formations. These contours were first drawn by the California Department of Water Resources (DWR, 1970) and have been subsequently updated based on new data, information, and interpretations by WEI.

The bottom of the Chino Valley's freshwater aquifer system is based on interpretations from borehole lithology, surface and borehole geophysical data, well construction details, and groundwater levels from each of the basins comprising the Chino Valley Basins: the Chino, Cucamonga, Six, and Spadra Basins. As such, following *Section 2.3.1 Gravity Data,* a description of the effective base of the freshwater aquifer is discussed for each Chino Valley Basins.

2.3.1 Gravity Data

The basement complex presumably underlies sedimentary bedrock in the western Chino Basin but at depths too great to play a factor in the shallow freshwater aquifers. Durham and Yerkes (1964) estimated a depth to the basement complex of several thousand feet and a contact of angular unconformity with the overlying sedimentary bedrock. Geophysical data supports this conceptualization. Figure 2-3 shows regional gravity data plotted and contoured as Bouguer anomalies with a contour interval of five milligals (MGal). The gravity data were collected in May 2007 from GEONET at the United States Gravity Data Repository System. The Bouguer anomalies in the Chino Valley Basins area range between -80 MGal in the western Chino Basin to about -55 MGal in the granitic Jurupa Mountains and La Sierra Hills. Gravity lows can be attributed to a greater thickness of low-density rock formations, such as loose sediments and sedimentary rocks. Note how the Bouguer anomaly contours have a similar shape to the contours of the bottom of the aquifer in Figure 2-2 with a trough of low values in the western Chino Basin. These gravity data are consistent with a deep sedimentary trough in the western Chino Basin with progressively shallower crystalline bedrock to the east and southeast toward the granitic Jurupa Mountains and La Sierra Hills.

2.3.2 Six Basins

In the Six Basins, the consolidated bedrock formations occur at depth underlying the water-bearing sediments and act as the effective base of the freshwater aquifer or bottom of aquifer. The bottom of

aquifer contours shown in Figure 2-2 are equivalent to the depth of the buried contact between the water-bearing sediments and the consolidated bedrock. The bottom of aquifer contours were drawn from lithologic descriptions of borehole cuttings that were recorded on well driller's reports and from borehole geophysical logs.

Figure 2-2 shows that in the Six Basins, the bottom of the aquifer is a network of troughs and ridges. The main features of the bottom of the aquifer are:

- A deep trough located northeast of the Indian Hill Fault that slopes from west to east.
- A west-to-east trending ridge located just north of the Indian Hill Fault.
- A ridge that trends southwest from the Indian Hill Fault just north of the Intermediate Fault.
- A deep trough in the southern portions of the Six Basins that slopes to the southeast.

The ridges appear to be related to fault movement. The troughs appear to be related to faulting and/or erosion by ancestral streams. Eckis speculated that the contact between the consolidated bedrock and the water-bearing sediments is unconformable, as indicated by an ever-present weathered zone in the consolidated bedrock directly underlying the contact with the water-bearing sediments (Eckis, 1934). This observed relationship suggests that the consolidated bedrock in the Six Basins area was undergoing erosion prior to deposition of the water-bearing sediments. Eckis reported that the weathered zone is about 50 feet thick and that beneath the weathered zone the bedrock is hard.

2.3.3 Cucamonga Basin

The sedimentary bedrock formations in the Cucamonga Basin are similar in texture and composition to the overlying water-bearing sediments, making the bottom of the aquifer contact between the two formations difficult to identify in borehole data alone. Slade (1997) correlated geophysical logs in and around the City of Upland area and was able to estimate that the contact between the consolidated bedrock and the older alluvium was approximately 600 feet below ground surface (bgs) near Red Hill and 600 to 700 feet bgs just north of the 210 freeway. Further investigation and the correlation of geophysical borehole data in this area indicate that the basement complex and water-bearing sediment contact may be as much as 1,000 feet deep at the intersection of Cucamonga Creek and the 210 freeway (WEI, 2012).

For the Cucamonga Basin, the bottom of the aquifer is represented as the contact between the older alluvium and consolidated bedrock formations (sedimentary bedrock formations or basement complex). The bottom of aquifer contours shown in Figure 2-2 were drawn from lithologic descriptions of borehole cuttings that were recorded on well driller's reports and from borehole geophysical logs. The bottom of aquifer in Cucamonga Basin shows an undulating topography that steeply slopes from the San Gabriel Mountains south toward the Chino Basin. Figure 2-2 shows that consolidated bedrock is encountered at depths ranging from zero feet in the northern parts of the basin, where it is exposed at the ground surface, to approximately 1,200 feet in the southern parts of the basin.

2.3.4 Chino Basin

On the east side of Chino Basin (east of Archibald Avenue), the contours of the bottom of the aquifer are based on depth to the basement complex. Figure 2-2 shows borehole locations in the eastern Chino Basin where the basement complex was penetrated at depths ranging from 35 to 1,100 feet below ground surface (ft-bgs). Since 2000, several new wells were drilled in the southeastern portion of Chino Basin that penetrated crystalline bedrock, including several HCMP monitoring wells and the e Chino Basin

Desalter Authority (CDA) production wells, and were used to refine the contours of the bottom of the aquifer in the southeastern portion of Chino Basin.

On the west side of the Chino Basin (west of Archibald Avenue), the determination of the bottom of the aquifer is not as straightforward. Figure 2-2 shows the locations of boreholes of depths 1,000 to 1,400 ft-bgs that did not penetrate the basement complex but terminated in highly weathered and consolidated sediments that may be sedimentary bedrock formations. These deep sedimentary bedrock formations are similar in texture and composition to the overlying water-bearing sediments, which make the contact between the formations difficult to identify in borehole data. Additional data is described below to justify the delineation between the water-bearing sediments and underlying consolidated bedrock.

2.3.4.1 Well Construction and Groundwater Level Data

Figure 2-2 shows deep wells in the Chino Basin, drilled deeper than 1,000 ft-bgs. All of the boreholes penetrated a similar sequence of sediments, including sands, gravels, silts, and clays. At some of these wells, spinner tests were performed after the well was developed. The spinner tests generally demonstrate that pumped groundwater enters wells primarily from shallower sediments (probably from the higher-permeability sediments of the Older Alluvium) with much smaller contributions from deeper sediments (probably from the lower-permeability sediments of the sedimentary bedrock formations). The deepest production wells in the western Chino Basin are about 1,200 ft-bgs.

Figure 2-2 also shows three well locations along Central Avenue in the western Chino Basin: City of Chino Hills well 19 (CH-19) is a deep production well (screened from 340-1,000 ft-bgs); and Ayala Park Extensometer Facility (AP) monitoring wells PA-7 (screened from 438-448 ft-bgs) and PB-2 (screened from 1,086-1,096 ft-bgs). Monitoring well PB-2 is screened about 100 feet below the deepest screens of CH-19. Both PA-7 and PB-2 are completed in sand and gravel units. Slug test data from PA 7 and PB-2 indicate that the hydraulic conductivity of PA-7 (48 ft/day) is much greater than that of PB-2 (0.5 ft/day). Figure 2-4 is a water level time-series chart that shows the water level responses at PA-7 and PB-2 to pumping at CH-19. Note the immediate drawdown of water levels at PA-7 to the initiation of pumping at CH-19 and the relatively delayed and muted drawdown of water levels at PB-2. The above observations indicate that pumping of the aquifer-system in the western Chino Basin above 1,000 ft-bgs causes:

- The horizontal flow of groundwater to pumping wells within the high-permeability sand and gravel units of the Older Alluvium, like those screened in PA-7 at 438-448 ft-bgs.
- The oblique and upward flow of groundwater to pumping wells within the deeper low-permeability sands and gravels of the sedimentary bedrock formations, like those screened in PB-2 at 1,086-1,096 ft-bgs.

2.3.4.2 Bedrock Fault

Another major feature of the bottom of the aquifer in the Chino Basin is the assumed "Bedrock Fault" that underlies Archibald Avenue. This bedrock fault has uplifted the crystalline bedrock of the basement complex in the eastern Chino Basin relative to the sedimentary bedrock and water-bearing sediments in the western Chino Basin. The evidence for this Bedrock Fault comes from well borehole data. Figure 2-5 shows the locations of hydrostratigraphic cross-sections (HSCS) developed for the 2020 Chino Valley Model. Figure 2-6a is a profile view of HSCS A-A' that crosses the Bedrock Fault in the southern Chino Basin. Note that the I-13 borehole (WEI ID 1206958) terminates in consolidated bedrock (crystalline bedrock) at a depth of about 320 ft-bgs. Approximately 4,500 ft to the northwest, the I-7 borehole (WEI ID 1206685) was drilled to a depth of 680 ft-bgs without penetrating consolidated

bedrock. This information and other similar observations were used to define the location and orientation of the assumed Bedrock Fault. The location and orientation of the Bedrock Fault and the existence of deep, low-permeability aquifers in the western Chino Basin are consistent with past work in this area.

2.3.4.3 Pomona Extensometer Facility

In January 2019, two boreholes were drilled in the City of Pomona to support the *2015 Workplan to Develop a Subsidence Management Plan for the Northwest MZ-1 Area.*[7] These boreholes were constructed with dual-nested piezometers for the purposes of monitoring both groundwater levels and aquifer-system deformation within Northwest MZ-1. The deeper of the two boreholes (PX2) was drilled to a total depth of 1,292 ft-bgs. Based on borehole lithology and borehole geophysical logs, our interpretations are that the borehole penetrated the full thickness of the water-bearing sediments and a portion of the underlying sedimentary bedrock. Drilling results from the PX2 borehole supports the concept that the bottom of the aquifer in the western Chino Basin includes the upper portion of the sedimentary bedrock formations. Figure 2-2 show the bottom of the aquifer at approximately 1,300 ft-bgs across most of the western portion of the Chino Basin.

2.3.5 Spadra Basin

The consolidated bedrock formations underlying the water-bearing sediments act as the bottom of aquifer in the Spadra Basin. The bottom of aquifer contours shown in Figure 2-2 are from the borehole lithologic descriptions of borehole cuttings that were recorded in well driller's reports. Each well driller's report was reviewed, and best efforts were made to identify the driller's interpretation of depth to borehole penetration of the consolidated bedrock formations. That said, the well drillers' interpretations are often subjective and poorly described with the typical terminology used to describe bedrock being: "hill formation," "rock," or "decomposed granite."

The bottom of aquifer contours depicted on Figure 2-2 show that the bottom of the aquifer in the Spadra Basin is a narrow trough aligned along the axis of the basin. A bedrock "narrows" is located at the southwestern end of Spadra Basin (i.e. the boundary with the Puente Basin) where the bottom of the aquifer appears to be less than 200 ft-bgs. The bottom of aquifer deepens to the east to over about 600 ft-bgs at the basin's eastern margins (i.e. the boundary with the Chino Basin). The eastward-sloping bedrock trough appears to be related to erosion by ancestral streams that flowed from west to east as the San Jose and Puente Hills were uplifted. Eckis (1934) speculated that the contact between the consolidated bedrock formations and the water-bearing sediments is unconformable, as indicated by an ever-present weathered zone in the consolidated bedrock directly underlying the contact with the water-bearing sediments. This observed relationship suggests that the consolidated bedrock in the Spadra Basin area was undergoing erosion prior to deposition of the water-bearing sediments. Eckis also reported that the weathered zone is about 50-feet thick and that beneath the weathered zone, the bedrock is hard. Fractured and weathered zones in the bedrock formations may yield water to wells locally, but the storage capacity is typically inadequate for sustained production.

2.4 Occurrence and Movement of Groundwater

Descriptions of the physical nature of the Chino Valley Basins, as groundwater reservoirs, are provided below with regard to basin boundaries, recharge, groundwater flow, internal barriers to groundwater flow, and discharge. In short, this section describes: 1) where groundwater occurs in the basins, 2) how

[7] http://www.cbwm.org/rep_engineering.htm

groundwater recharges and moves through the basins, and 3) where groundwater discharges from the basins.

2.4.1 Groundwater Recharge

The following are the major sources of recharge in the Chino Valley Basins:

- Deep infiltration of precipitation and applied water (DIPAW).
- Managed artificial recharge (MAR) of storm water, imported water, and recycled water at flood control and conservation basins.
- Infiltration of surface water discharge in unlined stream channels that traverse the basins from the San Gabriel Mountains to the Santa Ana River (Surface water includes storm and dry-weather discharges and imported water discharged to streams. The stream systems include: San Antonio/Chino Creeks, Cucamonga Creek, Day Creek, East Canyon, Etiwanda Creek, San Sevaine Creek, and the Temescal Wash. Specific to the Six Basins, the stream systems include the Thompson and Live Oak Creeks, which start in the San Gabriel Mountains and discharge to the San Gabriel River Watershed.)
- Infiltration of surface water discharges in the Santa Ana River. Surface water discharges include rising groundwater at the Riverside Narrows, storm and dry-weather discharge, imported water discharged to the Santa Ana River, and wastewater.
- Infiltration of surface water discharge in Temescal Wash. Surface water discharge includes storm and dry-weather discharges.
- Sub-surface inflow from the saturated sediments and fractures within the bounding mountains and hills that include the Chino and Puente Hills, San Gabriel Mountains, Jurupa Hills, Pedley Hills, La Sierra Hills, and Santa Ana Mountains.
- Subsurface inflow across the Rialto-Colton Fault.
- Subsurface inflow from the Riverside Basin through the Bloomington area.
- Deep infiltration of onsite wastewater disposal systems.
- Deep infiltration of leaks from municipal water systems.
- Deep infiltration from municipal separate storm sewer (MS4) systems.

The recharge components listed above are described in more detail in subsequent sections.

2.4.2 Groundwater Flow

Figure 2-7 is a groundwater elevation contour map for the Chino Valley Basins for spring 2019 (Chino Basin) and fall 2018 (Spadra, Six, and Cucamonga Basins) that shows the general groundwater flow pattern (perpendicular to the contours) for the basins in the model domain. A comparison of this contour map to groundwater elevation contour maps from other periods shows that the contours have been generally consistent over time and under different hydrologic conditions.

For the Six Basins area, groundwater flow generally mimics surface drainage patterns: from the forebay areas of high elevation in the near the San Gabriel Mountains towards pumping wells and areas of discharge near the San Gabriel River. Along this general flow path, groundwater encounters bedrock ridges and barriers to flow that deflect and retard it. As groundwater mounds behind bedrock ridges and/or fault barriers, it flows within the shallower sediments over and across these obstructions into downgradient basins. From the Six Basins Strategic Plan report, WEI determined that there are two major groundwater flow systems in the Six Basins: the San Antonio and the Live Oak groundwater flow systems (WEI, 2017).

Groundwater within the Cucamonga Basin generally flows as a single continuous system controlled by production patterns and recharge. In the State of the Cucamonga Basin report, WEI (WEI, 2012) showed that in the western part of the basin, groundwater generally flows south-southeast from the boundary with the San Gabriel Mountains to the Red Hill-Etiwanda Avenue Fault and roughly parallel to the West Cucamonga Barrier. In the eastern part of the basin, groundwater generally flows south-southwest to the Red Hill-Etiwanda Avenue Fault.

For the Chino Basin, groundwater flow mimics surface drainage patterns: from the forebay areas of high elevation in the north and east flanking the San Gabriel and Jurupa Mountains towards pumping wells and areas of discharge near the Santa Ana River within Prado Basin. While considered one basin from geologic and legal perspectives, the OBMP hydrologically subdivided the Chino Basin into five groundwater-flow systems called management zones in the OBMP. Water resource management activities that occur in one management zones will have limited impacts on the other management zones. For this reason, the five district hydrologic units have been termed "management zones." Figure 2-1 shows the five management zones in the Chino Basin included in the OBMP. Nearing the southwestern (lowest) portion of the basin, these flow systems become less distinct as all groundwater flow within Chino Basin converges and rises beneath the Prado Basin.

The eastern boundary of the Spadra Basin is a natural groundwater divide that extends from the eastern tip of the San Jose Hills southward to the Puente Hills. The groundwater divide is evidenced by groundwater elevations measured at wells in the Six Basins, Chino Basin, and Spadra Basin. Groundwater flowing westward from the divide enters the Spadra Basin; groundwater flowing eastward from the mound enters the Chino Basin. The location of the groundwater divide is transient and can shift east or west depending on the rate of groundwater flow from the Six Basins and changes in groundwater levels in the Spadra Basin and/or Chino Basin. The southwestward flowing groundwater that is not pumped ultimately migrates as underflow through the bedrock narrows into the Puente Basin.

2.4.3 Groundwater Discharge

Groundwater discharge from the Chino Valley Basins includes:

- Groundwater pumping from wells
- Rising groundwater within Prado Basin and potentially other locations along the Santa Ana River, depending on climate and season
- Rising groundwater in the Six Basins from the southern portion of the Pomona Basin—along the San Jose Fault
- Evapotranspiration in the Chino Basin along the Santa Ana River and its tributaries where groundwater is near or at the ground surface
- Evapotranspiration in the Six Basins and where groundwater is near or at the ground surface
- Subsurface discharge from the Spadra Basin to the Puente Basin

The discharge components listed above are described in more detail in subsequent sections.

2.4.4 Basin Boundaries

The physical boundaries of the Chino Valley Basins are shown in Figure 2-1 and include:

- **San Gabriel Mountain Front.** The northern boundary of the Chino Valley Basins is the nearly impermeable Basement Complex that outcrops along the front of the San Gabriel Mountains. The Cucamonga Fault Zone strikes along the front of the San Gabriel Mountains as a steep reverse fault that separates the Basement Complex from the alluvial plain of the Chino Valley.

Vertical movement on this fault zone has been upthrown on the northern side, which is partially responsible for the uplift of the San Gabriel Mountains and the down drop of the valley floor.

- **Contact with the Main San Gabriel Basin.** The western boundary of the Six Basins is the contact with the Main San Gabriel Basin. This boundary is somewhat arbitrary in that the water-bearing sediments are continuous across this boundary. This boundary is approximately aligned with a "bedrock shelf" (Eckis, et al., 1932; Eckis, 1934). Eckis reported that during periods of low groundwater levels, the water-bearing sediments are drained above the bedrock shelf, which then completely separates the Six Basins from the Main San Gabriel Basin (1934). During periods of higher groundwater levels, a flattened mound of groundwater exists above the bedrock shelf and acts as a groundwater divide between the Six Basins and the Main San Gabriel Basin. Groundwater west of the divide flows southwestward within the Main San Gabriel Basin. Groundwater east of the divide flows south and east within the Six Basins.
- **Puente Hills/Chino Hills.** The Chino Fault extends from the northwest to the southeast along the western boundary of the Chino Basin. It is, in part, responsible for uplift of the Puente Hills and Chino Hills, which form a continuous belt of low hills west of the fault. The Chino and Puente Hills, which are primarily composed of consolidated sedimentary rocks, form a low permeability barrier to groundwater flow.
- **San Jose Hills.** The southern boundary of the Six Basins is the impermeable Basement Complex and the consolidated Sedimentary Bedrock that outcrops along the northern edge of the San Jose Hills. Eckis and Gross speculate that an unnamed fault may exist along the northern front of the San Jose Hills that uplifted the hills and depressed the Pomona Basin (Eckis, et al., 1932).
- **San Jose Fault.** The eastern boundary of the Six Basins is the San Jose Fault. The San Jose Fault is considered to be a buried fault that offsets bedrock at depth and acts as a barrier to groundwater flow between the Six Basins and the Chino Basin. The location of the San Jose Fault was refined by WEI (2017) using remote-sensing techniques, specifically, Interferometric Synthetic Aperture Radar (InSAR). Groundwater elevation differences are on the order of several hundred feet on opposite sides of the fault (Eckis, 1934; WEI, 2017; DWR, 1970); Groundwater levels can be more than 400 feet higher in the Six Basins compared to groundwater levels in the Chino Basin. Groundwater seeps across the San Jose Fault as underflow from the Six Basins to the Chino Basin, especially during periods of high groundwater elevations within the Six Basins.
- **Extension of the Rialto-Colton Fault north of Barrier J.** Little well data exist to support the extension of the Rialto-Colton Fault north of Barrier J (although hydraulic gradients are steep through this area). Groundwater flowing south out of Lytle Creek Canyon, in part, is deflected by Barrier J and likely flows across the extension of the Rialto-Colton Fault north of Barrier J and into the Chino Basin.
- **Rialto-Colton Fault to the northeast.** The Rialto-Colton Fault separates the Rialto-Colton Basin from the Chino and Riverside Basins. This fault is a known barrier to groundwater flow along much of its length—especially in its northern reaches (south of Barrier J) where groundwater elevations can be hundreds of feet higher within the Rialto-Colton Basin (Dutcher, et al., 1963; Woolfenden, et al., 1997; DWR, 1970). The disparity in groundwater elevations across the fault decreases to the south. To the north of Slover Mountain, a gap in the Rialto-Colton Fault exists. Groundwater within the Rialto-Colton Basin passes through this gap to form a broad groundwater mound (divide) in the vicinity of Bloomington and, hence, is called the Bloomington Divide (Gosling, 1967; DWR, 1970; Dutcher, et al., 1963).
- **Bloomington Divide to the east.** A flattened mound of groundwater exists beneath the Bloomington area as a likely result of groundwater flow from the Rialto-Colton Basin through a gap in the Rialto-Colton Fault north of Slover Mountain (DWR, 1970; Gosling, 1967; Dutcher, et al., 1963). This mound of groundwater extends from the gap in the Rialto-Colton Fault

southwest towards the northeast tip of the Jurupa Mountains. Groundwater to the northwest of this divide recharges the Chino Basin and flows westward, staying north of the Jurupa Mountains. Groundwater southeast of the divide recharges the Riverside Basins and flows southwest towards the Santa Ana River.

- **Jurupa Mountains and Pedley Hills to the southeast.** The Jurupa Mountains and Pedley Hills are primarily composed of impermeable bedrock and form a barrier to groundwater flow that separates the Chino Basin from the Riverside Basins.
- **La Sierra Hills to the south.** The La Sierra Hills outcrop south of the Santa Ana River, are primarily composed of impermeable crystalline bedrock, and form a barrier to groundwater flow between the Chino Basin and the Arlington and Riverside Basins.
- **Shallow bedrock at the Riverside Narrows to the southeast.** Between the communities of Pedley and Rubidoux, impermeable bedrock outcrops on either side of the Santa Ana River narrows considerably. In addition, the alluvial thickness underlying the Santa Ana River thins to approximately 100 feet or less (i.e. shallow bedrock). This area of narrow and shallow bedrock along the Santa Ana River is commonly referred to as the Riverside Narrows. Groundwater upgradient of the Riverside Narrows within the Riverside Basins is forced to the surface and becomes rising water within the Santa Ana River (Eckis, 1934). Downstream of the Riverside Narrows, the bedrock configuration widens and deepens, and surface water within the Santa Ana River can infiltrate to become groundwater in the Chino Basin.

2.4.5 Internal Barriers to Groundwater Flow

The internal boundaries of the Chino Valley Basins are shown in Figure 2-1 and include:

- **Indian Hill Fault and Intermediate Fault (Six Basins).** The Indian Hill Fault separates the northern forebay areas of the Six Basins from the southern areas of groundwater discharge. This fault has been identified by others based on offsets in bedrock, offsets in groundwater elevations, and differences in the behavior of groundwater elevations on either side of the fault (Eckis, 1934; LACFCD, 1937; Eckis, et al., 1932; DWR, 1970). WEI (2017) showed estimates of vertical land surface deformation from InSAR that the Intermediate Fault in the Pomona Basin parallels the San Jose Fault and that offsets in groundwater elevations across this fault indicate its effectiveness as a barrier to groundwater flow.
- **West Cucamonga Barrier (Chino Basin – Cucamonga Basin).** The western boundary of the Cucamonga Basin has been established using groundwater elevation time-histories and InSAR. Vertical land surface displacement was estimated for the period between January 1996 and April 2000. During this period, groundwater levels in the western part of Cucamonga Basin decreased over 50 feet. Over the same period, groundwater levels in the Chino Basin (across the West Cucamonga Barrier) had little to no change. The InSAR, coupled with groundwater elevation time-histories, suggests that there is a physical barrier between the western portion of the Cucamonga Basin and the Chino Basin (WEI, 2017).
- **Red Hill-Etiwanda Avenue Fault (Cucamonga Basin – Chino Basin).** The Red Hill-Etiwanda Avenue Fault is a recently active fault, evidenced by recognizable fault scarps such as Red Hill at the extreme southern extent of the fault near Foothill Boulevard. The fault is a known barrier to groundwater flow, and groundwater elevation differences on the order of several hundred feet on opposite sides of the fault are typical (Eckis, 1934; DWR, 1970). Groundwater seeps across the Red Hill-Etiwanda Avenue Fault as underflow from the Cucamonga Basin to the Chino Basin, especially during periods of high groundwater elevations within the Cucamonga Basin.
- **Riley Barrier (Chino Basin).** Within the Chino Basin's boundaries, there is one documented barrier to groundwater flow. The barrier exists within the deep aquifer-system of the western Chino Basin and was named the "Riley Barrier" by Watermaster to recognize Francis Riley (a

retired USGS hydrogeologist) for his invaluable contributions to the design and implementation of the subsidence management program in MZ-1. The barrier is shown on Figure 2-1 and is aligned with the historical zone of ground fissuring in MZ-1. A more extensive discussion of the Riley Barrier can be found in the MZ-1 Summary Report (WEI, 2006).

- **Flow system boundary with Temescal Basin to the south.** A comparison of groundwater elevation contour maps over time suggests a consistent distinction between flow systems within the lower Chino Basin and Temescal Basin. As groundwater within Chino Basin flows southwest into the Prado Basin area, it converges with groundwater flowing northwest out of the Temescal Valley (Temescal Basin). These groundwaters commingle and flow southwest toward Prado Dam and can rise to become surface water in the Prado Basin. This area of convergence of Chino and Temescal groundwater is indistinct and probably varies with changes in climate and production patterns. As a result, the boundary that separates the Chino Basin from the Temescal Basin was drawn along the legal boundary of the Chino Basin (Chino Basin Municipal Water District v. City of Chino, et al., San Bernardino Superior Court, No. 164327).
- **Spadra Basin (Spadra Basin – Chino Basin).** A natural groundwater divide near the City of Pomona separates the Chino Basin from the Spadra Basin to the west. The divide, which extends from the eastern tip of the San Jose Hills southward to the Puente Hills, is produced by groundwater seepage from the Pomona Basin across the southern portion of the San Jose Fault (Eckis, 1934).

2.5 Aquifer Systems

The Chino Valley Basins are alluvial groundwater reservoirs composed of interbedded layers of gravel, sand, silt, and clay—or layers that are a combination of one or more of these sediment types. The layers that are composed mainly of gravel and sand are permeable, and groundwater flows through the interconnected pore space within these layers towards pumping wells. These layers of gravel and sand are referred to as "aquifers." The layers that are composed mainly of silt and clay are poorly permeable, and groundwater does not flow freely within these layers toward pumping wells. These layers of silt and clay are referred to as "aquitards." Aquitards store groundwater and can transmit appreciable amounts of groundwater to the adjacent aquifers through vertical drainage.

Groundwater can exist within an aquifer-system under two different physical conditions: unconfined and confined. Where the groundwater table is exposed to the atmosphere through the overlying unsaturated zone, the aquifer-system is unconfined, and the groundwater table can rise and fall freely under the stresses of recharge and pumping. Where deeper groundwater is separated from the atmosphere by significant thicknesses of aquitards, the aquifer-system is confined, and the groundwater can be under a pressure head that is higher than the top of the aquifer. Depending on the spatial distribution of the aquitards, and their effectiveness as "confining layers," a groundwater reservoir can be vertically stratified into multiple aquifer-systems that have different physical and chemical characteristics.

The saturated sediments within the Chino Valley Basins can be considered one groundwater reservoir, but the reservoir is sub-divided into distinct aquifer-systems based on the physical and hydraulic characteristics of the aquifer-system sediments and the contained groundwater. Of the five groundwater basins encompassing the Chino Valley Basins, the Chino Basin is the largest—both areally and in terms of basin storage. For this reason and for the purposes of this report, the discussion below on aquifer-systems and hydrostratigraphy (Section 2.5.1) is specific to the Chino Basin. For specific descriptions of the aquifer-systems comprising the Six and Cucamonga Basins, see WEI (2017) and WEI (2012), respectively.

From a simplistic standpoint, the aquifer-systems that comprise the Chino Basin consist of a shallow aquifer-system and at least one deep aquifer-system. The sediments that comprise the shallow aquifer-system are almost fully saturated in the southern portion of the Chino Basin. Depth to groundwater increases to the north to provide a thick vadose zone for percolating groundwater in the Chino Basin's forebay regions. The sediments that comprise the deep aquifer-system are always fully saturated.

The shallow aquifer-system is generally characterized by unconfined to semi-confined groundwater conditions, high permeability within its sand and gravel units, and high concentrations of dissolved solids and nitrate (especially in the southern portions of the Chino Basin). The deep aquifer-system is generally characterized by confined groundwater conditions, lower permeability within its sand and gravel units, and lower concentrations of dissolved solids and nitrate. Where depth-specific data are available, piezometric head tends to be higher in the shallow aquifer-system, indicating a downward vertical hydraulic gradient.

To illustrate the above generalizations, Figure 2-2 shows the location of City of Chino Hills Well 1A and Well 1B. These two wells are physically located within 30 feet of each other on the west side of the Chino Basin, but their non-pumping water-level time histories are distinctly different. Figure 2-8 displays the water-level time series of Well 1A (perforated within the shallow aquifer-system). Well 1A maintains a relatively stable water level that fluctuates annually by about 20-30 feet and a depth to water of about 80 feet-bgs. Comparatively, Well 1B, perforated within the deep aquifer-system, has a depth to water of about 220 feet-bgs and displays a wildly fluctuating piezometric level that can vary seasonally by as much as 250 feet. The piezometric level fluctuations observed in the deep aquifer-system are typical of confined groundwater conditions where small changes in storage (caused by pumping in this case) can generate large changes in piezometric levels.

Wells 1A and 1B also have significant differences in water quality. Nitrate concentrations in Wells 1A and 1B have historically averaged eight mg/L (1997 to 2017) and one mg/L (1997 to 2009), respectively. Total dissolved solids (TDS) concentrations in 1A and 1B have averaged 295 mg/L (1997 to 2017) and 170 mg/L (1997 to 2009), respectively. Arsenic concentrations are relatively high in the deep aquifer-system (averaging 80 micrograms per liter [µg/L] in Well 1B from 1999 to 2009 compared to non-detectable in Well 1A from 1997 to 2017). Similar vertical water quality gradients have been noted between deep and shallow groundwater in the area of the Chino Desalter well fields (GSS, 2001; Dennis Williams, GSS, pers. comm., 2003).

At the Ayala Park Extensometer Facility (Figure 2-2), there are 11 piezometers with screens of 5-20 feet in length that were completed at various depths, ranging from 139-1,229 ft-bgs. Slug tests were performed at a number of these piezometers to determine, among other objectives, the permeabilities of the sediments at various depths within the total aquifer system. Figure 2-6b is a hydrostratigraphic cross-section that includes the deep borehole at Ayala Park and some of the slug test results at the piezometers. In general, the piezometers in the shallow aquifer-system (less than about 350 ft-bgs) display relatively high hydraulic conductivities of 20 to 27 ft/day. The piezometers within the deep aquifer-system display relatively low hydraulic conductivities of 1.6 to 0.5 ft/day. A notable exception is a piezometer that was completed in a gravelly sand in the uppermost portion of the deep aquifer system (438-448 ft-bgs), which displays a relatively high hydraulic conductivity of 48 ft/day, indicating the existence of some higher permeability zones within the deep aquifer-system.

The distinction between aquifer systems is most pronounced within the west-southwest portions of the Chino Basin. This is likely because of the abundance of fine-grained sediments in the southwest (multiple layers of clays and silts). Groundwater flowing from high-elevation forebay areas in the north and east become confined beneath these fine-grained sediments in the west-southwest, and these sediments effectively isolate the shallow aquifer-system from the deep aquifer-system(s). The three-dimensional extent of these fine-grained sedimentary units and their effectiveness as confining layers has never been

mapped in detail across the Chino Basin. However, the following data and information were used to estimate the lateral extent of these units:

- Geologic descriptions from well completion reports in the Chino Basin confirm the predominance of fine-grained sediments in the west-southwest portion of the Chino Basin and the predominance of coarser-grained sediments in the north and east portions of Chino Basin.
- Historical flowing artesian conditions were mapped in the early 1900s in the southwest portion of the Chino Basin (Mendenhall, 1905; 1908; Fife, et al., 1976), indicating the existence of confining layers in these areas.
- Remote sensing studies were conducted to analyze land subsidence in Chino Basin (Peltzer, 1999a; 1999b). These studies employed InSAR, which utilizes radar imagery from an Earth-orbiting spacecraft to map ground surface deformation. InSAR indicates the occurrence of persistent subsidence across the western portion of Chino Basin from 1992 to 2018. It is likely that this subsidence is due to the compaction of fine-grained sediments, resulting from lower pore pressures within the aquifer-system (WEI, 2003a; 2019)
- North and east of these areas, the distinction between aquifer-systems is less pronounced because the fine-grained layers in the west-southwest thin and/or pinch-out to the north and east, and much of the shallow aquifer-system sediments are unsaturated in the forebay regions of Chino Basin.

2.5.1 Hydrostratigraphy of the Chino Basin

The analysis and documentation of Chino Basin stratigraphy, occurrence and movement of groundwater, and aquifer-system characteristics have allowed Watermaster to create a hydrostratigraphic conceptual model of the basin. Watermaster created a hydrostratigraphic model in 2003, which was subsequently updated in 2007 and 2013 (WEI, 2007; 2015). For the 2020 model update, the existing 11 hydrostratigraphic cross-sections were revised based on new data and hydrogeologic cross-sections and two additional hydrostratigraphic cross-sections were prepared to further refine the Chino Basin's geometry and hydrostratigraphy.

The plan-view locations of these cross-sections are shown in Figure 2-5, and the hydrostratigraphic cross-sections are included in Appendix A. Three representative hydrostratigraphic cross-sections: A-A', G-G', and J-J' are shown in Figures 2-6a, 2-6b, and 2-6c. Plotted on the representative hydrostratigraphic cross-sections are selected well and borehole data (where available), including borehole lithology, short-normal resistivity logs, well casing perforations, specific capacities, slug and spinner test results, water quality, and piezometric levels. In the descriptions of each model layer (see below), specific examples from individual wells and hydrostratigraphic cross-sections are discussed to highlight certain characteristics of the hydrostratigraphic units, but the delineation of these layers in three dimensions was drawn from a holistic analysis of the entire dataset. In other words, the layer boundaries do not always and exactly match specific observations at every well on every hydrostratigraphic cross-section but do honor the general patterns of the Chino Basin's depositional environment and hydrostratigraphy.

Prior to the 2020 model update, the Chino Basin aquifer-system was generalized into three hydrostratigraphic units: Layer 1, Layer 2, and Layer 3. The delineations of these hydrostratigraphic units were based on analyses of hydrostratigraphic cross-sections and other geologic and hydrogeologic data. For the 2020 model update, the three-layer Chino Basin aquifer-system originally developed in 2003 was refined to a five-layer aquifer-system.

The main reasons for introducing two new layers into the 2020 model update are: 1) the additional layering reflects an improved understanding of the Chino Basin's hydrostratigraphy, particularly in the western portion of the Chino Basin; and 2) the new layers enable the model to better simulate land

subsidence across the Chino Basin. In general, the Chino Basin consists of a shallow unconfined aquifer and deep confined aquifers. Historical flowing artesian conditions were mapped in the early 1900s in the southwest portion of the Chino Basin (Mendenhall, 1905; 1908; Fife, et al., 1976), which indicates the existence of confining layers in these areas. Likewise, review of water level time-series, water quality data, and aquifer testing data support confined groundwater conditions in the western portion of Chino Basin. It has also been demonstrated in the *Annual Report of the Ground-Level Monitoring Committee*[7] that the observed aquifer-system deformation in the Managed Area is a result of groundwater pumping from the deep and confined aquifer-system. Similarly, in Northwest MZ-1, available evidence indicates that the most likely mechanism behind the observed subsidence in Northwest MZ-1 is the compaction of fine-grained sediment layers (aquitards) within the aquifer-system.

2.5.1.1 Layer 1

Layer 1 consists of the upper 100-730 feet of sediments and is generally representative of the shallow aquifer-system. Layer 1 sediments are typically coarse-grained (sand and gravel layers) and, where saturated, transmit large quantities of groundwater to wells due to high hydraulic conductivities. On the west side of Chino Basin, Layer 1 sediments are composed of a greater fraction of finer-grained sediments (silt and clay layers), especially in the uppermost 100 feet. Layer 1 water quality is generally poor in the southern portion of the Chino Basin with relatively high concentrations of TDS and nitrate. Water quality is generally excellent in the northern portions of the Chino Basin.

Figure 2-6c displays the profile view of cross-section J-J', which is aligned southwest-northeast and illustrates the thickening of Layer 1 in the northeastern direction at the expense of Layer 2. The thickening of Layer 1 is supported by the observation that the silt and clay layers, which are typical of Layer 2 sediments in the southwestern Chino Basin, become thinner and less abundant in the eastern and northeastern portions of the Chino Basin.

Figure 2-6b displays the profile view of cross-section G-G', which is aligned southeast-northwest and bisects MZ-1. This hydrostratigraphic cross-section displays three of the newly installed HCMP monitoring wells (HCMP-3, 4, and 6) and the piezometers at Ayala Park (AP Piezometer), which were used to refine the layer geometries in the southern Chino Basin. The monitoring wells are nested piezometers that allow for depth-specific monitoring of the aquifer-system. Note the vertical stratification of groundwater quality in Figure 2-6b (and other cross-sections with vertically distinct groundwater quality data). The relatively high TDS and nitrate concentrations in the shallow aquifer-system (Layer 1) decrease significantly with depth, especially in the southern portions of the Chino Basin.

Figure 2-6a displays the profile view of hydrostratigraphic cross-section A-A', which is aligned west-east and bisects the southern portion of the Chino Basin through the Chino 1 Desalter well field. Note the depth of the well screens relative to the water quality and specific capacity data. The wells with shallow well screens have relatively high TDS and nitrate concentrations while the wells with deeper well screens have relatively low TDS and nitrate concentrations. The same pattern can be observed in the specific capacity data: wells with shallow screens have relatively high specific capacities, indicating relatively high permeability in the shallow aquifer-system; wells with deeper screens have relatively low specific capacities, indicating relatively low permeability in the deep aquifer-system.

2.5.1.2 Layer 2

Layer 2, where present, is an approximately a 10 to 80 foot-thick aquitard that represents the deep aquifer-system's upper confining layer. Layer 2 consists predominantly of silt and clay layers that directly underlie Layer 1. The fine-grained layers representing Layer 2 were identified using borehole logs penetrating the thickness of at least Layers 1 and 2 and geophysical logs. Layer 2 was correlated between wells across the western portion of the Chino Basin based primarily on the geophysical logs' (i.e.

resistivity log) "signatures" for fine-grained materials, borehole lithologic log descriptions, and well screen interval(s) placement.

Figure 2-6c displays the profile view of hydrostratigraphic cross-section J-J' and illustrates that Layer 2 is spatially restricted to the western portion of Chino Basin and "pinches out" to the northeast as Layer 1 thickens. This pinching-out is supported by the observation that the silt and clay layers, which are typical of Layer 2 sediments in the southwestern portion of the Chino Basin, become thinner and less abundant in the eastern and northeastern portions of the Chino Basin.

2.5.1.3 Layer 3

Layer 3 consists of 40-700 feet of sediments underlying Layer 1 or Layer 2 (if Layer 2 is present) and is representative of the upper portion of the deep aquifer-system. Layer 3 is generally characterized by an abundance of fine-grained sediments (silt and clay layers), confined groundwater conditions, and lower permeabilities and better water quality than in Layer 1 (relatively low TDS and nitrate concentrations—especially in the southern Chino Basin). Figure 2-6c displays the profile view of cross-section J-J' and illustrates that Layer 3 thins to the northeast and east as Layer 1 thickens.

The confined groundwater conditions of Layer 3 and the low concentrations of TDS and nitrate are best illustrated in Figures 2-6a and 2-6b (hydrostratigraphic cross-sections A-A' and G-G') and in Figure 2-8. Figure 2-6a shows well CH-1B located in southwestern Chino Basin and screened across Layers 2 and 3. The water-level time series for CH-1B (Figure 2-8) displays a fluctuating piezometric level that varies seasonally by as much as 250 feet – mainly in response to nearby pumping. These water-level fluctuations are typical of confined groundwater conditions where small changes in storage (caused by pumping in this case) can generate large changes in piezometric levels. This is a consistent observation that can be seen in all wells screened exclusively in the deep aquifer-system in the southwestern Chino Basin and indicates the existence of an effective upper confining layer (Layer 2) separating the deep and shallow aquifer-systems.

2.5.1.4 Layer 4

Layer 4, where present, is approximately a 10 to 80-foot-thick aquitard that represents the deep aquifer-system's lower confining layer. Similar to Layer 2, Layer 4 consists predominantly of silt and clay layers. The fine-grained layers representing Layer 4 directly underlie Layer 3 and were identified using borehole logs, penetrate the upper portion of Layer 5 and geophysical logs. Layer 4 was correlated between wells across the western portion of the Chino Basin based primarily on the geophysical logs' (i.e. resistivity log) "signatures" for fine-grained materials, borehole lithologic log descriptions, and well screen interval(s) placement.

Figure 2-6c displays the profile view of hydrostratigraphic cross-section J-J' and illustrates that Layer 4, like Layer 2, is spatially restricted to the western portion of Chino Basin and pinches out to the northeast as Layer 1 thickens. This pinching-out is supported by the observation that the silt and clay layers comprising Layer 4 in the southwestern portion of the Chino Basin become thinner and less abundant in the eastern and northeastern portions of the Chino Basin.

2.5.1.5 Layer 5

Layer 5 consists of up to 900 feet of sediments underlying Layers 3 or 4 (if 4 is present) within the deep aquifer system. Layer 5 is generally characterized by an abundance of coarse-grained sediments (sand and gravel layers), but due to their greater age, consolidation, and state of weathering, these sediments have lower permeability than the coarse-grained sediments of Layers 1 and 3. Layer 5 likely has a portion of the sedimentary bedrock formations in the western Chino Basin, and in the eastern portion of the

basin, Layer 5 sediments are likely composed of the lower portion of the Older Alluvium. In the western Chino Basin, Layer 5 sediments underlie Layer 4 and represent the lower portion of the deep aquifer-system. In the eastern Chino Basin, Layer 5 sediments directly underlie Layer 3 and represent the deep aquifer-system. In the southeastern Chino Basin, Layer 5 thins to about 20 feet east/southeast of the assumed Bedrock Fault toward the Jurupa Mountains and La Sierra Hills.

The best example of Layer 5 characteristics is observed at the Ayala Park Piezometer/Extensometer Facility. In Figure 2-6b, note the coarse-grained nature of the deep sediments, the very low concentrations of TDS and nitrate, and the very low hydraulic conductivity at PB-2 as estimated from slug tests. In other regions of the Chino Basin, some of these same observations for Layer 5 can be seen in the lithologic data, geophysical logs, and the spinner test results.

2.5.2 Creation of a Three-Dimensional Hydrostratigraphic Model

At each well, on each hydrostratigraphic cross-section, the bottom elevations of all the five layers were plotted on maps, and the layer bottom elevations were compared against the layer bottom elevations from the 2013 model. The 2013 model layer (three layers) bottom elevations were then modified to five layers based on the updated hydrostratigraphic geometry for the Chino Basin. The elevation contours for the bottom of Layers 1 through 5 are shown in Figures 2-9a through 2-9e. The five-layer bottom elevation contours were modified from the 2013 model layer bottom elevation and/or new layer bottom elevations were digitized in ArcGIS and converted to point values. The Geostatistical Analyst extension of ArcGIS was used to interpolate between the point values to create rasters (grids) of the layer bottom elevations. These rasters represent the updated hydrostratigraphic model of the Chino Basin and were used as input files for the hydrostratigraphic geometry in the 2020 model update.

2.6 Aquifer Properties

Hydraulic conductivity is the measure of a fluid's ability to flow through a medium. The value relates to fluid density (ρ), dynamic viscosity (μ), and the effective grain size (d_{10}) in unconsolidated deposits, as depicted in the following equation developed by Hubbert (1940):

$$K = \frac{C d_{10}^{2} \rho g}{\mu}$$

Where, C is an empirical constant of proportionality. This definition of hydraulic conductivity suggests that its value increases with the median grain size. However, the empirical constant C must be adjusted to account for the aquifer properties and other properties that affect groundwater flow.

Specific yield is important in determining the volume of water in storage in an aquifer. This characteristic can be determined by laboratory analyses of undisturbed samples of aquifer material. However, quicker, less costly alternatives to these laboratory analyses can be developed (Robson, 1993). Many investigations, for example Robson (1993) and Johnson (1967), showed that the values of specific yield are not proportionally related to grain size.

As straightforward methods for estimating aquifer properties are not easily applicable, a sediment texture analysis method was used to develop initial estimates of horizontal and vertical hydraulic conductivity and storage properties for the 2020 CVM. The method is described in Section 2.6.2.

As stated in Section 2.5, the saturated sediments within the Chino Valley Basins can be considered as one groundwater reservoir, but the reservoir is sub-divided into distinct aquifer-systems based on the physical and hydraulic characteristics of the aquifer-system sediments and the contained groundwater.

Of the five groundwater basins encompassing the Chino Valley Basins, the Chino Basin is the largest—both areally and in terms of basin storage. For this reason and for the purposes of this report, the discussion below on aquifer-properties is specific to the Chino Basin. For specific descriptions of the compilation of well data, classification of texture for aquifer sediments, and geostatistical model approach to estimate the spatial distribution of hydraulic conductivity and specific yield, see WEI (2017) and (2012), respectively.

2.6.1 Compilation of Existing Well Data

Textural analysis in this model update relied on lithological data from well driller's logs. Our investigations on geologic setting and stratigraphy have shown that driller's logs can provide valid textural information and help to configure a groundwater basin's hydrostratigraphy. For the 2013 model, WEI reviewed up to about 1,100 drillers' logs in the Chino Basin. For the 2020 CVM, about 70 additional driller's logs were collected and reviewed. Where possible, drillers' logs were located, and lithologic descriptions were assigned model layers based on depth intervals.

2.6.2 Classification of Texture and Reference Hydraulic Values for Aquifer Sediments

Hydraulic properties are closely related to the lithology of aquifers. In other words, each textural class has its own hydraulic properties. This allows assigning appropriate values of hydraulic parameters based on textural class. Several databases have been developed for this purpose, including RAWLS (Rawls, et al., 1982), ROSETTA (Schaap, et al., 1998), and CARSEL (Carsel, et al., 1988).

Many authors (Bouwer, 1978; Prudic, 1991; Reese, et al., 2000; Kuniansky, et al., 1998; Domenico, et al., 1997; Freeze, et al., 1979; Johnson, 1967) relate material grain-size class texture to hydraulic property values. Based on the published information from these references and locally available data, a reference table was developed. The table relates 80 lithological descriptions to the values of specific yield and saturated hydraulic conductivity. These 80 lithological descriptions cover a wide range of sediments: from boulders/cobbles, to gravels and sands, to clays and silts, and to lava flows, granites, and shales.

With the reference table and lithologic descriptions from the well drillers' logs, the following procedure is used to determine the hydraulic properties at well locations and within each layer:

- Determine the historical highest or potential highest water table in the basin of interest.
- Define the model layer bottom elevations.
- Determine the thickness for each sediment texture in a layer.
- Use the reference table to assign hydraulic properties based on lithologic descriptions.
- Calculate the thickness-weighted horizontal and vertical hydraulic conductivity and specific yield at each valid well in each layer using the formulas below:

$$K_h = \sum_{i=1}^{n} \frac{K_i b_i}{b}$$

$$K_v = b / \sum_{i=1}^{n} \frac{b_i}{K_i}$$

$$S_y = \sum_{i=1}^{n} \frac{S_{yi} b_i}{b}$$

Where K_h is the average horizontal conductivity in the layer, K_i is the hydraulic conductivity of i bed, b_i is the thickness of i bed, b is the total thickness of the aquifer in a layer, K_v is average vertical hydraulic conductivity in a layer, S_y is average specific yield in a layer, and S_{yi} is the specific yield for i bed.

Using this method, specific yield, horizontal hydraulic conductivity, and vertical hydraulic conductivity values were computed for each layer at each well location.

In addition to the method described above, WEI has collected various pumping test results in the Chino and Temescal Basins as well as in various other basins located in Santa Ana River Watershed. The pumping test results that are deemed to be reliable were used as prior information in the calibration process.

2.6.3 Geostatistical Model Approach

Geostatistics is a set of applications and statistical techniques used to analyze spatial and temporal correlations of variables distributed in space and time. Applications include modeling geological heterogeneities such as the heterogeneity and distribution of hydraulic properties.

WEI used a geostatistical method termed the best linear unbiased estimation (BLUE) to estimate the spatial distribution of hydraulic conductivity and specific yield. "Best" means the estimates with minimal variance or estimation error. "Unbiased" means the average value of the estimates in repeated sampling equals the true parameter. Like other simple spatial interpolation methods, such as inverse-distance method, BLUE is a linear estimator but it takes the observed spatial correlation structure into account. Because of this, BLUE not only has the capability of producing a prediction field, but also provides some measure of the certainty or accuracy of the predictions. This method can also integrate physical constraints and combine multiple data sources.

The core of the BLUE method, or Kriging method, is to configure the data spatial structure using a semivariogram model. The underlying principle of semivariogram model is that, on average, two observations closer together are more similar than two observations further apart. Because the underlying data have preferred orientations, values may change more quickly in one direction than another. As such, the semivariogram is a function of direction.

The procedure to generate the Kriging-estimated hydraulic properties was as follows:

1. Compute each hydraulic parameter's value in each layer at each well.
2. Conduct semivariogram analyses of hydraulic properties, determine their spatial variation structure, and obtain the best-fitted semivariogram spatial structure model and parameters.
3. Conduct the Kriging computation based on the hydraulic property value at each well location. During the processes, the best-fit semivariogram model and parameters are used to generate hydraulic property grids in each layer in the model domain.
4. Check the uncertainty of estimated hydraulic properties.

2.6.4 Specific Yield

The spatial data distribution of specific yield was the first property estimated. A semivariogram model was generated for specific yield based on the lithologic descriptions from about 1,170 representative well logs. The Kriging method that implemented the semivariogram model was used to make a prediction for specific yield across the Chino Basin and in each layer. The specific yield rasters are limited to the spatial extent of their respective layers and are shown in Figures 2-10a through 2-10e.

Figures 2-10a displays the spatial distribution of specific yield for Layer 1. Specific yield is highest (up to 20 percent) in the northern and eastern portions of the Chino Basin. A belt of similarly high specific

yield runs north of the Jurupa Mountains from Fontana toward the Prado Basin. This belt may represent coarse-grained sediments deposited by an ancestral Santa Ana River or Lytle Creek. The lowest specific yields in Layer 1 (8 to 10 percent) are on the west side of the Chino Basin. This area overlaps the historical artesian area and likely represents the shallow fine-grained sediments that historically acted as confining layers.

Figure 2-10c displays the spatial distribution of specific yield for Layer 3. Specific yield is highest, ranging up to 15 percent, in the central portions of the Chino Basin. Specific yield is lowest, ranging down to 5 percent, on the west side of the Chino Basin. The areas of relatively low specific yield overlap the historical artesian area and the areas of historical subsidence and may represent the fine-grained sediments that have experienced compaction due to reduced pore pressures.

Figure 2-10e displays the spatial distribution of specific yield for Layer 5. The primary observation in Layer 5 is a generally higher specific yield in the Fontana area relative to a lower specific yield in the western Chino Basin. This observation is consistent with Watermaster's current hydrostratigraphic conceptual model where the deep aquifer-system sediments of the western Chino Basin represent the highly weathered and partially consolidated sedimentary bedrock formations, and the deep sediments of the northern Chino Basin represent the more recent coarse-grained sediments of the Older Alluvium.

2.6.5 Horizontal Hydraulic Conductivity

The horizontal hydraulic conductivity of water-bearing sediments is a measure of their capacity to transmit water. Generally, sands and gravels have high hydraulic conductivities while clays and silts have low hydraulic conductivities. A semivariogram model was generated for horizontal hydraulic conductivity based on lithologic descriptions from about 1,170 representative well logs. The Kriging method that implemented the semivariogram model was used to make a prediction for horizontal hydraulic conductivity across the Chino Basin and in each layer. The horizontal hydraulic conductivity rasters are limited to the spatial extent of their respective layers and are shown in Figures 2-11a through 2-11e.

Figure 2-11a displays spatial distribution of horizontal hydraulic conductivity for Layer 1. Horizontal hydraulic conductivities are highest in the northern (70-100 ft/day) and eastern (60-80 ft/day) portions of the Chino Basin. A belt of similarly high horizontal hydraulic conductivity runs north of the Jurupa Mountains from Fontana toward the Prado Flood Control Basin. This belt may represent coarse-grained sediments deposited by an ancestral Santa Ana River or Lytle Creek. Horizontal hydraulic conductivity in Layer 1 is the lowest on the west side of the Chino Basin.

Figure 2-11c displays the spatial distribution of horizontal hydraulic conductivity for Layer 3. Horizontal hydraulic conductivities are highest, ranging up to 120 ft/day, in the central portions of the Chino Basin. Horizontal hydraulic conductivities are lowest on the west side of the Chino Basin.

Figure 2-11e displays the spatial distribution of horizontal hydraulic conductivity for Layer 5. Horizontal hydraulic conductivities are generally higher in the Fontana area relative to lower values in the western Chino Basin.

2.6.6 Vertical Hydraulic Conductivity

The average vertical hydraulic conductivity in a layer will be very low when a clay bed is present. This can also be observed from the equation used to compute average or equivalent vertical hydraulic conductivity for a stratified material. A semivariogram model was generated for vertical hydraulic conductivity based on lithologic descriptions from about 1,170 representative well logs. The Kriging method that implemented the semivariogram model was used to make a prediction for vertical hydraulic

conductivity across the Chino Basin and in each layer. The vertical hydraulic conductivity rasters are limited to the spatial extent of their respective layers and are shown in Figures 2-12a through 2-12e.

Figure 2-12a displays the spatial distribution of vertical hydraulic conductivity for Layer 1. Vertical hydraulic conductivities are high in the northern (15-28 ft/day) and eastern (22-35 ft/day) portions of the Chino Basin. A belt of relatively high vertical hydraulic conductivity (15-28 ft/day) runs north of the Jurupa Mountains from Fontana toward the Prado Basin. This belt is similar to those of specific yield and horizontal hydraulic conductivity. Vertical hydraulic conductivity in Layer 1 is the lowest on the west side of the Chino Basin. This area contains many interbedded clays in Layer 1.

Figure 2-12c displays the spatial distribution of vertical hydraulic conductivity for Layer 3. Vertical hydraulic conductivities are highest in the central and in eastern portions of the Chino Basin. Vertical hydraulic conductivities are very low on the west side of the Chino Basin. This area overlaps the historical artesian area and the area of historical subsidence in the Chino Basin.

Figure 2-12e displays the spatial distribution of vertical hydraulic conductivity for Layer 5. Vertical hydraulic conductivities are high in the north and lower in the western and southern portions of the Chino Basin.

2.7 Land Subsidence in the Chino Basin

One of the earliest indications of land subsidence in the Chino Basin was the appearance of ground fissures in the City of Chino. These fissures appeared as early as 1973, but an accelerated occurrence of ground fissuring ensued after 1991 and resulted in damage to existing infrastructure. Figure 2-13 shows the locations of the fissures within Chino Basin Management Zone 1 (MZ-1). Scientific studies of the area attributed the fissuring phenomenon to differential land subsidence, caused by pumping of the underlying aquifer system and the consequent drainage and compaction of aquitard sediments (Fife, et al., 1976; Kleinfelder, 1993; Kleinfelder, 1996; Geomatrix, 1994; GEOSCIENCE, 2002).

In 2000, Watermaster approved the Implementation Plan for the Peace Agreement, which called for an aquifer-system and land subsidence investigation in the southwestern region of MZ-1 to support the development of a subsidence management plan. From 2001-2005, Watermaster developed, coordinated, and conducted the investigation under the guidance of the MZ-1 Technical Committee, which was composed of representatives from all major MZ-1 producers and their technical consultants. The investigation included collecting and analyzing the information necessary to understand the extent, rate, and mechanisms of subsidence and fissuring, and using that information to develop a management plan to abate future subsidence and fissuring or reduce it to tolerable levels.

The methods, results, conclusions, and recommendations of the investigation are described in detail in the MZ-1 Summary Report (WEI, 2006) and the MZ-1 Subsidence Management Plan (CBWM, 2007). The MZ-1 Subsidence Management Plan identified other areas in the Chino Basin where subsidence and potential ground fissuring are a concern. Figure 2-13 also shows the locations of these "Areas of Subsidence Concern," including: Central MZ-1, Northwest MZ-1, the Northeast Area, and the Southeast Area. Figure 2-14 shows vertical ground motion measured by InSAR across the western Chino Basin for the time-period between 2011 and 2019.

Subsidence in Northwest MZ-1 was first identified as a concern in the MZ-1 Summary Report. Since 2007, Watermaster has been monitoring vertical ground motion via InSAR and piezometric levels with transducers at selected wells in the area. Figure 2-15 is a time-series chart that shows the long-term history of vertical ground motion within Northwest MZ-1. These data indicate that about 1.2 ft of subsidence has occurred in this area from 1992 through 2019—an average rate of about 0.05 ft/yr. The chart also shows piezometric levels at wells in the area from 1930-2019. From about 1930 to 1978,

piezometric levels in Northwest MZ-1 declined by about 200 feet. Since then, piezometric levels have recovered but have remained below 1930 levels. The observed and continuous subsidence that occurred during the 1992-2019 period cannot be explained entirely by concurrent changes in piezometric levels. A plausible explanation for the subsidence is that thick, slow-draining aquitards are compacting in response to the historical declines in piezometric levels that occurred from 1930 to 1978.

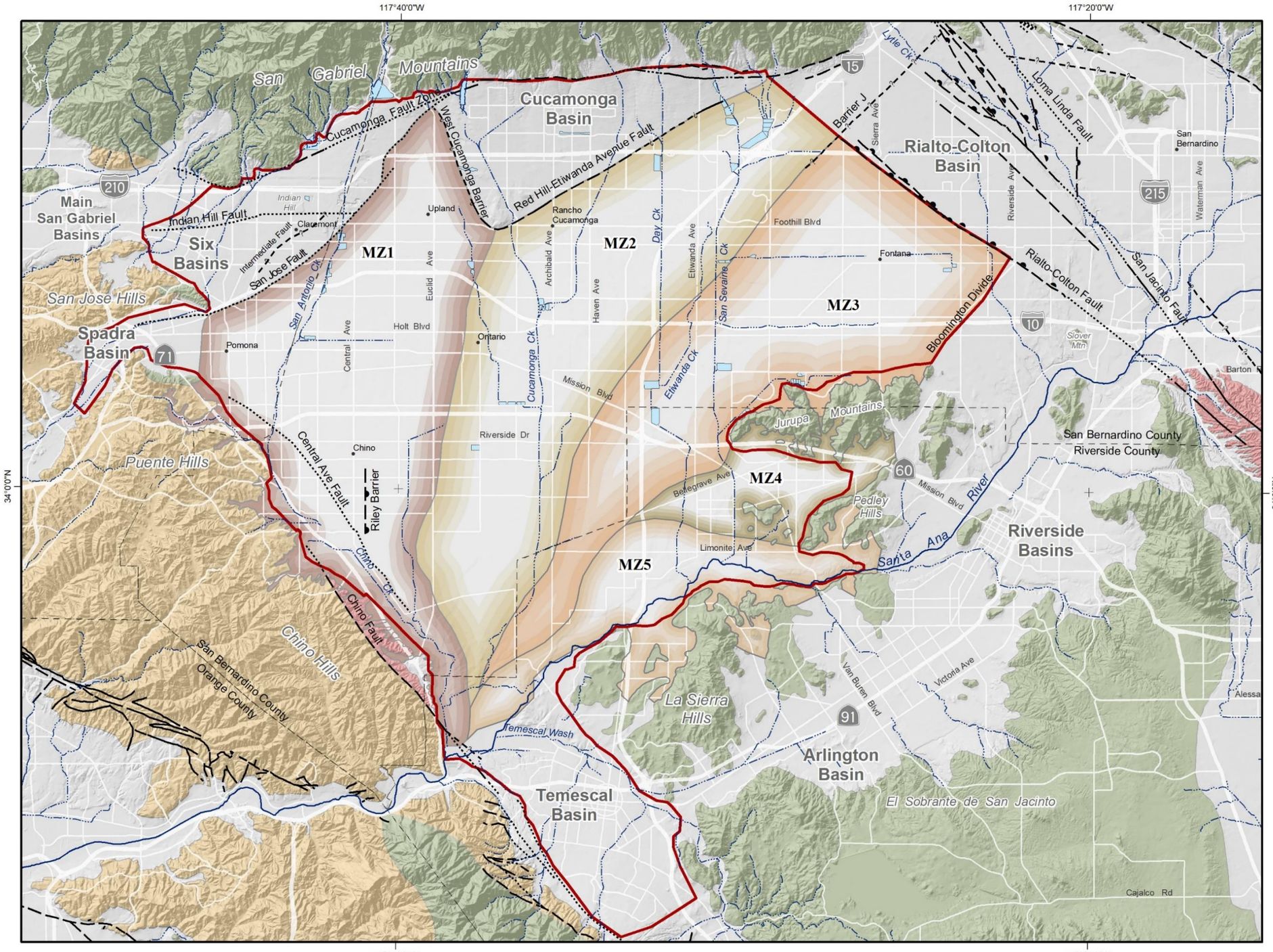

Chino Basin Management Zones as Defined in the OBMP

Chino Valley Basins Groundwater Flow Model Boundary

Streams & Flood Control Channels

Flood Control & Conservation Basins

Geology

Water-Bearing Sediments

Quaternary Alluvium

Consolidated Bedrock

Plio-Pleistocene Sedimentary Rocks

Cretaceous to Miocene Sedimentary Rocks

Pre-Tertiary Igneous and Metamorphic Rocks

Fault (solid where accurately located; dashed where approximately located or inferred; dotted where concealed)

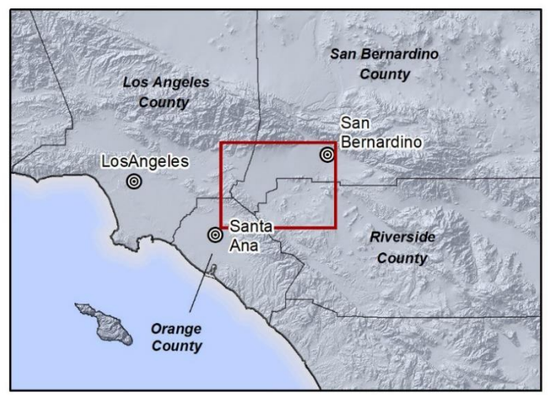

Produced by:

WEI
Wildermuth Environmental, Inc.

Author: MJC
Date: 1/22/2020
Document Name: Figure_2-1_20200109_Geology

0 1 2 3 4 5 Miles
0 2 4 6 8 KM

Prepared for:

2020 Safe Yield Recalculation

Chino Basin Watermaster
Partners in Basin Management

Geologic Map and Boundaries of the Chino Valley Basin

Figure 2-1

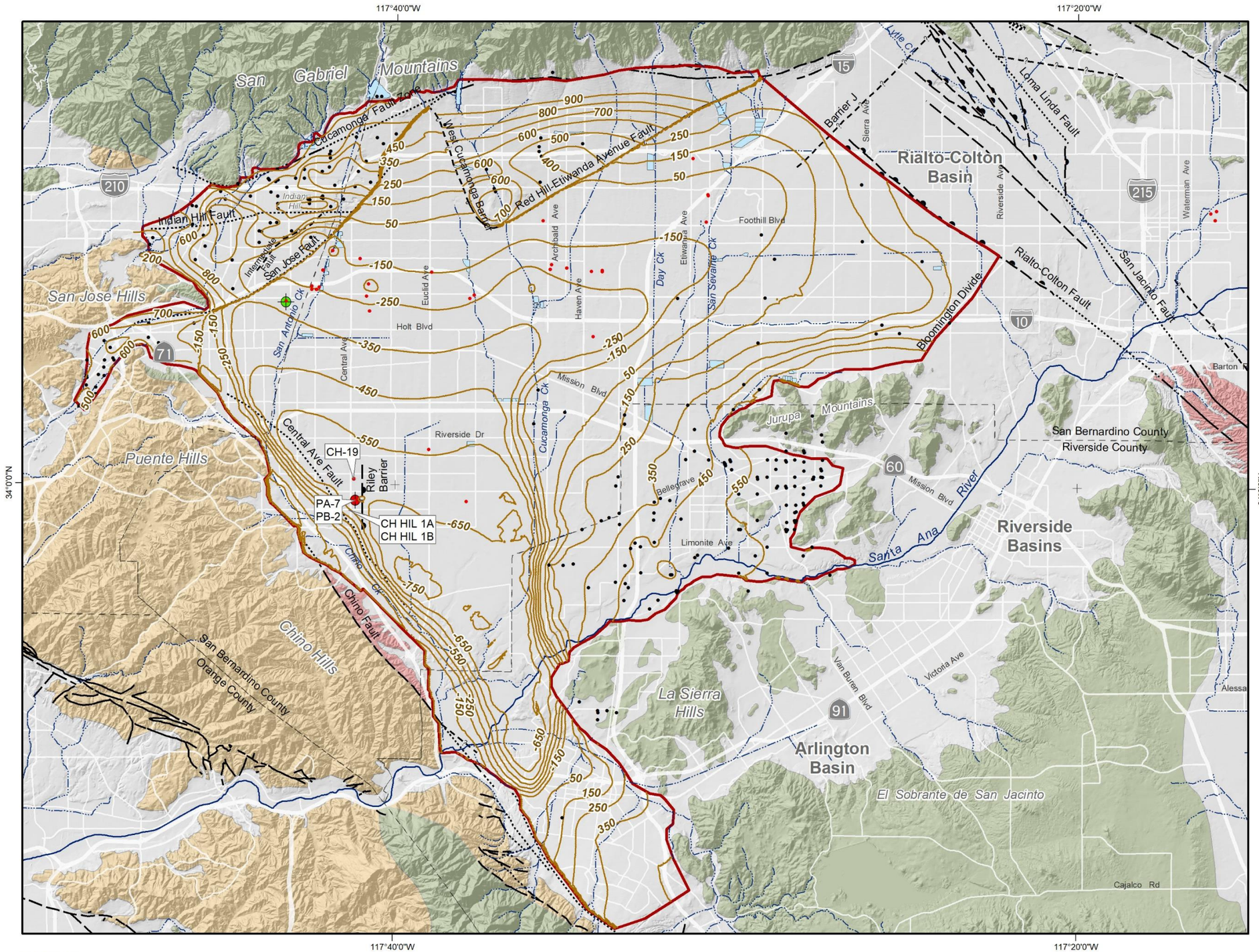

Produced by:

WEI
Wildermuth Environmental, Inc.

Author: MJC
Date: 1/22/2020
Document Name: Figure_2-2_20200115_BOA

0 1 2 3 4 5 Miles
0 2 4 6 8 KM

Prepared for:

2020 Safe Yield Recalculation

Chino Basin Watermaster
Partners in Basin Management

Effective Base of the Freshwater Aquifer Chino Valley Basin

Figure 2-2

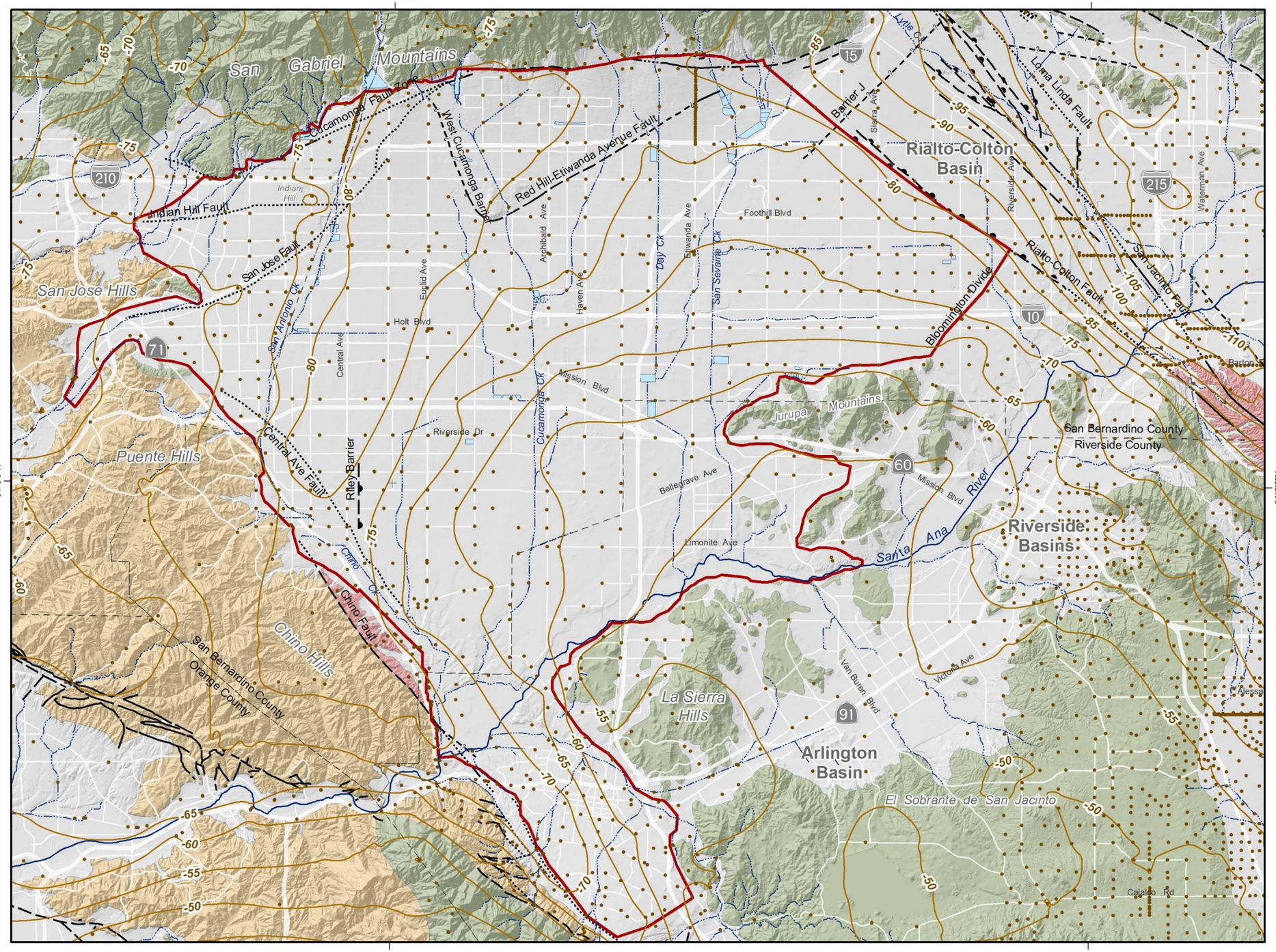

-50- Lines of Equal Bouguer Gravity Anomalies (milligals)

Gravity Station

Chino Valley Basins Groundwater Flow Model Boundary

Streams & Flood Control Channels

Flood Control & Conservation Basins

Geology

Water-Bearing Sediments

Quaternary Alluvium

Consolidated Bedrock

Plio-Pleistocene Sedimentary Rocks

Cretaceous to Miocene Sedimentary Rocks

Pre-Tertiary Igneous and Metamorphic Rocks

Fault (solid where accurately located; dashed where approximately located or inferred; dotted where concealed)

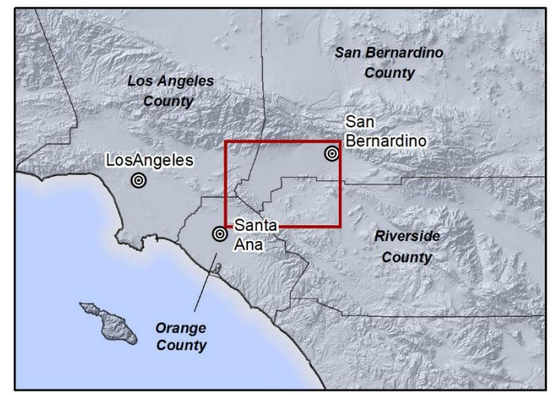

Produced by:

WEI
WILDERMUTH ENVIRONMENTAL, INC.

Author: MJC
Date: 1/22/2020
Document Name: Figure_2-3_20200113_Gravity

0 1 2 3 4 5 Miles
0 2 4 6 8 KM

Prepared for:

2020 Safe Yield Recalculation

CHINO BASIN WATERMASTER
Partners in Basin Management

Bouguer Gravity Map
Chino Valley Basin

Figure 2-3

Figure 2-4

Depth-Dependent Piezometric Response to Pumping

Southwestern Chino Basin

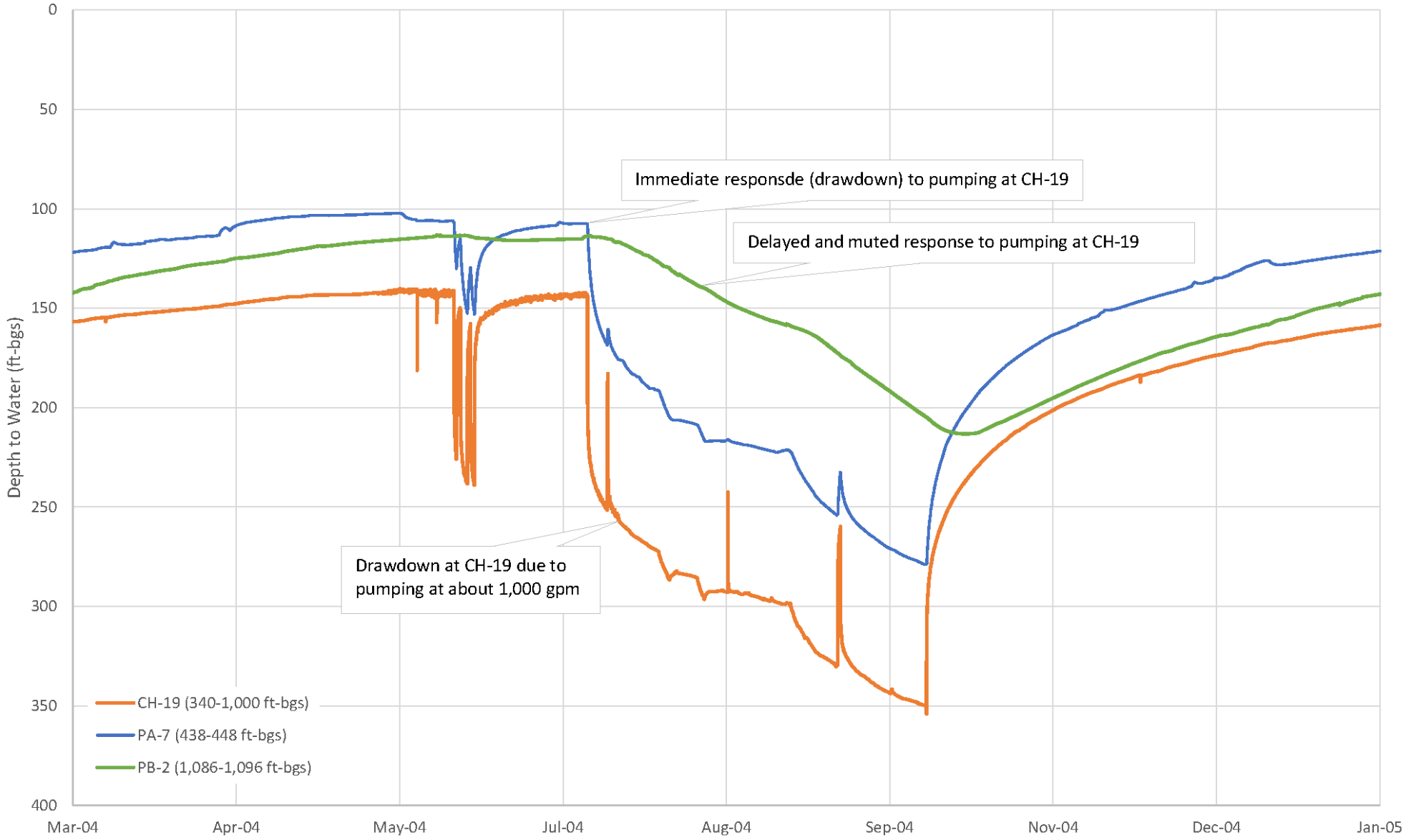

1/22/2020 -- 3:00 PM

Figure2-x_MZ1_DTWex

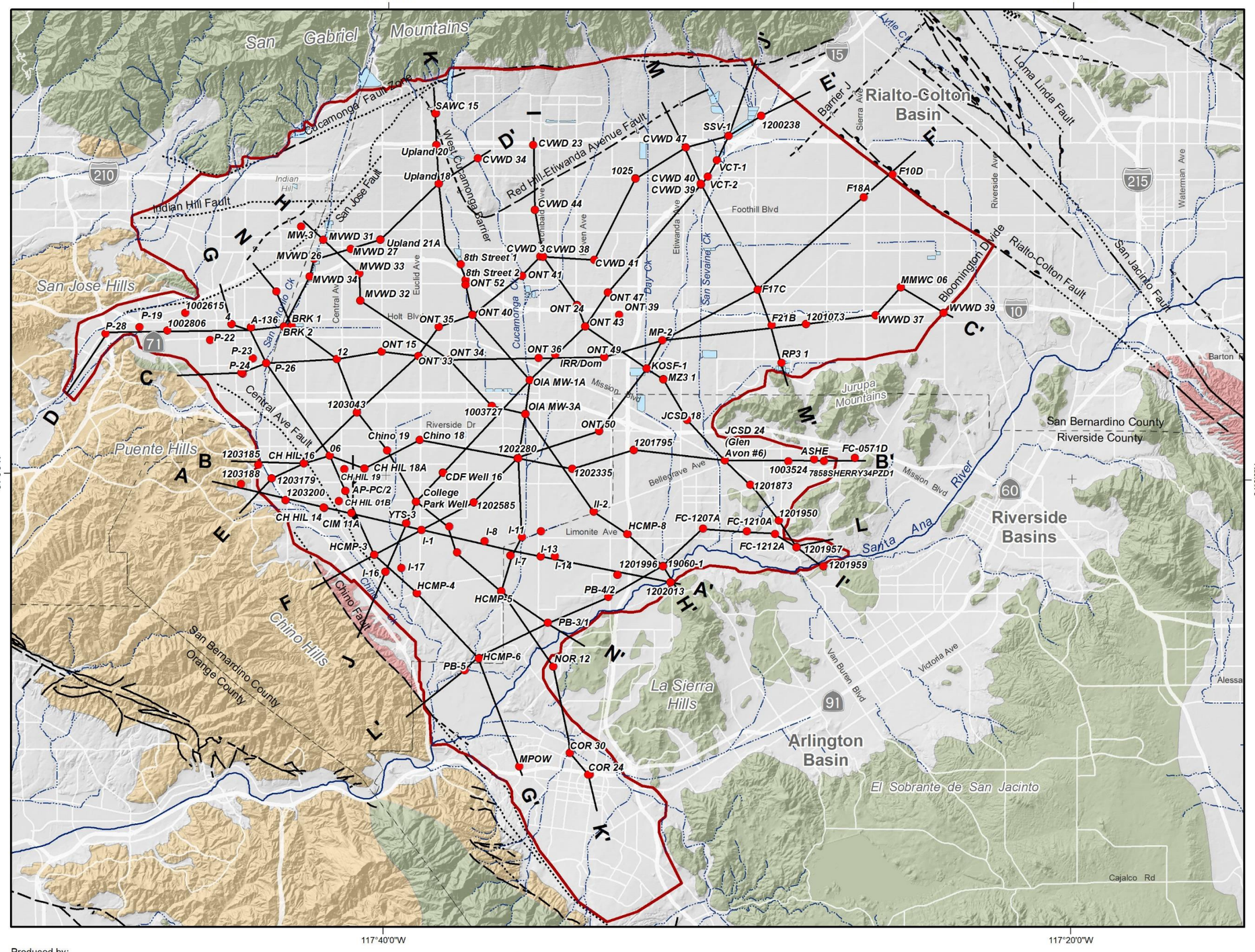

Hydrostratigraphic Cross-Section Profile Line

Borehole Used in Hydrostratigraphic Cross-Section

Chino Valley Basins Groundwater Flow Model Boundary

Streams & Flood Control Channels

Flood Control & Conservation Basins

Geology

Water-Bearing Sediments

Quaternary Alluvium

Consolidated Bedrock

Plio-Pleistocene Sedimentary Rocks

Cretaceous to Miocene Sedimentary Rocks

Pre-Tertiary Igneous and Metamorphic Rocks

Fault (solid where accurately located; dashed where approximately located or inferred; dotted where concealed)

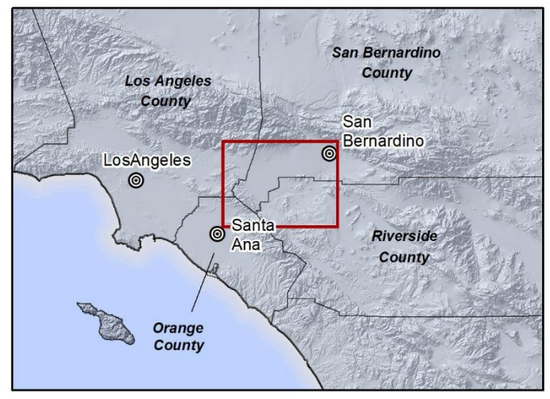

Produced by:

WEI Wildermuth Environmental, Inc.

Author: MJC

Date: 1/22/2020

Document Name: Figure_2-5_20200113_XS

Prepared for:

2020 Safe Yield Recalculation

Chino Basin Watermaster — Partners in Basin Management

Map View of the Hydrostratigraphic Cross-Sections

Figure 2-5

A (WEST) **A' (SOUTHEAST)**

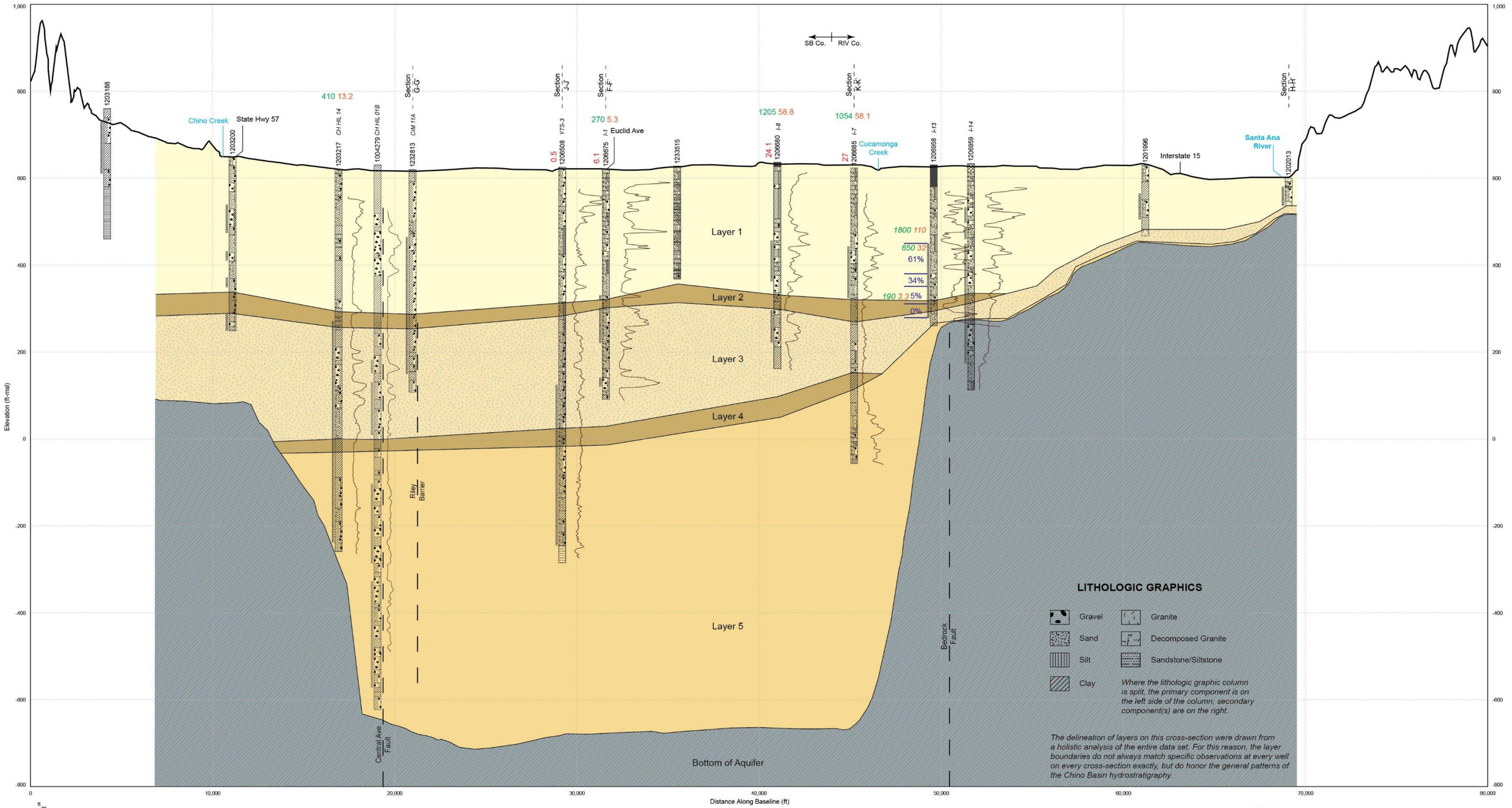

LITHOLOGIC GRAPHICS

- Gravel
- Sand
- Silt
- Clay
- Granite
- Decomposed Granite
- Sandstone/Siltstone

Where the lithologic graphic column is split, the primary component is on the left side of the column; secondary component(s) are on the right.

The delineation of layers on this cross-section were drawn from a holistic analysis of the entire data set. For this reason, the layer boundaries do not always match specific observations at every well on every cross-section exactly, but do honor the general patterns of the Chino Basin hydrostratigraphy.

ft
200
100
50
0
VERTICAL SCALE
2,000 4,000 6,000 ft
HORIZONTAL SCALE
VERTICAL EXAGGERATION 24:1

BOREHOLE LEGEND

1xxxxxx = WEI's HydroDaVE Database Well ID

Well Screen Interval

Resistivity Electrical Log

50 % Spinner Log Analysis (percent of flow from depth interval)

27.2 Specific Capactiy (gpm/ft)

Average Water Quality (1999-2019; mg/l)

TDS NO_3-N Well Discharge Sample

TDS NO_3-N Depth-specific Sample (sampled during borehole drilling)

HYDROSTRATIGRAPHIC LEGEND

- Layer 1 - Shallow aquifer-system
- Layer 2 - Upper confining unit in the deep aquifer-system
- Layer 3 - Upper portion of the deep aquifer-system
- Layer 4 - Lower confining unit in the deep aquifer-system
- Layer 5 - Lower portion of the deep aquifer-system
- Effective base of the freshwater aquifer-system

WEI
WILDERMUTH ENVIRONMENTAL, INC.

Hydrostratigraphic Cross-section: A-A'

Figure 2-6a

G (NORTH) **G' (SOUTH)**

Interstate 10
Section D-D'
Section C-C'
LA Co. SB Co.
Section B-B'
Section A-A'
Section F-F'
SB Co. RIV Co.
Section L-L'
352 18.1
San Antonio Creek
State Hwy 60
236 6.6
Prado Basin
Euclid Ave
Mill Creek
Santa Ana River
Temescal Creek
State Hwy 91
1201251 4
1002686 A-136
1002704 P-23
1002703 P-26
1004176 06
1203158 CH HIL 19
Ayala Park Piezometers
AP-PC2 Borehole Lithology
1206428
1232813 CIM 11A
1207980 HCMP-3
1224811 I-17
1207981 HCMP-4
1207983 HCMP-5
1206682 MPOW
Layer 1
Layer 2
Layer 3
Layer 4
Layer 5
550 20.7
1482 31.9
1941 83.3
331 2.7
331 7.7
360 2.2
372 1.9
372 0.3
PA-10 27
390 10
PA-7 48
300 2.3
PB-1
PB-2 0.5
170 9.24
San Jose Fault
Riley Barrier
Bottom of Aquifer
Elevation (ft-msl)
Distance Along Baseline (ft)

LITHOLOGIC GRAPHICS

- Gravel
- Sand
- Silt
- Clay
- Granite
- Decomposed Granite
- Sandstone/Siltstone

Where the lithologic graphic column is split, the primary component is on the left side of the column; secondary component(s) are on the right.

The delineation of layers on this cross-section were drawn from a holistic analysis of the entire data set. For this reason, the layer boundaries do not always match specific observations at every well on every cross-section exactly, but do honor the general patterns of the Chino Basin hydrostratigraphy.

BOREHOLE LEGEND

1xxxxxx = WEI's HydroDaVE Database Well ID

Well Screen Interval

Resistivity Electrical Log

50 Hydraulic Conductivity Data (from slug tests ft/day)

Average Water Quality (1997-2019; mg/l)

TDS NO_3-N Well Discharge Sample

TDS NO_3-N Depth-specific Sample (sampled during borehole drilling)

VERTICAL SCALE: ft 200, 100, 50, 0
HORIZONTAL SCALE: 2,000 4,000 6,000 ft
VERTICAL EXAGGERATION 25:1

HYDROSTRATIGRAPHIC LEGEND

- Layer 1 - Shallow aquifer-system
- Layer 2 - Upper confining unit in the deep aquifer-system
- Layer 3 - Upper portion of the deep aquifer-system
- Layer 4 - Lower confining unit in the deep aquifer-system
- Layer 5 - Lower portion of the deep aquifer-system
- Effective base of the freshwater aquifer-system

WEI
Wildermuth Environmental, Inc.

Hydrostratigraphic Cross-section: G-G'

Figure 2-6b

Report: FENCE_ELCGSPERFS - D, ILL File: 2019_CBWM_GWMODEL_UPDATE_V1.GPJ 4/29/2019

J (SOUTHWEST)

J' (NORTHEAST)

Elevation (ft-msl)

Distance Along Baseline (ft)

Section A-A'
Section N-N
Section K-K'
Section I-I'
Section E-E'

Prado Basin
State Hwy 71
Chino Creek
Euclid Blvd
State Hwy 60
West Cucamonga Creek
Cucamonga Creek
Interstate 10
Interstate 15
Day Creek
Foothill Blvd
Interstate 15
State Hwy 210
San Sevaine Creek

1222970 I-16
1206508 YTS-3
1206674 College Park Well
1208673 CDF Well 16
1220159 OIA MW-1A
1201125 IRR/DOM
1220169 ONT 43
1206945 ONT 45
1207948 ONT 47
1207929 CVWD 40
1223003 VCT-1
1223001 SSV-1

193 1.7
213 0.9
353 1.4
207 2.9
387 14.3
203 1.3
310 5.1

Layer 1
Layer 2
Layer 3
Layer 4
Layer 5

Chino Fault
Central Ave Fault
Bedrock Fault
Cucamonga Fault Zone

Bottom of Aquifer

LITHOLOGIC GRAPHICS

- Gravel
- Sand
- Silt
- Clay
- Granite
- Decomposed Granite
- Sandstone/Siltstone

Where the lithologic graphic column is split, the primary component is on the left side of the column; secondary component(s) are on the right.

The delineation of layers on this cross-section were drawn from a holistic analysis of the entire data set. For this reason, the layer boundaries do not always match specific observations at every well on every cross-section exactly, but do honor the general patterns of the Chino Basin hydrostratigraphy.

BOREHOLE LEGEND

1xxxxxx = WEI's HydroDaVE Database Well ID

Well Screen Interval

Resistivity Electrical Log

Average Water Quality (2004-2019; mg/l)

TDS NO_3-N Well Discharge Sample

TDS NO_3-N Depth-specific Sample (sampled during borehole drilling)

HYDROSTRATIGRAPHIC LEGEND

- Layer 1 - Shallow aquifer-system
- Layer 2 - Upper confining unit in the deep aquifer-system
- Layer 3 - Upper portion of the deep aquifer-system
- Layer 4 - Lower confining unit in the deep aquifer-system
- Layer 5 - Lower portion of the deep aquifer-system
- Effective base of the freshwater aquifer-system

VERTICAL SCALE: ft 200 100 50 0; 2,000 4,000 6,000 ft HORIZONTAL SCALE

VERTICAL EXAGGERATION 22:1

WEI Wildermuth Environmental, Inc.

Hydrostratigraphic Cross-section: J-J'

Figure 2-6c

Report FENCE - ELOGS/PSFIS - D_ILL File: 2019_CBWM_GWMODEL_UPDATE_V1.GPJ 4/25/2019

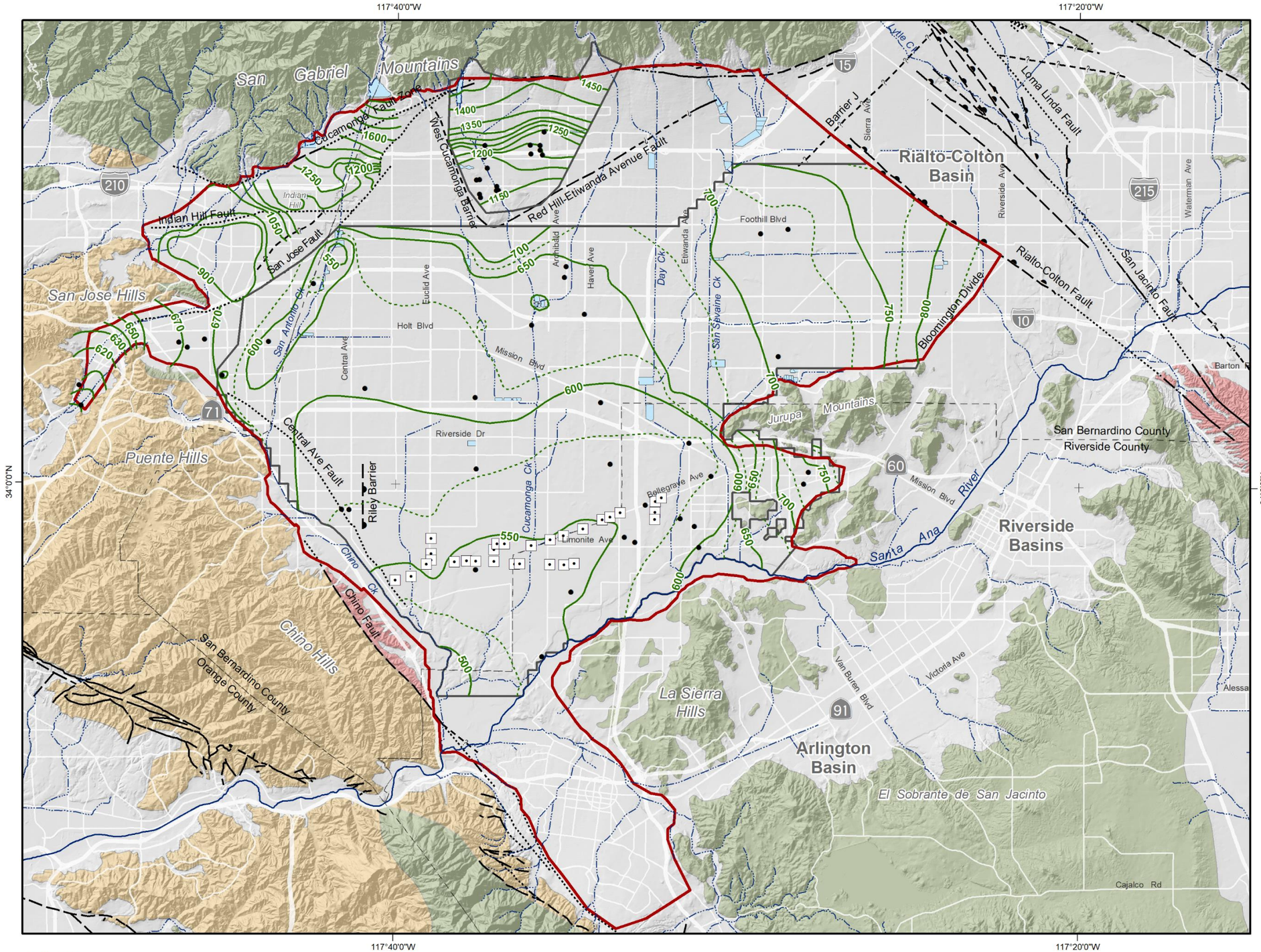

Groundwater-Elevation Contours
(feet above mean sea-level)
Chino Basin: Spring 2018
Spadra Basin: Fall 2018
Six Basins: Fall 2018
Cucamonga Basin: Fall 2018

Boundary of Contoured Area
(contours are not shown outside of this boundary due to lack of groundwater-level data)

Well with Groundwater Level Time History

Chino Basin Desalter Well

Chino Valley Basins
Groundwater Flow Model Boundary

Streams & Flood Control Channels

Flood Control & Conservation Basins

Geology

Water-Bearing Sediments

Quaternary Alluvium

Consolidated Bedrock

Plio-Pleistocene Sedimentary Rocks

Cretaceous to Miocene Sedimentary Rocks

Pre-Tertiary Igneous and Metamorphic Rocks

Fault (solid where accurately located; dashed where approximately located or inferred; dotted where concealed)

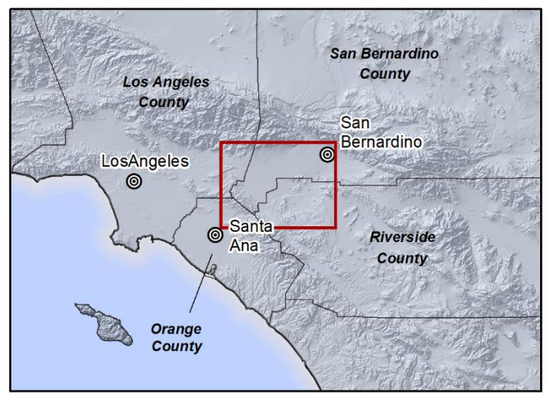

Produced by:

WEI
Wildermuth Environmental, Inc.

Author: MB
Date: 5/11/2020
Document Name: Figure_2-7_20200115_WL

0 1 2 3 4 5 Miles
0 2 4 6 8 KM

Prepared for:

2020 Safe Yield Recalculation

Chino Basin Watermaster
Partners in Basin Management

Groundwater-Elevation Contours Chino Valley Basin

Figure 2-7

Figure 2-8

Water-Level Time Histories (Non-Pumping)

City of Chino Hills 1A and 1B

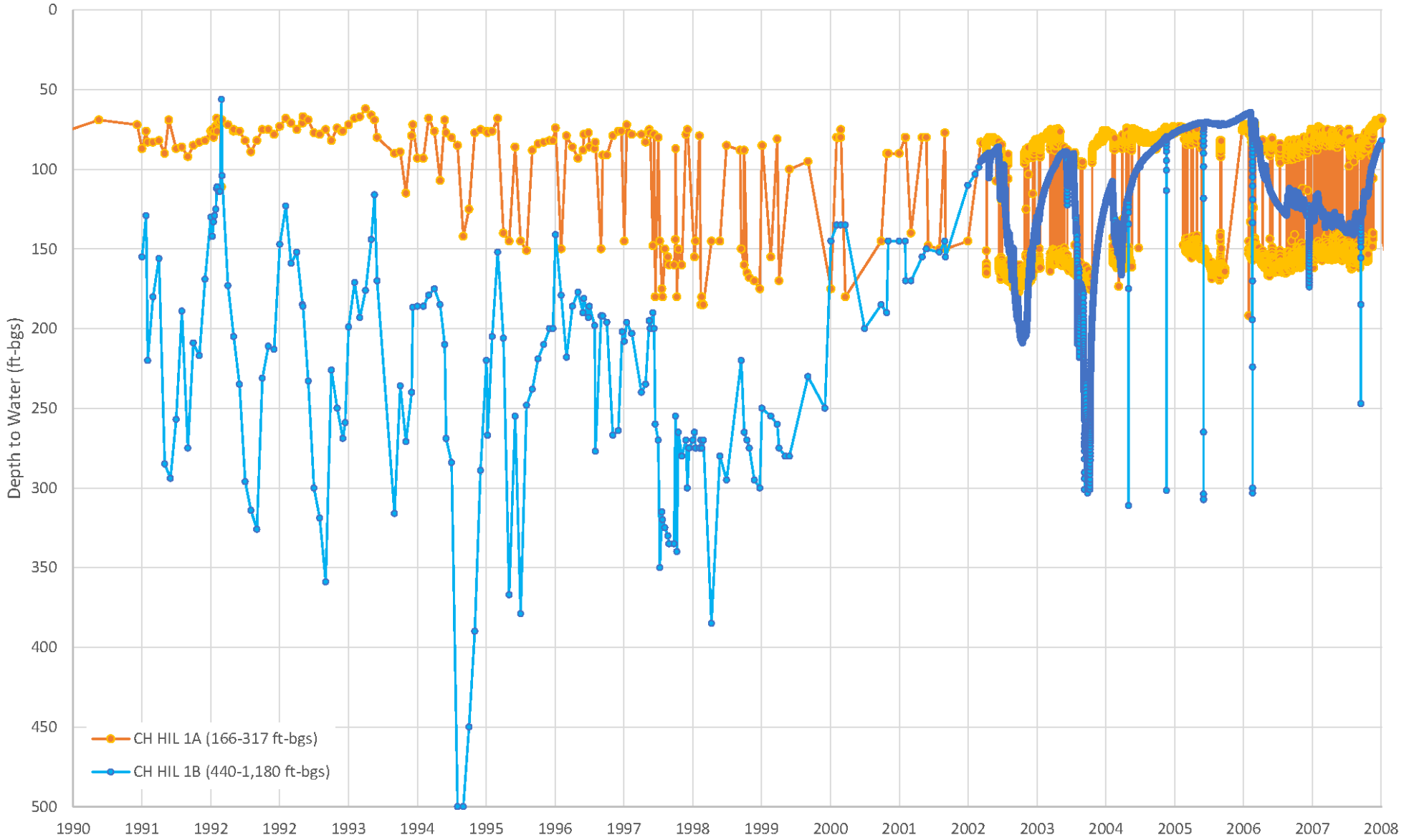

1/22/2020 -- 3:17 PM
Figure2-x_MZ1_DTWex

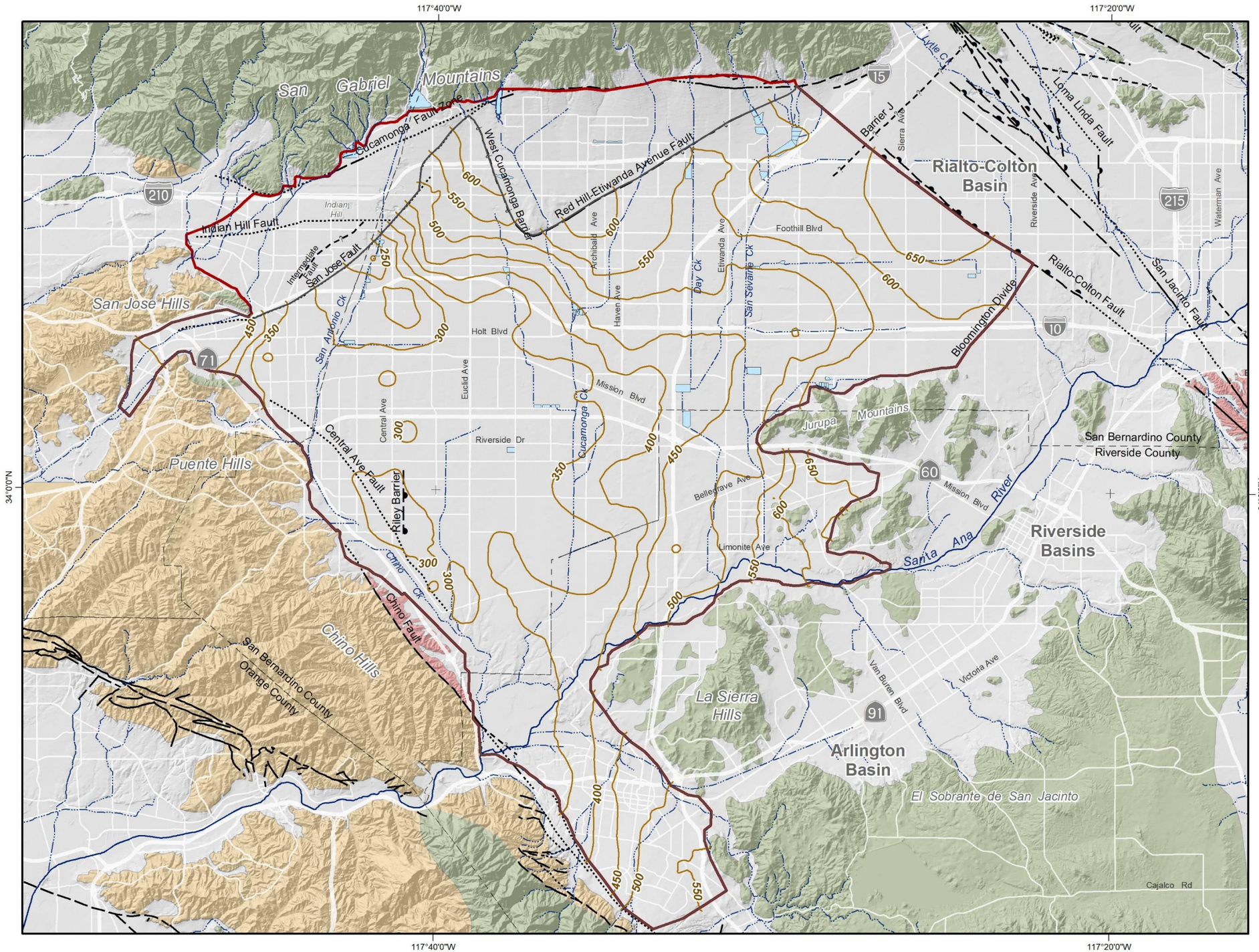

-600- Equal Elevation Contour of the Model Layer 1 (ft-above msl)

Layer 1 Hydrogeologic Boundary Extent

Chino Valley Basins Groundwater Flow Model Boundary

Streams & Flood Control Channels

Flood Control & Conservation Basins

Geology

Water-Bearing Sediments

Quaternary Alluvium

Consolidated Bedrock

Plio-Pleistocene Sedimentary Rocks

Cretaceous to Miocene Sedimentary Rocks

Pre-Tertiary Igneous and Metamorphic Rocks

Fault (solid where accurately located; dashed where approximately located or inferred; dotted where concealed)

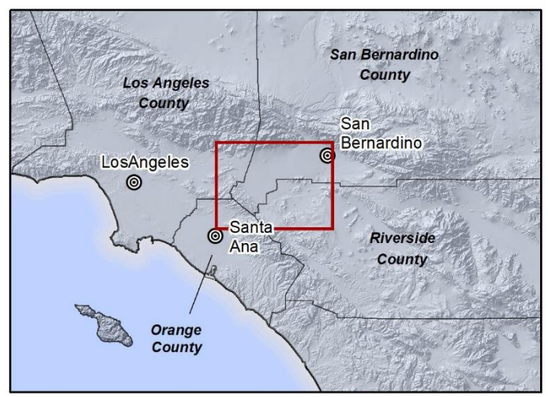

Produced by:

WEI Wildermuth Environmental, Inc.

Author: MJC

Date: 1/22/2020

Document Name: Figure_2-9a_20200117_L1btm

0 1 2 3 4 5 Miles

0 2 4 6 8 KM

Prepared for:

2020 Safe Yield Recalculation

Chino Basin Watermaster — Partners in Basin Management

Layer 1 Bottom Elevation for Chino Basin

Figure 2-9a

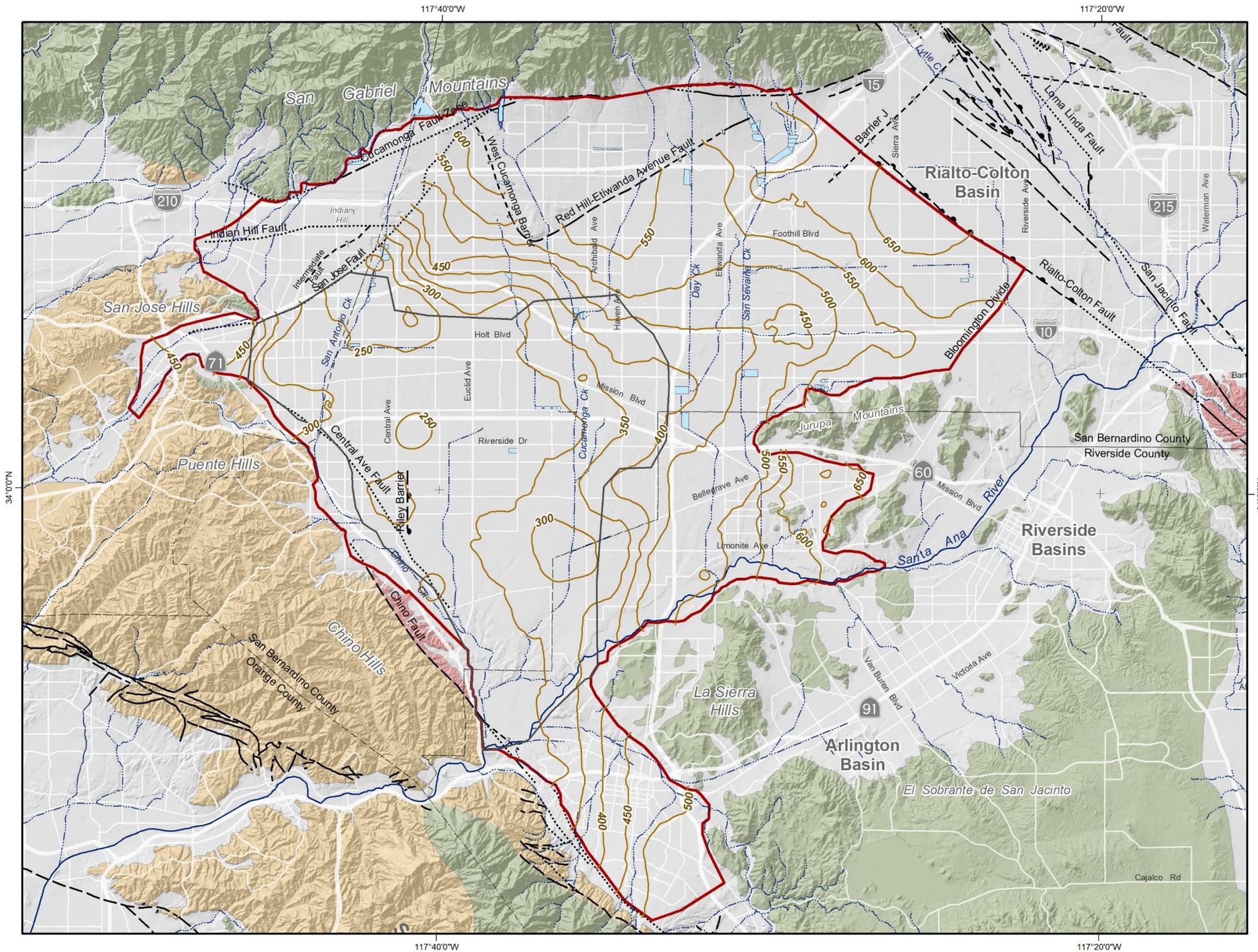

–600– Equal Elevation Contour of the Model Layer 2 (ft-above msl)

Layer 2 Hydrogeologic Boundary Extent

Chino Valley Basins Groundwater Flow Model Boundary

Streams & Flood Control Channels

Flood Control & Conservation Basins

Geology

Water-Bearing Sediments

Quaternary Alluvium

Consolidated Bedrock

Plio-Pleistocene Sedimentary Rocks

Cretaceous to Miocene Sedimentary Rocks

Pre-Tertiary Igneous and Metamorphic Rocks

Fault (solid where accurately located; dashed where approximately located or inferred; dotted where concealed)

Produced by:

WEI
WILDERMUTH ENVIRONMENTAL, INC.

Author: MJC
Date: 1/22/2020
Document Name: Figure_2-9b_20200117_L2btm

0 1 2 3 4 5 Miles
0 2 4 6 8 KM

Prepared for:

2020 Safe Yield Recalculation

CHINO BASIN WATERMASTER
Partners in Basin Management

Layer 2 Bottom Elevation for Chino Basin

Figure 2-9b

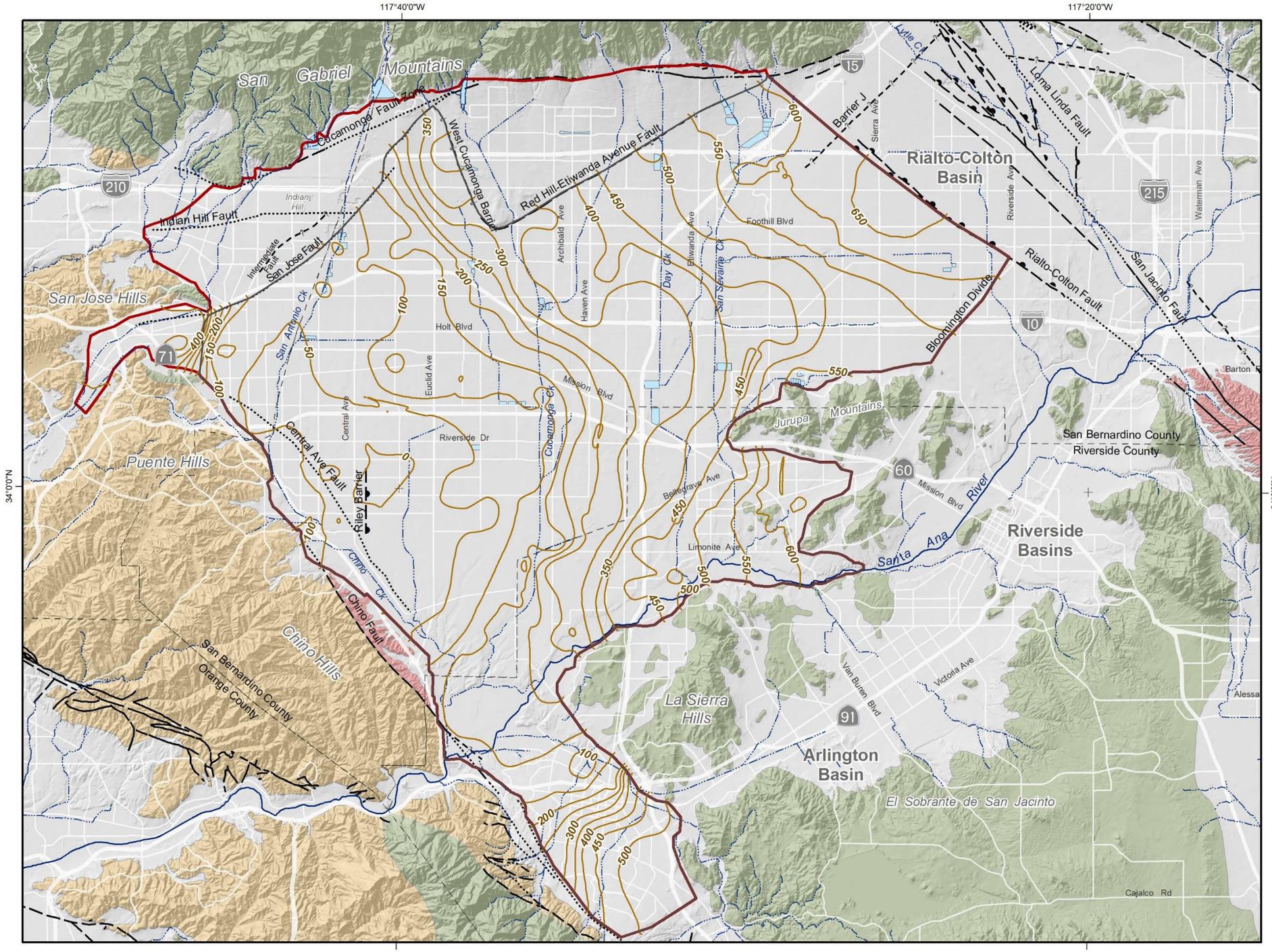

Produced by:

WEI
WILDERMUTH ENVIRONMENTAL, INC.

Author: MJC
Date: 1/22/2020
Document Name: Figure_2-9c_20200117_L3btm

0 1 2 3 4 5 Miles
0 2 4 6 8 KM

Prepared for:

2020 Safe Yield Recalculation

CHINO BASIN WATERMASTER
Partners in Basin Management

-600- Equal Elevation Contour of the Model Layer 3 (ft-above msl)

Layer 3 Hydrogeologic Boundary Extent

Chino Valley Basins Groundwater Flow Model Boundary

Streams & Flood Control Channels

Flood Control & Conservation Basins

Geology

Water-Bearing Sediments

Quaternary Alluvium

Consolidated Bedrock

Plio-Pleistocene Sedimentary Rocks

Cretaceous to Miocene Sedimentary Rocks

Pre-Tertiary Igneous and Metamorphic Rocks

Fault (solid where accurately located; dashed where approximately located or inferred; dotted where concealed)

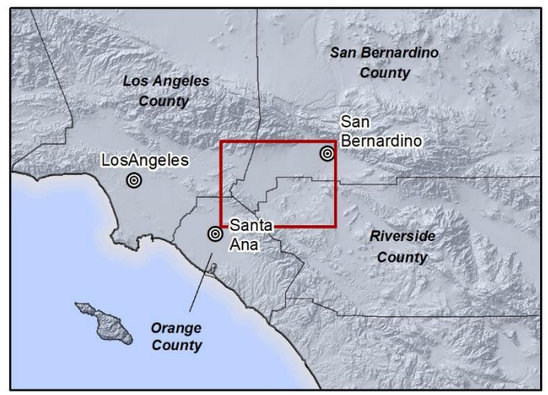

Layer 3 Bottom Elevation for Chino Basin

Figure 2-9c

117°40'0"W

117°20'0"W

34°0'0"N

San Gabriel Mountains

Cucamonga Fault Zone

West Cucamonga Barrier

Red Hill-Etiwanda Avenue Fault

Barrier J

Lytle Ck

Loma Linda Fault

Rialto-Colton Basin

Indian Hill Fault

Intermediate Fault

San Jose Fault

San Jose Hills

San Antonio Ck

Holt Blvd

Archibald Ave

Haven Ave

Day Ck

Etiwanda Ave

San Sevaine Ck

Foothill Blvd

Riverside Ave

Sierra Ave

Waterman Ave

Rialto-Colton Fault

San Jacinto Fault

Bloomington Divide

Barton

Central Ave Fault

Riley Barrier

Euclid Ave

Central Ave

Riverside Dr

Cucamonga Ck

Mission Blvd

Jurupa Mountains

San Bernardino County

Riverside County

Puente Hills

Bellegrave Ave

Limonite Ave

Mission Blvd

Santa Ana River

Riverside Basins

Chino Ck

Chino Fault

Chino Hills

San Bernardino County

Orange County

La Sierra Hills

Van Buren Blvd

Victoria Ave

Arlington Basin

El Sobrante de San Jacinto

Cajalco Rd

Alessa

210

15

215

10

71

60

91

50

100

150

200

250

300

350

400

450

500

550

600

650

0

117°40'0"W

117°20'0"W

34°0'0"N

-600- Equal Elevation Contour of the Model Layer 4 (ft-above msl)

Layer 4 Hydrogeologic Boundary Extent

Chino Valley Basins Groundwater Flow Model Boundary

Streams & Flood Control Channels

Flood Control & Conservation Basins

Geology

Water-Bearing Sediments

Quaternary Alluvium

Consolidated Bedrock

Plio-Pleistocene Sedimentary Rocks

Cretaceous to Miocene Sedimentary Rocks

Pre-Tertiary Igneous and Metamorphic Rocks

Fault (solid where accurately located; dashed where approximately located or inferred; dotted where concealed)

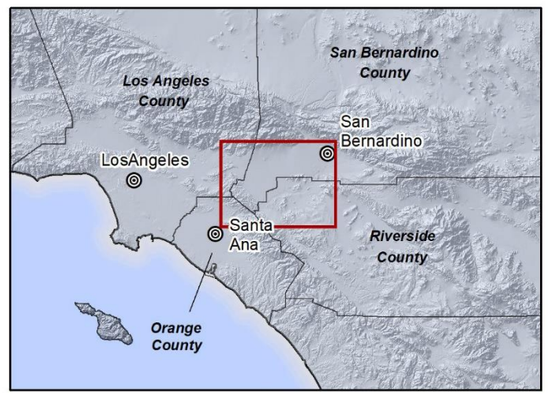

Produced by:

WEI
WILDERMUTH ENVIRONMENTAL, INC.

Author: MJC

Date: 1/22/2020

Document Name: Figure_2-9d_20200117_L4btm

0 1 2 3 4 5 Miles

0 2 4 6 8 KM

Prepared for:

2020 Safe Yield Recalculation

CHINO BASIN WATERMASTER
Partners in Basin Management

Layer 4 Bottom Elevation for Chino Basin

Figure 2-9d

117°40'0"W

117°20'0"W

34°0'0"N

San Gabriel Mountains

Cucamonga Fault Zone

West Cucamonga Barrier

Red Hill-Etiwanda Avenue Fault

Barrier J

Lytle Ck

Loma Linda Fault

Rialto-Colton Basin

Indian Hill

Indian Hill Fault

Intermediate Fault

San Jose Fault

San Jose Hills

San Antonio Ck

Archibald Ave

Haven Ave

Day Ck

Etiwanda Ave

San Sevaine Ck

Foothill Blvd

Riverside Ave

Sierra Ave

Waterman Ave

Rialto-Colton Fault

San Jacinto Fault

Bloomington Divide

Holt Blvd

Euclid Ave

Central Ave

Central Ave Fault

Riley Barrier

Mission Blvd

Cucamonga Ck

Riverside Dr

Jurupa Mountains

San Bernardino County

Riverside County

Puente Hills

Bellegrave Ave

Limonite Ave

Santa Ana River

Riverside Basins

Chino Ck

Chino Fault

Chino Hills

San Bernardino County

Orange County

La Sierra Hills

Van Buren Blvd

Victoria Ave

Arlington Basin

El Sobrante de San Jacinto

Cajalco Rd

Barton R

Alessa

-300 -200 -100 0 -100 -200 -300 -400 -500 -600 -700 -500 -400 -300 -200 -100 0 100 200 300 400 500 100 200 300 400 100 200

71 210 15 215 10 60 91

-600- Equal Elevation Contour of the Model Layer 5 (ft-above msl)

Layer 5 Hydrogeologic Boundary Extent

Chino Valley Basins Groundwater Flow Model Boundary

Streams & Flood Control Channels

Flood Control & Conservation Basins

Geology

Water-Bearing Sediments

Quaternary Alluvium

Consolidated Bedrock

Plio-Pleistocene Sedimentary Rocks

Cretaceous to Miocene Sedimentary Rocks

Pre-Tertiary Igneous and Metamorphic Rocks

Fault (solid where accurately located; dashed where approximately located or inferred; dotted where concealed)

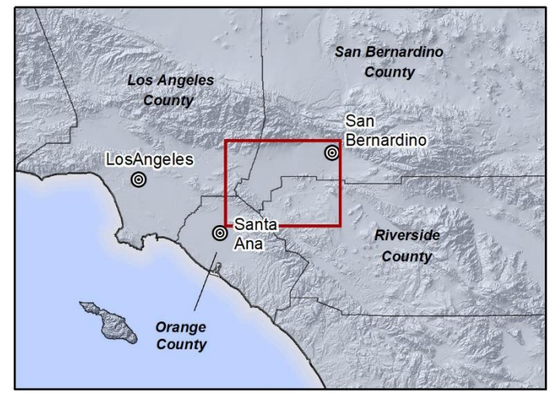

Produced by:

WEI Wildermuth Environmental, Inc.

Author: MJC

Date: 1/22/2020

Document Name: Figure_2-9e_20200117_L5btm

0 1 2 3 4 5 Miles

0 2 4 6 8 KM

Prepared for:

2020 Safe Yield Recalculation

Chino Basin Watermaster — Partners in Basin Management

Layer 5 Bottom Elevation for Chino Basin

Figure 2-9e

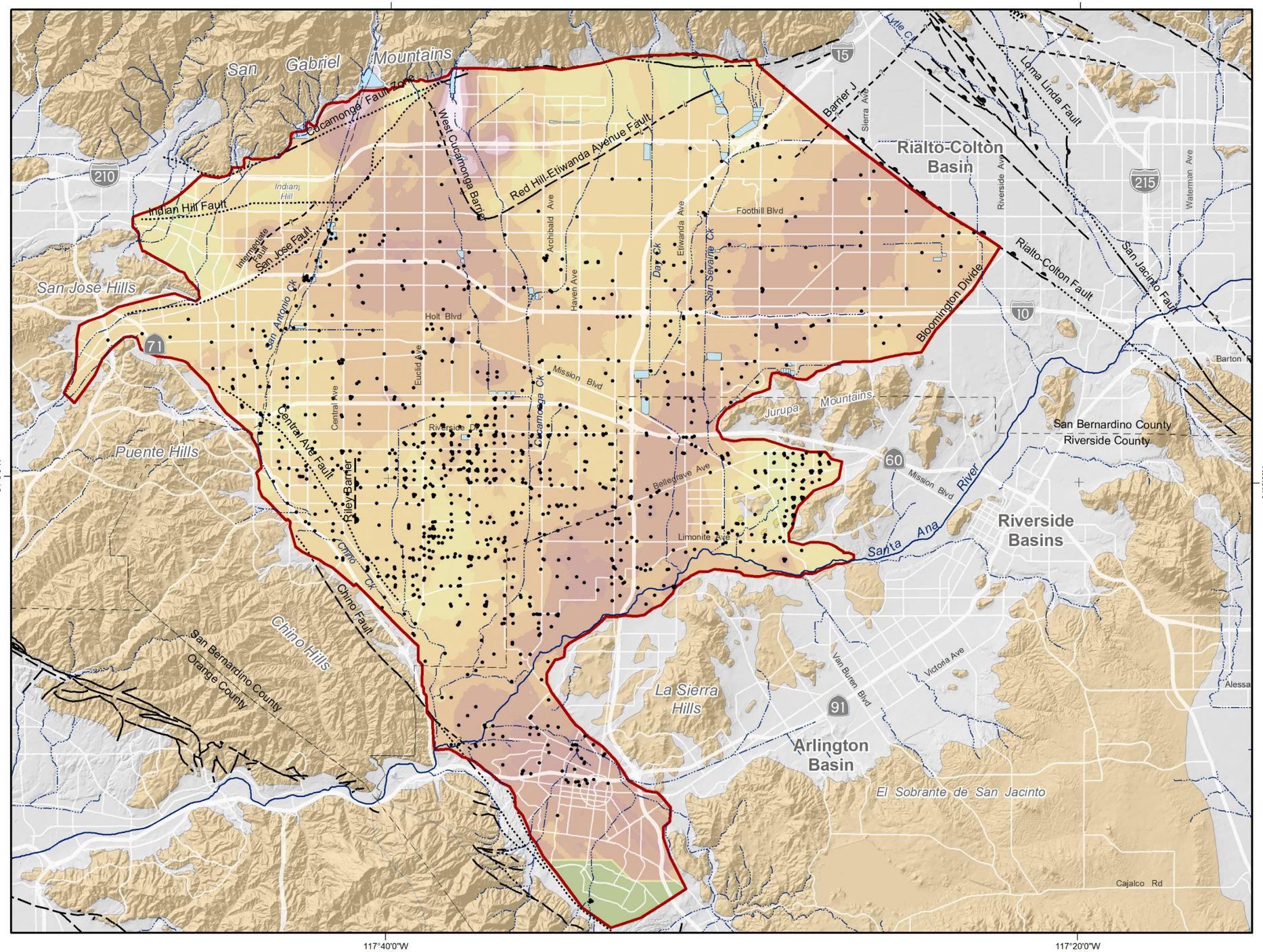

Initial Estimated Specific Yield
Layer 1

- 0.001 - 0.025
- 0.026 - 0.05
- 0.051 - 0.075
- 0.076 - 0.1
- 0.101 - 0.125
- 0.126 - 0.15
- 0.151 - 0.175
- 0.176 - 0.199
- 0.2 - 0.224
- 0.225 - 0.249

Borehole with Lithologic Data used to Estimate Specific Yield

Chino Valley Basins Groundwater Flow Model Boundary

Streams & Flood Control Channels

Flood Control & Conservation Basins

Geology

Water-Bearing Sediments

Quaternary Alluvium

Consolidated Bedrock

Undifferentiated Pre-Tertiary to Early Pleistocene Igneous, Metamorphic, and Sedimentary Rocks

Fault (solid where accurately located; dashed where approximately located or inferred; dotted where concealed)

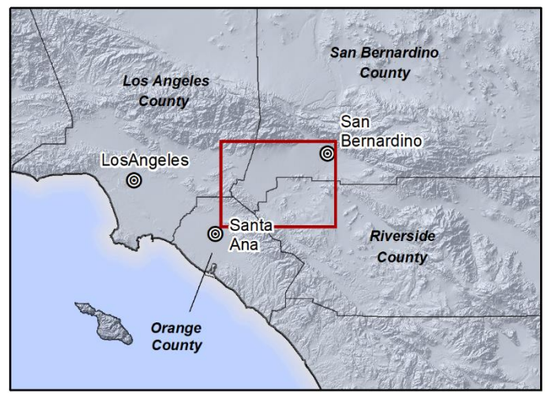

Produced by:

WEI
Wildermuth Environmental, Inc.

Author: MAB
Date: 4/29/2020
Document Name: Figure_2-10a_20200120_L1Sy

0 1 2 3 4 5 Miles
0 2 4 6 8 KM

Prepared for:

2020 Safe Yield Recalculation

Chino Basin Watermaster
Partners in Basin Management

Layer 1 Initial and Pre-calibrated Specific Yield Based on Borehole Lithology and Lithologic Modeling

Figure 2-10a

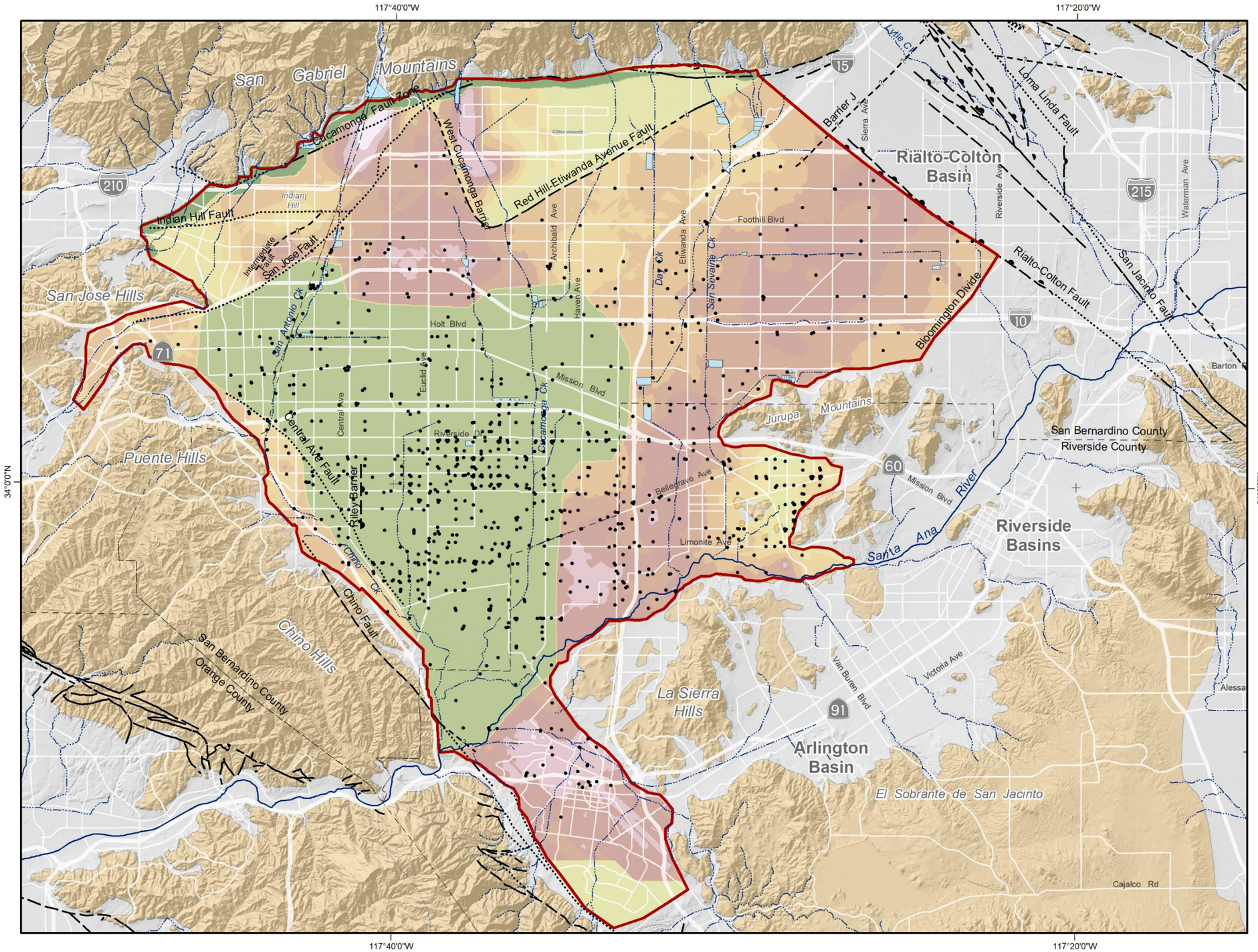

Initial Estimated Specific Yield
Layer 2

- 0.001 - 0.022
- 0.023 - 0.044
- 0.045 - 0.066
- 0.067 - 0.088
- 0.089 - 0.109
- 0.11 - 0.131
- 0.132 - 0.153
- 0.154 - 0.175
- 0.176 - 0.196
- 0.197 - 0.218

Borehole with Lithologic Data used to Estimate Specific Yield

Chino Valley Basins Groundwater Flow Model Boundary

Streams & Flood Control Channels

Flood Control & Conservation Basins

Geology

Water-Bearing Sediments

Quaternary Alluvium

Consolidated Bedrock

Undifferentiated Pre-Tertiary to Early Pleistocene Igneous, Metamorphic, and Sedimentary Rocks

Fault (solid where accurately located; dashed where approximately located or inferred; dotted where concealed)

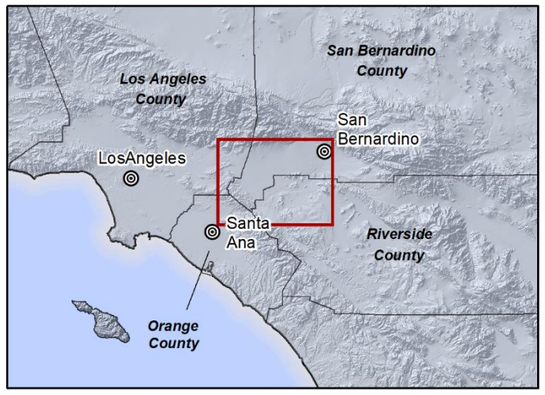

Produced by:

WEI
WILDERMUTH ENVIRONMENTAL, INC.

Author: MAB
Date: 4/29/2020
Document Name: Figure_2-10b_20200120_L2Sy

0 1 2 3 4 5 Miles
0 2 4 6 8 KM

Prepared for:

2020 Safe Yield Recalculation

CHINO BASIN WATERMASTER
Partners in Basin Management

Layer 2 Initial and Pre-calibrated Specific Yield Based on Borehole Lithology and Lithologic Modeling

Figure 2-10b

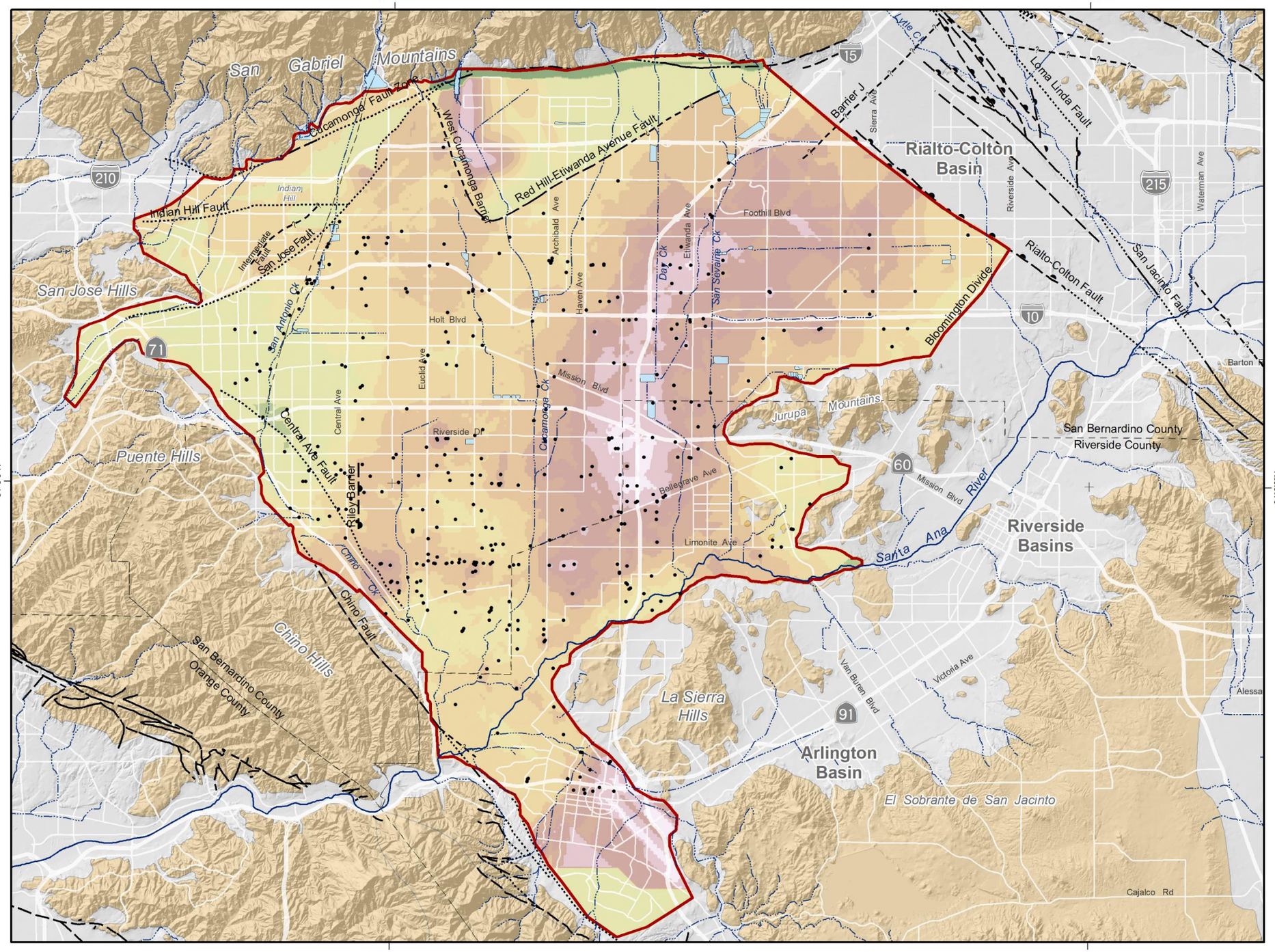

Initial Estimated Specific Yield
Layer 3

- 0 - 0.023
- 0.024 - 0.045
- 0.046 - 0.067
- 0.068 - 0.089
- 0.09 - 0.112
- 0.113 - 0.134
- 0.135 - 0.156
- 0.157 - 0.179
- 0.18 - 0.201
- 0.202 - 0.223

Borehole with Lithologic Data used to Estimate Specific Yield

Chino Valley Basins Groundwater Flow Model Boundary

Streams & Flood Control Channels

Flood Control & Conservation Basins

Geology

Water-Bearing Sediments

Quaternary Alluvium

Consolidated Bedrock

Undifferentiated Pre-Tertiary to Early Pleistocene Igneous, Metamorphic, and Sedimentary Rocks

Fault (solid where accurately located; dashed where approximately located or inferred; dotted where concealed)

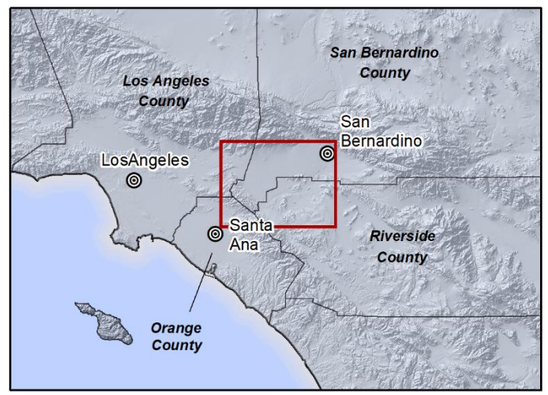

Produced by:

WEI
Wildermuth Environmental, Inc.

Author: MAB
Date: 4/29/2020
Document Name: Figure_2-10c_20200120_L3Sy

0 1 2 3 4 5 Miles
0 2 4 6 8 KM

Prepared for:

2020 Safe Yield Recalculation

Chino Basin Watermaster
Partners in Basin Management

Layer 3 Initial and Pre-calibrated Specific Yield Based on Borehole Lithology and Lithologic Modeling

Figure 2-10c

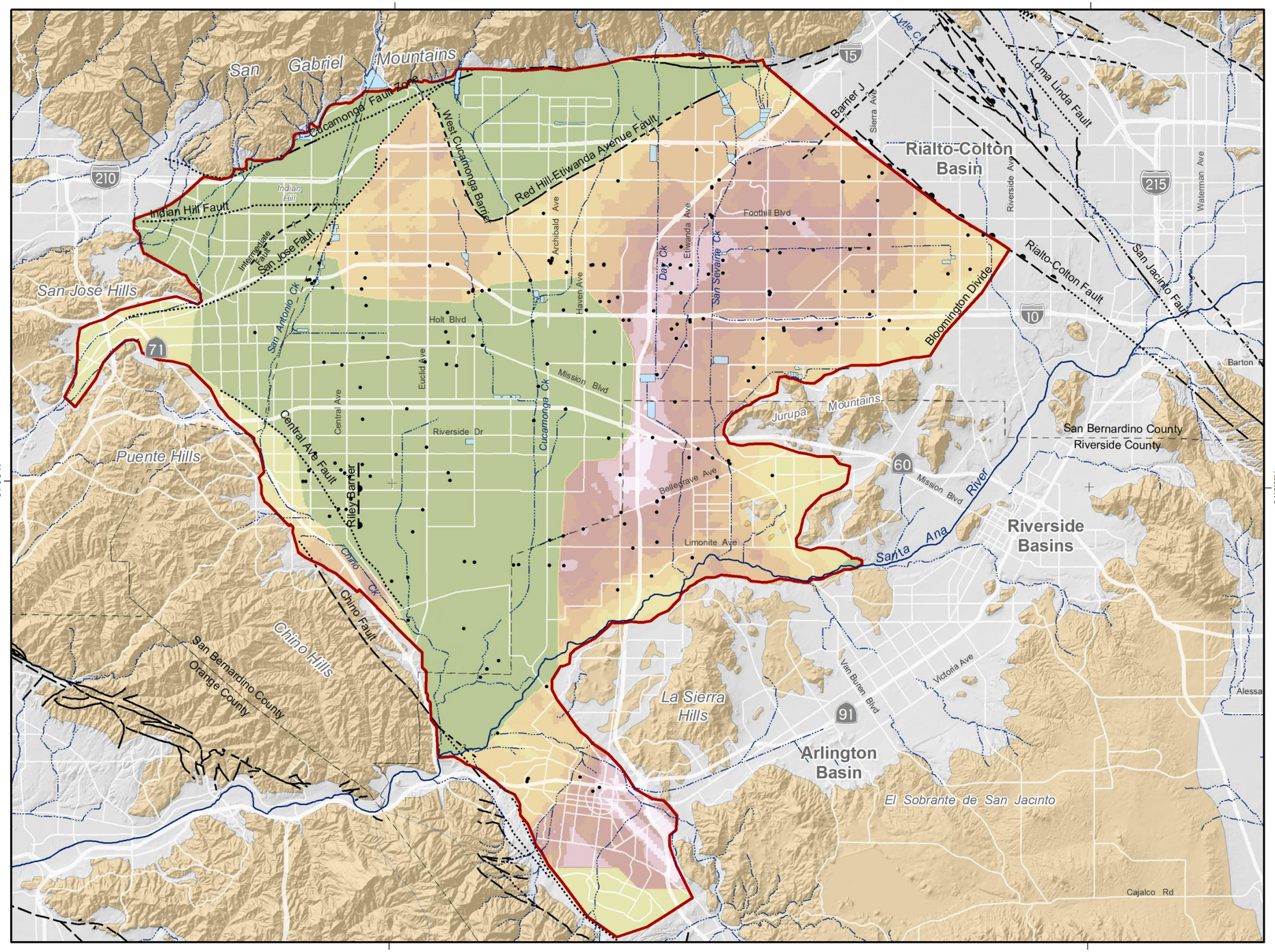

Initial Estimated Specific Yield
Layer 4

- 0 - 0.023
- 0.024 - 0.045
- 0.046 - 0.067
- 0.068 - 0.089
- 0.09 - 0.112
- 0.113 - 0.134
- 0.135 - 0.156
- 0.157 - 0.179
- 0.18 - 0.201
- 0.202 - 0.223

Borehole with Lithologic Data used to Estimate Specific Yield

Chino Valley Basins Groundwater Flow Model Boundary

Streams & Flood Control Channels

Flood Control & Conservation Basins

Geology

Water-Bearing Sediments

Quaternary Alluvium

Consolidated Bedrock

Undifferentiated Pre-Tertiary to Early Pleistocene Igneous, Metamorphic, and Sedimentary Rocks

Fault (solid where accurately located; dashed where approximately located or inferred; dotted where concealed)

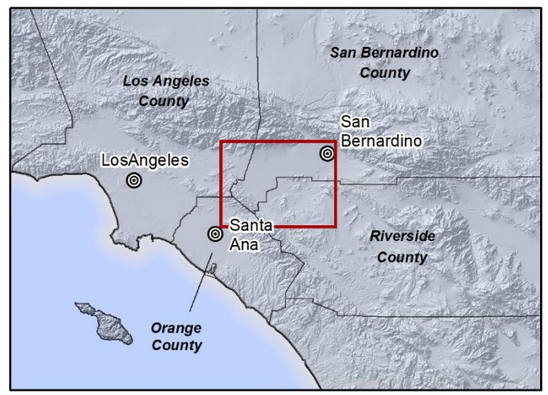

Produced by:

WEI
WILDERMUTH ENVIRONMENTAL, INC.

Author: MAB
Date: 4/29/2020
Document Name: Figure_2-10d_20200120_L4Sy

0 1 2 3 4 5 Miles
0 2 4 6 8 KM

Prepared for:

2020 Safe Yield Recalculation

CHINO BASIN WATERMASTER
Partners in Basin Management

Layer 4 Initial and Pre-calibrated Specific Yield Based on Borehole Lithology and Lithologic Modeling

Figure 2-10d

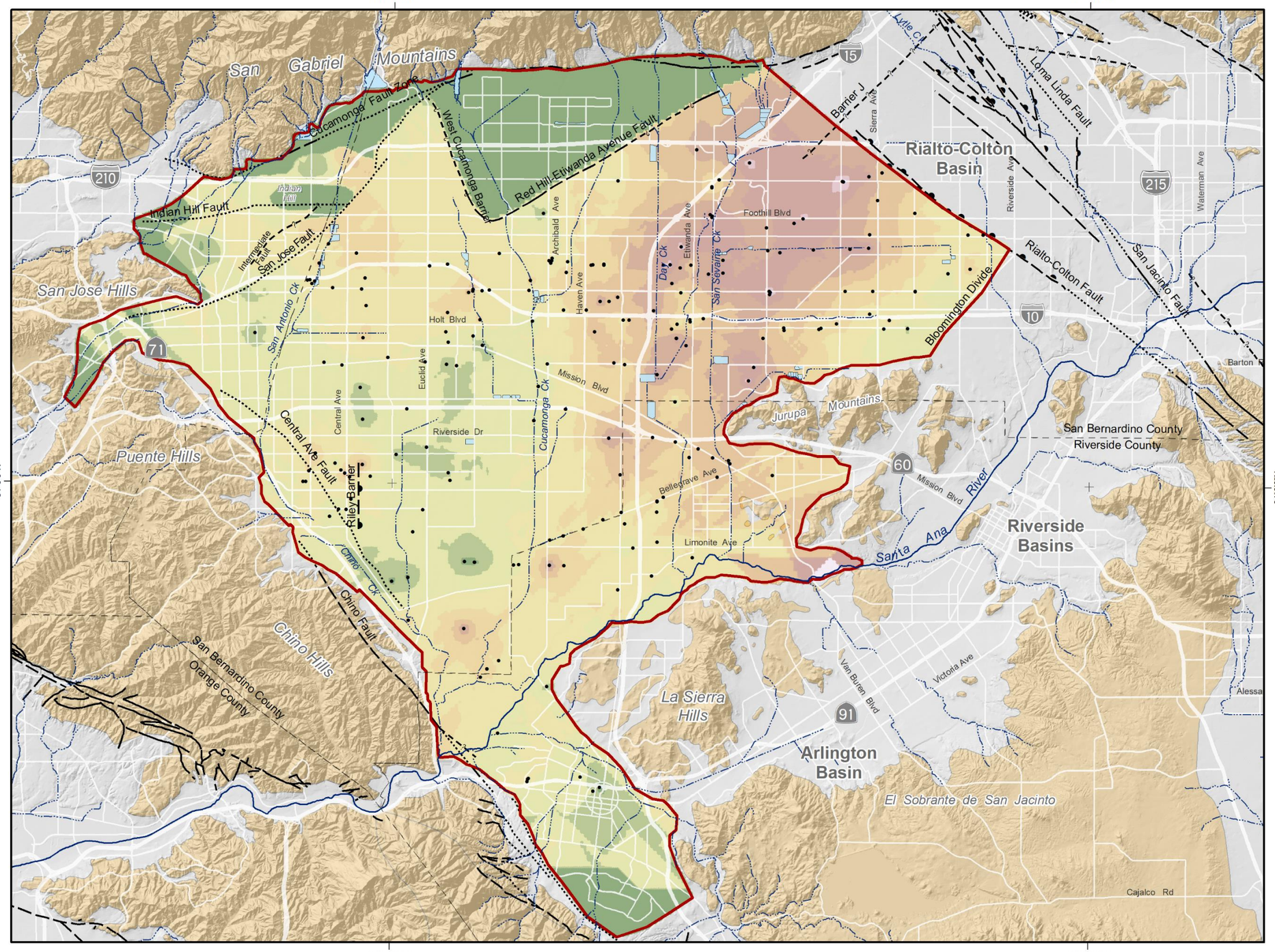

Initial Estimated Specific Yield
Layer 5

- 0.042 - 0.062
- 0.063 - 0.082
- 0.083 - 0.102
- 0.103 - 0.122
- 0.123 - 0.142
- 0.143 - 0.162
- 0.163 - 0.183
- 0.184 - 0.203
- 0.204 - 0.223
- 0.224 - 0.243

Borehole with Lithologic Data used to Estimate Specific Yield

Chino Valley Basins Groundwater Flow Model Boundary

Streams & Flood Control Channels

Flood Control & Conservation Basins

Geology

Water-Bearing Sediments

Quaternary Alluvium

Consolidated Bedrock

Undifferentiated Pre-Tertiary to Early Pleistocene Igneous, Metamorphic, and Sedimentary Rocks

Fault (solid where accurately located; dashed where approximately located or inferred; dotted where concealed)

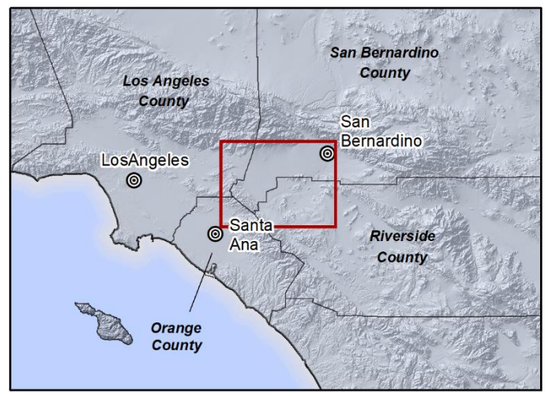

Produced by:

WEI
WILDERMUTH ENVIRONMENTAL, INC.

Author: MAB
Date: 4/29/2020
Document Name: Figure_2-10e_20200120_L5Sy

0 1 2 3 4 5 Miles
0 2 4 6 8 KM

Prepared for:

2020 Safe Yield Recalculation

CHINO BASIN WATERMASTER
Partners in Basin Management

Layer 5 Initial and Pre-calibrated Specific Yield Based on Borehole Lithology and Lithologic Modeling

Figure 2-10e

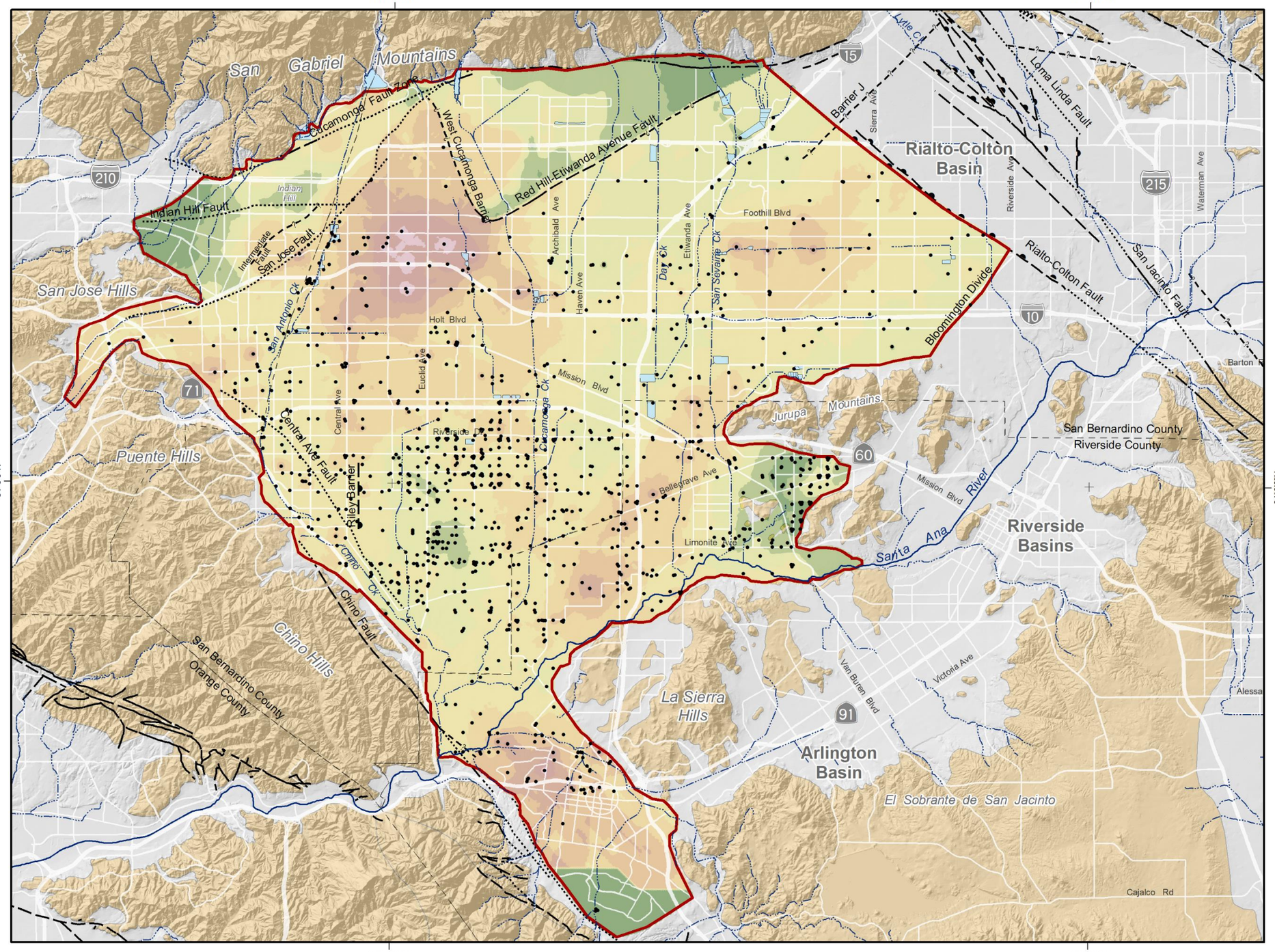

Initial Estimated Horizontal Hydraulic Conductivity
Layer 1
(ft/day)

- 3 - 21
- 22 - 40
- 41 - 58
- 59 - 76
- 77 - 95
- 96 - 113
- 114 - 132
- 133 - 150
- 151 - 168
- 169 - 187

Borehole with Lithologic Data used to Estimate Horizontal Hydraulic Conductivity

Chino Valley Basins Groundwater Flow Model Boundary

Streams & Flood Control Channels

Flood Control & Conservation Basins

Geology

Water-Bearing Sediments

Quaternary Alluvium

Consolidated Bedrock

Undifferentiated Pre-Tertiary to Early Pleistocene Igneous, Metamorphic, and Sedimentary Rocks

Fault (solid where accurately located; dashed where approximately located or inferred; dotted where concealed)

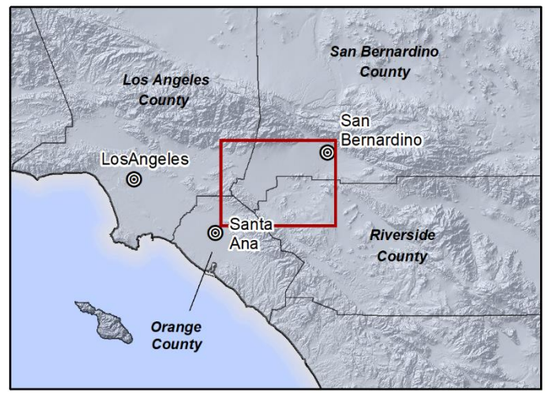

Produced by:

WEI
WILDERMUTH ENVIRONMENTAL, INC.

Author: MAB
Date: 4/29/2020
Document Name: Figure_2-11a_20200120_L1Kh

0 1 2 3 4 5 Miles
0 2 4 6 8 KM

Prepared for:

2020 Safe Yield Recalculation

CHINO BASIN WATERMASTER
Partners in Basin Management

Layer 1 Initial and Pre-calibrated Horizontal Hydraulic Conductivity Based on Borehole Lithology and Lithologic Modeling

Figure 2-11a

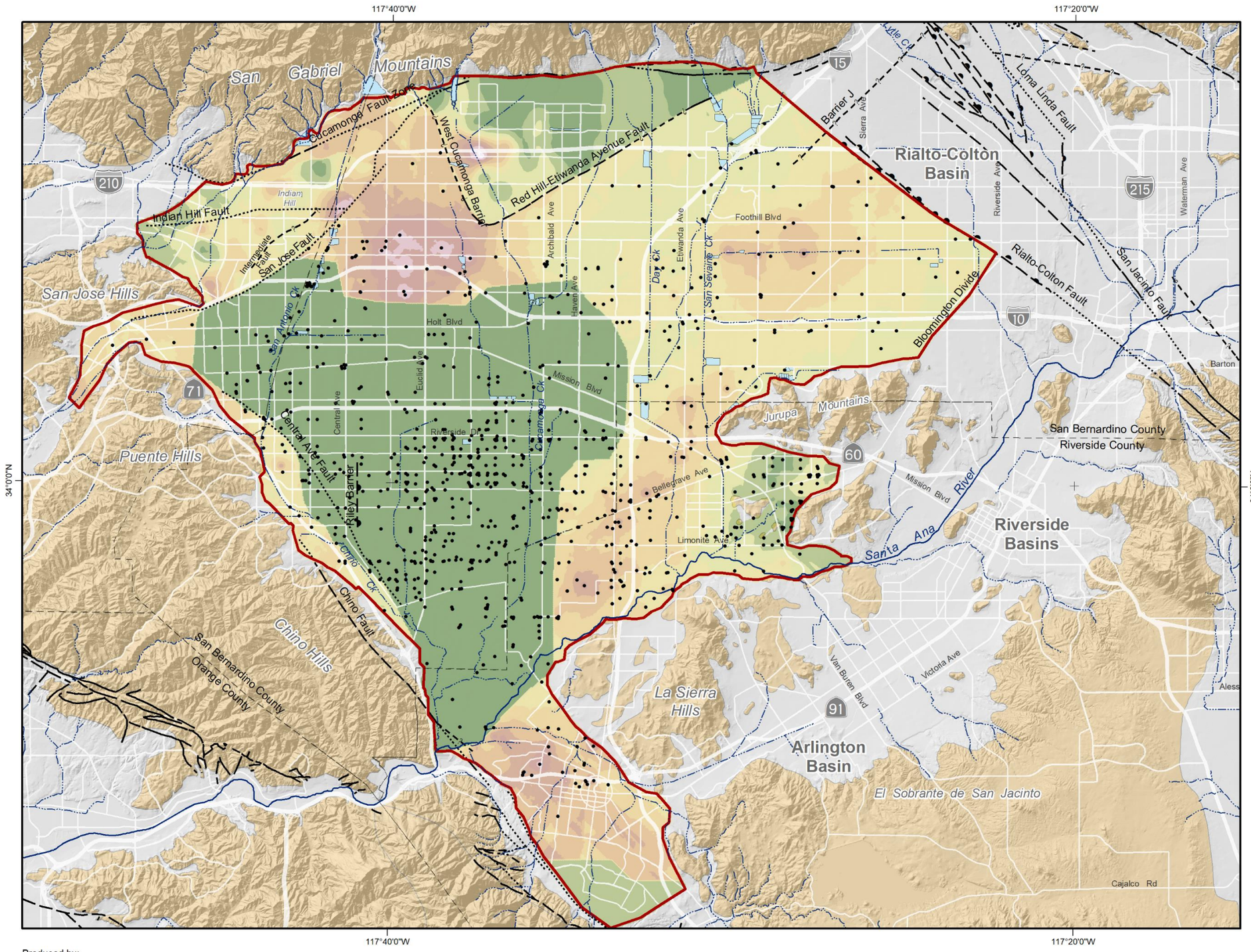

Initial Estimated Horizontal Hydraulic Conductivity
Layer 2
(ft/day)

- 0 - 19
- 20 - 37
- 38 - 56
- 57 - 75
- 76 - 93
- 94 - 112
- 113 - 131
- 132 - 150
- 151 - 168
- 169 - 187

Borehole with Lithologic Data used to Estimate Horizontal Hydraulic Conductivity

Chino Valley Basins Groundwater Flow Model Boundary

Streams & Flood Control Channels

Flood Control & Conservation Basins

Geology

Water-Bearing Sediments

Quaternary Alluvium

Consolidated Bedrock

Undifferentiated Pre-Tertiary to Early Pleistocene Igneous, Metamorphic, and Sedimentary Rocks

Fault (solid where accurately located; dashed where approximately located or inferred; dotted where concealed)

Produced by:

WEI
WILDERMUTH ENVIRONMENTAL, INC.

Author: MAB
Date: 4/29/2020
Document Name: Figure_2-11b_20200120_L2Kh

0 1 2 3 4 5 Miles
0 2 4 6 8 KM

Prepared for:

2020 Safe Yield Recalculation

CHINO BASIN WATERMASTER
Partners in Basin Management

Layer 2 Initial and Pre-calibrated Horizontal Hydraulic Conductivity Based on Borehole Lithology and Lithologic Modeling

Figure 2-11b

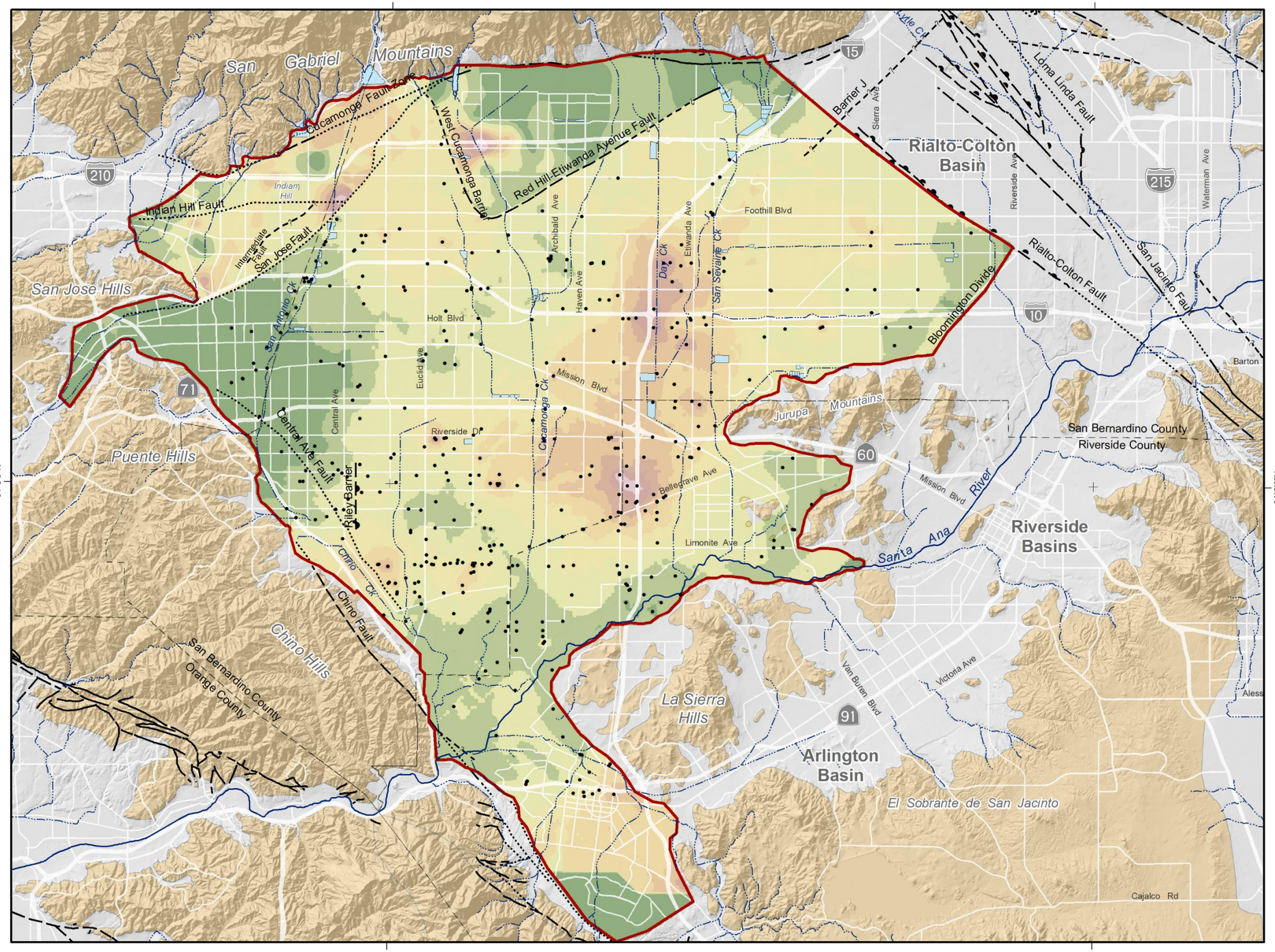

Initial Estimated Horizontal Hydraulic Conductivity
Layer 3
(ft/day)

- 3 - 22
- 23 - 41
- 42 - 60
- 61 - 79
- 80 - 99
- 100 - 118
- 119 - 137
- 138 - 156
- 157 - 175
- 176 - 195

Borehole with Lithologic Data used to Estimate Horizontal Hydraulic Conductivity

Chino Valley Basins Groundwater Flow Model Boundary

Streams & Flood Control Channels

Flood Control & Conservation Basins

Geology

Water-Bearing Sediments

Quaternary Alluvium

Consolidated Bedrock

Undifferentiated Pre-Tertiary to Early Pleistocene Igneous, Metamorphic, and Sedimentary Rocks

Fault (solid where accurately located; dashed where approximately located or inferred; dotted where concealed)

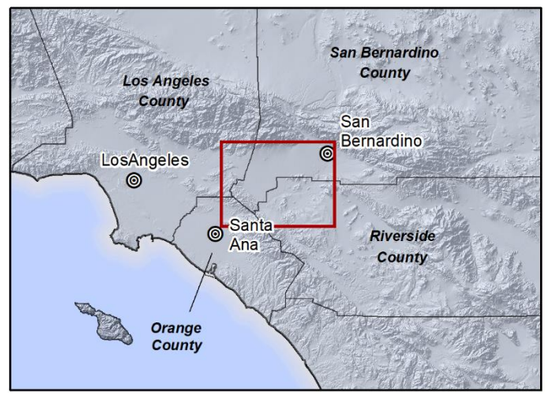

Produced by:

WEI
WILDERMUTH ENVIRONMENTAL, INC.

Author: MAB
Date: 4/29/2020
Document Name: Figure_2-11c_20200120_L3Kh

0 1 2 3 4 5 Miles
0 2 4 6 8 KM

Prepared for:

2020 Safe Yield Recalculation

CHINO BASIN WATERMASTER
Partners in Basin Management

Layer 3 Initial and Pre-calibrated Horizontal Hydraulic Conductivity Based on Borehole Lithology and Lithologic Modeling

Figure 2-11c

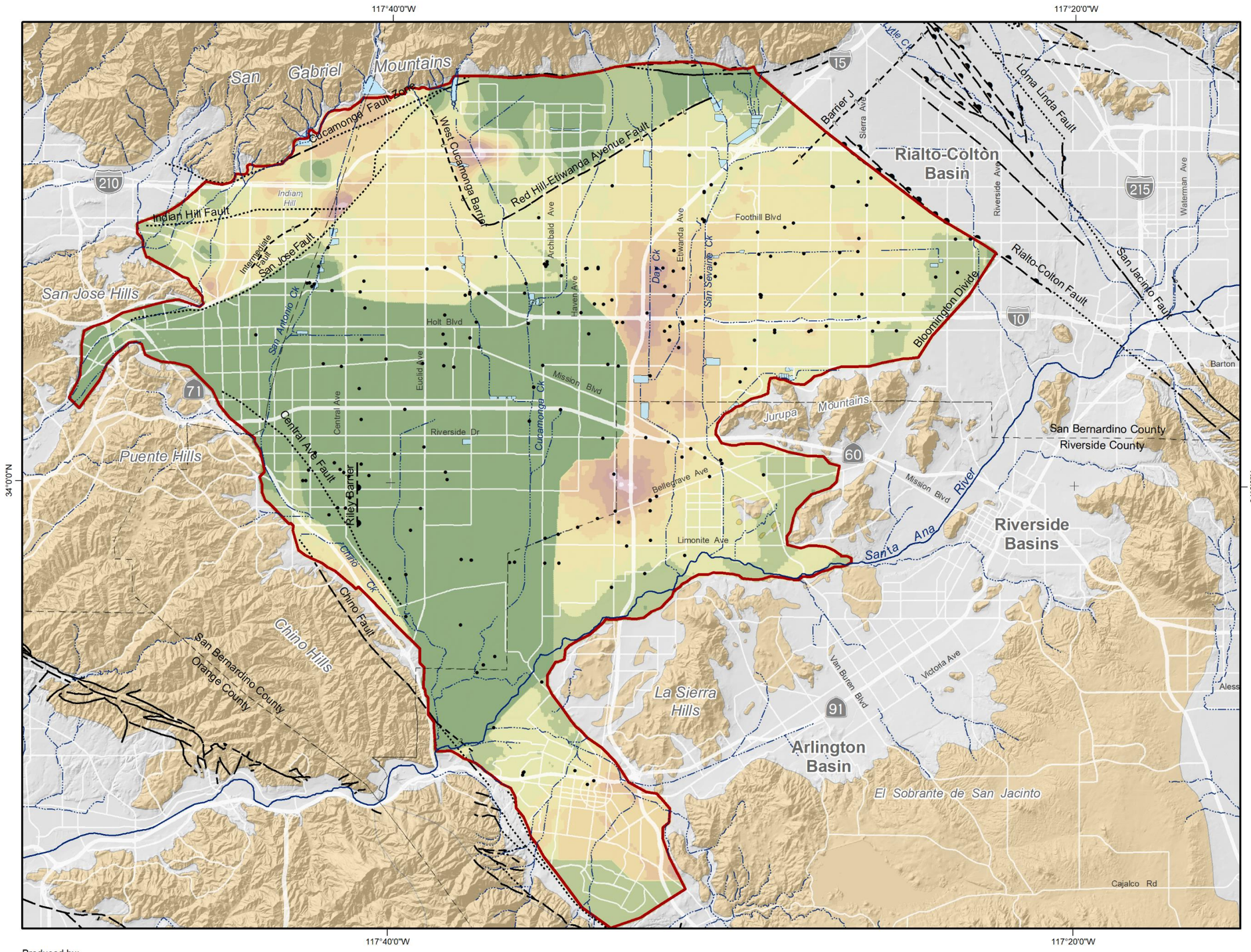

Initial Estimated Horizontal Hydraulic Conductivity
Layer 4
(ft/day)

- 0 - 20
- 21 - 39
- 40 - 58
- 59 - 78
- 79 - 97
- 98 - 117
- 118 - 136
- 137 - 156
- 157 - 175
- 176 - 195

Borehole with Lithologic Data used to Estimate Horizontal Hydraulic Conductivity

Chino Valley Basins Groundwater Flow Model Boundary

Streams & Flood Control Channels

Flood Control & Conservation Basins

Geology

Water-Bearing Sediments

Quaternary Alluvium

Consolidated Bedrock

Undifferentiated Pre-Tertiary to Early Pleistocene Igneous, Metamorphic, and Sedimentary Rocks

Fault (solid where accurately located; dashed where approximately located or inferred; dotted where concealed)

Produced by:

WEI
WILDERMUTH ENVIRONMENTAL, INC.

Author: MAB
Date: 4/29/2020
Document Name: Figure_2-11d_20200120_L4Kh

0 1 2 3 4 5 Miles
0 2 4 6 8 KM

Prepared for:

2020 Safe Yield Recalculation

CHINO BASIN WATERMASTER
Partners in Basin Management

Layer 4 Initial and Pre-calibrated Horizontal Hydraulic Conductivity Based on Borehole Lithology and Lithologic Modeling

Figure 2-11d

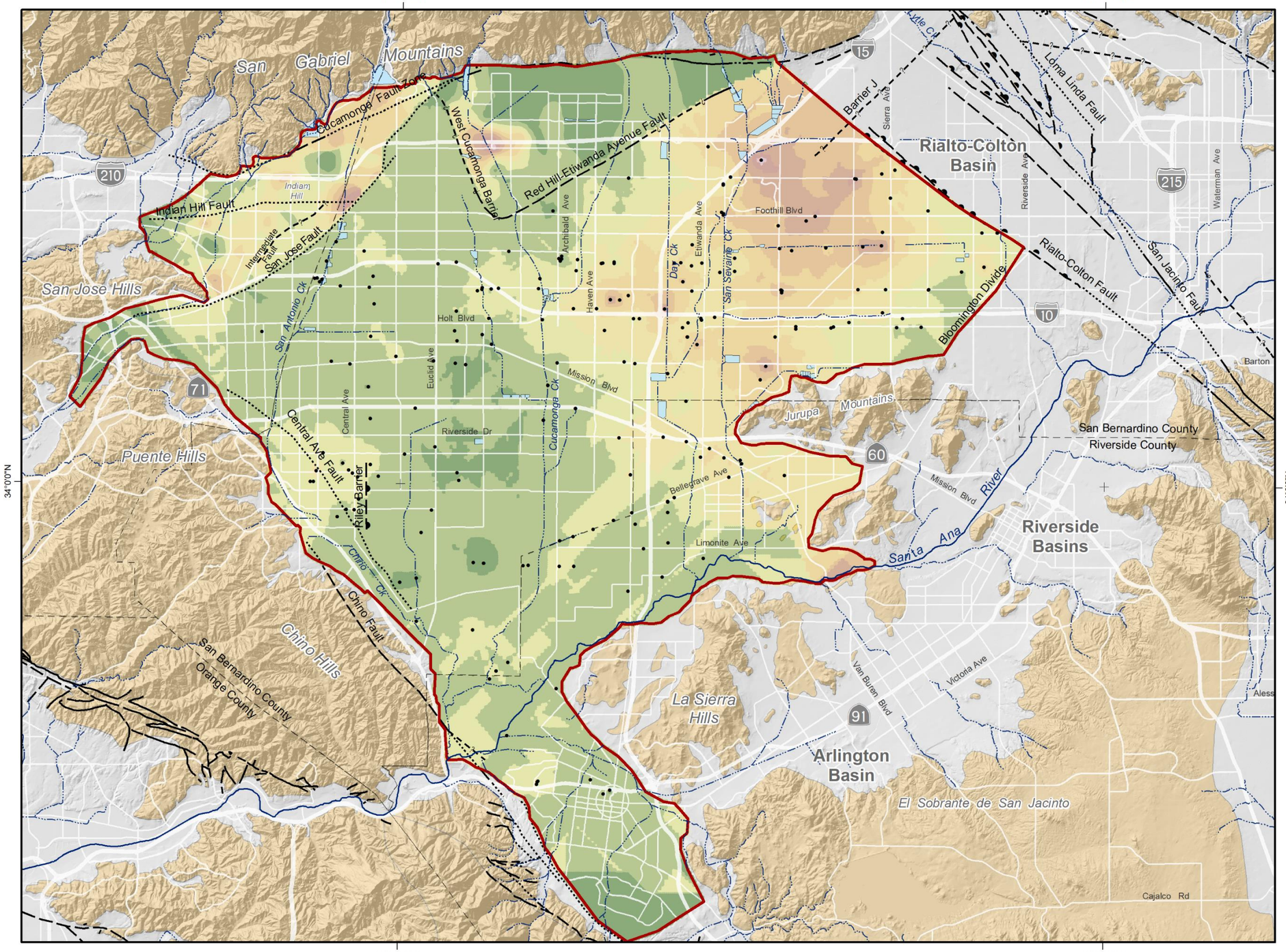

Initial Estimated Horizontal Hydraulic Conductivity
Layer 5
(ft/day)

- 3 - 24
- 25 - 45
- 46 - 65
- 66 - 86
- 87 - 107
- 108 - 128
- 129 - 149
- 150 - 170
- 171 - 190
- 191 - 211

Borehole with Lithologic Data used to Estimate Horizontal Hydraulic Conductivity

Chino Valley Basins Groundwater Flow Model Boundary

Streams & Flood Control Channels

Flood Control & Conservation Basins

Geology

Water-Bearing Sediments

Quaternary Alluvium

Consolidated Bedrock

Undifferentiated Pre-Tertiary to Early Pleistocene Igneous, Metamorphic, and Sedimentary Rocks

Fault (solid where accurately located; dashed where approximately located or inferred; dotted where concealed)

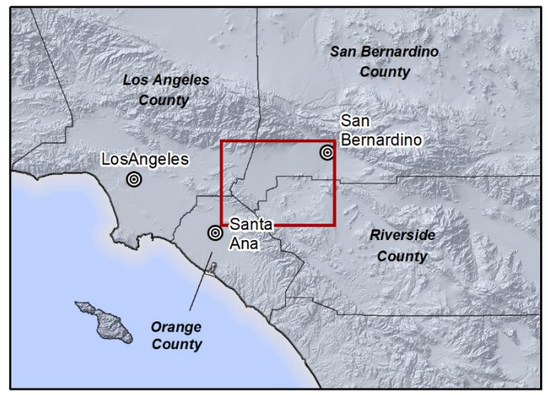

Produced by:

WEI
Wildermuth Environmental, Inc.

Author: MAB
Date: 4/29/2020
Document Name: Figure_2-11e_20200120_L5Kh

0 1 2 3 4 5 Miles
0 2 4 6 8 KM

Prepared for:

2020 Safe Yield Recalculation

Chino Basin Watermaster
Partners in Basin Management

Layer 5 Initial and Pre-calibrated Horizontal Hydraulic Conductivity Based on Borehole Lithology and Lithologic Modeling

Figure 2-11e

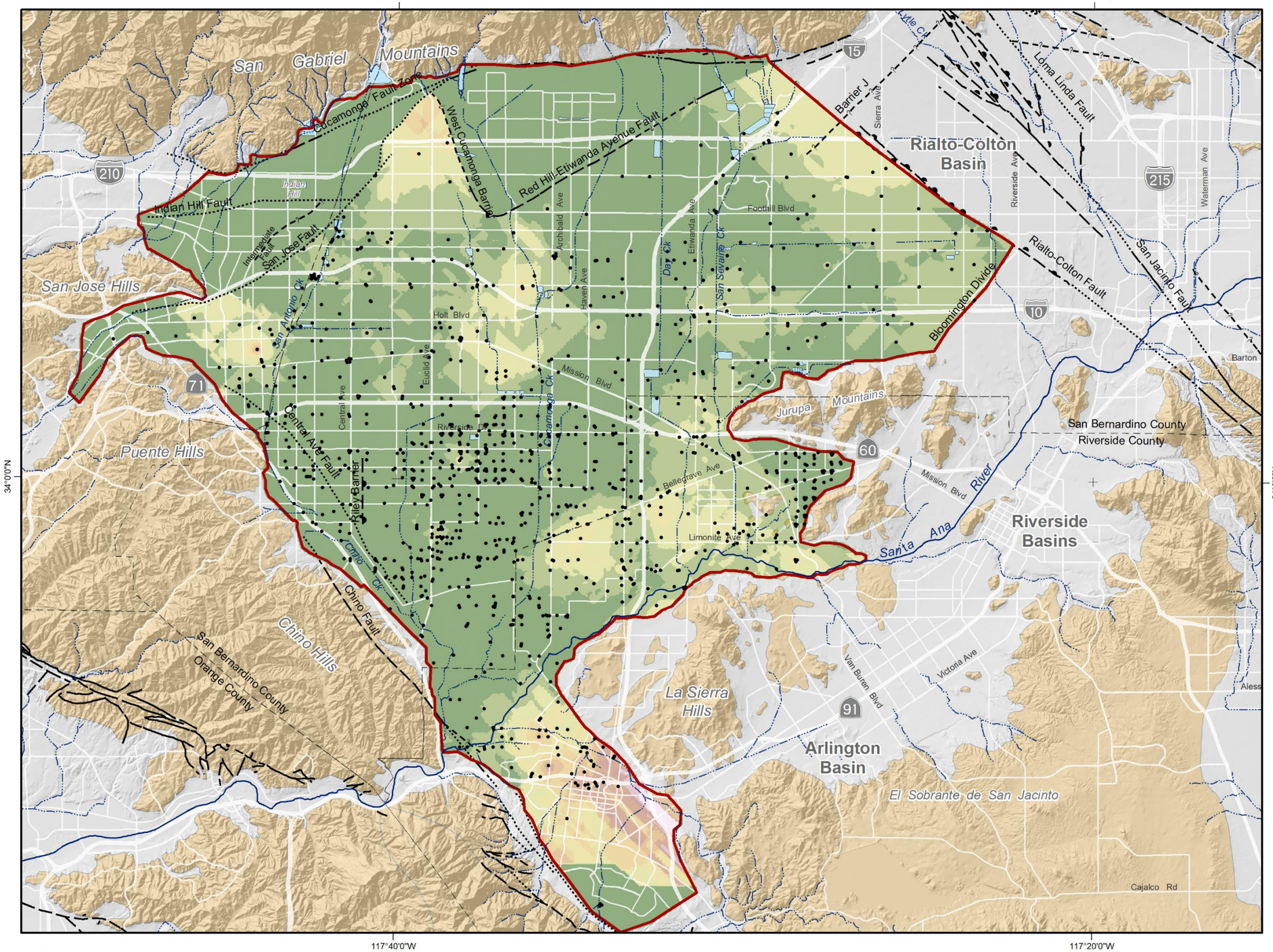

Initial Estimated Vertical Hydraulic Conductivity
Layer 1
(ft/day)

- 0.01 - 9
- 10 - 19
- 20 - 28
- 29 - 37
- 38 - 46
- 47 - 56
- 57 - 65
- 66 - 74
- 75 - 84
- 85 - 93

Borehole with Lithologic Data used to Estimate Vertical Hydraulic Conductivity

Chino Valley Basins Groundwater Flow Model Boundary

Streams & Flood Control Channels

Flood Control & Conservation Basins

Geology

Water-Bearing Sediments

Quaternary Alluvium

Consolidated Bedrock

Undifferentiated Pre-Tertiary to Early Pleistocene Igneous, Metamorphic, and Sedimentary Rocks

Fault (solid where accurately located; dashed where approximately located or inferred; dotted where concealed)

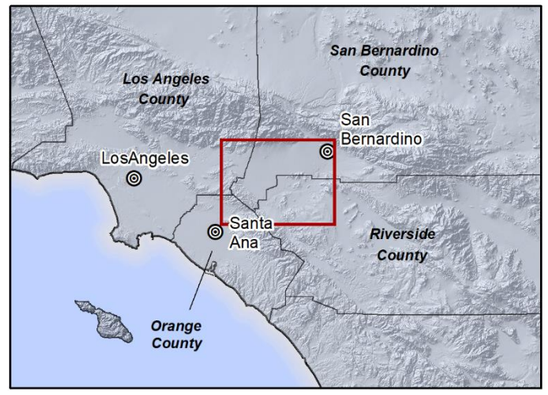

Produced by:

WEI
Wildermuth Environmental, Inc.

Author: MAB
Date: 4/29/2020
Document Name: Figure_2-12a_20200120_L1Kv

0 1 2 3 4 5 Miles
0 2 4 6 8 KM

Prepared for:

2020 Safe Yield Recalculation

Chino Basin Watermaster
Partners in Basin Management

Layer 1 Initial and Pre-calibrated Vertical Hydraulic Conductivity Based on Borehole Lithology and Lithologic Modeling

Figure 2-12a

117°40'0"W

117°20'0"W

34°0'0"N

San Gabriel Mountains

Cucamonga Fault Zone

West Cucamonga Barrier

Red Hill-Etiwanda Avenue Fault

Barrier J

Rialto-Colton Basin

Loma Linda Fault

Indian Hill Fault

Indian Hill

Intermediate Fault

San Jose Fault

San Jose Hills

Foothill Blvd

Archibald Ave

Haven Ave

Etiwanda Ave

Day Ck

San Sevaine Ck

Riverside Ave

Waterman Ave

Rialto-Colton Fault

San Jacinto Fault

Bloomington Divide

San Antonio Ck

Holt Blvd

Euclid Ave

Central Ave

Central Ave Fault

Mission Blvd

Riverside Dr

Cucamonga Ck

Jurupa Mountains

San Bernardino County

Riverside County

Puente Hills

Riley Barrier

Bellegrave Ave

Limonite Ave

Mission Blvd

Santa Ana River

Riverside Basins

Chino Ck

Chino Fault

Chino Hills

San Bernardino County

Orange County

La Sierra Hills

Van Buren Blvd

Victoria Ave

Arlington Basin

El Sobrante de San Jacinto

Cajalco Rd

Barton

Aless

15

210

215

10

71

60

91

117°40'0"W

117°20'0"W

34°0'0"N

Initial Estimated Vertical Hydraulic Conductivity
Layer 2
(ft/day)

- 0.01 - 9
- 10 - 19
- 20 - 28
- 29 - 37
- 38 - 46
- 47 - 56
- 57 - 65
- 66 - 74
- 75 - 84
- 85 - 93

Borehole with Lithologic Data used to Estimate Vertical Hydraulic Conductivity

Chino Valley Basins Groundwater Flow Model Boundary

Streams & Flood Control Channels

Flood Control & Conservation Basins

Geology

Water-Bearing Sediments

Quaternary Alluvium

Consolidated Bedrock

Undifferentiated Pre-Tertiary to Early Pleistocene Igneous, Metamorphic, and Sedimentary Rocks

Fault (solid where accurately located; dashed where approximately located or inferred; dotted where concealed)

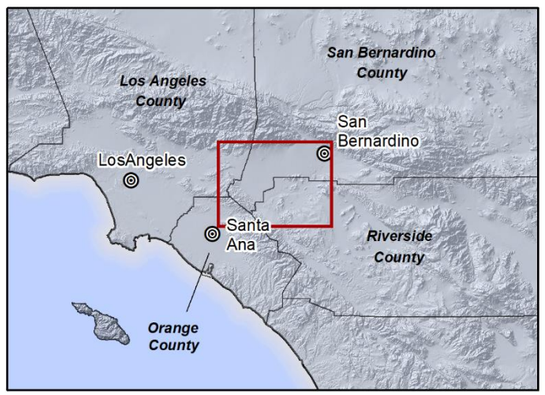

Produced by:

WEI
Wildermuth Environmental, Inc.

Author: MAB
Date: 4/29/2020
Document Name: Figure_2-12b_20200120_L2Kv

0 1 2 3 4 5 Miles
0 2 4 6 8 KM

Prepared for:

2020 Safe Yield Recalculation

Chino Basin Watermaster
Partners in Basin Management

Layer 2 Initial and Pre-calibrated Vertical Hydraulic Conductivity Based on Borehole Lithology and Lithologic Modeling

Figure 2-12b

117°40'0"W

117°20'0"W

34°0'0"N

San Gabriel Mountains

Cucamonga Fault Zone

West Cucamonga Barrier

Red Hill-Etiwanda Avenue Fault

Barrier J

Rialto-Colton Basin

Loma Linda Fault

Indian Hill Fault

Indian Hill

Intermediate Fault

San Jose Fault

San Jose Hills

Foothill Blvd

Archibald Ave

Haven Ave

Day Ck

Etiwanda Ave

San Sevaine Ck

Riverside Ave

Waterman Ave

Rialto-Colton Fault

San Jacinto Fault

Bloomington Divide

Holt Blvd

San Antonio Ck

Euclid Ave

Central Ave

Central Ave Fault

Mission Blvd

Cucamonga Ck

Riverside Dr

Jurupa Mountains

Barton

San Bernardino County

Riverside County

Puente Hills

Riley Barrier

Bellegrave Ave

Limonite Ave

Mission Blvd

Santa Ana River

Riverside Basins

Chino Ck

Chino Fault

Chino Hills

San Bernardino County

Orange County

La Sierra Hills

Van Buren Blvd

Victoria Ave

Arlington Basin

El Sobrante de San Jacinto

Cajalco Rd

Aless

15

210

215

10

71

60

91

0 1 2 3 4 5 Miles

0 2 4 6 8 KM

Initial Estimated Vertical Hydraulic Conductivity
Layer 3
(ft/day)

- 0.01 - 17
- 18 - 34
- 35 - 51
- 52 - 68
- 69 - 85
- 86 - 102
- 103 - 119
- 120 - 136
- 137 - 153
- 154 - 170

Borehole with Lithologic Data used to Estimate Vertical Hydraulic Conductivity

Chino Valley Basins Groundwater Flow Model Boundary

Streams & Flood Control Channels

Flood Control & Conservation Basins

Geology

Water-Bearing Sediments

Quaternary Alluvium

Consolidated Bedrock

Undifferentiated Pre-Tertiary to Early Pleistocene Igneous, Metamorphic, and Sedimentary Rocks

Fault (solid where accurately located; dashed where approximately located or inferred; dotted where concealed)

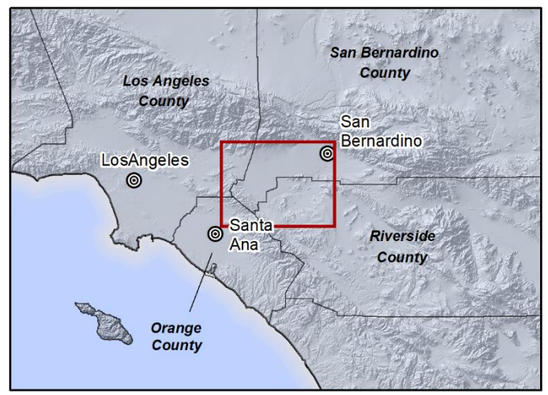

Produced by:

WEI
Wildermuth Environmental, Inc.

Author: MAB
Date: 4/29/2020
Document Name: Figure_2-12c_20200120_L3Kv

Prepared for:

2020 Safe Yield Recalculation

Chino Basin Watermaster
Partners in Basin Management

Layer 3 Initial and Pre-calibrated Vertical Hydraulic Conductivity Based on Borehole Lithology and Lithologic Modeling

Figure 2-12c

117°40'0"W

117°20'0"W

34°0'0"N

San Gabriel Mountains

Cucamonga Fault Zone

West Cucamonga Barrier

Red Hill-Etiwanda Avenue Fault

Barrier J

Rialto-Colton Basin

Loma Linda Fault

Indian Hill Fault

Indian Hill

Intermediate Fault

San Jose Fault

San Jose Hills

San Antonio Ck

Archibald Ave

Haven Ave

Day Ck

Etiwanda Ave

San Sevaine Ck

Foothill Blvd

Riverside Ave

Waterman Ave

Rialto-Colton Fault

San Jacinto Fault

Bloomington Divide

Holt Blvd

Euclid Ave

Central Ave

Central Ave Fault

Mission Blvd

Cucamonga Ck

Riverside Dr

Jurupa Mountains

San Bernardino County

Riverside County

Barton

Puente Hills

Riley Barrier

Bellegrave Ave

Limonite Ave

Mission Blvd

River

Santa Ana

Riverside Basins

Chino Ck

Chino Fault

Chino Hills

San Bernardino County

Orange County

La Sierra Hills

Van Buren Blvd

Victoria Ave

Arlington Basin

El Sobrante de San Jacinto

Cajalco Rd

Aless

15

210

215

10

71

60

91

117°40'0"W

117°20'0"W

34°0'0"N

Initial Estimated Vertical Hydraulic Conductivity
Layer 4
(ft/day)

- 0.01 - 17
- 18 - 34
- 35 - 51
- 52 - 68
- 69 - 85
- 86 - 102
- 103 - 119
- 120 - 136
- 137 - 153
- 154 - 170

Borehole with Lithologic Data used to Estimate Vertical Hydraulic Conductivity

Chino Valley Basins Groundwater Flow Model Boundary

Streams & Flood Control Channels

Flood Control & Conservation Basins

Geology

Water-Bearing Sediments

Quaternary Alluvium

Consolidated Bedrock

Undifferentiated Pre-Tertiary to Early Pleistocene Igneous, Metamorphic, and Sedimentary Rocks

Fault (solid where accurately located; dashed where approximately located or inferred; dotted where concealed)

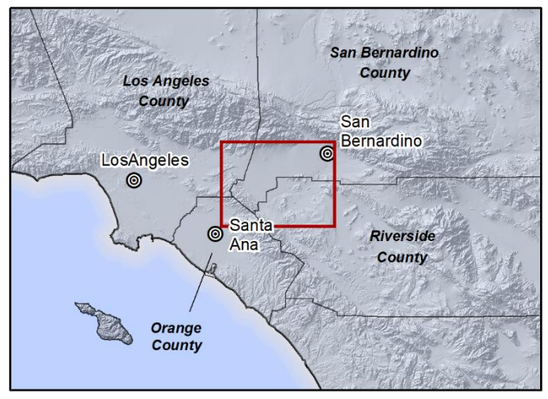

Produced by:

WEI
Wildermuth Environmental, Inc.

Author: MAB
Date: 4/29/2020
Document Name: Figure_2-12d_20200120_L4Kv

0 1 2 3 4 5 Miles
0 2 4 6 8 KM

Prepared for:

2020 Safe Yield Recalculation

Chino Basin Watermaster
Partners in Basin Management

Layer 4 Initial and Pre-calibrated Vertical Hydraulic Conductivity Based on Borehole Lithology and Lithologic Modeling

Figure 2-12d

117°40'0"W

117°20'0"W

34°0'0"N

San Gabriel Mountains

Cucamonga Fault Zone

West Cucamonga Barrier

Red Hill-Etiwanda Avenue Fault

Barrier J

Rialto-Colton Basin

Loma Linda Fault

Indian Hill Fault

Indian Hill

Intermediate Fault

San Jose Fault

San Jose Hills

San Antonio Ck

Foothill Blvd

Archibald Ave

Haven Ave

Day Ck

Etiwanda Ave

San Sevaine Ck

Riverside Ave

Waterman Ave

Rialto-Colton Fault

San Jacinto Fault

Bloomington Divide

Holt Blvd

Euclid Ave

Central Ave

Central Ave Fault

Mission Blvd

Cucamonga Ck

Riverside Dr

Jurupa Mountains

Barton

San Bernardino County

Riverside County

Puente Hills

Riley Barrier

Bellegrave Ave

Limonite Ave

Mission Blvd

Santa Ana River

Riverside Basins

Chino Ck

Chino Fault

Chino Hills

San Bernardino County

Orange County

La Sierra Hills

Van Buren Blvd

Victoria Ave

Arlington Basin

El Sobrante de San Jacinto

Cajalco Rd

15

210

71

60

91

215

10

0 1 2 3 4 5 Miles

0 2 4 6 8 KM

Initial Estimated Vertical Hydraulic Conductivity
Layer 5
(ft/day)

- 0.01 - 16
- 17 - 32
- 33 - 47
- 48 - 63
- 64 - 79
- 80 - 94
- 95 - 110
- 111 - 126
- 127 - 142
- 143 - 157

Borehole with Lithologic Data used to Estimate Vertical Hydraulic Conductivity

Chino Valley Basins Groundwater Flow Model Boundary

Streams & Flood Control Channels

Flood Control & Conservation Basins

Geology

Water-Bearing Sediments

Quaternary Alluvium

Consolidated Bedrock

Undifferentiated Pre-Tertiary to Early Pleistocene Igneous, Metamorphic, and Sedimentary Rocks

Fault (solid where accurately located; dashed where approximately located or inferred; dotted where concealed)

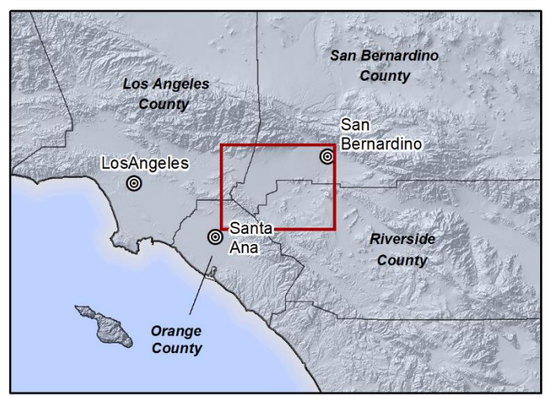

Produced by:

WEI
WILDERMUTH ENVIRONMENTAL, INC.

Author: MAB
Date: 4/29/2020
Document Name: Figure_2-12e_20200120_L5Kv

Prepared for:

2020 Safe Yield Recalculation

CHINO BASIN WATERMASTER
Partners in Basin Management

Layer 5 Initial and Pre-calibrated Vertical Hydraulic Conductivity Based on Borehole Lithology and Lithologic Modeling

Figure 2-12e

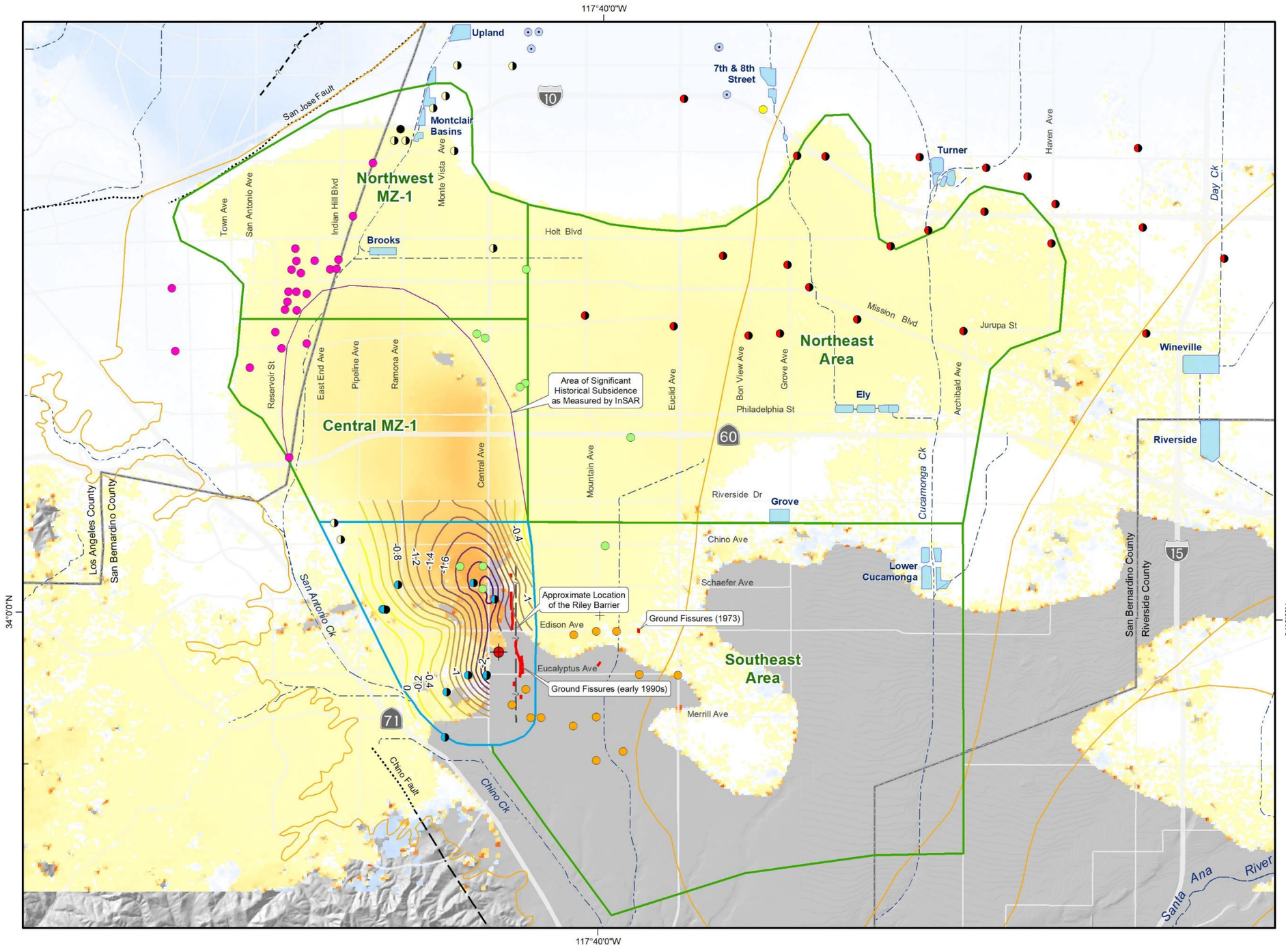

Contours of Relative Change in Land Surface Elevation as Estimated by Leveling Surveys 1987 to 1999

0.0 ft

-2.2 ft

Relative Change in Land Surface Elevation as Measured by InSAR Oct-1993 to Dec-1995

+ 1 ft

0

- 1 ft

InSAR absent or incoherent

OBMP Management Zones

- Ayala Park Extensometer Facility
- Managed Area
- Areas of Subsidence Concern
- Flood Control and Conservation Basins

Active Pumping Wells by Owner - 1987 to 1999

- California Institution for Men
- City of Chino
- City of Chino Hills
- City of Ontario
- City of Pomona
- City of Upland
- Golden State Water Company
- Monte Vista Water District
- San Antonio Water Company

Fault (solid where accurately located; dashed where approximately located or inferred; dotted where concealed)

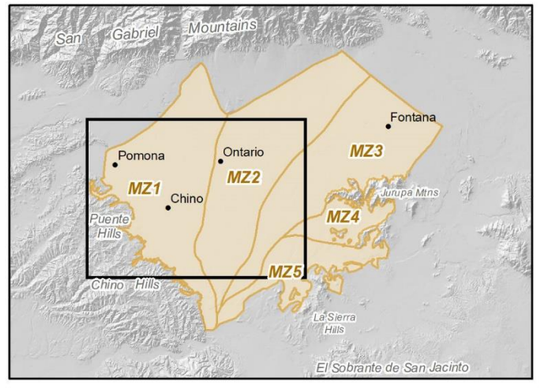

Produced by:

WEI
Wildermuth Environmental, Inc.

Author: NWS
Date: 1/22/2020
Document Name: Figure_2-13_20200115_Subsidence

0 1 2 Miles

0 1 2 KM

Prepared for:

2020 Safe Yield Recalculation

Chino Basin Watermaster
Partners in Basin Management

Historical Land Surface Deformation in Management Zone 1
1987-1999

Figure 2-13

117°40'0"W

34°0'0"N

Author: NWS Date: 1/22/2020 Document Name: Figure_2-14_20200115_Subsidence_v2

Relative Change in Land Surface Elevation
as Estimated by InSAR
(March 2011 to March 2019)

+ 0.25 ft

0 ft

- 0.25 ft

InSAR absent or incoherent

Average Annual Groundwater Pumping
April 1, 2011 to March 31, 2019
(afy)

0 - 100

100 - 500

500 - 1,000

1,000 - 2,000

>2,000

Average Annual Basin Recharge
FY 2011 to FY 2018
(afy)

0

<1,000

1,000 - 2,500

2,500 - 5,000

Managed Area

Areas of Subsidence Concern

Historical Ground Fissures

Approximate Location of the Riley Barrier

Fault (solid where accurately located; dashed where approximately located or inferred; dotted where concealed)

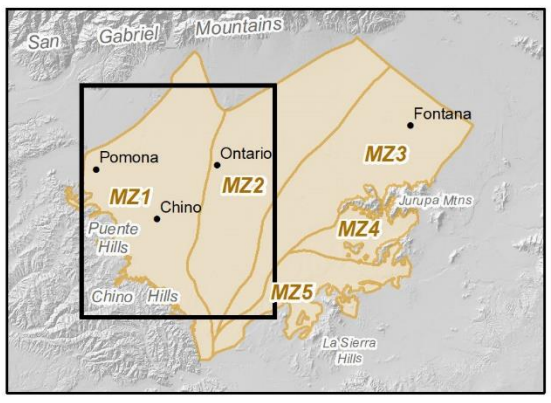

WEI
Wildermuth Environmental, Inc.

0 1 2 Miles

0 1 2 Kilometers

2020 Safe Yield Recalculation

Vertical Ground Motion across the Western Chino Basin
2011/19

Figure 2-14

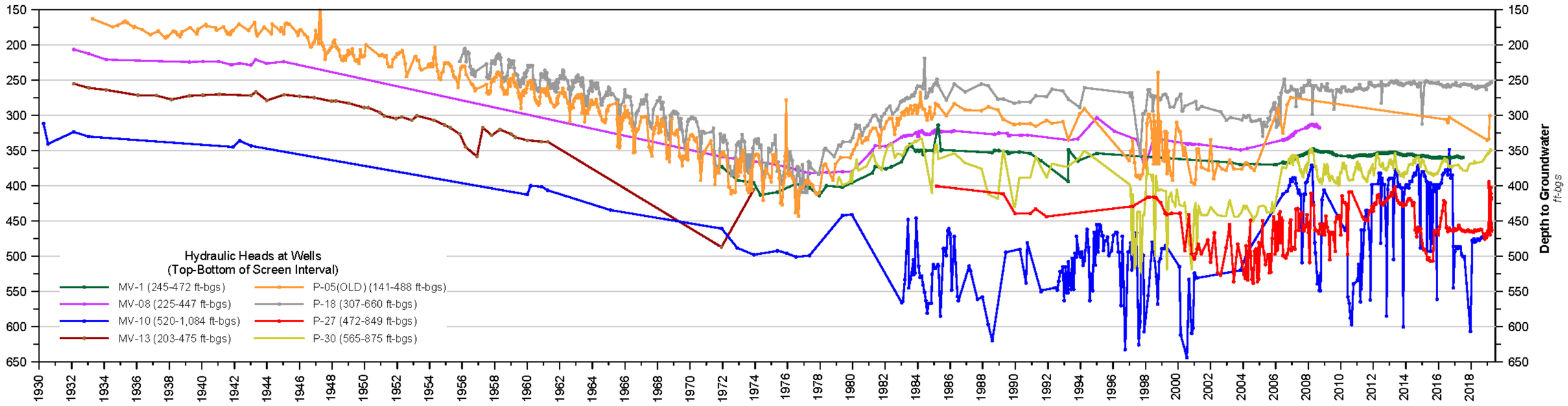

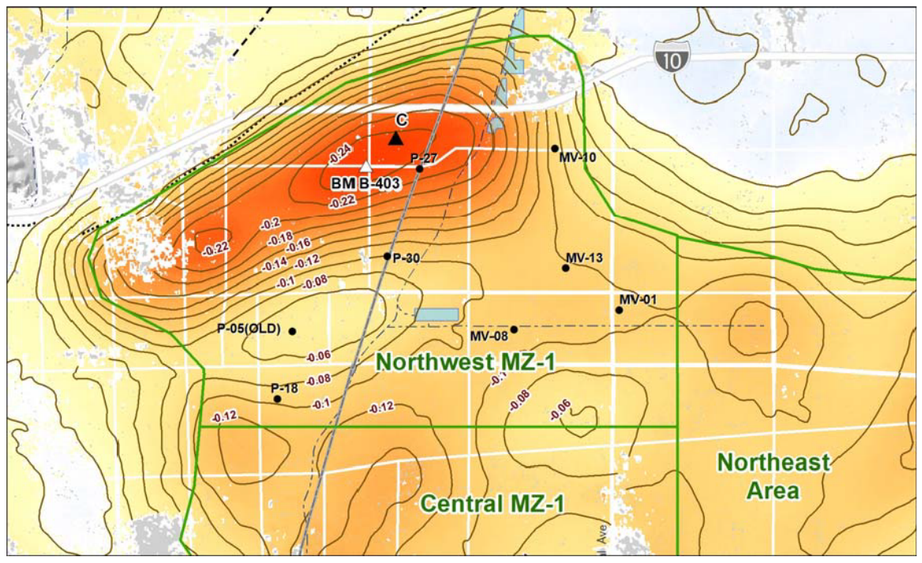

InSAR from March 2011 to March 2019

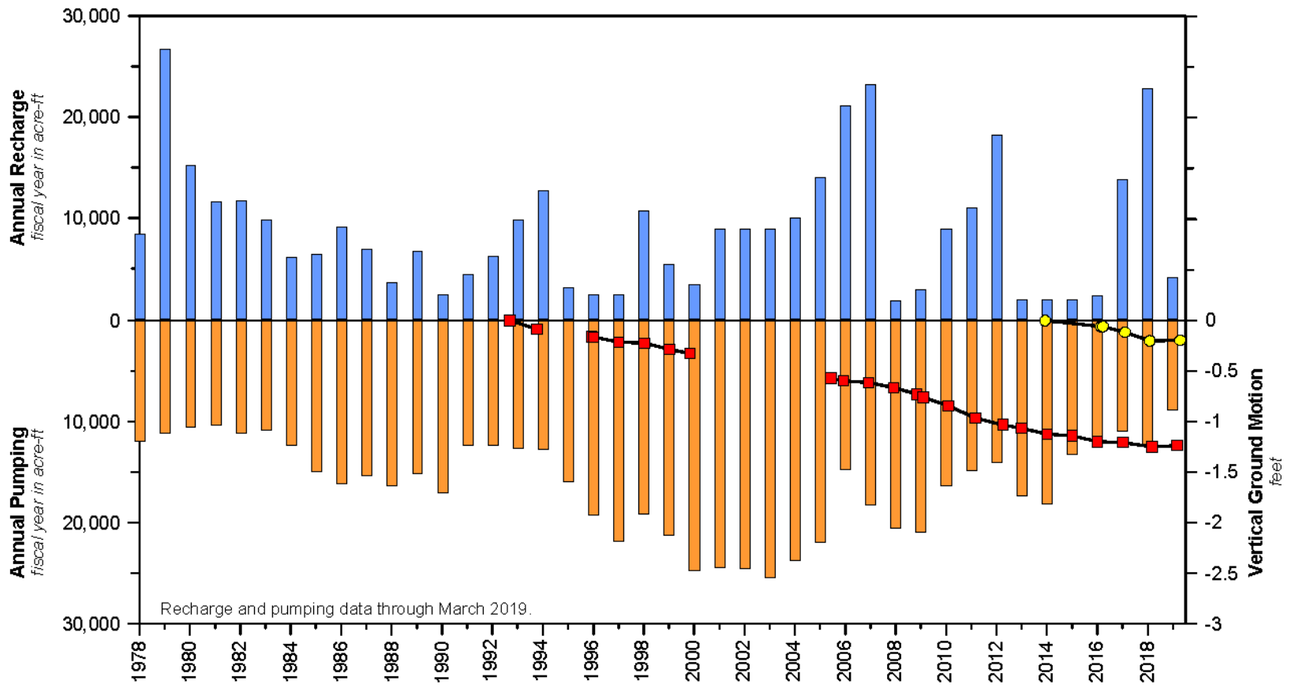

Vertical Ground-Motion
(Cumulative Displacement)
- BM B-403
- InSAR at Point C

Recharge and Pumping

Recharge of Recycled Water, Storm-water,* and Imported Water at the College Heights, Upland, Montclair, and Brooks Recharge Basins; and, at MVWD ASR Wells
*Storm-water is an estimated amount prior to fiscal year 2004/05

Groundwater Pumping from Wells in the Northwest MZ-1 Area

WEI
Wildermuth Environmental, Inc.

2020 Safe Yield Recalculation

Chino Basin Watermaster
Partners in Basin Management

History of Land Subsidence in Northwest MZ-1

Figure 2-15

3.1 Water Budget

The 2020 CVM watershed includes the Santa Ana River Watershed between the MWD crossing (USGS gage 11066460) and Prado Dam (USGS gage 11074500). Figure 3-1 shows the 2020 CVM watershed boundary and the active domain of the 2020 CVM. Water enters the 2020 CVM watershed in the form of precipitation, surface water inflows that originate from outside the watershed including the Santa Ana River and Temescal Wash gaged inflows, imported water and as subsurface inflows on the east side of the 2020 CVM Watershed. Water leaves the watershed through surface water outflow at Prado Dam, evapotranspiration, and export from the watershed.

As stated in Section 1, the primary objectives of this investigation are to calculate the Safe Yield of the Chino Basin and to provide Watermaster with updated planning and analysis tools to continue its administration of the Judgment, OBMP implementation and regulatory compliance demonstrations. This section introduces the water budget concept as the primary tool to estimate Safe Yield and the data used with computational tools to prepare the water budget.

> "A water budget takes into account the storage and movement of water between the four physical systems of the hydrologic cycle, the atmospheric system, the land surface system, the river and stream system, and the groundwater system. A water budget is a foundational tool used to compile water inflows (supplies) and outflows (demands). It is an accounting of the total groundwater and surface water entering and leaving a basin or user-defined area. The difference between inflows and outflows is a change in the amount of water stored." (DWR, 2016)

Water budgets are a fundamental tool for the sustainable management of groundwater. Figure 3-2 illustrates the recharge and discharge components included in the water budget. All the hydrologic components included in Figure 3-2 were considered in this investigation. The four physical systems shown in Figure 3-2 are represented in the 2020 CVM. The atmospheric and surface water systems include hydrologic processes that receive precipitation and imported water into the 2020 CVM watershed, produce streamflow and recharge in the 2020 CVM and outflow from it. The vadose and saturated zones included in the groundwater system.

The term *recharge component* is used to describe an inflow to the basin and *discharge component* is used to describe an outflow from the basin. Recharge components consist of subsurface boundary inflows; streambed recharge; the MAR of storm, imported, and recycled waters; and areal recharge. Areal recharge consists of the deep infiltration of precipitation and applied water and onsite wastewater disposal systems (septic tank leach fields and cesspools; collectively DIPAW). Discharge components consist of subsurface outflows, groundwater pumping, evapotranspiration and rising groundwater discharge to streams.

Table 3-1 lists the recharge and discharge components of the water budget applicable to this investigation and compares them to their calculation methods and the data required by those methods. The methods include the direct use of observed data, numerical models, or the combined use of data and models. The models are described in Section 4, the model's precise uses are described in Section 5 and the model results are described in Sections 6 and 7.

3.1.1 Data and Methods for Estimation of Recharge Components

3.1.1.1 Subsurface Inflow from Adjacent Groundwater Basins

Subsurface inflow to the active 2020 CVM domain occurs from the Riverside Basin through the Bloomington divide, located in the eastern-most part of the active 2020 CVM domain (see Figure 2-1). Subsurface outflow from the active 2020 CVM domain to the Puente Basin occurs from the Spadra Basin located in the westernmost part of the active 2020 CVM domain (see Figure 2-1).

For the calibration period, these subsurface flows were computed by the 2020 CVM based on historical time series of groundwater elevations at wells located in or just outside the 2020 CVM domain on these boundaries and calibrated hydraulic conductivities in the 2020 CVM adjacent to these boundaries. For planning scenarios, the subsurface inflow from the Riverside Basin was assumed equal to be the average subsurface inflow from the last five years from the calibration period, and the subsurface outflow from the Spadra Basin was assumed equal to be the average subsurface outflow from the last five years from the calibration period.

For calibration and planning scenarios, subsurface inflow from the Rialto Basin was assumed to be 1,480 afy, which is equal the value used in the calibration and planning scenarios of the 2013 Chino Basin model.

For calibration and planning scenarios, the subsurface inflow from the Arlington Basin to the Temescal Basin was assumed to the 810 afy, based on the development and application of the Arlington Basin Model (WEI, 2009), which is equal to the value used in the calibration and planning scenarios of the 2013 Chino Basin model.

3.1.1.2 Subsurface Inflow from Adjacent Hills and Mountains, MAR of Stormwater

The HSPF and R4 watershed models were used to estimate surface water discharge from precipitation throughout the 2020 CVM watershed and the DIPAW from the soil (root) zone. The model-estimated DIPAW for watersheds that are tributary to and not overlying the groundwater basins was assumed to be the subsurface inflow from these areas to the 2020 CVM proximate to the discharge point of the watershed to the groundwater basin. Surface water discharges estimated by these models were routed through the stream systems that overlie the active 2020 CVM domain and these models were used to estimate stormwater recharge proximate the streams. The data requirements of these models include the following: land use and associated properties (imperviousness, irrigation practices), hydrologic soil type, topography, surface water drainage system (channel alignment, hydraulic properties and operating scheme), surface water discharge measurements (boundary inflows and for calibration), precipitation, and ET and evaporation.

3.1.1.3 Streambed Recharge in the Santa Ana River and its Lower Tributaries

The MODFLOW NWT model is the groundwater model used to estimate the Chino Valley groundwater system response to historical and projected recharge and discharge stresses. The model estimated responses include groundwater levels, riparian vegetation ET and surface water flow in the Santa Ana River and its lower tributaries. Lower tributaries refer to unlined streams tributary and adjacent to the Santa Ana River. In calculating surface water discharge, the model estimates stream recharge in losing reaches and rising groundwater in gaining reaches. The measured surface water discharges tributary to the Santa Ana River and the lower tributaries include boundary inflow estimates for the Santa Ana River measured at MWD crossing (USGS gage 11066460), Temescal Wash (USGS gage 11072000), and

wastewater discharges to the Santa Ana River and its tributaries. R4/HSPF estimated stormwater discharge to the lower tributaries. Measured surface water discharges at below Prado Dam (USGS gage 11074500) were used for 2020 CVM calibration.

3.1.1.4 MAR

MAR of stormwater occurs in flood control and conservation basins and was estimated with the R4 /HSPF models for 1978 through 2004 and in the planning scenarios and is therefore dependent on the same data as the R4 and HSPF models described above. MAR of stormwater for 2005 through 2018 is based on estimates provided by IEUA. MAR of recycled and imported water are measured values in the calibration period and planning estimates in the planning scenarios.

3.1.2 Data and Methods for Estimating the Discharge Components

3.1.2.1 Groundwater Pumping

Overlying agricultural groundwater pumping was estimated: by the R4 model for the period 1978 through 2004 and in the planning scenarios and is therefore dependent on the same data as the R4; and with pumping estimates provided by the Chino Basin Watermaster that relies on meters install at some wells and water duty method for the other wells. Groundwater pumping by municipal and industrial users was measured data reported by the individual M&I entities for calibration and planning estimates provided by the individual M&I entities for planning scenarios.

3.1.2.2 ET

ET was estimated with the MODFLOW NWT model, and it depends in part on model-estimated groundwater levels, the location of the riparian vegetation, and the ET characteristics used by the model in its ET calculations. In the calibration period, the riparian area delineation varies and is based on historical aerial photographs and prior investigations (WEI, 2015; 2018). For the planning scenarios, the riparian areas were assumed constant—the same as the 2018 delineation.

3.1.2.3 Groundwater Discharge to the Santa Ana River and its Lower Tributaries

Groundwater discharge to the Santa Ana River and lower tributaries was estimated with the MODFLOW NWT model in the process described above for streambed recharge in the Santa Ana River and its lower tributaries.

3.2 Description of the Hydrologic Data Used in this investigation

The major data types required for this investigation—described below—include: land use, soils, drainage, precipitation, ET and evaporation, tributary and non-tributary surface water discharges, MAR, and model-specific hydrologic process parameters.[8] Adjustments to precipitation, ET and surface water boundary inflows due to climate change are discussed in Section 7. Figure 3-3 shows the watersheds for the major stream systems in the 2020 CVM watershed and USGS gaging stations.

[8] The R4 code and R4 model-specific hydrologic process parameters can be accessed here: https://github.com/weiwater/R4 and https://github.com/weiwater/WLAM, respectively.

3.2.1 Land Use, Irrigation Practices and Imperviousness

Land use and the activities that occur on land influence the amount of precipitation that contributes to surface water discharge and the amount of precipitation that can infiltrate and become groundwater. Figures 3-4a through 3-4c illustrate general land use types in the 2020 CVM watershed for 1975, 2017, and 2040, respectively, corresponding to the land uses that occurred at the beginning and end of the calibration period (1975 and 2017, respectively) and the beginning and of the planning period through assumed buildout (2017 and 2040, respectively). Land use maps for the period of 1949 through 2040 are included in Appendix B. Table 3-2 summarizes the land use time history in the Chino Basin and similar tables are included in Appendix B for the other 2020 CVM basins. These data were obtained from the Department of Water Resources, San Bernardino County, and the Southern California Association of Governments. Table 3-3 lists, by land use in the Chino Basin, the assumed imperviousness, crop ET, and irrigation efficiencies used in this investigation. Figure 3-5 graphically shows the land use transition and projected imperviousness for the Chino Basin; similar charts are included in Appendix B for the other 2020 CVM basins. Inspection of the land use time histories each of these basins shows the gradual transition from agricultural and native uses to urban uses and the associated increase in imperviousness. The total imperviousness of the Chino Basin is estimated to have increased from 18 percent in 1975 to about 56 percent in 2017 and is projected to reach about 60 percent by 2030. The hydrologic implications of this land use transition are significant as demonstrated in Sections 6 and 7.

3.2.2 Hydrologic Soil Type

The Natural Resources Conservation Service (NRCS) has compiled comprehensive soil surveys for the entire United States and has developed hydrologic tools to simulate hydrologic processes based on these soil surveys. Figure 3-6 shows the spatial distribution of the NRCS hydrologic soil groups within 2020 CVM watershed.[9] The soil texture, runoff and infiltration characteristics of these hydrologic soil groups are described below:

- Group A – consists of sand, loamy sand or sandy loam types of soils. It has low runoff potential and high infiltration rates even when thoroughly wetted. They consist chiefly of deep, well to excessively drained sands or gravels and have a high rate of water transmission.
- Group B – consists of silt loam or loam types of soils. It has a moderate infiltration rate when thoroughly wetted and consists chiefly of moderately deep to deep, moderately well to well drained soils with moderately fine to moderately coarse textures.
- Group C – consists of sandy clay loam. They have low infiltration rates when thoroughly wetted and consist chiefly of soils with a layer that impedes downward movement of water and soils with moderately fine to fine structure.
- Group D – consists of clay loam, silty clay loam, sandy clay, silty clay, or clay types of soils. This hydrologic soil group has the highest runoff potential.

Hydrologic soil group, land use, and other data are used in the R4 model to estimate how much precipitation becomes runoff and how much infiltrates into the soil.

3.2.3 Surface Water Drainage Systems

Streams originating in the San Gabriel Mountains flow southwestward towards the San Gabriel watershed or southward to the Santa Ana River. While in the mountains these stream channels are naturally occurring until they approach the valley floor where they transform to engineered systems that

[9] The hydrologic soils groups developed by the NRCS can be accessed here: https://www.nrcs.usda.gov/wps/portal/nrcs/detail/soils/survey/office/ssr12/tr/?cid=nrcs144p2_027279

include dams and debris basins with outlet controls, improved channels, diversion structures and flood control and conservation basins.

Prior to the implementation of the OBMP in 2000, and in response to rapid urbanization, the Los Angeles County Flood Control District (LACFCD), San Bernardino County Flood Control District (SBCFCD), and the US Army Corps of Engineers (USACE) constructed flood control projects that efficiently captured and conveyed stormwater to the San Gabriel and Santa Ana Rivers to reduce potential flooding, effectively eliminating the groundwater recharge that formerly took place in the unimproved stream channels and flood plains. These flood control projects included concrete lining of major drainages and the construction of retention basins to temporarily store stormwater and release it in 24 hours or less. Some provisions were made to mitigate the loss of recharge from these flood control projects at that time, but these provisions failed to achieve the groundwater recharge that took place prior to the construction of these flood control projects. Figure 3-7 shows the locations of the major channels that drain the Chino Basin area and their concrete lining time history.

The routing of surface water discharge through natural and engineered channel systems was simulated with the R4 model (described in Section 4 and elsewhere) to estimate surface discharge and recharge throughout the 2020 CVM domain. As-built drawings were obtained and field surveys were conducted in prior investigations (WEI, 1998; 2013; 2018) to develop subwatershed boundaries, channel and flood control and conservation basin geometry and facility operating schemes for use in HSPF and R4 surface water simulations.

3.2.4 Surface Water Discharge Measurements

Tributary discharges refer to surface water entering the 2020 CVM watershed as measured at the Santa Ana River at the MWD crossing and the Temescal Wash entering the watershed in Corona. Daily discharge estimates were obtained from the USGS through the USGS National Water Information System.[10] Non-tributary discharges include discharges from imported water pipelines and wastewater treatment plants to stream channels in the 2020 CVM watershed. Figure 3-8 shows the locations of USGS streamflow gages, wastewater treatment plants and their points of discharge, imported water pipelines, and surface water treatment plants. Table 3-4 lists these discharge points, their types, recording periods. With the exception of imported water discharged to the stream system for conveyance to Orange County, all imported water discharged to the stream system is diverted and recharged into flood control and conservation basins in the Chino Basin. Non-tributary discharge estimates of imported water were obtained from the Chino Basin Watermaster, IEUA, Six Basins Watermaster, and Santa Ana River Watermaster. Non-tributary discharge estimates by wastewater treatment plants to stream channels were obtained from the California Integrated Water Quality System,[11] annual reports of the Santa Ana River Watermaster, and the IEUA.

Figure 3-9 shows the time history of measured tributary and non-tributary inflows to the Santa Ana River for the calibration period of 1978 through 2018. The storm water discharges originating in the 2020 CVM in the reach of the Santa Ana River between the MWD Crossing and Prado Dam are not included in Figure 3-9.

[10] Stream discharge data from the National Water Information System can be accessed here: https://waterdata.usgs.gov/nwis/sw

[11] Wastewater discharge data from California Integrated Water Quality System can be accessed here: https://www.waterboards.ca.gov/ciwqs/publicreports.html#enforce

3.2.5 Precipitation

Precipitation is a primary source of water for the 2020 CVM watershed. Estimates of precipitation over the 2020 CVM model domain were developed from precipitation stations operated by the LACFCD, SBCFCD, Riverside County Flood Control and Water Conservation District, NOAA, and others, and gridded precipitation data products produced by the PRISM Climate Group and NOAA.[12] Figure 3-10 shows the locations of the precipitation stations that were used in this investigation, and Table 3-4 lists them along with their owners. Figure 3-11 shows the PRISM Climate Group and NOAA's NEXRAD grids over the 2020 CVM watershed. The monthly gridded precipitation estimates from the PRISM Climate Group were used to inform the spatial distribution of daily precipitation developed from precipitation stations for the period prior to the availability of gridded daily precipitation estimates from NEXRAD. NEXRAD estimates of daily precipitation were used starting in 2002.

Figure 3-12 shows the spatial distribution of the long-term average annual precipitation in the 2020 CVM watershed based on PRISM. The long-term average annual precipitation in the watershed ranges from 12 to 24 inches per year on the valley floor and from 24 to 42 inches per year in the San Gabriel Mountains. Figure 3-13 shows the annual precipitation time series of precipitation over the 2020 CVM watershed and the associated cumulative departure from mean (CDFM) precipitation for the period 1896 to 2018, a period of 122 years. The average precipitation over the 2020 CVM watershed ranged from a low of about 4 inches per year in 2007 to a high of 39 inches per year in 2005 and averaged about 17.5 inches per year over the calibration period. Figure 3-14 is an annual dry-period frequency duration plot that shows the precipitation frequency and return period of dry periods of various durations for the period of 1896 through 2018. The dry period of 2007 through 2016 is the driest ten-year period in the historical record. The dry period of 1999 through 2018 is the driest twenty-year period in the historical record.

Daily precipitation data were used with the HSPF and R4 models to estimate the water entering the surface water system, stormwater recharge in unlined channels and flood control and conservation basins, DIPAW and stormwater discharge to the Santa Ana River.

3.2.6 ET and Pan Evaporation

Potential ET (ET_0) is the ability of the atmosphere to remove water from the ground surface through evaporation and transpiration processes assuming no control on water supply. Actual ET is water that is actually removed from a ground surface due to the evaporation and transpiration processes. ET by naturally occurring vegetation and agricultural/urban vegetation is a significant outflow of water from the 2020 CVM watershed. ET_0 estimates near the 2020 CVM watershed were obtained from the California Irrigation Management Information System (CIMIS) stations located in Pomona and Riverside.[13] Figure 3-10 shows the locations of the CIMIS and pan evaporation stations that were used in this investigation and Table 3-5 lists them. The ET_0 estimates were used with published crop coefficients to estimate actual ET for the naturally occurring and agricultural/urban vegetation associated with the land uses in the 2020 CVM watershed. The daily ET_0 across the 2020 CVM watershed was estimated from the Pomona and Riverside CIMIS station ET_0 estimates using a spatial-temperature interpolation algorithm. Figure 3-15 shows the time history of ET_0 estimates at these CIMIS stations.

[12] Gridded data products from the PRISM Climate Group and NOAA can be accessed respectively at http://www.prism.oregonstate.edu and https://www.ncdc.noaa.gov/data-access/radar-data/nexrad.

[13] ET_0 data from the California Irrigation Management Information System can be accessed here: https://cimis.water.ca.gov

For the period prior to these CIMIS stations becoming active, ET_0 was estimated by regression relationships developed at these stations with evaporation at Puddingstone reservoir.

Pan evaporation data from a Thompson-class evaporation pan, located at Puddingstone reservoir,[14] was used in this investigation to estimate evaporation losses from surface water impounded in flood control and conservation basins. Figure 3-16 shows the time history of pan evaporation at the Puddingstone reservoir.

3.2.7 MAR Measurement

Figure 3-8 shows the locations of recharge facilities where MAR occurs in the Chino Basin. Figure 3-17 illustrates the time series of MAR in the Chino Basin. Estimates of MAR in the 2020 CVM domain were obtained from the entities that conduct recharge operations as summarized below.

- Starting in 2005, IEUA prepared estimates of stormwater captured at the major stormwater detention and recharge facilities in the Chino Basin. IEUA measures imported and recycled recharge at the recharge facilities in the Chino Basin where this recharge occurs.
- The San Antonio Water Company prepares measures imported water recharged in the Cucamonga Basin
- PVPA and Los Angeles County Flood Control District prepare stormwater recharge estimates in the Six Basins. And, the Three Valleys Municipal Water District measures imported water recharged in the Six Basins.
- The City of Corona measures wastewater recharged in the Temescal Basin.

3.2.8 Measured and Estimated Groundwater Pumping

With one exception, Groundwater pumping estimates were obtained from the all pumpers through the Chino Basin and Six Basins Watermasters, the City of Corona and the Cucamonga Valley Water District. The exception is overlying agricultural pumping in the Chino Basin which was estimated with R4 model for the period 1978 through 2004. Figure 3-18 shows the time history of groundwater pumping in the Chino Basin.

3.2.9 Groundwater Level Measurements

Groundwater level measurements were obtained from the all pumpers through the Chino Basin and Six Basins Watermasters, the City of Corona, Cucamonga Valley Water District, City of Riverside, USGS, and West Valley Water District. All these data are stored in the Chino Basin Watermaster's HydroDaVE^{sm} database system.

[14] Pan evaporation data from the LACFCD can be obtained by contacting County of Los Angeles Department of Public Works Stormwater Engineering Division P.O. Box 1460 Alhambra, CA 91802-1460 (626) 458-6120

Table 3-1 Comparison of Water Budget Terms to Determination Methods and Data Required to Estimate Them

	Water Budget Term Estimated from Direct Observation, Model or Both	Data Used in the Development of Recharge and Discharge Components								
		Land use	Hydrologic Soil Type	Surface Water Drainage System	Surface Water Discharge Measurement	Precipitation	ET and Evaporation	MAR	Groundwater Pumping	Groundwater Level Measurement
Recharge Components										
Subsurface boundary inflow from adjacent groundwater basins	Both, and prior information									◆
Subsurface boundary inflow from adjacent hills and mountains	Models	◆	◆	◆	◆	◆	◆			
Deep infiltration of precipitation and applied water	Model	◆	◆	◆	◆	◆	◆			
Streambed recharge in San Gabriel Mountain tributaries	Model	◆	◆	◆	◆	◆	◆			
Streambed recharge in the Santa Ana River and lower tributaries	Model	◆	◆	◆	◆	◆	◆			
MAR -- Stormwater	Both	◆	◆	◆	◆	◆	◆	◆		
MAR -- Recycled water	Data							◆		
MAR -- Imported water	Data							◆		
Discharge Components										
Groundwater pumping -- overlying agricultural	Both	◆	◆			◆	◆		◆	
Groundwater M&I									◆	
ET	Both	◆	◆			◆	◆			
Groundwater discharge to the Santa Ana River and lower tributaries.	Model	□				□	□			

Note. Prior information means other prior investigations

Table 3-2 Historical and Projected Land Use in the Chino Basin

(acres unless indicated otherwise)

Land Use Type	1957	1963	1975	1984	1990	1993	2000	2005	2012	2017	2020	2030	2040
Non-Irrigated Field Crops, Pasture, Fruits and Nut	3,903	695	3,312	1,337	1,051	936	738	376	299	204	198	175	160
Irrigated Field Crops, Pasture, Fruits and Nuts	35,975	33,932	26,343	18,006	14,502	14,623	9,832	6,794	5,331	4,499	5,150	4,343	3,826
Irrigated and Non-Irrigated Citrus	11,271	5,567	3,474	1,263	1,466	1,239	919	825	161	179	285	207	2
Irrigated Vineyard	13,195	21,728	14,796	9,618	3,181	2,403	932	764	486	487	50	0	0
Non-Irrigated Vineyard	232	12	31	17	188	170	140	99	80	82	75	73	73
Dairies and Feedlots	2,627	5,387	7,009	8,130	8,521	8,384	7,992	6,546	5,479	5,253	2,906	1,951	0
Medium and High Density Urban Residential	8,741	15,338	22,860	29,578	35,482	35,864	40,535	44,995	48,199	48,712	50,869	50,869	50,869
Special Impervious	1,397	1,731	3,884	5,662	6,166	6,486	8,012	8,480	10,323	10,351	10,425	10,431	10,432
Native Vegetation	54	57	268	930	143	243	236	259	790	647	202	202	202
Low Density Urban Residential	1,294	4,426	2,431	6,668	10,826	10,983	11,036	11,565	10,230	10,407	10,286	10,286	10,286
Commercial	1,682	2,976	2,897	6,904	9,104	10,033	15,970	18,867	20,490	20,838	21,610	21,268	21,268
Industrial	1,802	2,107	2,705	5,560	9,169	9,601	10,398	10,466	13,393	13,705	14,681	14,464	14,464
Undeveloped	58,725	46,262	44,876	38,893	32,531	31,877	25,652	23,531	19,545	18,574	18,166	17,675	16,814
Phreatophyte	3,433	4,110	5,028	5,649	5,012	4,478	4,471	3,990	3,977	4,890	4,891	4,891	4,891
Golf Course, Developed Parks, Schools	0	0	347	1,456	2,095	2,221	2,888	3,120	2,324	2,278	1,930	1,976	2,317
Dairy Wash Water Spray	0	0	4,010	4,497	4,842	4,739	4,520	3,419	3,080	3,080	1,706	1,110	0
Future Urban Development	0	0	0	0	0	0	0	0	0	0	842	4,401	8,729
Total	144,328	144,329	144,270	144,165	144,279	144,279	144,269	144,094	144,186	144,187	144,273	144,319	144,331
Aggregated Area by Land Use Group (acres)													
Agricultural	67,201	67,322	58,974	42,867	33,750	32,494	25,072	18,823	14,917	13,785	10,371	7,857	4,061
Urban	14,916	26,578	35,124	55,827	72,842	75,187	88,839	97,491	104,957	106,291	110,643	113,694	118,364
Undeveloped + Native Vegetation	62,211	50,429	50,172	45,471	37,686	36,598	30,359	27,780	24,311	24,111	23,259	22,767	21,906
Total	144,328	144,329	144,270	144,165	144,279	144,279	144,269	144,094	144,186	144,187	144,273	144,319	144,331
Aggregated Area by Land Use Group (percent of total)													
Agricultural	47%	47%	41%	30%	23%	23%	17%	13%	10%	10%	7%	5%	3%
Urban	10%	18%	24%	39%	50%	52%	62%	68%	73%	74%	77%	79%	82%
Undeveloped + Native Vegetation	43%	35%	35%	32%	26%	25%	21%	19%	17%	17%	16%	16%	15%
Total	100%	100%	100%	100%	100%	100%	100%	100%	100%	100%	100%	100%	100%
Aggregated imperviousness by Land Use Group													
Agricultural	1%	1%	1%	1%	0%	0%	0%	0%	0%	0%	0%	0%	0%
Urban	8%	13%	18%	28%	36%	38%	45%	50%	55%	56%	58%	60%	62%
Undeveloped + Native Vegetation	1%	1%	1%	1%	1%	1%	0%	0%	0%	0%	0%	0%	0%
Total	10%	15%	20%	30%	37%	39%	46%	51%	56%	56%	59%	60%	62%

Table 3-3 Imperviousness and Irrigation Assumptions for Land Uses in the Chino Basin

Land Use Type	Total Imperviousness (%)	Crop Evapotranspiration (ft/yr)	Crop Evapotranspiration Satisfied by Irrigation (ft/yr)	Irrigation Efficiency (%)
Non-Irrigated Field Crops, Pasture, Fruits and Nut	2	3.98	0.00	na
Irrigated Field Crops, Pasture, Fruits and Nuts	2	3.98	3.26	55 75
Irrigated and Non-Irrigated Citrus	2	2.59	2.59	60 80
Irrigated Vineyard	2	3.03	2.13	60 75
Non-Irrigated Vineyard	2	2.75	0.00	na
Dairies and Feedlots	2	0.00	0.00	na
Medium and High Density Urban Residential	75	3.10	3.10	75 75
Native Vegetation	2	0.82	0.00	na
Low Density Urban Residential	30	3.10	3.10	75 75
Commercial	90	3.10	3.10	75 75
Industrial	90	3.10	3.10	75 75
Special Impervious	95	3.10	3.10	na
Undeveloped	2	1.46	0.00	na

Table 3-4 Precipitation Stations

Station		Recording Period		Elevation (ft)	Agency
ID	Name	Start	End		
1026	Ontario Fire Station	6/1/1933	5/1/2001	986	SBCFCD
1034	Claremont Pomona College	7/15/1896	10/1/1989	1196	SBCFCD
1019AUTO	Upland - Chapel	9/10/1959	Active	1601	SBCFCD
1021AUTO	Mira Loma Space Center	11/29/1966	Active	804	SBCFCD
1067	Chino Substation - Edison	10/15/1926	10/1/1983	670	SBCFCD
1079	Chino - Imbach	6/15/1928	10/1/1987	642	SBCFCD
1085	San Antonio Heights C.D.F.	6/15/1943	Active	1901	SBCFCD
1175	Alta Loma Forney	7/18/1956	6/22/1982	1865	SBCFCD
2017AUTO	Fontana 5N (Getchell)	8/8/1958	Active	1959	SBCFCD
2194	Fontana Union Water Company - Townsite	10/15/1925	Active	1289	SBCFCD
2005B	Declez	3/14/1943	11/17/1950	1115	SBCFCD
2037AUTO	Lytle Creek Ranger Station	7/15/1930	Active	2730	SBCFCD
2159AUTO	Lytle Creek at Foothill Boulevard	1/23/1947	Active	1225	SBCFCD
2198	San Bernardino City - Lytle Creek	10/2/1926	Active	1225	SBCFCD
007	Arlington	1/10/1962	2/20/2000	805	RCFCD&WCD
044	Corona North	11/14/1949	Active	638	RCFCD&WCD
100	La Sierra	11/14/1954	2/20/2000	712	RCFCD&WCD
102	Lake Mathews	9/7/1958	Active	1400	RCFCD&WCD
177	Riverside East	11/6/1924	Active	986	RCFCD&WCD
178	Riverside North	9/17/1947	Active	800	RCFCD&WCD
179	Riverside South	1/10/1896	Active	840	RCFCD&WCD
250	Woodcrest	11/14/1955	5/23/1999	1557	RCFCD&WCD
265	Indian Hills	7/22/1986	Active	840	RCFCD&WCD
035	Chase & Taylor	7/1/1929	Active	1055	RCFCD&WCD
075	Temescal Canyon Wash	4/11/1905	5/16/1999	1220	RCFCD&WCD
071	Gavilan Springs	12/18/1977	2/28/1997	2050	RCFCD&WCD
067	Elsinore	8/23/1897	Active	1285	RCFCD&WCD
202	Santiago Peak	11/10/2001	Active	5638	RCFCD&WCD

Table 3-5 CIMIS and Evaporation Stations

Station		Recording Period		Elevation (ft)	Agency
ID	Name	Start	End		
78	Pomona	3/14/1989	Active	720	CIMIS
82	Claremont	4/13/1989	9/26/2007	1620	CIMIS
44	Riverside	6/2/1985	Active	1020	CIMIS
96C	Puddingstone Reservoir	9/1929	Active	1030	LACPWD

The start date of Puddingstone Reservoir is from CA DWR Bulletin No. 54-A, "Evaporation from Water Surfaces in California, Basic Data, 1948, Table 260

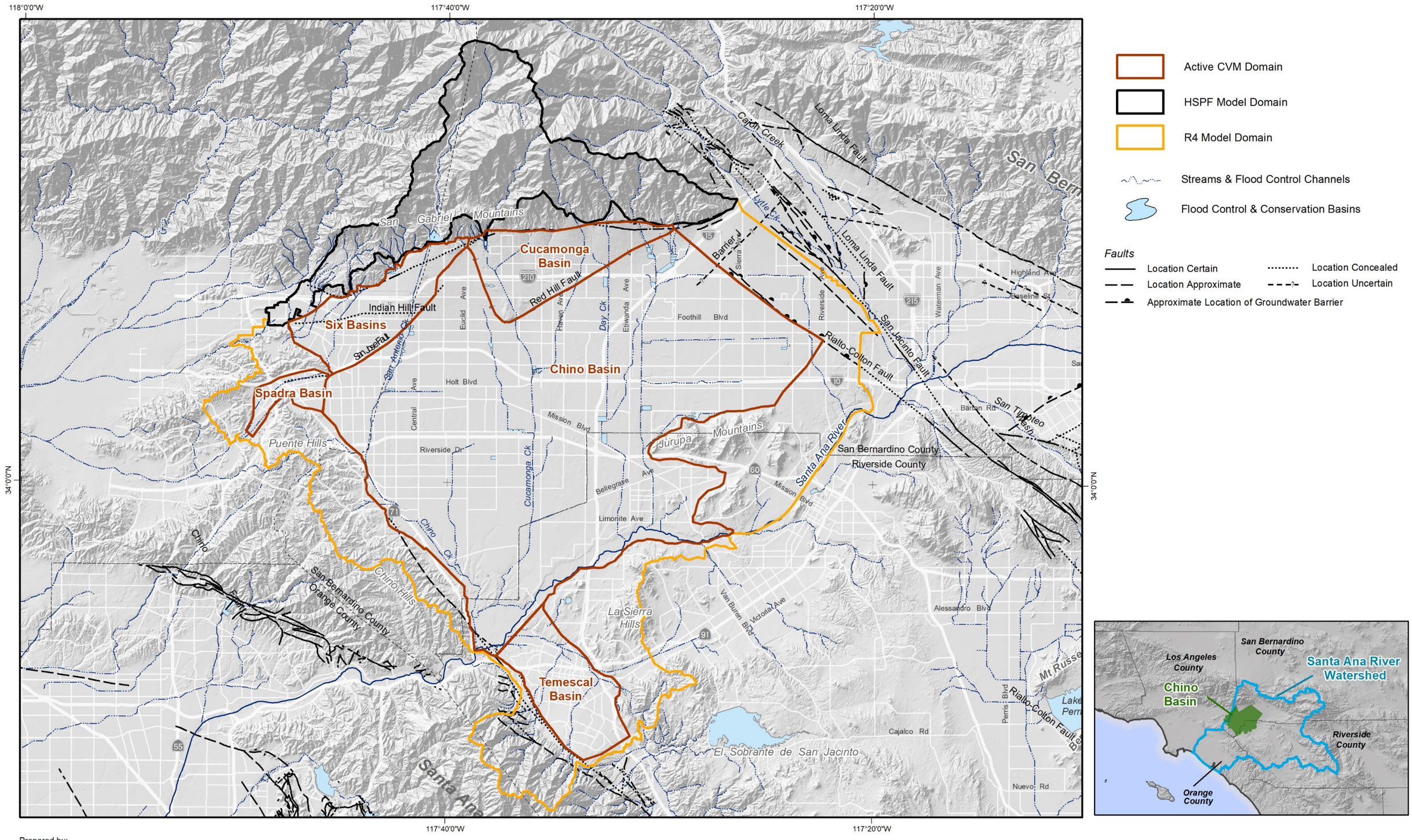

Prepared by:

WEI
Wildermuth Environmental, Inc.

Author: LS
Date: 3/21/2020
File: Figure 3-1 Surface and ground domain.mxd

0 1 2 3 4 5 Miles
0 2 4 6 8 Km

Prepared for:

2020 Safe Yield Recalculation

Chino Basin Watermaster
Partners in Basin Management

CVM Surface Water Models and Groundwater Model Domains

Figure 3-1

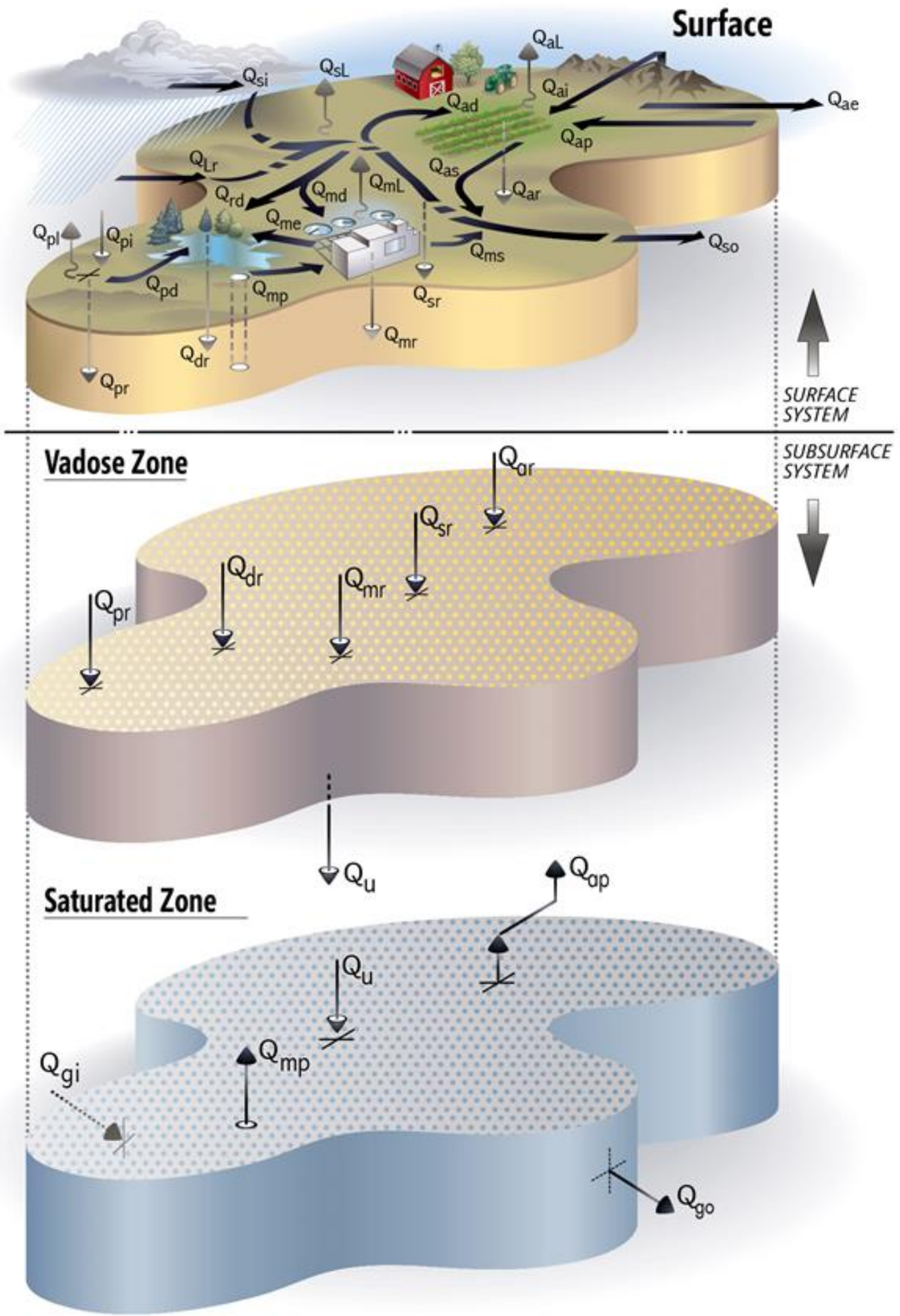

Figure 3-2 Water Budget Components

Surface Water System			Groundwater System		
Precipitation System			*Unsaturated Zone*		
Q_{pi}	=	precipitation falling on a management area	Q_{pr}	=	precipitation recharging the unsaturated zone
Q_{pL}	=	consumptive losses of precipitation	Q_{dr}	=	diversions recharging the unsaturated zone
Q_{Lr}	=	local runoff entering the stream system	Q_{sr}	=	stream flow recharging the unsaturated zone
Q_{pd}	=	local runoff diverted for recharge	Q_{mr}	=	M&I return flows recharging the unsaturated zone
Q_{pr}	=	percolation of precipitation	Q_{ar}	=	agricultural return flows recharging the unsaturated zone
			Q_{u}	=	flow leaving the unsaturated zone
Stream System					
Q_{si}	=	stream flow entering a management area			
Q_{Lr}	=	local runoff from the precipitation			
Q_{rd}	=	stream flow diverted for artificial recharge			
Q_{md}	=	stream flow diverted for M&I use	*Saturated Zone*		
Q_{ad}	=	stream flow diverted for agriculture use	Q_{gi}	=	groundwater inflow to the saturated zone
Q_{sL}	=	consumptive losses of stream flow	Q_{u}	=	flow entering the saturated zone from the unsaturated zone
Q_{ms}	=	M&I return waters entering the stream system	Q_{go}	=	groundwater outflow from the saturated zone
Q_{as}	=	agricultural return waters entering the stream system	Q_{mp}	=	water pumped for M&I use
Q_{so}	=	stream flow leaving a management area	Q_{ap}	=	water pumped for agricultural use
Q_{sr}	=	stream flow recharging the groundwater system			
Recharge System					
Q_{rd}	=	stream flow diverted for artificial recharge			
Q_{pd}	=	local runoff diverted for artificial recharge			
Q_{dr}	=	total diversions for artificial recharge			
M&I Water Use System					
Q_{md}	=	stream flow diverted for M&I use			
Q_{mp}	=	groundwater pumped for M&I use			
Q_{mi}	=	water imported for M&I use			
Q_{mL}	=	consumptive losses during M&I use			
Q_{ms}	=	M&I return waters discharged to the stream system			
Q_{me}	=	M&I waters exported to other management areas			
Q_{mr}	=	M&I return waters recharging the groundwater system			
Agricultural Water Use System					
Q_{ad}	=	stream flow diverted for agricultural use			
Q_{ap}	=	groundwater pumped for agricultural use			
Q_{ai}	=	water imported for agricultural use			
Q_{aL}	=	consumptive losses during agricultural use			
Q_{as}	=	agricultural return flows discharged to the stream system			
Q_{ae}	=	agricultural waters exported to other management			
Q_{ar}	=	agricultural waters recharging the groundwater system			

WEI
Wildermuth Environmental, Inc.

118°0'0"W
117°40'0"W
117°20'0"W
34°0'0"N

Cucamonga Basin
Six Basins
Chino Basin
Spadra Basin
Temescal Basin
San Gabriel Mountains
Puente Hills
Chino Hills
La Sierra Hills
Jurupa Mountains
El Sobrante de San Jacinto
Indian Hill Fault
Red Hill Fault
San Jose Fault
Chino Fault
Cajon Creek
Lytle Ck
Loma Linda Fault
Barrier J
Rialto-Colton Fault
San Timoteo Wash
Santa Ana River
San Antonio Ck
Day Ck
Cucamonga Ck
Chino Ck
Foothill Blvd
Holt Blvd
Riverside Dr
Mission Blvd
Limonite Ave
Bellegrave Ave
Euclid Ave
Haven Ave
Etiwanda Ave
Central Ave
Riverside Ave
Waterman Ave
Highland Ave
Baseline St
Van Buren Blvd
Victoria Ave
Alessandro Blvd
Cajalco Rd
Nuevo Rd
Perris Blvd
San Bernardino County
Riverside County
Orange County
Mt Russ
Lak
Per

Watersheds in the Chino Valley Model

- Cucamonga Creek
- Day Creek
- Prado Basin Headlands
- San Antonio/Chino Creek
- San Gabriel Rivier
- San Sevaine Creek
- Temescal Wash

- Streamflow Gages
- Wastewater Discharge Point
- Active CVM Domain
- HSPF Model Domain
- R4 Model Domain
- Streams and Flood Control Channels
- Flood Control & Conservation Basins

Faults

- Location Certain
- Location Approximate
- Approximate Location of Groundwater Barrier
- Location Concealed
- Location Uncertain

Prepared by:

WEI
Wildermuth Environmental, Inc.

Author: LS
Date: 3/21/2020
File: Figure 3-3 WW Discharge etc.mxd

0 1 2 3 4 5 Miles
0 2 4 6 8 Km

Prepared for:

2020 Safe Yield Recalculation

Chino Basin Watermaster
Partners in Basin Management

Watershed, Streams, Wastewater Discharge Points and USGS Streamflow Gages

Figure 3-3

117°40'0"W

117°20'0"W

34°0'0"N

General Land Use Type

- Agriculture
- Dairy
- Urban
- Vacant
- Riparian Vegetation

- Active CVM Domain
- HSPF Model Domain
- R4 Model Domain
- Streams & Flood Control Channels

Prepared by:

WEI
Wildermuth Environmental, Inc.

Author: LS
Date: 3/21/2020
File: Figure 3-4a LU1975.mxd

0 1 2 3 4 5 Miles
0 2 4 6 8 Km

Prepared for:

2020 Safe Yield Recalculation

Chino Basin Watermaster
Partners in Basin Management

General Land Use 1975

Figure 3-4a

117°40'0"W

117°20'0"W

34°0'0"N

General Land Use Type

- Agriculture
- Dairy
- Urban
- Vacant
- Riparian Vegetation

- Active CVM Domain
- HSPF Model Domain
- R4 Model Domain
- Streams & Flood Control Channels

Prepared by:

WEI
Wildermuth Environmental, Inc.

Author: LS
Date: 3/21/2020
File: Figure 3-4b LU2017.mxd

0 1 2 3 4 5 Miles
0 2 4 6 8 Km

Prepared for:

2020 Safe Yield Recalculation

Chino Basin Watermaster
Partners in Basin Management

General Land Use 2017

Figure 3-4b

117°40'0"W

117°20'0"W

34°0'0"N

General Land Use Type

- Agriculture
- Dairy
- Urban
- Vacant
- Riparian Vegetation

- Active CVM Domain
- HSPF Model Domain
- R4 Model Domain
- Streams & Flood Control Channels

Prepared by:

WEI
Wildermuth Environmental, Inc.

Author: LS
Date: 3/21/2020
File: Figure 3-4c LU2040.mxd

0 1 2 3 4 5 Miles
0 2 4 6 8 Km

Prepared for:

2020 Safe Yield Recalculation

Chino Basin Watermaster
Partners in Basin Management

Projected General Land Use 2040

Figure 3-4c

Figure 3-5 Historical and Projected Land Use in the Chino Basin

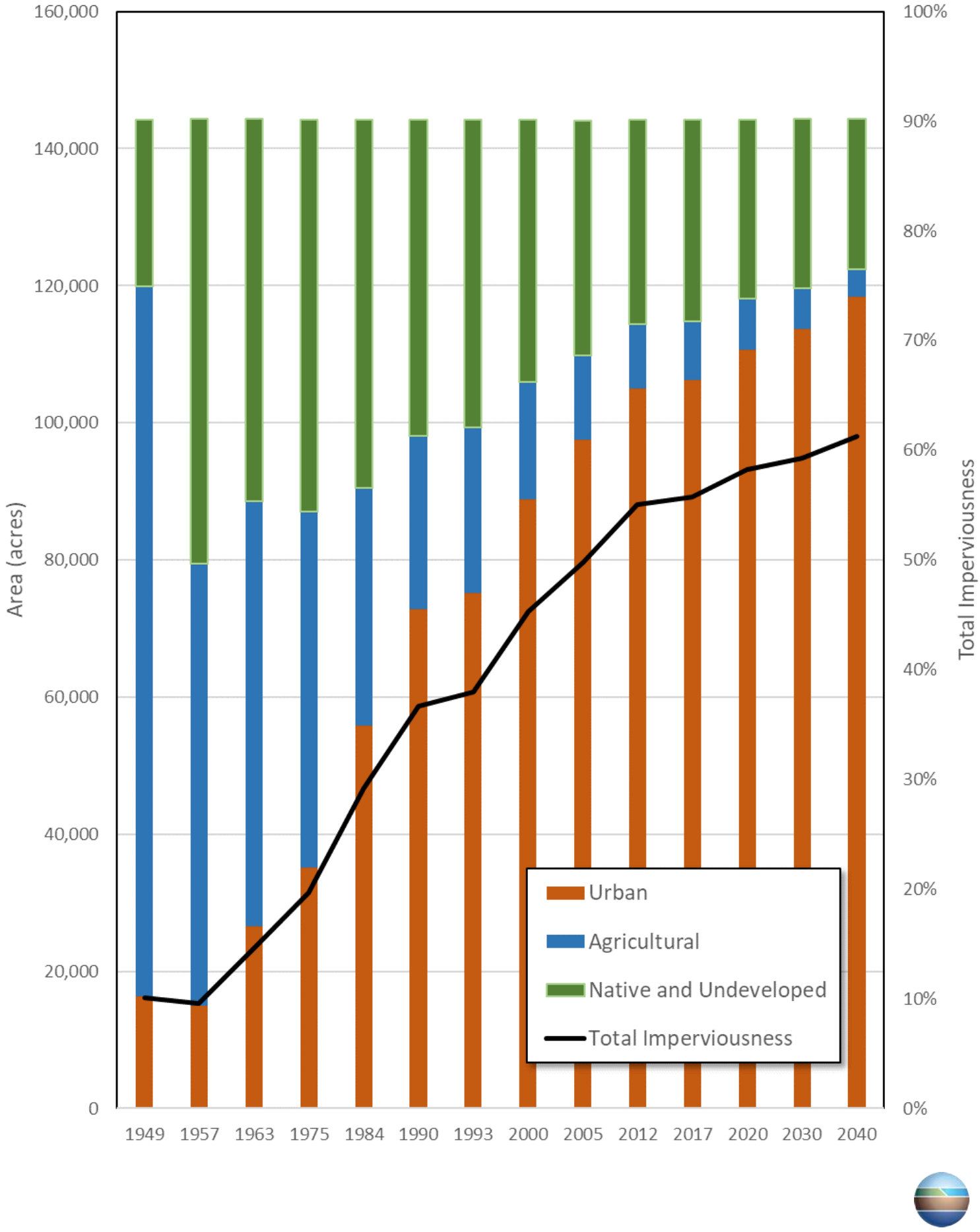

117°40'0"W
117°20'0"W
34°0'0"N

National Resource Conservation Service Hydrologic Soil Groups

- A
- B
- C
- D

- HSPF Model Domain
- R4 Model Domain
- Streams and Flood Control Channels

San Dimas Wash
Walnut Creek
Puente Creek
San Jose Creek
BREA CR
Fullerton Creek
Carbon Canyon Creek
Santiago Creek
San Antonio Creek
Chino Creek
Cucamonga Creek
West Cucamonga Creek
Deer Creek
Day Creek
San Sevaine Creek
Cypress Channel
Cucamonga Creek
West Fontana Channel
Declez Channel
Arlington Channel
Temescal Wash
Santa Ana River
Cajon Creek
Lytle Creek
East Twin Creek
Warm Creek
City Creek
San Timoteo Wash
San Bernardino County
Riverside County
Orange County

Prepared by:

WEI
WILDERMUTH ENVIRONMENTAL, INC.

Author: LS
Date: 1/23/2020
File: Figure 3-6.mxd

0 1 2 3 4 5 Miles
0 2 4 6 8 Km

Prepared for:

2020 Safe Yield Recalculation

CHINO BASIN WATERMASTER
Partners in Basin Management

National Resource Conservation Service Hydrologic Soil Groups

Figure 3-6

Periods in Which Channels were Concrete Lined

- 1950-1959
- 1960-1969
- 1970-1979
- 1980-1989
- 1990-1999

- Active CVM Domain
- HSPF Model Domain
- R4 Model Domain
- Streams & Flood Control Channels
- Flood Control & Conservation Basins

Faults

- Location Certain
- Location Approximate
- Approximate Location of Groundwater Barrier
- Location Concealed
- Location Uncertain

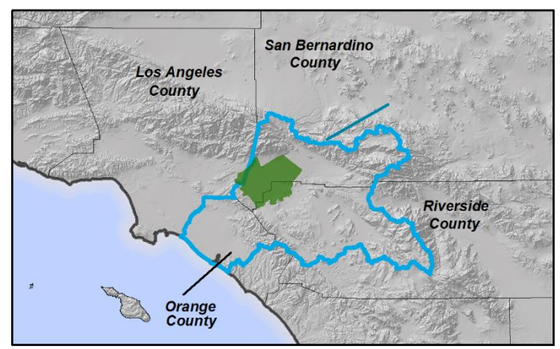

Prepared by:

WEI
Wildermuth Environmental, Inc.

Author: LS
Date: 5/7/2020
File: Figure 3-7 Channel Lining.mxd

0 1 2 3 4 5 Miles
0 2 4 6 8 Km

Prepared for:

2020 Safe Yield Recalculation

Chino Basin Watermaster
Partners in Basin Management

Time History of Channel Lining in the Chino and Cucamonga Basins

Figure 3-7

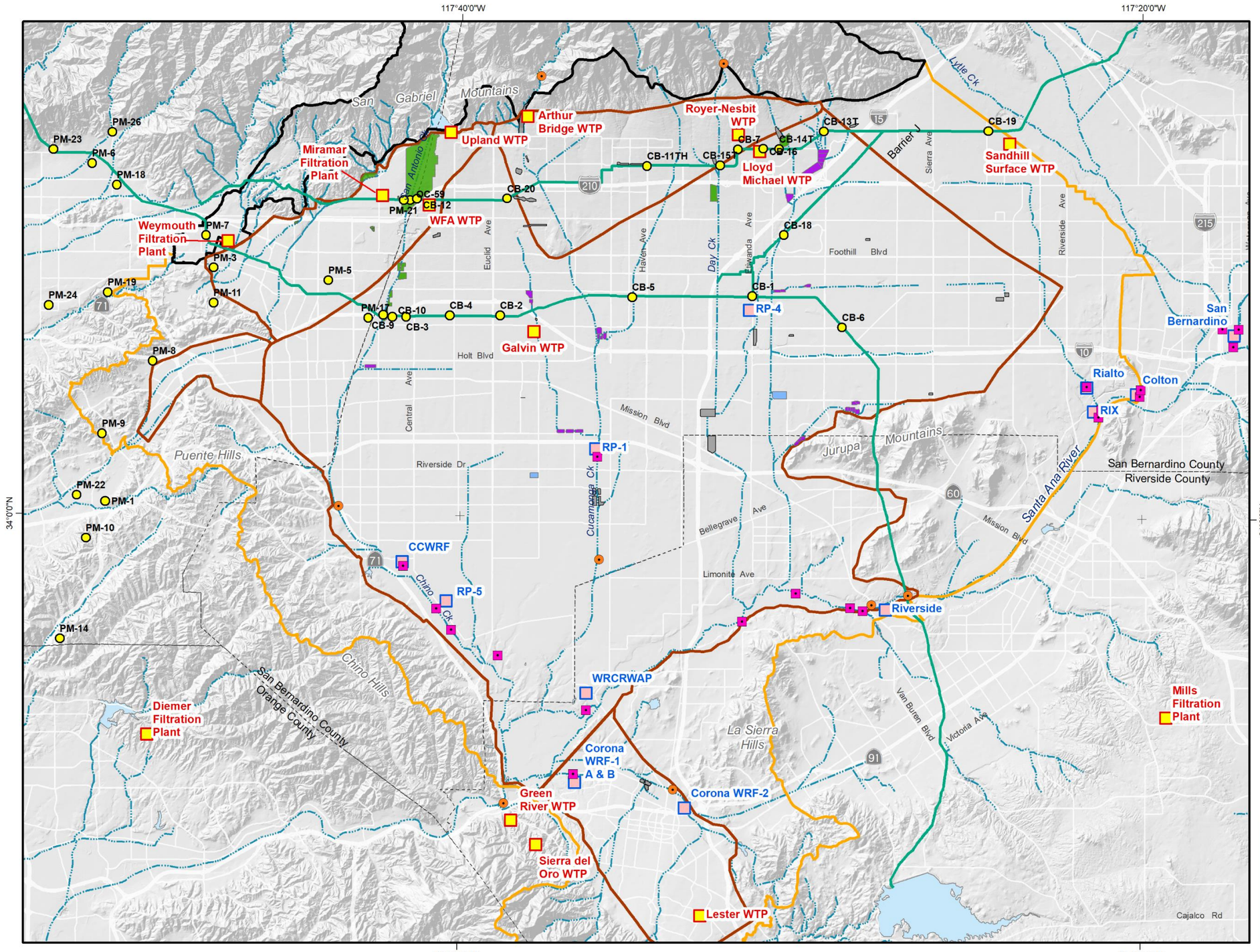

Wastewater Treatment Plant

Imported Water Treatment Plant

Wastewater Discharge Point

Imported Water Pipeline

MWD Service Connection/Turnout

Streamflow Gage

Spreading Basins

Storm, Imported & Recycled Water

Storm Water

Storm & Imported Water

Other

Other Features

Active CVM

R4 Model Domain

HSPF Model Domain

Santa Ana Watershed Rivers

Prepared by:

WEI
Wildermuth Environmental, Inc.

Author: LS
Date: 5/11/2020
File: Figure 3-8 Storm_imported_recycled.mxd

0 1 2 3 4 5 Miles

0 2 4 6 8 Km

Prepared for:

2020 Safe Yield Recalculation

Chino Basin Watermaster
Partners in Basin Management

Imported Water Pipelines, Turnouts, Surface Water Treatment Plants, Spreading Basins, Wastewater Treatment Plants and Their Points of Discharge

Figure 3-8

Figure 3-9 Time History of Tributary and Non-Tributary Discharges to the Santa Ana River

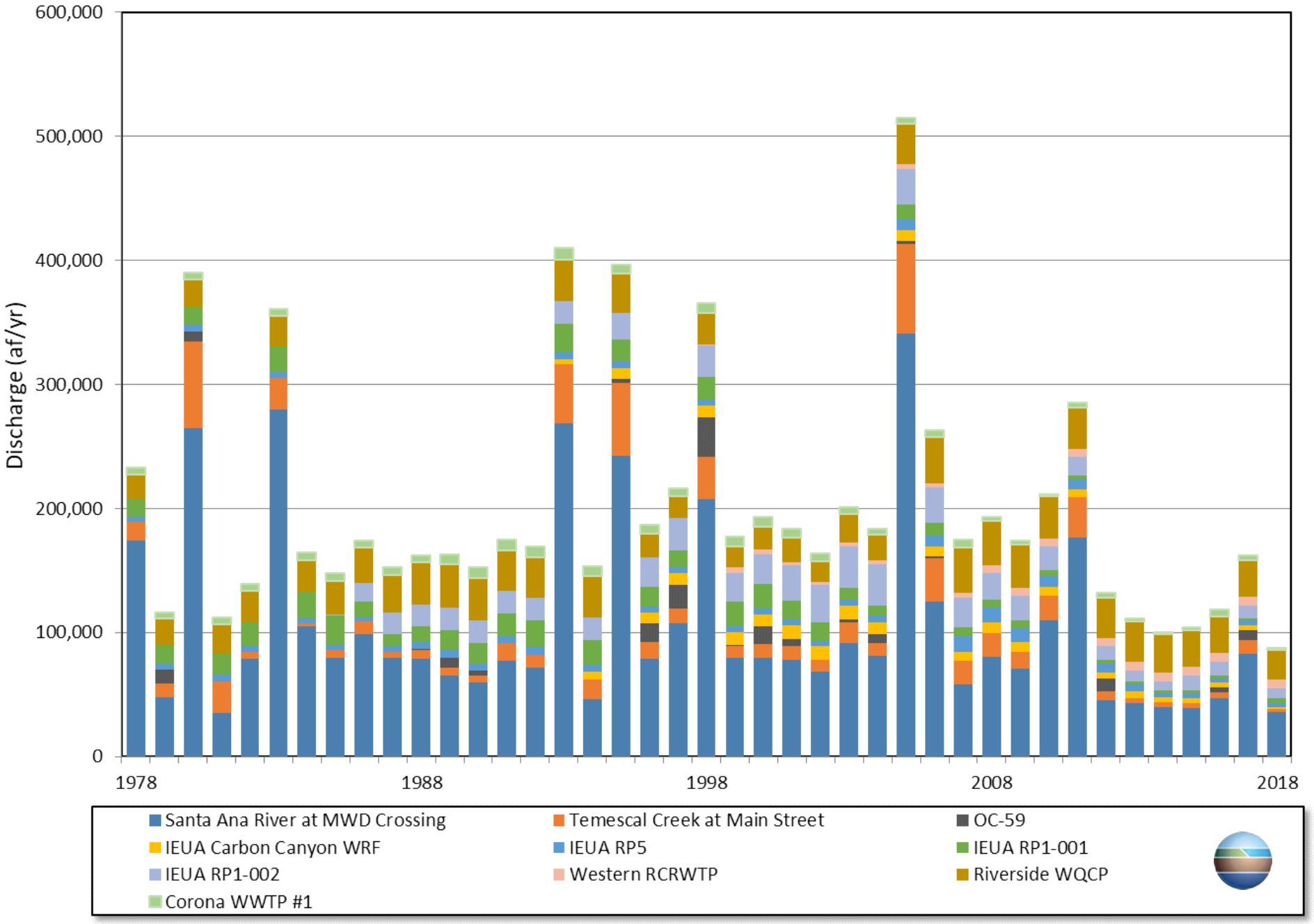

117°40'0"W
117°20'0"W
34°0'0"N

ID# 2037AUTO
ID# 2017AUTO
ID# 1085
Cucamonga Basin
Claremont
ID# 1019AAUTO
ID# 1175
ID# 2198
Puddingstone Res
Six Basins
ID# 1034
ID# 2194
ID# 2159AUTO
ID# 2005B
Pomona
Spadra Basin
ID# 1026
ID# 1021AUTO
Chino Basin
ID# 178
ID# 265
ID# 1067
ID# 1079
ID# 177
ID# 179
U.C. Riverside
ID# 100
ID# 044
La Sierra Hills
ID# 250
Temescal Basin
ID# 035
ID# 102
El Sobrante de San Jacinto
San Gabriel Mountains
Puente Hills
Chino Hills
Jurupa Mountains
Cajon Creek
Santa Ana River
San Bernardino County
Riverside County
Orange County
Foothill Blvd
Holt Blvd
Mission Blvd
Limonite Ave
Bellegrave Ave
Victoria Ave
Sierra Ave
Riverside Ave
Euclid Ave
Central Ave
Etiwanda Ave
Day Ck
San Ant. Ck
Cucamonga Ck
Chino Ck

CIMIS Weather Station
Evaporation Station
Precipitation Station
Active CVM Domain
HSPF Model Domain
R4 Model Domain
Streams & Flood Control Channels
Flood Control & Conservation Basins

Prepared by:
WEI
Wildermuth Environmental, Inc.

Author: LS
Date: 3/21/2020
File: Figure 3-10 Precip_CIMIS_Evap.mxd

0 1 2 3 4 5 Miles
0 2 4 6 8 Km

Prepared for:
2020 Safe Yield Recalculation

Chino Basin Watermaster
Partners in Basin Management

Location of Precipitation, CIMIS and Evaporation Stations

Figure 3-10

117°40'0"W

117°20'0"W

34°0'0"N

PRISM Precipitation Data Grid

NEXRAD Precipitation Data Grid

Active CVM Domain

HSPF Model Domain

R4 Model Domain

Prepared by:

WEI
WILDERMUTH ENVIRONMENTAL, INC.

Author: LS
Date: 3/21/2020
File: Figure 3-11 PRISM_NEXRAD.mxd

0 1 2 3 4 5 Miles

0 2 4 6 8 Km

Prepared for:

2020 Safe Yield Recalculation

CHINO BASIN WATERMASTER
Partners in Basin Management

PRISM and NEXRAD Grid Systems

Figure 3-11

117°40'0"W

117°20'0"W

34°0'0"N

Cucamonga Basin

Six Basins

Spadra Basin

Chino Basin

Temescal Basin

Redlands Blvd

San Jac

Contour of Long-Term Average Annual Precipitation (in)

Value

High : 55

Low : 0

Active CVM Domain

HSPF Model Domain

R4 Model Domain

Prepared by:

WEI
WILDERMUTH ENVIRONMENTAL, INC.

Author: LS
Date: 3/21/2020
File: Figure 3-12 Average_Precip.mxd

0 1 2 3 4 5 Miles

0 2 4 6 8 Km

Prepared for:

2020 Safe Yield Recalculation

CHINO BASIN WATERMASTER
Partners in Basin Management

Long-Term Average Annual Precipitation in the Chino Valley, 1896 - 2018

Figure 3-12

Figure 3-13 Time History of Annual Precipitation on the CVM Watershed and Associated Cumulative Departure From Mean Annual Precipitation

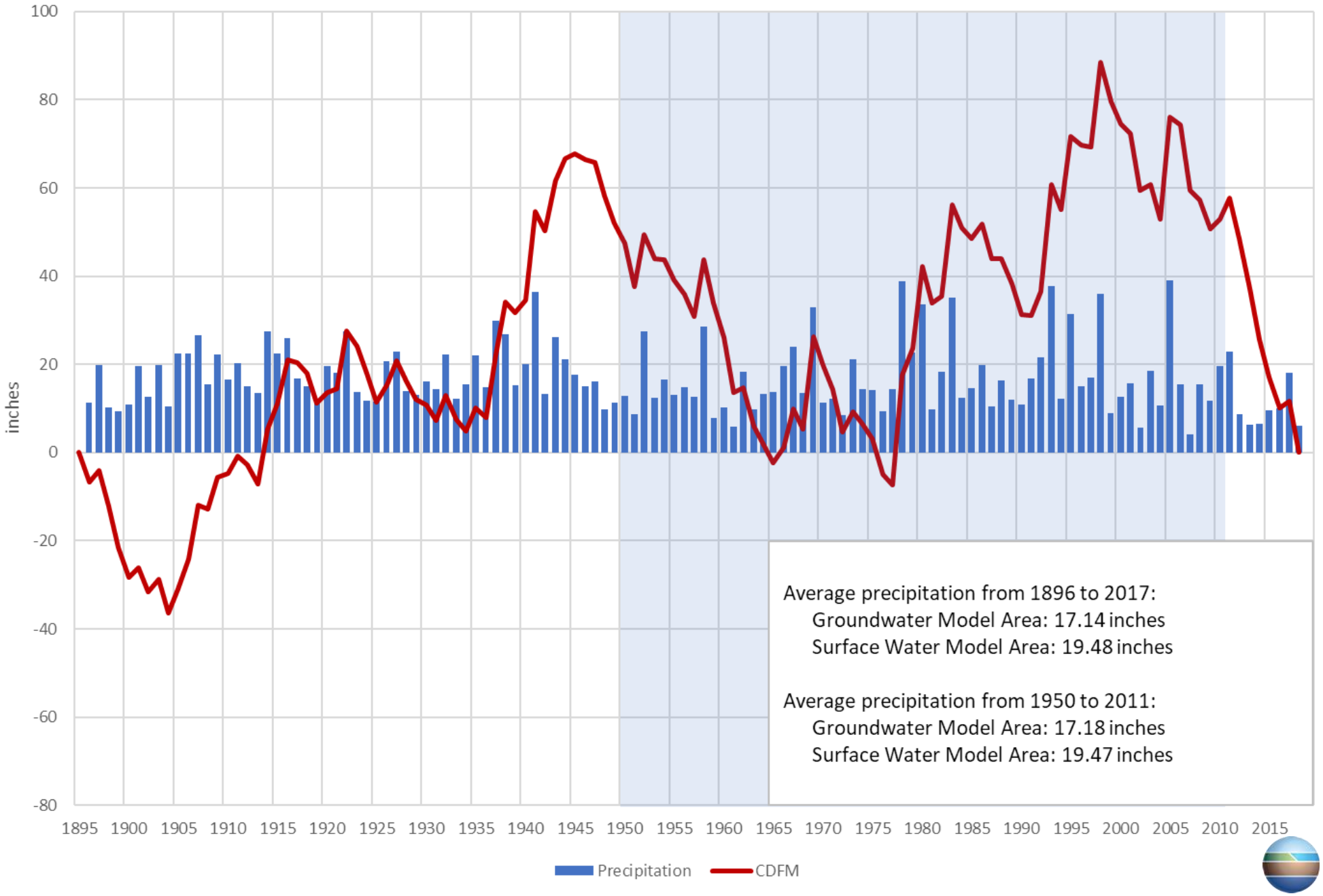

Figure 3-14 Dry Period Recurrence Interval

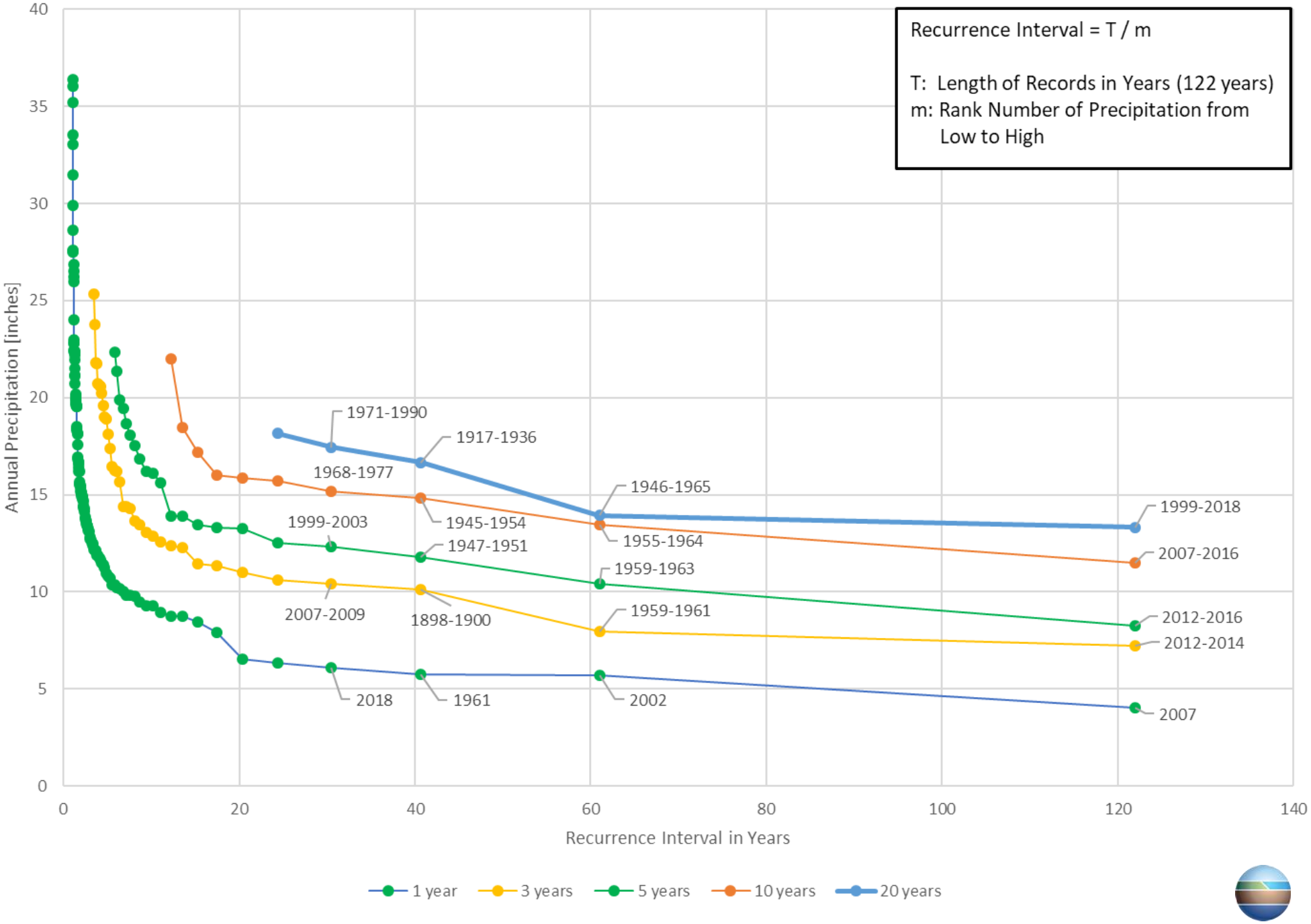

Figure 3-15 Time History of Estimated ET at CIMIS Stations

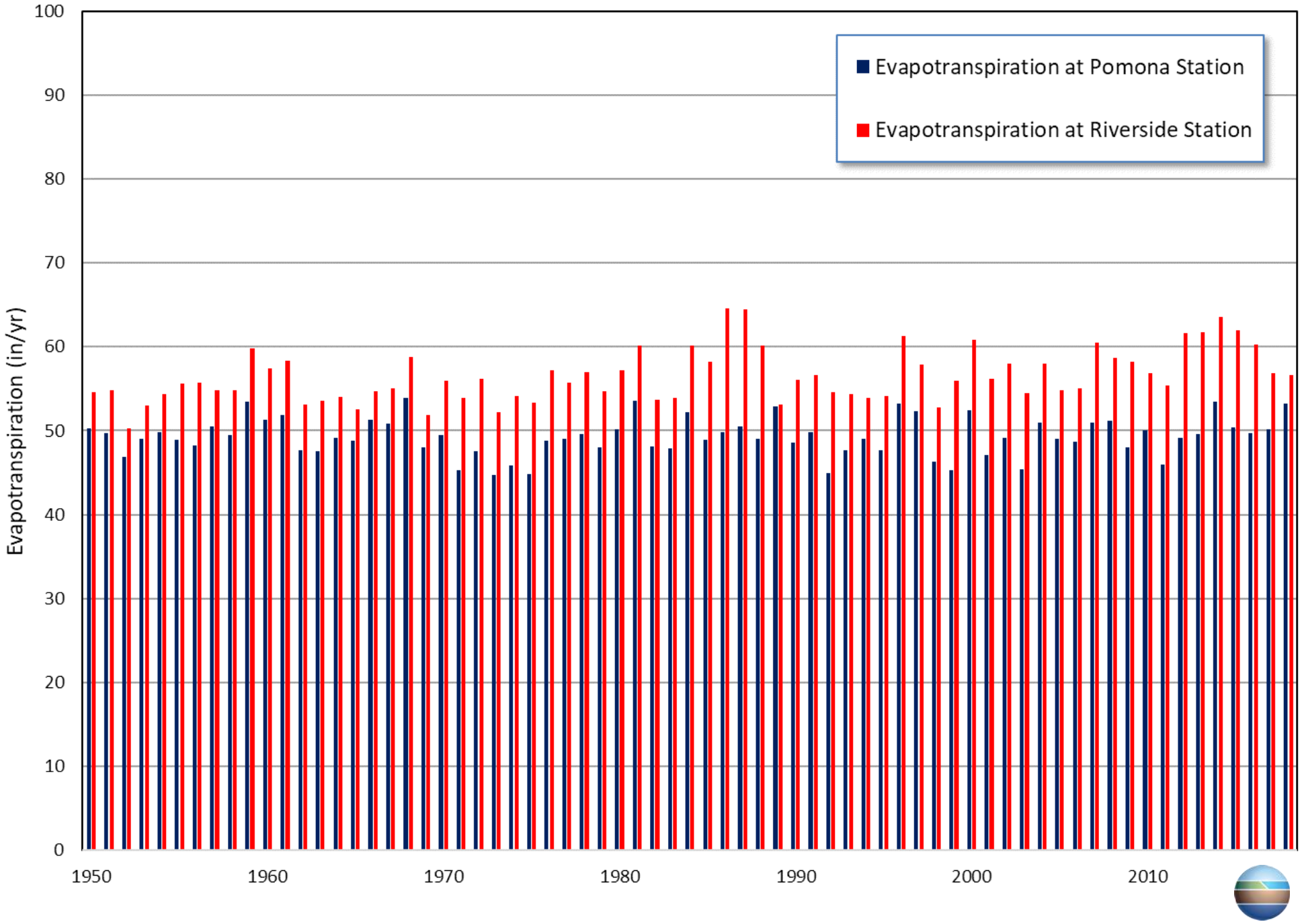

Figure 3-16 Time History of Pan Evaporation at Puddingstone Reservoir

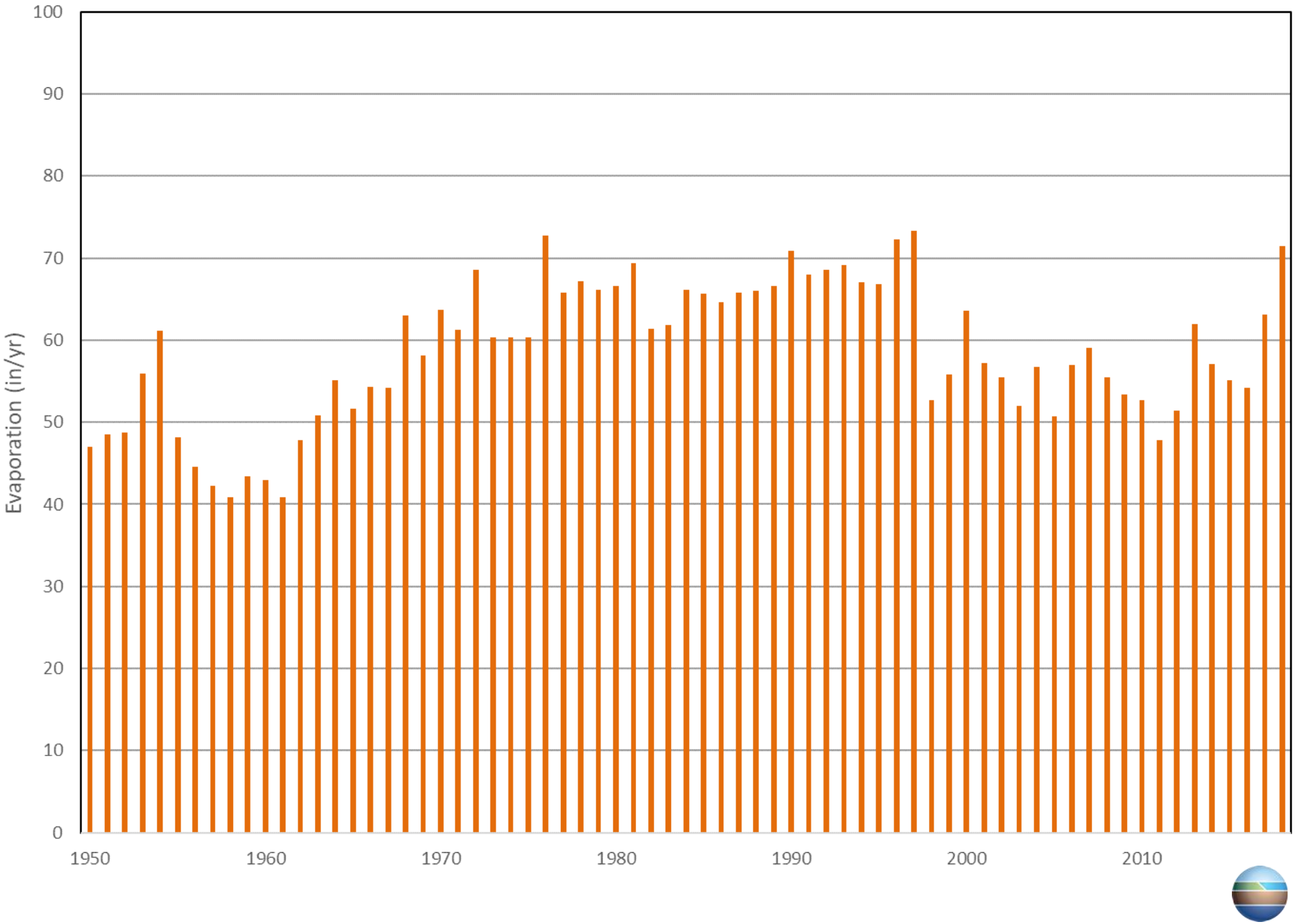

Figure 3-17 Time History of Managed Recharge in the Chino Basin in the Judgment Period

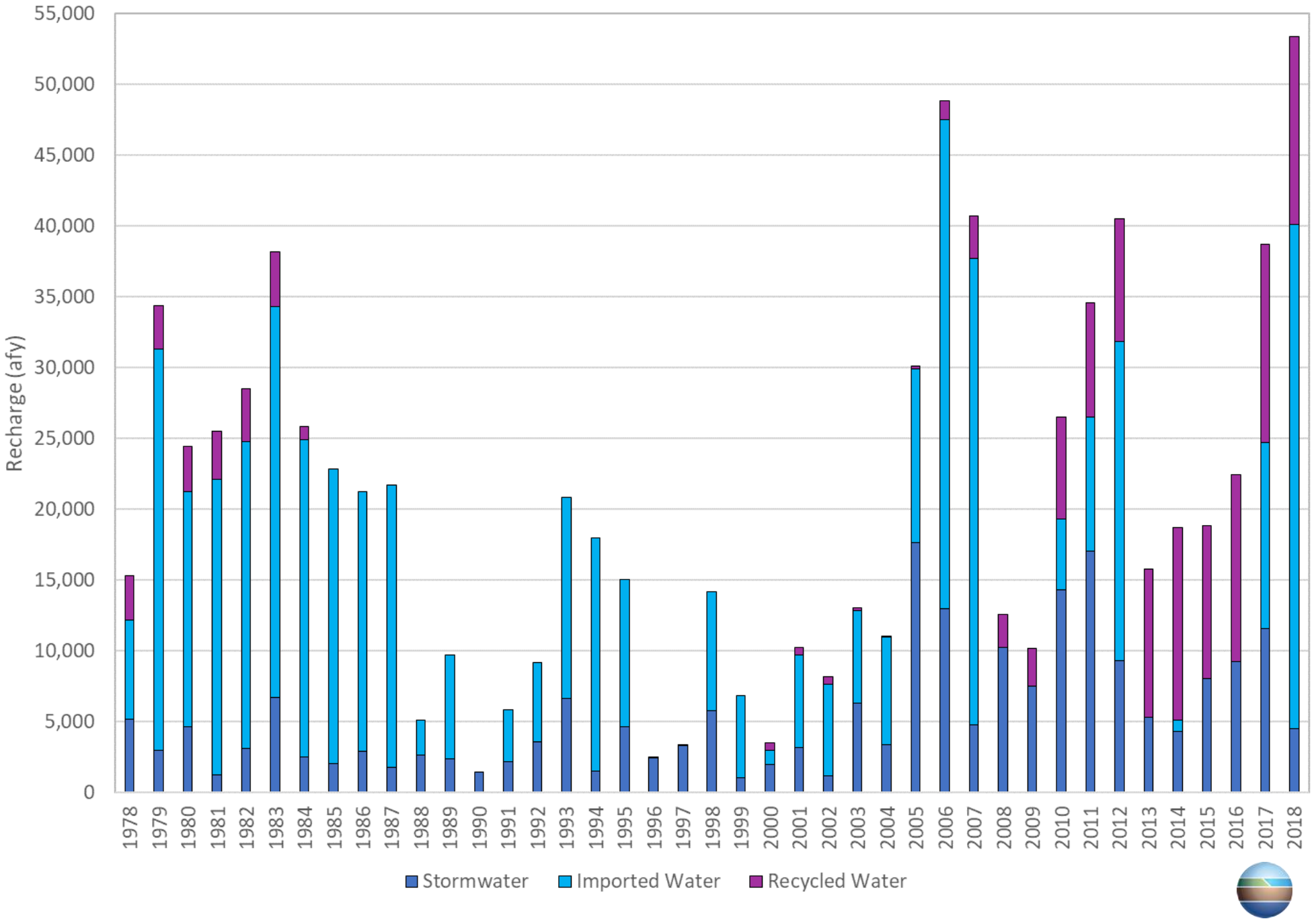

Figure 3-18 Time History of Groundwater Pumping in the Chino Basin in the Judgment Period

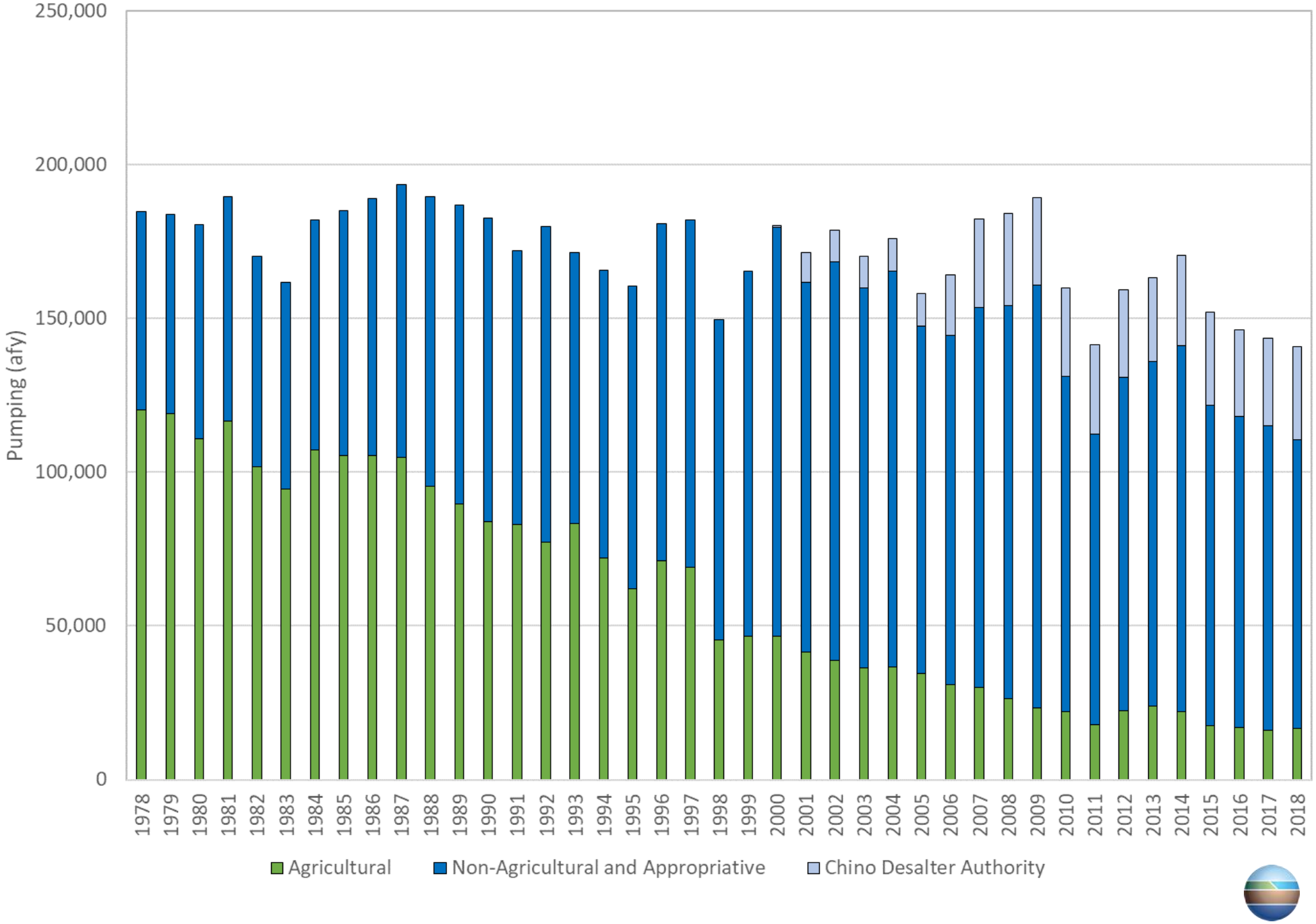

Section 4 – Computer Codes

This section describes the computer codes used in the development of the 2020 CVM and the Safe Yield calculation. The 2020 CVM relies on five codes to represent the physical processes in the 2020 CVM aquifer systems:

- San Gabriel Mountain Hydrology: HSPF (Bicknell, et al., 2005).
- Runoff, surface water flow, stormwater recharge, agricultural pumping, applied water and soil zone process: R4 (WEI, 2007). [15]
- Vadose zone flow HYDRUS-2D (Simunek, et al., 1999).
- Groundwater flow: MODFLOW (McDonald, et al., 1988; Mehl, et al., 2001) and MODFLOW-NWT (Niswonger, et al., 2011).
- Parameter estimation and calibration: PEST and SENSAN (Doherty, 2019).

4.1 HSPF

The Hydrological Simulation Program-FORTRAN, known as HSPF, is a numerical model developed to simulate hydrologic and water quality processes in natural and man-made water systems. It is used in the planning, design, and operation of water resources systems. HSPF uses the time history of precipitation, temperature, evaporation, evapotranspiration and parameters related to land use patterns, soil characteristics, and agricultural practices to simulate the processes that occur in a watershed. The initial result of an HSPF simulation is a time history of the quantity and quality of water transported over the land surface and through various soil zones to streams. Runoff flow rate, sediment loads, nutrients, pesticides, toxic chemicals, and other quality constituent concentrations can be predicted. The model uses these results and stream channel information to simulate instream processes. From this, HSPF produces a time history of water quantity and quality at any point in the watershed.

HSPF models for the San Gabriel Mountain streams were initially development of the Cucamonga and Six Basins models in 2014 and they have been updated and improved to support the recent update and recalibration of the Six Basins Model. Specifically, HSPF produces surface water discharge estimates to San Gabriel Mountain streams that enter the 2020 CVM domain and subsurface inflows along the San Gabriel Mountain front to the Cucamonga and Six Basins. Upon entering the 2020 CVM domain, the surface water discharge estimates are routed through the 2020 CVM domain with the R4 model.

4.2 R4 Surface Water Simulation Model

The R4 Model[15] is a comprehensive suite of hydrologic simulation modules that were developed by WEI to support hydrologic decision support processes and groundwater modeling. R4 was used in this investigation to calculate areal recharge from precipitation and irrigation and storm water recharge that occurs along pervious stream bottoms and in stormwater management basins and to estimate agricultural pumping when pumping records were unavailable.

The origin of this model can be traced to the Chino Basin Water Conservation District and Watermaster. These agencies wanted to estimate the volume of stormwater recharge that occurred in recharge basins, flood retention basins, and unlined streams in the Chino Basin. WEI developed a simulation model that estimates runoff from daily precipitation, routes the runoff through the Chino Basin drainage systems,

[15] Documentation for the R4 Model is included as Appendix A in the report entitled: "2007 CBWM Model Documentation and Evaluation of the Peace II project Description (WEI, 2007). The model is in the public domain and can be downloaded from https://github.com/weiwater/R4

calculates recharge on a daily basis, and produces reports that summarize recharge performance. This model was initially developed in 1994 for the western portion of the Chino Basin (Wildermuth, 1995) and was expanded to the entire Chino Basin in 1996 (WEI, 1998). Subsequently, it was used in the Chino Basin to estimate the recharge performance of proposed flood control and conservation basin improvements and the recharge benefits of improved basin maintenance (Black & Veatch, 2001). The model was expanded to include water quality simulations and applied to the Wasteload Allocation Investigation for the Santa Ana Watershed (WEI, 2002). The root zone simulation module is used to estimate irrigation applied to land surface based on variable vegetation types, ET_0, and irrigation practices using a soil moisture model; and the deep infiltration of precipitation and applied water (DIPAW).

The model has been used for groundwater models developed by WEI, including several models of the Chino Basin for the period 2003 through 2020 (WEI, 2003; 2007; 2008; 2009; 2015; 2018), the Beaumont Basin (WEI, 2008b), the Arlington Basin (WEI, 2007), the Cucamonga Basin (WEI, 2014), Six Basins (WEI, 2017; 2020), and the Temescal Basin (WEI, 2013). The R4 model has also been used in recharge master plans investigation in the Chino and Temescal Basins (WEI, 2002; 2010; 2013) in indirect potable reuse investigations in the Beaumont Basin, Chino Basin, San Bernardino Basin Area (WEI, 2006a; 2008b; 2010a) and the wasteload allocation investigation for the Santa Ana River Watershed (WEI, 2002; 2008c).

The rainfall module consists of several procedures that prepare hydrologic data, including precipitation, evaporation, evapotranspiration, and land surface features data, such as land use, hydrologic soil type, vegetation, etc. The study area is subdivided sub watersheds called hydrologic sub areas (HSAs) delineated based on topography, land use, hydrologic soil group, vegetation, drainage features, and urban stormwater management plans.

The runoff module calculates daily runoff from precipitation data for each HSA using a modified Soil Conservation Service (SCS) method. The runoff module summarizes data and prepares two files: runoff for the router module and the infiltration of precipitation to the soil zone for the root zone module.

The router module collects stormwater runoff from each HSA, point discharge data (e.g. wastewater discharge from treatment plants), and boundary inflow data, and routes these combined flows through drainage systems. This module, using natural and improved channel geometry data, calculates infiltration through pervious stream bottoms, simulates operation of flood control/conservation basins using the Modified Puls method, calculates the infiltration of water in flood control/conservation basins, and calculates evaporation from the free water surface of streams and flood control/conservation basins.

The root zone module is a soil moisture accounting model that is integrated with the runoff module. It estimates the evapotranspiration requirements for vegetation types and uses the estimated precipitation infiltration provided by runoff module to estimate the irrigation water requirement. Infiltrated precipitation and applied irrigation water, after abstraction by ET, are then routed through the root zone on a daily time step. When the volume of water in the root zone exceeds the field capacity the water in excess of the field capacity is discharged from the root zone to vadose zone.

4.3 HYDRUS-2D

HYDRUS-2D (Simunek, et al., 1999) is a Microsoft Windows-based modeling environment for the analysis of water flow and solute and heat transport in variably saturated porous media. The HYDRUS-2D model was used in conjunction with another tool (see Section 5.2.4.1) to simulate unsaturated flow in the vadose zone in the 2020 CVM. This program numerically solves the Richards equation for saturated-unsaturated flow and the Fickian-based advection-dispersion equations for heat and solute transport. This program can be used to analyze water and solute movement in unsaturated, partially saturated, or fully saturated porous media.

4.4 MODFLOW-NWT

The USGS has developed a wide range of computer models to simulate saturated and unsaturated subsurface flow, solute transport, and chemical reactions in groundwater systems. The most widely used of these models is MODFLOW, which simulates three-dimensional groundwater flow using the finite-difference method. Although it was conceived solely as a groundwater flow model in 1984 and released in 1988 (McDonald, et al., 1988), MODFLOW's modular structure has provided a robust framework for the integration of additional simulation capabilities that build on and enhance its original scope. The family of MODFLOW-related models now includes capabilities for simulating coupled groundwater/surface water systems and solute transport.

MODFLOW-NWT (Niswonger, et al., 2011) was chosen for this project because 1) it has extensive publicly available documentation, 2) it has sustained rigorous USGS and academic peer review, 3) it has a long history of development and use, 4) it is widely used around the world in public and private sectors, and 5) it can easily operate with additional simulation tools published by others.

HSPF, R4 and HYDRUS-2D are used to create recharge and discharge stresses on the groundwater basins in the 2020 CVM. MODFLOW is used to estimate the groundwater basin's response to these stresses.

4.5 PEST and SENSAN

PEST[16] (Doherty, 2019), an acronym for Parameter ESTimation, is a computer code for model calibration and predictive analysis. During a calibration process, PEST applies the Gauss-Marquardt-Levenberg algorithm to adjust model parameter values for which the sum of weighted squared deviations between model-calculated and observed values is reduced to a minimum. The mathematics of PEST is further described in Section 6 of this report. PEST has been successfully applied in many fields of the geophysical sciences, including groundwater modeling. It has been proven to be a robust tool and was therefore applied to the Chino Basin groundwater model.

SENSAN (Doherty, 2019), an acronym for SENSitivity ANalysis, is a command-line program that provides the ability to carry out multiple model runs in parallel. WEI operates a parallel computer system with several processors where key model output from each run are recorded for later analysis. This allows for very complex multiple parameter sensitivity analyses to be completed in a much shorter time period.

PEST and SENSAN were chosen for this project because 1) they reduce modeling time and significantly increase the value of the results, 2) the software has extensive publicly available documentation, 3) it has a strong history of development, and 4) it is considered a standard in the groundwater industry and has been incorporated into most MODFLOW model processors.

[16] PEST is in the public domain and can be downloaded from http://www.pesthomepage.org/

This section describes how the hydrogeologic conceptual model described in Section 2 and the hydrologic data described in Section 3 were translated into numerical surface and ground water models. First the surface water models are described followed by the groundwater model. The topics discussed in this section include the 2020 CVM domain (model domain) and grid (model grid), the assignment of hydraulic properties to the model grid, the initial conditions, boundary conditions, and the description of the specific MODFLOW packages used to simulate recharge and discharges stresses, internal barriers and to evaluate parameter sensitivity.

5.1 Surface Water Models

Figure 3-1 shows the HSPF and R4 model domains. The HSPF model was used to estimate daily discharge from precipitation from the San Gabriel Mountains to valley floor and the estimated surface discharge became inflow to R4 domain over the valley floor. Figure 5-1 shows the hydrologic sub-areas (HSAs) for the HSPF and R4 models. There are 39 HSAs for the San Gabriel mountain watersheds and 344 HSA for the rest of the 2020 CVM surface water domain. Note that in the prior Safe Yield recalculation the Chino Basin included 180 HSAs. The 2020 CVM has a much more refined drainage system delineation. The refined HSA delineation was developed to more accurately represent the drainage system and capture the historical and projected changes in land use and associated cultural conditions. The number of land use types used in the prior Safe Yield recalculation was 14 and the number of land use types used in the in the 2020 CVM is 17. The number of land use types was increased to be able to more accurately estimate storm water discharge, irrigation demands and DIPAW.

The HSPF and R4 watershed models were used to estimate stormwater discharge and route these discharges routed through the stream systems that overlie the active 2020 CVM domain and to estimate stormwater recharge in streams and flood control and conservation basins. Stormwater MAR was estimated with the HSPF and R4 models for 1978 through 2004 and in the planning scenarios. Stormwater MAR for 2005 through 2018 is based on estimates of stormwater diversions provided by IEUA. The model-estimated DIPAW for watersheds that are tributary to and not overlying the groundwater basins was assumed to be the subsurface inflow from these areas to the 2020 CVM proximate to the discharge point of the watershed to the groundwater basin. The hydrologic data required by these models were described in Section 3.

5.2 Groundwater Model

The topics discussed in this section include the 2020 CVM domain (model domain) and grid (model grid), the assignment of hydraulic properties to the model grid, the initial conditions, boundary conditions, and the description of the specific MODFLOW packages used to simulate recharge and discharges stresses, internal barriers and to evaluate parameter sensitivity.

5.2.1 Model Domain and Grid

The model domain and the model grid are shown in Figure 5-2. The model grid consists of 577 rows, 648 columns, and five layers. Horizontally, each cell has a dimension of 60 by 60 meters (196 by 196 feet). This fine cell size was selected to model the curvature of drawdown near wells, recharge basins and streams. The grid cells are designated as "inactive" outside the model domain and as "active" inside the domain. There is a total of 904,668 active cells.

The spatial extent of the model domain was determined by the saturated extent and thickness of the aquifer system: the extent was limited to regions where the saturated thickness was greater than about

40 feet. The saturated thickness was determined based on groundwater levels at the start of the calibration period and the elevation of the effective base of the aquifer systems.

The aquifer system in the Chino Basin is represented by five layers. The discretization of these layers is discussed in Section 2.5. The top layer (Layer 1) is simulated as an unconfined layer ranging from 32 feet and to 1,405 feet in thickness. Layer 2 is a confining unit generally ranging from 40-65 feet in the central part of the Chino Basin and pinching out in the northern and eastern part of the Chino Basin. Layer 3 is simulated as a confined aquifer ranging from 5 to 345 feet in thickness. Layer 4 is a confining unit generally ranging from 20 feet to 55 feet in thickness in the west and middle of Chino Basin and pinching out east of MZ2. Layer 5 is simulated as a confined aquifer ranging from 10 feet and to 903 feet in thickness.

The Six Basins consists of three layers and the Cucamonga and Spadra Basins consist of two layers.

5.2.2 Time Discretization and Calibration Period

The transient stress period of the model is one month. The calibration period chosen for the development of the 2020 CVM was July 1, 1977 through June 30, 2018. The July 1, 1977 start date was selected because the hydrologic data used in the calibration of the Cucamonga and Six Basins models was available starting in the fiscal year 1978.

5.2.3 Hydraulic Properties and Zonation

The hydraulic properties used in the model include horizontal hydraulic conductivity, vertical hydraulic conductivity, specific yield for an unconfined aquifer (Layer 1), and the specific storage for confined aquifers (Layers 2 through 5). In Section 2.6, hydraulic properties of aquifers and their spatial distribution in the 2020 CVM basins were shown at model-cell scale based on a lithological model. However, other factors, such as sorting and compaction can also affect the values of hydraulic properties. Sorting is the process by which sediment grains are selected and separated according to the grain size by the agents of transportation. Sediment sorting is directly related to the environment of deposition. For example, well-sorted sands or gravels in a river channel typically have higher porosity and higher hydraulic conductivity than found in glacial deposits. And, compaction with depth reduces the pore space resulting in lower porosity, lower hydraulic conductivity and lower specific yield. In the 2020 CVM basins, the depositional environments include alluvial fans, river channels, floodplains, and lakes.

To represent sediment sorting and compaction and to reduce the number of parameters to a manageable level, the model domain was subdivided into a number of parameter zones. Parameter zonation is a way to reduce the number of estimated parameters and thus make inverse modeling computationally tractable. Hydraulic parameter zonation is based on 1) geologic and geomorphologic conditions, 2) hydrogeological conditions, 3) the location of calibration wells, and 4) the capability of the numerical tools and computer resources. Figures 5-3a through 5-3e show the parameter zones for Layers 1 through 5, respectively. Horizontal hydraulic conductivity, vertical hydraulic conductivity, specific yield in unconfined Layer 1, and specific storage in confined aquifer layers were assumed to have the same zonation. These parameter zones were constructed to represent similar depositional environments.

The hydraulic property values in each cell of the model were then calculated by MODFLOW based on the following equations:

$$K_h(i,j,k) = XK_h(zone) \times KH(i,j,k)$$

$$K_v(i,j,k) = XK_v(zone) \times KV(i,j,k)$$

$$S_y(i,j,k) = XS_y(zone) \times SY(i,j,k)$$

Where i, j, and k represent row, column, and layer in the model domain; $XK_h(zone)$, $XK_v(zone)$, and $XS_y(zone)$ are parameter zone coefficients that are used to scale the initial cell estimates of horizontal hydraulic conductivity, vertical hydraulic conductivity, and specific yield or specific storage derived from the lithological model. KH, KV, and SY are the initial cell and layers-specific estimates of horizontal hydraulic conductivity, vertical hydraulic conductivity, and specific yield or specific storage derived from the lithological model. The calculated parameter value for any cell is the product of the parameter zone coefficient and the initial hydraulic parameter value derived from the lithological model for cells within the parameter zone. This allows for the model to have a heterogeneous K_h, K_v, S_y and S_s.. The model parameters $XK_h(zone)$, $XK_v(zone)$ and $XS_y(zone)$ are adjusted in the calibration processes.

As shown in Figures 5-3a through 5-3e, Layers 1 and 2 have 35 parameter zones (12 in the Chino Basin) Layer 3 has 17 parameter zones (10 in the Chino Basin), and Layers 4 and 5 have 9 parameter zones (8 in the Chino Basin). Table 5-1a lists the initial parameter estimates and ranges based on the lithology model. Table 5-1b lists the initial parameter estimates and ranges used to start the calibration.

5.2.4 Initial Condition

An initial condition is required to solve numerical groundwater flow problems. In the 2020 CVM these correspond to the initial storage in the vadose zone and the initial piezometric elevations in the saturated zone for each model layer.

5.2.4.1 Initial Condition in the Vadose Zone

The vadose zone extends from the bottom of the root zone to the groundwater table. DIPAW discharging from the root zone flows through the vadose zone to the groundwater table. The pore space in the vadose zone is variably saturated. The speed at which groundwater flows through the vadose zone is slower than in the saturated zone in part because it is variably saturated and because vertical hydraulic conductivity is generally lower than horizontal hydraulic conductivity. Storage space in the vadose zone buffers the variability in DIPAW caused by variable precipitation and irrigation. Vadose zone hydraulics cannot be directly simulated in MODFLOW for a basin as large and lithologically complex as the 2020 CVM. A simplified vadose zone routing scheme was developed and implemented in the 2020 CVM at the model cell level.

A detailed investigation of vadose zone travel (lag) time from the root zone to the water table was done for the evaluation of the Peace II Agreement and was reported in *2007 CBWM Groundwater Model Documentation and Evaluation of the Peace II Project Description.* (WEI, 2007). In that work, the lag time was estimated based on the time it took for a conservative tracer injected into the vadose zone at the root zone to travel to the water table. The HYDRUS-2D model was used to estimate lag time at several boreholes with detailed lithologic descriptions and located in the 2013 Model domain. For the boreholes that were investigated, the primary factor contributing to lag time was vadose zone thickness. These lag times were then generalized throughout the Chino Basin model domain based on vadose thickness and individual lag times were estimated for each model cell. Figure 5-4 shows the location of the boreholes where the HYDRUS-2D models were constructed and it shows contours of equal lag time. In Figure 5-4, the contours were based on the estimated lag time at the modeled boreholes and scaled across the 2020 CVM based on vadose zone thickness. The lag time ranges from about one to four years near the Santa Ana River to over 30 years in the Upland area and typically ranges from 5 to 30 years in other areas.

Several routing formulations were evaluated for the work reported in 2007.[17] Two candidate routing models were tested: linear reservoir and volume averaging. In a linear reservoir approach, the discharge from a reservoir is proportional to storage. The discharge from a linear reservoir is:

$$D_{w,t} = K \times (S^{t-1} + \Upsilon \times D_{r,t})$$

$$S^{t} = S^{t-1} + D_{r,t} - D_{w,t}$$

Where $D_{w,t}$ is the DIPAW discharge to water table for the period t, K is a constant of proportionality (storage coefficient), S^{t-1} is the storage in the vadose zone at the beginning of time period t, S^{t} is the storage in the vadose zone at the end of time period t, and Υ ranges from 0 to 1 and typically would be assigned a value of 0.5. In words, the DIPAW to the water table for period t is equal to constant times sum of the volume of water stored in the vadose zone at the beginning time period t (denoted by the superscript $t-1$) plus some fraction of the DIPAW discharging from the root zone during the period. After the DIPAW to the saturated zone is computed, the water stored in the vadose zone at the end of the time period S^{t} (denoted by the superscript t) is updated and becomes the starting storage for the next stress period. The challenges in implementing this method are the estimation of the initial storage in the vadose zone and the storage coefficient K. It was difficult to calibrate and created unrealistic volumes of water stored in the vadose zone.

In a volume averaging approach, the estimate of the DIPAW discharge to the water table is assumed equal to the volume average DIPAW leaving the root zone over a period of time equal to the lag time

$$D_{w,t} = (1/n) \times \sum_{j=t-n}^{t} D_{r,j}$$

Where $D_{w,t}$ is the DIPAW discharge to water table for the period t, n is the lag time (in years) divided by the model time step (less than one year), $D_{r,j}$ is the DIPAW discharging from the root zone and the summation occurs for all DIPAW at the root zone that occurs during the lag time. In other words, for a model cell with a 10-year lag time and one-month stress period, the DIPAW at the water table would be equal to the average of the prior 120 months of DIPAW at the root zone. In this method, there is no explicit calculation of the water stored in the vadose zone. The challenge in implementing this method is that it requires a long time-history of DIPAW at the root zone that predates the start of a simulation period.

In the work reported in 2007, and after experimentation and calibration, the volume averaging approach was used. The DIPAW time series at the root zone was estimated for several decades preceding the calibration period to provide a long enough DIPAW time series to cover the long lag times in the northern part of the Chino Basin. The resulting Chino Basin model was calibrated very well. The same vadose routing approach used in the calibration of the 2013 model was subsequently used to estimate Safe Yield and to evaluate the basin response in subsequent planning investigations. We continued the use of the volume averaging routing method in 2020 CVM. A 35-year time history of DIPAW at the root zone is required to calculate the DIPAW at the root zone in 1978 for the parts of the 2020 CVM with the greatest vadose thicknesses. This was accomplished by estimating the DIPAW at the root zone

[17] Documentation for the use and application of HYDRUS for the 2007 CBWM Model and the 2013 Watermaster Model is included as Appendix B in (WEI, 2007).

from 1950 through 1977 with the updated R4 model. The DIPAW at the root zone for the period 1943 through 1949 was assumed equal to the DIPAW at the root zone from the prior Safe Yield recalculation.

5.2.4.2 Initial Condition in the Saturated Zone

The initial condition for the saturated zone was the groundwater elevation at the beginning of calibration period (July 1, 1977); the initial condition for the Chino Basin was assumed to be equal to the July 1, 1977 estimated groundwater elevations from the prior Safe Yield investigation (WEI, 2015). For the Cucamonga Six and Spadra Basins, the initial condition was based on historic groundwater elevation observations. Figures 5-5a, 5-5b and 5-5c show groundwater level elevation contour maps that represent the initial condition of the 2020 CVM for layers 1, 3, and 5, respectively. In Chino Basin, the initial groundwater elevation in Layers 2 and 4 were assumed to be same as those in Layers 1 and 3, respectively.

5.2.5 Boundary Conditions

Boundary conditions are necessary in solving numerical groundwater flow problems. Ideally, the model domain is bound by identifiable hydrogeologic features that can be quantified relative to the groundwater system. These boundaries can also occur within the active model domain (e.g. wells and creek). Table 5-2 lists the model boundaries, the associated boundary conditions, and the MODFLOW packages utilized to simulate those boundary conditions. Figure 5-6 shows the boundary types in the calibration period.

5.2.5.1 Subsurface Inflow from Mountain Boundaries

As mentioned in Section 4, the HSPF model was used to estimate subsurface inflow from San Gabriel Mountains to the Cucamonga and Six Basins. The R4 model was used to estimate subsurface inflows from the Chino Hills, Puente Hills, La Sierra Hills, Pedley Hills, Santa Ana Mountain and the Jurupa Mountains.

5.2.5.2 Subsurface Inflow from Adjacent Groundwater Basins

Groundwater discharges from the Riverside Basin to the Chino Basin through the so-called Bloomington Divide area (Gosling, 1967). Recent investigations (WEI, 2003; 2006; 2015; Geoscience, 2019) have demonstrated that subsurface inflow from the Riverside Basin provides significant inflow to the Chino Basin. Figure 5-7 shows the locations of wells with historical water level in the immediate vicinity of the boundary between the Riverside and Chino Basins. Figure 5-8 shows that the groundwater level time histories for wells that straddle the boundary of the Chino and Riverside Basins. Review of these time histories in Figure 5-8 indicate that the water levels east of the Riverside-Chino Basin boundary (WVWD 18/18A, WVWD 29 and Hagin) are about 20 feet higher than the groundwater levels observed at wells located west of the boundary (WMWD 20, 28/Larch and NA_1002114) and that the time histories on both sides of the boundary temporally track each other. The persistent east to west gradient, similar groundwater level histories and the lack of known physical barrier to groundwater flow suggest an open boundary between the basins and that groundwater discharges from the Riverside Basin to the Chino Basin. This boundary condition in the 2020 CVM was set as a time-variant specified head boundary for the calibration period, and as a constant specified flow boundary for planning alternatives. The hydraulic conductivity of Layers 1, 3 and 5 adjacent to this boundary and the subsurface inflow from the Riverside Basin were estimated in calibration using the observed groundwater levels located in the Riverside Basin near the boundary.

Subsurface inflow from the Rialto Basin that occurs across the Rialto-Colton Fault was assumed to be the same value estimated in the calibration of the 2013 Model and is equal to 1,480 afy. The inflow at

the south side of the Rialto Fault is assumed to 715 afy, and at the north side of Rialto Fault is assumed to be 765 afy, while the middle part of the Rialto Fault is a no-flow boundary.

Subsurface inflow from the Arlington Basin to the Temescal Basin was estimated based on the Arlington Basin Model, ranges from 617 afy to 1,139 afy with average value of 807 afy.

All subsurface boundary inflows were simulated with the MODFLOW Flow and Head Boundary (FHB) Package that is described Section 5.2.6.1 below.

5.2.5.3 Recharge from San Gabriel Mountain Streams Tributary to the Santa Ana River

Storm water discharge originates in the San Gabriel Mountains and flows south across the model domain to the Santa Ana River. The HSPF model was used to estimate the daily surface water discharge of the San Gabriel Mountains. The R4 model combined the HSPF daily stormwater discharge estimates with the R4-estimatd daily stormwater discharge from precipitation over the model domain and routed the stormwater through the drainage system overlying the 2020 CVM. The time history of land use changes and drainage improvements were incorporated into the R4 simulations. The R4 model estimated the surface water recharge in unlined drainage channels and stormwater management (flood control and conservation) basins. The R4 model was calibrated against observed streamflow data in Chino and Cucamonga Creeks and IEUA-estimated storm water capture at flood control and conservation basins.

Historical estimates of imported and recycled water are also recharged in stormwater management basins.

All recharge in streams that originate in the San Gabriel Mountains and flows south across the model domain to the Santa Ana River (except the lower reaches where surface water and groundwater interaction can occur) and recharge of imported and recycled were simulated with the MODFLOW Flow and Head Boundary (FHB) Package that is described Section 5.2.6.1 below.

5.2.5.4 Surface Water and Groundwater Interaction in the Santa Ana River and Its Lower Tributaries

Figure 5-9 shows the stream channels in the model domain where MODFLOW calculates streamflow based on boundary inflows and depth to groundwater. The boundary inflows include (1) estimated daily discharges from USGS stations on the Santa Ana River at MWD Crossing near the Riverside Narrows and on Temescal Creek at Main Street, (2) estimated daily discharges from wastewater treatment plants, (3) R4 Model estimated daily discharges from tributary San Gabriel Mountain streams, and (4) imported water deliveries to Orange County. These discharges were described in Section 3. The surface water and groundwater interaction in the Santa Ana River and its lower tributaries were simulated with the MODFLOW Streamflow-Routing 2 (SFR2) Package that is described in Section 5.2.6.2 below.

The network of streams defined in the SFR2 Package is divided into reaches and segments. A stream reach is a section of a stream that is associated with a finite-difference cell used to model ground-water flow and transport. A segment consists of a series of contiguous reaches where flows can be routed.

The streambed elevations along creeks and channels were extracted from the 2015 LiDAR data along Santa Ana River with 1-meter resolution (US Army Corps of Engineers, 2015). The channel geometry along Santa Ana River and Prado Basin is defined by an eight-point cross section in each of the stream segments by using these 2015 LiDAR data.

The stream stage in each reach was computed using Manning's equation prior to calculating leakage to or from the aquifer. The stage for each reach was calculated using the specified inflow into the stream

segment. The initial slope of the stream channel was computed based on the 10-meter DEM. The stream channel slopes were further adjusted as needed to ensure a decreasing slope. The estimates of Manning's roughness coefficient were based on the streambed characteristics of the Santa Ana River and its tributaries (Barnes, 1967); the estimated values range from 0.025 to 0.04.

5.2.5.5 Groundwater Pumping

Groundwater pumping and injection were simulated with the MODFLOW Well (WEL) Package described in Section 5.2.6.3 below.

5.2.5.6 DIPAW

After routing DIPAW through the vadose zone, DIPAW recharge was simulated with the MODFLOW Recharge (RCH) Package described in Section 5.2.6.4 below.

5.2.5.7 Evapotranspiration

Evapotranspiration in riparian areas was simulated with the MODFLOW Evapotranspiration Segments (ETS) Package described in Section 5.2.6.5 below.

5.2.5.8 Internal Barriers

The faults that separate the Chino Basin, Cucamonga and Six Basins as well as internal faults and barriers within these basins (internal barriers), were simulated as horizontal flow barriers with the MODFLOW Horizontal-Flow Barrier (HFB) Package described in Section 5.2.6.6 below. The estimated hydraulic conductivity values for these barriers were adjusted through model calibration.

5.2.6 MODFLOW Packages for Boundary Conditions

5.2.6.1 Flow and Head Boundary Package (FHB)

The Flow and Head Boundary (HFB) Package (Leake, et al., 1997) can be used to simulate specified flow or head boundary conditions that vary with time. In the 2020 CVM, the FHB Package was used to simulate specified subsurface inflows, storm water recharge, supplemental recharge, and streambed percolation along unlined channels of upper Santa Ana River tributaries that cross the model domain.

5.2.6.2 Streamflow-Routing Package (SFR2)

The SFR2 Package (Niswonger, et al., 2006) was used to simulate the Santa Ana River and the lower reaches of some of its tributaries in the Prado Basin. The SFR2 Package routes surface flow and calculates recharge to and discharge from the aquifer based on the elevation of a streambed, water level in the stream, hydraulic head in the aquifer, and hydraulic conductivity of the streambed. The shift from recharge of the aquifer to discharge to the stream occurs at the point where the hydraulic head in the aquifer equals the water level in the stream.

5.2.6.3 Well Package (WEL)

The Well Package (McDonald, et al., 1988) was used to simulate the withdrawal of water from aquifers by wells. The Well Package can also be used to simulate any other source of withdrawal or recharge that occurs at a known rate, including specified flow boundaries. This package uses a constant flow rate for each stress period.

5.2.6.4 Recharge Package (RCH)

The RCH Package (McDonald, et al., 1988) is designed to simulate areally distributed recharge to the ground-water system. Most commonly, areal recharge occurs as a result of precipitation and irrigation water that percolates to the ground-water system. The recharge value represents the amount of water that goes into the groundwater system and not the amount of precipitation. Three recharge options are supported by MODFLOW: "Recharge only at the top layer", "Recharge at specified vertical cells", and "Recharge at highest active cells." The RCH Package was used to simulate the DIPAW with the option "Recharge at highest active cells."

5.2.6.5 Evapotranspiration Segments Package (ETS)

The ETS Package (Banta, 2000) was used in the model to simulate the discharge of groundwater by ET in the Prado Basin and along the Santa Ana River riparian area. For the remainder of the study area, it was assumed that ET from groundwater does not occur from the saturated zone because depth to groundwater exceeds the extinction depth.

The ETS Package simulates ET with a relationship between the ET rate and depth to groundwater. The relation of evapotranspiration rate to depth to groundwater is conceptualized as a segmented line between an evaporation surface, where the evapotranspiration rate reaches a maximum, and an elevation located at an extinction depth below the evaporation surface, where the evapotranspiration rate reaches zero. The user may define as many intermediate segment endpoints as desired to state the relation of evapotranspiration rate to hydraulic head between these two elevations. When MODFLOW solves for groundwater elevations, the evapotranspiration rate of a model cell is determined by using the user-defined relationship of evapotranspiration rate to the calculated depth.

5.2.6.6 Horizontal-Flow Barrier Package (HFB)

The Horizontal-Flow Barrier (HFB) Package (Hsieh, et al., 1993) simulates thin low-permeability geologic features that impede the horizontal flow of groundwater. These geologic features are approximated as a series of horizontal-flow barriers conceptually situated on the boundaries between pairs of adjacent cells in the finite-difference grid. The key assumption underlying the FHB package is that the width of the barrier is negligibly small in comparison with the horizontal dimensions of the cells in the grid. Barrier width is not explicitly considered in the HFB package, but is included implicitly in the user-specified value of hydraulic conductivity. Furthermore, the barrier is assumed to have zero storage capacity. Its sole function is to lower the horizontal conductance between the cells that it separates. In the 2020 CVM, this package was used to simulate the behavior of internal faults and barriers that separate the Cucamonga and Six Basins from the Chino Basin and other internal barriers.

5.2.7 Other MODFLOW Packages

5.2.7.1 Preconditioned Conjugate-Gradient Package (PCG) and the Newton Solver (NWT)

The Preconditioned Conjugate-Gradient package (PCG) was selected as the numerical solver in the MODFLOW model during most of the calibration effort, as it runs faster than other solvers under the same convergence criteria and it was necessary due to the thousands of simulations required for sensitivity analyses and parameter estimation. The Newton Solver was used for final calibration simulations and all planning simulations.

5.2.7.2 Sensitivity Process (SEN) and Observation Process (OBS)

The Sensitivity Process (Hill, et al., 2000) was used to calculate the sensitivity of hydraulic heads throughout the model with respect to specified parameters using the accurate sensitivity-equation method. These are called grid sensitivities. The Observation Process uses the grid sensitivities to calculate sensitivities for the simulated values associated with the observations. These are called observation sensitivities. Observation sensitivities are used to calculate a number of statistics that can be used (1) to diagnose inadequate data, (2) to identify parameters that probably cannot be estimated by regression using the available observations. In addition, observation sensitivities may be used to evaluate the utility of proposed new data in future.

Prior to executing model calibration, the observation sensitivity values were calculated, and used to guide the selection of calibration wells ensuring that adequate observation sensitivities exist in the selected wells.

Table 5-1a The Initial Parameter Estimates and Ranges based on the lithology model

Zone	Layer	Horizontal Hydraulic Conductivity (ft/day)			Vertical Hydraulic Conductivity (ft/day)			Specific Yield (-)		
		Min	Max	Mean	Min	Max	Mean	Min	Max	Mean
1	1	3.23E+01	1.84E+02	6.54E+01	3.87E-02	3.23E+01	9.45E+00	7.88E-02	1.88E-01	1.33E-01
2	1	3.32E+01	7.15E+01	5.50E+01	1.74E+00	2.26E+01	1.05E+01	9.89E-02	1.61E-01	1.32E-01
3	1	3.20E+01	1.83E+02	9.78E+01	1.35E-01	5.04E+01	1.19E+01	7.98E-02	1.95E-01	1.42E-01
4	1	3.29E+01	1.51E+02	7.04E+01	1.47E+00	3.34E+01	1.06E+01	8.67E-02	1.92E-01	1.41E-01
5	1	3.15E+01	1.55E+02	7.92E+01	1.00E-02	8.67E+01	6.15E+00	8.06E-02	1.77E-01	1.22E-01
6	1	2.79E+01	1.71E+02	7.07E+01	1.02E-02	6.10E+01	9.48E+00	7.21E-02	1.86E-01	1.27E-01
7	1	3.89E+01	1.20E+02	6.80E+01	1.06E-02	3.47E+01	4.18E+00	8.07E-02	1.83E-01	1.26E-01
8	1	2.63E+01	1.19E+02	5.46E+01	1.00E-02	1.76E+01	2.54E+00	7.16E-02	1.52E-01	1.03E-01
9	1	4.35E+01	1.68E+02	8.70E+01	1.25E-02	4.30E+01	1.36E+01	9.69E-02	2.11E-01	1.56E-01
10	1	4.26E+01	1.04E+02	6.60E+01	1.89E-02	2.24E+01	6.88E+00	1.05E-01	1.85E-01	1.41E-01
11	1	5.42E+01	1.74E+02	1.02E+02	1.51E+00	9.28E+01	4.53E+01	1.24E-01	2.15E-01	1.75E-01
12	1	2.00E+01	1.46E+02	7.68E+01	1.50E+00	9.28E+01	2.75E+01	5.00E-02	2.07E-01	1.31E-01
13	1	3.34E+01	1.23E+02	6.85E+01	1.00E-02	1.94E+01	2.86E+00	6.93E-02	1.42E-01	1.09E-01
14	1	5.11E+00	1.06E+02	4.64E+01	6.33E-01	4.10E+01	1.47E+01	3.78E-02	2.07E-01	1.10E-01
1	2	2.94E+01	1.77E+02	6.54E+01	3.87E-02	3.23E+01	9.45E+00	5.66E-02	1.84E-01	1.33E-01
2	2	3.35E+01	7.24E+01	5.50E+01	1.74E+00	2.26E+01	1.05E+01	9.39E-02	1.61E-01	1.32E-01
3	2	1.24E+00	1.87E+02	9.75E+01	1.22E-01	5.04E+01	1.19E+01	2.52E-02	1.96E-01	1.41E-01
4	2	3.76E+00	1.56E+02	7.03E+01	1.40E-01	3.34E+01	1.06E+01	3.60E-02	1.90E-01	1.40E-01
5	2	1.00E-01	1.31E+02	3.74E-01	1.00E-02	1.71E+01	2.64E-02	1.51E-02	1.55E-01	3.03E-02
6	2	1.00E-01	8.88E+01	2.49E-01	1.00E-02	2.30E+01	3.13E-02	3.00E-02	1.41E-01	3.02E-02
7	2	1.00E-01	7.52E+01	3.45E-01	1.00E-02	2.35E+01	3.88E-02	3.00E-02	1.55E-01	3.04E-02
8	2	1.00E-01	7.37E+01	3.74E-01	1.00E-02	3.92E+00	2.20E-02	3.00E-02	1.09E-01	3.04E-02
9	2	3.39E+00	1.66E+02	8.67E+01	1.25E-02	4.30E+01	1.37E+01	3.51E-02	2.11E-01	1.56E-01
10	2	1.00E-01	9.49E+01	4.26E-01	1.00E-02	1.83E+01	7.73E-02	3.00E-02	1.46E-01	3.05E-02
11	2	7.34E+00	1.75E+02	1.02E+02	9.55E-01	9.28E+01	4.53E+01	4.10E-02	2.14E-01	1.74E-01
12	2	1.27E+00	1.49E+02	7.67E+01	3.28E-01	9.28E+01	2.75E+01	3.22E-02	2.06E-01	1.31E-01
13	2	4.43E+00	1.26E+02	6.77E+01	1.00E-02	1.94E+01	2.83E+00	3.48E-02	1.41E-01	1.08E-01
14	2	5.25E+00	1.08E+02	4.66E+01	6.33E-01	4.10E+01	1.47E+01	3.81E-02	2.00E-01	1.09E-01
1	3	1.61E+01	1.74E+02	6.33E+01	1.00E-02	6.21E+01	2.49E+01	3.95E-02	2.21E-01	1.40E-01
2	3	3.28E+00	5.95E+01	4.09E+01	1.60E+00	1.96E+01	8.17E+00	4.98E-02	1.31E-01	9.92E-02
3	3	2.66E+01	1.70E+02	7.30E+01	1.00E-02	1.18E+02	2.02E+01	2.76E-02	2.12E-01	1.25E-01
4	3	5.99E+00	1.47E+02	4.86E+01	2.83E-02	1.43E+02	1.28E+01	2.50E-02	2.06E-01	1.04E-01
5	3	7.27E+00	6.66E+01	2.53E+01	1.00E-02	3.23E+01	2.25E+00	4.00E-02	1.23E-01	6.73E-02
6	3	2.18E+01	1.56E+02	5.56E+01	9.59E-01	1.47E+02	1.90E+01	6.20E-02	1.88E-01	1.09E-01
7	3	1.95E+01	1.30E+02	6.26E+01	9.81E-02	6.68E+01	1.53E+01	6.54E-02	2.12E-01	1.21E-01
8	3	1.52E+01	1.95E+02	6.48E+01	1.19E+00	1.23E+02	3.84E+01	4.40E-02	2.23E-01	1.32E-01
9	3	2.26E+01	8.01E+01	3.89E+01	1.66E+00	2.15E+01	1.14E+01	7.53E-02	1.23E-01	9.65E-02
10	3	2.00E+01	1.32E+02	5.97E+01	1.21E+00	1.70E+02	4.06E+01	5.00E-02	2.18E-01	1.26E-01
11	3	7.73E+00	8.95E+01	3.91E+01	5.90E-01	7.88E+01	1.72E+01	4.00E-02	1.58E-01	8.45E-02
1	4	1.67E+01	1.74E+02	6.34E+01	1.00E-02	6.21E+01	2.49E+01	4.84E-02	2.21E-01	1.40E-01
2	4	3.28E+00	5.95E+01	4.10E+01	1.60E+00	1.96E+01	8.21E+00	4.98E-02	1.31E-01	9.93E-02
3	4	7.01E-01	1.70E+02	7.37E+01	1.00E-02	1.18E+02	2.26E+01	2.42E-02	2.12E-01	1.26E-01
4	4	1.00E-01	1.08E+02	2.61E-01	1.00E-02	5.85E+01	5.95E-02	3.00E-02	1.85E-01	3.02E-02
5	4	1.00E-01	4.53E+01	2.11E-01	1.00E-02	6.44E+00	1.76E-02	3.00E-02	8.69E-02	3.02E-02
6	4	1.00E-01	7.87E+01	2.11E-01	1.00E-02	6.33E+01	7.56E-02	3.00E-02	1.42E-01	3.01E-02

Table 5-1a The Initial Parameter Estimates and Ranges based on the lithology model

Zone	Layer	Horizontal Hydraulic Conductivity (ft/day)			Vertical Hydraulic Conductivity (ft/day)			Specific Yield (-)		
		Min	Max	Mean	Min	Max	Mean	Min	Max	Mean
7	4	1.00E-01	1.04E+02	3.74E-01	1.00E-02	4.82E+01	1.50E-01	3.00E-02	1.69E-01	3.05E-02
8	4	1.00E-01	4.60E+01	2.91E-01	1.00E-02	1.72E+01	5.35E-02	3.00E-02	1.03E-01	3.03E-02
9	4	3.75E+00	1.32E+02	5.96E+01	5.60E-01	1.70E+02	4.05E+01	3.50E-02	2.18E-01	1.26E-01
1	5	3.14E+01	2.11E+02	9.46E+01	1.15E-02	1.57E+02	3.70E+01	6.16E-02	2.26E-01	1.64E-01
2	5	2.90E+01	1.13E+02	5.41E+01	1.11E+00	1.31E+01	4.29E+00	7.46E-02	1.45E-01	1.09E-01
3	5	1.20E+01	1.80E+02	5.57E+01	1.00E-02	4.46E+01	1.26E+01	6.15E-02	2.12E-01	1.29E-01
4	5	1.72E+01	1.39E+02	3.95E+01	1.03E-02	3.32E+01	7.43E+00	6.39E-02	1.73E-01	1.04E-01
5	5	2.60E+01	8.51E+01	4.36E+01	8.43E-01	8.46E+00	2.74E+00	7.49E-02	1.61E-01	1.02E-01
6	5	1.51E+01	6.92E+01	3.09E+01	1.28E+00	2.87E+01	6.71E+00	5.43E-02	1.89E-01	9.31E-02
7	5	1.20E+01	7.29E+01	3.65E+01	2.42E+00	4.86E+01	1.80E+01	4.87E-02	2.05E-01	1.12E-01
8	5	2.93E+01	5.33E+01	4.35E+01	1.53E+00	1.96E+01	1.16E+01	8.37E-02	1.37E-01	1.15E-01
9	5	1.32E+01	6.95E+01	3.51E+01	1.50E+00	2.95E+01	8.16E+00	4.23E-02	1.21E-01	8.23E-02

Table 5-1b The Initial Parameter Estimates and Ranges Used to Start the Calibration

Zone	Layer	Horizontal Hydraulic Conductivity (ft/day)			Vertical Hydraulic Conductivity (ft/day)			Specific Yield[1] or Specific Storage[1] (-)		
		Min	Max	Mean	Min	Max	Mean	Min	Max	Mean
1	1	8.79E+01	5.00E+02	1.78E+02	1.94E-02	1.62E+01	4.74E+00	8.20E-02	1.96E-01	1.38E-01
2	1	4.08E+01	8.77E+01	6.74E+01	8.72E-01	1.13E+01	5.25E+00	1.03E-01	1.68E-01	1.38E-01
3	1	1.86E+01	1.07E+02	5.69E+01	6.75E-02	2.52E+01	5.97E+00	3.66E-02	8.98E-02	6.52E-02
4	1	5.02E+01	2.30E+02	1.07E+02	7.38E-01	1.67E+01	5.32E+00	3.98E-02	8.83E-02	6.46E-02
5	1	2.79E+01	1.38E+02	7.02E+01	1.82E-04	1.58E+00	1.12E-01	5.85E-02	1.28E-01	8.87E-02
6	1	1.33E+01	8.13E+01	3.36E+01	1.85E-04	1.11E+00	1.73E-01	5.24E-02	1.35E-01	9.23E-02
7	1	5.95E+01	1.83E+02	1.04E+02	1.55E-03	5.07E+00	6.10E-01	6.14E-02	1.40E-01	9.62E-02
8	1	2.10E+01	9.48E+01	4.36E+01	1.82E-04	3.21E-01	4.62E-02	5.45E-02	1.16E-01	7.87E-02
9	1	5.22E+01	2.02E+02	1.04E+02	6.25E-03	2.15E+01	6.82E+00	7.37E-02	1.61E-01	1.19E-01
10	1	3.44E+01	8.37E+01	5.32E+01	2.75E-03	3.26E+00	1.00E+00	8.30E-02	1.45E-01	1.11E-01
11	1	4.37E+01	1.40E+02	8.22E+01	2.20E-01	1.35E+01	6.61E+00	9.74E-02	1.69E-01	1.37E-01
12	1	9.56E+00	6.97E+01	3.67E+01	2.19E-01	1.35E+01	4.01E+00	5.45E-02	2.25E-01	1.43E-01
13	1	2.66E+01	9.82E+01	5.46E+01	1.82E-04	3.52E-01	5.20E-02	4.30E-02	8.79E-02	6.76E-02
14	1	6.13E+00	1.27E+02	5.57E+01	3.17E-01	2.05E+01	7.35E+00	2.88E-02	1.57E-01	8.34E-02
1	2	8.00E+01	4.81E+02	1.78E+02	1.84E-02	1.53E+01	4.49E+00	3.40E-05	1.10E-04	7.97E-05
2	2	4.10E+01	8.88E+01	6.74E+01	8.26E-01	1.08E+01	4.97E+00	5.63E-05	9.66E-05	7.94E-05
3	2	7.22E-01	1.09E+02	5.67E+01	5.81E-02	2.39E+01	5.65E+00	1.51E-05	1.18E-04	8.49E-05
4	2	5.73E+00	2.37E+02	1.07E+02	6.63E-02	1.59E+01	5.04E+00	2.16E-05	1.14E-04	8.43E-05
5	2	1.00E-03	1.31E+00	3.74E-03	2.57E-05	4.39E-02	6.80E-05	6.50E-08	6.69E-07	1.31E-07
6	2	1.00E-03	8.88E-01	2.49E-03	2.57E-05	5.91E-02	8.05E-05	1.30E-07	6.08E-07	1.31E-07
7	2	1.00E-03	7.52E-01	3.45E-03	2.43E-05	5.72E-02	9.42E-05	1.30E-07	6.71E-07	1.31E-07
8	2	1.00E-03	7.37E-01	3.74E-03	2.43E-05	9.53E-03	5.34E-05	1.30E-07	4.73E-07	1.31E-07
9	2	4.07E+00	1.99E+02	1.04E+02	3.75E-03	1.29E+01	4.10E+00	7.02E-08	4.23E-07	3.12E-07
10	2	8.06E-02	7.65E+01	3.44E-01	3.00E-03	5.50E+00	2.32E-02	6.00E-07	2.91E-06	6.10E-07
11	2	5.92E+00	1.41E+02	8.21E+01	2.87E-01	2.78E+01	1.36E+01	8.20E-08	4.28E-07	3.49E-07
12	2	6.05E-01	7.11E+01	3.67E+01	9.85E-02	2.78E+01	8.25E+00	6.44E-08	4.12E-07	2.62E-07
13	2	4.43E-02	1.26E+00	6.77E-01	2.43E-05	4.70E-02	6.89E-03	1.50E-07	6.10E-07	4.66E-07
14	2	6.30E+00	1.30E+02	5.59E+01	1.90E-01	1.23E+01	4.40E+00	7.63E-08	4.00E-07	2.18E-07
1	3	6.38E+00	6.87E+01	2.51E+01	4.75E-03	2.95E+01	1.18E+01	2.37E-05	1.33E-04	8.41E-05
2	3	1.30E+00	2.35E+01	1.62E+01	7.61E-01	9.31E+00	3.88E+00	2.99E-05	7.87E-05	5.95E-05
3	3	1.05E+01	6.71E+01	2.89E+01	4.75E-03	5.63E+01	9.61E+00	1.66E-05	1.27E-04	7.53E-05
4	3	1.04E+00	2.56E+01	8.47E+00	7.28E-06	3.67E-02	3.30E-03	1.08E-07	8.90E-07	4.51E-07
5	3	3.14E-01	2.88E+00	1.09E+00	2.43E-07	7.85E-04	5.46E-05	1.73E-07	5.32E-07	2.91E-07
6	3	9.41E-01	6.73E+00	2.40E+00	2.46E-04	3.77E-02	4.89E-03	2.68E-07	8.10E-07	4.70E-07
7	3	6.75E+00	4.51E+01	2.17E+01	2.52E-05	1.72E-02	3.93E-03	1.31E-07	4.24E-07	2.42E-07
8	3	5.28E+00	6.75E+01	2.25E+01	5.65E-01	5.82E+01	1.83E+01	8.80E-08	4.47E-07	2.64E-07
9	3	2.83E-01	1.00E+00	4.86E-01	4.97E-01	6.46E+00	3.42E+00	1.51E-06	2.47E-06	1.93E-06
10	3	3.94E+00	2.60E+01	1.18E+01	3.64E-01	5.10E+01	1.22E+01	1.00E-07	4.36E-07	2.52E-07
11	3	6.93E-01	8.03E+00	3.51E+00	1.52E-04	2.02E-02	4.42E-03	1.73E-07	6.83E-07	3.65E-07
1	4	6.61E+00	6.87E+01	2.51E+01	4.75E-03	2.95E+01	1.18E+01	2.91E-05	1.33E-04	8.41E-05
2	4	1.30E+00	2.35E+01	1.62E+01	7.61E-01	9.31E+00	3.90E+00	2.99E-05	7.87E-05	5.96E-05
3	4	2.77E-01	6.71E+01	2.92E+01	4.75E-03	5.63E+01	1.07E+01	1.45E-05	1.27E-04	7.57E-05
4	4	1.00E-03	1.08E+00	2.61E-03	2.57E-06	1.50E-02	1.53E-05	1.30E-07	8.00E-07	1.31E-07
5	4	1.00E-03	4.53E-01	2.11E-03	2.43E-07	1.56E-04	4.27E-07	1.30E-07	3.75E-07	1.30E-07
6	4	1.00E-03	7.87E-01	2.11E-03	2.57E-06	1.63E-02	1.94E-05	1.30E-07	6.14E-07	1.30E-07

Table 5-1b The Initial Parameter Estimates and Ranges Used to Start the Calibration

Zone	Layer	Horizontal Hydraulic Conductivity (ft/day)			Vertical Hydraulic Conductivity (ft/day)			Specific Yield[1] or Specific Storage[1] (-)		
		Min	Max	Mean	Min	Max	Mean	Min	Max	Mean
7	4	1.00E-03	1.04E+00	3.74E-03	3.00E-03	1.44E+01	4.51E-02	6.00E-07	3.38E-06	6.09E-07
8	4	4.32E-03	1.99E+00	1.26E-02	3.00E-03	5.17E+00	1.61E-02	6.00E-07	2.07E-06	6.06E-07
9	4	1.62E-01	5.70E+00	2.58E+00	1.68E-01	5.10E+01	1.22E+01	7.00E-07	4.36E-06	2.52E-06
1	5	5.03E+00	3.38E+01	1.51E+01	2.12E-03	2.90E+01	6.80E+00	8.20E-07	3.01E-06	2.18E-06
2	5	8.58E+00	3.35E+01	1.60E+01	3.73E-01	4.41E+00	1.45E+00	9.92E-07	1.93E-06	1.45E-06
3	5	1.67E+00	2.50E+01	7.74E+00	2.44E-03	1.09E+01	3.07E+00	6.95E-06	2.39E-05	1.46E-05
4	5	5.56E-01	4.49E+00	1.28E+00	1.59E-04	5.11E-01	1.14E-01	1.04E-06	2.82E-06	1.69E-06
5	5	5.85E+00	1.91E+01	9.80E+00	2.95E-06	2.96E-05	9.58E-06	7.00E-07	1.51E-06	9.55E-07
6	5	3.40E+00	1.55E+01	6.94E+00	4.48E-04	1.00E-02	2.35E-03	8.86E-07	3.07E-06	1.52E-06
7	5	4.19E+00	2.55E+01	1.28E+01	9.32E-02	1.87E+00	6.94E-01	7.94E-07	3.34E-06	1.83E-06
8	5	1.02E+01	1.86E+01	1.52E+01	5.90E-02	7.53E-01	4.45E-01	6.64E-07	1.09E-06	9.13E-07
9	5	4.61E+00	2.42E+01	1.23E+01	1.01E-01	1.98E+00	5.48E-01	2.23E-06	6.40E-06	4.34E-06

(1) Specific yield values are displayed for layer 1. Specific storage values are displayed for layers 2 to 5.

Table 5-2 Boundary Conditions

Geographic Name	Boundary Condition	MODFLOW Package	Source
San Gabriel Mountain Front to Cucamonga and Six Basins	Specified Flow[1]	FHB[5]	HSPF
Puente Hills/Chino Hills	Specified Flow[2]	FHB	R4
La Sierra Hills	Specified Flow[2]	FHB	R4
Hole Lake	Specified Flow[2]	FHB	R4
Jurupa Mountains and Pedley Hills	Specified Flow[2]	FHB	R4
Bloomington Divide	Specified Head and Flow[3]	FHB	Measured Water Levels
Rialto-Colton Fault	Constant Specified Flow	FHB	Estimated
Santa Ana Mountains	Specified Flow[2]	FHB	R4
Arlington Narrows	Specified Flow[2]	FHB	Arlington Model
DIPAW	Specified Flow[2]	RCH[6]	R4
Wells	Specified Flow[2]	WEL[7]	Measured and estimated by R4
Santa Ana River and its lower tributaries	Head-dependent Flow[4]	SFR2[8]	Inflow to streams estimated by R4
San Gabriel Mountain Tributaries	Specified Flow[2]	FHB	R4
MAR of imported and recycled waters	Specified Flow[2]	FHB	IEUA measured
MAR Stormwater	Specified Flow[2]	FHB	Measured and estimated by R4
Riparian evapotranspiration	Head-dependent Flow[4]	ETS[9]	See Section 3

1. Constant specified flow and time-variant specified flow
2. Time-variant specified flow
3. Time-variant specified head for calibration period and constant specified flow for planning alternatives
4. Flow rates are dependent on the simulated hydraulic heads
5. FHB – Flow and Head Boundary Package
6. RCH – Recharge Package
7. WEL – Well Package
8. SFR2 – Stream-Routing Package
9. ETS – Evapotranspiration Segments Package

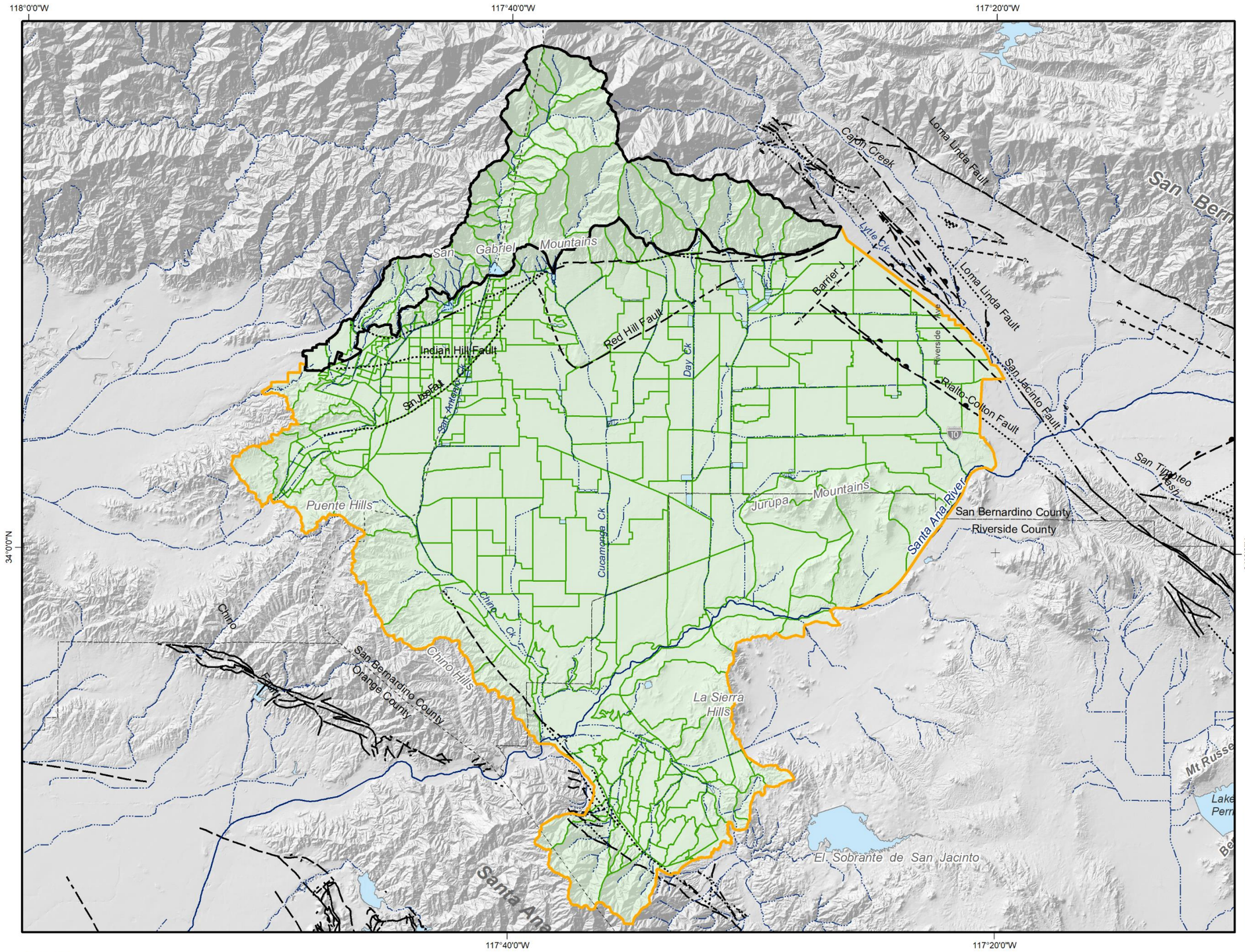

HSPF Model Domain

R4 Model Domain

Hydrologic Sub Area

Streams & Flood Control Channels

Flood Control & Conservation Basins

Faults

- Location Certain
- Location Approximate
- Approximate Location of Groundwater Barrier
- Location Concealed
- Location Uncertain

Prepared by:

WEI
WILDERMUTH ENVIRONMENTAL, INC.

Author: LS
Date: 3/31/2020
File: Figure 5-1 HSA NEW.mxd

0 1 2 3 4 5 Miles
0 2 4 6 8 Km

Prepared for:

2020 Safe Yield Recalculation

CHINO BASIN WATERMASTER
Partners in Basin Management

Hydrologic Sub Areas in the CVM Watershed Domain

Figure 5-1

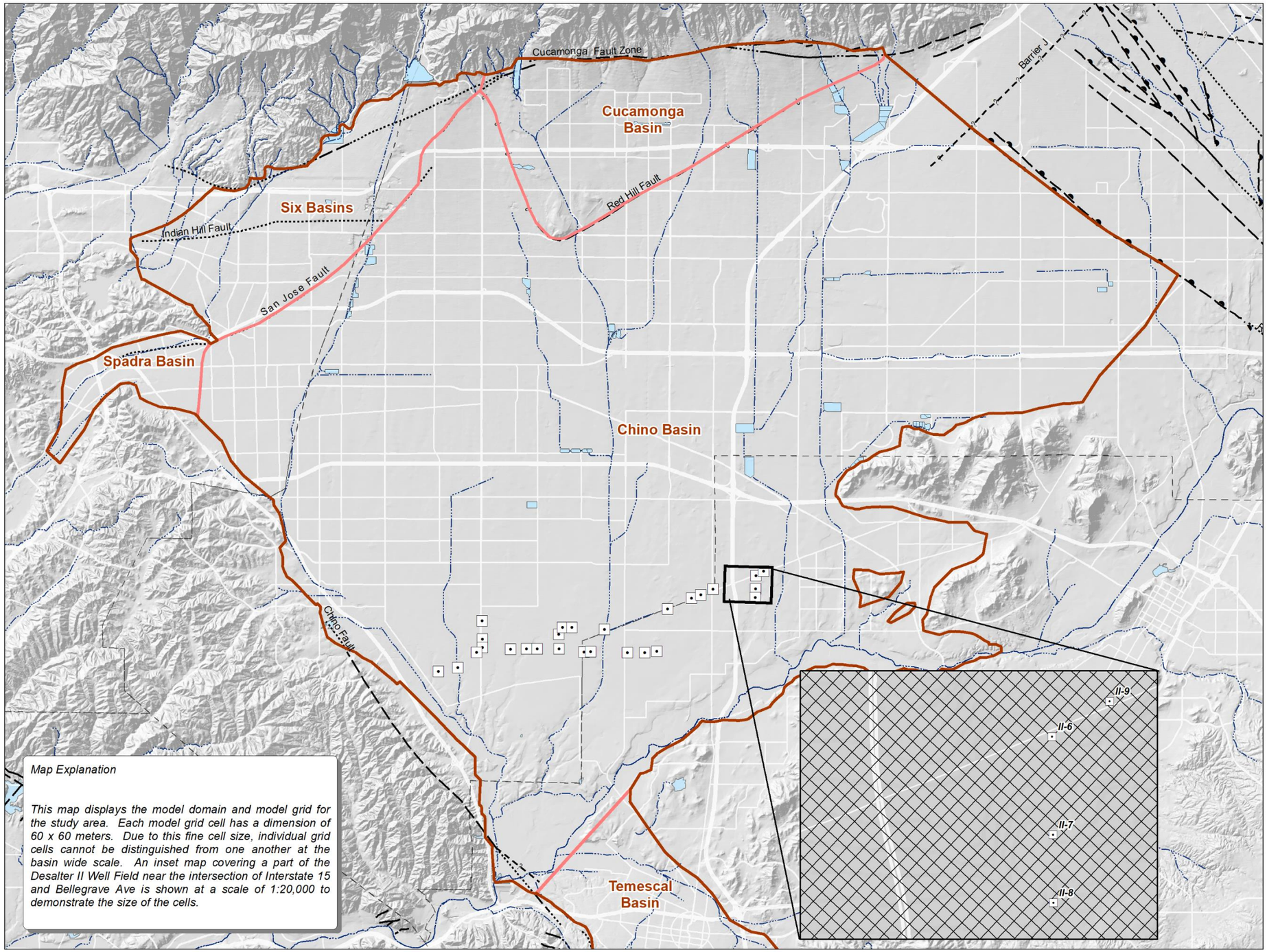

CVM Domain

Active CVM Domain

CVM Internal Basin Boundaries

CVM Grid

Chino Desalter Authority Well

Streams & Flood Control Channels

Flood Control & Conservation Basins

Faults

Location Certain

Location Concealed

Location Approximate

Location Uncertain

Approximate Location of Groundwater Barrier

Prepared by:

WEI
Wildermuth Environmental, Inc.

Author: LS
Date: 4/1/2020
File: Figure 5-2 model_domain_grid.mxd

0 1 2 3 4 5 Miles

0 2 4 6 8 Km

Prepared for:

2020 Safe Yield Recalculation

Chino Basin Watermaster
Partners in Basin Management

Map of CVM Domain and Grid

Figure 5-2

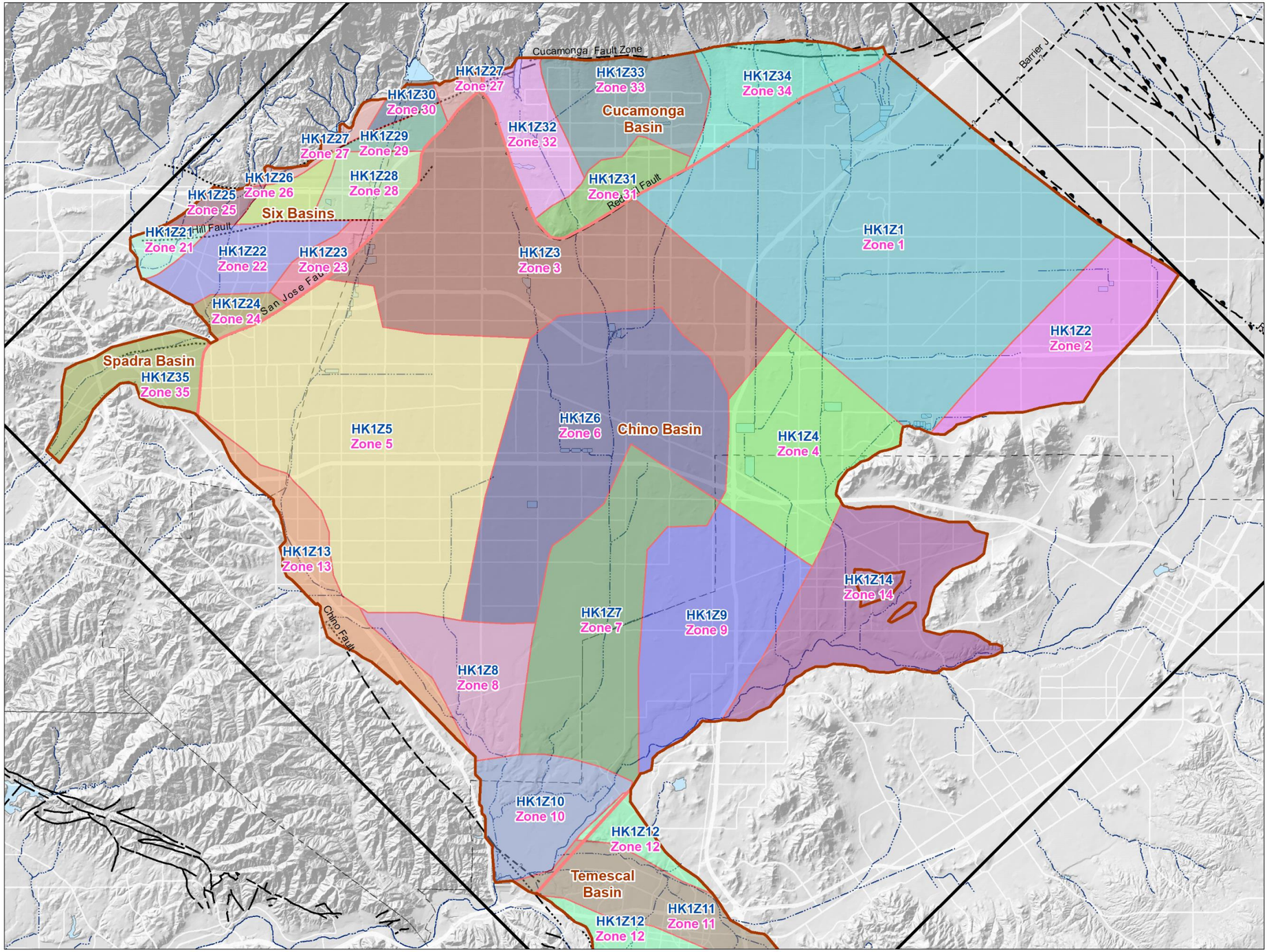

Parameter Zone

CVM Domain

Active CVM Domain

CVM Internal Basin Boundaries

Streams & Flood Control Channels

Flood Control & Conservation Basins

Faults

Location Certain

Location Approximate

Approximate Location of Groundwater Barrier

Location Concealed

Location Uncertain

Prepared by:

WEI
Wildermuth Environmental, Inc.

Author: LS
Date: 4/1/2020
File: Figure 5-3a par_zone.mxd

0 1 2 3 4 5 Miles

0 2 4 6 8 Km

Prepared for:

2020 Safe Yield Recalculation

Chino Basin Watermaster
Partners in Basin Management

CVM Hydraulic Parameter Zonation Layer 1

Figure 5-3a

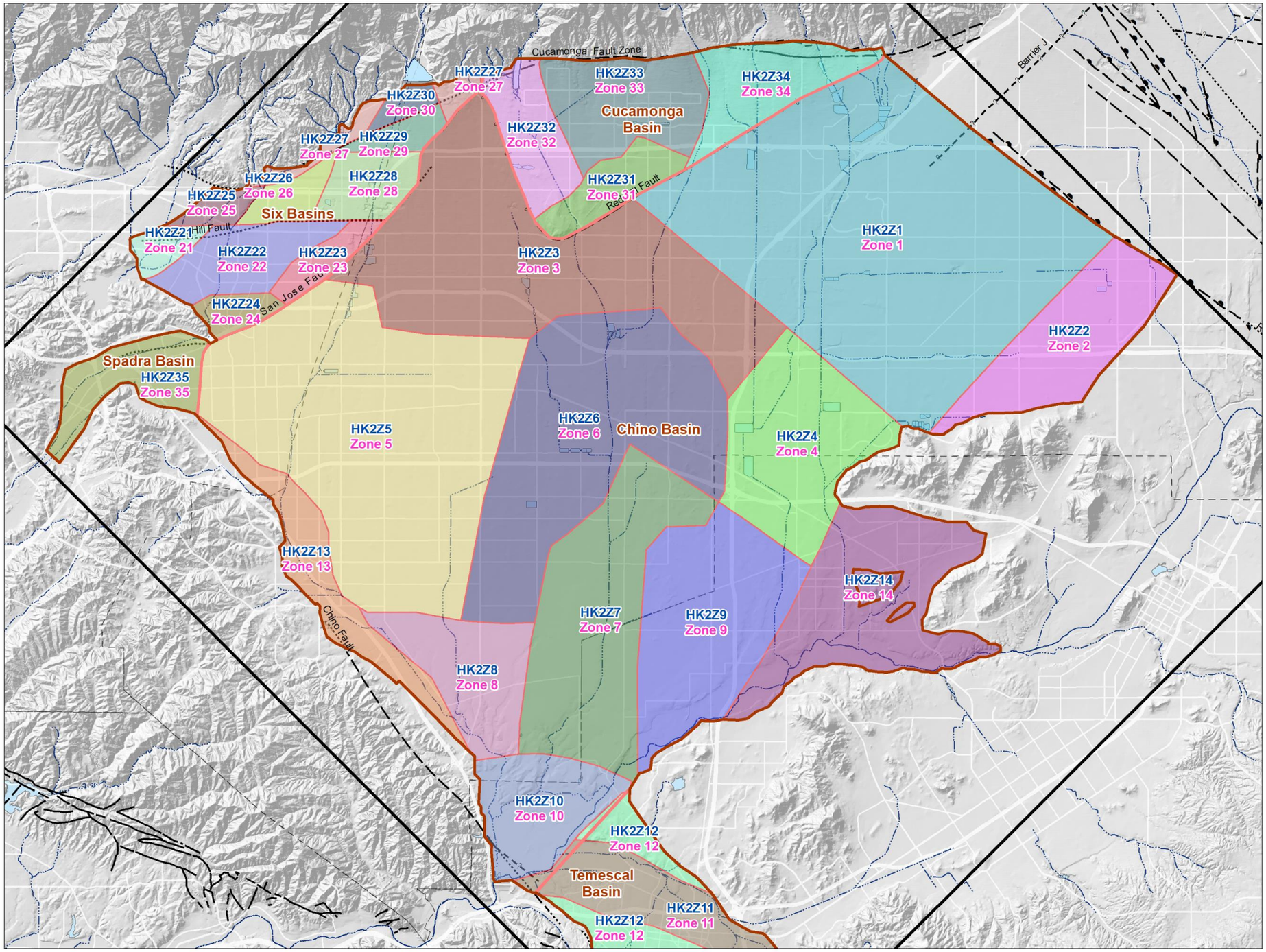

Parameter Zone

CVM Domain

Active CVM Domain

CVM Internal Basin Boundaries

Streams & Flood Control Channels

Flood Control & Conservation Basins

Faults

Location Certain

Location Concealed

Location Approximate

Location Uncertain

Approximate Location of Groundwater Barrier

Prepared by:

WEI
Wildermuth Environmental, Inc.

Author: LS
Date: 4/1/2020
File: Figure 5-3b par_zone.mxd

0 1 2 3 4 5 Miles

0 2 4 6 8 Km

Prepared for:

2020 Safe Yield Recalculation

Chino Basin Watermaster
Partners in Basin Management

CVM Hydraulic Parameter Zonation Layer 2

Figure 5-3b

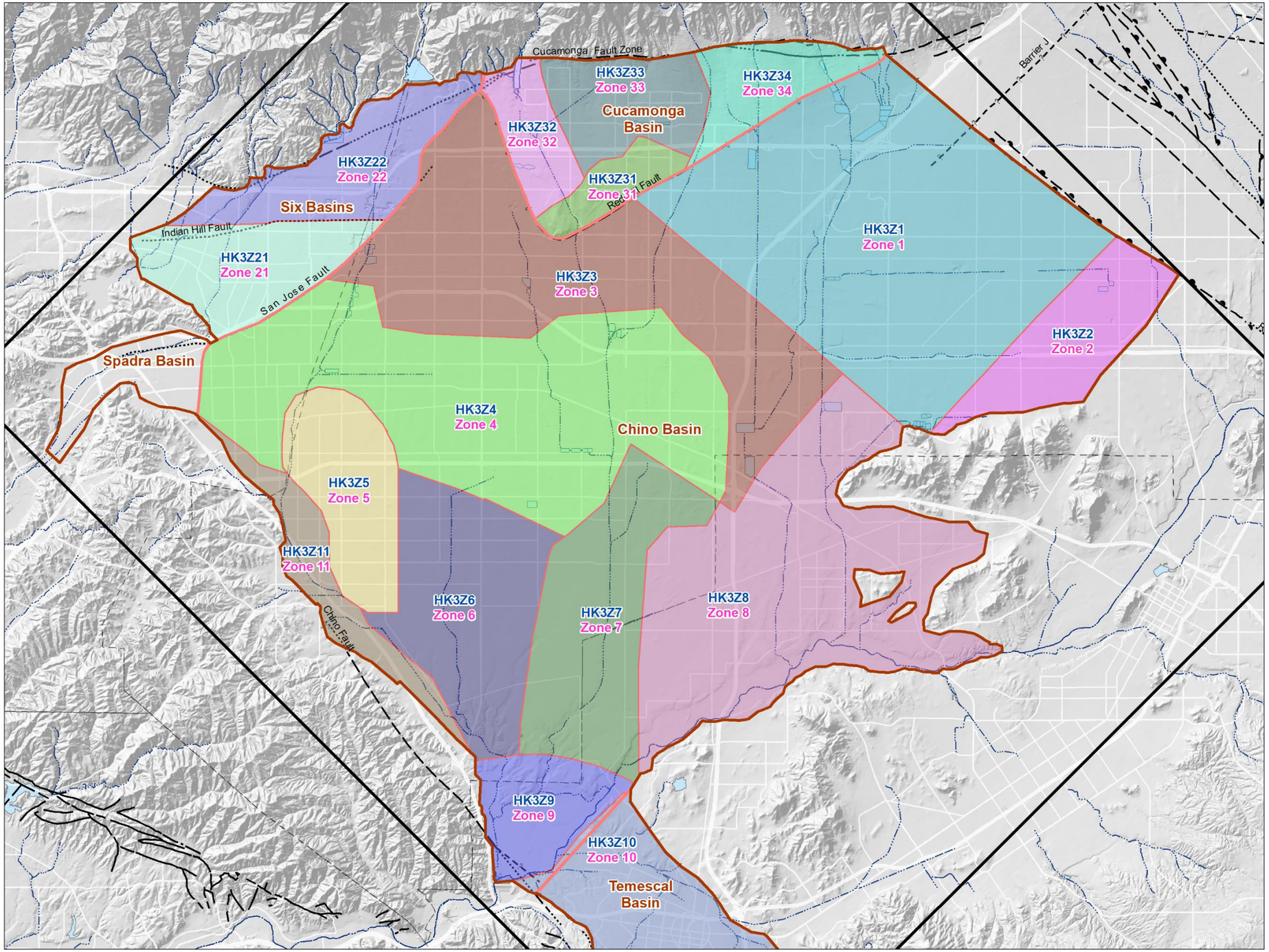

Parameter Zone

CVM Domain

Active CVM Domain

CVM Internal Basin Boundaries

Streams & Flood Control Channels

Flood Control & Conservation Basins

Faults

Location Certain

Location Concealed

Location Approximate

Location Uncertain

Approximate Location of Groundwater Barrier

Prepared by:

WEI
Wildermuth Environmental, Inc.

Author: LS
Date: 4/1/2020
File: Figure 5-3c par_zone.mxd

0 1 2 3 4 5 Miles

0 2 4 6 8 Km

Prepared for:

2020 Safe Yield Recalculation

Chino Basin Watermaster
Partners in Basin Management

CVM Hydraulic Parameter Zonation
Layer 3

Figure 5-3c

Parameter Zone

CVM Domain

Active CVM Domain

CVM Internal Basin Boundaries

Streams & Flood Control Channels

Flood Control & Conservation Basins

Faults

Location Certain

Location Concealed

Location Approximate

Location Uncertain

Approximate Location of Groundwater Barrier

Cucamonga Basin

Six Basins

Spadra Basin

Chino Basin

Temescal Basin

HK4Z1 Zone 1

HK4Z2 Zone 2

HK4Z3 Zone 3

HK4Z4 Zone 4

HK4Z5 Zone 5

HK4Z6 Zone 6

HK4Z7 Zone 7

HK4Z8 Zone 8

HK4Z9 Zone 9

Cucamonga Fault Zone

Red Hill Fault

Indian Hill Fault

San Jose Fault

Chino Fault

Barrier J

Prepared by:

WEI
Wildermuth Environmental, Inc.

Author: LS
Date: 4/1/2020
File: Figure 5-3d par_zone.mxd

0 1 2 3 4 5 Miles

0 2 4 6 8 Km

Prepared for:

2020 Safe Yield Recalculation

Chino Basin Watermaster
Partners in Basin Management

CVM Hydraulic Parameter Zonation Layer 4

Figure 5-3d

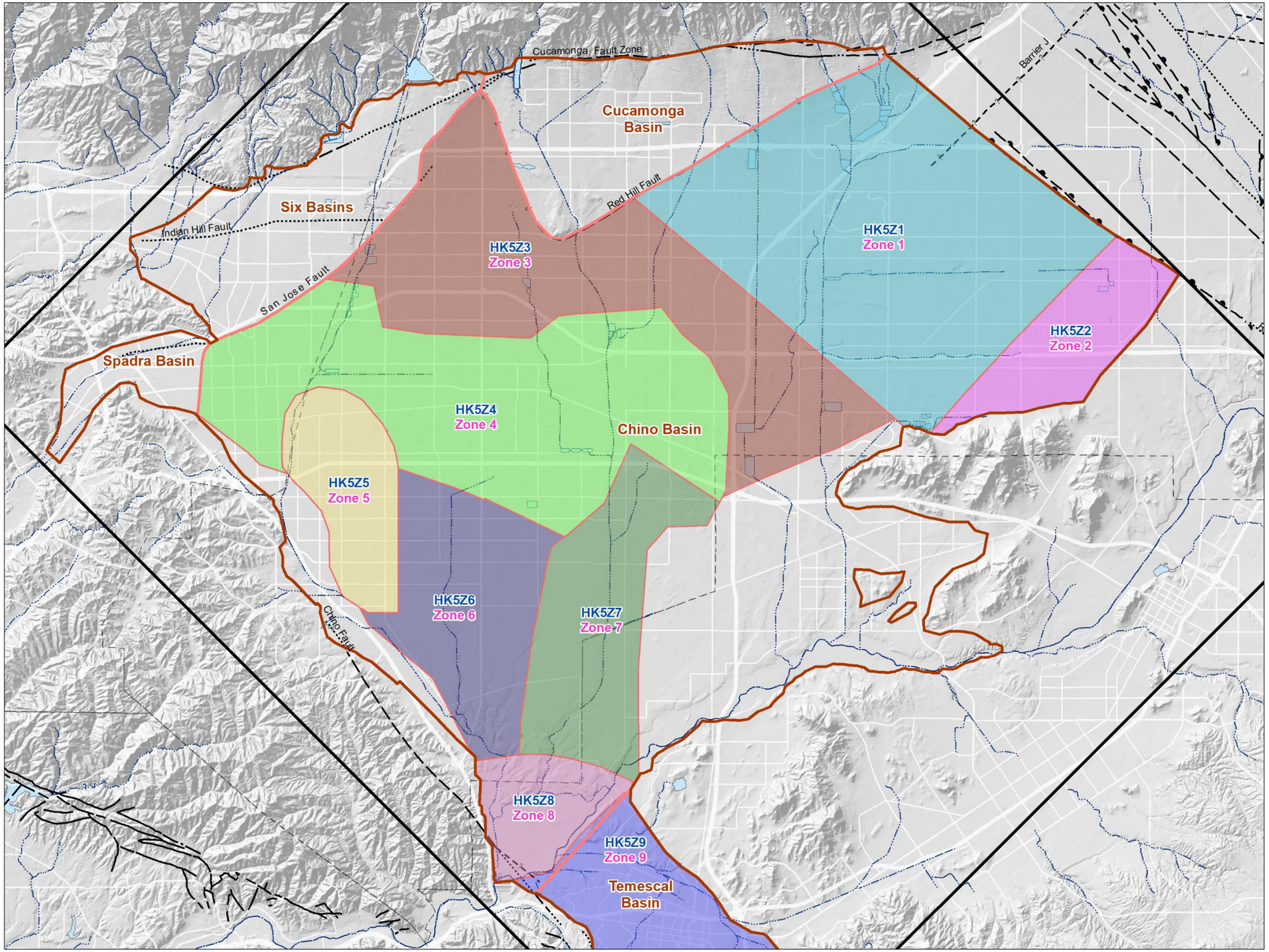

Parameter Zone

CVM Domain

Active CVM Domain

CVM Internal Basin Boundaries

Streams & Flood Control Channels

Flood Control & Conservation Basins

Faults

Location Certain

Location Concealed

Location Approximate

Location Uncertain

Approximate Location of Groundwater Barrier

Prepared by:

WEI
Wildermuth Environmental, Inc.

Author: LS
Date: 4/1/2020
File: Figure 5-3e par_zone.mxd

0 1 2 3 4 5 Miles

0 2 4 6 8 Km

Prepared for:

2020 Safe Yield Recalculation

Chino Basin Watermaster
Partners in Basin Management

CVM Hydraulic Parameter Zonation Layer 5

Figure 5-3e

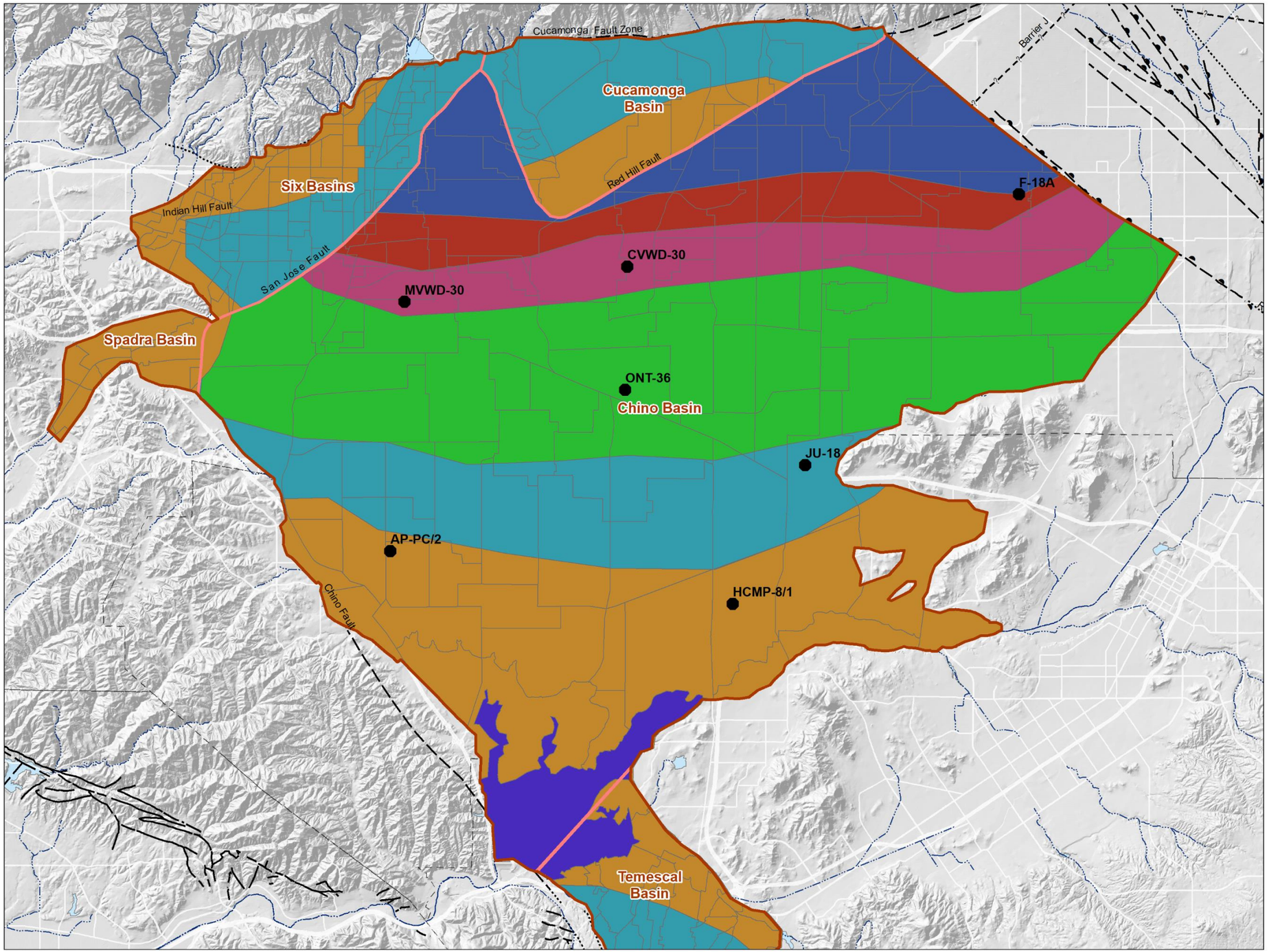

DIPAW Lag Zone by Year

- 0-4
- 5-10
- 11-15
- 16-20
- 21-25
- 26-30
- 31-36

- Boreholes Used in HYDRUS-2D
- Hydrologic Sub-Area (HSA)
- Active CVM Domain
- CVM Internal Basin Boundaries

- Streams & Flood Control Channels
- Flood Control & Conservation Basins

Faults

- Location Certain
- Location Approximate
- Location Concealed
- Location Uncertain
- Approximate Location of Groundwater Barrier

Prepared by:

WEI
Wildermuth Environmental, Inc.

Author: LS
Date: 4/1/2020
File: Figure 5-4 Lagtime.mxd

0 1 2 3 4 5 Miles
0 2 4 6 8 Km

Prepared for:

2020 Safe Yield Recalculation

Chino Basin Watermaster
Partners in Basin Management

Lag Time Distribution in the Active CVM Domain

Figure 5-4

Hydraulic Head Contours
(ft above mean sea-level)

Appropriative Pool Pumping Wells

- City of Chino
- City of Chino Hills
- City of Ontario
- City of Pomona
- City of Upland
- Cucamonga Valley Water District
- Fontana Water Company
- Jurupa Community Services District
- Monte Vista Water District
- Other Appropriators

Chino Desalter Authority Wells

Wells in Six Basin and Cucamonga Basin with Water Level Data from April-July of 1977

Streams & Flood Control Channels

Flood Control & Conservation Basins

Active CVM Domain

CVM Internal Basin Boundaries

OBMP Management Zones

Faults

- Location Certain
- Location Approximate
- Approximate Location of Groundwater Barrier
- Location Concealed
- Location Uncertain

Prepared by:

WEI
Wildermuth Environmental, Inc.

Author: LS
Date: 5/11/2020
File: Figure 5-5a 1977GWE_layer1.mxd

0 1 2 3 4 5 Miles
0 2 4 6 8 Km

Prepared for:

2020 Safe Yield Recalculation

Chino Basin Watermaster
Partners in Basin Management

Hydraulic Head Contours
Initial Condition Hydraulic Head Map
Layer 1 - July 1977

Figure 5-5a

Hydraulic Head Contours
(ft above mean sea-level)

Appropriative Pool Pumping Wells

- City of Chino
- City of Chino Hills
- City of Ontario
- City of Pomona
- City of Upland
- Cucamonga Valley Water District
- Fontana Water Company
- Jurupa Community Services District
- Monte Vista Water District
- Other Appropriators

Chino Desalter Authority Wells

Wells in Six Basin and Cucamonga Basin with Water Level Data from April-July of 1977

Streams & Flood Control Channels

Flood Control & Conservation Basins

Active CVM Domain

CVM Internal Basin Boundaries

OBMP Management Zones

Faults

- Location Certain
- Location Approximate
- Approximate Location of Groundwater Barrier
- Location Concealed
- Location Uncertain

Prepared by:

WEI
Wildermuth Environmental, Inc.

Author: LS
Date: 5/11/2020
File: Figure 5-5b 1977GWE_layer2.mxd

0 1 2 3 4 5 Miles
0 2 4 6 8 Km

Prepared for:

2020 Safe Yield Recalculation

Chino Basin Watermaster
Partners in Basin Management

Hydraulic Head Contours
Initial Condition Hydraulic Head Map
Layer 3 - July 1977

Figure 5-5b

Hydraulic Head Contours
(ft above mean sea-level)

Appropriative Pool Pumping Wells

- City of Chino
- City of Chino Hills
- City of Ontario
- City of Pomona
- City of Upland
- Cucamonga Valley Water District
- Fontana Water Company
- Jurupa Community Services District
- Monte Vista Water District
- Other Appropriators

Chino Desalter Authority Wells

Streams & Flood Control Channels

Flood Control & Conservation Basins

Active CVM Domain

CVM Internal Basin Boundaries

OBMP Management Zones

Faults

- Location Certain
- Location Approximate
- Approximate Location of Groundwater Barrier
- Location Concealed
- Location Uncertain

Prepared by:

WEI
Wildermuth Environmental, Inc.

Author: LS
Date: 5/11/2020
File: Figure 5-5c 1977GWE_layer3.mxd

0 1 2 3 4 5 Miles
0 2 4 6 8 Km

Prepared for:

2020 Safe Yield Recalculation

Chino Basin Watermaster
Partners in Basin Management

Hydraulic Head Contours
Initial Condition Hydraulic Head Map
Layer 5 - July 1977

Figure 5-5c

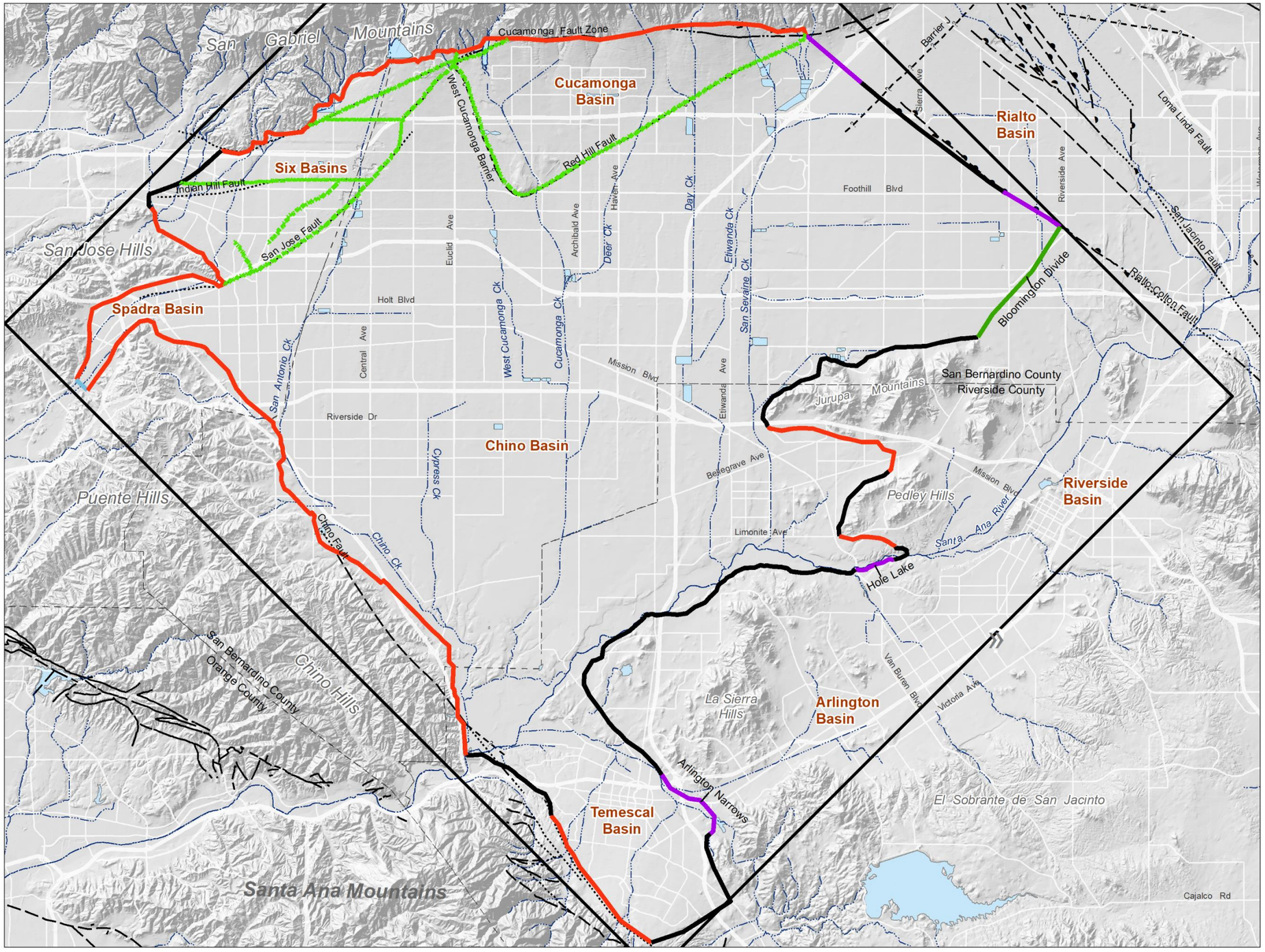

Prepared by:

WEI
Wildermuth Environmental, Inc.

Author: LS
Date: 4/1/2020
File: Figure 5-6 bndry_cond.mxd

0 1 2 3 4 5 Miles
0 2 4 6 8 Km

Prepared for:

2020 Safe Yield Recalculation

Chino Basin Watermaster
Partners in Basin Management

CVM Boundary Conditions

Figure 5-6

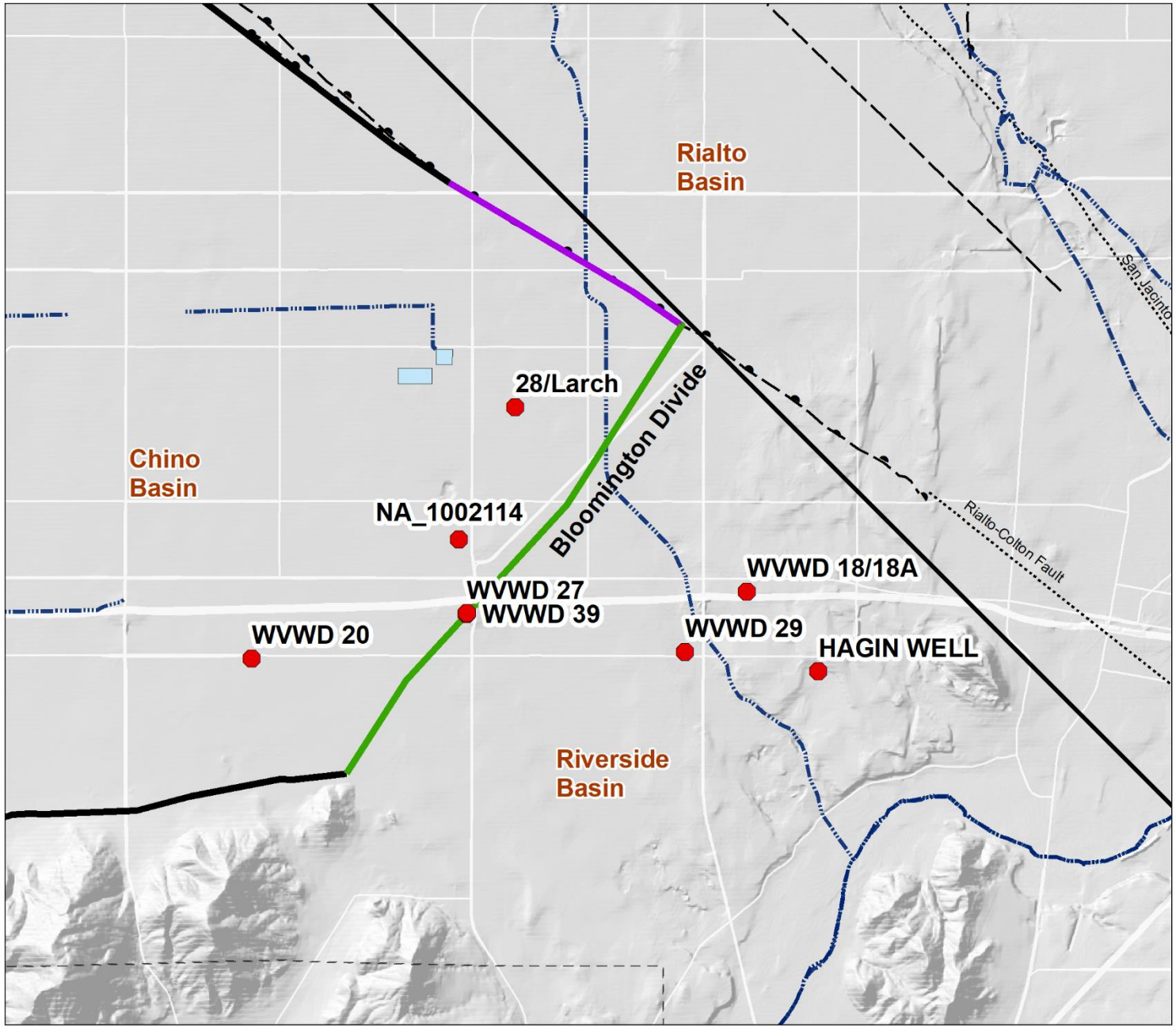

Well with HIstorical Water Levels in Figure 5-7

No-Flow Boundary

Specified Flow Boundary

Specified Head Boundary

CVM Domain

Streams & Flood Control Channels

Flood Control & Conservation Basins

Faults

Location Certain

Location Approximate

Approximate Location of Groundwater Barrier

Location Concealed

Location Uncertain

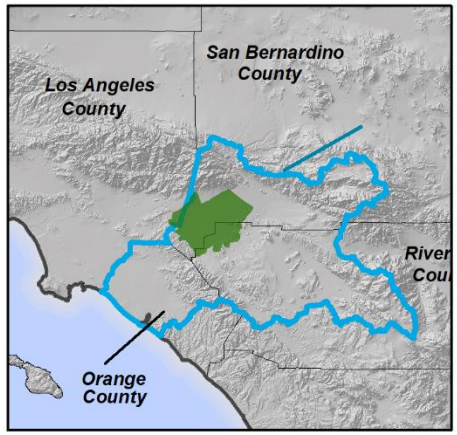

Prepared by:

WEI
WILDERMUTH ENVIRONMENTAL, INC.

Author: LS
Date: 4/1/2020
File: Figure 5-7 blm_div.mxd

0 1 Miles
0 2 Km

Prepared for:

2020 Safe Yield Recalculation

Location of Wells With Historical Water Level Records
Bloomington Divide Area

Figure 5-7

Figure 5-8
Comparison of Groundwater Level Across the Bloomington Divide

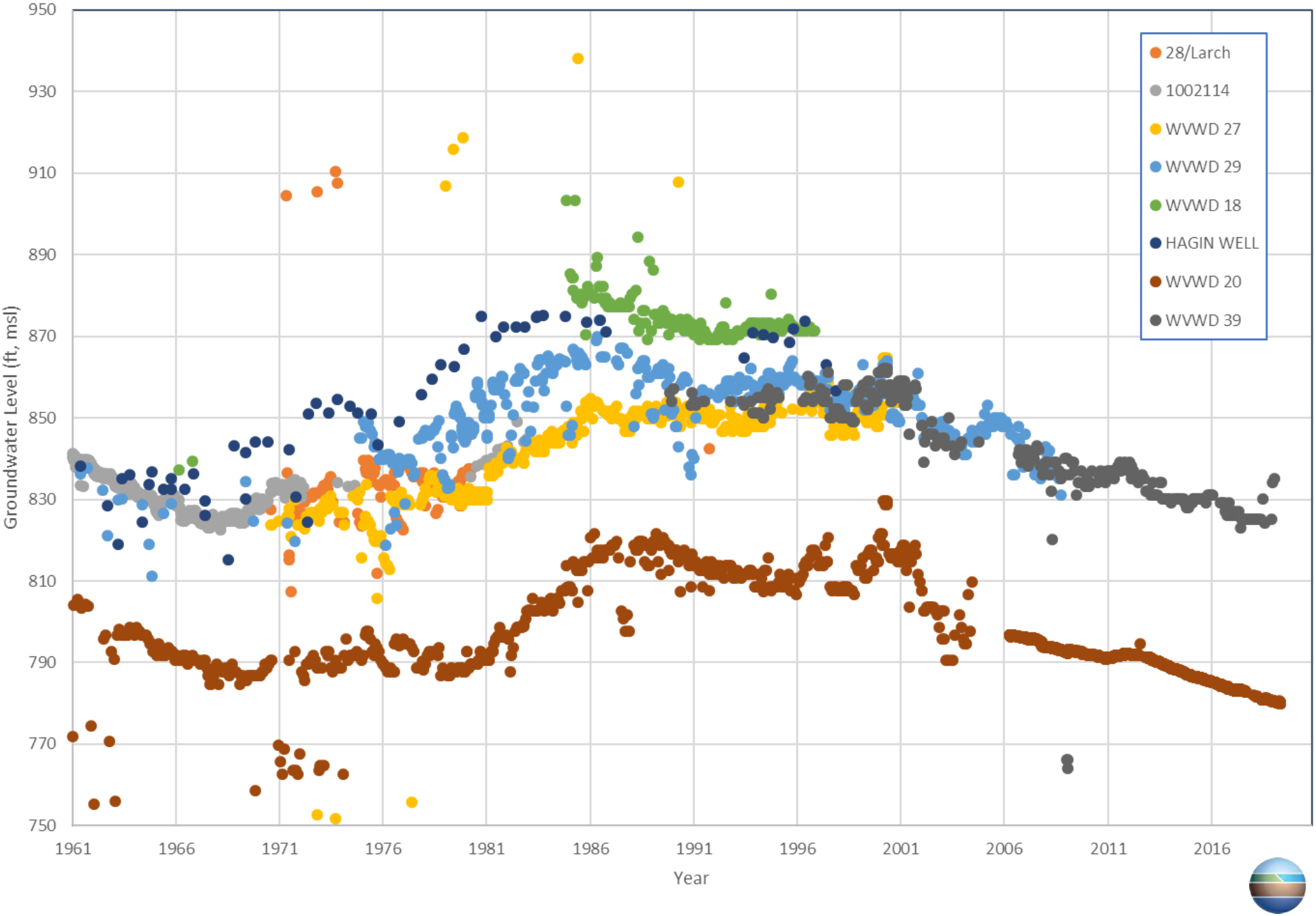

IEUA CCWRF
WTP
IEUA RP-5
WTP
IEUA RP-1
WTP
WRCWRA TP
WTP
Corona TP 1B
WTP
Riverside TP
WTP
Santa Ana River at MWD Crossing
Temescal Wash at Main Street
Chino Fault

Stream Chennels Where MODFLOW SFR2 Package is Used
WTP Recycled Water Discharge Location
Surface Water Discharge Location
Active CVM Domain
CVM Domain
Streams & Flood Control Channels
Flood Control & Conservation Basins

Faults
Location Certain
Location Concealed
Location Approximate
Location Uncertain
Approximate Location of Groundwater Barrier

Prepared by:
WEI
Wildermuth Environmental, Inc.

Author: LS
Date: 4/1/2020
File: Figure 5-9 Stream Package.mxd

0 1 2 3 4 5 Miles
0 2 4 6 8 Km

Prepared for:
2020 Safe Yield Recalculation
Chino Basin Watermaster
Partners in Basin Management

SFR2 Package for Stream Segments where Simulation of Groundwater and Surface Water Interaction Occurs

Figure 5-9

The purpose of model calibration is to estimate the best set of the model parameters and to use them estimate the water budget. Calibration is the process of adjusting model parameters to produce the best match between simulated and observed system responses that include time series of surface water discharge and groundwater levels at wells. During the process of calibration, model parameters are adjusted (subject to reasonable bounds) with manual methods and/or automatic parameter estimation techniques to match observed surface water discharge at gaging stations and water levels at wells.

The HSPF and R4 models were calibrated manually to match surface water discharges at gaging stations and estimated recharge at flood control and water conservation basins. After the R4 model was calibrated for surface water, the R4 root zone module was manually calibrated to match urban irrigation demands. This section describes the calibration results for these models.

MODFLOW-2000 (Harbaugh et al, 2000), UCODE_2014 (Poeter, et al., 2014), and PEST (Doherty, 2019b) provide means to automate parameter estimation and evaluate the resulting model. Automatic parameter estimation is often referred to as inverse modeling. Numerical inverse methods are widely used in hydrology and are discussed in numerous scientific publications and books, for example Carrera, et al. (1986a; 1986b; 1986c), Doherty (2015), Neuman (1973), and Yeh (1986). The calibration of the 2020 CVM involves both manual calibration and inverse modeling with PEST. As described in Section 4, PEST was selected due to its robust calibration capabilities. This section describes the procedure for calibrating the groundwater flow model; defines the objective function, minimization algorithm, and sensitivity analysis; discusses calibration data selection, calibration and residual analysis; and presents the historical water budget for the calibration period.

6.1 Calibration Criteria

The difference between the measured and computed system responses at the calibration points are termed residuals. The sum of the squared-weighted residuals is the objective function used in this calibration effort. Calibration concluded when the objective function could no longer be practically minimized. One estimate of the goodness of fit for model calibration is the coefficient of determination (R^2 or R-square) statistic. In words, the coefficient of determination is the fraction of the observed variance that is explained by the model.

Another estimate of the goodness of fit for model calibration is the Nash-Sutcliffe efficiency (NSE) index (Nash, et al., 1970). The NSE index is a normalized statistic that determines the relative magnitude of the residual variance (*noise*) compared to the measured data variance (*information*). The NSE index indicates how well the plot of observed versus simulated data fits the *perfect-fit* line. Servat, et al. (1991) found the NSE index to be the best objective function for reflecting the overall fit of a hydrograph.

The NSE index is computed as shown below:

$$NSE = 1 - \frac{\sum_{i=1}^{n}(h_m - h_s)_i^2}{\sum_{i=1}^{n}(h_m - \bar{h}_m)_i^2}$$

Where h_m is the measured (observed) head or discharge value, h_s is the simulated counterpart, and n is the number of measured values.

Nash-Sutcliffe efficiencies range from $-\infty$ to 1 (inclusive), with the NSE index equal to 1 being the optimal value. Values between 0.0 and 1.0 are generally viewed as acceptable levels of performance,

whereas values < 0.0 indicate that the mean observed value is a better predictor than the simulated value, which indicates unacceptable performance. Moriasi, et al. (2007) provided a thorough literature review of reported model performance ratings for NSE and recommended following performance ratings for models with monthly time steps: $-\infty$ to 0.5 as unsatisfactory; 0.5 to 0.65 as satisfactory; 0.65 to 0.75 as good; 0.75 to 1.0 as very good.

The NSE index was used herein for two major reasons: (1) it is recommended for use by ASCE (1993) and Legates et al. (1999), and (2) it is commonly used, which provides extensive information on reported values. Sevat et al. (1991) found the NSE index to be the best objective function for reflecting the overall fit of a hydrograph.

6.2 Calibration of the Surface Water Models

6.2.1 Calibration to Estimated Discharge and Diversions

The locations of gaging stations used to calibrate the surface water models are shown in Figure 6-1. The table below lists the gaging stations that were used to calibrate the HSPF and R4 models and their respective R^2 and NSE indexes. These models were calibrated manually. With the exception of Live oak Canyon that overlies the Six Basins and discharges to the San Gabriel River watershed, calibration matches are characterized as good to very good. Figures 6-2 and 6-3 are scatter plots that show the goodness of fit of the gaging station estimates of monthly surface water discharge to model estimated monthly discharge for Chino Creek and Cucamonga Creek, respectively.

Statistics for Surface Water Model Calibration

Gaging Station	Watershed Type	Model	R^2	NSE
Live Oak Canyon (LACFCD)	SGM	HSPF	0.29	0.05
San Antonio Creek at San Antonio Creek Dam (USACE)	SGM	HSPF	0.69	0.64
Cucamonga Creek near Mira Loma (USGS 11073495)	SGM	HSPF	0.85	0.84
Day Creek near Etiwanda (USGS 11067000)	SGM	HSPF	0.69	0.67
Chino Creek at Schaefer Avenue (USGS 11073360)	Valley Floor	R4	0.91	0.95
Cucamonga Creek near Mira Loma (USGS 11073495)	Valley Floor	R4	0.81	0.77

IEUA operates a series of flood control and conservation Basins in the Chino Basin the locations of which are shown in Figure 6-1. IEUA estimates the amount of stormwater diverted into these basins using a variety of water level sensors, other observations and assumptions of basin infiltration rates and reports the diversions as monthly totals. The R4 model was calibrated to match its estimates of stormwater recharge to IEUA diversion estimates. Facility information that is input to the R4 model include diversion rating curves for basin inlets, elevation-area-storage curves, outlet ratings curves and depth dependent infiltration rates and evaporation data. The table below lists these basins and the R^2 achieved in calibration. NSE indices were not calculated because the sample size was small.

Review of these figures and statistics indicate that the calibration of the R4 model for surface water discharge, streambed recharge and recharge in flood control and water conservation basins ranges from unsatisfactory (three basins), satisfactory (two basins) and good to very good (eight basins). As to this calibration two things are worth noting.

- The R4 model computes recharge taking into account evaporation, infiltration and overflow. IEUA estimates diversion using measured water surface elevation data and other which is sometimes incomplete and other assumption, ignores evaporation and cannot account for inflows that are less than the infiltration rates. The R4 estimates of recharge and IEUA diversion estimates are not exactly the same thing.
- The R4 model assumes a constant albeit complicated set of operating rules consistent with an operating agreement between the San Bernardino County Flood Control District (SBCFCD), Watermaster and Chino Basin Water Conservation District. In practice and with approval with the SBCFCD, IEUA deviates from the operating rules in the agreement to maximize recharge without compromising safety.

Flood Control and Conservation Basins used to Calibrate the Surface Water Models

Flood Control and Conservation Basin	R^2
Upland Basin	0.79
Montclair Basins	0..88
Brook Street Basin	0.84
$7^{th}/8^{th}$ Street Basins	0.68
Ely Basins	0.56
Turner Basins	0.64
Lower Day Basin	0.86
Etiwanda Debris Basin	0.67
Victoria Basin	0.81
San Sevaine Basins	0.83
Banana/Hickory Basins	0.27
RP3 Basins	0.14
Declez Basin	0.35
Grove Basin	0.34

6.2.2 Calibration of Urban Irrigation Demand

The R4 model is used to estimate DIPAW at the root zone. To do that reliably, the R4 model needs to be able to estimate the magnitude and timing of irrigation. The R4 root zone module determines the demand for irrigation based on soil moisture storage available for use by vegetation and it schedules irrigation to ensure there is adequate moisture for the vegetation. IEUA collects monthly water demand and water sources used by all its member agencies and sewerage inflow estimates to their treatment plants. These data can be used with dry-weather discharge estimates from USGS gages on Chino and Cucamonga Creeks, and estimated OWDS discharges to estimate urban irrigation demand. The monthly

urban irrigation demand in each sewershed is estimated to be equal to the total potable supply to the sewershed minus the sum of sewage inflow to the plants plus OWDS discharge plus dry-weather discharge. The R4 root zone module is calibrated to match this estimate of urban irrigation in each sewershed and then generalized to the remainder of the 2020 CVM watershed. Figures 6-4a and 6-4b show the IEUA estimated total monthly water supply to the RP1/RP4 and RP2/CC/RP5 sewersheds, respectively, and the efficacy of the potable supply including the R4-estimated urban irrigation supply. The green bars show the R4-estimated urban irrigation supply and demonstrate the ability of the R4 model to replicate the urban irrigation demand and the historical seasonality. Figures 6-5a and 6-5b are scatter plots that show the IEUA estimated total monthly water supply to the RP1/RP4 and RP2/CC/RP5 sewersheds, respectively, and efficacy of the potable water supply. The table below shows the R^2 and NSE indices achieved in the R4 model calibration. Review of these figures and statistics indicate that the calibration of the R4 model for scheduling irrigation during the calibration period ranges from satisfactory to very good.

Statistics for the R4 Calibration of Urban Irrigation Demand

Sewershed	R2	NSE
RP1/RP4	0.76	0.74
RP2/CC/RP5	0.71	0.68

6.3 Calibration of the Groundwater Model

6.3.1 Model Calibration Procedure and Strategy

The parameter estimation program PEST Version 17 (Doherty, 2019) was used to calibrate the 2020 CVM that includes the Chino Basin, Cucamonga Basin, Six-Basin, Spadra Basin, and Temescal Basin. The major steps in the model calibration process include:

1. Numerical Formulation of Conceptual Model. Calibration starts with the development of model conceptualization and mathematical-numerical descriptions of relevant physical processes. First, the conceptual model is converted to a numerical model. The numerical conversion includes the definition of the model aquifer geometry, the assignment of initial and boundary conditions, discretization in space and time, and the selection of hydraulic parameter zonation and heterogeneity. Next, forward modeling is conducted to check the water balance and for possible errors caused in the process of conceptual model conversion. Finally, modeling results are checked to see whether the numerical model can simulate the groundwater system's behavior under measured conditions. All the model parameters, including the model inputs that can be parameterized, are then fixed at their best estimates. Forward modeling is solved by the MODFLOW-2000 groundwater model.
2. Sensitivity Analysis. The next step is to determine which model parameters should be calibrated. Model parameters include the hydraulic properties of the aquifer, boundary conditions, as well as any other features of the model that can be parameterized. The parameters that are subjected to inverse modeling should be selected based on the importance of the parameters, which can be measured by parameter sensitivity. The model parameters with high sensitivity coefficients should be determined as accurately as possible. For this reason, a sensitivity analysis is conducted to determine the importance of model parameters before inverse modeling commences. Because parameter sensitivities vary in each iterative optimization process, sensitivity analyses are conducted in all steps of the calibration process.
3. Selection of Calibration Data. Calibration data include observed groundwater elevations at wells and surface water discharge at gages. Model output and measured data are compared only at

discrete points in space and time—the calibration data points. The difference between the measured and computed system responses at the calibration points are termed residuals. The sum of the squared-weighted residuals is the objective function used in this calibration effort. Calibration is a numerically guided iterative process that adjusts estimates of model parameters to minimize this objective function.

4. Forward Modeling. A MODFLOW simulation is carried out with current parameter values to obtain the simulated water levels that correspond to measured water levels.
5. Parameter Estimation. PEST uses the Marquardt-Levenberg method to minimize the objective function by iteratively updating the model parameters until a user-specified maximum number of iterations is reached or when the objective function can no longer be reduced. At the end of the parameter estimation process, the forward modeling run is carried out with updated parameters. Details of the Marquardt-Levenberg method are given in the PEST book (Doherty, 2015) and the PEST user's manual (Doherty, 2019; 2019b).
6. Analysis of Residuals**.** Residuals are analyzed geographically and at individual wells to determine bias, systematic errors and model validity

6.3.2 Selection of Calibration Data

The calibration period is July 1, 1977 through June 30, 2018 or fiscal year 1977/78 through fiscal year 2017/18. This period because the historical data used to calibrate the Cucamonga and Six Basins models that were incorporated with the Chino Basin model into the 2020 CVM started in 1978. The 42-year includes major land use transition and the wettest and driest period in the instrument record.

The model was calibrated by comparing measured and model estimated groundwater-level and historic surface water discharge into Prado Dam reservoir. Groundwater-level measurements were selected based on the following criteria:

- Wells used in calibration should be geographically distributed to evenly weight the calibration across the model domain.
- Wells used in calibration should be screened vertically distributed to evenly weight the calibration across model layers.
- Water level measurements at wells should be relatively evenly distributed over time.

For the 2020 CVM, over 30,000 water-level measurements from 153 wells were used in calibration. To ensure that the water level measurements were distributed evenly over time, and to avoid bias toward high-frequency water level measurements, a subset of water level measurements were selected for calibration purposes and the selected water levels are at least 15-days apart.

Surface water discharge at Santa Ana River below Prado Dam and stage observations for the Prado Dam reservoir pool were used by the Army Corps of Engineers to estimate the total discharge into Prado Dam reservoir. This reconstructed monthly inflow hydrograph was used as a calibration target for 2020 CVM.

Figure 6-6 shows selected calibration well locations. Table 6-1 lists the owners, names, coordinates, and screen layers of these wells. For calibration wells that span multiple model layers, a weight was assigned to the water levels of each layer to derive a final value for comparison to the observed data. Weights were assigned to layers based on the thickness of the aquifer and the estimated hydraulic conductivity.

6.3.3 Sensitivity Analysis and Covariance Matrix

Parameter sensitivity measures the impact of a small parameter change on the calculated system response and objective function. If a small model parameter change results in a significant change in the objective

function, the parameter is regarded as highly sensitive. PEST calculates sensitivities for values of hydraulic head throughout the model using the Jacobian matrix. Certain parameter values, such as those parameters related to storage coefficients and hydraulic conductivity, differ greatly in orders of magnitude, and their parameter sensitivities are not directly comparable. PEST scales the elements of the Jacobian matrix by the magnitude of the parameter value to make parameter sensitivities comparable with one another. This feature allows for measuring the sensitivity of a calibration point and measuring the importance of the parameters.

The sensitivity analysis was conducted in two steps. At the beginning, all model parameters were selected to compute their sensitivities. This is called the primal sensitivity analysis. The purpose is to exclude insensitive parameters from the final adjusted parameter set. During this process, the covariance matrix from the sensitivity analysis was checked. The covariance matrix of model parameters describes the statistical correlations between pairs of parameters. If two parameters show a strong correlation, they cannot be determined independently. For example, if two parameters are negatively (inversely) correlated, a similar system response is obtained by concurrently increasing one and decreasing the other parameter. For example, the vertical hydraulic conductivity in layer 3 in the City of Chino area is negatively correlated to the vertical hydraulic conductivity in layer 2 and layer 4. Based on the results of the primal sensitivity analysis, insensitive parameters and one of the paired correlated parameters are excluded from the list of calibration parameters.

A total of 112 parameters were selected through the primal sensitivity analysis. The results of the primal sensitivity analysis indicated that the hydraulic conductivities of San Jose Fault and Redhill Fault play an important role for the 2020 CVM, as does for the hydraulic conductivity in the Bloomington Divide area.

6.3.4 PEST Settings and Calibration Results

All of the efforts taken within a calibration process are ultimately evaluated on the success or failure of meeting three conditions: (1) the groundwater system processes and geometry are adequately represented and simulated, (2) weighted true errors are independent, and (3) errors in the observation data used for calibration are independent (Hill, et al., 2005). As to condition 3, it was assumed that the water level measurements were taken by numerous personnel, representing numerous agencies, and that these measurements would therefore have random errors. It was also assumed that there are no natural processes that might make these observations biased. In this report, only conditions 1 and 2 are addressed.

6.3.4.1 PEST Settings

Forward simulation of the flow model for the calibration period requires about 40 minutes of computational time. Since the model output, as it corresponds to the calibration points, depends on the estimation of parameters and the fit can be improved by appropriately changing model parameters, several strategies were used to find a parameter set that iteratively yields smaller values of the objective function. These strategies resulted in good matches between simulated and measured data and reasonable parameter estimates, not only in their values but also in comparison to other parameters in space. The major steps used in PEST inverse modeling are described below.

The initial model parameter values were derived and estimated based on the parameter estimates of the model used in the prior Safe Yield calculation (WEI, 2015), the Six Basins Strategic Plan (WEI, 2017), and unpublished modeling results for the Cucamonga Basin. Some initial hydraulic parameter estimates were developed from aquifer stress tests and sinner log tests.

As described in Section 4 and in this section, the Levenberg-Marquardt algorithm was used to minimize the objective function. It is necessary to note how to make the best choice for the Marquardt parameter (λ), as it is referred to in PEST. The choices for this value depend on how well-scaled the initial problem is. Marquardt recommends starting with a value λ and a factor ν>1 (Marquardt, 1963). When λ becomes large, this algorithm acts as the steepest-descent algorithm. When λ is zero, it is reduced to the Gauss-Newton method, which is better suited for small residuals. During iteration, the algorithm decreases or increases the parameter λ value through multiplication or division by ν to accelerate convergence. Based on theoretical study of the algorithm as well as trial and error, the initial λ value was set to 10.0 and ν was fixed at 2.0.

The parameter-updated step size was limited in PEST's settings. During any optimization iteration, the objective function reduction rate was set to be less than 30 percent. This setting prevented the minimization algorithm from moving too far beyond the region in which the linearity assumption is justified. The parameter maximum relative and factor change limits were also set to prevent the parameter adjustment from overshooting.

Upper and lower parameter bounds were set to limit the parameters to a reasonable range. These bounds were chosen based published literature (Freeze, et al., 1979; Fetter, 2001) and available aquifer stress tests. The upper and lower bounds, combined with the step size limitation and parameter selection (discussed below), made the calibration process stable and the results reasonable.

Error analyses for several trial inverse modeling runs revealed that some of the hydraulic parameters are highly correlated with others. To settle this correlation challenge, the correlation coefficients among parameters were examined after primal sensitivity and some of the parameters that were strongly correlated to others were excluded. In addition, prior information was incorporated into the estimation process. Aquifer stress test were used, where available for initial parameter estimates.

6.3.4.2 Calibration Results

Table 6-2 contains the final calibrated parameter values. Appendix E contains maps that show the spatial distribution of calibrated parameters and a table that compares hydraulic conductivity estimates from aquifer stress tests to initial and final calibrated values. The simulated water levels are computed based on these calibrated parameter values.

Figures 6-7a, 6-7b, and 6-7c show the simulated and measured water levels for calibration wells in Chino Basin, Cucamonga Basin, and Six Basins, respectively. The coefficient of determination R^2 is 0.932 for Chino Basin, 0.823 for Cucamonga Basin, and 0.954 for Six Basins. The NSE index is 0.957 for Chino Basin, 0.859 for Cucamonga Basin, and 0.945 for Six Basins. All points are distributed closely around the diagonal line, indicating good inverse modeling performance and a robust calibration.

Further exploration of the model results indicates that the poor matches in the City of Chino area occur at deep wells screened in layers 3 and 5 of the so-called "big shoe" area. Figure 6-7d shows the measured groundwater elevations versus model-estimated groundwater elevations for wells in this area. This scatter plot shows that these poor correlations occur at Chino Hills Wells 07C, 15B, and 19. Pumping events at these wells were relatively short compared to long-term pumping at most municipal wells. Groundwater levels fluctuated significantly when pumping started and stopped. Groundwater elevation data at these wells do not correlate temporarily with the stress periods used in the model which contributes to the lack of correlation.

The calibrated model also resulted in a good fit to the total observed stream discharge into the Prado Dam reservoir. Figure 6-8a is a time-history plot of the model-estimated stream inflow to Prado versus the total Prado inflow estimated by US Army Corps of Engineers (USACE). Figure 6-8b is a scatter plot

of model-estimated discharge into the Prado Dam reservoir versus the USACE-estimated inflow; the diagonal red line on the plot indicates a perfect match between the model- and USACE-estimated discharge values. The coefficient of determination R^2 is 0.946 and the NSE index is 0.945.

Using the entire calibration dataset, the coefficient of determination R^2 is 0.93; that is, the model can explain 93 percent of the variance observed in groundwater level observations. By this criterion the calibration is considered very good.

Appendix C contains time-history plots of simulated and measured water levels for the calibration wells during the calibration period. The time-history plots are useful indicators the quality of calibration as they show model-calculated water levels compared to measured water levels at a single location. Overall, the time-history plots in Appendix C show a good match between the simulated and measured values, indicating that trends within the aquifer are being simulated well.

The high values for the coefficient of determination and NSE index for the groundwater levels and surface water discharge into the Prado Dam reservoir indicate that the model parameterization and the water budget for the 2020 CVM are accurate: it would not be possible to achieve good calibration in the groundwater basin and the surface water system, as indicated by the high values for the coefficient of determination and NSE index, if the model parameterization and the water budget were not accurate.

Another, more visceral way to think about it is realize that the only groundwater level information that is input to the model as data is the initial groundwater elevation assumed on July 1, 1978 over the model domain and the time series of boundary elevations (based on well observation) along the edge of the model in the Bloomington Divide area near Riverside and the Spadra Basin boundary in Orange County. That the 2020 CVM can closely estimate the groundwater levels and discharge into the Prado Basin throughout the calibration period means that the model parameterization and the recharge and discharge components in the 2020 CVM are an accurate representation of what occurred during the calibration period.

6.3.5 Residual Analysis

Residual analysis is critical in evaluating the performance of calibration. Minimizing the objective function using the Levenberg-Marquardt algorithm may lead to the best-estimate parameters for a given groundwater flow model. However, this does not imply that a real groundwater system is properly represented by a model. If a conceptual model fails to reproduce the salient features of a system, the given calibrated model may not be able to match the observed data as expected. Residual analysis can reveal potential trends in residuals, indicating a systematic error in a model or the data, and can point out aspects of a model that require modification.

Statistics on hydraulic head residuals aid in the evaluation of model calibration. The following table lists the hydraulic-head residual statistics in Chino Basin.

- The mean of the residuals is expected to be close to zero. A large positive or negative mean indicates that groundwater elevations are systematically under-predicted or over-predicted by the model.
- The median value indicates that half of the residuals are less than 2.793 feet and that half of them are greater.
- The minimum and maximum values are the greatest residuals and occur in the City of Chino area for deeply constructed wells where calibration data are limited.

Descriptive Residual Statistics

Statistic	Value
Mean	0.061
Median	2.793
Minimum	-239.936
Maximum	135.19

Figure 6-9 shows the residual distribution in the Chino Basin part of the 2020 CVM. The figure illustrates that the mean of the residuals is around 0.06, which is near zero, with a standard deviation of about 21 feet.

The Cucamonga, Six, Spadra, and Temescal Basins are included in the 2020 CVM and they contribute subsurface inflow to the Chino Basin. Thus, these basins need to be well calibrated to ensure the reliability of the subsurface inflow estimates to the Chino Basin. Figures 6-10a through 6-10d show the residual distributions in Cucamonga Basin, Six Basins, Spadra Basin, and Temescal Basin, respectively. The residual distributions show the calibrated 2020 CVM was able to reproduce the behavior of these groundwater basins during the calibration period. The residual distribution shown in Figures 6-9 and 6-10a through 6-10d are random. Figure 6-11 shows spatial distribution of average residuals for each calibration well. Review of Figure 6-6 indicates that there is no spatial bias in estimating groundwater levels.

6.3.6 Historical Water Budget

The information presented in Sections 2, 3 and this section used in a series of models to develop the water budget for all the basins in the 2020 CVM for the historical calibration period. Note that as mention previously in this report, only the Chino Basin water budget will be discussed herein. The final water budget for the Chino Basin was derived after the 2020 CVM was calibrated as it contains certain recharge and discharge components that were estimated with the 2020 CVM. Table 6-3 includes the annual time series of recharge, discharge, change in storage and net recharge for the period July 1, 1978 through June 30, 2018. Individual recharge and discharge components with a column heading of "I" were input directly into the 2020 CVM and components with a column heading "R" are computational results produced by the 2020 CVM. The historical water budget for the calibration period consisting of the individual components are described in the following text.

6.3.6.1 Recharge Components

Recharge components include: subsurface inflow from adjacent mountain areas and groundwater basin; storm water recharge in natural channels and flood control/conservation basins; DIPAW, the artificial recharge of imported and recycled water; and deep infiltration of discharge from OWDSs that include septic tank leach fields and cesspools. These recharge components were estimated from basic data described in Section 3 and hydrologic model computations and were finalized in during the 2020 CVM calibration.

6.3.6.1.1 Subsurface Inflow to the Chino Basin

Subsurface inflow was computed with the HSPF model for the San Gabriel Mountains that contribute subsurface inflow to the Cucamonga and Six Basins. Subsurface inflow from the Chino, Puente and Jurupa Hills was estimated with R4 model. Subsurface inflow from the Rialto basin was assumed to be the same values as used in the prior Safe Yield calculation of 1,480 afy. The subsurface boundary inflow

from the Riverside Basin through the Bloomington Divide was computed in the 2020 CVM using a time series of observed groundwater elevations in the Riverside Basin just upgradient of the model boundary. Subsurface boundary inflows to the Chino Basin from the Cucamonga, Six, Spadra and Temescal Basins were computed in calibration by the 2020 CVM.

6.3.6.1.2 Areal Recharge in the Chino Basin

Areal recharge includes DIPAW and OWDS. Both components are combined and routed through the vadose zone and reported in Table 6-3 as DIPAW.

6.3.6.1.2.1 DIPAW

WEI estimated DIPAW at the root zone with the R4 model and routed this recharge through the vadose zone with a separate routing model that uses a time and volume-weighted averaging scheme to simulate the buffering effects of vadose zone storage. DIPAW occurs when soil moisture exceeds field capacity. Field capacity is the maximum volume of water that can be stored in the soil zone against the force of gravity. Soil moisture in excess of field capacity is assumed to infiltrate beyond the root zone and migrate through the vadose zone to the saturated zone.

DIPAW estimates were based on land use, soil type, irrigable area, evapotranspiration, precipitation, and applied water. The initial estimate of applied water for urban areas was estimated from reports prepared by the IEUA.[18] Final estimates of applied water for urban irrigation were developed by calibrating the R4 model and extending the calibration results to non-IEUA areas in the Chino Basin. DIPAW estimates for agricultural, native, and undeveloped areas (land in transition from vacant and agricultural uses to urban uses) were based on vegetation type and associated root zone depth, soil type, permeable area, irrigable area, evapotranspiration, and precipitation. Evapotranspiration was estimated for various vegetation types based on published unit consumptive use rates, crop coefficients, and potential ET estimates from CIMIS.

6.3.6.1.2.2 Deep Infiltration of OWDS Discharge

Areal recharge from OWDS was estimated based on data collected from the counties and cities that showed, by year, which land parcels were developed and not sewered. The discharge rates associated with the OWDS are based on estimates developed on unit sewage generation developed from IEUA data. Appendix B contains information to support the OWDS estimates.

6.3.6.1.2.3 Areal Recharge Calibration

Within the Chino Basin, the travel time from these sources to the water table varies depending on water application rate, vadose zone thickness, lithology of the vadose zone, and land use. The vadose zone is over 600 feet thick in the northern Chino Basin and it is less than 20 feet thick near the Santa Ana River. The greater the vadose zone thickness the greater the travel time through the vadose zone. The HYDRUS-2D model was used to estimate the time required for DIPAW to transit the vadose zone and that travel time informs the vadose zone routing model. The lag time distribution developed with HYDRUS 2D modeling work was adjusted manually during calibration and the lag time distribution shown in Figure 5-4 produced the best calibration result. Note that this is the same process that was used in the prior Safe Yield recalculation

Figure 6-12a compares the time history of DIPAW discharging from the root zone and DIPAW discharging to the saturated zone to the estimated storage in the vadose. Review of this figure indicates that part of the DIPAW discharging to the saturated zone is derived from a reduction in storage in the

[18] These are reports prepared by the IEUA to determine the total dissolved solids increment in water use and wastewater treatment. These reports are filed with the Santa Ana Regional Board.

vadose zone which would be expected when cultural conditions are changing. Figure 6-12b shows the relationship between end of year vadose zone storage and DIPAW discharging to the saturated zone. This figure contains callouts to notably wet years and the associated increase in vadose zone storage following the wet years – the vadose zone response to wet years diminishes over time due to changes in cultural conditions as would be expected

Table 6-3 lists the time series of DIPAW reaching the saturated zone and statistics to characterize it. During the calibration period, DIPAW was about 52 percent of total recharge, averaged about 106,900 afy and ranged from a minimum of 69,500 afy to a maximum of 133,500 afy. Two things influence the trends in DIPAW: precipitation and cultural conditions. There are peaks in DIPAW resulting from the 1978 to 1983 and 1993 to 1998 wet periods, a general downward trend due to the urbanization of agricultural and vacant lands, and an extreme dry period following 1998. Figure 6-13 compares the estimated annual precipitation over the Chino Basin and the R4 Model estimated DIPAW at the root zone. Review of Figure 6-13 shows that DIPAW is declining over time relative to precipitation. This occurs due to a decrease in pervious area and reduction in applied water that occurs as agricultural/natural/vacant land uses are replaced with urban land uses. The implications of the decline in DIPAW due to changes in cultural conditions relative to precipitation is discussed in Section 7.

6.3.6.1.3 Streambed Infiltration and MAR

Streambed recharge occurs in unlined stream channels and in flood retention and water conservation basins. Most of the major stream channels in the Chino Basin were concrete-lined as of March 2003 (WEI, 2018). The R4 Model was used to estimate the storm water recharge in stream channels and in flood control and conservation basins. The 2020 CVM was used to estimate surface water recharge in the Santa Ana River and its lower unlined tributaries.

6.3.6.1.3.1 Streambed Infiltration from Santa Ana River

Surface water flow in the Santa Ana River consists of a base flow and storm flow. Base flow occurs throughout the year, and it consists of rising groundwater and wastewater discharged to the river. Storm flow occurs in response to precipitation and stormwater releases from the Seven Oaks and San Antonio Dam during and after precipitation events have passed. Past groundwater modeling and groundwater level observations have demonstrated that throughout most of the Santa Ana River reach in the Chino Basin, the river is a significant source of recharge and that the amount of streambed infiltration is dependent in part on groundwater pumping in the southern part of the basin and the magnitude of surface water discharge in the river. Surface water discharge at the Riverside Narrows, as characterized by the USGS gage at the MWD Crossing consists of occasional stormwater, consistently occurring rising groundwater from the Riverside Basin and wastewater discharged upstream of the Riverside Narrows by the Cities of Colton, Rialto and San Bernardino. Within the Chino Basin, wastewater is discharged by the Cities of Corona and Riverside, the IEUA and the WRCWRA. Table 6-3 lists the time history of Santa Ana River streambed infiltration and statistics to characterize it. During the calibration period, Santa Ana River streambed infiltration was about 34 percent of total recharge, averaged about 32,400 afy and ranged from a minimum of 25,400 afy to a maximum of 38,000 afy.

6.3.6.1.3.2 Streambed Infiltration from Santa Ana River Tributaries

Streambed infiltration of stormwater flows occur in unlined Santa Ana River tributaries that flow from the San Gabriel Mountains to the Santa Ana River. As described previously in this section, most of these streams have been lined during the period of the late 1950s through the 1990s and as a result this source of recharge declined significantly. Table 6-3 lists the time history of streambed infiltration from unlined Santa Ana River tributaries and statistics to characterize it. During the calibration period, unlined Santa Ana River tributaries infiltration was about 2 percent of total recharge, averaged about 3,900 afy, and ranged from a minimum of 80 afy to a maximum of 24,500 afy.

6.3.6.1.3.3 MAR

MAR is storm, recycled and imported waters that are diverted or delivered to flood control and conservation basins for recharge. Managed stormwater recharge contributes to Safe Yield. Stormwater recharge in flood control and conservation basins was estimated with the R4 Model from 1978 through 2004, after which stormwater recharge estimates from the IEUA were used. Recycled water is recharged to augment yield. Imported water is recharged to meet Watermaster replenishment obligations, and for temporary storage in Storage and Recovery programs. Table 6-3 lists the time history of MAR and statistics to characterize it. The table below summarizes the MAR for storm, recycled and imported waters during the calibration period.

Summary of MAR during the Calibration Period (afy)

Statistic	Storm	Recycled	Imported	Total
Total	223,013	131,900	472,281	827,193
Percent of total recharge	2.7%	1.6%	5.6%	9.9%
Average	5,439	3,217	11,519	20,175
Maximum	17,648	13,394	35,621	53,327
Minimum	1,007	0	0	1,430

6.3.6.1.4 Total Recharge

Total recharge is the sum of all the individual recharge components. Table 6-3 lists the time history of total recharge and statistics to characterize it. During the calibration period, total recharge averaged about 204,000 afy and ranged from a minimum of about 166,000 afy to a maximum of about 271,000 afy.

6.3.6.2 Discharge Components

6.3.6.2.1 Groundwater Pumping

Estimates of groundwater production were developed from the records of the Chino Basin Watermaster for the Chino Basin, previous modeling reports, crop transpiration requirements, and diary operation records. Groundwater production was categorized into four groups in the Chino Basin. Agricultural users include dairymen, farmers, and the State of California. Overlying non-agricultural water users include industrial and other non-agricultural overlying water users. Appropriative users include cities, water districts, and private water companies. The Chino Desalter Authority (CDA) is a large groundwater pumper in the southern Chino Basin, and after treatment, most of the produced groundwater is served to Appropriators. Table 6-3 lists the groundwater production time history for the calibration period. In Table 6-3, the annual pumping by the Overlying Non-Agricultural and Appropriative pools were combined.

Agricultural pumping was estimated during the period from 1978 to 2004 with the R4 Model because reliable historical records were not available. Watermaster installed meters at most of the agricultural wells from 2001 through 2004. After 2004, the historical records of agricultural pumping became available and were used.

For the period 1978 through 2004, agricultural pumping for irrigation and dairy operations were estimated on daily time steps with the R4 Model and aggregated to the monthly time steps used in the groundwater model. Agricultural pumping was determined by estimating the crop demand (after precipitation) and diary demands and subtracting any non-groundwater source of water, such as water

in the soil profile, surface water, or dairy wash water. Land use data from 1949, 1957, 1963, 1975, 1984, 1990, 2000, and 2006 were used to calculate agricultural pumping. Irrigation demands can be satisfied by rainfall, groundwater, and other sources. Groundwater pumping for irrigation is estimated as the water needed by the crops minus the water supplied through non-groundwater sources.

Before fiscal year 2005, dairy pumping was estimated based on cow counts from the RWQCB and the USDA. From fiscal year 2005 forward, dairy pumping estimates were based on production estimates provided by Watermaster.

Estimates of pumping by the Overlying Non-Agricultural Pool, Appropriative Pool, and CDA were based on production estimates provided by Watermaster.

Table 6-3 lists the time history of groundwater pumping and statistics to characterize it. Groundwater pumping during the calibration period is summarized in the table below.

Summary of Groundwater Pumping During the Calibration Period (afy)

Statistic	CDA	Overlying Non Ag and Appropriative Pools	Overlying Agricultural Pool	Total
Total	418,208	4,133,457	2,484,952	7,036,617
Percent of total discharge	4.9%	48.6%	29.2%	82.8%
Average	10,200	100,816	60.609	171,625
Maximum	30,116	137,345	120,072	193,504
Minimum	0	64,771	16,191	140,768

6.3.6.2.2 Evapotranspiration

Evapotranspiration (ET) is the combination of water loss due to evaporation from the soil and transpiration from plants. In most of the study area, ET that occurs from the soil zone is accounted for with R4 Model. ET that occurs from the saturated zone is explicitly computed by the 2020 CVM within the Prado Basin area and along the Santa Ana River in the southern part of the Chino Basin and northern part of the Temescal Basin. Table 6-3 lists the time history of riparian vegetation ET and statistics to characterize it. During the calibration period, riparian vegetation ET was about 8.6 percent of total discharge, averaged about 17,800 afy, and ranged from a minimum of 16,100 afy to a maximum of 19,300 afy. The time history of increasing riparian ET estimated by the model corresponds to increases in wastewater discharge to the Santa Ana River and its tributaries and changes in the spatial extent of riparian vegetation in the Prado Basin and Santa Ana River.

6.3.6.2.3 Rising Groundwater

Rising groundwater can occur in the Santa Ana River and its unlined tributaries in the southern Chino Basin and northern Temescal Basin when the hydraulic head beneath unlined streams exceeds the elevation of the streambed. The magnitude of rising groundwater varies seasonally, being greater in the winter and lesser in the summer. Rising groundwater cannot be directly calculated from existing monitoring programs. The available data consist of surface water discharge monitoring stations on the Santa Ana River at the MWD Crossing located at the Riverside Narrows, Temescal Wash at Main Street, and the Santa Ana River at below Prado Dam. Measured non-tributary discharges include recycled water

discharges from the Cities of Corona and Riverside, the IEUA, and the Western Riverside County Water Reclamation Authority plant; Arlington Desalter discharge; and State Project water discharges by OCWD to San Antonio Creek in Upland. Between the MWD Crossing and Prado Dam, there are few measurements of surface water discharge that can be used to define reaches of rising groundwater or streambed recharge. The great stands of riparian vegetation along the Santa Ana River and within the Prado Basin area are likely to contribute to the seasonal variation of base flow in the Santa Ana River and may impact rising groundwater in the Prado Basin area. Table 6-3 lists the time history of rising groundwater discharge and statistics to characterize it. During the calibration period, rising groundwater discharge was about 8.7 percent of total discharge, averaged about 18,000 afy, and ranged from a minimum of 12,600 afy to a maximum of 29,800 afy.

6.3.6.2.4 Total Discharge

Total discharge is the sum of all the individual discharge components. Table 6-3 lists the time history of total discharge and statistics to characterize it. Total discharge during the calibration period averaged about 207,400 afy and ranged from a minimum of about 172,800 afy to a maximum of about 226,200 afy.

6.3.6.3 Change in Storage

The annual change in storage is equal to the annual recharge minus the annual discharge. Table 6-3 lists the time history of the annual change in storage and statistics to characterize it. Figure 6-14 shows the time history of total recharge, total discharge and cumulative change in storage. Starting from the initial storage estimate on July 1, 1977, storage increased through 1986 by 292,000 af in response to the recharge of imported water and the 1978-1983 wet period. Storage declined afterwards through 1992 to about 205,000 af above the initial storage estimate due to the 1984-1992 dry period. Storage increased in response to the 1993-1998 wet period, reaching in 1995 about 244,000 af above the initial storage estimate and thereafter generally declined by the end of the calibration period to about 129,700 af below the initial storage estimate. The decline in storage that occurs after 1998 is the result of an extended dry period starting in 1999 and extending through 2018, the Parties use of water in storage to offset the CDA replenishment obligation, controlled overdraft allowed in the Judgment and reoperation allowed in the Peace II Agreement.

6.3.6.4 Total Basin Storage

The total water in storage in the Chino Basin was estimated based on the model estimated head in each model layer and the calibrated model parameters of specific yield and specific storage. The amount of water in storage for each model layer, the vadose zone, and the total water in storage is summarized in the table below.

The change in storage in the saturated zone during the calibration period was about -129,700 af or about -1.04 percent of the water in storage in the basin on July 1, 2018. This includes the controlled overdraft permitted in the Judgment and the reoperation water dedicated to desalter replenishment. The change in storage in the vadose zone is estimated to be about -318,888 af and this decline is result of changes in cultural conditions and drought.

Summary of Groundwater in Storage July 1, 2018 (af)

Model Layer	Effective Porosity	Compression	Total Storage
1	3,506,002	36,264	3,542,266
2	257,877	11,155	269,031
3	2,042,190	70,004	2,112,194
4	137,756	7,230	144,986
5	6,209,553	76,430	6,285,983
Subtotal Saturated Zone	12,153,377	201,083	12,354,460
Vadose Zone	255,576	na	255,576
Total Storage	12,408,953	201,083	12,610,036

6.3.7 Net Recharge

Net recharge, as used herein, is the exploitable inflow to a groundwater basin over a specified period, either under historical conditions or in a future projection under prescribed operating conditions, and it is a result of the hydrology, cultural conditions, and water management practices of the time period. Net recharge is equal to recharge minus uncontrolled discharge and excludes the recharge of supplemental water. Algebraically:

$$Net\ recharge = \Delta S/\Delta t + O_p - I_{ar}$$

Where O_p and I_{ar} are the average groundwater pumping and average supplemental water recharge over the base period, respectively. The derivation of net recharge is presented in Section 1. The last column in the right in Table 6-3 lists the annual time history of net recharge and statistics to characterize it. The table below summarizes it by decade.

Summary of Net Recharge by Decade in the Calibration Period

Statistic	1981 – 1990	1991 - 2000	2001 - 2010	2011 - 2018
Total	1,795,341	1,564,469	1,347,682	1,014,020
Average	179,534	156,447	134,768	126,753
Maximum	205,202	170,010	145,373	146,530
Minimum	156,526	138,476	124,374	113,206

The net recharge decline throughout the calibration period is due to changes in cultural conditions caused by the conversion agricultural and vacant land uses to urban land uses. Figure 6-15 illustrates the time history of change in DIPAW discharging to the vadose zone and compares it to time histories of pervious land cover, precipitation and applied irrigation water, and the ten-year moving average of precipitation and applied irrigation water on pervious land cover. The amount of DIPAW discharged to the vadose zone decreases with decreasing pervious area as would be expected with the changes in cultural conditions. The decline in DIPAW is exacerbated by the 20-year dry-period that started in 1999 and extended through 2018.

Figure 6-16 is similar to Figure 6-15 except that it compares model estimated net recharge over the calibration period to time histories of pervious land cover, precipitation, and applied irrigation water on

pervious land, and ten-year moving average of precipitation and applied irrigation water applied on pervious land. The net recharge projected for the 2011 through 2020 period from the prior Safe Yield calculation was estimated to be 135,000 afy based on the long-term average precipitation for cultural conditions expected during this period. The primary driver for the reduction in net recharge during the 2011 through 2020 period were changes in cultural conditions during the entirety of the calibration period and extremely low precipitation that occurred during the last 20 years of the calibration period.

Table 6-1 Calibration Wells

Well ID	Well Name	Screened Layer	Latitude	Longitude	Well Type	Owner	Basin
1207066	Offsite MW1	1	34.0450	-117.5068	Monitoring	Alcoa	Chino
1207069	Offsite MW4	1	34.0528	-117.4804	Monitoring	Alcoa	Chino
1206682	I-10	13	33.9762	-117.6143	Production	Chino Basin Desalter Authority	Chino
1206962	II-2	1	33.9861	-117.5666	Production	Chino Basin Desalter Authority	Chino
1206952	AP-PA/7	1	33.9938	-117.6869	Monitoring	Chino Basin Watermaster	Chino
1206955	AP-PA/10	1	33.9938	-117.6869	Monitoring	Chino Basin Watermaster	Chino
1002645	14	1,3,5	34.0580	-117.6820	Production	City of Chino	Chino
1002743	09	1,3,5	34.0382	-117.6831	Production	City of Chino	Chino
1004185	13	1,3	34.0117	-117.6657	Production	City of Chino	Chino
1206674	15	1,3,5	34.0121	-117.7043	Production	City of Chino	Chino
1206686	YMCA	1	33.9964	-117.6805	Production	City of Chino	Chino
1004179	CH HIL 17	1,3,5	34.0053	-117.6922	Production	City of Chino Hills	Chino
1004217	CH HIL 07C	3,5	34.0007	-117.7088	Production	City of Chino Hills	Chino
1203149	CH HIL 18A	3,5	34.0029	-117.6780	Production	City of Chino Hills	Chino
1203158	CH HIL 19	3,5	34.0025	-117.6879	Production	City of Chino Hills	Chino
1203214	CH HIL 15B	3,5	33.9898	-117.6932	Production	City of Chino Hills	Chino
1203215	CH HIL 15A	1,3	33.9898	-117.6931	Production	City of Chino Hills	Chino
1003613	NOR 11	1	33.9846	-117.5563	Production	City of Norco	Chino
1002254	ONT 31	1,3,5	34.0556	-117.5274	Production	City of Ontario	Chino
1002305	ONT 20	1,3	34.0789	-117.5586	Production	City of Ontario	Chino
1002319	ONT 09	1,3,5	34.0868	-117.6503	Production	City of Ontario	Chino
1002328	ONT 04	1,3,5	34.0774	-117.6274	Production	City of Ontario	Chino
1002343	ONT 07	4	34.0623	-117.6084	Production	City of Ontario	Chino
1002346	ONT 11	1,3,5	34.0553	-117.6248	Production	City of Ontario	Chino
1002371	ONT 08	1	34.0474	-117.5950	Production	City of Ontario	Chino
1002372	ONT 36	1,3,5	34.0481	-117.5937	Production	City of Ontario	Chino
1002623	P-30	1,3	34.0667	-117.7170	Production	City of Pomona	Chino
1002654	P-16	1	34.0571	-117.7275	Production	City of Pomona	Chino
1002685	P-24(OLD)	1,3	34.0411	-117.7377	Production	City of Pomona	Chino
1203062	P-29	1,3	34.0262	-117.7296	Production	City of Pomona	Chino
1002313	Upland 09	1,3,5	34.0876	-117.6417	Production	City of Upland	Chino
1002531	Upland 08	1,3	34.0950	-117.6813	Production	City of Upland	Chino
1002205	CVWD 35	1	34.1067	-117.5154	Production	Cucamonga Valley Water District	Chino
1002312	CVWD 3	1,3,5	34.0845	-117.5849	Production	Cucamonga Valley Water District	Chino
1002081	F31A	3,5	34.1212	-117.4529	Production	Fontana Water Company	Chino
1002082	F18A	3,5	34.1137	-117.4361	Production	Fontana Water Company	Chino
1002085	F35A	3	34.0948	-117.4402	Production	Fontana Water Company	Chino
1002101	FU28	1	34.0921	-117.4105	Production	Fontana Water Company	Chino
1002153	FU6	1,3	34.0557	-117.4448	Production	Fontana Water Company	Chino
1002213	F30A	1,3,5	34.1045	-117.4759	Production	Fontana Water Company	Chino
1002242	F21A	1	34.0628	-117.4807	Production	Fontana Water Company	Chino
1002554	Margarita #1	1	34.0814	-117.7075	Production	Golden State Water Company	Chino
1202872	MW-2	1	33.9469	-117.6330	Undetermined	Inland Empire Utilities Agency	Chino
1207980	HCMP-3/1	1	33.9681	-117.6730	Monitoring	Inland Empire Utilities Agency	Chino
1207982	HCMP-5/1	1	33.9534	-117.6112	Monitoring	Inland Empire Utilities Agency	Chino
1207983	HCMP-6/1	1	33.9265	-117.6217	Monitoring	Inland Empire Utilities Agency	Chino
1207984	HCMP-7/1	1	33.9566	-117.5810	Monitoring	Inland Empire Utilities Agency	Chino
1207985	HCMP-8/1	1	33.9770	-117.5500	Monitoring	Inland Empire Utilities Agency	Chino
1208082	T-2/1	1	34.0727	-117.5972	Monitoring	Inland Empire Utilities Agency	Chino
1208799	MZ3 1/1	1	34.0398	-117.5331	Monitoring	Inland Empire Utilities Agency	Chino
1223006	VCT-2/2	1	34.1217	-117.5119	Monitoring	Inland Empire Utilities Agency	Chino
1232871	PB-7/2	1	33.9418	-117.6542	Monitoring	Inland Empire Utilities Agency	Chino
1232872	PB-7/1	1	33.9418	-117.6542	Monitoring	Inland Empire Utilities Agency	Chino
1003502	JCSD 16	1	34.0146	-117.5213	Production	Jurupa Community Services District	Chino
1002646	MVWD 08	1	34.0595	-117.7015	Production	Monte Vista Water District	Chino
1002722	MVWD 02	1,3,5	34.0482	-117.7006	Production	Monte Vista Water District	Chino
1202866	83240-DOM	1	33.9516	-117.6529	Production	Orange County Flood Control	Chino
1232806	OCWD-PDE4	1	33.9193	-117.6168	Monitoring	Orange County Water District	Chino
1002321	SAWC 18	1	34.0777	-117.6616	Production	San Antonio Water Company	Chino
1003582	03	1	34.0018	-117.5150	Production	Santa Ana River Water Company	Chino
1003630	07	1	33.9836	-117.5209	Undetermined	Santa Ana River Water Company	Chino
1003665	01A	1	33.9739	-117.5356	Undetermined	Santa Ana River Water Company	Chino
1207215	FC-936A2	1	34.0008	-117.4688	Monitoring	State of California, Department of	Chino
1002536	West End 1	1	34.0942	-117.6726	Production	West End Consolidated Water Co.	Chino
1002150	WVWD 20	1,3	34.0628	-117.4213	Production	West Valley Water District	Chino
1002209	Tamco	1	34.0933	-117.5282	Undetermined	Ameron International Corp.	Chino
1206514	Dom	1	34.0113	-117.5934	Production	Archibald Ranch Community Church	Chino
1206512	Dairy/Dom	1	34.0065	-117.6275	Production	Basque American Dairy	Chino
1202226	Dairy/Dom	1	34.0164	-117.6147	Production	Bekendam, Hank	Chino
1003856	9200-DOM	1	33.9999	-117.6078	Production	Borba, John	Chino
1202293	DOM	1	34.0107	-117.5764	Production	Boschma & Son Dairy	Chino
1206751	NA_1206751	1	33.9679	-117.6412	Production	Bouma, Ewoude	Chino
1002219	Cal Speedway 1	1,3,5	34.0896	-117.5099	Production	California Speedway	Chino
1003878	73000-1	1	33.9802	-117.6576	Production	California Youth Authority	Chino
1201166	MIL M-03	1	34.0350	-117.5605	Monitoring	County of San Bernardino	Chino
1003983	NA_1003983	1,3	33.9684	-117.6475	Production	County of San Bernardino, Dept. Of	Chino
1206472	CMG/PTI/J&A	1	33.9323	-117.6096	Production	Cow-west Dairy	Chino
1207026	MW-11	1	34.0536	-117.6450	Monitoring	General Electric Corporation	Chino
1202479	DAIRY DOM	1	33.9906	-117.6471	Production	Southern California Agricultural	Chino

Table 6-1 Calibration Wells

Well ID	Well Name	Screened Layer	Latitude	Longitude	Well Type	Owner	Basin
1206471	DOM	1	33.9775	-117.4980	Production	En Sue, Liau	Chino
1003810	ELEC-DAIRY-	1	33.9967	-117.5626	Production	Falloncrest Farms	Chino
1206525	NA_1206525	1	34.0175	-117.6374	Production	Gutierrez, Ernesto	Chino
1206630	ABANDONED	1	33.9542	-117.6338	Undetermined	H & R Barthelemy Dairy	Chino
1202576	DOM	1	33.9900	-117.6160	Production	Lee, Henrietta	Chino
1202861	IRRIGATION-	1	33.9568	-117.6455	Undetermined	Lizzaraga, Frank	Chino
1004058	5-Mtr#	1	33.9572	-117.5934	Undetermined	Michel, Louise	Chino
1201917	4	1	33.9827	-117.5494	Production	Mobile Community Management	Chino
1202809	74200-IRR	1	33.9685	-117.6369	Production	Stark, Everett	Chino
1004207	03	1,3	33.9967	-117.6719	Production	State of California, California	Chino
1004299	09	1,3	33.9756	-117.6673	Production	State of California, California	Chino
1206765	MW-24I	1	33.9843	-117.6865	Monitoring	State of California, California	Chino
1206766	MW-24S	1	33.9845	-117.6865	Monitoring	State of California, California	Chino
1206477	DOM/Office	1	33.9465	-117.5961	Production	Sterling Leasing Inc.	Chino
1206619	Dom	1	33.9422	-117.6302	Production	Stueve Brothers Farms	Chino
1207088	Archibald 1	1	33.9303	-117.5950	Monitoring	United States, Geological Survey	Chino
1202774	AG#6-	1	33.9759	-117.6236	Production	Unknown	Chino
1202650	81400-IRR	1	33.9899	-117.5783	Production	Van Dam, Bas	Chino
1206507	ABANDONED	1	33.9571	-117.6664	Undetermined	Van Leeuwen, John	Chino
1203019	EAST 1-D-1	1	33.9516	-117.5652	Production	Van Leeuwen, William	Chino
1003607	DOMESTIC	1	33.9922	-117.5450	Production	Vernola, Pat	Chino
1000554	Upland 15	1	34.1371	-117.6357	Production	City of Upland	Cucamonga
1000525	CVWD 27	1	34.1436	-117.5539	Production	Cucamonga Valley Water District	Cucamonga
1000539	CVWD 13	1	34.1435	-117.5962	Production	Cucamonga Valley Water District	Cucamonga
1000543	CVWD 15	1	34.1380	-117.5981	Production	Cucamonga Valley Water District	Cucamonga
1000568	CVWD 19	1	34.1331	-117.6254	Production	Cucamonga Valley Water District	Cucamonga
1000573	CVWD 20	1	34.1252	-117.6210	Production	Cucamonga Valley Water District	Cucamonga
1000590	CVWD 23	1	34.1342	-117.5969	Production	Cucamonga Valley Water District	Cucamonga
1002287	CVWD 10	1	34.1196	-117.6193	Production	Cucamonga Valley Water District	Cucamonga
1000555	SAWC 16	1	34.1467	-117.6444	Production	San Antonio Water Company	Cucamonga
1006968	SAWC 32	1	34.1602	-117.6394	Production	San Antonio Water Company	Cucamonga
1000629	NA_1000629	2	34.1463	-117.7002	Undetermined	Adams And Garner	Six Basin
1201189	Cartwright	1	34.1019	-117.7577	Production	City of La Verne	Six Basin
1224787	Old Baldy	1	34.1033	-117.7715	Production	City of La Verne	Six Basin
1224789	Walnut	1	34.0976	-117.7754	Production	City of La Verne	Six Basin
1224790	La Verne	2	34.1186	-117.7509	Production	City of La Verne	Six Basin
1002432	P-20	2	34.1142	-117.7258	Production	City of Pomona	Six Basin
1002489	P-09B	1	34.1031	-117.7349	Production	City of Pomona	Six Basin
1002494	P-13	2	34.1065	-117.7295	Production	City of Pomona	Six Basin
1002594	P-01A	1	34.0816	-117.7450	Monitoring	City of Pomona	Six Basin
1002604	P-03	1	34.0830	-117.7515	Production	City of Pomona	Six Basin
1201224	P-07	1	34.0819	-117.7397	Production	City of Pomona	Six Basin
1000647	Indian Hill	2	34.1244	-117.7205	Production	Golden State Water Company	Six Basin
1000651	Pomello #1	2	34.1357	-117.7001	Production	Golden State Water Company	Six Basin
1002507	Dreher #1	1	34.0999	-117.7279	Production	Golden State Water Company	Six Basin
1002517	Del Monte #1	1	34.0938	-117.7145	Production	Golden State Water Company	Six Basin
1002723	Alamosa #2	2	34.1330	-117.7002	Production	Golden State Water Company	Six Basin
1208146	Campbell #1	2	34.1189	-117.7292	Production	Golden State Water Company	Six Basin
1208148	College #2	1	34.1014	-117.7103	Production	Golden State Water Company	Six Basin
1208151	Mills #1	2	34.1175	-117.7059	Production	Golden State Water Company	Six Basin
1000639	SAWC 26	2	34.1262	-117.6845	Production	San Antonio Water Company	Six Basin
1000672	SAWC 28	2	34.1359	-117.6807	Monitoring	San Antonio Water Company	Six Basin
1207955	SAWC 33	2	34.1514	-117.6794	Production	San Antonio Water Company	Six Basin
1224766	MW-1	2	34.1416	-117.6876	Monitoring	Six Basins Watermaster	Six Basin
1224767	MW-2	2	34.1219	-117.6980	Monitoring	Six Basins Watermaster	Six Basin
1002448	NA_1002448	2	34.1164	-117.7481	Undetermined	Unknown	Six Basin
1002505	NA_1002505	2	34.0984	-117.7259	Undetermined	Unknown	Six Basin
1002784	NA_1002784	2	34.0945	-117.7838	Undetermined	Unknown	Six Basin
1002794	NA_1002794	1	34.0911	-117.7705	Undetermined	Unknown	Six Basin
1230774	MW-2	2	34.1003	-117.7867	Monitoring	Victor Graphics	Six Basin
1000621	Upland Foothill	2	34.1414	-117.6735	Production	West End Consolidated Water Co.	Six Basin
1002386	Lemon Heights	2	34.1214	-117.6798	Production	West End Consolidated Water Co.	Six Basin
1002395	Mountain View	2	34.1162	-117.6936	Production	West End Consolidated Water Co.	Six Basin
1224293	MW-14Y	1	34.0932	-117.7377	Monitoring	Xerox Corporation	Six Basin
1237127	Well 1	1	34.0621	-117.7967	Production	California State Polytechnic	Spadra
1002815	P-28	1	34.0567	-117.8046	Production	City of Pomona	Spadra
1203259	P-31 (OGT-3)	1	34.0598	-117.7858	Production	City of Pomona	Spadra
1002811	NA_1002811	1	34.0608	-117.7873	Undetermined	Unknown	Spadra
1004636	COR 06	1	33.8734	-117.5566	Production	City of Corona	Temescal
1004907	COR 08	1	33.8781	-117.5607	Production	City of Corona	Temescal
1004914	COR 15	1	33.8830	-117.5829	Production	City of Corona	Temescal
1004920	COR 11	1	33.8831	-117.6017	Production	City of Corona	Temescal
1004949	COR 14	1	33.8731	-117.5868	Production	City of Corona	Temescal
1222093	Corona CG-1	1	33.8667	-117.5377	Monitoring	Riverside County Waste	Temescal

Table 6-2 Final Calibrated Parameter Values

Zone	Layer	Horizontal Hydraulic Conductivity (ft/day)			Vertical Hydraulic Conductivity (ft/day)			Specific Yield[1] or Specific Storage[1] (-)		
		Min	Max	Mean	Min	Max	Mean	Min	Max	Mean
1	1	8.01E+01	4.56E+02	1.62E+02	2.01E-02	1.67E+01	4.90E+00	6.67E-02	1.59E-01	1.12E-01
2	1	3.65E+01	7.85E+01	6.04E+01	9.01E-01	1.17E+01	5.43E+00	8.38E-02	1.37E-01	1.12E-01
3	1	2.56E+01	1.47E+02	7.83E+01	6.98E-02	2.61E+01	6.18E+00	4.86E-02	1.19E-01	8.64E-02
4	1	2.36E+01	1.08E+02	5.04E+01	7.63E-01	1.73E+01	5.50E+00	5.28E-02	1.17E-01	8.56E-02
5	1	2.45E+01	1.21E+02	6.16E+01	3.39E-04	2.94E+00	2.08E-01	9.06E-02	1.99E-01	1.37E-01
6	1	2.74E+01	1.68E+02	6.94E+01	3.45E-04	2.07E+00	3.21E-01	8.11E-02	2.09E-01	1.43E-01
7	1	6.92E+01	2.13E+02	1.21E+02	1.55E-03	5.07E+00	6.10E-01	6.50E-02	1.48E-01	1.02E-01
8	1	6.54E+00	2.95E+01	1.36E+01	3.39E-04	5.98E-01	8.60E-02	5.77E-02	1.23E-01	8.33E-02
9	1	4.58E+01	1.77E+02	9.16E+01	6.25E-03	2.15E+01	6.82E+00	7.80E-02	1.70E-01	1.26E-01
10	1	1.48E+01	3.61E+01	2.29E+01	2.75E-03	3.26E+00	1.00E+00	1.18E-01	2.06E-01	1.57E-01
11	1	1.89E+01	6.03E+01	3.55E+01	2.20E-01	1.35E+01	6.61E+00	1.38E-01	2.40E-01	1.95E-01
12	1	9.56E+00	6.97E+01	3.67E+01	2.19E-01	1.35E+01	4.01E+00	4.27E-02	1.77E-01	1.12E-01
13	1	8.29E+00	3.06E+01	1.70E+01	3.39E-04	6.55E-01	9.67E-02	3.68E-02	7.52E-02	5.78E-02
14	1	5.38E+00	1.12E+02	4.88E+01	3.17E-01	2.05E+01	7.35E+00	3.05E-02	1.66E-01	8.83E-02
1	2	8.00E+01	4.81E+02	1.78E+02	1.67E-02	1.39E+01	4.07E+00	3.40E-05	1.10E-04	7.97E-05
2	2	4.10E+01	8.88E+01	6.74E+01	7.49E-01	9.75E+00	4.51E+00	5.63E-05	9.66E-05	7.94E-05
3	2	7.22E-01	1.09E+02	5.67E+01	5.27E-02	2.17E+01	5.12E+00	1.51E-05	1.18E-04	8.49E-05
4	2	5.73E+00	2.37E+02	1.07E+02	6.01E-02	1.44E+01	4.57E+00	2.16E-05	1.14E-04	8.43E-05
5	2	3.92E-03	5.13E+00	1.47E-02	7.14E-06	1.22E-02	1.89E-05	5.39E-08	5.54E-07	1.08E-07
6	2	3.92E-03	3.48E+00	9.76E-03	7.14E-06	1.64E-02	2.24E-05	1.07E-07	5.04E-07	1.08E-07
7	2	3.92E-03	2.95E+00	1.35E-02	1.74E-05	4.09E-02	6.74E-05	1.07E-07	5.56E-07	1.09E-07
8	2	3.92E-03	2.89E+00	1.47E-02	1.74E-05	6.82E-03	3.82E-05	1.07E-07	3.92E-07	1.09E-07
9	2	4.07E+00	1.99E+02	1.04E+02	4.62E-03	1.59E+01	5.04E+00	5.14E-08	3.10E-07	2.28E-07
10	2	6.07E-02	5.76E+01	2.59E-01	3.69E-03	6.78E+00	2.86E-02	4.43E-07	2.15E-06	4.50E-07
11	2	4.46E+00	1.06E+02	6.19E+01	3.53E-01	3.43E+01	1.67E+01	6.00E-08	3.13E-07	2.55E-07
12	2	6.05E-01	7.11E+01	3.67E+01	1.21E-01	3.43E+01	1.02E+01	4.72E-08	3.02E-07	1.92E-07
13	2	1.74E-01	4.95E+00	2.66E+00	1.74E-05	3.37E-02	4.93E-03	1.25E-07	5.05E-07	3.86E-07
14	2	6.30E+00	1.30E+02	5.59E+01	2.34E-01	1.51E+01	5.42E+00	5.58E-08	2.93E-07	1.60E-07
1	3	2.03E+01	2.19E+02	7.97E+01	4.75E-03	2.95E+01	1.18E+01	1.90E-05	1.06E-04	6.74E-05
2	3	4.13E+00	7.49E+01	5.15E+01	7.61E-01	9.31E+00	3.88E+00	2.39E-05	6.31E-05	4.77E-05
3	3	3.35E+01	2.13E+02	9.19E+01	4.75E-03	5.63E+01	9.61E+00	1.33E-05	1.02E-04	6.03E-05
4	3	3.70E+00	9.05E+01	3.00E+01	4.01E-06	2.02E-02	1.81E-03	1.04E-07	8.59E-07	4.35E-07
5	3	7.88E-01	7.22E+00	2.74E+00	4.36E-07	1.41E-03	9.79E-05	1.67E-07	5.13E-07	2.81E-07
6	3	2.36E+00	1.69E+01	6.02E+00	1.36E-04	2.07E-02	2.69E-03	2.59E-07	7.82E-07	4.54E-07
7	3	1.02E+01	6.84E+01	3.29E+01	1.39E-05	9.46E-03	2.16E-03	5.29E-07	1.71E-06	9.79E-07
8	3	8.01E+00	1.02E+02	3.41E+01	5.65E-01	5.82E+01	1.83E+01	3.56E-07	1.81E-06	1.07E-06
9	3	6.16E-02	2.18E-01	1.06E-01	4.97E-01	6.46E+00	3.42E+00	1.51E-06	2.47E-06	1.93E-06
10	3	3.94E+00	2.60E+01	1.18E+01	3.64E-01	5.10E+01	1.22E+01	4.05E-07	1.77E-06	1.02E-06
11	3	6.93E-01	8.03E+00	3.51E+00	8.34E-05	1.11E-02	2.44E-03	1.67E-07	6.59E-07	3.52E-07
1	4	6.61E+00	6.87E+01	2.51E+01	1.05E-03	6.51E+00	2.60E+00	1.82E-05	8.30E-05	5.27E-05
2	4	1.30E+00	2.35E+01	1.62E+01	1.68E-01	2.05E+00	8.60E-01	1.87E-05	4.93E-05	3.73E-05
3	4	2.77E-01	6.71E+01	2.92E+01	1.05E-03	1.24E+01	2.37E+00	9.08E-06	7.95E-05	4.74E-05
4	4	1.13E-03	1.22E+00	2.94E-03	1.20E-06	7.02E-03	7.14E-06	5.44E-07	3.36E-06	5.48E-07
5	4	1.13E-03	5.09E-01	2.37E-03	3.16E-07	2.04E-04	5.56E-07	5.44E-07	1.57E-06	5.47E-07
6	4	1.13E-03	8.86E-01	2.37E-03	1.20E-06	7.59E-03	9.07E-06	5.44E-07	2.58E-06	5.46E-07
7	4	1.13E-03	1.17E+00	4.21E-03	7.35E-04	3.54E+00	1.11E-02	6.00E-07	3.38E-06	6.09E-07
8	4	4.25E-03	1.96E+00	1.24E-02	7.35E-04	1.27E+00	3.93E-03	6.00E-07	2.07E-06	6.06E-07
9	4	1.60E-01	5.60E+00	2.53E+00	4.12E-02	1.25E+01	2.98E+00	7.00E-07	4.36E-06	2.52E-06
1	5	8.36E+00	5.62E+01	2.52E+01	2.12E-03	2.90E+01	6.80E+00	5.75E-06	2.11E-05	1.53E-05
2	5	9.53E+00	3.73E+01	1.78E+01	3.73E-01	4.41E+00	1.45E+00	6.96E-06	1.36E-05	1.01E-05
3	5	2.53E+00	3.80E+01	1.17E+01	2.44E-03	1.09E+01	3.07E+00	7.18E-06	2.47E-05	1.51E-05
4	5	3.04E-01	2.46E+00	6.98E-01	1.59E-04	5.11E-01	1.14E-01	3.22E-06	8.72E-06	5.22E-06
5	5	5.39E-01	1.76E+00	9.04E-01	2.95E-06	2.96E-05	9.58E-06	5.89E-06	1.27E-05	8.03E-06
6	5	3.14E-01	1.43E+00	6.41E-01	4.48E-04	1.00E-02	2.35E-03	2.74E-06	9.51E-06	4.69E-06
7	5	3.10E+00	1.89E+01	9.46E+00	9.32E-02	1.87E+00	6.94E-01	2.45E-06	1.03E-05	5.66E-06
8	5	7.59E+00	1.38E+01	1.13E+01	5.90E-02	7.53E-01	4.45E-01	6.64E-06	1.09E-05	9.13E-06
9	5	3.42E+00	1.80E+01	9.09E+00	1.01E-01	1.98E+00	5.48E-01	2.23E-06	6.40E-06	4.34E-06

(1) Specific yield values are displayed for layer 1. Specific storage values are displayed for layers 2 to 5.

Table 6-3 Water Budget for the Chino Basin for the Calibration Period (af)

Fiscal Year	Recharge														Discharge						Change in Storage		Net Recharge
	R	I	R	R	R	R	R	I	R	I	I	I	I		I	I	I	R	R				
	Subsurface Inflow							Deep Infiltration of Precipitation and Applied Water	Santa Ana River Streambed Infiltration	Streambed Infiltration from Santa Ana River Tributaries	Managed Aquifer Recharge			Total Recharge	Groundwater Pumping			Riparian Veg ET	Rising Groundwater	Total Discharge	Annual	Cumulative	
	Bloomington Divide	Chino/Puente Hills, Jurupa Hills, and Rialto Basin	Net Temescal Basin	Pomona Basin	Claremont Basin	Cucamonga Basin	Spadra Basin				Storm Water	Recycled Water	Imported Water		CDA Pumping	Overlying Non Ag and Appropriative Pools	Overlying Agricultural Pool						
1978	11,404	8,811	2,502	2,278	2,277	12,032	961	117,423	37,046	24,456	5,183	3,175	6,952	234,499	0	64,771	120,072	16,951	14,495	216,289	18,210	18,210	192,927
1979	11,002	9,659	3,101	2,867	2,574	11,628	576	122,211	33,871	15,620	2,951	3,049	28,347	247,456	0	65,008	118,922	17,257	12,619	213,805	33,651	51,861	186,185
1980	12,497	10,790	3,420	2,922	2,578	11,567	498	126,236	38,002	20,253	4,662	3,232	16,537	253,195	0	69,503	110,885	16,404	14,897	211,689	41,505	93,366	202,125
1981	13,071	10,955	4,216	3,024	2,585	11,537	476	126,479	30,545	7,647	1,219	3,451	20,850	236,055	0	72,927	116,470	17,194	13,035	219,626	16,429	109,795	181,525
1982	13,337	11,289	4,987	2,892	2,470	11,401	480	126,714	33,792	11,112	3,096	3,726	21,641	246,937	0	68,404	101,624	16,868	13,389	200,284	46,652	156,447	191,313
1983	13,316	10,685	5,161	3,008	2,597	11,552	496	132,273	35,436	18,011	6,703	3,873	27,590	270,704	0	67,259	94,508	16,139	17,899	195,805	74,898	231,346	205,202
1984	14,378	9,829	6,112	3,222	2,752	11,871	511	133,497	29,048	8,724	2,472	982	22,400	245,799	0	74,726	107,238	16,642	17,412	216,018	29,782	261,127	188,363
1985	13,577	8,729	6,343	3,085	2,561	11,887	526	128,408	30,446	6,257	2,032	0	20,782	234,631	0	79,626	105,444	16,810	14,364	216,243	18,388	279,515	182,676
1986	12,428	9,439	6,192	3,007	2,456	11,668	549	127,728	33,461	6,062	2,903	0	18,327	234,221	0	83,822	105,254	16,877	15,805	221,757	12,463	291,979	183,212
1987	11,951	8,844	6,493	2,944	2,379	11,309	553	121,909	32,772	2,874	1,789	0	19,938	223,754	0	88,675	104,829	17,090	14,383	224,976	-1,222	290,756	172,344
1988	11,385	7,674	5,839	2,790	2,274	10,771	538	122,069	34,246	2,925	2,641	0	2,485	205,637	0	94,222	95,264	17,187	15,603	222,276	-16,640	274,117	170,361
1989	11,408	7,528	5,339	2,681	2,214	10,364	529	120,836	31,310	1,422	2,393	0	7,332	203,357	0	97,218	89,511	17,407	14,798	218,935	-15,578	258,539	163,820
1990	11,788	7,121	4,579	2,536	2,124	10,448	509	115,495	31,487	433	1,430	0	0	187,950	0	98,914	83,775	17,482	13,942	214,113	-26,163	232,376	156,526
1991	12,630	6,656	4,009	2,421	2,092	10,335	474	113,633	33,477	712	2,198	0	3,634	192,271	0	88,986	83,073	17,525	14,171	203,756	-11,484	220,891	156,941
1992	13,286	7,250	3,737	2,438	2,136	10,393	442	112,979	34,141	1,028	3,598	0	5,568	196,997	0	102,664	77,336	17,736	14,905	212,640	-15,643	205,248	158,788
1993	13,611	8,300	2,863	2,725	2,434	10,588	423	116,794	37,980	2,239	6,619	0	14,224	218,800	0	88,040	83,284	17,404	17,162	205,889	12,910	218,159	170,010
1994	13,637	8,223	3,621	2,994	2,560	10,871	425	117,935	30,748	650	1,486	0	16,448	209,597	0	93,564	72,115	18,155	15,589	199,423	10,174	228,333	159,405
1995	13,478	9,217	2,488	2,899	2,507	10,967	428	119,075	35,361	1,538	4,662	0	10,375	212,995	0	98,173	62,171	17,711	19,136	197,191	15,803	244,136	165,773
1996	13,289	9,146	3,546	3,017	2,560	11,015	455	117,398	29,441	709	2,425	0	82	193,085	0	109,609	71,220	18,429	18,553	217,811	-24,726	219,410	156,021
1997	13,292	9,072	3,290	2,829	2,430	10,883	481	116,836	30,483	1,007	3,305	0	16	193,925	0	112,998	68,968	18,564	18,917	219,448	-25,523	193,887	156,427
1998	13,650	8,754	2,402	2,803	2,417	10,727	503	117,046	33,821	1,637	5,780	0	8,352	207,895	0	104,141	45,302	18,238	22,456	190,138	17,757	211,644	158,848
1999	13,956	8,514	3,516	2,936	2,489	10,756	494	115,042	26,381	519	1,007	0	5,839	191,449	0	118,738	46,730	19,035	22,794	207,298	-15,849	195,795	143,780
2000	14,451	7,890	2,858	2,707	2,341	10,563	508	109,843	27,081	499	1,985	507	997	182,232	523	133,086	46,538	18,938	23,315	222,400	-40,168	155,628	138,476
2001	14,556	7,970	3,132	2,532	2,254	10,223	525	107,823	25,419	598	3,162	500	6,538	185,230	9,470	120,396	41,429	18,717	26,464	216,476	-31,245	124,382	133,011
2002	15,177	7,242	3,565	2,467	2,206	10,028	517	102,792	25,922	230	1,148	505	6,493	178,292	10,173	129,760	38,650	18,472	26,544	223,599	-45,307	79,075	126,279
2003	15,747	6,518	2,932	2,377	2,145	9,868	504	102,305	28,672	859	6,284	185	6,548	184,945	10,322	123,471	36,507	18,157	26,630	215,087	-30,142	48,934	133,425
2004	16,088	6,780	1,994	2,407	2,123	9,860	492	99,010	27,465	536	3,357	49	7,607	177,768	10,480	128,548	36,809	18,069	27,669	221,574	-43,807	5,127	124,374
2005	14,346	7,918	721	2,643	2,336	9,816	481	99,647	30,922	5,917	17,648	158	12,259	204,813	10,595	112,943	34,503	17,178	29,844	205,064	-251	4,876	145,373
2006	14,568	7,648	1,891	3,152	2,571	9,897	467	99,823	30,439	1,806	12,940	1,303	34,567	221,073	19,819	113,553	30,812	17,561	24,576	206,321	14,752	19,627	143,065
2007	15,150	7,607	1,268	2,911	2,413	9,826	412	96,008	29,276	79	4,745	2,993	32,960	205,647	28,529	123,695	29,919	18,276	21,441	221,859	-16,212	3,415	129,978
2008	15,044	7,346	1,173	2,627	2,240	9,842	384	93,275	31,703	1,530	10,205	2,340	0	177,709	30,116	127,696	26,280	18,358	20,003	222,453	-44,744	-41,329	137,008
2009	15,271	7,363	696	2,509	2,178	9,950	414	91,489	33,318	839	7,512	2,684	0	174,220	28,456	137,345	23,386	18,561	18,475	226,223	-52,003	-93,331	134,500
2010	15,584	6,402	562	2,448	2,167	9,809	441	88,512	35,285	1,939	14,273	7,210	5,000	189,632	28,964	108,983	22,038	18,686	18,067	196,739	-7,107	-100,438	140,669
2011	15,960	6,889	557	2,601	2,299	9,891	452	88,763	36,213	3,358	17,052	8,065	9,465	201,564	28,941	94,413	18,042	18,739	18,765	178,901	22,663	-77,775	146,530
2012	15,577	6,971	1,397	2,713	2,317	9,820	441	84,009	34,463	463	9,271	8,634	22,560	198,637	28,230	108,501	22,412	19,282	15,649	194,074	4,563	-73,212	132,511
2013	15,144	6,651	1,516	2,676	2,203	9,748	426	80,130	33,536	243	5,271	10,479	0	168,023	27,380	111,748	24,074	17,348	13,871	194,421	-26,398	-99,610	126,325
2014	15,067	6,355	1,371	2,645	2,144	9,548	440	78,395	34,301	241	4,299	13,593	795	169,195	29,626	118,849	22,131	17,426	13,348	201,380	-32,185	-131,795	124,032
2015	15,230	5,760	1,217	2,547	2,096	8,721	458	75,817	34,907	421	8,001	10,840	0	166,014	30,022	104,317	17,552	17,580	13,585	183,056	-17,042	-148,837	124,009
2016	15,716	5,015	1,057	2,498	2,062	7,809	449	73,547	36,134	476	9,236	13,222	0	167,221	28,191	101,301	16,908	17,824	14,147	178,371	-11,150	-159,988	122,028
2017	15,967	5,587	1,529	2,462	2,056	8,311	423	72,874	35,805	1,920	11,575	13,934	13,150	185,593	28,284	98,960	16,191	17,869	15,261	176,565	9,028	-150,960	125,379
2018	15,711	5,385	2,306	2,510	2,072	8,041	388	69,532	32,664	2,165	4,494	13,212	35,621	194,101	30,088	93,904	16,776	18,147	13,914	172,828	21,272	-129,687	113,206
Statistics for the Calibration Period 1978 through 2018																							
Total	572,725	325,781	125,499	111,751	95,688	426,142	19,947	4,381,613	1,326,822	159,955	223,013	131,900	472,281	8,373,116	418,208	4,133,457	2,484,952	728,293	737,893	8,502,803	-		6,302,749
Percent	6.8%	3.9%	1.5%	1.3%	1.1%	5.1%	0.2%	52.3%	15.8%	1.9%	2.7%	1.6%	5.6%	100.0%	4.9%	48.6%	29.2%	8.6%	8.7%	100.0%			
Average	13,969	7,946	3,061	2,726	2,334	10,394	487	106,869	32,362	3,901	5,439	3,217	11,519	204,222	10,200	100,816	60,609	17,763	17,997	207,385	-3,163		153,726
Median	13,956	7,674	2,932	2,707	2,317	10,393	480	113,633	33,318	1,530	4,299	507	7,607	198,637	0	101,301	46,730	17,711	15,805	212,640	-7,107		156,021
Maximu	16,088	11,289	6,493	3,222	2,752	12,032	961	133,497	38,002	24,456	17,648	13,934	35,621	270,704	30,116	137,345	120,072	19,282	29,844	226,223	74,898	291,979	205,202
Minimum	11,002	5,015	557	2,278	2,056	7,809	384	69,532	25,419	79	1,007	0	0	166,014	0	64,771	16,191	16,139	12,619	172,828	-52,003	-159,988	113,206

Note: column heading R means model results and column heading I means model input

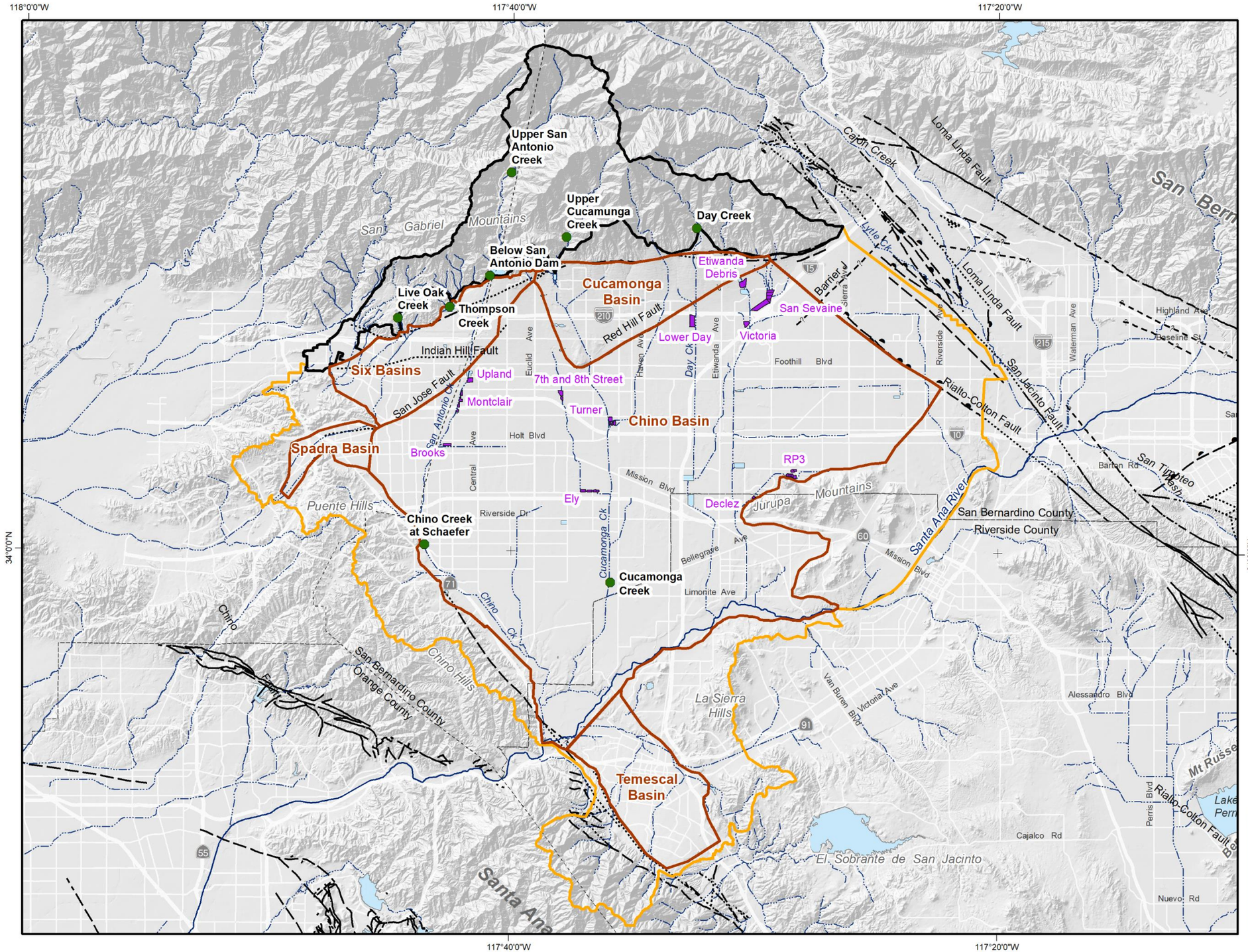

Prepared by:

WEI
Wildermuth Environmental, Inc.

Author: LS
Date: 4/1/2020
File: Figure 6-1 Calibrate SWM.mxd

0 1 2 3 4 5 Miles
0 2 4 6 8 Km

Prepared for:

2020 Safe Yield Recalculation

Chino Basin Watermaster
Partners in Basin Management

Location Map for Gaging Stations and Flood Control and Conservation Basins Used to Calibrate the HSPF and R4 Models

Figure 6-1

Figure 6-2 Scatter Plot of R4-Estimated Monthly Discharge and USGS-Estimated Discharge for Chino Creek at Schaefer Avenue

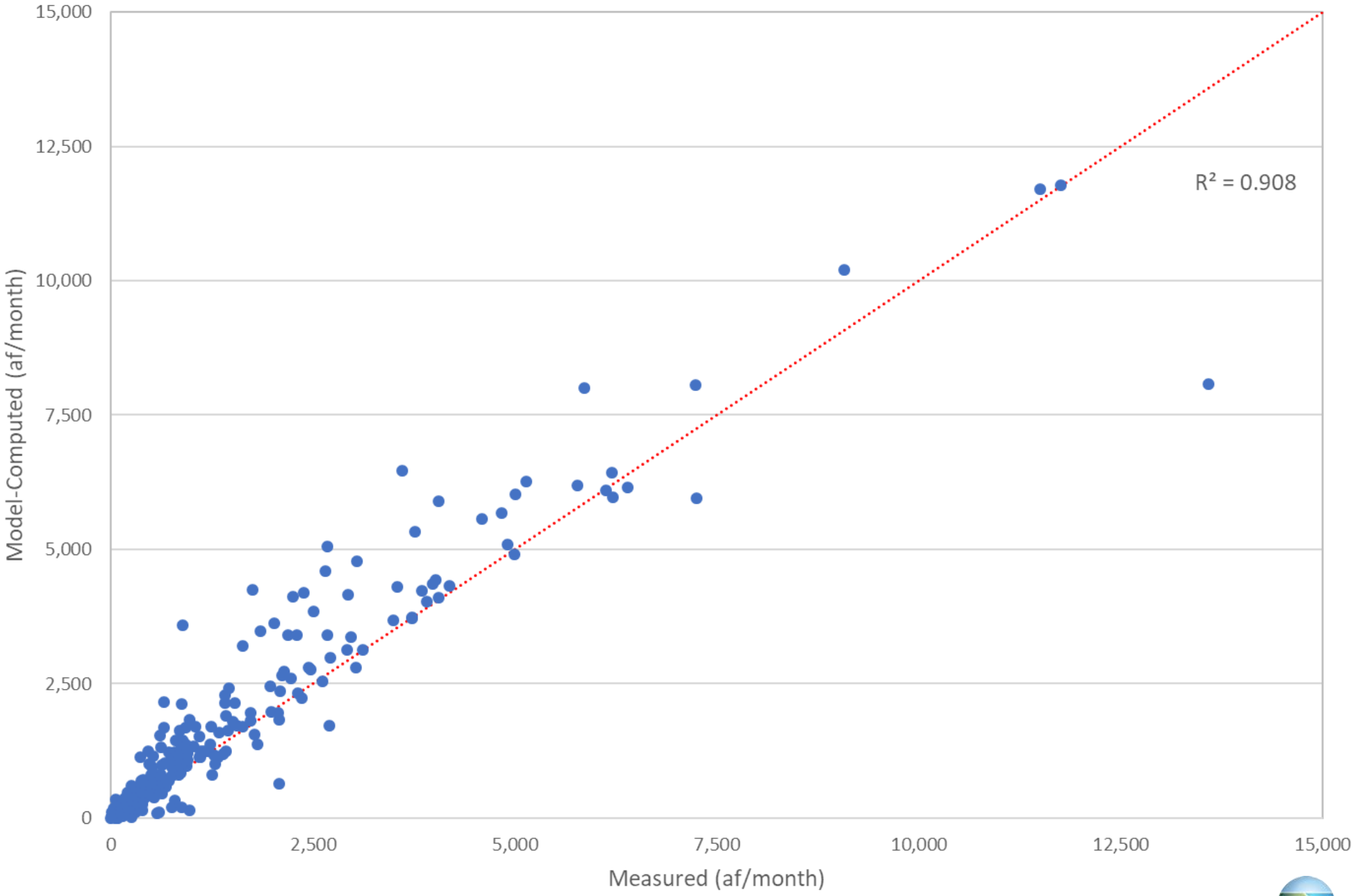

Figure 6-3 Scatter Plot of R4-Estimated Monthly Discharge and USGS-Estimated Discharge for Cucamonga Creek near Mira Loma

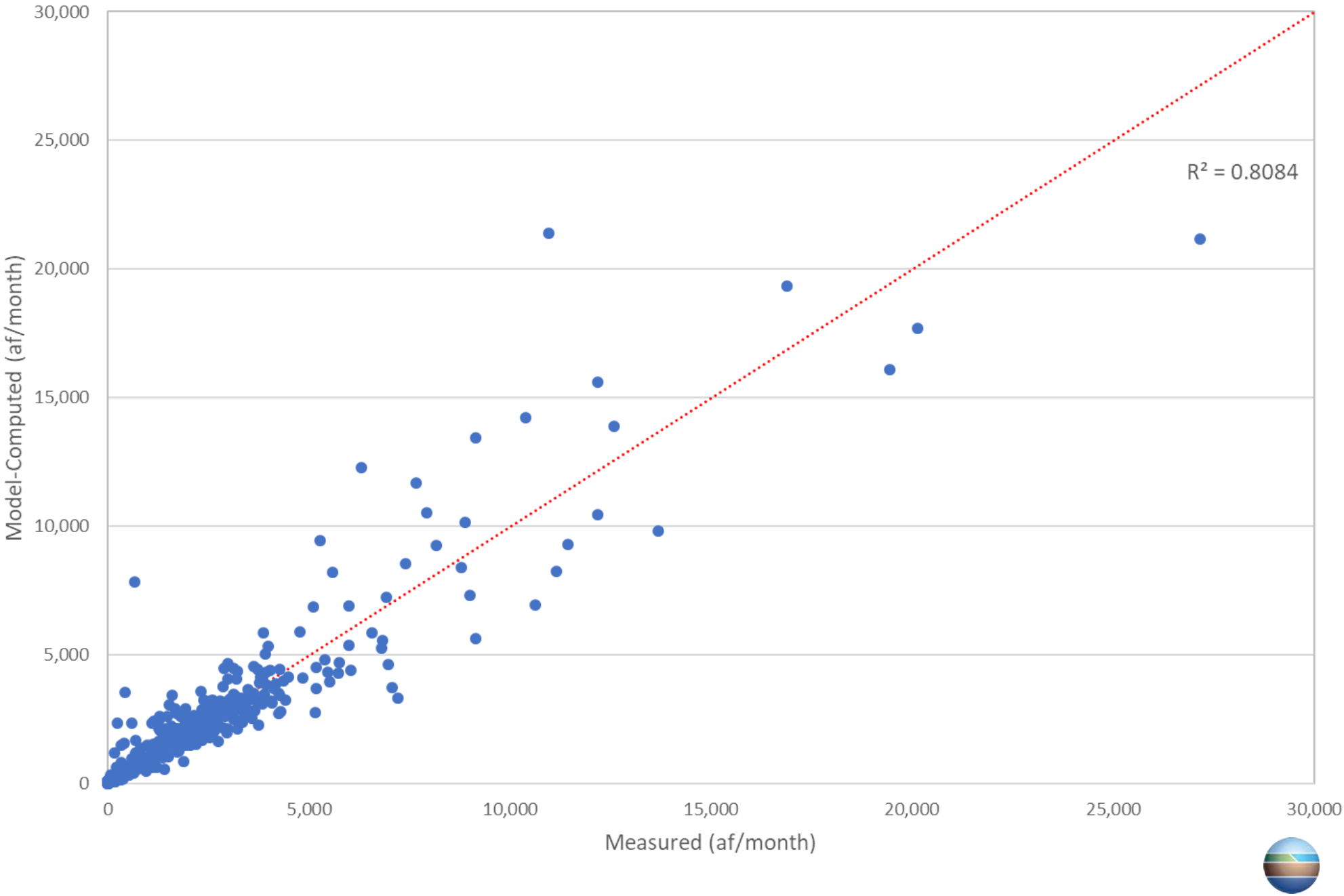

Figure 6-4a Total Water Supply to the RP1/RP4 Sewershed and the Efficacy of the Supply

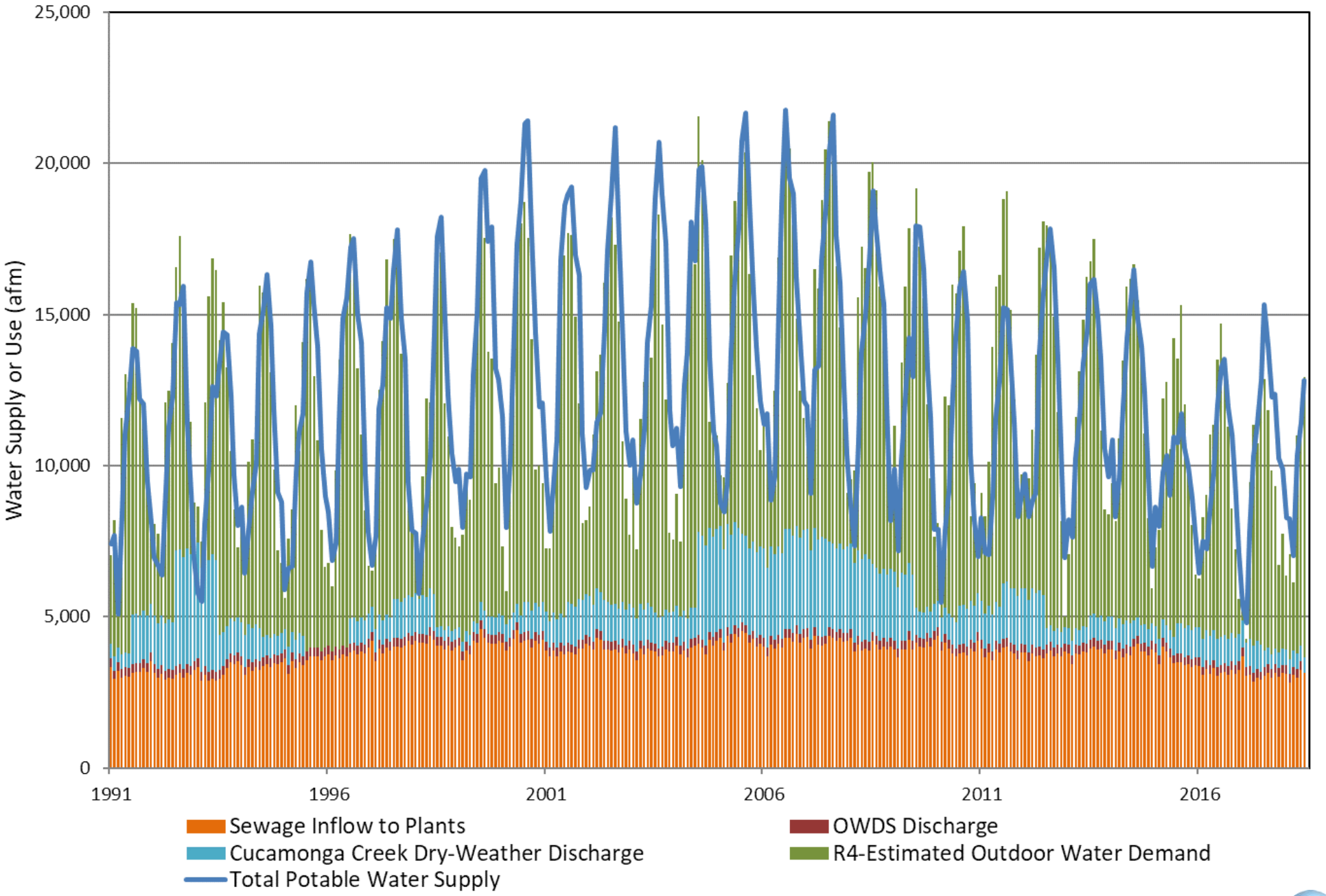

Figure 6-4b Total Water Supply to the RP2/CC/RP5 Sewershed and the Efficacy of the Supply

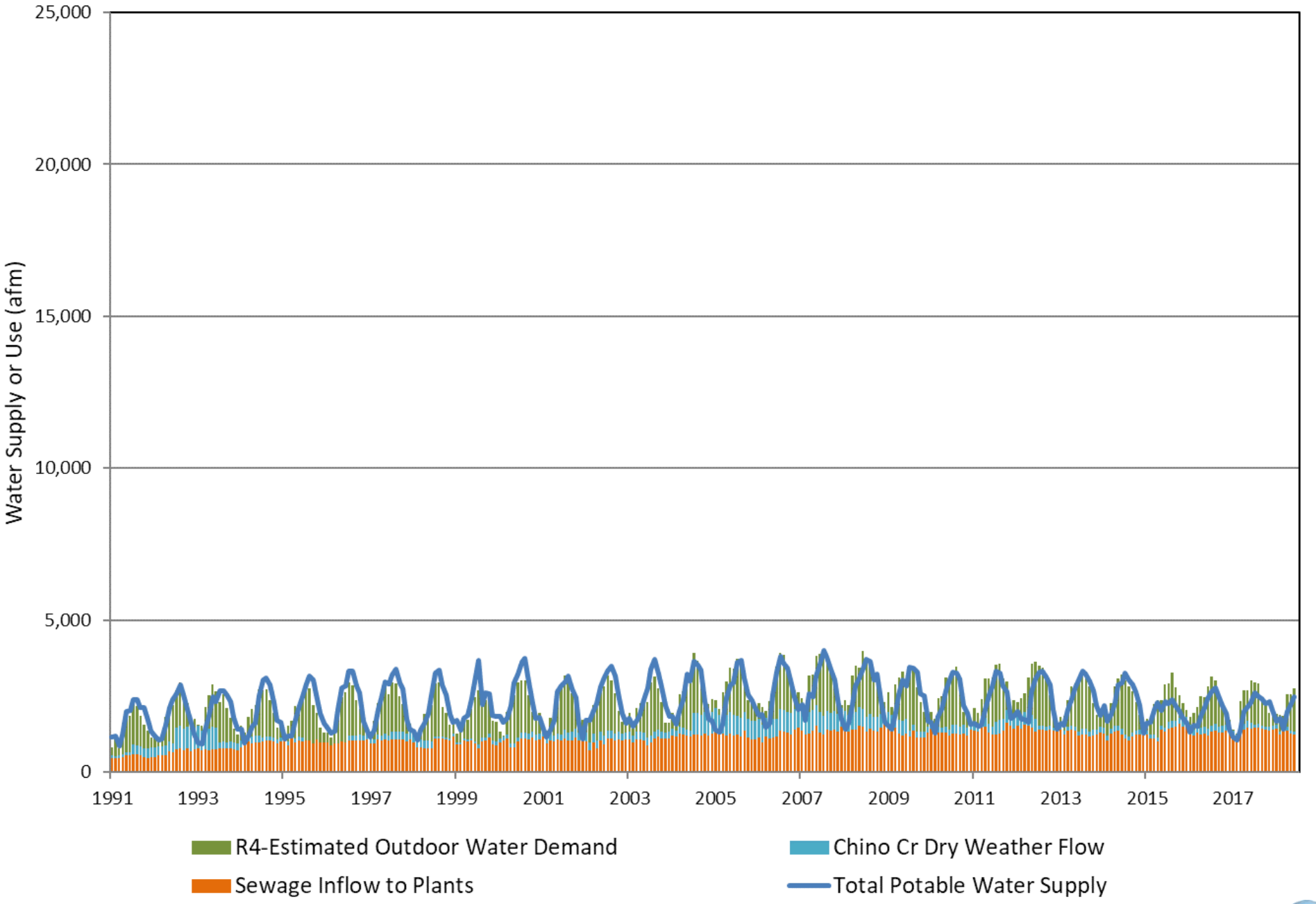

Figure 6-5a Scatter Plot of IEUA Estimated Water Supply and the R4-Estimated Water Supply for the RP1/RP4 Sewershed

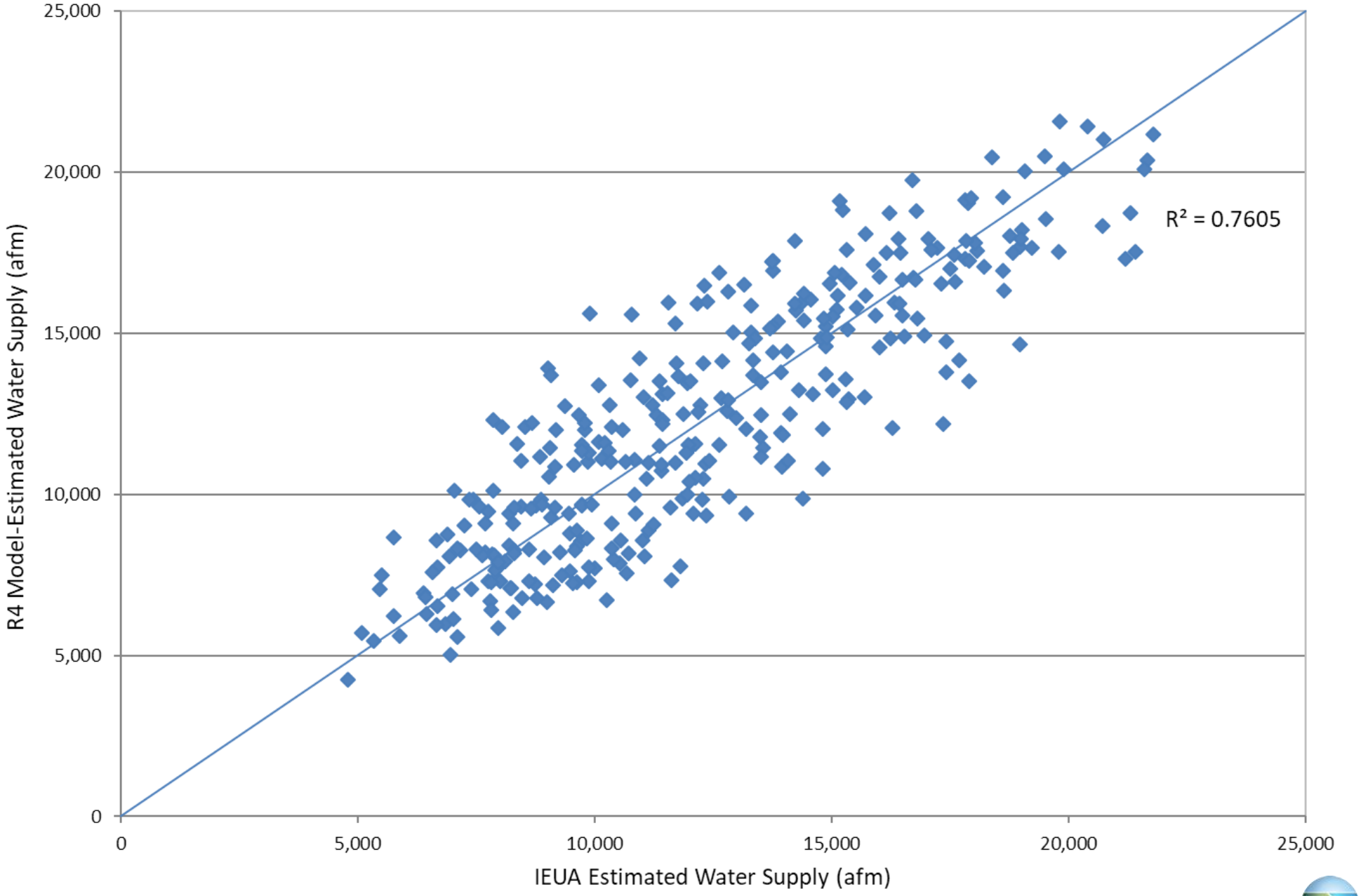

Figure 6-5b Scatter Plot of IEUA Estimated Water Supply and the R4-Estimated Water Supply for the RP2/CC/RP5 Sewershed

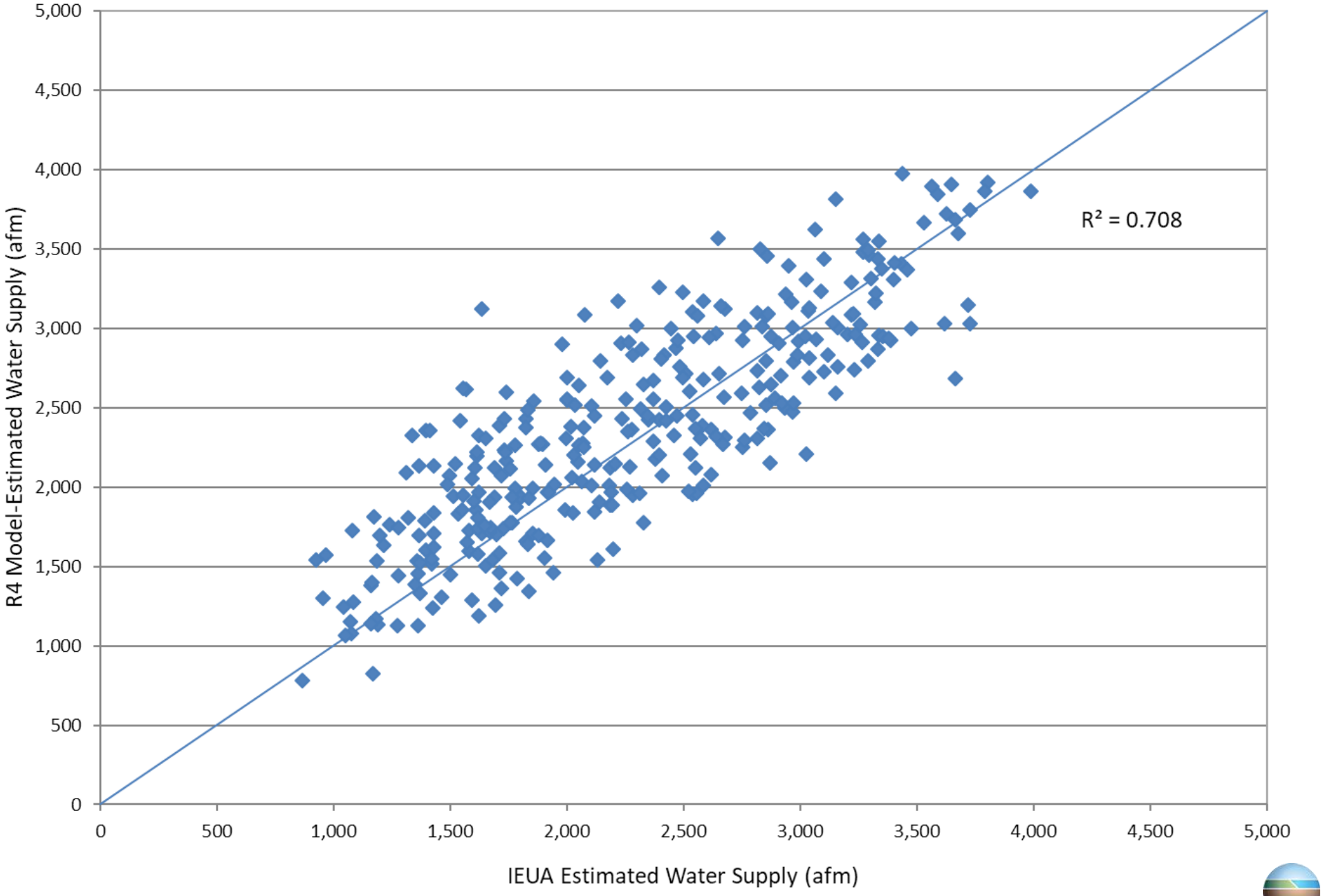

Groundwater Model Calibration Wells

- City of Chino
- City of Chino Hills
- City of Corona
- City of Ontario
- City of Pomona
- City of Upland
- Cucamonga Valley Water District
- Fontana Water Company
- Jurupa Community Services District
- Monte Vista Water District
- CDA
- Other

Streams & Flood Control Channels

Flood Control & Conservation Basins

Water Service Area

OBMP Management Zones

Faults

- Location Certain
- Location Approximate
- Approximate Location of Groundwater Barrier
- Location Concealed
- Location Uncertain

Prepared by:

WEI
Wildermuth Environmental, Inc.

Author: LS
Date: 4/1/2020
File: Figure 6-6 Calibration Wells.mxd

0 1 2 3 4 5 Miles
0 2 4 6 8 Km

Prepared for:

2020 Safe Yield Recalculation

Chino Basin Watermaster
Partners in Basin Management

Location of Calibration Wells
Chino Valley Model

Figure 6-6

Figure 6-7a
Comparison of Simulated and Measured Water Levels in the Wells of Chino Basin

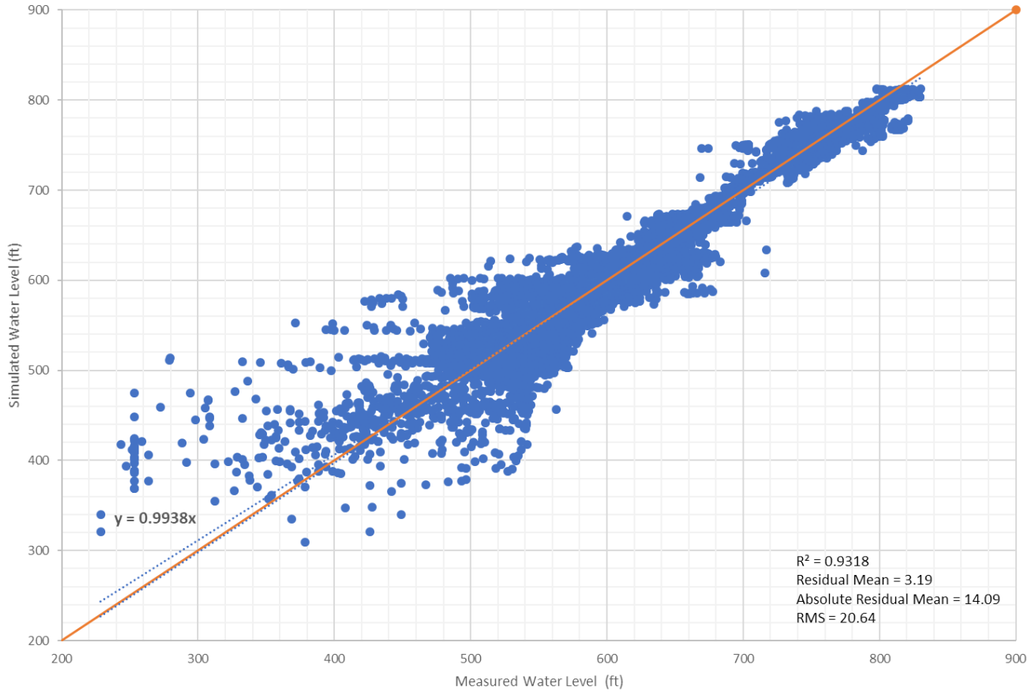

Figure 6-7b
Comparison of Simulated and Measured Water Levels in the Wells of Cucamonga Basin

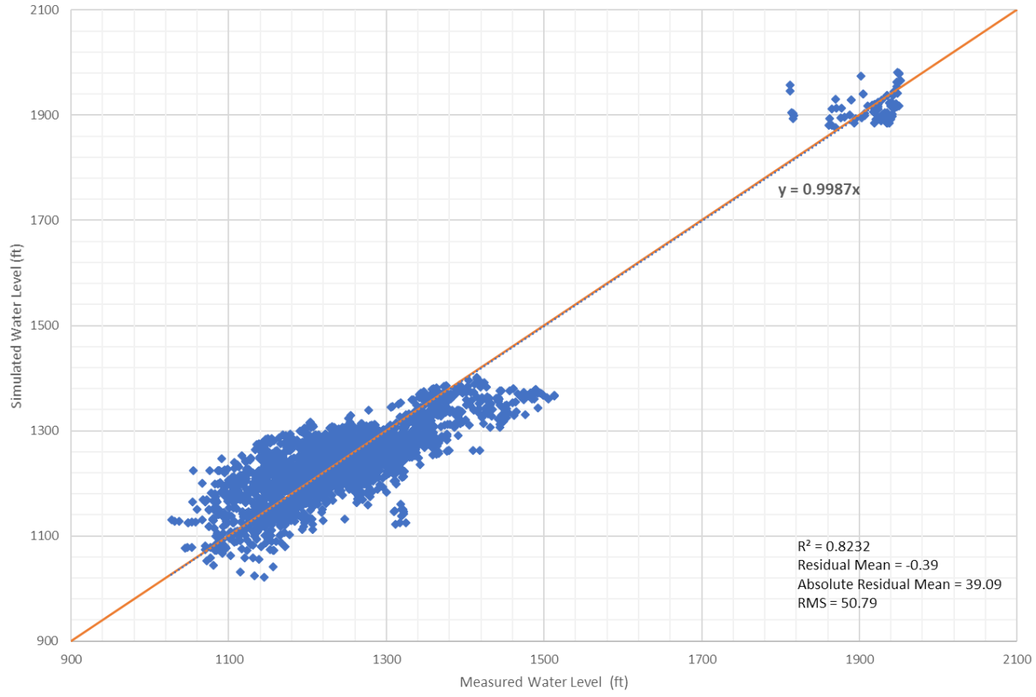

Figure 6-7c
Comparison of Simulated and Measured Water Levels in the Wells of Six Basin

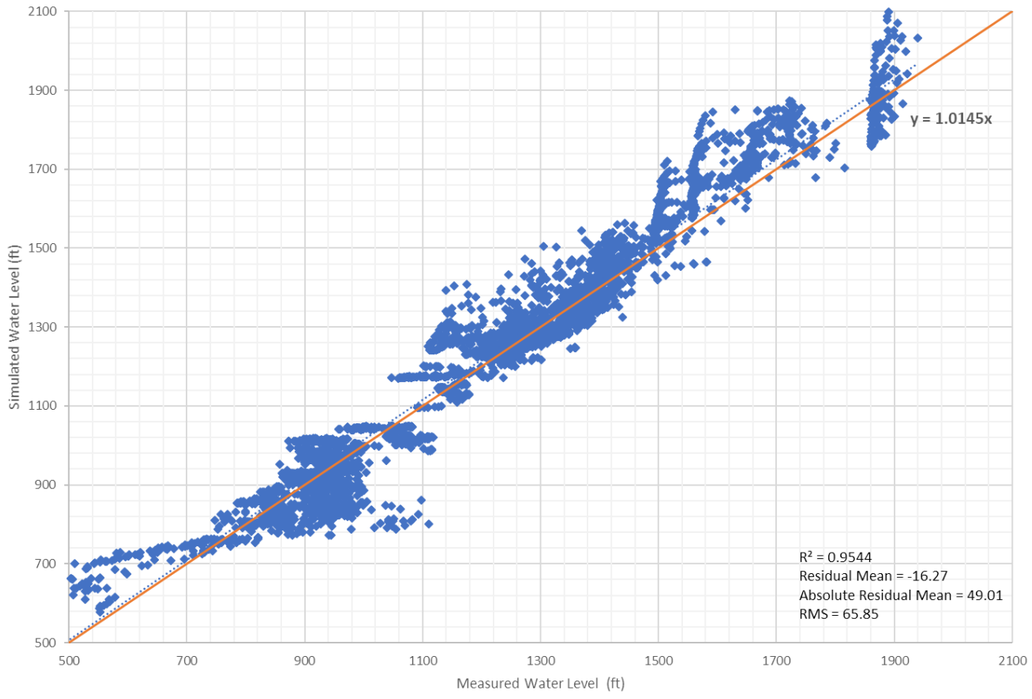

Figure 6-7d
Comparison of Simulated and Measured Water Levels in the Selected Chino Hills Wells with the other Wells of Chino Basin

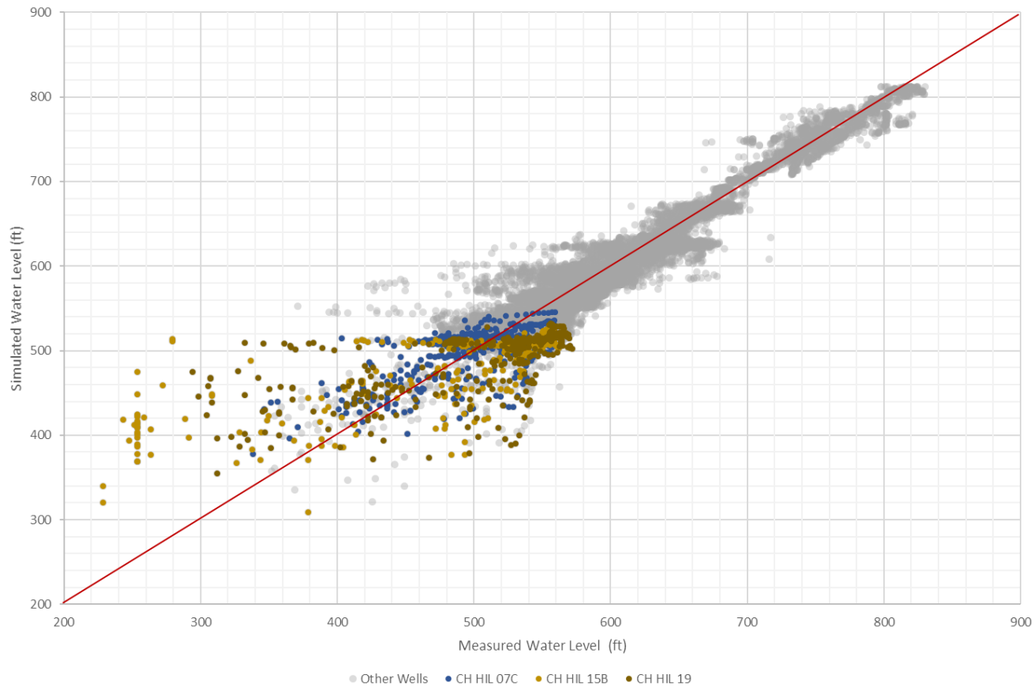

Figure 6-8a
MODFLOW Estimated Stream Flow and Measured Stream Flow Below the Prado Dam

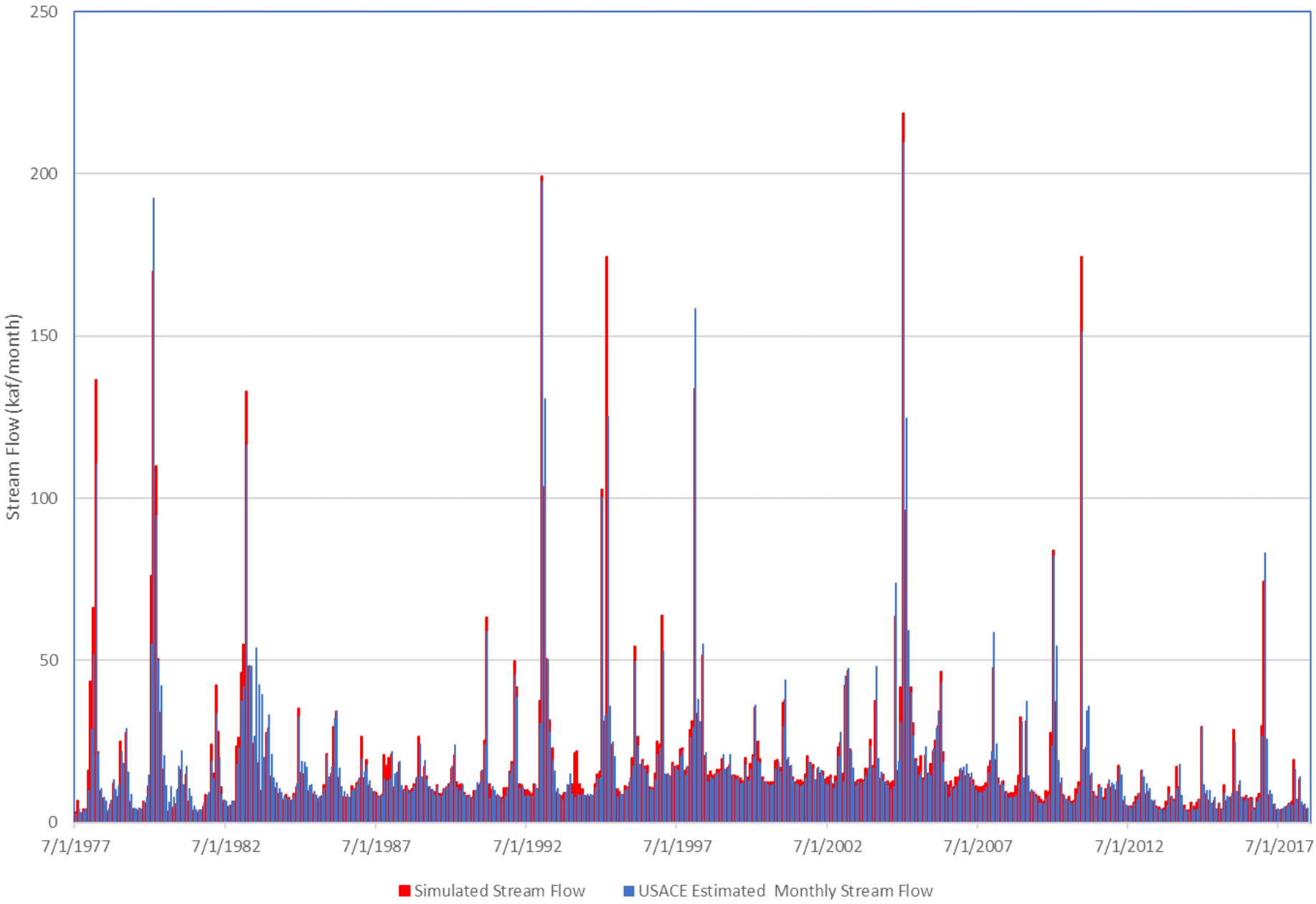

Figure 6-8b
Comparison of Simulated Stream Flow at Prado Dam to Total Prado Inflow Estimated by USACE

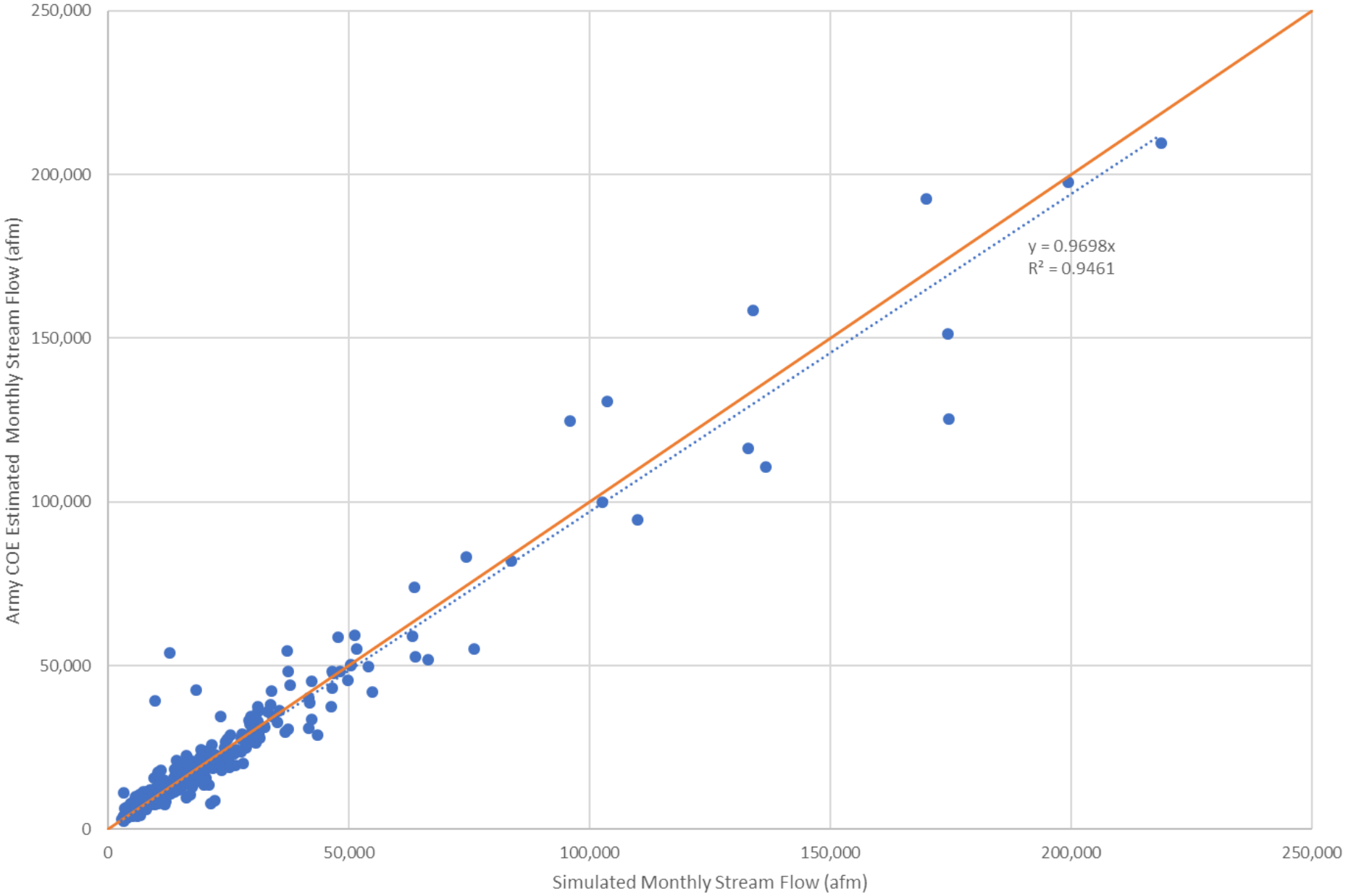

Figure 6-9
Residual Relative Freqency Histogram in Chino Basin

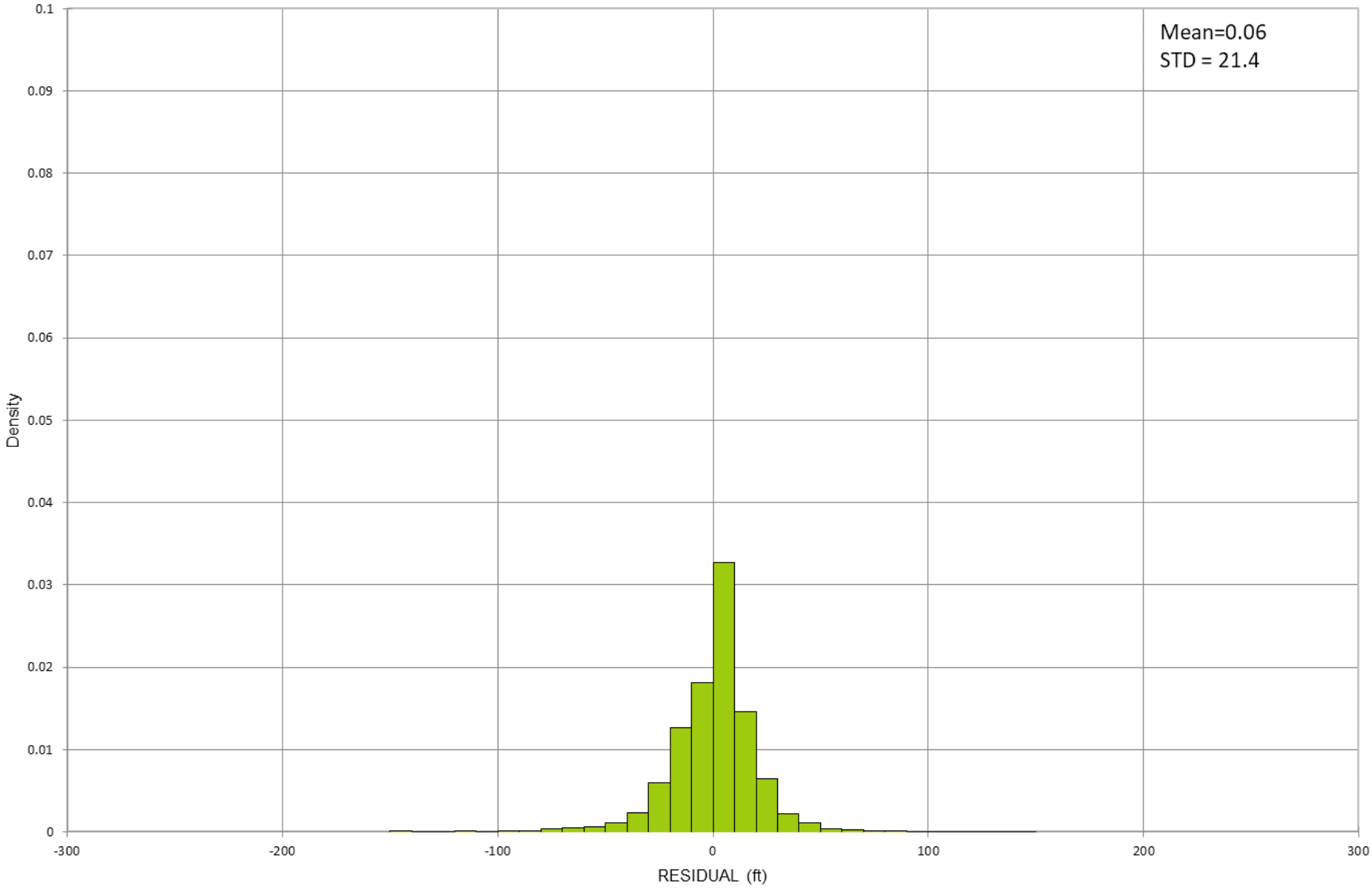

Figure 6-10a
Residual Relative Freqency Histogram in Cucamonga Basin

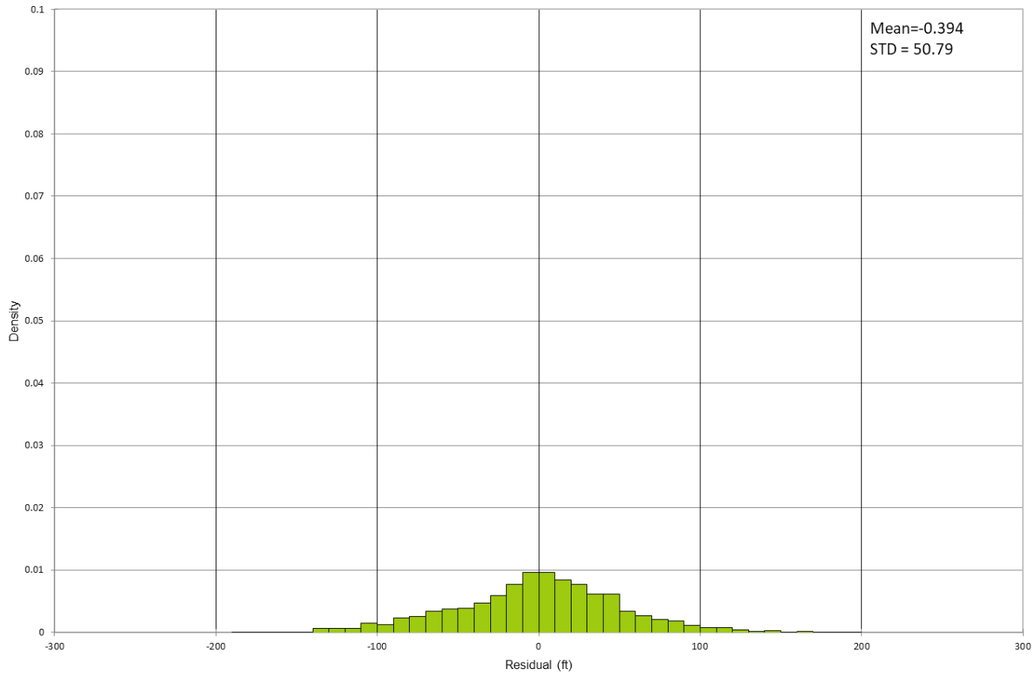

Figure 6-10b
Residual Relative Freqency Histogram in Six Basins

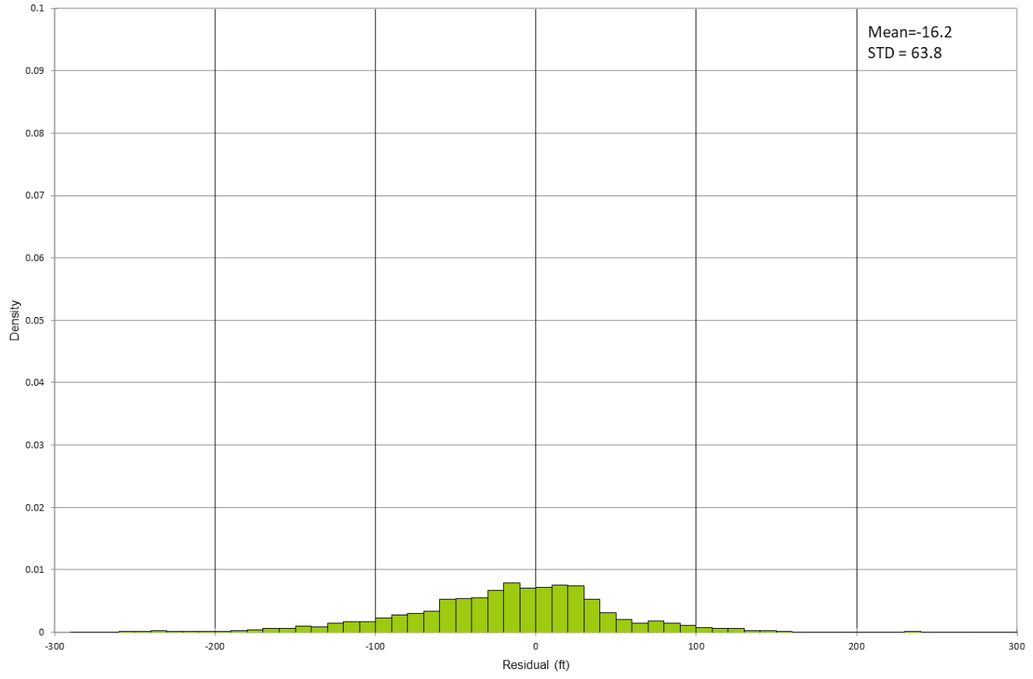

Figure 6-10c
Residual Relative Freqency Histogram in Spadra Basin

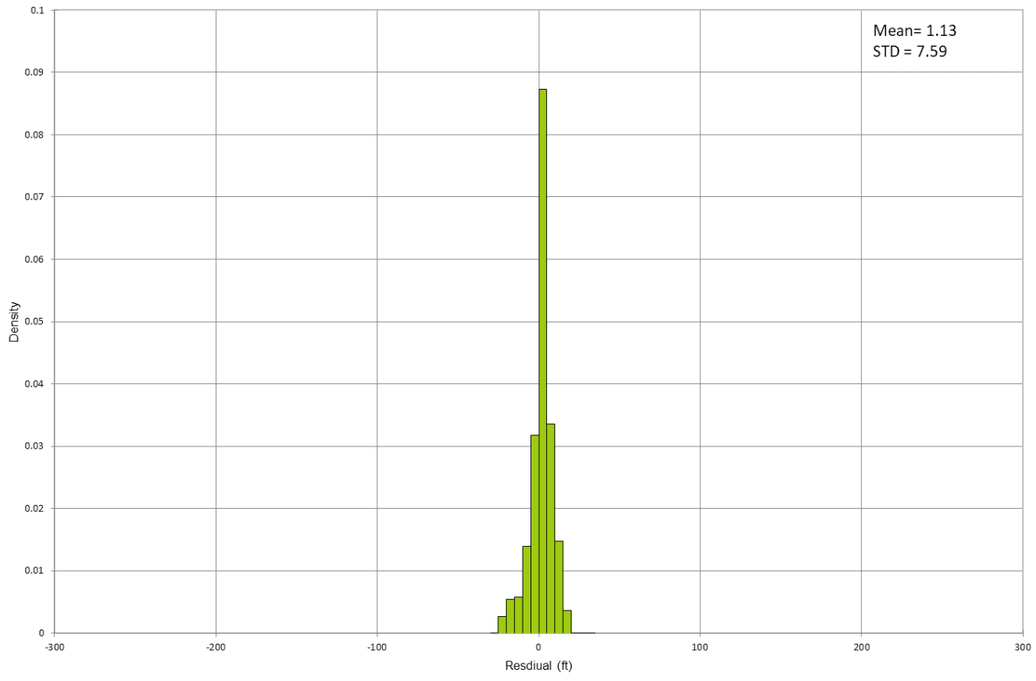

Figure 6-10d
Residual Relative Freqency Histogram in Temescal Basin

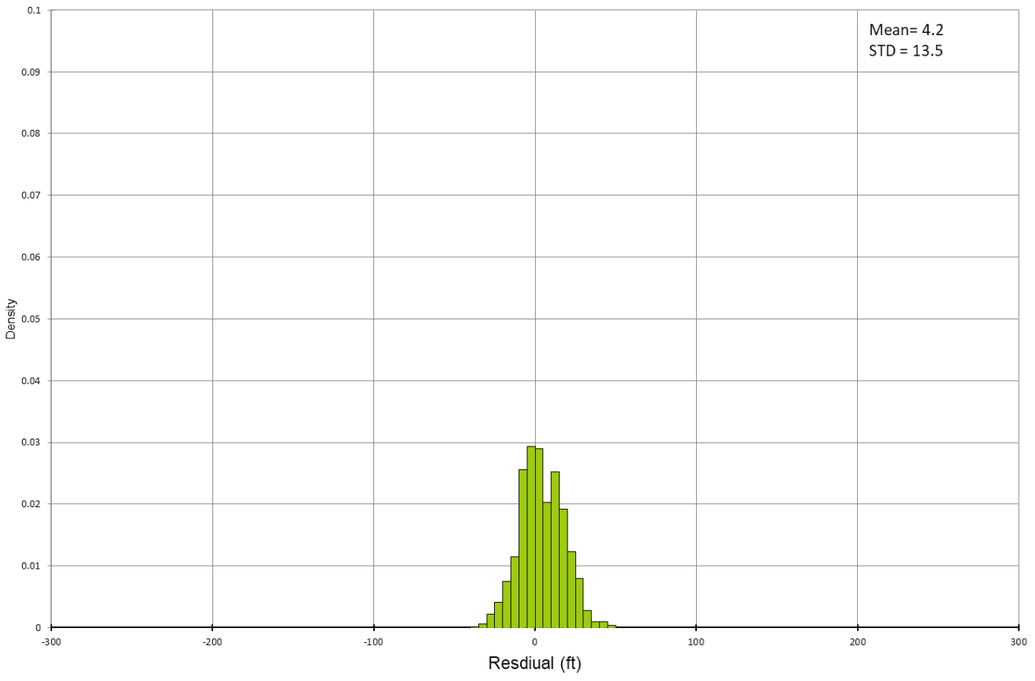

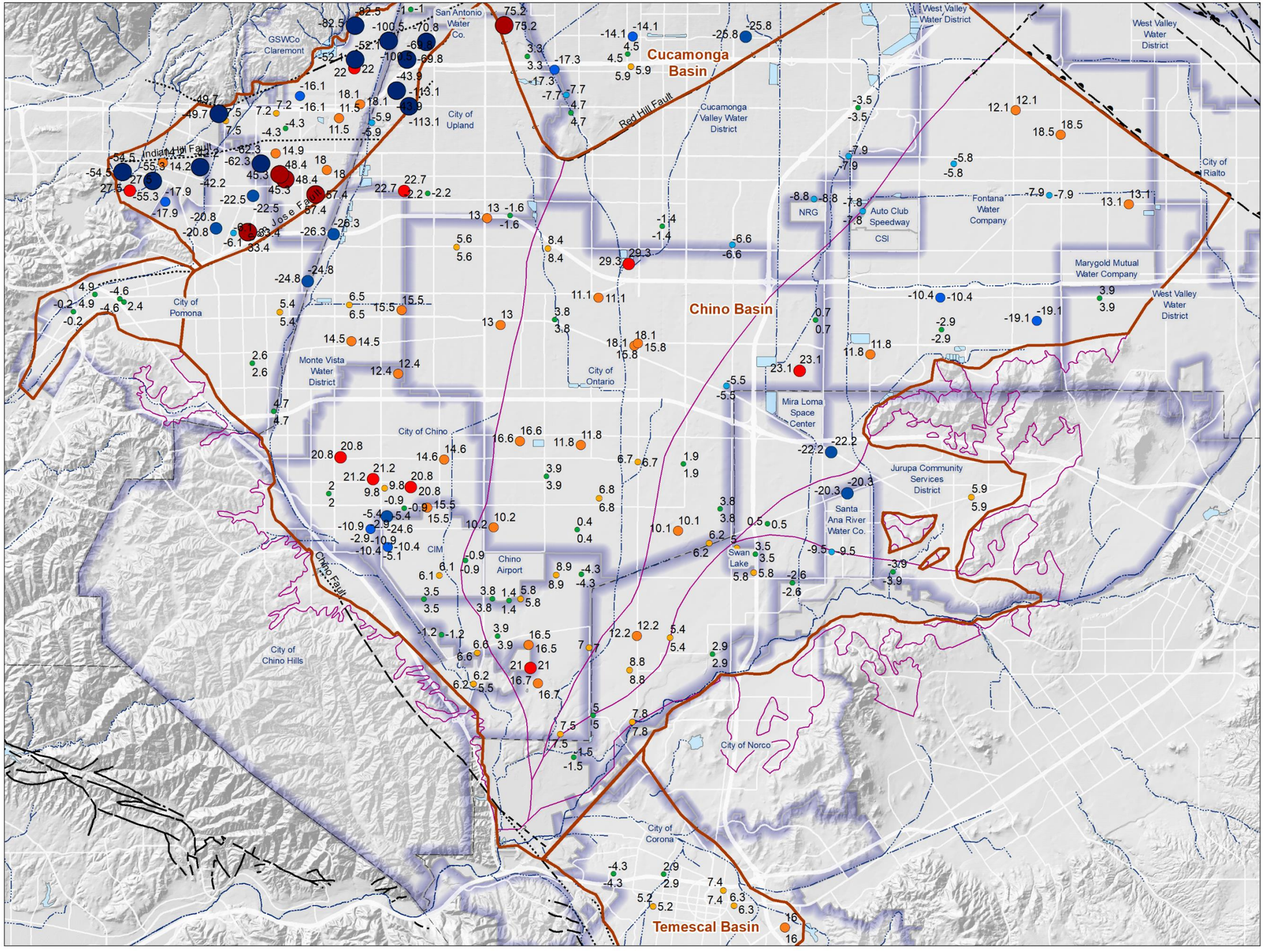

Mean Residual Error

- < -30
- -30 - -20
- -20 - -10
- -10 - -5
- -5 - 5
- 5 - 10
- 10 - 20
- 20 - 30
- >30

Streams & Flood Control Channels

Flood Control & Conservation Basins

Water Service Area

OBMP Management Zones

Faults

- Location Certain
- Location Concealed
- Location Approximate
- Location Uncertain
- Approximate Location of Groundwater Barrier

Prepared by:

WEI
WILDERMUTH ENVIRONMENTAL, INC.

Author: LS
Date: 5/11/2020
File: Figure 6-11 Mean Residual.mxd

0 1 2 3 4 5 Miles
0 2 4 6 8 Km

Prepared for:

2020 Safe Yield Recalculation

CHINO BASIN WATERMASTER
Partners in Basin Management

Mean Residual Error of Calibration Wells

Figure 6-11

Figure 6-12a Discharge to and from Vadose Zone and End of Year Vadose Zone Storage for Calibration Period

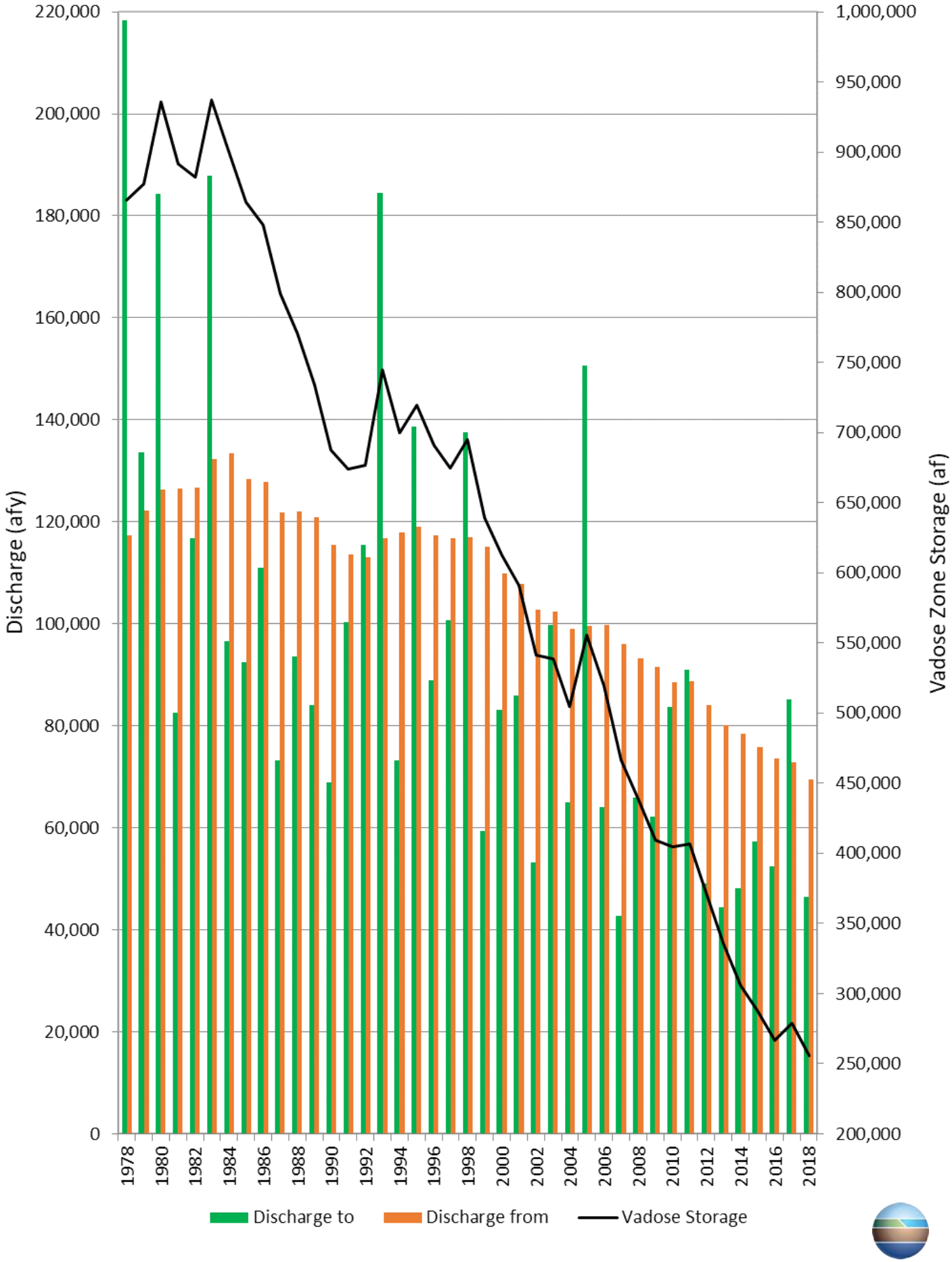

Figure 6-12b Relationship of End of Year Vadose Zone Storage to DIPAW Discharge to Saturated Zone for the Calibration Period

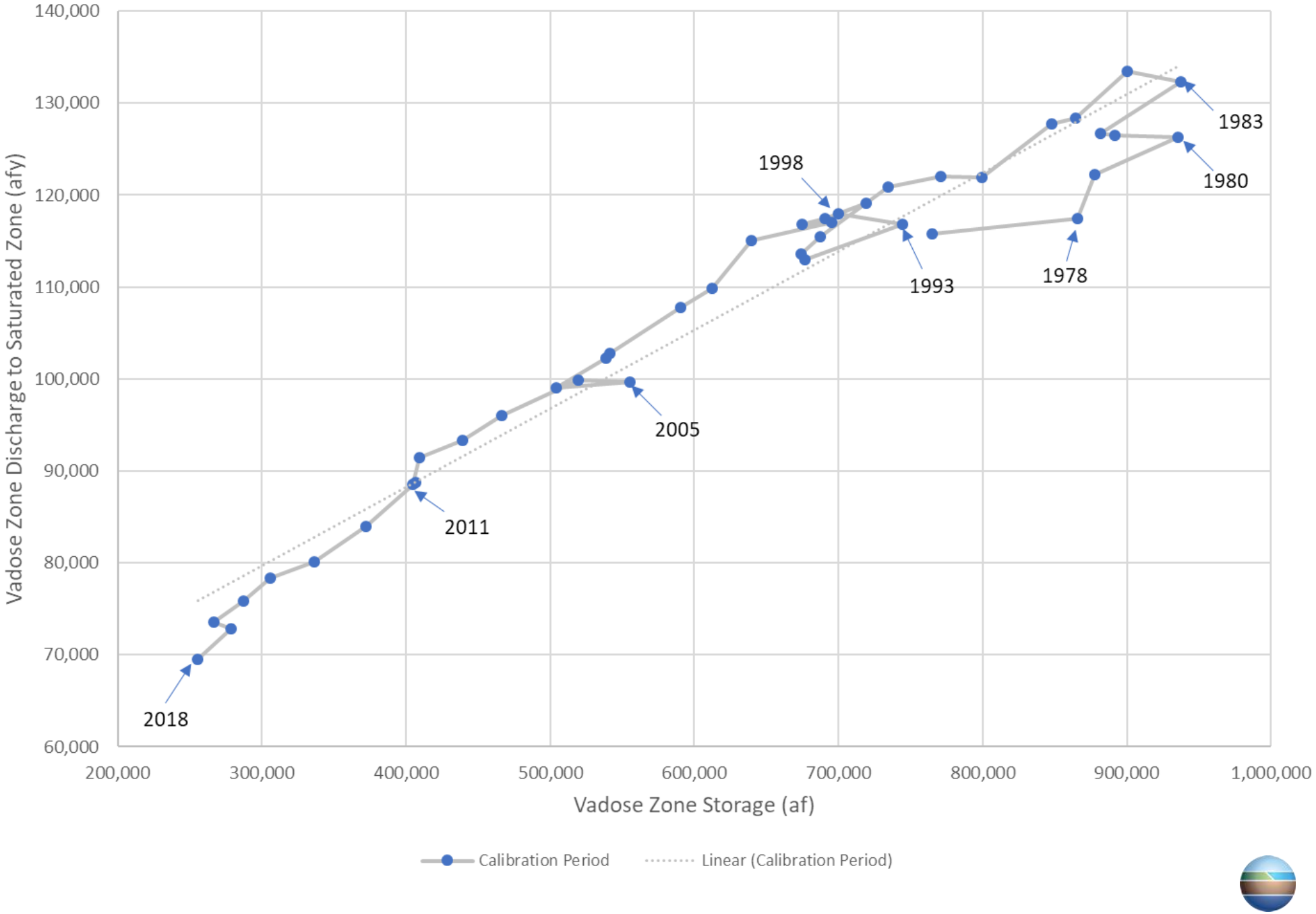

Figure 6-13 Comparison of Historical Basin Precipitation to Historical DIPAW

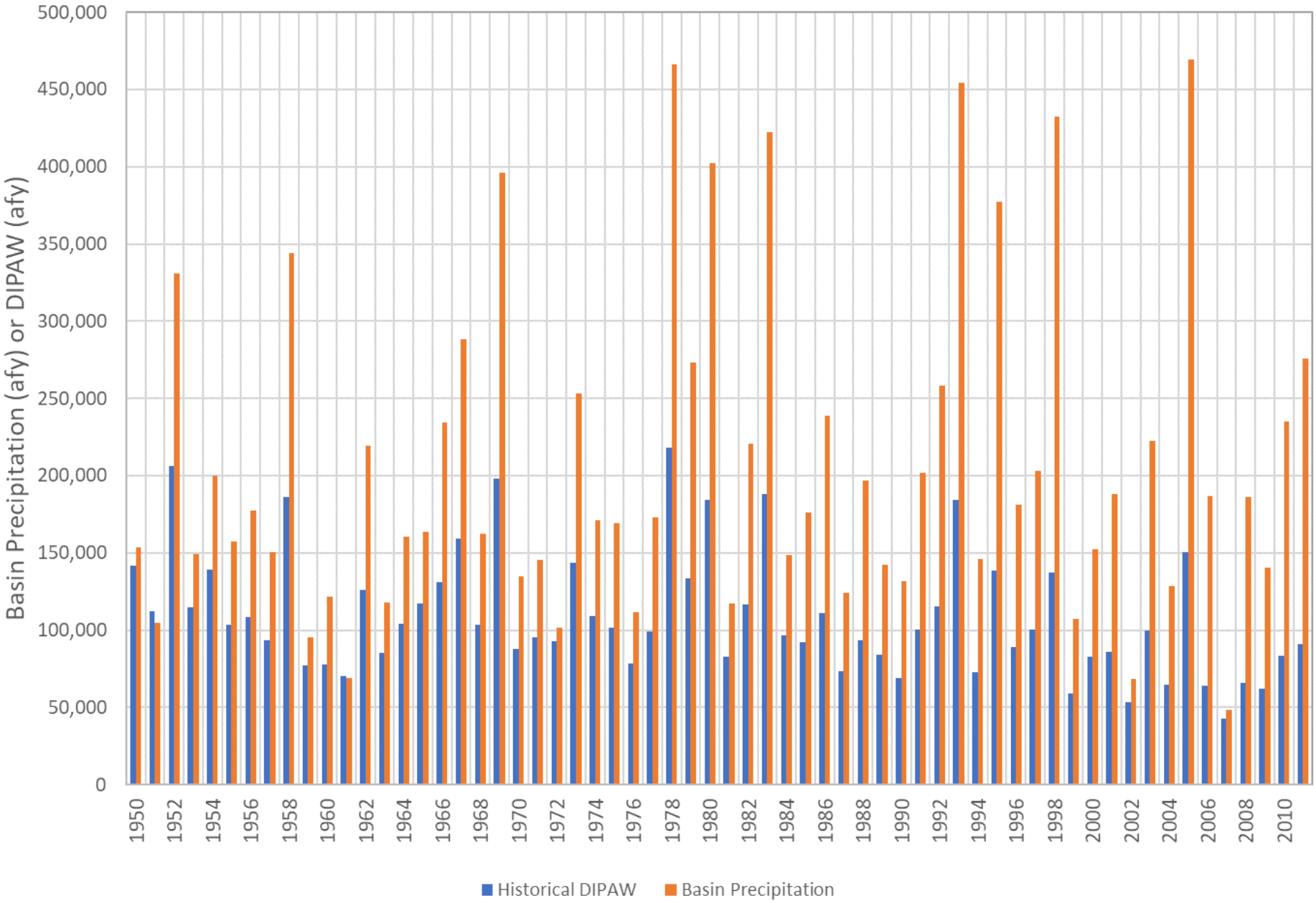

Figure 6-14 Total Recharge, Discharge, and Change in Storage in the Chino Basin During the Calibration Period

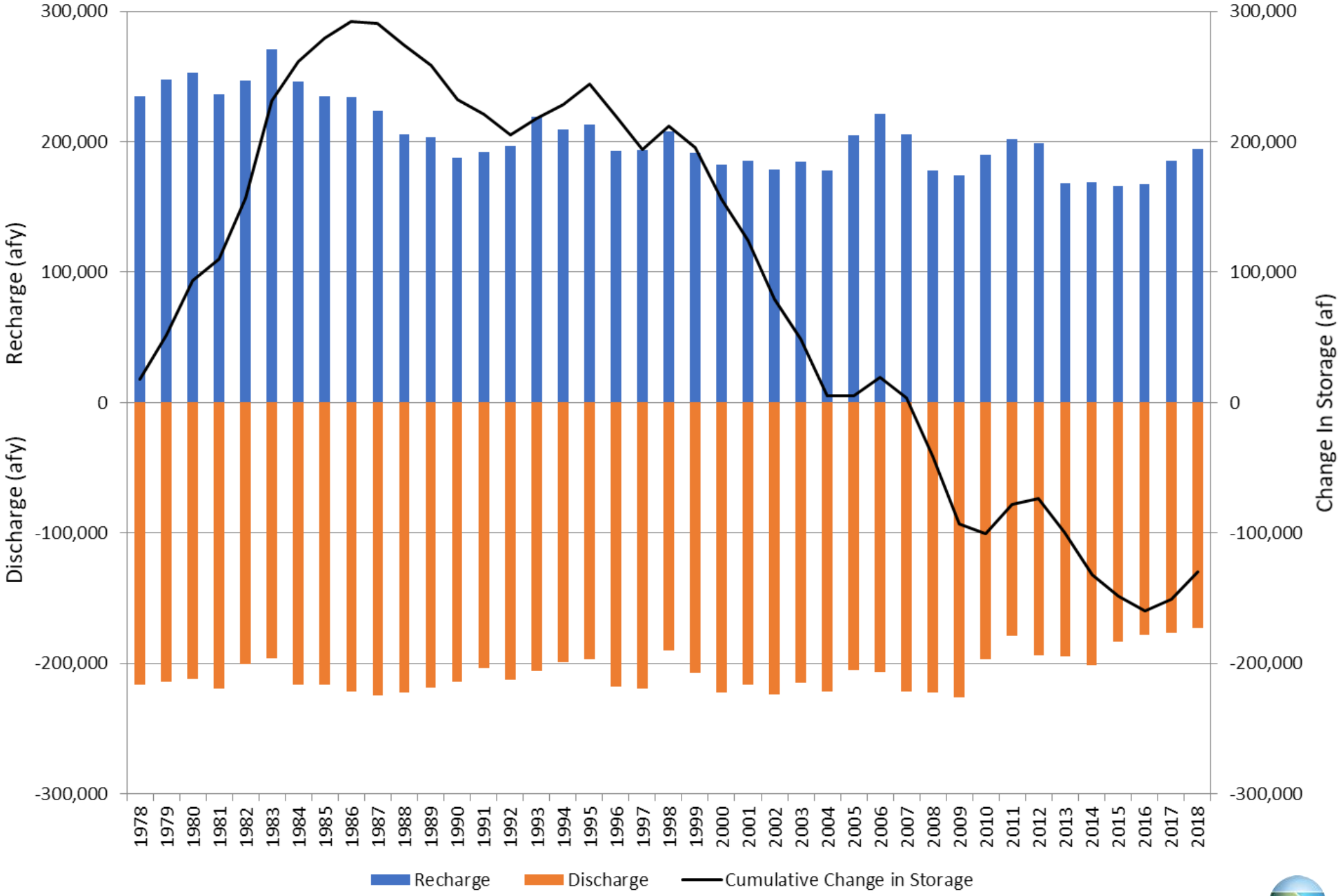

Figure 6-15
Comparison of DIPAW Discharge to the Saturated Zone from the Prior and 2020 Safe Yield Recalculations to Precipitation and Applied Water over Pervious Area for the Calibration Period

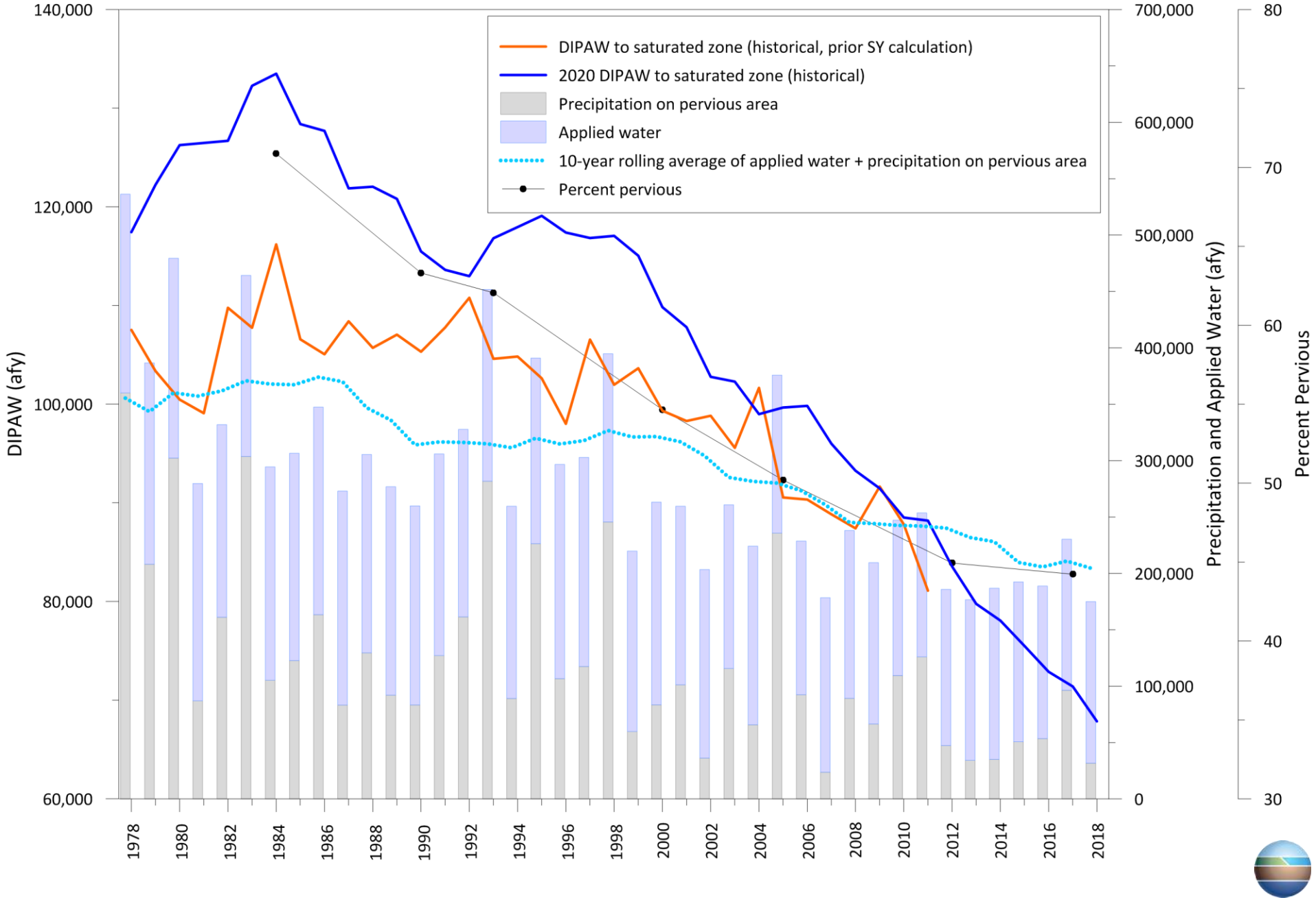

Figure 6-16
Comparison of Net Recharge from the Prior and 2020 Safe Yield Recalculations
to Precipitation and Applied Water over Pervious Area for the Calibration Period

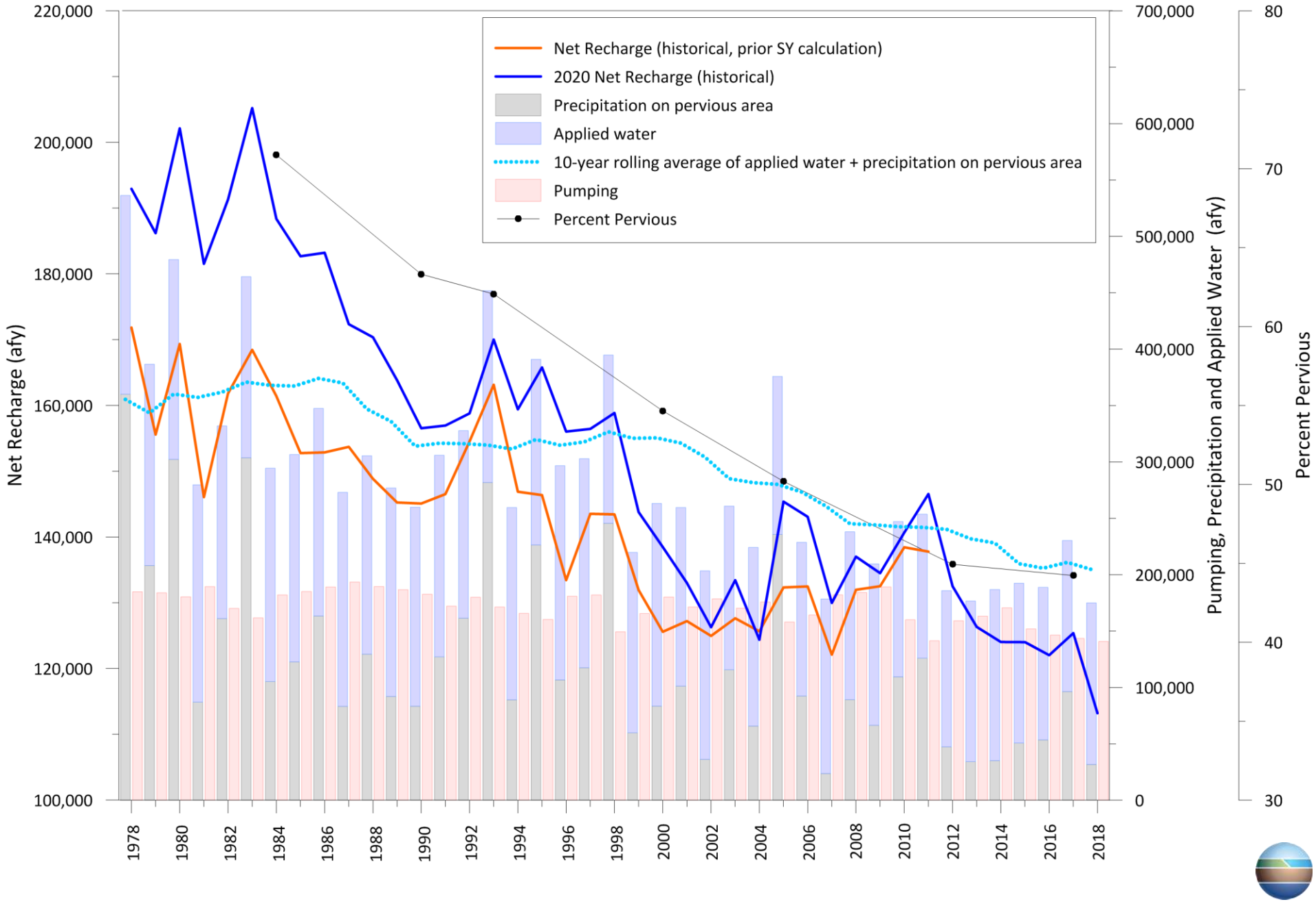

7.1 Application of the Court-Approved Methodology to Calculate Safe Yield

The Safe Yield calculation methodology used in the 2020 Safe Yield calculation is documented in a technical memorandum dated August 15, 2015 and was subsequently approved by the Court on April 28, 2017. The methodology is described below.

> "The methodology to redetermine the Safe Yield for 2010/11 and the recommended methodology for future Safe Yield evaluations is listed below. This methodology is consistent with professional custom, standard and practice, and the definition of Safe Yield in the Judgment and the Physical Solution.
>
> 1. Use the data collected during 2000/01 to 2009/10 (and in the case of subsequent resets newly collected data) in the re-calibration process for the Watermaster's groundwater-flow model.
> 2. Use a long-term historical record of precipitation falling on current and projected future land uses to estimate the long-term average net recharge to the Basin.
> 3. Describe the current and projected future cultural conditions, including, but not limited to the plans for pumping, stormwater recharge and supplemental-water recharge.
> 4. With the information generated in [1] through [3] above, use the groundwater-flow model to redetermine the net recharge to the Chino Basin taking into account the then existing current and projected future cultural conditions.
> 5. Qualitatively evaluate whether the groundwater production at the net recharge rate estimated in [4] above will cause or threaten to cause "undesirable results" or "Material Physical Injury". If groundwater production at net recharge rate estimated in [4] above will cause or threaten to cause "undesirable results" or "Material Physical Injury" then Watermaster will identify and implement prudent measures necessary to mitigate "undesirable results" or "Material Physical Injury", set the value of Safe Yield to ensure there is no "undesirable results" or "Material Physical Injury", or implement a combination of mitigation measures and a changed Safe Yield."

Each of these steps has been completed and documented herein as follows:

- The calibration period used for this model is July 1, 1977 through June 30, 2018 and is inclusive of the July 1, 2000 through June 30, 2010 period and the subsequent historical period through June 30, 2018 as required in Step 1. The hydrologic period used in the calibration is documented in Section 3 and the calibration is documented in Section 6.
- The long-term historical records of precipitation and ET_0, adjusted for climate change developed in Step 2 is documented in Section 7.2.
- The historical and projected land use is described in Section 3 and remaining components of cultural conditions developed in Step 3 are documented in Section 7.3.
- The projected net recharge to the basin developed in Step 4 is documented in Section 7.4.
- An evaluation of undesirable results and MPI developed in Step 5 is described in Section 7.5.

7.2 Long-Term Historical Records Used to Estimate Net Recharge

For use in SGMA-related water budget development and groundwater modeling, DWR (2018) provides climate change datasets in the form of change factors of precipitation, ET_0, and surface runoff based on 20 global climate projections. According to the *Guidance for Climate Data Change Use During Groundwater Sustainability Plan Development* (DWR, 2018), change factor ratios were calculated as the future scenario (2030 or 2070) divided by the 1995 historical temperature detrended (1995 HTD) scenario. The 1995 HTD scenario represents historical climate conditions where the observed temperature increasing trend is removed.

The change factors are provided as monthly time-series over the period of 1915 to 2011 for each grid cell of the DWR's Variable Infiltration Capacity (VIC) model, which covers the State of California. Figure 7-1 shows a portion of the VIC model grid, the 2020 CVM boundary (in black) and the domains of the HSPF and R4 models used to estimate surface water discharge and most of the recharge stresses in the 2020 2020 CVM.

In this investigation, the historical precipitation and ET_0 datasets for the period 1950 to 2011 were used to estimate net recharge and Safe Yield. This is the latest 62-year period that overlaps the change factor time series provided by the DWR and for which the average annual precipitation over the 2020 CVM domain and watershed area are equal to their respective long-term precipitation averages. Figure 3-11 shows the cumulative departure from mean (CDFM) precipitation curves for the 2020 CVM domain and watershed area. These CDFM curves are based on the PRISM monthly precipitation datasets at 30-arcsec (800 meters) grid resolution. The average annual precipitation for this period for the 2020 CVM domain is about 17.18 inches; and for the 2020 CVM watershed area is about 19.47 inches, the latter being greater due to the orographic effects caused by the San Gabriel Mountains. The average annual precipitation for the entire historical record of 1895 through 2018 is about 17.14 inches for the 2020 CVM domain; and for the 2020 CVM watershed area is about 19.48 inches– virtually identical to the 1950 through 2011 period.

Figures 7-2a and 7-2b illustrate the statistics of the change factors for precipitation for 2030 and 2070 conditions, respectively. Figures 7-3a and 7-3b illustrate the statistics of the change factors for the ET_0 for 2030 and 2070 conditions, respectively. These figures are based on the change factor values for the VIC model cells that overly the 2020 CVM model domain over the period of 1950 to 2011. The average value of those change factor values is displayed on the upper-right corner of each figure. Review of these charts indicates that average precipitation is projected to decrease, and average ET_0 is projected to increase.

The following procedure was used to apply the change factors to the 2020 CVM for the 2020 Safe Yield recalculation:

1. For the current (2018) cultural condition:
    a. The HSPF and R4 models are executed with the most recent (2017) land use data and the daily precipitation and ET_0 datasets from 1950 to 2011 with a change factor of 1.
    b. The average monthly DIPAW, stormwater discharge to streams, and stormwater recharge are calculated based on the results of the HSPF and R4 simulations.
    c. The Santa Ana River and Temescal Wash discharges are adjusted to remove upstream historical wastewater discharges, multiplied with the surface runoff change factor of 1 and adjusted to include projected 2018 wastewater discharges.
2. For the 2030 cultural condition:

a. The HSPF models are executed with the 2030 land use data and the daily precipitation and ET_0 datasets from 1950 to 2011, and the estimated surface runoff is multiplied with the surface runoff change factor for 2030.
b. The Santa Ana River and Temescal Wash discharges are adjusted to remove upstream historical wastewater discharges, multiplied with the surface runoff change factor for 2030 and adjusted to include projected 2030 wastewater discharges.
c. The daily precipitation and ET_0 datasets from 1950 to 2011 are multiplied with the change factors of 2030.
d. The R4 model is executed with the 2030 land use data and the modified precipitation and ET_0 datasets.
e. The average monthly DIPAW, stormwater discharge to streams, and stormwater recharge are calculated based on the results of the HSPF and R4 simulations.

3. For the 2040 cultural condition:
   a. The HSPF models are executed with the 2040 land use data and the daily precipitation and ET_0 datasets from 1950 to 2011, and the estimated surface runoff is multiplied with the surface runoff change factor for 2040.
   b. The Santa Ana River and Temescal Wash discharges are adjusted to remove upstream historical wastewater discharges, multiplied with the surface runoff change factor for 2040 and adjusted to include projected 2040 wastewater discharges.
   c. The daily precipitation and ET_0 datasets from 1950 to 2011 are multiplied with the change factors of 2040.
   d. The R4 model is executed with the 2040 land use data and the modified precipitation and ET_0 datasets.
   e. The average monthly DIPAW, stormwater discharge to streams, and stormwater recharge are calculated based on the results of the HSPF and R4 simulations.
4. For the 2070 cultural condition:
   a. The HSPF models are executed with the 2070 land use data and the daily precipitation and ET_0 datasets from 1950 to 2011, and the estimated surface runoff is multiplied with the surface runoff change factor for 2070.
   b. The Santa Ana River and Temescal Wash discharges are adjusted to remove upstream historical wastewater discharges, multiplied with the surface runoff change factor for 2040 and adjusted to include projected 2070 wastewater discharges.
   c. The daily precipitation and ET_0 datasets from 1950 to 2011 are multiplied with the change factors of 2070.
   d. The R4 model is executed with the 2070 land use data and the modified precipitation and ET_0 datasets.
   e. The average monthly DIPAW, stormwater discharge to streams, and stormwater recharge are calculated based on the results of the HSPF and R4 simulations.
5. Apply the estimated DIPAW, stormwater discharge to streams, and stormwater recharge to the 2020 CVM.
   a. The estimated average monthly DIPAW and the stormwater discharge values are linearly interpolated between 2018, 2030, 2040, and 2070 cultural conditions (based on the simulation time), and the results are used as input to the 2020 CVM.

7.3 Present and Projected Future Cultural Conditions

The 2020 CVM was used to project net recharge, groundwater levels and the state of hydraulic control for the 2019 through 2050 period. A planning scenario was developed to recalculate Safe Yield based on the recent planning work reported in the *2018 Storage Framework Investigation* and the *2020 Storage Management Plan*. This scenario, referred to herein as 2020 SYR1 is based on the water demands and

water supply plans provided by the Watermaster Parties, planning hydrology that incorporates climate change impacts on precipitation and ET_0, and assumptions regarding cultural conditions and future replenishment. The information and assumptions included in the planning scenario are described in this section.

7.3.1 Planning Scenario

Planning scenario 2020 SYR1 included cultural conditions representative of the period of 2018 through 2050 and uses a 62-year hydrologic period from 1950 through 2011. Scenario 2020 SYR1 assumed groundwater pumping would change over time based on groundwater pumping projections provided by the Watermaster Parties, and that replenishment and recharge operations would be conducted by Watermaster pursuant to the Judgment and Peace Agreement. Scenario 2020 SYR1 assumed the following:

- The planning period runs from July 1, 2018 through June 30, 2050.
- The economy continues to expand with the build-out of undeveloped land by 2040.
- The CDA expansion and related improvements will be completed in 2022, and re-operation will occur based on the current approved schedule through 2030.
- The 6,500 afy supplemental water recharge obligation for MZ1 will terminate in 2030. At the time of this investigation, it was assumed that this obligation will be satisfied through the recharge of imported water for the Dry-Year Yield Program that has already occurred and planned recycled water recharge planned to occur in MZ1 through 2030.
- Projected future recycled water recharge estimates were provided by the IEUA.
- Projected future stormwater recharge estimates were based on R4 Model simulations incorporating planned 2013 Recharge Master Plan Update (RMPU) improvements that are assumed operational in 2023 and the existing and projected cultural conditions. No increase in future stormwater recharge capacity was assumed beyond that planned in the 2013 RMPU.
- Pumping rights were based on the current and projected future Safe Yield.
- There is an active water market among the Chino Basin Parties where annual unpumped rights and stored water are conveyed among the Parties. This market resulted in reduced wet-water replenishment compared to the wet-water replenishment that would have occurred if there were no such market.

7.3.1.1 Groundwater Pumping Projections

In 2017, as part of the 2018 Storage Framework Investigation, Watermaster submitted a comprehensive data request to each Appropriative Pool party and some of the larger Overlying Non-Agricultural Pool pumpers, including:

- Arrowhead Mountain Spring Water Company (Arrowhead)
- City of Chino (Chino)
- City of Chino Hills, (Chino Hills)
- City of Norco (Norco)
- City of Ontario (Ontario)
- City of Pomona (Pomona)
- City of Upland (Upland)
- Cucamonga Valley Water District (CVWD)
- Fontana Water Company (FWC)
- Golden State Water Company (GSWC)

- Jurupa Community Services District (JCSD)
- Marygold Mutual Water Company
- Monte Vista Irrigation Company
- Monte Vista Water District (MVWD)
- Niagara Bottling, LLC (Niagara)
- Santa Ana River Water Company (SARWC)
- San Antonio Water Company (SAWCo)
- San Bernardino County – Olympic Shooting Park
- West Valley Water District (WVWD)

Watermaster staff reviewed the Parties' responses and followed up for clarification, if necessary. The data provided by the Parties represents their best estimates of their demands and associated water supply plans. Individually and in aggregate, these water demands and associated supply plans are reasonable and the most reliable planning information available.

All agencies were requested to provide projections of the water sources that they would use to meet their demands on a monthly and annual basis for each planning year through 2050. Several Parties' water supply plans had projected water supplies that exceeded their demands. When this occurred, Watermaster staff conducted additional discussions to determine these Parties' projected Chino Basin groundwater pumping and established priorities of use for their other sources. The tables below show the historical (2015) and projected aggregate water demand and supply plans for all Chino Basin Parties, based on their responses to the data request, their 2015 Urban Water Management Plans (UWMPs), and other information obtained for the 2018 Storage Framework Investigation and the 2020 Storage Management Plan. The projected growth in water demand by the Appropriative Pool Parties drives the increase in aggregate water demand, as some Appropriative Pool Parties are projected to serve new urban water demands created by the conversion of agricultural and vacant land uses to urban uses.

The total water demand is projected to grow from about 329,200 afy in 2020 to about 416,600 afy by 2040. Recycled water for direct reuse is projected to increase from about 23,700 afy in 2020 to about 34,000 afy by 2040. The amount of imported water supplied by Metropolitan is projected to increase from about 90,900 afy in 2020 to about 113,000 afy by 2040.

Table 7-1 shows the groundwater pumping projection by producer. Note that the near-term CDA pumping projection for the early 2020s has been updated since the completion of the 2020 Storage Management Plan. The table below summarizes the projected groundwater pumping by pool.

Aggregate Water Supply Plan for Watermaster Parties and CDA

Water Source	2015 (Actual)	2020	2025	2030	2035	2040
Volume (afy)						
Chino Basin Groundwater	148,600	132,200	146,300	153,500	166,300	175,500
Non-Chino Basin Groundwater	51,400	55,700	61,700	63,300	65,000	66,800
Local Surface Water	8,100	19,700	19,700	19,700	19,700	19,700
Imported Water from Metropolitan	56,000	90,900	98,800	105,700	107200	113,000
Other Imported Water	6,900	7,000	7,200	7,300	7,500	7,600
Recycled Water for Direct Reuse	17,400	23,700	24,300	26,900	30,500	34,000
Total	288,400	329,200	358,000	376,400	396,200	416,600
Percentage						
Chino Basin Groundwater	52%	40%	41%	41%	42%	42%
Non-Chino Basin Groundwater	18%	17%	17%	17%	16%	16%
Local Surface Water	3%	6%	6%	5%	5%	5%
Imported Water from Metropolitan	19%	28%	28%	28%	27%	27%
Other Imported Water	2%	2%	2%	2%	2%	2%
Recycled Water for Direct Reuse	6%	7%	7%	7%	8%	8%
Total	100%	100%	100%	100%	100%	100%

Summary of Projected Groundwater Pumping by Pool and the CDA (afy)

Planning Year	Agricultural Pool	Overlying Non-Agricultural Pool[19]	Appropriative Pool and CDA	Total
2015 (Actual)	17,400	3,400	127,900	148,600
2020	15,700	3,900	121,600	141,200
2025	12,800	3,900	129,600	146,300
2030	10,000	3,900	139,600	153,500
2035	7,900	4,000	154,400	166,300
2040	4,800	4,000	166,700	175,500

[19] The number reported in this column is the total pumped by the Overlying Non-Agricultural Pool. General Electric Company, a member of the Overlying Non-Agricultural Pool, pumps about 1,700 afy that is treated and injected back into the Chino Basin. The net pumping by the Overly Non-Agricultural Pool is actually 1,700 afy less than reported in this table.

7.3.1.2 Methodology to Project Replenishment Obligations

Pursuant to the Judgment, Watermaster levies and collects assessments each year in amounts sufficient to purchase replenishment water to replace pumping by a pool during the preceding year in excess of that pool's allocated share of Safe Yield (Overlying Agricultural and Overlying Non-Agricultural Pools) or Operating Safe Yield (Appropriative Pool). Parties within the Overlying Non-Agricultural Pool can transfer stored water and/or unused Safe Yield rights among themselves with Watermaster approval to minimize their replenishment obligations. Appropriative Pool Parties can do the same within their Pool. After the completion of a fiscal year, Watermaster collects pumping and transfer records from all Parties to determine replenishment obligations created in the prior year. Projected future replenishment obligations are based on current and projected Safe Yield, groundwater augmentation as described above, and the transfer activity among the Parties. This process, as implemented in this investigation, is described below.

The 2020 Safe Yield recalculation investigation estimated the aggregate annual replenishment obligation using the following assumptions:

- On a go-forward basis, under-producers will transfer unused pumping rights and stored water to over-producers each year.
- Stored water will be used to meet future replenishment obligations prior to the purchase of wet-water for recharge.

An analysis of Watermaster assessment packages for fiscal years 2010/11 through 2016/17 conducted by Watermaster staff for the 2018 Storage Framework Investigation indicated that about 80 percent of replenishment obligations were satisfied from unused pumping rights and stored water. The remaining replenishment obligations were satisfied with wet-water recharge. Based on this finding, the following assumptions were used to project future replenishment obligations in this investigation:

- If aggregate pumping rights are greater than the projected aggregate pumping, then the under-pumping is credited to storage accounts and there is no wet-water recharge for replenishment.
- If the aggregate pumping rights are less than the projected aggregate pumping, then 80 percent of the replenishment obligation is debited to storage accounts with the remainder being satisfied through wet-water recharge.

Pumping rights are based on the following assumptions:

- The Safe Yield is 135,000 afy through 2020; thereafter, the Safe Yield is replaced with an estimate of Safe Yield based on projected net recharge and using the Safe Yield recalculation methodology approved by the Court[20].
- Reoperation water is allocated to the replenishment of desalter production, as provided for in the Peace II Agreement and by a 2017agreement among the Appropriative Pool following Court approval of Safe Yield. Reoperation water will be allocated to the replenishment of desalter production through 2030.
- Recycled water recharge was assumed to occur as projected by the IEUA as of June 2016[21] and modified in the near term based on recent actual recycled water recharge performance.

[20] See technical memorandum entitled Methodology to Reset Safe Yield Using Long-Term Average Hydrology and Current and Projected Future Cultural Conditions prepared by WEI, August 10, 2015.

[21] Email from Andy Campbell (IEUA) to WEI, June 2016.

In this investigation, it was assumed that when the aggregate annual replenishment obligation becomes positive, the replenishment obligation would be satisfied with 80 percent of the replenishment water from stored water and the remaining 20 percent from wet-water recharge and 100 percent by wet-water recharge when the water in managed storage is depleted. The aggregate water in managed storage for the Parties in the Overlying Non-Agricultural and Appropriative Pools on July 1, 2019 was 503,275 af.

7.3.2 Impacts of Drought and Future Water Conservation Vadose Zone Storage Initial Conditions

DIPAW is the largest single recharge component in the Chino Basin. Figure 7-4 shows the time history of historical DIPAW discharge to the saturated zone for the prior Safe Yield and 2020 Safe Yield recalculations. Note that that the historical period for the prior Safe Yield recalculation ends on June 30, 2011, and for the 2020 Safe Yield recalculation, it ends on June 30, 2018. The projected DIPAW for both of these recalculation efforts is also shown and extends from the end of their respective historic periods through June 30, 2050.

In the prior Safe Yield calculation, DIPAW discharge to the saturated zone is in the low 90,000s of afy near the end of the historic period ending in 2011 and remains in the low 90,000s of afy throughout the planning period. For the 2020 CVM, the historic period runs through 2018, and DIPAW discharge to the saturated zone is estimated to have decreased starting in 1999 from about 100,000 to about 70,000 afy in 2018, gradually increasing and asymptotically approaching about 86,000 afy in 2050. For the planning period, DIPAW discharge from the root zone to the vadose zone is about 86,000 afy for the entire planning period. The DIPAW discharge to the saturated zone decreases during the period of 2011 through 2018 due to drought and state-mandated outdoor water conservation that occurred during the latter part of drought period.

Figure 3-14 shows the dry-period (drought) recurrence intervals for historical precipitation falling on the 2020 CVM domain for the 122-year period 1897 through 2018 for various durations that include 1-, 3-, 5- 10- and 20-year contiguous and independent periods. Review of this figure indicates that the period from 1999 through 2018 contained the least precipitation observed in the instrumented historical record: The specific takeaways include:

- The 20-year dry period between 1999 through 2018 is the driest 20-year period in the historical record, and it has a return period of about once in 122 years (that is, it occurs on average once in 122 years).
- The 10-year dry period between 2007 through 2016 is the driest 10-year dry period in the historical record, and it has a return period of about once in 122 years.
- The 5-year dry period of 2012 through 2016 is the driest 5-year period, and it has a return period of about once in 122 years.

During the prior Safe Yield recalculation, the initial groundwater elevation, the initial groundwater storage in the saturated zone, and the initial storage in the vadose zone for the planning period were assumed to be equal to their respective values from the calibration period ending on June 30, 2011. This same assumption is included in this Safe Yield Recalculation: the initial groundwater storage in the saturated zone, and the initial storage in the vadose zone for the planning period were assumed to be equal to their respective values from the calibration period ending on June 30, 2018.

7.3.3 Conservation Related Impacts of Assembly Bill 1668 and Senate Bill 606

In 2018, the California legislature passed, and the Governor signed two pieces of legislation (AB 1668 & SB 606), collectively known as "Making Conservation a California Way of Life," to establish new water efficiency standards for purveyors. The outdoor water use component of the legislation, which takes direction from previous legislation establishing California's Model Water Efficient Landscape Ordinance (MWELO) and provides a computational mechanism for establishing an acceptable outdoor water use based on the following equation:

Acceptable water use equals Irrigable Area times ET_0 times ET adjustment factor (ETAF)

The ETAF is equal to the annual crop water coefficient divided by irrigation efficiency. The ETAF range from 0.8 for older landscapes to lower values for modern developments (0.45 for commercial/industrial/institutional water users and 0.55 for residential water users as described in the MWELO). During the 2020 Model calibration, we were able to estimate the average ETAF's in the IEUA service area and these ETAFs are listed in the table below.

ETAFs Assumed in Calibration and Planning Periods

Land Use Year and IEUA Sewersheds	ETAF
RP1/RP4 service areas	
1975 to 2000	1.14
2000 to 2012	1.11
2017	0.86
2020 to 2070	
Legacy urban	1.11
New residential	0.55
New commercial/industrial/institutional	0.44
Carbon Canyon/ RP5 service areas	
1975 to 2000	0.90
2000 to 2012	0.86
2017	0.60
2020 to 2070	
Legacy urban	0.86
New residential	0.55
New commercial/industrial/institutional	0.44

Pursuant to legislation, the urban irrigation ETAF will be established by the DWR in 2022 and implemented in 2023, and the ETAF will likely be reduced further in 2025 and 2030. At the present time, it's unclear whether the DWR will complete its work on time and/or if the CEQA process associated with the adoption of the ETAFs will be completed on time. It is also not clear what the ETAFs will be for the Chino Basin area. Reductions in ETAFs below the historical values shown in the table above will result in a decrease in DIPAW and subsequently net recharge and Safe Yield.

Because of these uncertainties, the impact of the new conservation legislation is not included in the 2020 Safe Yield calculation. Implementation of new ETAFs pursuant to legislation represents a significant change in cultural conditions and it will result in reduction in net recharge and Safe Yield.

7.4 Projected Water Budget and Net Recharge

The water budget estimated by simulating the 2020 SYR1 planning scenario with the calibrated 2020 CVM is summarized in Table 7-2. Note that as mention previously in this report, only the Chino Basin water budget will be discussed herein. The description of the recharge and discharge components and how each component was computed are identical to those described in Section 6 for the historic period water budget except for differences in subsurface inflow and MAR that are described below.

7.4.1 Subsurface Inflow to the Chino Basin

Subsurface inflow was computed in the planning period in an identical manner as the calibration period except for subsurface inflow from the Riverside Basin through the Bloomington Divide which was assumed equal to the average subsurface inflow from the last five years of the calibration period. Recall during calibration that this recharge component is based on the difference between observed groundwater elevations in the Riverside Basin near the model boundary and computed groundwater elevations in the Chino Basin and that the magnitude of this recharge was estimated to gradually increase over time as the groundwater elevations in the Chino Basin declined. It is uncertain that this increasing trend will occur in the future.

7.4.2 MAR

Stormwater recharge in flood control and conservation basins was estimated with the R4 model based on existing and planned 2013 RMPU facilities that are assumed to be fully operational in 2023. Recycled water is recharged to augment net recharge and the projected recycled water recharge is based on IEUA projections modified in the near term based on recent recharge history. Imported water is recharged to meet Watermaster's replenishment obligations only; no Storage and Recovery programs were included in the 2020 SYR1 scenario. Table 7-3 illustrates how the time history of imported water recharge for replenishment is computed using the methodology described in Section 7.3.1.2 Methodology to Project Replenishment Obligations.

7.4.3 Change in Storage

Figure 7-5 shows the annual recharge, discharge and cumulative storage change in the Basin for the 2020 SYR1 scenario. Storage decreases relative to July 1, 2018, the start of the planning period, throughout the entire planning period and ultimately declines by about 240,000 af. This decline is not overdraft – it occurs as the Parties use their water in managed storage to meet their replenishment obligation.

Figure 7-6 is similar to Figure 6-12a and it shows a comparison of the time history of DIPAW discharging from the root zone and DIPAW discharging to the saturated zone to the estimated end of year storage in the vadose for the calibration and planning periods. Review of this figure indicates that part of the DIPAW arriving at the saturated zone during the calibration period is derived from a reduction in storage in the vadose zone which would be expected when cultural conditions are changing. In the planning period the DIPAW discharge from the root zone is assumed to be the long-term average value through the planning period and that the storage in the vadose zone and DIPAW discharge to the saturated zone increase in response to the long-term average DIPAW discharge from the root zone.

Figure 7-7 shows the relationship between end of year vadose zone storage and DIPAW discharging to the saturated zone for the planning and calibration periods. This figure contains callouts to notably wet years in the calibration period and the associated increase in vadose zone storage following the wet years – the vadose zone response to wet years diminishes over time due to changes in cultural conditions as would be expected in the historical period. In the planning period (indicated by the orange color symbols and line), the DIPAW discharging to the saturated zone and vadose zone storage both increase. This means that over the long-term, with current and projected cultural conditions and climate change that the DIPAW discharge to the saturated zone will recover from the drought and oscillate around the long term DIPAW.

7.4.4 Net Recharge

The columns to the far right in Table 7-2 show the annual net recharge and ten-year average net recharge that is used to estimate Safe Yield. The table below summarizes the recharge and discharge components, change in storage, and net recharge by decade.

Decadal Averages of Recharge and Discharge Components, Change in Storage and Net Recharge for Scenario 2020 SYR1 (afy)

Hydrologic Components	2021 - 2030	2031 - 2040	2041 - 2050
Recharge Components			
Subsurface Inflow	37,929	40,326	40,892
Deep Infiltration of Precipitation and Applied Water (DIPAW)	75,826	81,822	84,407
Santa Ana River Streambed Infiltration	36,556	36,172	36,888
Streambed Infiltration from Santa Ana River Tributaries	549	548	547
MAR - Stormwater	13,522	14,269	14,212
MAR - Recycled and Imported	15,225	18,839	19,698
Period Average	179,607	191,977	196,644
Discharge Components			
Groundwater Pumping	148,524	166,871	173,679
Riparian Veg ET	18,668	19,142	19,316
Rising Groundwater	15,164	15,787	15,354
Period Average	182,356	201,800	208,348
Period Average Change in Storage	-2,749	-9,823	-11,704
Period Average Net Recharge	130,550	138,209	142,276

The net recharge for the period 2021 through 2030 is projected to be about 131,000 afy and increases to 138,000 for 2031 through 2040 and 142,000 afy for 2041 through 2050. The table below compares the projected decadal 10-year period average from the prior and 2020 Safe Yield calculations.

Comparison of Decadal Averages of Net Recharge from Prior and 2020 Safe Yield calculations (afy)

Period	Prior Safe Yield Calculation	2020 Safe Yield Calculation
2011 - 2020	135,000	125,000
2021 - 2030	134,000	131,000
2031 - 2040	140,000	138,000
2041 - 2050	142,000	142,000

Figure 7-6 is similar to Figure 6-15 except that it includes both the calibration and projection period. Like Figure 6-15, it illustrates the time history of change in DIPAW discharging to the vadose zone for the calibration and planning periods and compares it to time histories of pervious land cover, combined precipitation and applied irrigation water over pervious land and ten-year moving average of the combined precipitation and applied irrigation water on pervious land. (note that graph does not show precipitation in the projection period.) Over the calibration period, the amount of DIPAW discharged to at the root zone decreases over time with decreasing pervious area as would be expected. DIPAW discharge to the saturated zone after 2018 is shown as a nearly horizontal line and represents the projected DIPAW in the planning period. Pursuant to the Court-approved Safe Yield methodology, DIPAW in the planning period is assumed equal to long-term average DIPAW based on projected cultural conditions, long-term precipitation and ET_0, the latter two items adjusted for projected climate change impacts.

Figure 7-7 is similar to Figure 7-6 except that it compares model estimated net recharge over the calibration and planning periods to time histories of pervious land cover, combined precipitation and applied irrigation water on pervious land and the ten-year moving average of precipitation and applied irrigation water applied on pervious land cover (note that graph does not show precipitation in the projection period.) The primary driver for the reduction in net recharge during the 2021 through 2030 period were changes in cultural conditions prior to the planning period and extremely low precipitation that occurred during the 20 years prior to the planning period.

7.5 Projected Basin Response

This section describes the projected basin response that Watermaster must consider when setting the Safe Yield that include projected groundwater level, pumping sustainability, new land subsidence, and the state of hydraulic control.

7.5.1 Groundwater Level Projections

Figures 7-8a, 7-8b, and 7-8c show the groundwater elevation throughout the Chino Basin for July 2018, for model layers 1, 3 and 5, respectively, which is the initial groundwater elevation for the planning period. The projected change in groundwater elevations are illustrated in a series of maps as follows:

- Figures 7-9a through 7-9d show the projected change in groundwater elevation for model layer 1 for the periods 2018 to 2030, 2030 to 2040, 2040 to 2050, and cumulative period 2018 to 2050, respectively.
- Figures 7-10a through 7-10d show the projected change in groundwater elevation for model layer 3 for the periods 2018 to 2030, 2030 to 2040, 2040 to 2050, and cumulative period 2018 to 2050, respectively.

- Figures 7-11a through 7-11d show the projected change in groundwater elevation for model layer 5 for the periods 2018 to 2030, 2030 to 2040, 2040 to 2050, and cumulative period 2018 to 2050, respectively.

7.5.1.1 Layer 1 Groundwater Elevation Changes

Most of the 240,000 af of storage decline that occurs between 2018 and 2050 occurs in model layer 1 which is an unconfined aquifer. Review of Figures 7-9a through 7-9d reveals that:

- For the 2018 to 2030 period (Figure 7-9a), groundwater elevations are projected to decline west of central Ontario ranging from 0 to greater than 10 feet in the MVWD service area and in the CDA well fields. Groundwater elevations northeast of central Ontario are projected to increase slightly. The decline in storage projected for this period is about 38,000 af.
- For the 2030 to 2040 period (Figure 7-9b), groundwater elevations are projected to decline over most of Chino Basin by 10 feet or more primarily in the northeast Ontario, CVWD and FWC services areas. The decline in storage that projected for this period is about 93,000 af and cumulatively through 2040 is projected to be about 131,000 af.
- For the 2040 to 2050 period (Figure 7-9c), groundwater elevations are projected to decline over the entire Chino Basin ranging from 0 to about 10 feet in southeast Ontario and exceeding 10 feet in the JCSD services area. The decline in storage projected for this period is about 109,000 af and cumulatively through 2040 is projected to be about 240,000 af.
- Cumulatively for the 2018 to 2050 period (Figure 7-9d), groundwater elevations are projected to decline over the entire Chino Basin ranging from 0 to about 20 feet with an area stretching from the CVWD to JCSD service areas projected to decline up to 20 feet or more. There is an area in the eastern part of the JCSD service area where groundwater elevations are projected to increase.

7.5.1.2 Layer 3 Groundwater Elevations Changes

Review of Figures 7-10a through 7-10d reveals that:

- For the 2018 to 2030 period (Figure 7-10a), groundwater elevations are projected to decline west of central Ontario ranging from 0 to greater than 10 feet in parts of the MVWD and Chino service areas and, in the CDA well field. Groundwater elevations northeast of central Ontario, in the western part of MZ1 and the eastern part of the JCSD service area are projected to increase slightly.
- For the 2030 to 2040 period (Figure 7-10b), groundwater elevations are projected to decline over most of the basin generally decreasing by at least 10 feet throughout most of the Ontario and Fontana service areas and all of the CVWD service area.
- For the 2040 to 2050 period (Figure 7-10c), groundwater elevations are projected to decline over the entire Chino Basin ranging from 0 to about 10 feet or more in northwest JCSD service area.
- Cumulatively for the 2018 to 2050 period (Figure 7-10d), groundwater elevations are projected to decline over the entire Chino Basin ranging from 0 to more than 30 feet within area bounded by the CVWD , JCSD, Chino, MVWD and Upland service areas.

7.5.1.3 Layer 5 Groundwater Elevations Changes

Review of Figures 7-11a through 7-11d reveals that:

- For the 2018 to 2030 period (Figure 7-11a), groundwater elevations are projected to increase over most of the basin with slight declines projected in the northeast MVWD and southwest Upland services areas.
- For the 2030 to 2040 period (Figure 7-11b), groundwater elevations are projected to decline over most of Chino Basin by 10 or more feet or more in an area that stretches east from the center of MZ1.
- For the 2040 to 2050 period (Figure 7-11c), groundwater elevations are projected to decline over the entire Chino Basin ranging from 0 to about 10 feet in southeast Ontario.
- Cumulatively for the 2018 to 2050 period (Figure 7-11d), groundwater elevations are projected to decline in the Ontario, Upland, CVWD and FWC service areas ranging from 0 to over 20 feet. Groundwater elevations are projected to increase in the Pomona and parts of Chino and MVWD services areas.

7.5.1.4 Projected Groundwater Elevation Time Series at Selected Wells

Appendix D contains projected groundwater elevation time series for 167 Appropriator Party wells located throughout the Chino Basin for the 2020 SYR1 scenario.

7.5.2 Pumping Sustainability

The term *pumping sustainability*, as used herein, refers to the ability to produce water from a specific well at a desired production rate, given the groundwater level at that well and its well construction and current equipment details. The projected groundwater elevation time series shown Appendix D contain a pumping sustainability metric if provided by the Appropriator. Pumping sustainability metrics are defined for each well by well owner. Groundwater pumping at a well is assumed to be sustainable if the groundwater elevation at that well projected by the model is greater than the pumping sustainability metric. If the projected groundwater elevation falls below the sustainability metric, the owner will either lower the pumping equipment in their well, reduce pumping or a combination of the two. Pumping sustainability is characterized three ways based on the review of the groundwater elevation time series in Appendix D:

- Groundwater elevation at a well are projected to be greater than the sustainability metric by more than 50 feet throughout the planning period. Pumping sustainability is likely to be assured in this category.
- Groundwater elevation at a well are projected to be greater than the pumping sustainability metric by less than 50 feet at least once during the planning period. Wells in this category could potentially experience pumping sustainability challenges.
- Groundwater elevation at a well is projected to be less than the sustainability metric at least once during the planning period. Pumping sustainability is not assured in this category.

Table 7-4 summarizes the occurrence of potential and likely pumping sustainability challenges during the planning period. Using the criteria listed above, 40 of 167 wells have the potential to incur pumping sustainability challenges and 16 are likely to incur pumping sustainability challenges. Figure 7-12 shows the spatial and temporal distribution of projected likely pumping sustainability challenges. Most of the pumping sustainability challenges in the basin are the result of uncoordinated pumping amongst the Parties or construction of wellfields that cause significant interference and drawdown. In either case, pumping sustainability challenges that occur in the planning period can be mitigated by lowering pumping equipment, changing pumping patterns or a combination of the two.

7.5.3 Land Subsidence

To evaluate the risk of MPI due to subsidence over the entirety of MZ1, historical groundwater elevations were used to develop a groundwater elevation control surface (new land subsidence metric) throughout MZ1 that defined the likelihood of initiating new subsidence: if groundwater levels are greater than the new land subsidence metric, then new land subsidence would not occur; if groundwater levels fall below the new land subsidence metric, then new land subsidence could occur and cause MPI.

The western part of the basin is either susceptible to or actively experiencing land subsidence. The areas of current concern include the so-called "Managed Area" and the Northwest MZ1 area. Land subsidence in the "Managed Area" has been reduced to de minimis levels through the voluntary efforts of the Cities of Chino and Chino Hills. Land subsidence in Northwest MZ1, including parts of the Cities of Chino, Montclair, Ontario, and Pomona, is continuing, and Watermaster is currently in the process of developing a land subsidence management plan in this area. For purposes of this investigation, these legacy subsidence challenges are assumed managed and the focus of land subsidence evaluation for the Safe Yield calculation is to evaluate the potential for new land subsidence. In this investigation, we use the term new land subsidence to refer to land subsidence caused by the lowering of groundwater elevations below the current estimate of the preconsolidation stress.

Figure 7-13 shows the areal distribution of the difference between the projected groundwater elevations from the 2020 SYR1 scenario and preconsolidation stress. Review of the maps indicate that projected groundwater elevations are greater than the preconsolidation stress except for two small areas centered on wells where groundwater pumping can be modified to ensure no new land subsidence. Watermaster's land subsidence monitoring program will provide an early warning of the projected land subsidence before the subsidence becomes significant. For purposes of establishing the 2020 Safe Yield, no unmitigated new land subsidence is projection to occur.

7.5.4 State of Hydraulic Control

The projected state of hydraulic control was estimated with the 2020 CVM by simulating the Chino Basin's response to the 2020 SYR1 scenario. The attainment of hydraulic control is measured by demonstrating, from groundwater elevation data, either that all groundwater north of the desalter well fields cannot pass through the CDA well fields (total hydraulic containment standard) or that groundwater discharge through the CDA well fields is, in aggregate, less than 1,000 afy (de minimis standard). The Regional Board has agreed that compliance with the de minimis standard will be determined from groundwater monitoring data and the results of periodic calibrations of the Watermaster groundwater model and interpretations of the calibration results.

Figures 7-14 shows the location of the CDA wells in the southern part of the Basin. Groundwater elevation contours for model layer 1 and directional vectors that show the direction of groundwater flow. Groundwater discharge from the Chino-North Management Zone to the Prado Basin Management Zone and the Santa Ana River is projected to not be fully contained by the CDA wellfield in the area between the Chino Hills and CDA well I-17. Groundwater discharge through the CDA wellfield was estimated through the analysis of model projected cell-by-cell discharges through a "line of control" approximately perpendicular to the groundwater flow field and near the CDA wellfield. The annual discharge through the line of control is reduced by groundwater pumping in the flow field that occurs downgradient of the line of control. Figure 7-15 shows the historical and projected groundwater discharge through the line of control. Groundwater discharge through the line of control is projected to be less than the de minimis discharge threshold of 1,000 afy; hence, hydraulic control is projected to be maintained through 2050.

7.6 Recommended Safe Yield

Following the Court-ordered Safe Yield calculation methodology, Watermaster should recommend that the Court set the Safe Yield at 131,000 afy for the 2021 through 2030 period. No MPI or undesirable results are projected to occur if the Safe Yield were to be set at this value.

A deviation from the projected cultural conditions will likely occur if the State mandates reduced ETAFs as described in Section 7.3.3. Upon the State's promulgation of reduced ETAFs, Watermaster should evaluate the significance of any resulting change in cultural conditions, and, if cultural conditions are judged to have changed such that the Safe Yield would be changed by more than 2.5%, Watermaster should move the Court to reset the Safe Yield accordingly.

Table 7-1 Historical and Projected Groundwater Pumping in the Chino Basin (afy)

Producer	Historical Pumping										Pumping Projection (2019 Update)				
								Statistics (2013-2019)							
	2013	2014	2015	2016	2017	2018	2019	Min	Max	Mean	2020	2025	2030	2035	2040
Overlying Agricultural Pool															
Aggregate Agricultural Pool Pumping	23,946	22,063	17,361	16,904	17,786	18,827	15,572	15,572	23,946	*18,923*	15,678	12,788	9,968	7,907	4,808
Overlying Non-Agricultural Pool															
Ameron	59	18	29	30	25	-	-	18	59	*32*	-	-	-	-	-
Angelica Textile Service	48	37	26	28	20	-	-	20	48	*32*	-	-	-	-	-
California Speedway Corporation	509	436	454	300	410	438	389	300	509	*419*	500	500	500	500	500
California Steel Industries, Inc.	1,303	1,417	1,279	1,187	1,298	1,266	1419	1,187	1,419	*1,310*	1,450	1,450	1,470	1,500	1,530
General Electric Company	1,285	1,626	1,355	917	1,667	957	1127	917	1,667	*1,276*	1,667	1,667	1,667	1,667	1,667
NRG California South LP	470	290	221	204	211	212	18	18	470	*232*	232	232	232	232	232
Riboli Family and San Antonio Winery, Inc.	10	10	7	4	5	6	26	4	26	*10*	10	10	10	10	10
Southern Service Company	-	-	-	-	-	21	23	21	23	*22*	32	32	32	32	32
TAMCO	-	-	-	-	-	18	10	10	18	*14*	32	32	32	32	32
Subtotal Overlying Non-Agricultural Pool Pumping	*3,685*	*3,834*	*3,371*	*2,670*	*3,636*	*2,919*	*3,010*	*2,670*	3,834	*3,304*	*3,923*	*3,923*	*3,943*	*3,973*	*4,003*
Appropriative Pool															
Arrowhead Mountain Spring Water Company	413	379	426	356	367	308	285	285	426	362	400	400	400	400	400
City of Chino	7,022	6,725	6,546	5,010	4,972	5,162	4,315	4,315	7,022	5,679	8,262	9,696	11,058	11,945	14,355
City of Chino Hills	3,039	2,163	3,745	1,633	2,246	2,839	1,608	1,608	3,745	2,468	2,570	3,600	3,600	3,600	3,600
City of Ontario	21,146	21,980	17,675	22,849	24,840	26,280	20,722	17,675	26,280	22,213	12,363	14,514	17,947	23,715	31,016
City of Pomona	12,227	12,909	12,520	9,964	8,067	9,286	10,840	8,067	12,909	10,830	11,309	11,395	11,481	11,568	11,568
City of Upland	2,358	2,822	3,416	2,601	1,260	1,764	2,381	1,260	3,416	2,372	2,800	2,800	2,800	2,800	2,800
Cucamonga Valley Water District	18,740	16,122	14,640	20,537	16,562	6,838	9,624	6,838	20,537	14,723	12,755	13,687	13,859	19,282	19,282
Fontana Water Company	11,752	15,377	13,344	15,317	13,250	11,392	9,961	9,961	15,377	12,913	9,920	10,416	13,153	15,591	17,942
Jurupa Community Services District	17,411	18,406	12,805	9,284	11,498	15,286	13,894	9,284	18,406	14,083	10,310	12,310	14,310	14,310	14,310
Marygold Mutual Water Company	1,250	1,315	1,250	753	619	944	950	619	1,315	1,011	1,241	1,322	1,403	1,484	1,565
Monte Vista Water District	10,324	12,522	7,402	8,371	7,086	6,483	6,631	6,483	12,522	8,403	6,500	6,257	6,397	6,537	6,668
Niagara	1,000	1,343	1,860	1,775	1,532	1,571	1,683	1,000	1,860	1,537	1,537	1,537	1,537	1,537	1,537
San Antonio Water Company	1,540	1,159	1,479	1,031	538	428	376	376	1,540	936	1,232	1,232	1,232	1,232	1,232
San Bernardino County (Olympic Facility)	12	16	11	9	13	11	11	9	16	12	12	12	12	12	12
Golden State Water Company	1,059	736	720	807	850	148	0	0	1,059	617	374	374	374	374	374
Subtotal Appropriative Pool Pumping	*109,292*	*113,974*	*97,840*	*100,297*	*93,699*	*88,740*	*83,280*	*83,280*	*113,974*	*98,160*	*81,585*	*89,552*	*99,564*	*114,387*	*126,661*
Chino Desalter Authority															
Total Desalter Pumping	*27,098*	*29,282*	*30,022*	*28,191*	*28,284*	*30,088*	*31,233*	*27,098*	*31,233*	*29,171*	*40,000*	*40,000*	*40,000*	*40,000*	*40,000*
2020 SMP Projected Total Pumping	164,021	169,153	148,593	148,061	143,405	140,574	133,095	*133,095*	*169,153*	*149,557*	141,186	146,263	153,474	166,266	175,472
Less GE Injection											-1,667	-1,667	-1,667	-1,667	-1,667
2020 SMP Projected Net Total Basin Pumping											139,519	144,596	151,808	164,600	173,805
2018 SFI Projected Net Total Basin Pumping											144,527	149,468	154,302	167,722	176,765
Change in Projected Net Total Basin Pumping from the 2018 SFI Projection											-5,008	-4,872	-2,494	-3,122	-2,960

increase relative to 2018 SFI projection

decrease relative to 2018 SFI projection

Table 7-2 Water Budget for Scenario 2020 SYR1a for the Chino Basin (af)

Fiscal Year	Recharge														Discharge						Change in Storage		Net Recharge	10-Year Net Recharge
	I	I	R	R	R	R	R	I	R	I	I	I	I		I	I	I	R	R					
	Subsurface Inflow from							Deep Infiltration of Precipitation and Applied Water	Santa Ana River Streambed Infiltration	Streambed Infiltration from Santa Ana River Tributaries	Managed Aquifer Recharge			Total Recharge	Groundwater Pumping			Riparian Veg ET	Rising Groundwater	Total Discharge	Annual	Cumulative		
	Riverside Basin through Bloomington Divide	Chino/Puente Hills, Jurupa Hills, and Rialto Basin	Temescal Basin	Pomona Basin	Claremont Basin	Cucamonga Basin	Spadra Basin				Storm Water	Recycled Water	Imported Water		CDA Pumping	Overlying Non Ag and Appropriative Pools	Overlying Agricultural Pool							
2019	15,538	7,694	365	2,644	2,060	6,914	343	68,414	36,230	550	10,472	13,504	0	164,728	31,748	82,530	20,362	18,066	14,113	166,819	-2,092	-2,092	119,045	
2020	15,538	7,697	760	2,721	2,140	6,888	368	70,654	36,020	550	10,472	13,504	0	167,312	31,748	86,552	19,011	18,212	14,438	169,961	-2,650	-4,741	121,157	
2021	15,538	7,699	1,035	2,863	2,211	6,842	384	71,823	36,565	550	10,472	13,795	0	169,777	31,748	88,112	18,380	18,292	14,392	170,924	-1,147	-5,888	123,298	130,550
2022	15,538	7,701	1,204	2,990	2,253	6,850	395	73,046	36,843	550	10,472	14,087	0	171,929	39,366	89,682	17,811	18,371	14,502	179,732	-7,803	-13,691	124,969	130,550
2023	15,538	7,704	1,315	3,107	2,283	6,884	406	73,119	36,792	550	14,296	14,379	0	176,372	39,366	91,247	16,546	18,453	14,784	180,397	-4,025	-17,716	128,757	130,550
2024	15,538	7,706	1,401	3,220	2,305	6,962	415	73,798	36,877	549	14,296	14,670	0	177,738	39,366	92,815	15,269	18,547	14,866	180,863	-3,125	-20,840	129,655	130,550
2025	15,538	7,708	1,471	3,330	2,324	7,020	423	76,723	36,674	549	14,296	14,962	0	181,018	39,366	94,312	14,802	18,622	15,225	182,328	-1,309	-22,150	132,209	130,550
2026	15,538	7,711	1,530	3,436	2,339	7,105	429	77,507	36,520	549	14,296	15,253	0	182,215	39,366	95,834	14,038	18,709	15,436	183,384	-1,169	-23,319	132,815	130,550
2027	15,538	7,713	1,584	3,540	2,352	7,200	433	77,962	36,409	549	14,296	15,545	0	183,122	39,366	97,365	13,628	18,796	15,537	184,692	-1,569	-24,888	133,245	130,550
2028	15,538	7,715	1,638	3,641	2,365	7,325	436	77,884	36,320	549	14,296	15,837	160	183,703	39,366	98,886	13,455	18,882	15,587	186,177	-2,473	-27,362	133,237	130,550
2029	15,538	7,718	1,684	3,740	2,377	7,414	438	77,731	36,306	549	14,296	16,128	390	184,310	39,366	100,416	12,685	18,967	15,622	187,056	-2,746	-30,108	133,203	130,550
2030	15,538	7,720	1,731	3,830	2,387	7,527	440	78,662	36,253	549	14,204	16,420	621	185,882	39,366	101,941	11,971	19,042	15,685	188,004	-2,123	-32,230	134,114	130,550
2031	15,538	7,721	1,775	3,911	2,397	7,642	441	79,555	36,175	548	14,296	16,420	332	186,750	39,366	105,030	11,713	19,063	15,762	190,934	-4,184	-36,414	135,174	138,209
2032	15,538	7,722	1,815	3,981	2,405	7,778	441	80,269	36,123	548	14,290	16,420	843	188,176	39,366	108,122	11,550	19,080	15,797	193,915	-5,740	-42,154	136,036	138,209
2033	15,538	7,723	1,848	4,044	2,413	7,870	441	80,565	36,151	548	14,284	16,420	1,355	189,202	39,366	111,207	11,326	19,097	15,810	196,805	-7,603	-49,757	136,520	138,209
2034	15,538	7,724	1,879	4,101	2,420	7,980	441	81,379	36,168	548	14,278	16,420	1,867	190,743	39,366	114,302	10,637	19,115	15,800	199,219	-8,476	-58,233	137,542	138,209
2035	15,538	7,725	1,904	4,154	2,427	8,086	441	81,429	36,174	548	14,272	16,420	2,378	191,496	39,366	117,392	9,940	19,133	15,798	201,629	-10,133	-68,366	137,767	138,209
2036	15,538	7,726	1,930	4,203	2,434	8,210	440	82,433	36,147	548	14,266	16,420	2,747	193,042	39,366	119,817	9,160	19,152	15,800	203,295	-10,253	-78,618	138,924	138,209
2037	15,538	7,727	1,949	4,249	2,441	8,282	440	82,901	36,167	548	14,260	16,420	3,115	194,037	39,366	122,241	8,657	19,169	15,805	205,238	-11,201	-89,819	139,528	138,209
2038	15,538	7,729	1,966	4,292	2,447	8,371	440	83,073	36,195	548	14,254	16,420	3,483	194,756	39,366	124,662	8,464	19,187	15,790	207,469	-12,713	-102,532	139,876	138,209
2039	15,538	7,730	1,983	4,332	2,454	8,456	441	83,366	36,240	547	14,248	16,420	3,851	195,606	39,366	127,084	7,595	19,204	15,761	209,011	-13,404	-115,937	140,369	138,209
2040	15,538	7,731	1,995	4,371	2,461	8,561	442	83,255	36,183	547	14,242	16,420	4,219	195,965	39,366	129,505	6,643	19,223	15,750	210,487	-14,522	-130,459	140,352	138,209
2041	15,538	7,732	2,006	4,413	2,468	8,615	444	83,370	36,236	547	14,237	16,420	3,278	195,304	39,366	129,505	4,808	19,241	15,720	208,639	-13,335	-143,793	140,646	142,276
2042	15,538	7,733	2,014	4,453	2,476	8,685	446	83,850	36,336	547	14,231	16,420	3,278	196,008	39,366	129,505	4,808	19,259	15,659	208,596	-12,588	-156,382	141,393	142,276
2043	15,538	7,735	2,024	4,489	2,483	8,750	448	84,001	36,464	547	14,226	16,420	3,278	196,403	39,366	129,505	4,808	19,276	15,587	208,541	-12,137	-168,519	141,844	142,276
2044	15,538	7,736	2,033	4,524	2,491	7,605	451	84,202	36,586	547	14,220	16,420	3,278	195,630	39,366	129,505	4,808	19,293	15,504	208,476	-12,847	-181,365	141,134	142,276
2045	15,538	7,738	2,039	4,557	2,498	7,639	452	84,303	36,752	547	14,215	16,420	3,278	195,974	39,366	129,505	4,808	19,309	15,421	208,408	-12,433	-193,799	141,547	142,276
2046	15,538	7,739	2,044	4,587	2,504	7,718	454	84,378	36,942	547	14,209	16,420	3,278	196,357	39,366	129,505	4,808	19,324	15,322	208,324	-11,967	-205,766	142,014	142,276
2047	15,538	7,740	2,050	4,614	2,510	7,792	455	84,596	37,141	546	14,204	16,420	3,278	196,884	39,366	129,505	4,808	19,340	15,218	208,236	-11,352	-217,118	142,629	142,276
2048	15,538	7,742	2,056	4,640	2,516	7,912	456	84,923	37,303	546	14,199	16,420	3,278	197,527	39,366	129,505	4,808	19,356	15,119	208,154	-10,627	-227,744	143,354	142,276
2049	15,538	7,743	2,057	4,665	2,521	7,926	457	85,133	37,484	546	14,193	16,420	3,278	197,961	39,366	129,505	4,808	19,372	15,035	208,085	-10,124	-237,868	143,857	142,276
2050	15,538	7,744	2,060	4,688	2,527	7,988	458	85,317	37,638	546	14,188	16,420	3,278	198,390	39,366	129,505	4,808	19,387	14,957	208,023	-9,634	-247,502	144,347	142,276
Statistics for the Projection Period																								
Total	497,216	247,126	55,144	126,329	76,686	246,797	13,840	2,559,621	1,168,416	17,537	440,981	506,484	58,140	6,014,317	1,236,858	3,594,099	331,724	607,538	491,600	6,261,819	-247,502		4,350,556	
Percent	8.3%	4.1%	0.9%	2.1%	1.3%	4.1%	0.2%	42.6%	19.4%	0.3%	7.3%	8.4%	1.0%	100.0%	19.8%	57.4%	5.3%	9.7%	7.9%	100.0%				
Average	15,538	7,723	1,723	3,948	2,396	7,712	433	79,988	36,513	548	13,781	15,828	1,817	187,947	38,652	112,316	10,366	18,986	15,363	195,682	-7,734		135,955	
Median	15,538	7,725	1,891	4,127	2,424	7,748	441	81,404	36,328	548	14,245	16,420	2,123	191,120	39,366	115,847	10,288	19,124	15,562	200,424	-9,055		137,654	
Maximum	15,538	7,744	2,060	4,688	2,527	8,750	458	85,317	37,638	550	14,296	16,420	4,219	198,390	39,366	129,505	20,362	19,387	15,810	210,487	-1,147	-2,092	144,347	
Minimum	15,538	7,694	365	2,644	2,060	6,842	343	68,414	36,020	546	10,472	13,504	0	164,728	31,748	82,530	4,808	18,066	14,113	166,819	-14,522	-247,502	119,045	

Note: column heading R means model results and column heading I means model input

Table 7-3 Projected Groundwater Pumping, Pumping Rights, Replenishment and End-of-Year Volume in Managed Storage – 2020 SYR1 (af)

Fiscal Year ending June 30	Projected Groundwater Pumping per 2020 SMP Survey for Normal Year	Pumping Rights				Net Replenishment Obligation[2]	Replenishment from Storage[3]	Replenishment with Wet-Water Recharge	End-of-Year Managed Storage
		Safe Yield[1]	Reoperation Water Use to Offset the Desalter Replenishment Obligation	Recycled Water Recharge	Total				
(1)	(2)	(3)	(4)	(5)	(6) = (3)+(4)+(5)	(7) = (2)-(6)	(8)	(9)	$(10)_t = (10)_{t-1} - (7)_t + (9)_t$
2019									503,275
2020	139,519	135,000	12,500	13,504	161,004	-21,485	0	0	524,760
2021	140,534	130,550	12,500	13,795	156,845	-16,311	0	0	541,071
2022	141,550	130,550	12,500	14,087	157,137	-15,587	0	0	556,658
2023	142,565	130,550	12,500	14,379	157,429	-14,863	0	0	571,521
2024	143,581	130,550	12,500	14,670	157,720	-14,140	0	0	585,661
2025	144,596	130,550	12,500	14,962	158,012	-13,416	0	0	599,077
2026	146,038	130,550	5,000	15,253	150,804	-4,765	0	0	603,842
2027	147,481	130,550	5,000	15,545	151,095	-3,615	0	0	607,457
2028	148,923	130,550	5,000	15,837	151,387	-2,464	0	0	609,920
2029	150,365	130,550	5,000	16,128	151,679	-1,313	0	0	611,234
2030	151,808	130,550	5,000	16,420	151,970	-163	0	0	611,396
2031	154,366	138,209	0	16,420	154,629	-263	0	0	611,659
2032	156,924	138,209	0	16,420	154,629	2,296	1,836	459	609,823
2033	159,483	138,209	0	16,420	154,629	4,854	3,883	971	605,939
2034	162,041	138,209	0	16,420	154,629	7,412	5,930	1,482	600,009
2035	164,600	138,209	0	16,420	154,629	9,971	7,977	1,994	592,033
2036	166,441	138,209	0	16,420	154,629	11,812	9,450	2,362	582,583
2037	168,282	138,209	0	16,420	154,629	13,653	10,922	2,731	571,661
2038	170,123	138,209	0	16,420	154,629	15,494	12,395	3,099	559,266
2039	171,964	138,209	0	16,420	154,629	17,335	13,868	3,467	545,398
2040	173,805	138,209	0	16,420	154,629	19,176	15,341	3,835	530,057
2041	173,805	142,276	0	16,420	158,696	15,108	12,087	3,022	517,970
2042	173,805	142,276	0	16,420	158,696	15,108	12,087	3,022	505,883
2043	173,805	142,276	0	16,420	158,696	15,108	12,087	3,022	493,797
2044	173,805	142,276	0	16,420	158,696	15,108	12,087	3,022	481,710
2045	173,805	142,276	0	16,420	158,696	15,108	12,087	3,022	469,623
2046	173,805	142,276	0	16,420	158,696	15,108	12,087	3,022	457,536
2047	173,805	142,276	0	16,420	158,696	15,108	12,087	3,022	445,450
2048	173,805	142,276	0	16,420	158,696	15,108	12,087	3,022	433,363
2049	173,805	142,276	0	16,420	158,696	15,108	12,087	3,022	421,276
2050	173,805	142,276	0	16,420	158,696	15,108	12,087	3,022	409,189

503,275 af is the estimated volume in managed storage on June 30, 2019

1 -- Safe yield estimate from net recharge estimated in Scenario 1.

2 -- This is the annual net replenishment obligation based on the assumptions described in the 2018 SFI report; negative values mean aggregate underproduction and an increase in stored water accounts.

3 -- 80 percent of a positive replenishment obligation is satisfied from storage and 20 percent is satisfied by wet-water recharge.

Table 7-4 Pumping Sustainability Challenges at Specific Wells

Well Owner	Well Name	Projected Groundwater Level		Well Owner	Well Name	Projected Groundwater Level	
		<50 feet Above Metric	Below Metric			<50 feet Above Metric	Below Metric
CDA				JCSD			
	I-1	◆			6	◆	
	I-6	◆			8	◆	
	I-7	◆			11	◆	
	I-9	◆			12	◆	
	I-10	◆			13		◆
	I-13	◆			14	◆	
	I-14		◆		15	◆	
	I-15		◆		16	◆	
	II-1		◆		17	◆	
	II-3	◆			18	◆	
	II-4	◆			19	◆	
	II-6	◆			20	◆	
	II-9a	◆			22	◆	
Chino					25	◆	
	5	◆		Ontario			
Chino Hills					24	◆	
	15B	◆			29	◆	
CVWD					31		◆
	1	◆			36	◆	
	3	◆			37		◆
	5		◆		38		◆
	39	◆			39		◆
FWC					44	◆	
	F7A	◆			49	◆	
	F7A	◆			50	◆	
	F17B	◆		Pomona			
	F23A		◆		10B		◆
	F24A		◆		21		◆
	F26A		◆		26		◆
	F31A	◆					
	F44A	◆					
	F44B		◆				
	F44C	◆					

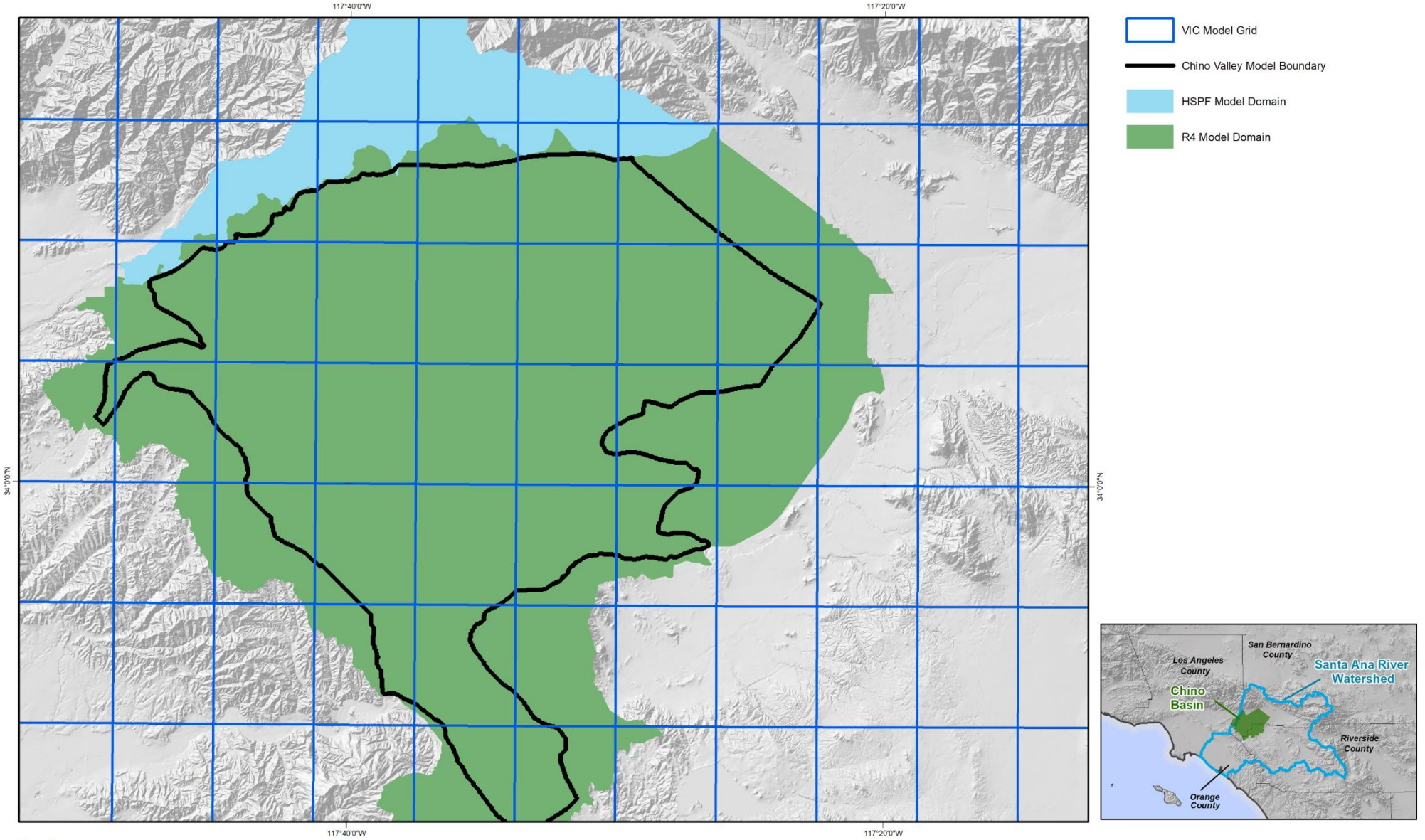

VIC Model Grid and Domains of the Chino Valley and Surface Water Models

Figure 7-1

Figure 7-2a: 2030 Monthly Precipitation Change Factor Probability Distribution for Chino, Cucamonga, Six Basins, Arlington, and Temescal Basins

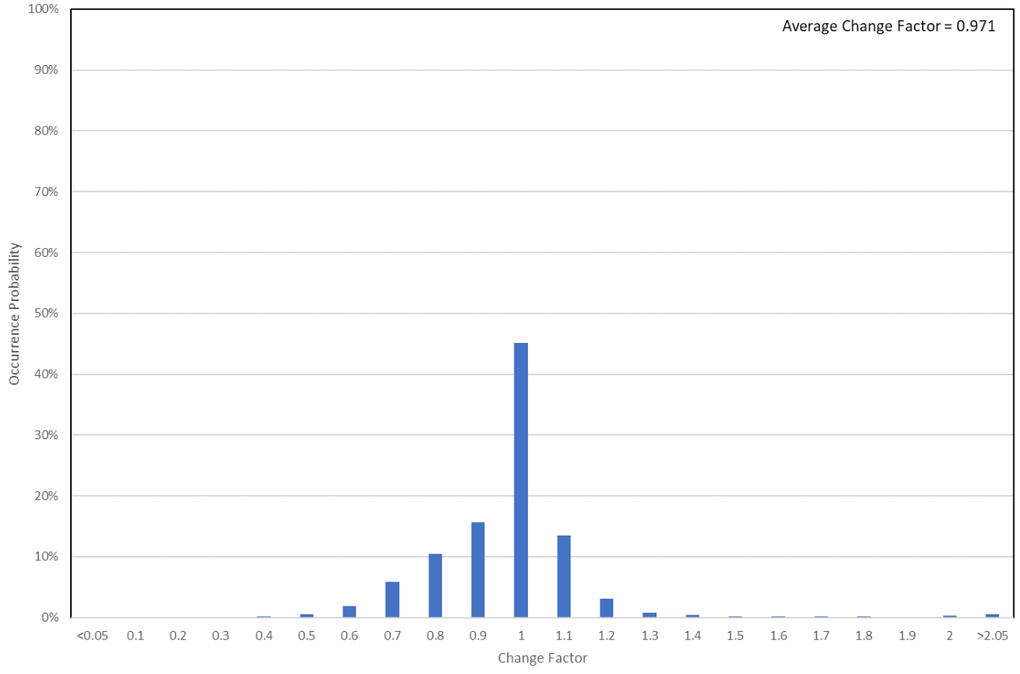

Figure 7-2b: 2070 Monthly Precipitation Change Factor Probability Distribution for Chino, Cucamonga, Six Basins, Arlington, and Temescal Basins

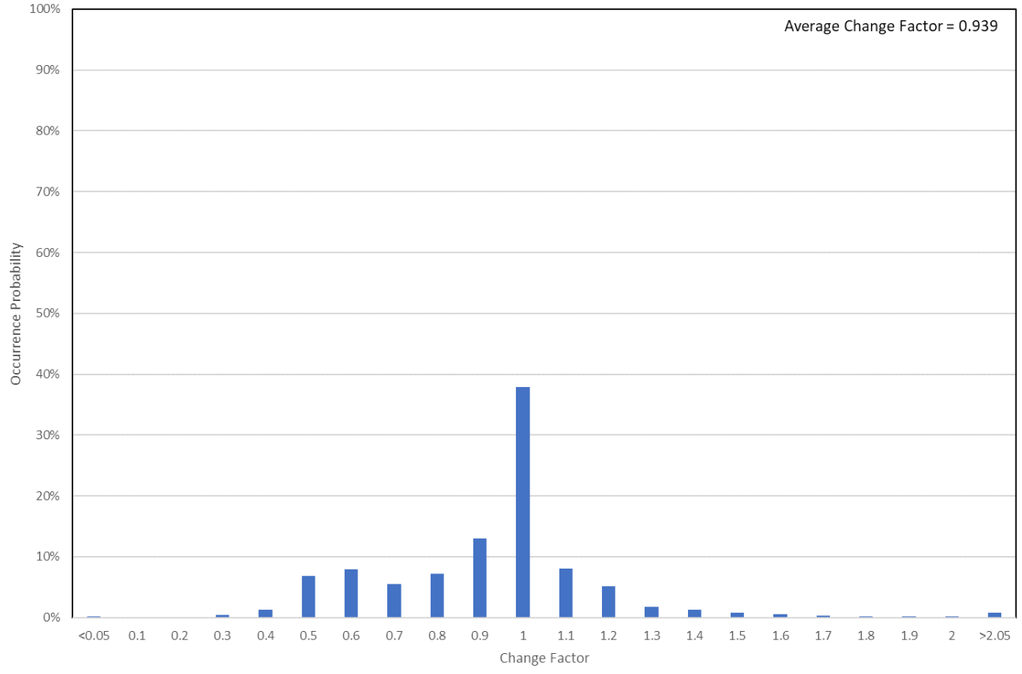

Figure 7-3a: 2030 Monthly Reference ET Change Factor Probability Distribution for Chino, Cucamonga, Six Basins, Arlington, and Temescal Basins

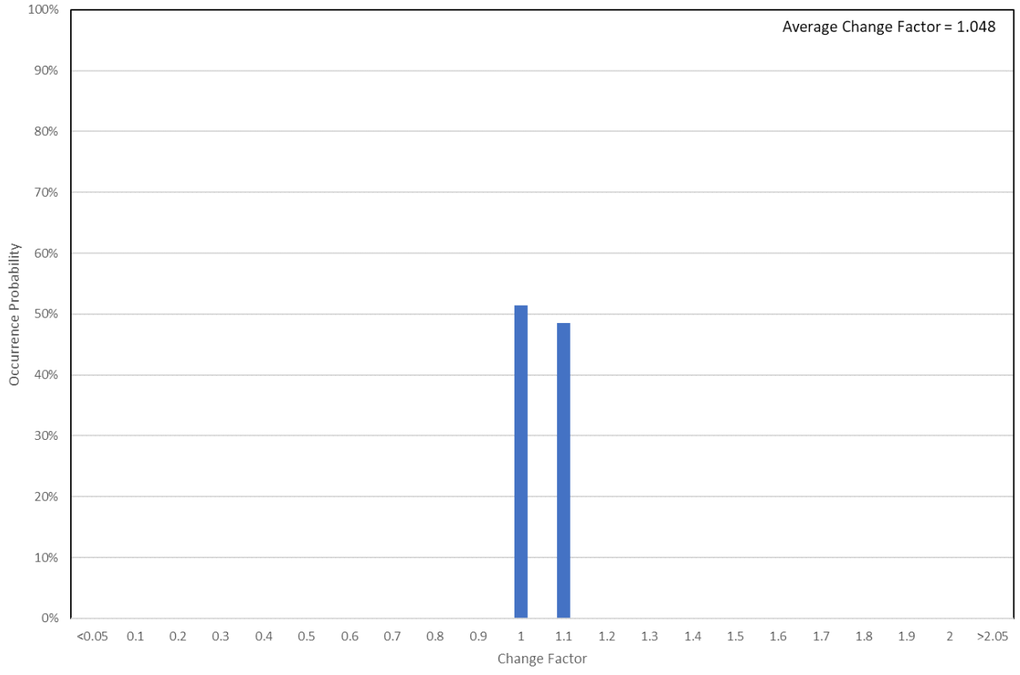

Figure 7-3b: 2070 Monthly Reference ET Change Factor Probability Distribution for Chino, Cucamonga, Six Basins, Arlington, and Temescal Basins

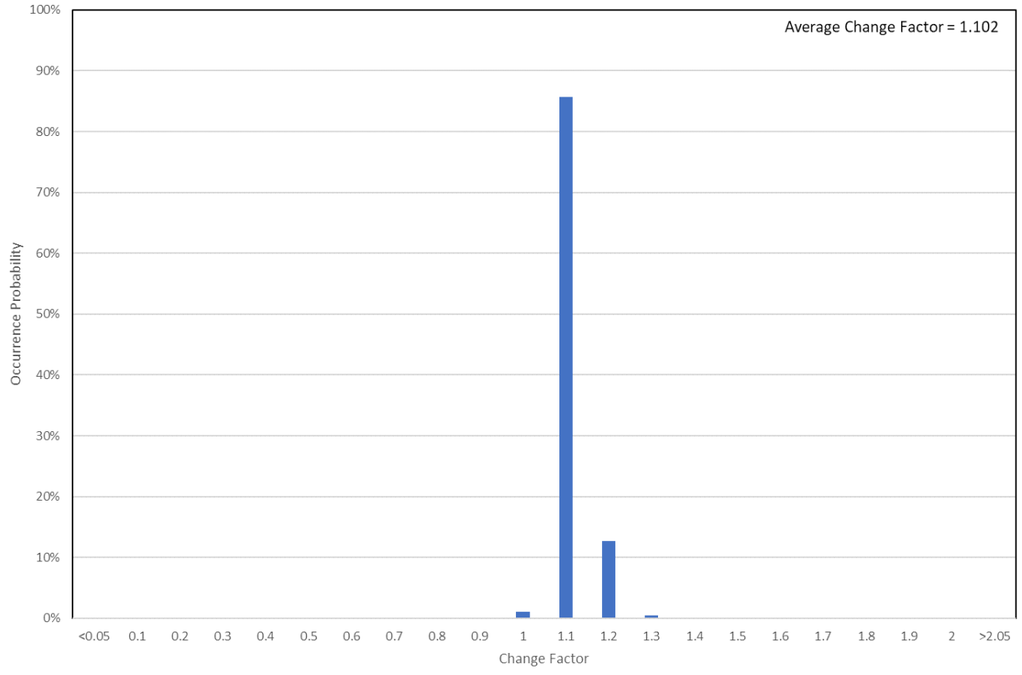

Figure 7-4 Comparison of DIPAW Discharging Out of the Vadose Zone to the Saturated Zone for the Prior and 2020 Safe Yield Investigations

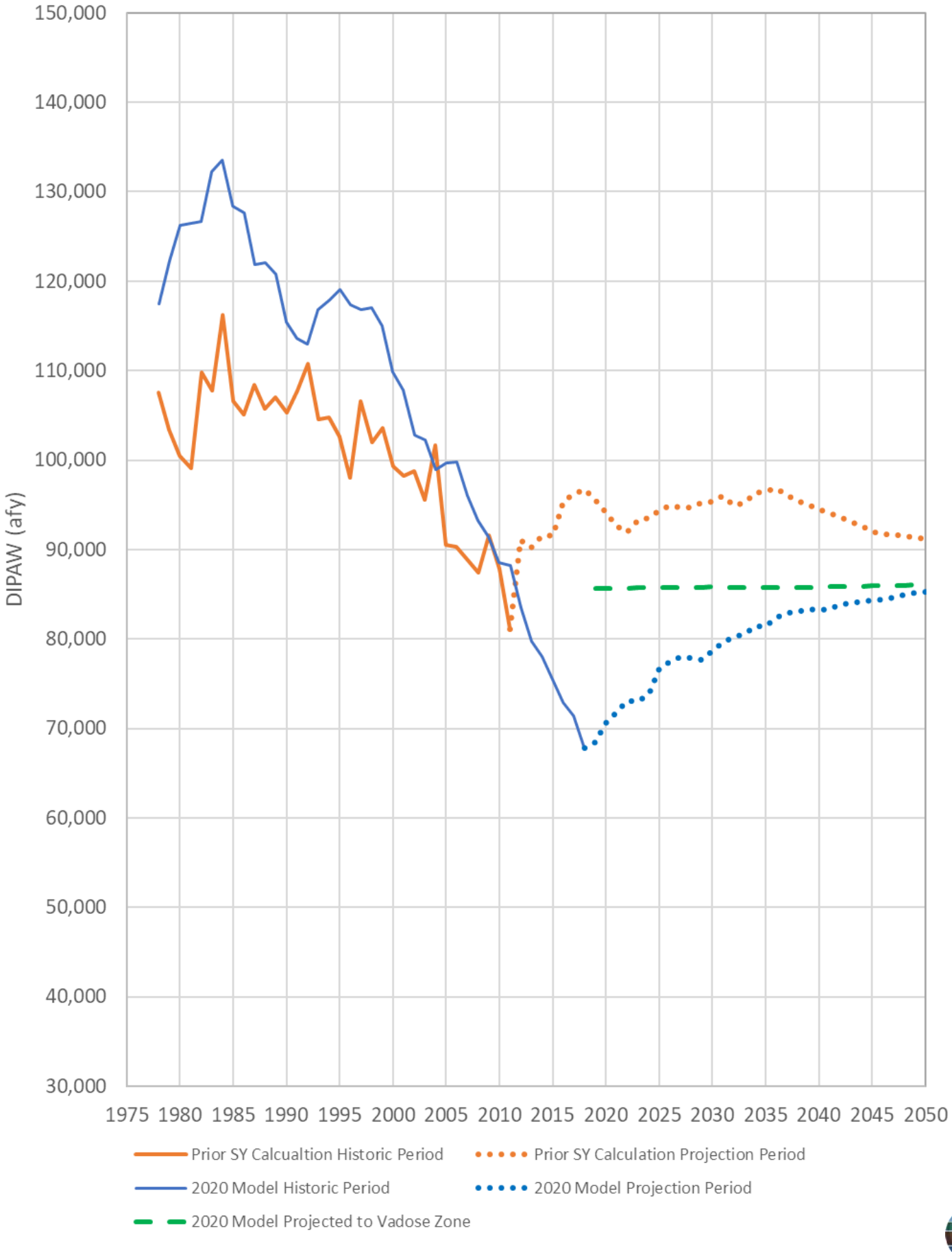

Figure 7-5 Total Recharge, Discharge, and Change in Storage for Scenario 2020 SYR1 in the Chino Basin

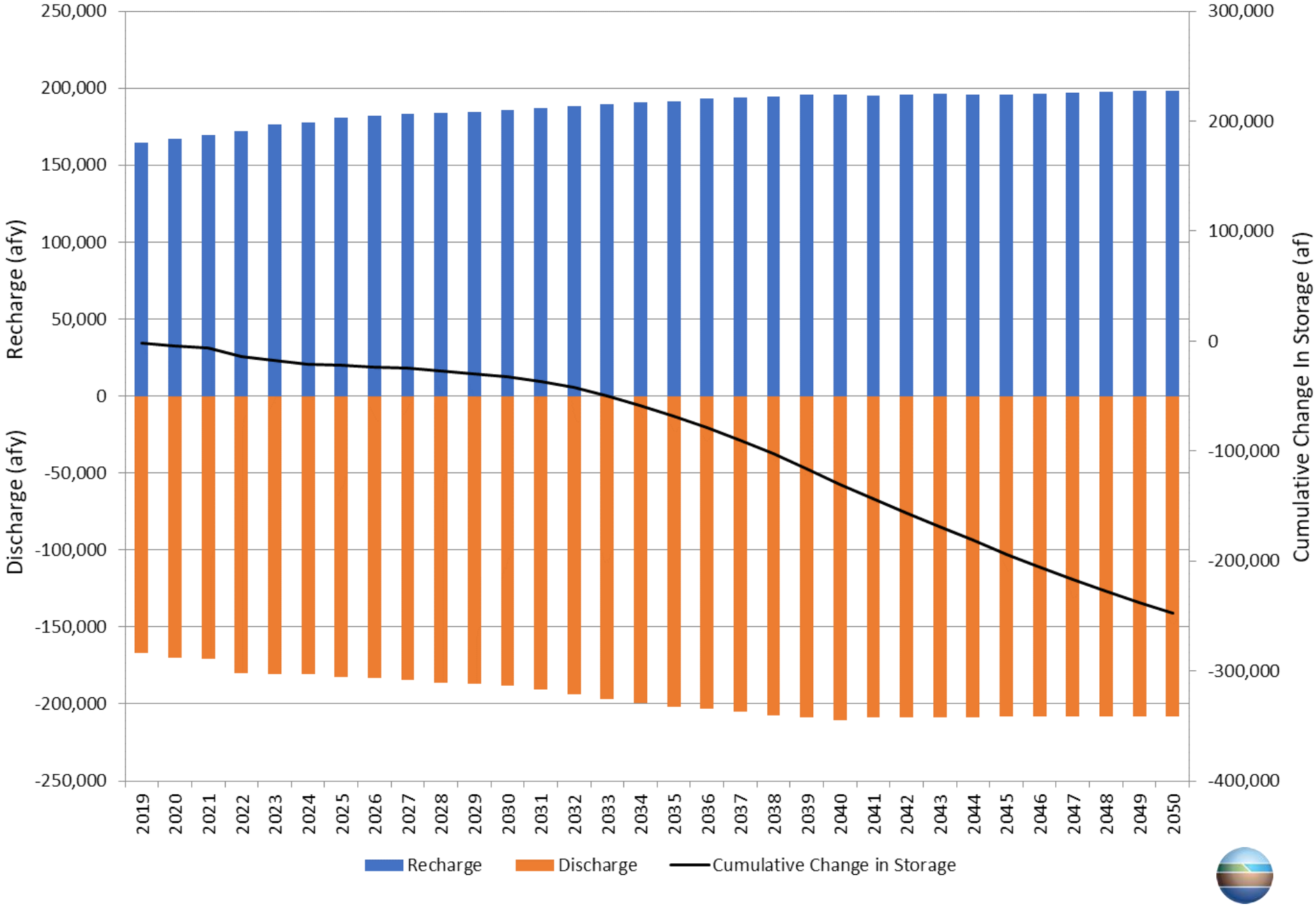

Figure 7-6 Discharge to and from Vadose Zone and End of Year Vadose Zone Storage for the Calibration and Planning Periods

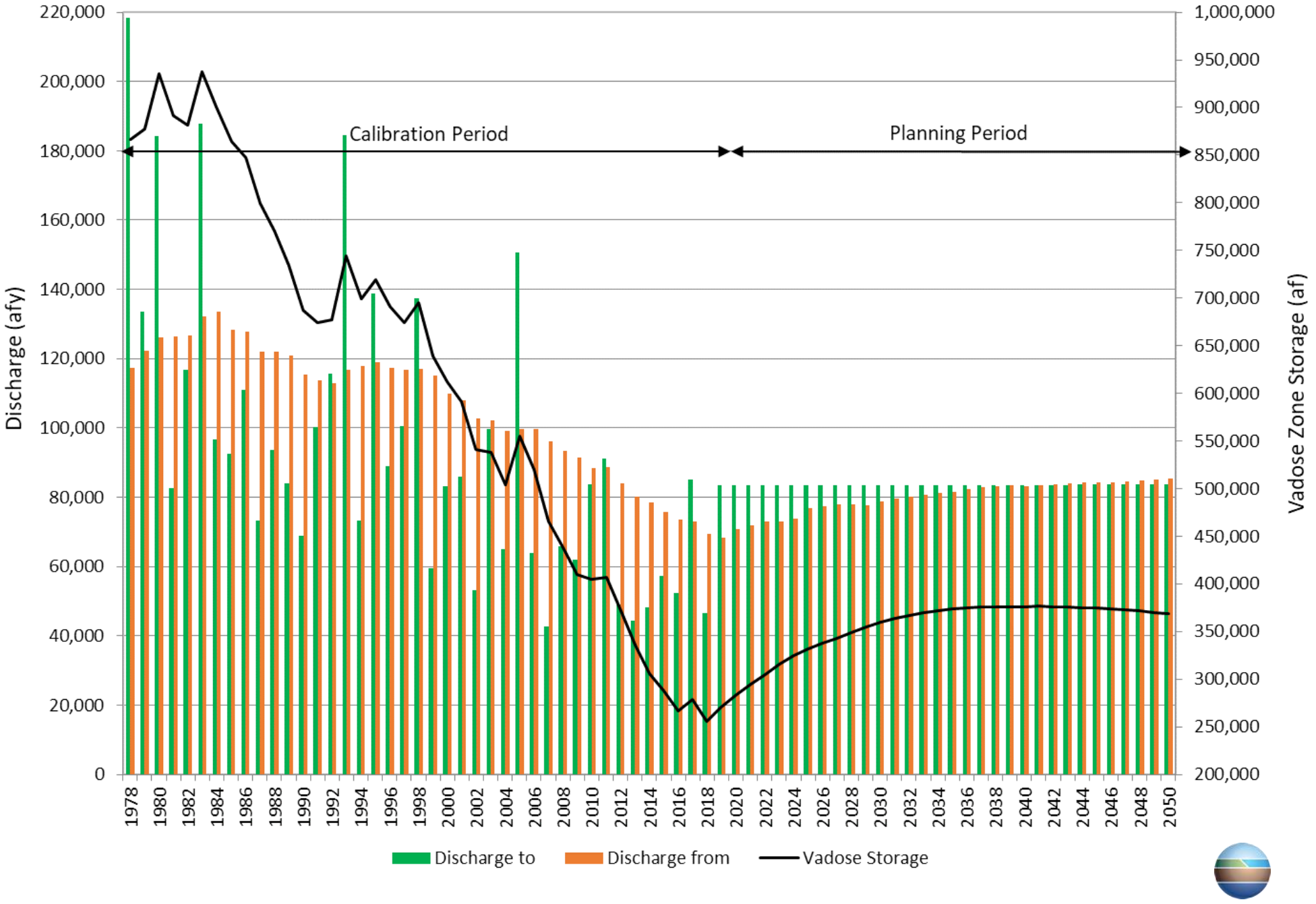

Figure 7-7 Relationship of End of Year Vadose Zone Storage to DIPAW Discharge to Saturated Zone for the Calibration and Planning Periods

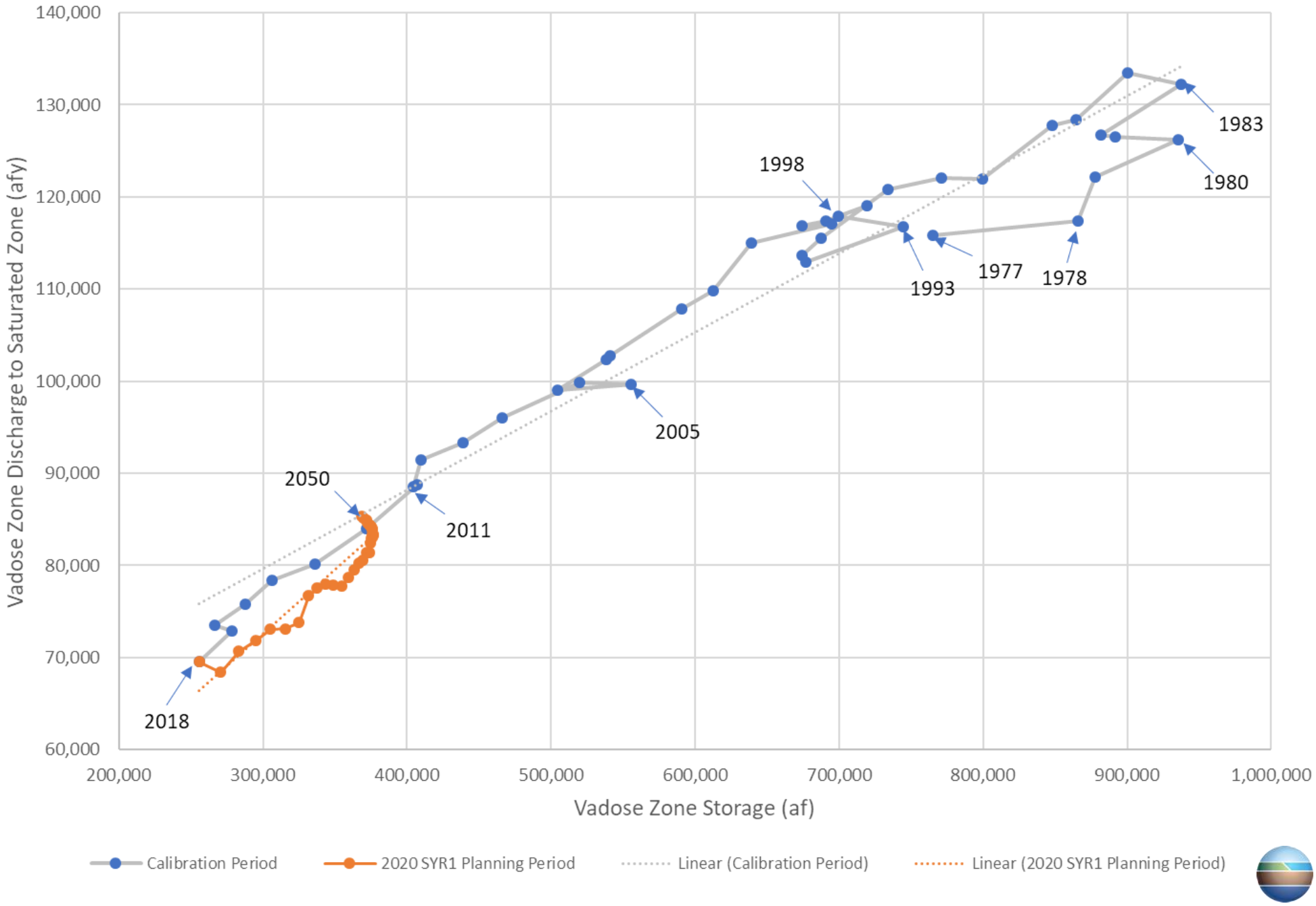

Hydraulic Head Contours (July 2018)
(ft above mean sea-level)

Appropriative Pool Pumping Wells

- City of Chino
- City of Chino Hills
- City of Ontario
- City of Pomona
- City of Upland
- Cucamonga Valley Water District
- Fontana Water Company
- Jurupa Community Services District
- Monte Vista Water District
- Other Appropriators

Chino Desalter Wells

Streams & Flood Control Channels

Flood Control & Conservation Basins

OBMP Management Zones

Faults

- Location Certain
- Location Approximate
- Approximate Location of Groundwater Barrier
- Location Concealed
- Location Uncertain

Prepared by:

WEI
WILDERMUTH ENVIRONMENTAL, INC.

Author: LS
Date: 3/11/2020
File: Figure 7-8a wl2018_1cont10.mxd

0 1 2 3 4 5 Miles
0 2 4 6 8 Km

Prepared for:

2020 Safe Yield Recalculation

CHINO BASIN WATERMASTER
Partners in Basin Management

Hydraulic Head Contours -- Layer 1
Scenario SYR1 - July 2018

Figure 7-8a

Hydraulic Head Contours (July 2018)
(ft above mean sea-level)

Appropriative Pool Pumping Wells

- City of Chino
- City of Chino Hills
- City of Ontario
- City of Pomona
- City of Upland
- Cucamonga Valley Water District
- Fontana Water Company
- Jurupa Community Services District
- Monte Vista Water District
- Other Appropriators

Chino Desalter Wells

Streams & Flood Control Channels

Flood Control & Conservation Basins

OBMP Management Zones

Faults

- Location Certain
- Location Approximate
- Approximate Location of Groundwater Barrier
- Location Concealed
- Location Uncertain

Prepared by:

WEI
WILDERMUTH ENVIRONMENTAL, INC.

Author: LS
Date: 3/11/2020
File: Figure 7-8b wl2018_3cont10.mxd

0 1 2 3 4 5 Miles
0 2 4 6 8 Km

Prepared for:

2020 Safe Yield Recalculation

CHINO BASIN WATERMASTER
Partners in Basin Management

Hydraulic Head Contours -- Layer 3
Scenario SYR1 - July 2018

Figure 7-8b

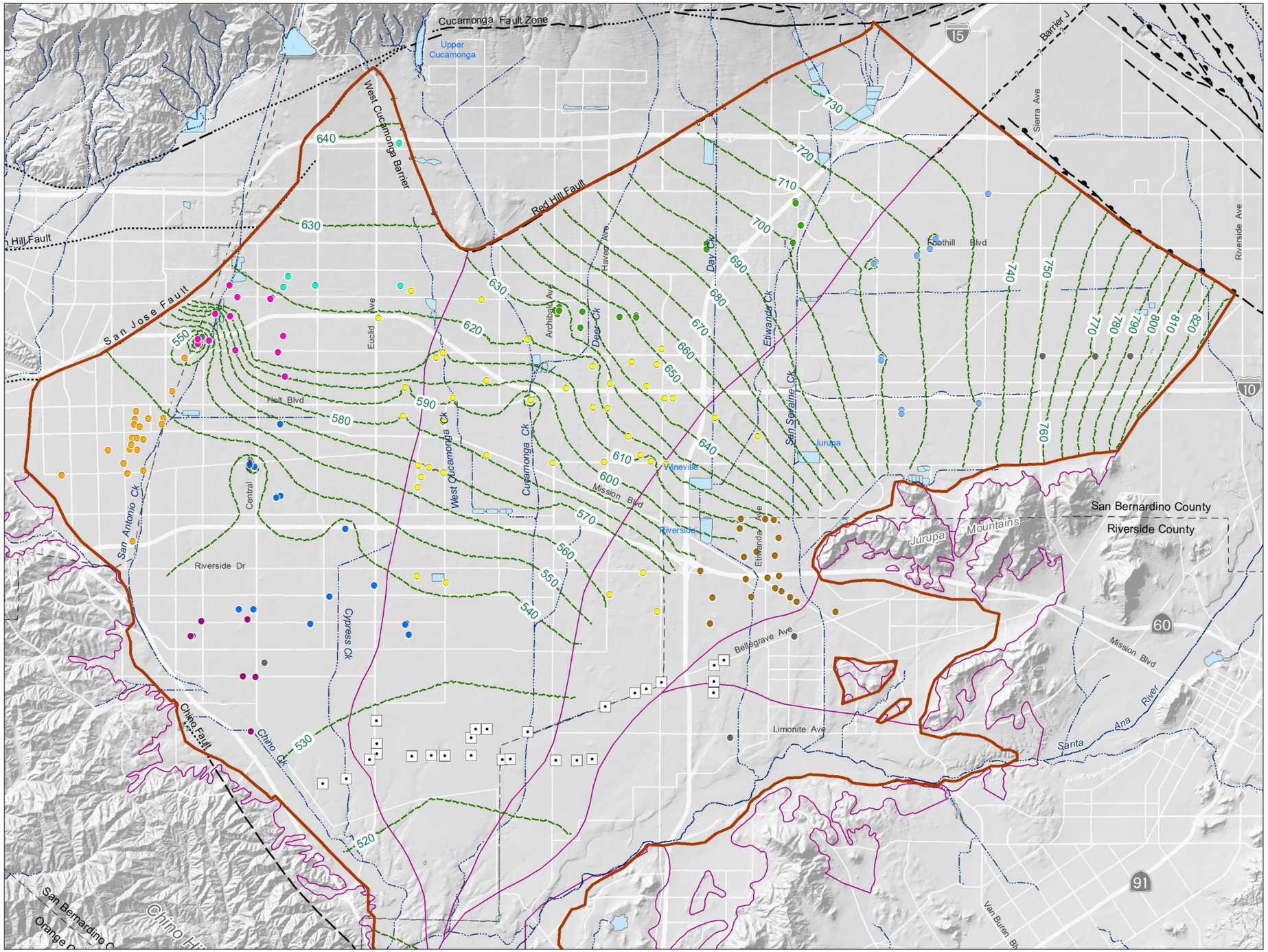

Hydraulic Head Contours (July 2018)
(ft above mean sea-level)

Appropriative Pool Pumping Wells

- City of Chino
- City of Chino Hills
- City of Ontario
- City of Pomona
- City of Upland
- Cucamonga Valley Water District
- Fontana Water Company
- Jurupa Community Services District
- Monte Vista Water District
- Other Appropriators

Chino Desalter Wells

Streams & Flood Control Channels

Flood Control & Conservation Basins

OBMP Management Zones

Faults

- Location Certain
- Location Approximate
- Approximate Location of Groundwater Barrier
- Location Concealed
- Location Uncertain

Prepared by:

WEI
WILDERMUTH ENVIRONMENTAL, INC.

Author: LS
Date: 3/11/2020
File: Figure 7-8c wl2018_5cont10.mxd

0 1 2 3 4 5 Miles
0 2 4 6 8 Km

Prepared for:

2020 Safe Yield Recalculation

CHINO BASIN WATERMASTER
Partners in Basin Management

Hydraulic Head Contours -- Layer 5
Scenario SYR1 - July 2018

Figure 7-8c

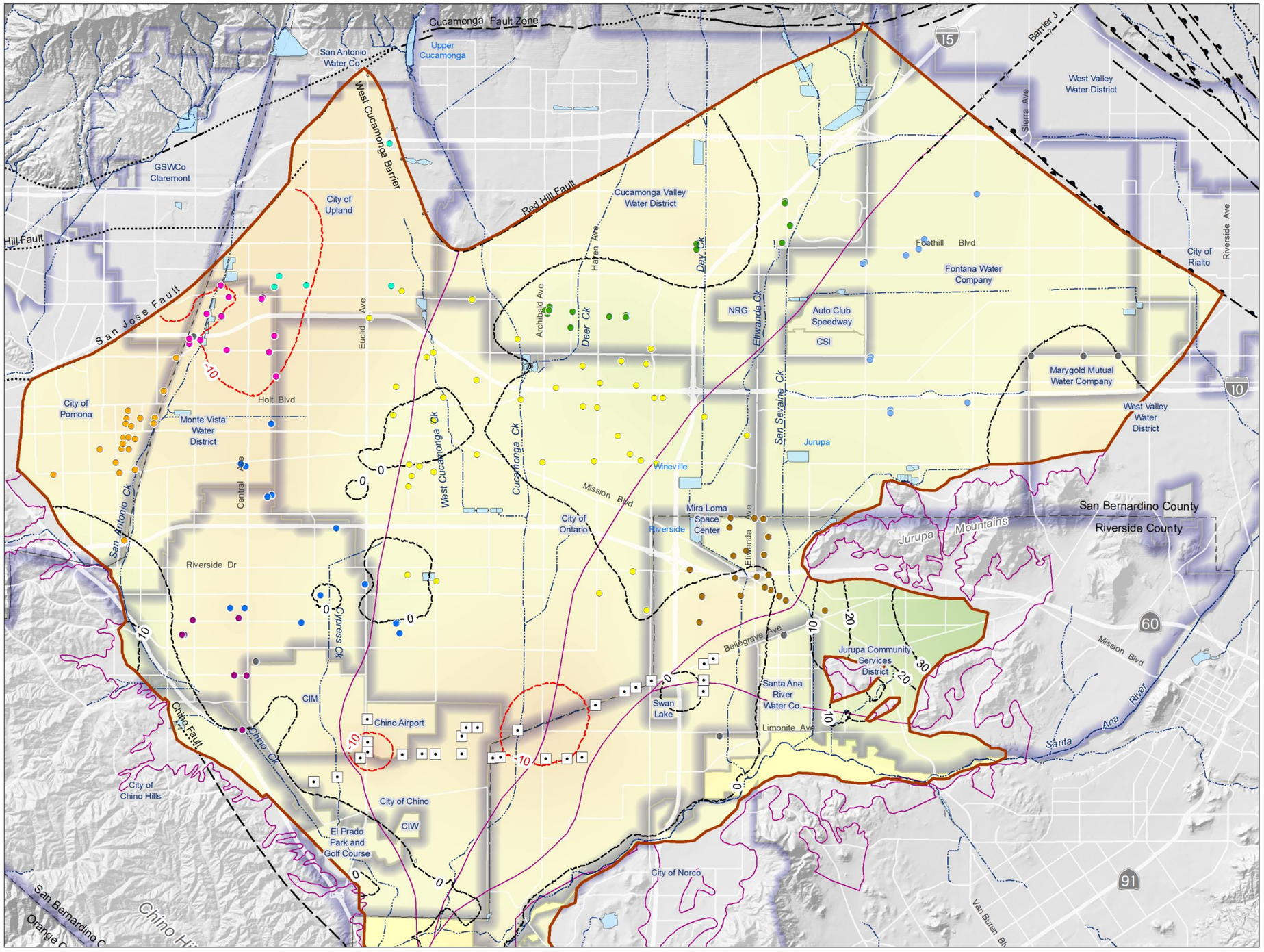

Contour of Hydraulic Head Change (ft) Positive Change
July 2018 to July 2030

Contour of Hydraulic Head Change (ft) Negative Change
July 2018 to July 2030

Hydraulic Head Change (ft) *July 2018 to July 2030*

100 — Increase
0
-100 — Decrease

Appropriative Pool Pumping Wells

- City of Chino
- City of Chino Hills
- City of Ontario
- City of Pomona
- City of Upland
- Cucamonga Valley Water District
- Fontana Water Company
- Jurupa Community Services District
- Monte Vista Water District
- Other Appropriators

Chino Desalter Wells

Streams & Flood Control Channels

Flood Control & Conservation Basins

Water Service Area

OBMP Management Zones

Faults

- Location Certain
- Location Approximate
- Approximate Location of Groundwater Barrier
- Location Concealed
- Location Uncertain

Prepared by:

WEI
WILDERMUTH ENVIRONMENTAL, INC.

Author: LS
Date: 3/11/2020
File: Figure 7-9a wl30minus18_1_SYR1a.mxd

0 1 2 3 4 5 Miles
0 2 4 6 8 Km

Prepared for:

2020 Safe Yield Recalculation

CHINO BASIN WATERMASTER
Partners in Basin Management

Projected Hydraulic Head Change -- Layer 1
Scenario SYR1 - July 2030 minus July 2018

Figure 7-9a

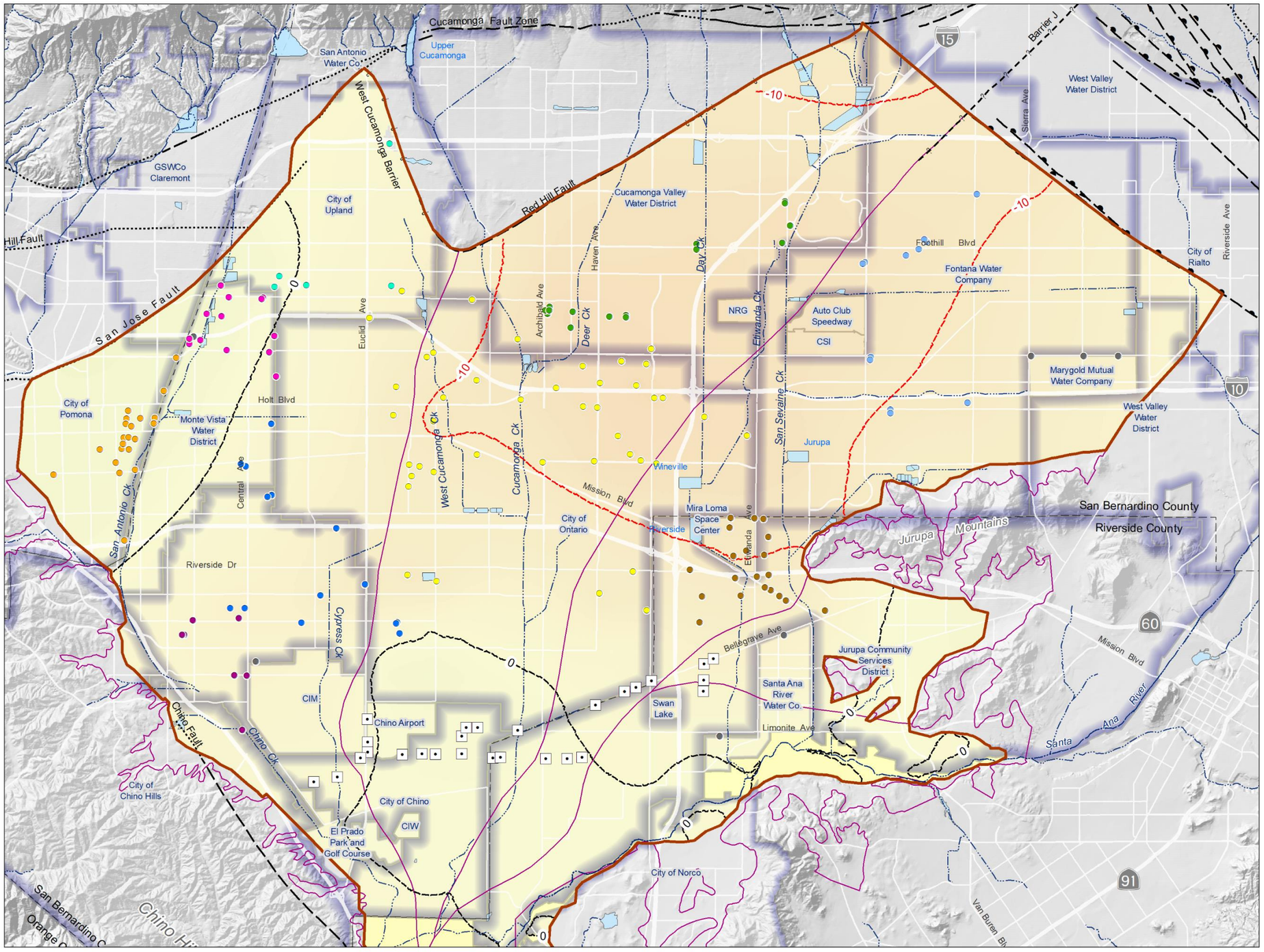

Contour of Hydraulic Head Change (ft) Positive Change
July 2030 to July 2040

Contour of Hydraulic Head Change (ft) Negative Change
July 2030 to July 2040

Hydraulic Head Change (ft) *July 2030 to July 2040*

100 — Increase
0
-100 — Decrease

Appropriative Pool Pumping Wells

- City of Chino
- City of Chino Hills
- City of Ontario
- City of Pomona
- City of Upland
- Cucamonga Valley Water District
- Fontana Water Company
- Jurupa Community Services District
- Monte Vista Water District
- Other Appropriators

Chino Desalter Wells

Streams & Flood Control Channels

Flood Control & Conservation Basins

Water Service Area

OBMP Management Zones

Faults

- Location Certain
- Location Approximate
- Approximate Location of Groundwater Barrier
- Location Concealed
- Location Uncertain

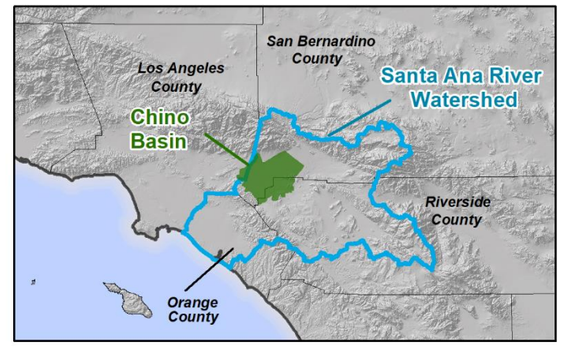

Prepared by:

WEI
Wildermuth Environmental, Inc.

Author: LS
Date: 3/11/2020
File: Figure 7-9b wl40minus30_1_SYR1a.mxd

0 1 2 3 4 5 Miles
0 2 4 6 8 Km

Prepared for:

2020 Safe Yield Recalculation

Chino Basin Watermaster — Partners in Basin Management

Projected Hydraulic Head Change -- Layer 1
Scenario SYR1 - July 2040 minus July 2030

Figure 7-9b

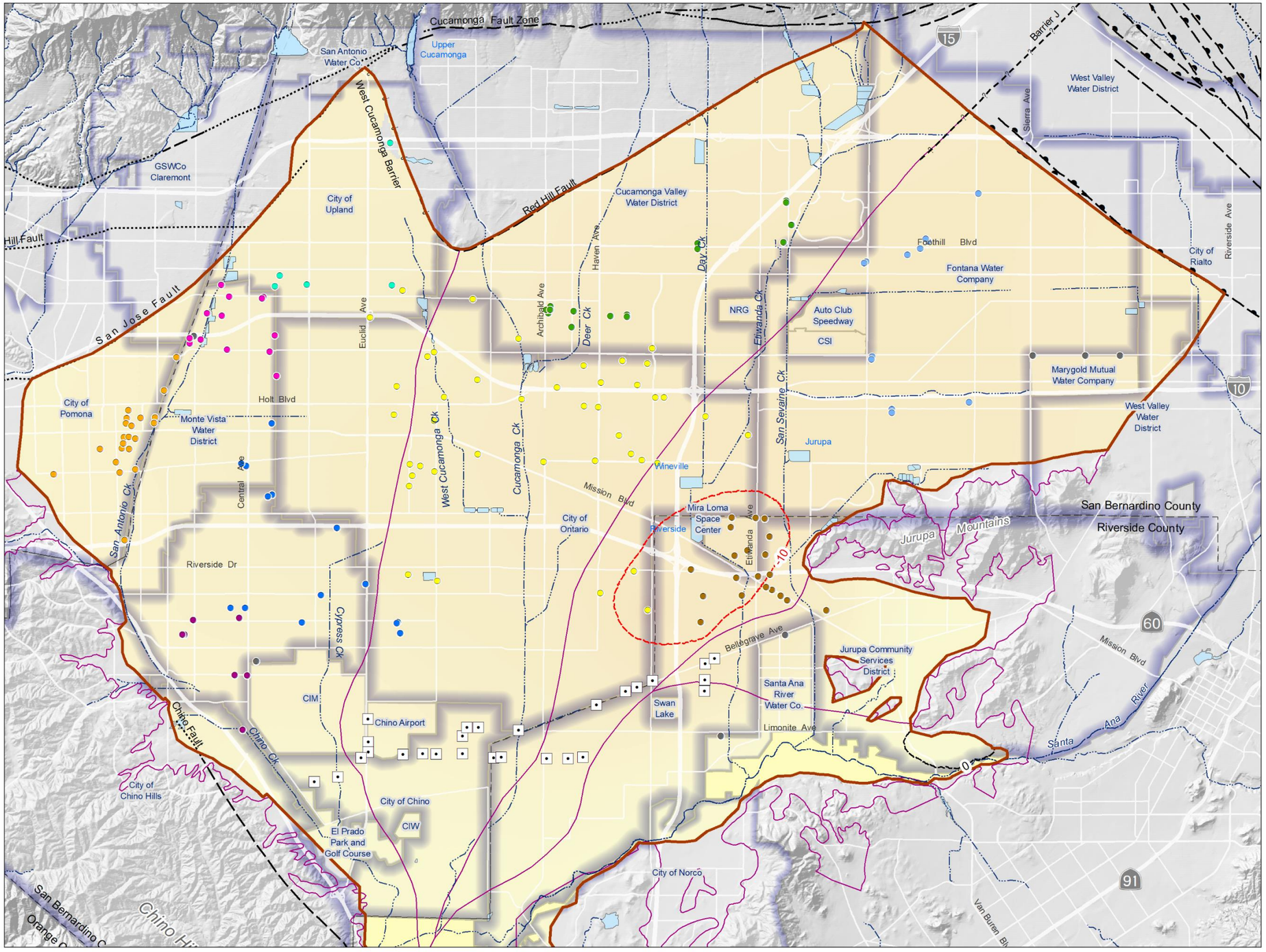

10 Contour of Hydraulic Head Change (ft) Positive Change
July 2040 to July 2050

10 Contour of Hydraulic Head Change (ft) Negative Change
July 2040 to July 2050

Hydraulic Head Change (ft) *July 2040 to July 2050*

100 Increase
0
-100 Decrease

Appropriative Pool Pumping Wells

- City of Chino
- City of Chino Hills
- City of Ontario
- City of Pomona
- City of Upland
- Cucamonga Valley Water District
- Fontana Water Company
- Jurupa Community Services District
- Monte Vista Water District
- Other Appropriators

Chino Desalter Wells

Streams & Flood Control Channels

Flood Control & Conservation Basins

Water Service Area

OBMP Management Zones

Faults

- Location Certain
- Location Approximate
- Approximate Location of Groundwater Barrier
- Location Concealed
- Location Uncertain

Prepared by:

WEI
WILDERMUTH ENVIRONMENTAL, INC.

Author: LS
Date: 3/11/2020
File: Figure 7-9c wl50minus40_1_SYR1a.mxd

0 1 2 3 4 5 Miles
0 2 4 6 8 Km

Prepared for:

2020 Safe Yield Recalculation

CHINO BASIN WATERMASTER
Partners in Basin Management

Projected Hydraulic Head Change -- Layer 1
Scenario SYR1 - July 2050 minus July 2040

Figure 7-9c

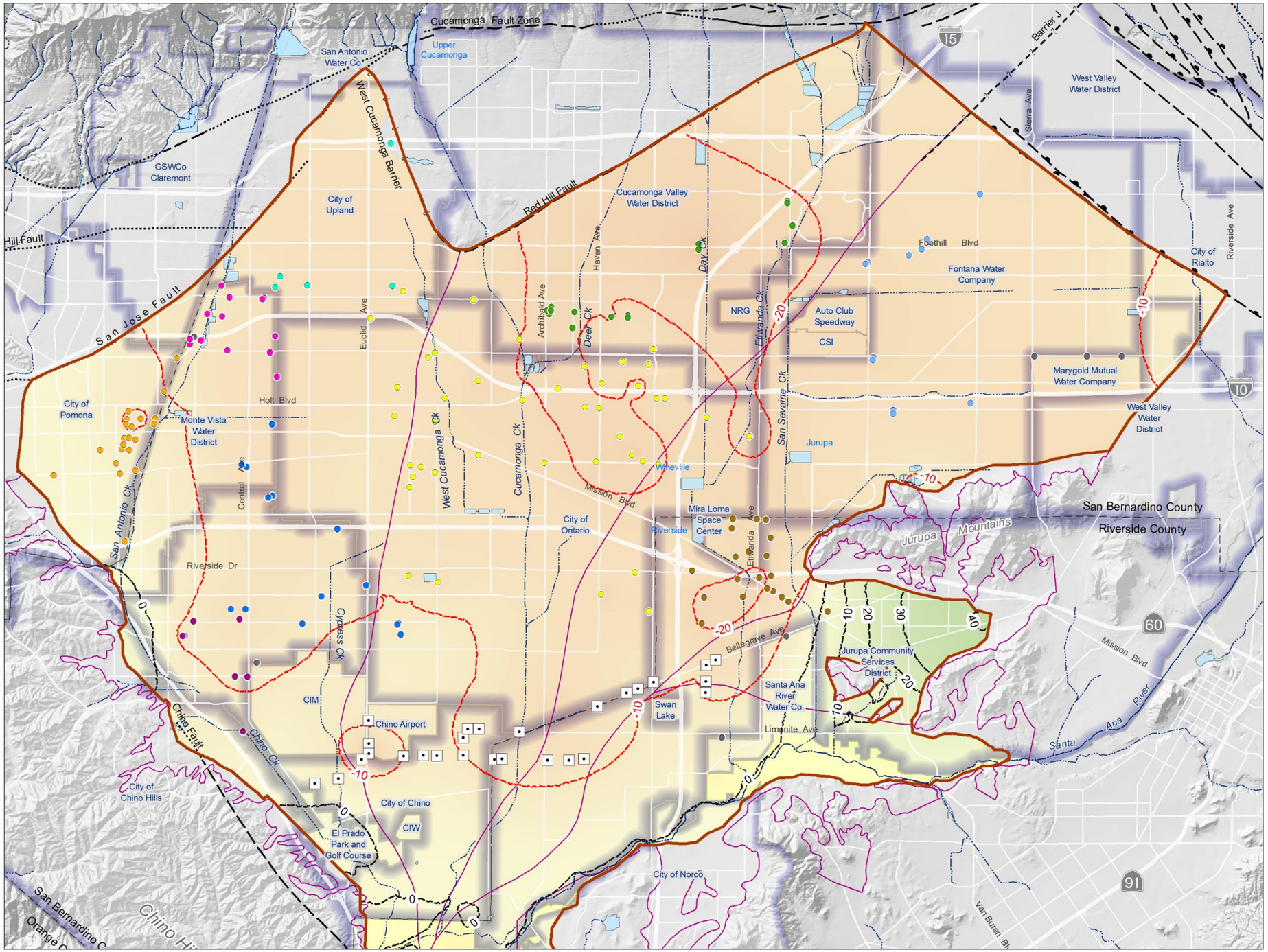

Contour of Hydraulic Head Change (ft) Positive Change
July 2018 to July 2050

Contour of Hydraulic Head Change (ft) Negative Change
July 2018 to July 2050

Hydraulic Head Change (ft) *July 2018 to July 2050*

100 — Increase
0
-100 — Decrease

Appropriative Pool Pumping Wells

- City of Chino
- City of Chino Hills
- City of Ontario
- City of Pomona
- City of Upland
- Cucamonga Valley Water District
- Fontana Water Company
- Jurupa Community Services District
- Monte Vista Water District
- Other Appropriators

Chino Desalter Wells

Streams & Flood Control Channels

Flood Control & Conservation Basins

Water Service Area

OBMP Management Zones

Faults

- Location Certain
- Location Approximate
- Approximate Location of Groundwater Barrier
- Location Concealed
- Location Uncertain

Prepared by:

WEI
Wildermuth Environmental, Inc.

Author: LS
Date: 3/11/2020
File: Figure 7-9d wl50minus18_1_SYR1a.mxd

0 1 2 3 4 5 Miles
0 2 4 6 8 Km

Prepared for:

2020 Safe Yield Recalculation

Chino Basin Watermaster
Partners in Basin Management

Projected Hydraulic Head Change -- Layer 1
Scenario SYR1 - July 2050 minus July 2018

Figure 7-9d

Contour of Hydraulic Head Change (ft) Positive Change
July 2018 to July 2030

Contour of Hydraulic Head Change (ft) Negative Change
July 2018 to July 2030

Hydraulic Head Change (ft) *July 2018 to July 2030*

100 — Increase
0
-100 — Decrease

Appropriative Pool Pumping Wells

- City of Chino
- City of Chino Hills
- City of Ontario
- City of Pomona
- City of Upland
- Cucamonga Valley Water District
- Fontana Water Company
- Jurupa Community Services District
- Monte Vista Water District
- Other Appropriators

Chino Desalter Wells

Streams & Flood Control Channels

Flood Control & Conservation Basins

Water Service Area

OBMP Management Zones

Faults

- Location Certain
- Location Approximate
- Approximate Location of Groundwater Barrier
- Location Concealed
- Location Uncertain

Prepared by:

WEI
WILDERMUTH ENVIRONMENTAL, INC.

Author: LS
Date: 3/11/2020
File: Figure 7-10a wl30minus18_3_SYR1a.mxd

0 1 2 3 4 5 Miles
0 2 4 6 8 Km

Prepared for:

2020 Safe Yield Recalculation

CHINO BASIN WATERMASTER
Partners in Basin Management

Projected Hydraulic Head Change -- Layer 3
Scenario SYR1 - July 2030 minus July 2018

Figure 7-10a

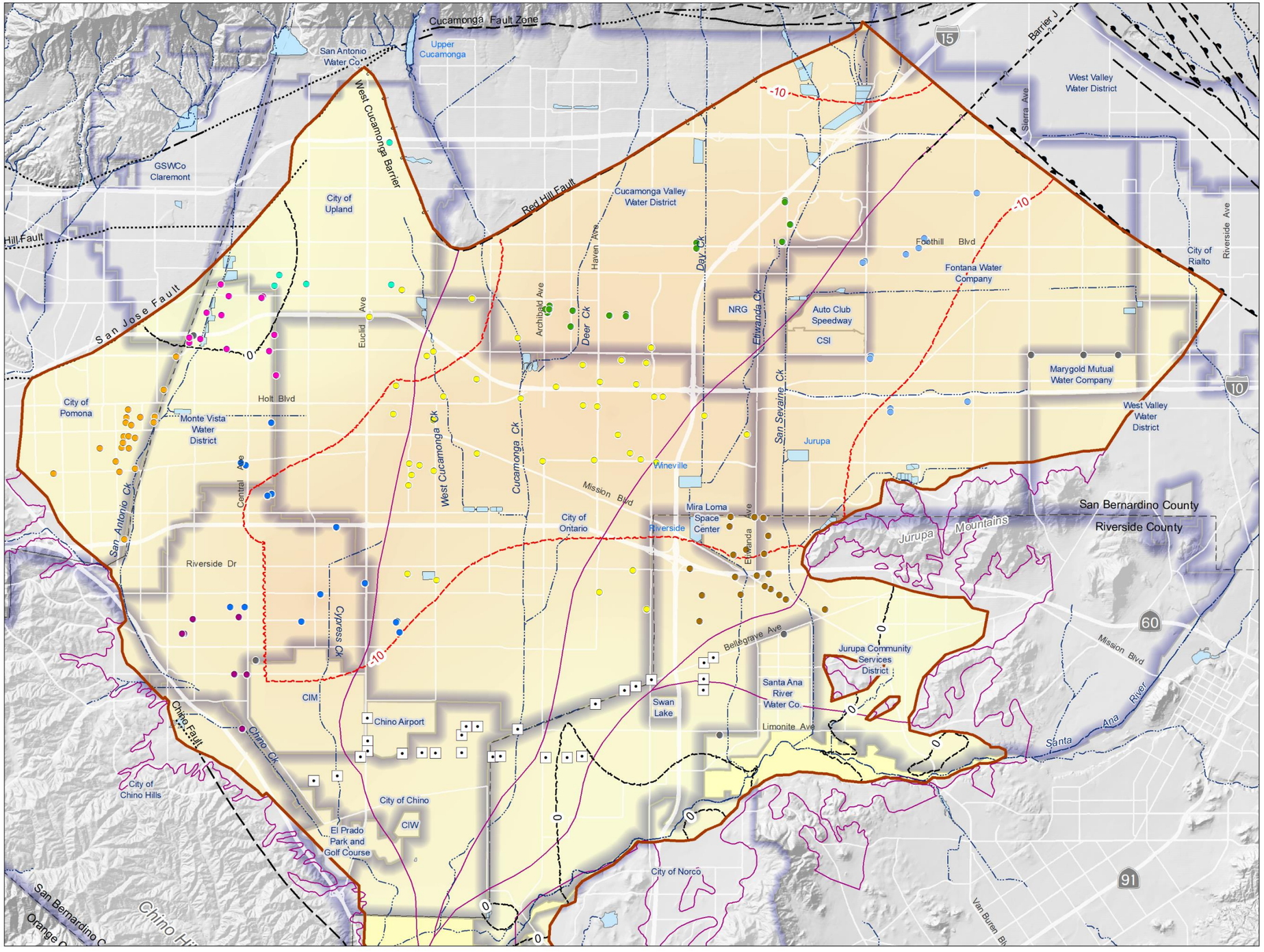

Contour of Hydraulic Head Change (ft) Positive Change
July 2030 to July 2040

Contour of Hydraulic Head Change (ft) Negative Change
July 2030 to July 2040

Hydraulic Head Change (ft) *July 2030 to July 2040*

100 — Increase
0
-100 — Decrease

Appropriative Pool Pumping Wells

- City of Chino
- City of Chino Hills
- City of Ontario
- City of Pomona
- City of Upland
- Cucamonga Valley Water District
- Fontana Water Company
- Jurupa Community Services District
- Monte Vista Water District
- Other Appropriators

Chino Desalter Wells

Streams & Flood Control Channels

Flood Control & Conservation Basins

Water Service Area

OBMP Management Zones

Faults

- Location Certain
- Location Approximate
- Approximate Location of Groundwater Barrier
- Location Concealed
- Location Uncertain

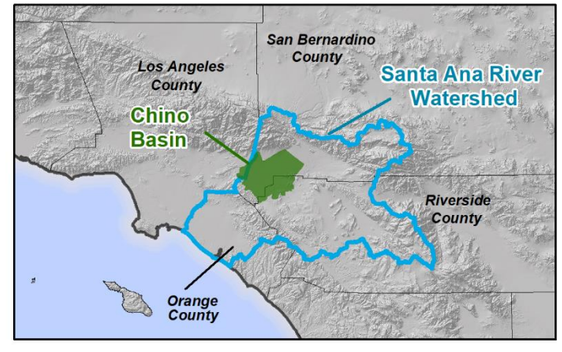

Prepared by:

WEI
Wildermuth Environmental, Inc.

Author: LS
Date: 3/11/2020
File: Figure 7-10b wl40minus30_3_SYR1a.mxd

0 1 2 3 4 5 Miles
0 2 4 6 8 Km

Prepared for:

2020 Safe Yield Recalculation

Chino Basin Watermaster — Partners in Basin Management

Projected Hydraulic Head Change -- Layer 3
Scenario SYR1 - July 2040 minus July 2030

Figure 7-10b

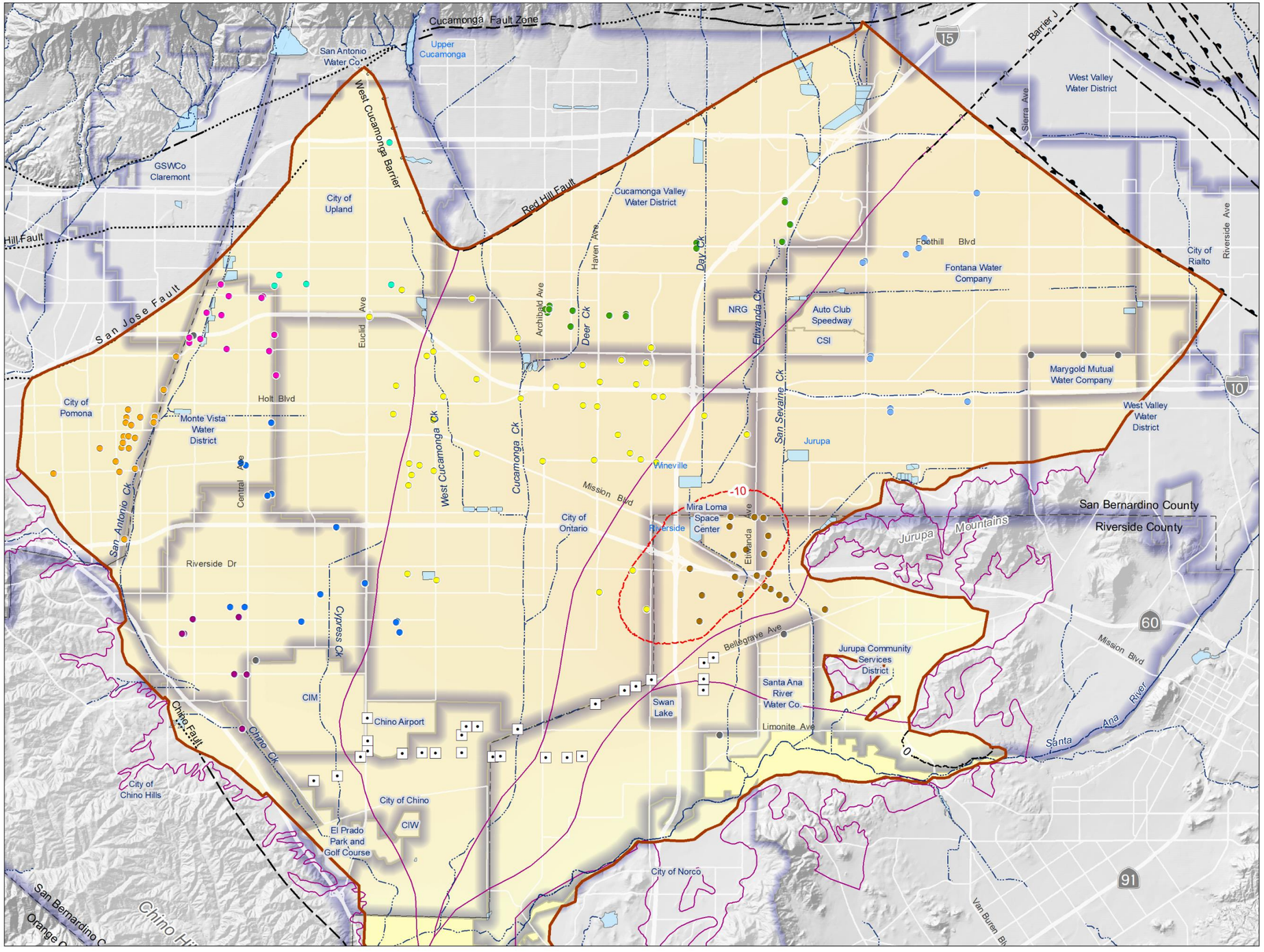

Contour of Hydraulic Head Change (ft) Positive Change
July 2040 to July 2050

Contour of Hydraulic Head Change (ft) Negative Change
July 2040 to July 2050

Hydraulic Head Change (ft) *July 2040 to July 2050*

100 — Increase
0
-100 — Decrease

Appropriative Pool Pumping Wells

- City of Chino
- City of Chino Hills
- City of Ontario
- City of Pomona
- City of Upland
- Cucamonga Valley Water District
- Fontana Water Company
- Jurupa Community Services District
- Monte Vista Water District
- Other Appropriators

Chino Desalter Wells

Streams & Flood Control Channels

Flood Control & Conservation Basins

Water Service Area

OBMP Management Zones

Faults

- Location Certain
- Location Approximate
- Approximate Location of Groundwater Barrier
- Location Concealed
- Location Uncertain

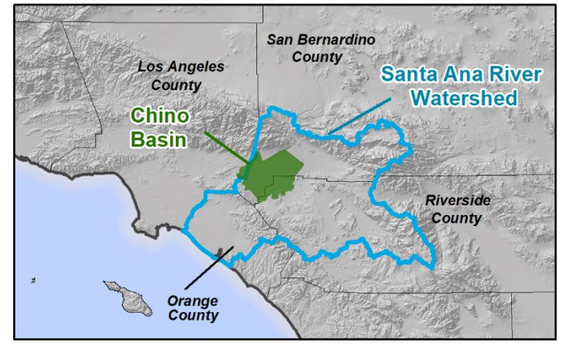

Prepared by:

WEI
Wildermuth Environmental, Inc.

Author: LS
Date: 3/11/2020
File: Figure 7-10c wl50minus40_3_SYR1a.mxd

0 1 2 3 4 5 Miles
0 2 4 6 8 Km

Prepared for:

2020 Safe Yield Recalculation

Chino Basin Watermaster
Partners in Basin Management

Projected Hydraulic Head Change -- Layer 3
Scenario SYR1 - July 2050 minus July 2040

Figure 7-10c

Contour of Hydraulic Head Change (ft) Positive Change
July 2018 to July 2050

Contour of Hydraulic Head Change (ft) Negative Change
July 2018 to July 2050

Hydraulic Head Change (ft) *July 2018 to July 2050*

100 — Increase
0
-100 — Decrease

Appropriative Pool Pumping Wells

- City of Chino
- City of Chino Hills
- City of Ontario
- City of Pomona
- City of Upland
- Cucamonga Valley Water District
- Fontana Water Company
- Jurupa Community Services District
- Monte Vista Water District
- Other Appropriators

Chino Desalter Wells

Streams & Flood Control Channels

Flood Control & Conservation Basins

Water Service Area

OBMP Management Zones

Faults

- Location Certain
- Location Approximate
- Approximate Location of Groundwater Barrier
- Location Concealed
- Location Uncertain

Prepared by:

WEI
WILDERMUTH ENVIRONMENTAL, INC.

Author: LS
Date: 3/11/2020
File: Figure 7-10d wl50minus18_3_SYR1a.mxd

0 1 2 3 4 5 Miles
0 2 4 6 8 Km

Prepared for:

2020 Safe Yield Recalculation

CHINO BASIN WATERMASTER
Partners in Basin Management

Projected Hydraulic Head Change -- Layer 3
Scenario SYR1 - July 2050 minus July 2018

Figure 7-10d

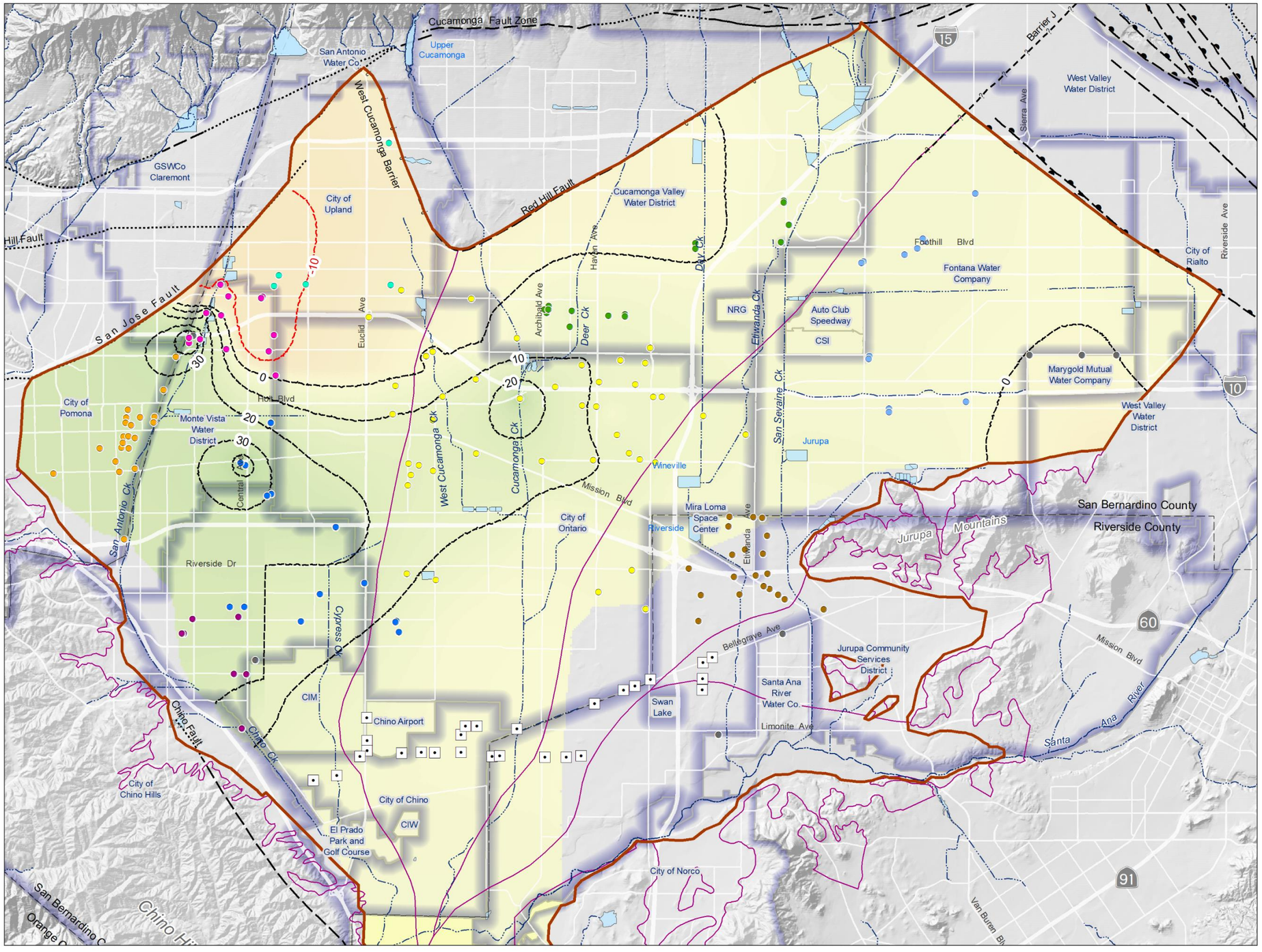

Contour of Hydraulic Head Change (ft) Positive Change
July 2018 to July 2030

Contour of Hydraulic Head Change (ft) Negative Change
July 2018 to July 2030

Hydraulic Head Change (ft) *July 2018 to July 2030*

100 — Increase
0
-100 — Decrease

Appropriative Pool Pumping Wells

- City of Chino
- City of Chino Hills
- City of Ontario
- City of Pomona
- City of Upland
- Cucamonga Valley Water District
- Fontana Water Company
- Jurupa Community Services District
- Monte Vista Water District
- Other Appropriators

Chino Desalter Wells

Streams & Flood Control Channels

Flood Control & Conservation Basins

Water Service Area

OBMP Management Zones

Faults

- Location Certain
- Location Approximate
- Approximate Location of Groundwater Barrier
- Location Concealed
- Location Uncertain

Prepared by:

WEI
WILDERMUTH ENVIRONMENTAL, INC.

Author: LS
Date: 3/11/2020
File: Figure 7-11a wl30minus18_5_SYR1a.mxd

0 1 2 3 4 5 Miles
0 2 4 6 8 Km

Prepared for:

2020 Safe Yield Recalculation

CHINO BASIN WATERMASTER
Partners in Basin Management

Projected Hydraulic Head Change -- Layer 5
Scenario SYR1 - July 2030 minus July 2018

Figure 7-11a

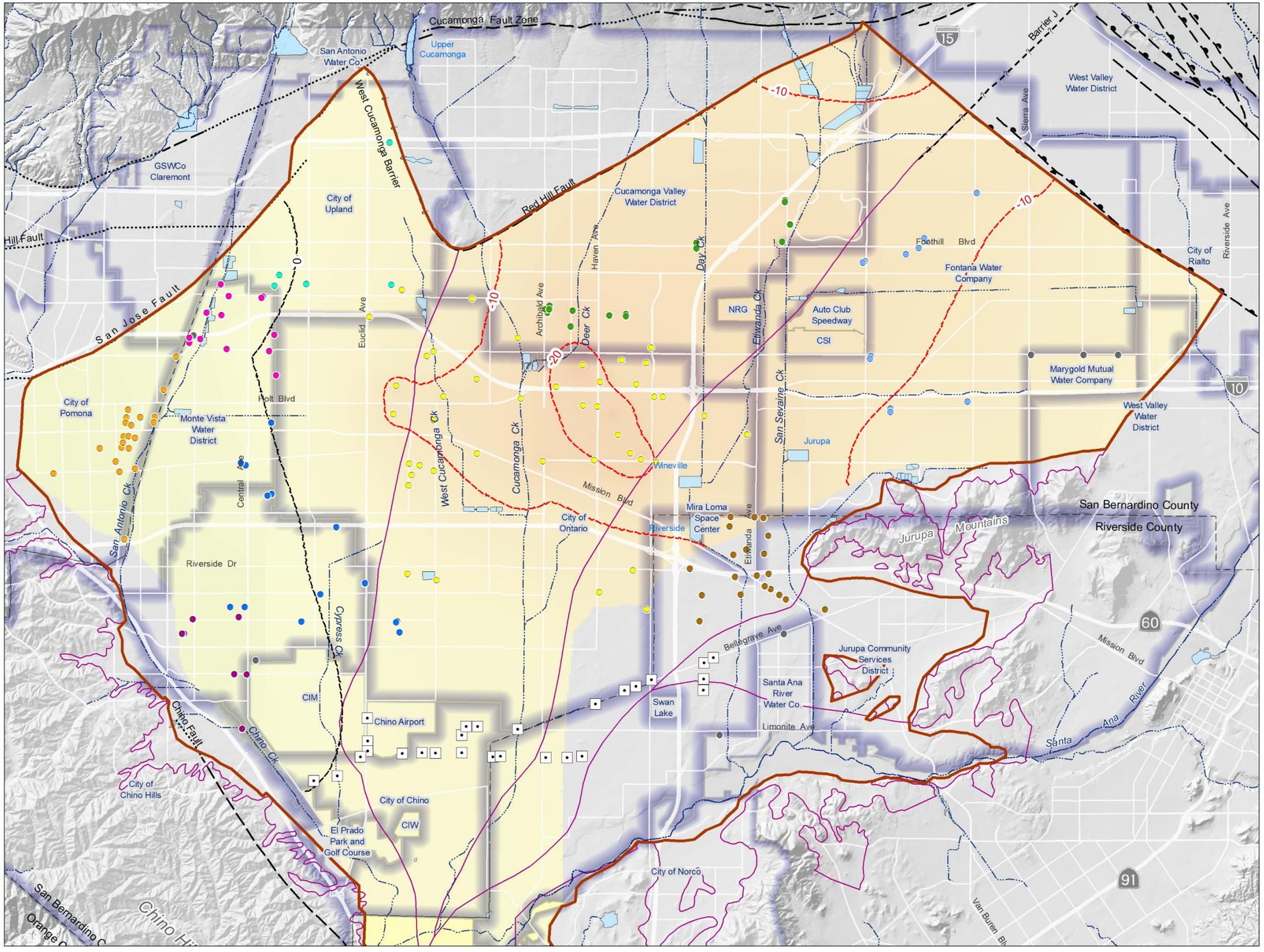

Contour of Hydraulic Head Change (ft) Positive Change
July 2030 to July 2040

Contour of Hydraulic Head Change (ft) Negative Change
July 2030 to July 2040

Hydraulic Head Change (ft) *July 2030 to July 2040*

100 — Increase
0
-100 — Decrease

Appropriative Pool Pumping Wells

- City of Chino
- City of Chino Hills
- City of Ontario
- City of Pomona
- City of Upland
- Cucamonga Valley Water District
- Fontana Water Company
- Jurupa Community Services District
- Monte Vista Water District
- Other Appropriators

Chino Desalter Wells

Streams & Flood Control Channels

Flood Control & Conservation Basins

Water Service Area

OBMP Management Zones

Faults

- Location Certain
- Location Approximate
- Approximate Location of Groundwater Barrier
- Location Concealed
- Location Uncertain

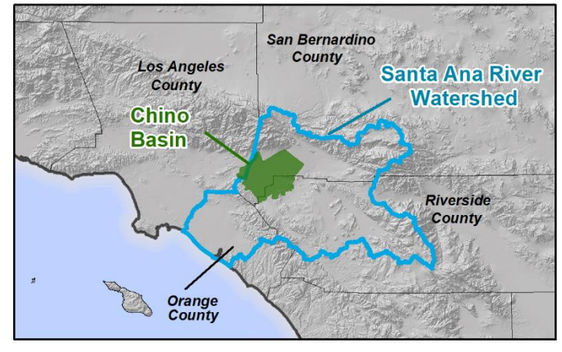

Prepared by:

WEI
WILDERMUTH ENVIRONMENTAL, INC.

Author: LS
Date: 3/11/2020
File: Figure 7-11b wl40minus30_5_SYR1a.mxd

0 1 2 3 4 5 Miles
0 2 4 6 8 Km

Prepared for:

2020 Safe Yield Recalculation

CHINO BASIN WATERMASTER
Partners in Basin Management

Projected Hydraulic Head Change -- Layer 5
Scenario SYR1 - July 2040 minus July 2030

Figure 7-11b

Contour of Hydraulic Head Change (ft) Positive Change
July 2040 to July 2050

Contour of Hydraulic Head Change (ft) Negative Change
July 2040 to July 2050

Hydraulic Head Change (ft) *July 2040 to July 2050*

100 — Increase
0
-100 — Decrease

Appropriative Pool Pumping Wells

- City of Chino
- City of Chino Hills
- City of Ontario
- City of Pomona
- City of Upland
- Cucamonga Valley Water District
- Fontana Water Company
- Jurupa Community Services District
- Monte Vista Water District
- Other Appropriators

Chino Desalter Wells

Streams & Flood Control Channels

Flood Control & Conservation Basins

Water Service Area

OBMP Management Zones

Faults

- Location Certain
- Location Approximate
- Approximate Location of Groundwater Barrier
- Location Concealed
- Location Uncertain

Prepared by:

WEI
Wildermuth Environmental, Inc.

Author: LS
Date: 3/11/2020
File: Figure 7-11c wl50minus40_5_SYR1a.mxd

0 1 2 3 4 5 Miles
0 2 4 6 8 Km

Prepared for:

2020 Safe Yield Recalculation

Chino Basin Watermaster — Partners in Basin Management

Projected Hydraulic Head Change -- Layer 5
Scenario SYR1 - July 2050 minus July 2040

Figure 7-11c

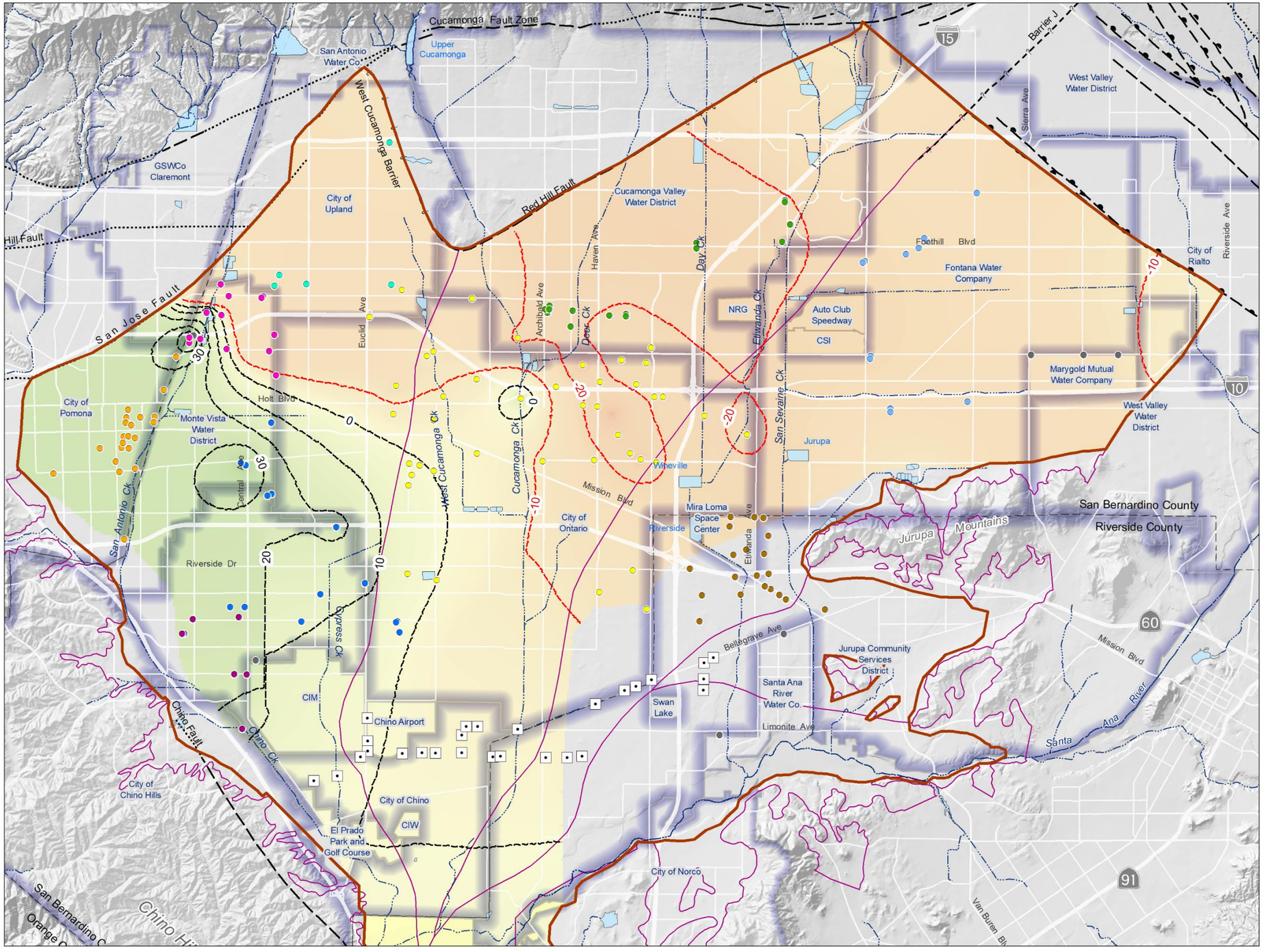

Contour of Hydraulic Head Change (ft) Positive Change
July 2018 to July 2050

Contour of Hydraulic Head Change (ft) Negative Change
July 2018 to July 2050

Hydraulic Head Change (ft) *July 2018 to July 2050*

100 — Increase
0
-100 — Decrease

Appropriative Pool Pumping Wells

- City of Chino
- City of Chino Hills
- City of Ontario
- City of Pomona
- City of Upland
- Cucamonga Valley Water District
- Fontana Water Company
- Jurupa Community Services District
- Monte Vista Water District
- Other Appropriators

Chino Desalter Wells

Streams & Flood Control Channels

Flood Control & Conservation Basins

Water Service Area

OBMP Management Zones

Faults

- Location Certain
- Location Approximate
- Approximate Location of Groundwater Barrier
- Location Concealed
- Location Uncertain

Prepared by:

WEI
WILDERMUTH ENVIRONMENTAL, INC.

Author: LS
Date: 3/11/2020
File: Figure 7-11d wl50minus18_5_SYR1a.mxd

0 1 2 3 4 5 Miles
0 2 4 6 8 Km

Prepared for:

2020 Safe Yield Recalculation

CHINO BASIN WATERMASTER
Partners in Basin Management

Projected Hydraulic Head Change -- Layer 5
Scenario SYR1 - July 2050 minus July 2018

Figure 7-11d

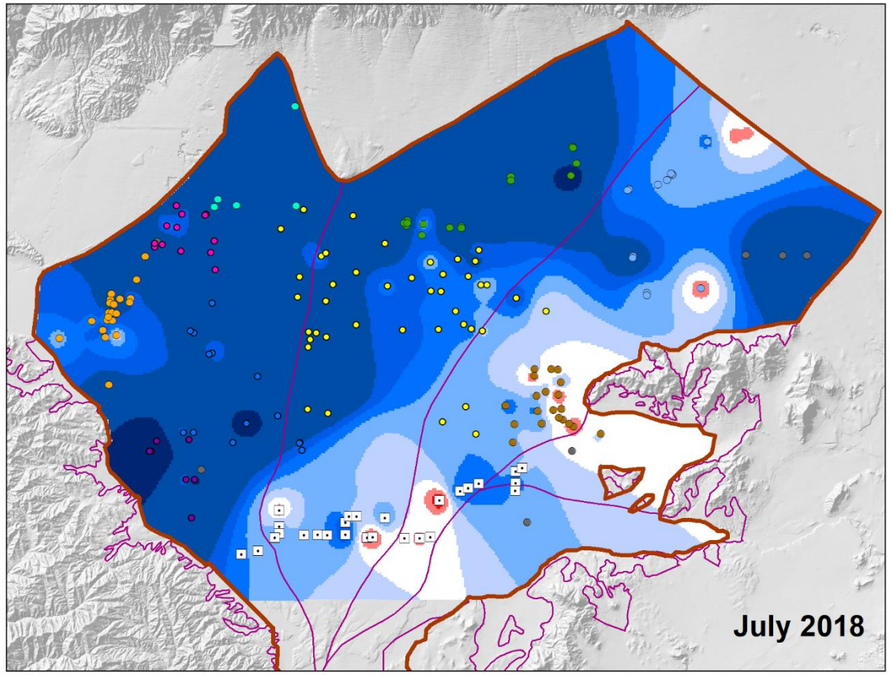

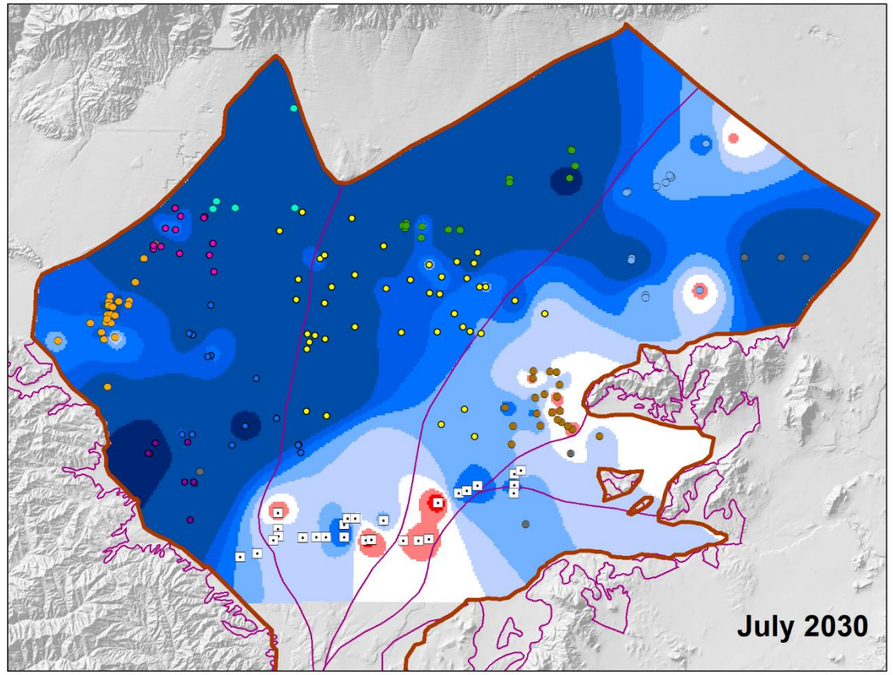

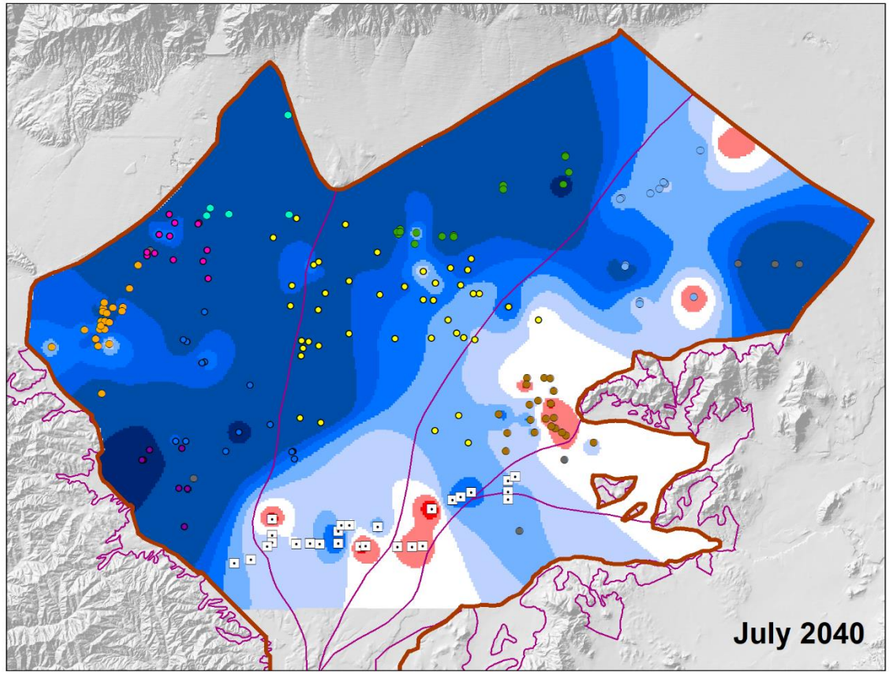

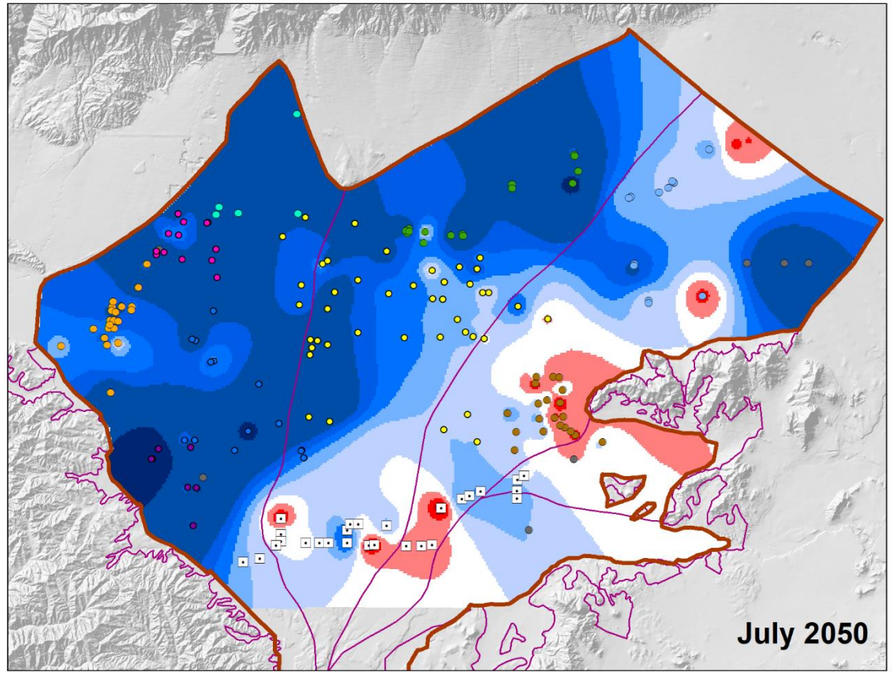

Projected Groundwater Level Minus Sustainability Metric (ft)

- -60 to -40
- -40 to -20
- -20 to 0
- 0 to 20
- 20 to 40
- 40 to 60
- 60 to 80
- 80 to 100
- 100 to 200
- 200 to 400

Appropriative Pool Pumping Wells

- City of Chino
- City of Chino Hills
- City of Ontario
- City of Pomona
- City of Upland
- Cucamonga Valley Water District
- Fontana Water Company
- Jurupa Community Services District
- Monte Vista Water District
- Other Appropriators

Chino Desalter Wells

OBMP Management Zones

MODFLOW Groundwater Flow Model Boundary (Active Model Domain)

Prepared by:

WEI
Wildermuth Environmental, Inc.

Author: LS
Date: 3/12/2020
File: Figure 7-X production_metric_quad_SYR1a.mxd

0 1 2 3 4 5 Miles
0 2 4 6 8 Km

Prepared for:

2020 Safe Yield Recalculation

Chino Basin Watermaster
Partners in Basin Management

Projected Groundwater Elevation in Chino Basin Compared to Production Sustainability Metric
Scenario SYR1

Figure 7-12

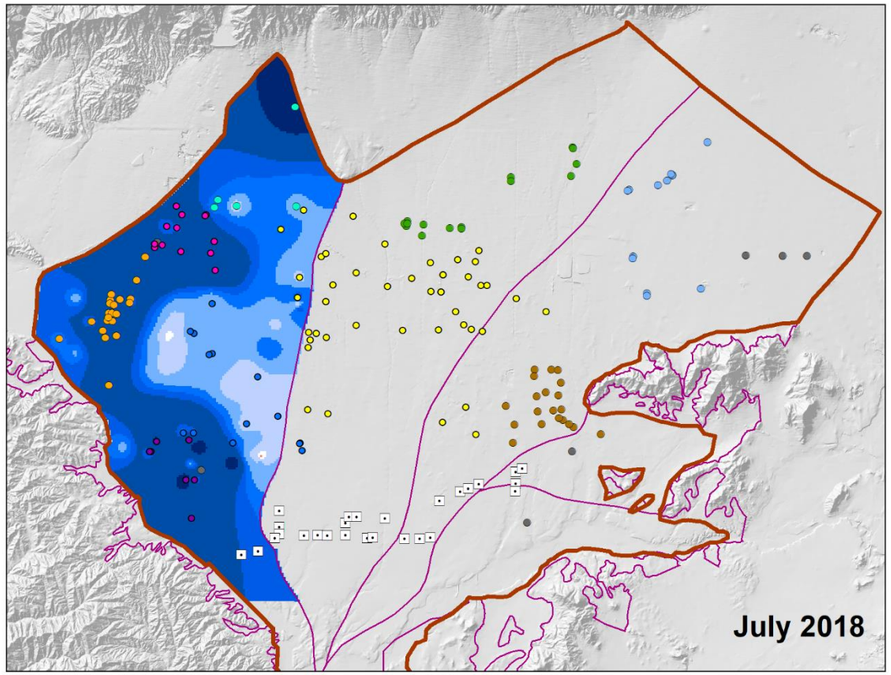

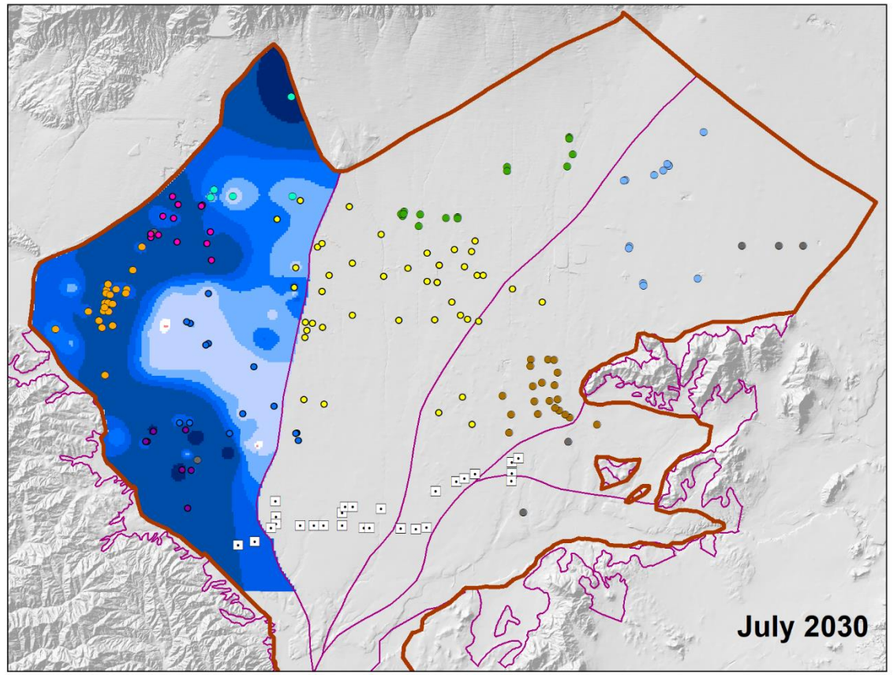

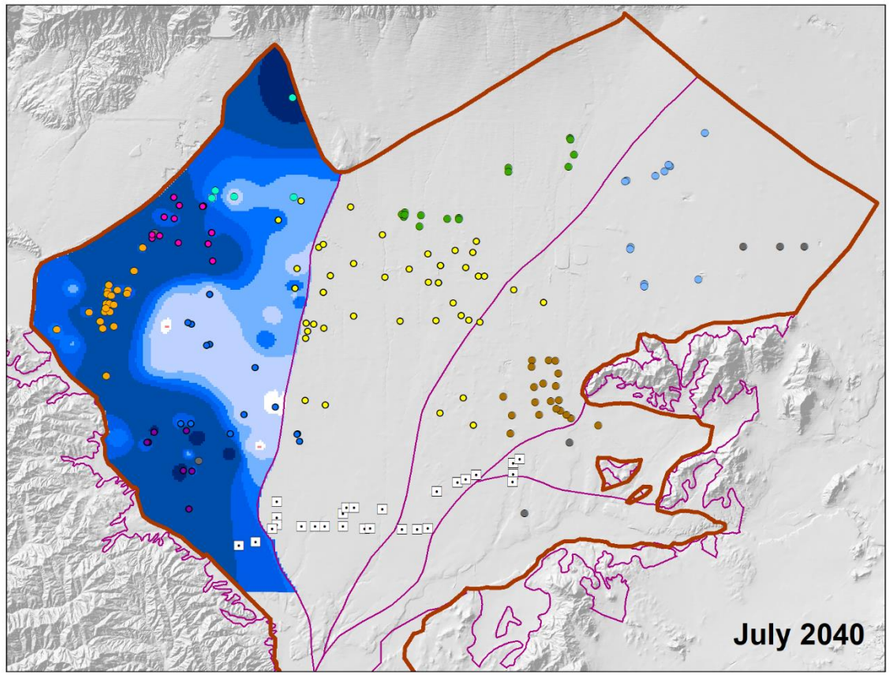

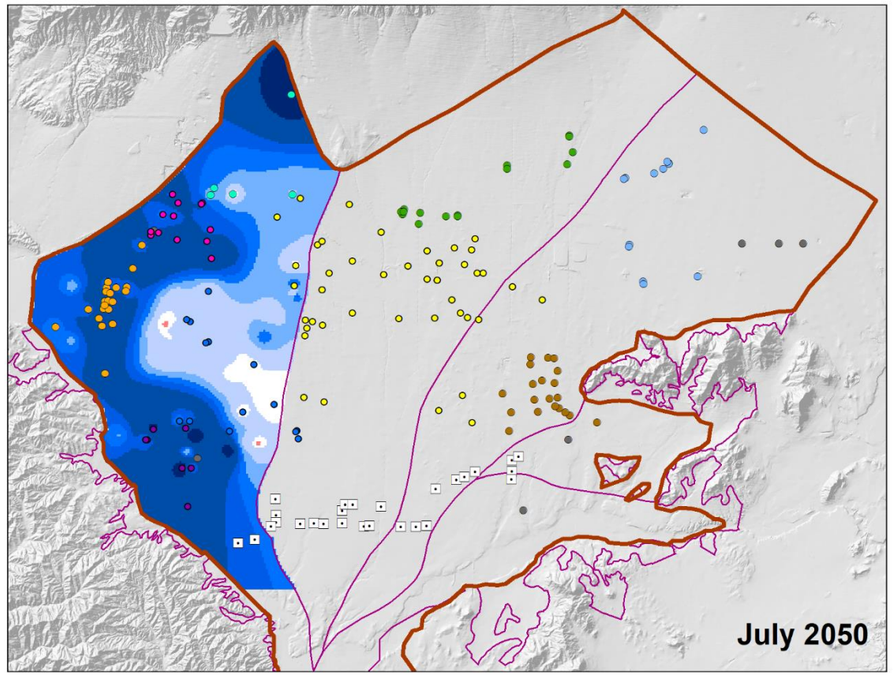

Projected Groundwater Level Minus Subsidence Metric (ft)

- -60 to -40
- -40 to -20
- -20 to 0
- 0 to 20
- 20 to 40
- 40 to 60
- 60 to 80
- 80 to 100
- 100 to 200
- 200 to 400

Appropriative Pool Pumping Wells

- City of Chino
- City of Chino Hills
- City of Ontario
- City of Pomona
- City of Upland
- Cucamonga Valley Water District
- Fontana Water Company
- Jurupa Community Services District
- Monte Vista Water District
- Other Appropriators

Chino Desalter Wells

OBMP Management Zones

MODFLOW Groundwater Flow Model Boundary (Active Model Domain)

Prepared by:

WEI
WILDERMUTH ENVIRONMENTAL, INC.

Author: LS
Date: 4/28/2020
File: Figure 7-13 subsidence_metric_quad_SYR1a.mxd

0 1 2 3 4 5 Miles
0 2 4 6 8 Km

Prepared for:

2020 Safe Yield Recalculation

CHINO BASIN WATERMASTER
Partners in Basin Management

Projected Groundwater Elevation in MZ1 Compared to Subsidence Metric
Scenario SYR1

Figure 7-13

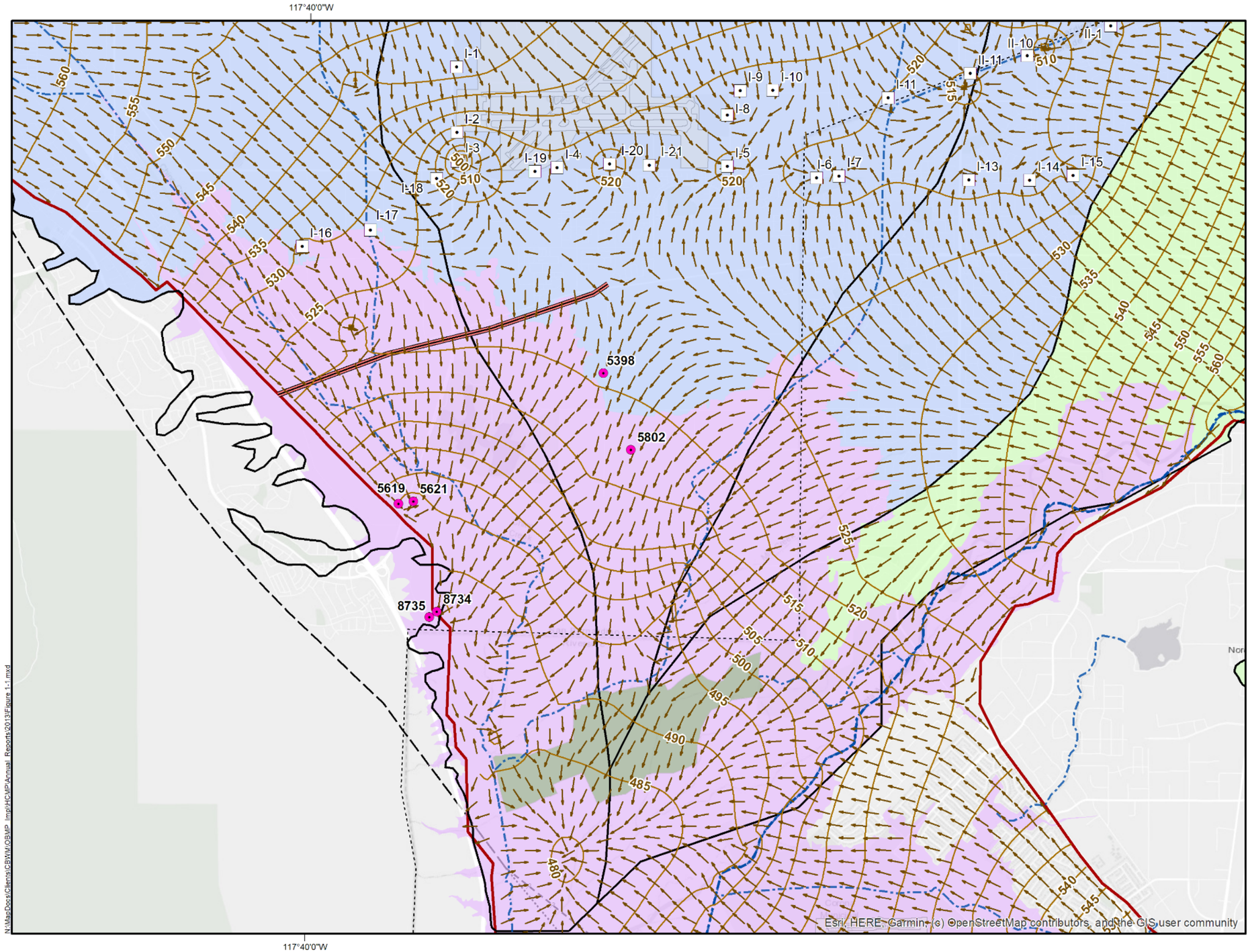

2030 Groundwater Flow Vector - Model Layer 1

2030 Groundwater Elevation Contours (feet above mean sea-level) - Model Layer 1

Line of Control for Assessment of Hydraulic Control

Chino Valley Basin Groundwater Flow Model Boundary

Chino Basin Desalter Authority Well

Pool 1 Wells Assumed Active Downgradient of the Line of Control - Labeled by XRef ID

Streams & Flood Control Channels

OCWD Wetlands

OBMP and Maximum-Benefit Groundwater Management Zones

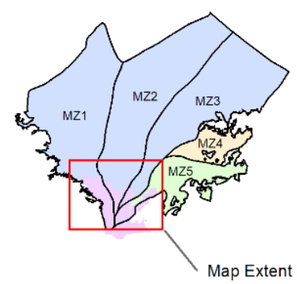

Chino Basin Maximum-Benefit Groundwater Management Zones

- Chino-North
- Chino-South
- Chino-East
- Prado Basin

WEI Wildermuth Environmental, Inc.

Author: VMW
Date: 20200311
File: Figure_7-5_GWE 2030

0 0.5 1 2 Miles

0 0.75 1.5 3 KM

Prepared for:

2020 Safe Yield Recalculation

Chino Basin Watermaster — Partners in Basin Management

Projected Groundwater Level Elevations and Flow Vectors for July 2030

Figure 7-14

Figure 7-15 Historical and Projected Groundwater Discharge from the Chino North Management Zone to Prado Basin Management Zone

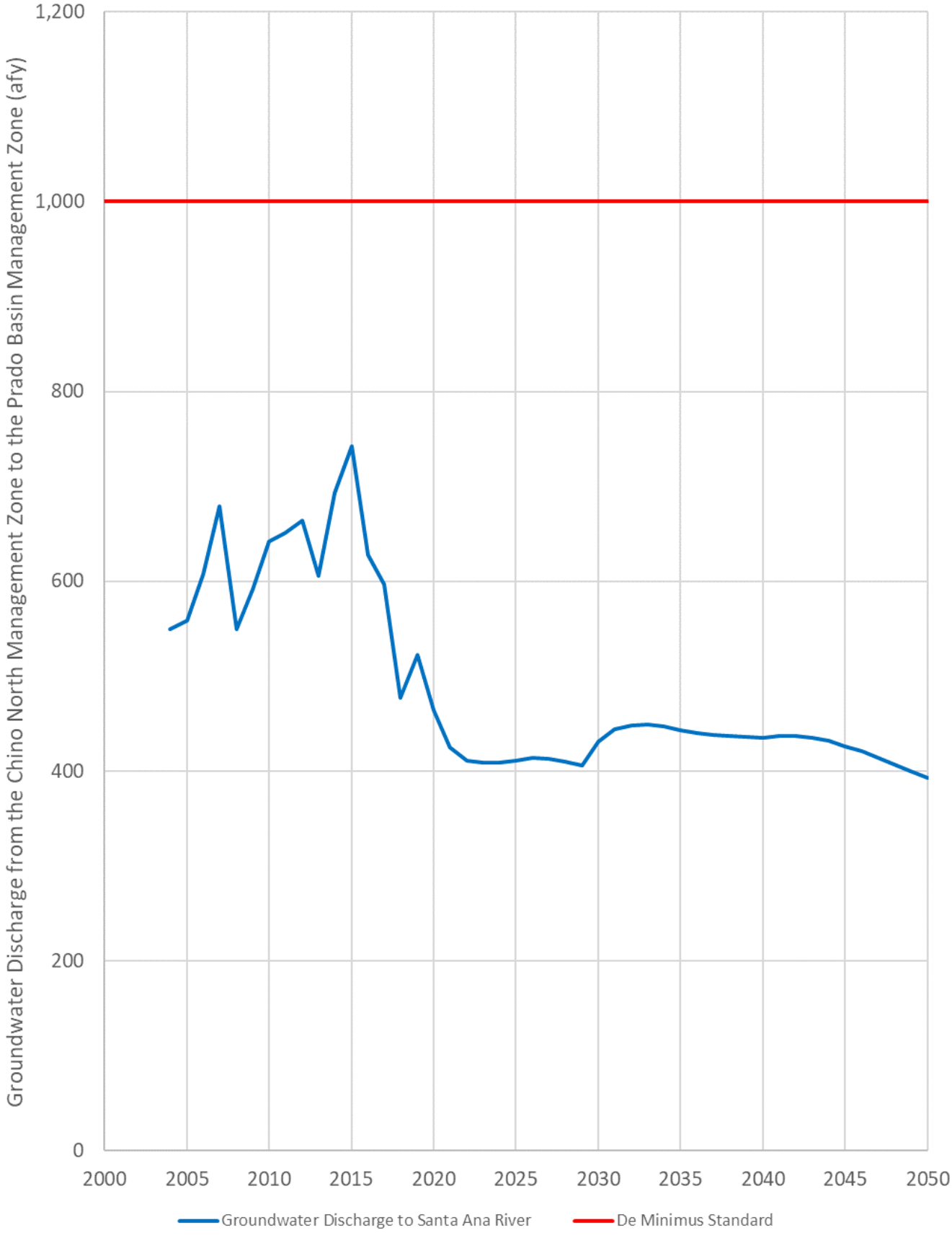

Section 8 – References

ASCE. 1993. *Criteria for evaluation of watershed models. J. Irrigation Drainage Eng. 119(3): 429-442.* 1993.

Banta, Edward R. 2000. *MODFLOW-2000, The U.S. Geological Survey Modular Ground-Water Model—Documentation of Packages for Simulating Evapotranspiration with a Segmented Function (ETS1) and Drains with Return Flow (DRT1).* Denver, CO : U.S. Geological Survey, 2000.

Barnes, Harry H. Jr. 1967. *Roughness Characteristics of Natural Channels. U.S. Geological Survey Water-Supply Paper 1849.* s.l. : USGS, 1967.

Bicknell, B. R., et al. 2005. *Hydrological Simulation Program - Fortran (HSPF). User's Manual for Release 12.2.* s.l. : U.S. EPA National Exposure Research Laboratory Athens, GA, in cooperation with U.S. Geological Survey, Water Resources Division, Reston,VA., 2005.

Black & Veatch. 2001. *Phase 2 (Chino Basin) Recharge Master Plan.* 2001.

Bouwer, H. 1978. *Groundwater Hydrology.* New York : McGraw-Hill Book, 1978. p. 480.

Carrera, Jesus and Neuman, Shlomo P. 1986a. Estimation of Aquifer Parameters Under Transient and Steady State Conditions: 1. Maximum Likelihood Method Incorporating Prior Information. *Water Resources Research.* 1986a, Vol. 22, 2, pp. 199-210.

—. 1986b. Estimation of Aquifer Parameters Under Transient and Steady State Conditions: 2. Uniqueness, Stability, and Solution Algorithms. *Water Resources Research.* 1986b, Vol. 22, 2, pp. 211-227.

—. 1986c. Estimation of Aquifer Parameters Under Transient and Steady State Conditions: 3. Application to Synthetic and Field Data. *Water Resources Research.* 1986c, Vol. 22, 2, pp. 228-242.

Carsel, R. F. and Parrish, R. S. 1988. Developing joint probability distributions of soil water retention characteristics. *Water Resources Research.* 1988, Vol. 24, 5, pp. 755-769.

CBWM. 2007. *Chino Basin Optimum Basin Management Program - Management Zone 1 Subsidence Management Plan.* s.l. : Chino Basin Watermaster, 2007.

Doherty, John. 2015. *Calibration and uncertainty analysis for complex environmental models.* Brisbane, Australia : Watermark Numerical Computing, 2015. p. 227. ISBN-13: 978-0-9943786-0-6.

—. 2019. *Model-Independent Parameter Estimation User Manual: 7th Edition published in 2018. Latest addtions: May 2019.* Brisbane, Australia : Watermark Numerical Computing, 2019.

—. 2019b. *Model-Independent Parameter Estimation User Manual: 7th Edition published in 2018. Latest addtions: May 2019.* Brisbane, Australia : Watermark Numerical Computing, 2019b.

—. 2019. *Model-Independent Parameter Estimation Version 17.* s.l. : Watermark Numerical Computing, 2019.

Domenico, Patrick A. and Schwartz, Franklin W. 1997. *Physical and Chemical Hydrogeology.* 2nd. s.l. : John Wiley & Sons, Inc., 1997. ISBN-13: 978-0471597629.

Durham, D. L. and Yerkes, R. F. 1964. *Geology and oil resources of the eastern Puente Hills area, southern California.* s.l. : U.S. Geological Survey, 1964.

Dutcher, L. C. and Moyle, Jr., W. R. 1963. *Preliminary Appraisal of the Test-Well Drilling Program in the Bloomington-Colton Area, San Bernardino County, California: USGS Closed-File Report, 15 p.* 1963.

Dutcher, L. C. and Garrett, A. A. 1963. *Geologic and hydrologic features of San Bernardino area, California, with special reference to underflow across the San Jacinto fault.* s.l. : U.S. Geological Survey Water-Supply Paper 1419., 1963. p. 114.

DWR. 2016. *Best Management Practices for the Sustaibable Management of Groundwater - Water Budget BMP.* s.l. : Department of Water Resources, 2016.

—. 2018. *Guidance for Climate Change Data Use During Groundwater Sustainability Plan Development. California Department of Water Resources, Sustainable Groundwater Management Program.* 2018.

—. 1970. *Meeting Water Demands in the Chino-Riverside Area, Appendix A: California Department of Water Resources Water Supply. Bulletin No. 104-3.* 1970. p. 108.

—. 2018. *Resource Guide - DWR-provided Climate Change Data and Guidance for Use During Groundwater Sustainability Plan Development. Department of Water Resources.* 2018.

Eckis, R. and Gross, P. L. K. 1932. *The Geology and Groundwater in Pomona and San Dimas Basins, Southern California. South Coastal Basin Investigation. 184 p.* 1932.

Eckis, R. 1934. *Geology and Ground Water Storage Capacity of Valley Fill, South Coastal Basin Investigation.* s.l. : California Department of Public Works, Division of Water Resources Bulletin No. 45, 1934. p. 273.

Fetter, C. W. 2001. *Applied Hydrogeology. 4th Edition.* s.l. : Prentice Hall, 2001.

Fife, D. L., et al. 1976. *Geologic hazards in southwestern San Bernardino County, California.* s.l. : California Division of Mines and Geology Special Report 113, 1976. p. 40.

Freeze, Allan R. and Cherry, John A. 1979. *Groundwater.* Upper Saddle River, NJ : Prentice-Hall, Inc., 1979. ISBN 978-0133653120.

Geomatrix. 1994. *Final report ground fissuring study, California Department of Corrections, California Institution for Men, Chino, California. Project No. 2360. 1994.* s.l. : Geomatrix Consultants, Inc., 1994.

GEOSCIENCE. 2002. *2002, Preliminary geohydrologic analysis of subsidence in the western portion of the Chino Basin. Prepared for the City of Chino Hills. August 2002.* s.l. : GEOSCIENCE, Support Services, Inc., 2002.

Geoscience. 2019. *Upper Santa Ana River Integrated Model TM No. 3: Model Calibration.* s.l. : Geoscience Support Services, Inc., 2019.

Gosling, A. W. 1967. *Patterns of subsurface flow in the Bloomington-Colton area, upper Santa Ana Valley, California.* s.l. : U.S. Geological Survey Hydrologic Investigation Atlas, HA-268, 1967.

Gosling, A. W. 1967. *Patterns of subsurface flow in the Bloomington-Colton area, upper Santa Ana Valley, California: U.S. Geological Survey Hydrologic Investigation Atlas, HA-268.* 1967.

Hill, Mary C. and Tiedeman, Claire R. 2005. *Effective Groundwater Model Calibration: With Analysis of Data, Sensitivities, Predictions, and Uncertainty.* s.l. : Wiley, 2005. 9780471776369.

Hill, Mary C., et al. 2000. *MODFLOW-2000, the U.S. Geological Survey modular ground-water model; user guide to the observation, sensitivity, and parameter-estimation processes and three post-processing programs.* Denver, CO. : s.n., 2000.

Hsieh, Paul A. and Freckleton, John R. 1993. *Documentation of a computer program to simulate horizontal-flow barriers using the U.S. Geological Survey's modular three dimensional finite-difference ground-water flow model.* Sacramento, California : U. S. Geological Survey, 1993.

Johnson, A. I. 1967. *Specific yield--compilation of specific yields for various materials.* s.l. : U.S. Geological Survey Water Supply Paper 1662-D, 1967. p. 74.

Kleinfelder. 1996. *Chino Basin subsidence and fissuring Study, Chino, California. Project No. 58-5264-02. March 1996.* . s.l. : Kleinfelder, Inc., 1996.

—. 1993. *Geotechnical investigation, regional subsidence and related ground fissuring, City of Chino, California. Project No. 58-3101-01. 1993.* s.l. : Kleinfelder, Inc.,, 1993.

Kuniansky, E. L. and Hamrick, S. T. 1998. *Hydrogeology and simulation of ground-water flow in the Paluxy aquifer in the vicinity of Landfills 1 and 3, US Air Force Plant 4, Fort Worth, Texas.* s.l. : U.S. Geological Survey Water-Resources Investigations Report 98, 1998.

LACFCD. 1937. *1936-37 Report on San Antonio Spreading Grounds investigation and ground water fluctuations and movements in the San Antonio Basins. October 1937.* 1937.

Larsen, E. S., et al. 1958. *Lead-alpha ages of the Mesozoic batholiths of western North America.* 1958. pp. 35-62.

Leake, Stanley. A. and Lilly, Michael R. 1997. *Documentation of a Computer Program (FHB1) for Assignment of Transient Specified-Flow and Specified-Head Boundaries in Applications of the Modular Finite-Difference Ground-Water Flow Model (MODFLOW).* Tucson, Arizona : U. S. Geological Survey, 1997.

Legates, D. R. and McCabe , G. J. . 1999. Evaluating the use of "goodness-of-fit" measures in hydrologic and hydroclimatic model validation. *Water Resources Res.* 1999, Vol. 35, 1, pp. 233-241.

Marquardt, Donald W. 1963. An Algorithm for Least-Squares Estimation of Nonlinear Parameters. *Journal of the Society for Industrial and Applied Mathematics.* 1963, Vol. 11, 2, pp. 431-441.

McDonald, Michael G. and Harbaugh, Arlen W. 1988. *MODFLOW, A modular three-dimensional finite difference ground-water flow model.* Reston, Virginia : U. S. Geological Survey, 1988.

Mehl, Steffen W. and Mary, Hill C. 2001. *MODFLOW-2000, the U. S. Geological Survey modular ground-water model; user guide to the Link-AMG (LMG) package for solving matrix equations using an algebraic multigrid solver.* Denver, Colorado : U. S. Geological Survey, 2001.

Mendenhall, W. C. 1905. *Development of underground waters in the western coastal-plain region of southern California.* s.l. : U.S. Geological Survey Water-Supply Paper 139, 1905. p. 105.

—. 1908. *Ground water and irrigation enterprises in the foothill belt, southern California.* s.l. : U.S. Geological Survey Water-Supply Paper 219, 1908. p. 180.

Moriasi, D. N., et al. 2007. Model Evaluation Guidelines for Systematic Quantification of Accuracy in Watershed Simulations. *American Society of Agricultural and Biological Engineers.* 2007, Vol. 50, 3, pp. 885-900.

Nash, J. E. and Sutcliffe, J. V. . 1970. River flow forecasting through conceptual models: Part 1. A discussion of principles. *J. Hydrology.* 1970, Vol. 10, 3, pp. 282-290.

Neuman, S. P. 1973. Saturated-unsaturated seepage by finite elements. 1973, pp. 2233-2251.

Niswonger, Richard G., Panday, Sorab and Ibaraki , Motomu. 2011. *MODFLOW-NWT, A Newton formulation for MODFLOW-2005: U.S. Geological Survey Techniques and Methods 6-A37, 44 p.* Reston, Virginia : U.S. Geological Survey, 2011.

Niswonger, Richard G. and Prudic, David E. 2006. *Documentation of the Streamflow-Routing (SFR2) Package to Include Unsaturated Flow Beneath Streams—A Modification to SFR1.* s.l. : U.S. Geological Survey, 2006.

Peltzer, G. 1999a. *Subsidence monitoring project: City of Chino. March 1999.* 1999a.

—. 1999b. *Subsidence monitoring project: City of Chino. May 1999.* 1999b.

Poeter, Eileen P., et al. 2014. *UCODE_2014, with new capabilities to define parameters unique to predictions, calculate weights using simulated values, estimate parameters with SVD, evaluate uncertainty with MCMC, and More. Report Number: GWMI 2014-02.* s.l. : Integrated Groundwater Modeling Center, 2014.

Prudic, D. E. 1991. *Estimates of hydraulic conductivity from aquifer-test analyses and specific-capacity data, Gulf Coast Regional Aquifer Systems, south-central United States,.* s.l. : U.S. Geological Survey Water-Resources Investigation Report 90-4121, 1991. p. 38.

Rawls, W. J., Brakensiek, D. L. and Saxton, K. E. 1982. Estimation of soil water properties. *Transactions of American Society of Agricultural Engineers.* 1982, Vol. 25, pp. 1316-1320.

Reese, R. S. and Cunningham, K. J. 2000. *Hydrogeology of the gray limestone aquifer in southern Florida.* s.l. : U.S. Geological Survey Water-Resources Investigations Report 99-4213, 2000. p. 244.

Robson, S. G. 1993. *Techniques for Estimating Specific Yield and Specific Retention from Grain-Size Data and Geophysical Logs from Clastic Bedrock Aquifers. Water-Resources Investigations Report 93-4198.* s.l. : USGS, 1993.

Schaap, M. G., Leij, F. J. and van Genuchten, M. Th. 1998. Neural network analyses for hierarchical prediction of soil hydraulic properties. *Soil Science Society of America Journal.* 1998, Vol. 62, 4, pp. 847-855.

Servat, Eric and Dezetter, Alain. 1991. Selection of calibration objective fonctions in the context of rainfall-ronoff modelling in a Sudanese savannah area. *Hydrological Sciences Journal.* 1991, Vol. 36, 4, pp. 307-330.

Sevat, E. and Dezetter, A. 1991. Selection of calibration objective functions in the context of rainfall-runoff modeling in a Sudanese savannah area. *Hydrological Sci. J.* 1991, Vol. 36, 4, pp. 307-330.

Simunek, J., Sejna, M. and van Genuchten, M. Th. . 1999. *The HYDRUS-2D software package for simulating two-dimensional movement of water, heat, and multiple solutes in variably saturated media.* Version 2.0 IGWMC - TPS - 53. Golden : International Groundwater Modeling Center, Colorado School of Mines, 1999. p. 251.

Slade. 1997. *Hydrological assessment of portions of the Chino, Claremont Heights and Cucamonga Groundwater Basins, San Bernardino County, California. Prepared for the City of Upland Public Works Department. September 1997. Richard C. Slade and Associates.* s.l. : Richard C. Slade and Associates, 1997.

The theory of Ground-water motion, EOS 21(2). **Hubbert, King M. 1940.** s.l. : American Geogeophysical Union, 1940.

Todd, David K. 1959. *Groundwater hydrology.* 1959.

US Army Corps of Engineers. 2015. *2015 LiDAR of Santa Ana River, holes filled with IFSAR data. Data requested on June 7, 2018; retrieved on July 2, 2018.* s.l. : US Army Corps of Engineers, Los Angeles District, Hydrology and Hydraulics Branch, 2015.

WEI. 2007. *2007 CBWM Groundwater Model Documentation and Evaluation of the Peace II Project Description.* s.l. : Wildermuth Environmental, Inc., 2007.

—. 2008c. *2008 Santa Ana River Wasteload Allocation Model Report. Prepared for the Basin Monitoring Program Task Force.* s.l. : Wildermuth Environmental, Inc., 2008c.

—. 2009. *2009 Production Optimization and Evaluation of the Peace II Project Description. Prepared for the Chino Basin Watermaster.* s.l. : Wildermuth Environmental, Inc., 2009.

—. 2010. *2010 Recharge Master Plan Update. Prepared for the Chino Basin Watermaster and Inland Empire Utilities Agency.* s.l. : Wildermuth Environmental, Inc., 2010.

—. 2012. *2012 State of the Cucamonga Basin. Prepared for City of Upland, Cucamonga Valley Water District, and San Antonio Water Company.* . s.l. : Wildermuth Environemental, Inc., 2012.

—. 2013. *2013 Amendment to 2010 Recharge Master Plan Update. Prepared for the Chino Basin Watermaster and Inland Empire Utilities Agency.* s.l. : Wildermuth Environmental, Inc., 2013.

—. 2015. *2013 Chino Basin Groundwater Model Update and Recalculation of the Safe Yield Pursuant to the Peace Agreement.* s.l. : Wildermuth Environmental, Inc., 2015.

—. 2019. *2018/19 Final Annual Report of the Ground Level Monitoring Committe. Prepared for Chino Basin Watermaster. November 2019.* s.l. : Wildermuth Environmental, Inc. , 2019.

—. 2008. *Analysis of Material Physical Injury from the Proposed Expansion of the Dry-Year Yield Program. Prepared for the Chino Basin Watermaster.* s.l. : Wildermuth Environmental, Inc., 2008.

—. 2003. *Chino Basin Dry-Year Yield Program Modeling Report. Prepared for the Chino Basin Watermaster and Inland Empire Utilities Agency.* s.l. : Wildermuth Environmental, Inc., 2003.

—. 2014. *Draft Cucamonga Basin Groundwater Model Report. Prepared for the Cucamonga Valley Water District.* s.l. : Wildermuth Environmental, Inc., 2014.

—. 2008b. *Draft Title 22 Engineering Report for Potential GRRPs in the Beaumont Basin. Prepared for the San Timoteo Watershed Management Agency.* s.l. : Wildermuth Environmental, Inc., 2008b.

—. 2003a. *Management Zone 1 (MZ-1) Interim Monitoring Program. Prepared for the Chino Basin Watermaster. January 2003. Wildermuth Environmental, Inc.* 2003a.

—. 2006. *Management Zone 1 Interim Monitoring Program: MZ-1 Summary Report. Prepared for the MZ-1 Technical Committee. February 2006.* s.l. : Wildermuth Environmental, Inc., 2006.

—. 1998. *Phase 1 Recharge Master Plan (Chino Basin). Prepared for the Chino Basin Watermaster and the Chino Basin Water Conservation District.* s.l. : Wildermuth Environmental, Inc., 1998.

—. 2010a. *Recycled Water Planning Investigation Report. Prepare for the San Bernardino Municipal Water Department.* s.l. : Wildermuth Environmental, Inc., 2010a.

—. 2019. *Storage Framework Investigation. Final Report October 2018. Revised in January 2019.* s.l. : Wildermuth Environmental, Inc., 2019.

—. 2018. *Storage Fremework Investigation. Final Report October 2018.* s.l. : Wildermuth Environmental, Inc., 2018.

—. 2017. *Strategic plan for the Six Basins. Prepared for Six Basins Watermaster. November 2017.* s.l. : Wildermuth Environmental, Inc., 2017.

—. 2002. *TIN/TDS Study – Phase 2B, Wasteload Allocation Investigation, Final Technical Memorandum. Prepared for the TIN/TDS Task Force.* s.l. : Wildermuth Environmental, Inc., 2002.

—. 2006a. *Title 22 Engineering Report, Phase II Recycled Water Groundwater Recharge Project. Prepared in association with DDB Engineering for the Inland Empire Utilities Agency.* s.l. : Wildermuth Environmental, Inc., 2006a.

—. 2020. *Unpublished modeling work for the recalibrated Six Basin Model; to be published in 2020. Prepared for the Six Basins Watermaster.* s.l. : Wildermuth Environmental, Inc., 2020.

Wildermuth, Mark J. 1995. *Annual Recharge Estimates at the Chino Basin, Water Conservation District Spreading Basins.* s.l. : Water Resource Engineers, 1995.

Woolfenden, L. R. and Kadhim, D. 1997. *Geohydrology and Water Chemistry in the Rialto-Colton Basin, San Bernardino County, California.* s.l. : : USGS Water-Resources Investigations Report 97-4012, 1997. p. 101.

Yeh, William W-G. 1986. Review of parameter identification procedures in groundwater hydrology: The inverse problem. *Water Resources Research.* 1986, Vol. 22, 2, pp. 95-108.

Appendix A

Hydrostratigraphic Cross Sections

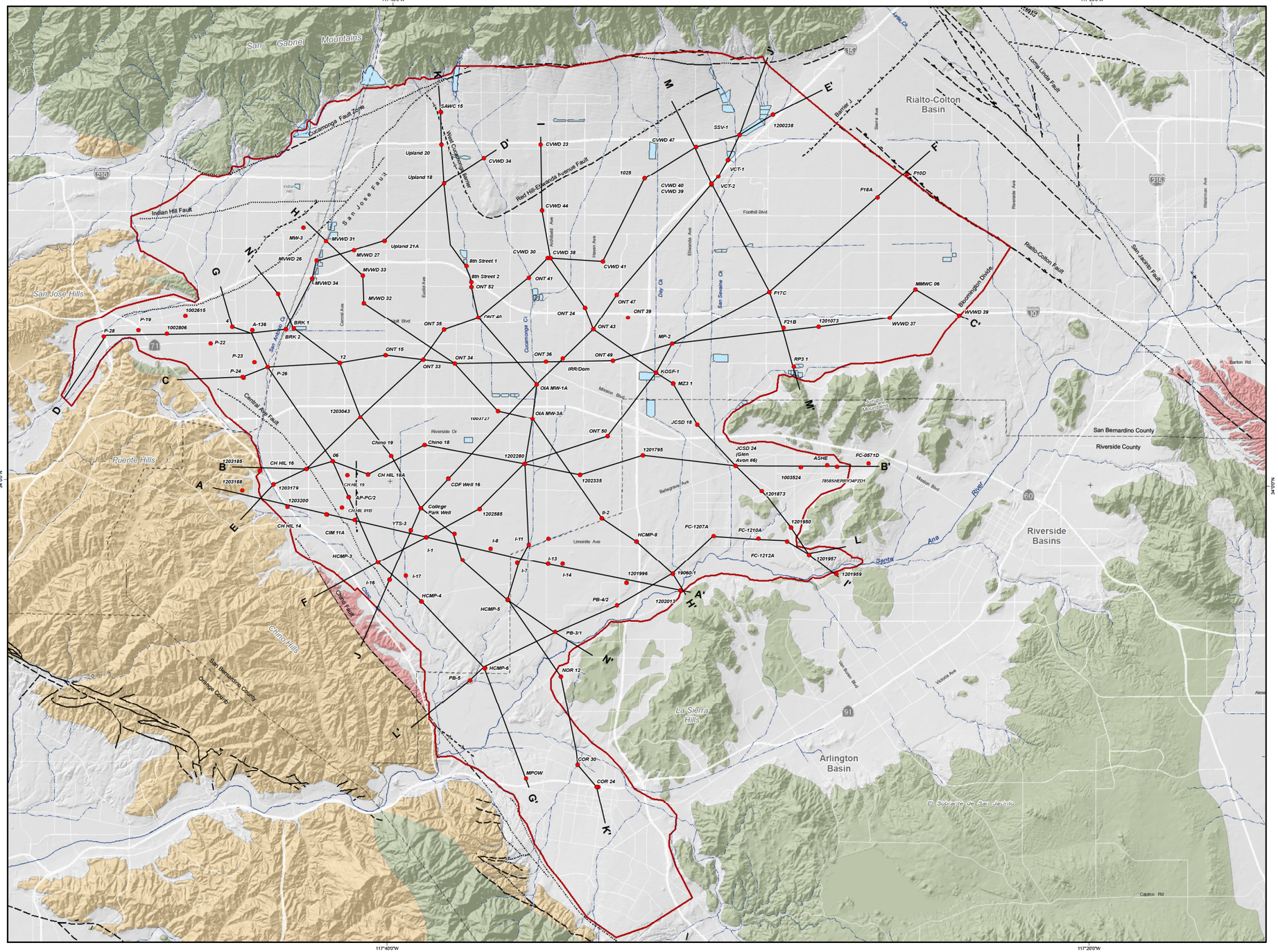

Hydrostratigraphic Cross-Section Profile Line

Borehole Used in Hydrostratigraphic Cross-Section

Chino Valley Basins Groundwater Flow Model Boundary

Streams & Flood Control Channels

Flood Control & Conservation Basins

Geology

Water-Bearing Sediments

Quaternary Alluvium

Consolidated Bedrock

Plio-Pleistocene Sedimentary Rocks

Cretaceous to Miocene Sedimentary Rocks

Pre-Tertiary Igneous and Metamorphic Rocks

Fault (solid where accurately located; dashed where approximately located or inferred; dotted where concealed)

Produced by:

WEI
Wildermuth Environmental, Inc.

Date: 1/23/2020

Document Name: Appendix_A-1_20200123_XS

0 1 2 3 4 5 Miles

0 2 4 6 8 KM

Prepared for:

2020 Safe Yield Recalculation

Chino Basin Watermaster
Partners in Basin Management

Map View of the Hydrostratigraphic Cross-Sections

Appendix A-1

A (WEST)

A' (SOUTHEAST)

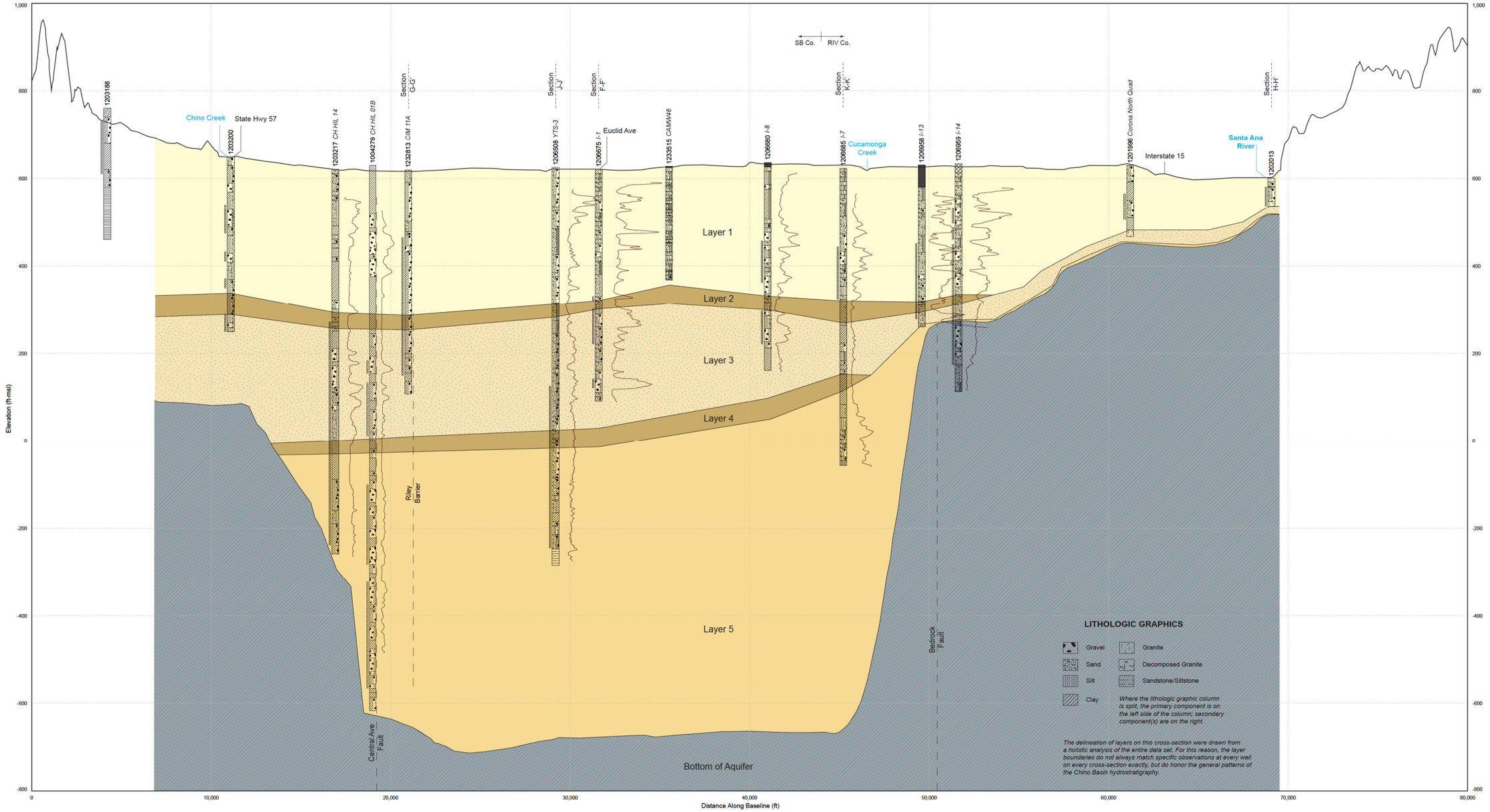

ft
200
100
50
0
VERTICAL SCALE
2,000
4,000
6,000 ft
HORIZONTAL SCALE
VERTICAL EXAGGERATION 24:1

BOREHOLE LEGEND

1xxxxxx = WEI's HydroDaVE Database Well ID

Well Screen Interval

Resistivity Electrical Log

HYDROSTRATIGRAPHIC LEGEND

- Layer 1 - Shallow aquifer system
- Layer 2 - Upper confining unit in the deep aquifer system
- Layer 3 - Upper portion of the deep aquifer system
- Layer 4 - Lower confining unit in the deep aquifer system
- Layer 5 - Lower portion of the deep aquifer system
- Effective base of the freshwater aquifer system

Hydrostratigraphic Cross-section: A-A'

Appendix A-2

B (WEST)

B' (EAST)

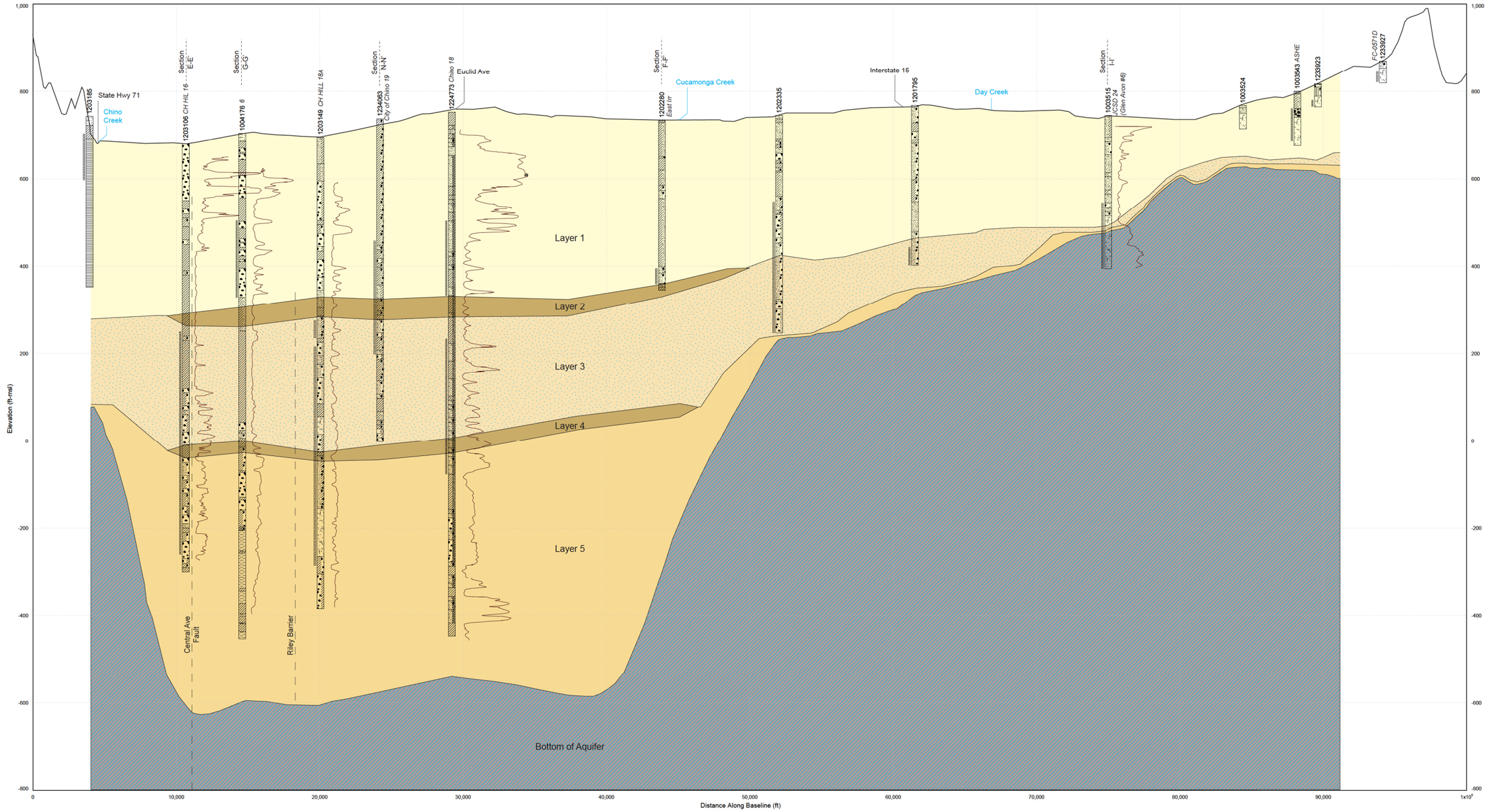

Report: FIGS - ELOGSPERF5 - D_LIL File: 2019_CBWM_GWMODEL_UPDATE_V1.GPJ 4/29/2019

ft
200
100
50
0
VERTICAL SCALE
2,000 4,000 6,000 ft
HORIZONTAL SCALE
VERTICAL EXAGGERATION 31:1

BOREHOLE LEGEND

1xxxxxx = WEI's HydroDaVE Database Well ID

Well Screen Interval

Resistivity Electrical Log

HYDROSTRATIGRAPHIC LEGEND

- Layer 1 - Shallow aquifer system
- Layer 2 - Upper confining unit in the deep aquifer system
- Layer 3 - Upper portion of the deep aquifer system
- Layer 4 - Lower confining unit in the deep aquifer system
- Layer 5 - Lower portion of the deep aquifer system
- Effective base of the freshwater aquifer system

Hydrostratigraphic Cross-section: B-B'

Appendix A-3

C (West)

C' (East)

Elevation (ft-msl)

Distance Along Baseline (ft)

State Hwy 71

Section G-G'

Section N-N'

Section E-E'

Section H-H'

Section M-M'

1201255 P-24B

1002703 P-26

San Antonio Creek

1002739 City of Chino 12

1002636 ONT 15

1002360 ONT 33

Euclid Ave

1002367 ONT 34

West Cucamonga Creek

Cucamonga Creek

1002372 ONT 36

1207952 ONT 49

Interstate 15

Day Creek

Etiwanda Creek

San Sevaine Creek

1232847 P-21B

1201073

1002109 WWD 37

Interstate 10

1221751 MWMC 06

WWD 39

1006993

Interstate 10

Layer 1

Layer 2

Layer 3

Layer 4

Layer 5

Bottom of Aquifer

LITHOLOGIC GRAPHICS

Gravel

Sand

Silt

Clay

Granite

Decomposed Granite

Sandstone/Siltstone

Where the lithologic graphic column is split, the primary component is on the left side of the column; secondary component(s) are on the right.

The delineation of layers on this cross-section were drawn from a holistic analysis of the entire data set. For this reason, the layer boundaries do not always match specific observations at every well on every cross-section exactly, but do honor the general patterns of the Chino Basin hydrostratigraphy.

BOREHOLE LEGEND

1xxxxxx = WEI's HydroDaVE Database Well ID

Well Screen Interval

Resistivity Electrical Log

HYDROSTRATIGRAPHIC LEGEND

- Layer 1 - Shallow aquifer system
- Layer 2 - Upper confining unit in the deep aquifer system
- Layer 3 - Upper portion of the deep aquifer system
- Layer 4 - Lower confining unit in the deep aquifer system
- Layer 5 - Lower portion of the deep aquifer system
- Effective base of the freshwater aquifer system

VERITCAL SCALE

HORIZONTAL SCALE

VERITCAL EXAGGERATION 33:1

Hydrostratigraphic Cross-section: C-C'

Appendix A-3

D (WEST) **D' (NORTHEAST)**

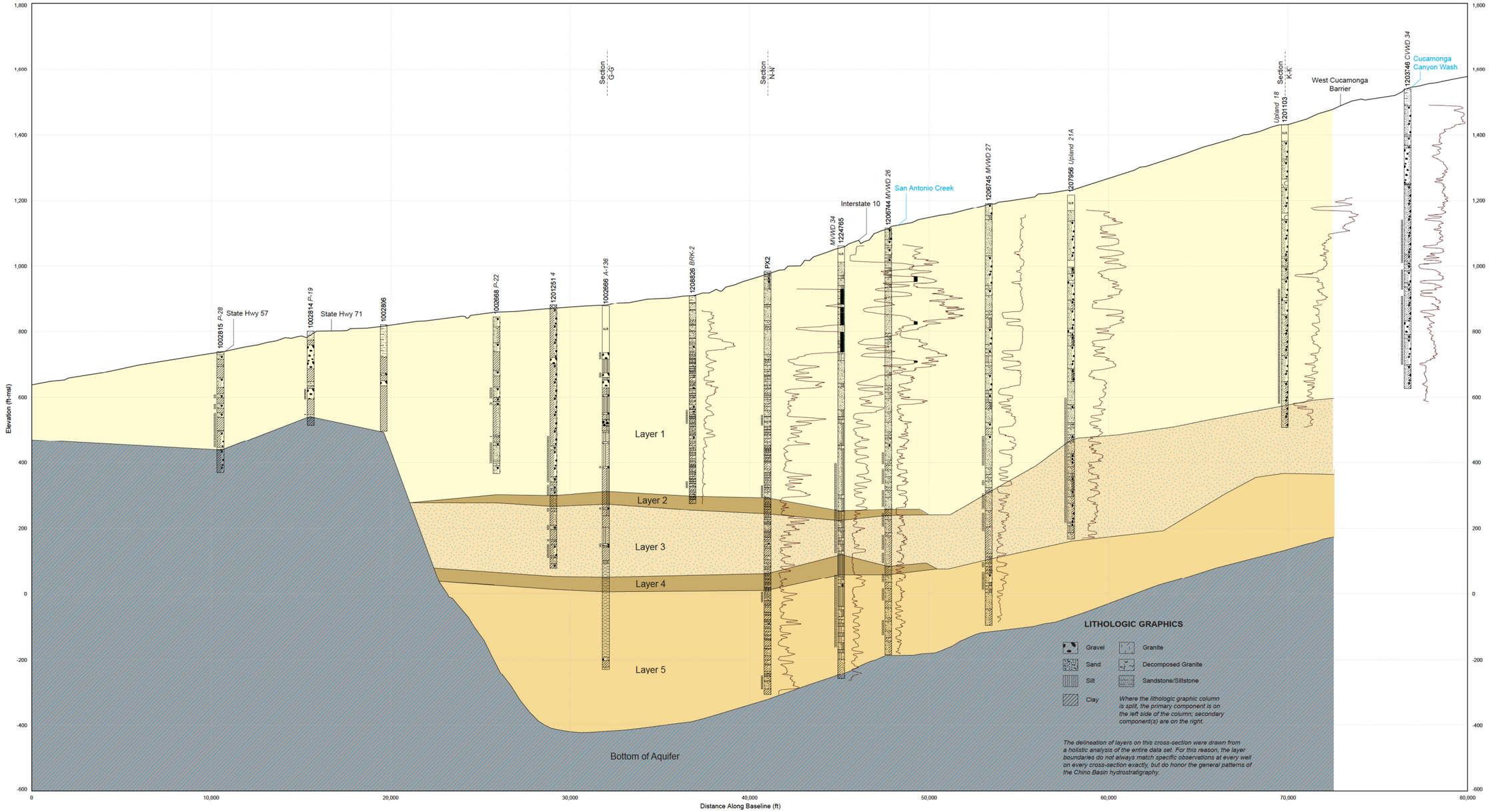

Report: FIN24_ELOGSFIEBF9 - D_LL - File: 2019_CBWM_GWMODEL_UPDATE_V1.GPJ - 4/29/2019

BOREHOLE LEGEND

1xxxxxx = WEI's HydroDaVE Database Well ID

Well Screen Interval

Resistivity Electrical Log

HYDROSTRATIGRAPHIC LEGEND

- Layer 1 - Shallow aquifer system
- Layer 2 - Upper confining unit in the deep aquifer system
- Layer 3 - Upper portion of the deep aquifer system
- Layer 4 - Lower confining unit in the deep aquifer system
- Layer 5 - Lower portion of the deep aquifer system
- Effective base of the freshwater aquifer system

ft
200
100
50
0
VERTICAL SCALE
2,000 4,000 6,000 ft
HORIZONTAL SCALE
VERTICAL EXAGGERATION 18:1

Hydrostratigraphic Cross-section: D-D'

Appendix A-4

E (WEST) **E' (NORTHEAST)**

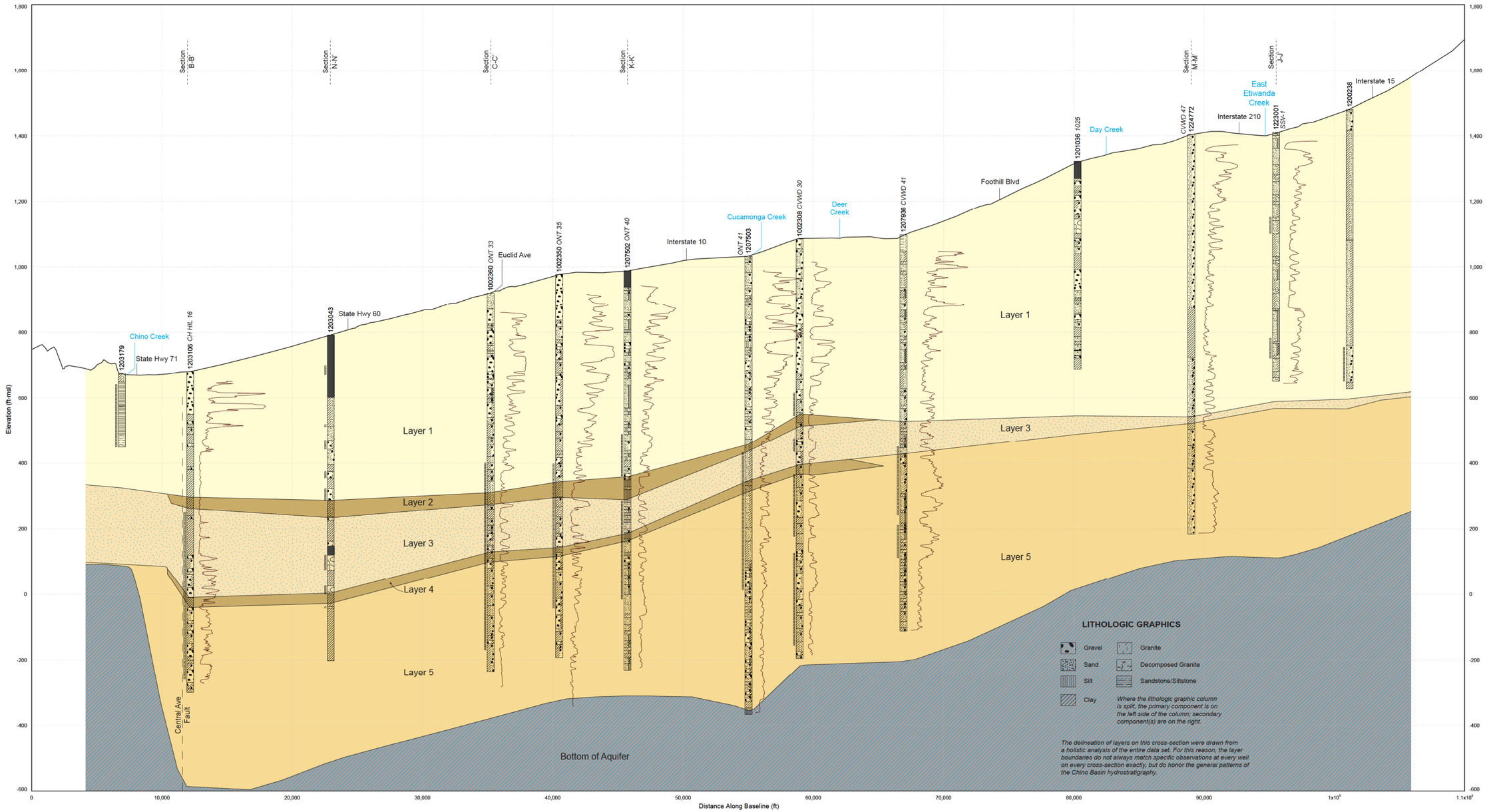

BOREHOLE LEGEND

1xxxxxx = WEI's HydroDaVE Database Well ID

Well Screen Interval

Resistivity Electrical Log

HYDROSTRATIGRAPHIC LEGEND

- Layer 1 - Shallow aquifer system
- Layer 2 - Upper confining unit in the deep aquifer system
- Layer 3 - Upper portion of the deep aquifer system
- Layer 4 - Lower confining unit in the deep aquifer system
- Layer 5 - Lower portion of the deep aquifer system
- Effective base of the freshwater aquifer system

VERTICAL SCALE: ft 200 100 50 0

HORIZONTAL SCALE: 2,000 4,000 6,000 ft

VERITCAL EXAGGERATION 25:1

Hydrostratigraphic Cross-section: E-E'

Appendix A-5

F (SOUTHWEST) **F' (NORTHEAST)**

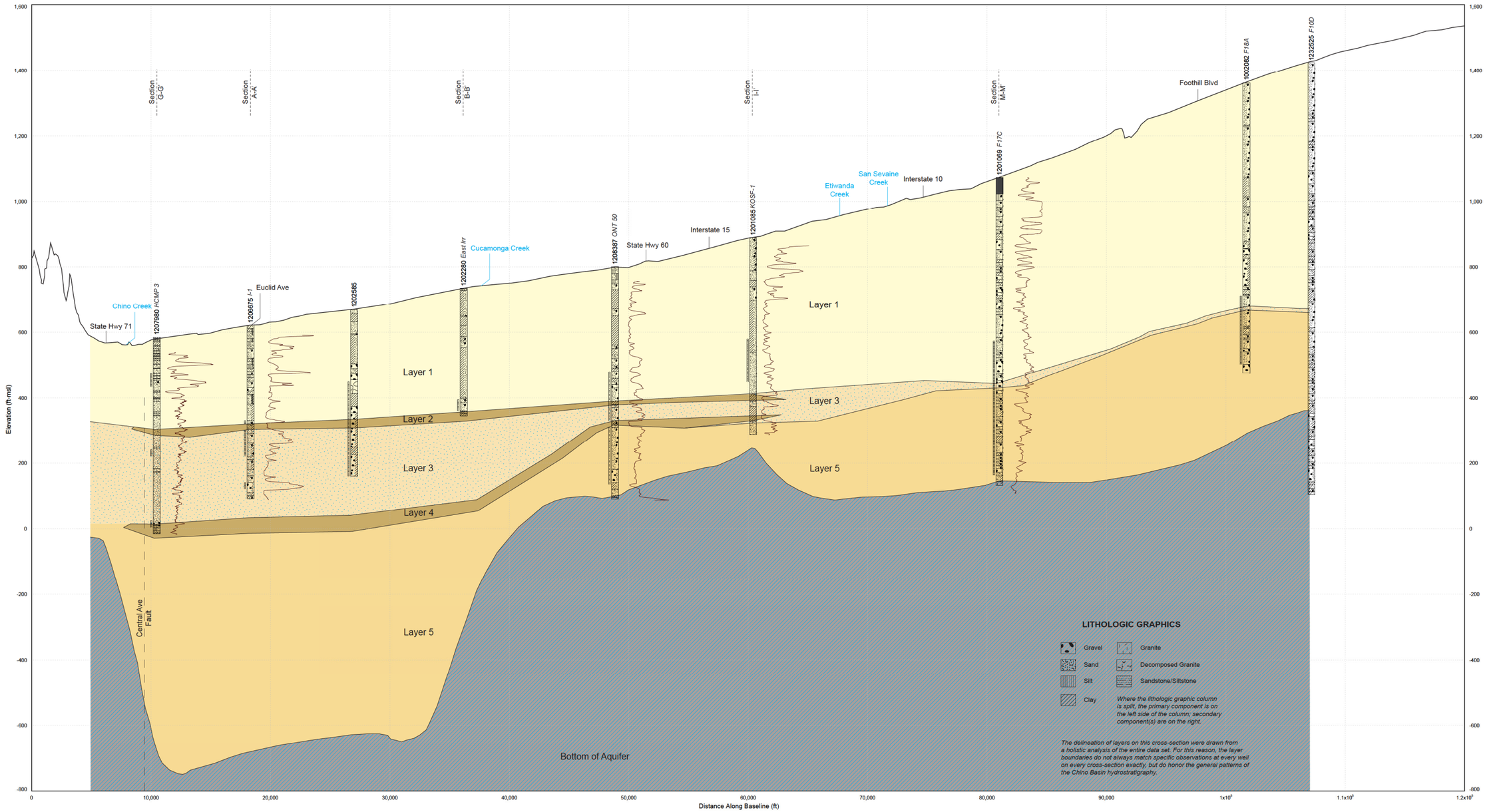

LITHOLOGIC GRAPHICS

Gravel	Granite
Sand	Decomposed Granite
Silt	Sandstone/Siltstone
Clay	

Where the lithologic graphic column is split, the primary component is on the left side of the column; secondary component(s) are on the right.

The delineation of layers on this cross-section were drawn from a holistic analysis of the entire data set. For this reason, the layer boundaries do not always match specific observations at every well on every cross-section exactly, but do honor the general patterns of the Chino Basin hydrostratigraphy.

BOREHOLE LEGEND

1xxxxxx = WEI's HydroDaVE Database Well ID

Well Screen Interval

Resistivity Electrical Log

HYDROSTRATIGRAPHIC LEGEND

- Layer 1 - Shallow aquifer system
- Layer 2 - Upper confining unit in the deep aquifer system
- Layer 3 - Upper portion of the deep aquifer system
- Layer 4 - Lower confining unit in the deep aquifer system
- Layer 5 - Lower portion of the deep aquifer system
- Effective base of the freshwater aquifer system

ft
200
100
50
0
VERTICAL SCALE
2,000 4,000 6,000 ft
HORIZONTAL SCALE
VERTICAL EXAGGERATION 25:1

Report: FENCE - ELOGSPERF5 - D_ILL File: 2019_CBWM_GWMODEL_UPDATE_V1.GPJ 4/26/2019

Hydrostratigraphic Cross-section: F-F'

Appendix A-6

G (NORTH) **G' (SOUTH)**

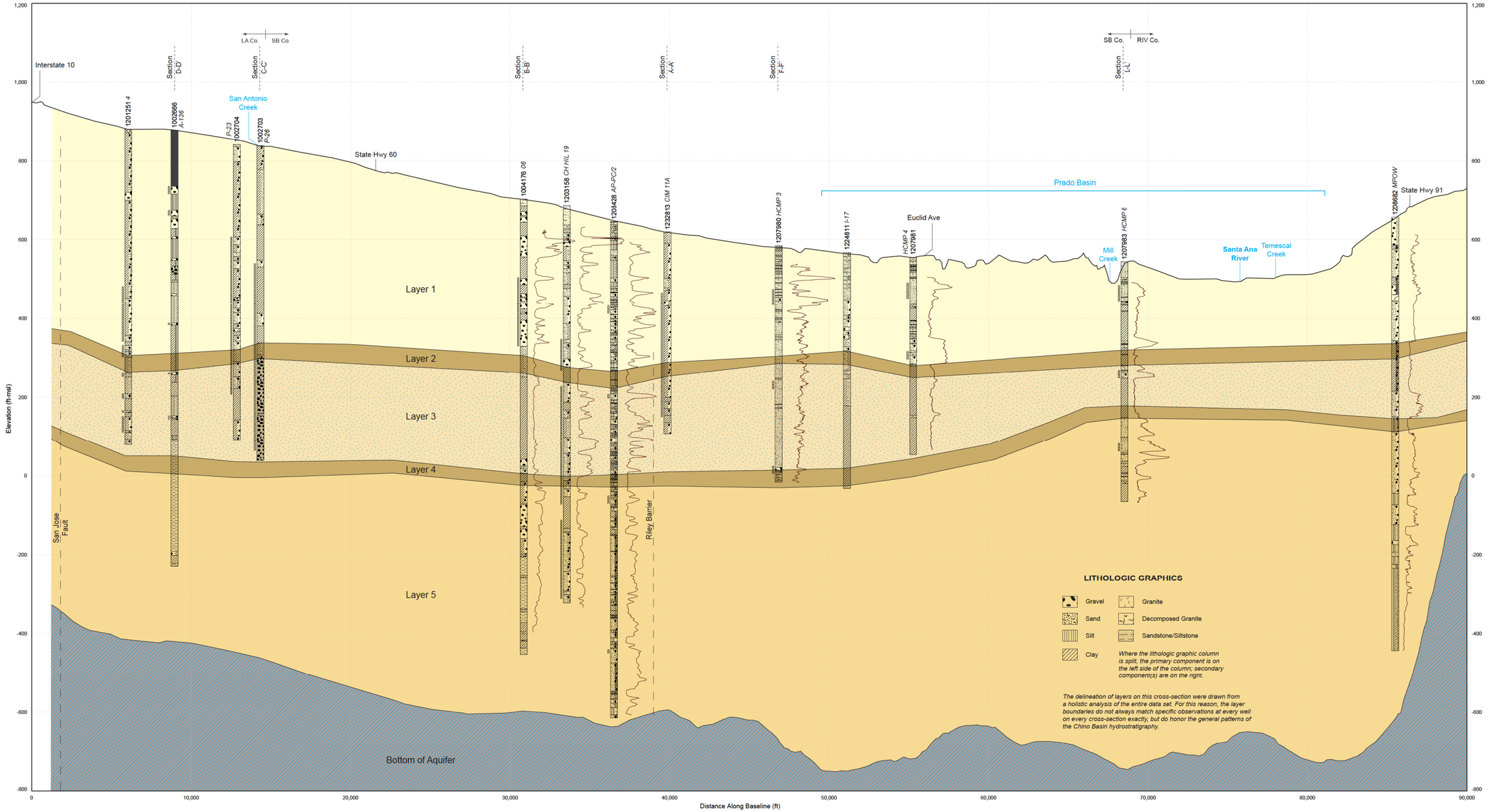

LITHOLOGIC GRAPHICS

Gravel	Granite
Sand	Decomposed Granite
Silt	Sandstone/Siltstone
Clay	

Where the lithologic graphic column is split, the primary component is on the left side of the column; secondary component(s) are on the right.

The delineation of layers on this cross-section were drawn from a holistic analysis of the entire data set. For this reason, the layer boundaries do not always match specific observations at every well on every cross-section exactly, but do honor the general patterns of the Chino Basin hydrostratigraphy.

BOREHOLE LEGEND

1xxxxxx = WEI's HydroDaVE Database Well ID

Well Screen Interval

Resistivity Electrical Log

HYDROSTRATIGRAPHIC LEGEND

- Layer 1 - Shallow aquifer system
- Layer 2 - Upper confining unit in the deep aquifer system
- Layer 3 - Upper portion of the deep aquifer system
- Layer 4 - Lower confining unit in the deep aquifer system
- Layer 5 - Lower portion of the deep aquifer system
- Effective base of the freshwater aquifer system

ft
200
100
50
0
VERTICAL SCALE
2,000 4,000 6,000 ft
HORIZONTAL SCALE
VERTICAL EXAGGERATION 25:1

Report FENCE - ELOSSHEIRFS - D_LLL File 2019_CBWM_GWMODEL_UPDATE_V1.GPJ 4/29/2019

Hydrostratigraphic Cross-section: G-G'

Appendix A-7

H (NORTHWEST) **H (SOUTHEAST)**

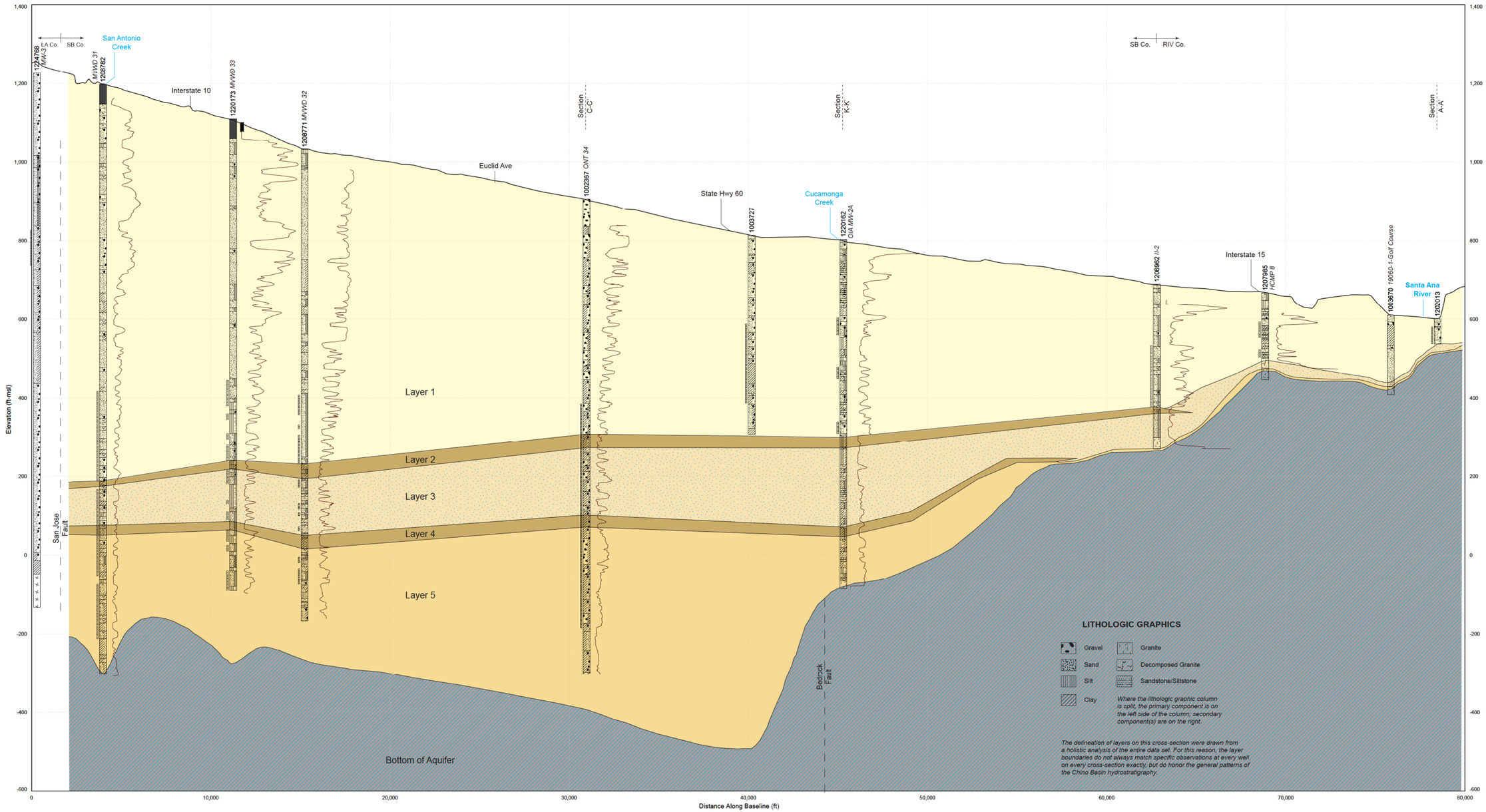

LITHOLOGIC GRAPHICS

- Gravel
- Sand
- Silt
- Clay
- Granite
- Decomposed Granite
- Sandstone/Siltstone

Where the lithologic graphic column is split, the primary component is on the left side of the column; secondary component(s) are on the right.

The delineation of layers on this cross-section were drawn from a holistic analysis of the entire data set. For this reason, the layer boundaries do not always match specific observations at every well on every cross-section exactly, but do honor the general patterns of the Chino Basin hydrostratigraphy.

BOREHOLE LEGEND

1xxxxxx = WEI's HydroDaVE Database Well ID

- Well Screen Interval
- Resistivity Electrical Log

HYDROSTRATIGRAPHIC LEGEND

- Layer 1 - Shallow aquifer system
- Layer 2 - Upper confining unit in the deep aquifer system
- Layer 3 - Upper portion of the deep aquifer system
- Layer 4 - Lower confining unit in the deep aquifer system
- Layer 5 - Lower portion of the deep aquifer system
- Effective base of the freshwater aquifer system

ft 200 100 50 0 VERTICAL SCALE

2,000 4,000 6,000 ft HORIZONTAL SCALE

VERTICAL EXAGGERATION 25:1

Revit FENCE - ELOSSPERS - D_ILL File 2019_CBWM_GWMODEL_UPDATE_V1.rvt 4/9/2019

Hydrostratigraphic Cross-section: H-H'

Appendix A-8

I (NORTH)

I' (SOUTHEAST)

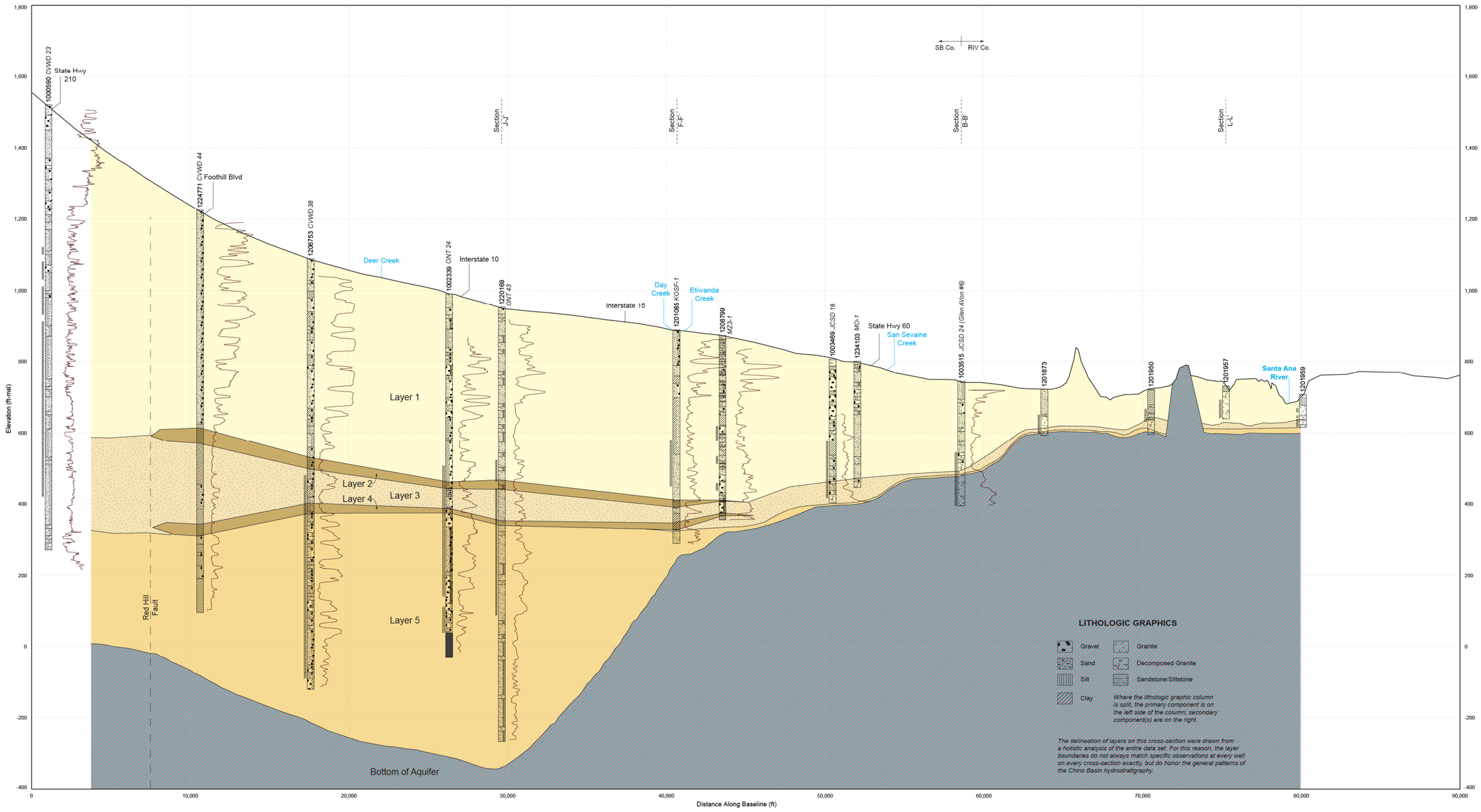

LITHOLOGIC GRAPHICS

- Gravel
- Sand
- Silt
- Clay
- Granite
- Decomposed Granite
- Sandstone/Siltstone

Where the lithologic graphic column is split, the primary component is on the left side of the column; secondary component(s) are on the right.

The delineation of layers on this cross-section were drawn from a holistic analysis of the entire data set. For this reason, the layer boundaries do not always match specific observations at every well on every cross-section exactly, but do honor the general patterns of the Chino Basin hydrostratigraphy.

BOREHOLE LEGEND

1xxxxxx = WEI's HydroDaVE Database Well ID

- Well Screen Interval
- Resistivity Electrical Log

HYDROSTRATIGRAPHIC LEGEND

- Layer 1 - Shallow aquifer system
- Layer 2 - Upper confining unit in the deep aquifer system
- Layer 3 - Upper portion of the deep aquifer system
- Layer 4 - Lower confining unit in the deep aquifer system
- Layer 5 - Lower portion of the deep aquifer system
- Effective base of the freshwater aquifer system

ft
200
100
50
0
VERTICAL SCALE
2,000
4,000
6,000 ft
HORIZONTAL SCALE
VERTICAL EXAGGERATION 22:1

Hydrostratigraphic Cross-section: I-I'

Appendix A-9

J (SOUTHWEST)

J' (NORTHEAST)

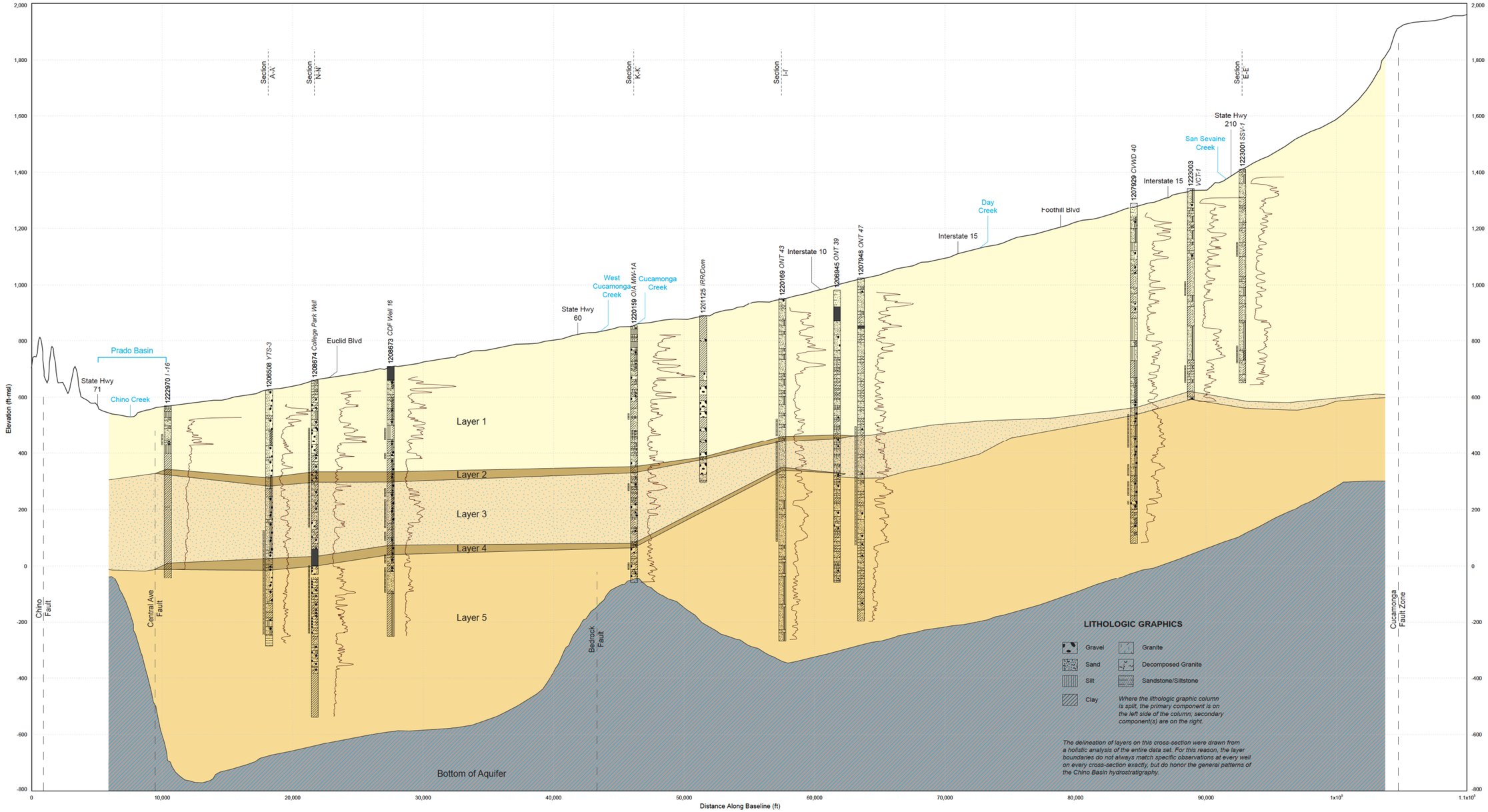

BOREHOLE LEGEND

1xxxxxx = WEI's HydroDaVE Database Well ID

Well Screen Interval

Resistivity Electrical Log

HYDROSTRATIGRAPHIC LEGEND

- Layer 1 - Shallow aquifer system
- Layer 2 - Upper confining unit in the deep aquifer system
- Layer 3 - Upper portion of the deep aquifer system
- Layer 4 - Lower confining unit in the deep aquifer system
- Layer 5 - Lower portion of the deep aquifer system
- Effective base of the freshwater aquifer system

ft
200
100
50
0
VERTICAL SCALE
2,000 4,000 6,000 ft
HORIZONTAL SCALE
VERTICAL EXAGGERATION 22:1

Report FENCE - ELOGSFENFS - D_ELL File 2019_CBWM_GWMODEL_UPDATE_V1.GPJ 4/29/2019

Hydrostratigraphic Cross-section: J-J'

Appendix A-10

K (NORTH) **K' (SOUTH)**

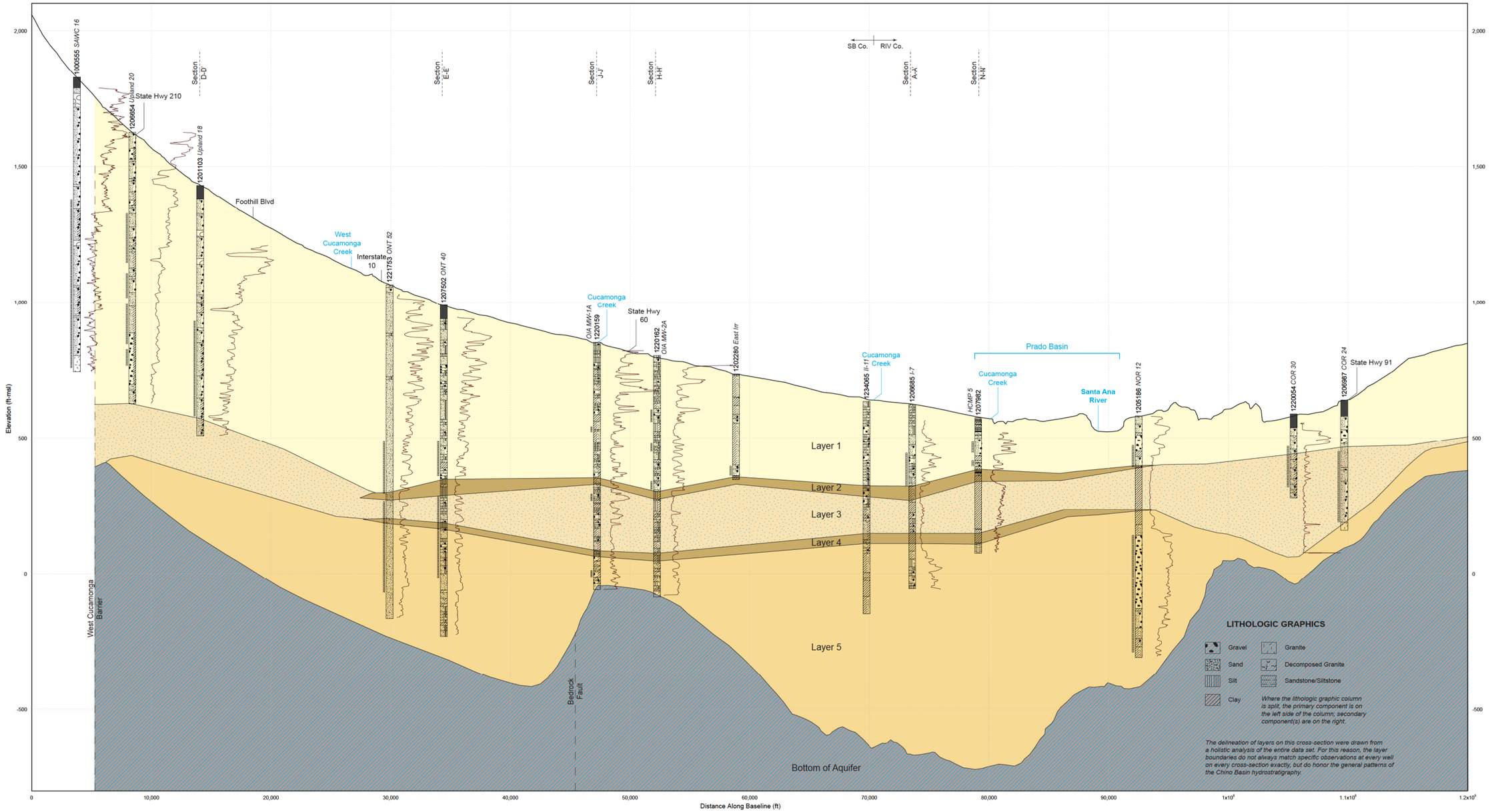

Report: FIG21 - ELOGSPERF5 - D_LIL File: 2019_CBWM_GWMODEL_UPDATE_VI.GPJ 4/29/2019

BOREHOLE LEGEND

1xxxxxx = WEI's HydroDaVE Database Well ID

Well Screen Interval

Resistivity Electrical Log

ft
300
200
100
0
VERTICAL SCALE
2,000 4,000 6,000 ft
HORIZONTAL SCALE
VERTICAL EXAGGERATION 14:1

HYDROSTRATIGRAPHIC LEGEND

- Layer 1 - Shallow aquifer system
- Layer 2 - Upper confining unit in the deep aquifer system
- Layer 3 - Upper portion of the deep aquifer system
- Layer 4 - Lower confining unit in the deep aquifer system
- Layer 5 - Lower portion of the deep aquifer system
- Effective base of the freshwater aquifer system

Hydrostratigraphic Cross-section: K-K'

Appendix A-11

L' (SOUTHWEST)

L' (EAST)

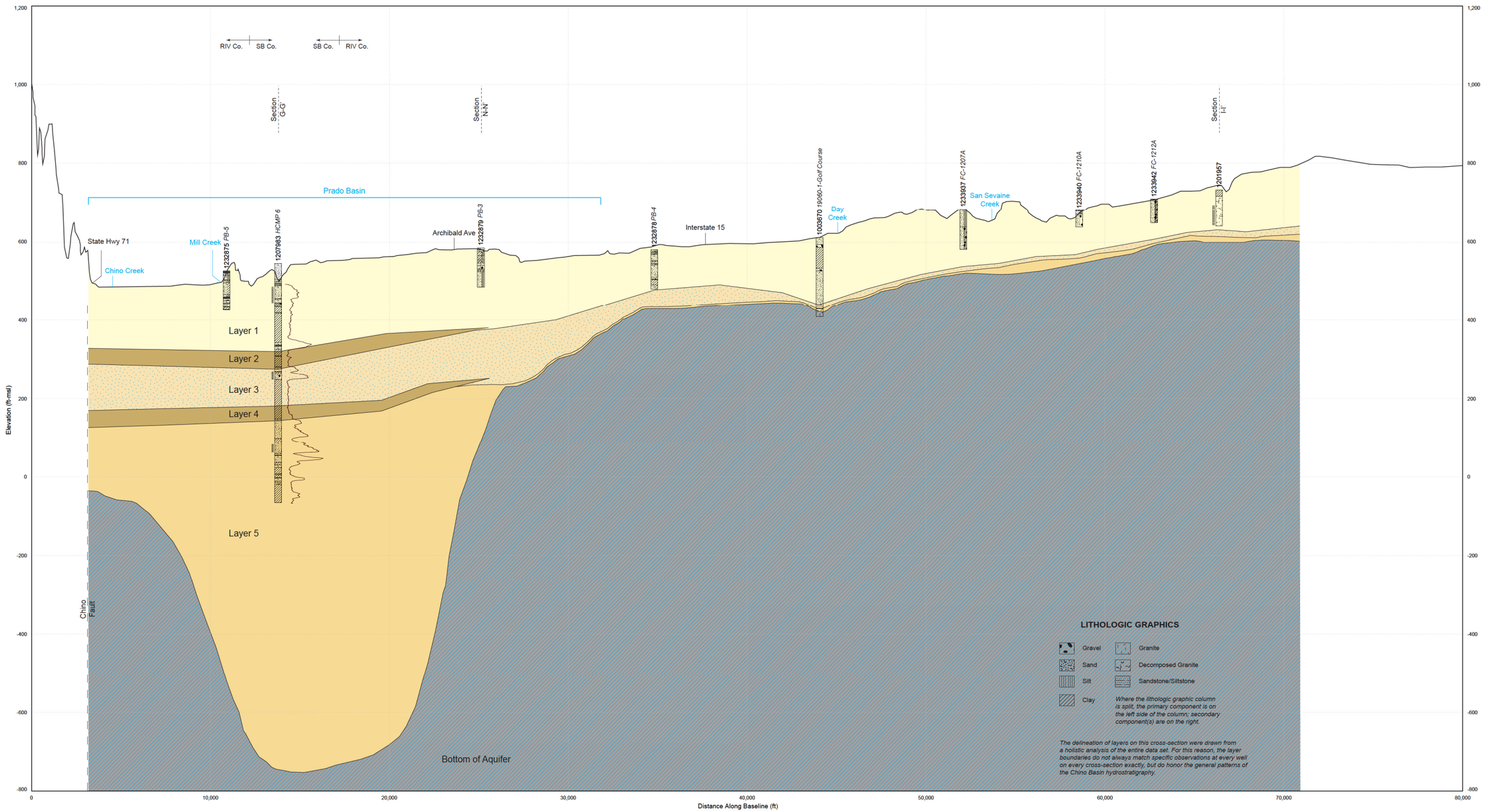

LITHOLOGIC GRAPHICS

- Gravel
- Sand
- Silt
- Clay
- Granite
- Decomposed Granite
- Sandstone/Siltstone

Where the lithologic graphic column is split, the primary component is on the left side of the column; secondary component(s) are on the right.

The delineation of layers on this cross-section were drawn from a holistic analysis of the entire data set. For this reason, the layer boundaries do not always match specific observations at every well on every cross-section exactly, but do honor the general patterns of the Chino Basin hydrostratigraphy.

BOREHOLE LEGEND

1xxxxxx = WEI's HydroDaVE Database Well ID

- Well Screen Interval
- Resistivity Electrical Log

HYDROSTRATIGRAPHIC LEGEND

- Layer 1 - Shallow aquifer system
- Layer 2 - Upper confining unit in the deep aquifer system
- Layer 3 - Upper portion of the deep aquifer system
- Layer 4 - Lower confining unit in the deep aquifer system
- Layer 5 - Lower portion of the deep aquifer system
- Effective base of the freshwater aquifer system

ft
200
100
50
0
VERTICAL SCALE
2,000
4,000
6,000 ft
HORIZONTAL SCALE
VERTICAL EXAGGERATION 22:1

Revit FENCE - ELOSSERS D_LIL File 2019_CBWM_GWMODEL_UPDATE_V1.rvt 6/17/2019

Hydrostratigraphic Cross-section: L-L'

Appendix A-12

M (NORTHWEST) **M' (SOUTHEAST)**

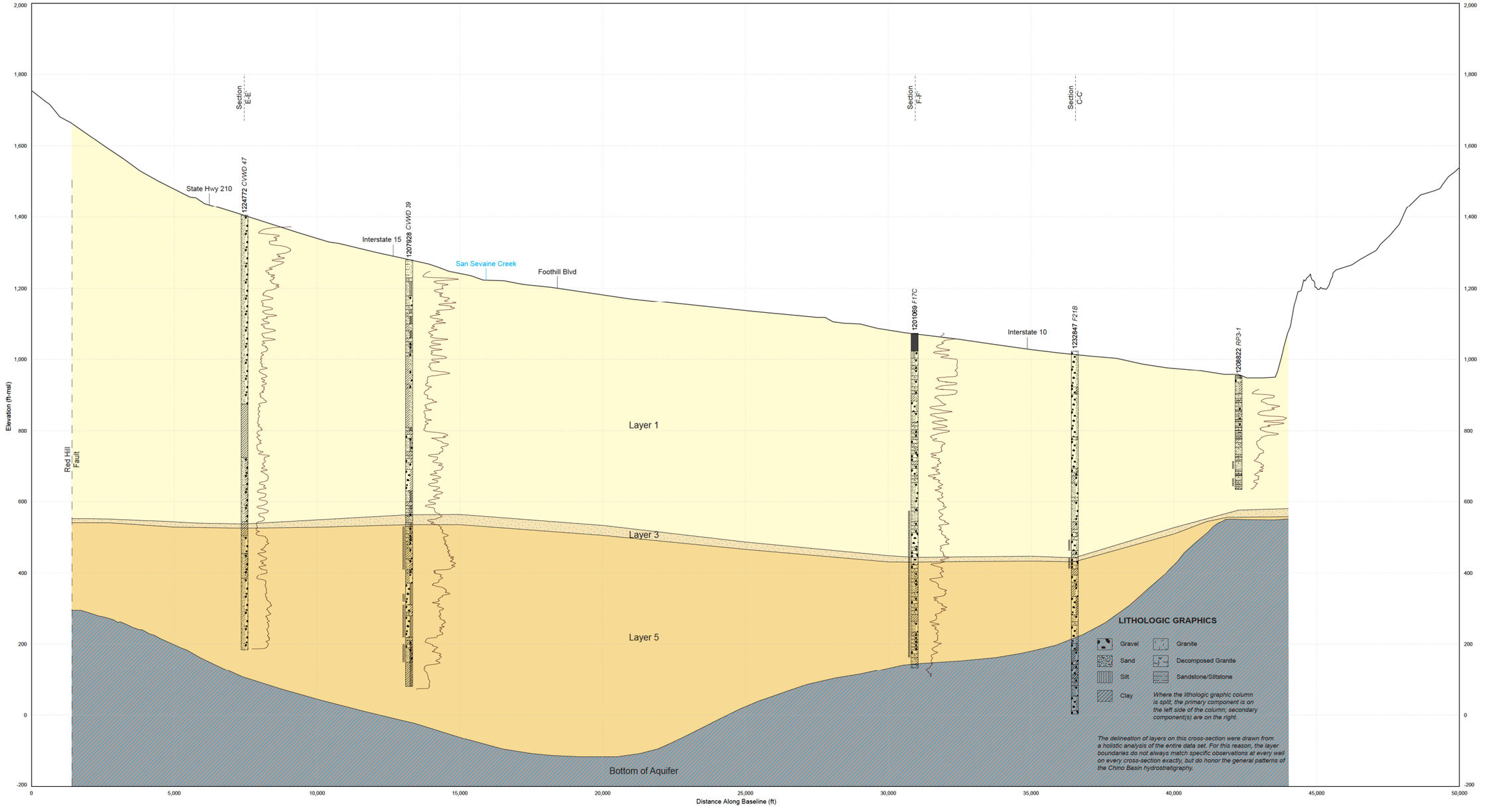

BOREHOLE LEGEND

1xxxxxx = WEI's HydroDaVE Database Well ID

Well Screen Interval

Resistivity Electrical Log

HYDROSTRATIGRAPHIC LEGEND

- Layer 1 - Shallow aquifer system
- Layer 2 - Upper confining unit in the deep aquifer system
- Layer 3 - Upper portion of the deep aquifer system
- Layer 4 - Lower confining unit in the deep aquifer system
- Layer 5 - Lower portion of the deep aquifer system
- Effective base of the freshwater aquifer system

ft
200
100
50
0
VERTICAL SCALE
1,000 2,000 3,000ft
HORIZONTAL SCALE
VERTICAL EXAGGERATION 12:1

Report: FRN21_ELOGSPREPS - D_LLL File: 2019_CBWM_GWMODEL_UPDATE_V1.GPJ 4/29/2019

Hydrostratigraphic Cross-section: M-M'

Appendix A-13

N (NORTHWEST) **N' (SOUTHEAST)**

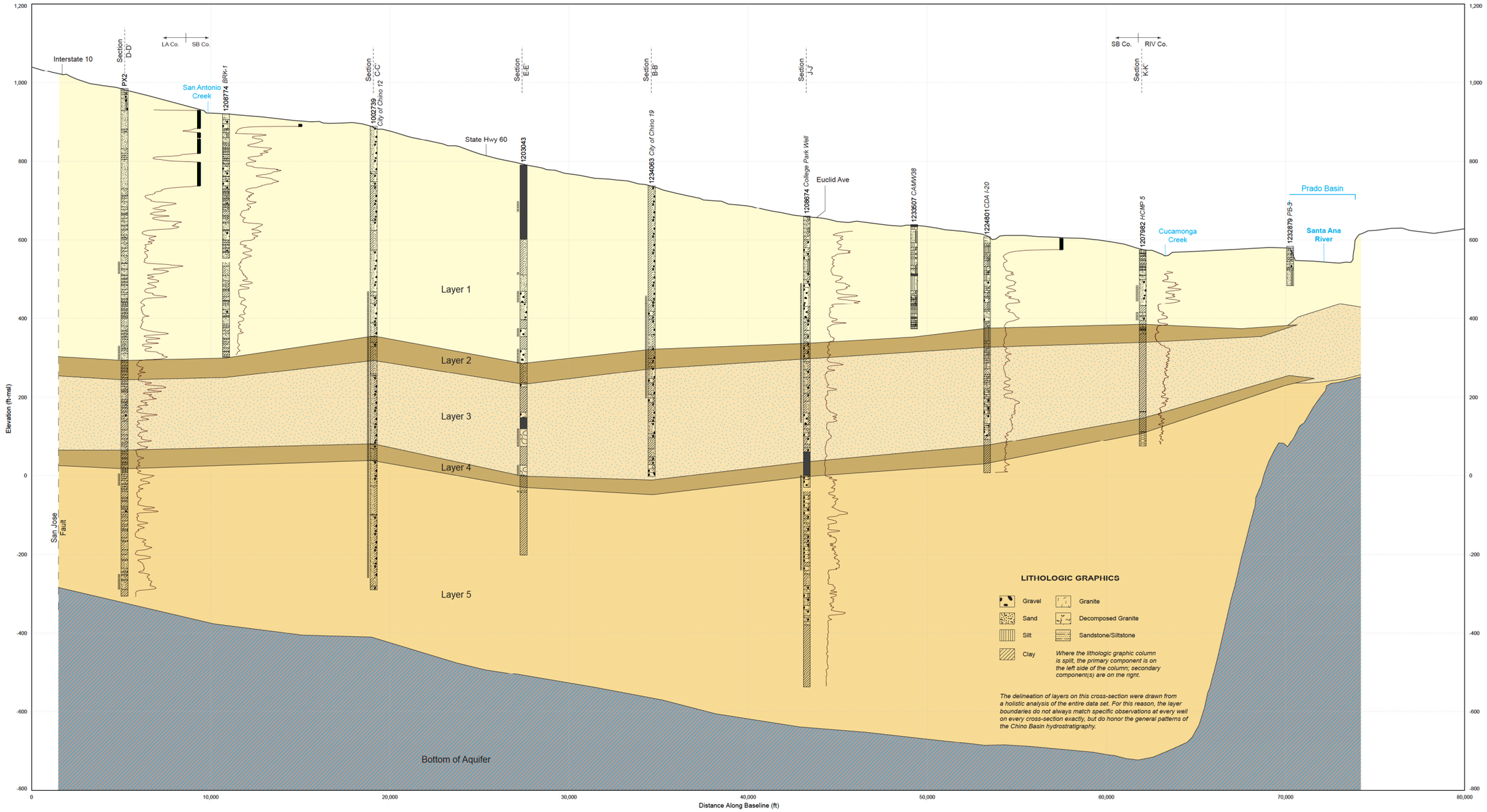

LITHOLOGIC GRAPHICS

Gravel	Granite
Sand	Decomposed Granite
Silt	Sandstone/Siltstone
Clay	

Where the lithologic graphic column is split, the primary component is on the left side of the column; secondary component(s) are on the right.

The delineation of layers on this cross-section were drawn from a holistic analysis of the entire data set. For this reason, the layer boundaries do not always match specific observations at every well on every cross-section exactly, but do honor the general patterns of the Chino Basin hydrostratigraphy.

BOREHOLE LEGEND

1xxxxxx = WEI's HydroDaVE Database Well ID

Well Screen Interval

Resistivity Electrical Log

HYDROSTRATIGRAPHIC LEGEND

- Layer 1 - Shallow aquifer system
- Layer 2 - Upper confining unit in the deep aquifer system
- Layer 3 - Upper portion of the deep aquifer system
- Layer 4 - Lower confining unit in the deep aquifer system
- Layer 5 - Lower portion of the deep aquifer system
- Effective base of the freshwater aquifer system

ft
200
100
50
0
VERTICAL SCALE
2,000 4,000 6,000 ft
HORIZONTAL SCALE
VERTICAL EXAGGERATION 22:1

Hydrostratigraphic Cross-section: N-N'

Appendix A-14

Appendix B

Supplemental Hydrologic Information

Appendix B Table of Contents

117°40'0"W

117°20'0"W

34°0'0"N

General Land Use Type

- Agriculture
- Dairy
- Urban
- Vacant
- Riparian Vegetation

- Active CVM Domain
- HSPF Model Domain
- R4 Model Domain
- Streams & Flood Control Channels

Prepared by:

WEI
Wildermuth Environmental, Inc.

Author: LS
Date: 3/21/2020
File: Figure B-1a LU1949.mxd

0 1 2 3 4 5 Miles
0 2 4 6 8 Km

Prepared for:

2020 Safe Yield Recalculation

Chino Basin Watermaster
Partners in Basin Management

General Land Use 1949

Figure B-1a

117°40'0"W

117°20'0"W

34°0'0"N

General Land Use Type

- Agriculture
- Dairy
- Urban
- Vacant
- Riparian Vegetation

- Active CVM Domain
- HSPF Model Domain
- R4 Model Domain
- Streams & Flood Control Channels

Prepared by:

WEI
Wildermuth Environmental, Inc.

Author: LS
Date: 3/21/2020
File: Figure B-1b LU1957.mxd

0 1 2 3 4 5 Miles
0 2 4 6 8 Km

Prepared for:

2020 Safe Yield Recalculation

Chino Basin Watermaster
Partners in Basin Management

General Land Use 1957

Figure B-1b

117°40'0"W

117°20'0"W

34°0'0"N

General Land Use Type

- Agriculture
- Dairy
- Urban
- Vacant
- Riparian Vegetation

- Active CVM Domain
- HSPF Model Domain
- R4 Model Domain
- Streams & Flood Control Channels

Prepared by:

WEI
Wildermuth Environmental, Inc.

Author: LS
Date: 3/21/2020
File: Figure B-1c LU1963.mxd

0 1 2 3 4 5 Miles
0 2 4 6 8 Km

Prepared for:

2020 Safe Yield Recalculation

Chino Basin Watermaster
Partners in Basin Management

General Land Use 1963

Figure B-1c

117°40'0"W

117°20'0"W

34°0'0"N

General Land Use Type

- Agriculture
- Dairy
- Urban
- Vacant
- Riparian Vegetation

- Active CVM Domain
- HSPF Model Domain
- R4 Model Domain
- Streams & Flood Control Channels

Prepared by:

WEI
Wildermuth Environmental, Inc.

Author: LS
Date: 3/21/2020
File: Figure B-1d LU1975.mxd

0 1 2 3 4 5 Miles
0 2 4 6 8 Km

Prepared for:

2020 Safe Yield Recalculation

Chino Basin Watermaster
Partners in Basin Management

General Land Use 1975

Figure B-1d

117°40'0"W

117°20'0"W

34°0'0"N

General Land Use Type

- Agriculture
- Dairy
- Urban
- Vacant
- Riparian Vegetation

- Active CVM Domain
- HSPF Model Domain
- R4 Model Domain
- Streams & Flood Control Channels

Prepared by:

WEI
Wildermuth Environmental, Inc.

Author: LS
Date: 3/21/2020
File: Figure B-1e LU1984.mxd

0 1 2 3 4 5 Miles
0 2 4 6 8 Km

Prepared for:

2020 Safe Yield Recalculation

Chino Basin Watermaster
Partners in Basin Management

General Land Use 1984

Figure B-1e

117°40'0"W

117°20'0"W

34°0'0"N

General Land Use Type

- Agriculture
- Dairy
- Urban
- Vacant
- Riparian Vegetation

- Active CVM Domain
- HSPF Model Domain
- R4 Model Domain
- Streams & Flood Control Channels

Prepared by:

WEI
Wildermuth Environmental, Inc.

Author: LS
Date: 3/21/2020
File: Figure B-1f LU1990.mxd

0 1 2 3 4 5 Miles
0 2 4 6 8 Km

Prepared for:

2020 Safe Yield Recalculation

Chino Basin Watermaster
Partners in Basin Management

General Land Use 1990

Figure B-1f

117°40'0"W

117°20'0"W

34°0'0"N

General Land Use Type

- Agriculture
- Dairy
- Urban
- Vacant
- Riparian Vegetation

- Active CVM Domain
- HSPF Model Domain
- R4 Model Domain
- Streams & Flood Control Channels

Prepared by:

WEI
Wildermuth Environmental, Inc.

Author: LS
Date: 3/21/2020
File: Figure B-1g LU2001.mxd

0 1 2 3 4 5 Miles
0 2 4 6 8 Km

Prepared for:

2020 Safe Yield Recalculation

Chino Basin Watermaster
Partners in Basin Management

General Land Use 2001

Figure B-1g

117°40'0"W

117°20'0"W

34°0'0"N

General Land Use Type

- Agriculture
- Dairy
- Urban
- Vacant
- Riparian Vegetation

- Active CVM Domain
- HSPF Model Domain
- R4 Model Domain
- Streams & Flood Control Channels

Prepared by:

WEI
Wildermuth Environmental, Inc.

Author: LS
Date: 3/21/2020
File: Figure B-1h LU2012.mxd

0 1 2 3 4 5 Miles
0 2 4 6 8 Km

Prepared for:

2020 Safe Yield Recalculation

Chino Basin Watermaster
Partners in Basin Management

General Land Use 2012

Figure B-1h

117°40'0"W

117°20'0"W

34°0'0"N

General Land Use Type

- Agriculture
- Dairy
- Urban
- Vacant
- Riparian Vegetation

- Active CVM Domain
- HSPF Model Domain
- R4 Model Domain
- Streams & Flood Control Channels

Prepared by:

WEI
Wildermuth Environmental, Inc.

Author: LS
Date: 3/21/2020
File: Figure B-1i LU2017.mxd

0 1 2 3 4 5 Miles
0 2 4 6 8 Km

Prepared for:

2020 Safe Yield Recalculation

Chino Basin Watermaster
Partners in Basin Management

General Land Use 2017

Figure B-1i

117°40'0"W

117°20'0"W

34°0'0"N

General Land Use Type

- Agriculture
- Dairy
- Urban
- Vacant
- Riparian Vegetation

- Active CVM Domain
- HSPF Model Domain
- R4 Model Domain
- Streams & Flood Control Channels

Prepared by:

WEI
Wildermuth Environmental, Inc.

Author: LS
Date: 3/21/2020
File: Figure B-1j LU2030.mxd

0 1 2 3 4 5 Miles
0 2 4 6 8 Km

Prepared for:

2020 Safe Yield Recalculation

Chino Basin Watermaster
Partners in Basin Management

Projected General Land Use 2030

Figure B-1j

117°40'0"W

117°20'0"W

34°0'0"N

General Land Use Type

- Agriculture
- Dairy
- Urban
- Vacant
- Riparian Vegetation

- Active CVM Domain
- HSPF Model Domain
- R4 Model Domain
- Streams & Flood Control Channels

Prepared by:

WEI
Wildermuth Environmental, Inc.

Author: LS
Date: 3/21/2020
File: Figure B-1k LU2040.mxd

0 1 2 3 4 5 Miles
0 2 4 6 8 Km

Prepared for:

2020 Safe Yield Recalculation

Chino Basin Watermaster
Partners in Basin Management

Projected General Land Use 2040

Figure B-1k

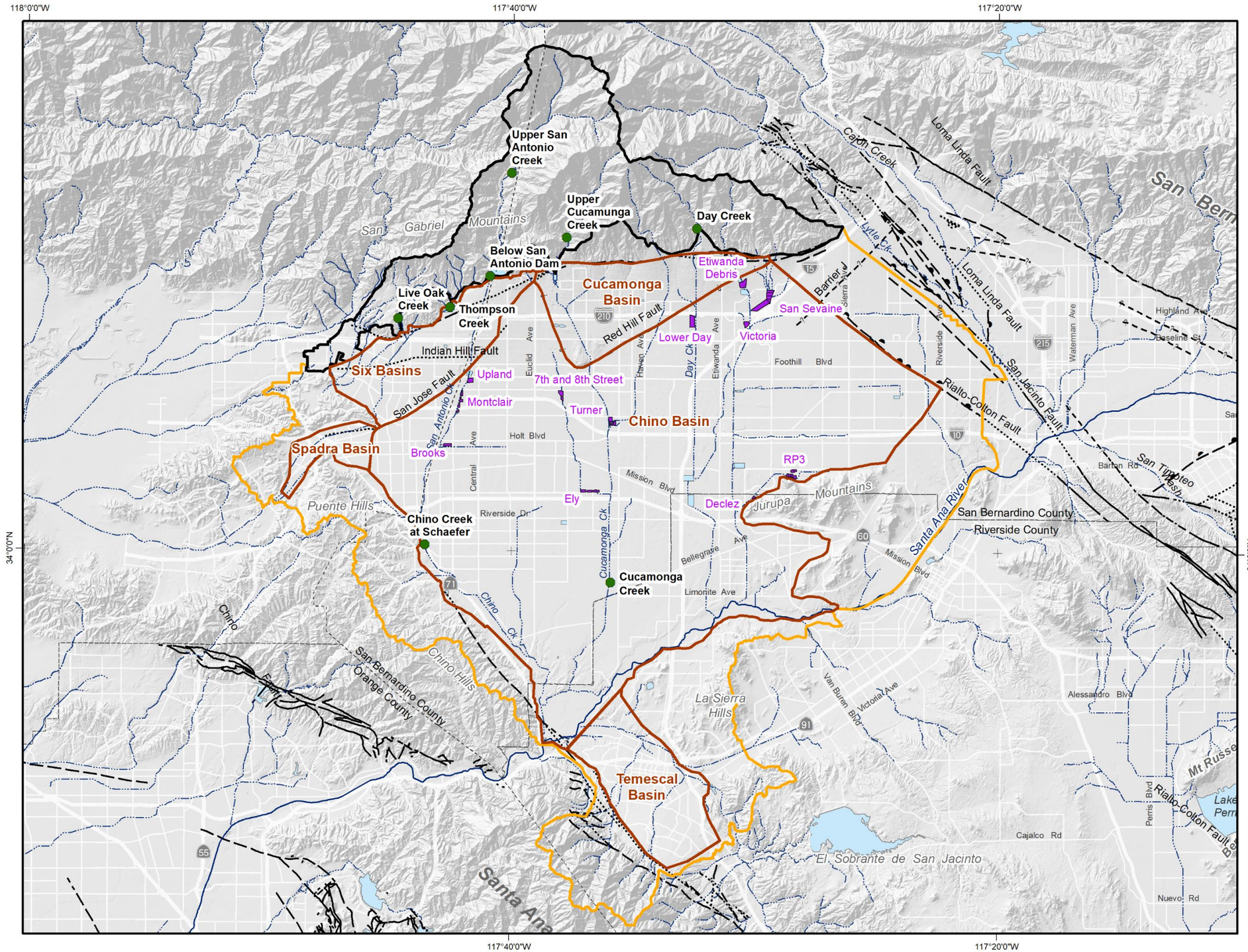

Prepared by:

WEI
Wildermuth Environmental, Inc.

Author: LS
Date: 4/1/2020
File: Figure B-2 Calibrate SWM.mxd

Prepared for:

2020 Safe Yield Recalculation

Chino Basin Watermaster
Partners in Basin Management

Location Map for Gaging Stations and Flood Control and Conservation Basins Used to Calibrate the HSPF and R4 Models

Figure B-2

Figure B-4: Annual Comparison of R4-Estimated Recharge to IEUA-Estimated Storm Water Diversion - Upland Basin

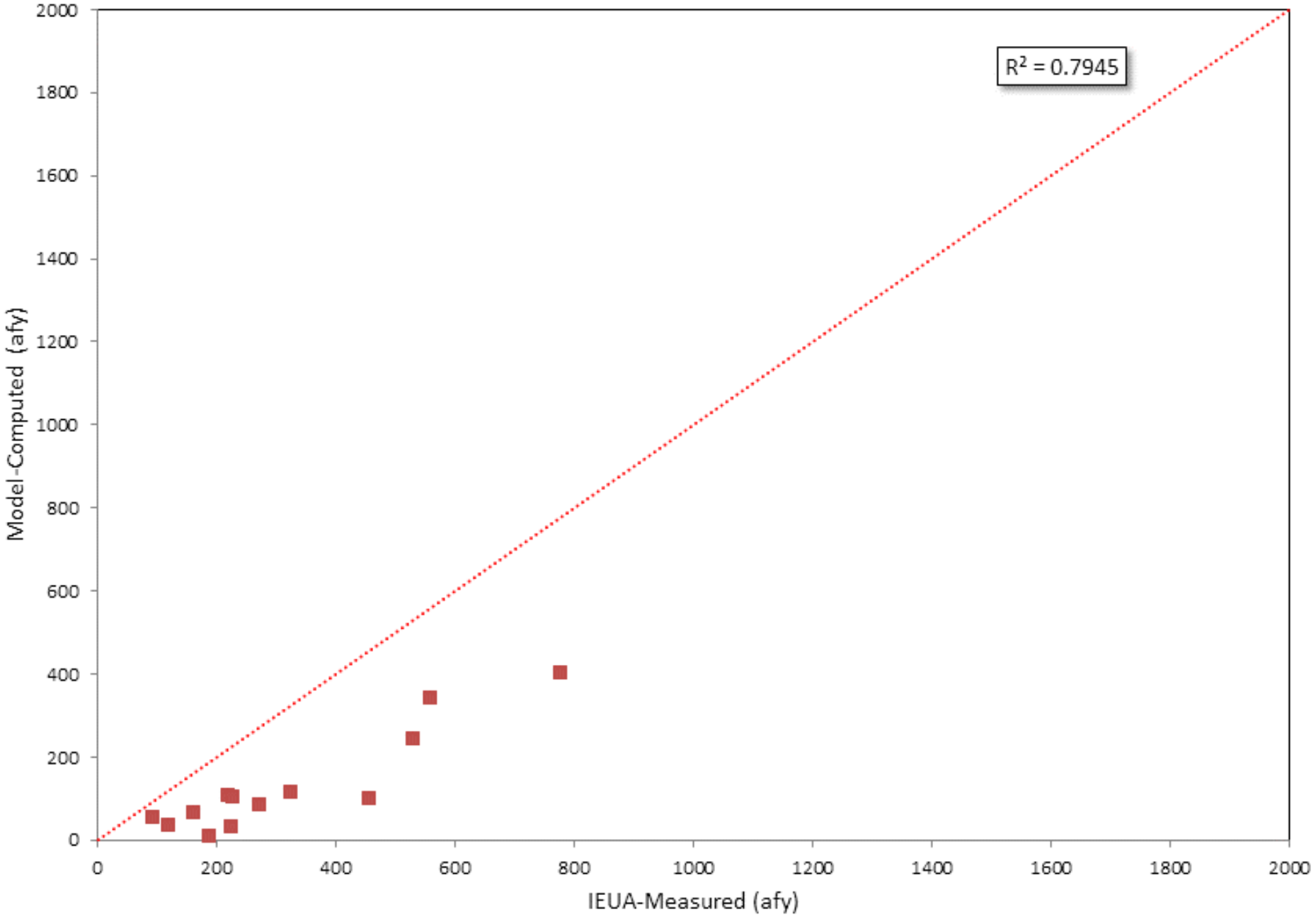

Figuer B-5: Annual Comparison of R4-Estimated Recharge to IEUA-Estimated Storm Water Diversion - Montclair Basins

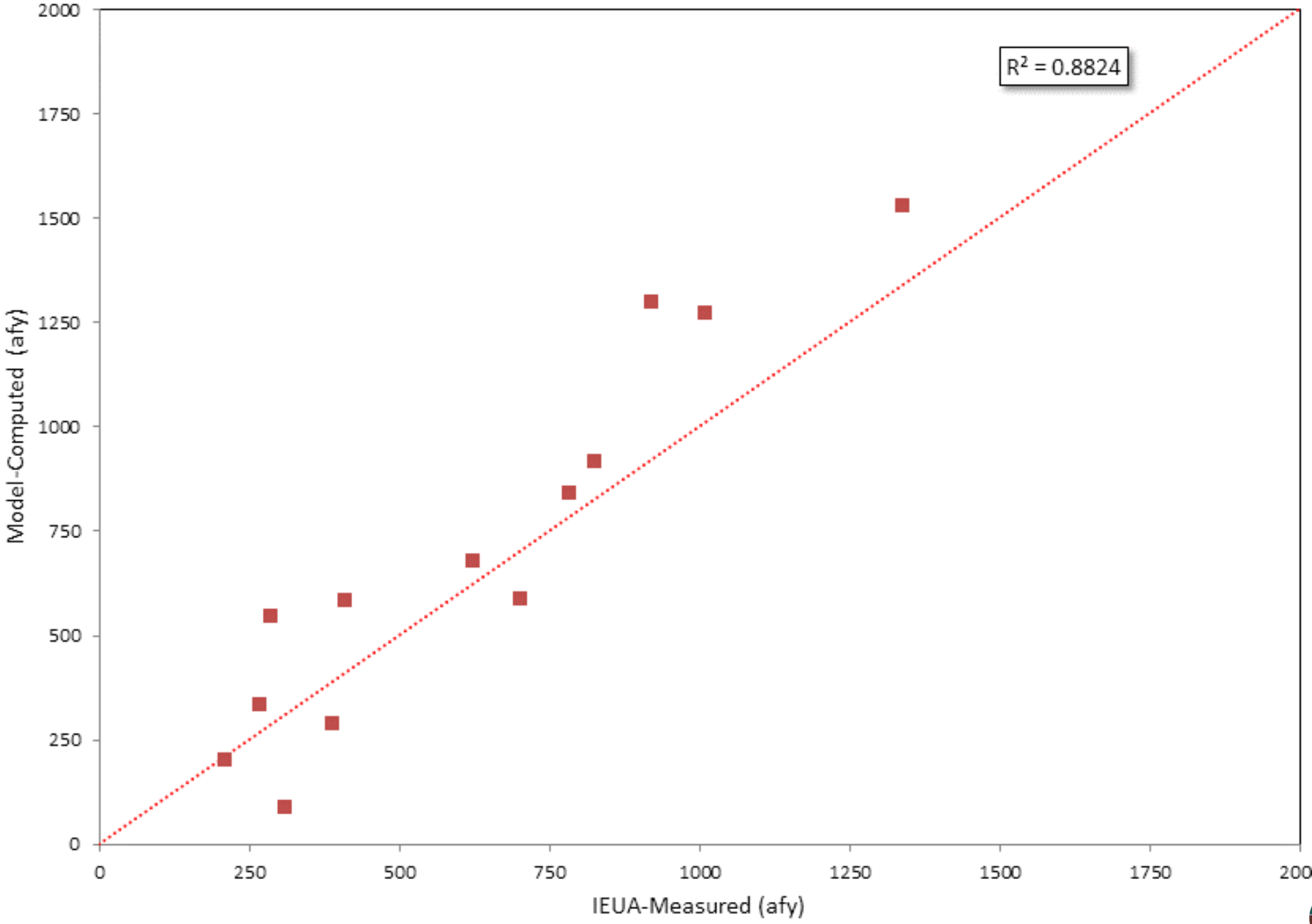

Figure B-6: Annual Comparison of R4-Estimated Recharge to IEUA-Estimated Storm Water Diversion - Brooks Street Basin

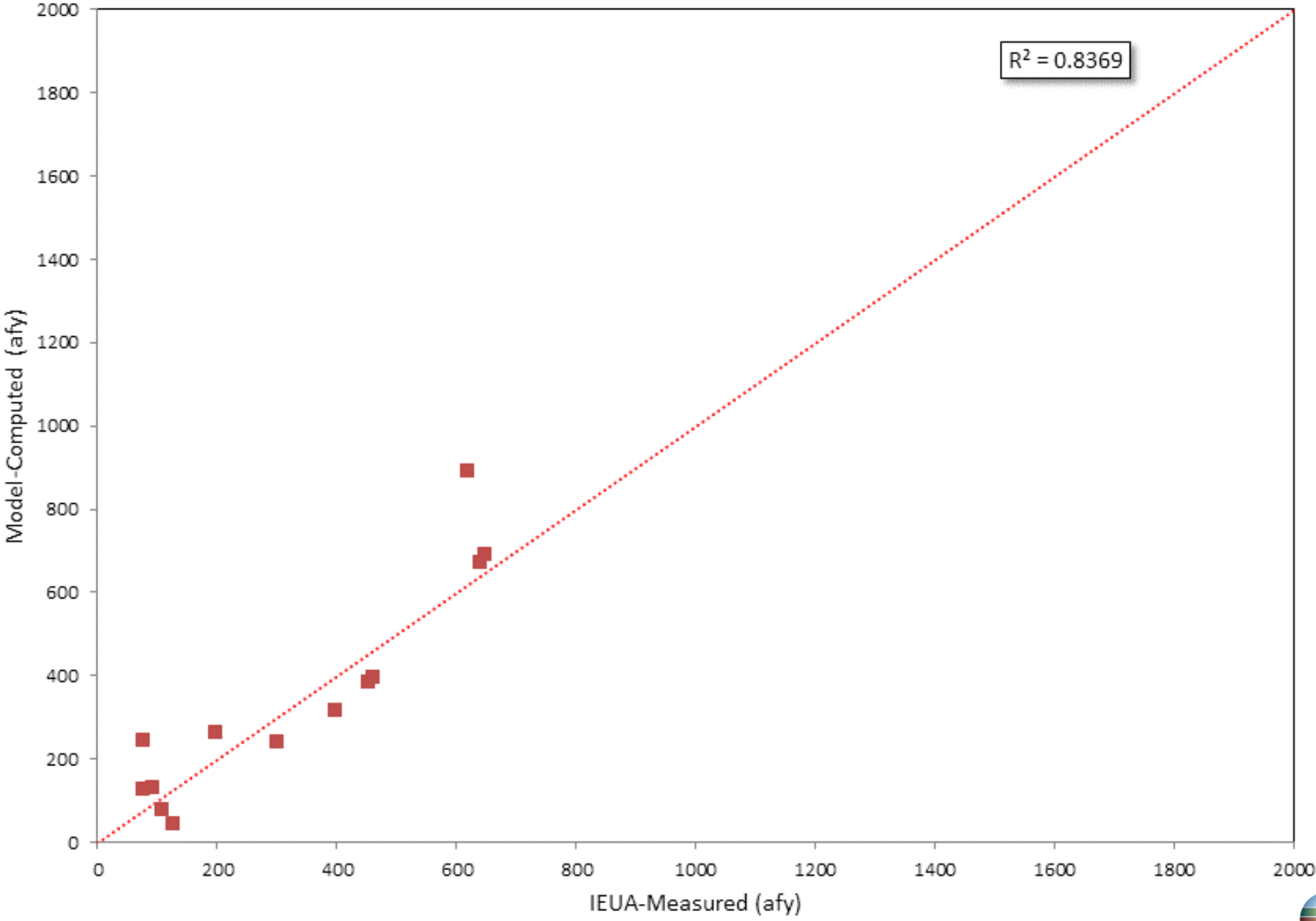

Figure B-7: Annual Comparison of R4-Estimated Recharge to IEUA-Estimated Storm Water Diversion - 8th and 7th Street Basins

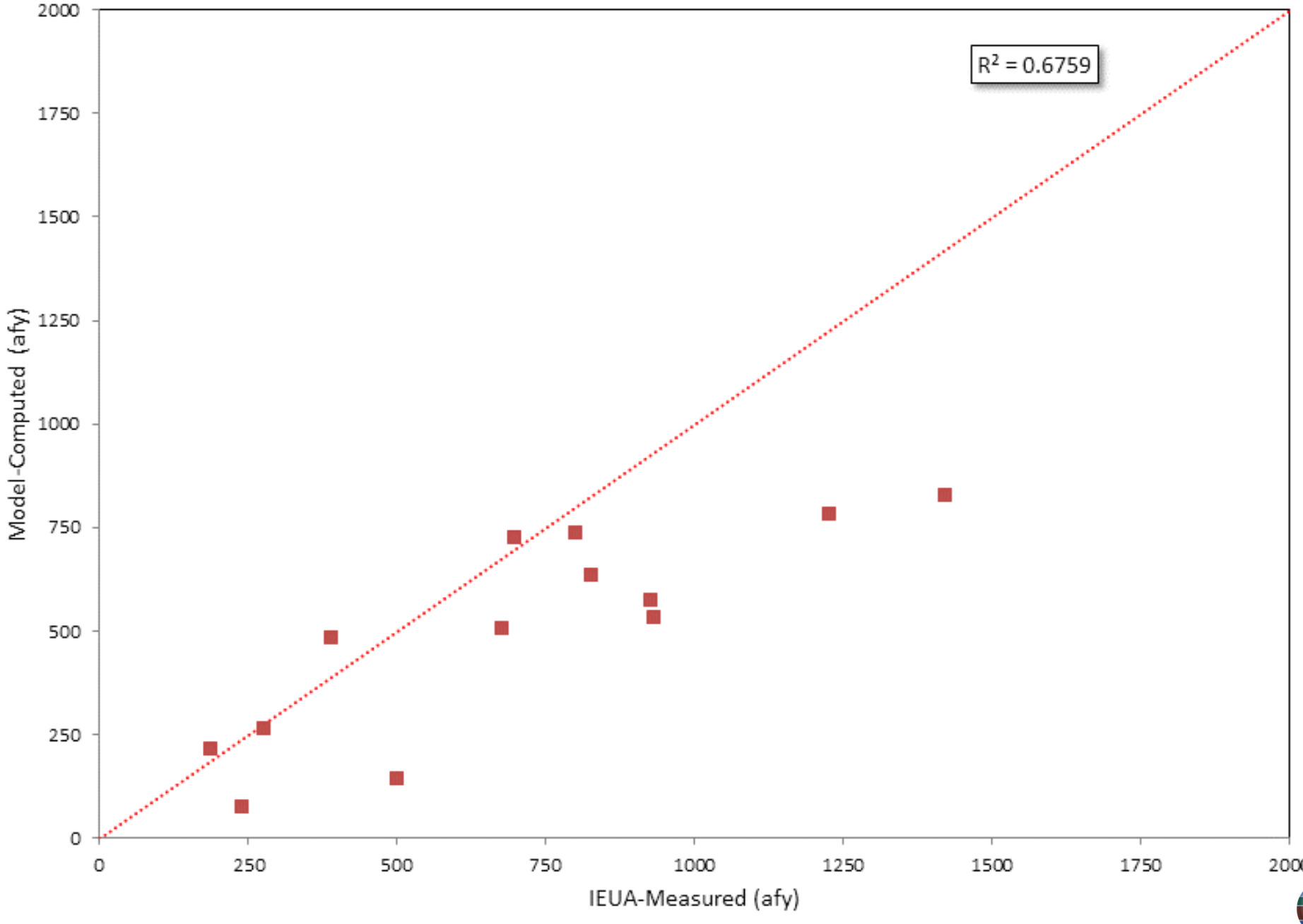

Figure B-8: Annual Comparison of R4-Estimated Recharge to IEUA-Estimated Storm Water Diversion - Ely Basins

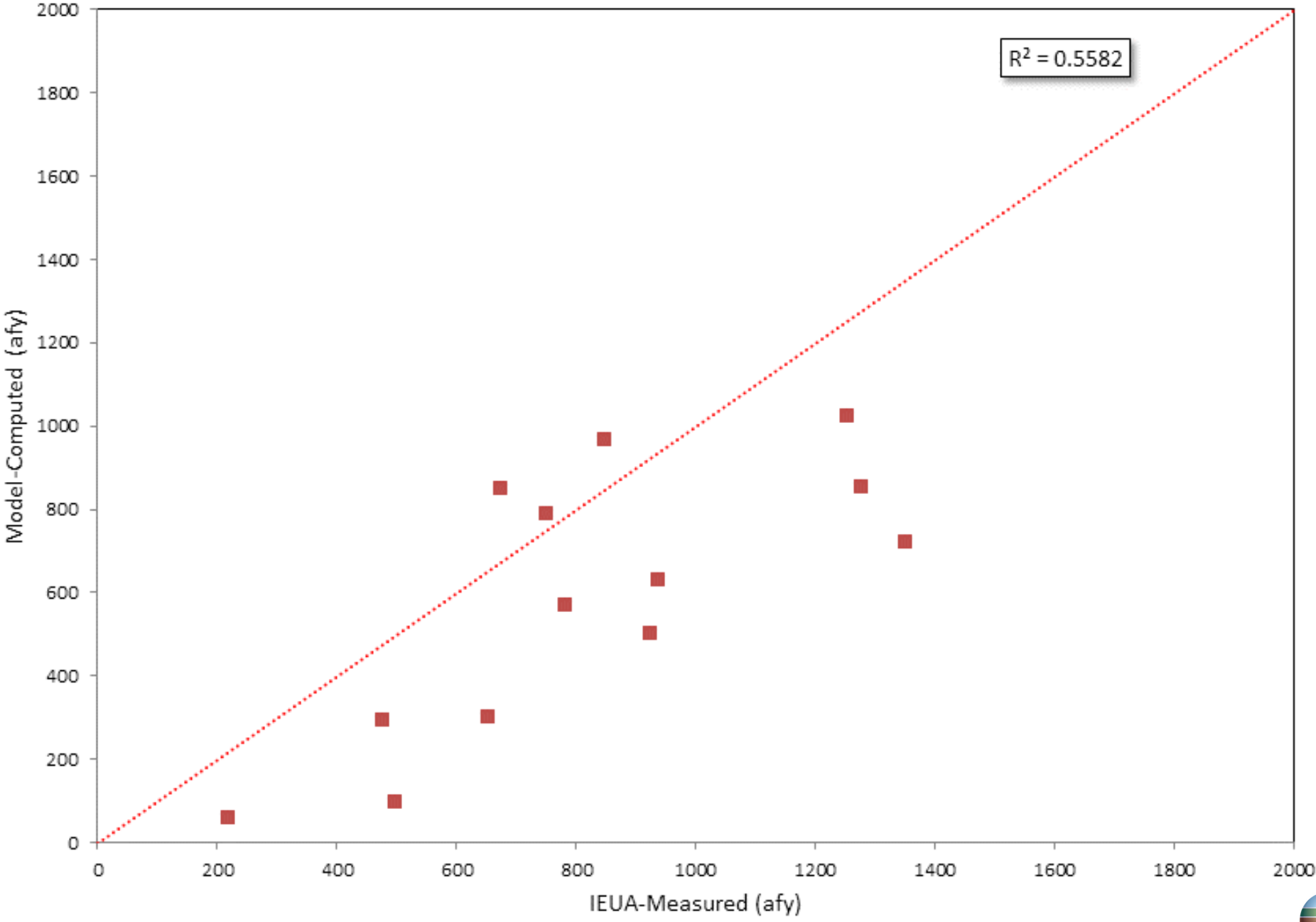

Figure B-9: Annual Comparison of R4-Estimated Recharge to IEUA-Estimated Storm Water Diversion - Turner Basins

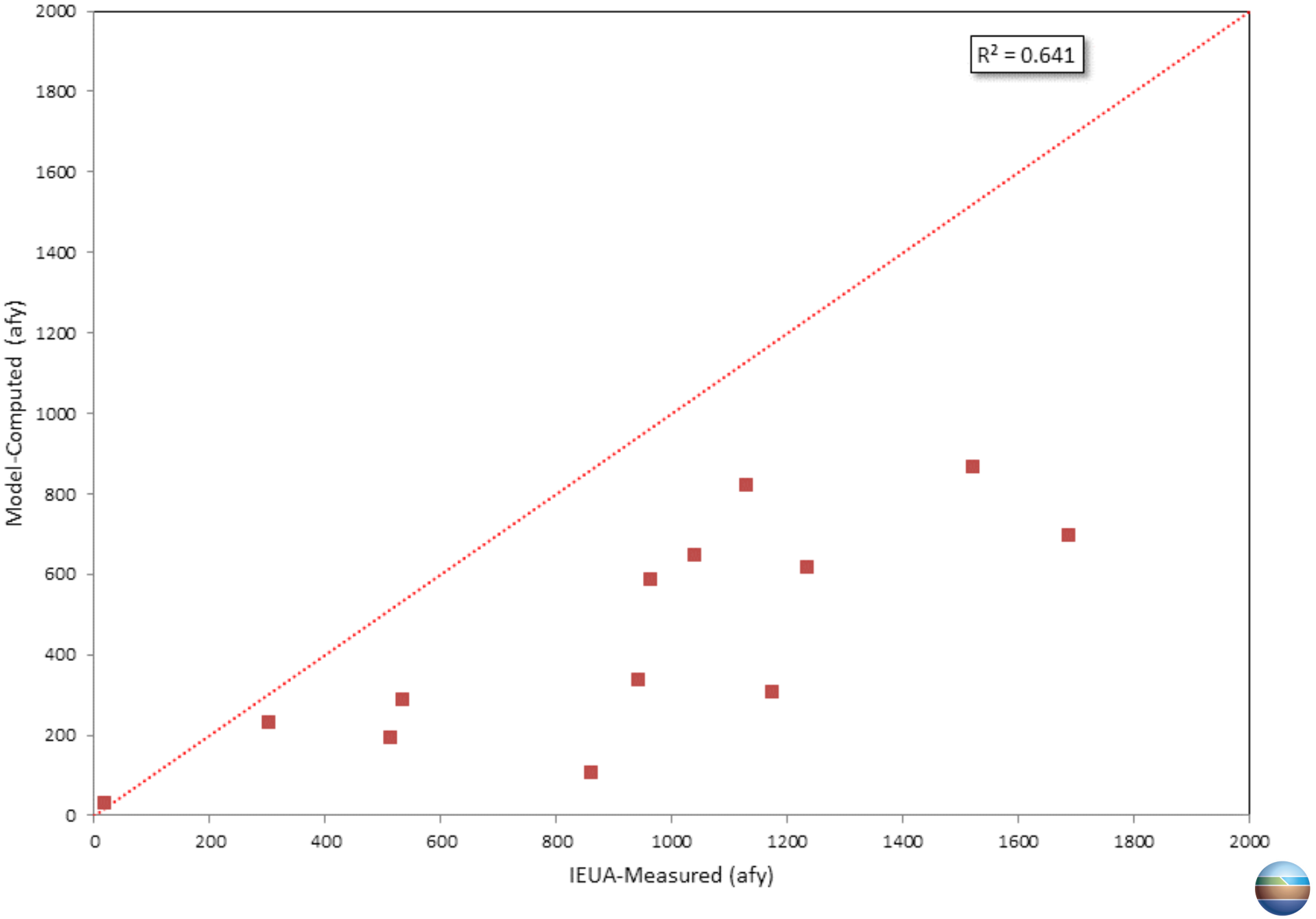

Figure B-10: Annual Comparison of R4-Estimated Recharge to IEUA-Estimated Storm Water Diversion - Lower Day Basin

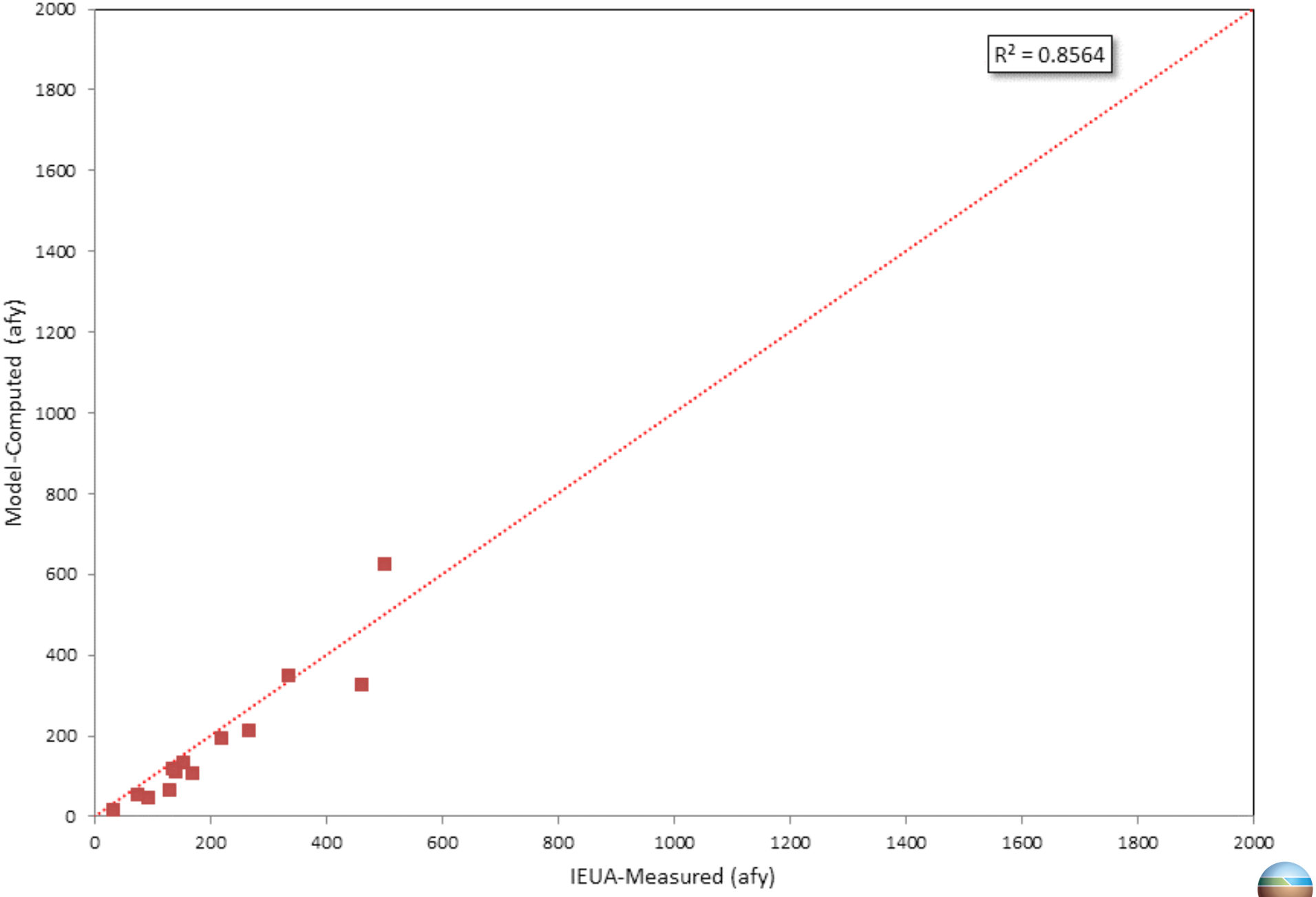

Figure B-11: Annual Comparison of R4-Estimated Recharge to IEUA-Estimated Storm Water Diversion - Etiwanda Debris Basin

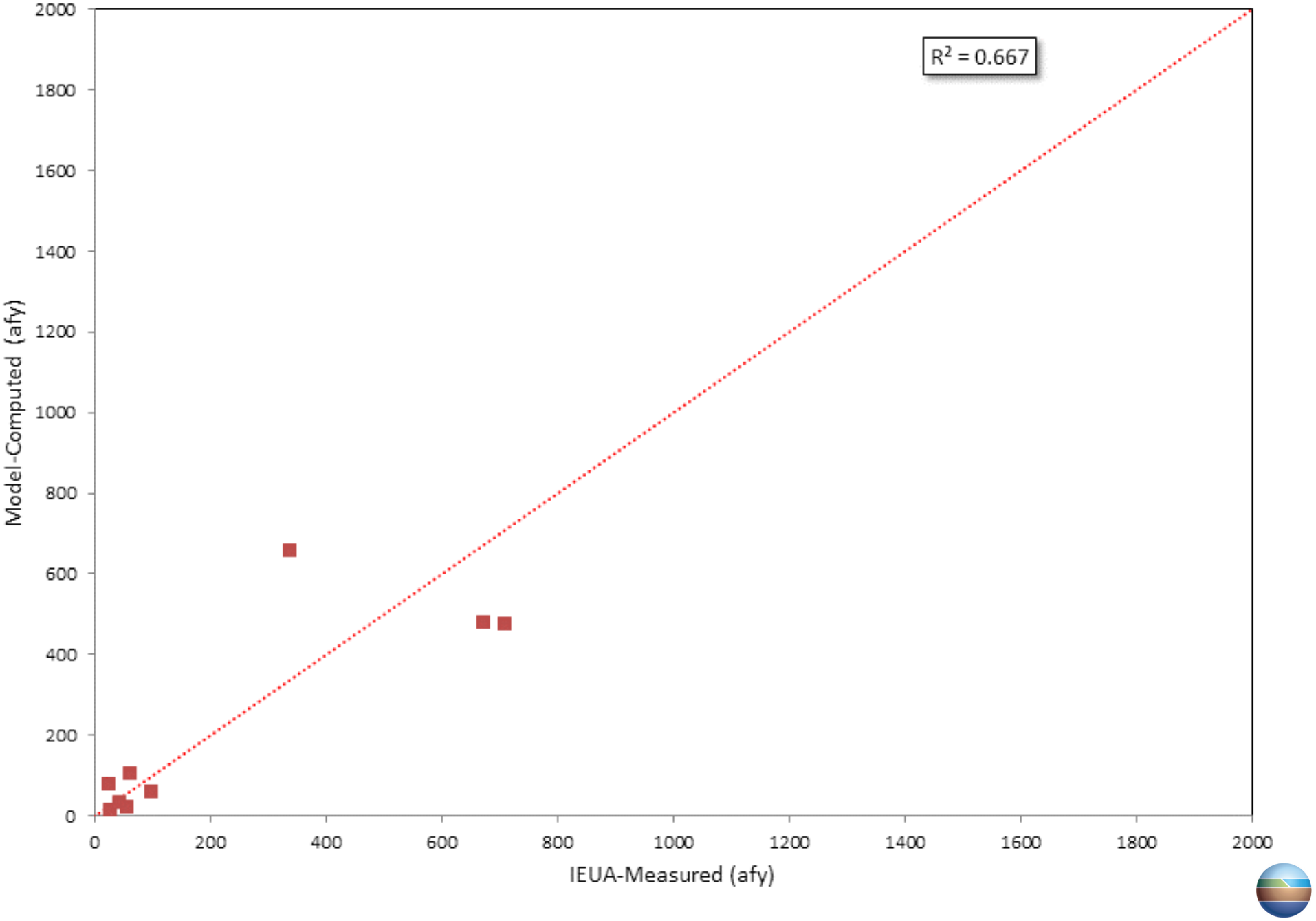

Figure B-12: Annual Comparison of R4-Estimated Recharge to IEUA-Estimated Storm Water Diversion - Victoria Basin

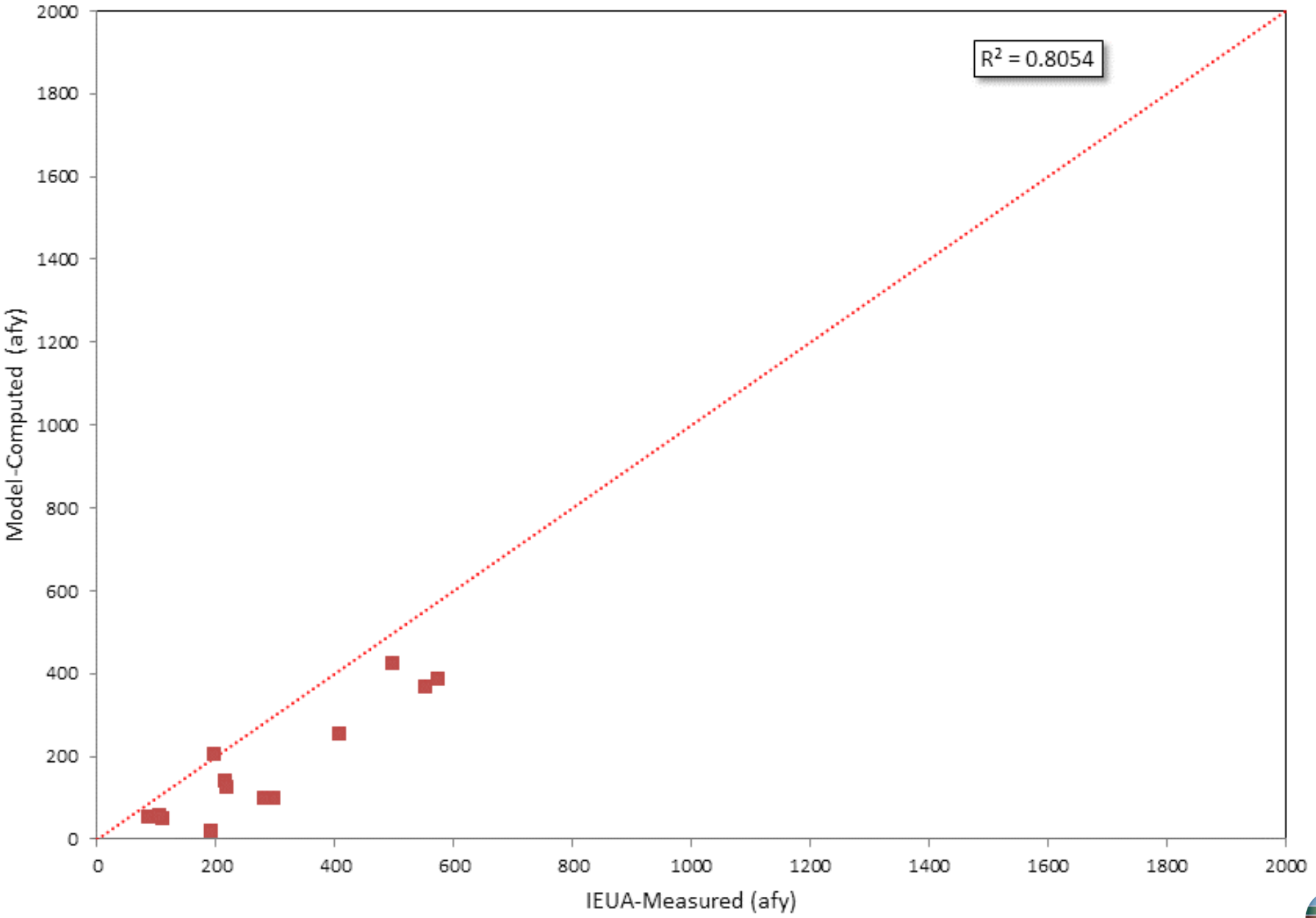

Figure B-13: Annual Comparison of R4-Estimated Recharge to IEUA-Estimated Storm Water Diversion - San Sevaine Basins

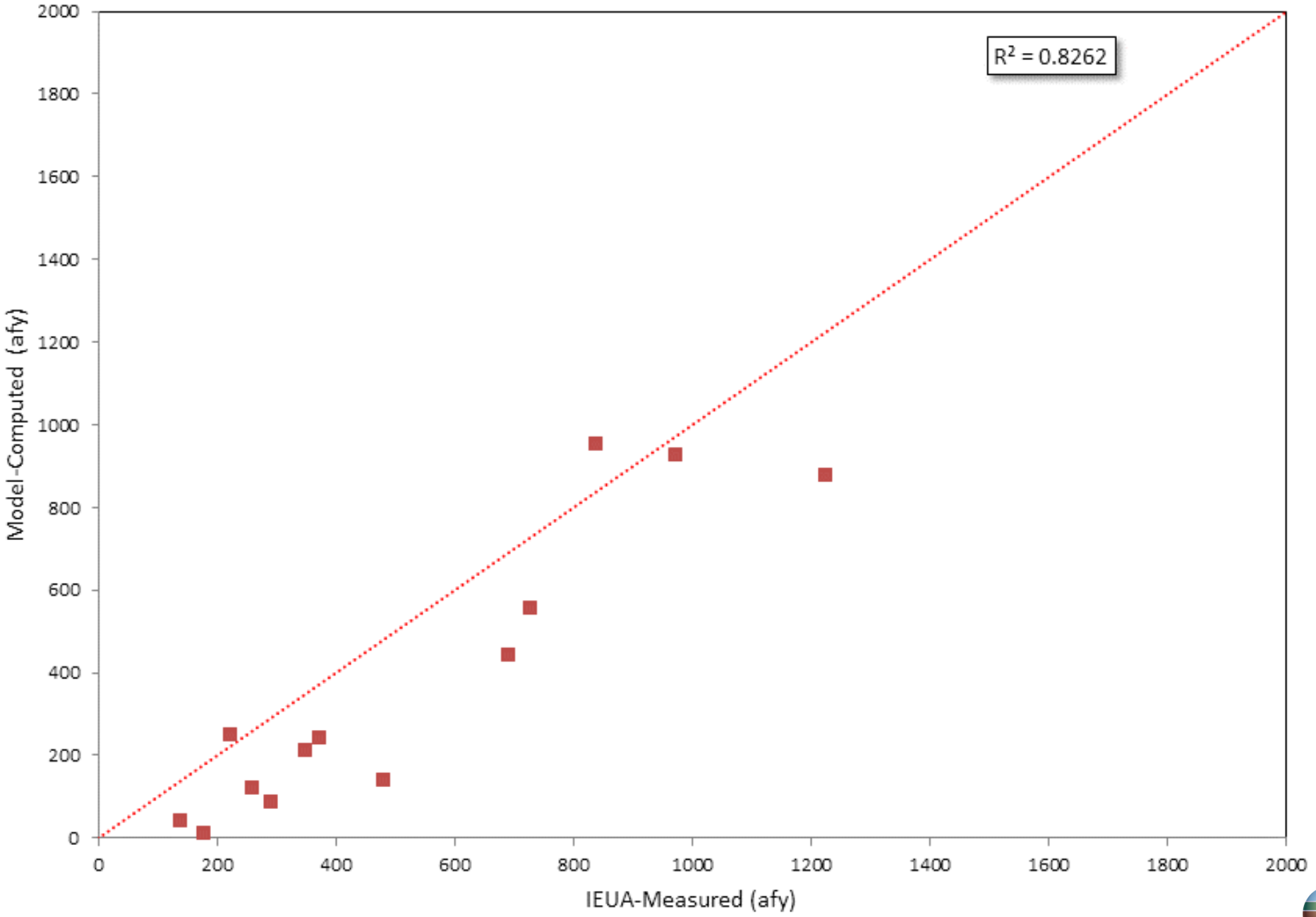

Figure B-14: Annual Comparison of R4-Estimated Recharge to IEUA-Estimated Storm Water Diversion - Banana/Hickory Basins

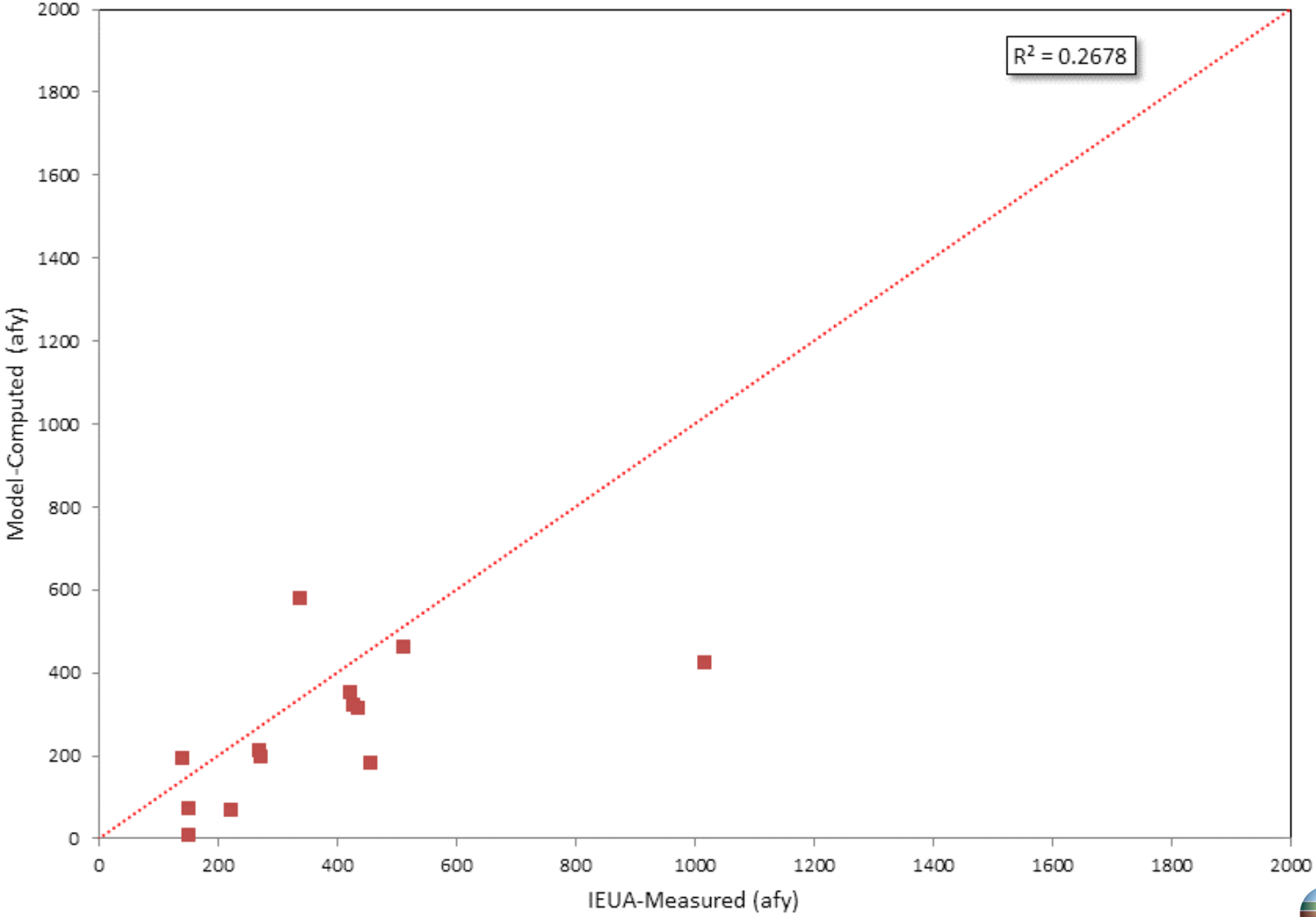

Figure B-15: Annual Comparison of R4-Estimated Recharge to IEUA-Estimated Storm Water Diversion - RP3 Basins

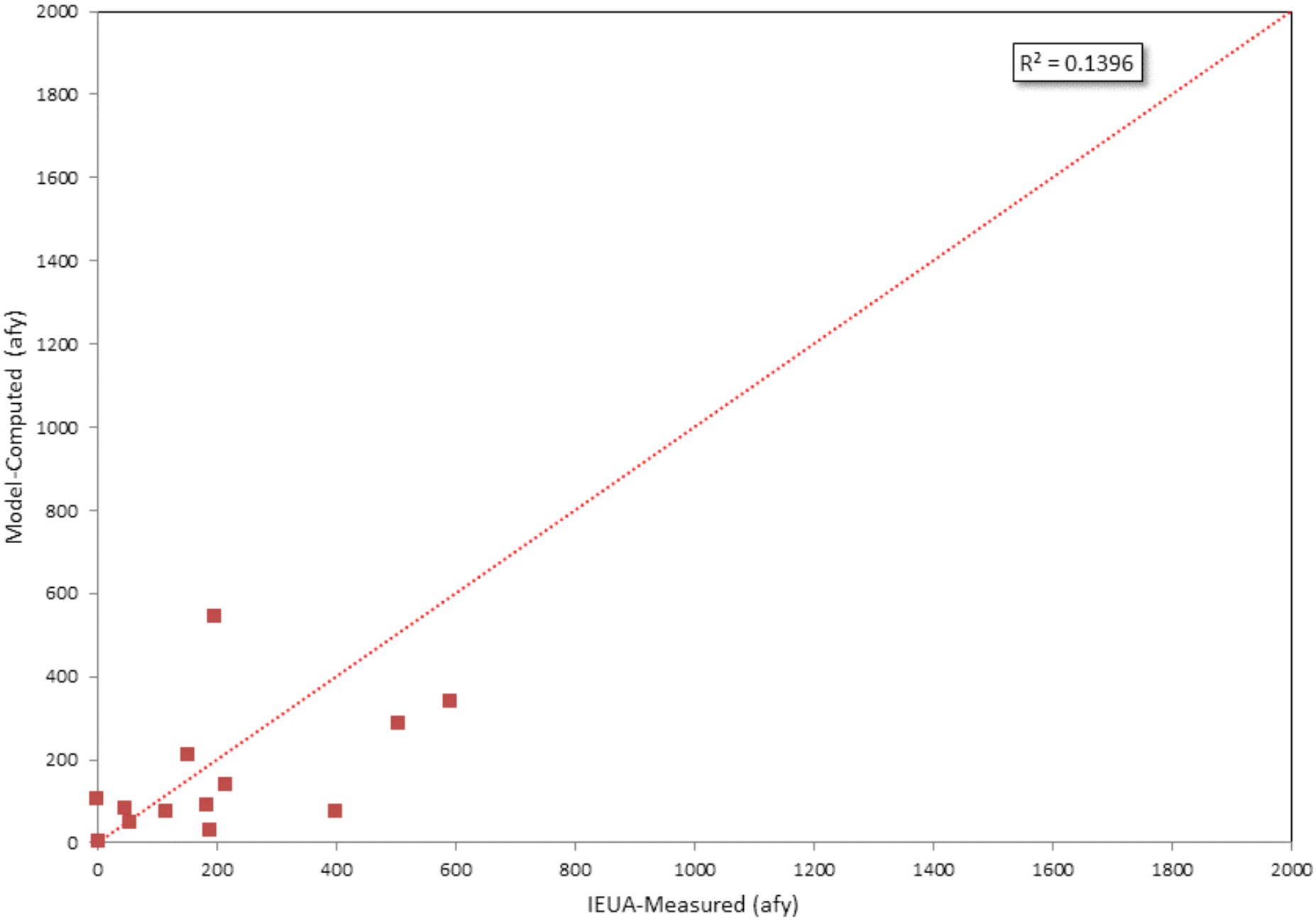

Figure B-16: Annual Comparison of R4-Estimated Recharge to IEUA-Estimated Storm Water Diversion - Declez Basins

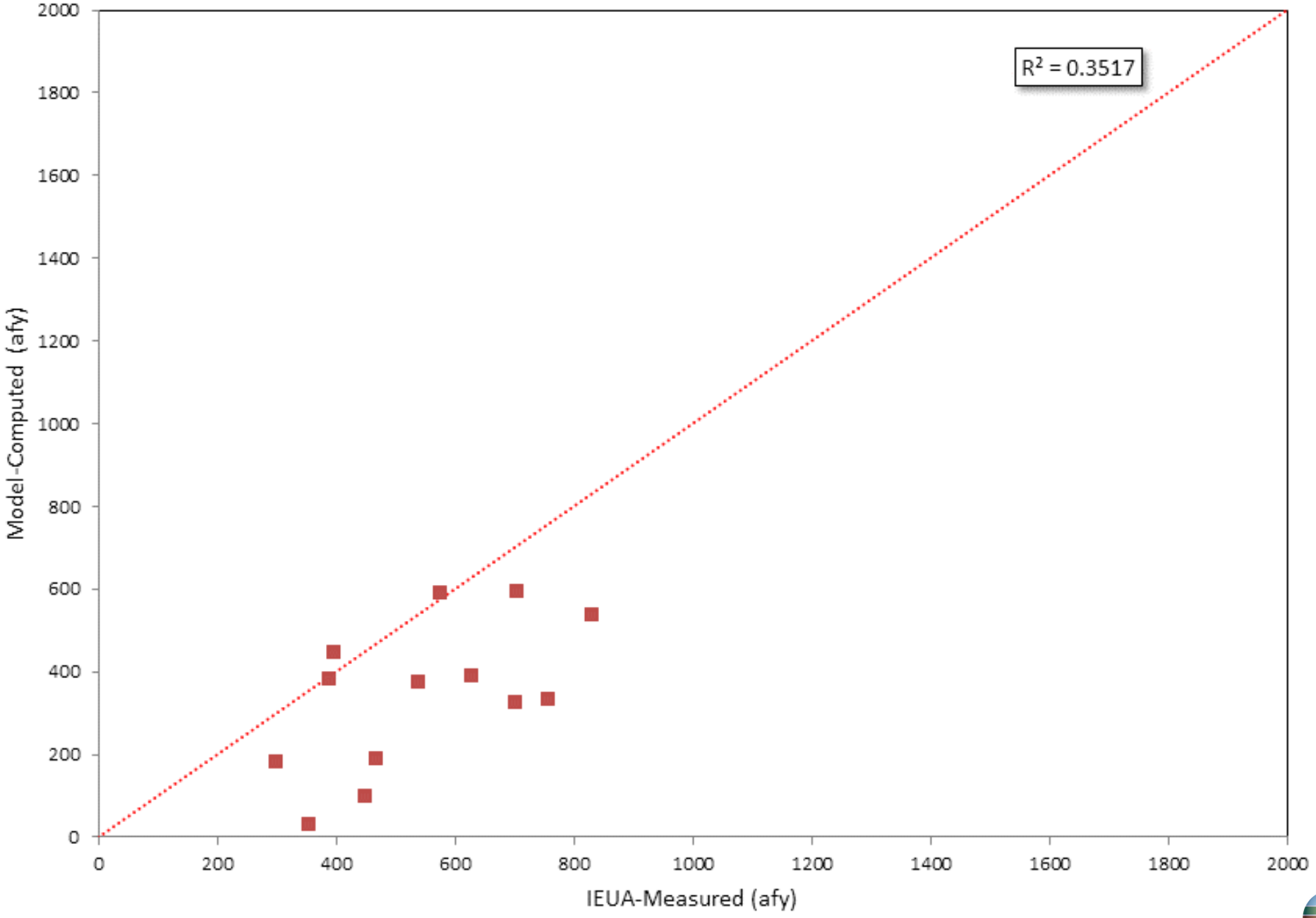

Figure B-17: Annual Comparison of R4-Estimated Recharge to IEUA-Estimated Storm Water Diversion - Grove Basin

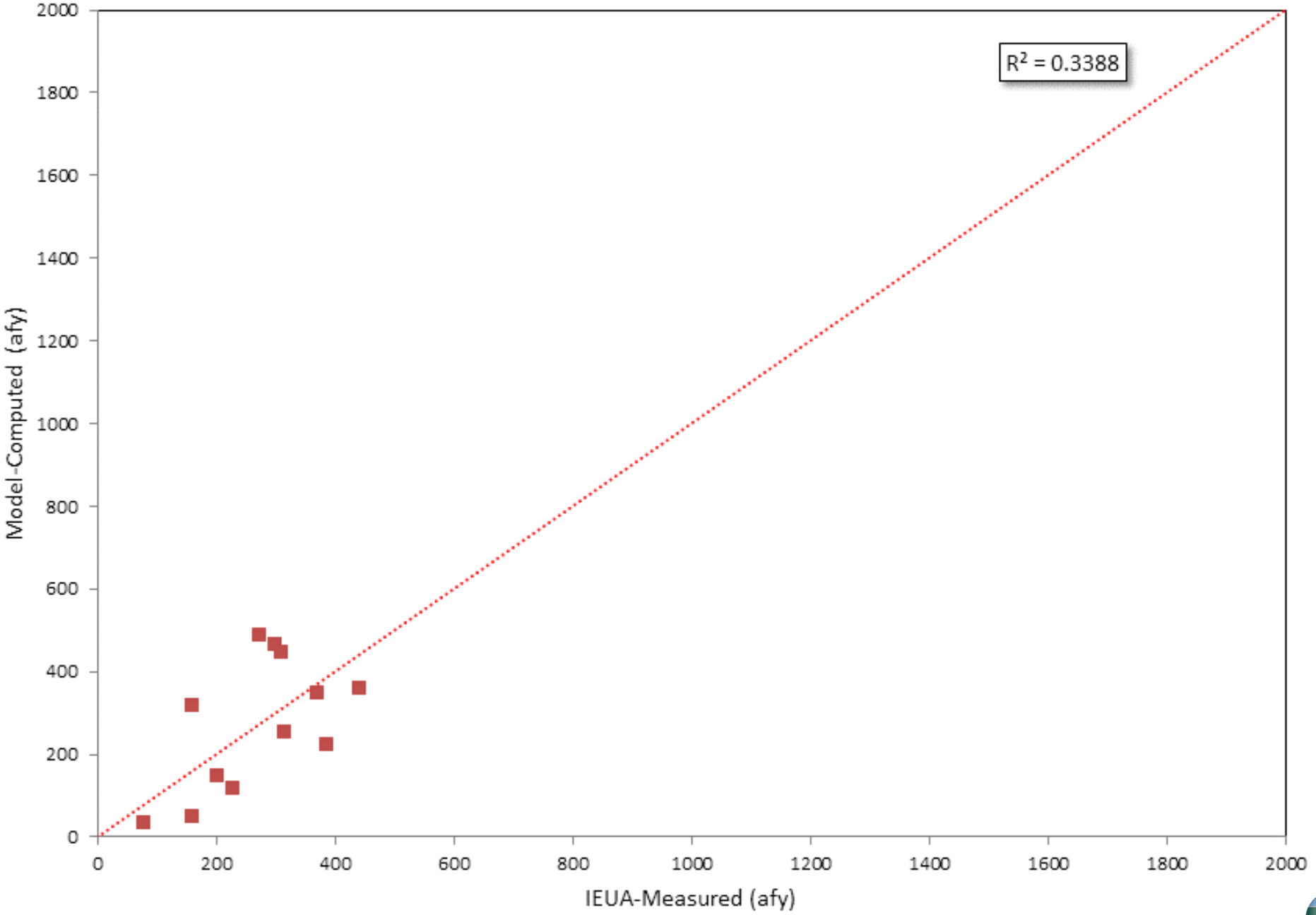

TECHNICAL MEMORANDUM

February 6, 2020

RE: Riparian Vegetation Evapotranspiration

Objective

This technical memorandum (TM) describes how the amount of water consumed by the riparian vegetation in Prado through evapotranspiration (ET) was estimated as well as how the model calculates the portion of this amount that is derived from groundwater.

Estimating Evapotranspiration Rates

In order to estimate the amount of water consumed by the riparian vegetation through ET for the model calibration period of fiscal 1978 through 2018, we estimated the extent and density of the riparian vegetation along the Santa Ana River within the Chino Basin Groundwater Model domain for a range of years spanning the model calibration period. In addition to the years 1974, 1994, and 2006 which were used in the 2013 model, we added the extent and density for the years of 1985, 1999, and 2019. Figure B-18-1 shows the extent, area, and density for these six years. The following steps explain how we determined the extent and spatial density of the riparian vegetation shown in Figure B-18-1.

1. Obtained and assembled historical aerial photos of the Santa Ana River that covered the entire, or most of the model domain area for the years 1974, 1985, 1994, 1999, 2006, and 2019.
2. Geo-referenced aerial photos in Arc Map if needed.
3. In ArcMap, imported: existing land use shapefiles that were assembled or digitized for the Chino Basin modeling work and displayed the land use types associated with the riparian vegetation; or existing shapefiles of riparian vegetation extents.
4. For each aerial photo year, the land use or riparian vegetation extent shapefile closest to the year of the aerial photo was used as an initial estimate of the extent of the riparian vegetation along the River, and then modified to match the extent of the riparian vegetation as shown in the aerial photo to create a riparian vegetation extent shapefile for each year.
5. In Arc Map, the aerial photos and shapefiles of the riparian vegetation extent for all years were overlain by a 1,320 by 1,320-meter grid, and each grid was assigned a number.
6. For each year, the area of riparian vegetation within each grid cell was calculated in ArcMap.

23692 Birtcher Dr.
Lake Forest, CA 92630

7. For each individual year, the density of the riparian vegetation for each grid cell was evaluated visually using the aerial photo, and an estimate of the density of the riparian vegetation area for each grid cell was recorded as a percentage.
8. The density estimate analysis described in step 7 was performed independently by two to three different people.
9. The three density estimates for each year and each grid cell were averaged, to get a final estimate of density for each grid cell for each year.
10. For each year, an area-weighted density was calculated for the entire extent of riparian vegetation. This average density was used to adjust the expected ET rate for vegetation.

As determined in the USGS Open File Report 96-4241 (Lines et al, 1996), the annual consumptive use of groundwater and surface water by riparian vegetation varies based on the aerial density of the vegetation. The area-weighted density of the riparian vegetation determined for each of the six years was used to determine the effective ET rate of the riparian vegetation based on the approach adopted in USGS Open File Report 96-4241 and its findings. The effective ET rate is equal to the unit ET rate for a 100 percent riparian coverage times the vegetation density.

The unit ET rates used for riparian vegetation in the CVM are from the evapotranspiration analysis on the Prado Basin prepared by Merkel (2006) for the southern Cottonwood Riparian Forest and southern Willow Scrub habitats and are in ft/day for each month. The table below lists the monthly maximum ET rates for the for the years 1974, 1985, 1994, 1999, 2006, and 2019:

Riparian Vegetation ET ft/day

	Jan	Feb	Mar	Apr	May	Jun	Jul	Aug	Sep	Oct	Nov	Dec
1974	0.00432	0.00486	0.00774	0.01764	0.02036	0.02328	0.02499	0.02455	0.01879	0.00644	0.00445	0.00340
1985	0.00432	0.00486	0.00774	0.01764	0.02036	0.02328	0.02499	0.02455	0.01879	0.00644	0.00445	0.00340
1994	0.00432	0.00486	0.00774	0.01764	0.02036	0.02328	0.02499	0.02455	0.01879	0.00644	0.00445	0.00340
1999	0.00432	0.00486	0.00774	0.01764	0.02036	0.02328	0.02499	0.02455	0.01879	0.00644	0.00445	0.00340
2006	0.00432	0.00486	0.00774	0.01764	0.02036	0.02328	0.02499	0.02455	0.01879	0.00644	0.00445	0.00340
2019	0.00389	0.00438	0.00696	0.01588	0.01833	0.02095	0.02249	0.02210	0.01691	0.00580	0.00400	0.00306

Finally, we spatially and temporally interpolate between the years 1974, 1985, 1994, 1999, 2006, and 2019 to create a monthly time series of maximum ET rates spanning the entire calibration period. These maximum ET rates were used in the MODFLOW Segmented Function Evapotranspiration (ETS1) package to calculate the percentage of ET derived from groundwater.

Relationship between depth to groundwater and the rate of evapotranspiration from groundwater

The 2020 model used the MODFLOW Segmented Function Evapotranspiration (ETS1) package to calculate the percentage of maximum ET derived from groundwater. The ETS1 package is an improvement from the MODFLOW Evapotranspiration (EVT) package, used in the 2013 model, because it allows for a more realistic relationship between depth to groundwater and the rate of ET from groundwater. Figure B-18-2 compares the depth to groundwater vs the rate of ET from groundwater curves used in the CVM to the one used in the 2013 model. The main differences between the two curves are listed below:

1. Previously, in the 2013 model, when the water level was above the ground surface, the rate of ET from groundwater was equal to the maximum ET rate. However, at high water-table elevations, the root system becomes oxygen deficient and transpiration rates decrease until the plants die of anoxia (Maddock et al. 2012). To better simulate this behavior, in the 2020 model, when the water level was at or above the ground surface, the ET rate from groundwater decreased from the maximum ET rate when the water level was at the ground surface to zero when the water level was 5 ft or greater above the ground surface..
2. Previously, in the 2013 model, the extinction depth, which is the depth to groundwater below which the roots cannot obtain water and the ET rate from groundwater is zero, was set to 30 ft. However, the literature suggests that the extinction depth of shallow-rooted riparian vegetation like cottonwoods and willows, which are the dominant species found in the Prado Basin, more commonly ranges from 10 to 25 ft (Leake et al. 2008, Ma et al. 2001, Springer et al. 1999, Stamos et al. 2001). Therefore, the 2CVMused an extinction depth of 20ft below the ground surface.

References

Leake, Stanley A., Pool, Donald R., Leenhouts, James M. 2008. Simulated Effects of Ground-Water Withdrawals and Artificial Recharge on Discharge to Streams, Springs, and Riparian Vegetation in the Sierra Vista Subwatershed of the Upper San Pedro Basin, Southeastern Arizona: Scientific Investigations Report 2008–5207. U.S. Department of the Interior and U.S. Geological Survey.

Lines, Gregory C. and Bilhorn, Thomas W. 1996. Riparian Vegetation and Its Water Use During 1995 Along the Mojaven River, Southern California: Water-Resources Investigation Report 96-4241. U.S. Geological Survey

Ma, T.S., Hathaway, D.L., Hobson, A. 2001. MODFLOW Simulation of Transient Surface Water/Groundwater Interactions in a Shallow Riparian Zone Using HEC-2-Based Water Surface Profiles. MODFLOW 2001 and Other Modeling Odysseys, International Groundwater Modeling Center (IGWMC), Colorado School of Mines, Golden, Colorado, September 11-14, 2001. In MODFLOW 2001 and Other Modeling Odysseys, Proceedings. 425-431.

Maddock, Thomas, III, Baird, K.J., Hanson, R.T., Schmid, Wolfgang, Ajami, Hoori. 2012. RIP-ET: A riparian evapotranspiration package for MODFLOW-2005: U.S. Geological Survey Techniques and Methods 6-A39.

Merkel and Associates. 2006. Evapotranspiration Analysis of the Prado Basin Santa Ana River, California. Prepared for Wildermuth Environmental, Inc.

Springer, Abraham E., Wright, Julie M., Shafroth, Patrick B., Stromberg, Juliet C., Patten, Duncan T. 1999. Coupling groundwater and riparian vegetation model to assess effects of reservoir releases. Water Resources Research. Vol. 35, No.12, pp. 3621-3630.

Stamos, Christina L., Martin, Peter, Nishikawa, Tracy, Cox, Brett F. 2001. Simulation of Ground-Water Flow in the Mojave River Basin, California: Water-Resources Investigations Report. U.S. Geological Survey.The objective of this technical memorandum is to describe the steps to calculate the volume of groundwater discharged from aquitards due to land subsidence in the Management Zone 1 (MZ1) of the Chino Valley Watershed.

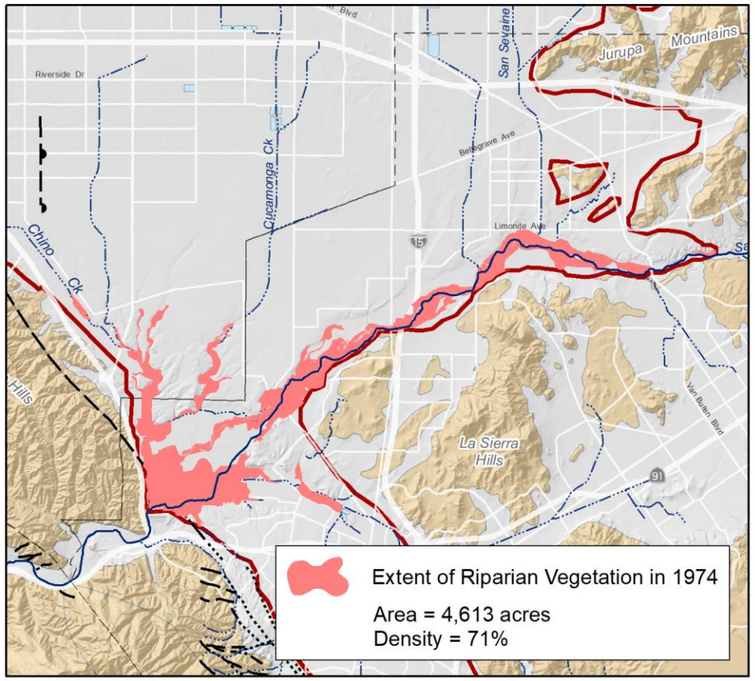

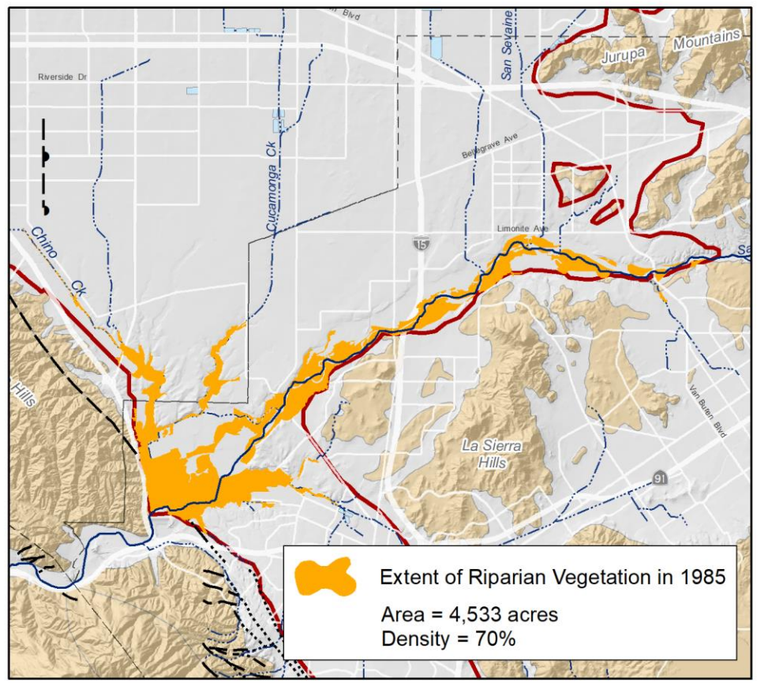

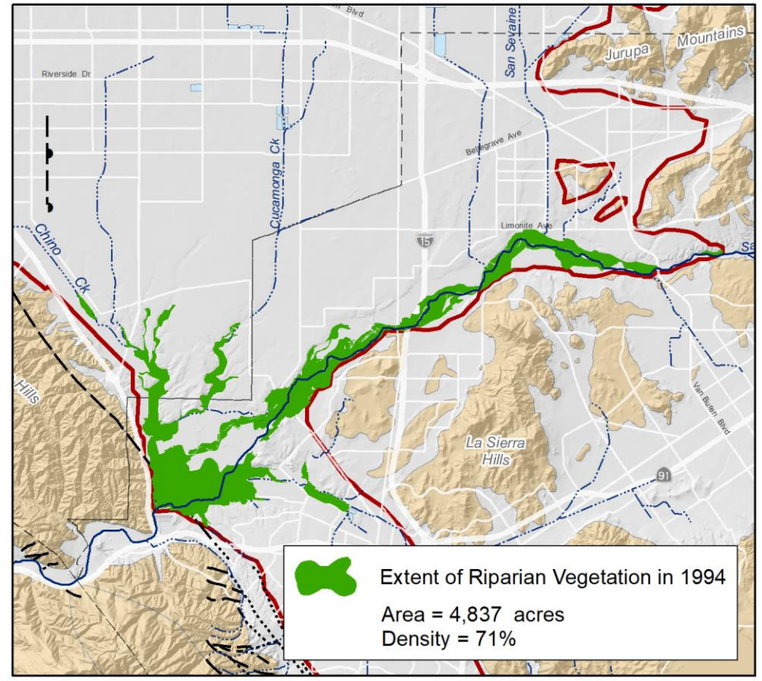

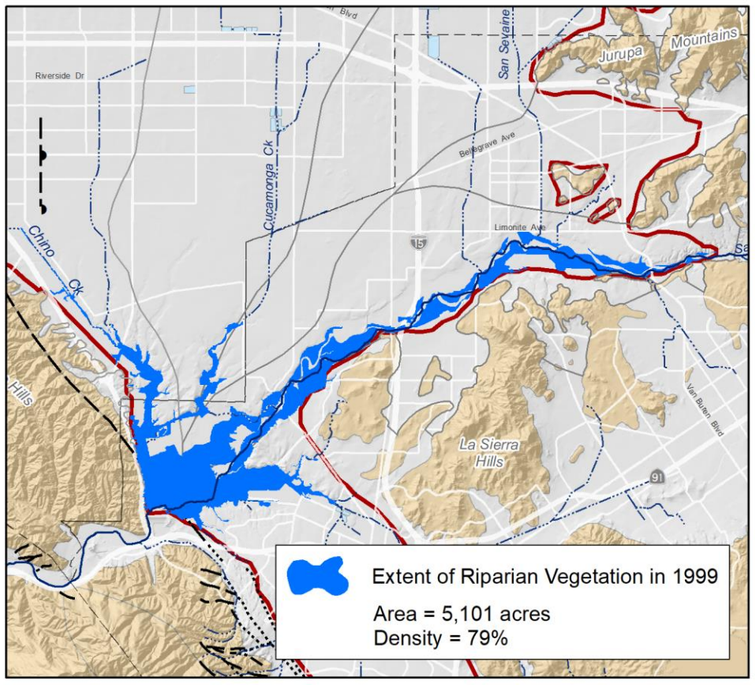

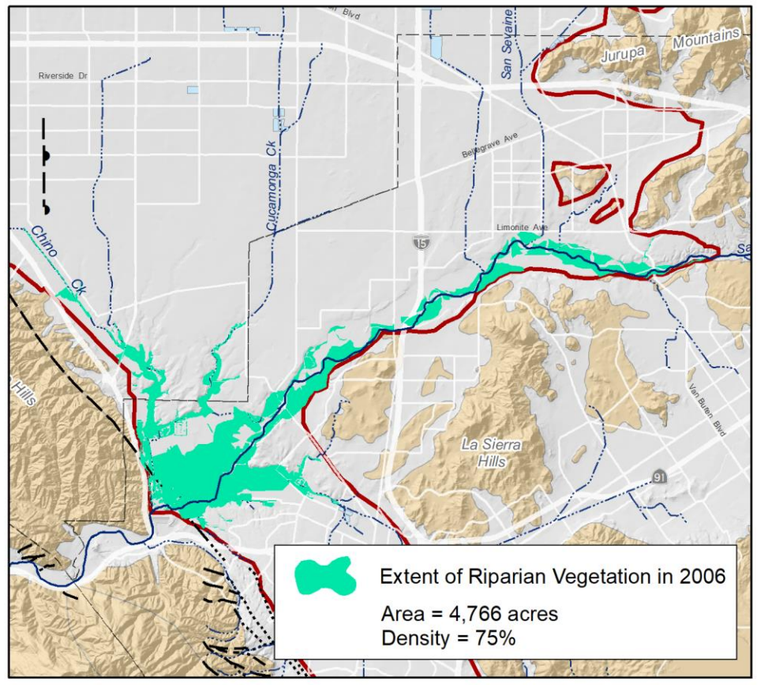

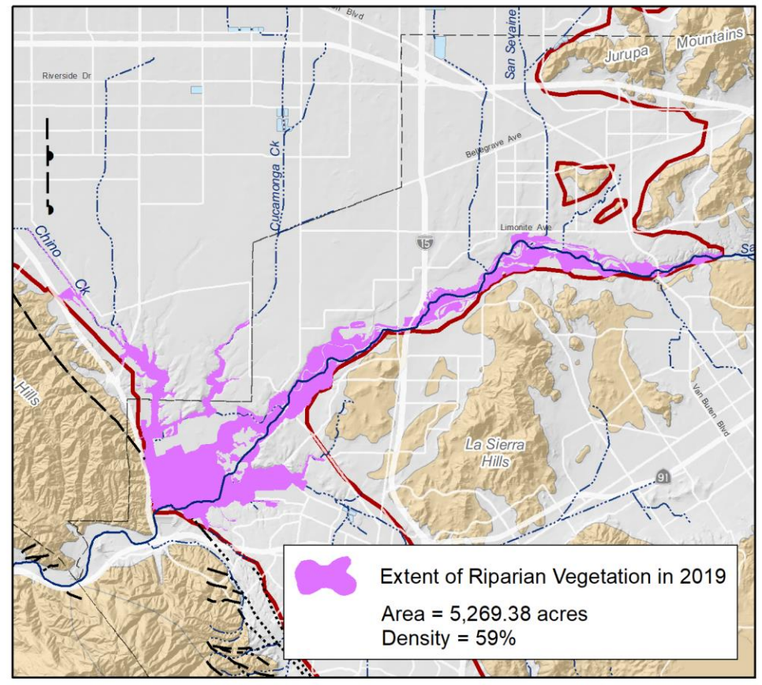

Produced by:

WEI
Wildermuth Environmental, Inc.

Date: 4/1/2020

Document Name: Figure B-18-1 Riparian Veg

0 1 2 3 4 5 Miles

0 1 2 3 4 KM

Chino Basin Watermaster

2020 Safe Yield Recalculation

Extent of Riparian Vegetation

1974, 1985, 1944, 1999, 2006, and 2019

Figure B-18-1

Figure B-18-2: Relationship Between Depth to Groundwater and Rate of Evapotranspiration from Groundwater for MODFLOW's ETS and EVT Packages

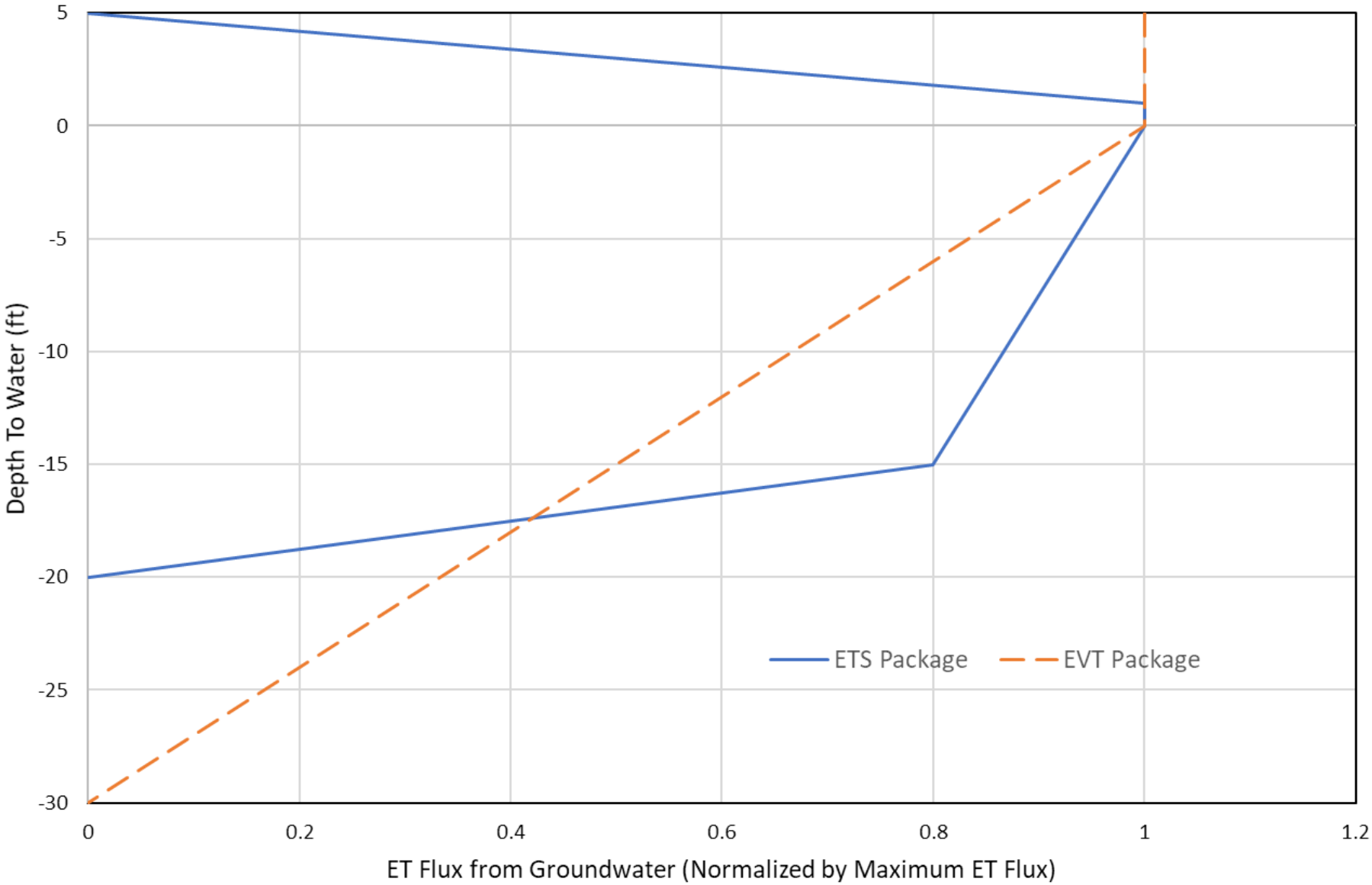

TECHNICAL MEMORANDUM

February 11, 2020

RE: Technical Memorandum for Onsite Wastewater Disposal Systems

Objective

The objective of this technical memorandum is to describe the steps to estimate the septic tank recharge values that were used in the Chino Valley Model for 2020 Safe Yield Recalculation.

Calculation Methodology and Assumptions

The following steps were carried out to estimate the volume of groundwater recharge from septic tanks.

1. The data of the parcels with existing septic tanks were collected. The attached figure below shows the locations of those parcels and the boundary of the groundwater model for 2020 Safe Yield Recalculation.
2. The septic tank parcel data were overlaid on the groundwater model. The numbers of septic tank parcels within each of the model cells were determined.
3. For each model cell, the number of septic tank parcels was multiplied with the following numbers. The results were added to the groundwater recharge flux of that model cell.

   1978 to 2008: 270 gallons/day
   2009 to 2014: 206 gallons/day
   2014 forward: 180 gallons/day

Wildermuth Environmental, Inc.
23692 Birtcher Dr.
Lake Forest, CA 92630

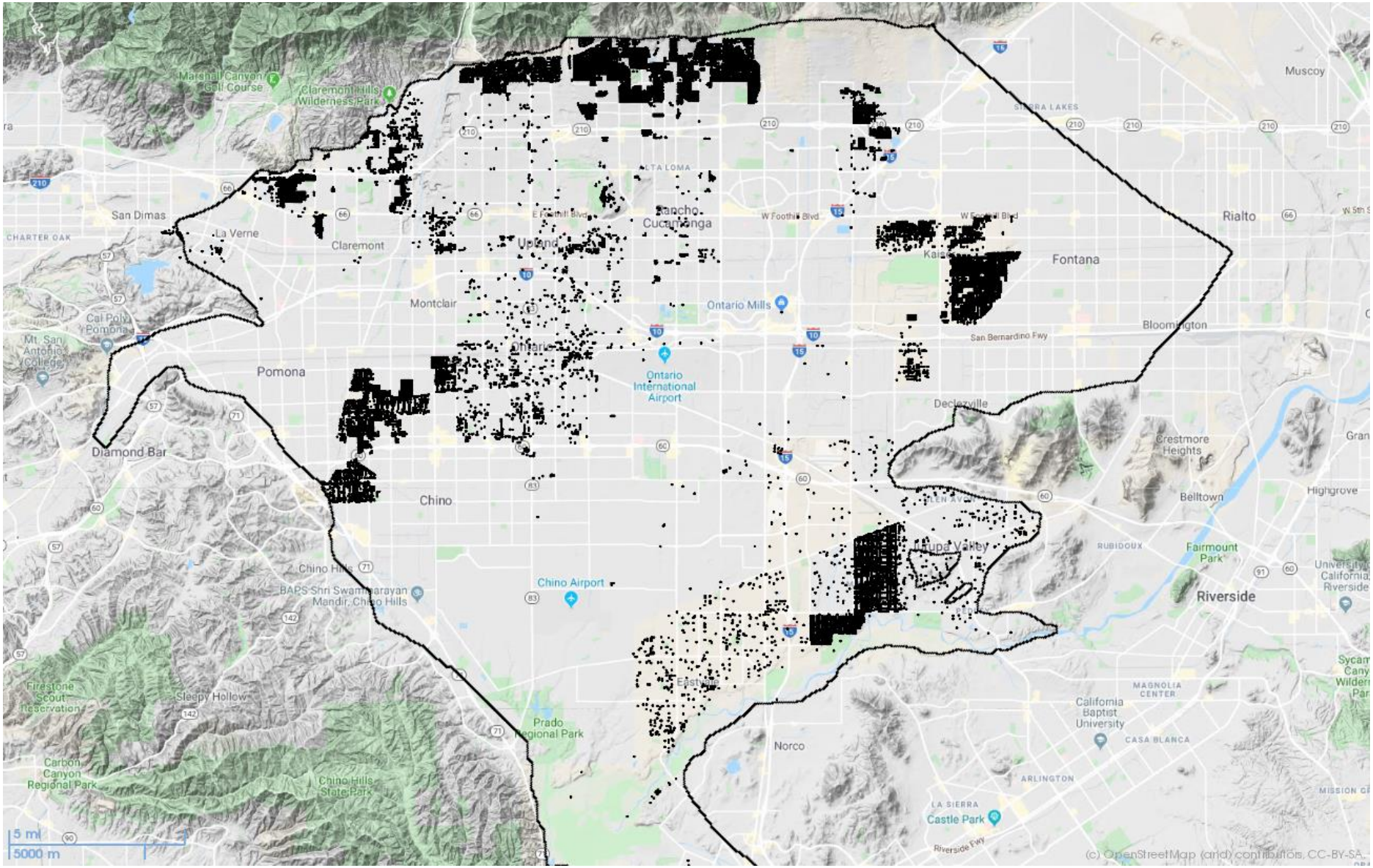

Figure B-19 Parcels with Existing Septic Tanks

TECHNICAL MEMORANDUM

February 11, 2020

RE: Groundwater discharged from aquitards due to land subsidence

Objective

The objective of this technical memorandum is to describe the steps to calculate the volume of groundwater discharged from aquitards due to land subsidence in the Management Zone 1 (MZ1) of the Chino Valley Watershed.

Calculation Methodology and Assumptions

The volume of groundwater discharged from aquitards caused by land subsidence is assumed to be equal to the volume of land surface displacement. The following steps were carried out for the calculation.

1. The LiDAR data of the cumulative land surface displacement from March 2011 to March 2019 was rasterized. The shaded area of the figure below shows the coverage of the rasterized LiDAR data. This area corresponds to the area of greatest recent land subsidence in the Chino Basin
2. The rasterized LiDAR data was imported to the model cells (of the Chino Valley Model for 2020 Safe Yield Recalculation). The volume of land surface displacement at a model cell is equal to the product of the cell area and the vertical displacement in that cell.
3. The volume of displacement for an area of interest is equal sum of the cellular volumes calculated in step 3 over the area of interest.
4. The volume of groundwater discharged from aquitards due to land subsidence of all active model cells within MZ1 is calculated as 1,445 af or 181 afy.
5. The volume of groundwater discharged from aquitards due to land subsidence of all active model cells within the rasterized LiDAR coverage is calculated as 2100 af or 263 afy.

As to the Chino Basin, the average recharge created by land subsidence in the last 8 years was about 181 afy and the average total recharge, exclusive of recharge contributed by land subsidence in the planning period is estimated to be about 188,000 afy. If the rate of land subsidence continued throughout the planning period, it would contribute about 0.09 percent of the total recharge over the planning period and thus subsidence is not projected to be a significant source of recharge to the basin for the 2020 Safe Yield calculation. Since the magnitude of this recharge is negligible and Watermaster is currently developing a land subsidence plan to abate or minimize future land subsidence, the contribution from land subsidence was excluded from the 2020 Safe Yield calculation

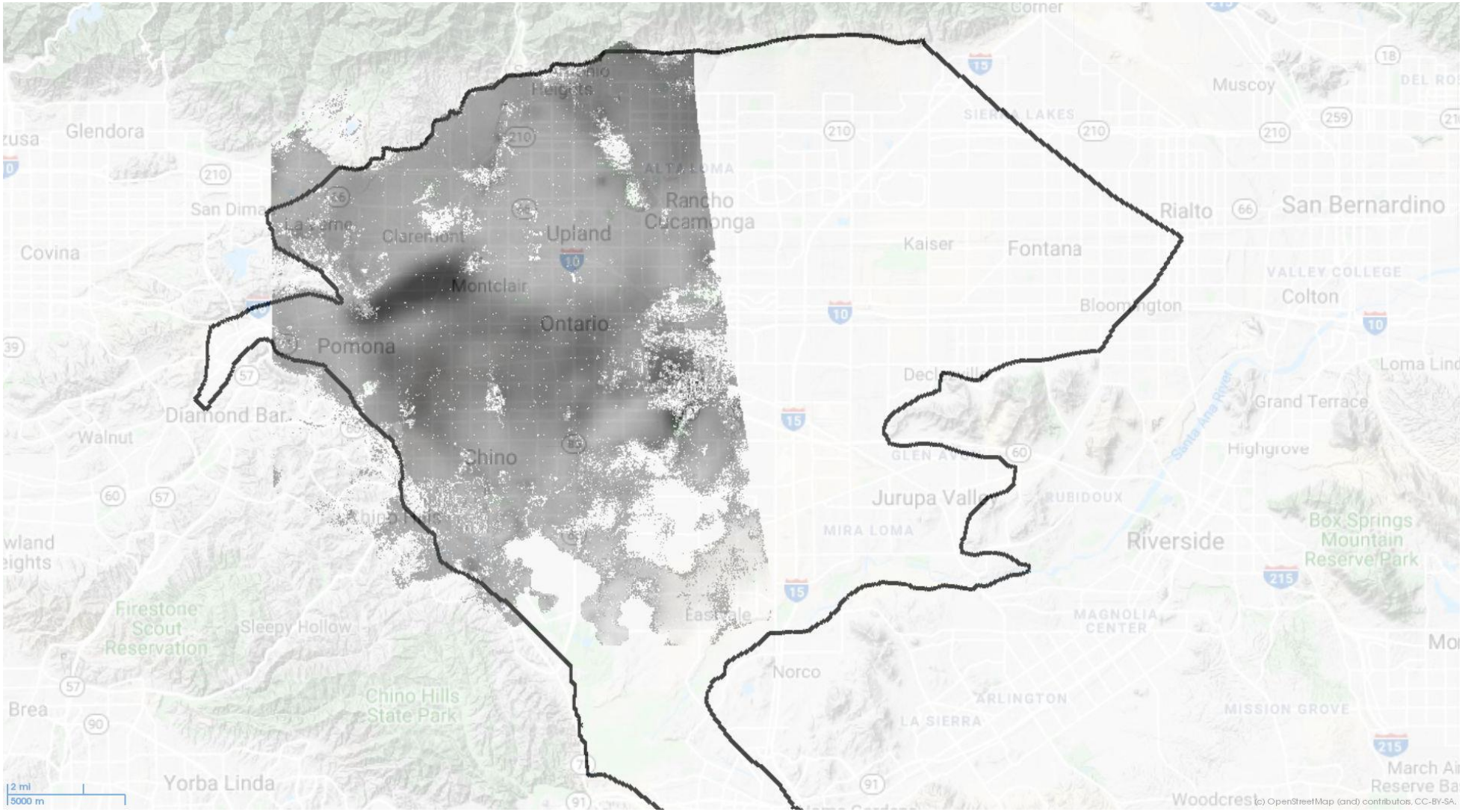

Figure B-20 Coverage of the Rasterized LiDAR Data

Appendix C

Time-History Plots of Simulated and Measured Groundwater Elevations in the Wells Used in Model Calibration 1977 - 2018

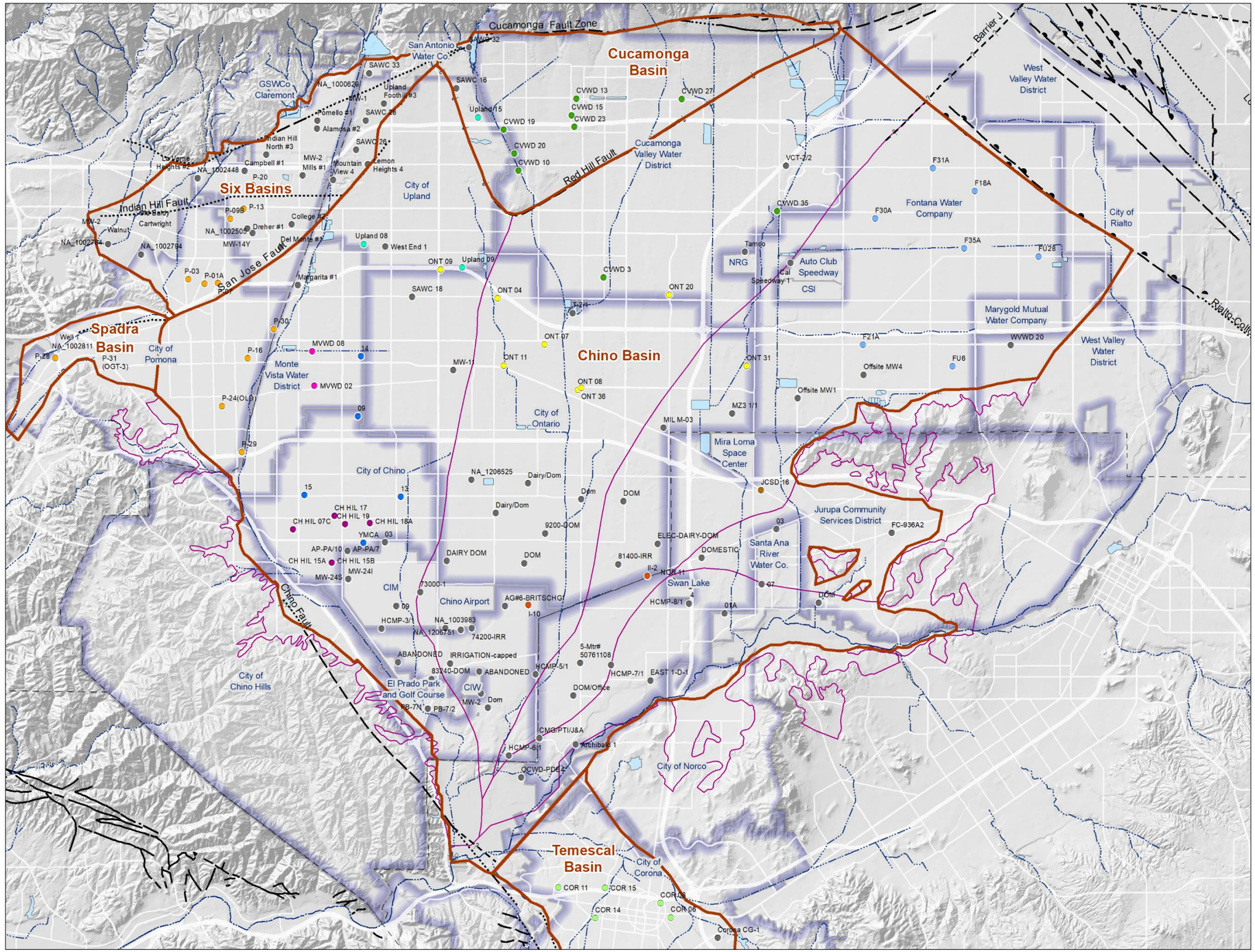

Groundwater Model Calibration Wells

- City of Chino
- City of Chino Hills
- City of Corona
- City of Ontario
- City of Pomona
- City of Upland
- Cucamonga Valley Water District
- Fontana Water Company
- Jurupa Community Services District
- Monte Vista Water District
- CDA
- Other

Streams & Flood Control Channels

Flood Control & Conservation Basins

Water Service Area

OBMP Management Zones

Faults

- Location Certain
- Location Approximate
- Approximate Location of Groundwater Barrier
- Location Concealed
- Location Uncertain

Prepared by:

WEI
Wildermuth Environmental, Inc.

Author: LS
Date: 3/13/2020
File: Figure C-1 Calibration Wells.mxd

0 1 2 3 4 5 Miles
0 2 4 6 8 Km

Prepared for:

2020 Safe Yield Recalculation

Chino Basin Watermaster
Partners in Basin Management

Location of Calibration Wells
Chino Valley Model

Figure C-1

Appendix C-1
Comparison of Measured and Simulated Groundwater Water Level
in the Alcoa's Well Offsite MW1

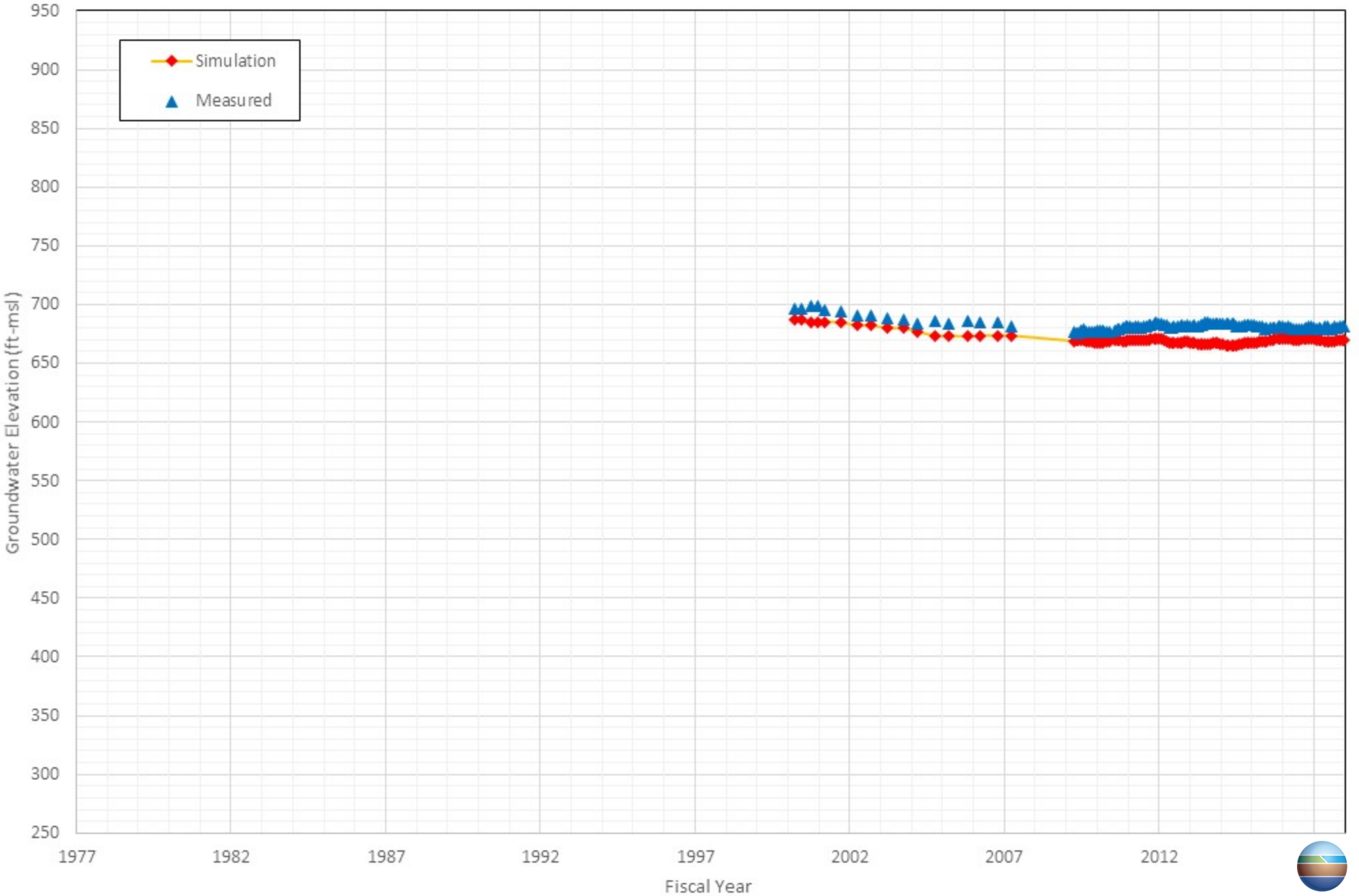

Appendix C-2
Comparison of Measured and Simulated Groundwater Water Level
in the Alcoa's Well Offsite MW4

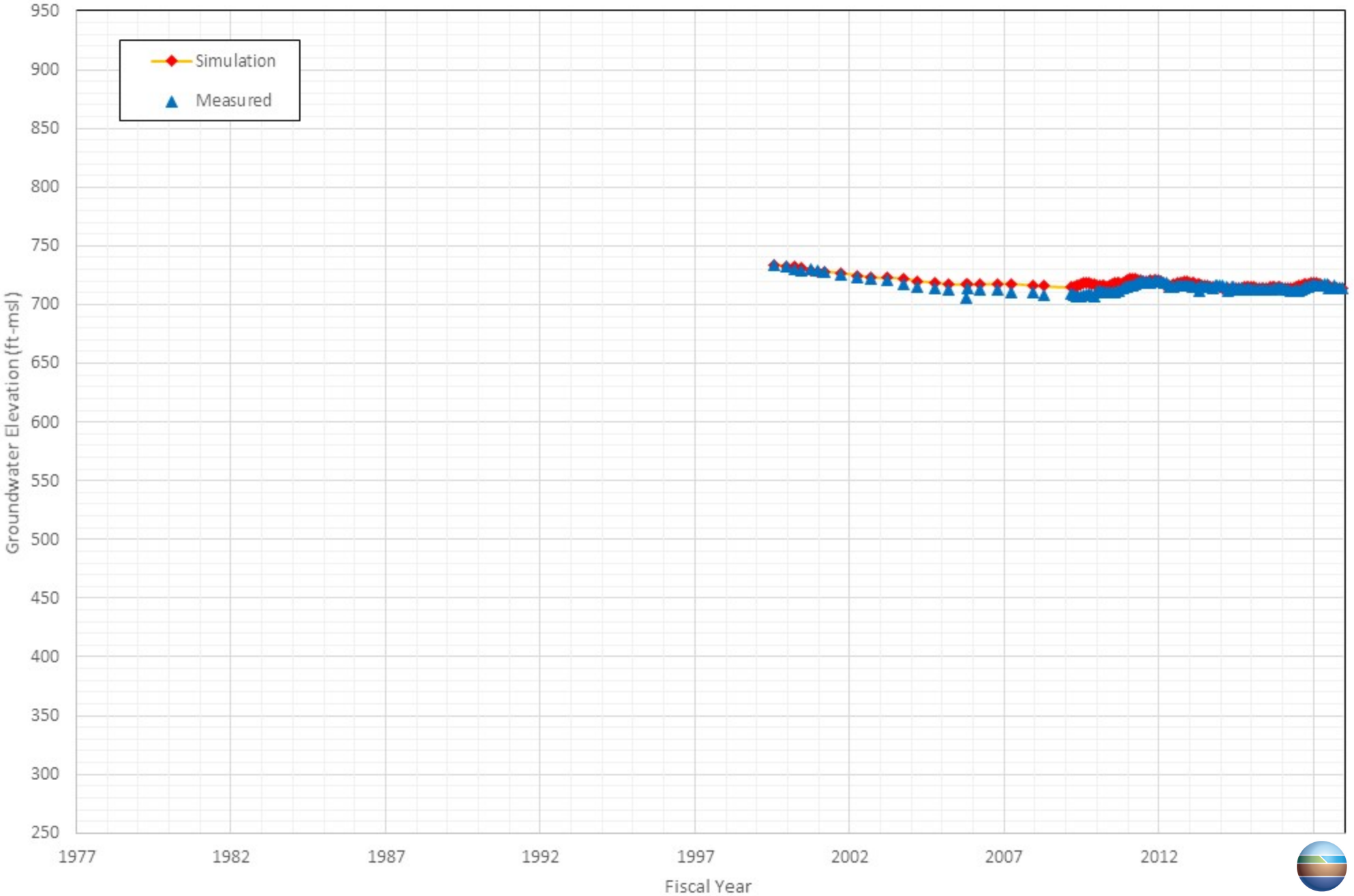

Appendix C-3
Comparison of Measured and Simulated Groundwater Water Level
in the Ameron International Corp.'s Well Tamco

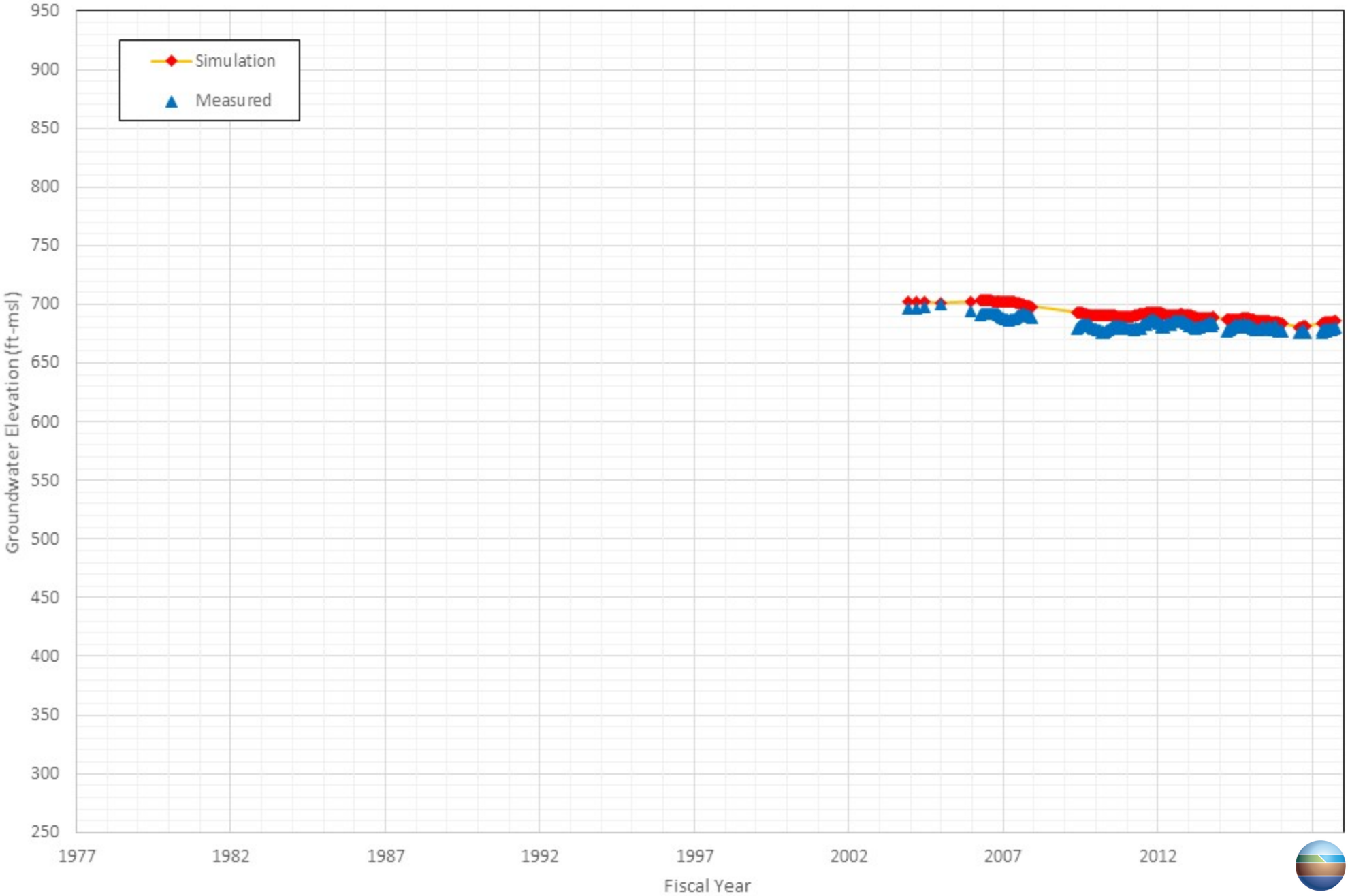

Appendix C-4
Comparison of Measured and Simulated Groundwater Water Level
in the California Speedway's Well Cal Speedway 1

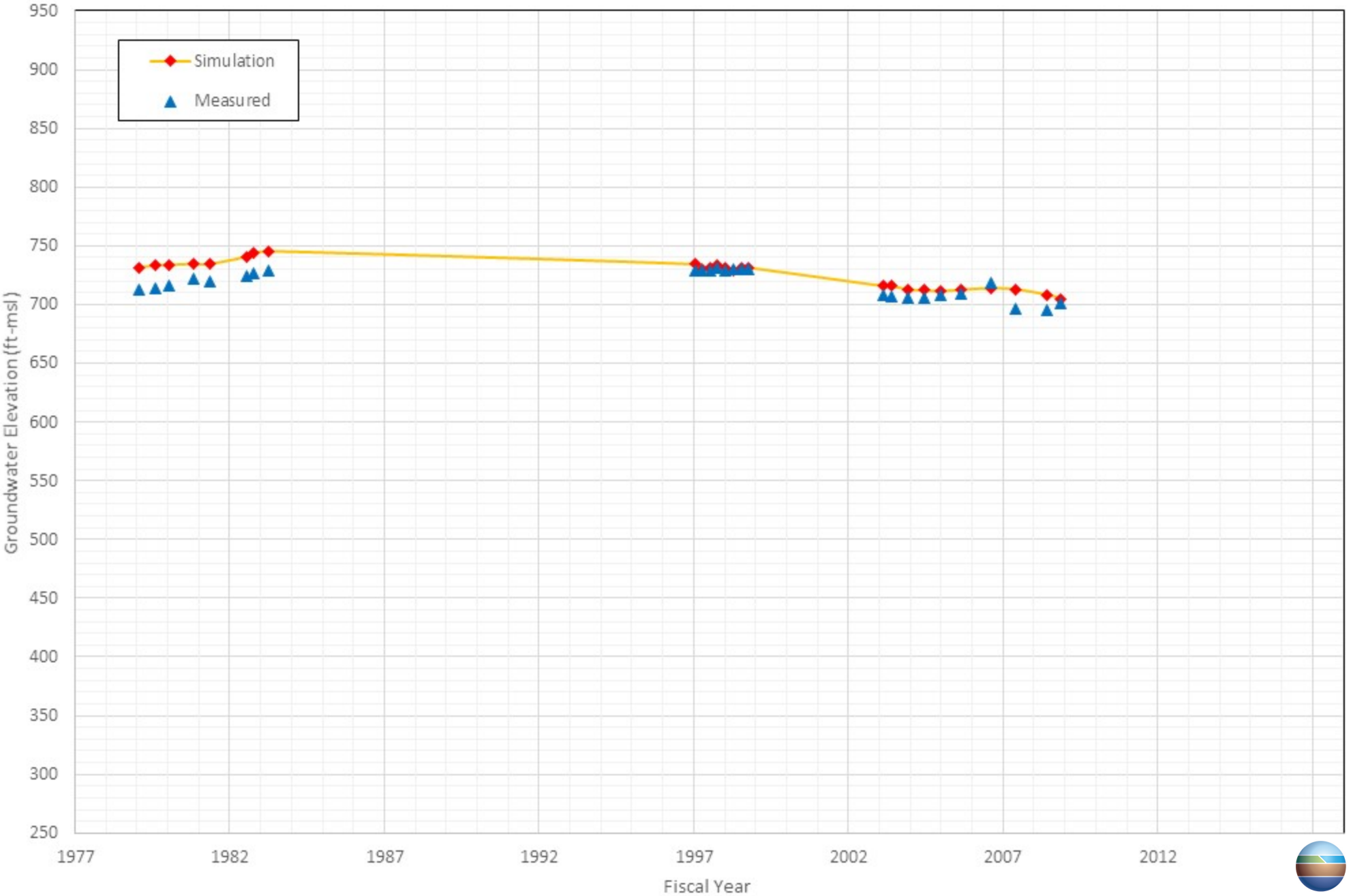

Appendix C-5
Comparison of Measured and Simulated Groundwater Water Level
in the California Youth Authority's Well 73000-1

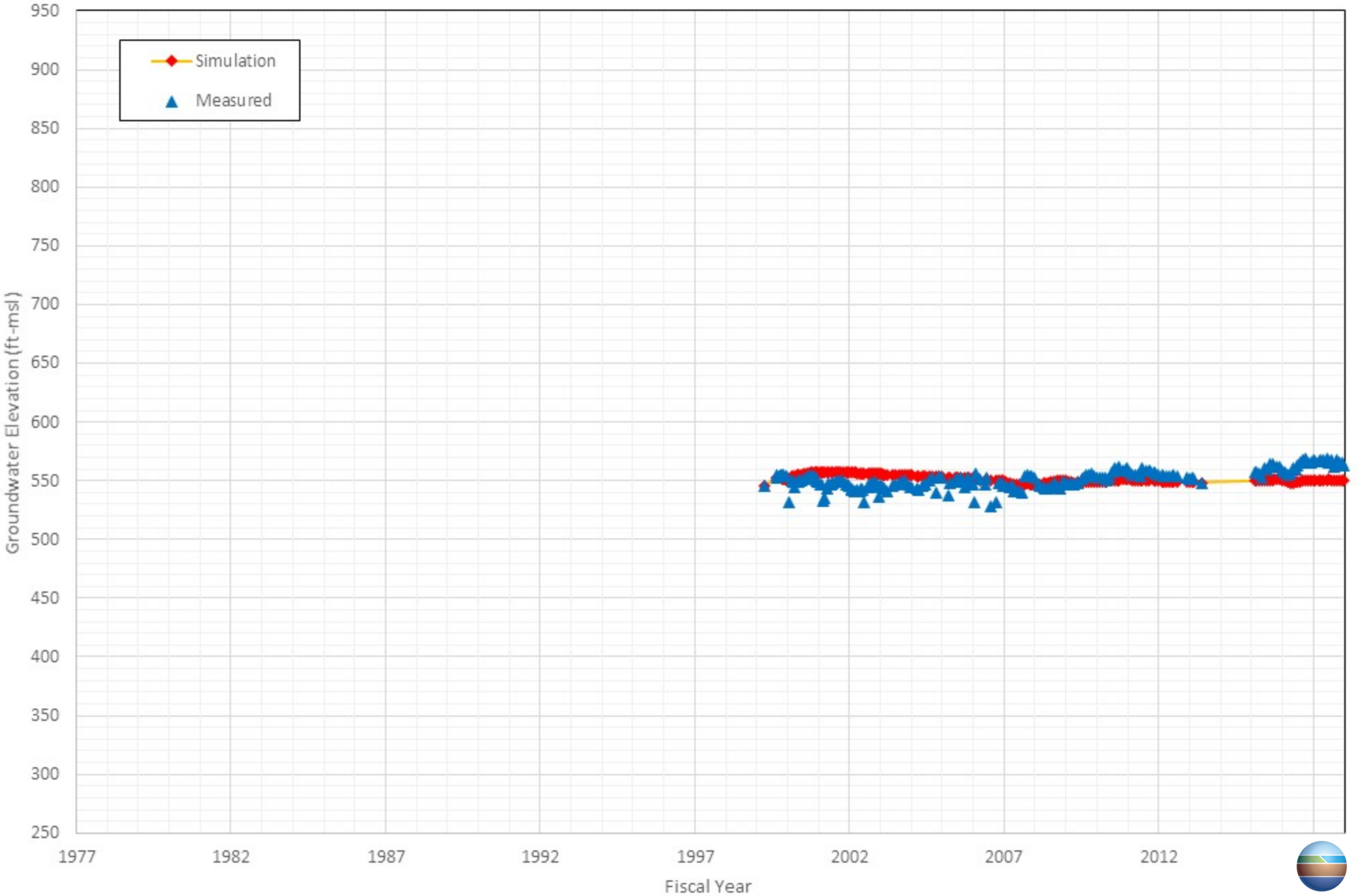

Appendix C-6
Comparison of Measured and Simulated Groundwater Water Level
in the Chino Basin Watermaster's Well AP-PA/10

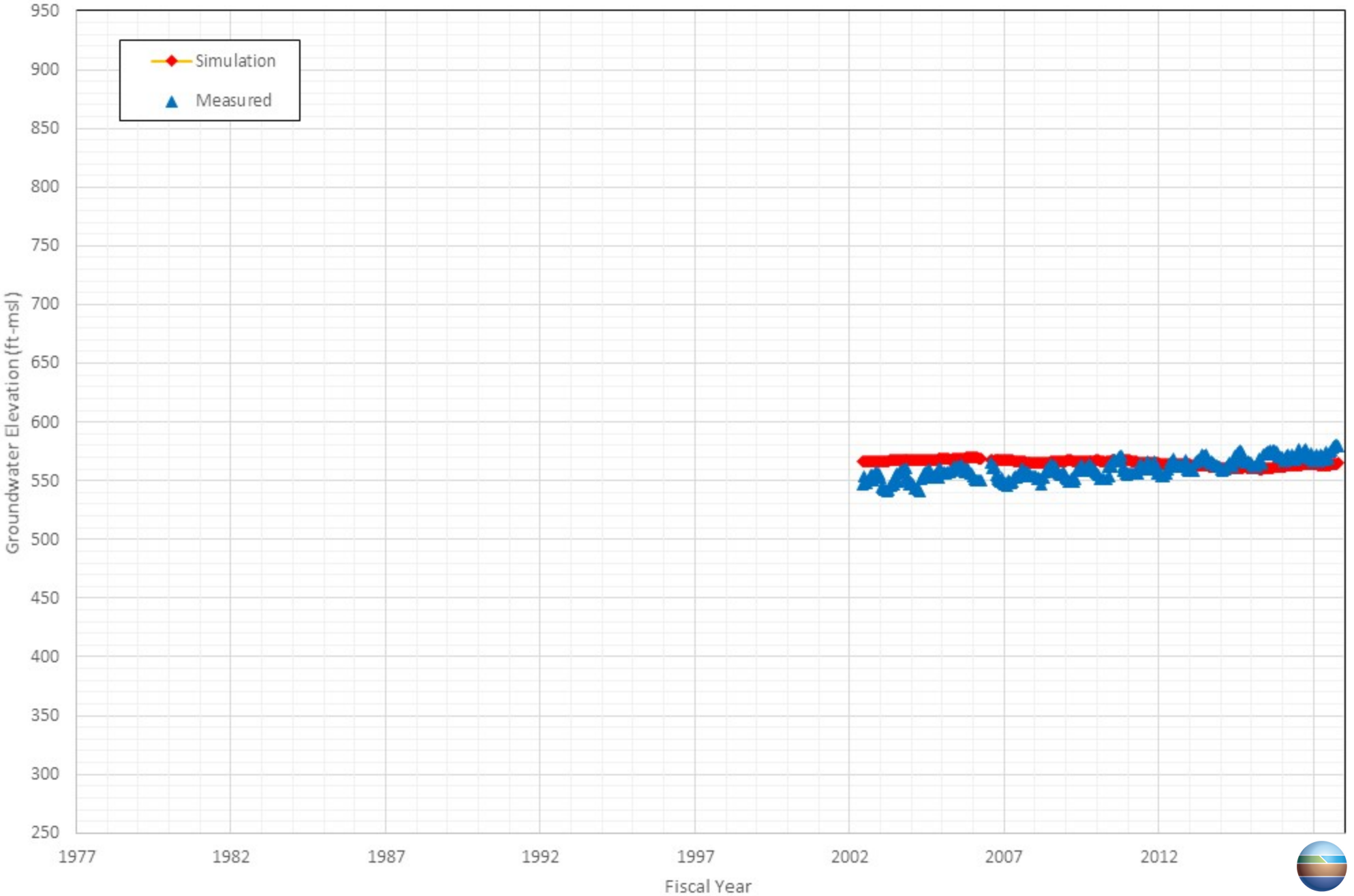

Appendix C-7
Comparison of Measured and Simulated Groundwater Water Level
in the Chino Basin Watermaster's Well AP-PA/7

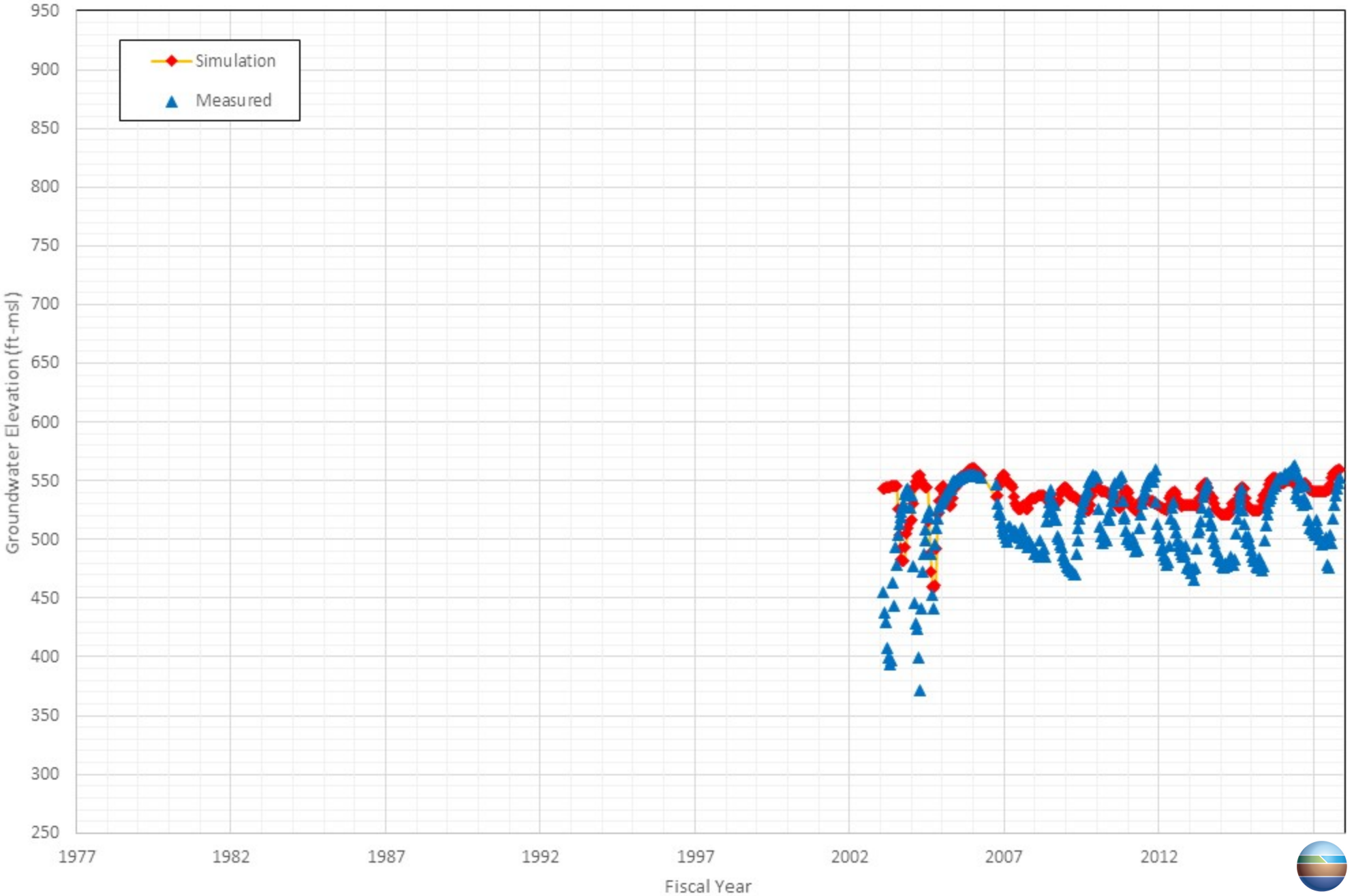

Appendix C-8
Comparison of Measured and Simulated Groundwater Water Level
in the Chino Basin Desalter Authority's Well I-10

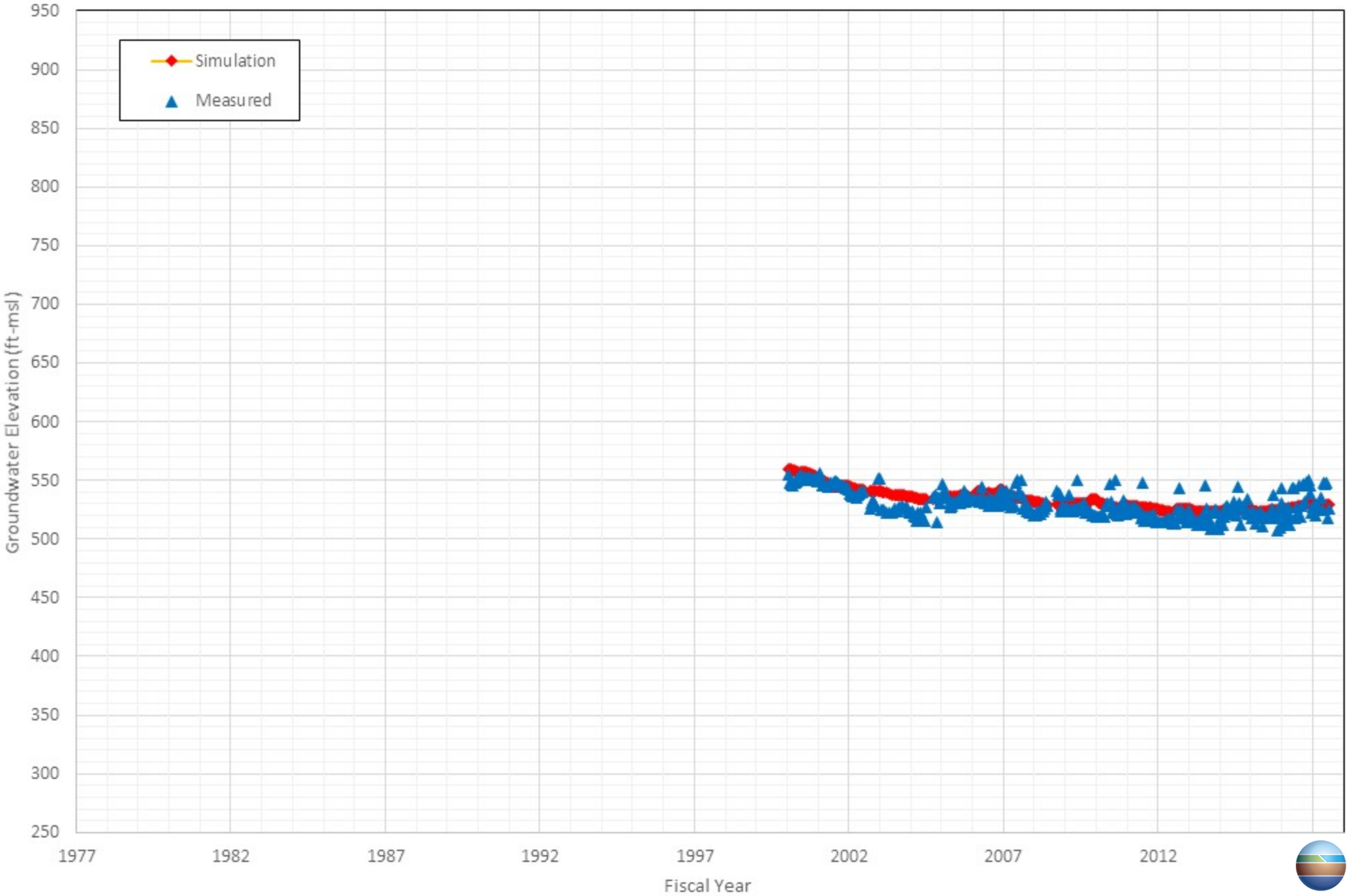

Appendix C-9
Comparison of Measured and Simulated Groundwater Water Level
in the Chino Basin Desalter Authority's Well II-2

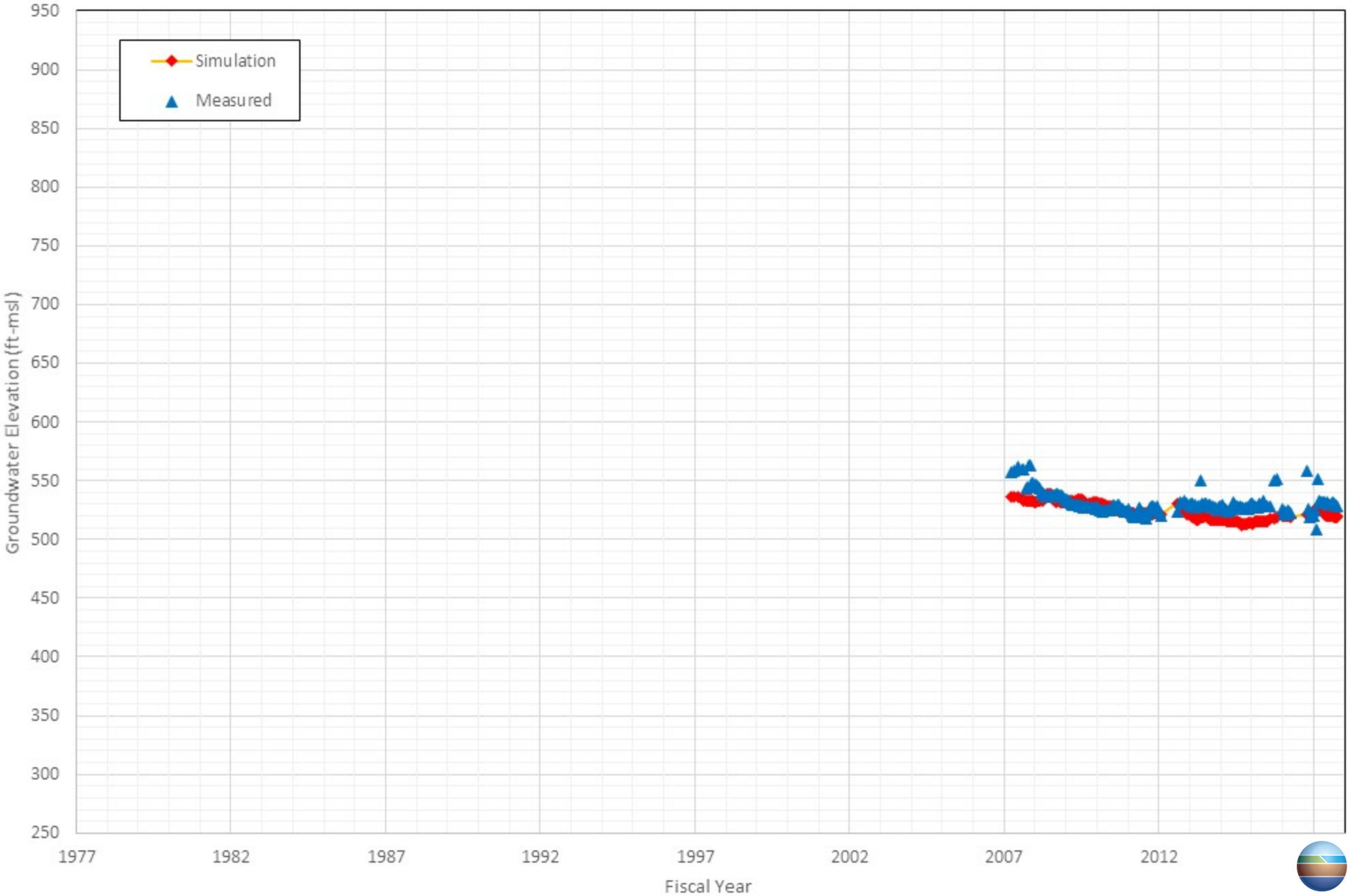

Appendix C-10
Comparison of Measured and Simulated Groundwater Water Level
in the City of Chino's Well 09

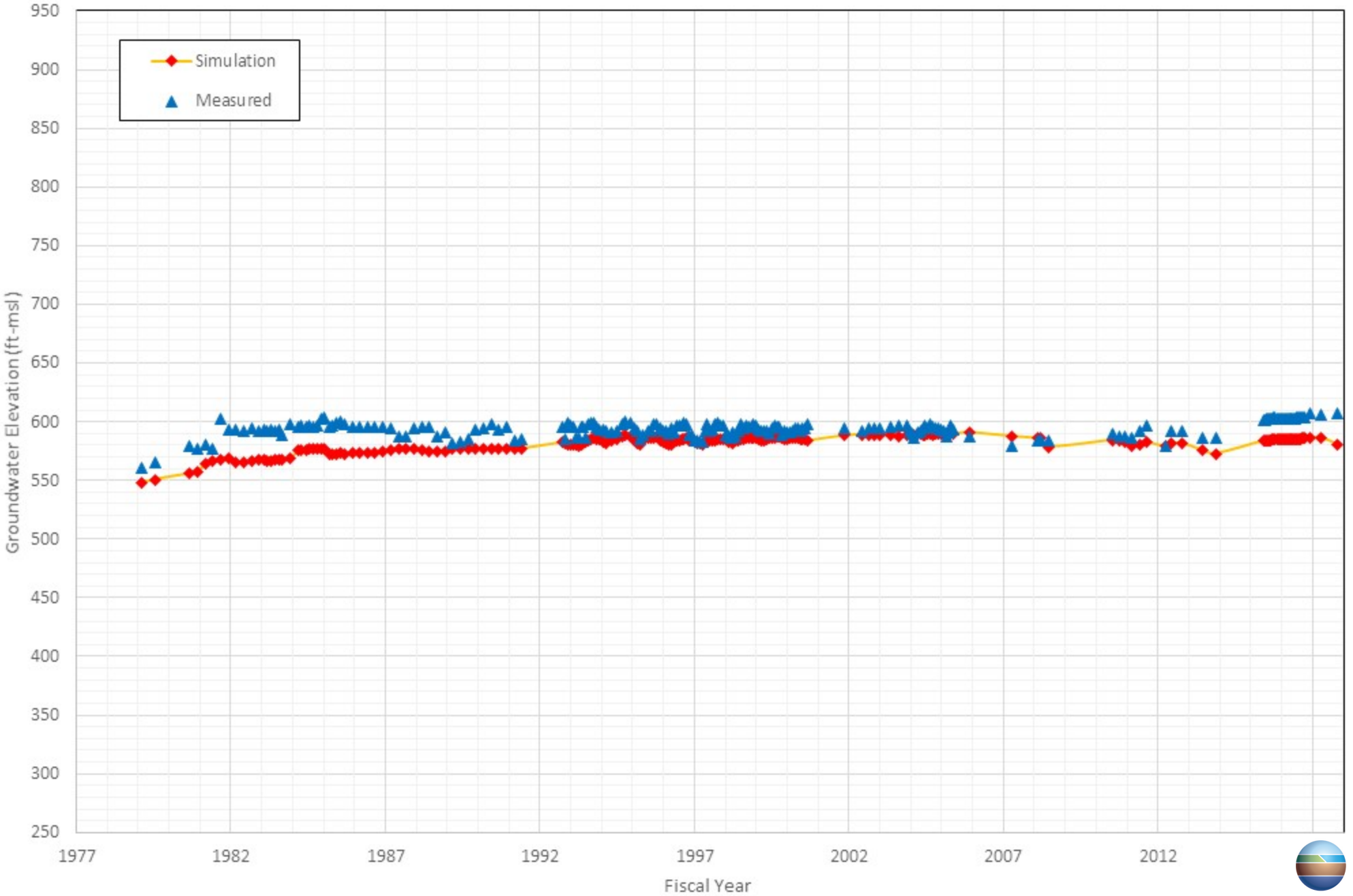

Appendix C-11
Comparison of Measured and Simulated Groundwater Water Level
in the City of Chino's Well 13

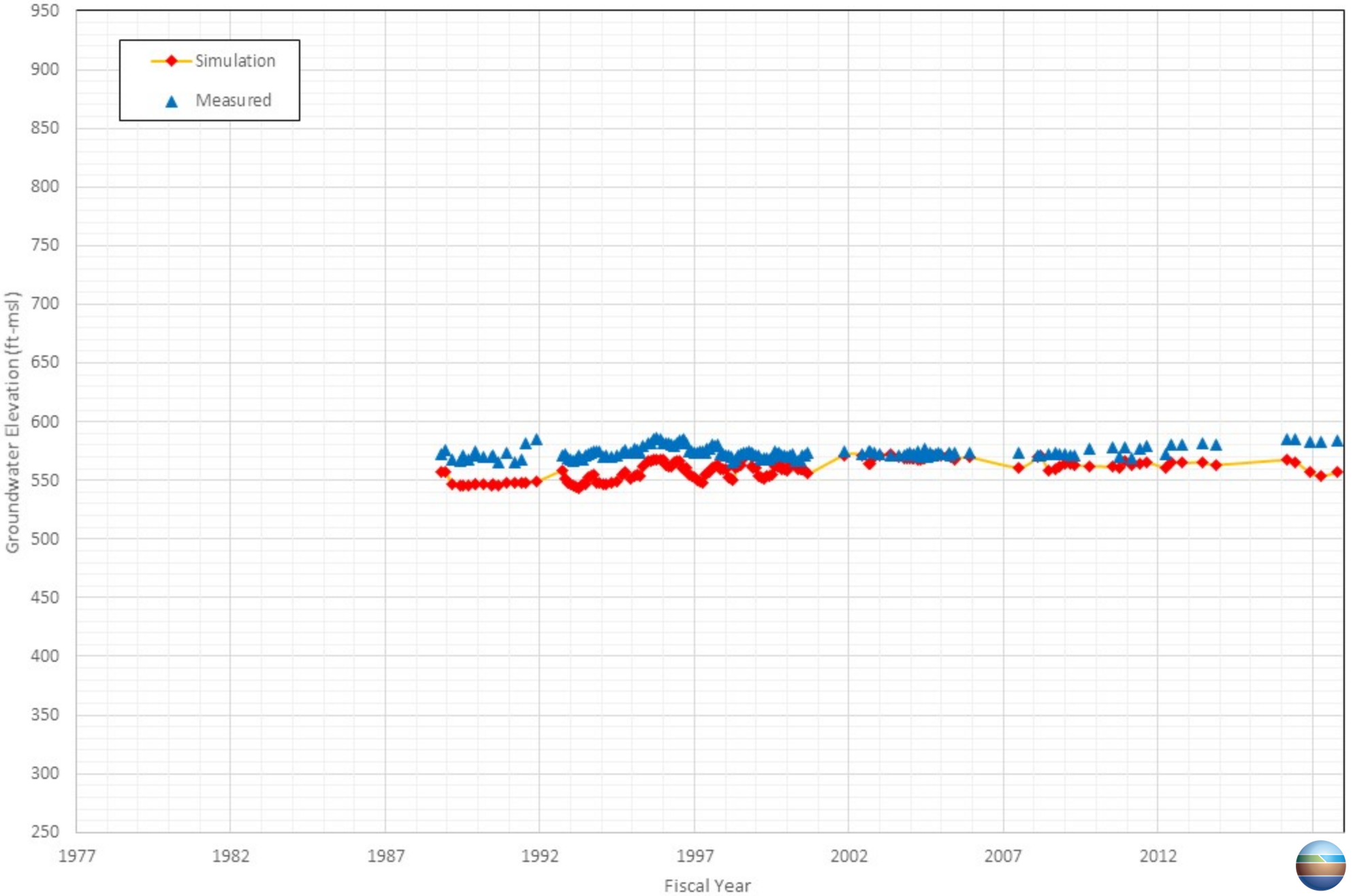

Appendix C-12
Comparison of Measured and Simulated Groundwater Water Level
in the City of Chino's Well 14

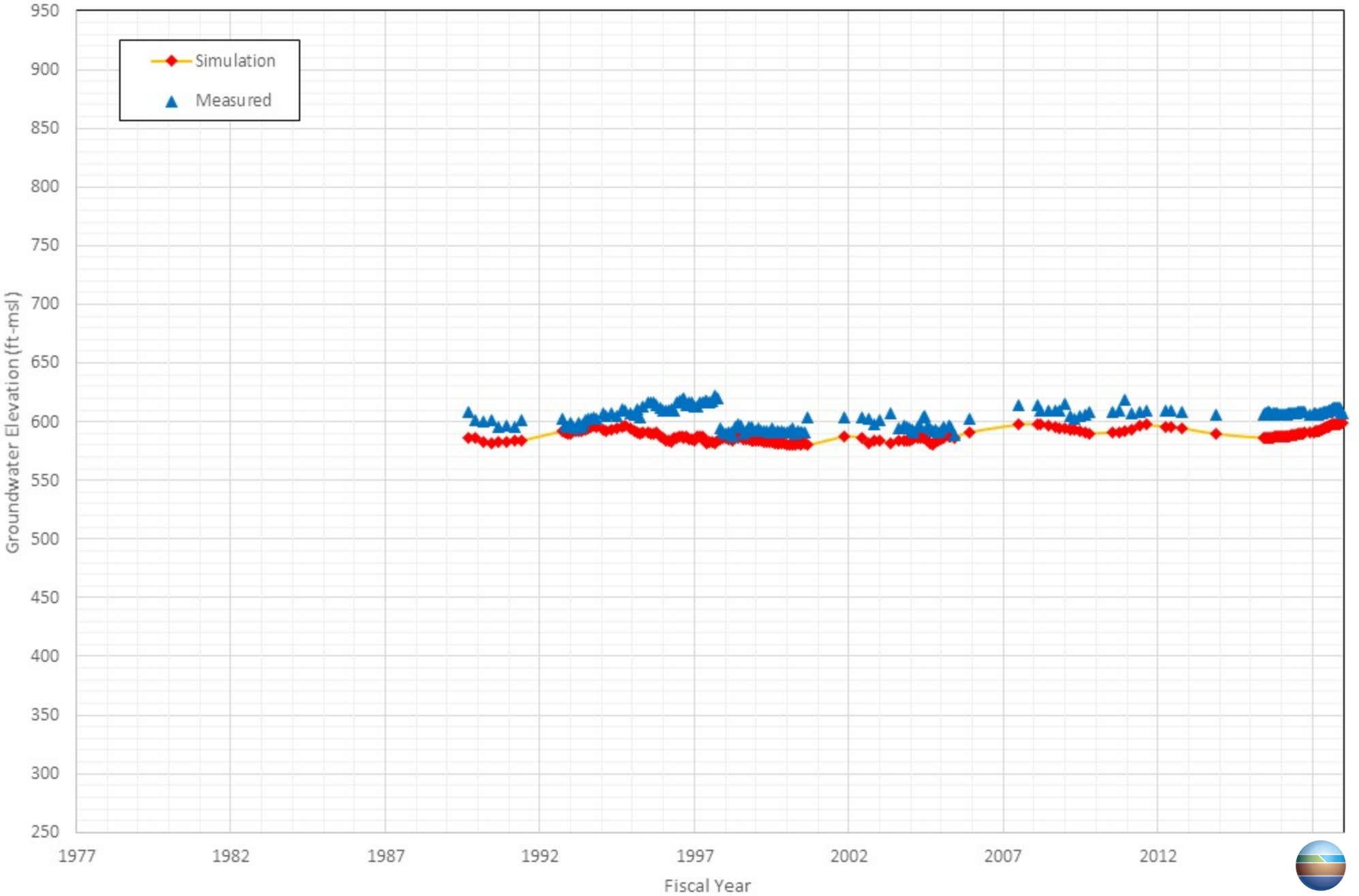

Appendix C-13
Comparison of Measured and Simulated Groundwater Water Level
in the City of Chino's Well 15

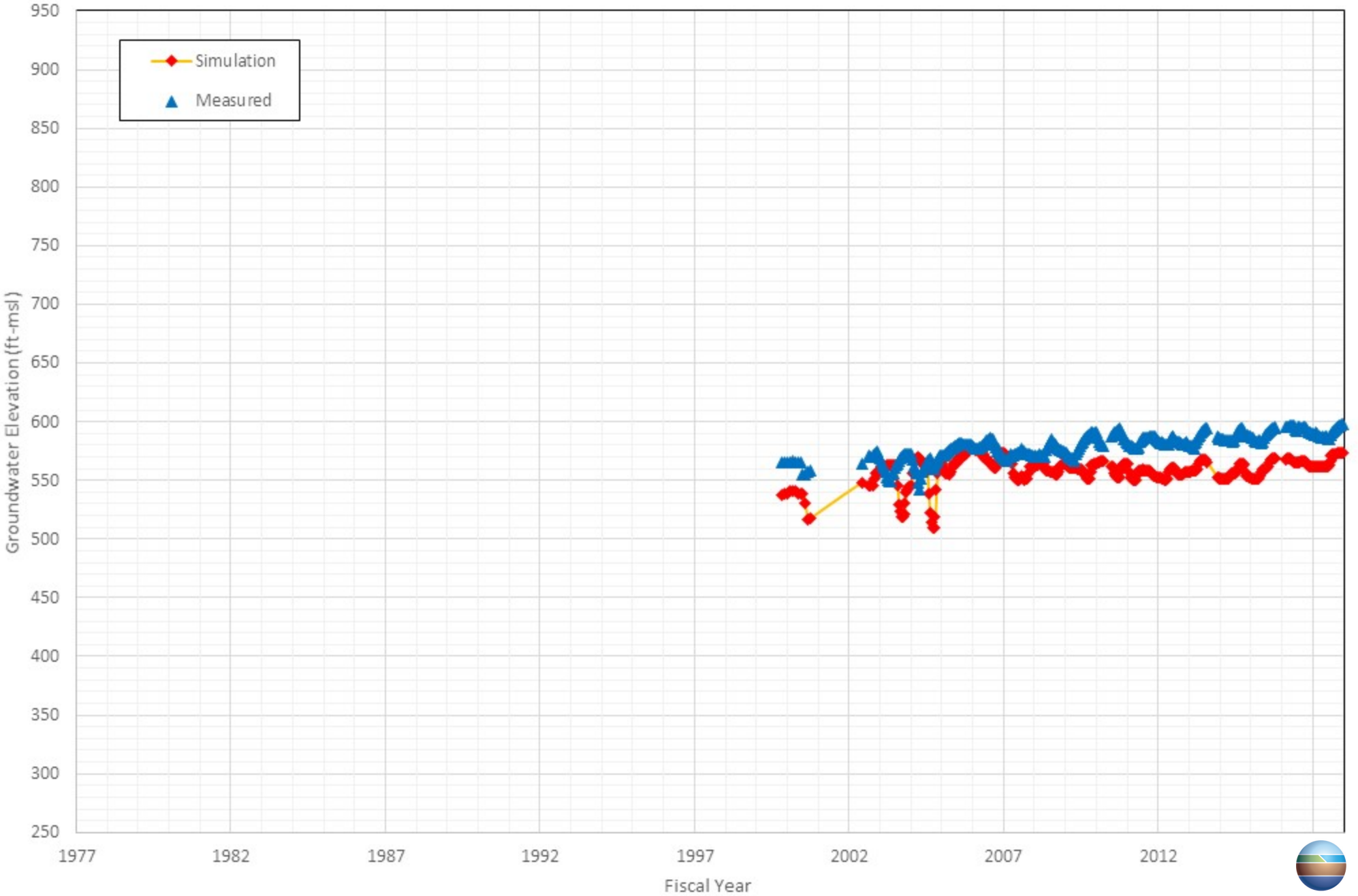

Appendix C-14
Comparison of Measured and Simulated Groundwater Water Level
in the City of Chino's Well YMCA

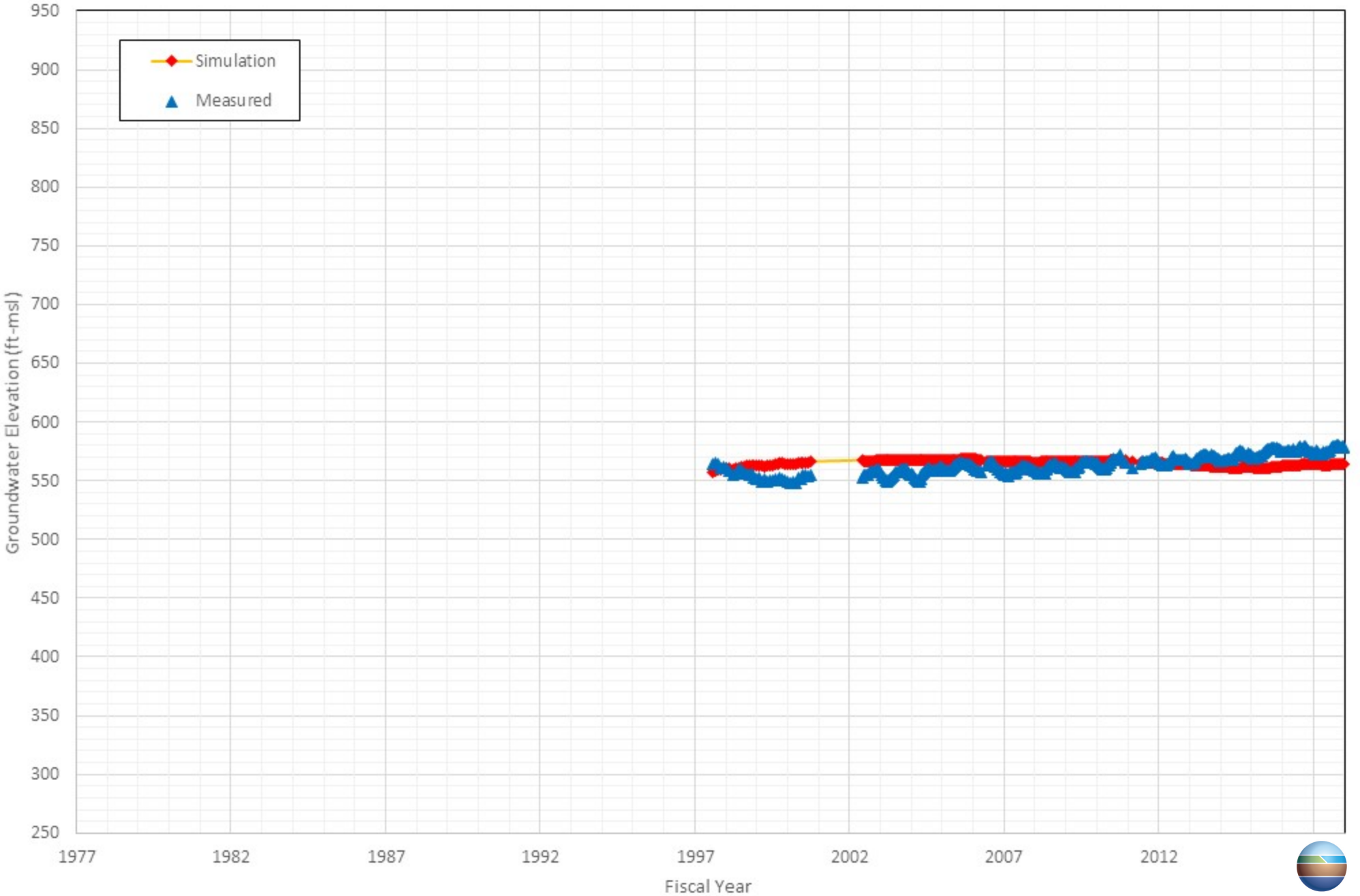

Appendix C-15
Comparison of Measured and Simulated Groundwater Water Level
in the City of Chino Hills's Well CH HIL 07C

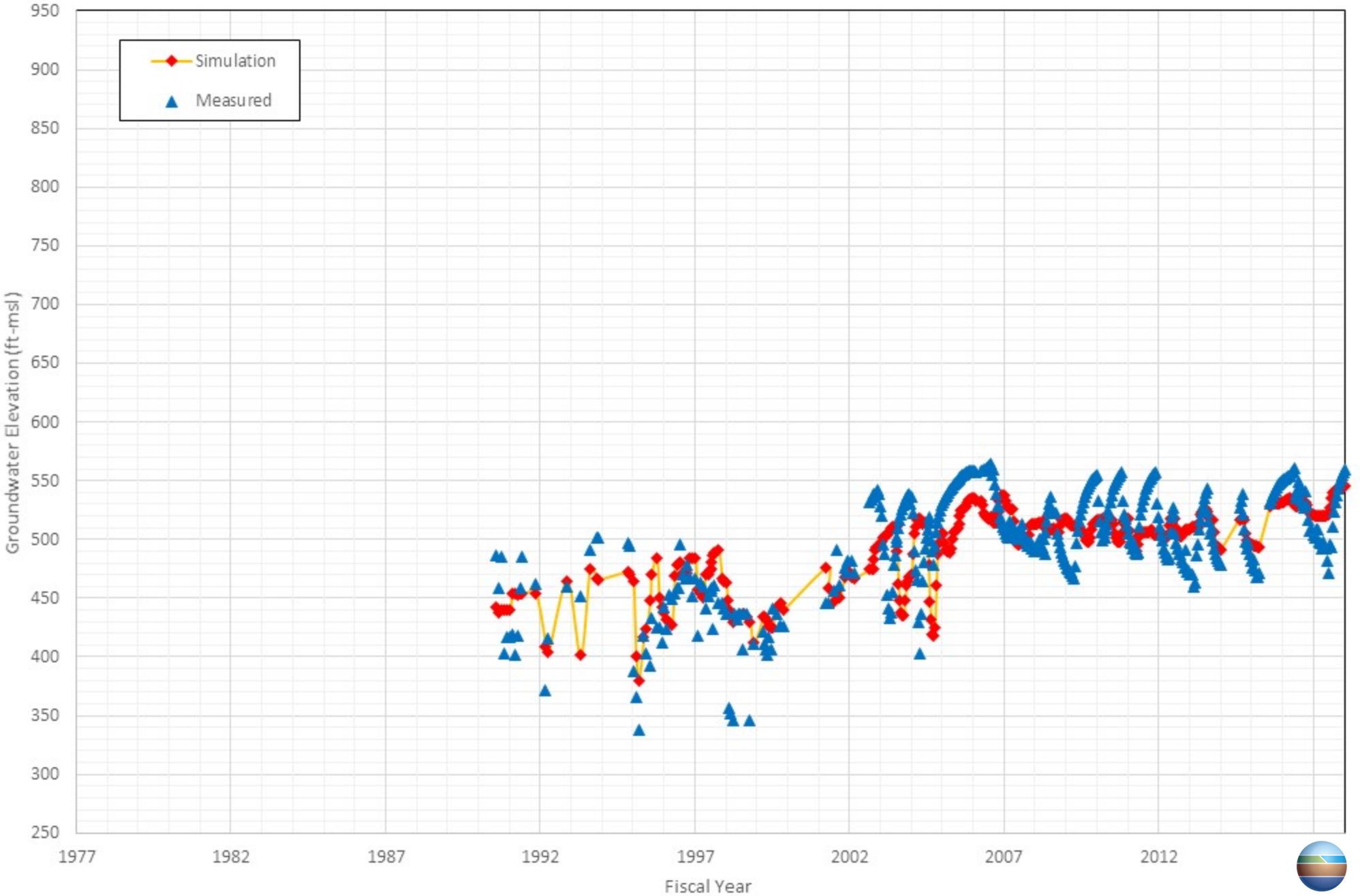

Appendix C-16
Comparison of Measured and Simulated Groundwater Water Level
in the City of Chino Hills's Well CH HIL 15A

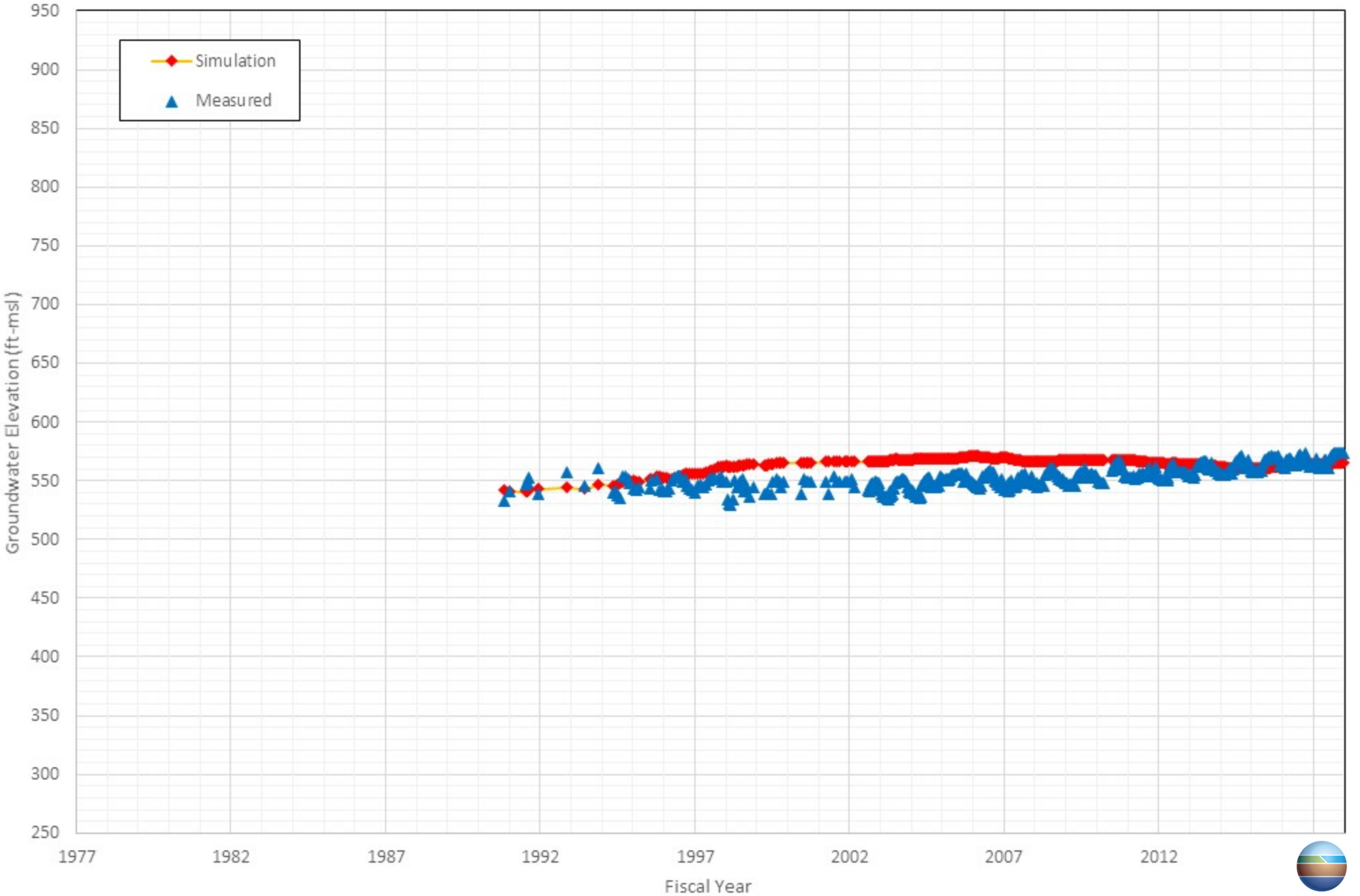

Appendix C-17
Comparison of Measured and Simulated Groundwater Water Level
in the City of Chino Hills's Well CH HIL 15B

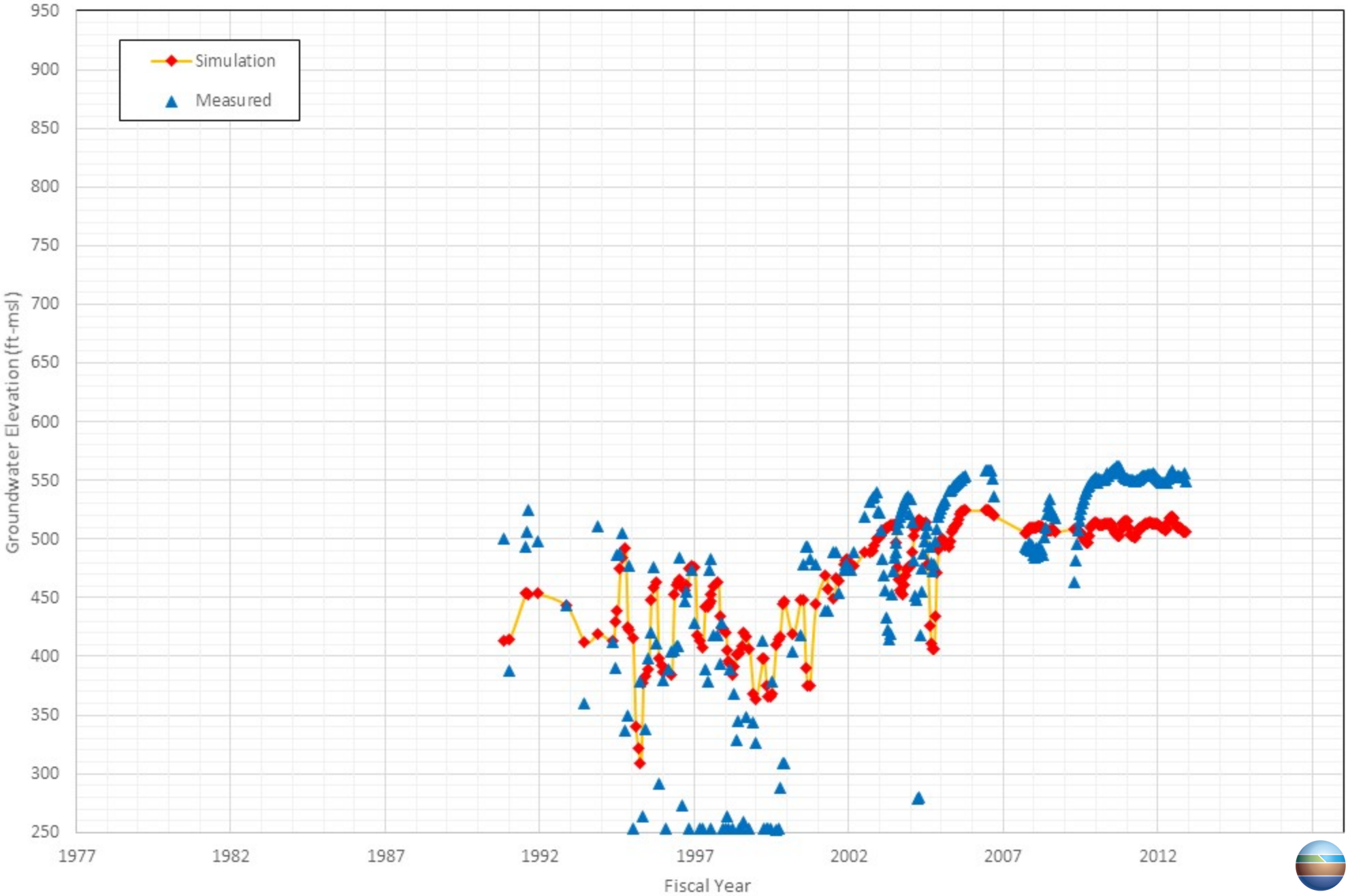

Appendix C-18
Comparison of Measured and Simulated Groundwater Water Level
in the City of Chino Hills's Well CH HIL 17

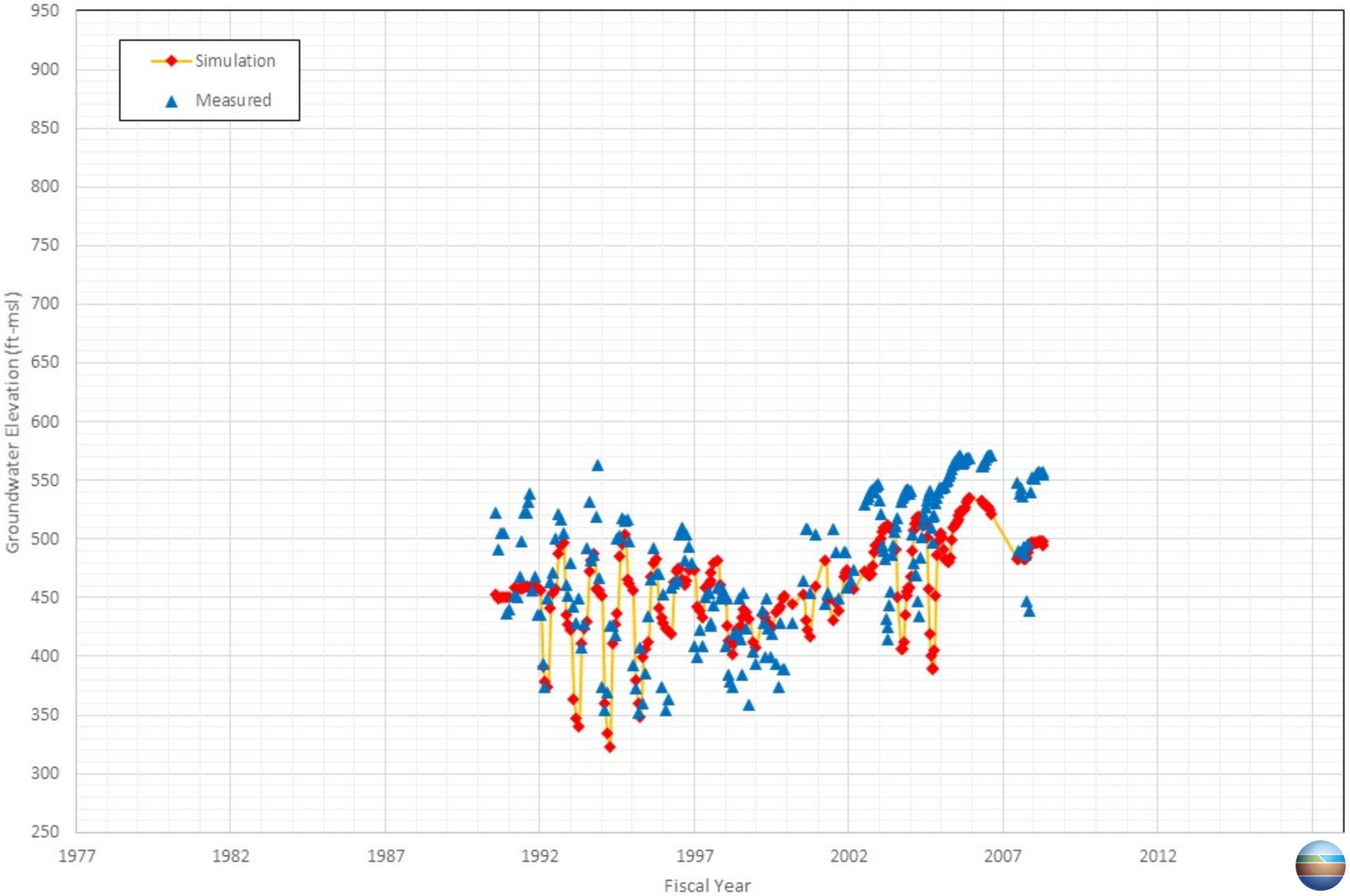

Appendix C-19
Comparison of Measured and Simulated Groundwater Water Level
in the City of Chino Hills's Well CH HIL 18A

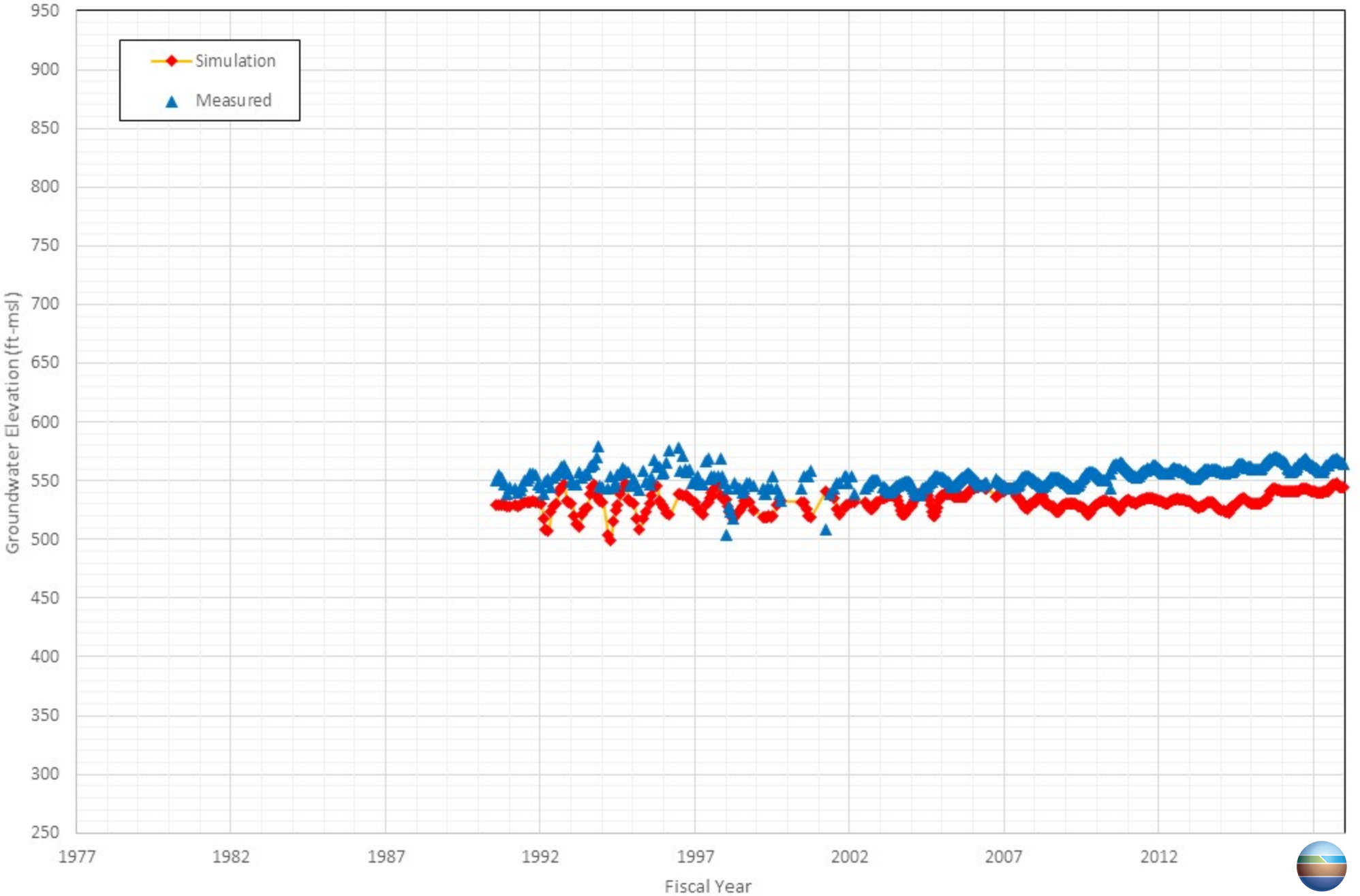

Appendix C-20
Comparison of Measured and Simulated Groundwater Water Level
in the City of Chino Hills's Well CH HIL 19

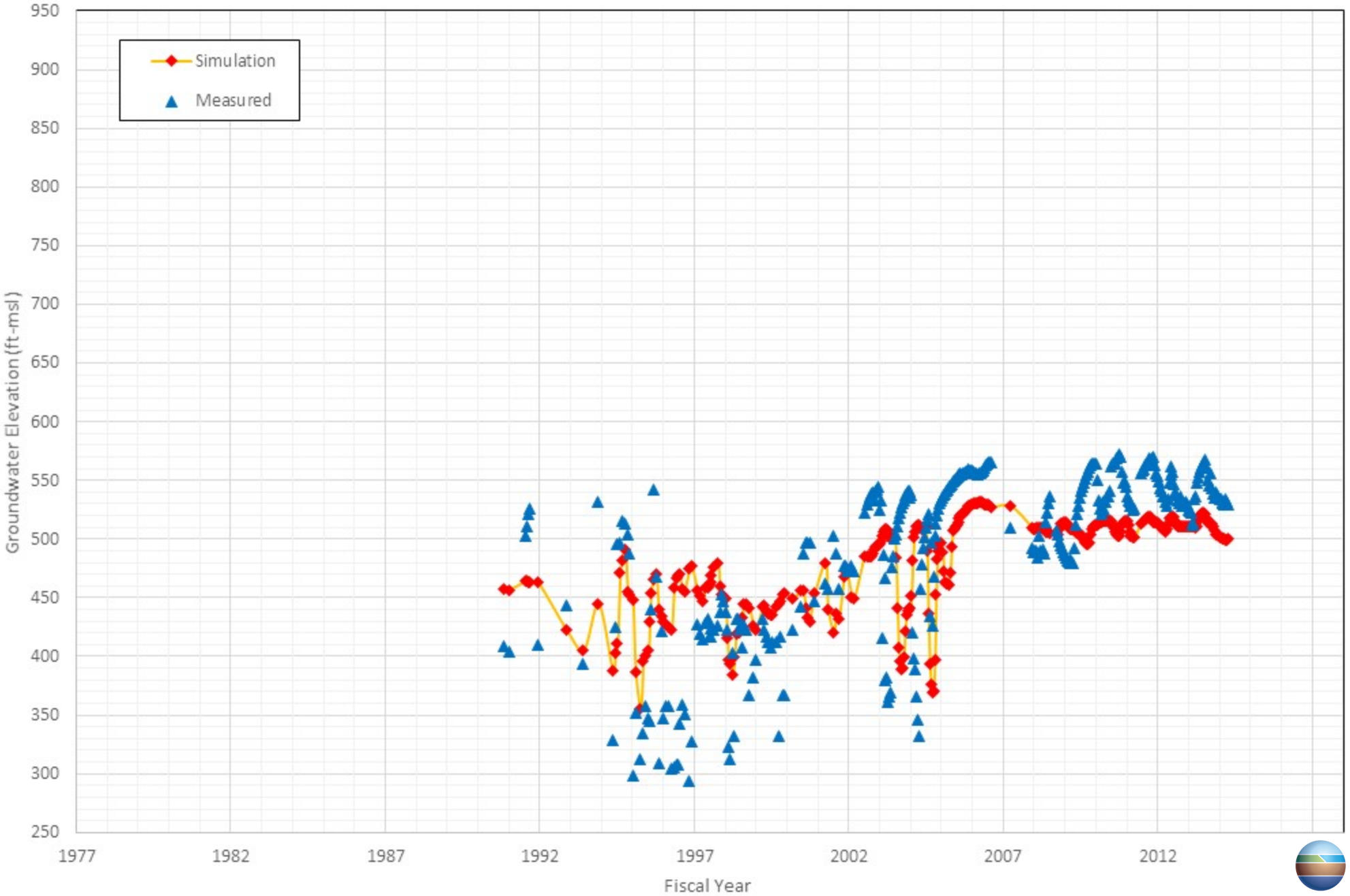

Appendix C-21
Comparison of Measured and Simulated Groundwater Water Level
in the Inland Empire Utilities Agency's Well HCMP-6/1

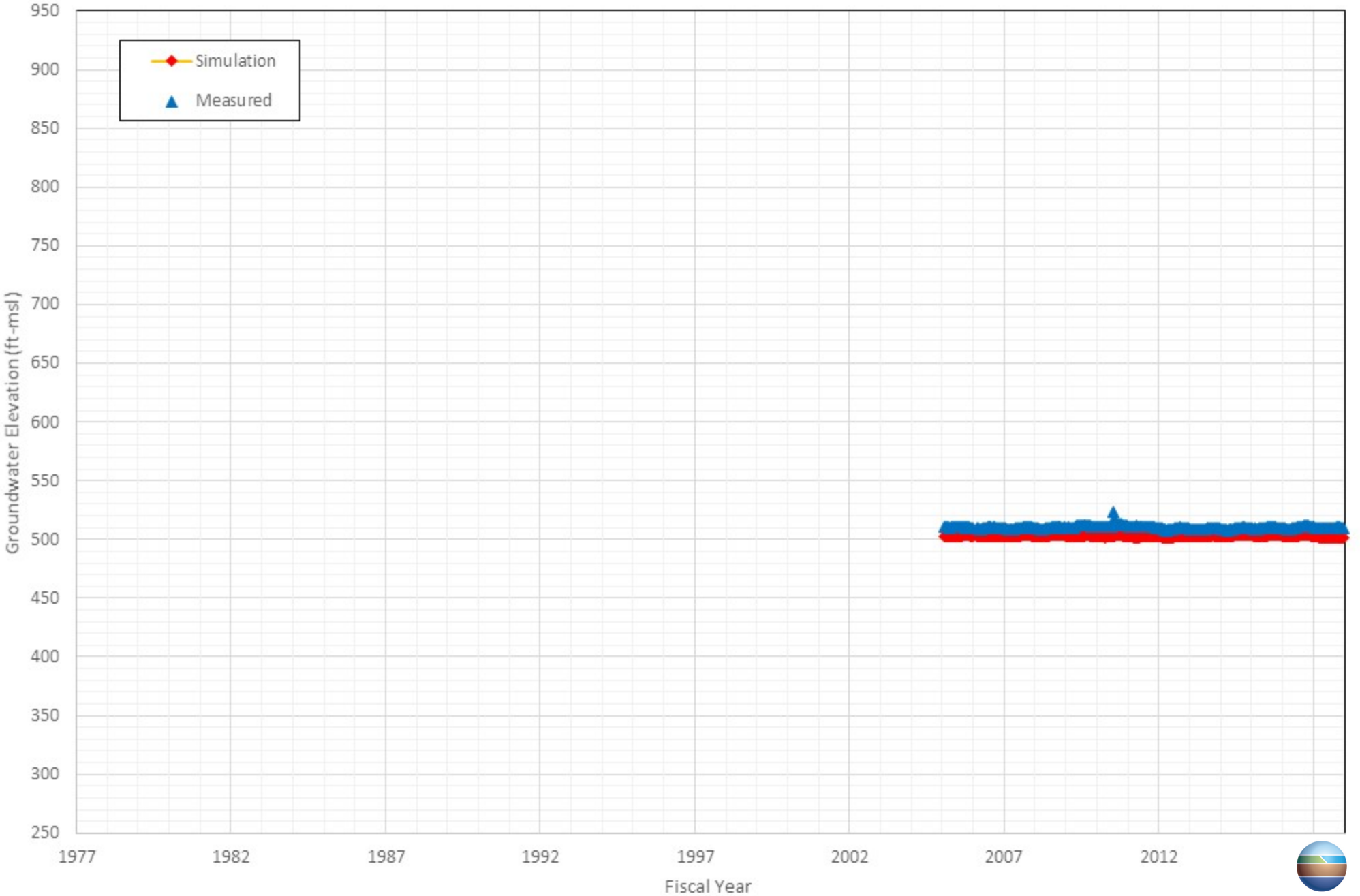

Appendix C-22
Comparison of Measured and Simulated Groundwater Water Level
in the Inland Empire Utilities Agency's Well MZ3 1/1

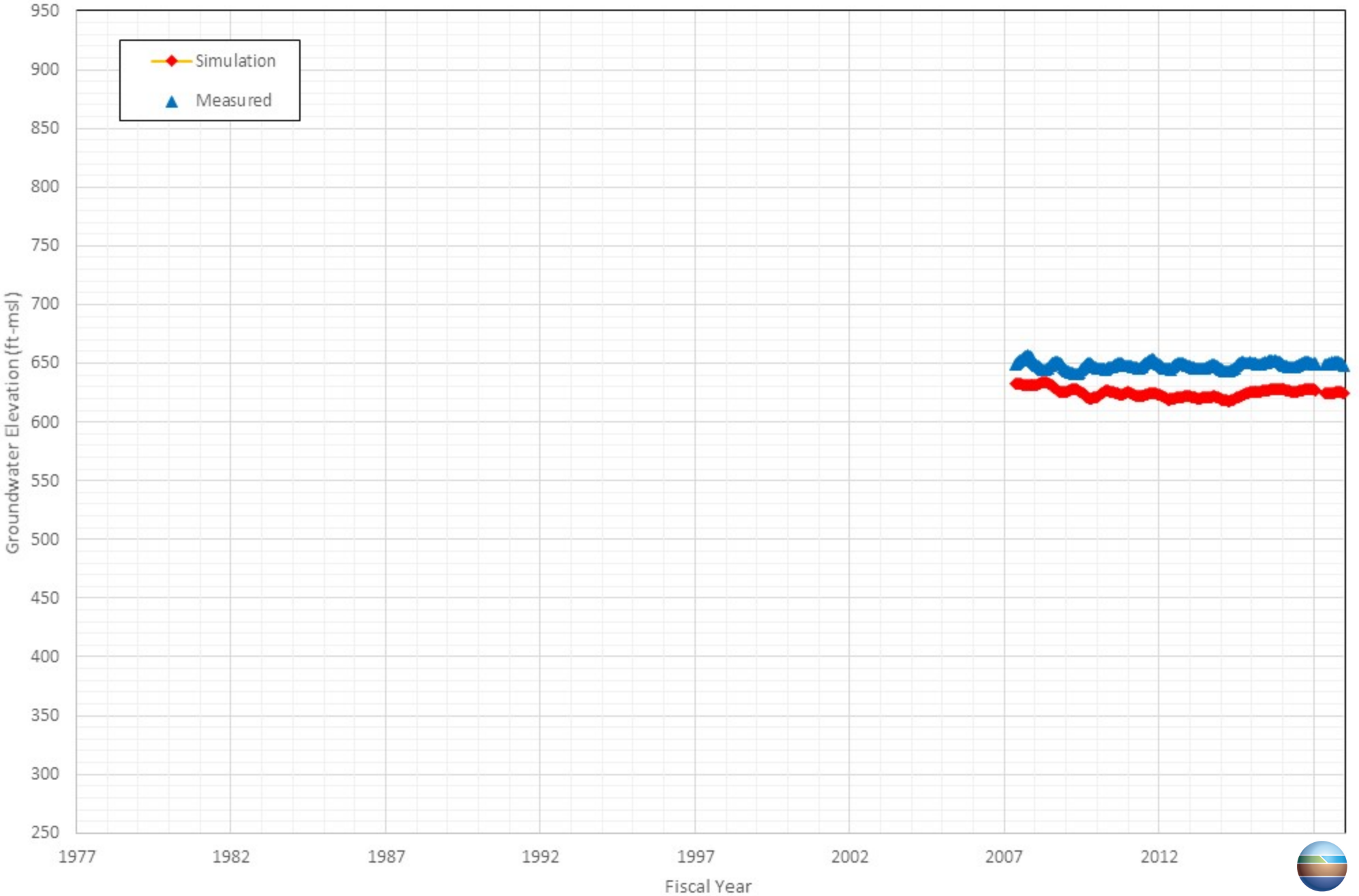

Appendix C-23
Comparison of Measured and Simulated Groundwater Water Level
in the Inland Empire Utilities Agency's Well T-2/1

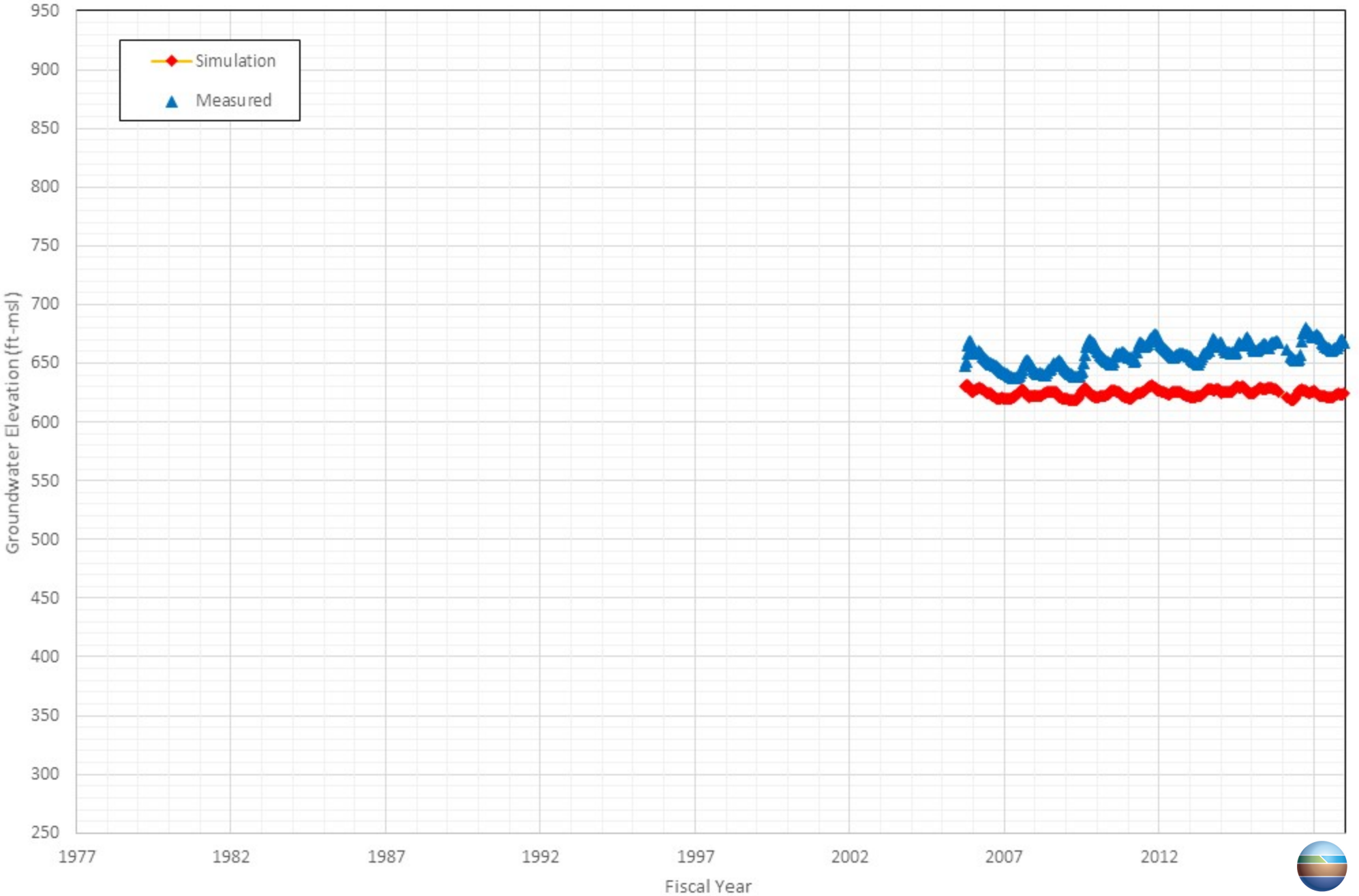

Appendix C-24
Comparison of Measured and Simulated Groundwater Water Level
in the Inland Empire Utilities Agency's Well VCT-2/2

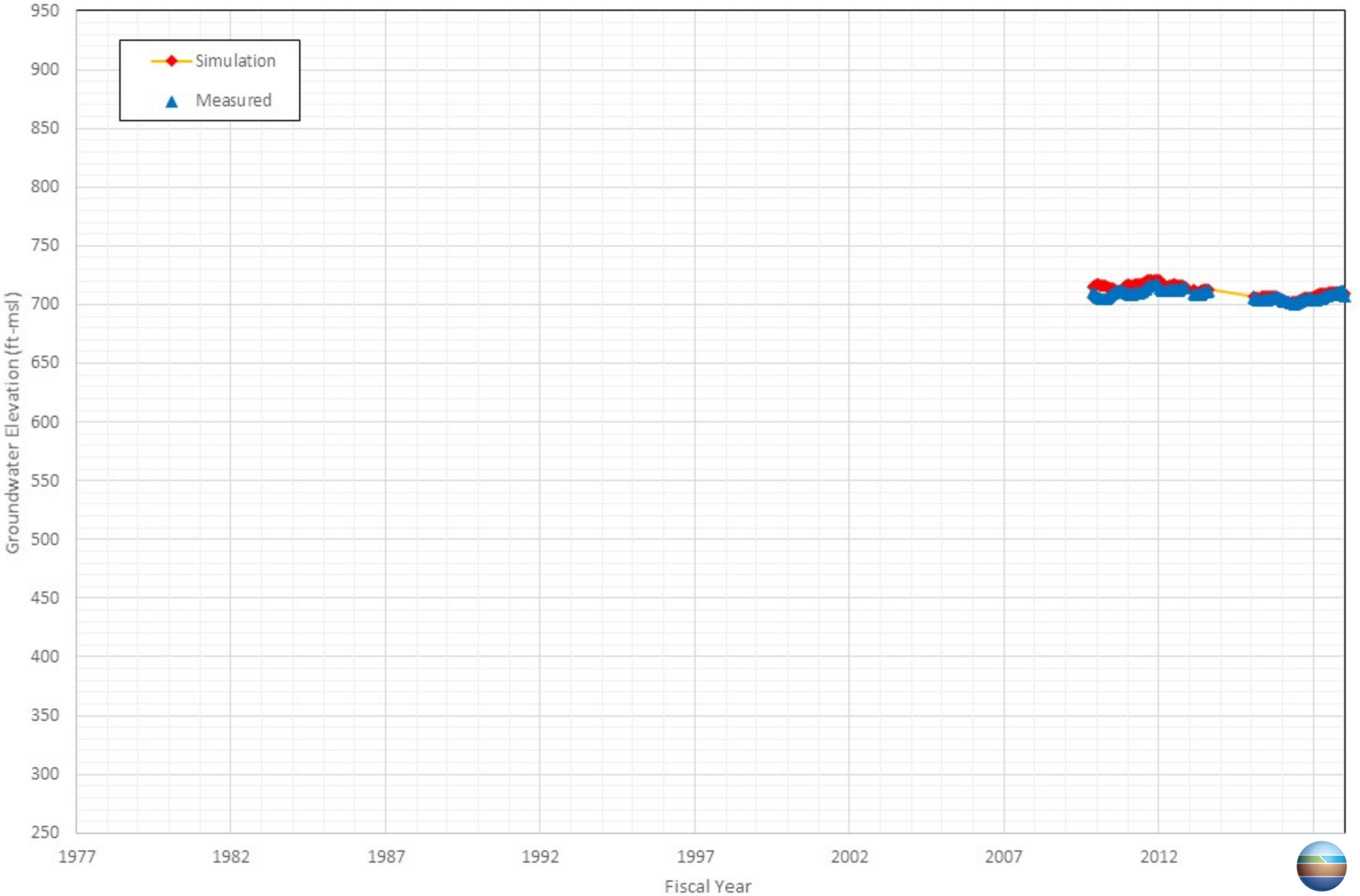

Appendix C-25
Comparison of Measured and Simulated Groundwater Water Level
in the City of Norco's Well NOR 11

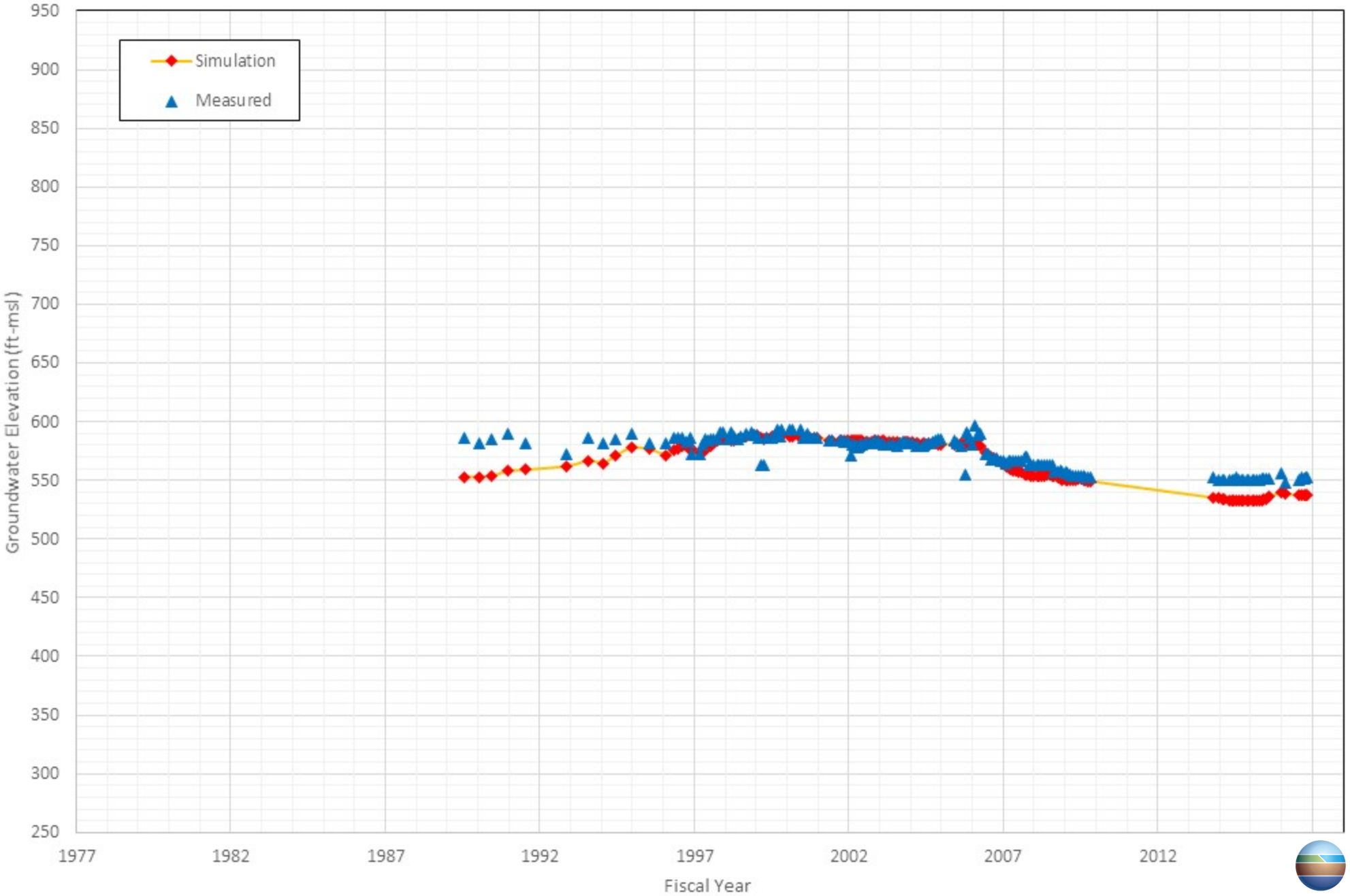

Appendix C-26
Comparison of Measured and Simulated Groundwater Water Level
in the City of Ontario's Well ONT 04

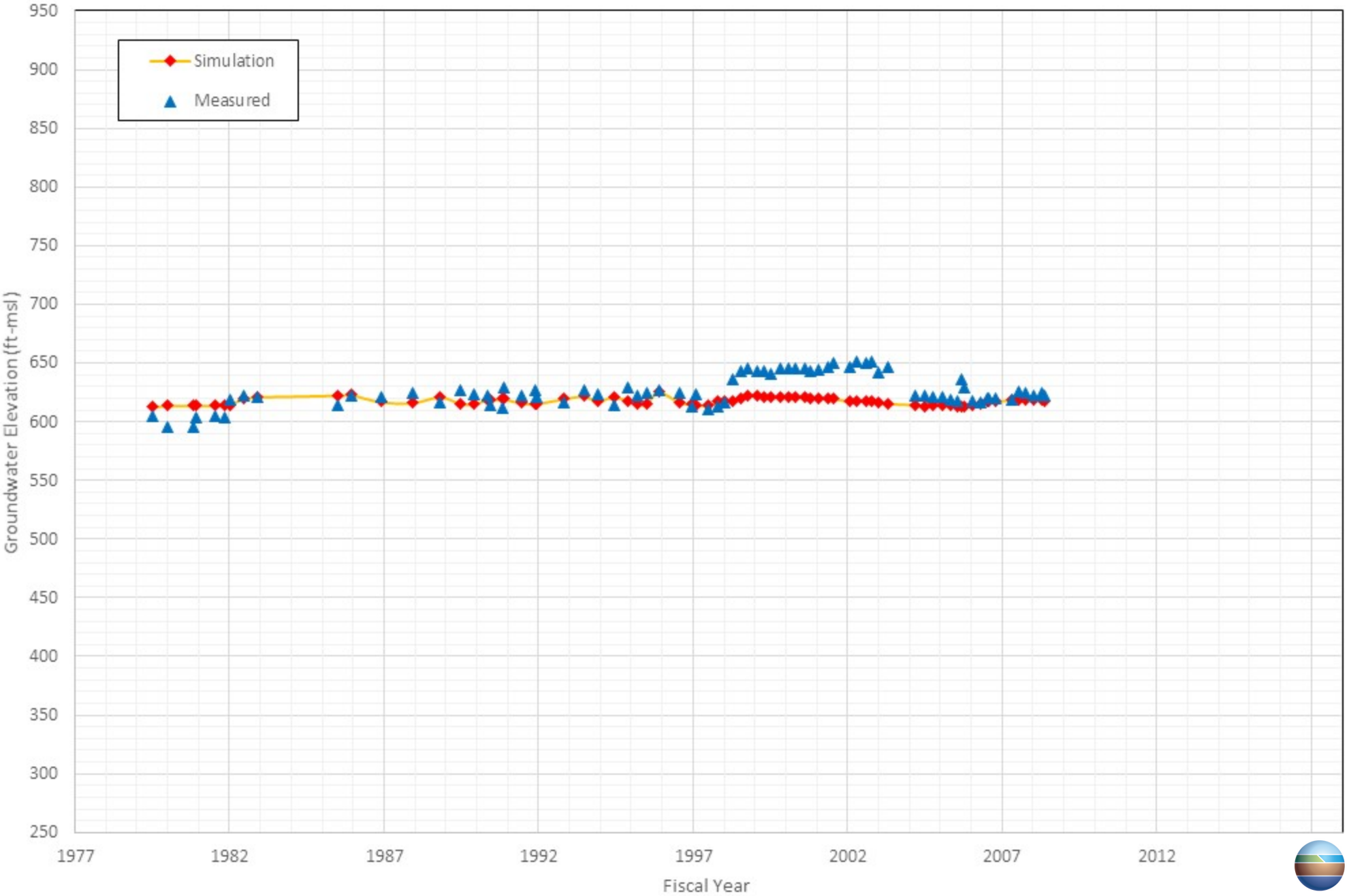

Appendix C-27
Comparison of Measured and Simulated Groundwater Water Level
in the City of Ontario's Well ONT 07

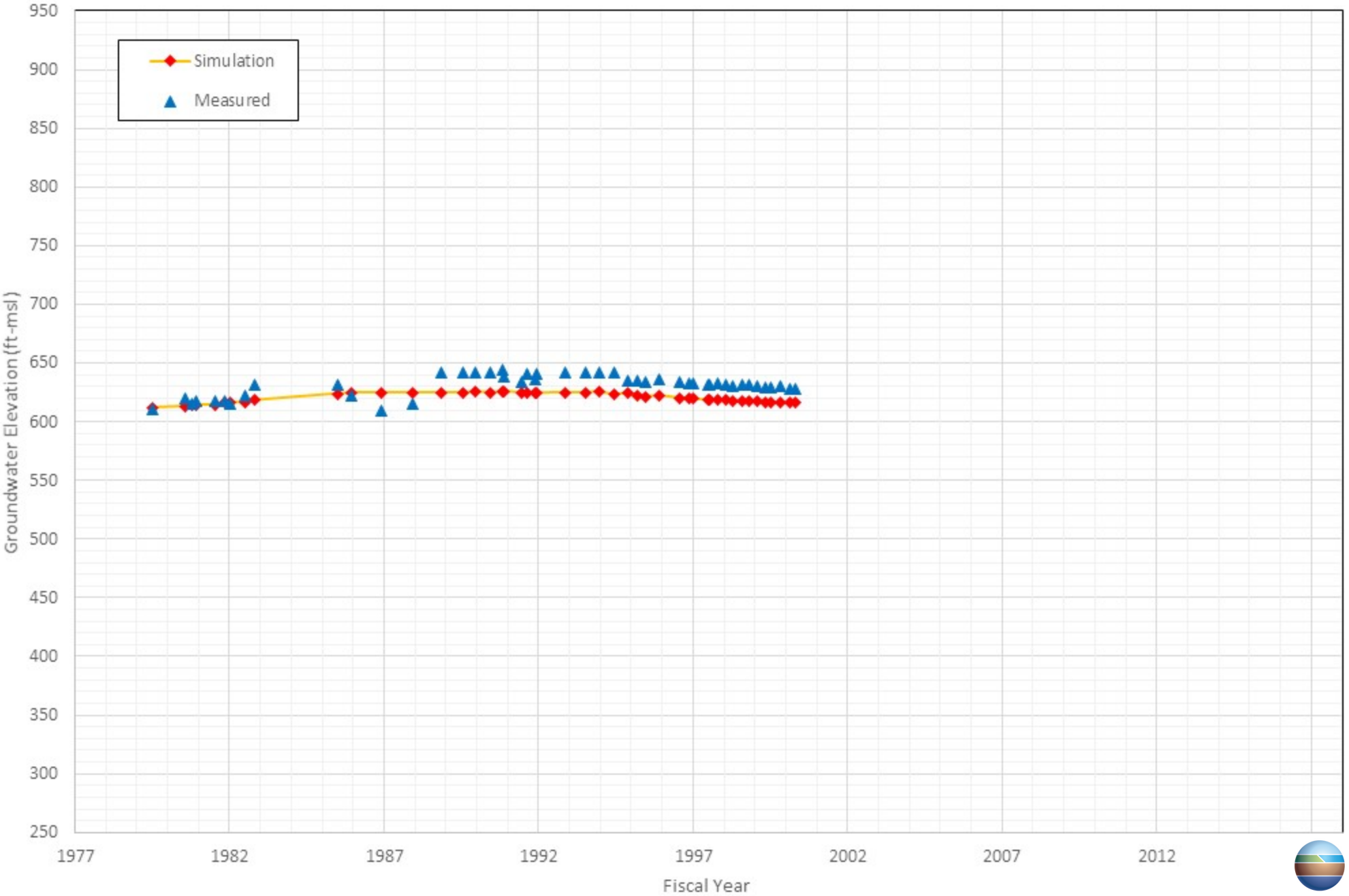

Appendix C-28
Comparison of Measured and Simulated Groundwater Water Level
in the City of Ontario's Well ONT 08

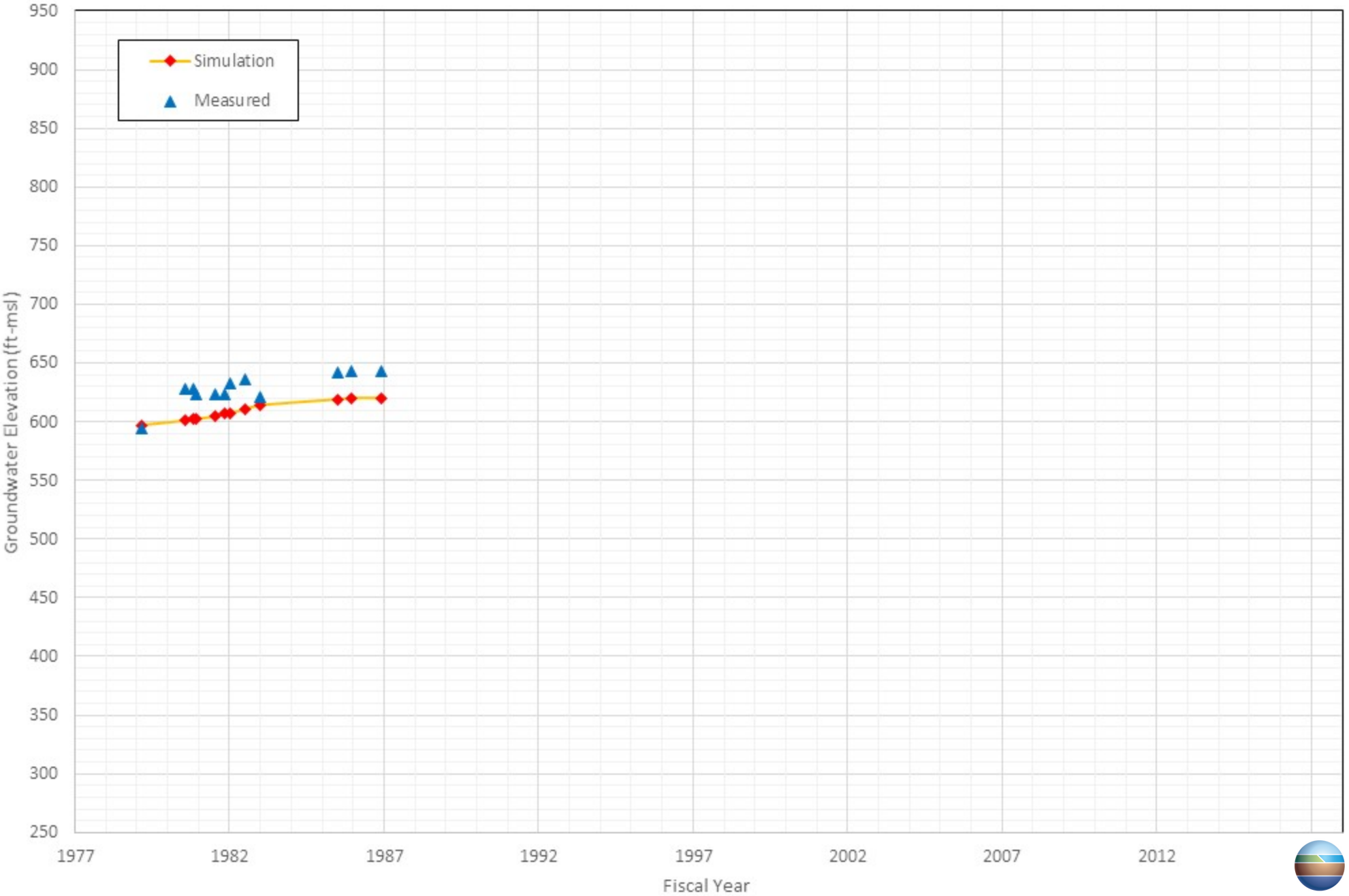

Appendix C-29
Comparison of Measured and Simulated Groundwater Water Level
in the City of Ontario's Well ONT 09

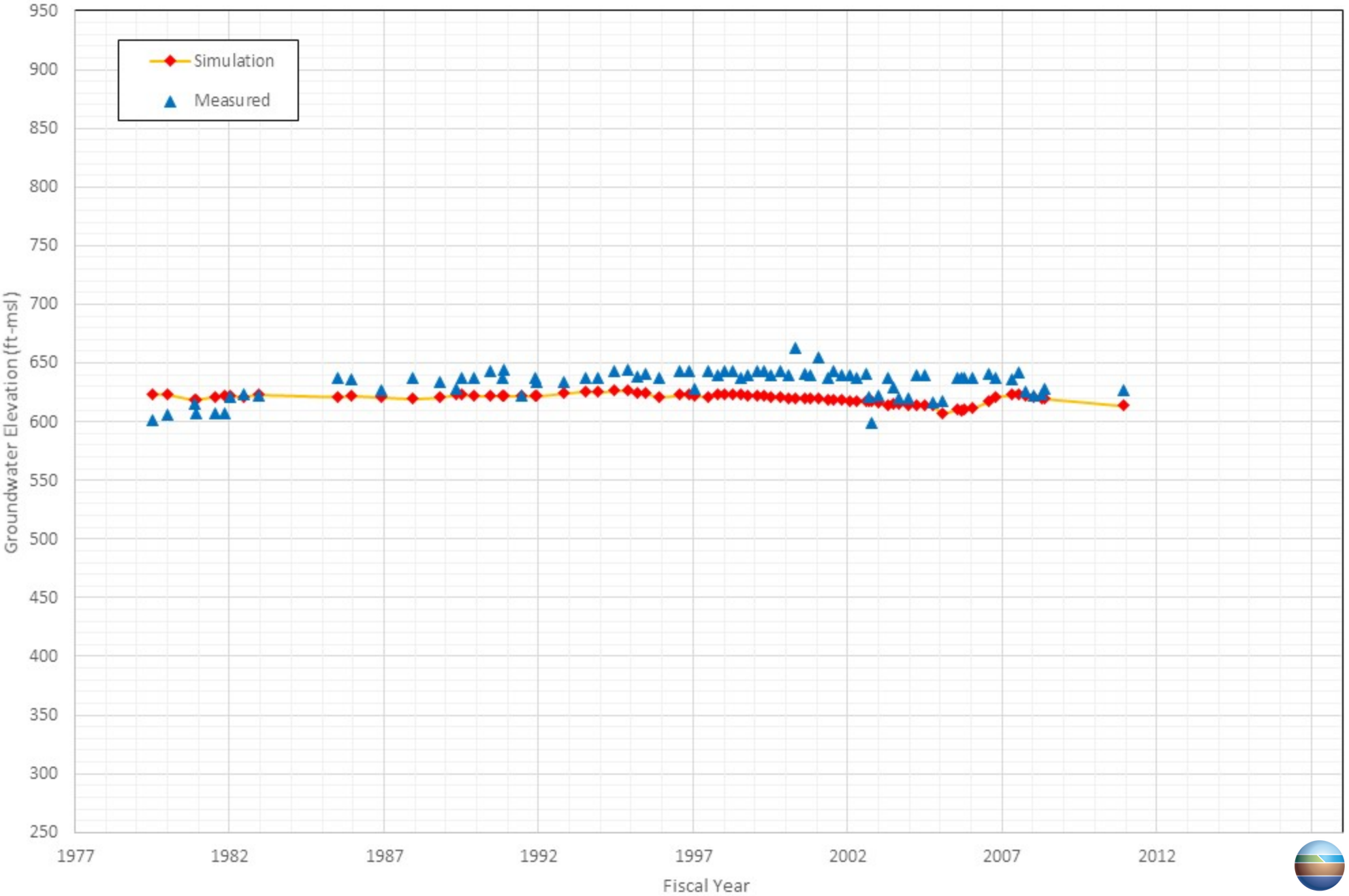

Appendix C-30
Comparison of Measured and Simulated Groundwater Water Level
in the City of Ontario's Well ONT 11

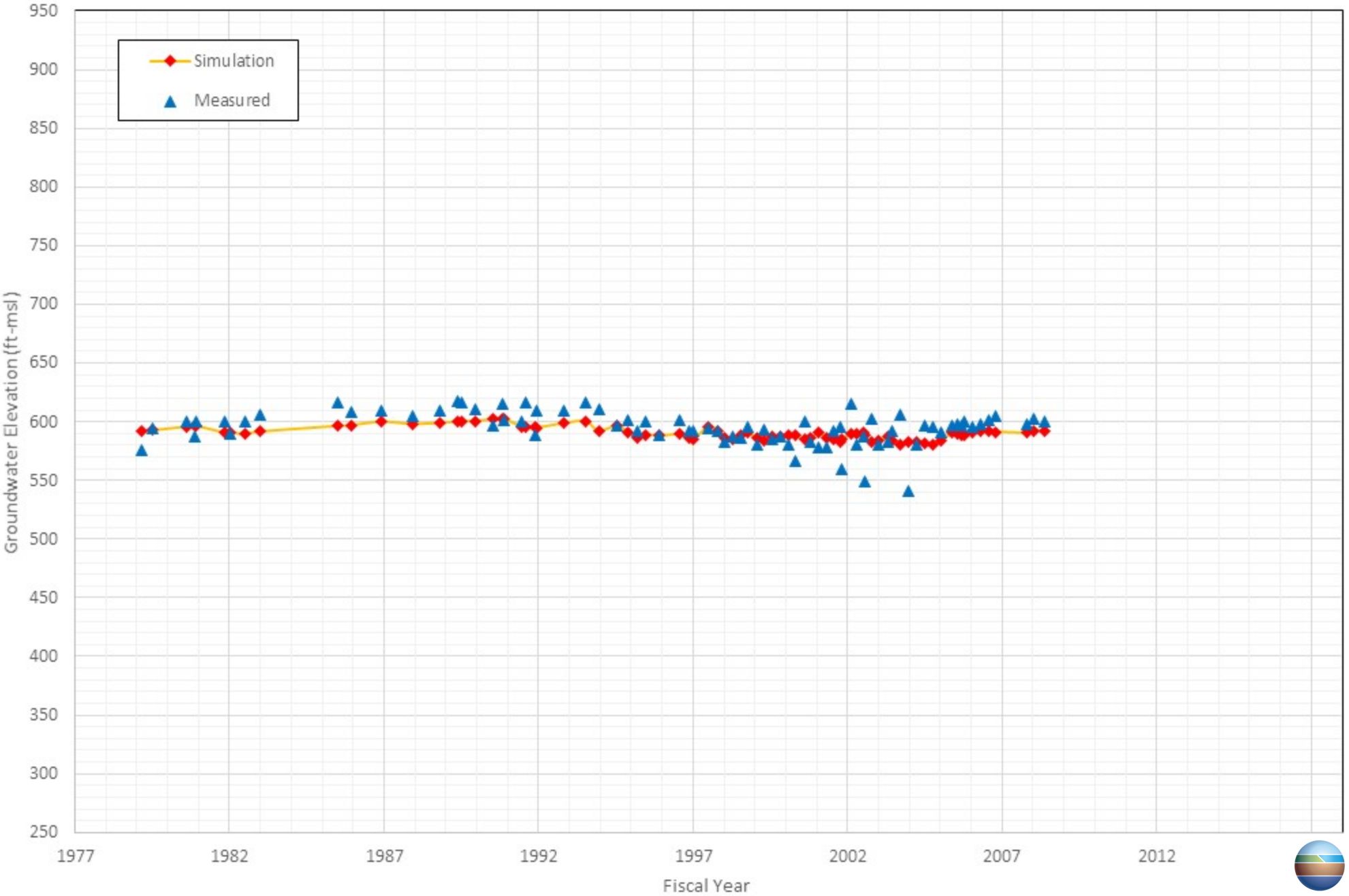

Appendix C-31
Comparison of Measured and Simulated Groundwater Water Level
in the City of Ontario's Well ONT 20

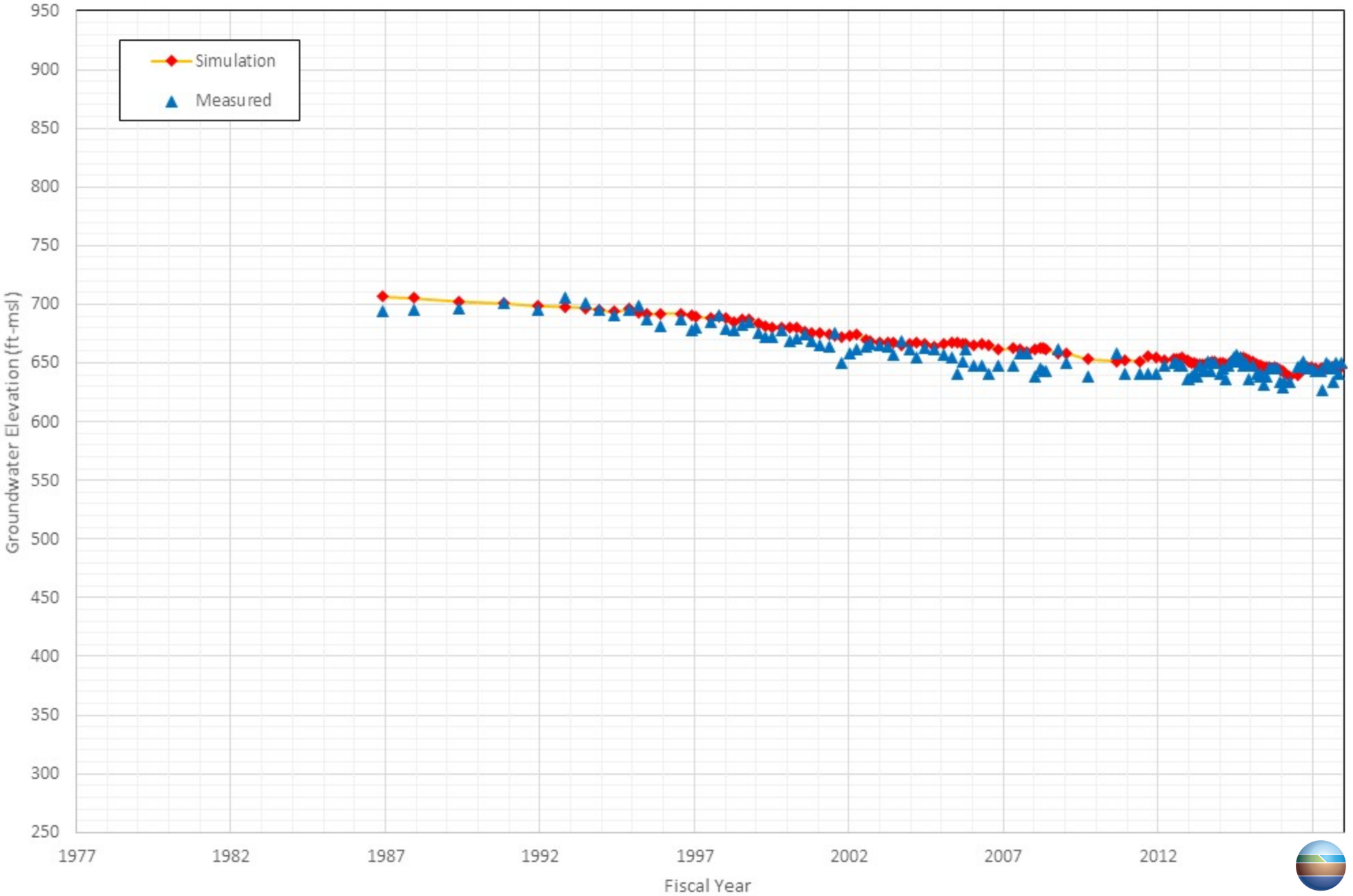

Appendix C-32
Comparison of Measured and Simulated Groundwater Water Level
in the City of Ontario's Well ONT 31

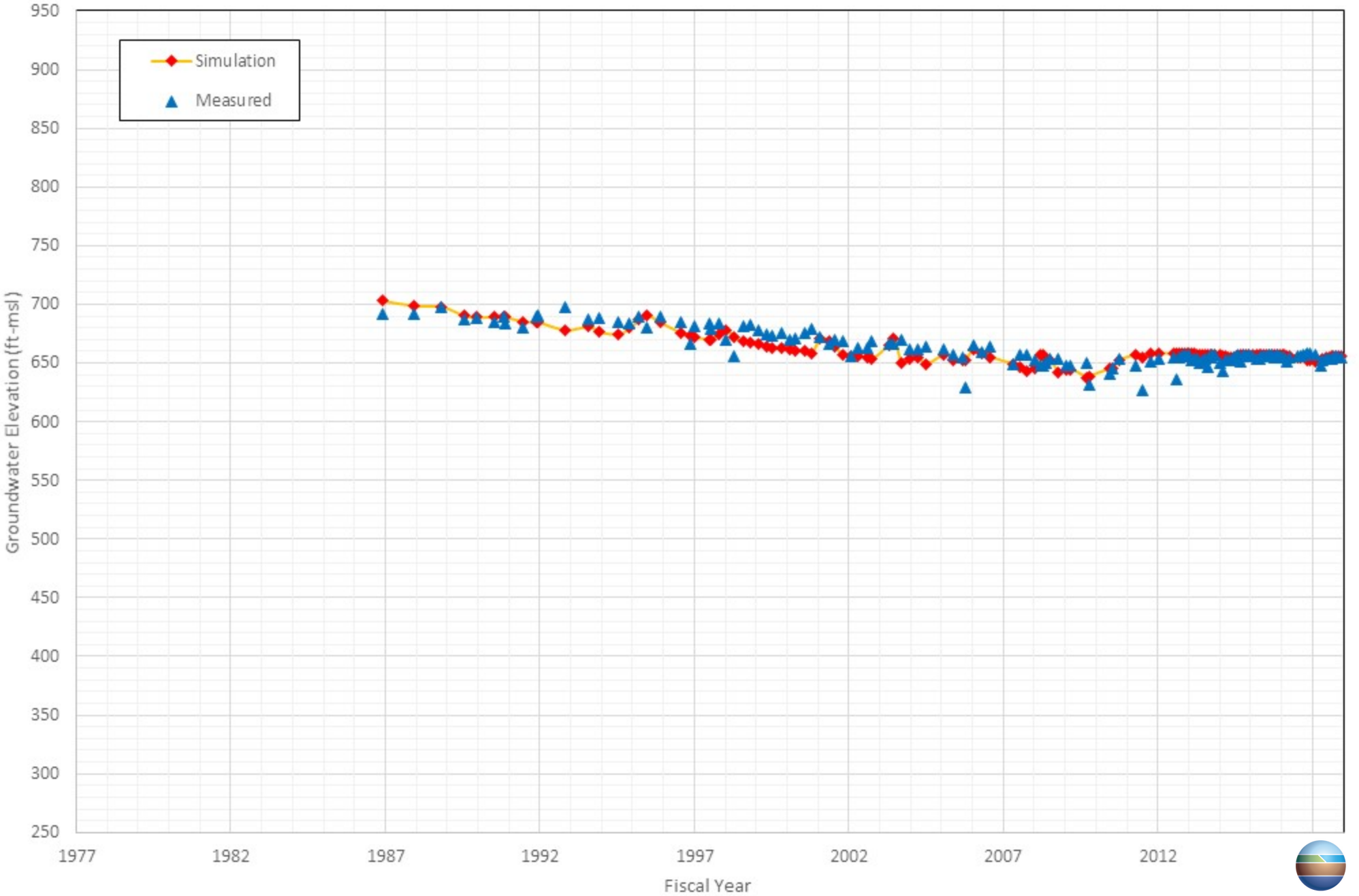

Appendix C-33
Comparison of Measured and Simulated Groundwater Water Level
in the City of Ontario's Well ONT 36

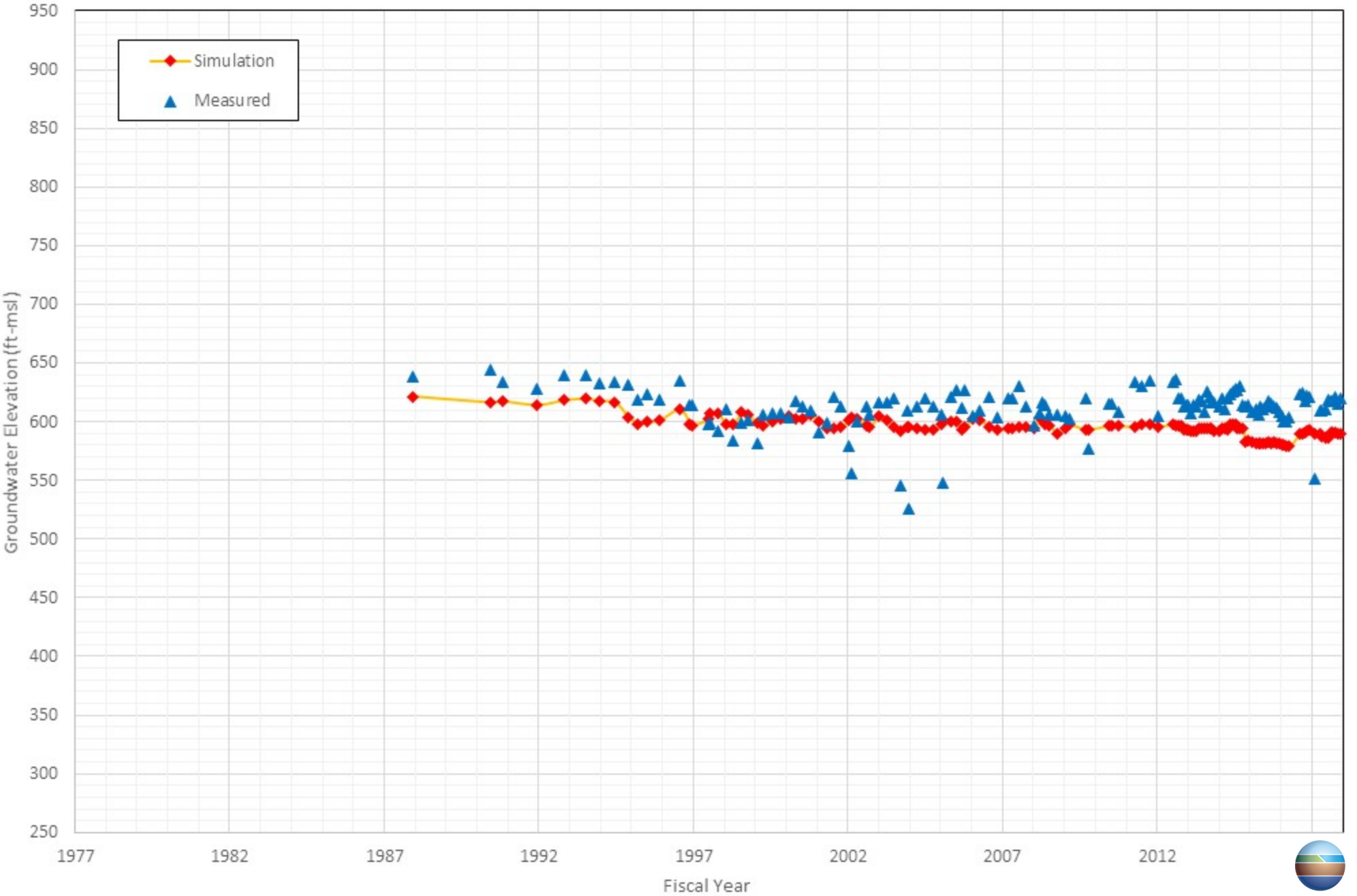

Appendix C-34
Comparison of Measured and Simulated Groundwater Water Level
in the City of Pomona's Well P-16

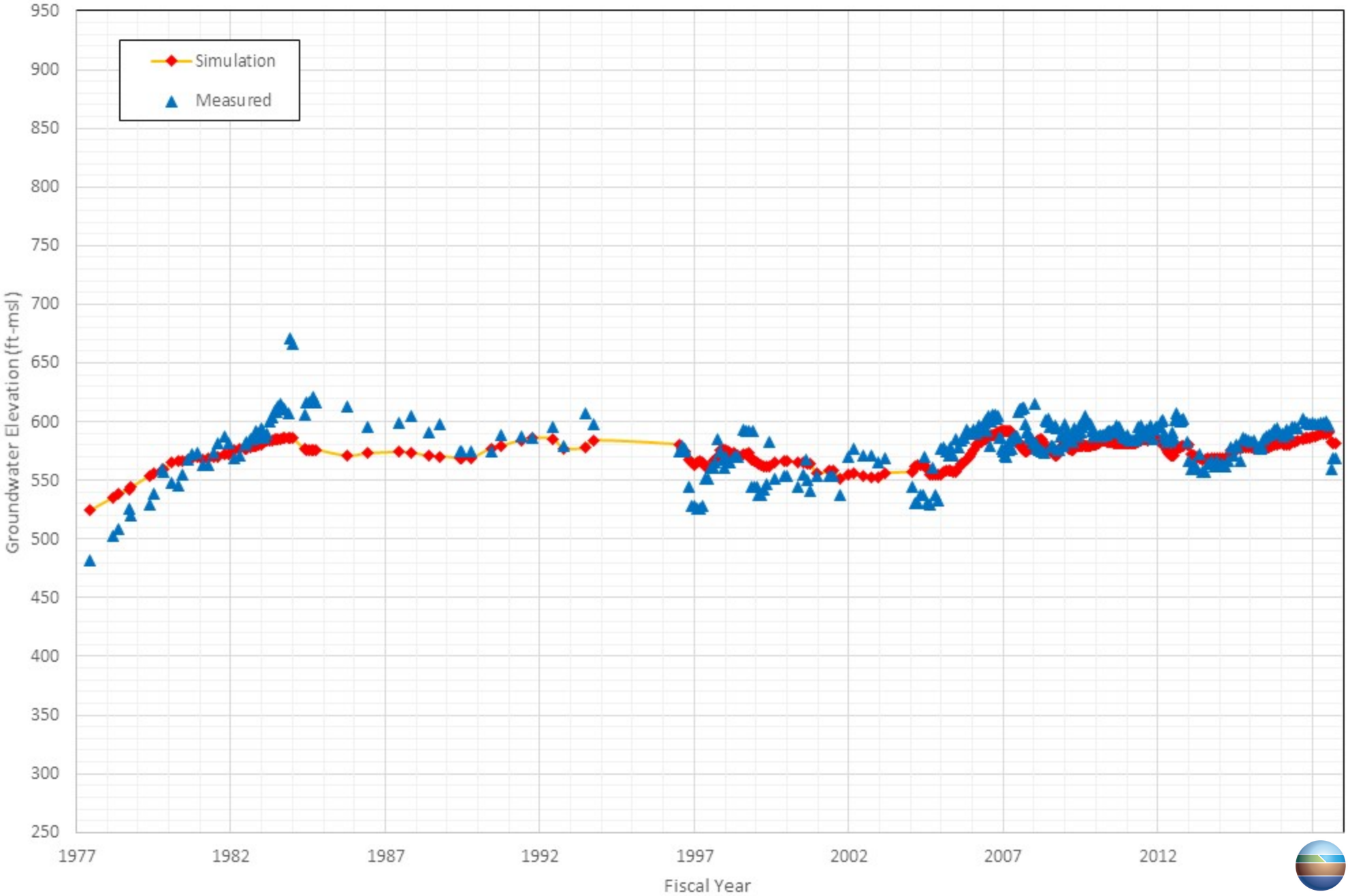

Appendix C-35
Comparison of Measured and Simulated Groundwater Water Level
in the City of Pomona's Well P-24(OLD)

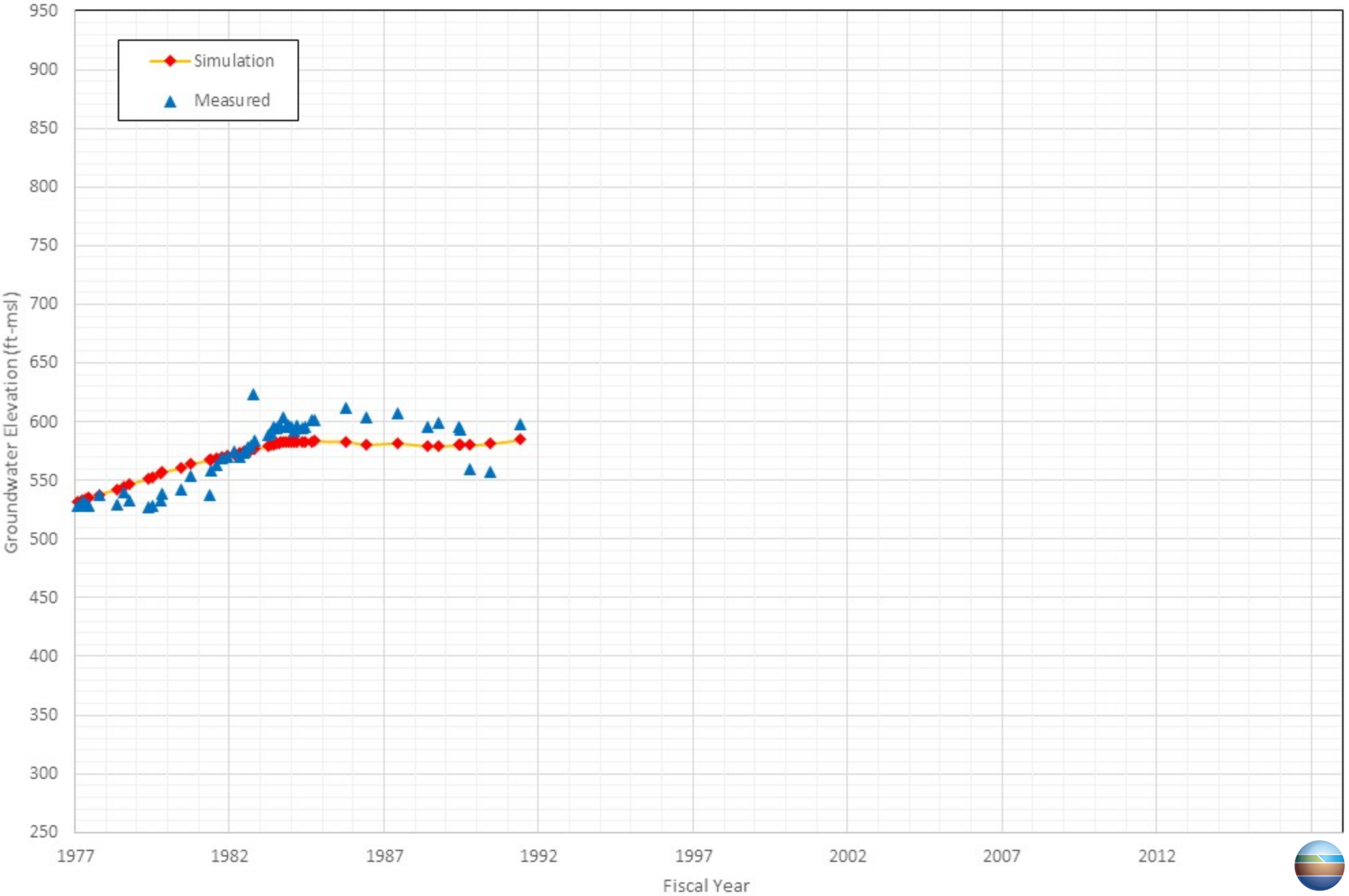

Appendix C-36
Comparison of Measured and Simulated Groundwater Water Level
in the City of Pomona's Well P-29

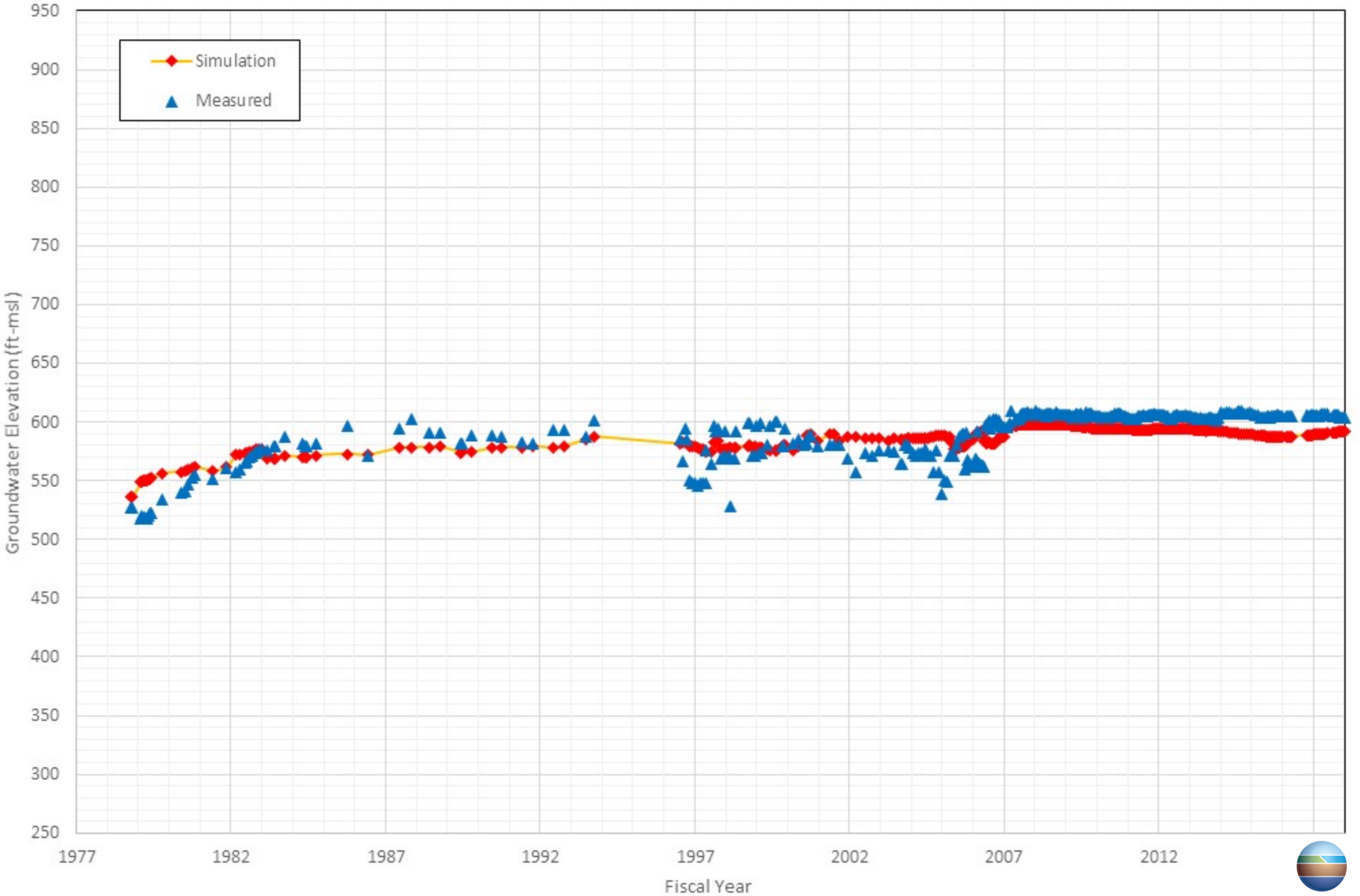

Appendix C-37
Comparison of Measured and Simulated Groundwater Water Level
in the City of Pomona's Well P-30

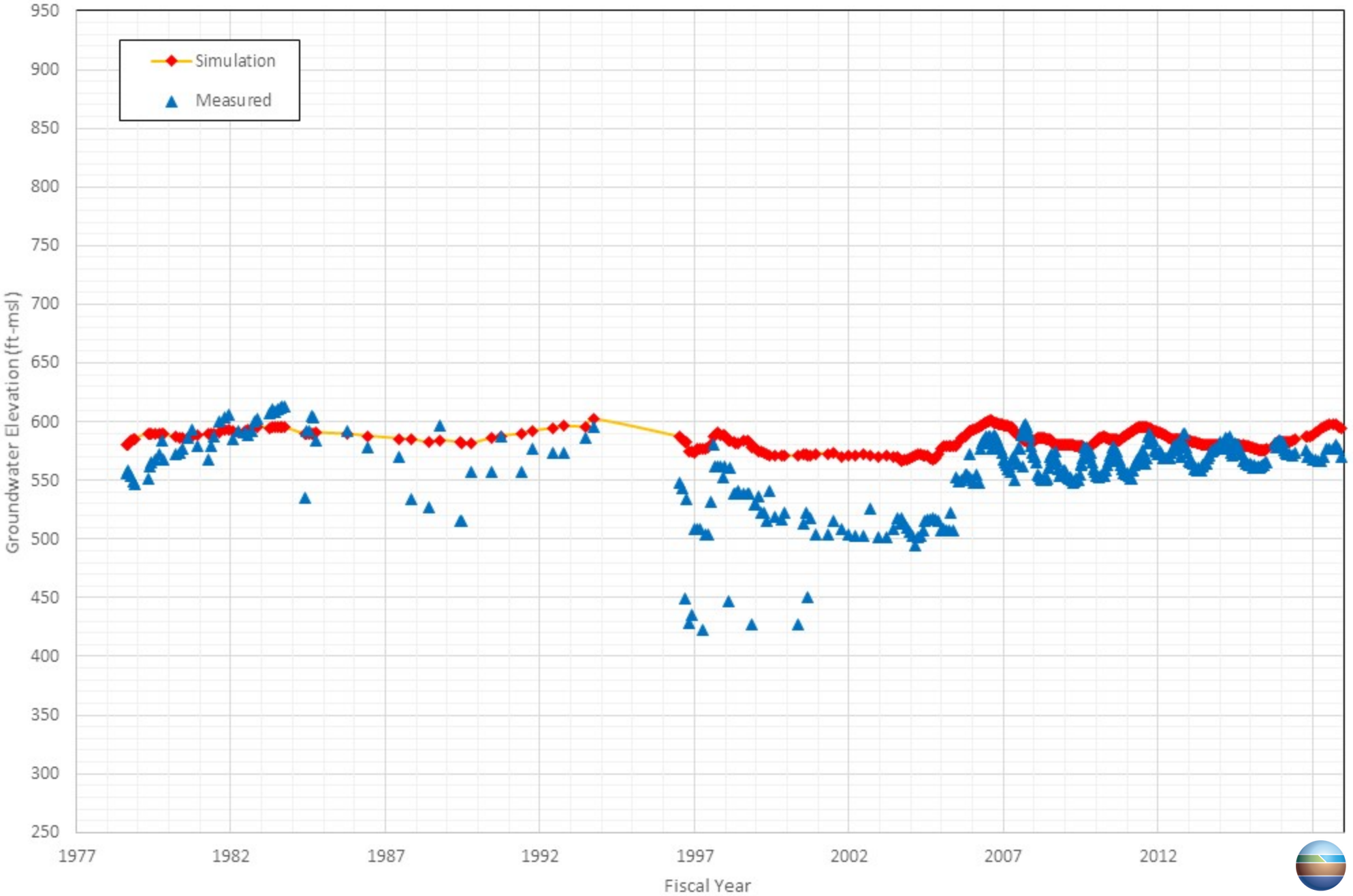

Appendix C-38
Comparison of Measured and Simulated Groundwater Water Level
in the City of Upland's Well Upland 08

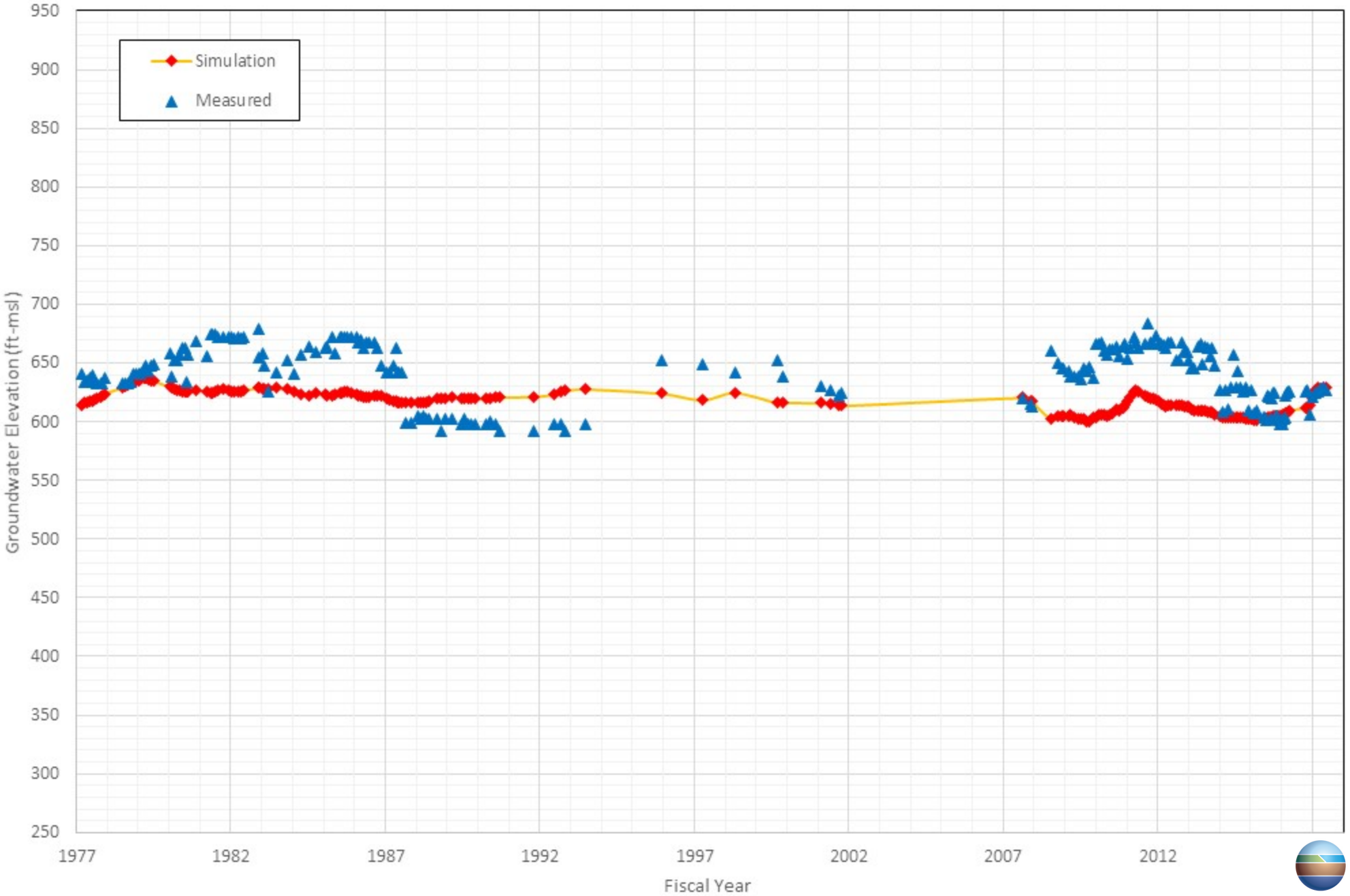

Appendix C-39
Comparison of Measured and Simulated Groundwater Water Level
in the City of Upland's Well Upland 09

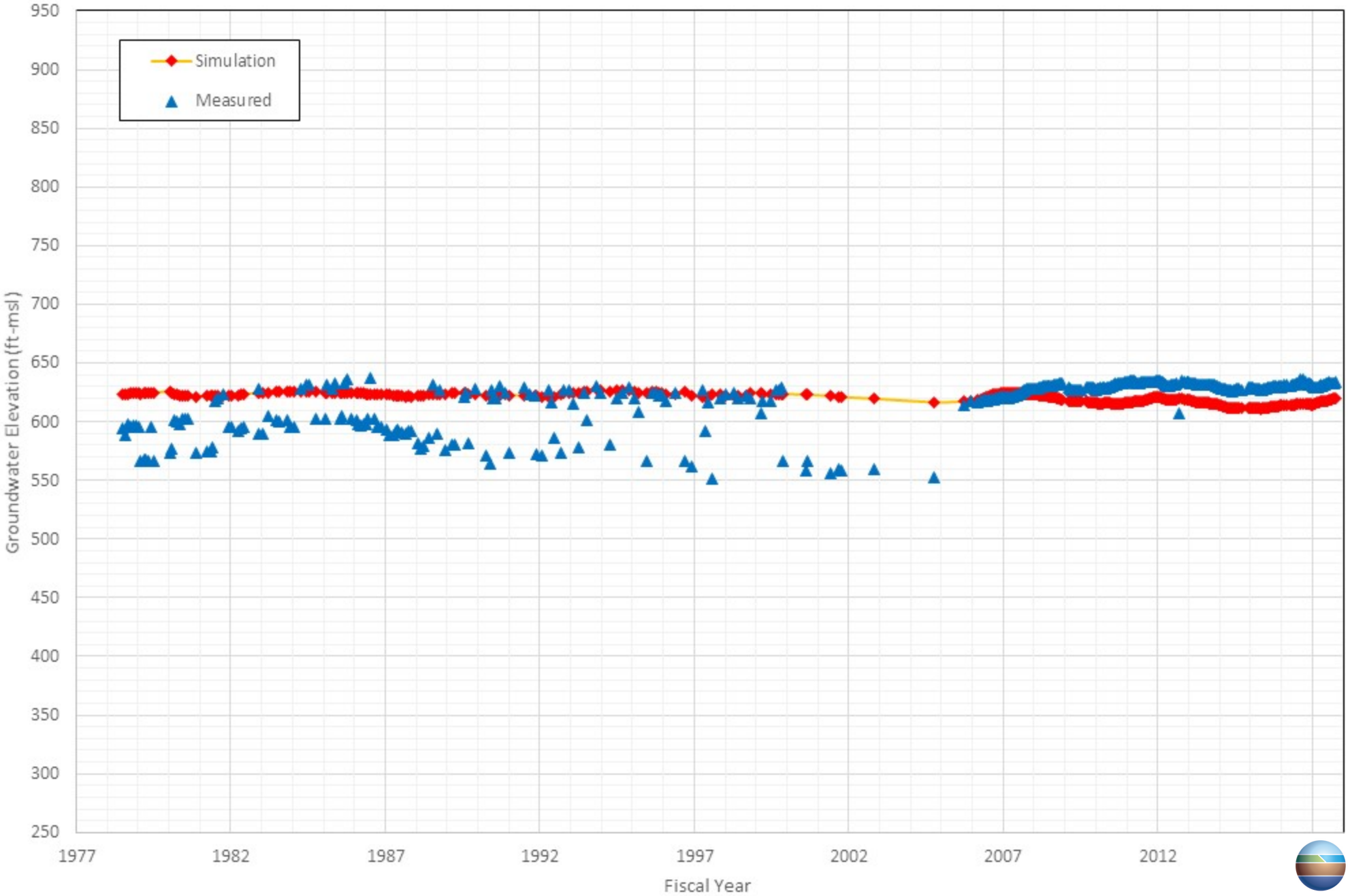

Appendix C-40
Comparison of Measured and Simulated Groundwater Water Level
in the County of San Bernardino's Well MIL M-03

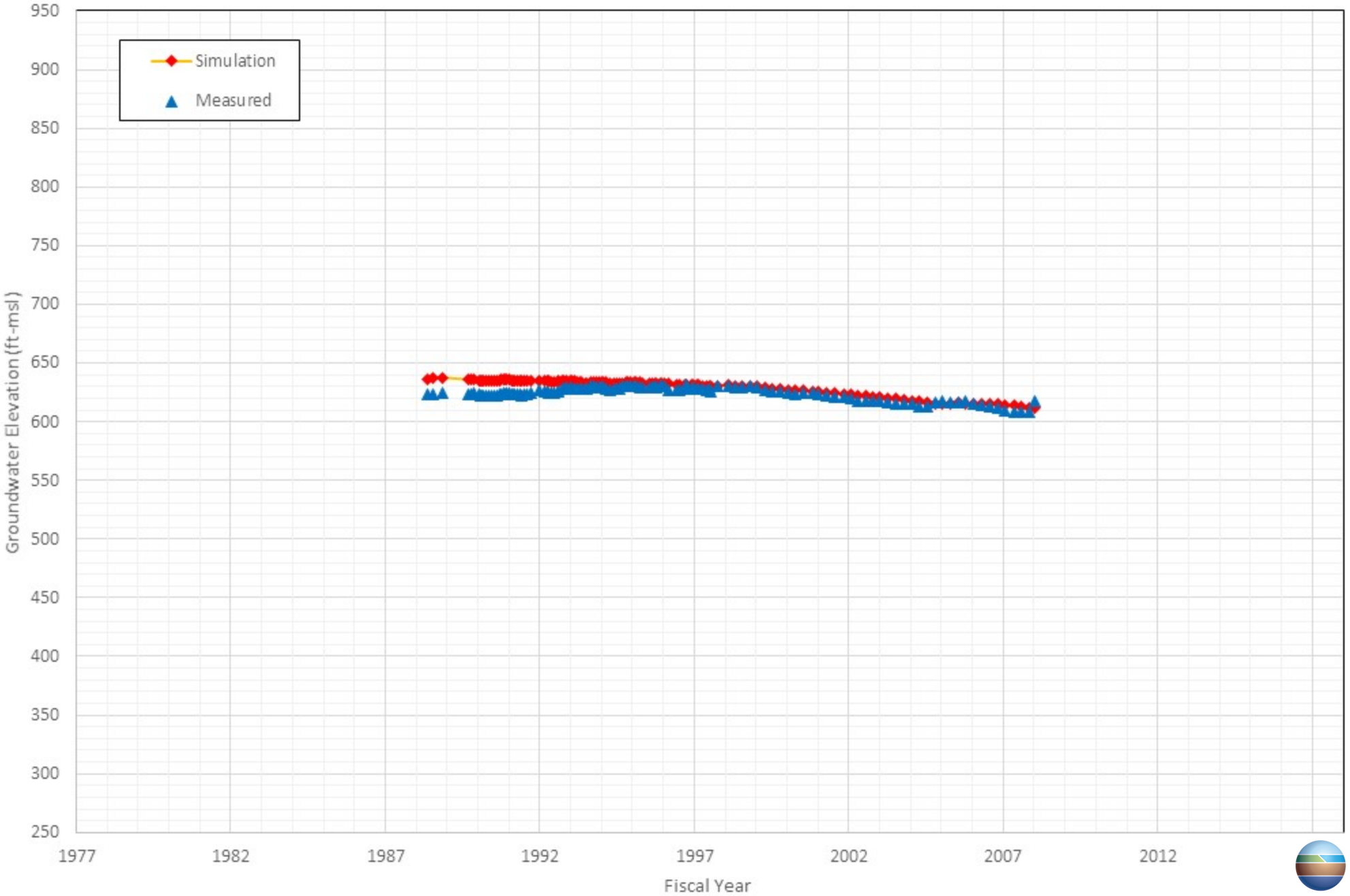

Appendix C-41
Comparison of Measured and Simulated Groundwater Water Level
in the County of San Bernardino, Dept. Of Airports's Well NA_1003983

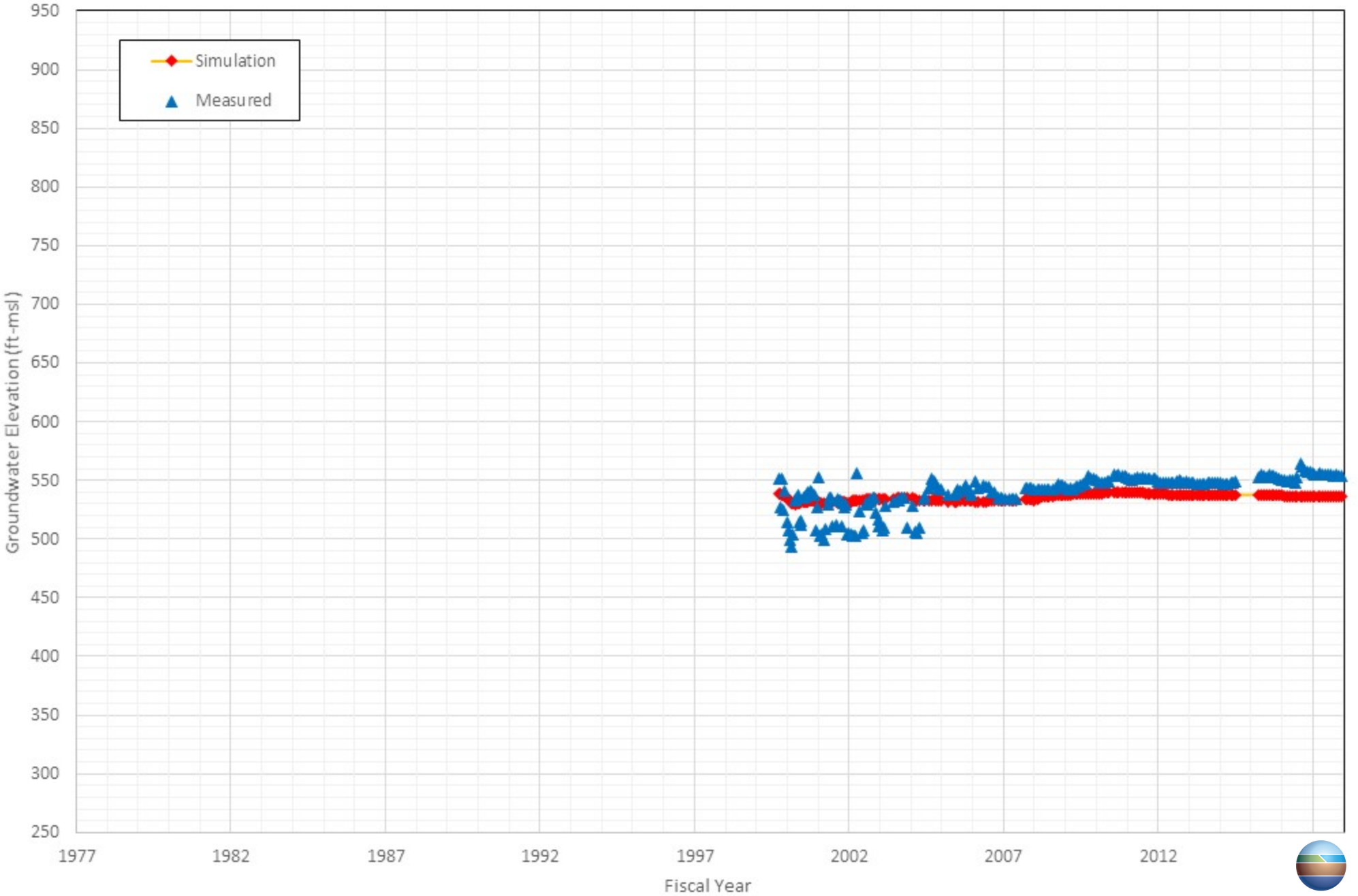

Appendix C-42
Comparison of Measured and Simulated Groundwater Water Level
in the Cucamonga Valley Water District's Well CVWD 3

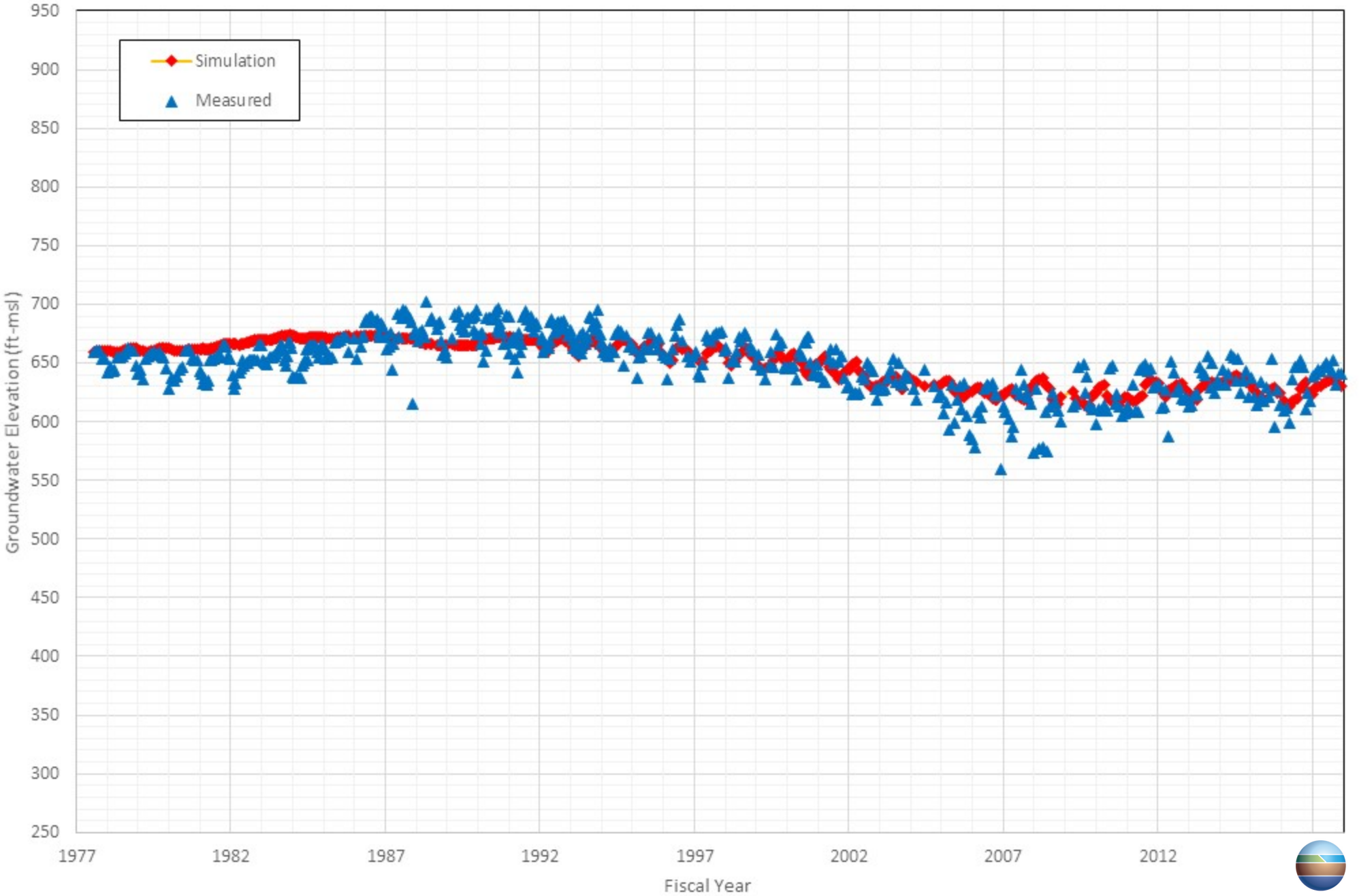

Appendix C-43
Comparison of Measured and Simulated Groundwater Water Level
in the Cucamonga Valley Water District's Well CVWD 35

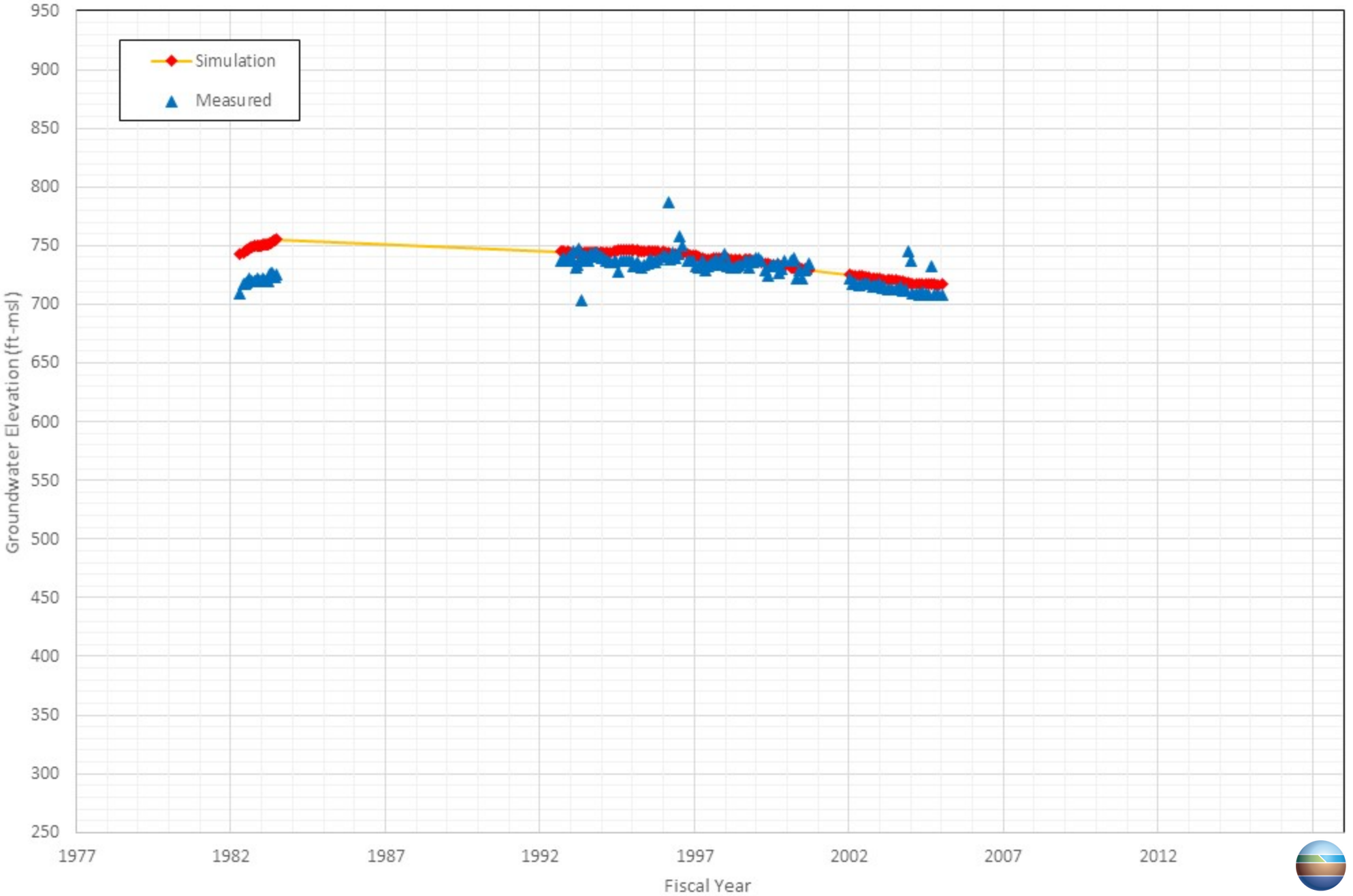

Appendix C-44
Comparison of Measured and Simulated Groundwater Water Level
in the Fontana Water Company's Well F18A

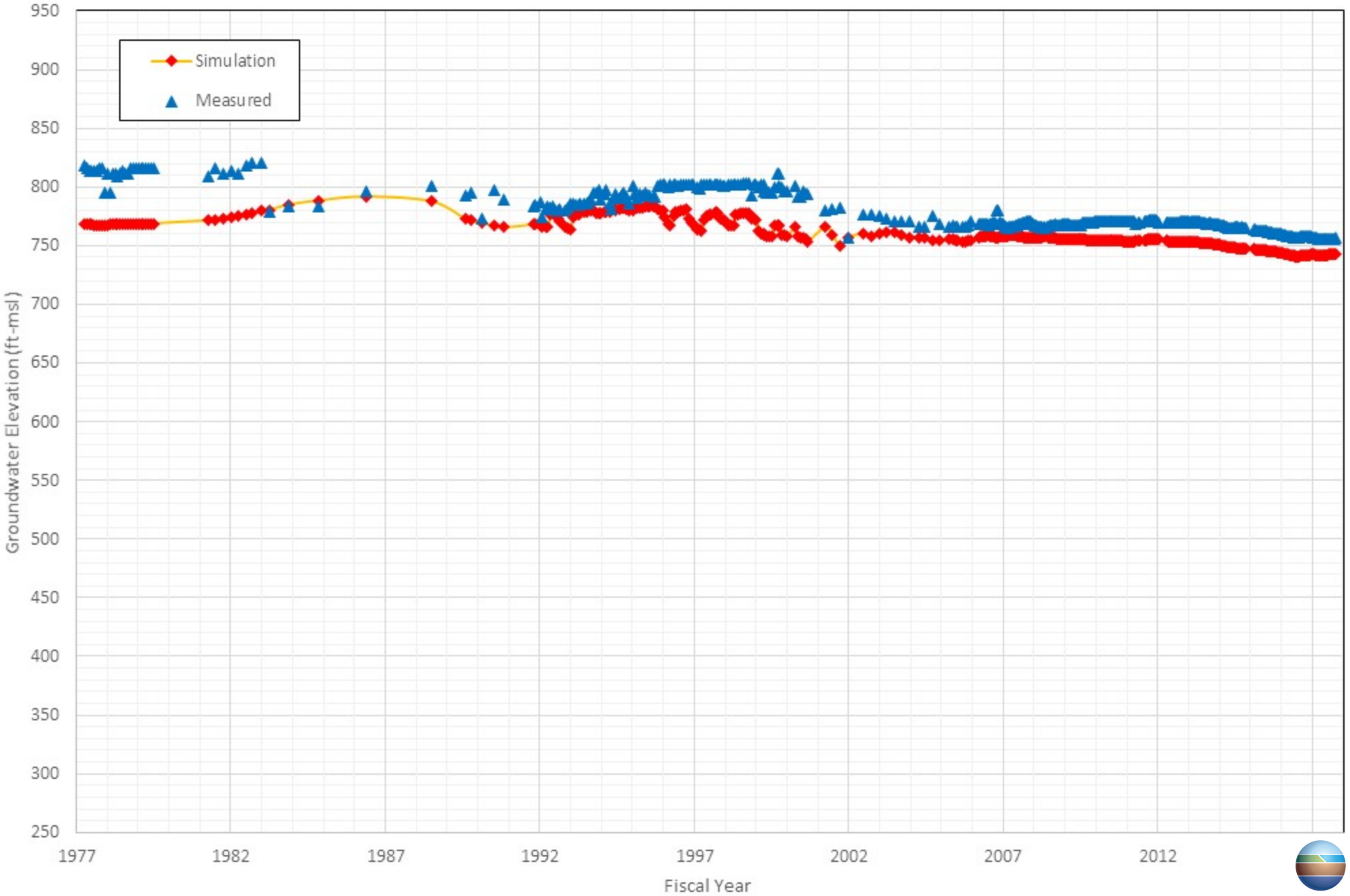

Appendix C-45
Comparison of Measured and Simulated Groundwater Water Level
in the Fontana Water Company's Well F21A

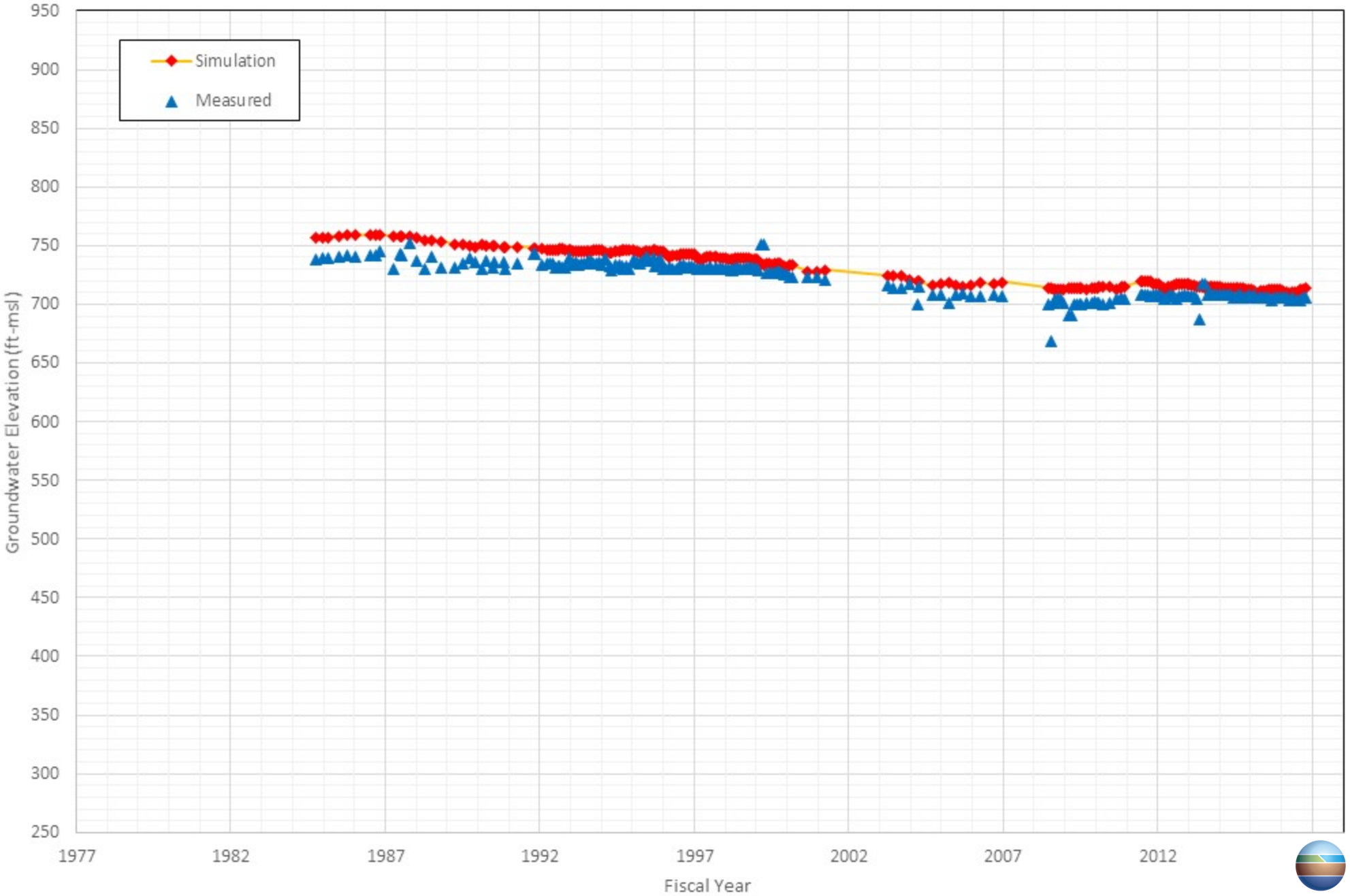

Appendix C-46
Comparison of Measured and Simulated Groundwater Water Level
in the Fontana Water Company's Well F30A

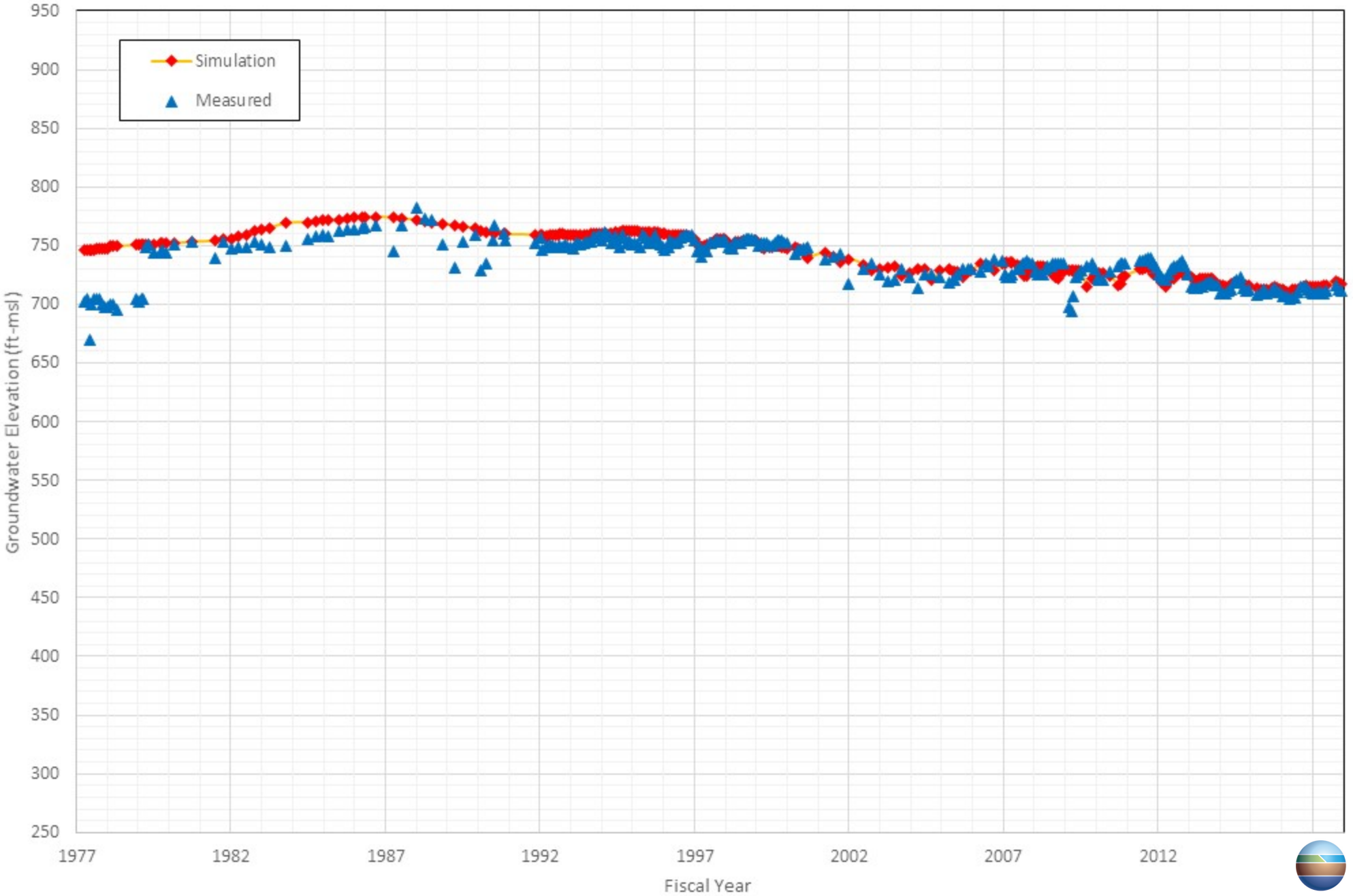

Appendix C-47
Comparison of Measured and Simulated Groundwater Water Level
in the Fontana Water Company's Well F31A

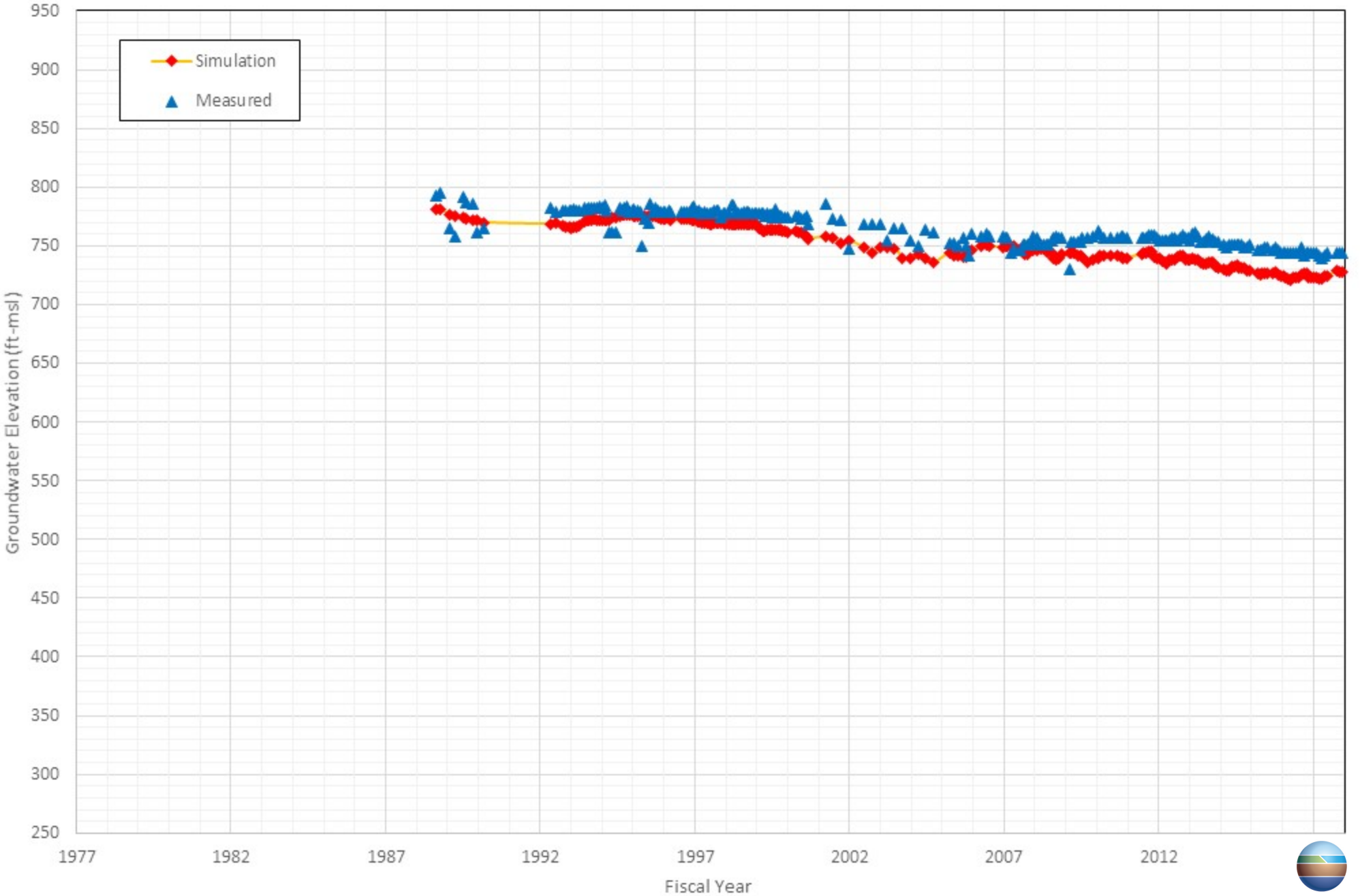

Appendix C-48
Comparison of Measured and Simulated Groundwater Water Level
in the Fontana Water Company's Well F35A

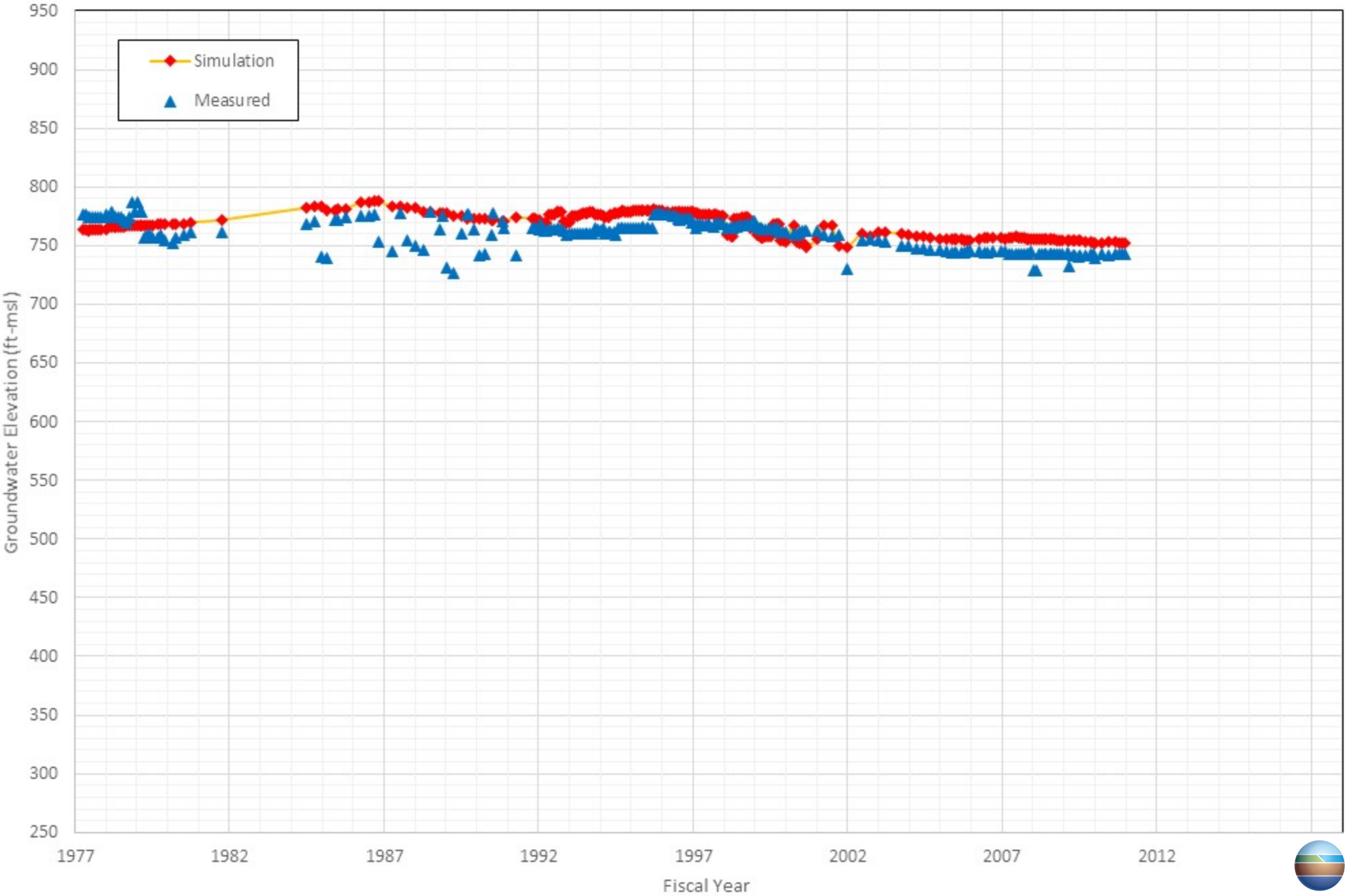

Appendix C-49
Comparison of Measured and Simulated Groundwater Water Level
in the Fontana Water Company's Well FU28

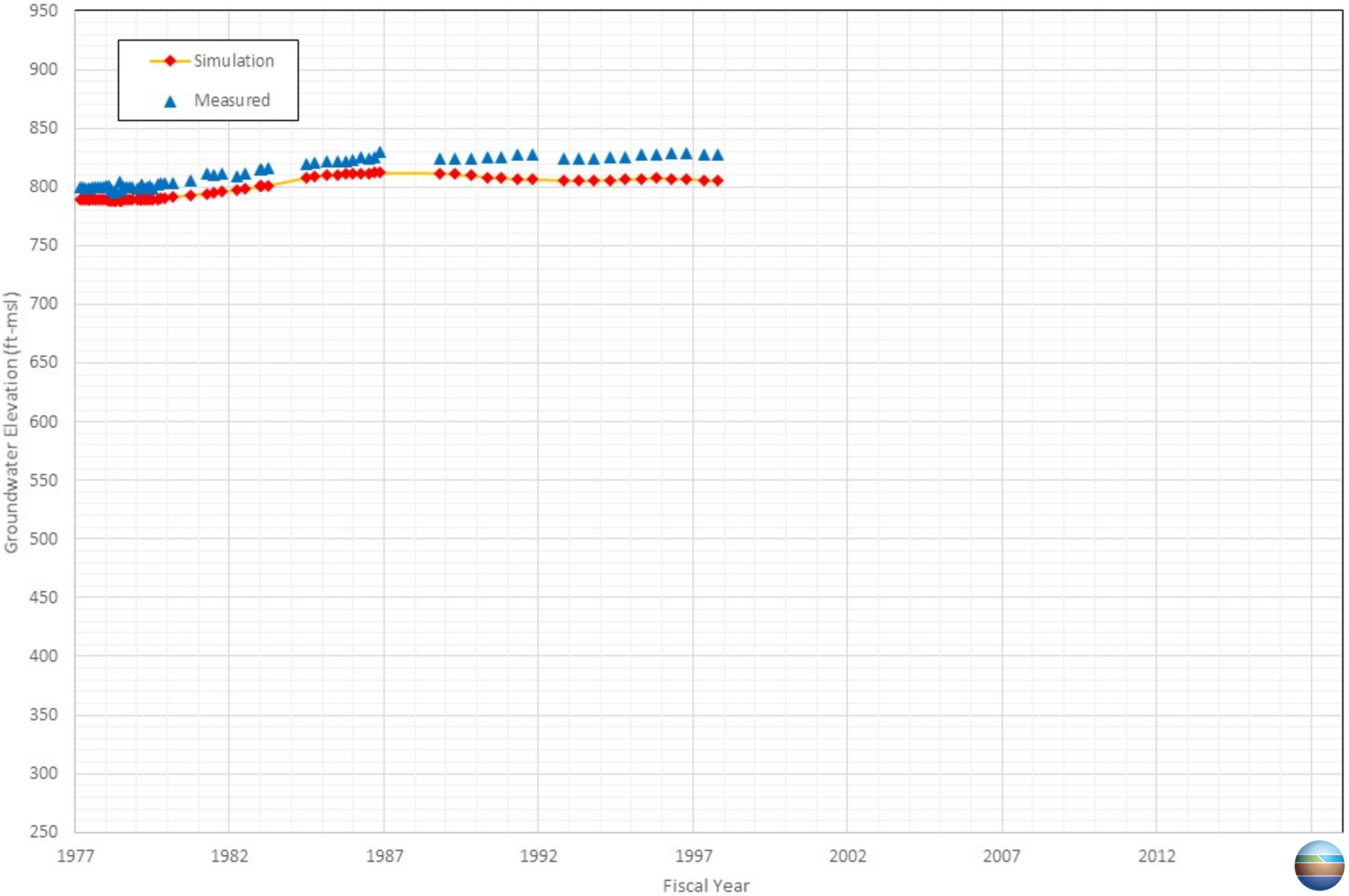

Appendix C-50
Comparison of Measured and Simulated Groundwater Water Level
in the Fontana Water Company's Well FU6

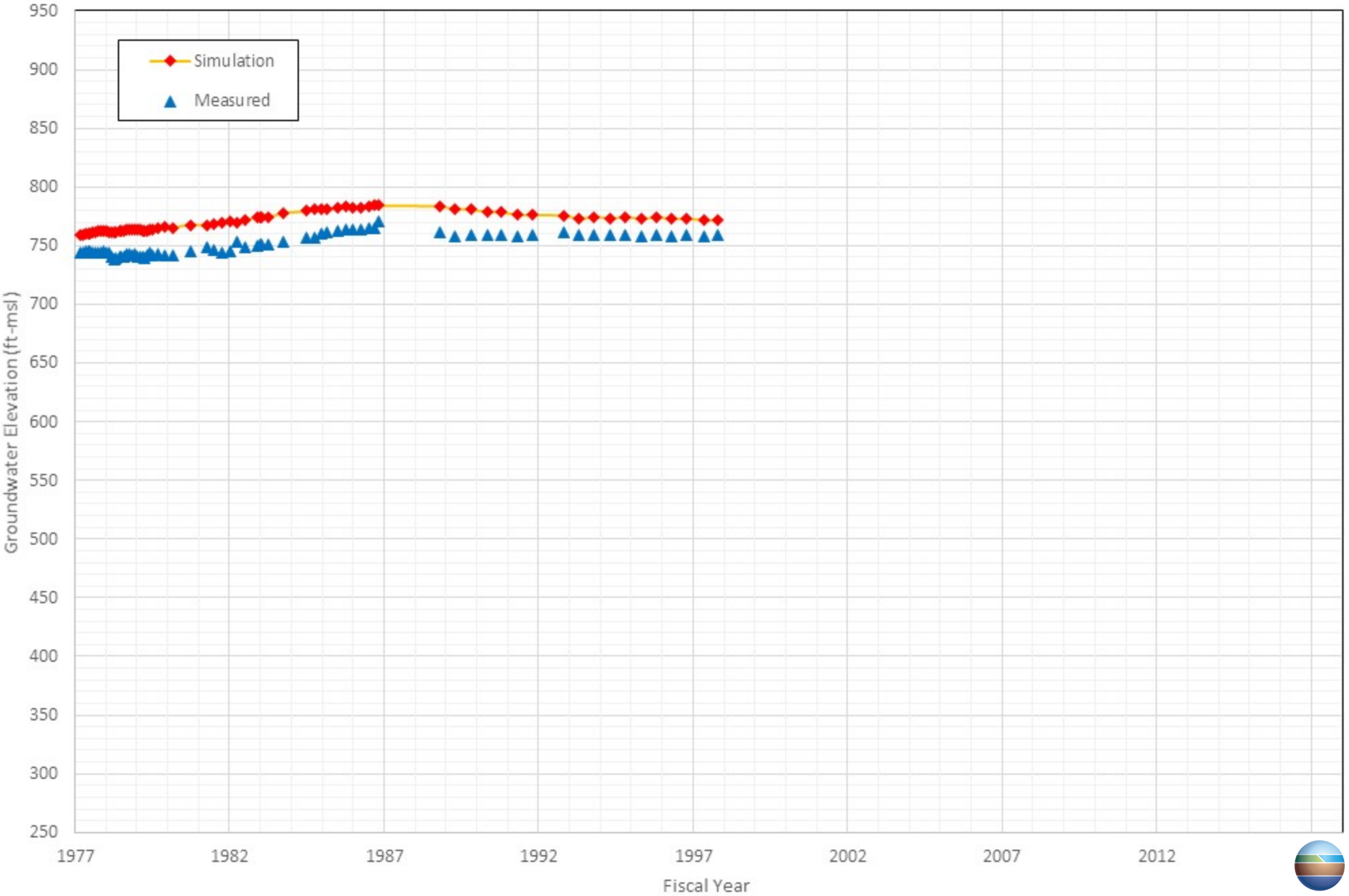

Appendix C-51
Comparison of Measured and Simulated Groundwater Water Level
in the General Electric Corporation's Well MW-11

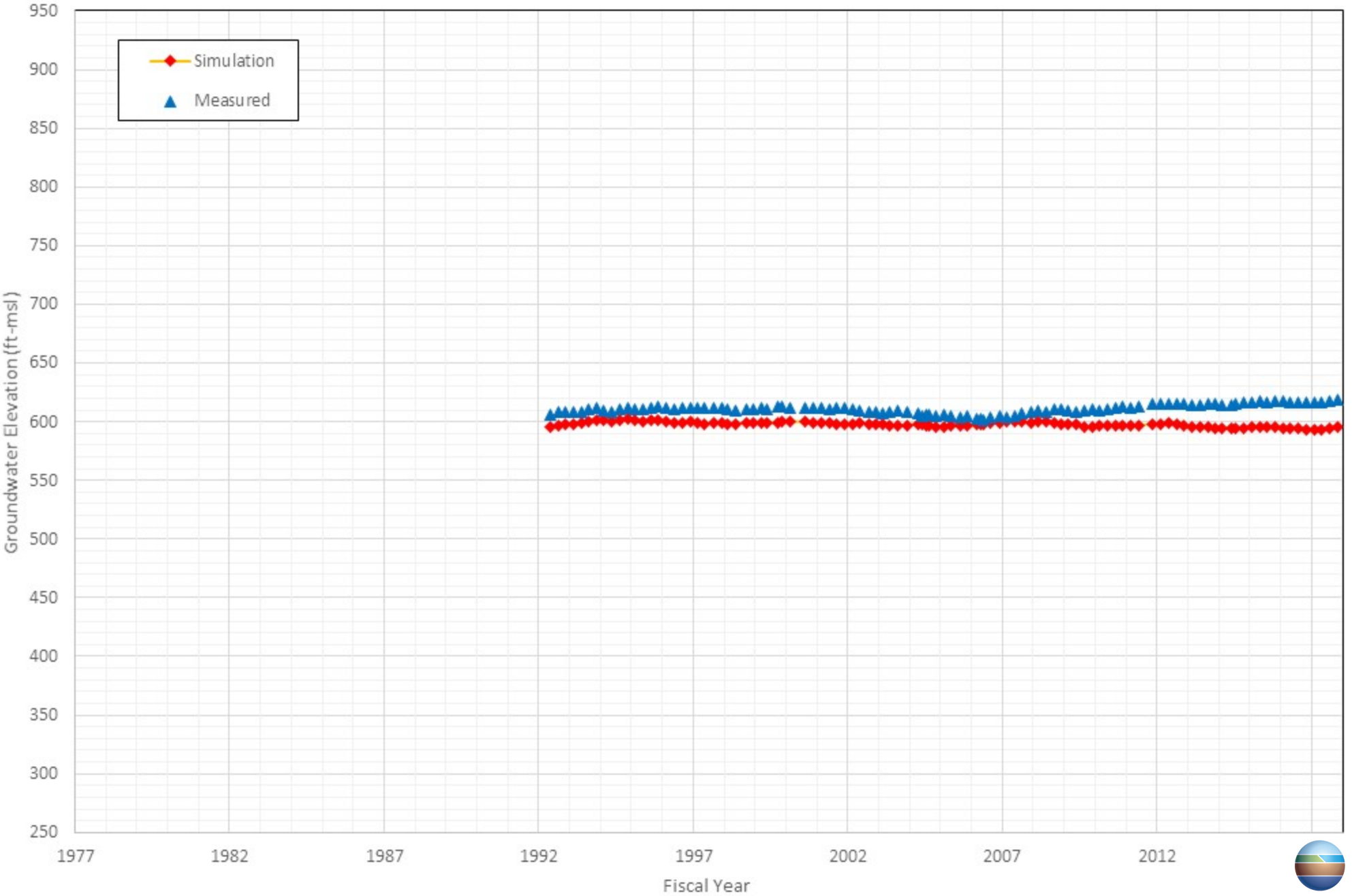

Appendix C-52
Comparison of Measured and Simulated Groundwater Water Level
in the Golden State Water Company's Well Margarita #1

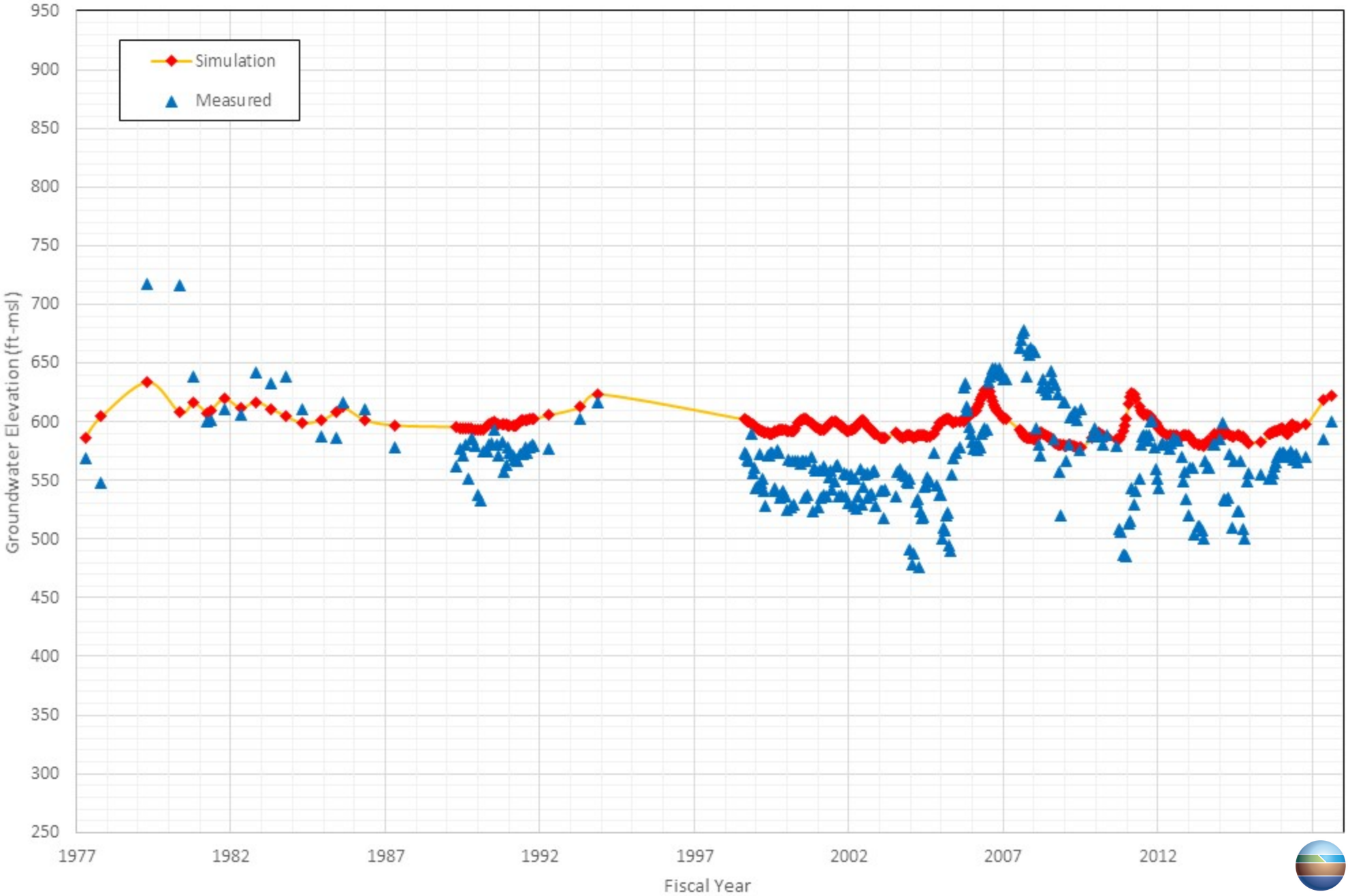

Appendix C-53
Comparison of Measured and Simulated Groundwater Water Level
in the Inland Empire Utilities Agency's Well HCMP-3/1

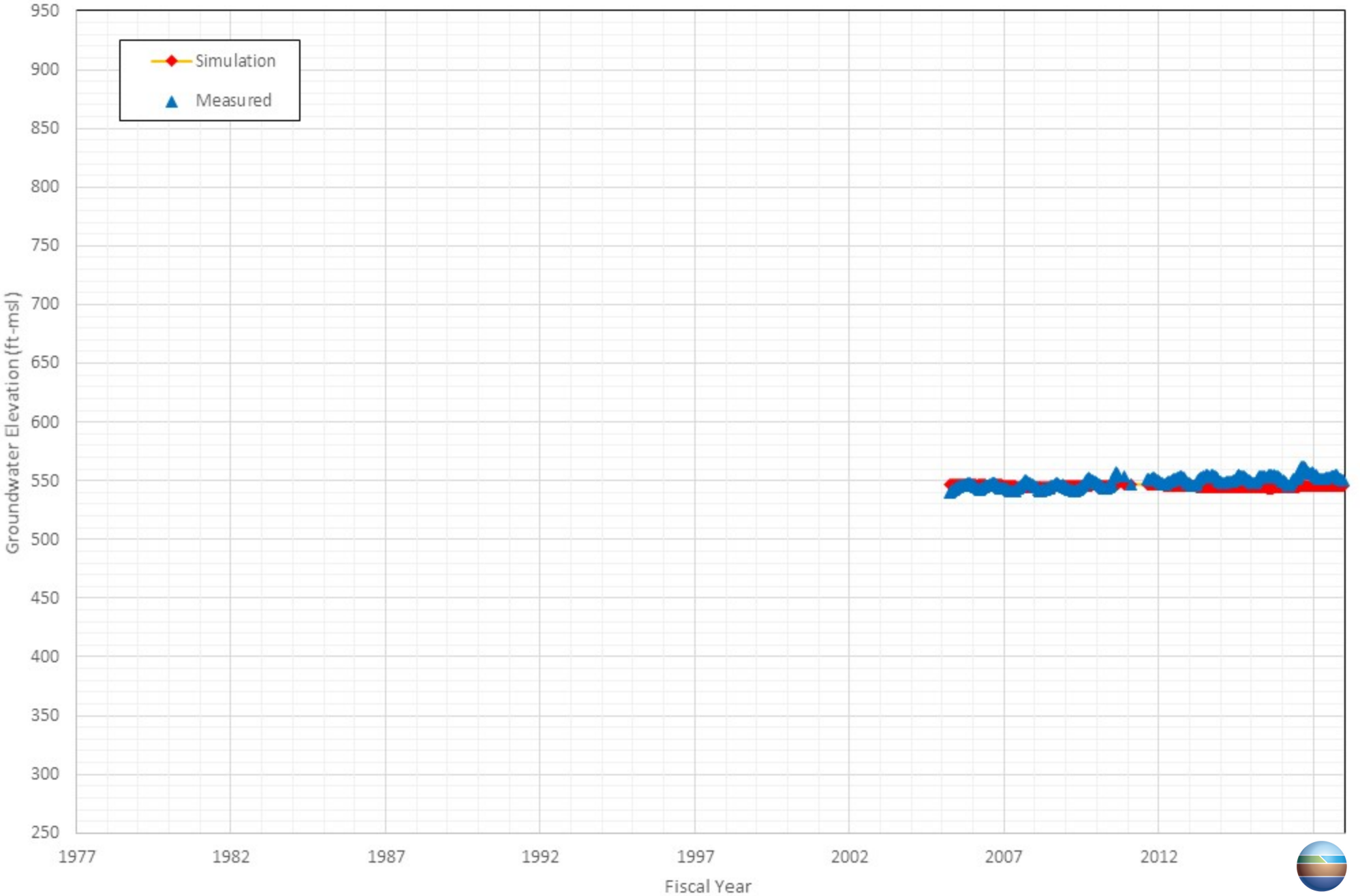

Appendix C-54
Comparison of Measured and Simulated Groundwater Water Level
in the Inland Empire Utilities Agency's Well HCMP-5/1

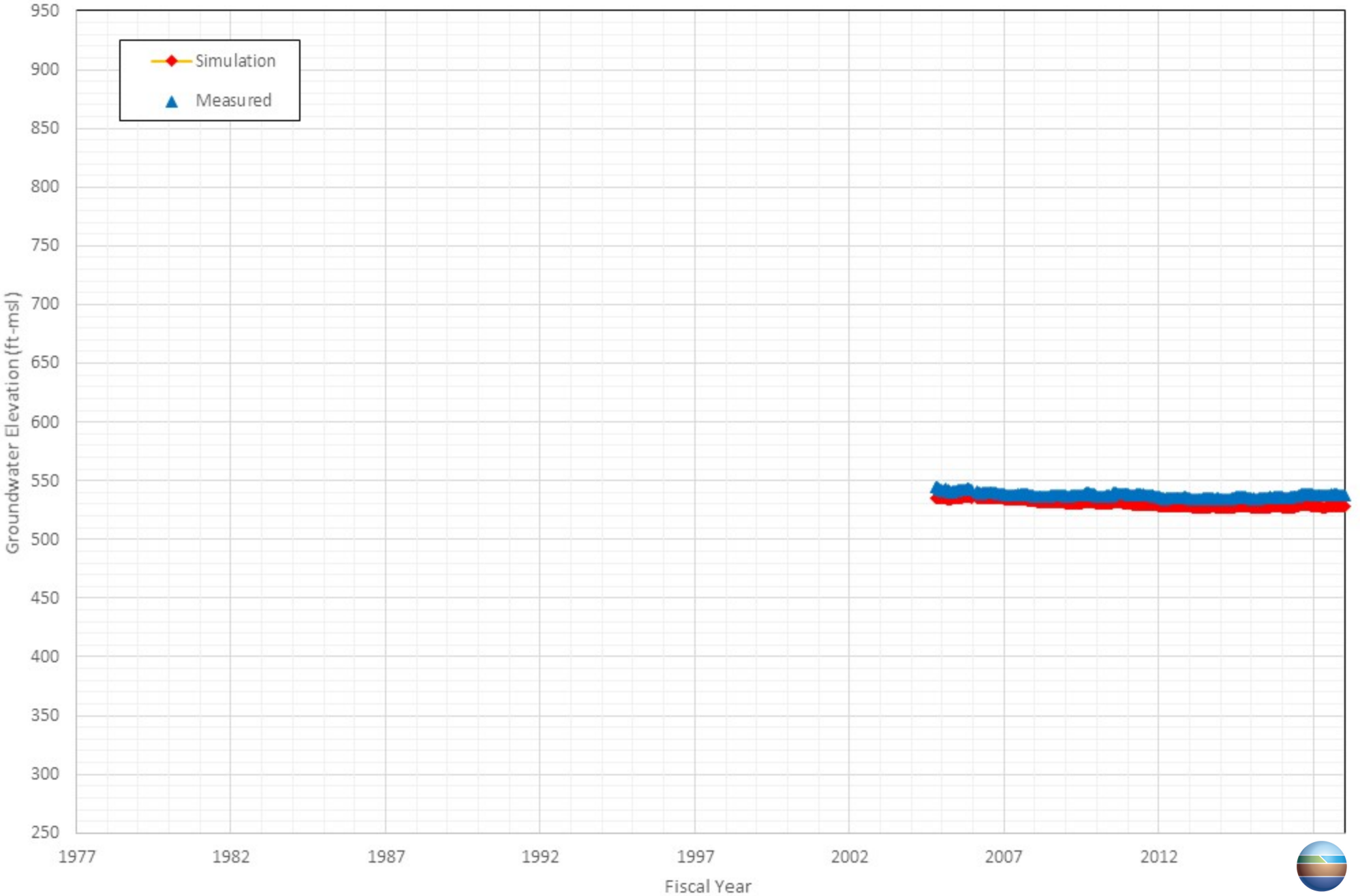

Appendix C-55
Comparison of Measured and Simulated Groundwater Water Level
in the Inland Empire Utilities Agency's Well HCMP-7/1

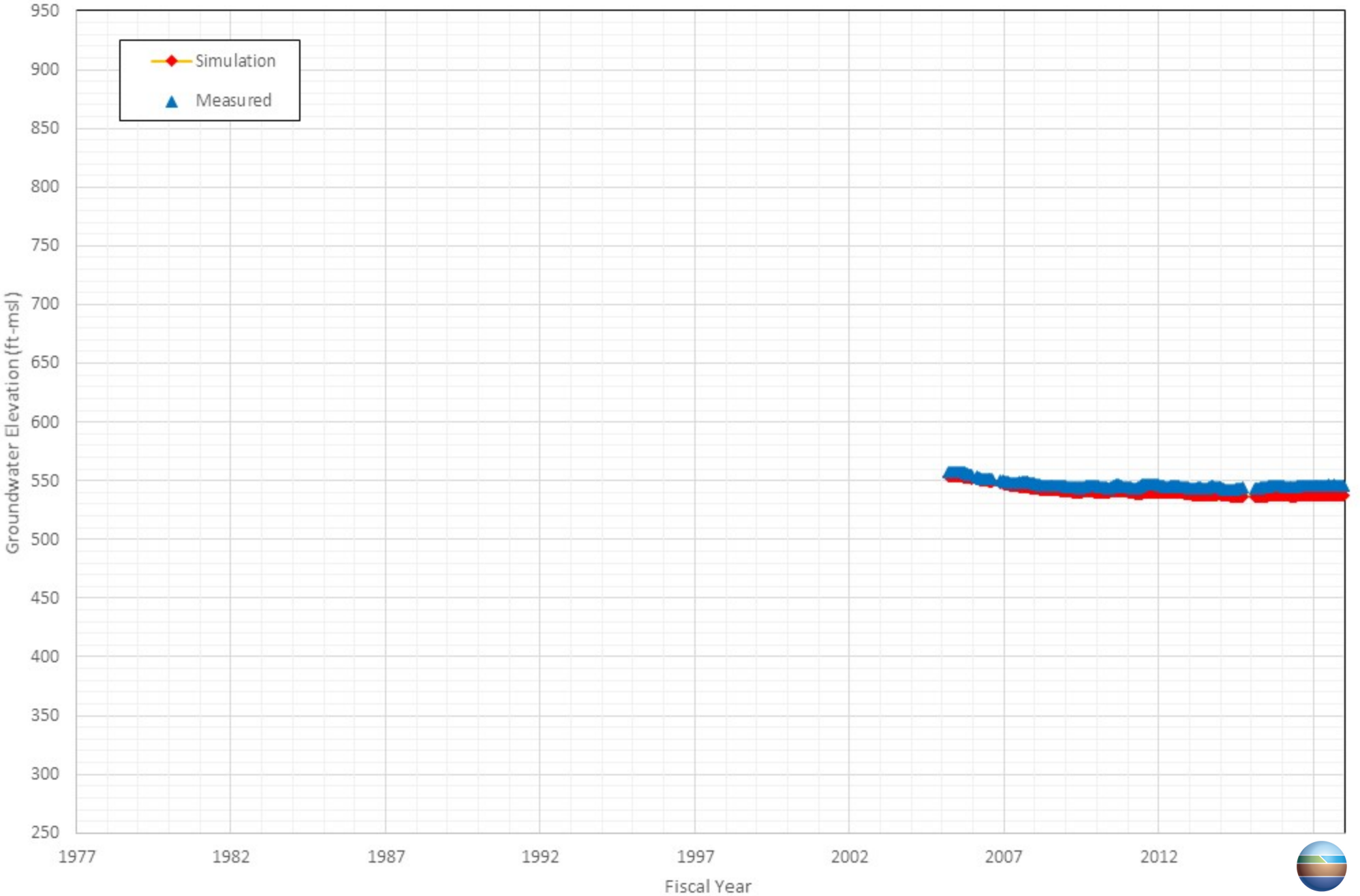

Appendix C-56
Comparison of Measured and Simulated Groundwater Water Level
in the Inland Empire Utilities Agency's Well HCMP-8/1

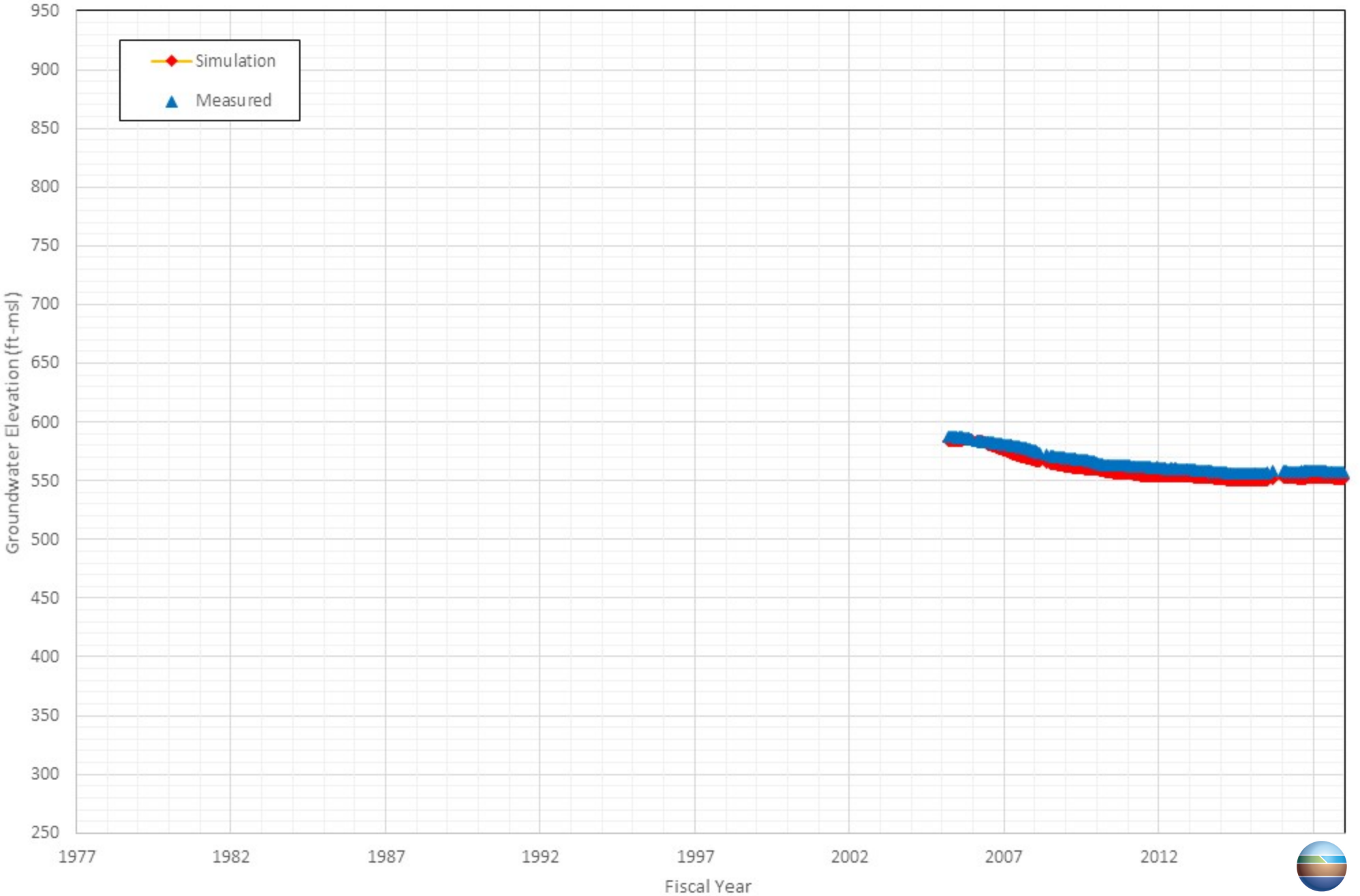

Appendix C-57
Comparison of Measured and Simulated Groundwater Water Level
in the Inland Empire Utilities Agency's Well MW-2

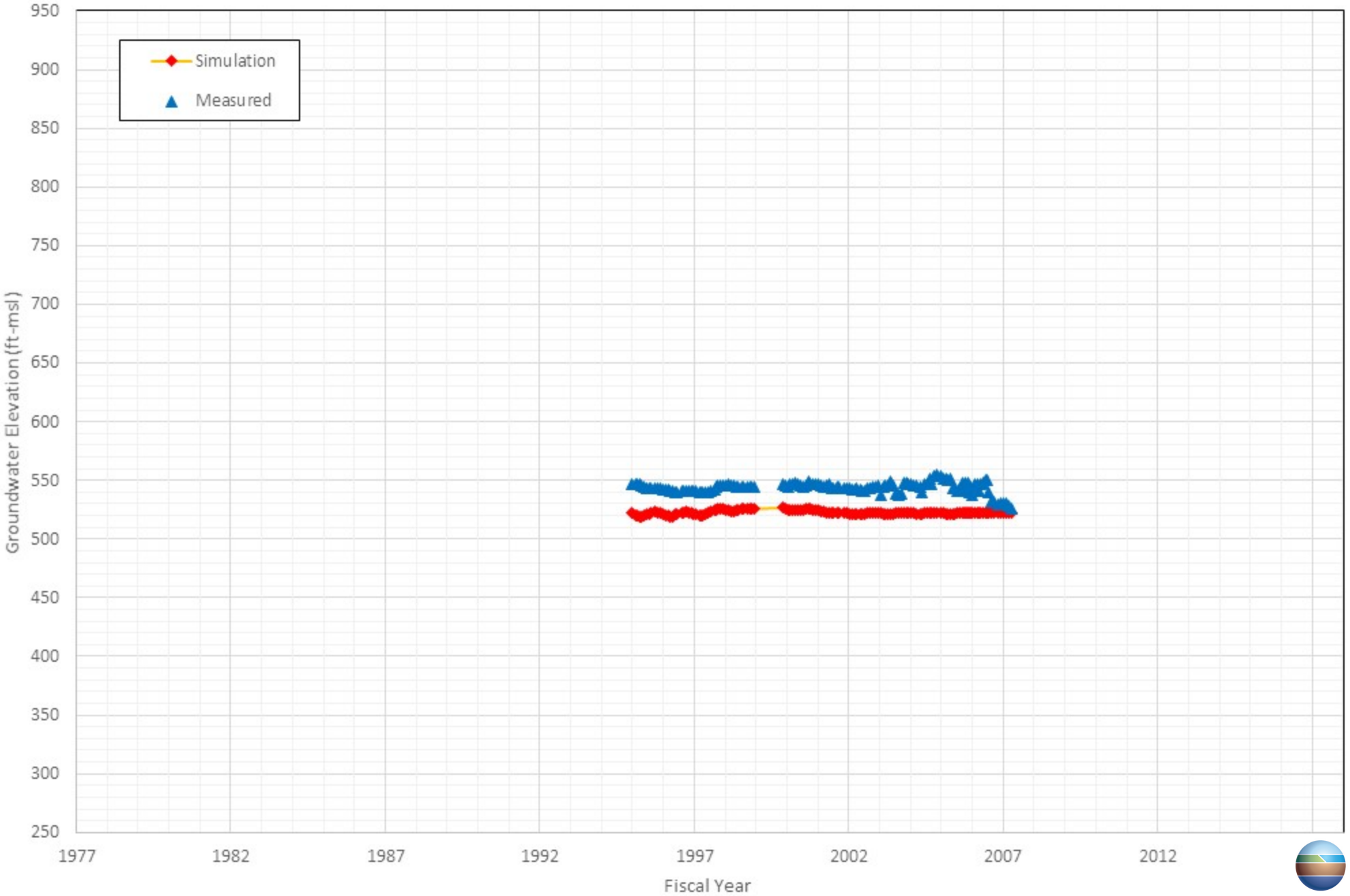

Appendix C-58
Comparison of Measured and Simulated Groundwater Water Level
in the Inland Empire Utilities Agency's Well PB-7/1

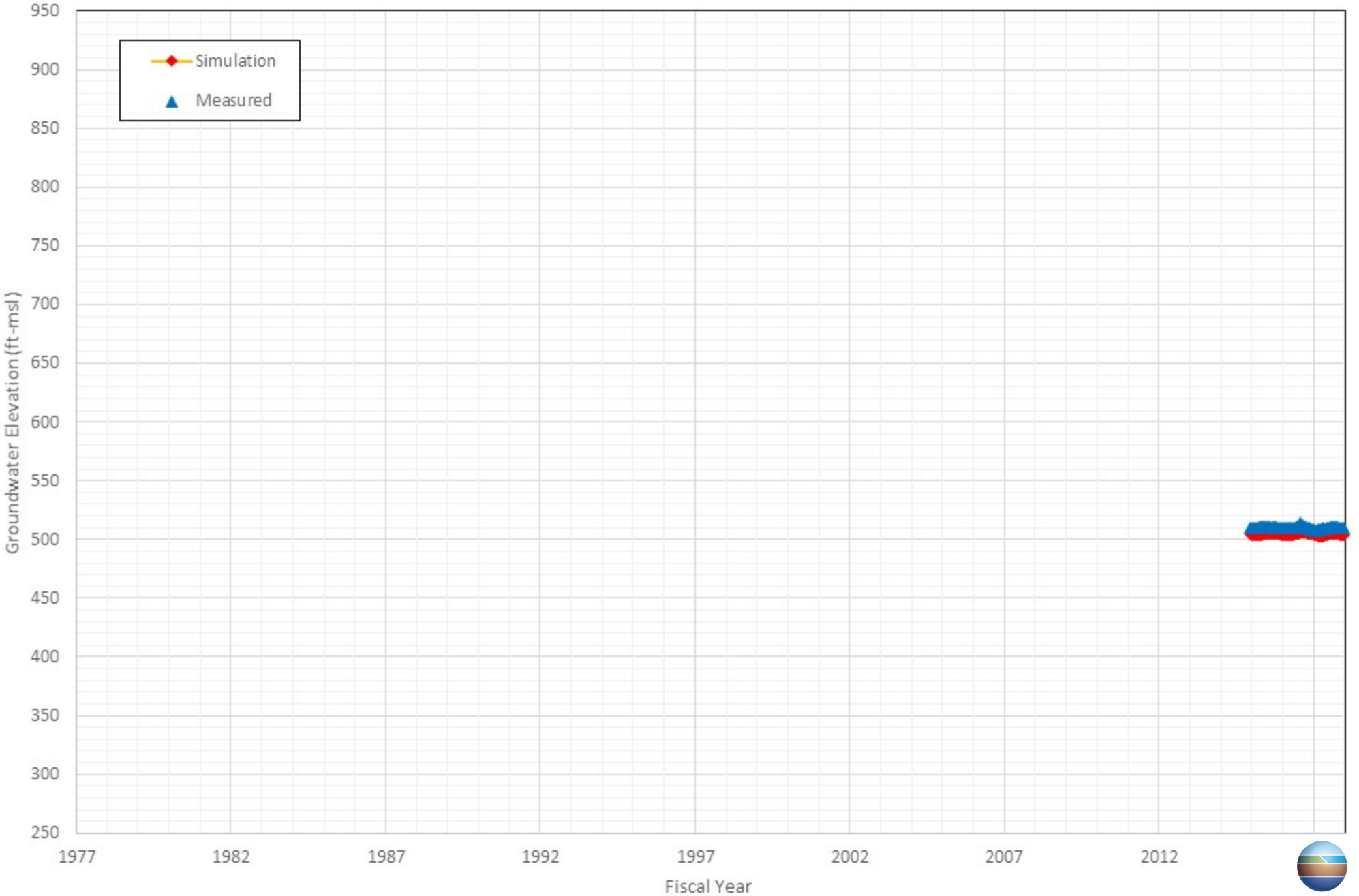

Appendix C-59
Comparison of Measured and Simulated Groundwater Water Level
in the Inland Empire Utilities Agency's Well PB-7/2

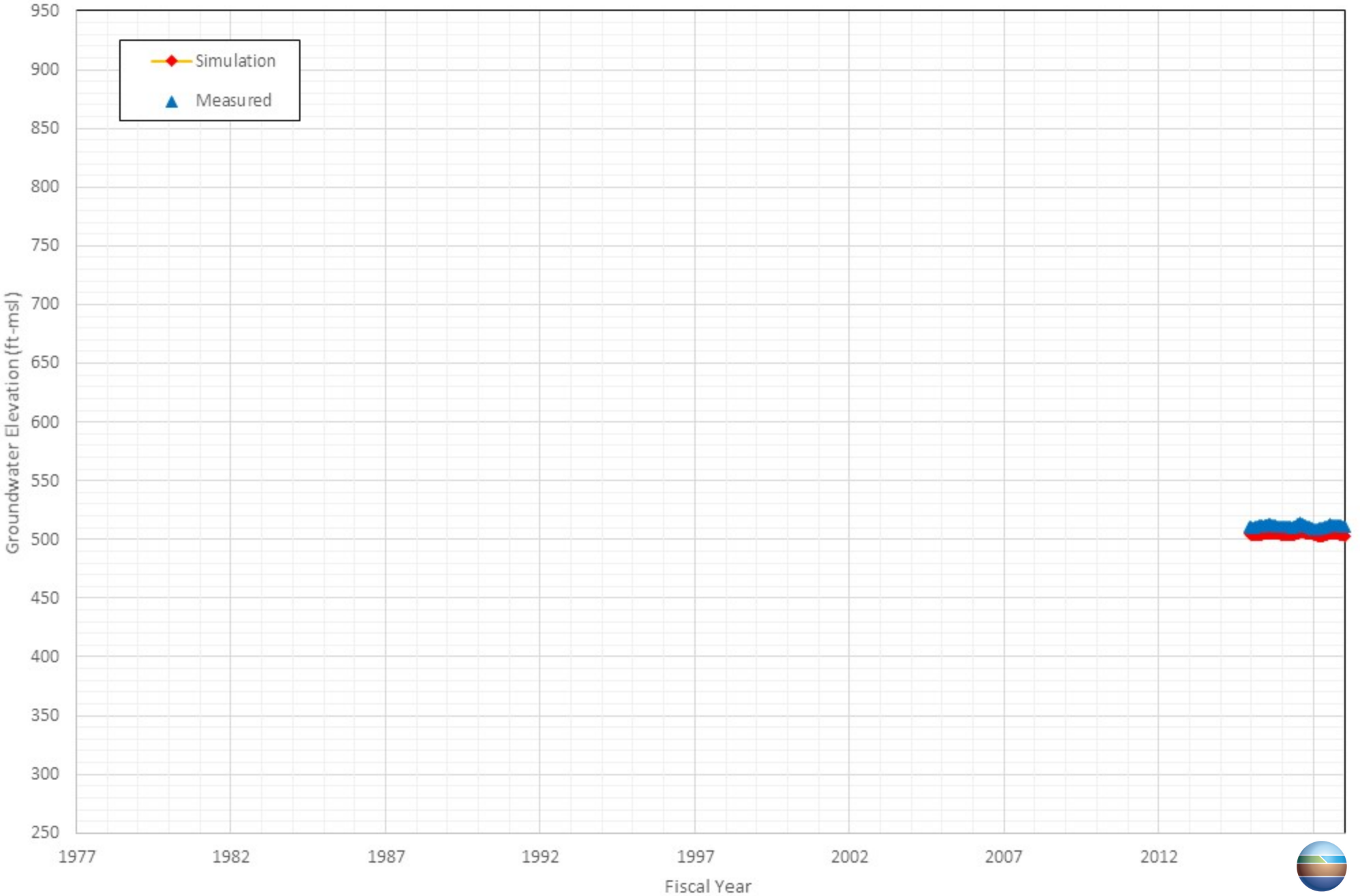

Appendix C-60
Comparison of Measured and Simulated Groundwater Water Level
in the Jurupa Community Services District's Well JCSD 16

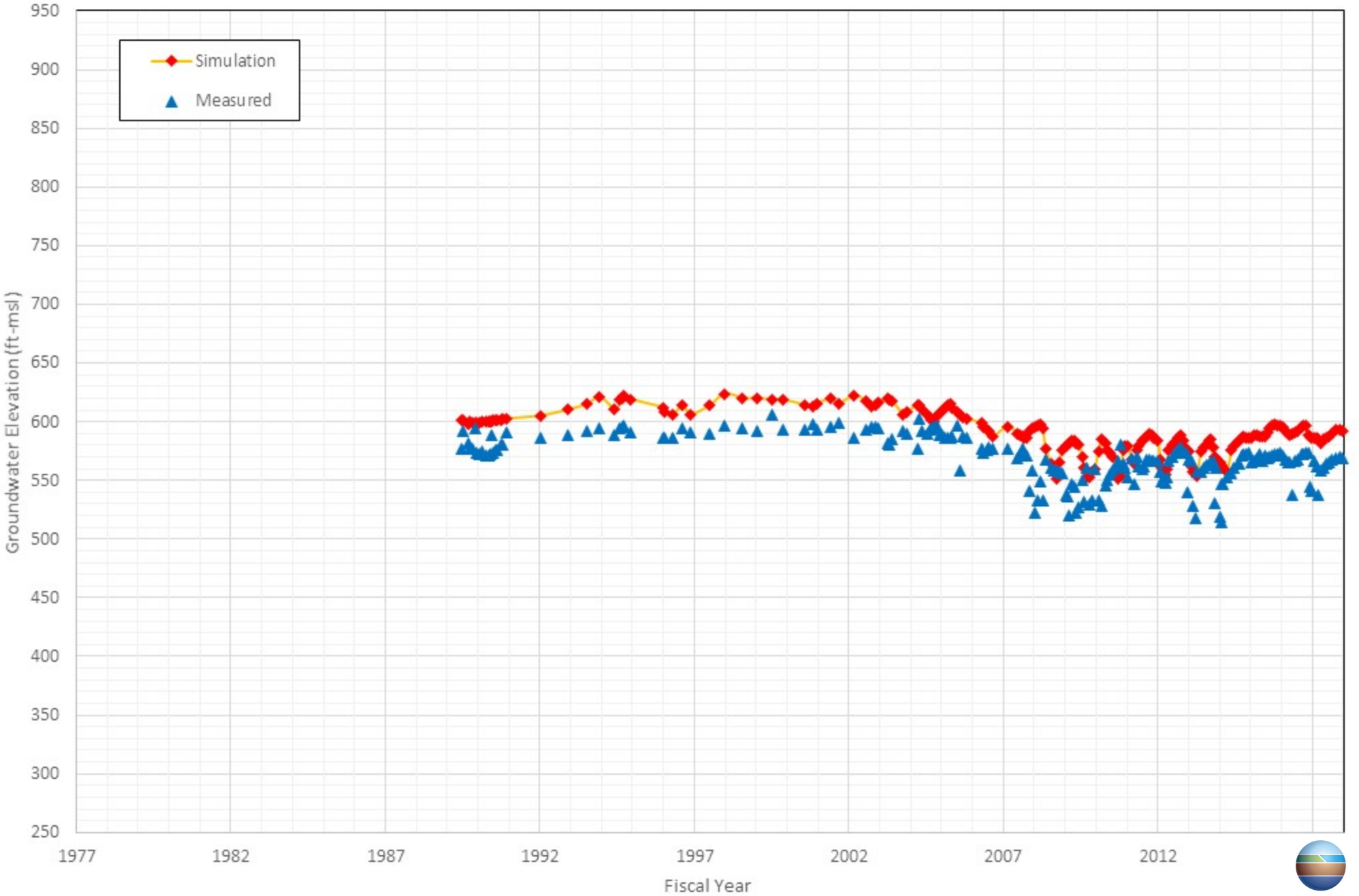

Appendix C-61
Comparison of Measured and Simulated Groundwater Water Level
in the Monte Vista Water District's Well MVWD 02

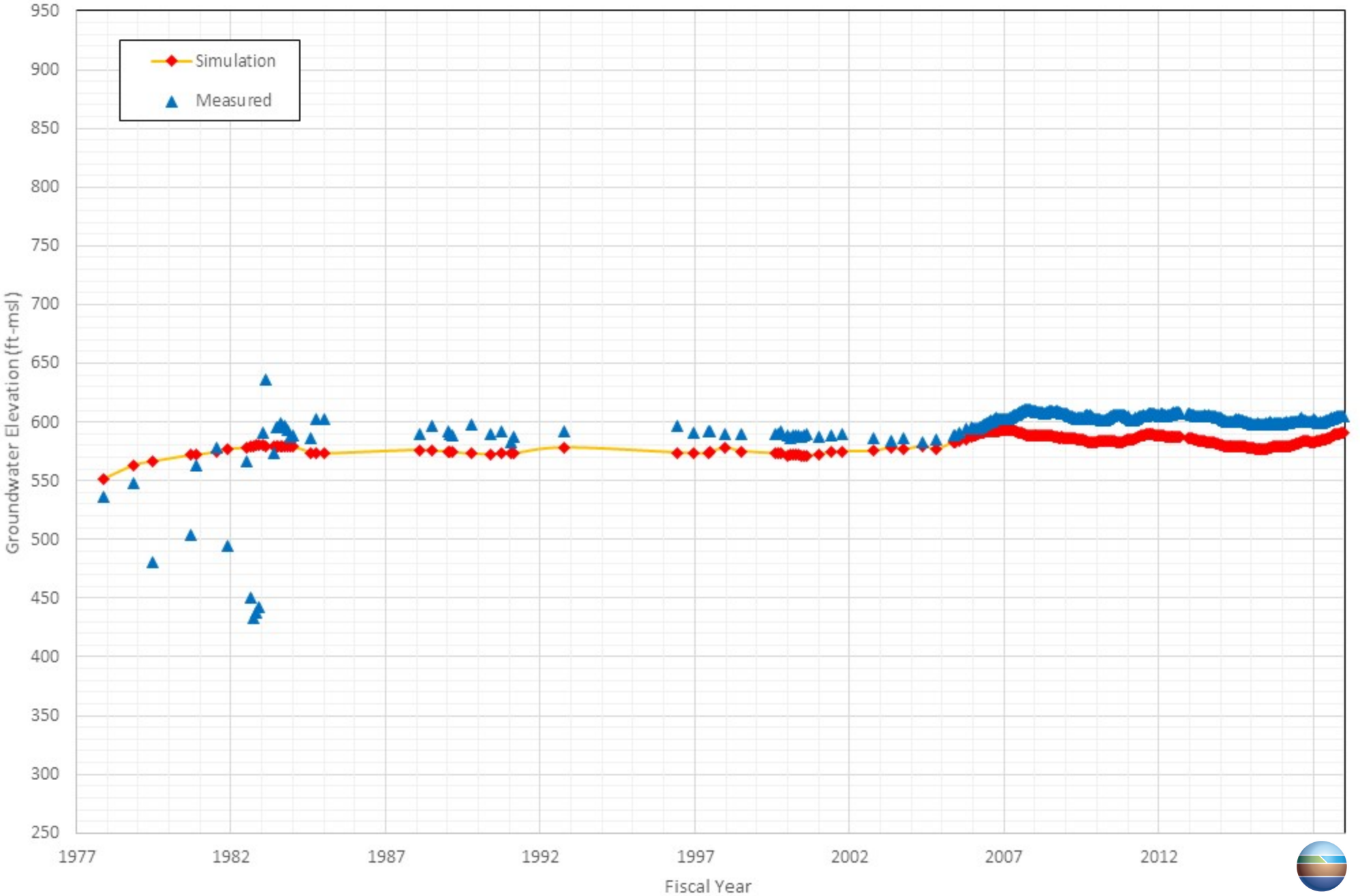

Appendix C-62
Comparison of Measured and Simulated Groundwater Water Level
in the Monte Vista Water District's Well MVWD 08

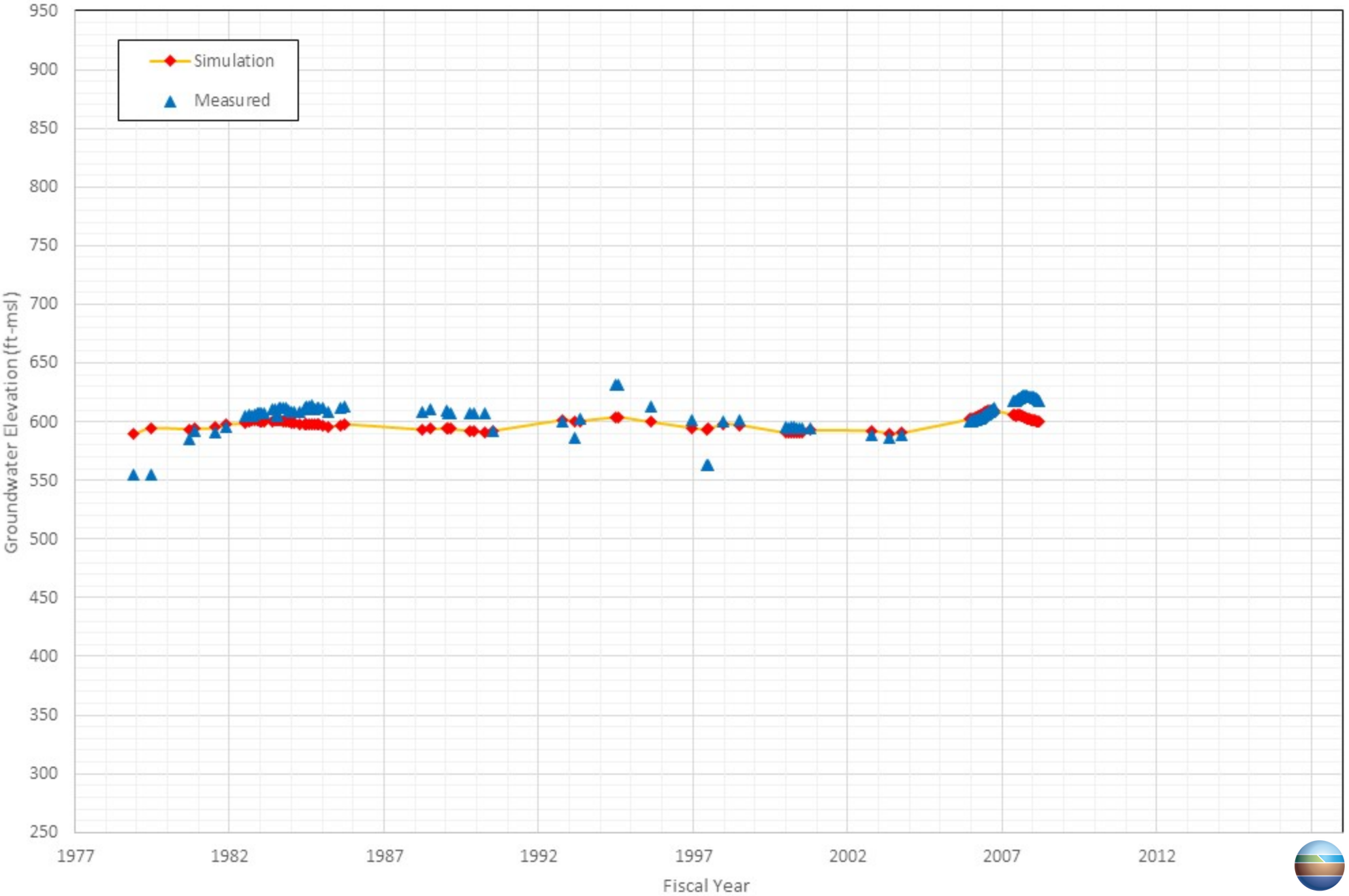

Appendix C-63
Comparison of Measured and Simulated Groundwater Water Level
in the West Valley Water District's Well WVWD 20

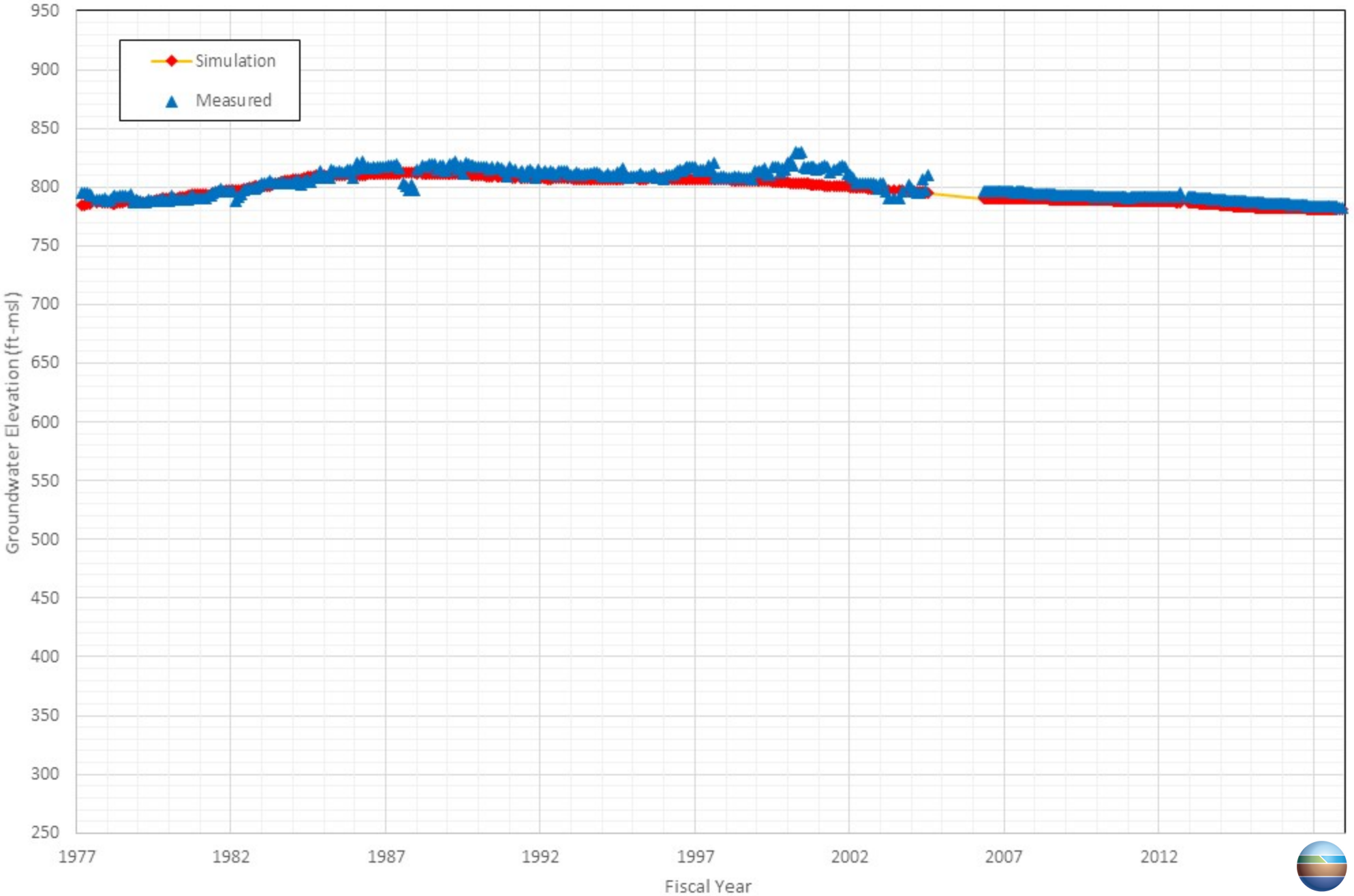

Appendix C-64
Comparison of Measured and Simulated Groundwater Water Level
in the Orange County Flood Control District's Well 83240-DOM

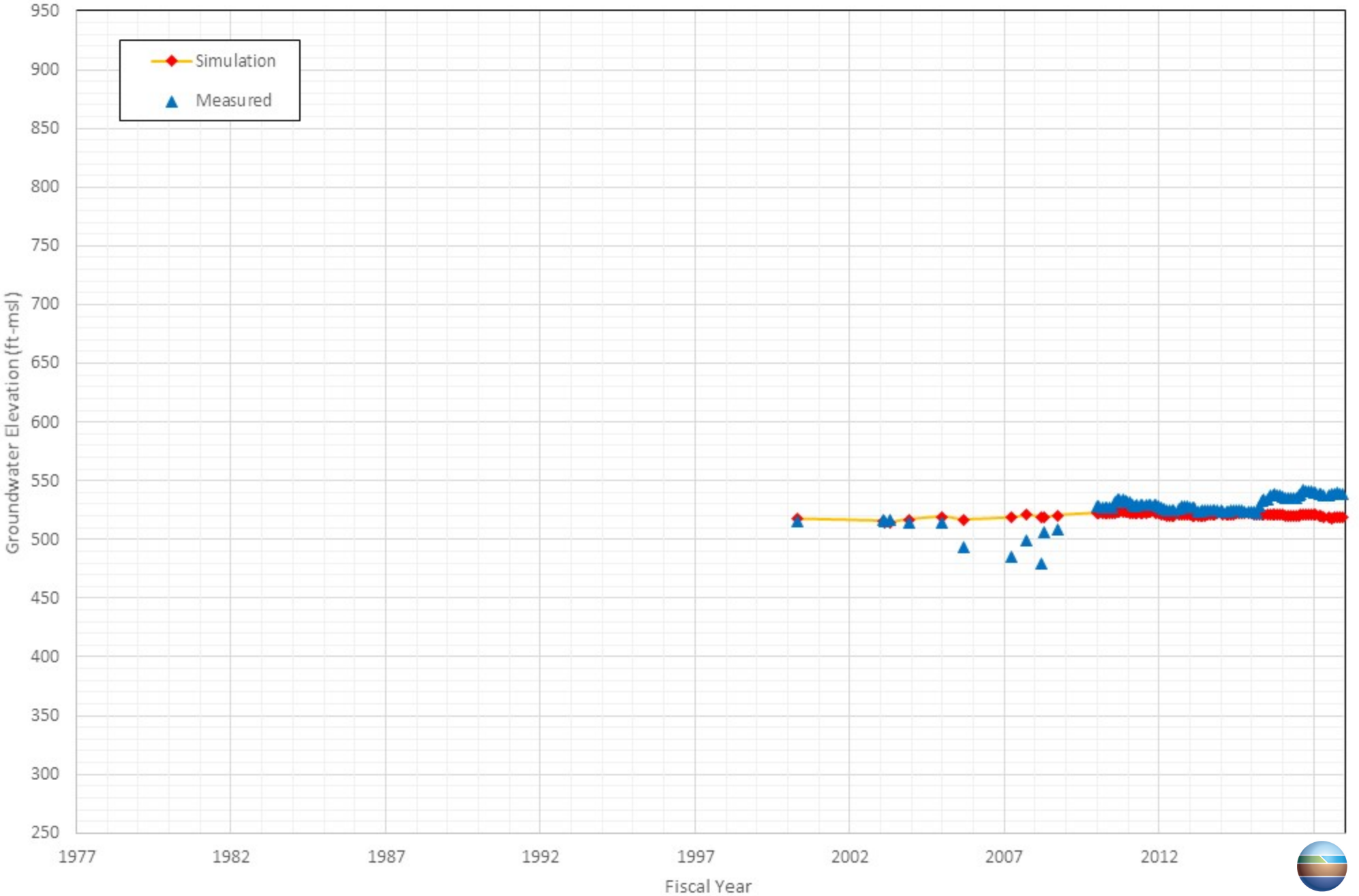

Appendix C-65
Comparison of Measured and Simulated Groundwater Water Level
in the Orange County Water District's Well OCWD-PDE4

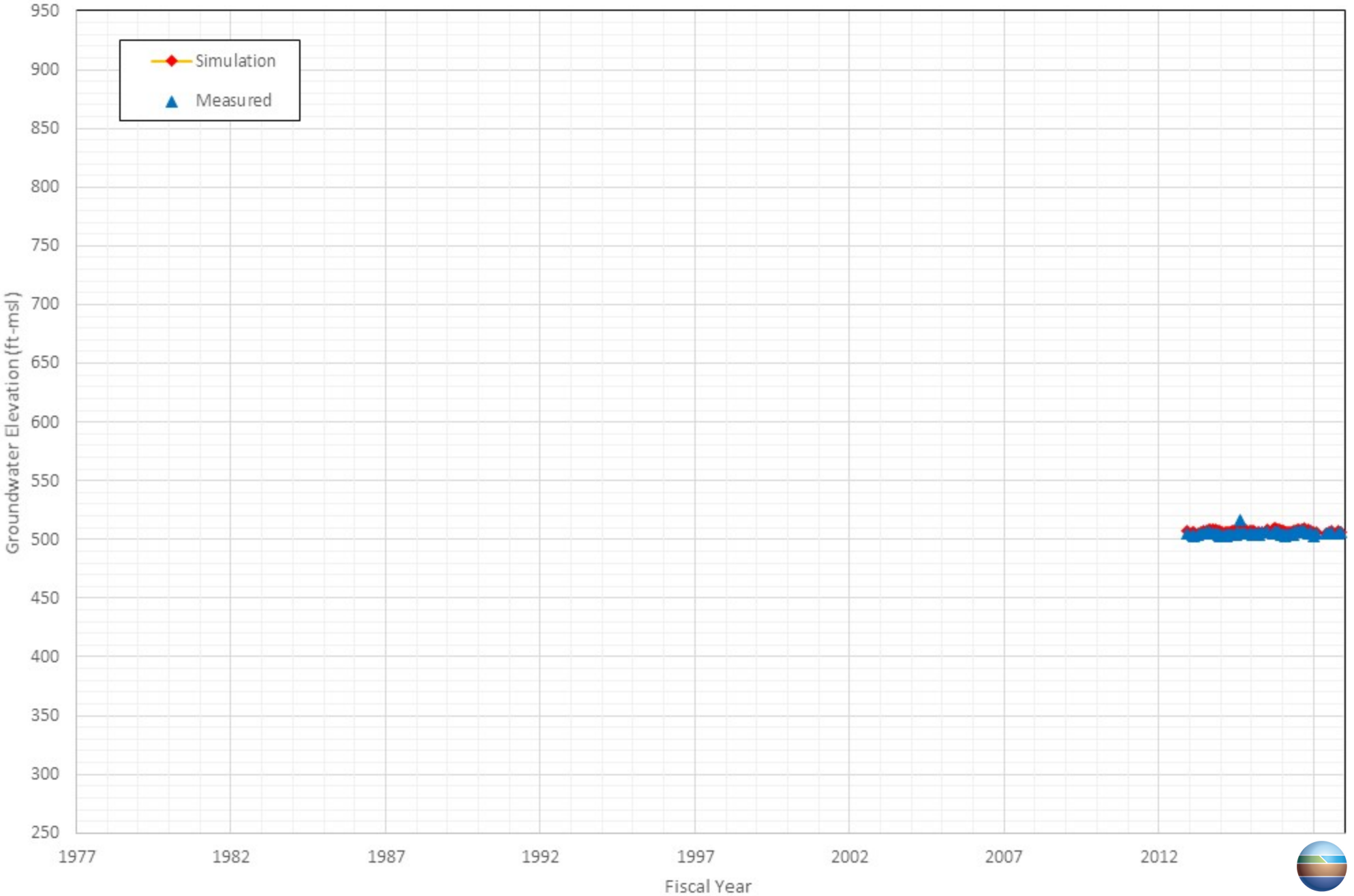

Appendix C-66
Comparison of Measured and Simulated Groundwater Water Level
in the Santa Ana River Water Company's Well 01A

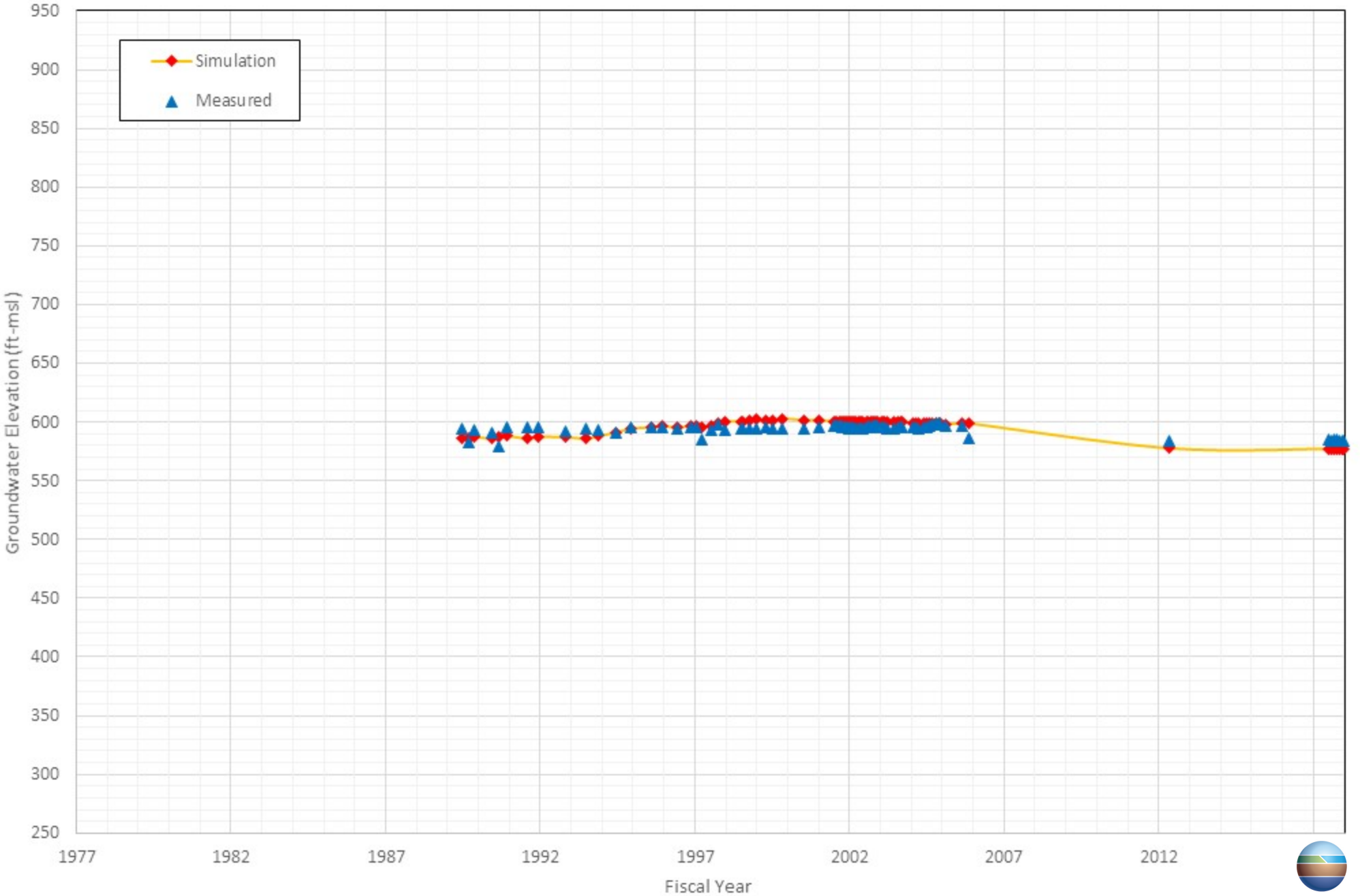

Appendix C-67
Comparison of Measured and Simulated Groundwater Water Level
in the Santa Ana River Water Company's Well 03

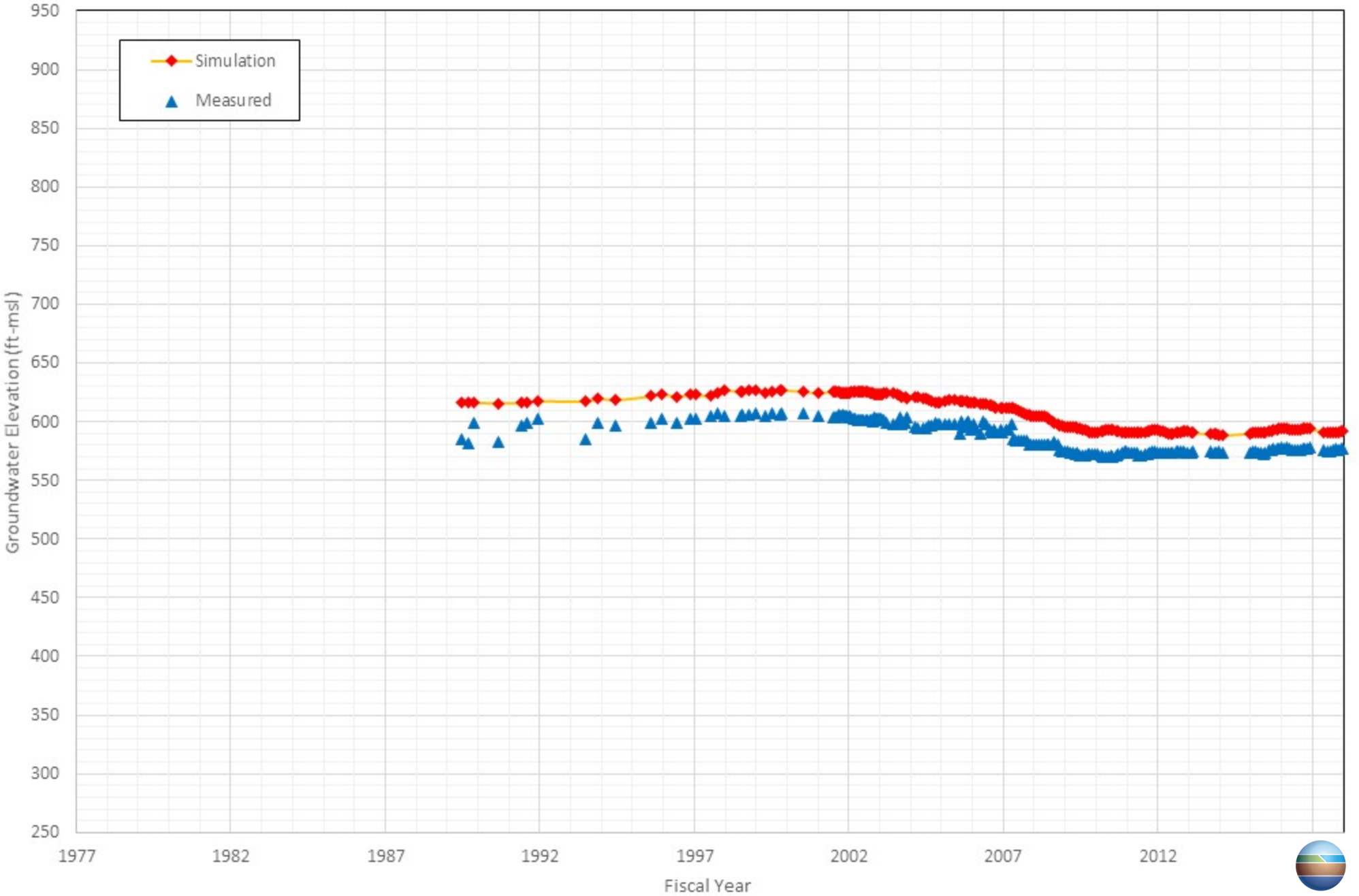

Appendix C-68
Comparison of Measured and Simulated Groundwater Water Level
in the Santa Ana River Water Company's Well 07

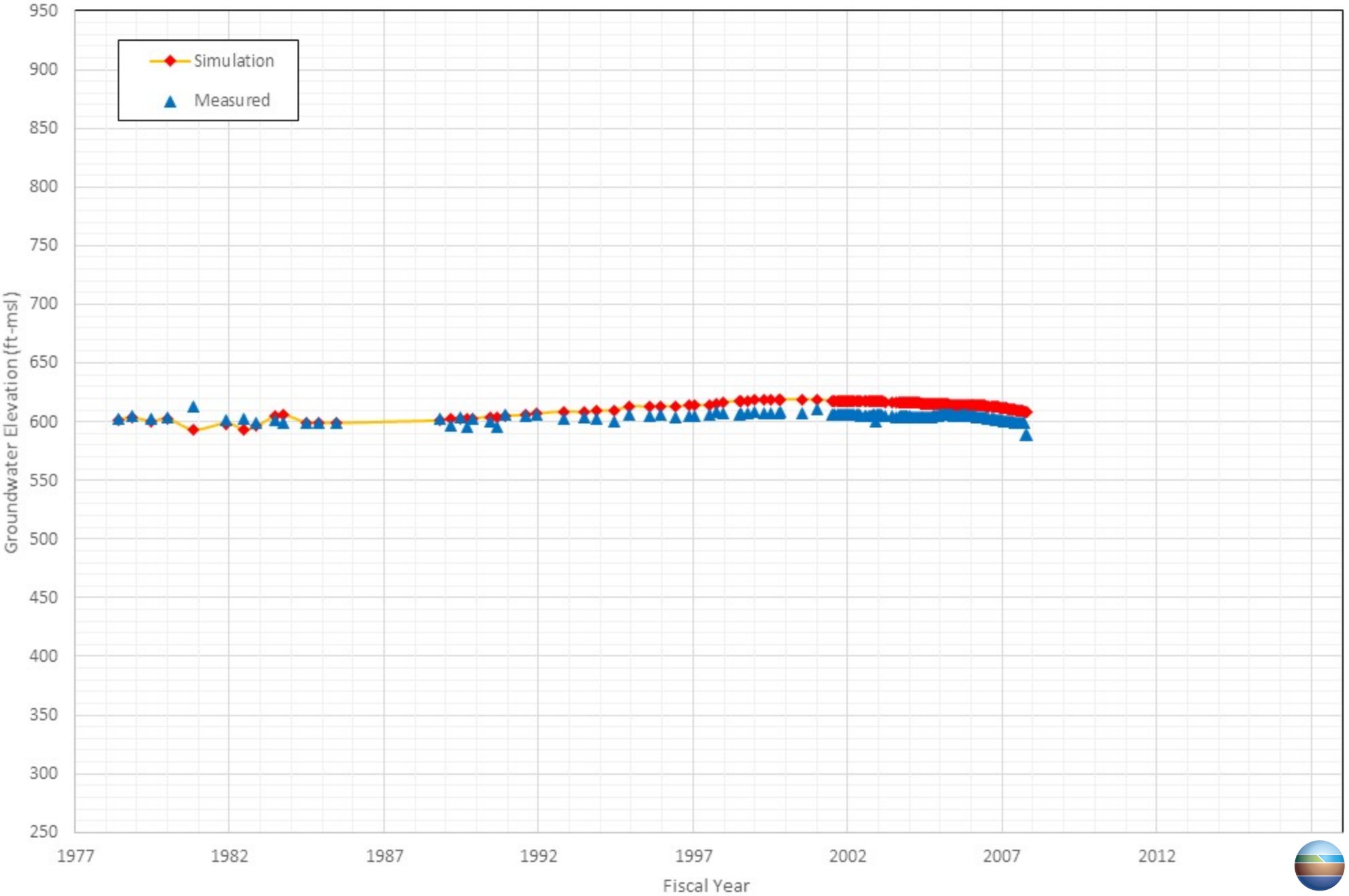

Appendix C-69
Comparison of Measured and Simulated Groundwater Water Level
in the San Antonio Water Company's Well SAWC 18

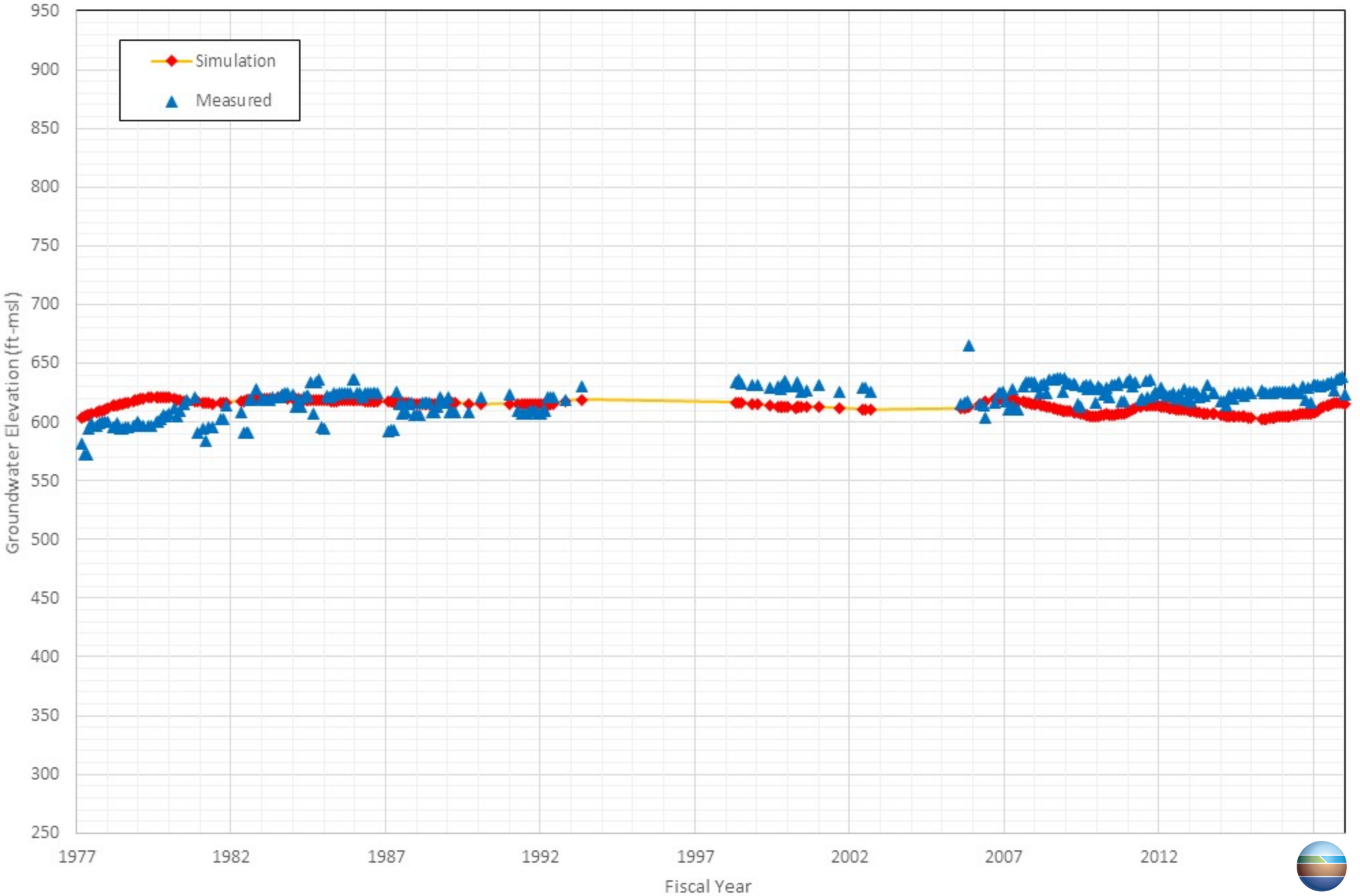

Appendix C-70
Comparison of Measured and Simulated Groundwater Water Level
in the State of California, California Institution for Men's Well 03

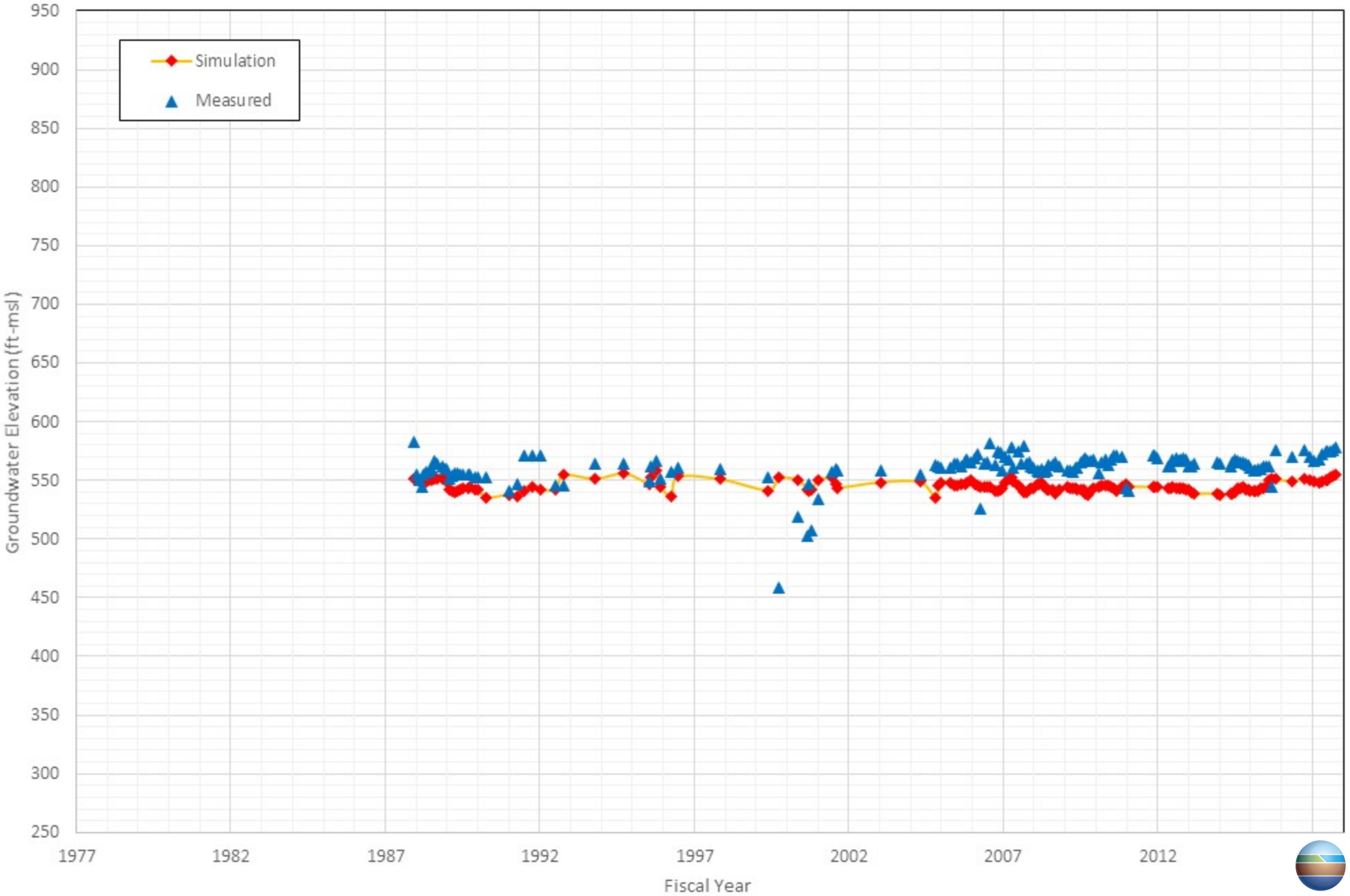

Appendix C-71
Comparison of Measured and Simulated Groundwater Water Level
in the State of California, California Institution for Men's Well 09

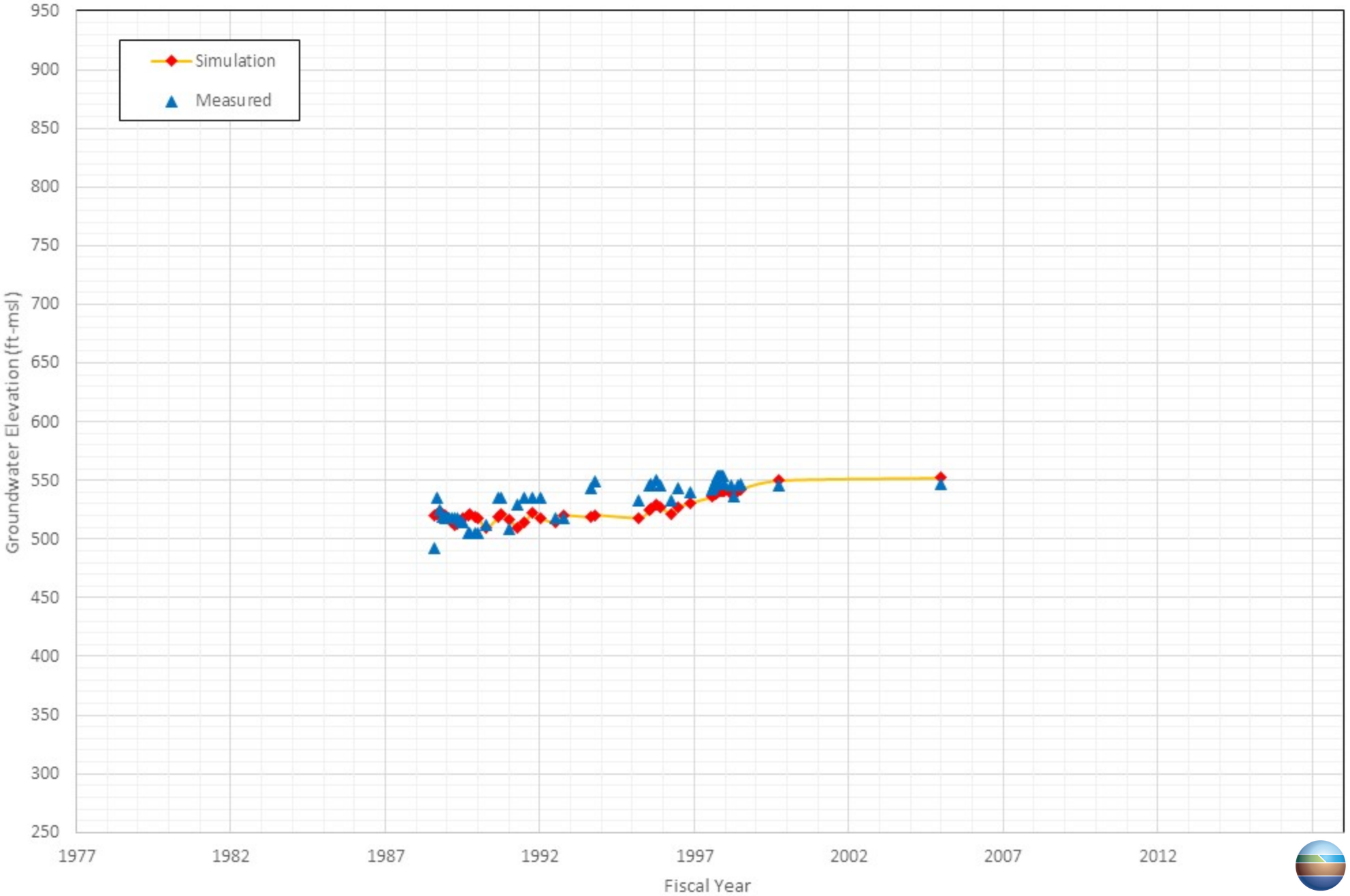

Appendix C-72
Comparison of Measured and Simulated Groundwater Water Level
in the State of California, California Institution for Men's Well MW-24I

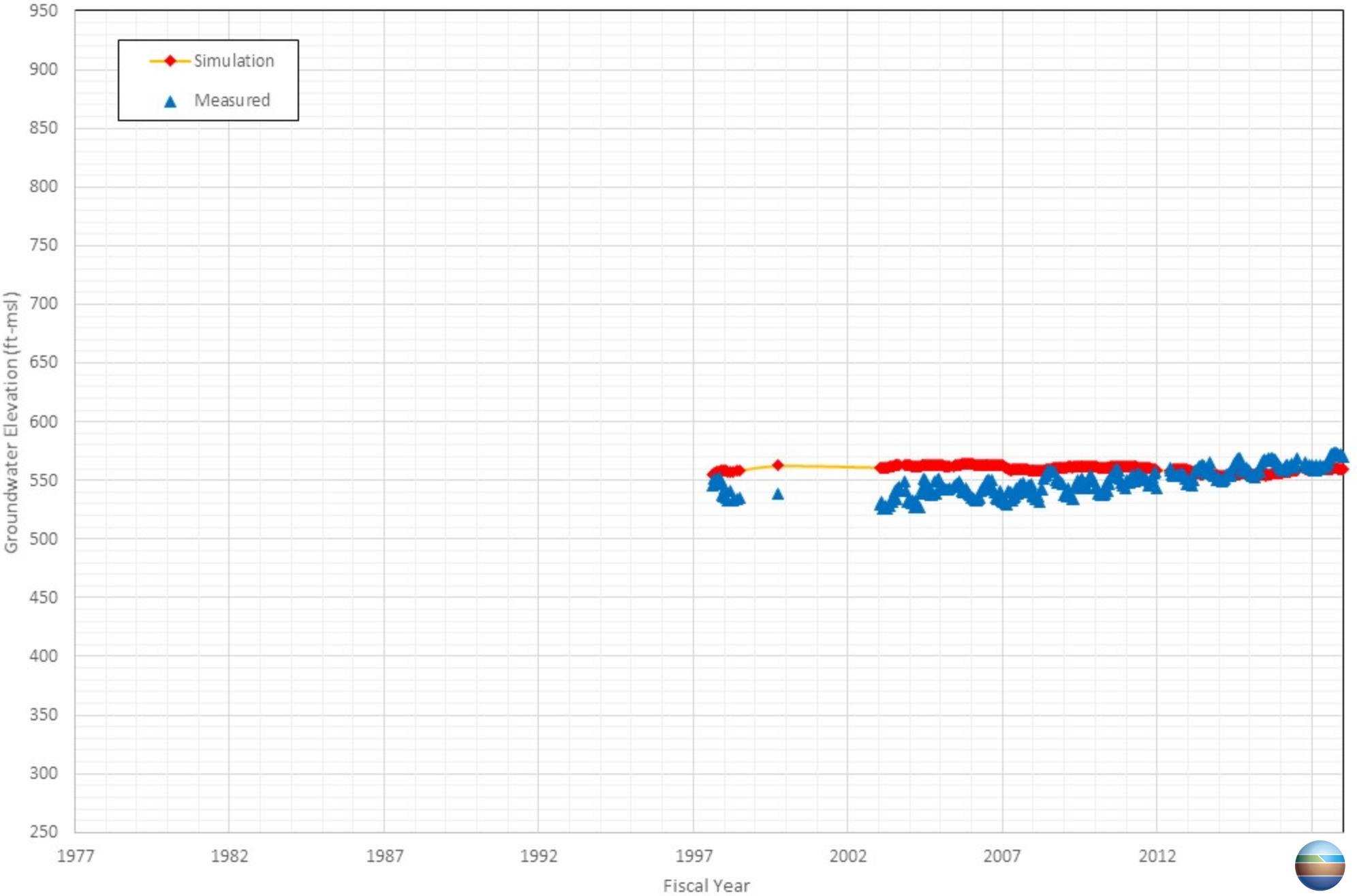

Appendix C-73
Comparison of Measured and Simulated Groundwater Water Level
in the State of California, California Institution for Men's Well MW-24S

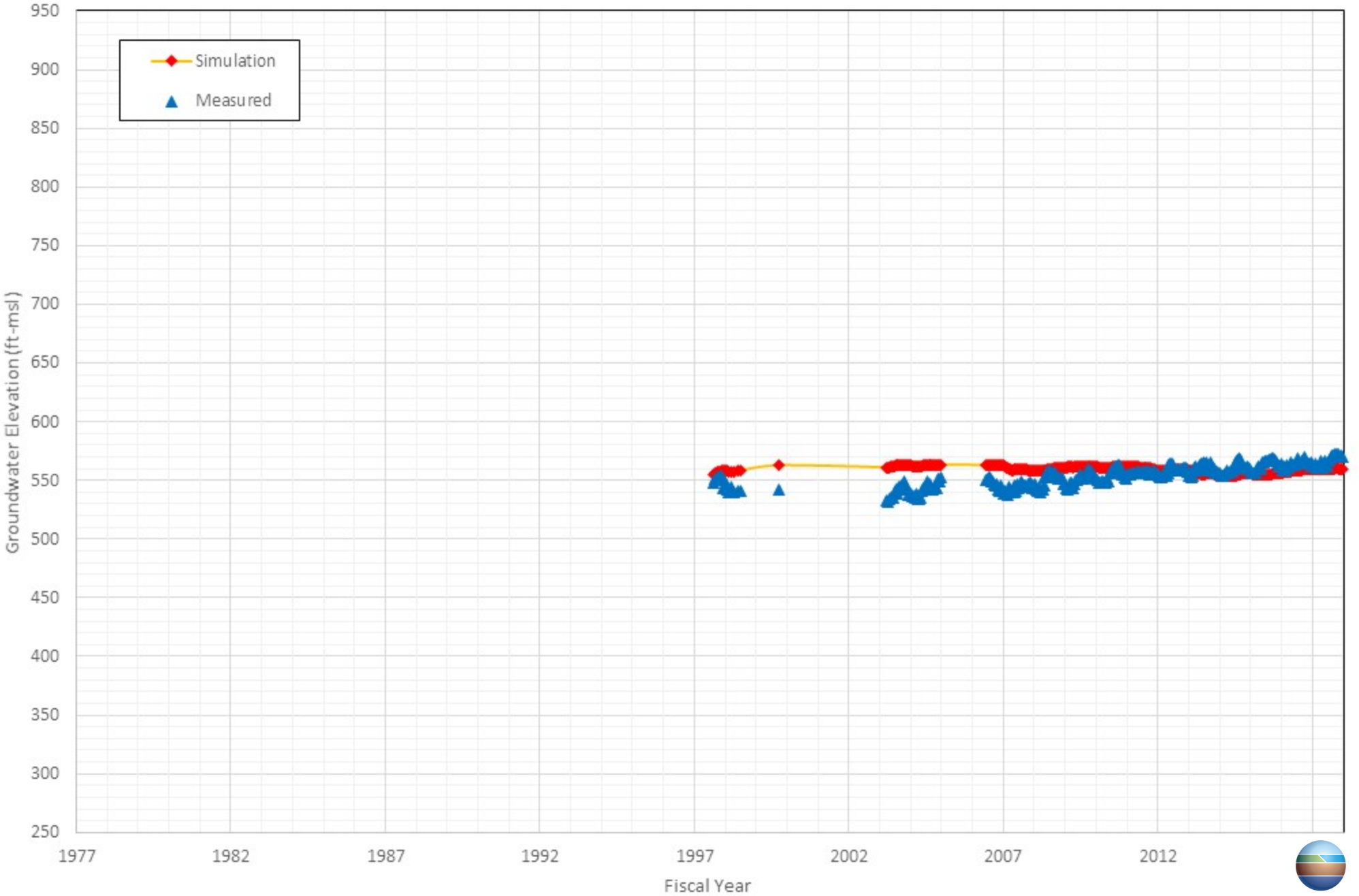

Appendix C-74
Comparison of Measured and Simulated Groundwater Water Level
in the State of California, Department of Toxic Substances Control's Well FC-936A2

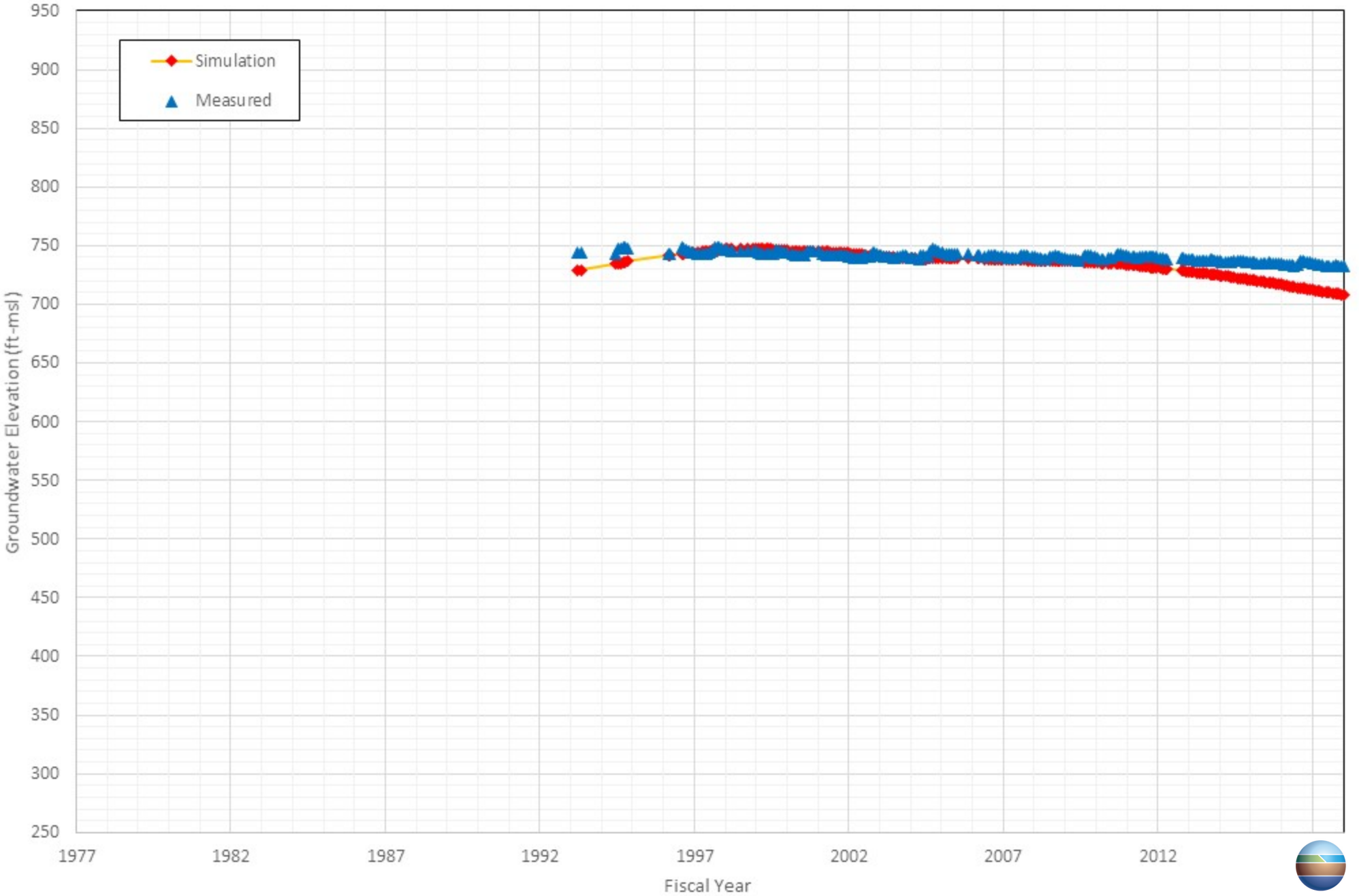

Appendix C-75
Comparison of Measured and Simulated Groundwater Water Level
in the United States, Geological Survey (USGS)'s Well Archibald 1

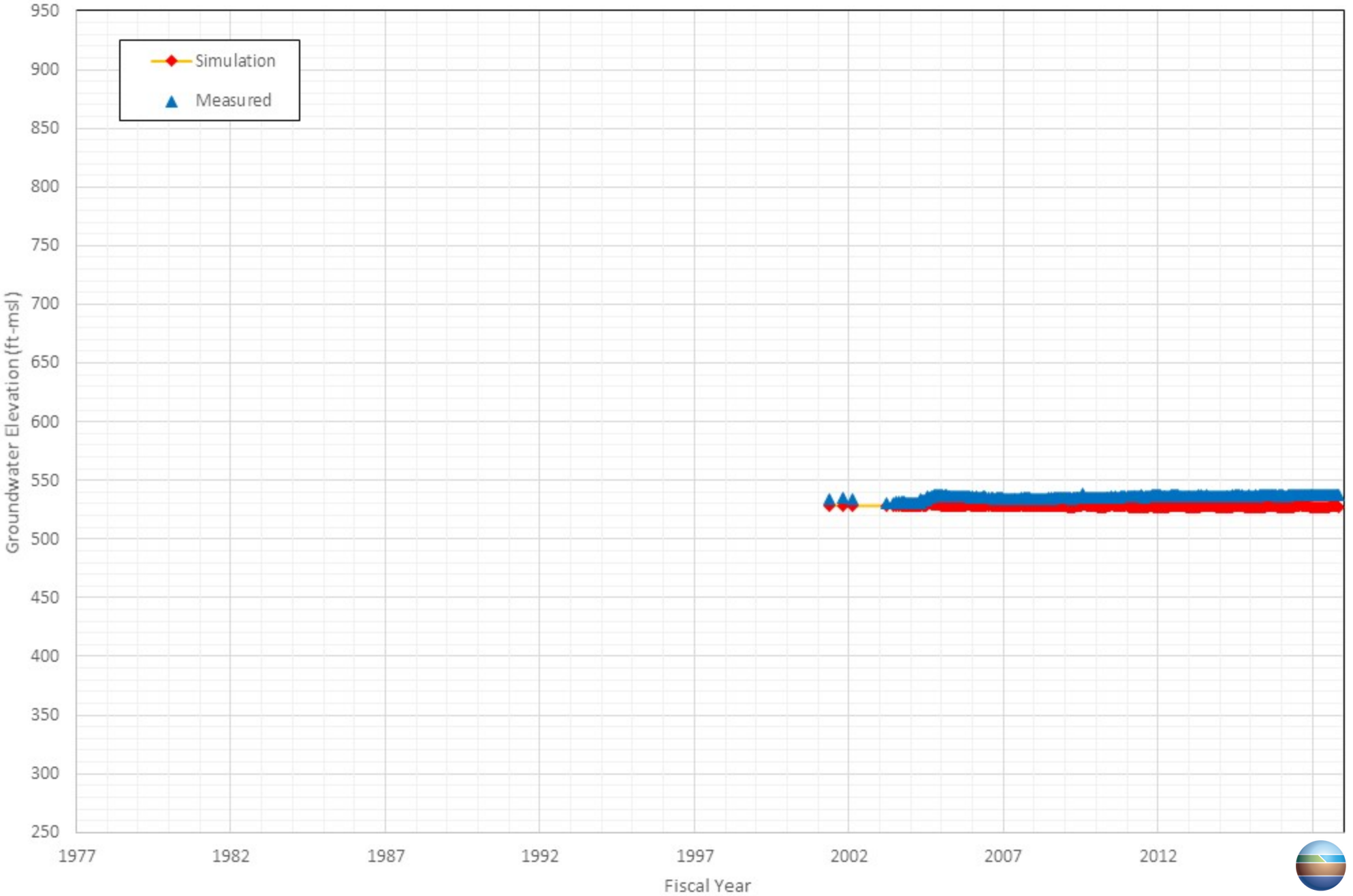

Appendix C-76
Comparison of Measured and Simulated Groundwater Water Level
in the West End Consolidated Water Co.'s Well West End 1

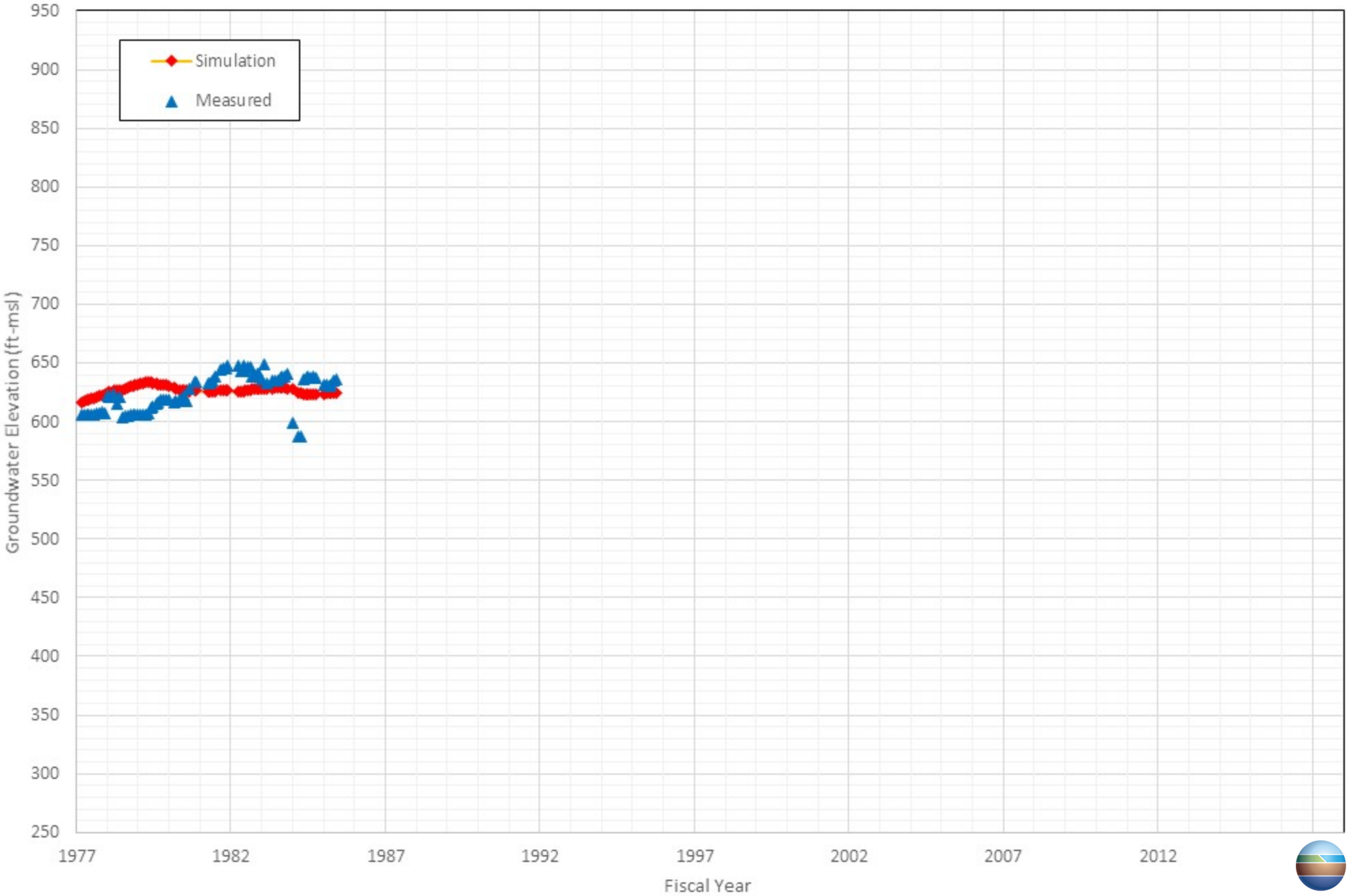

Appendix C-77
Comparison of Measured and Simulated Groundwater Water Level
in the Archibald Ranch Community Church's Well Dom

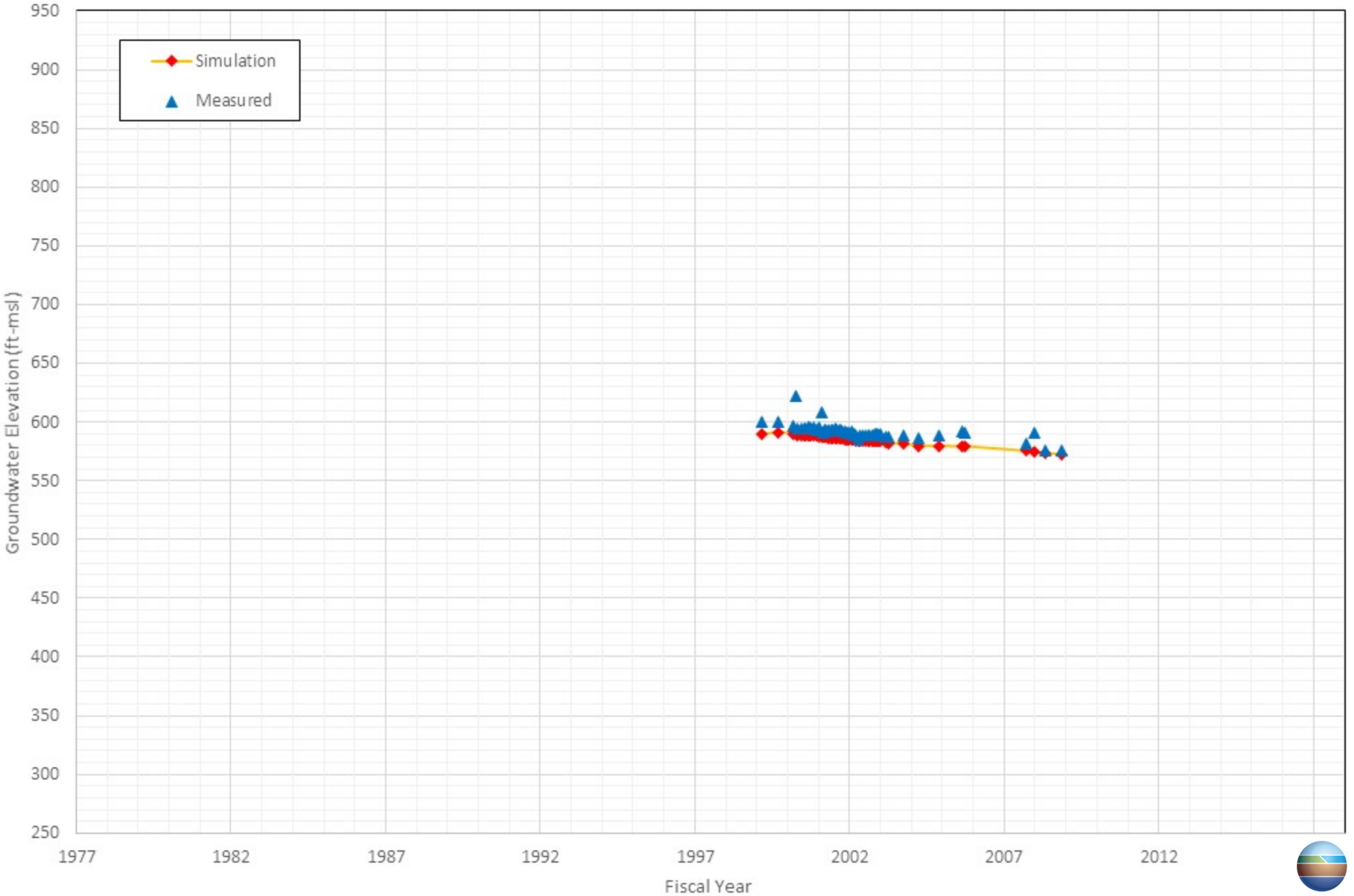

Appendix C-78
Comparison of Measured and Simulated Groundwater Water Level
in the Basque American Dairy's Well Dairy/Dom

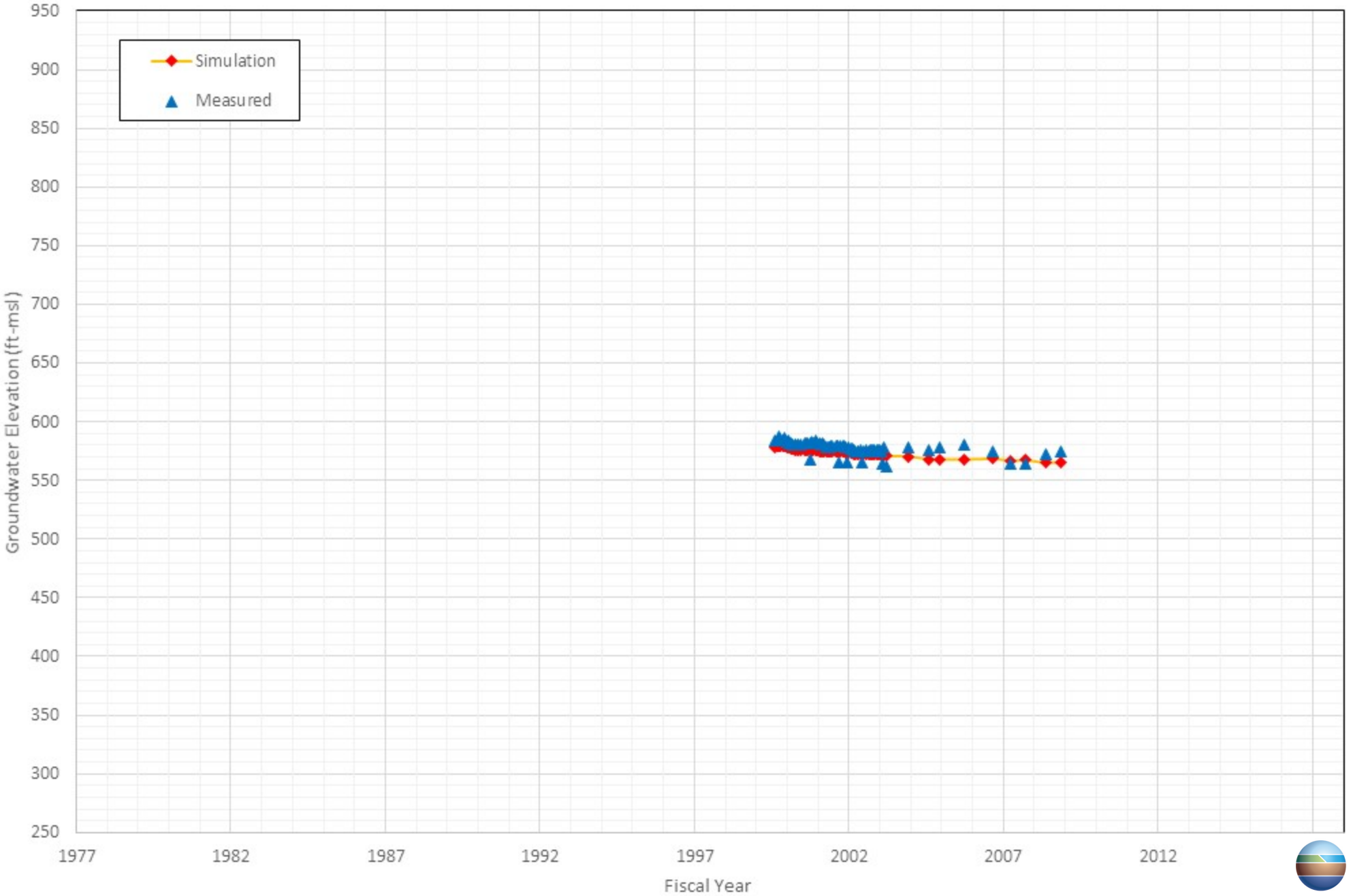

Appendix C-79
Comparison of Measured and Simulated Groundwater Water Level
in the Bekendam, Hank's Well Dairy/Dom

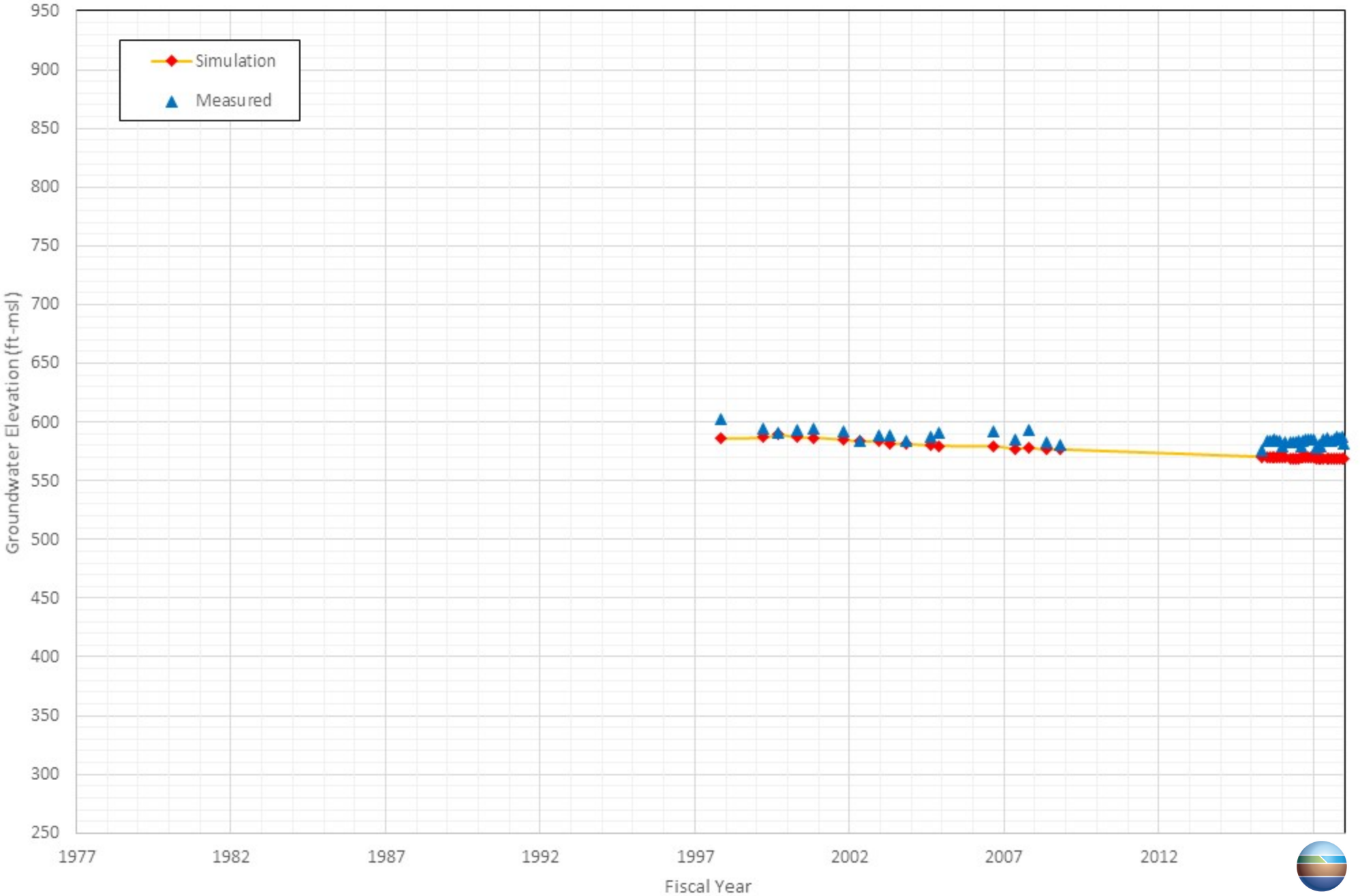

Appendix C-80
Comparison of Measured and Simulated Groundwater Water Level
in the Borba, John's Well 9200-DOM

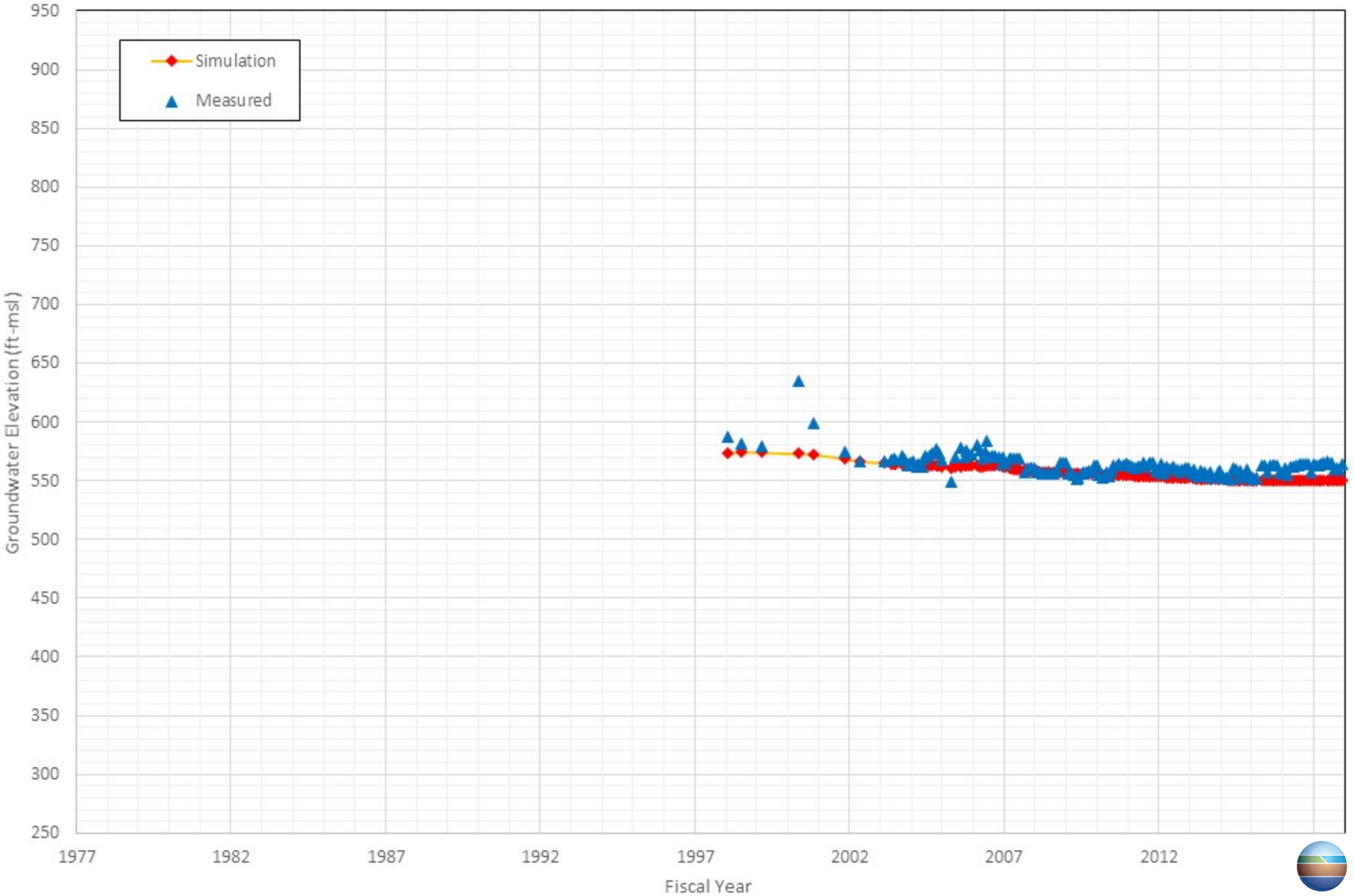

Appendix C-81
Comparison of Measured and Simulated Groundwater Water Level
in the Boschma & Son Dairy's Well DOM

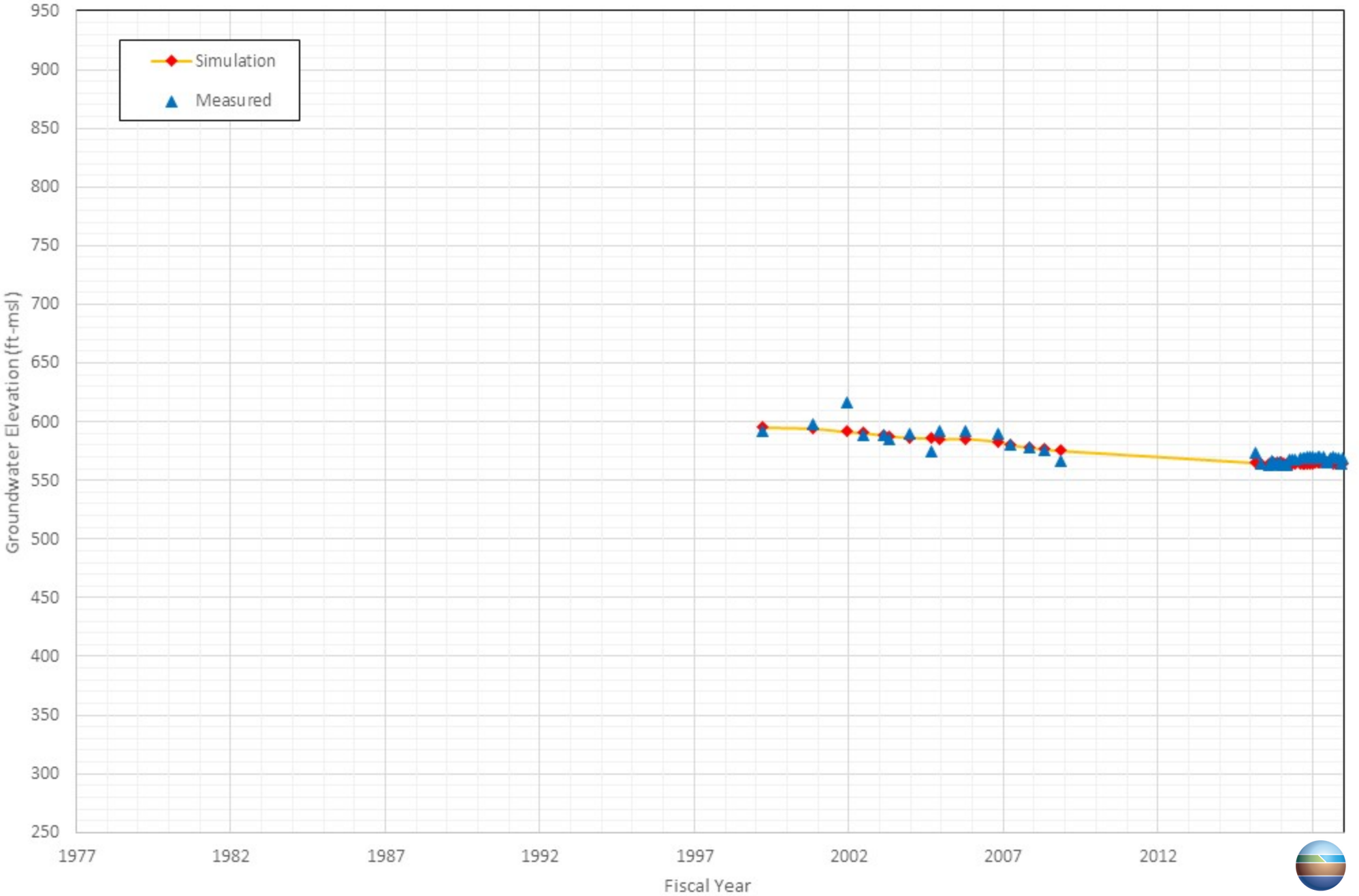

Appendix C-82
Comparison of Measured and Simulated Groundwater Water Level
in the Bouma, Ewoude's Well NA_1206751

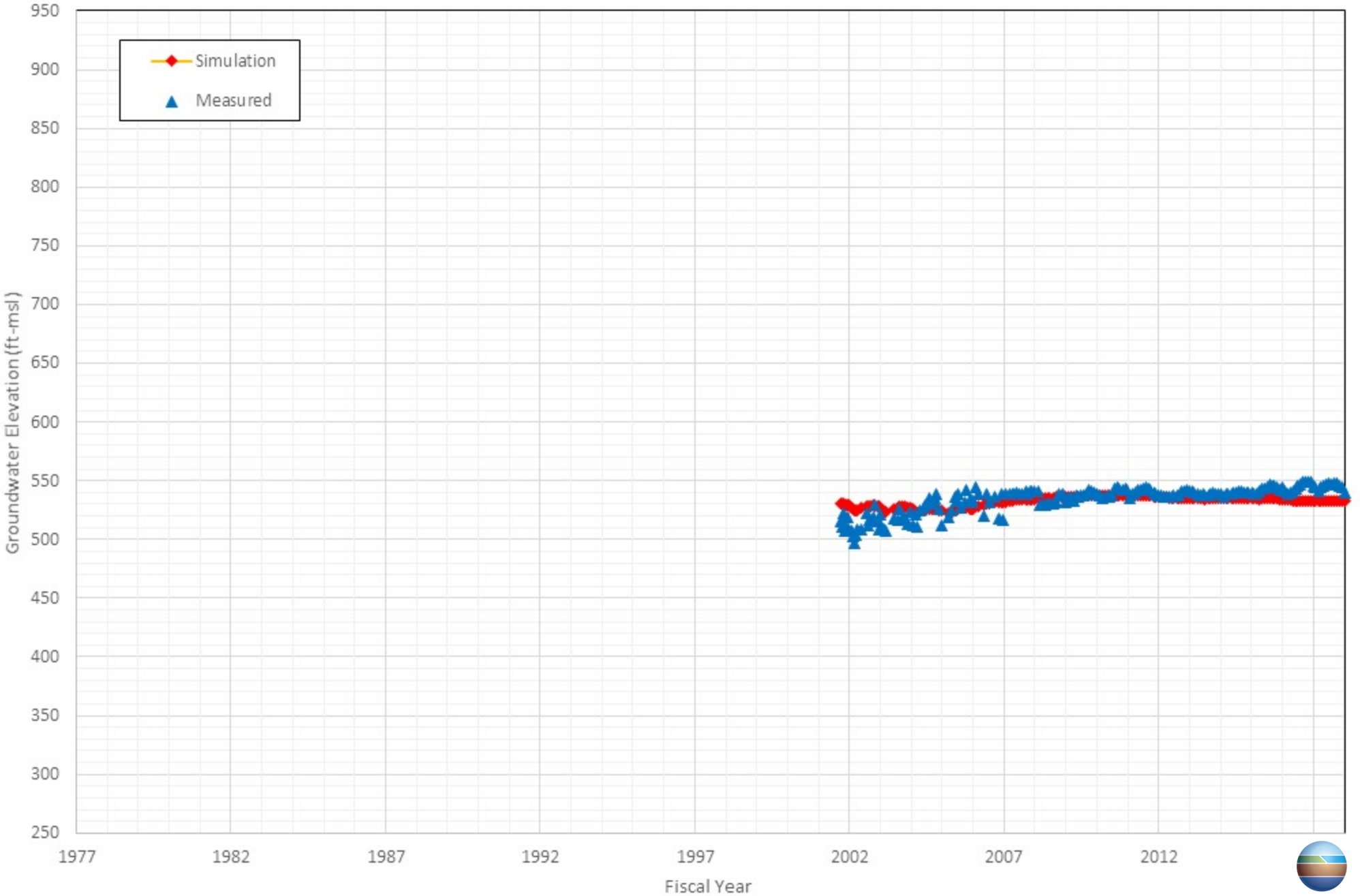

Appendix C-83
Comparison of Measured and Simulated Groundwater Water Level
in the Cow-west Dairy's Well CMG/PTI/J&A

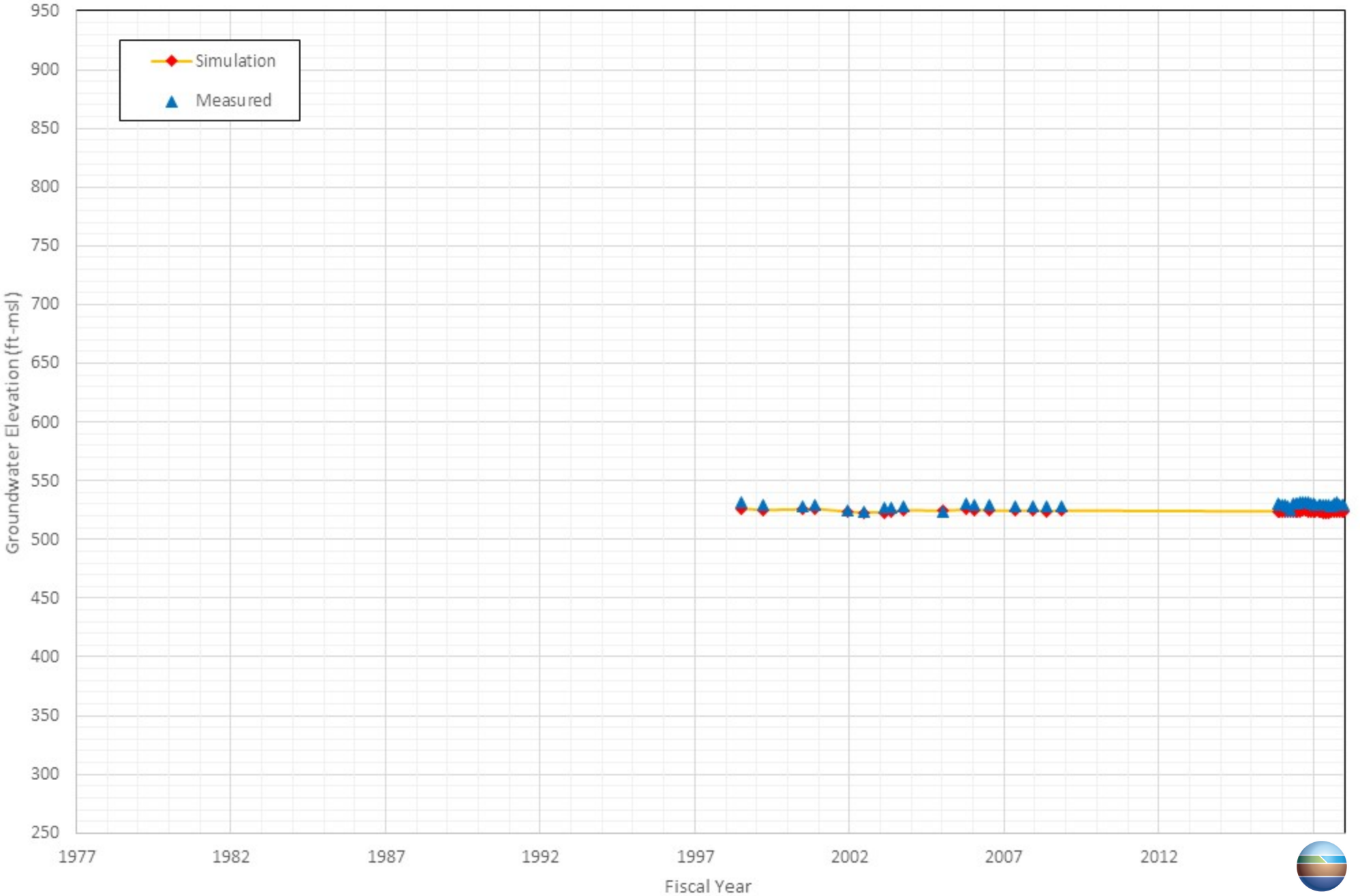

Appendix C-84
Comparison of Measured and Simulated Groundwater Water Level
in the En Sue, Liau's Well DOM

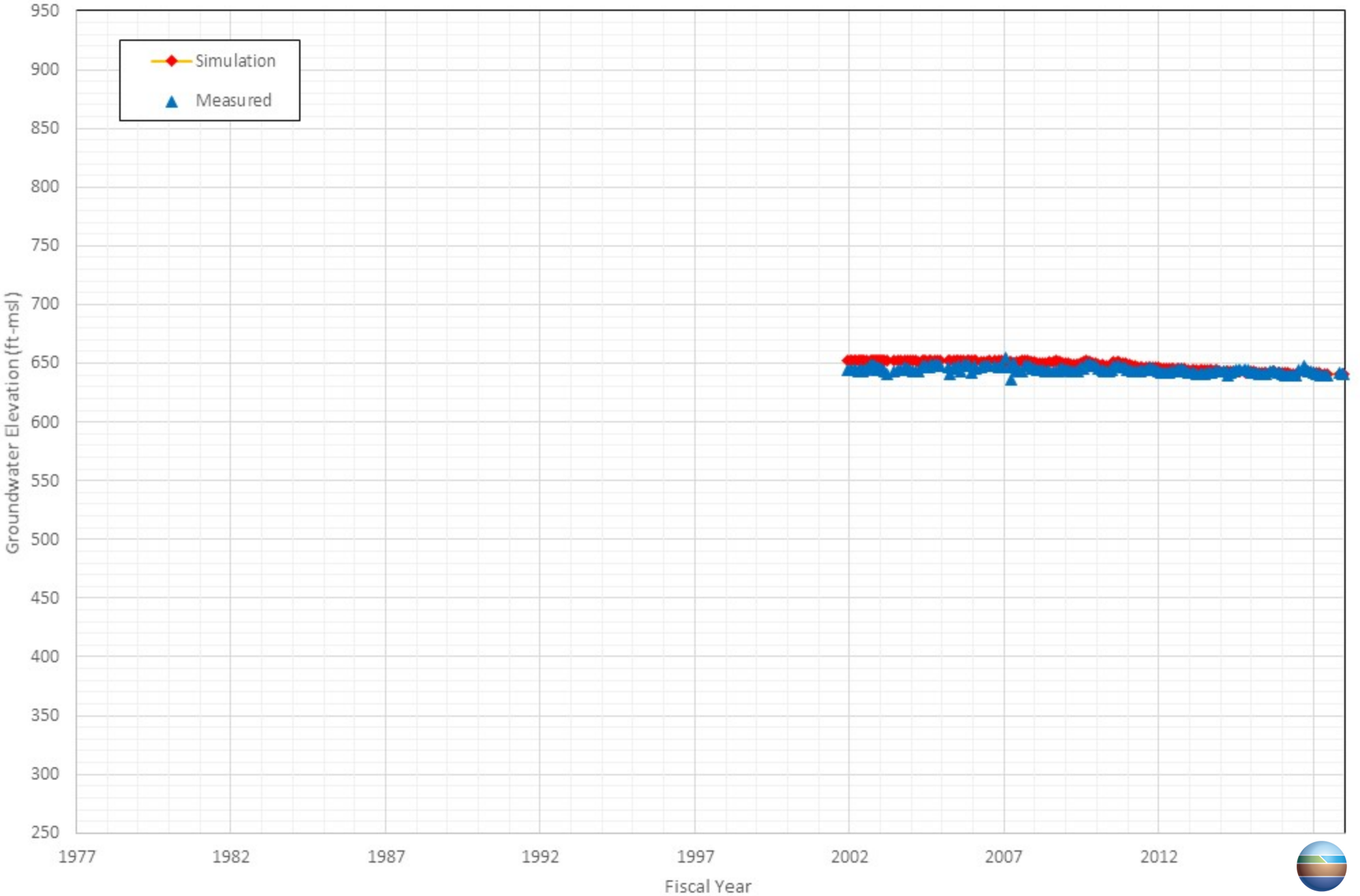

Appendix C-85
Comparison of Measured and Simulated Groundwater Water Level
in the Falloncrest Farms's Well ELEC-DAIRY-DOM

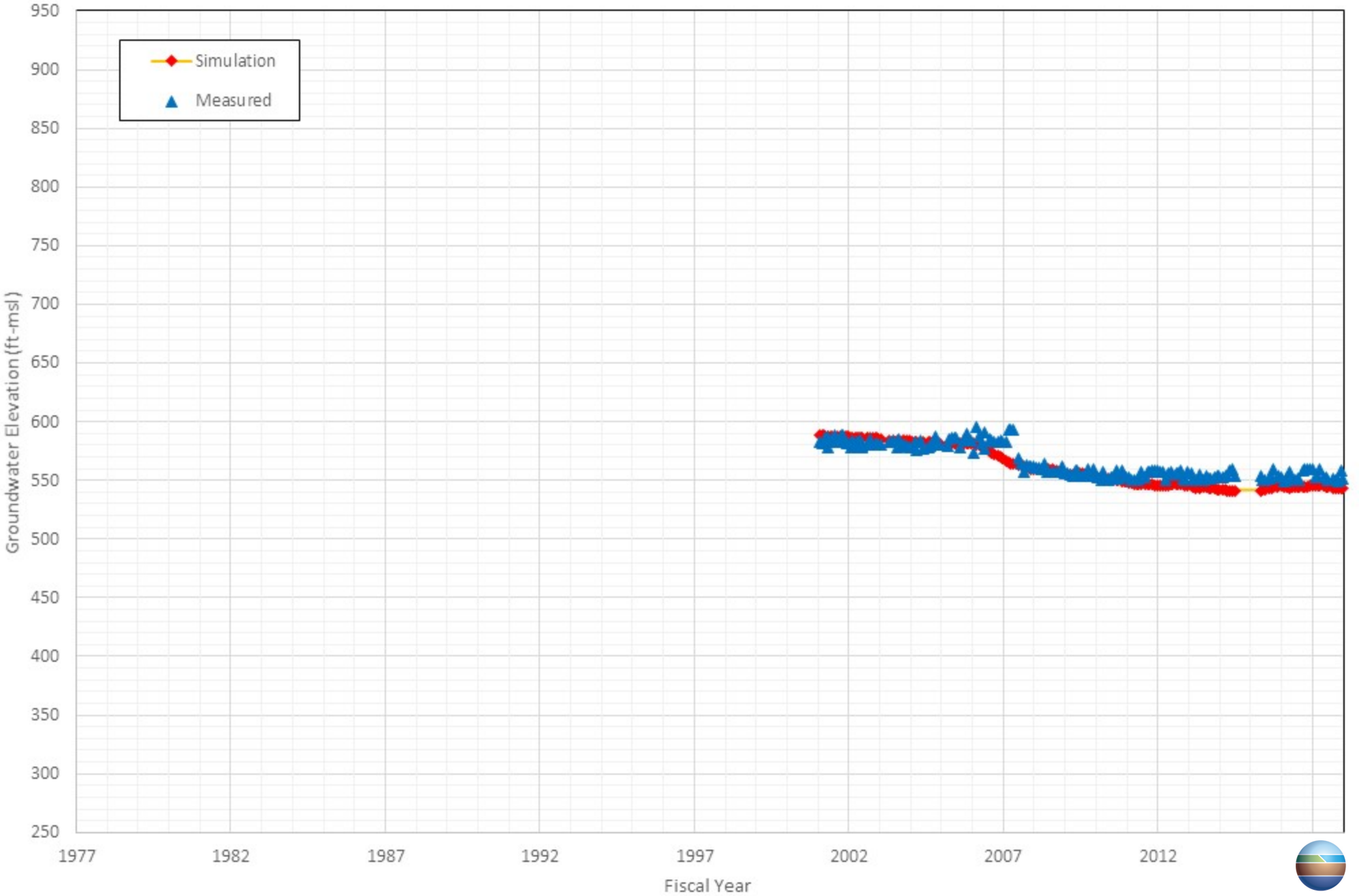

Appendix C-86
Comparison of Measured and Simulated Groundwater Water Level
in the Gutierrez, Ernesto's Well NA_1206525

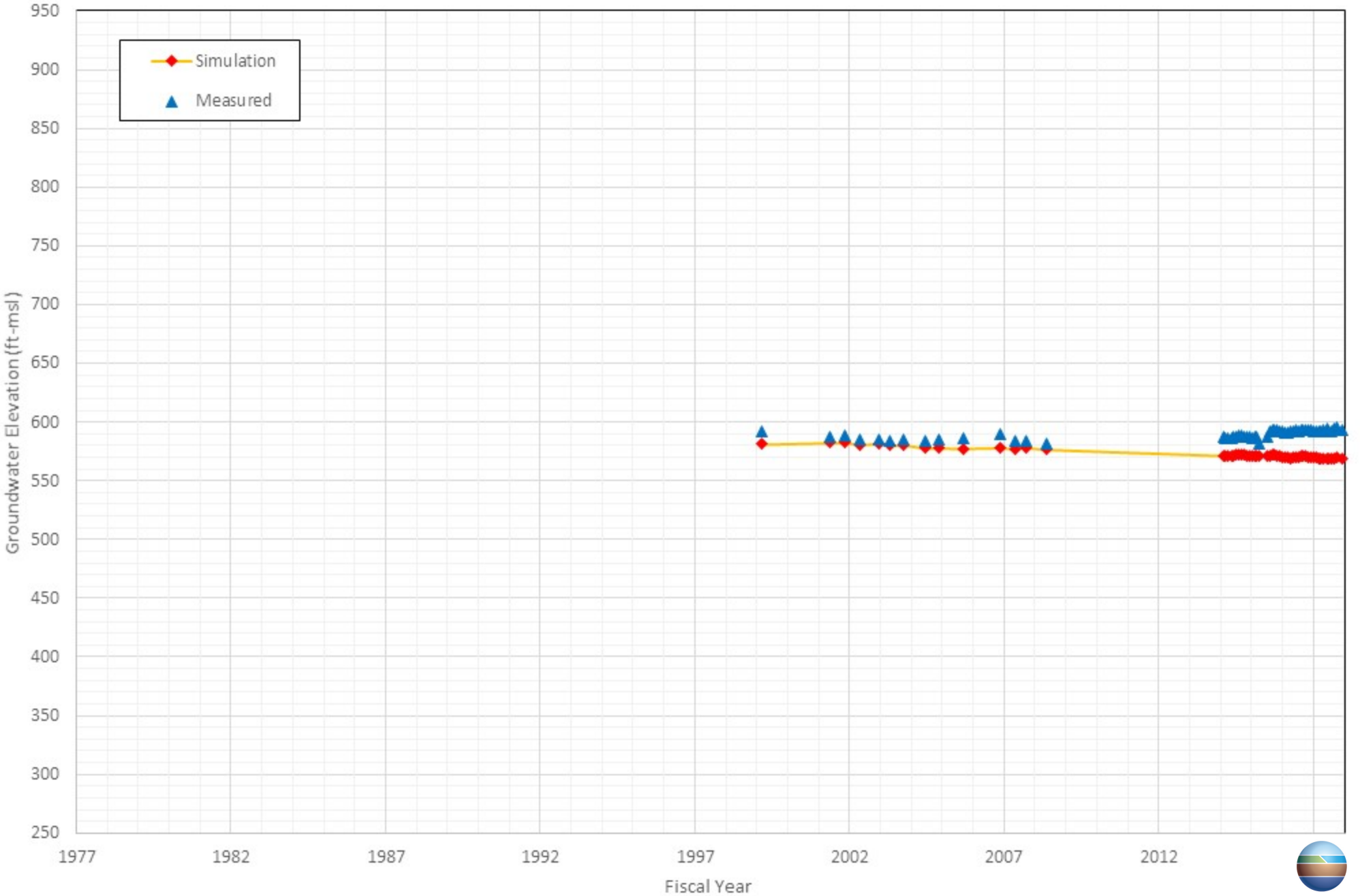

Appendix C-87
Comparison of Measured and Simulated Groundwater Water Level
in the H & R Barthelemy Dairy's Well ABANDONED

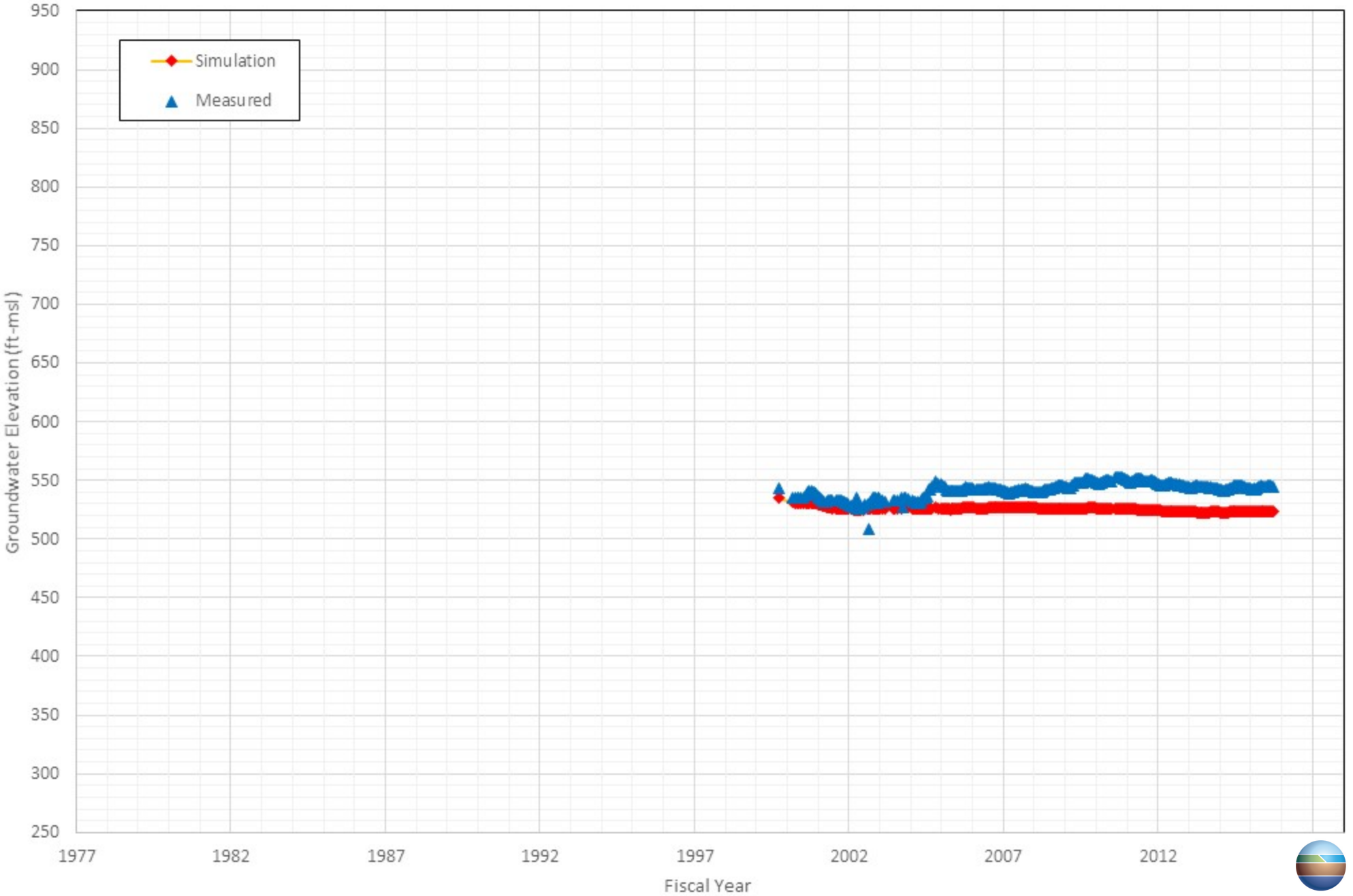

Appendix C-88
Comparison of Measured and Simulated Groundwater Water Level
in the Lee, Henrietta's Well DOM

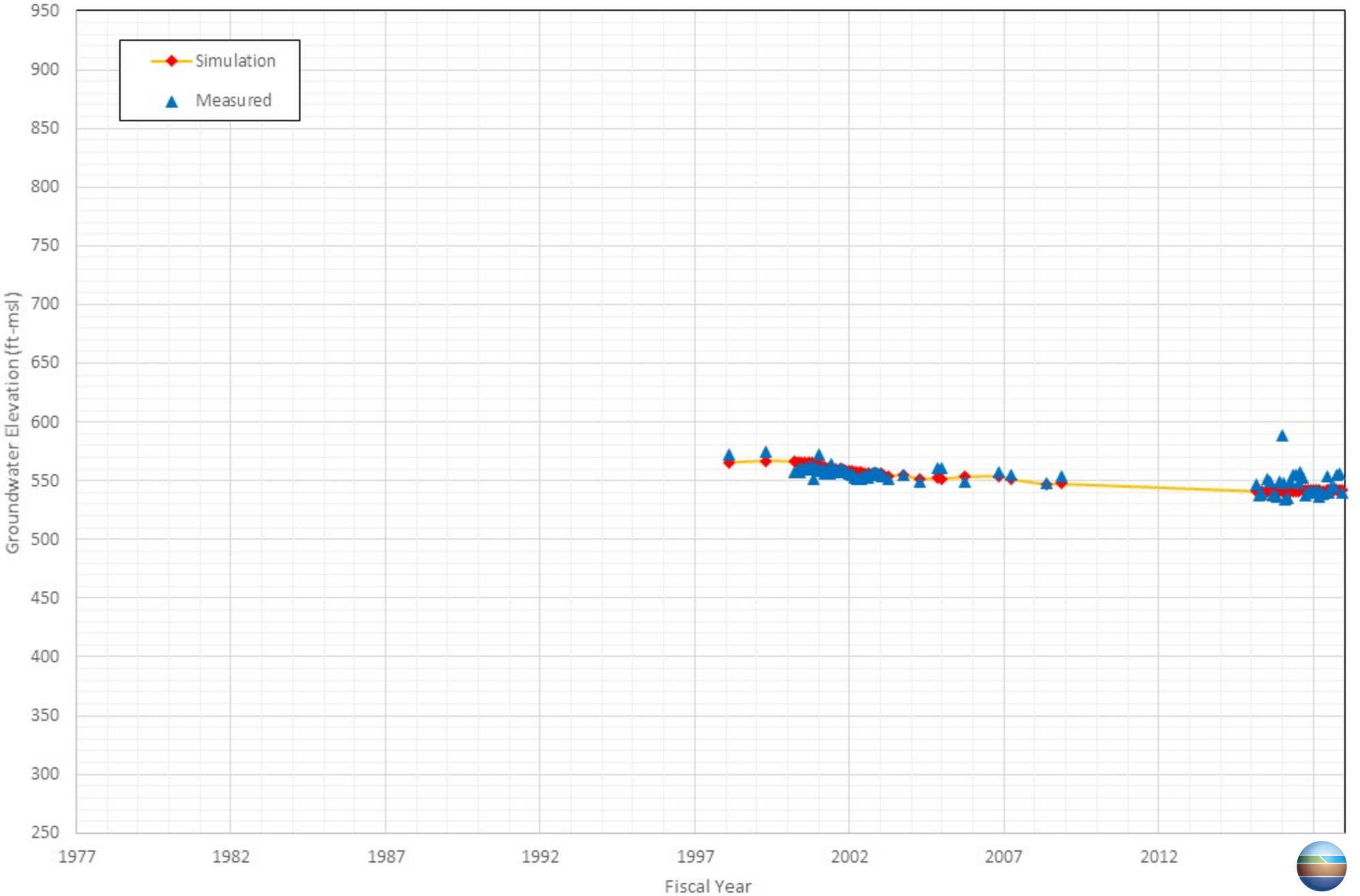

Appendix C-89
Comparison of Measured and Simulated Groundwater Water Level
in the Lizzaraga, Frank's Well IRRIGATION-capped

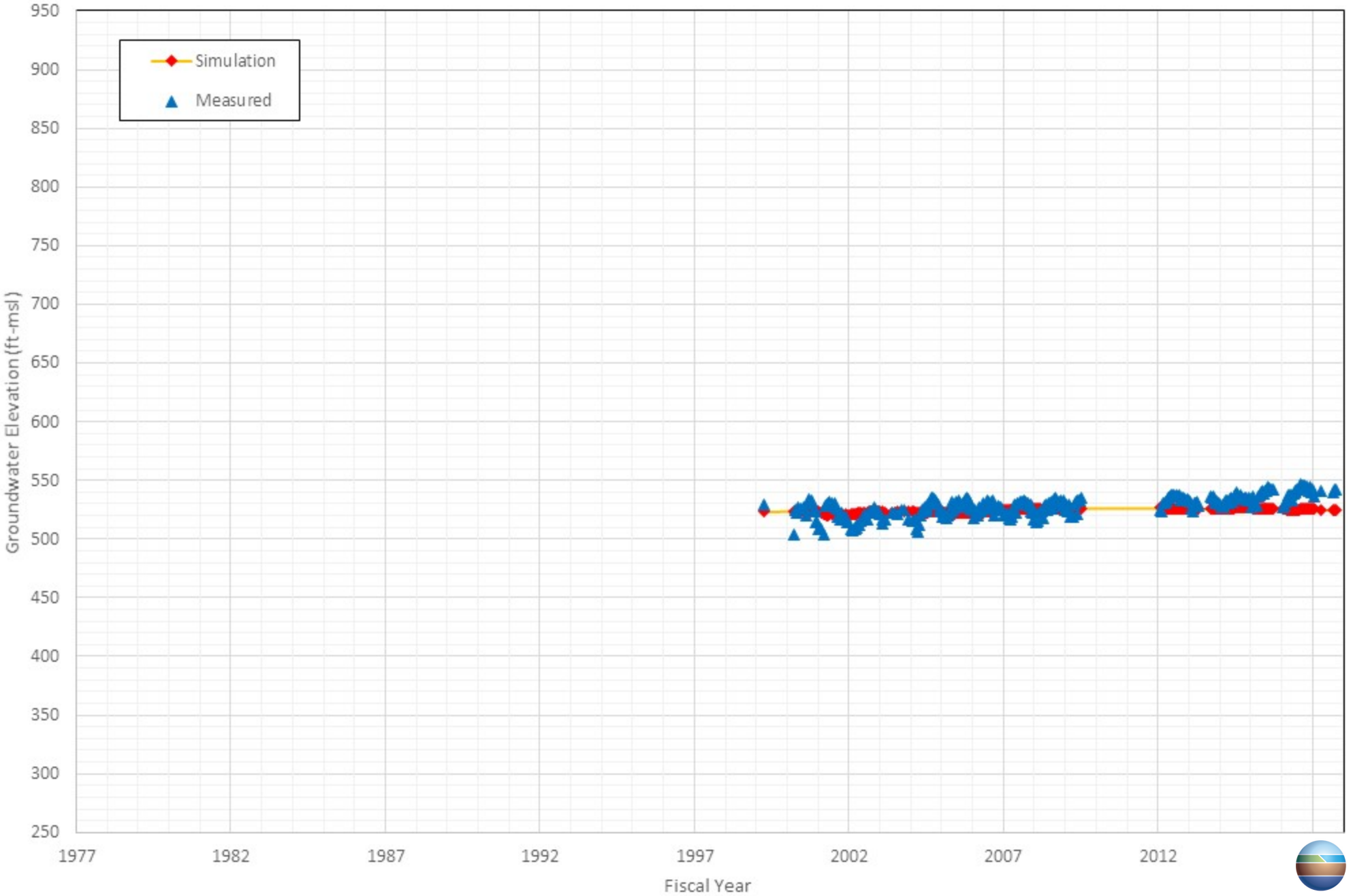

Appendix C-90
Comparison of Measured and Simulated Groundwater Water Level
in the Michel, Louise's Well 5-Mtr# 50761108

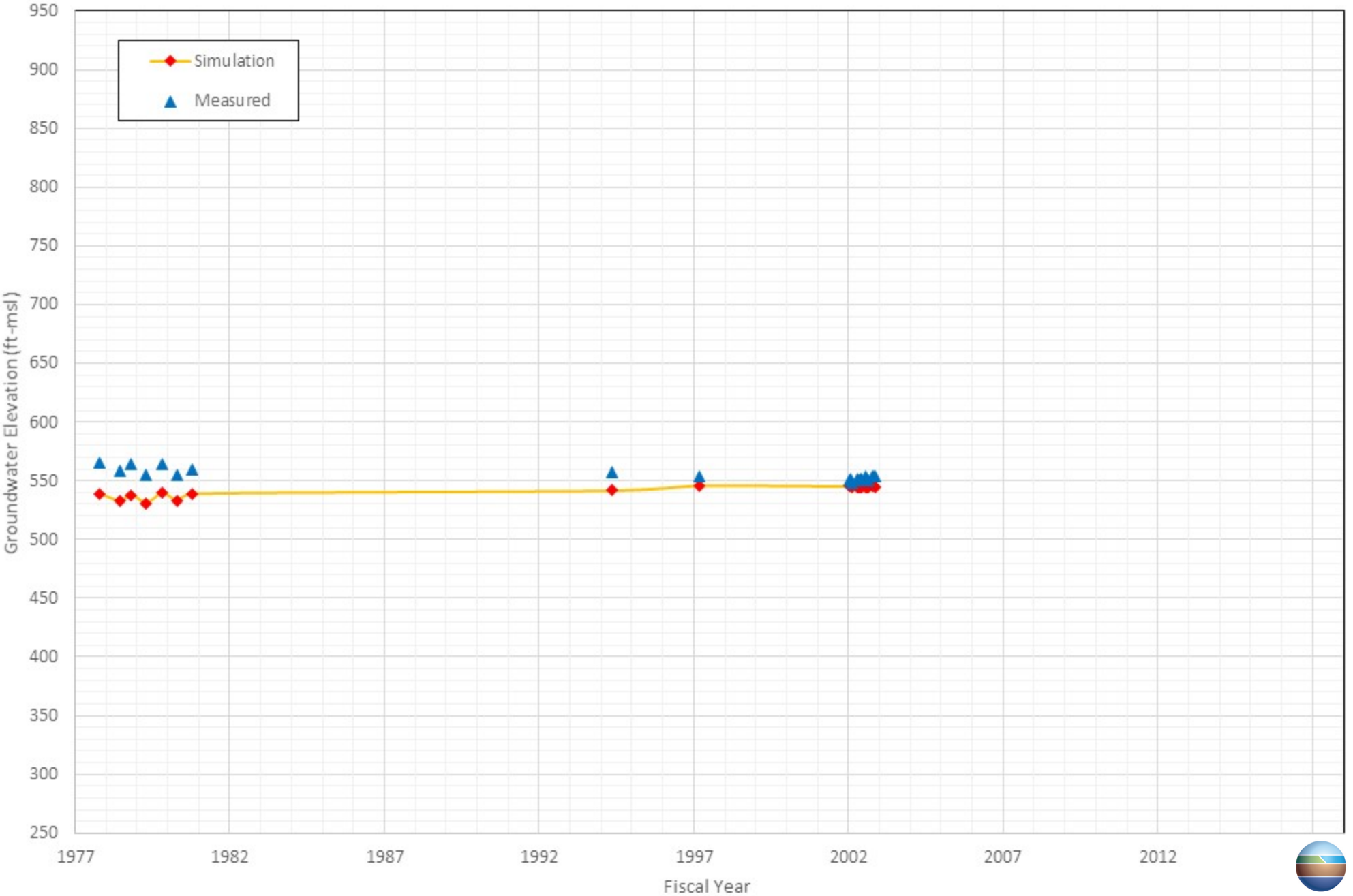

Appendix C-91
Comparison of Measured and Simulated Groundwater Water Level
in the Mobile Community Management Company's Well 4

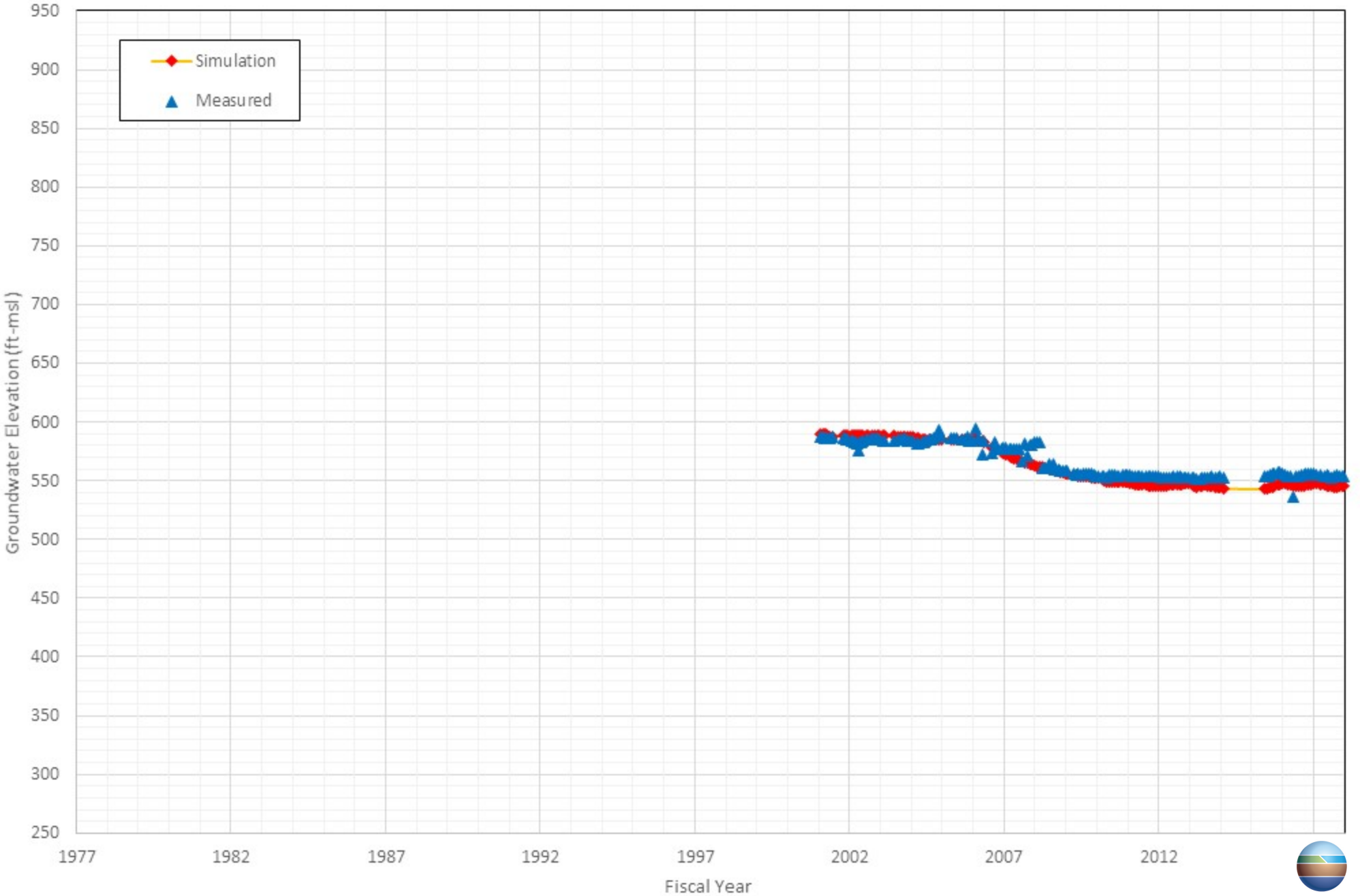

Appendix C-92
Comparison of Measured and Simulated Groundwater Water Level
in the Southern California Agricultural Land Fnd.'s Well DAIRY DOM

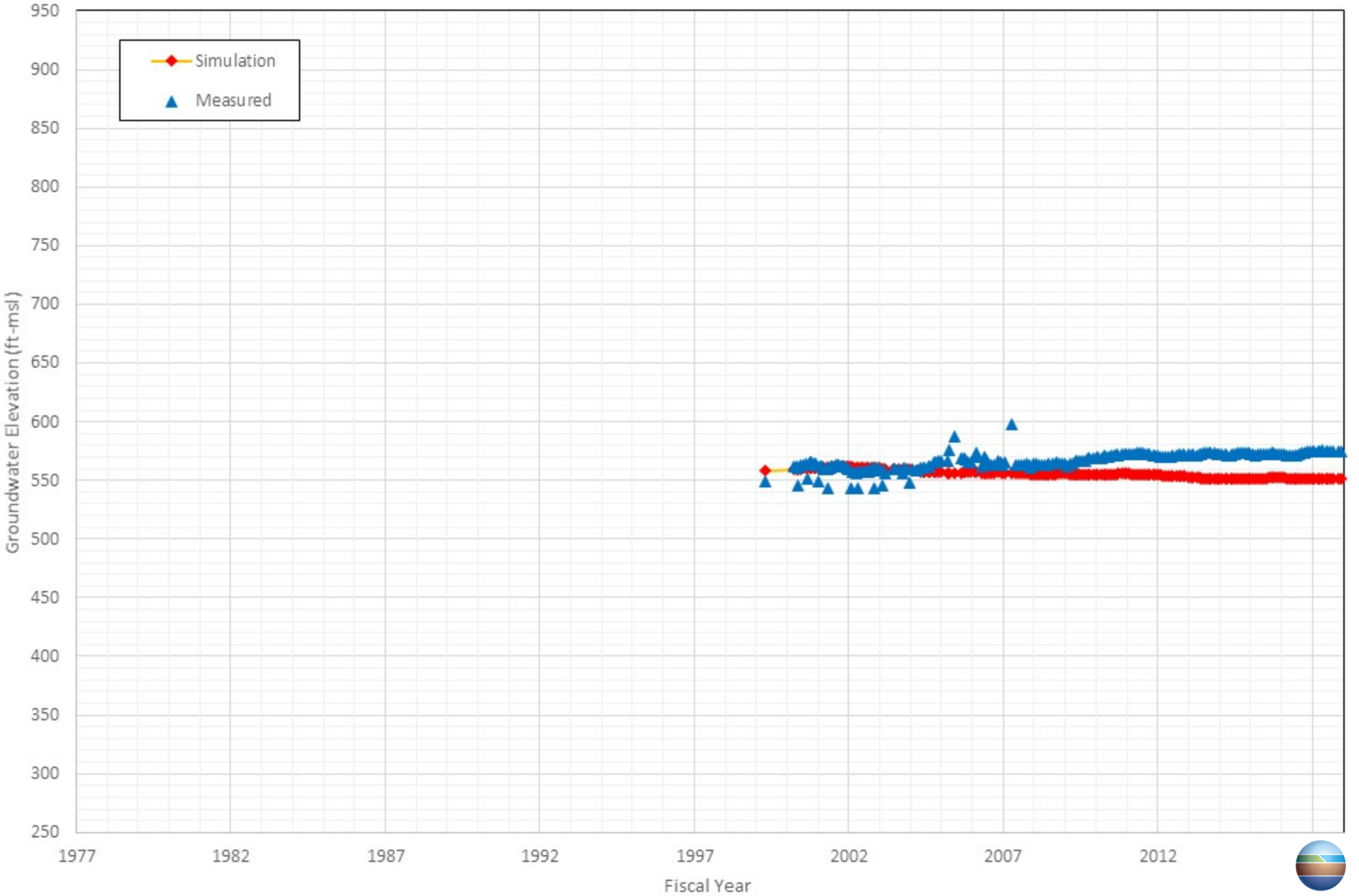

Appendix C-93
Comparison of Measured and Simulated Groundwater Water Level
in the Stark, Everett's Well 74200-IRR

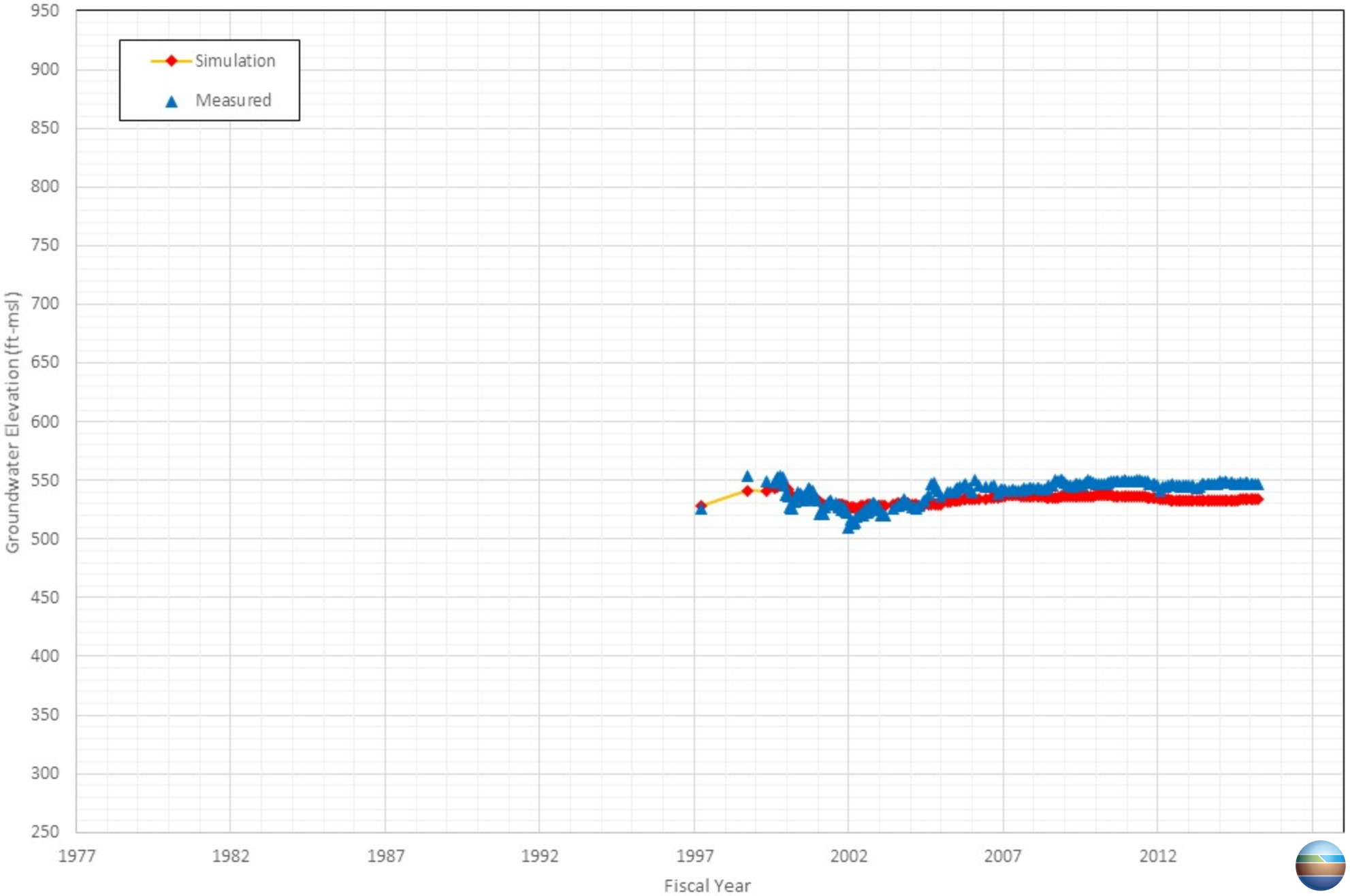

Appendix C-94
Comparison of Measured and Simulated Groundwater Water Level
in the Sterling Leasing Inc's Well DOM/Office

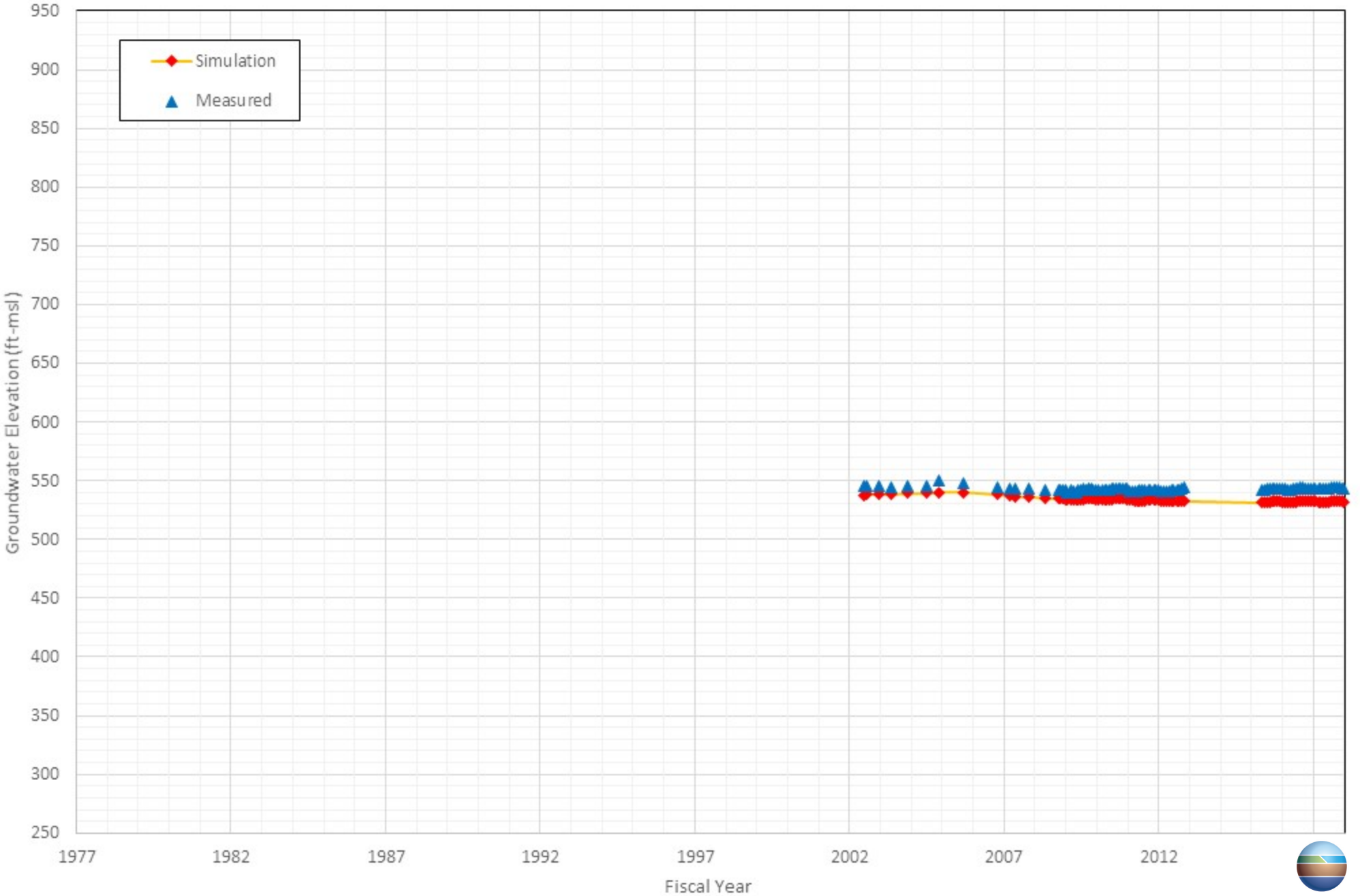

Appendix C-95
Comparison of Measured and Simulated Groundwater Water Level
in the Stueve Brothers Farms's Well Dom

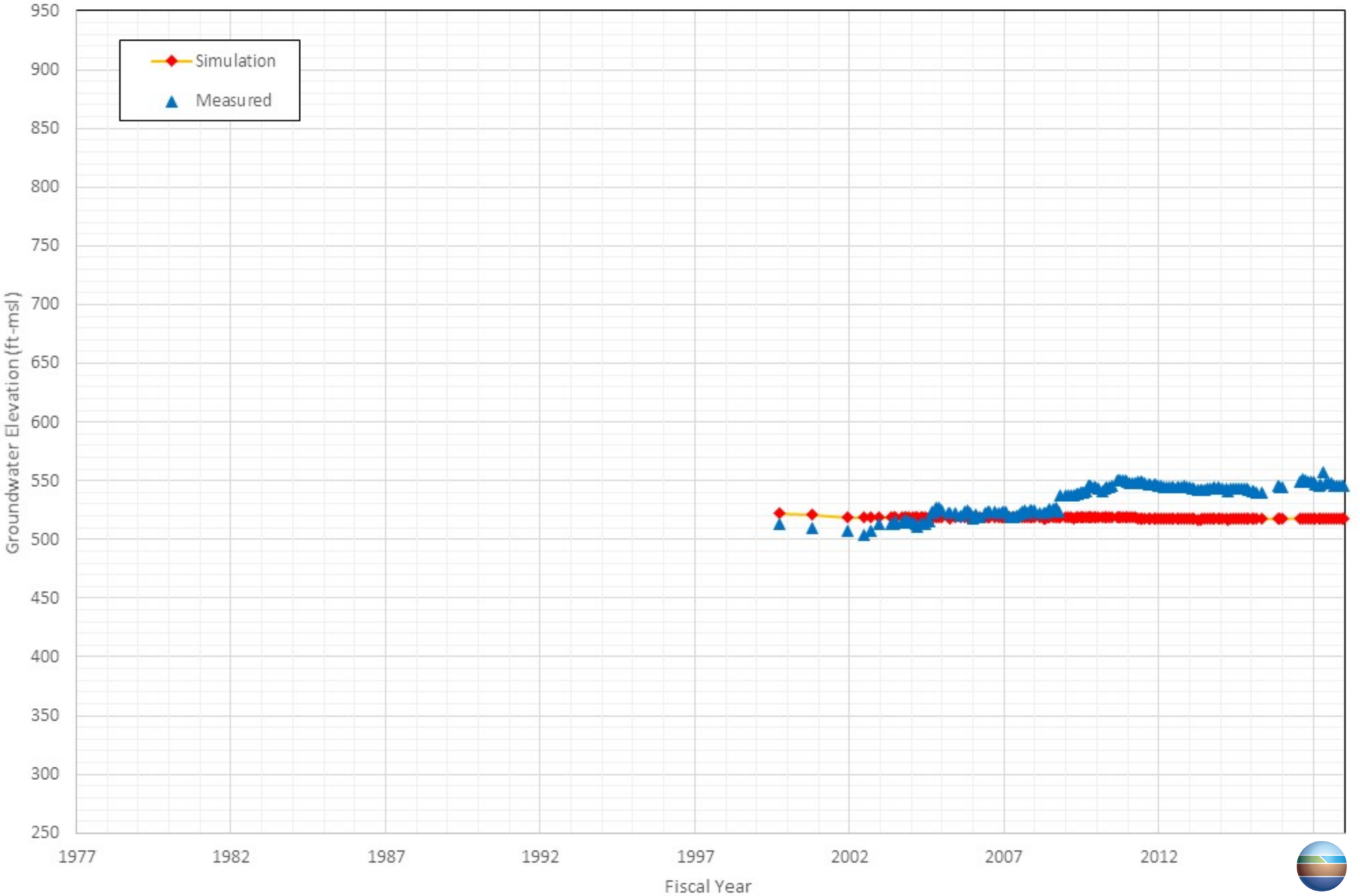

Appendix C-96
Comparison of Measured and Simulated Groundwater Water Level
in the Unknown's Well AG#6-BRITSCHGI

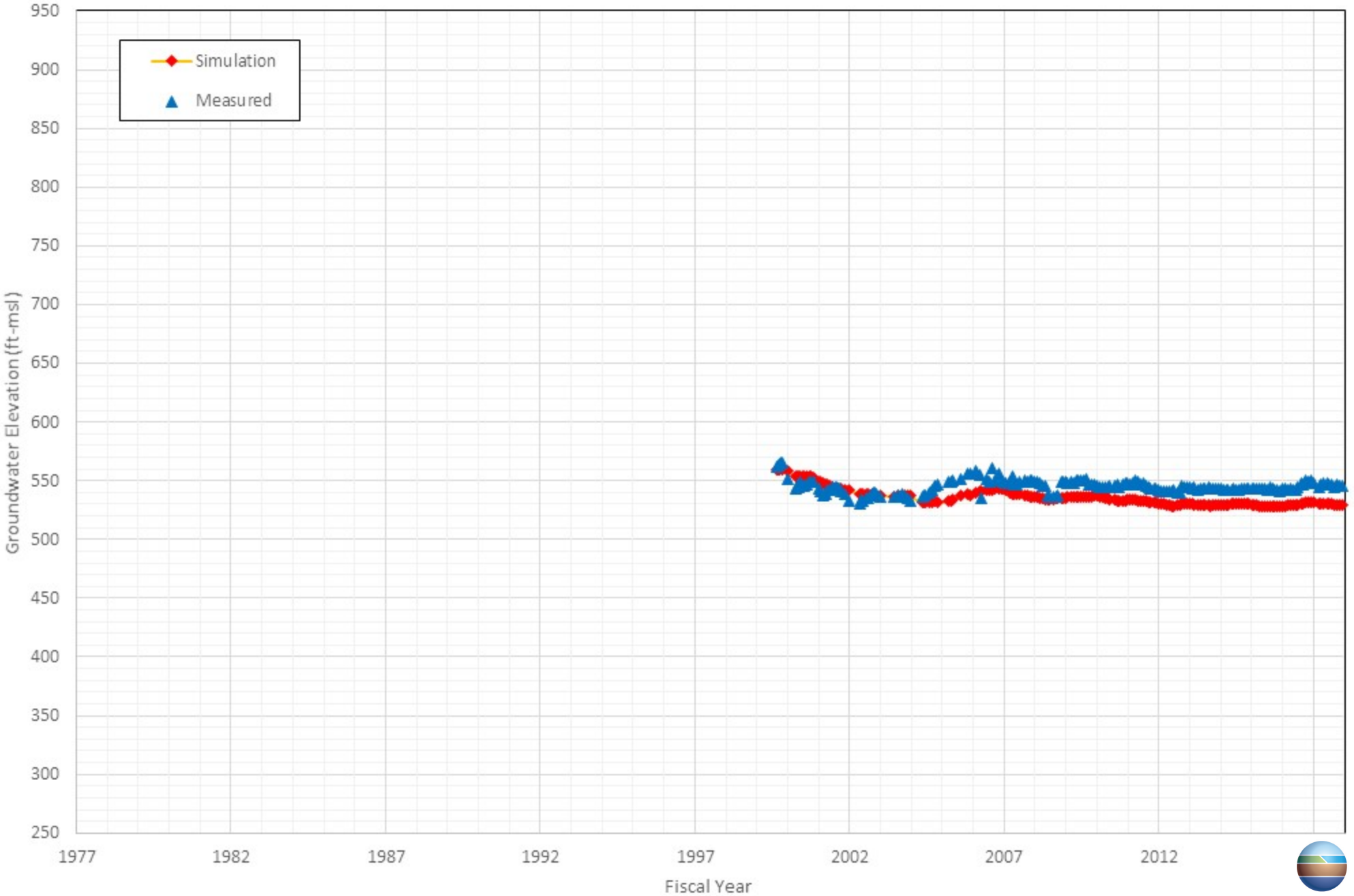

Appendix C-97
Comparison of Measured and Simulated Groundwater Water Level
in the Van Dam, Bas's Well 81400-IRR

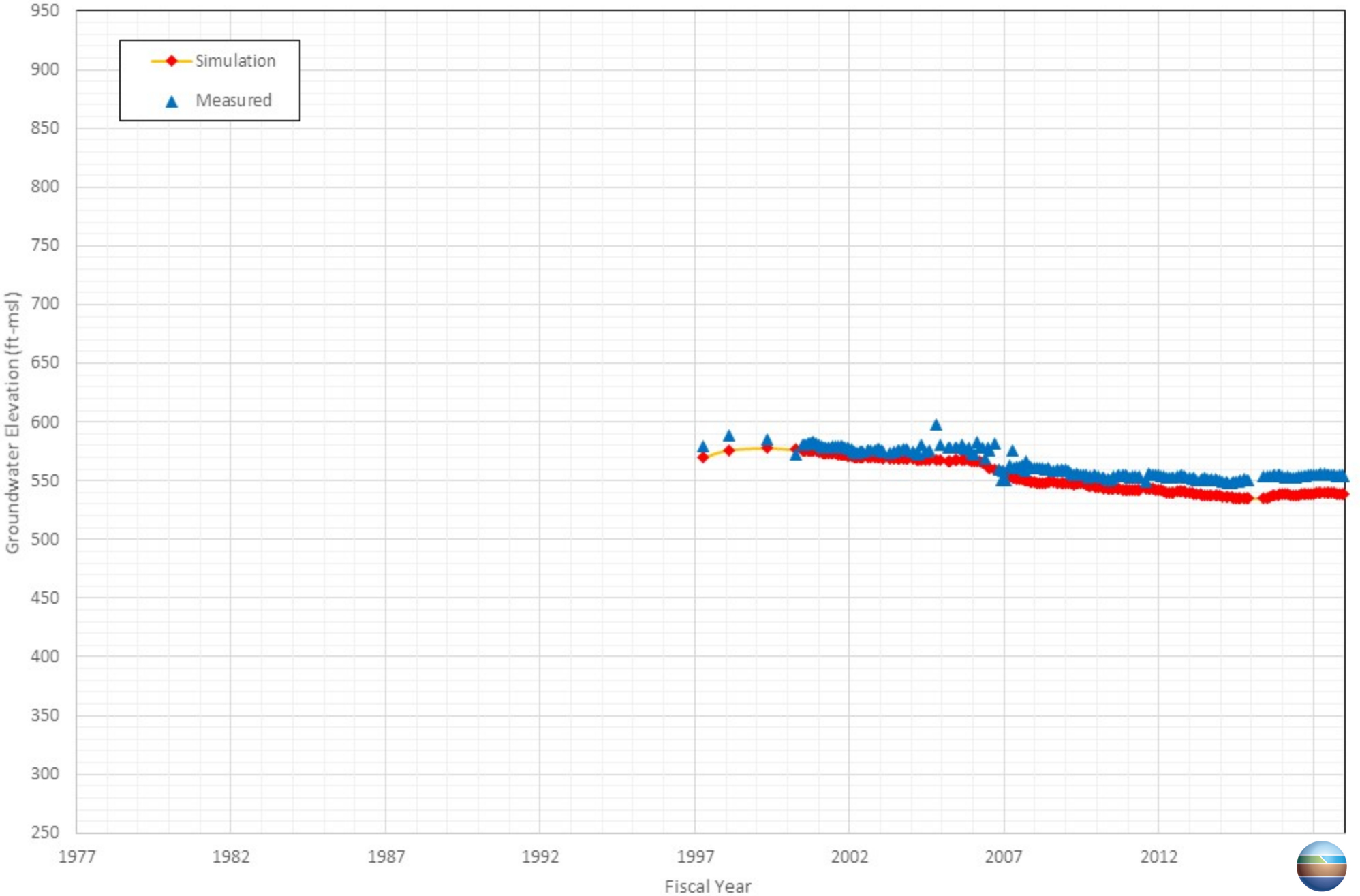

Appendix C-98
Comparison of Measured and Simulated Groundwater Water Level
in the Van Leeuwen, John's Well ABANDONED

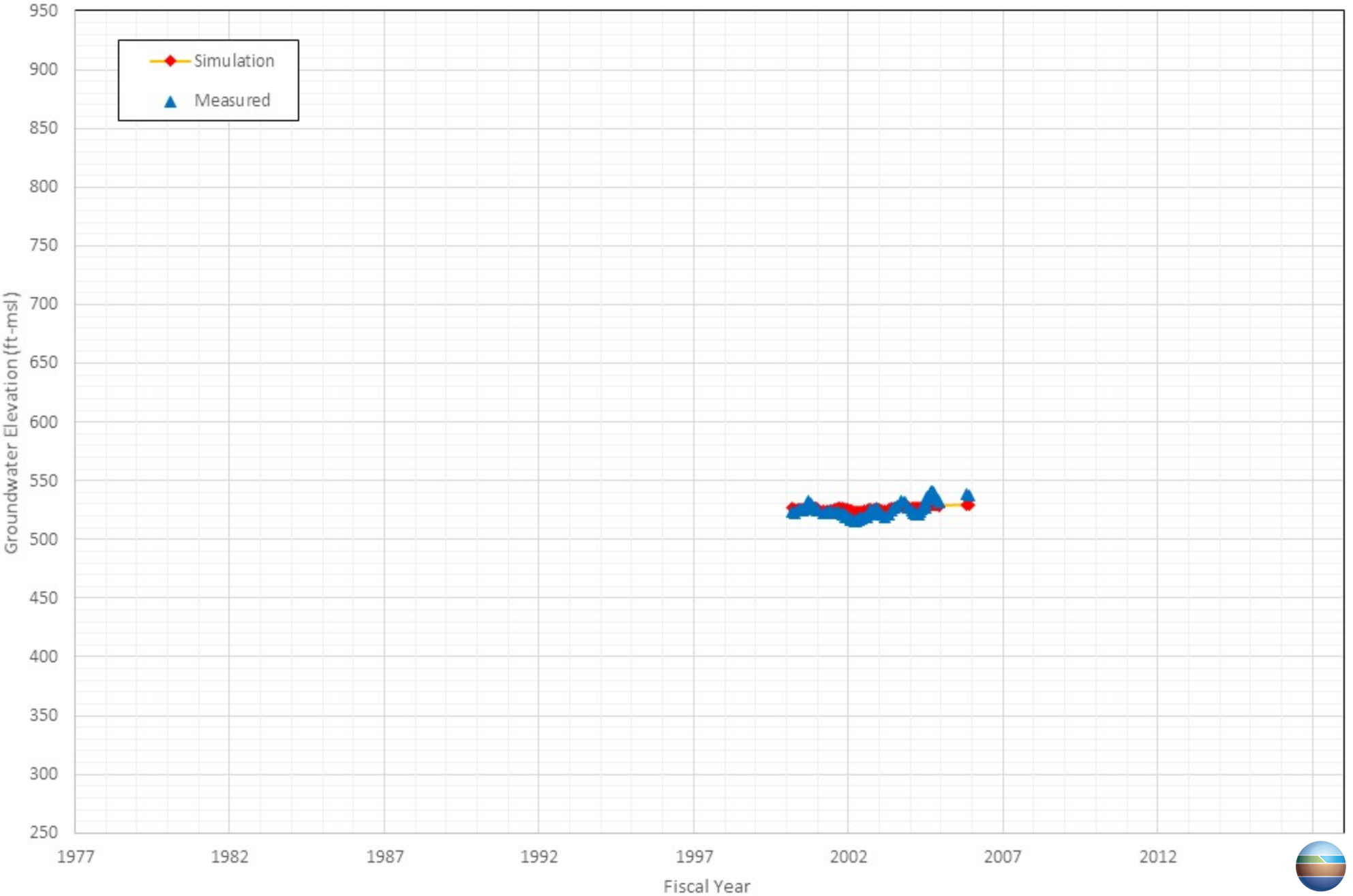

Appendix C-99
Comparison of Measured and Simulated Groundwater Water Level
in the Van Leeuwen, William's Well EAST 1-D-1

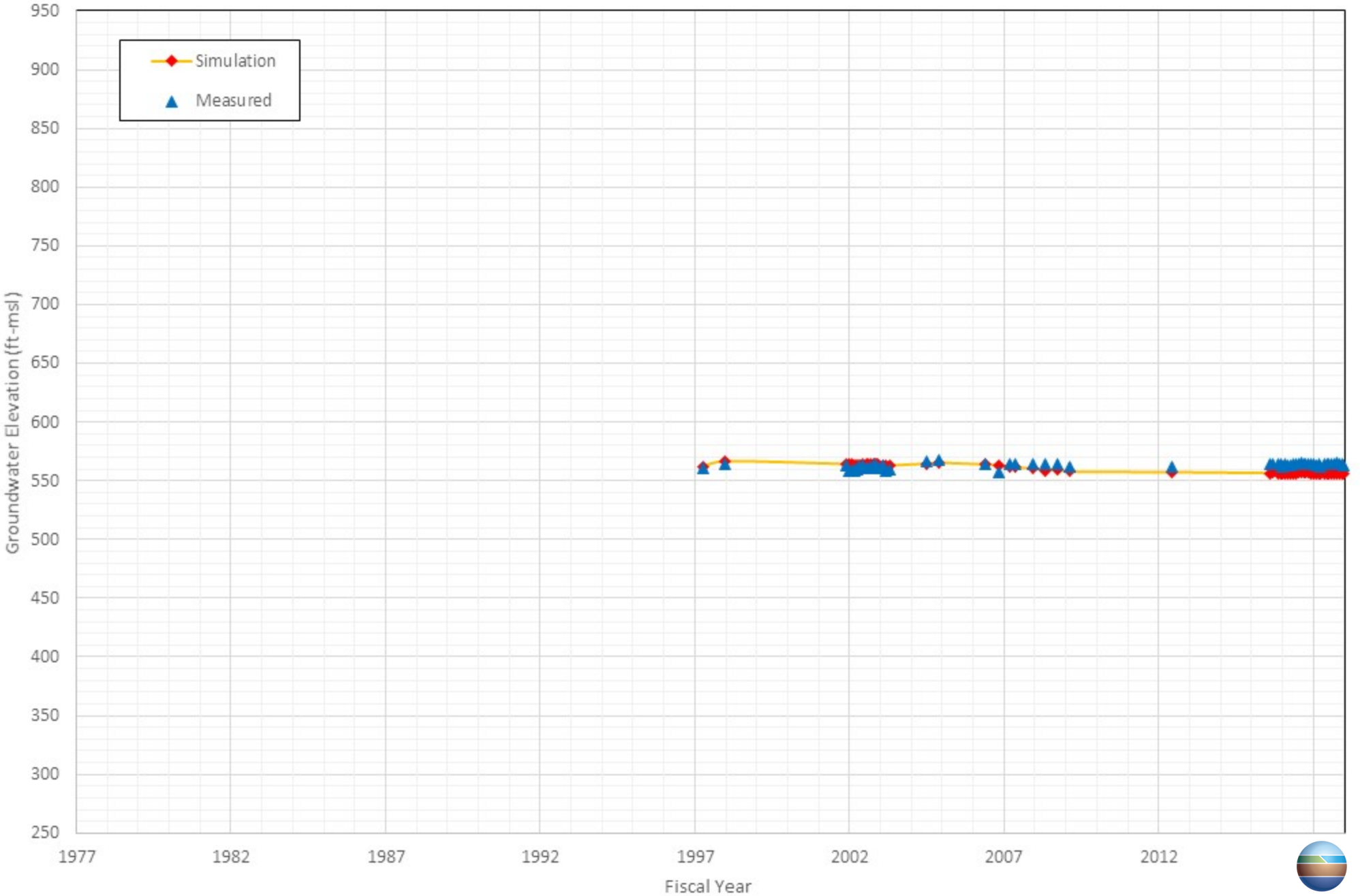

Appendix C-100
Comparison of Measured and Simulated Groundwater Water Level
in the Vernola, Pat's Well DOMESTIC

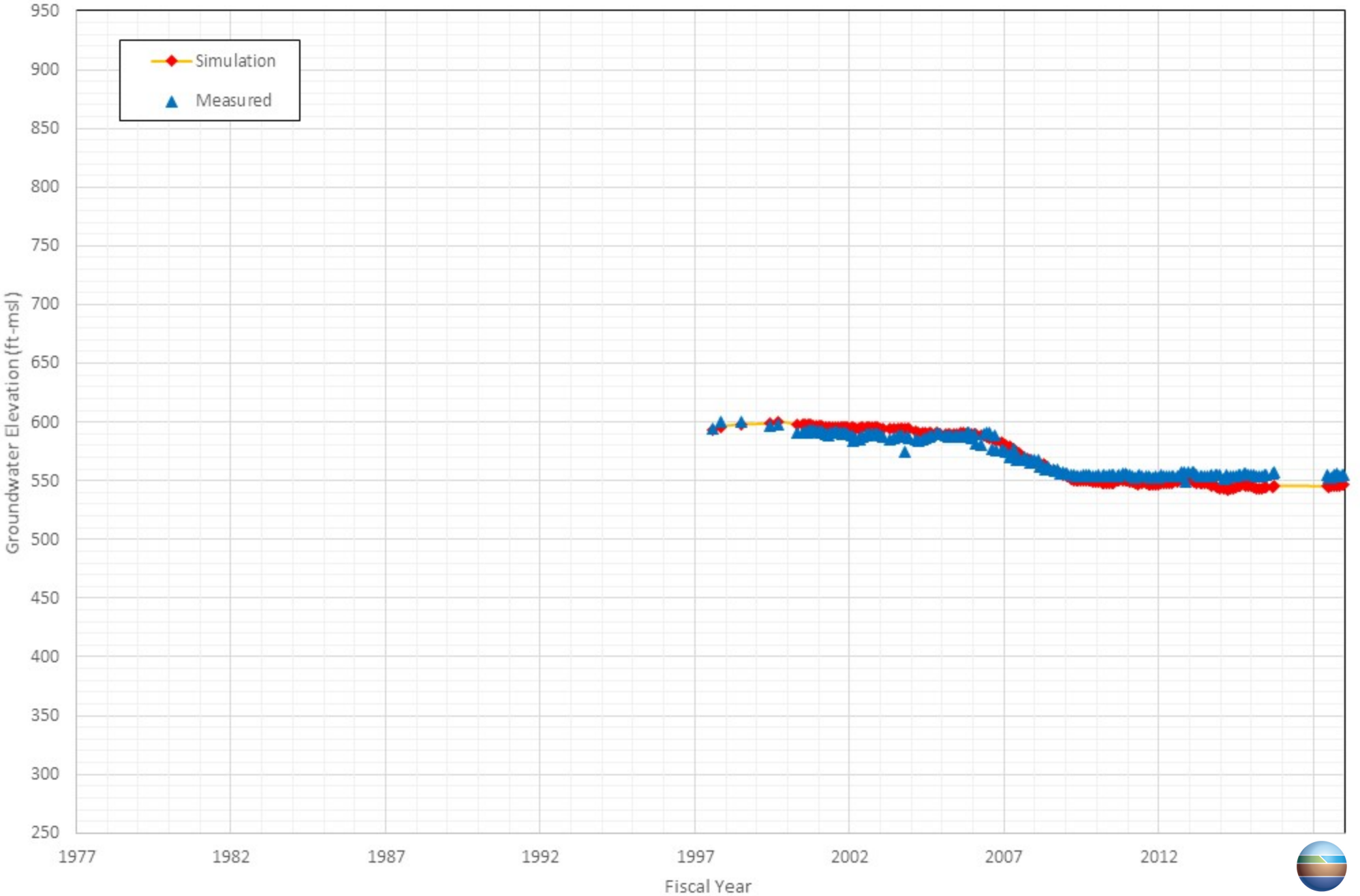

Appendix C-101
Comparison of Measured and Simulated Groundwater Water Level
in the City of Pomona's Well P-28

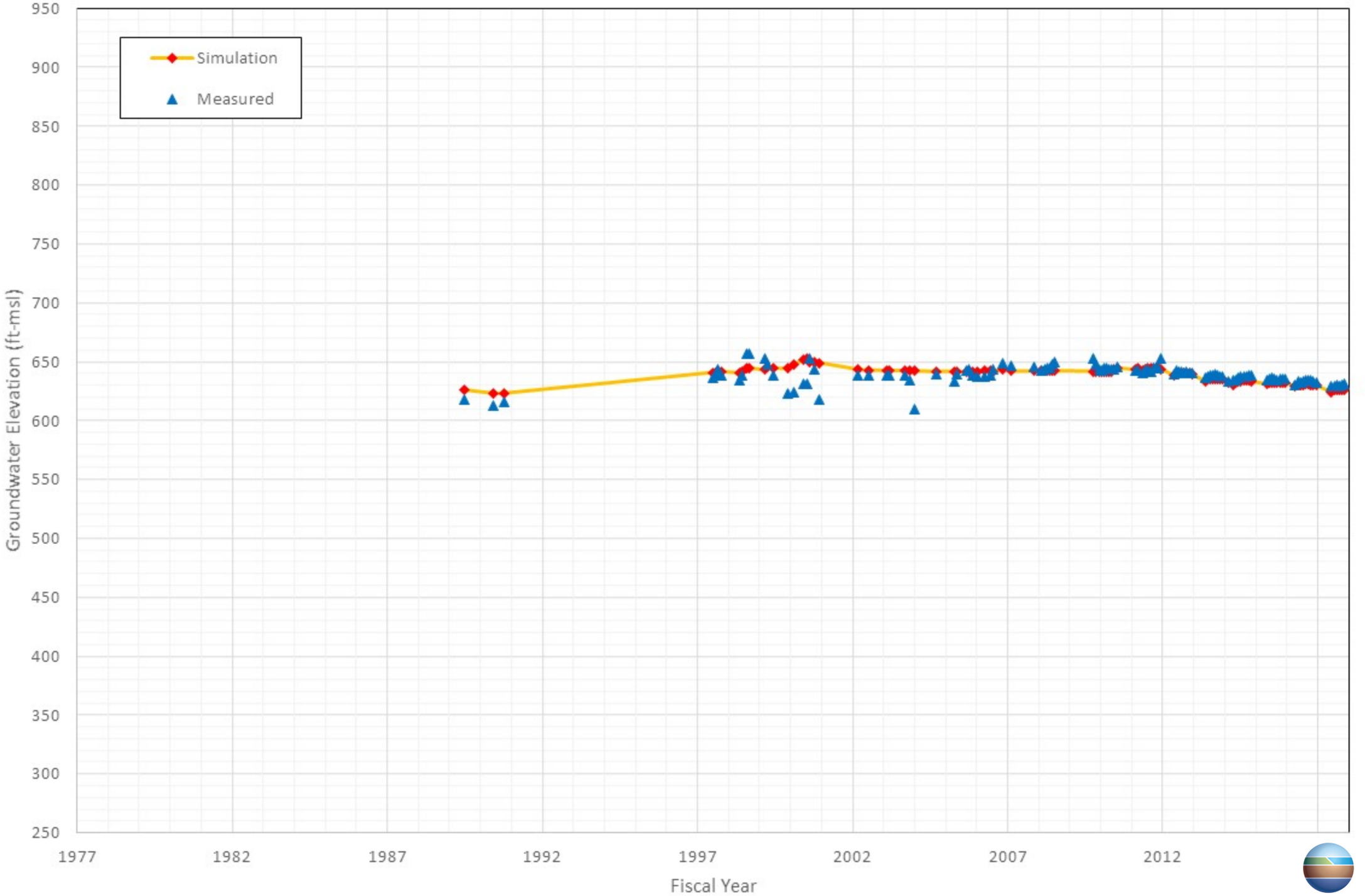

Appendix C-102
Comparison of Measured and Simulated Groundwater Water Level
in the California State Polytechnic University, Pomona's Well Well 1

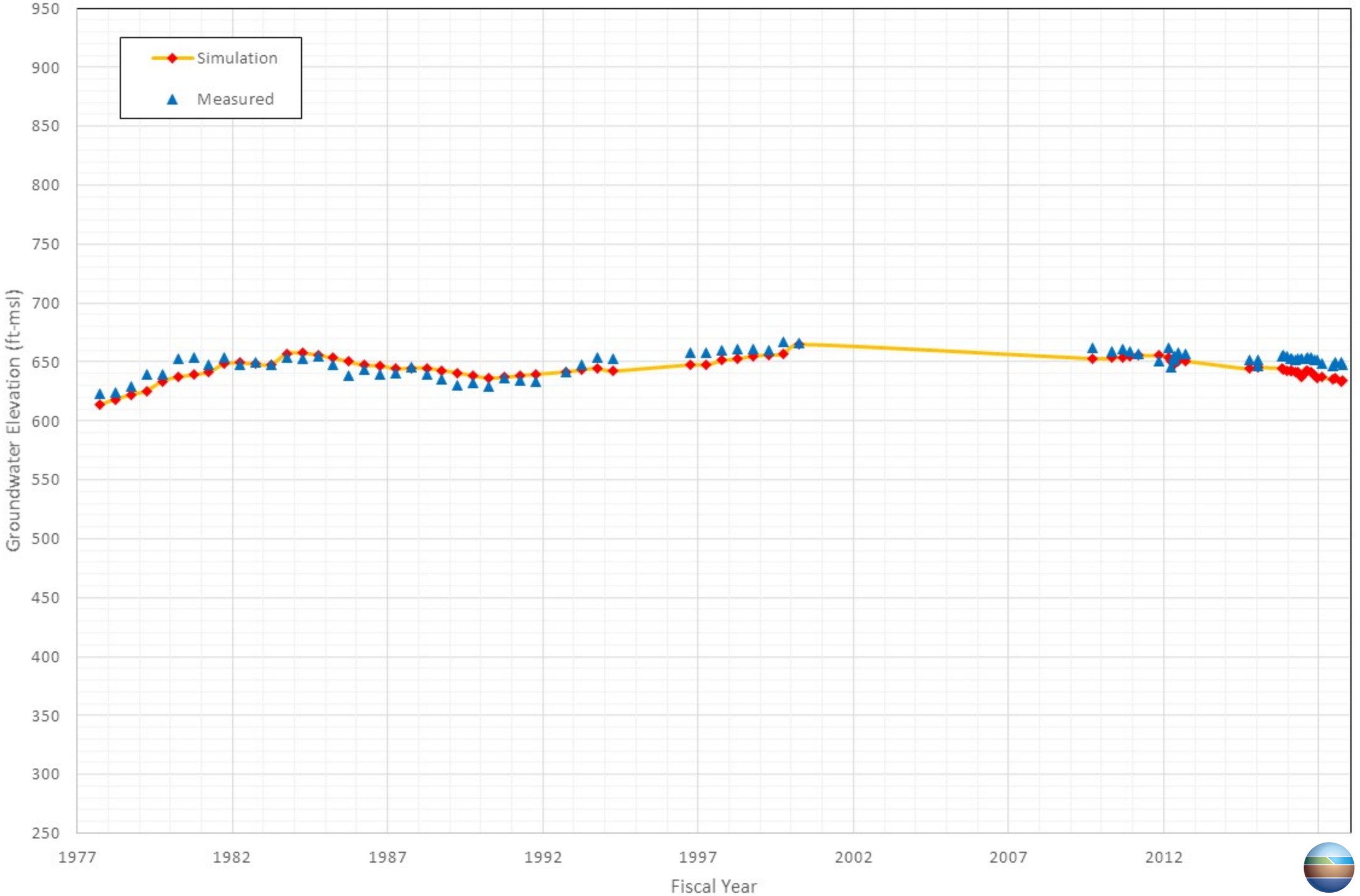

Appendix C-103
Comparison of Measured and Simulated Groundwater Water Level
in the Unknown's Well NA_1002811

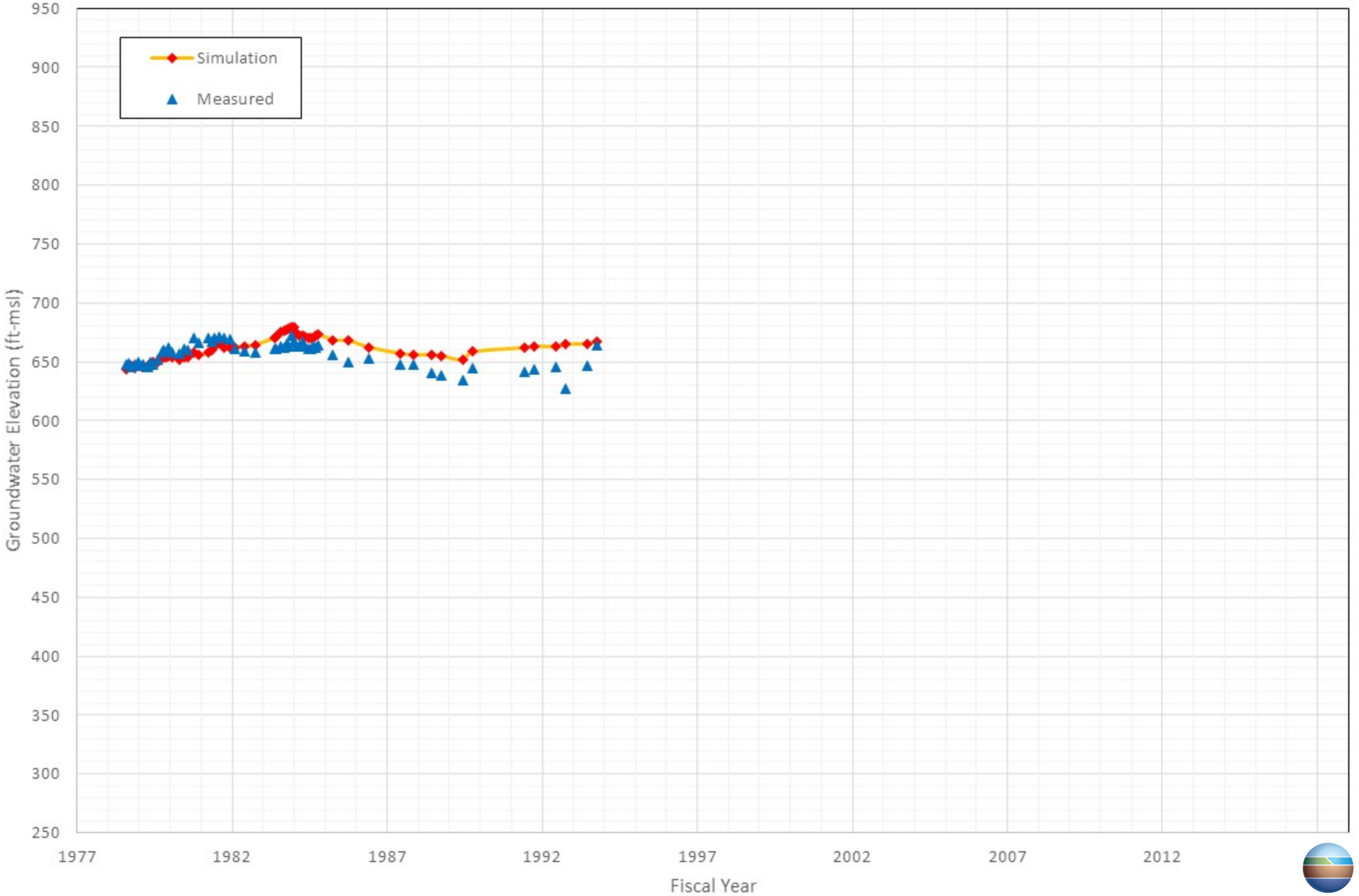

Appendix C-104
Comparison of Measured and Simulated Groundwater Water Level
in the City of Pomona's Well P-31 (OGT-3)

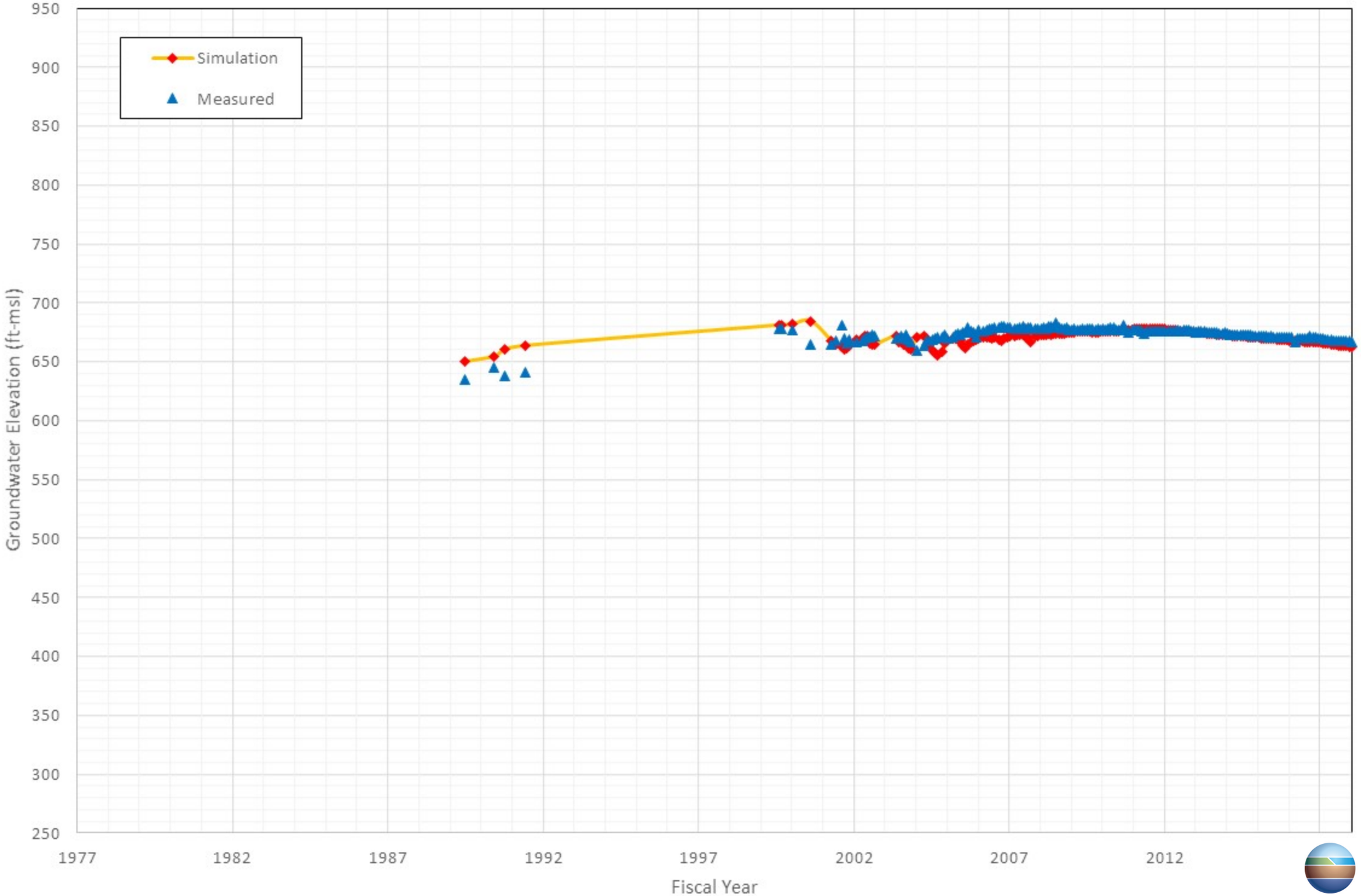

Appendix D

Time-History Plots of Projected Groundwater Elevations in Select Wells for the 2020 SYR1 Scenario

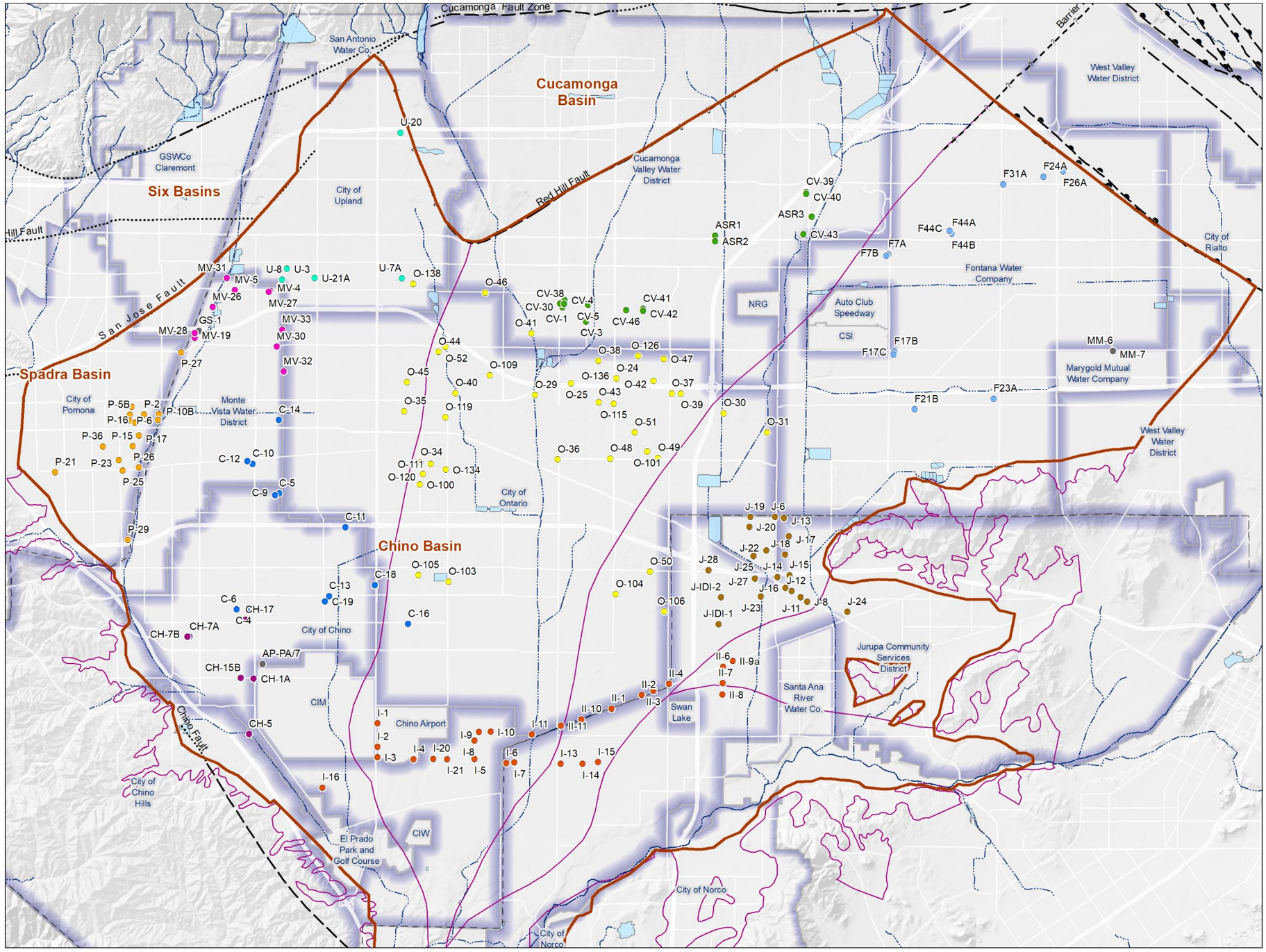

Groundwater Model Wells

- City of Chino
- City of Chino Hills
- City of Corona
- City of Ontario
- City of Pomona
- City of Upland
- Cucamonga Valley Water District
- Fontana Water Company
- Jurupa Community Services District
- Monte Vista Water District
- CDA
- Other

Streams & Flood Control Channels

Flood Control & Conservation Basins

Water Service Area

OBMP Management Zones

Faults

- Location Certain
- Location Approximate
- Approximate Location of Groundwater Barrier
- Location Concealed
- Location Uncertain

Prepared by:

WEI
WILDERMUTH ENVIRONMENTAL, INC.

Author: LS
Date: 4/1/2020
File: Figure F-1 SYR Hydrograph Wells.mxd

Prepared for:

2020 Safe Yield Recalculation

Location of Wells with Groundwater Elevation Time Series in the Planning Period in Appendix D

Figure D-1

Appendix D-1
Projected Groundwater Elevation for Scenarios 1
CDA Well CDA I-1

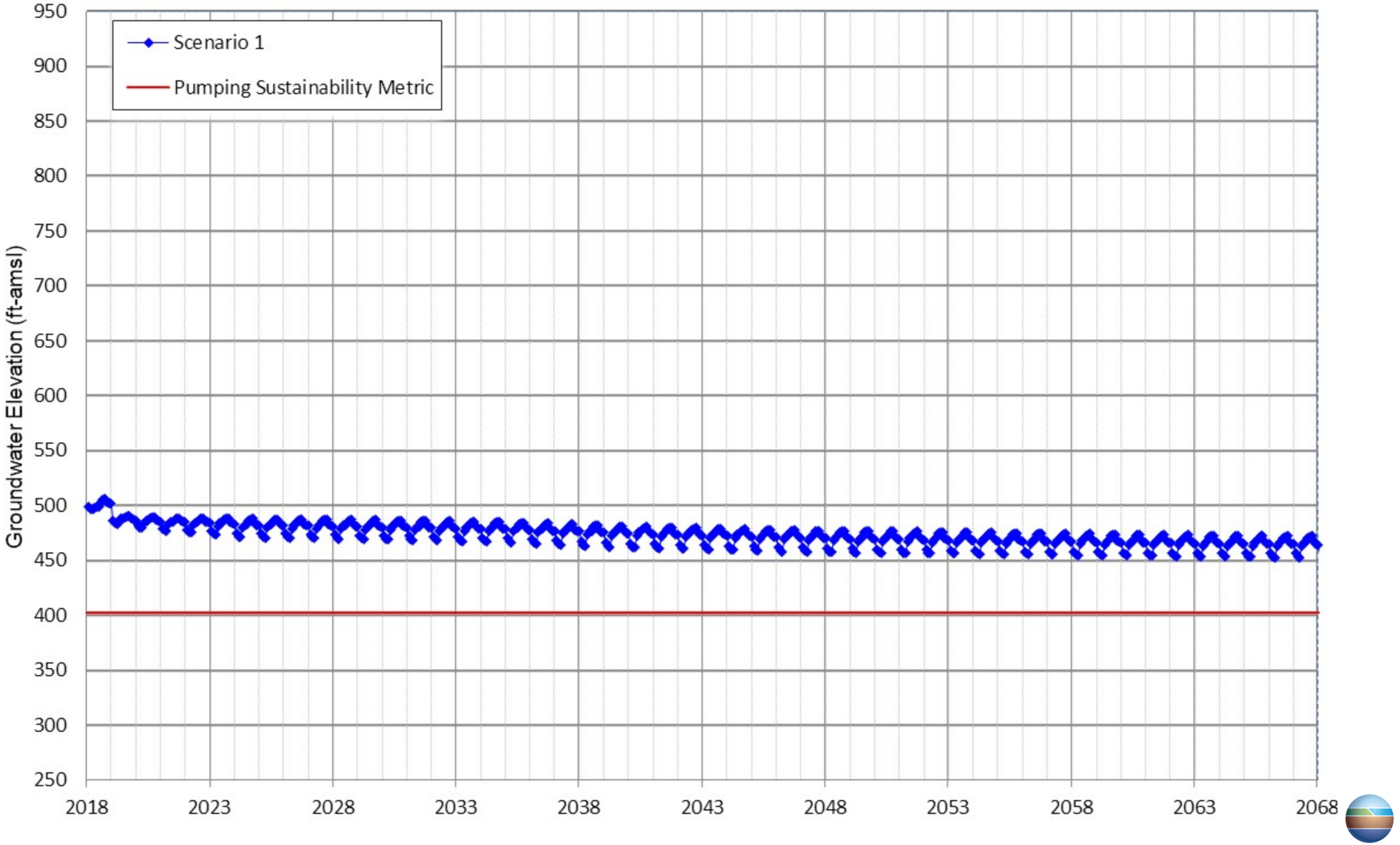

Appendix D-2
Projected Groundwater Elevation for Scenarios 1
CDA Well CDA I-2

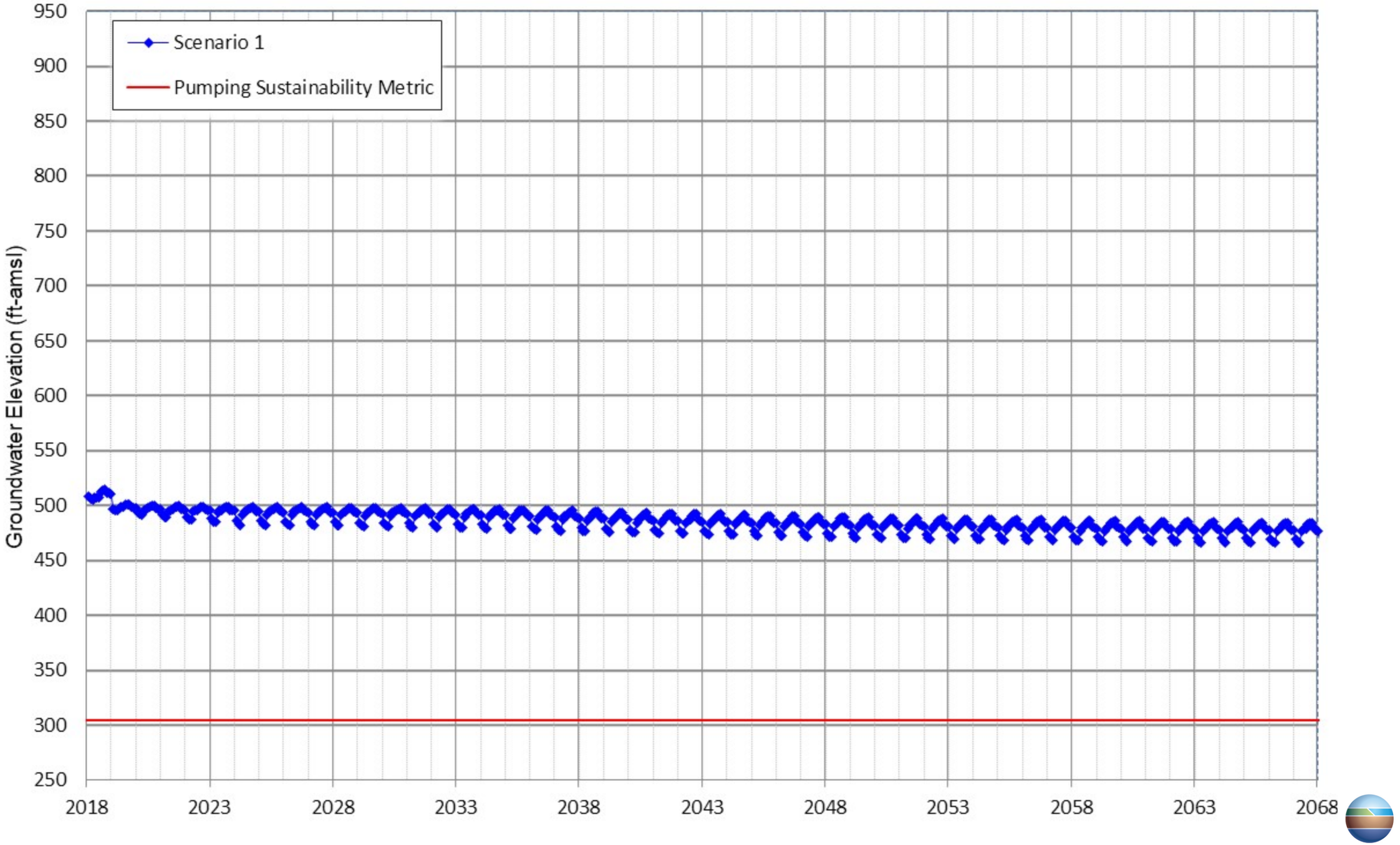

Appendix D-3
Projected Groundwater Elevation for Scenarios 1
CDA Well CDA I-3

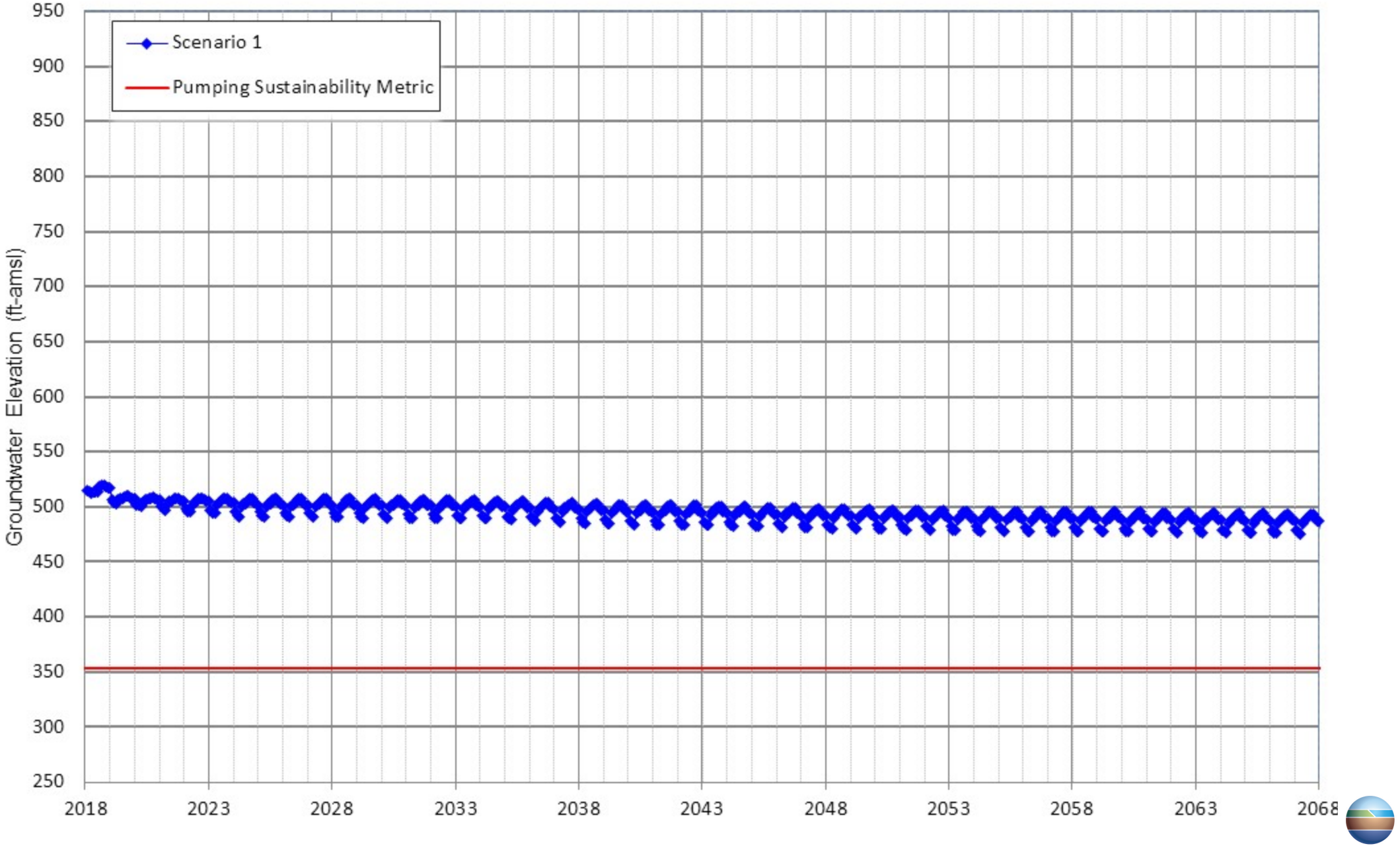

Appendix D-4
Projected Groundwater Elevation for Scenarios 1
CDA Well CDA I-4

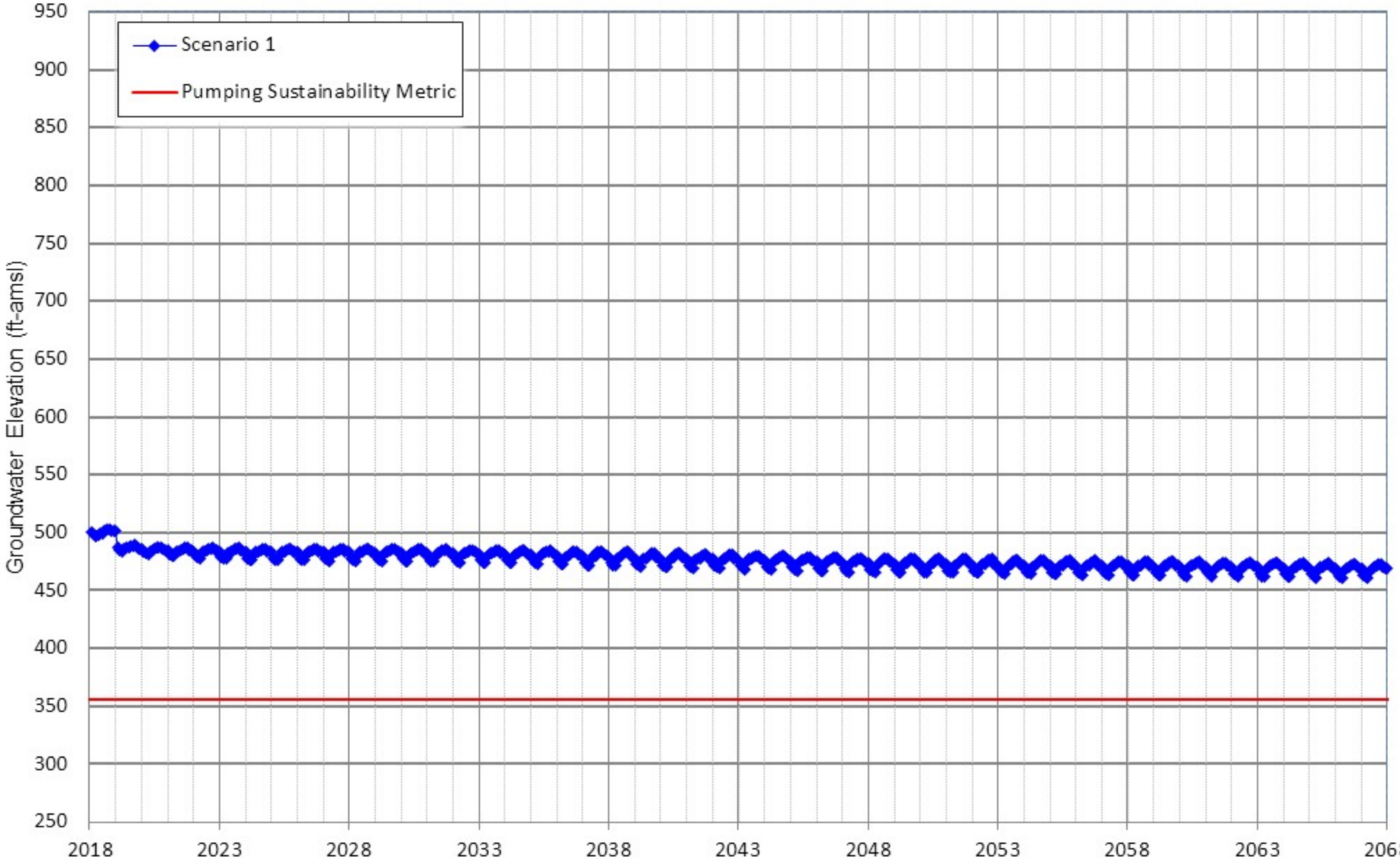

Appendix D-5
Projected Groundwater Elevation for Scenarios 1
CDA Well CDA I-5

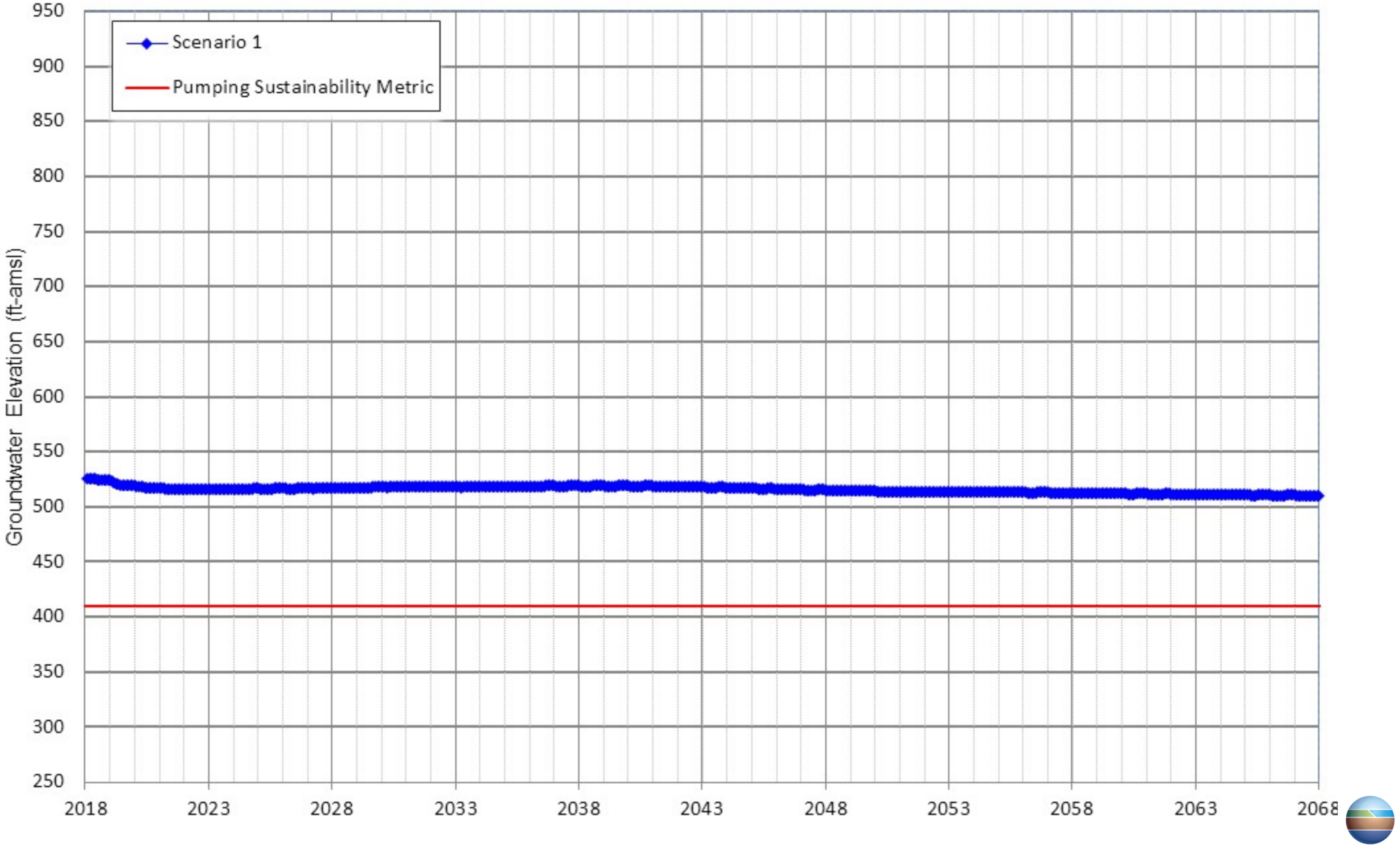

Appendix D-6
Projected Groundwater Elevation for Scenarios 1
CDA Well CDA I-6

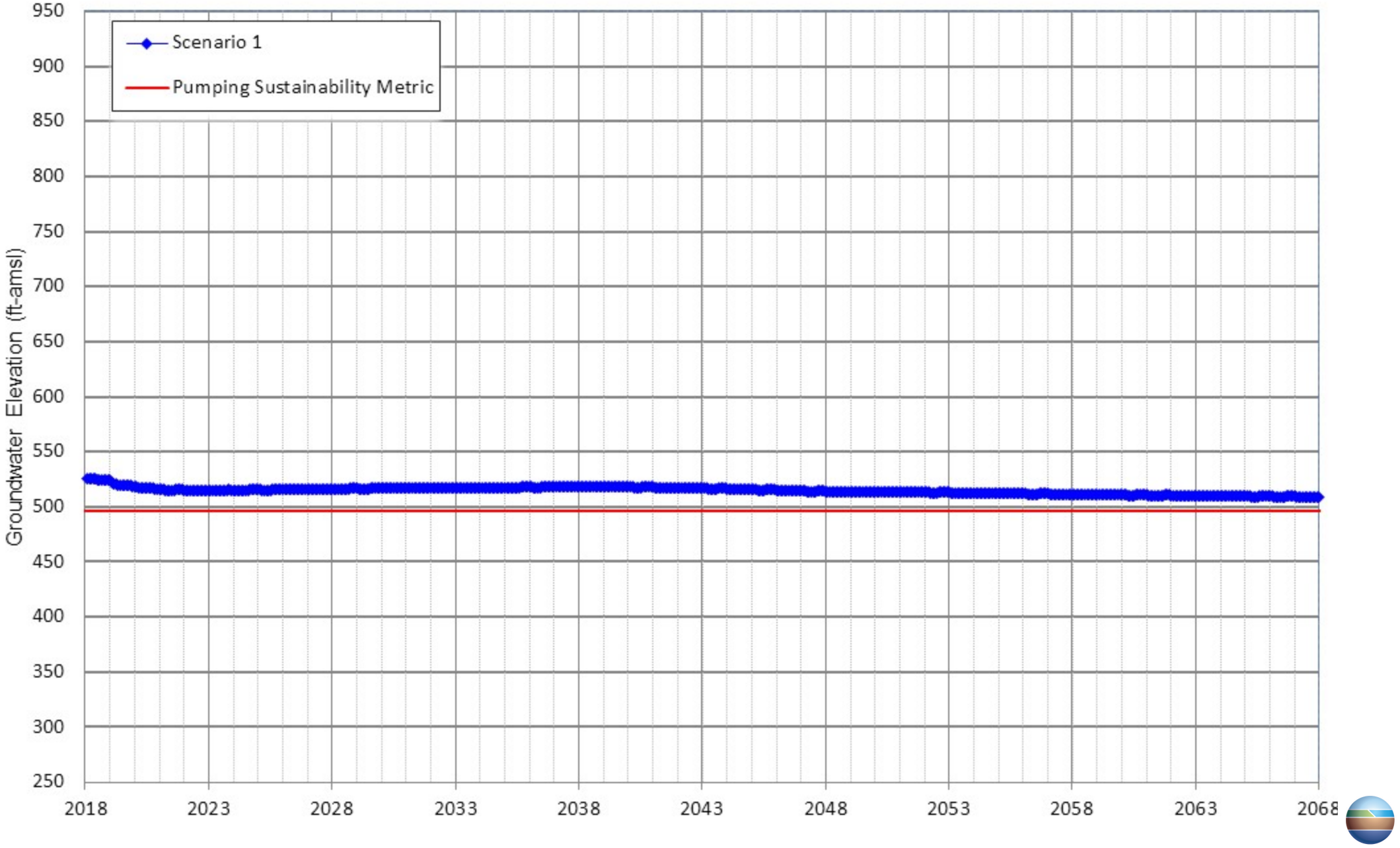

Appendix D-7
Projected Groundwater Elevation for Scenarios 1
CDA Well CDA I-7

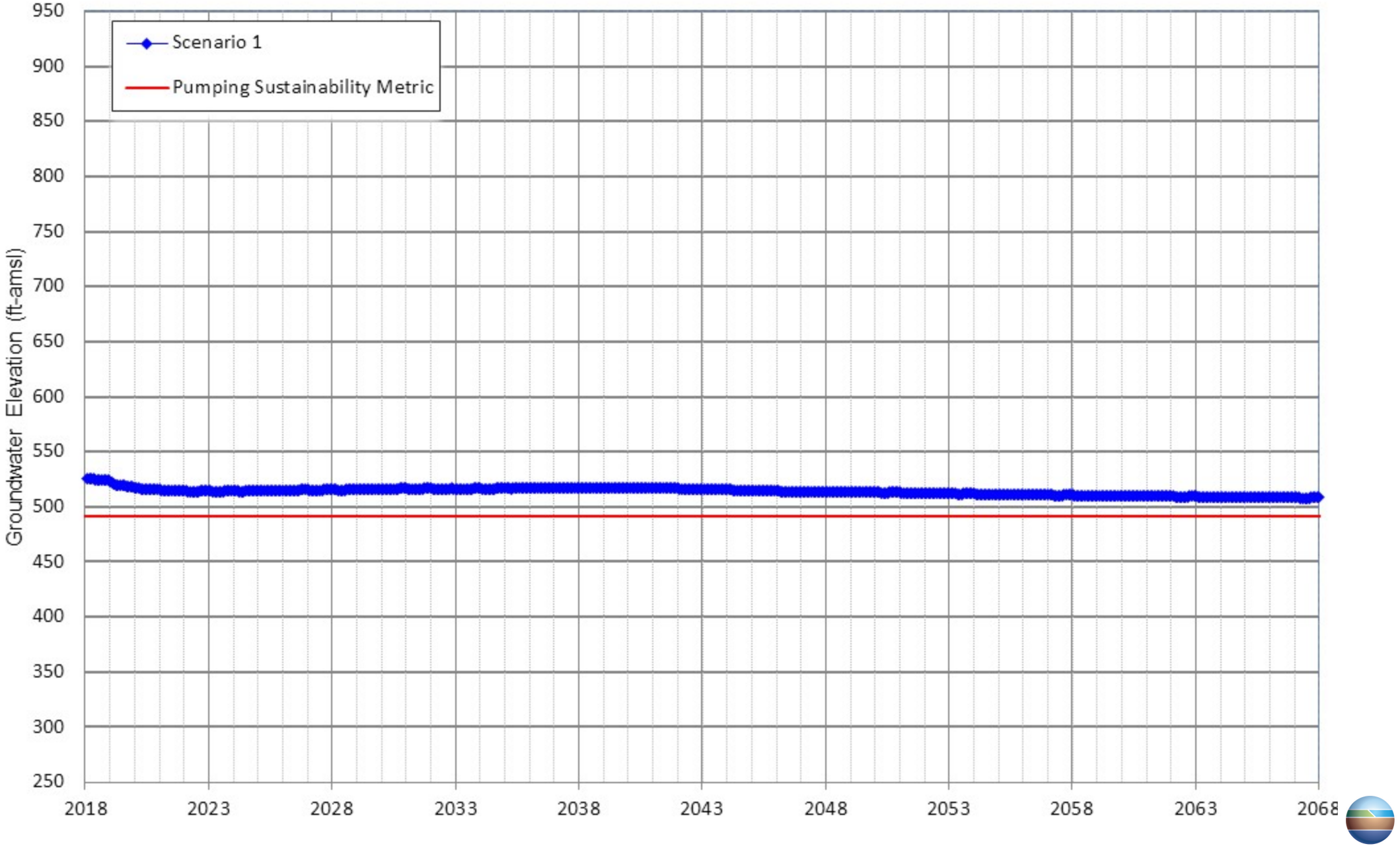

Appendix D-8
Projected Groundwater Elevation for Scenarios 1
CDA Well CDA I-8

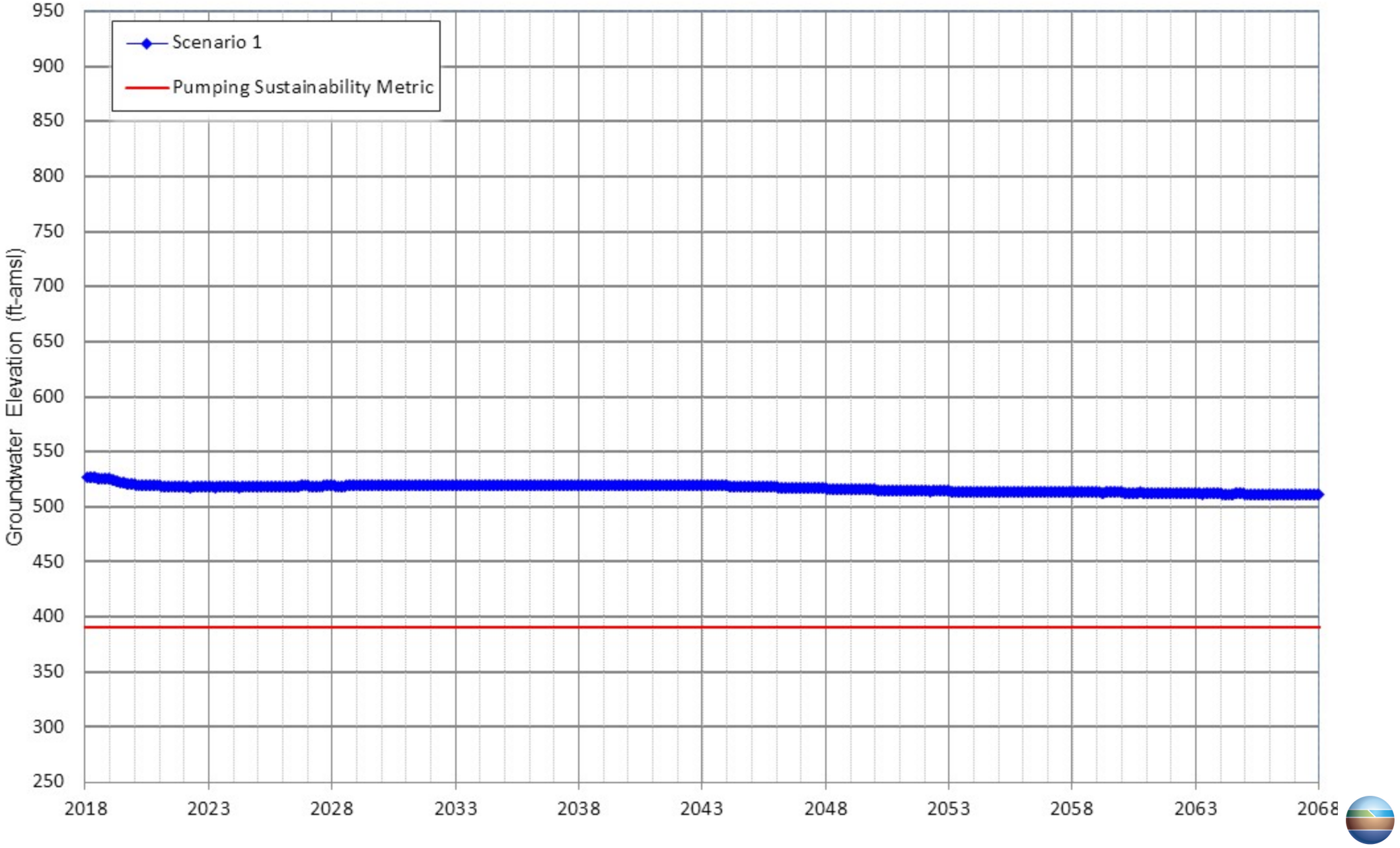

Appendix D-9
Projected Groundwater Elevation for Scenarios 1
CDA Well CDA I-9

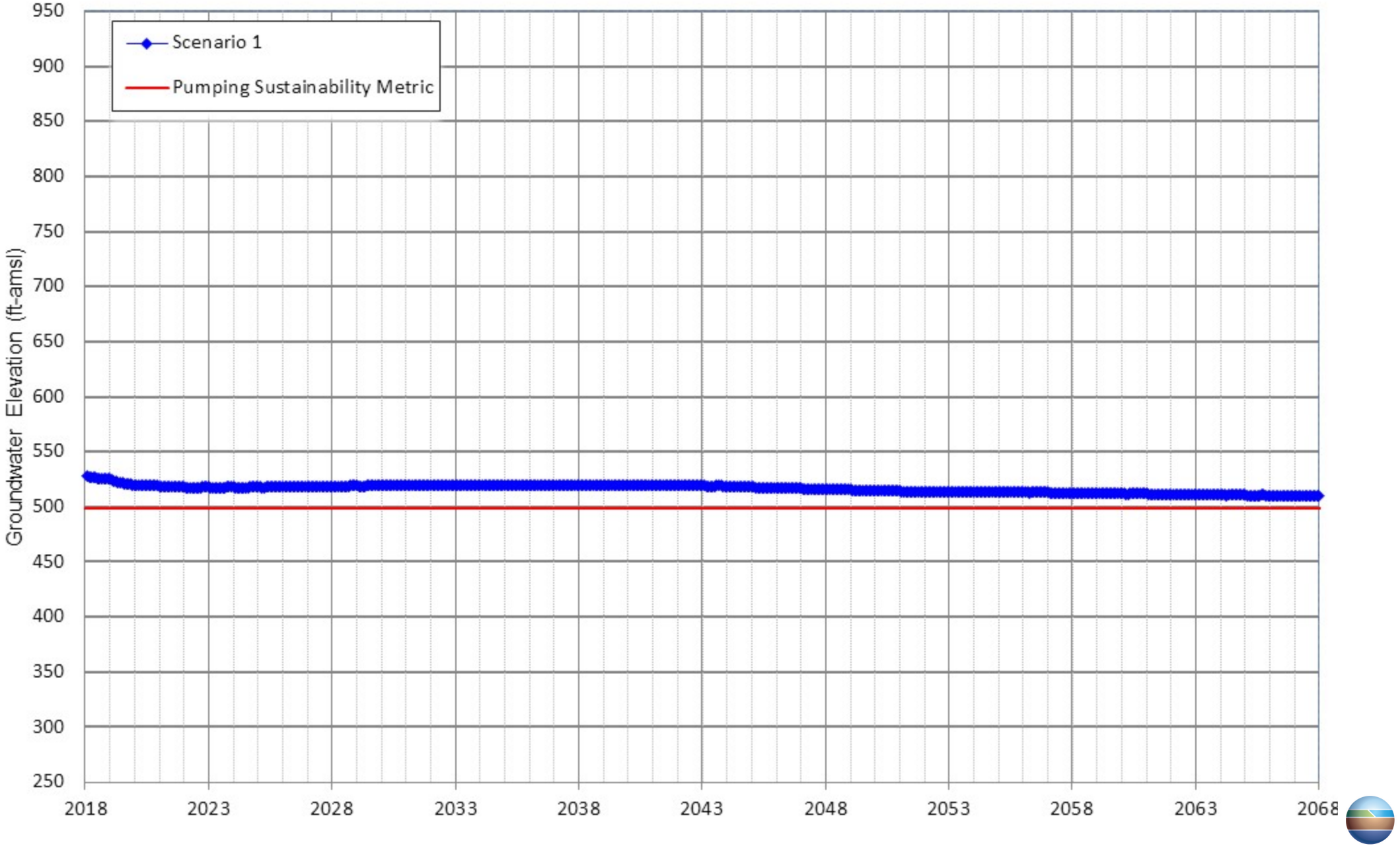

Appendix D-10
Projected Groundwater Elevation for Scenarios 1
CDA Well CDA I-10

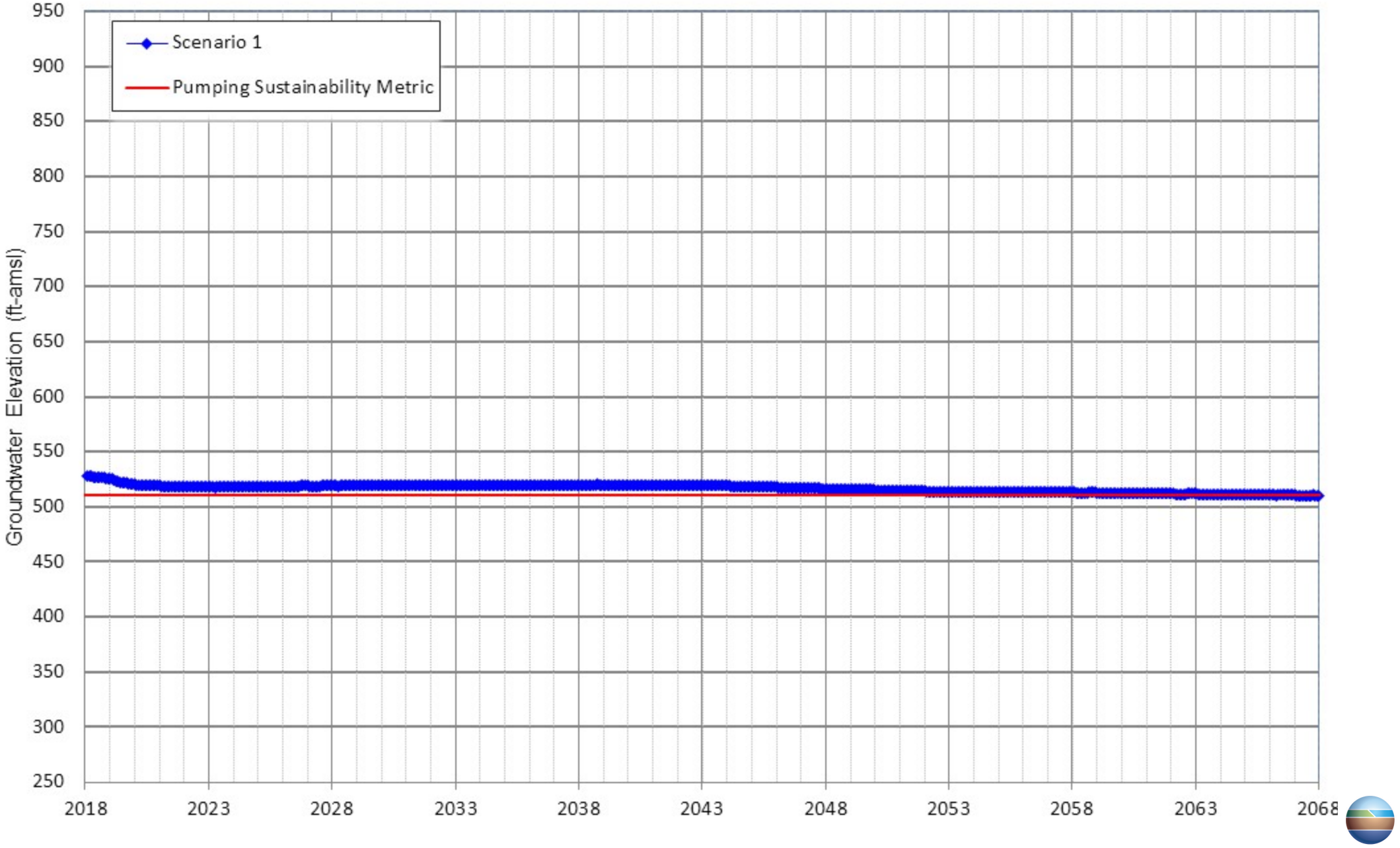

Appendix D-11
Projected Groundwater Elevation for Scenarios 1
CDA Well CDA I-11

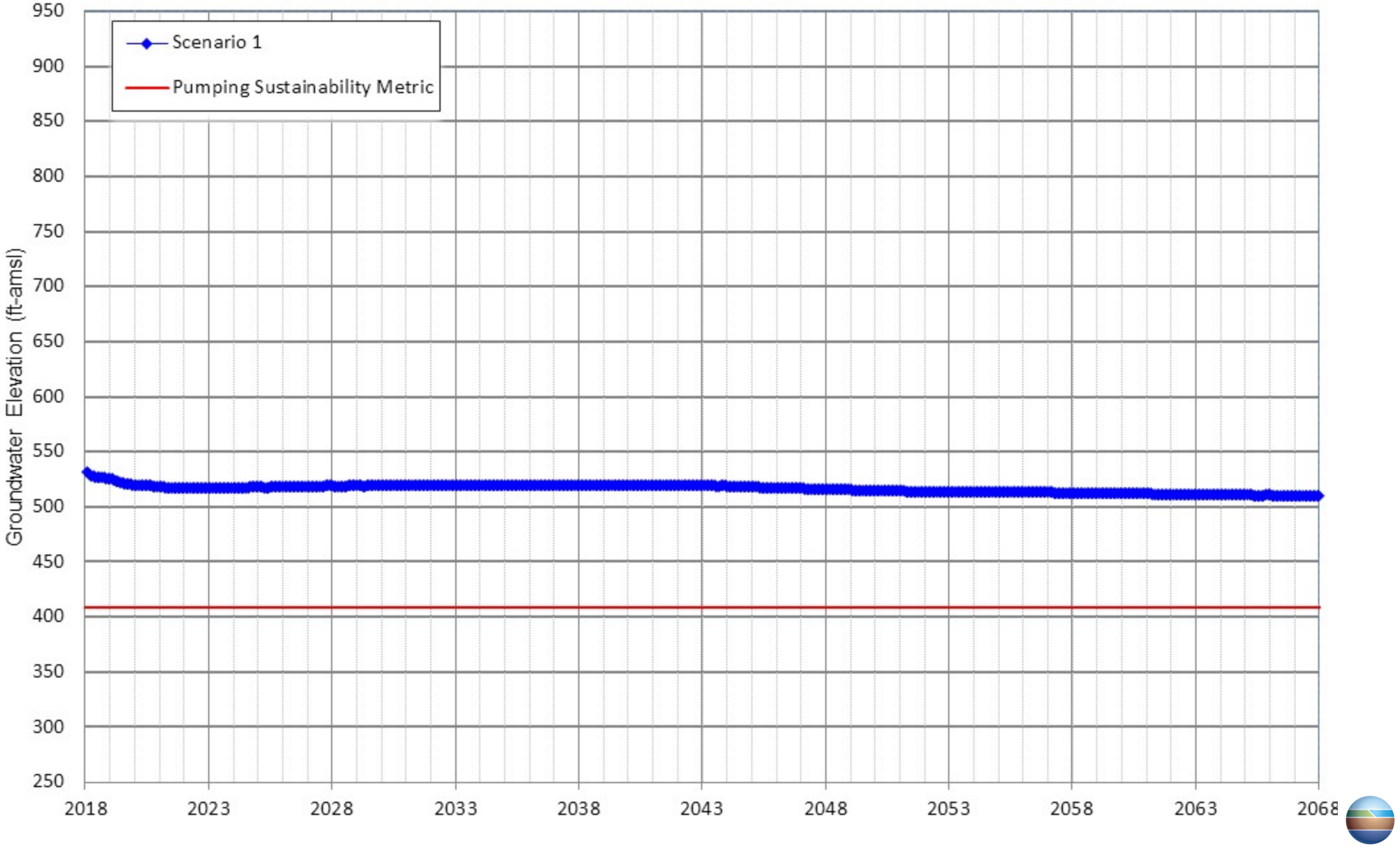

Appendix D-12
Projected Groundwater Elevation for Scenarios 1
CDA Well CDA I-13

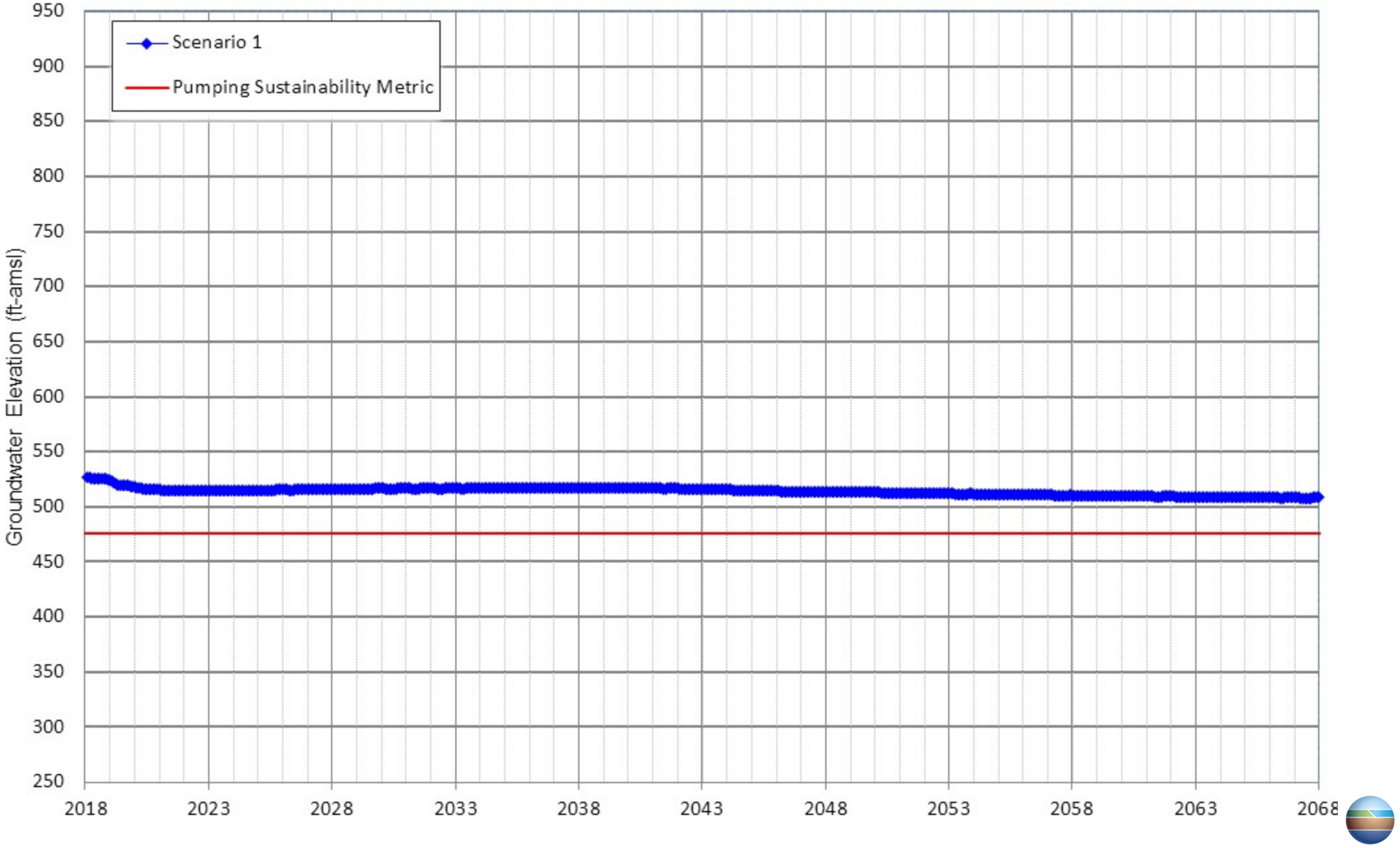

Appendix D-13
Projected Groundwater Elevation for Scenarios 1
CDA Well CDA I-14

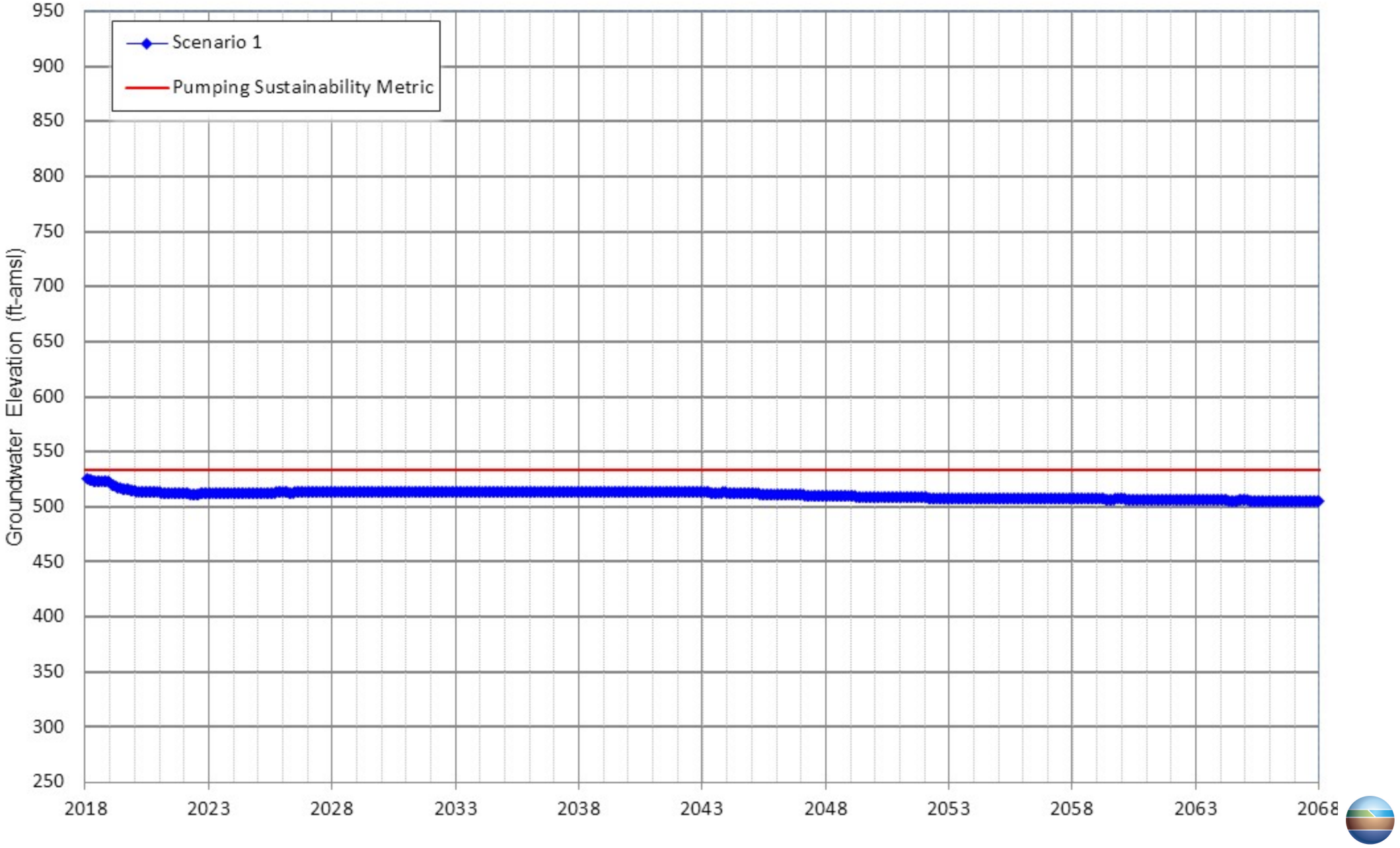

Appendix D-14
Projected Groundwater Elevation for Scenarios 1
CDA Well CDA I-15

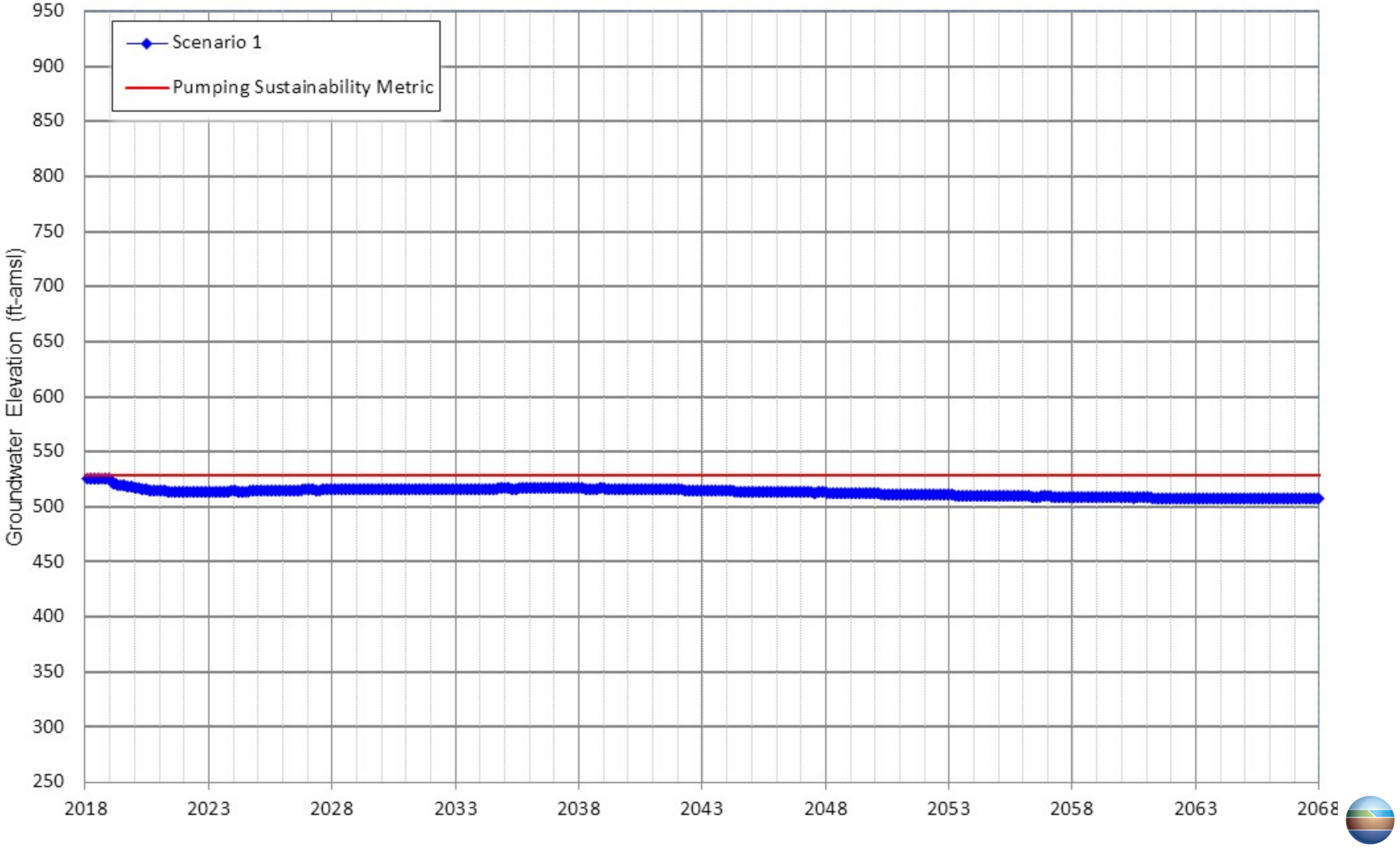

Appendix D-15
Projected Groundwater Elevation for Scenarios 1
CDA Well CDA I-16

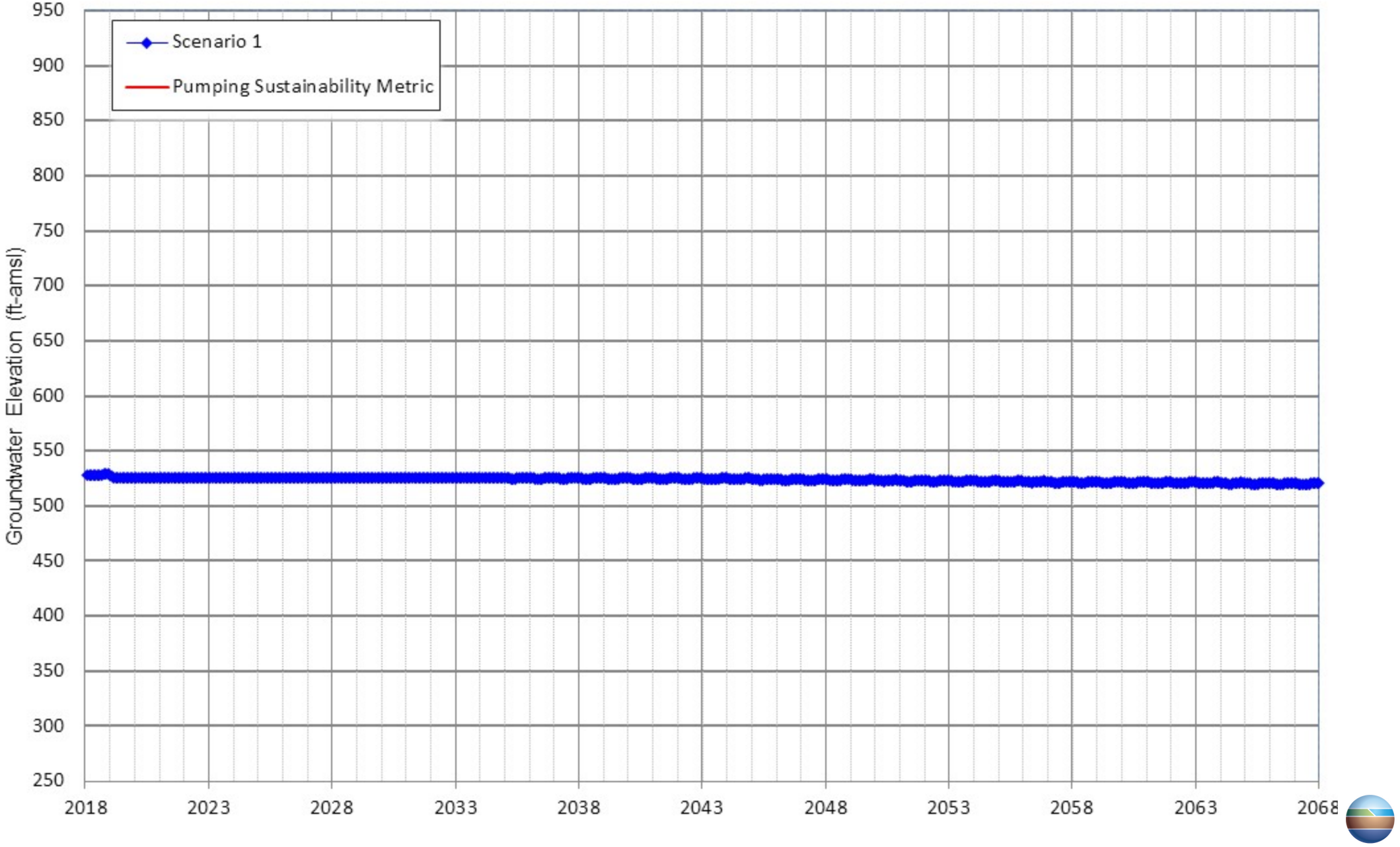

Appendix D-16
Projected Groundwater Elevation for Scenarios 1
CDA Well CDA I-20

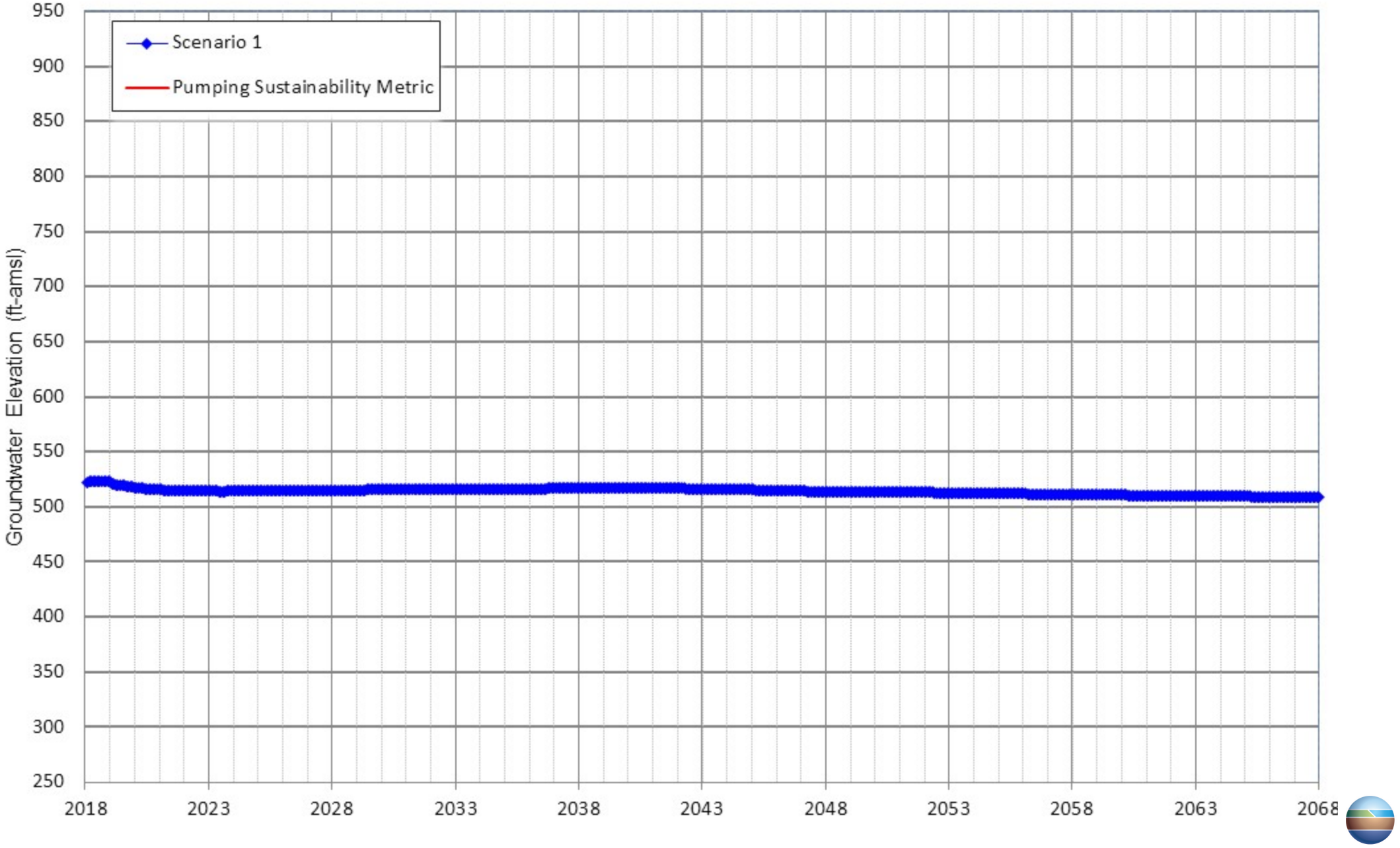

Appendix D-17
Projected Groundwater Elevation for Scenarios 1
CDA Well CDA I-21

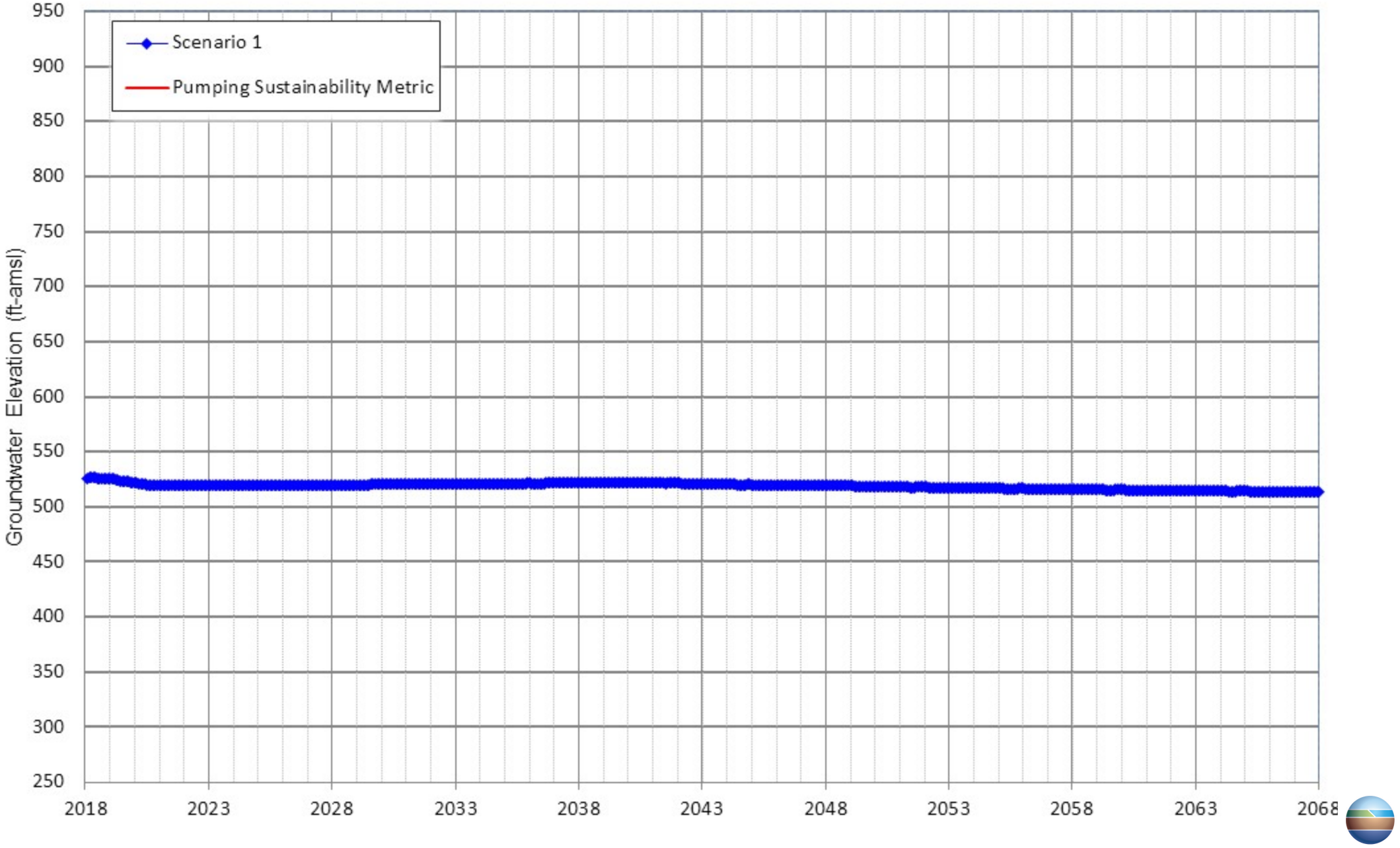

Appendix D-18
Projected Groundwater Elevation for Scenarios 1
CDA Well CDA II-1

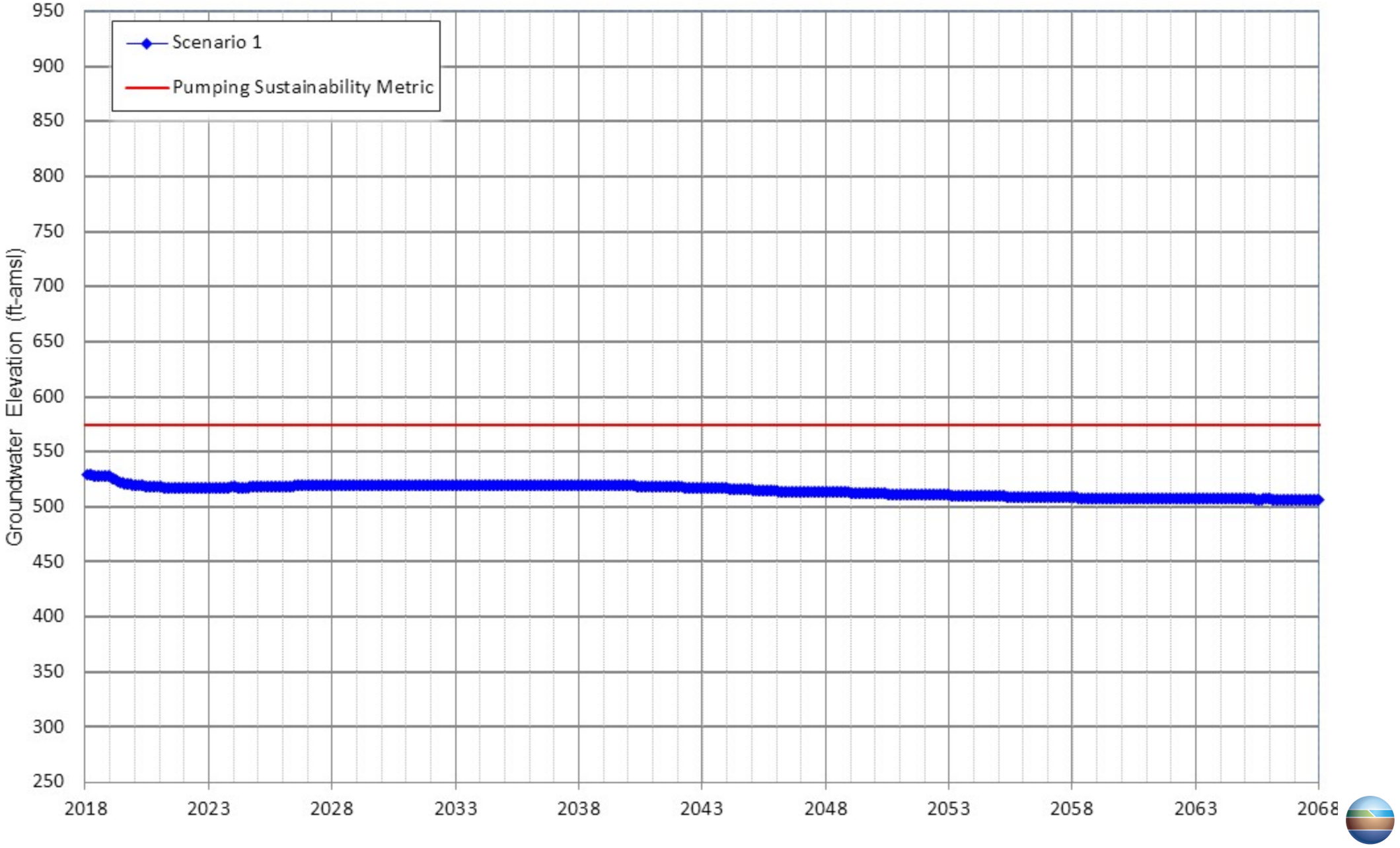

Appendix D-19
Projected Groundwater Elevation for Scenarios 1
CDA Well CDA II-2

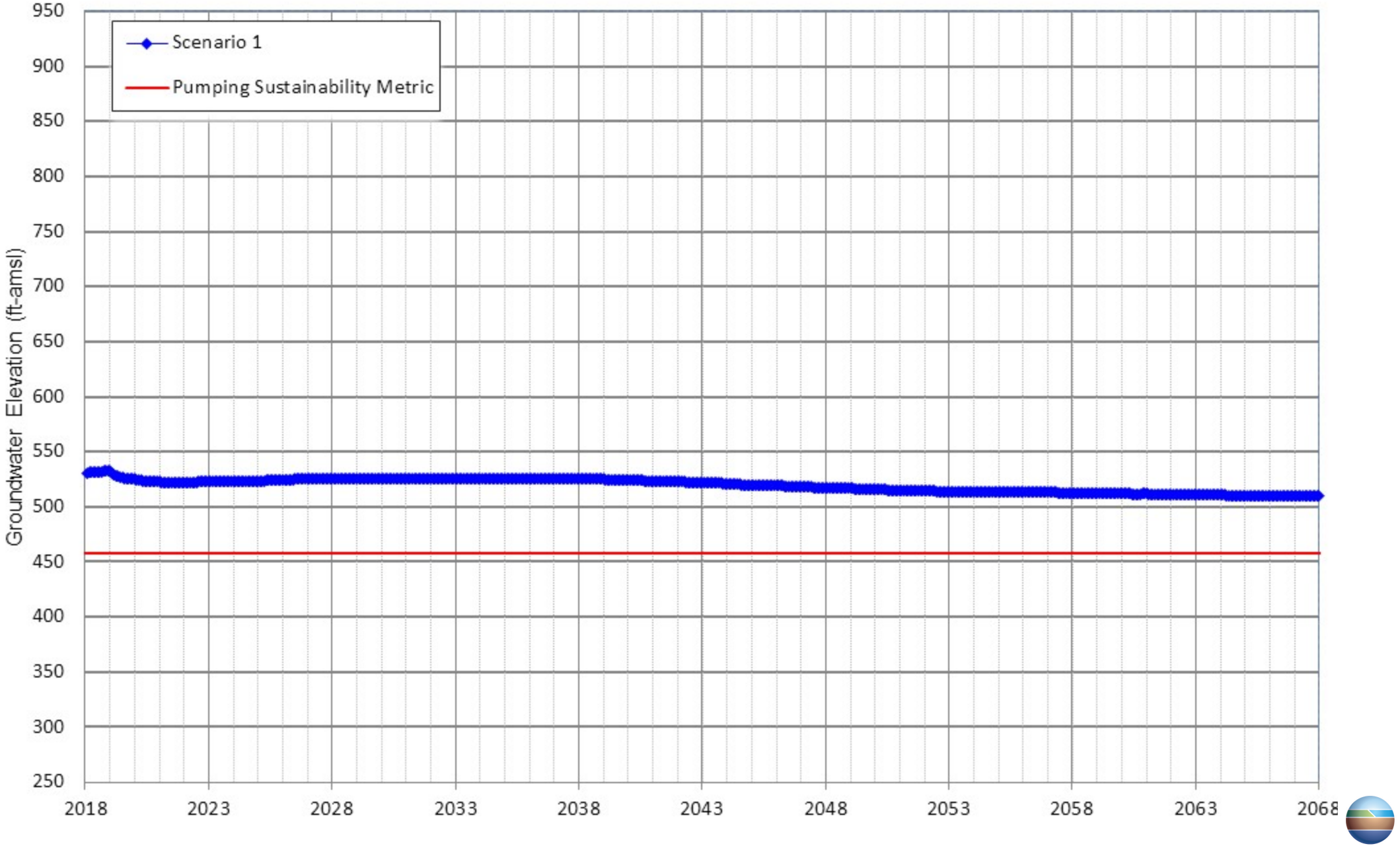

Appendix D-20
Projected Groundwater Elevation for Scenarios 1
CDA Well CDA II-3

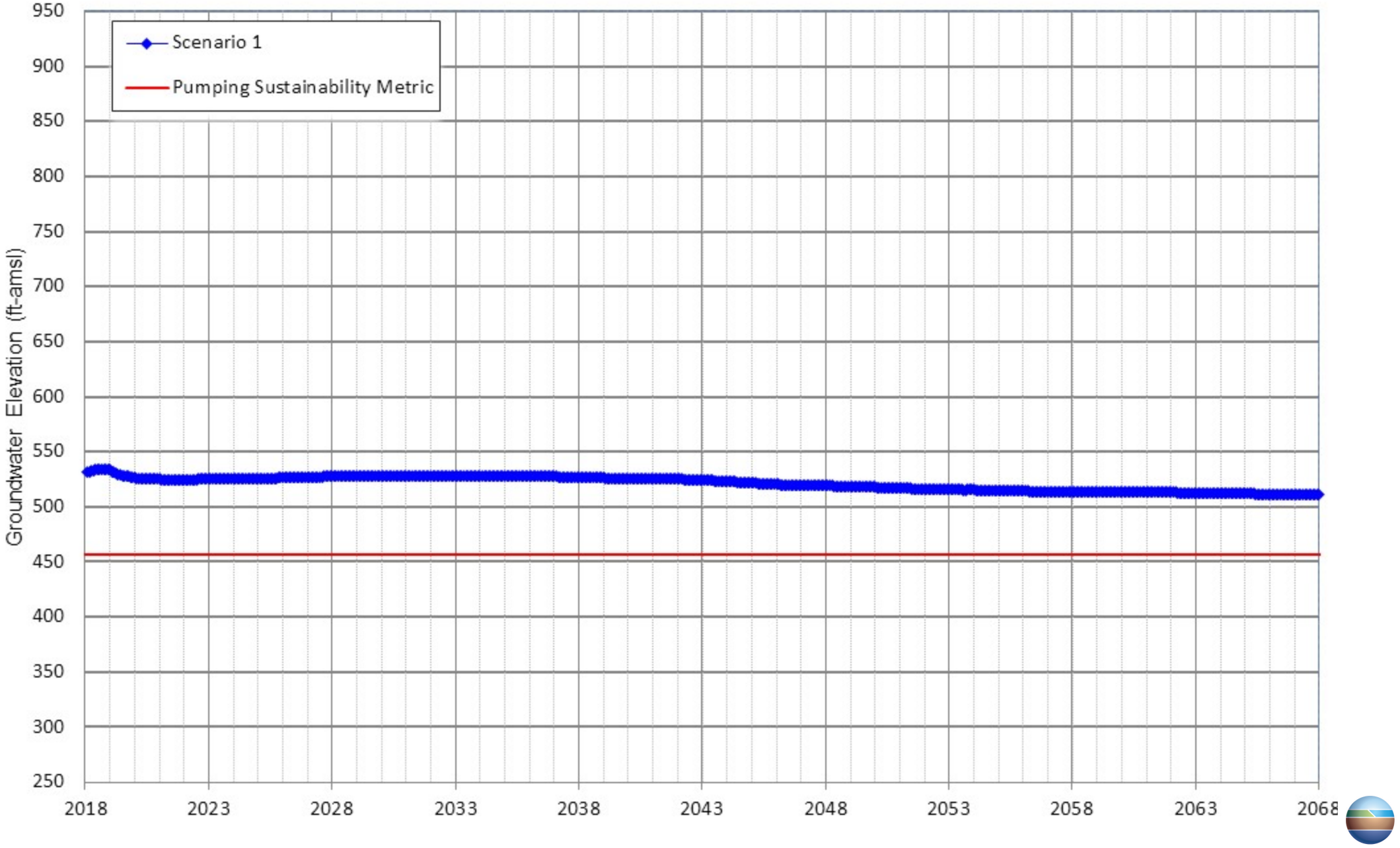

Appendix D-21
Projected Groundwater Elevation for Scenarios 1
CDA Well CDA II-4

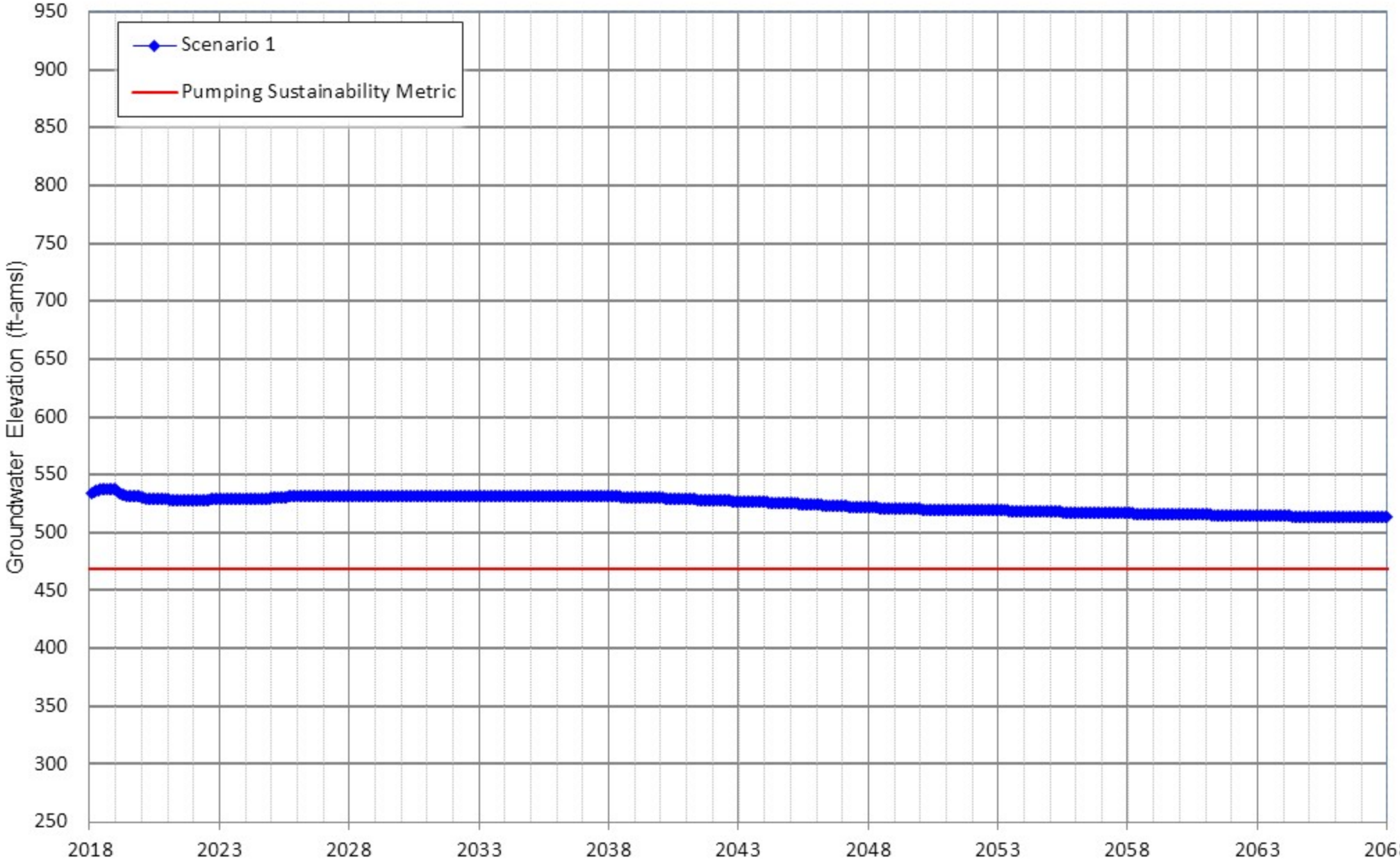

Appendix D-22
Projected Groundwater Elevation for Scenarios 1
CDA Well CDA-II-6

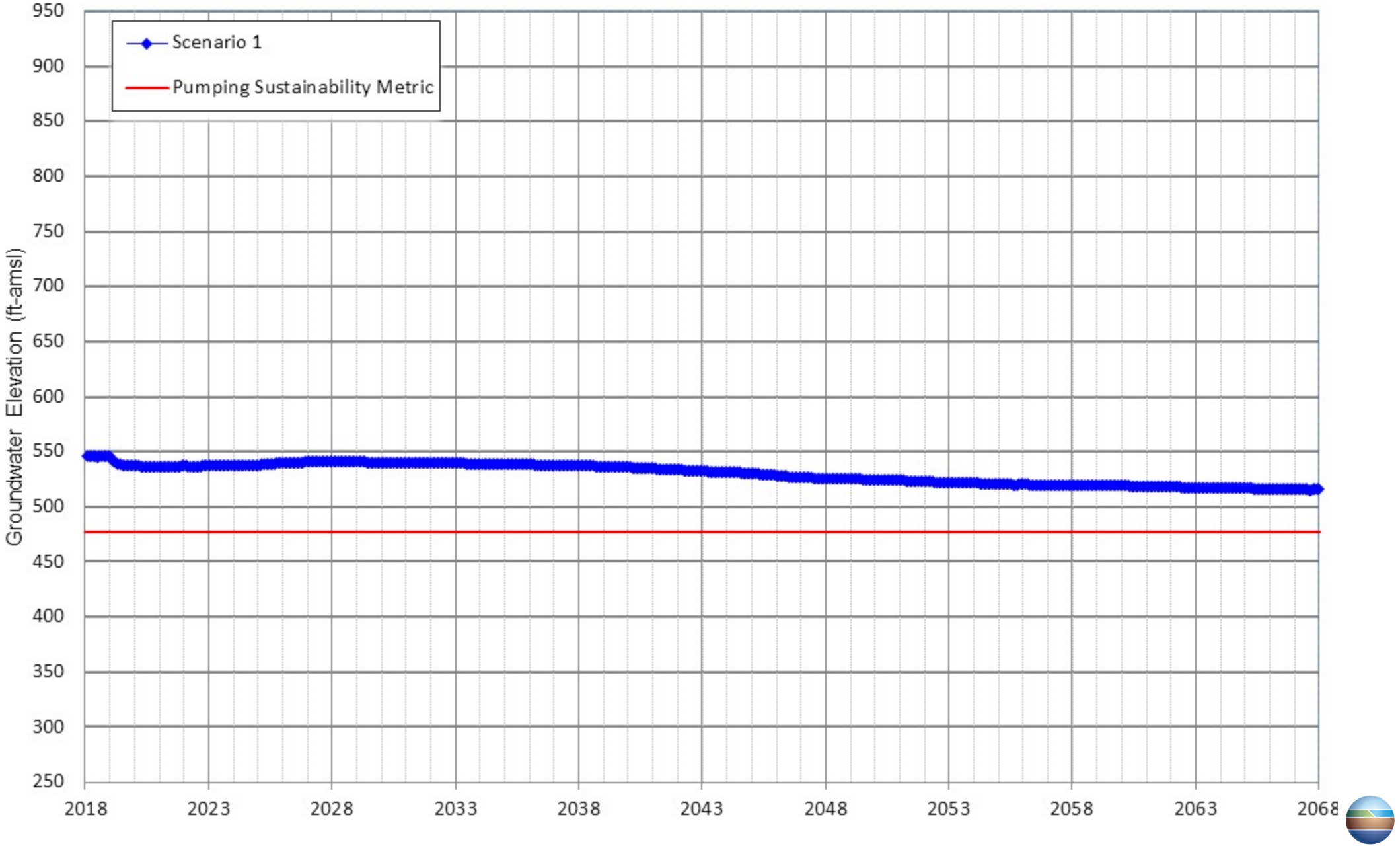

Appendix D-23
Projected Groundwater Elevation for Scenarios 1
CDA Well CDA II-7

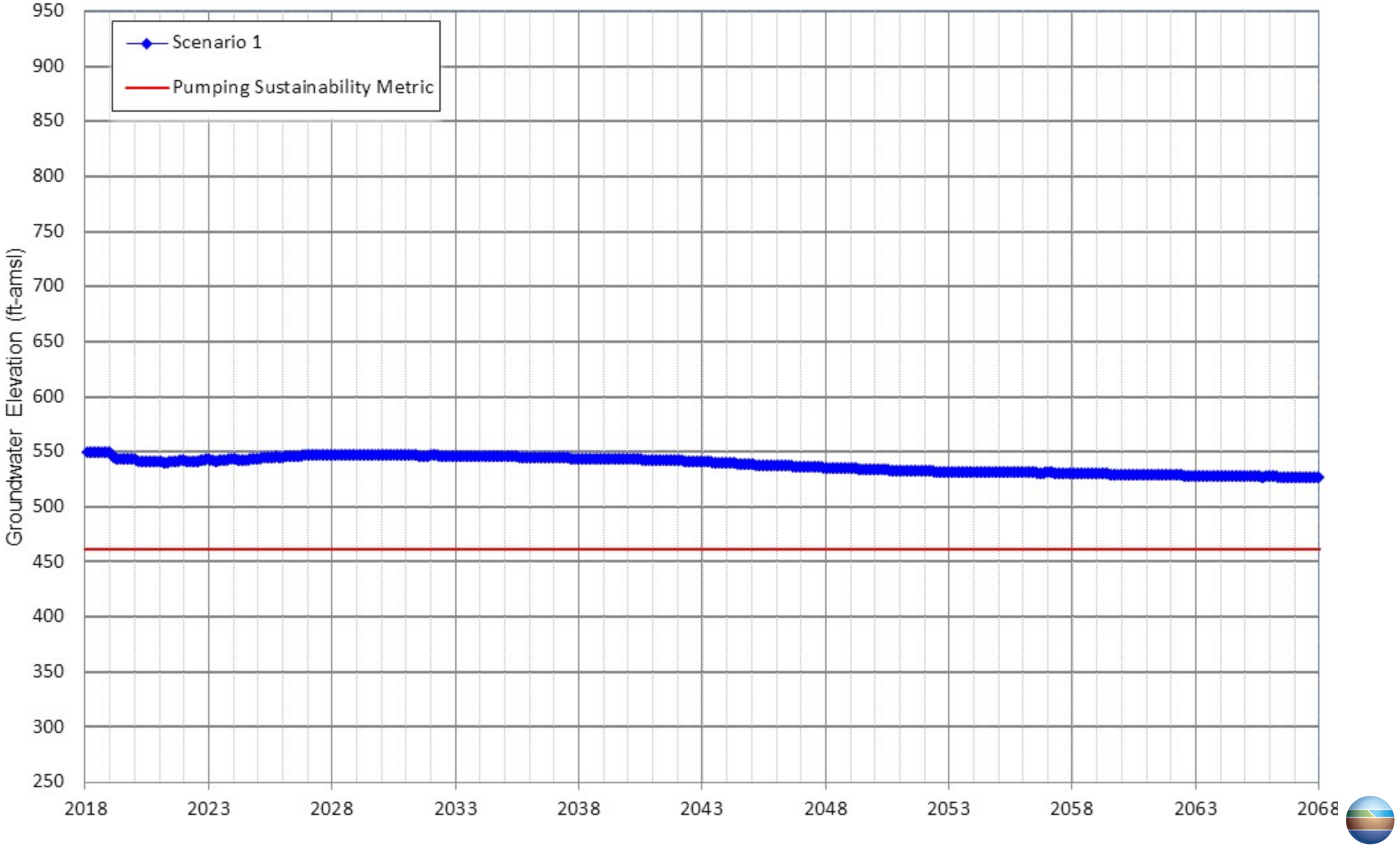

Appendix D-24
Projected Groundwater Elevation for Scenarios 1
CDA Well CDA-II-8

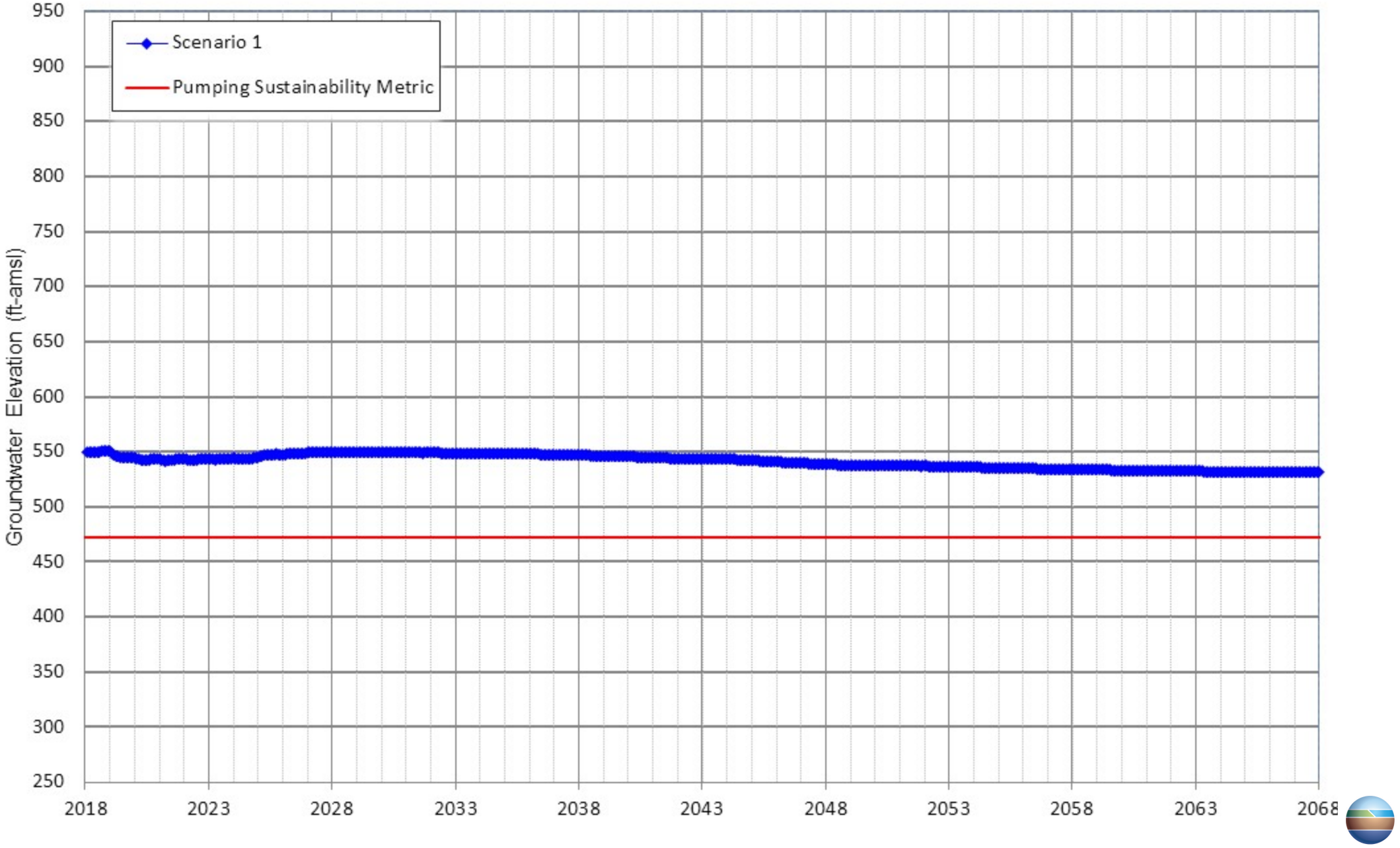

Appendix D-25
Projected Groundwater Elevation for Scenarios 1
CDA Well CDA-II-9a

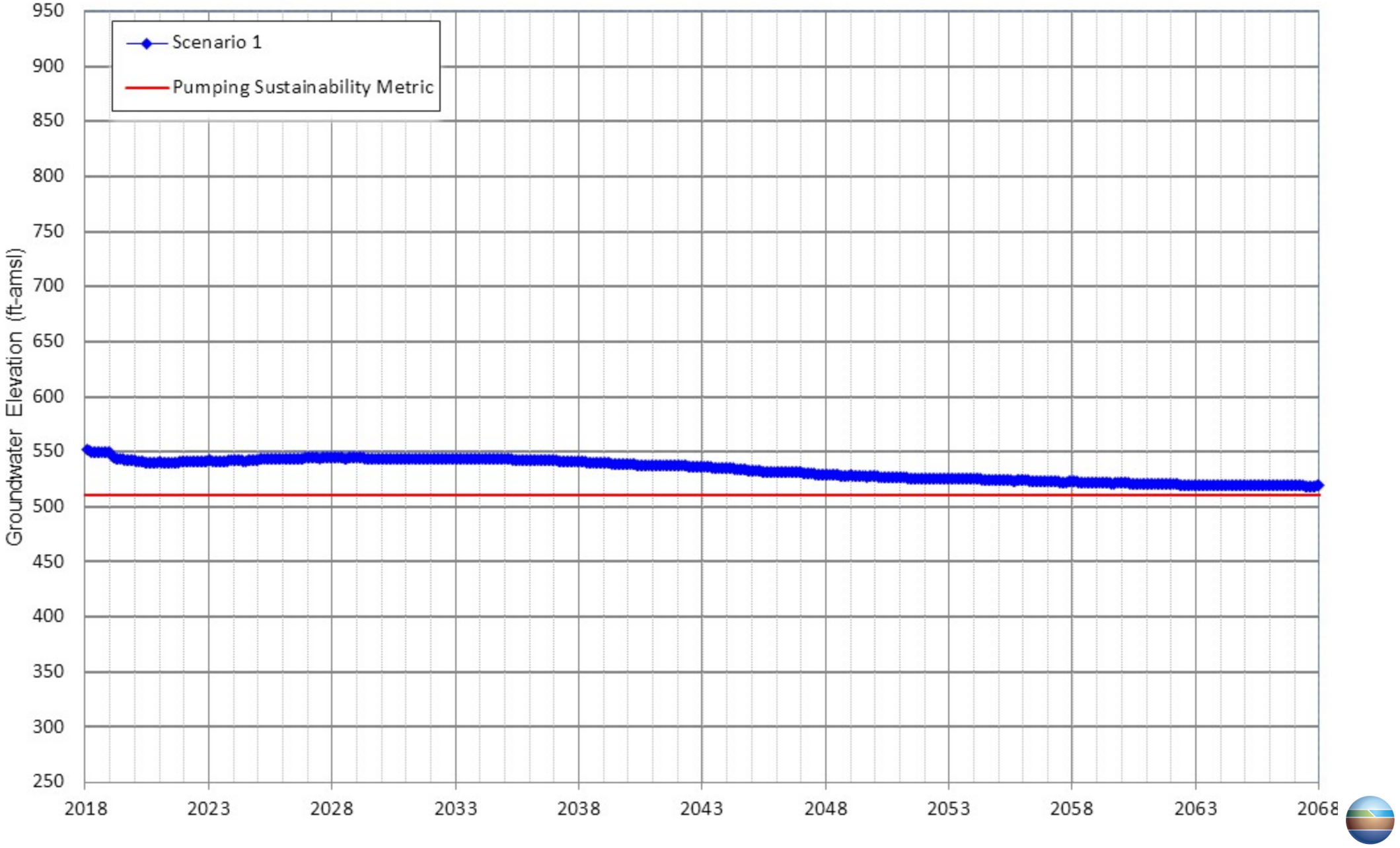

Appendix D-26
Projected Groundwater Elevation for Scenarios 1
CDA Well CDA II-10

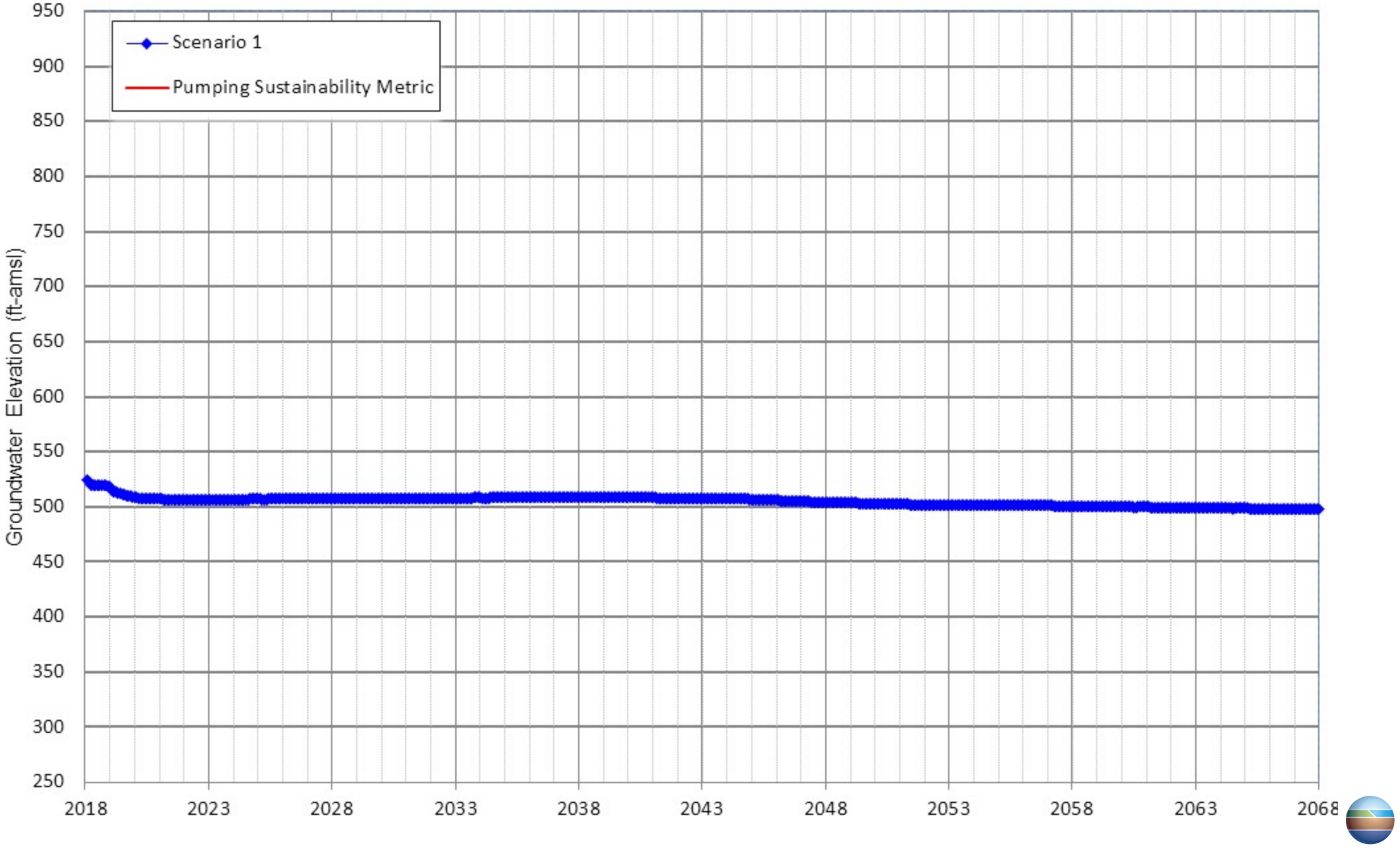

Appendix D-27
Projected Groundwater Elevation for Scenarios 1
CDA Well CDA II-11

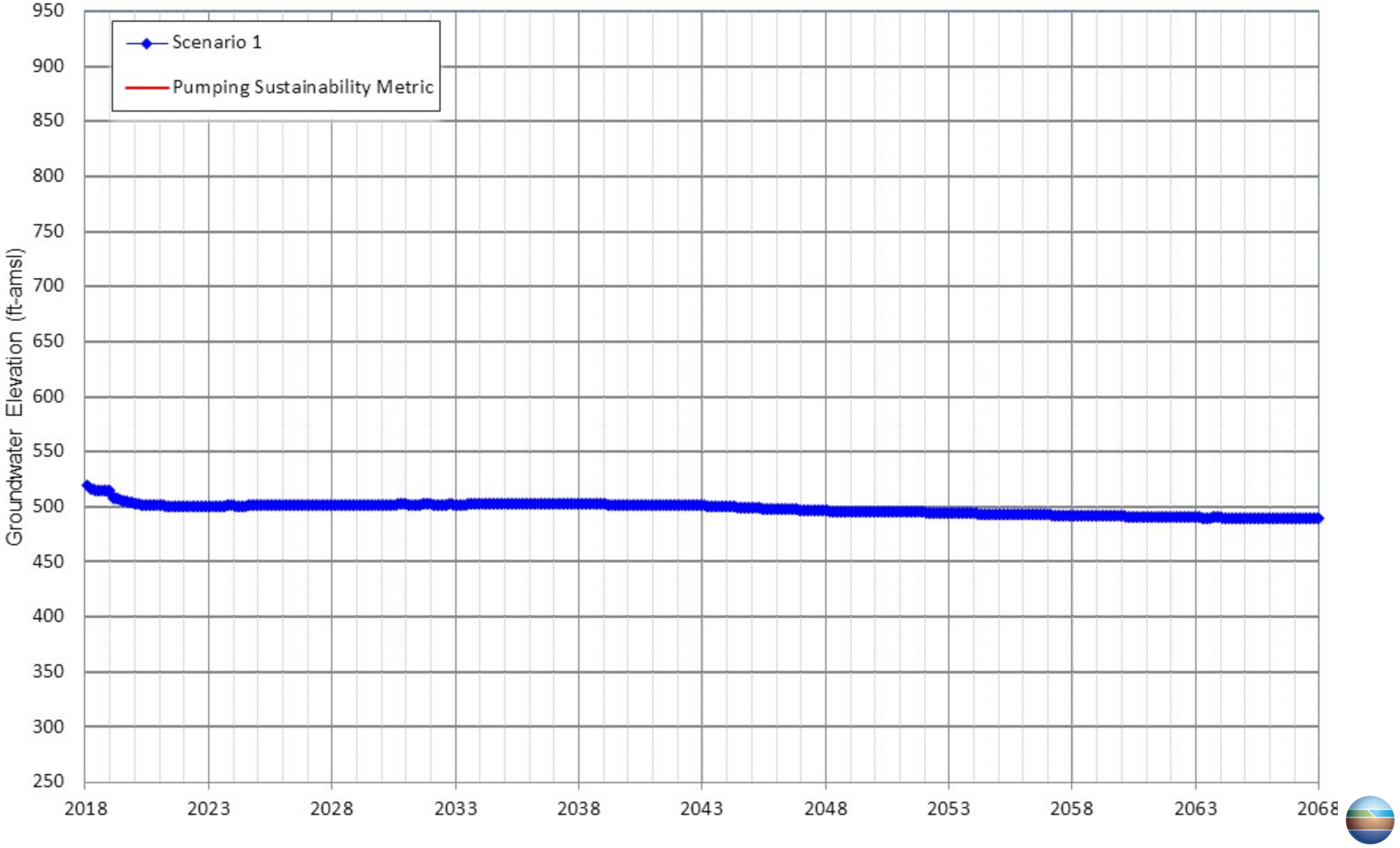

Appendix D-28
Projected Groundwater Elevation for Scenarios 1
City of Chino Hills Well 1A

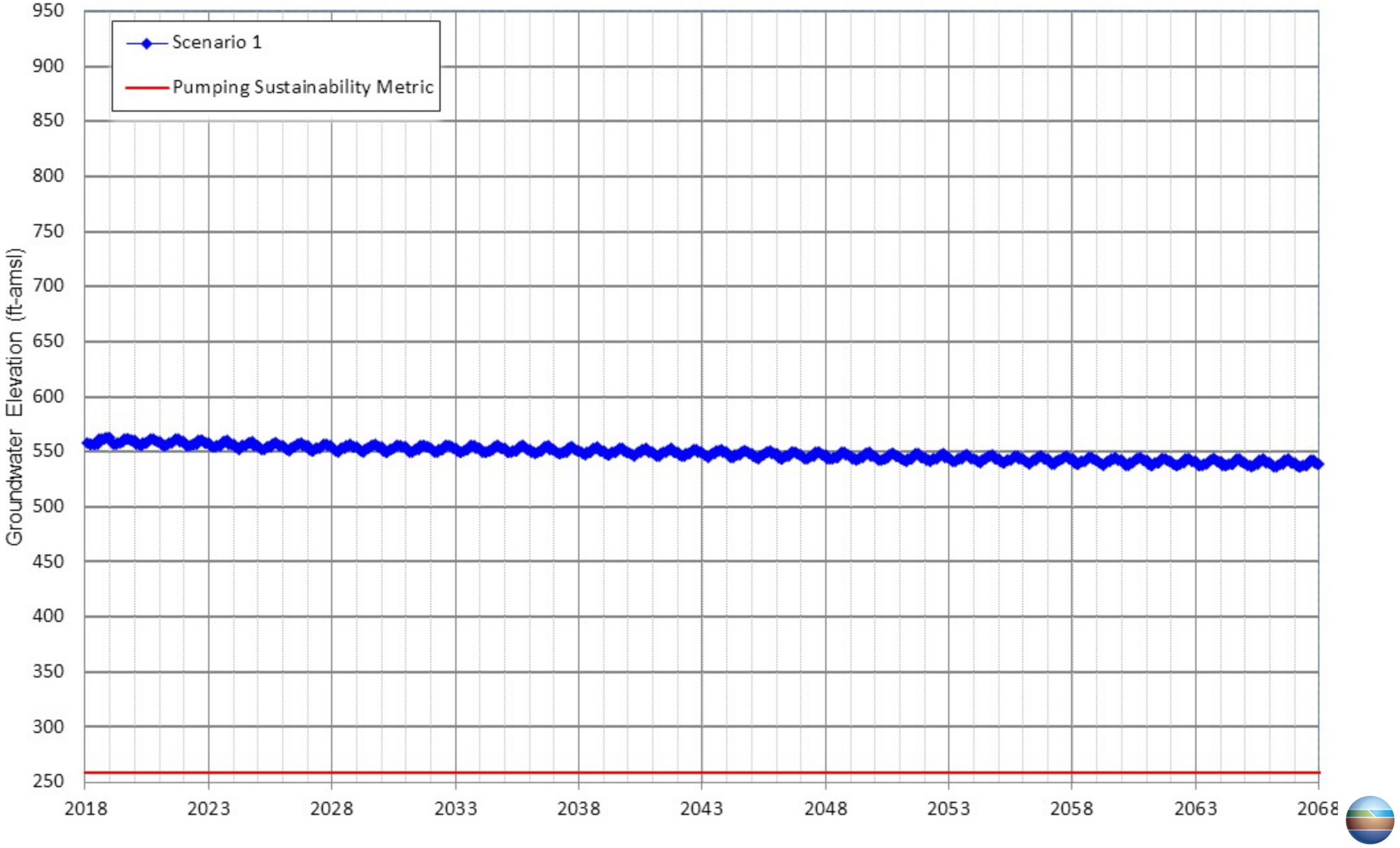

Appendix D-29
Projected Groundwater Elevation for Scenarios 1
City of Chino Hills Well 5

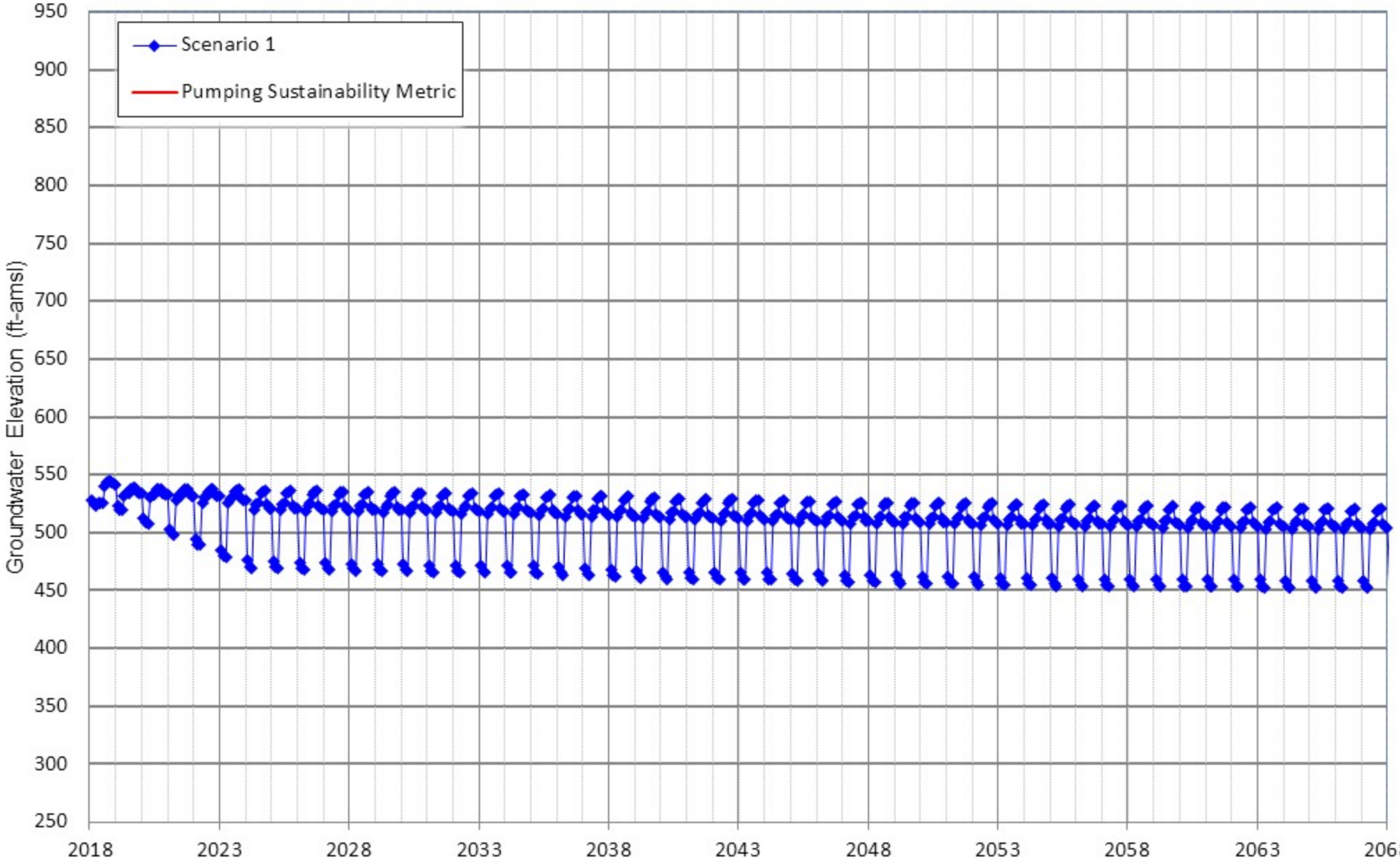

Appendix D-30
Projected Groundwater Elevation for Scenarios 1
City of Chino Hills Well 7A

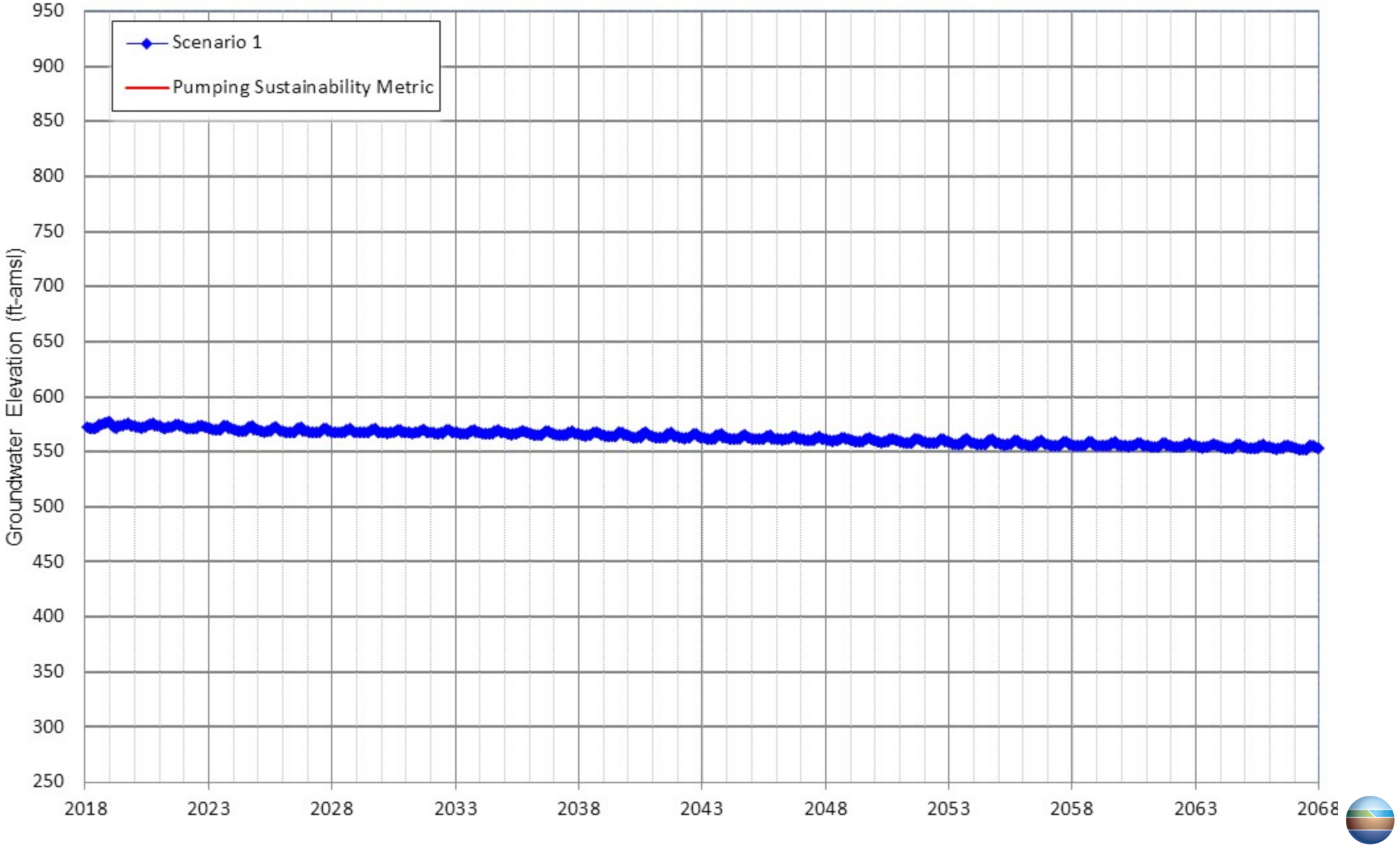

Appendix D-31
Projected Groundwater Elevation for Scenarios 1
City of Chino Hills Well 7B

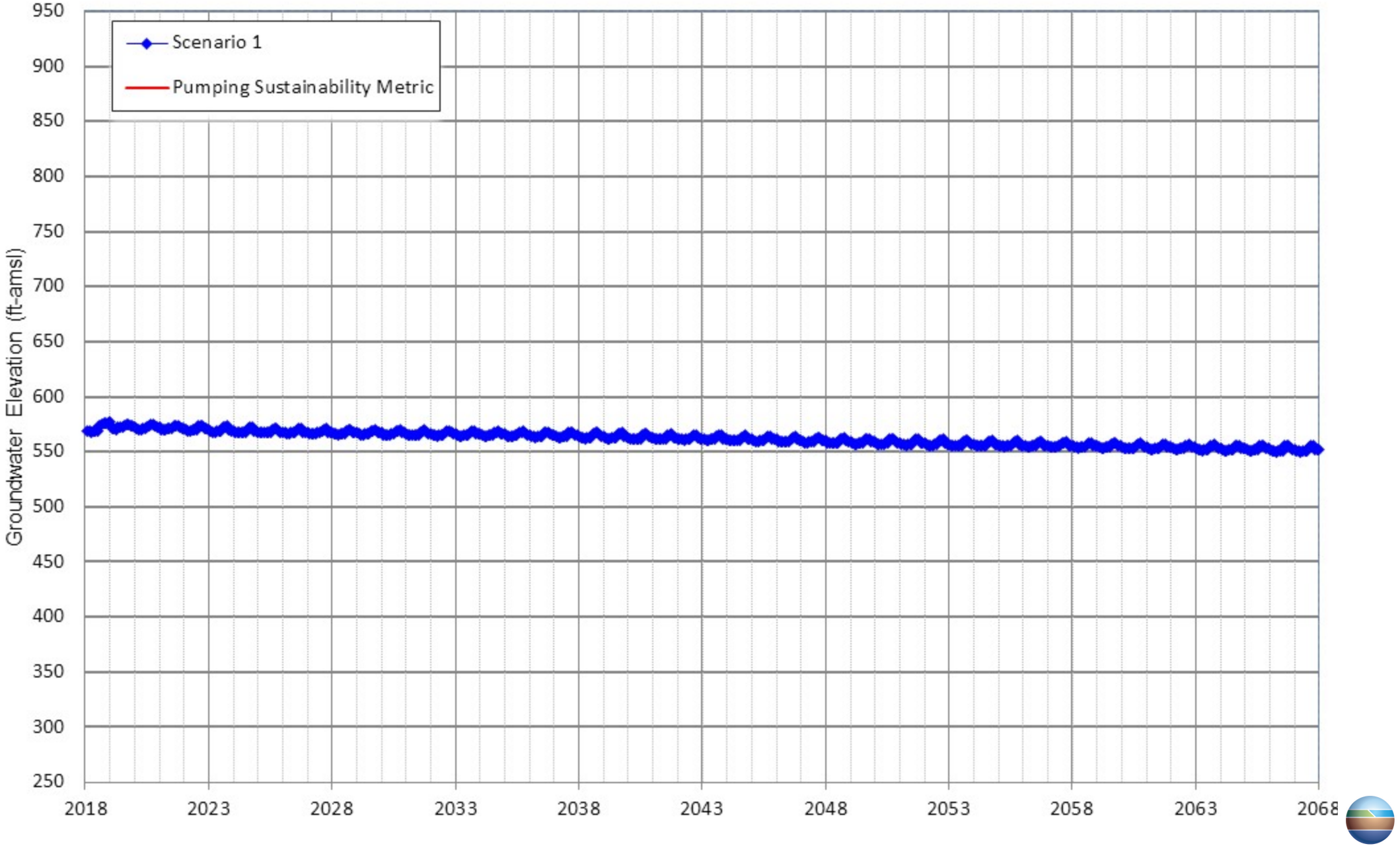

Appendix D-32
Projected Groundwater Elevation for Scenarios 1
City of Chino Hills Well 15B

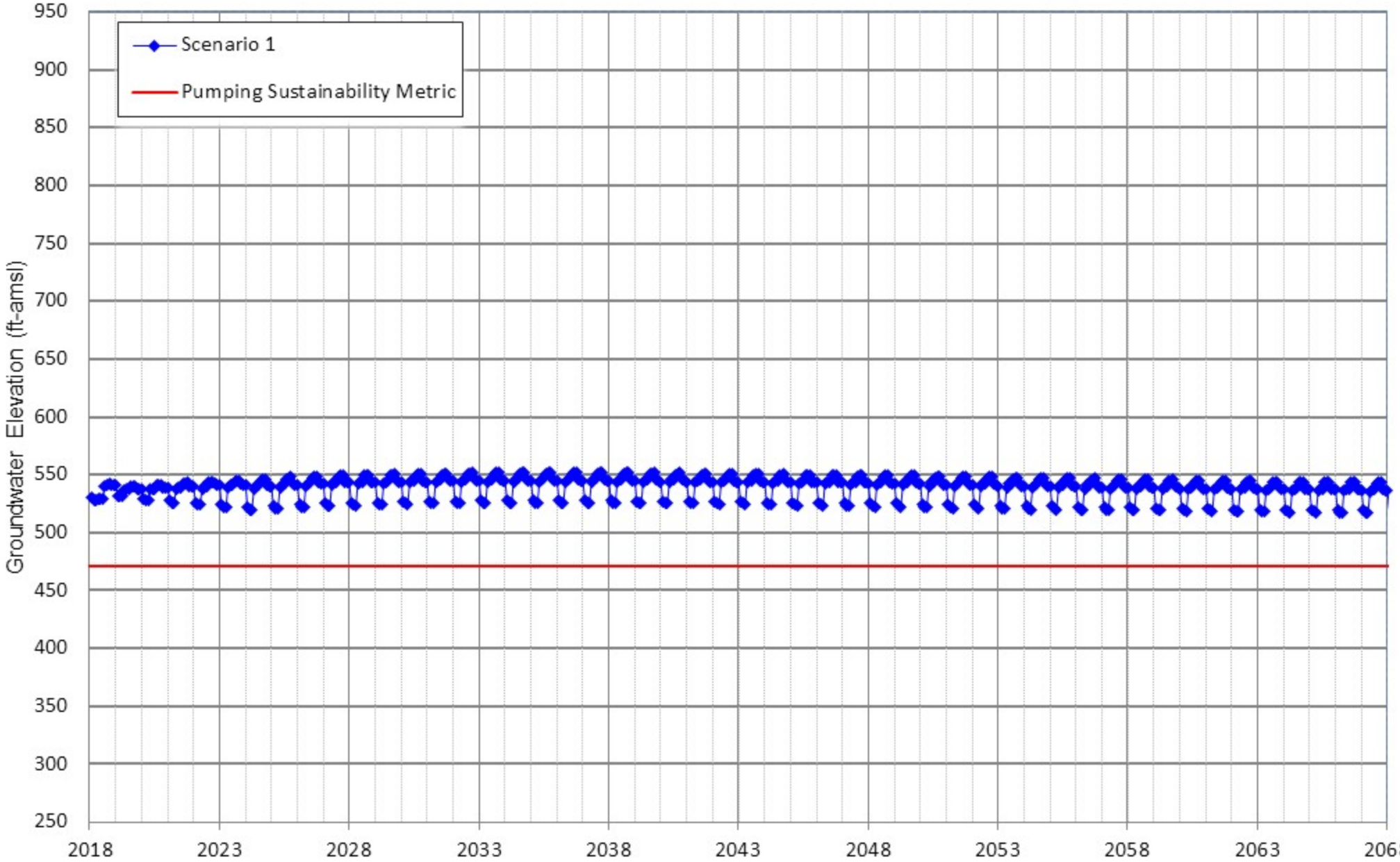

Appendix D-33
Projected Groundwater Elevation for Scenarios 1
City of Chino Hills Well 17

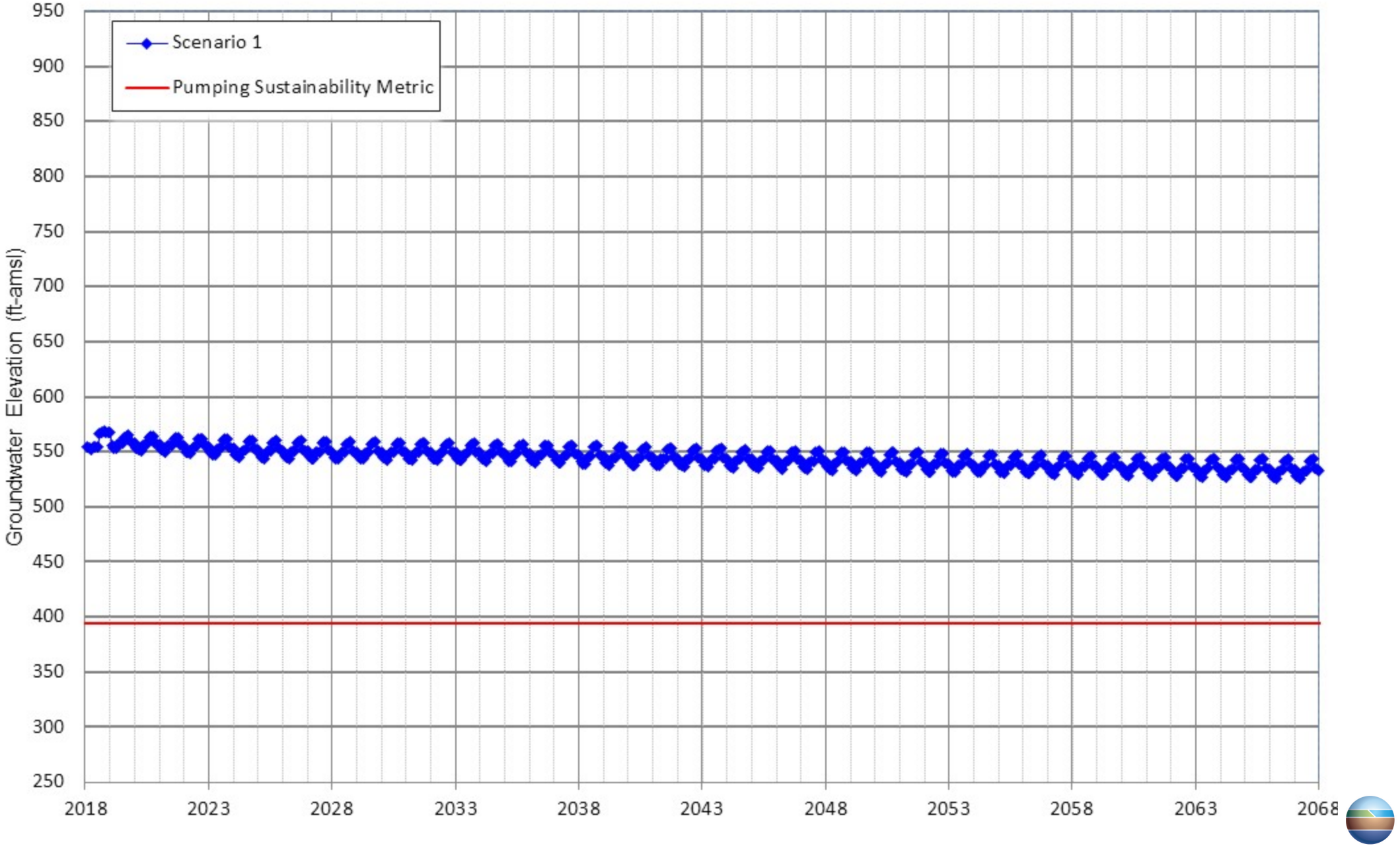

Appendix D-34
Projected Groundwater Elevation for Scenarios 1
City of Chino Well 4

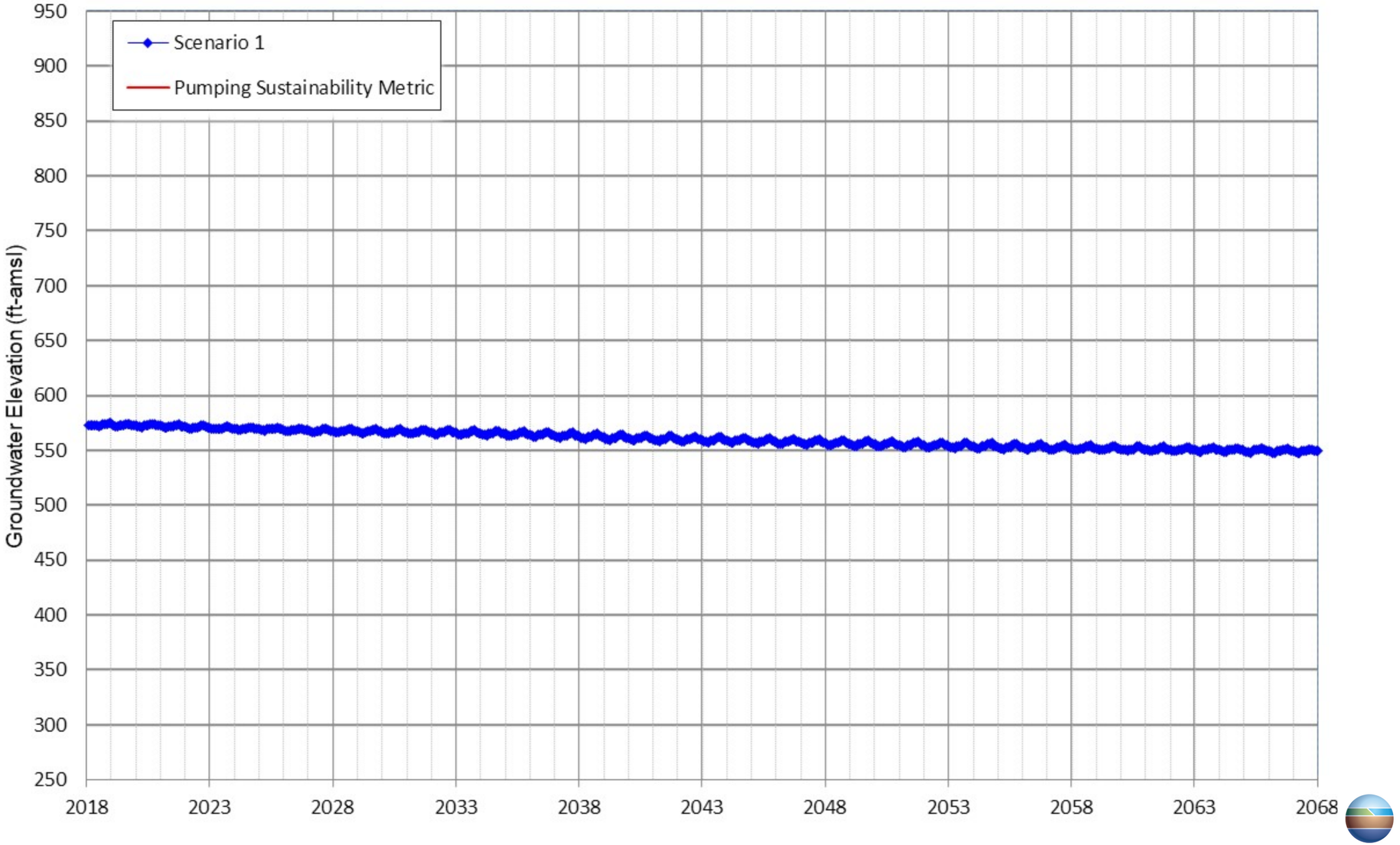

Appendix D-35
Projected Groundwater Elevation for Scenarios 1
City of Chino Well 5

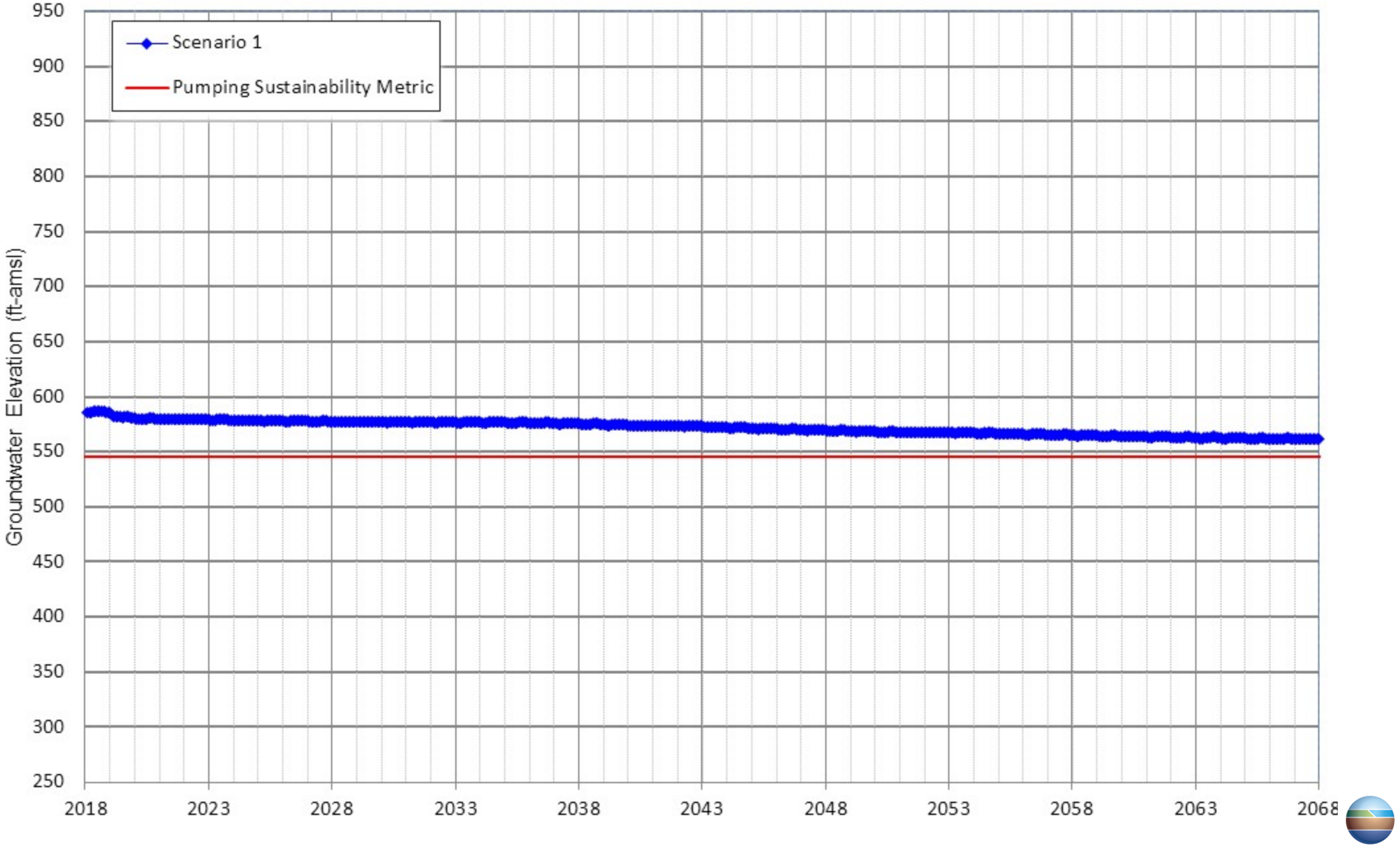

Appendix D-36
Projected Groundwater Elevation for Scenarios 1
City of Chino Well 6

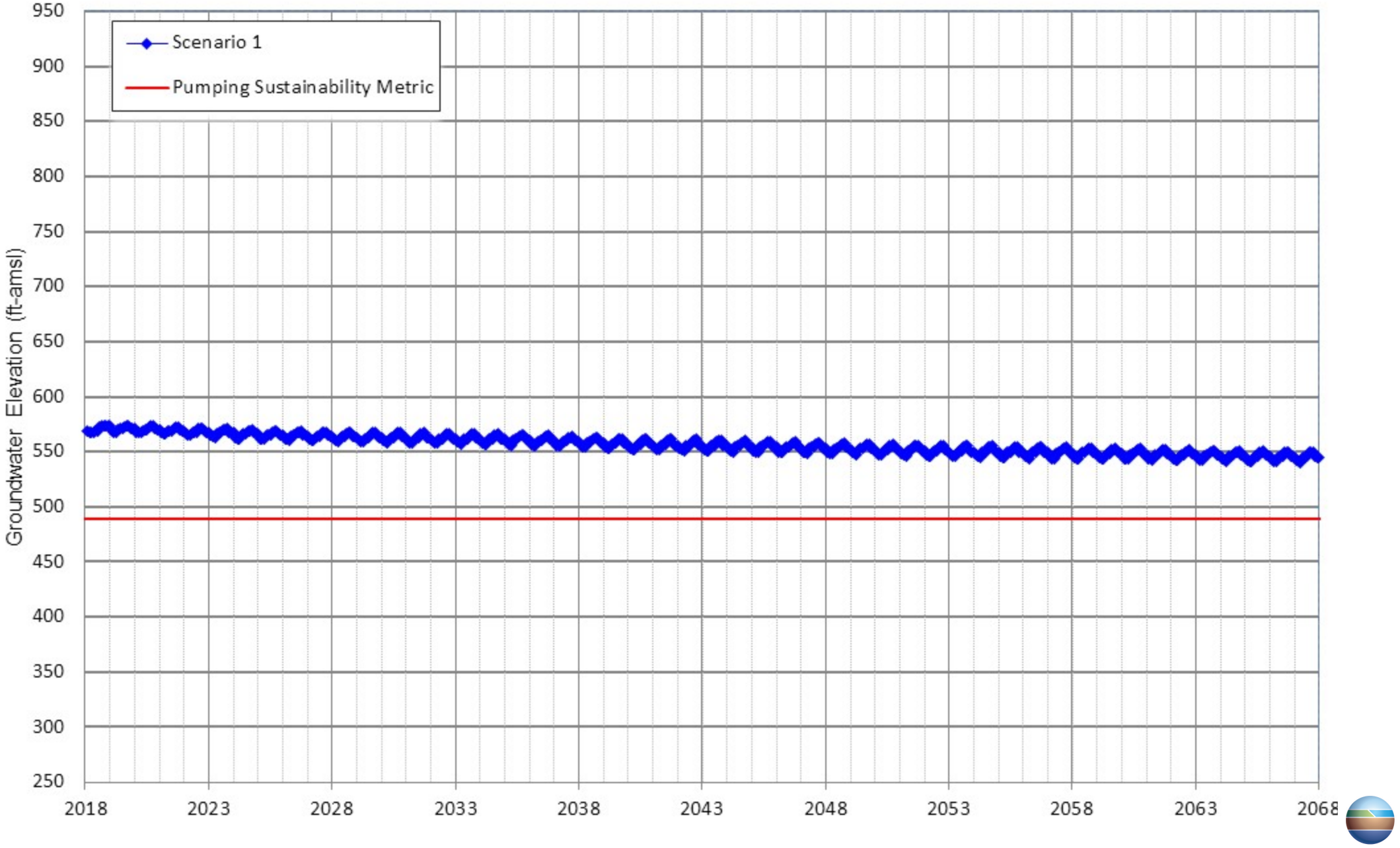

Appendix D-37
Projected Groundwater Elevation for Scenarios 1
City of Chino Well 9

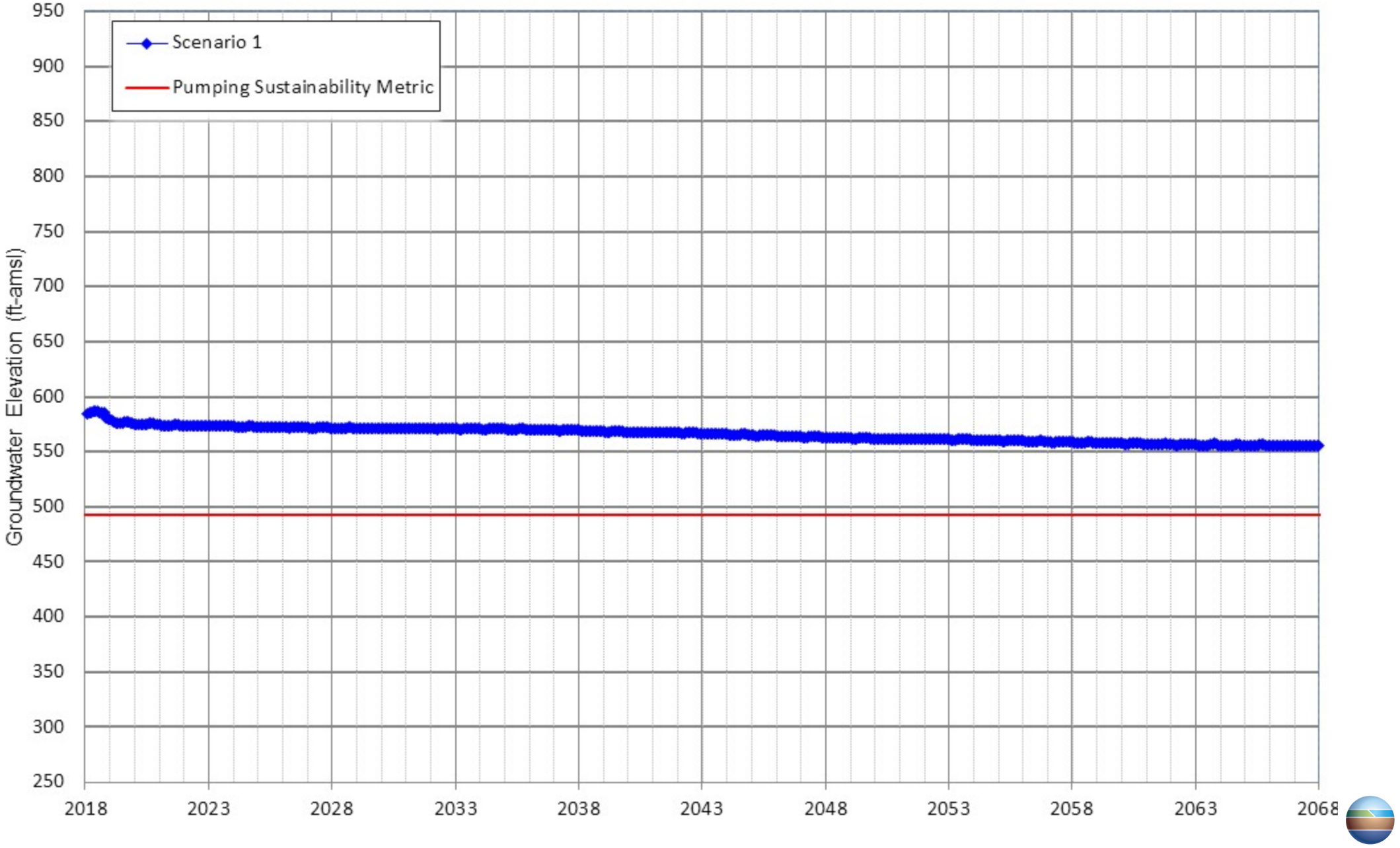

Appendix D-38
Projected Groundwater Elevation for Scenarios 1
City of Chino Well 10

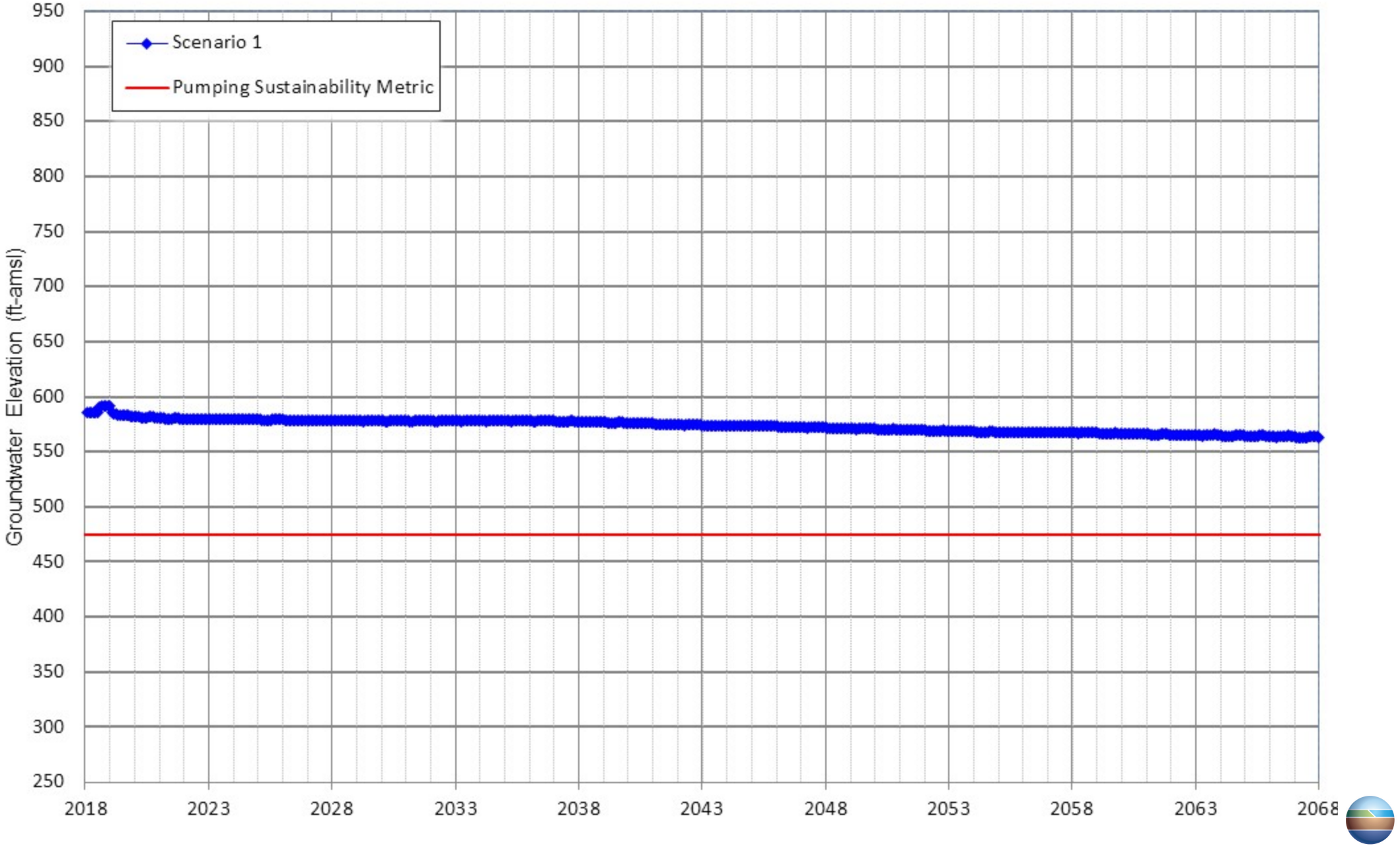

Appendix D-39
Projected Groundwater Elevation for Scenarios 1
City of Chino Well 11

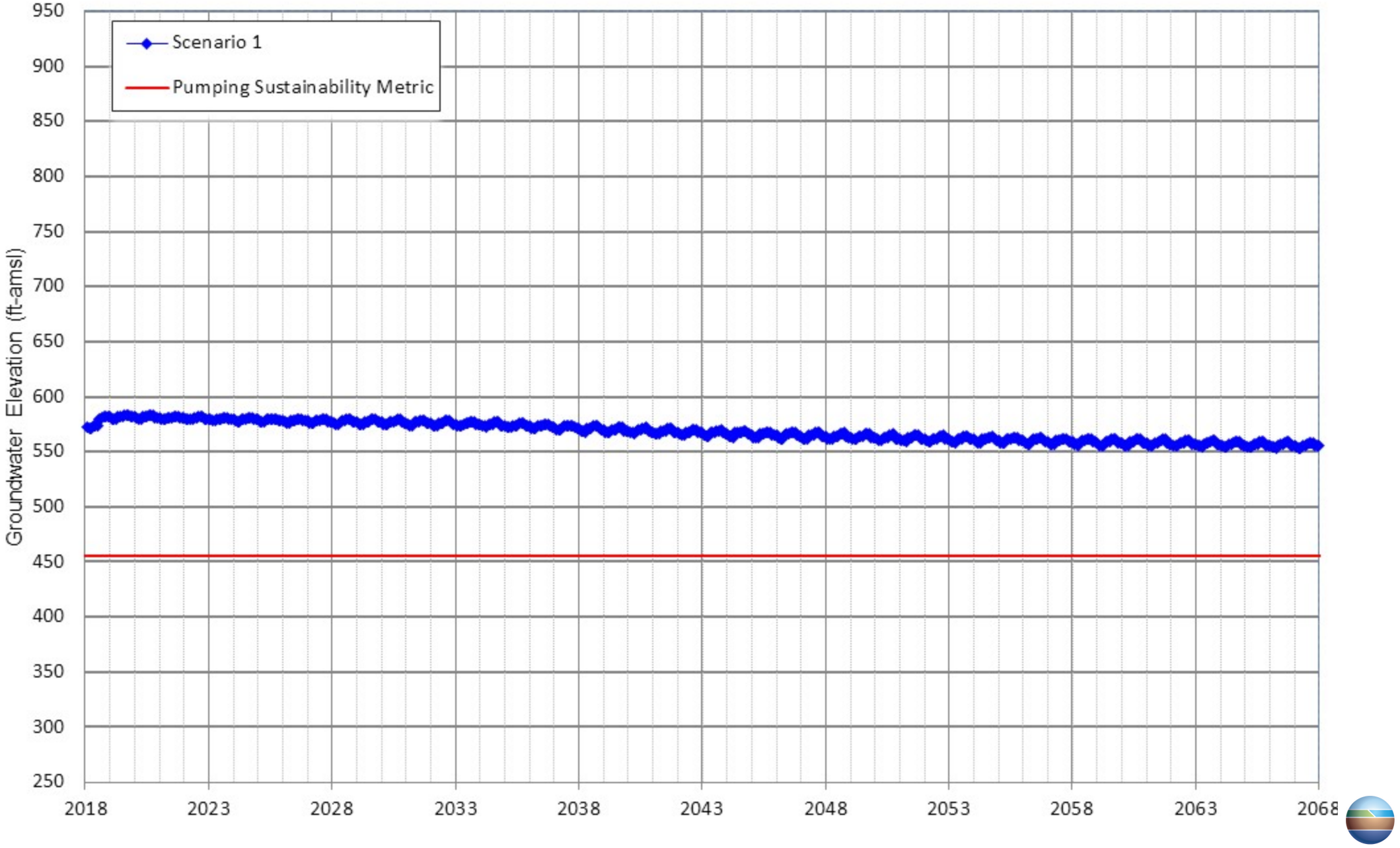

Appendix D-40
Projected Groundwater Elevation for Scenarios 1
City of Chino Well 12

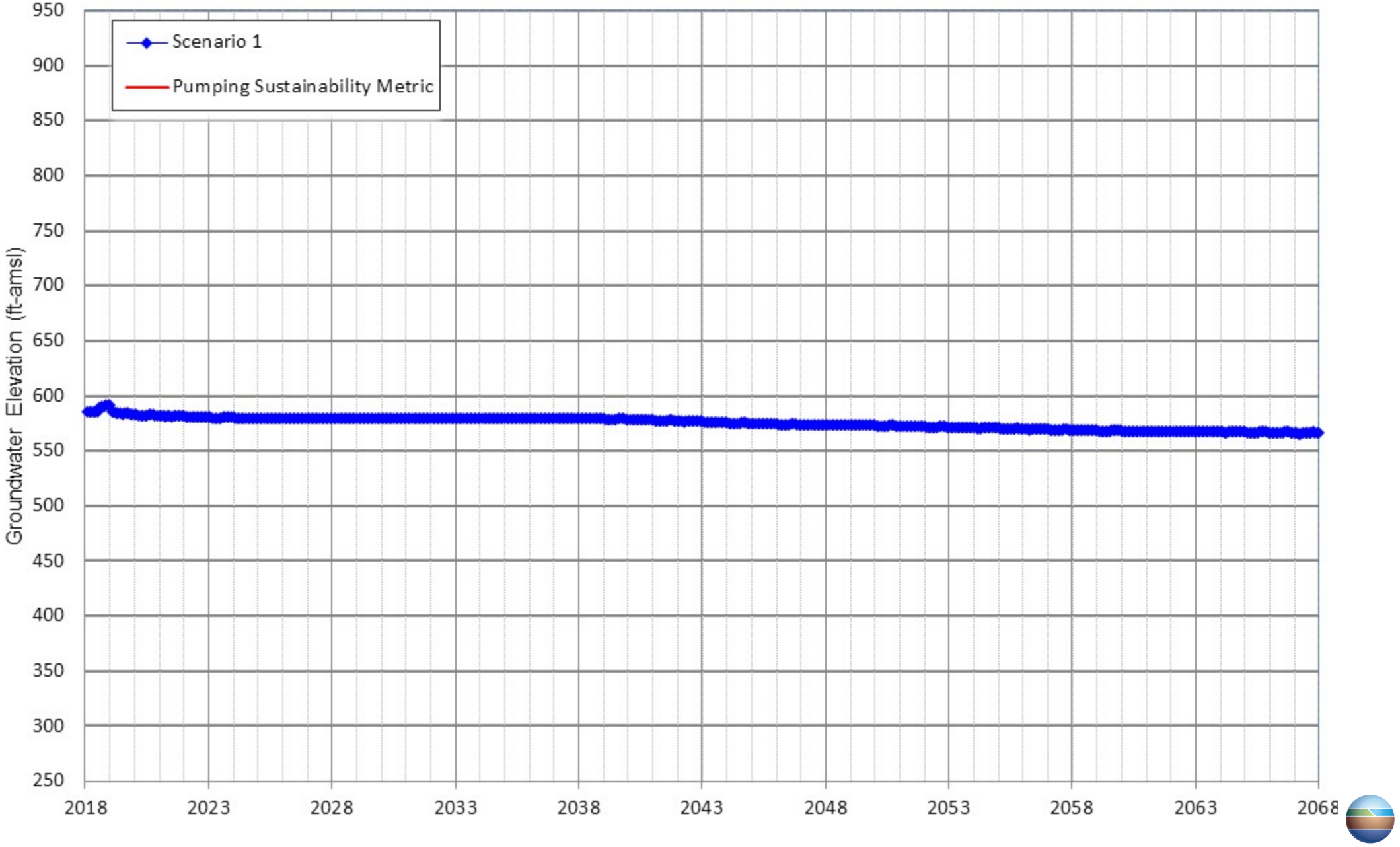

Appendix D-41
Projected Groundwater Elevation for Scenarios 1
City of Chino Well 13

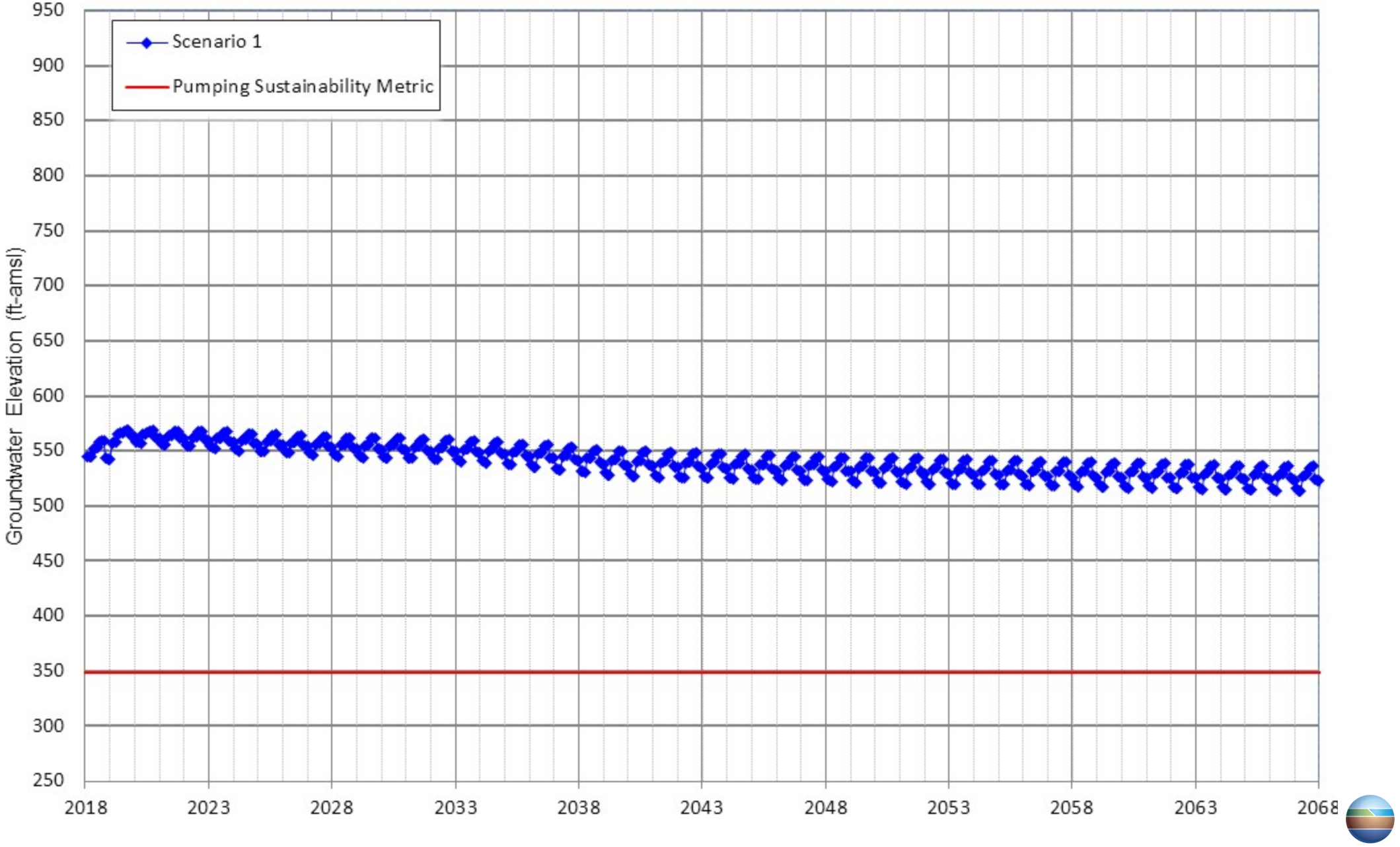

Appendix D-42
Projected Groundwater Elevation for Scenarios 1
City of Chino Well 14

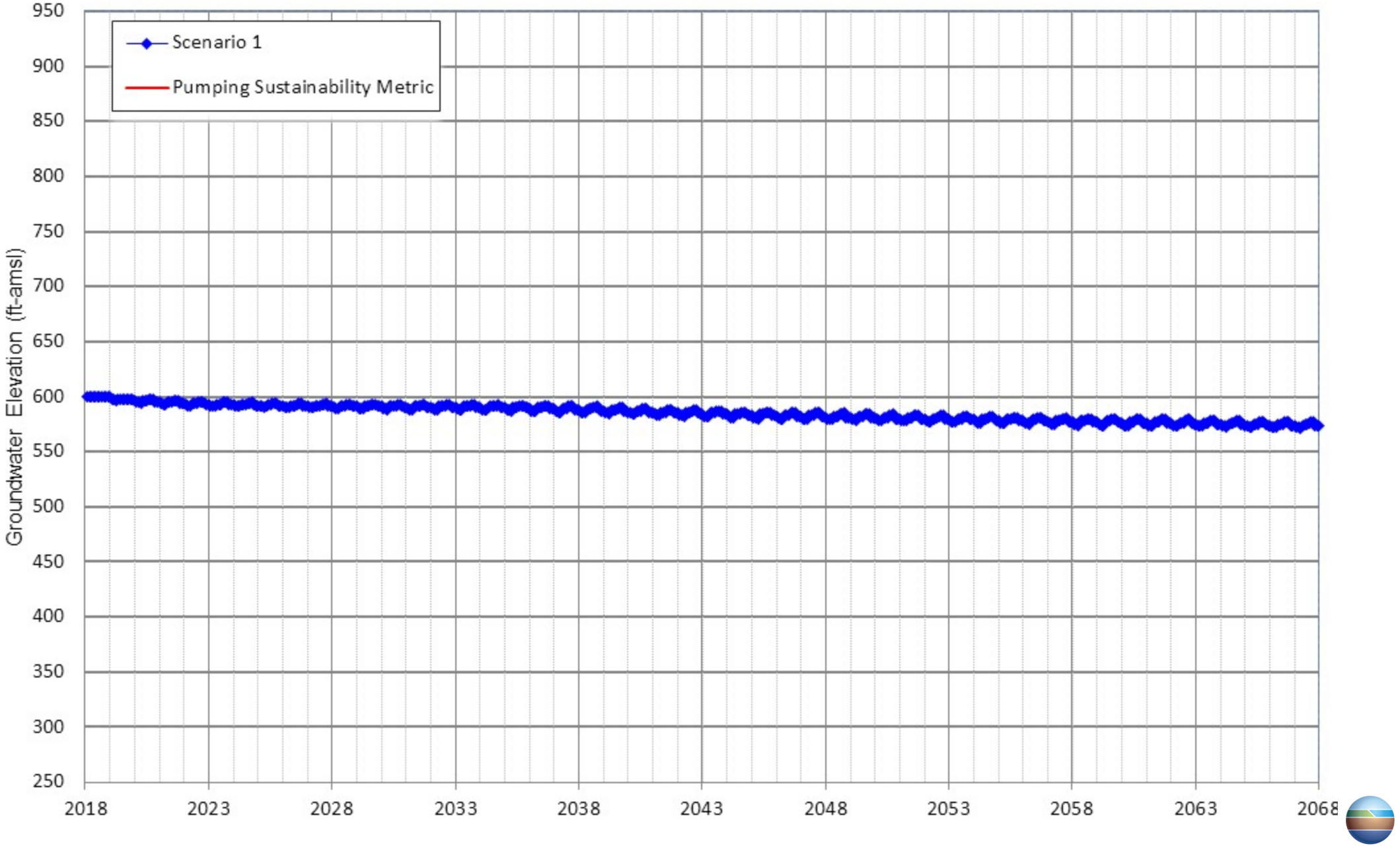

Appendix D-43
Projected Groundwater Elevation for Scenarios 1
City of Chino Well 16

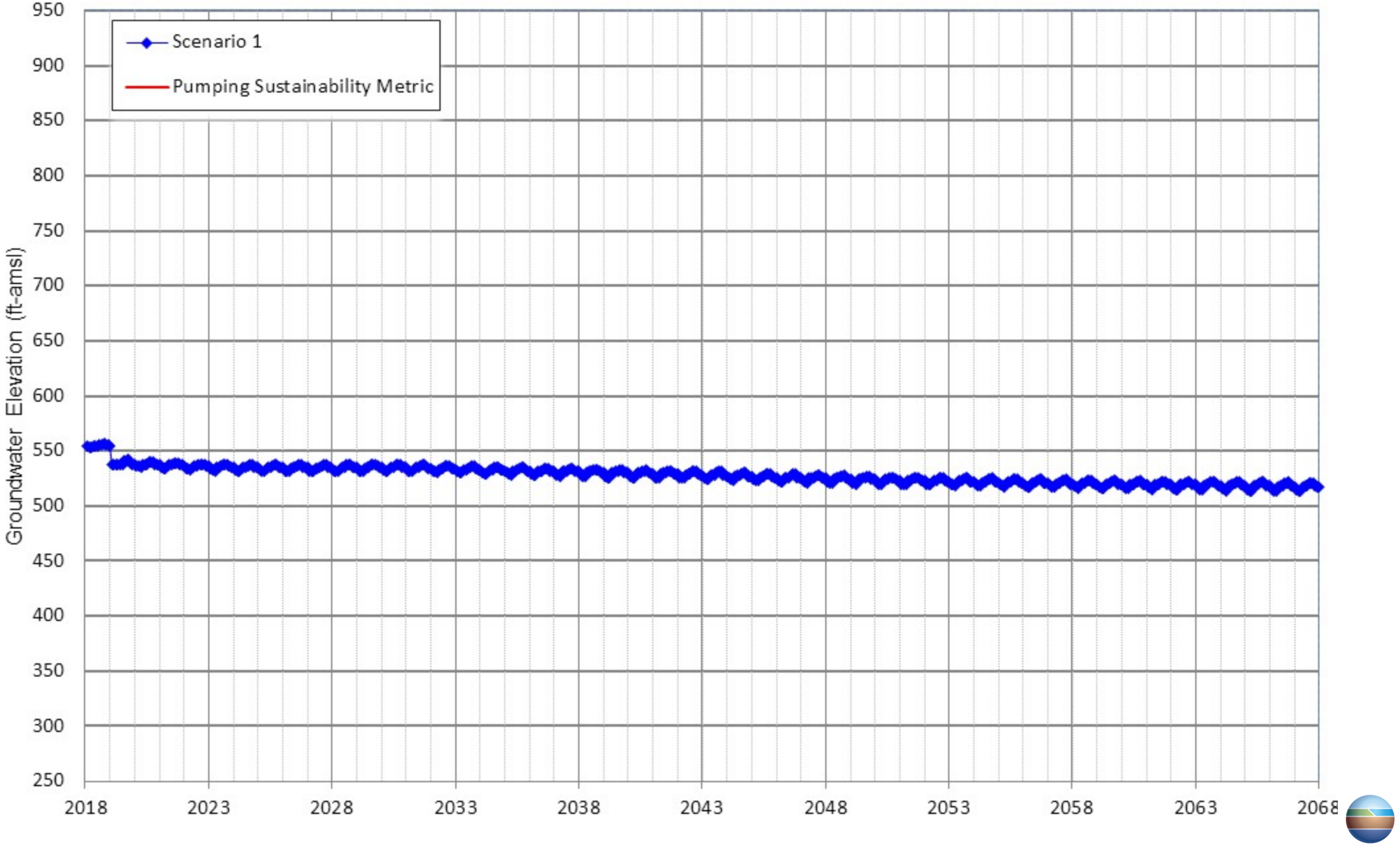

Appendix D-44
Projected Groundwater Elevation for Scenarios 1
City of Chino Well 19

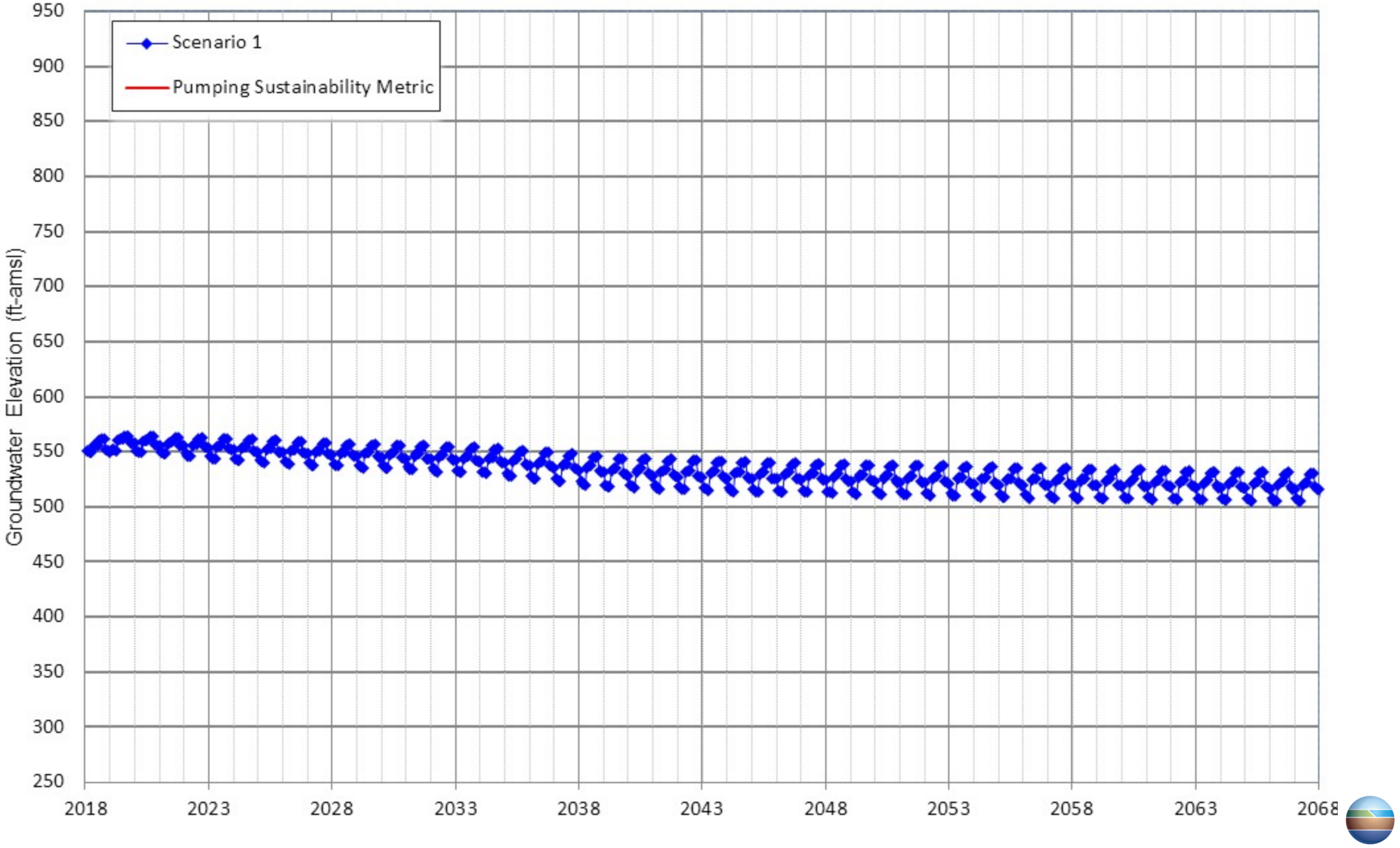

Appendix D-45
Projected Groundwater Elevation for Scenarios 1
City of Chino Well 18

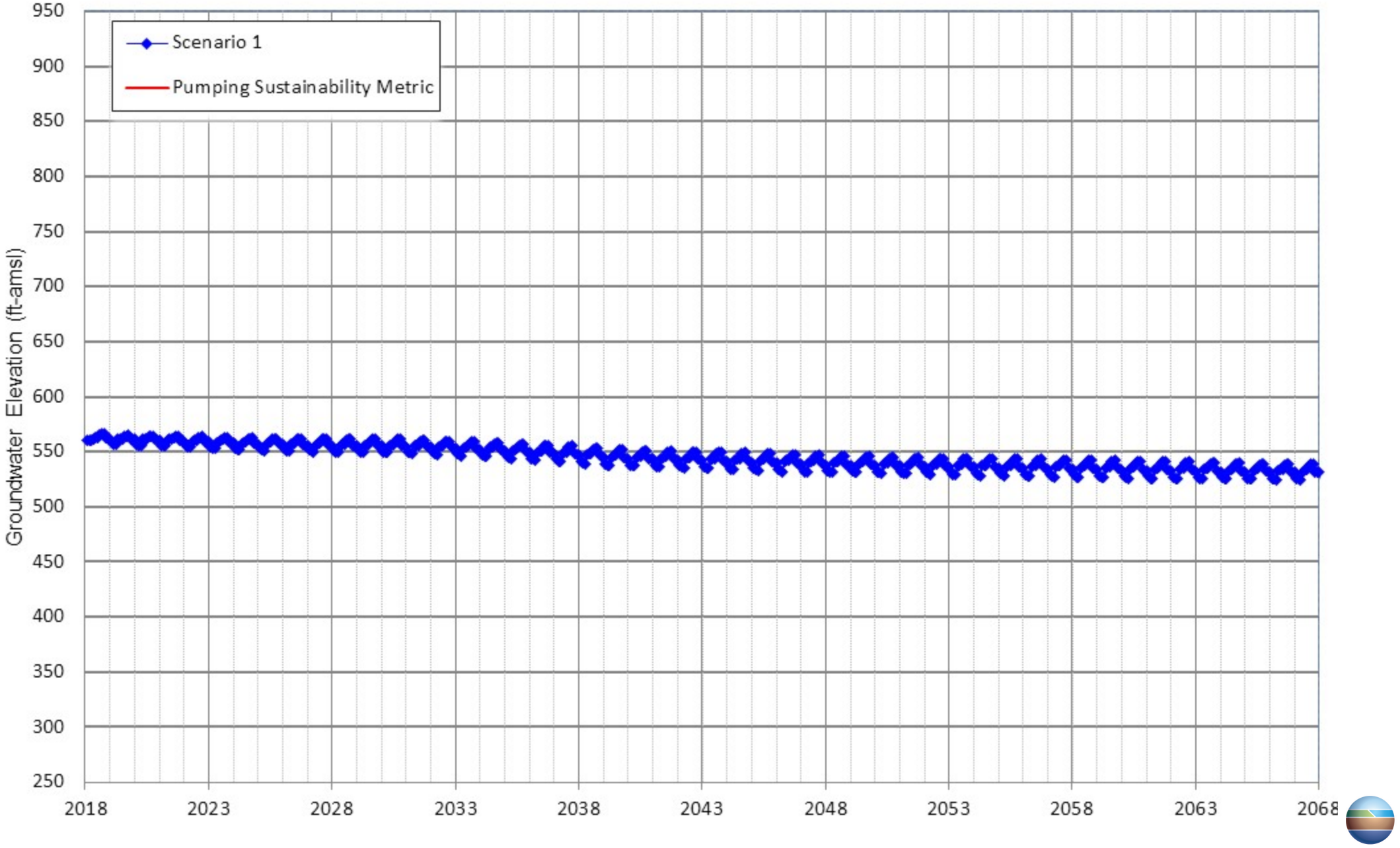

Appendix D-46
Projected Groundwater Elevation for Scenarios 1
CVWD Well CB-1

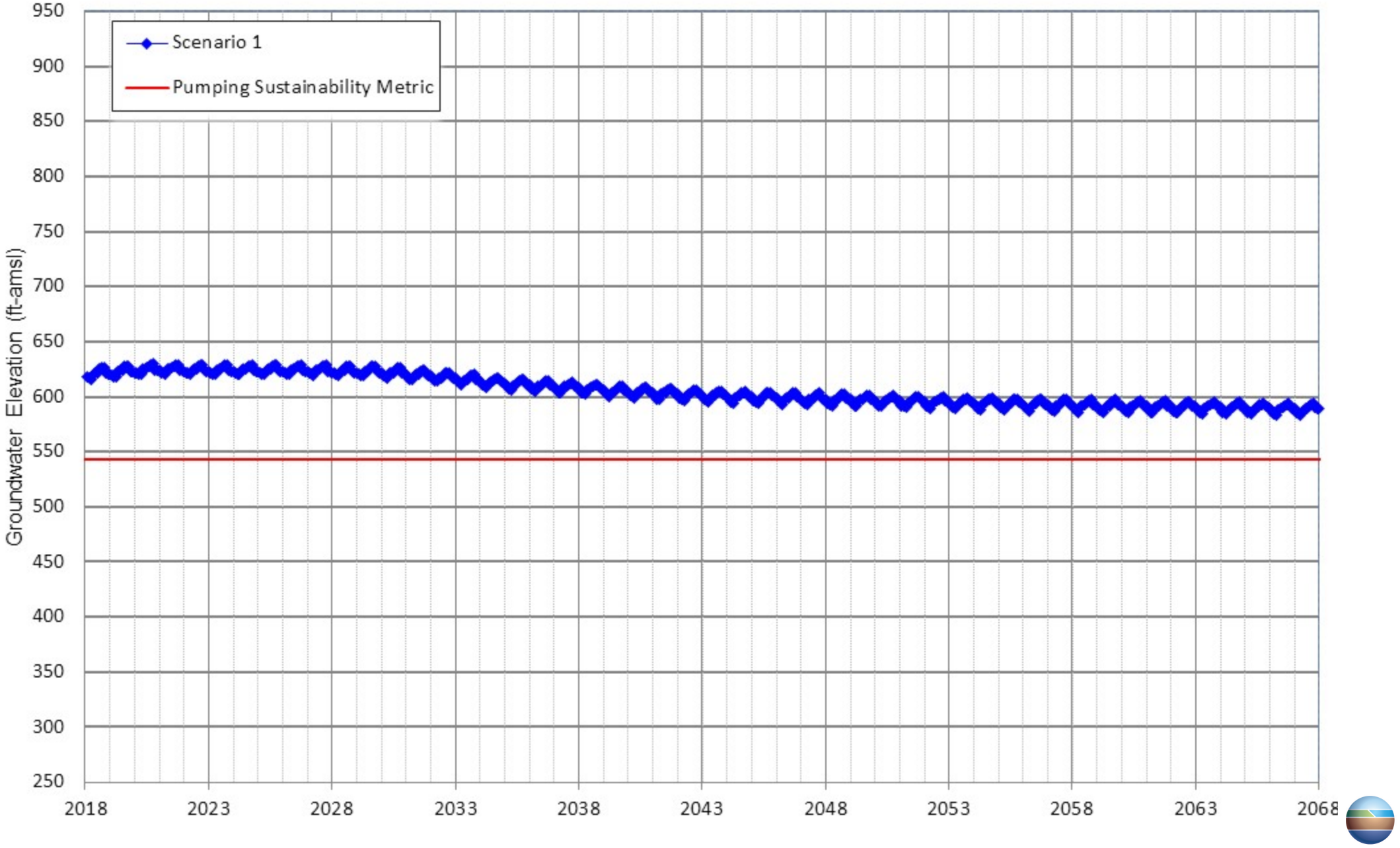

Appendix D-47
Projected Groundwater Elevation for Scenarios 1
CVWD Well CB-3

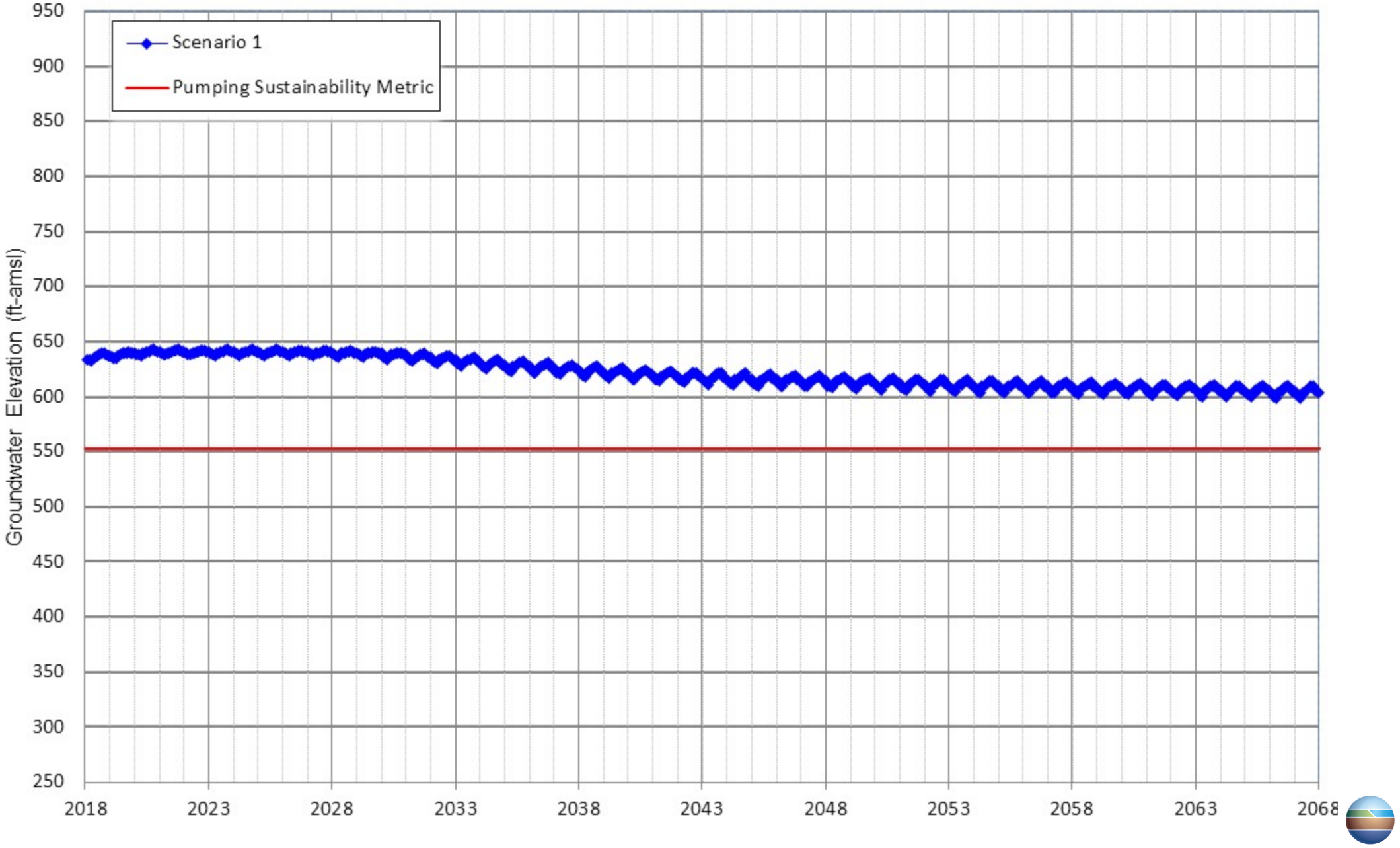

Appendix D-48
Projected Groundwater Elevation for Scenarios 1
CVWD Well CB-4

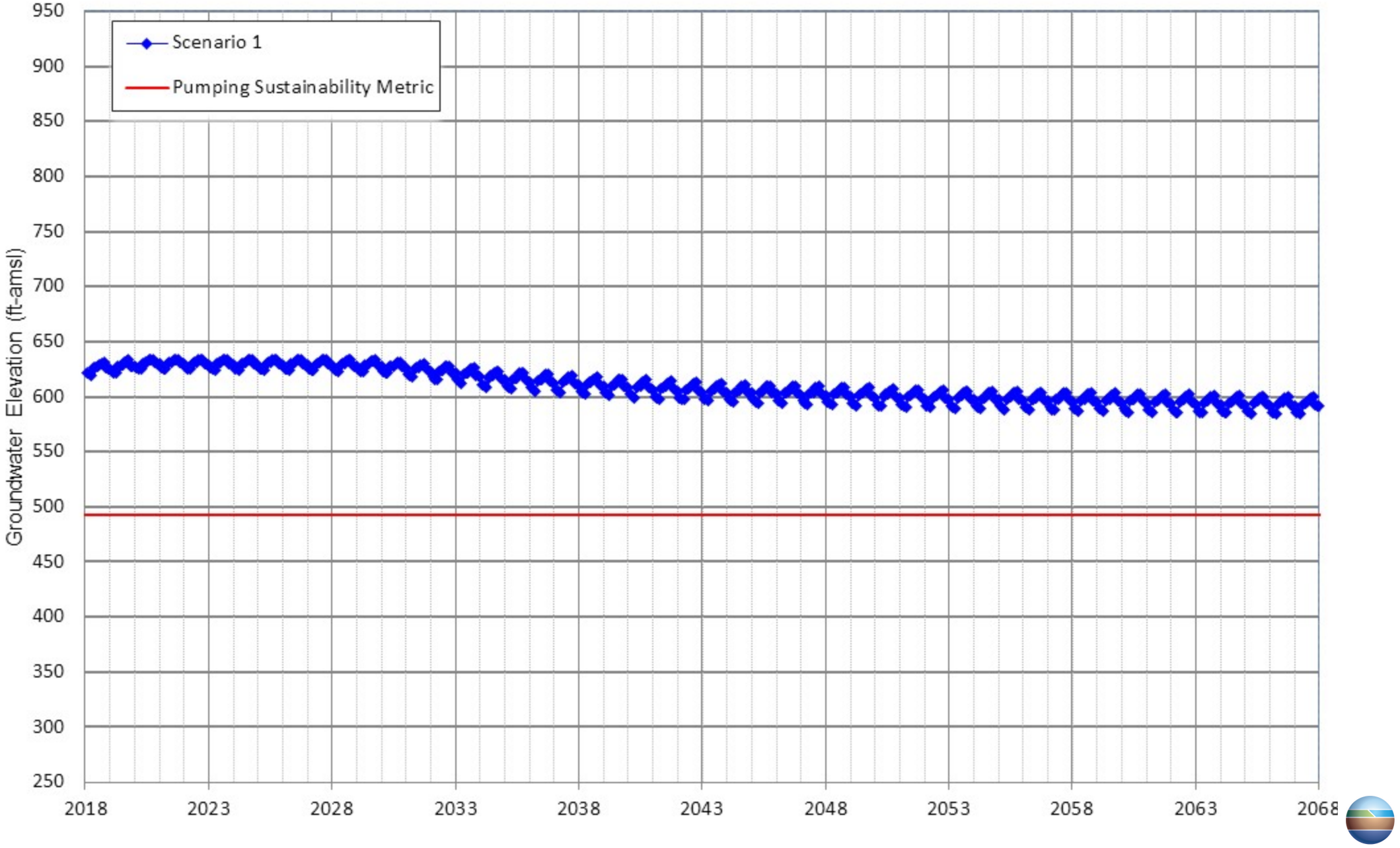

Appendix D-49
Projected Groundwater Elevation for Scenarios 1
CVWD Well CB-5

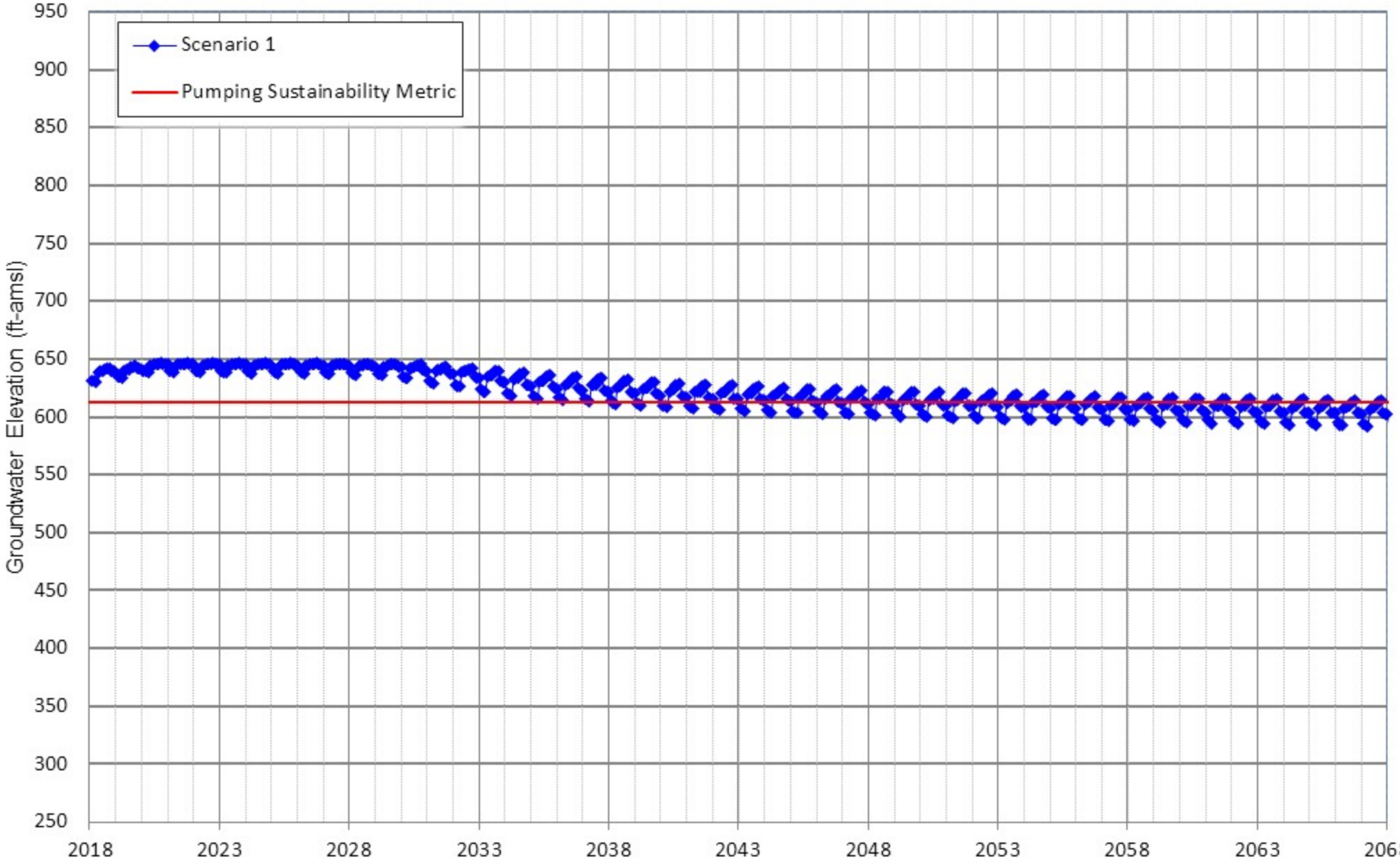

Appendix D-50
Projected Groundwater Elevation for Scenarios 1
CVWD Well CB-30

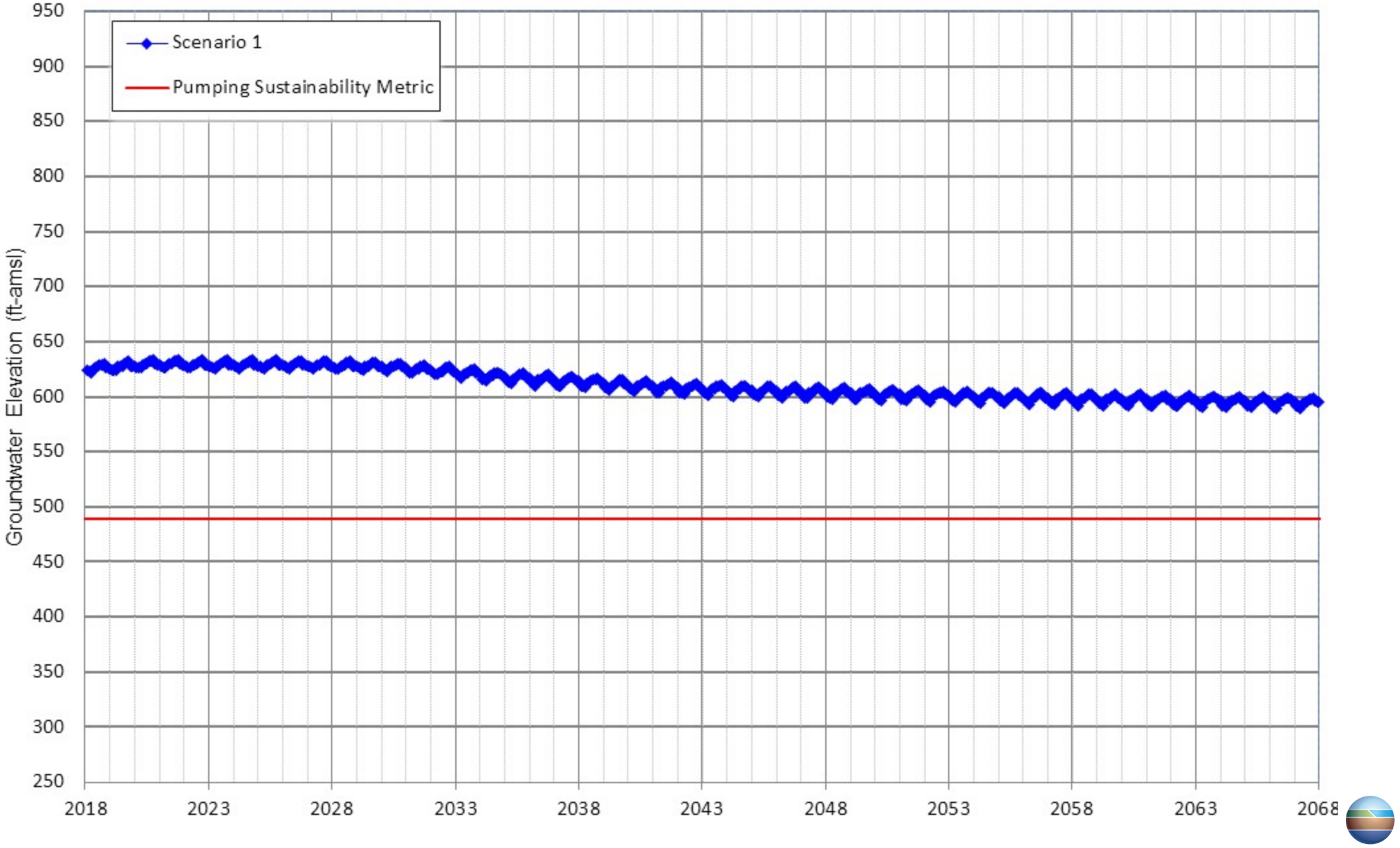

Appendix D-51
Projected Groundwater Elevation for Scenarios 1
CVWD Well CB-38

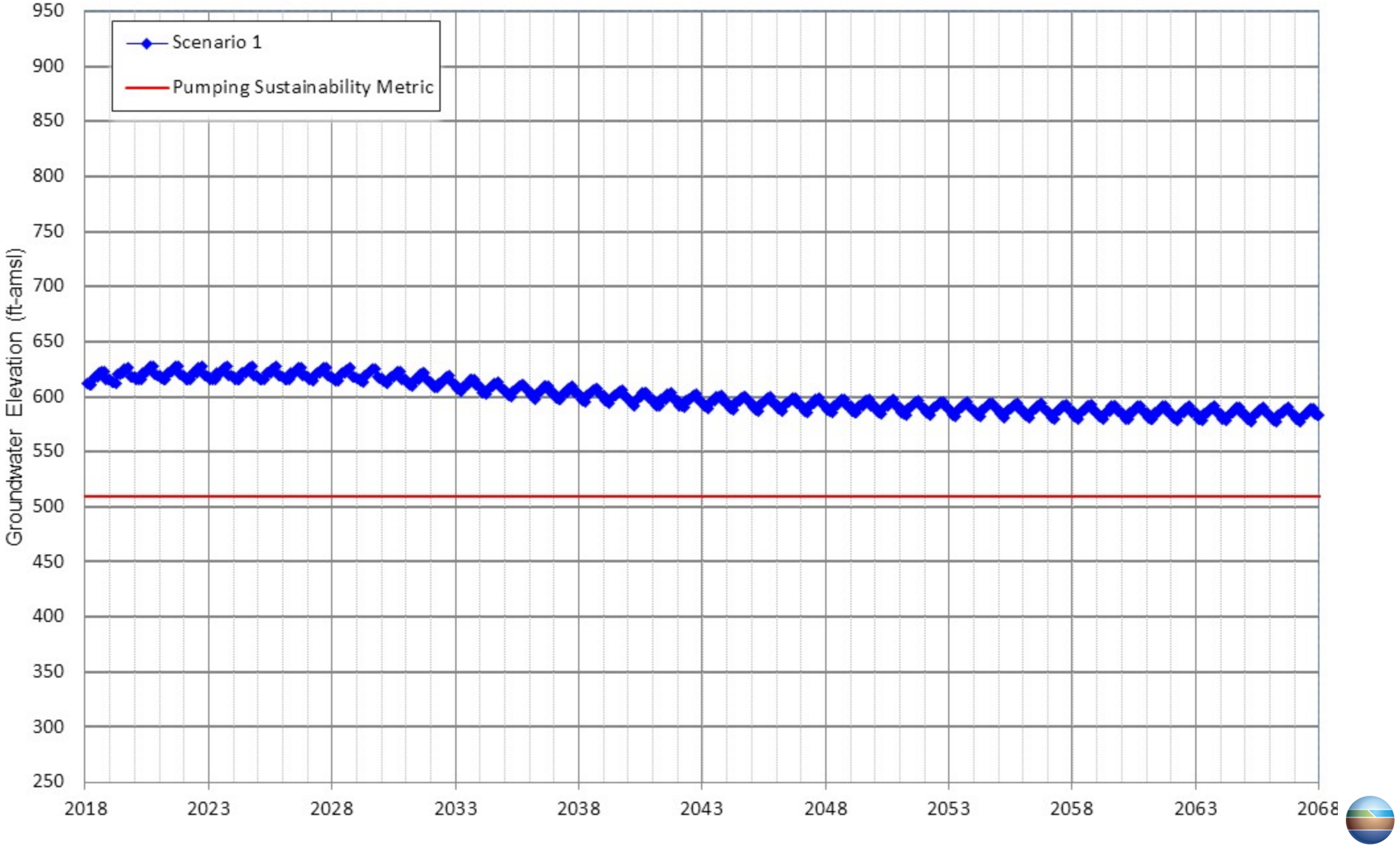

Appendix D-52
Projected Groundwater Elevation for Scenarios 1
CVWD Well CB-39

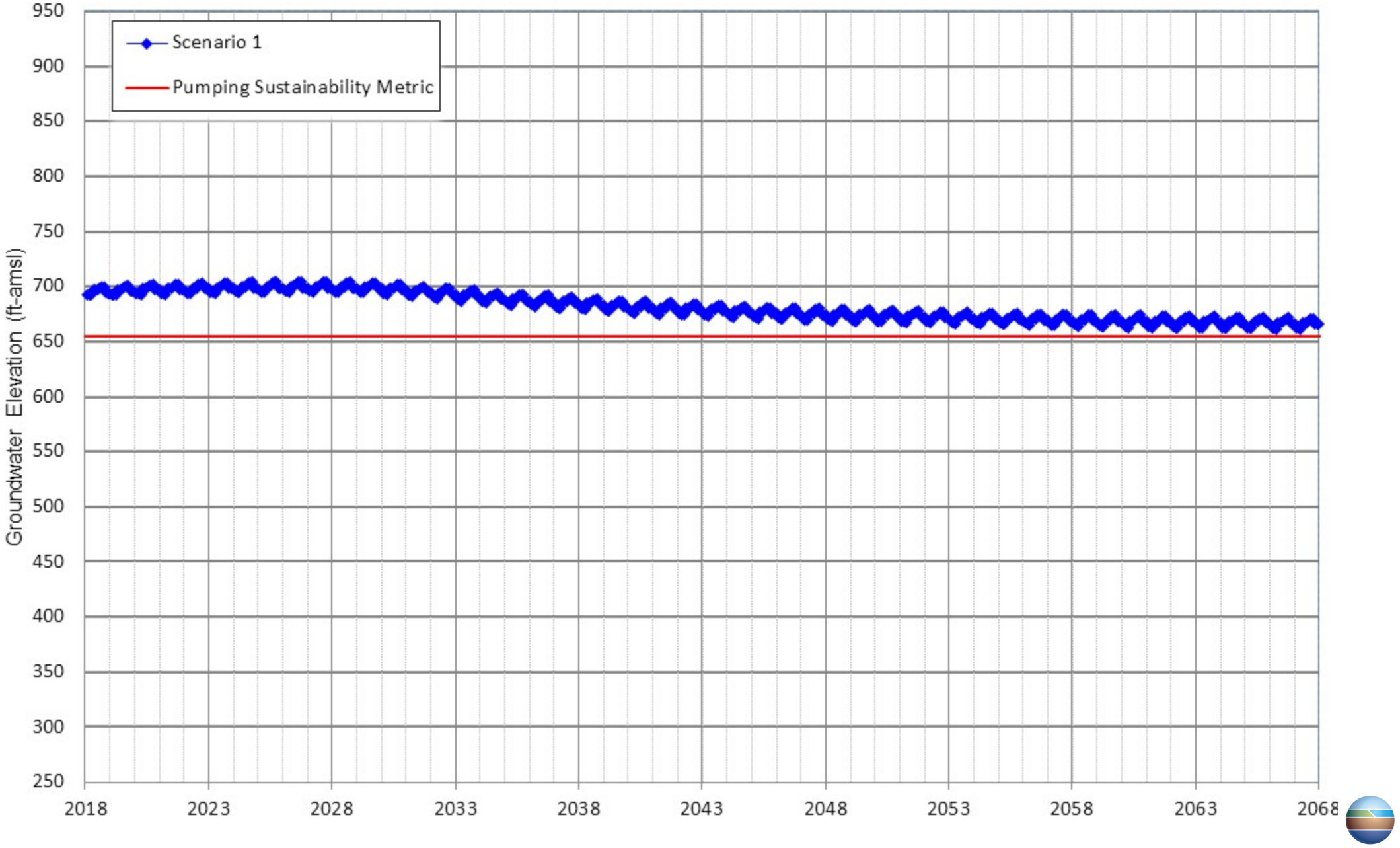

Appendix D-53
Projected Groundwater Elevation for Scenarios 1
CVWD Well CB-40

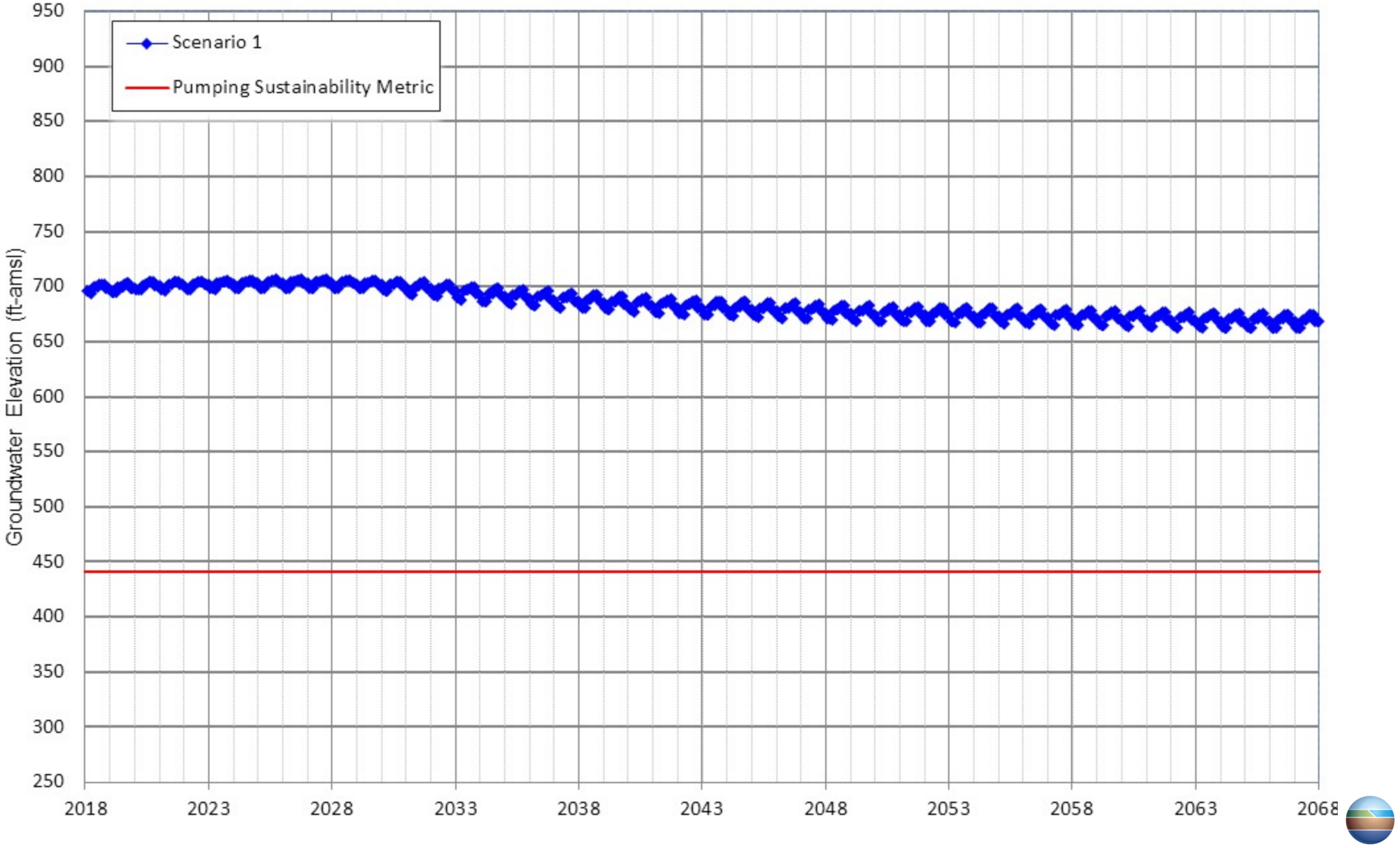

Appendix D-54
Projected Groundwater Elevation for Scenarios 1
CVWD Well CB-41

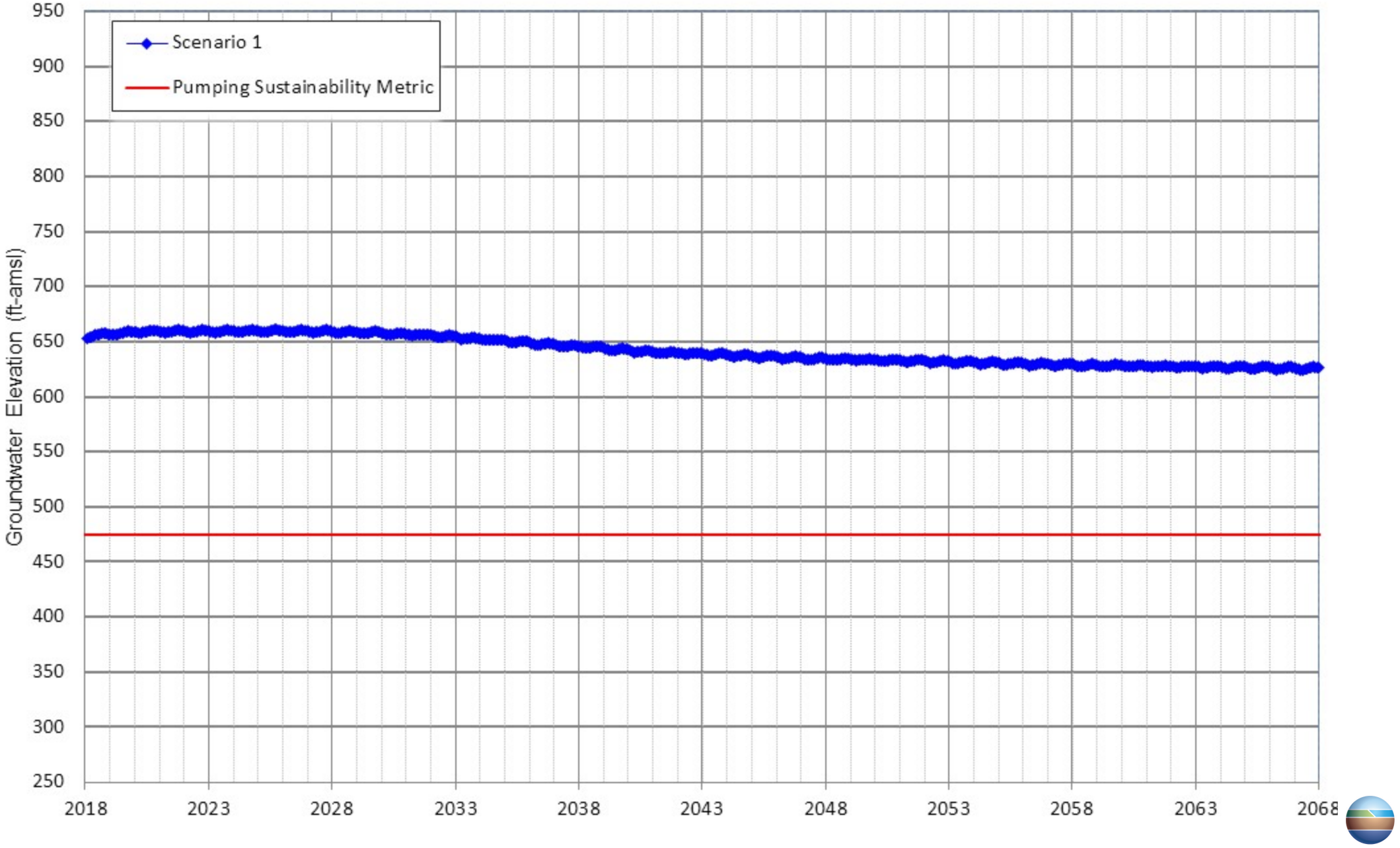

Appendix D-55
Projected Groundwater Elevation for Scenarios 1
CVWD Well CB-42

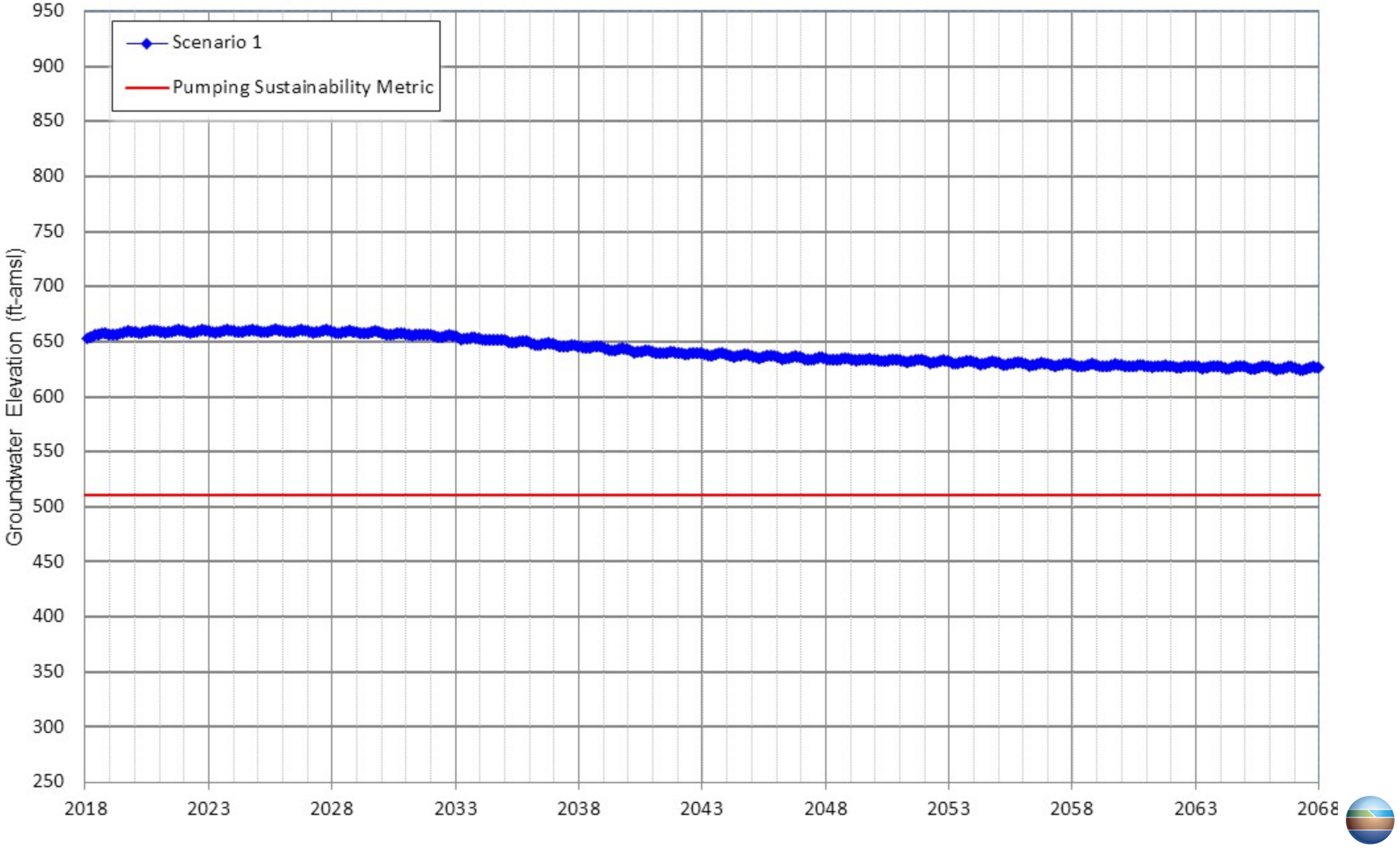

Appendix D-56
Projected Groundwater Elevation for Scenarios 1
CVWD Well CB-43

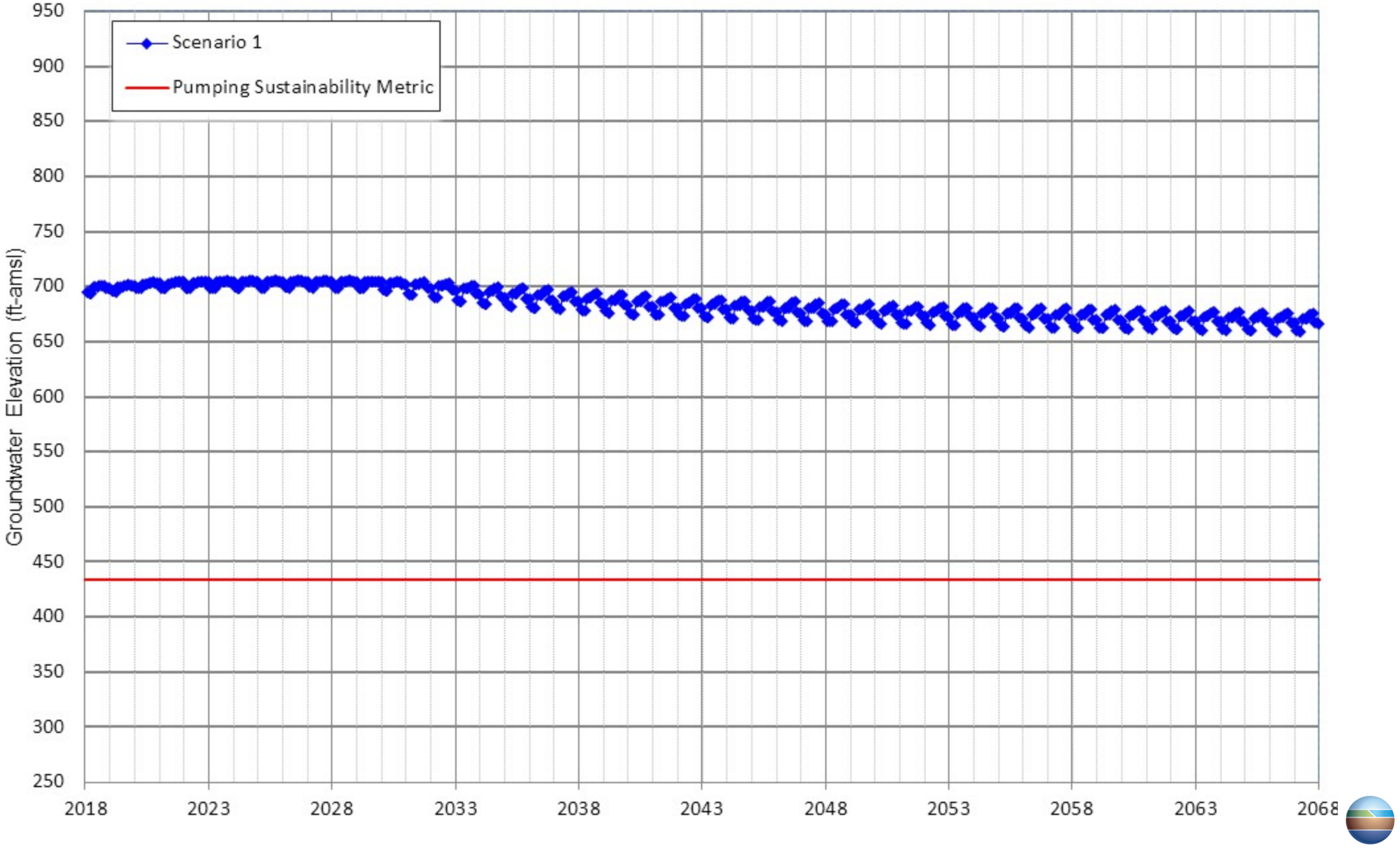

Appendix D-57
Projected Groundwater Elevation for Scenarios 1
CVWD Well CB-46

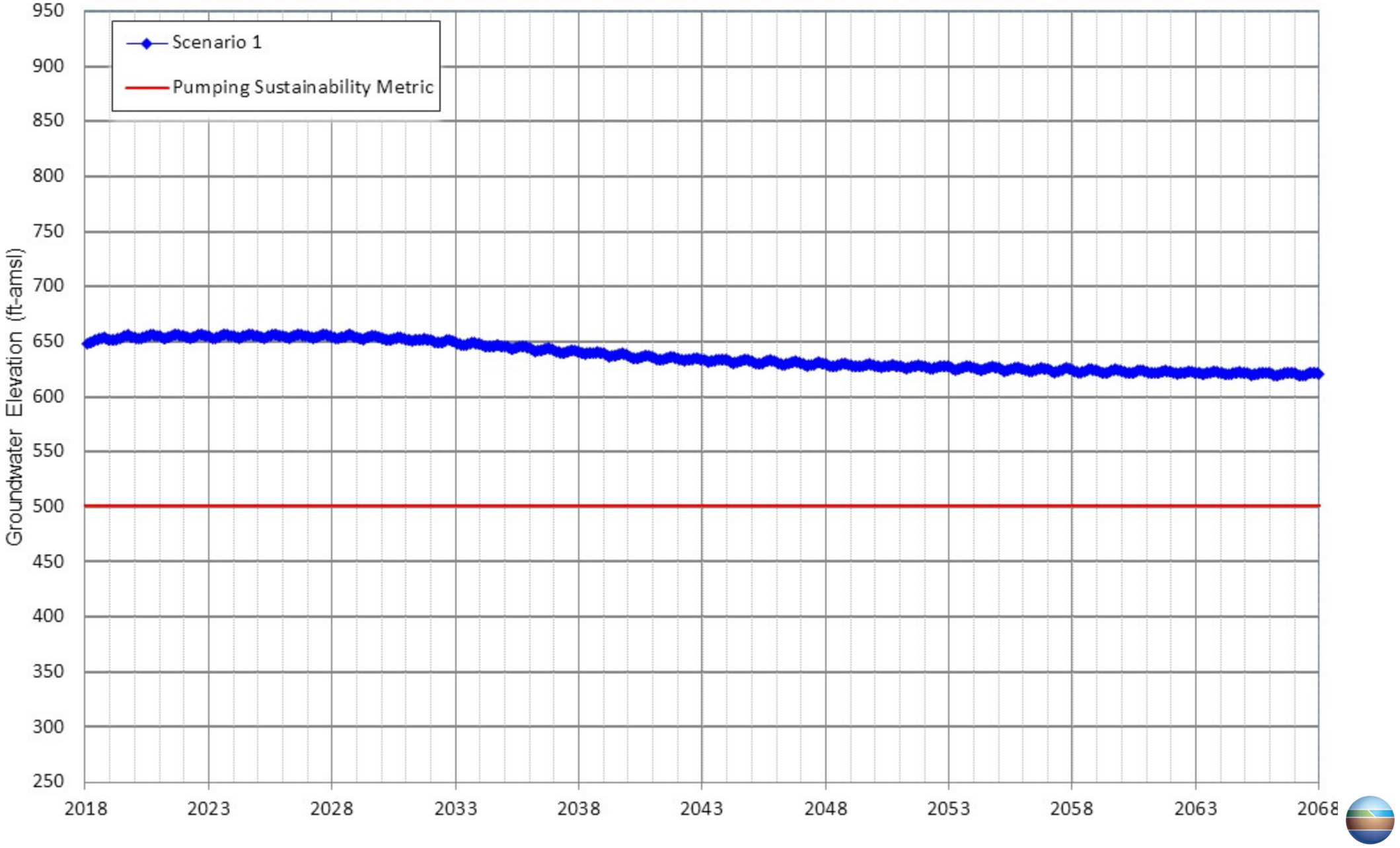

Appendix D-58
Projected Groundwater Elevation for Scenarios 1
CVWD Well ASR1- CB-49

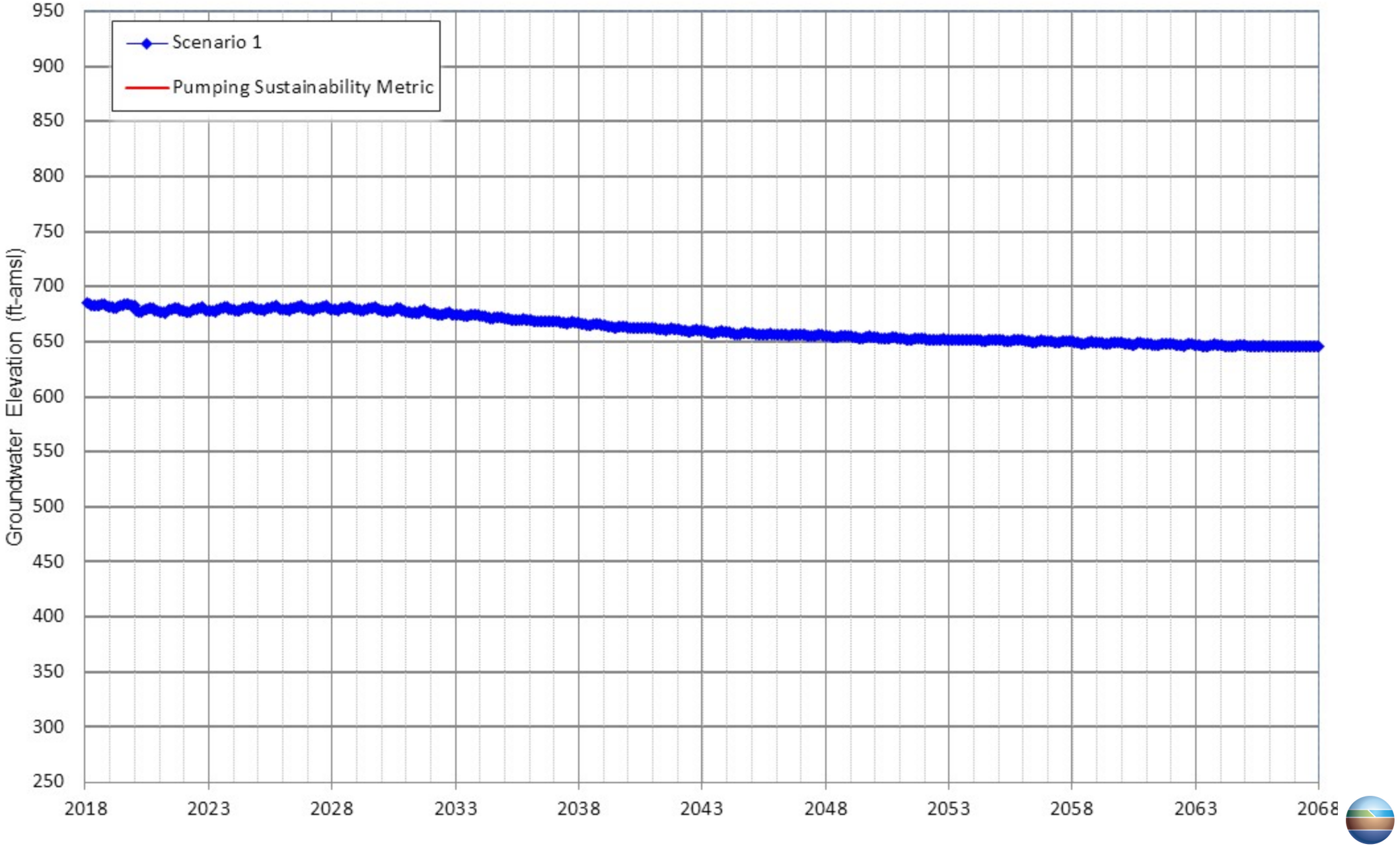

Appendix D-59
Projected Groundwater Elevation for Scenarios 1
CVWD Well ASR2-CB-50

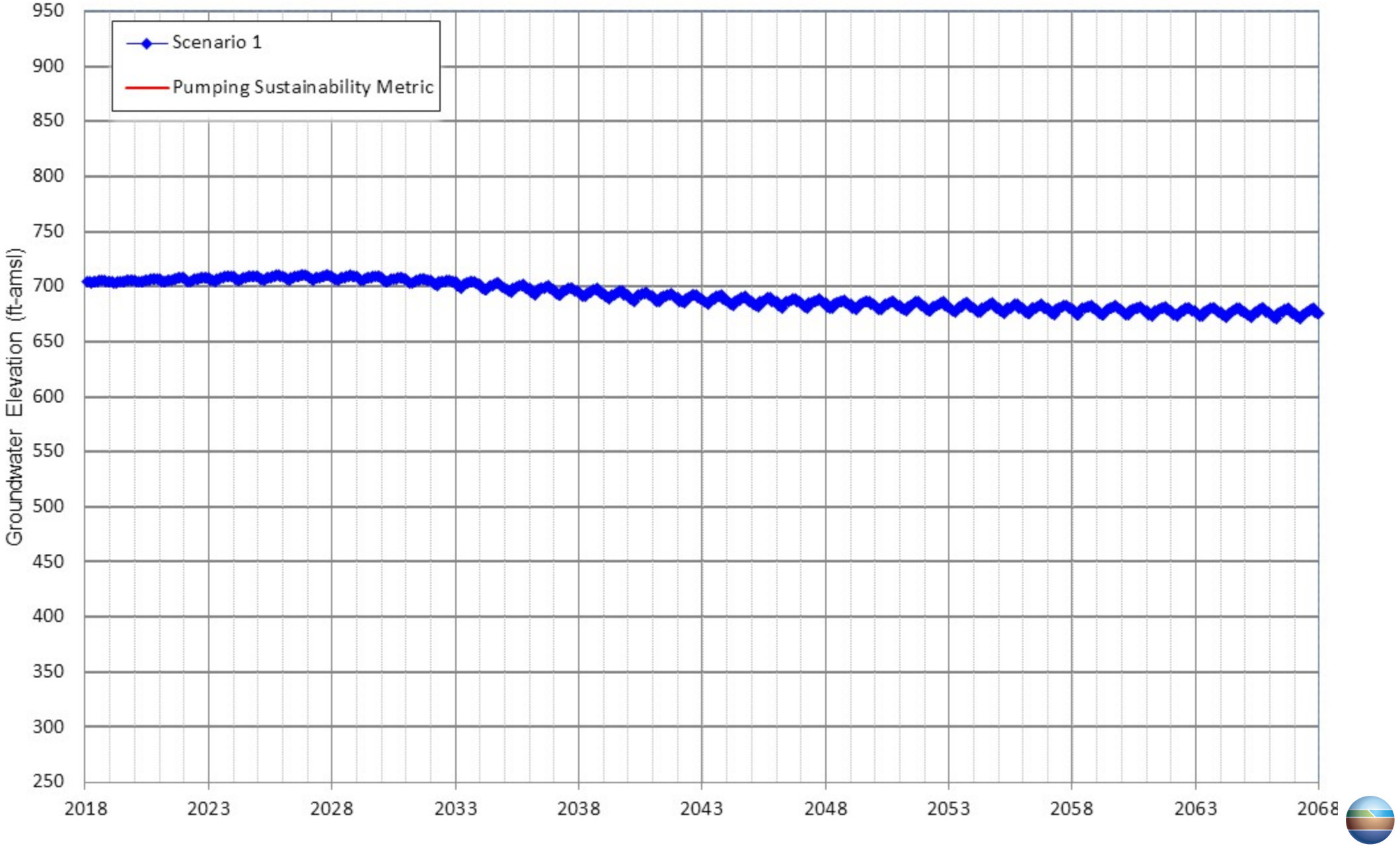

Appendix D-60
Projected Groundwater Elevation for Scenarios 1
CVWD Well ASR3-CB-48

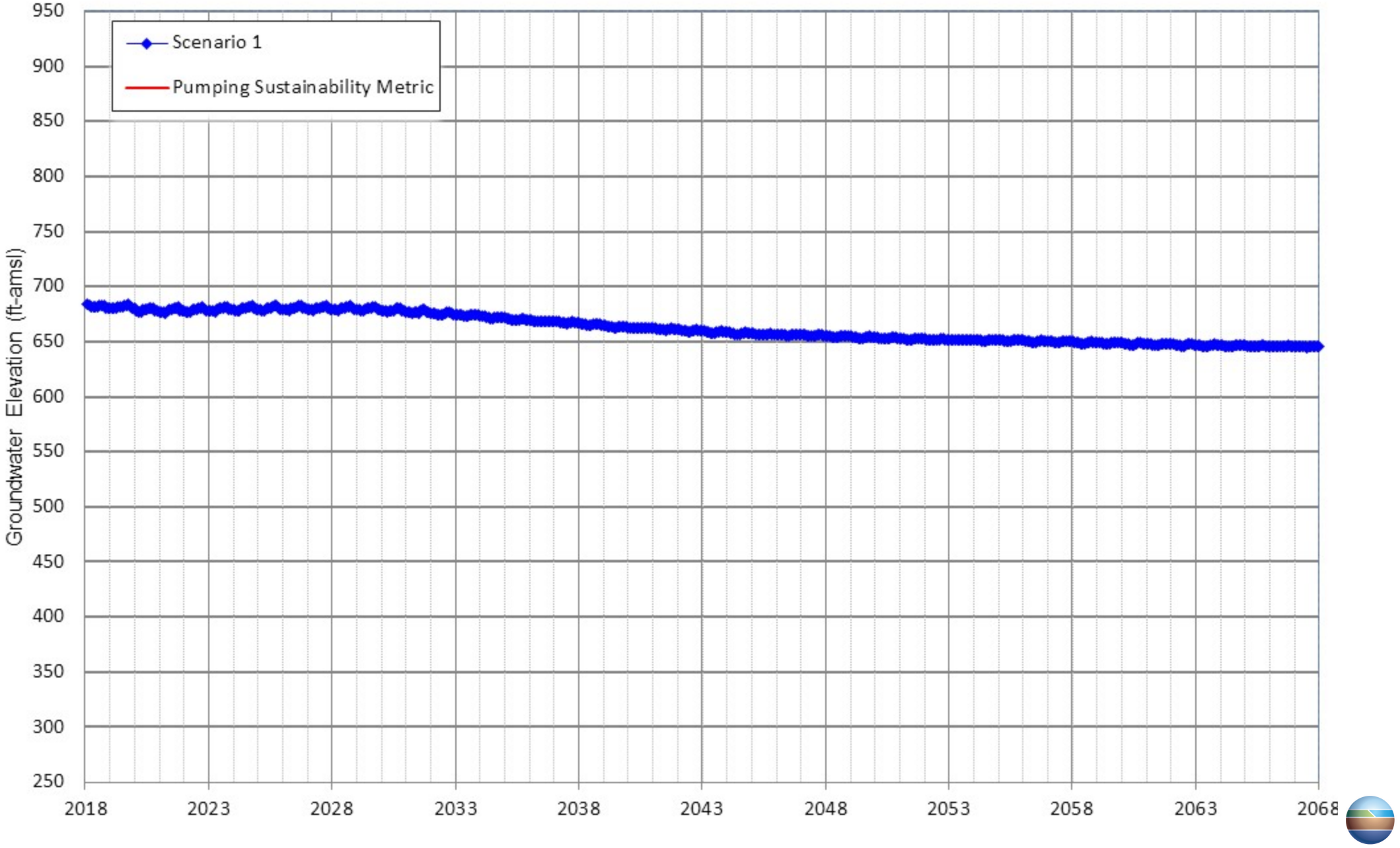

Appendix D-61
Projected Groundwater Elevation for Scenarios 1
FWC Well F7A

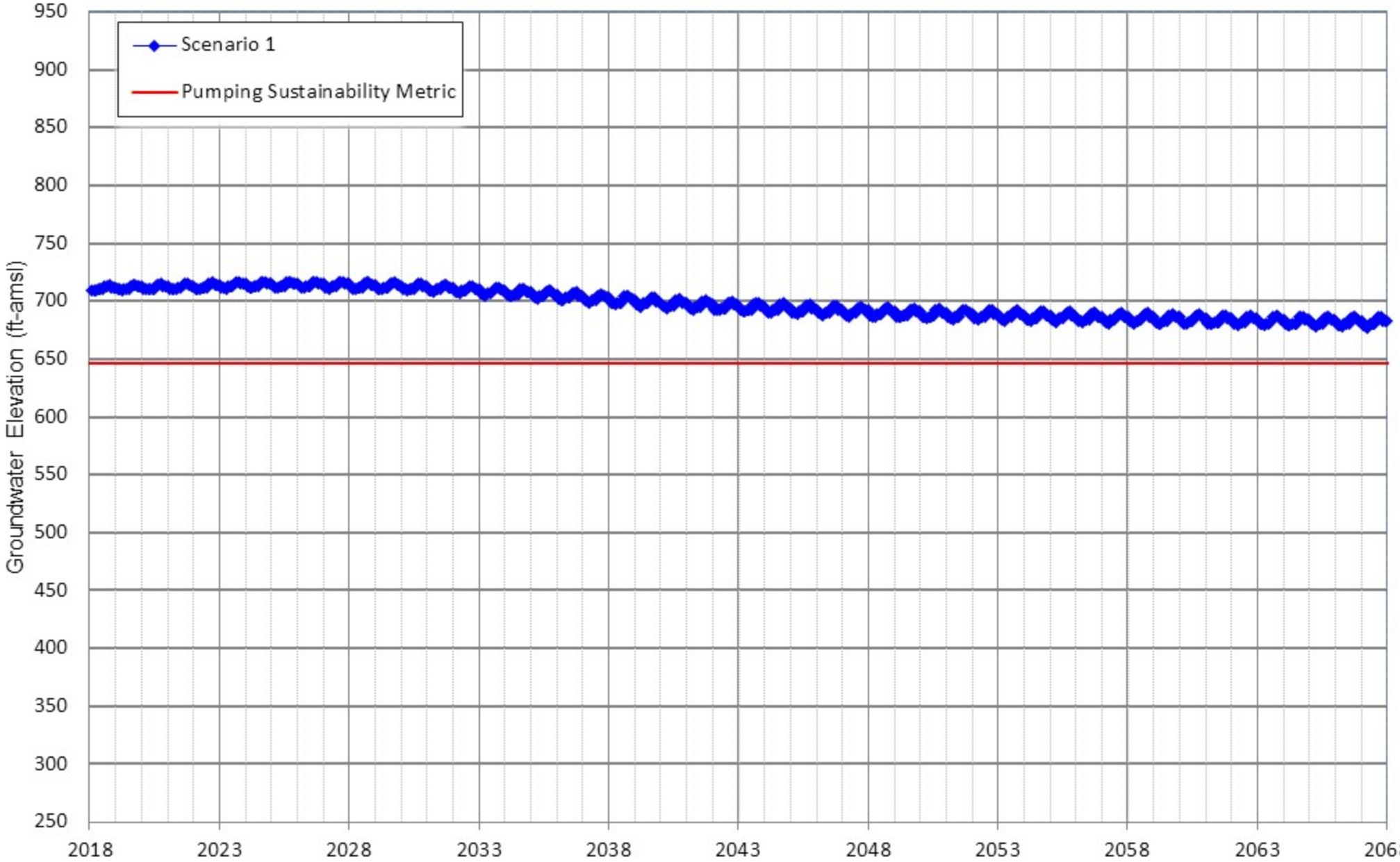

Appendix D-62
Projected Groundwater Elevation for Scenarios 1
FWC Well F7B

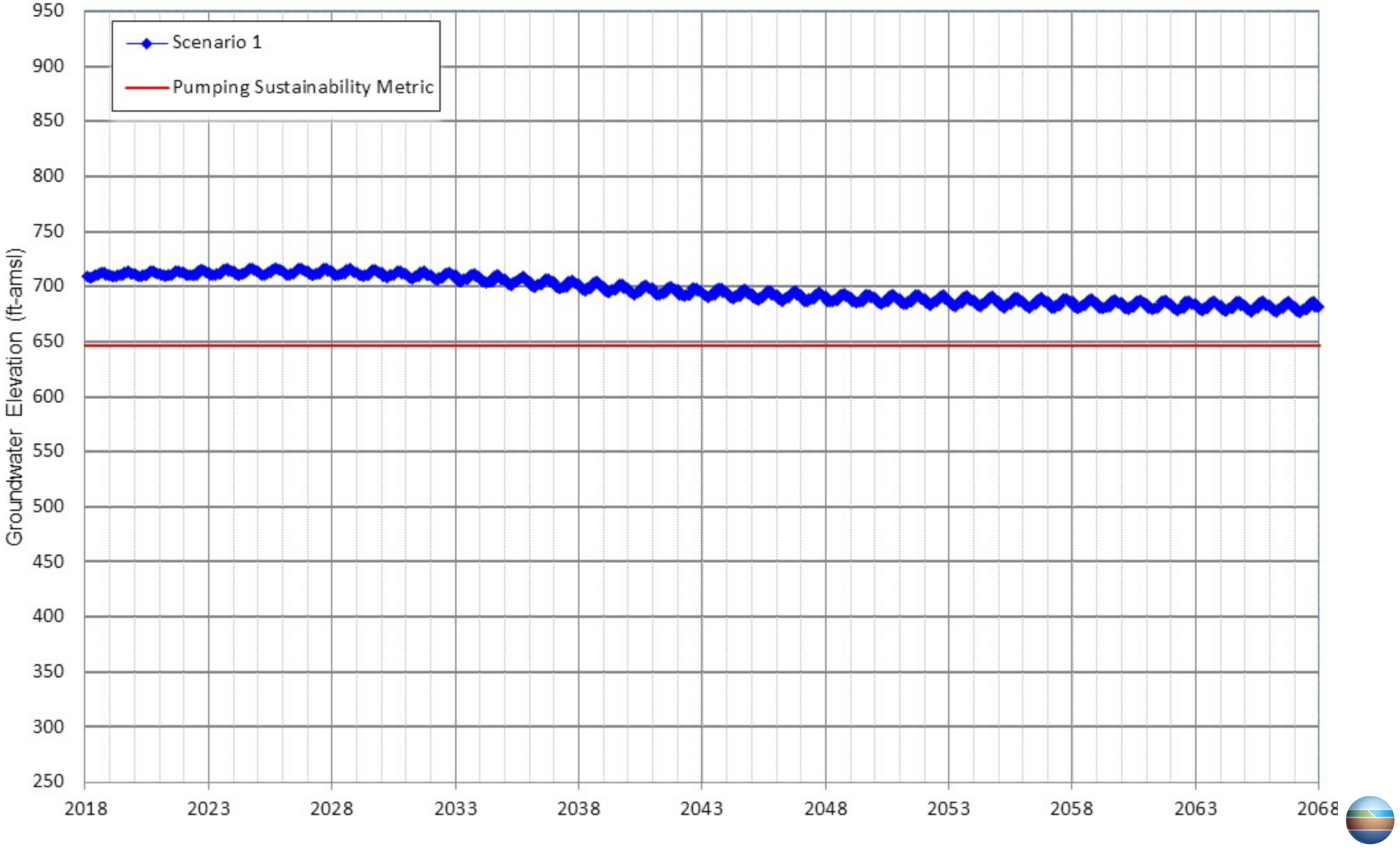

Appendix D-63
Projected Groundwater Elevation for Scenarios 1
FWC Well F17B

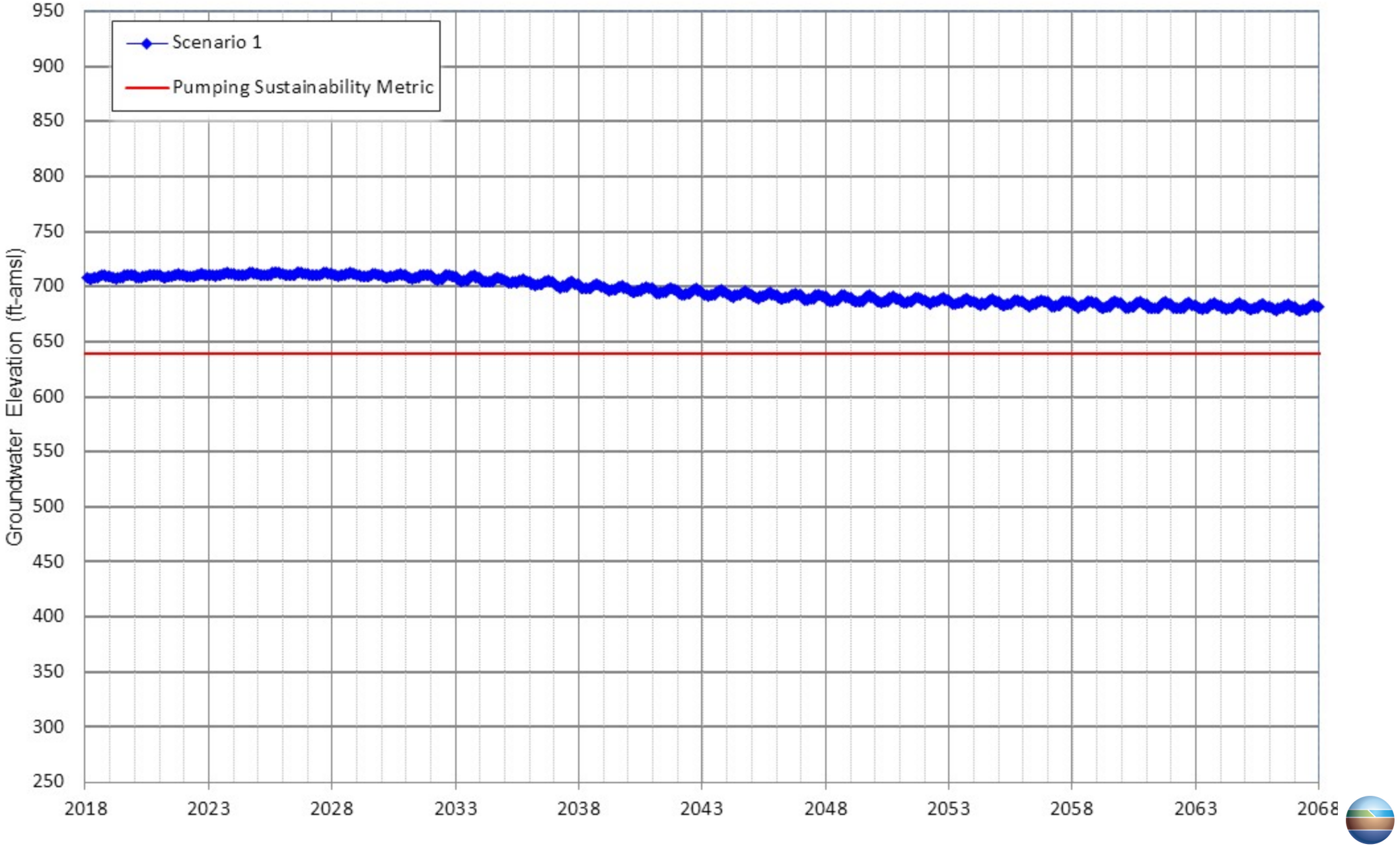

Appendix D-64
Projected Groundwater Elevation for Scenarios 1
FWC Well F17C

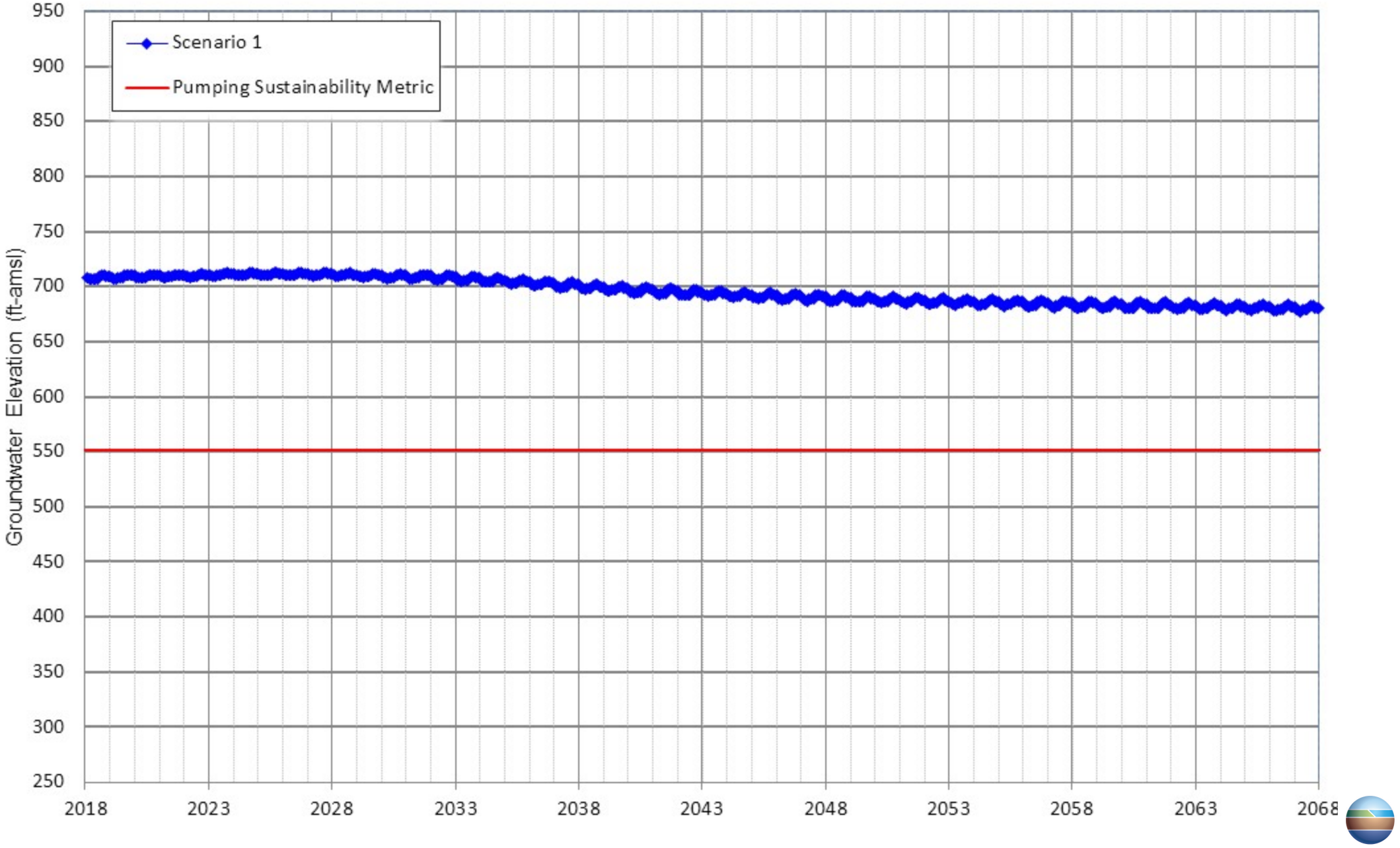

Appendix D-65
Projected Groundwater Elevation for Scenarios 1
FWC Well F21B

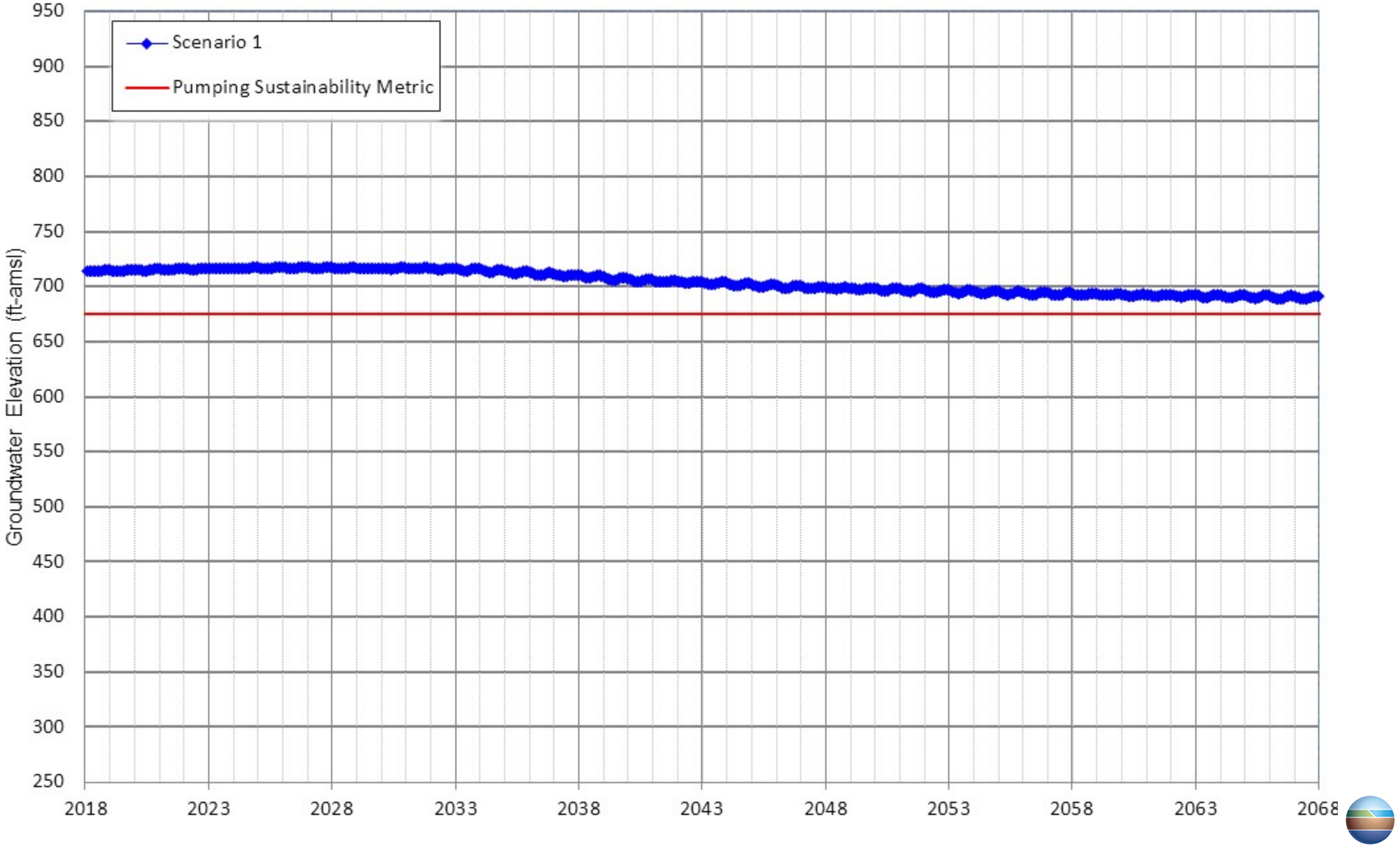

Appendix D-66
Projected Groundwater Elevation for Scenarios 1
FWC Well F23A

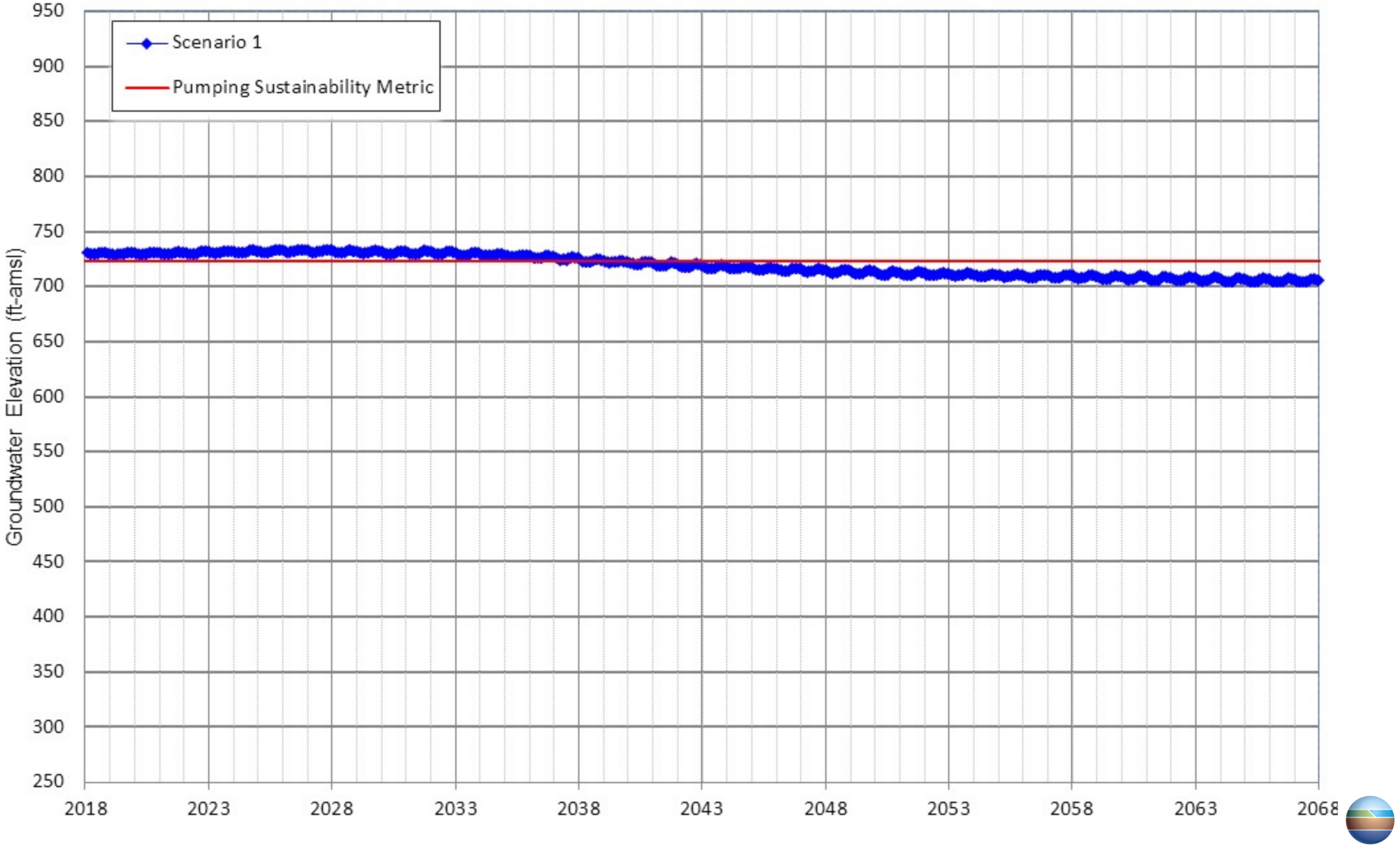

Appendix D-67
Projected Groundwater Elevation for Scenarios 1
FWC Well F24A

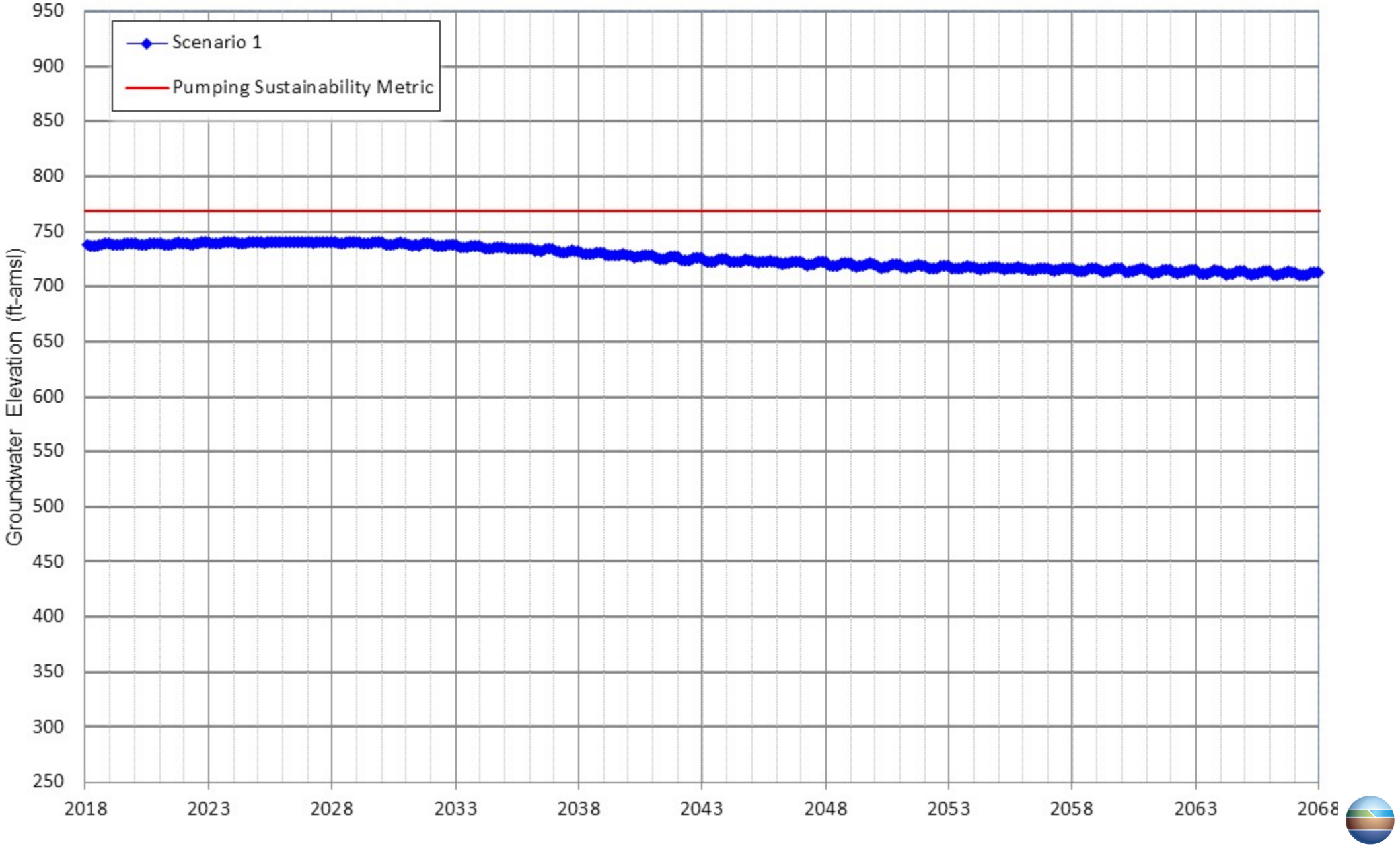

Appendix D-68
Projected Groundwater Elevation for Scenarios 1
FWC Well F26A

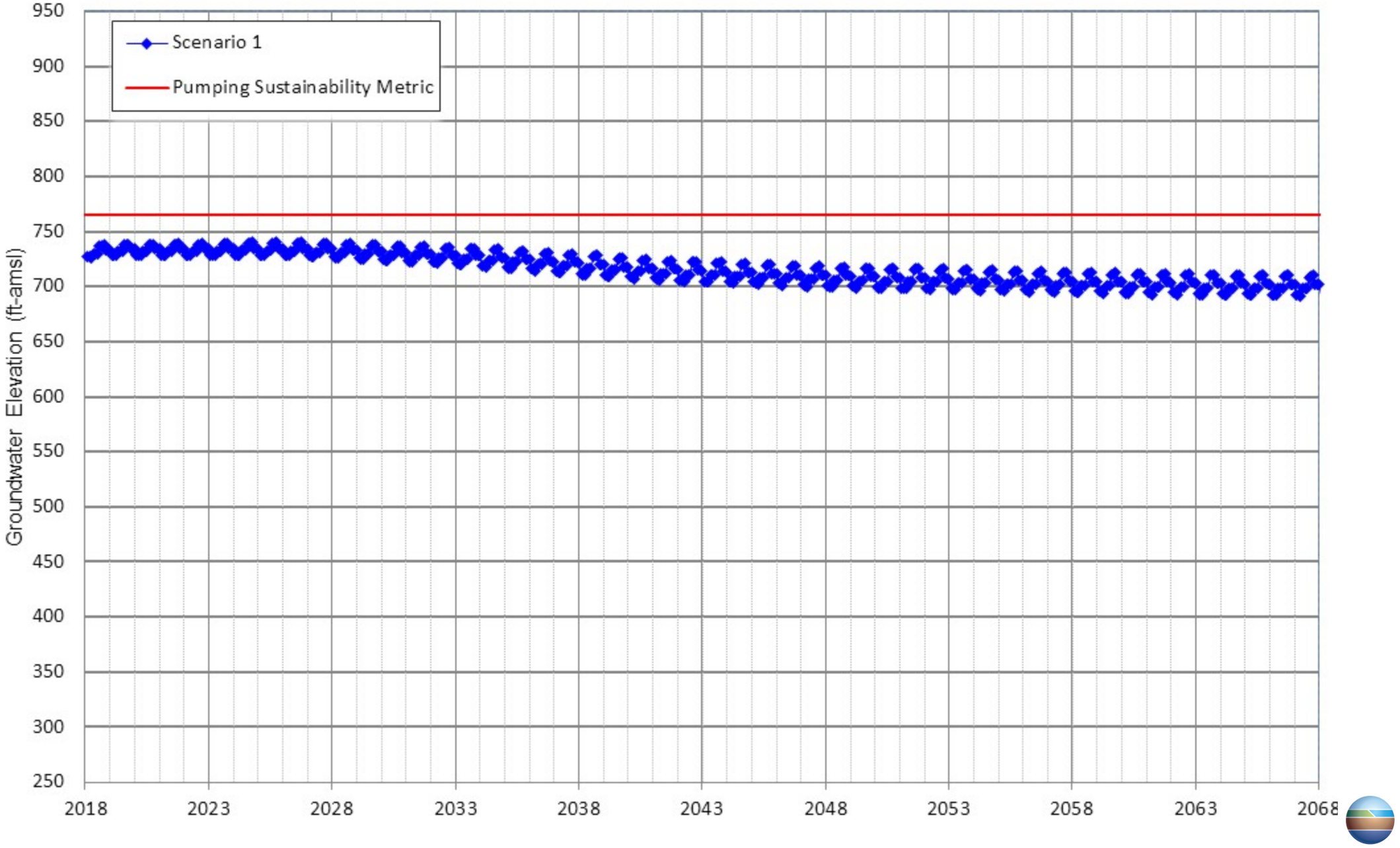

Appendix D-69
Projected Groundwater Elevation for Scenarios 1
FWC Well F31A

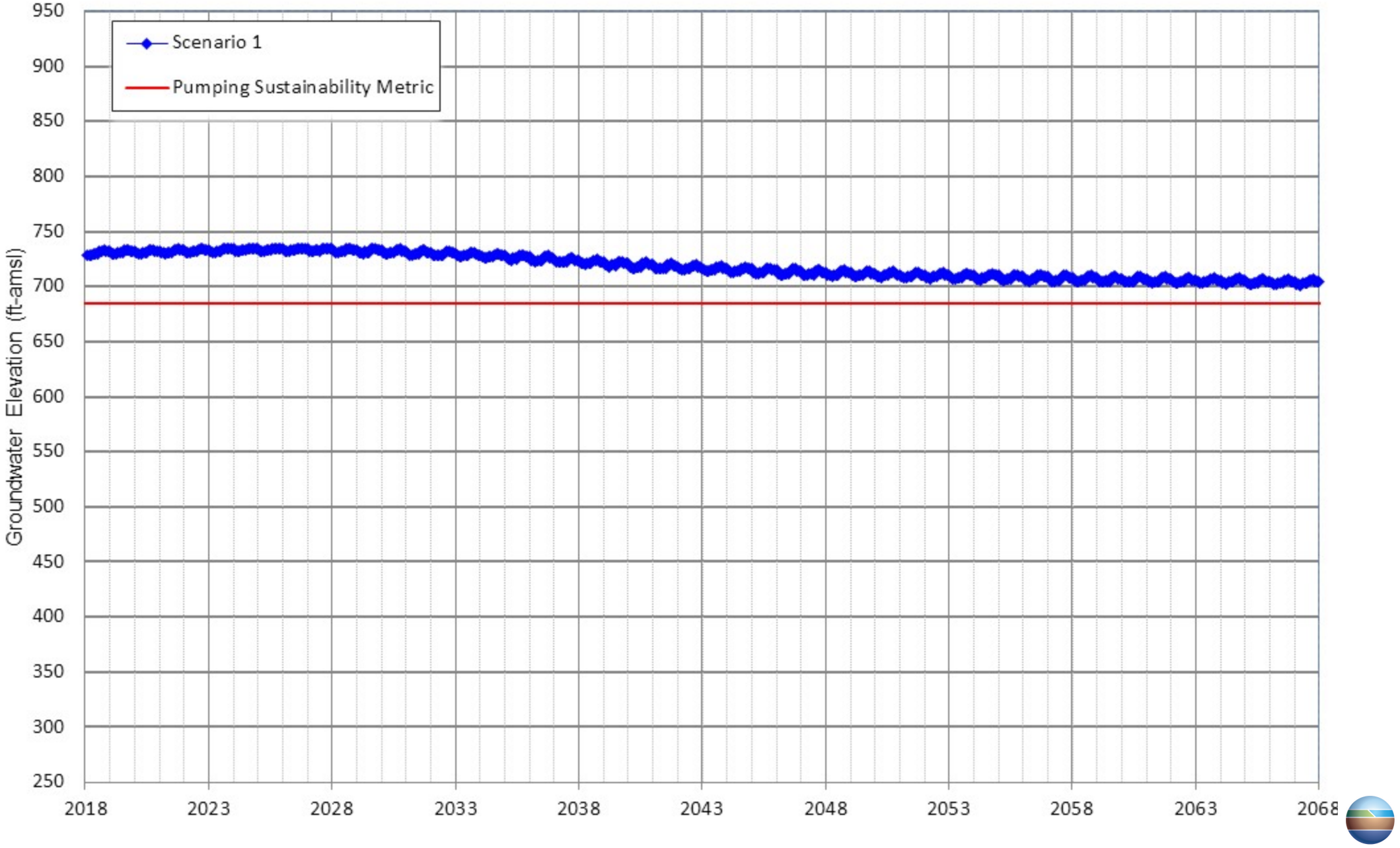

Appendix D-70
Projected Groundwater Elevation for Scenarios 1
FWC Well F44A

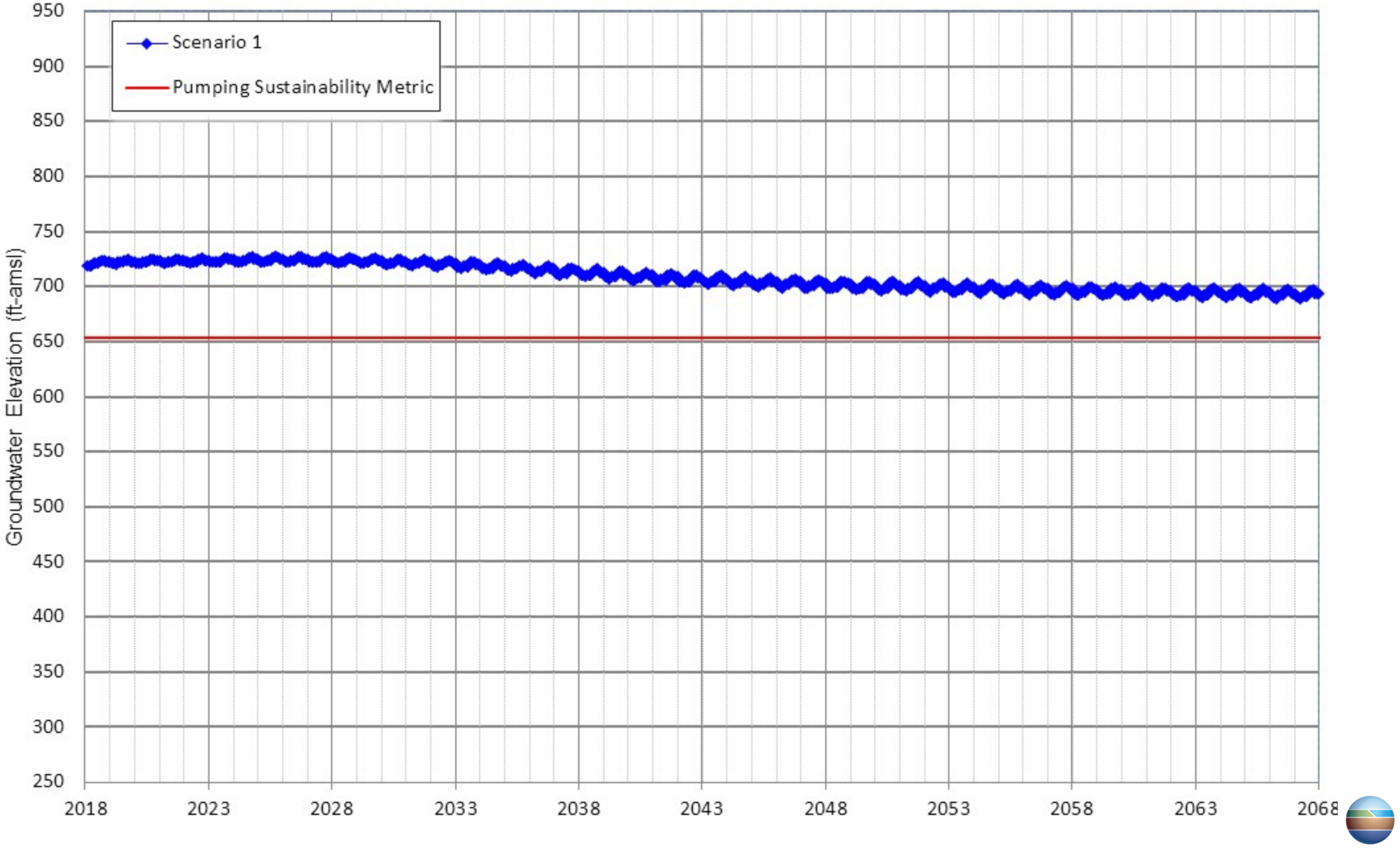

Appendix D-71
Projected Groundwater Elevation for Scenarios 1
FWC Well F44B

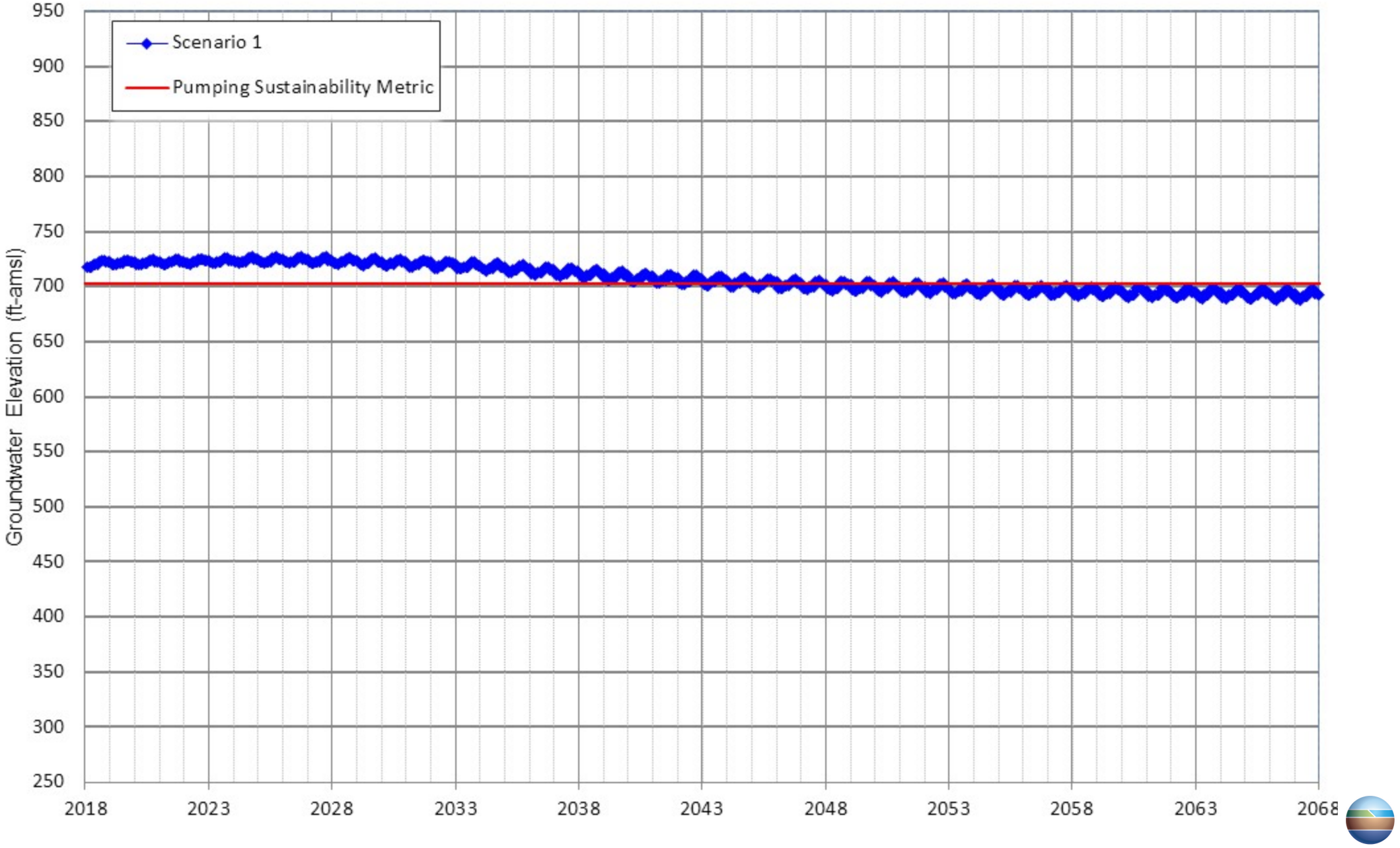

Appendix D-72
Projected Groundwater Elevation for Scenarios 1
FWC Well F44C

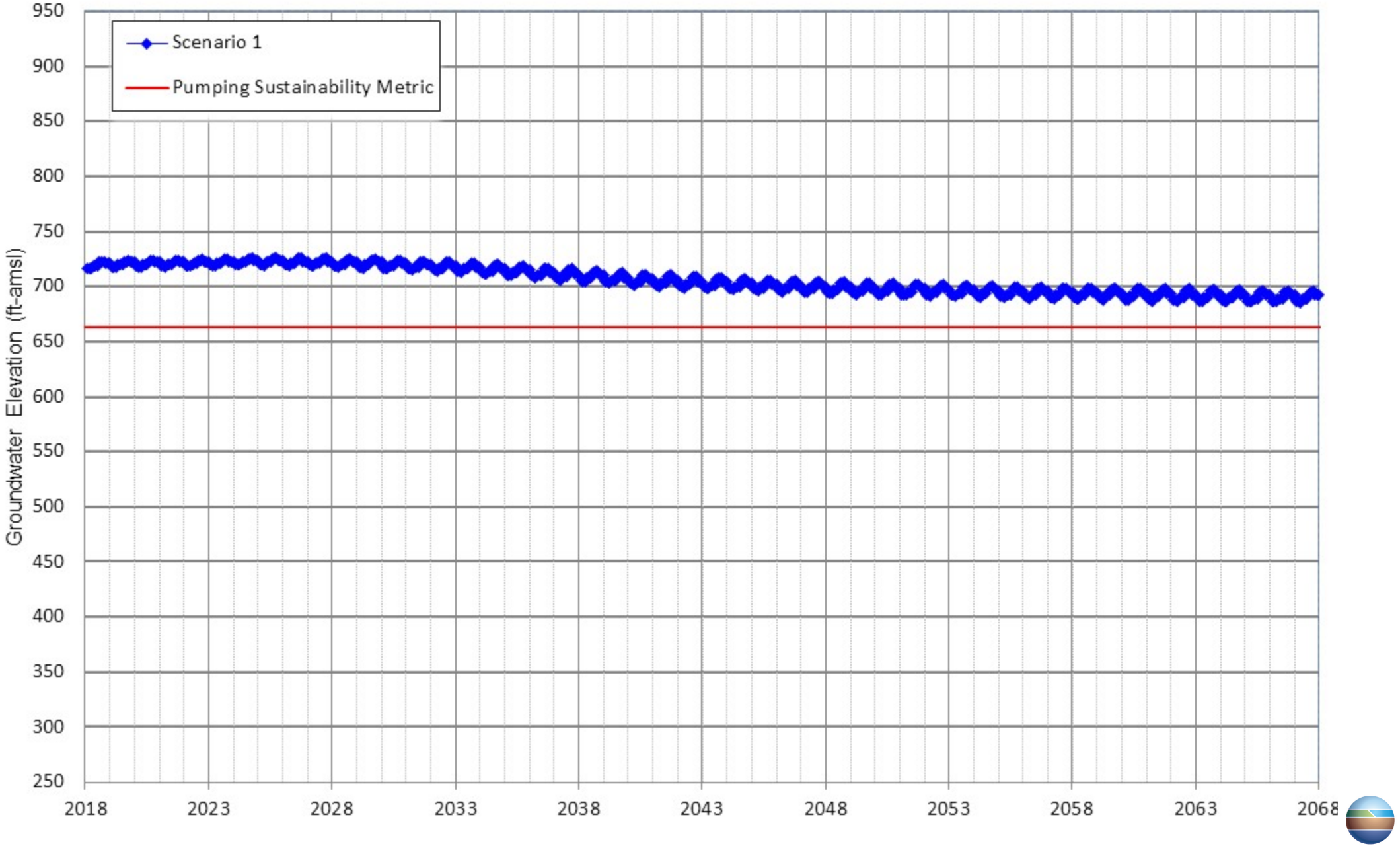

Appendix D-73
Projected Groundwater Elevation for Scenarios 1
GSWC Well #1

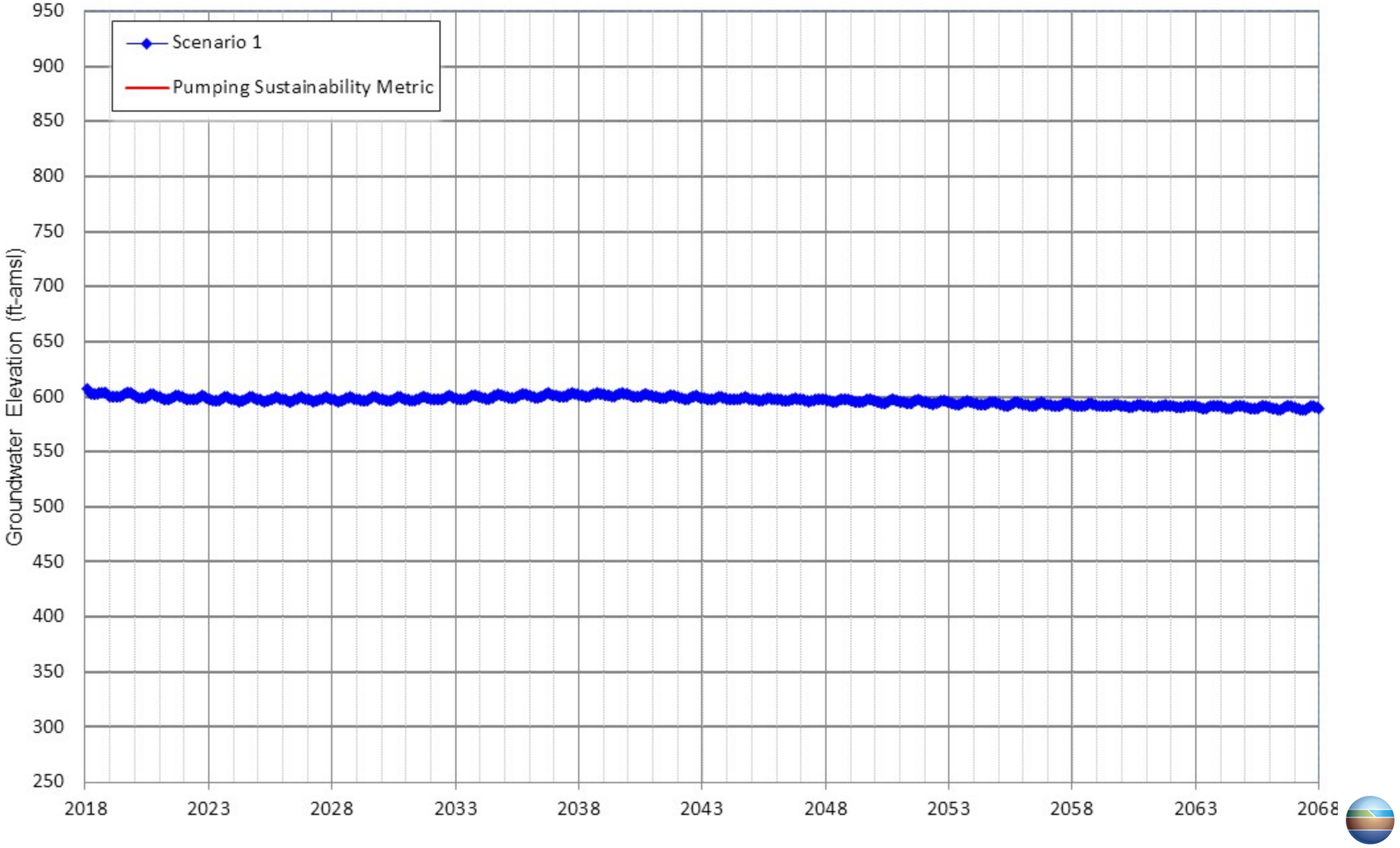

Appendix D-74
Projected Groundwater Elevation for Scenarios 1
JCSD Well 6

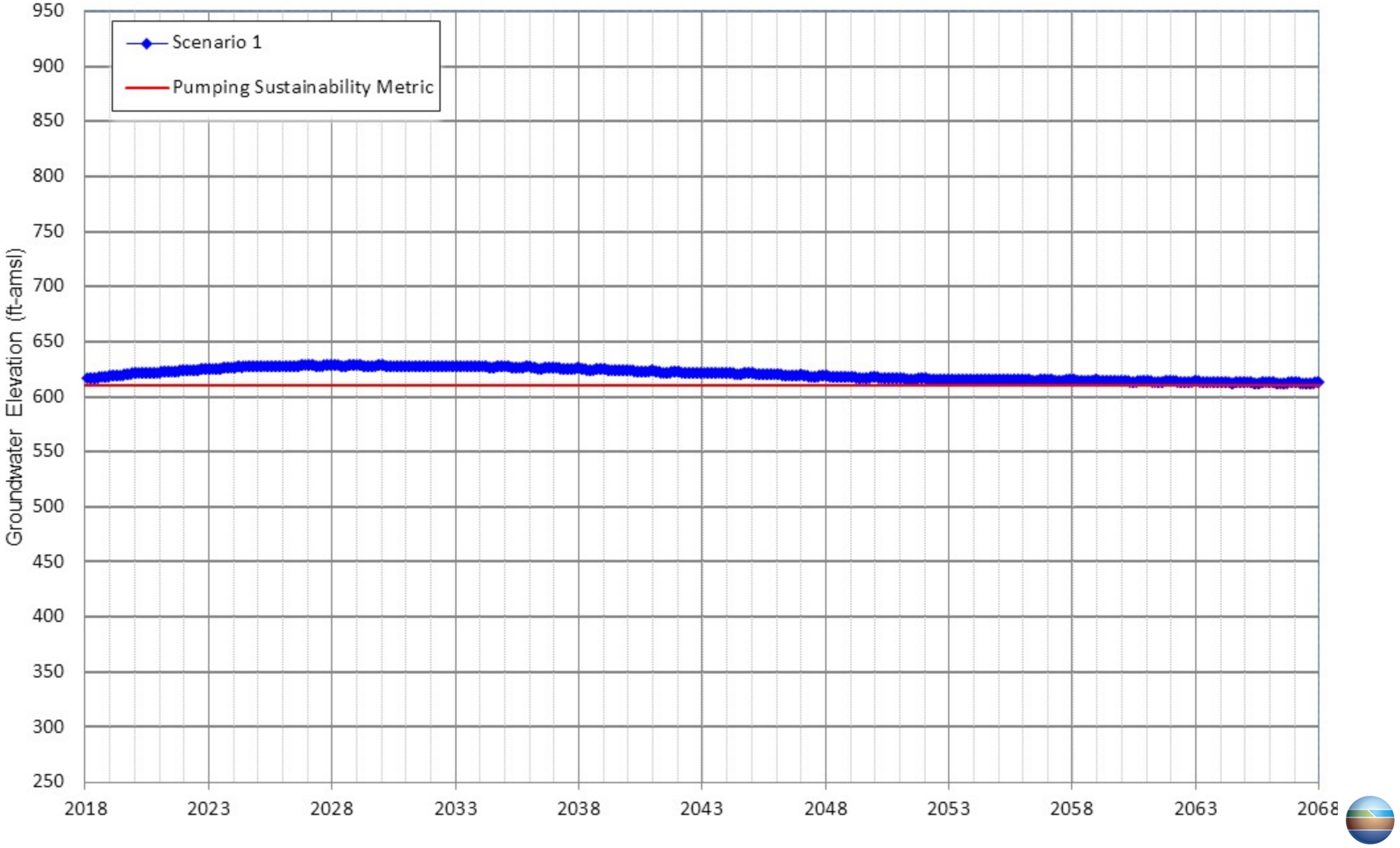

Appendix D-75
Projected Groundwater Elevation for Scenarios 1
JCSD Well 8

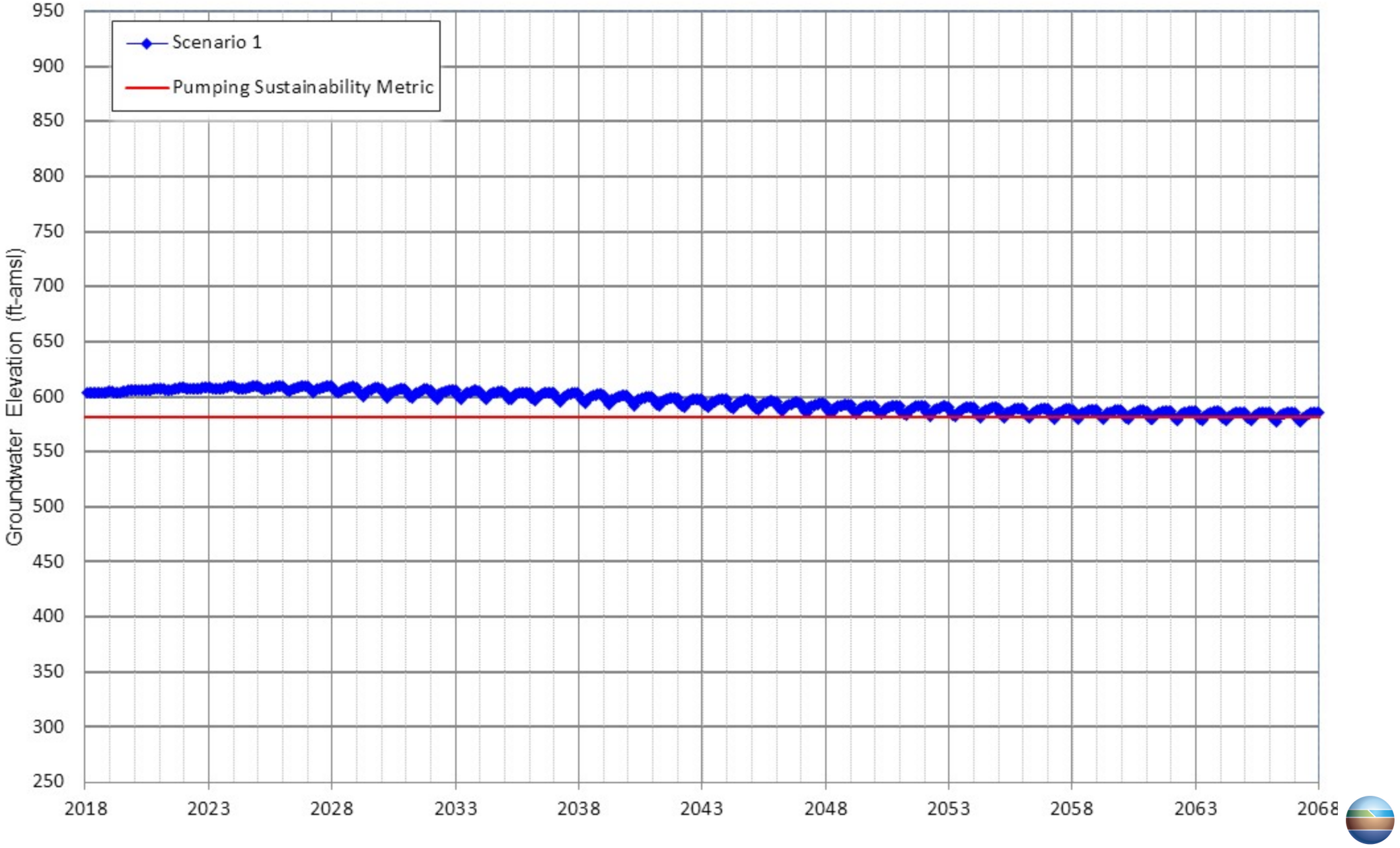

Appendix D-76
Projected Groundwater Elevation for Scenarios 1
JCSD Well 11

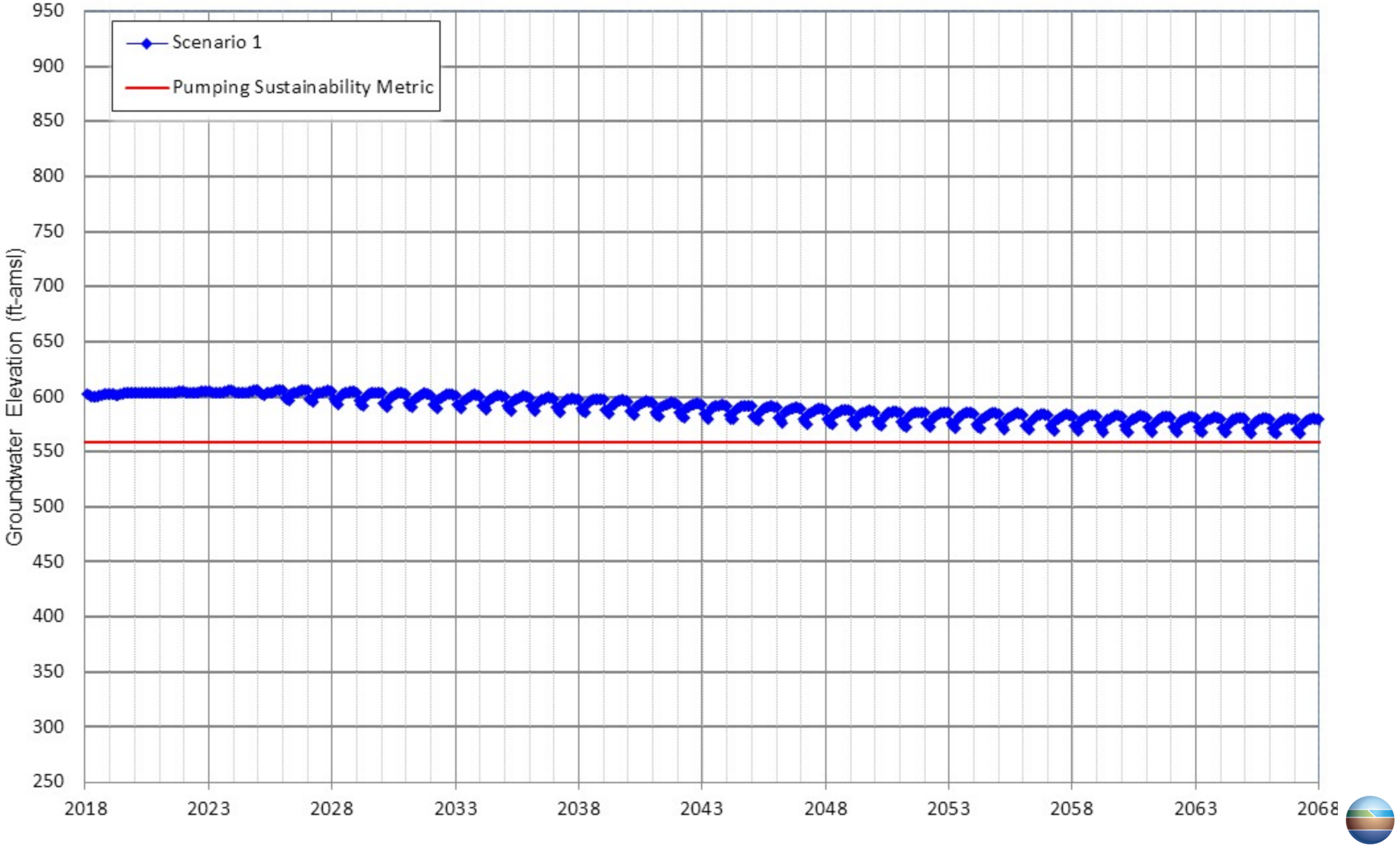

Appendix D-77
Projected Groundwater Elevation for Scenarios 1
JCSD Well 12

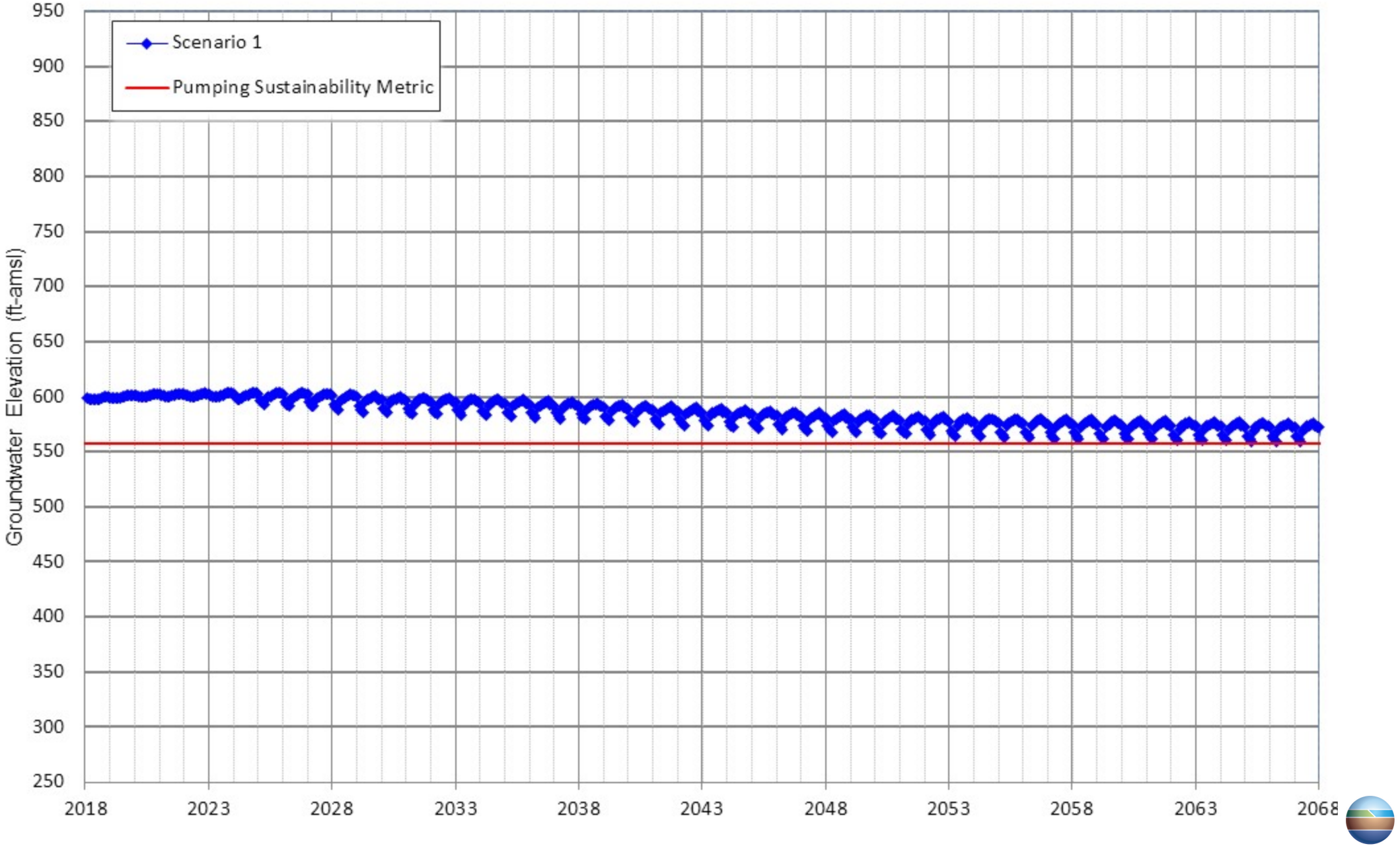

Appendix D-78
Projected Groundwater Elevation for Scenarios 1
JCSD Well 13

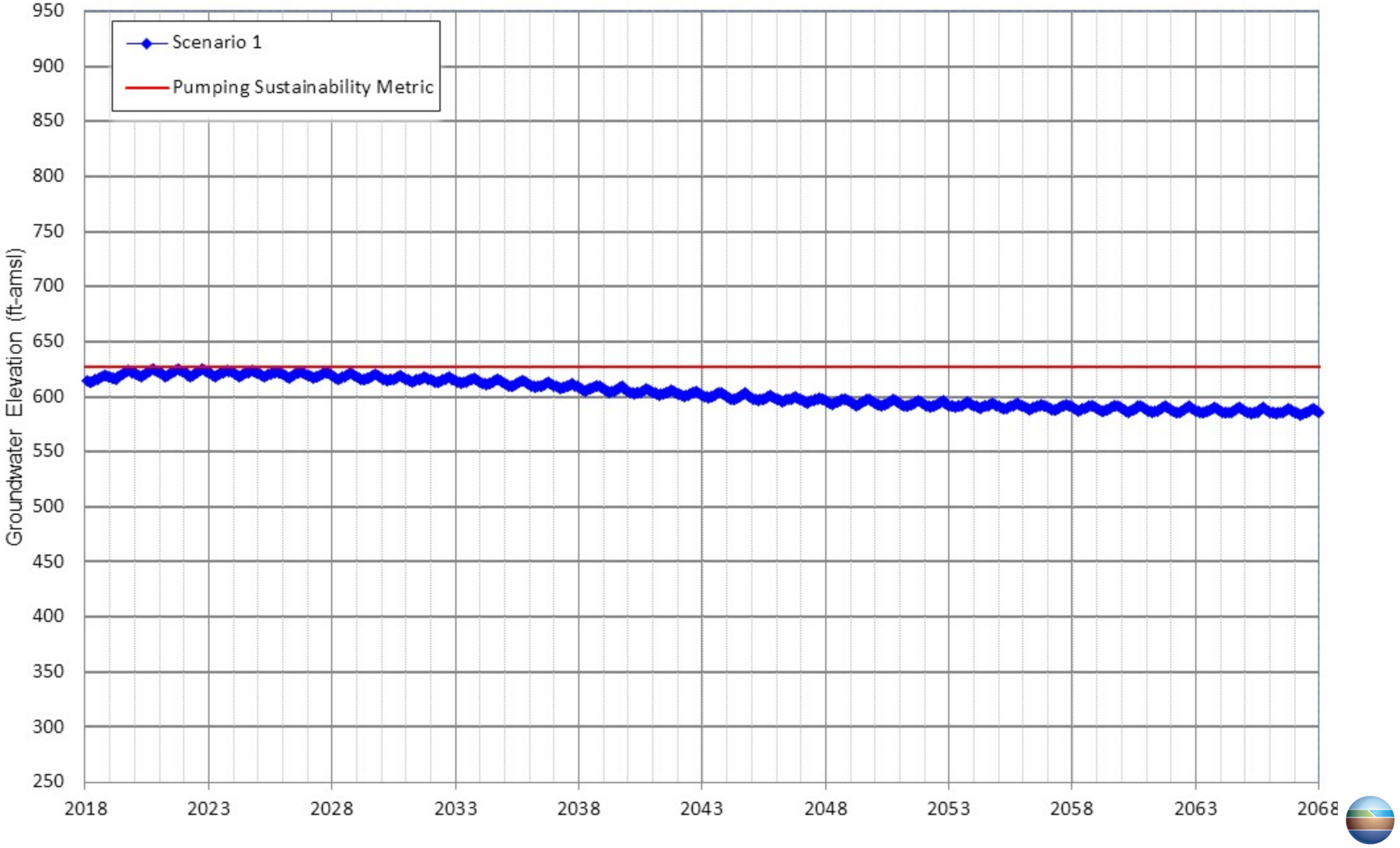

Appendix D-79
Projected Groundwater Elevation for Scenarios 1
JCSD Well 14

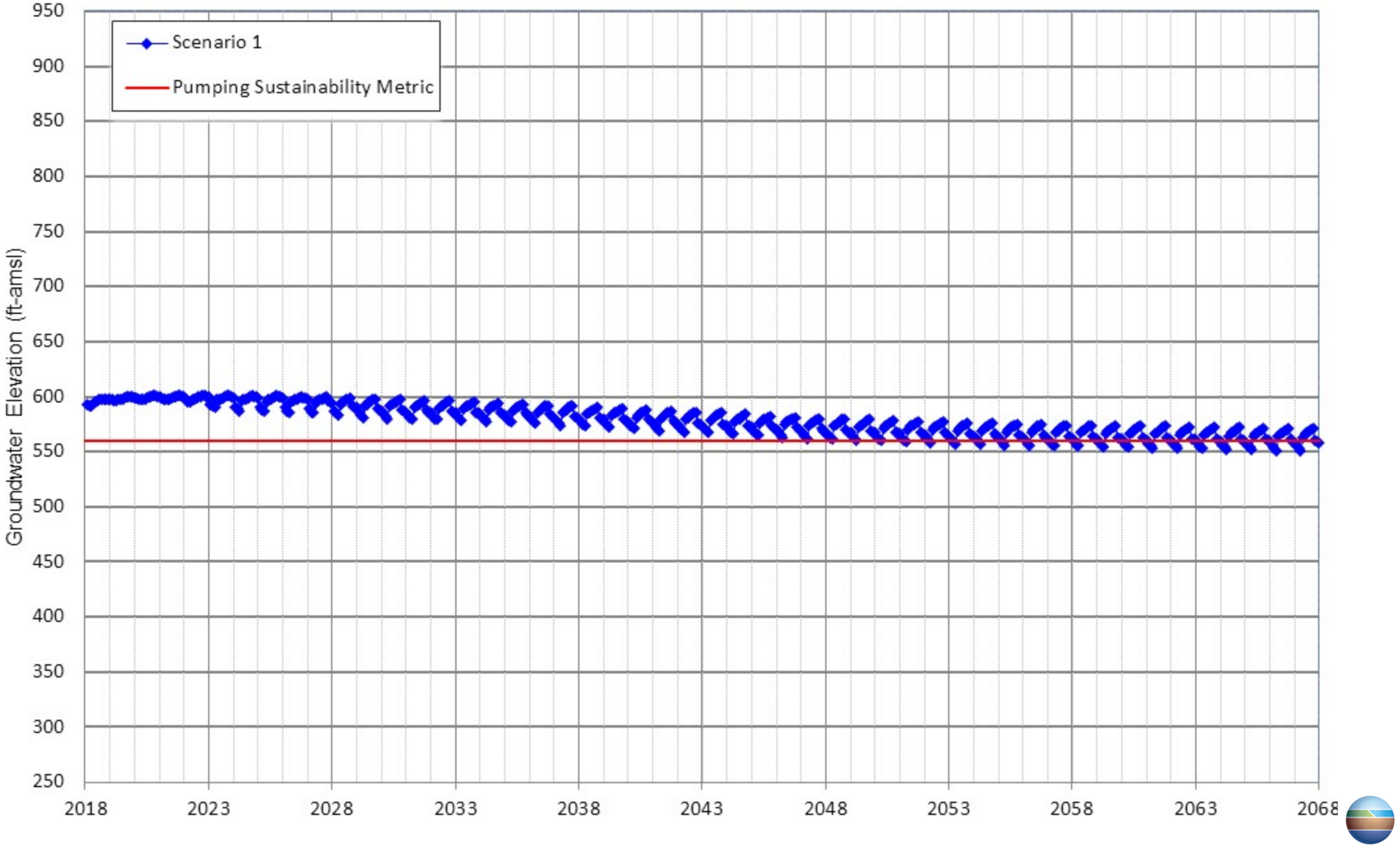

Appendix D-80
Projected Groundwater Elevation for Scenarios 1
JCSD Well 15

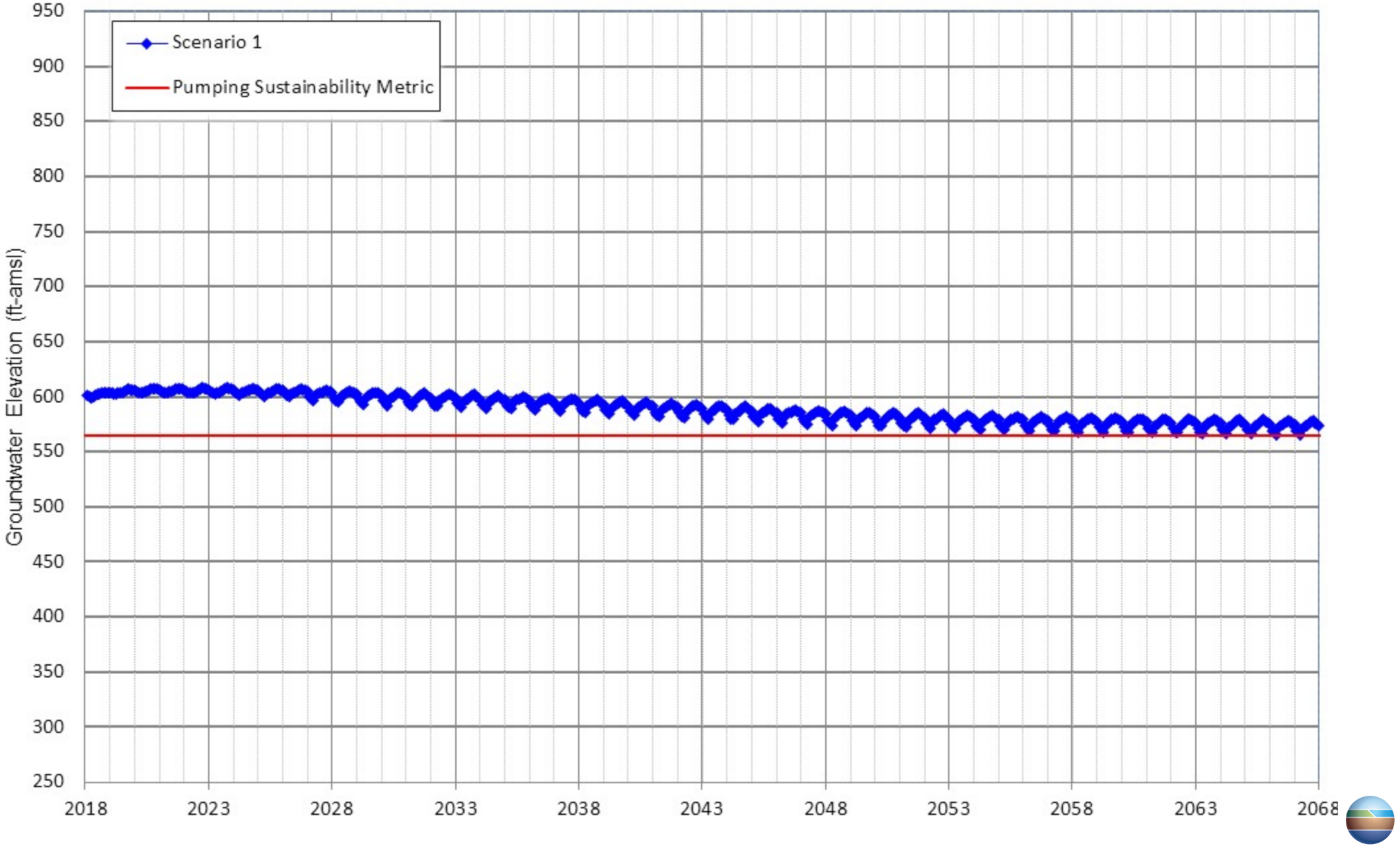

Appendix D-81
Projected Groundwater Elevation for Scenarios 1
JCSD Well 16

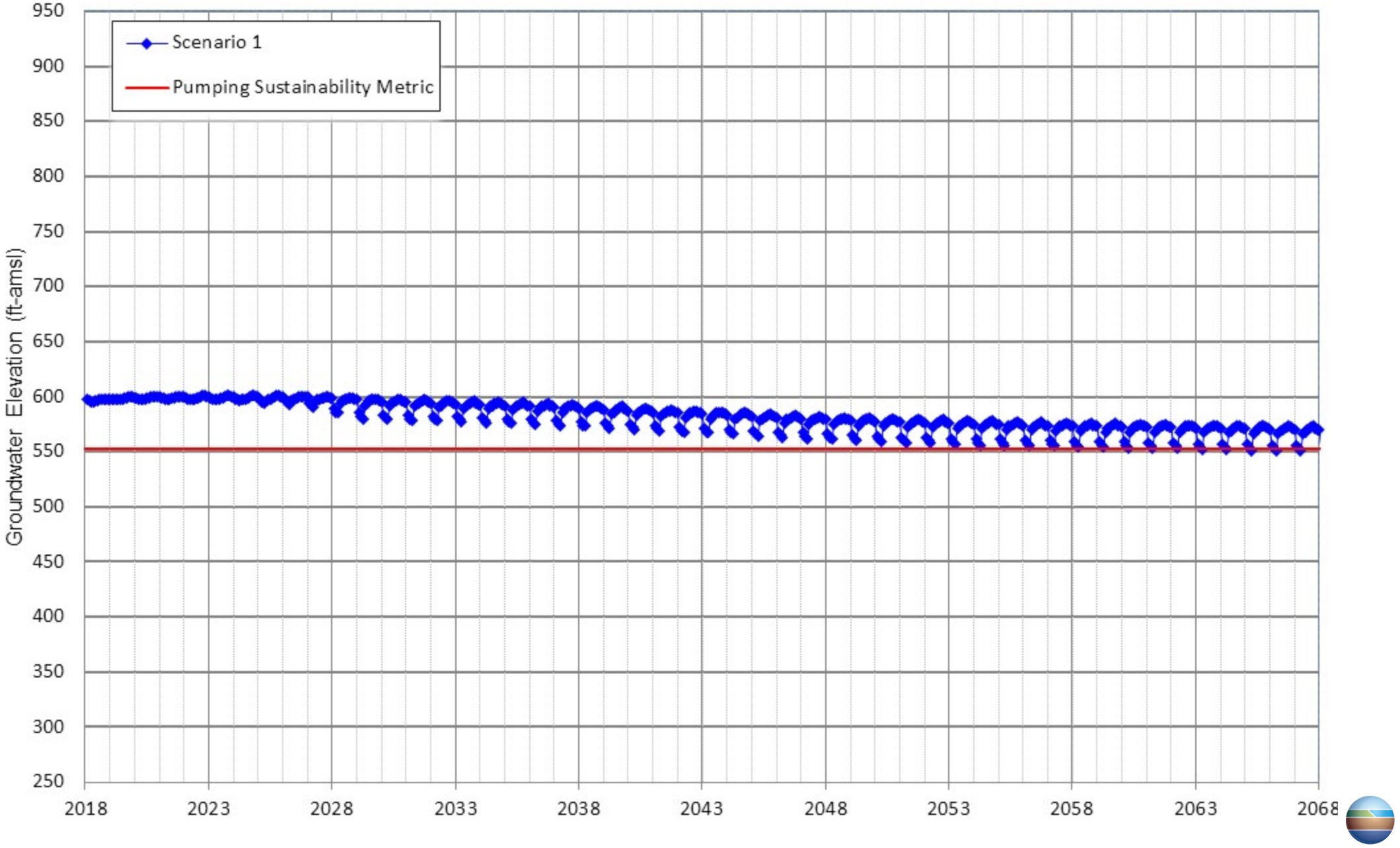

Appendix D-82
Projected Groundwater Elevation for Scenarios 1
JCSD Well 17

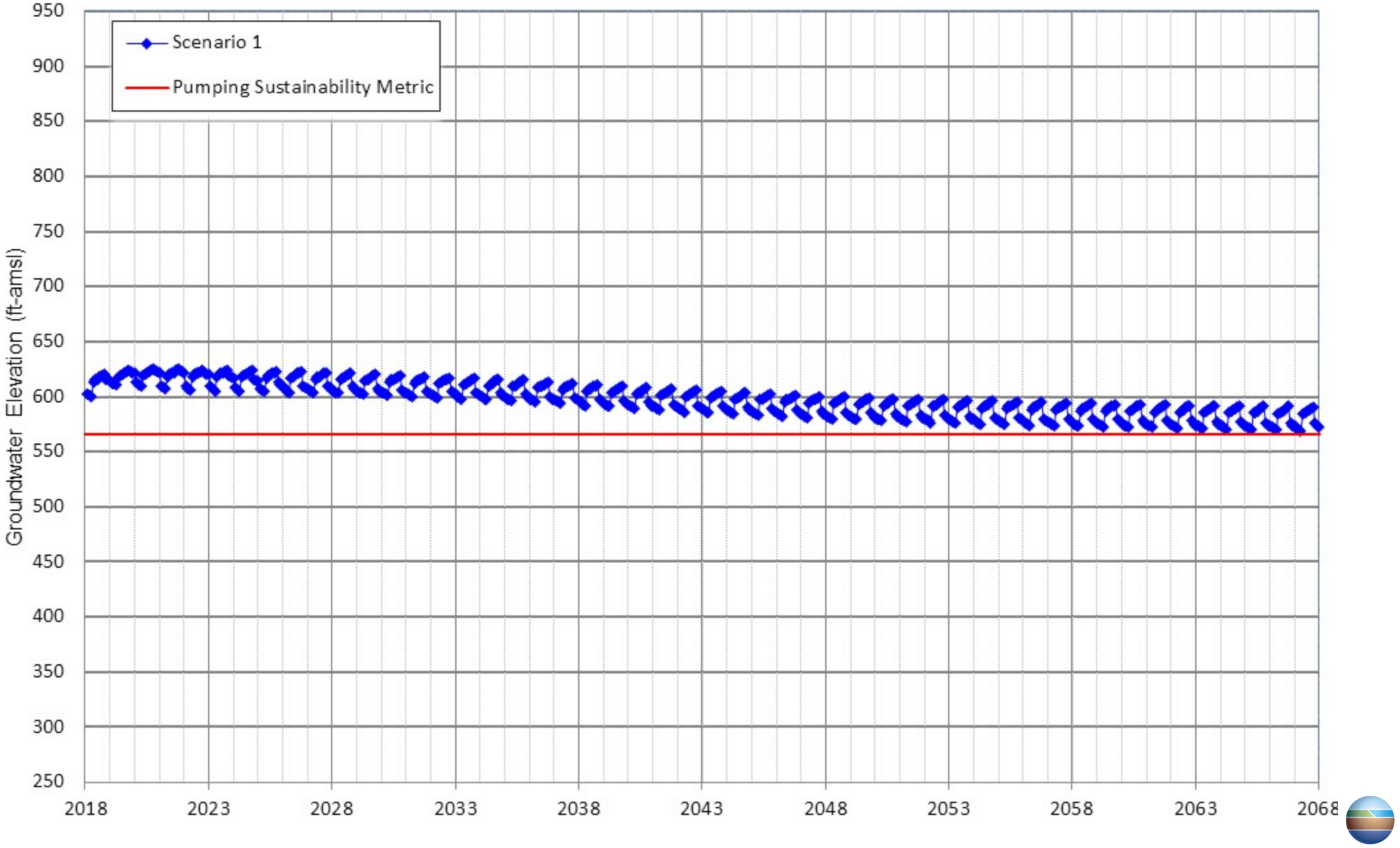

Appendix D-83
Projected Groundwater Elevation for Scenarios 1
JCSD Well 18

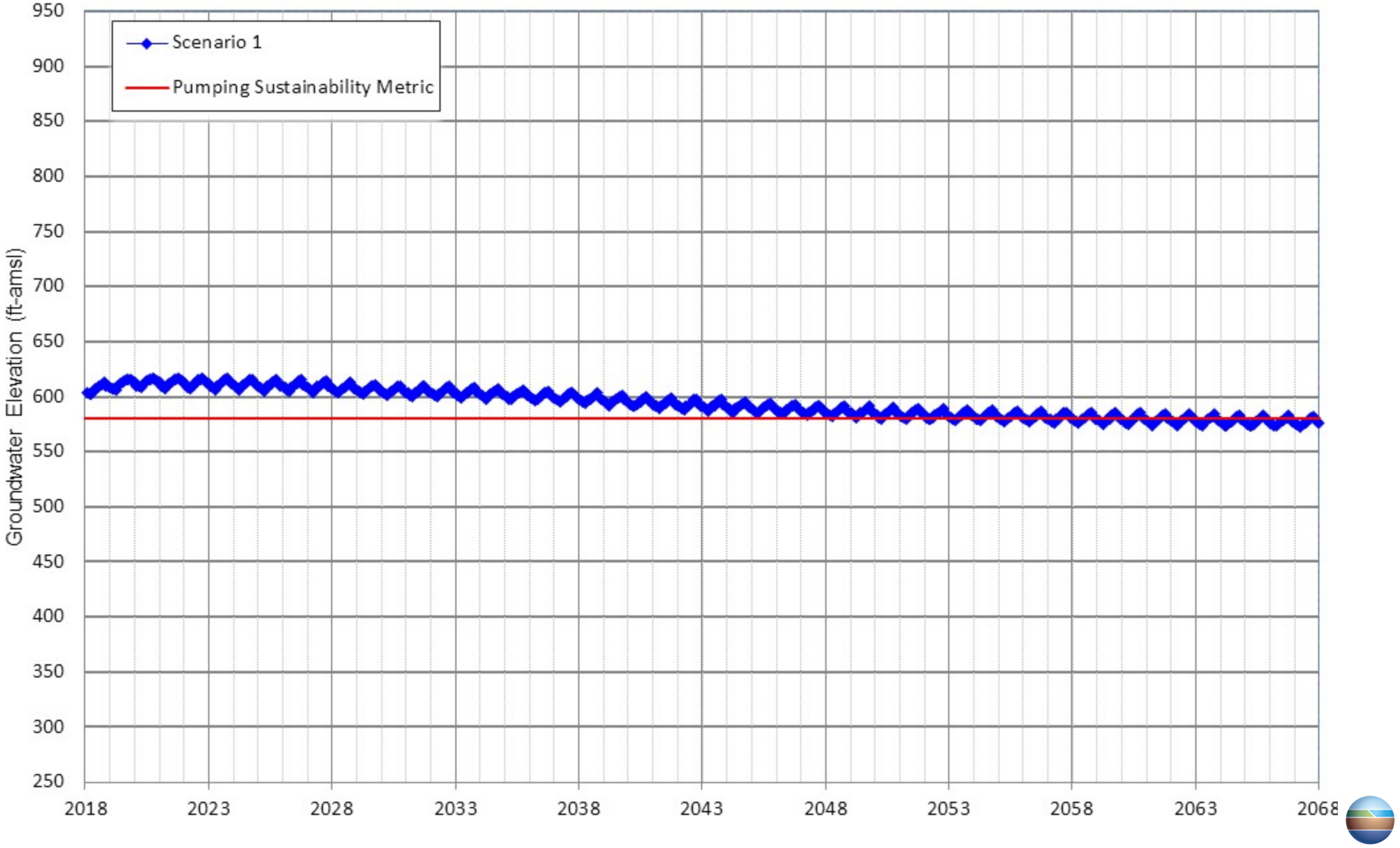

Appendix D-84
Projected Groundwater Elevation for Scenarios 1
JCSD Well 19

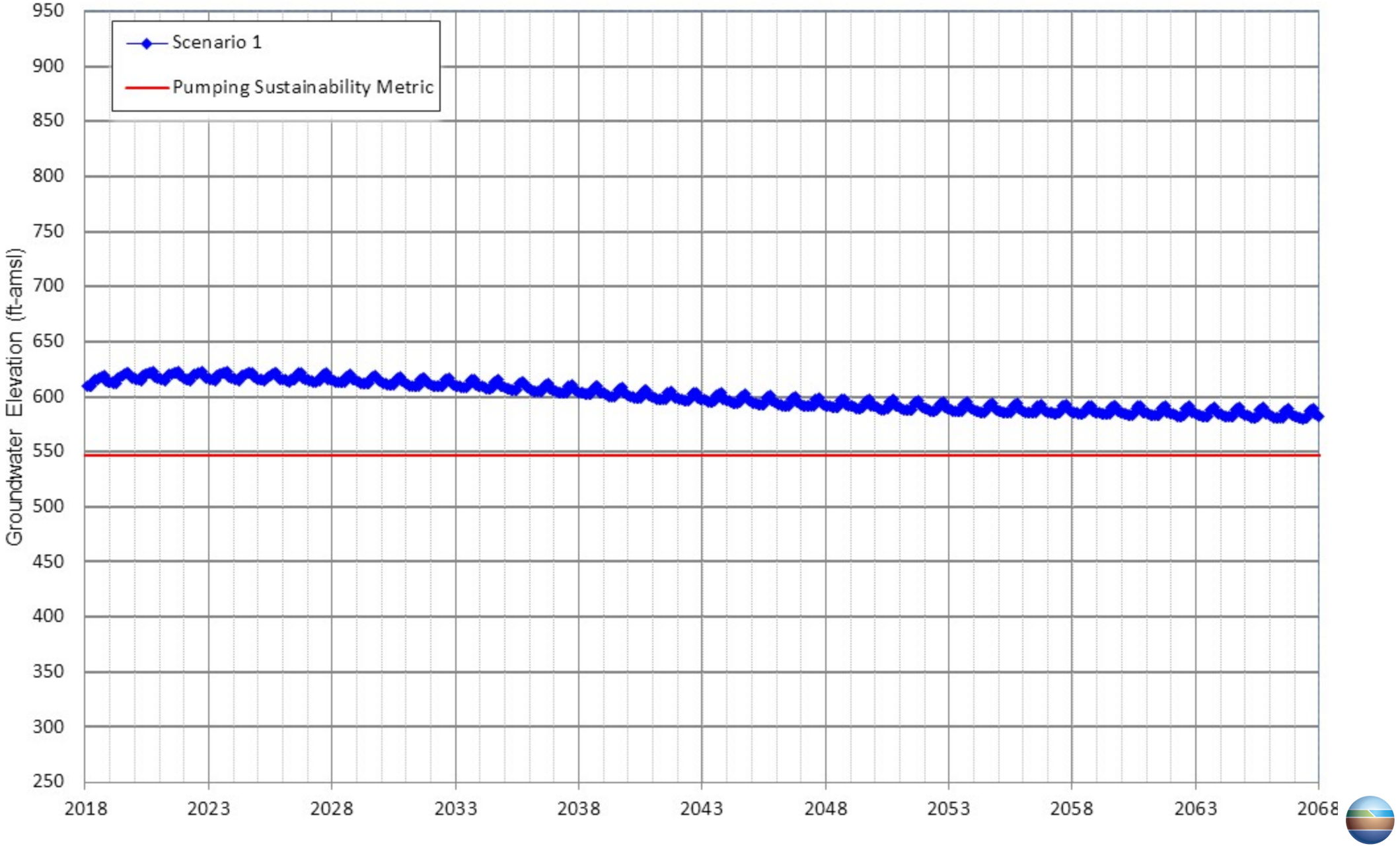

Appendix D-85
Projected Groundwater Elevation for Scenarios 1
JCSD Well 20

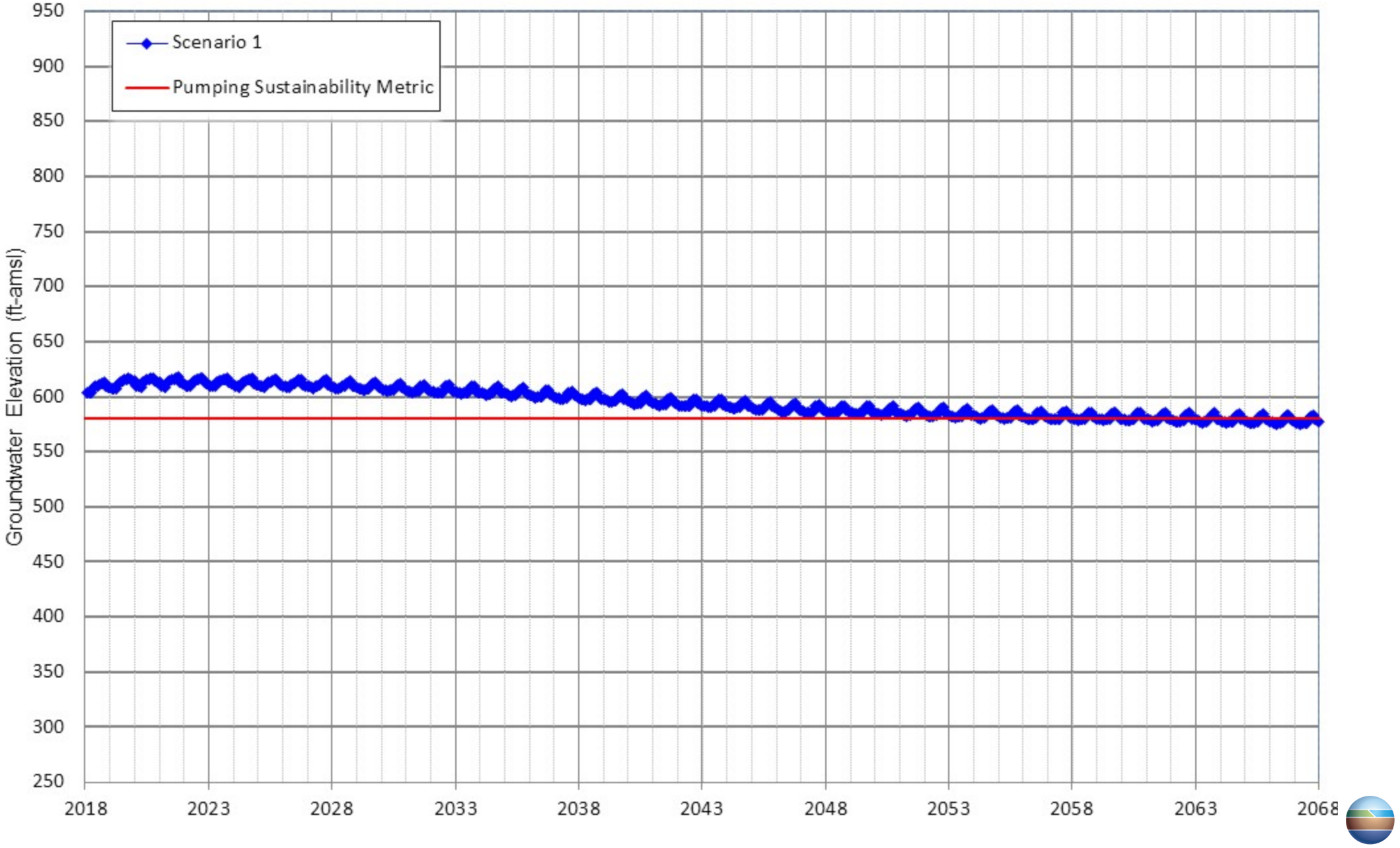

Appendix D-86
Projected Groundwater Elevation for Scenarios 1
JCSD Well 22

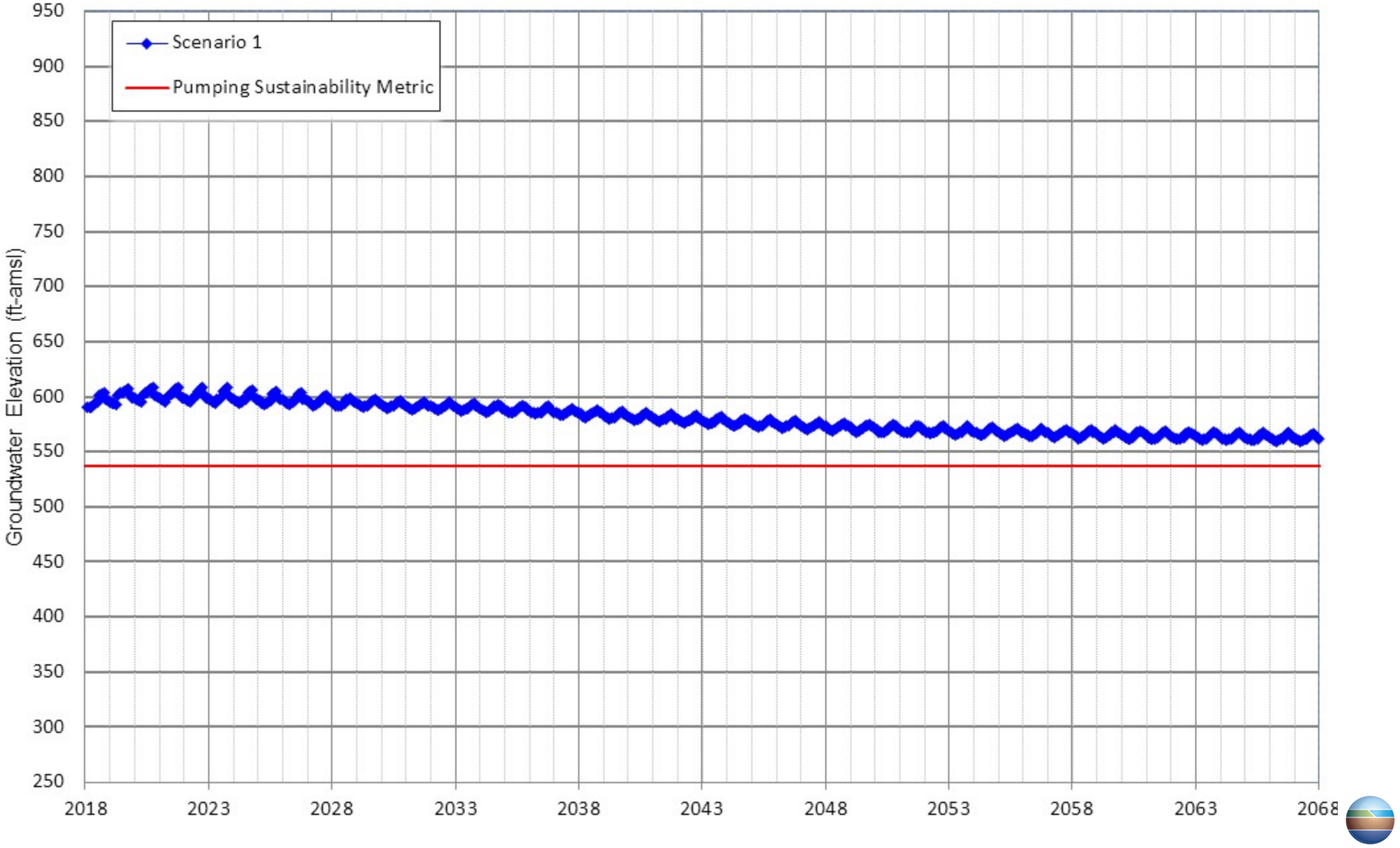

Appendix D-87
Projected Groundwater Elevation for Scenarios 1
JCSD Well 23

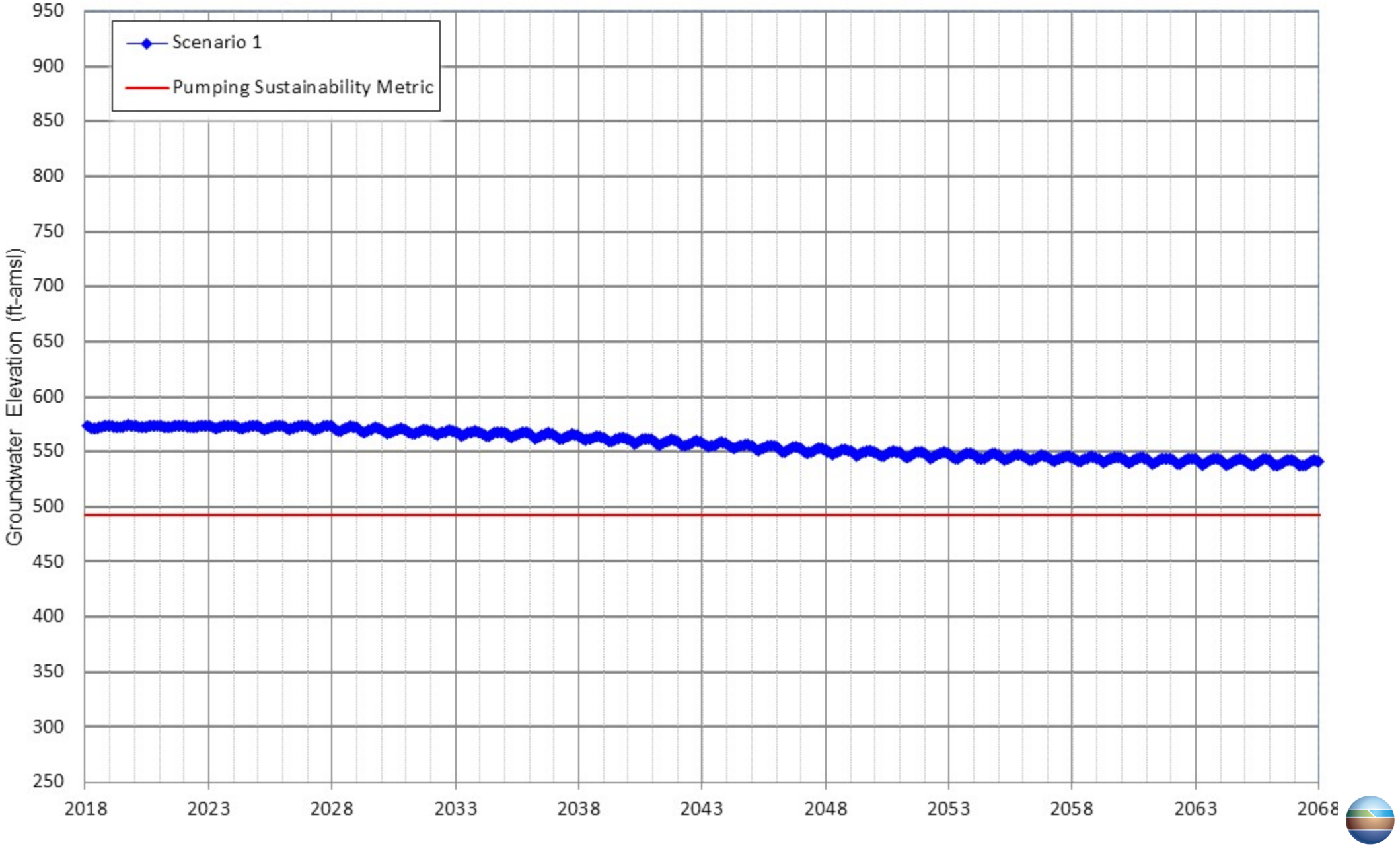

Appendix D-88
Projected Groundwater Elevation for Scenarios 1
JCSD Well 24

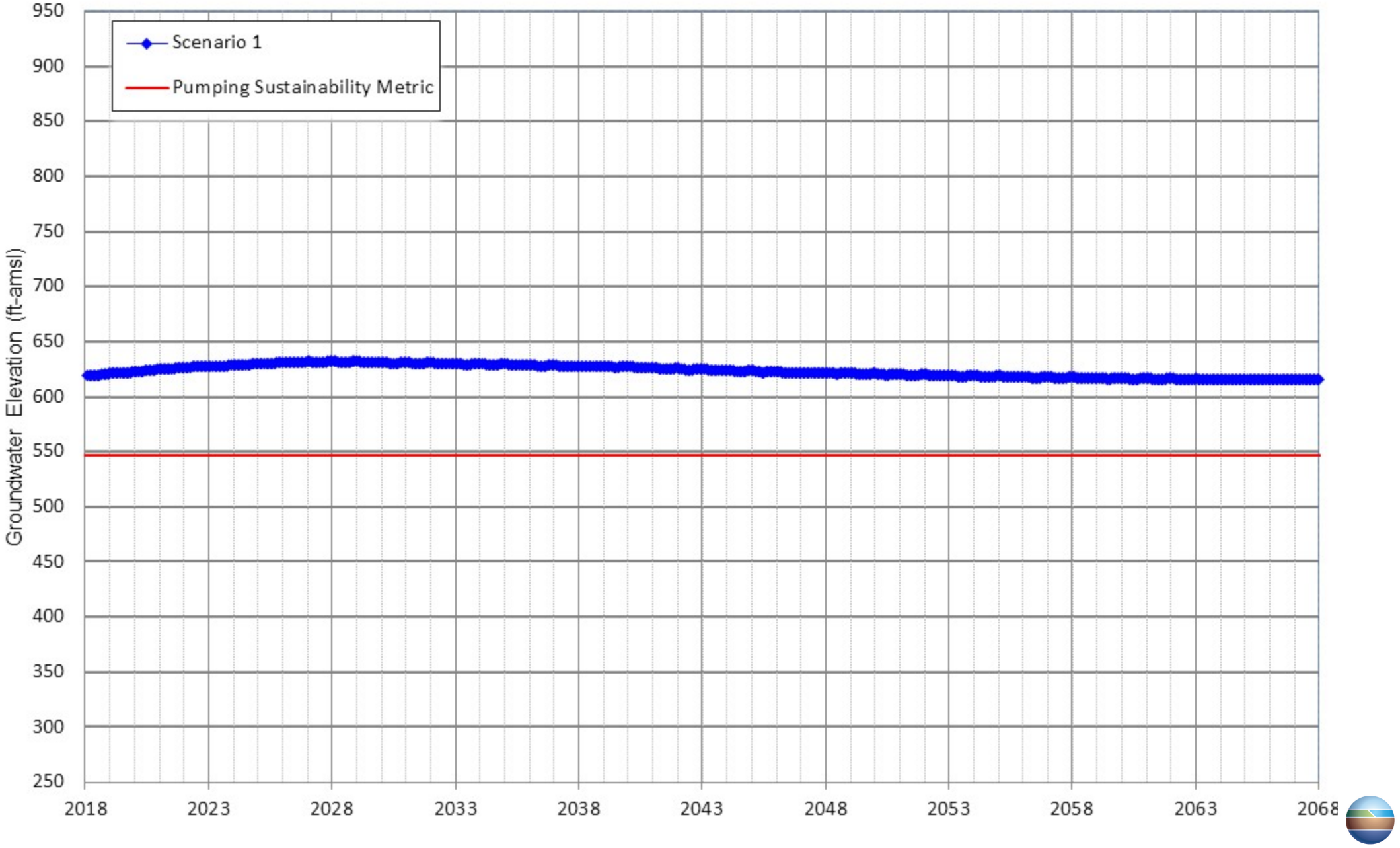

Appendix D-89
Projected Groundwater Elevation for Scenarios 1
JCSD Well 25

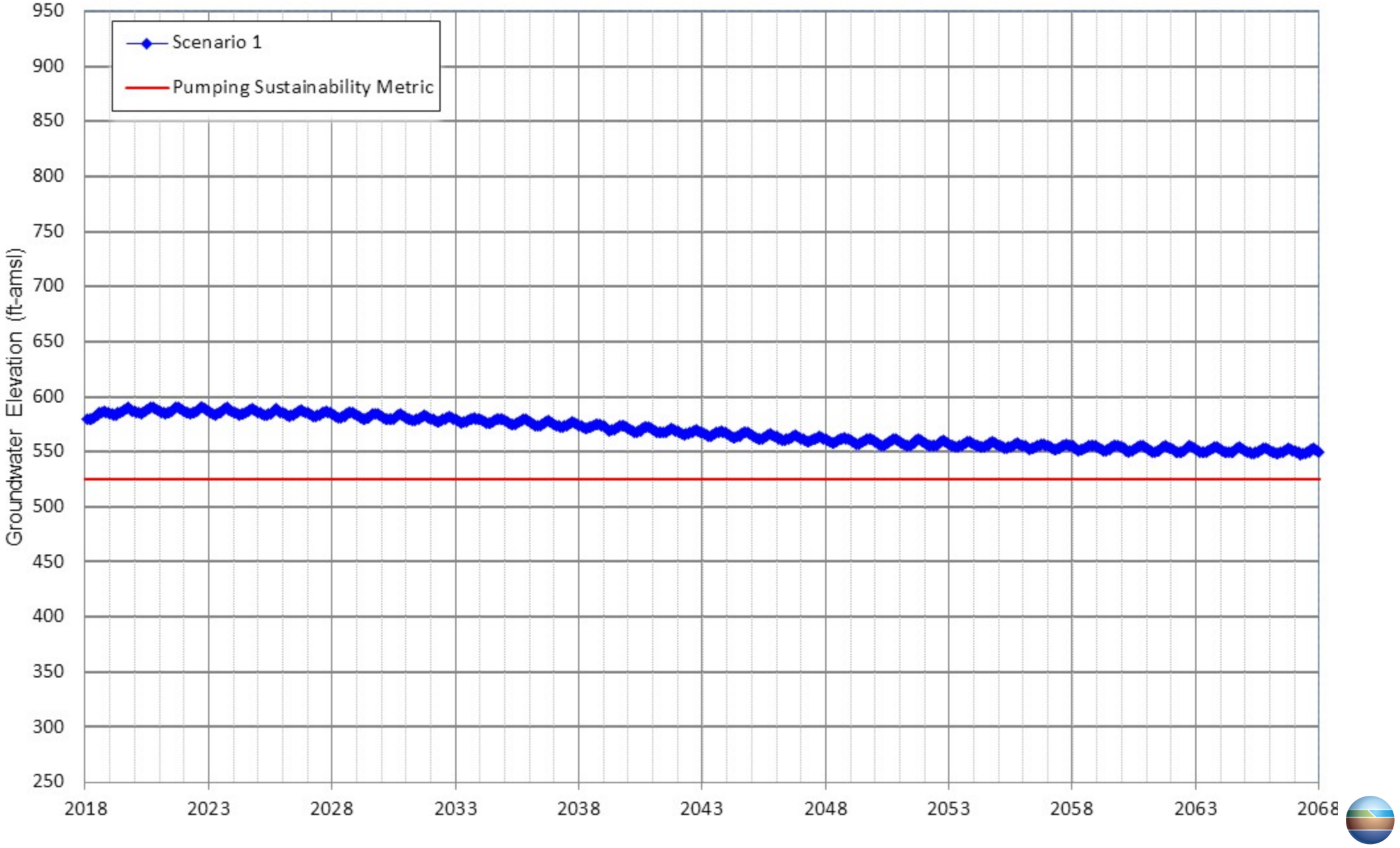

Appendix D-90
Projected Groundwater Elevation for Scenarios 1
JCSD Well 27

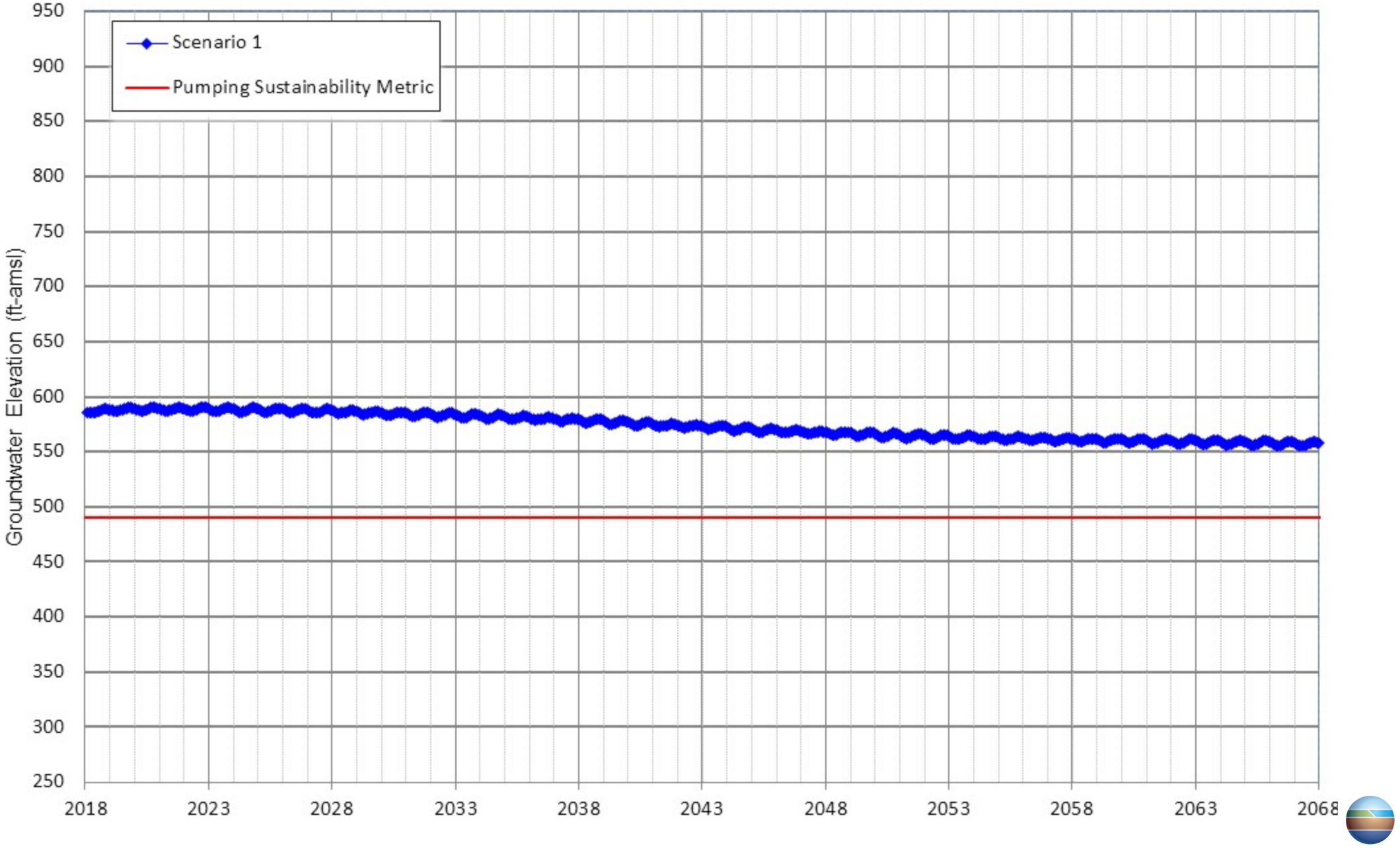

Appendix D-91
Projected Groundwater Elevation for Scenarios 1
JCSD Well 28

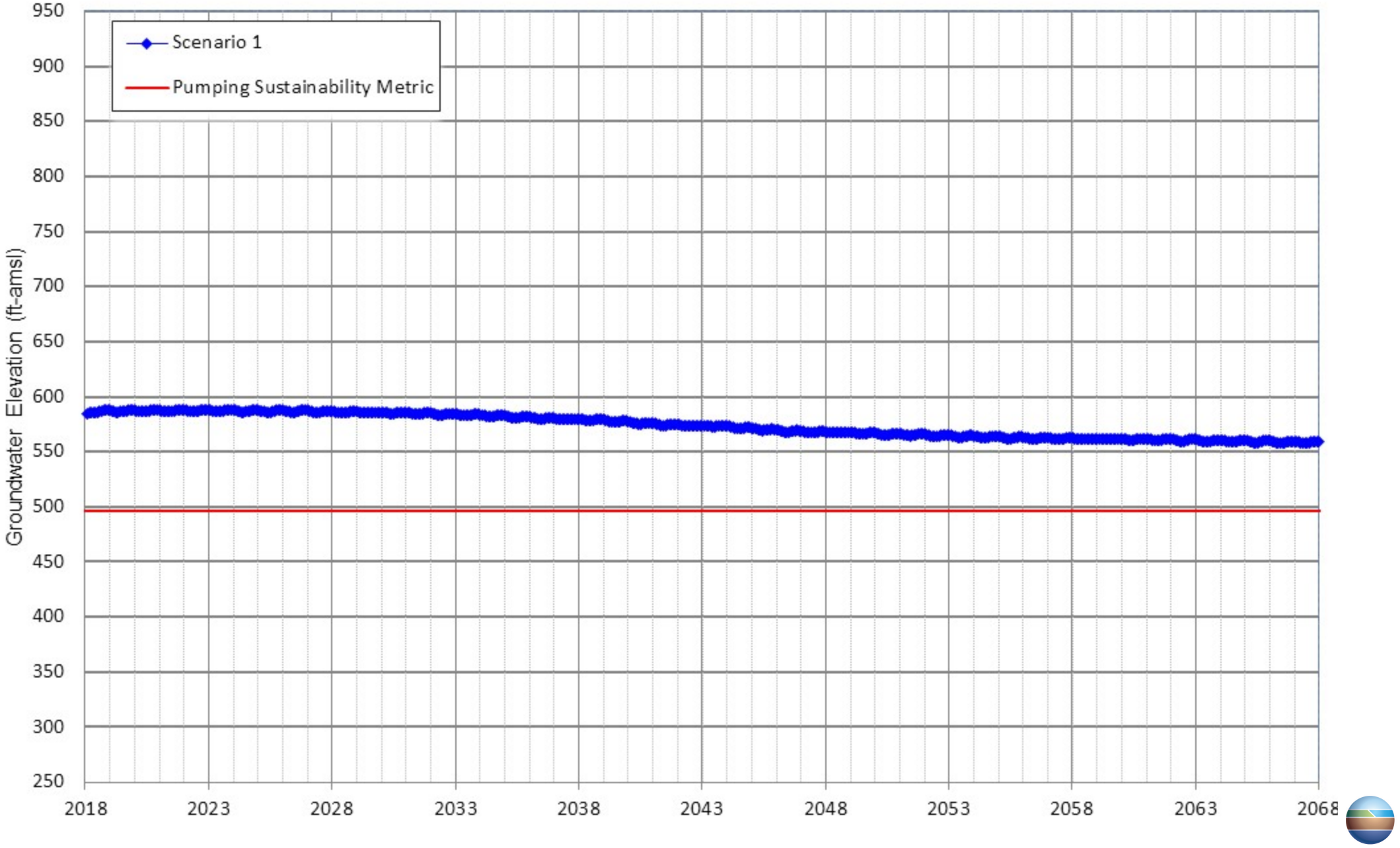

Appendix D-92
Projected Groundwater Elevation for Scenarios 1
JCSD Well IDI-1

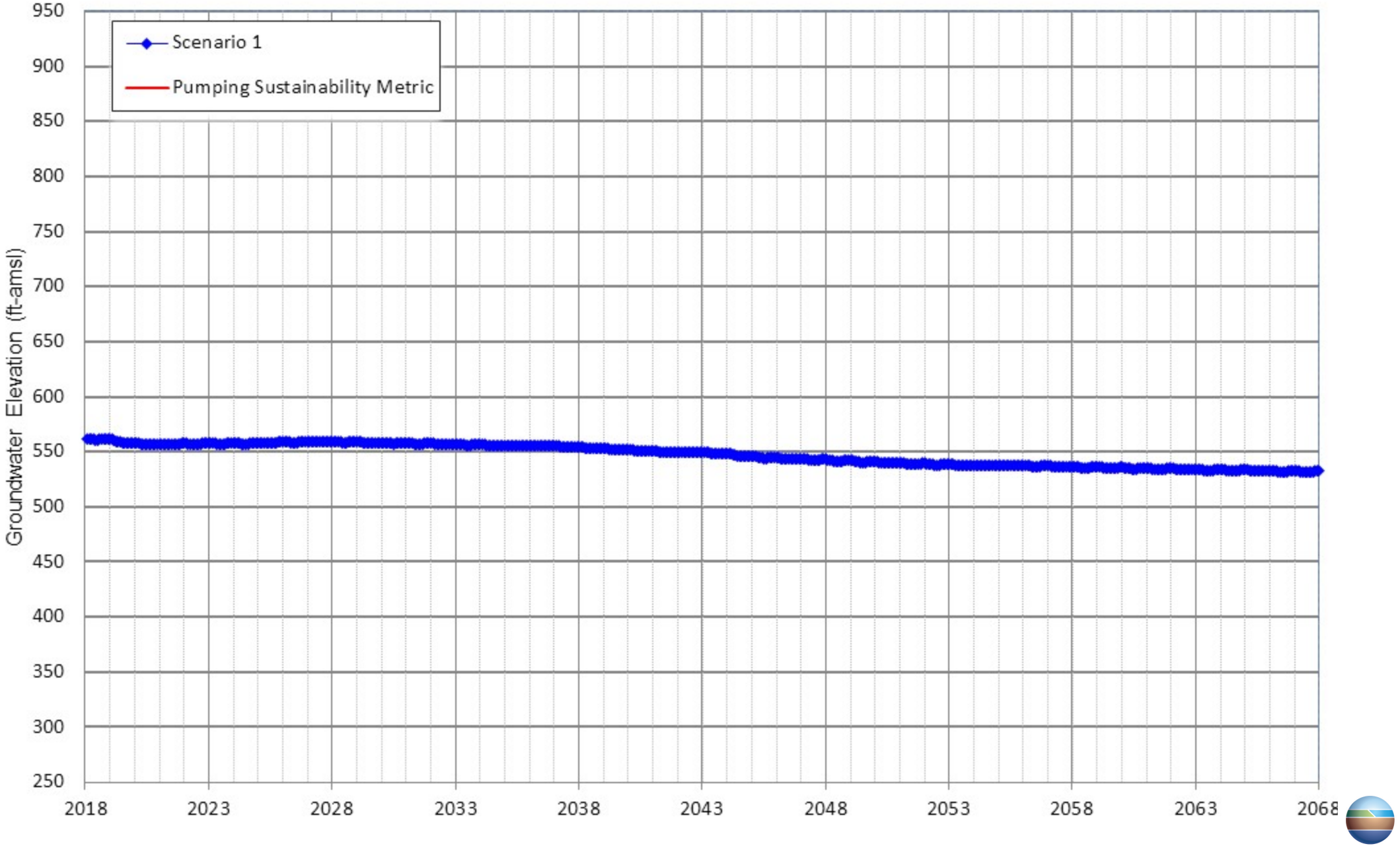

Appendix D-93
Projected Groundwater Elevation for Scenarios 1
JCSD Well IDI-2

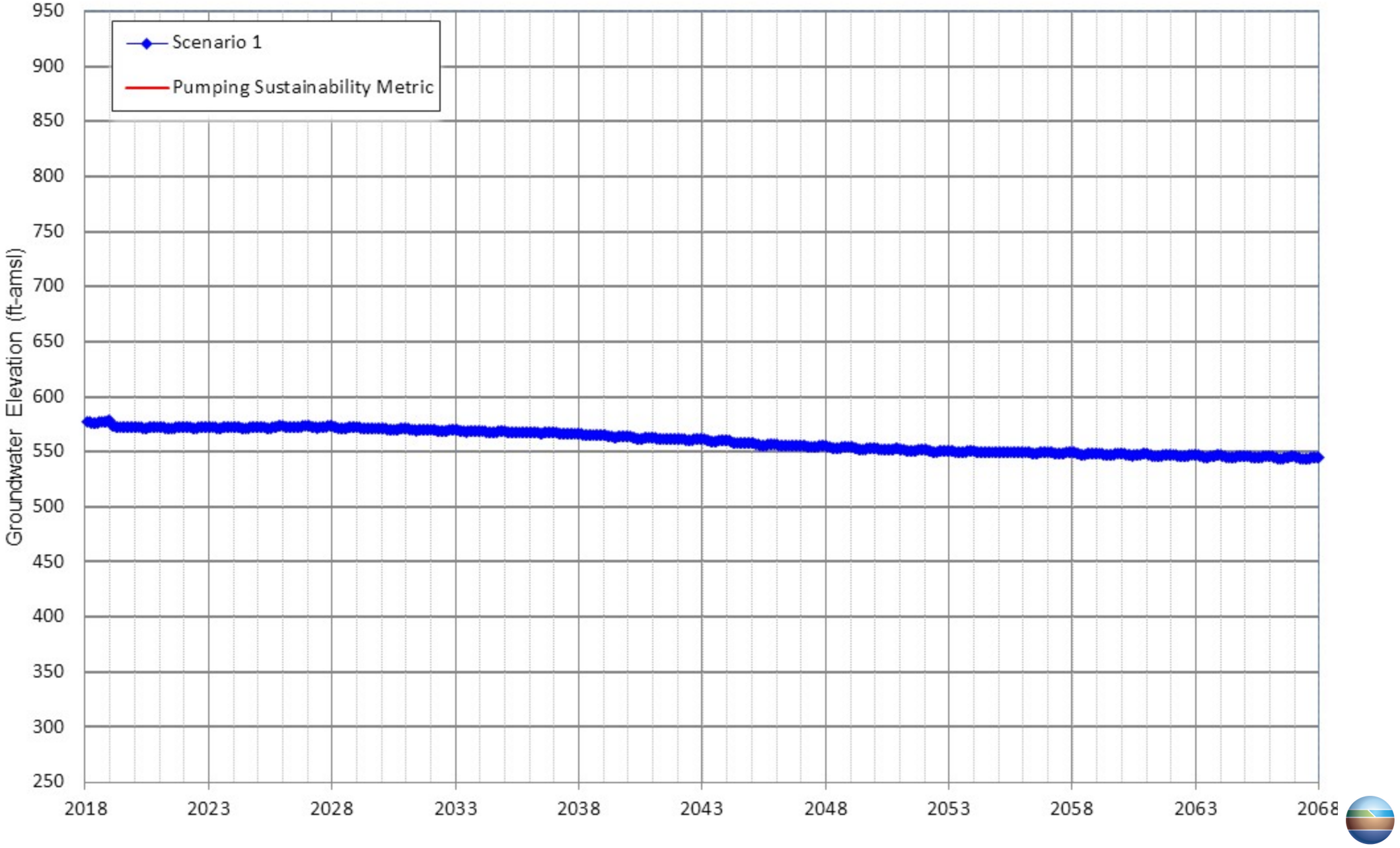

Appendix D-94
Projected Groundwater Elevation for Scenarios 1
MMWC Well 6

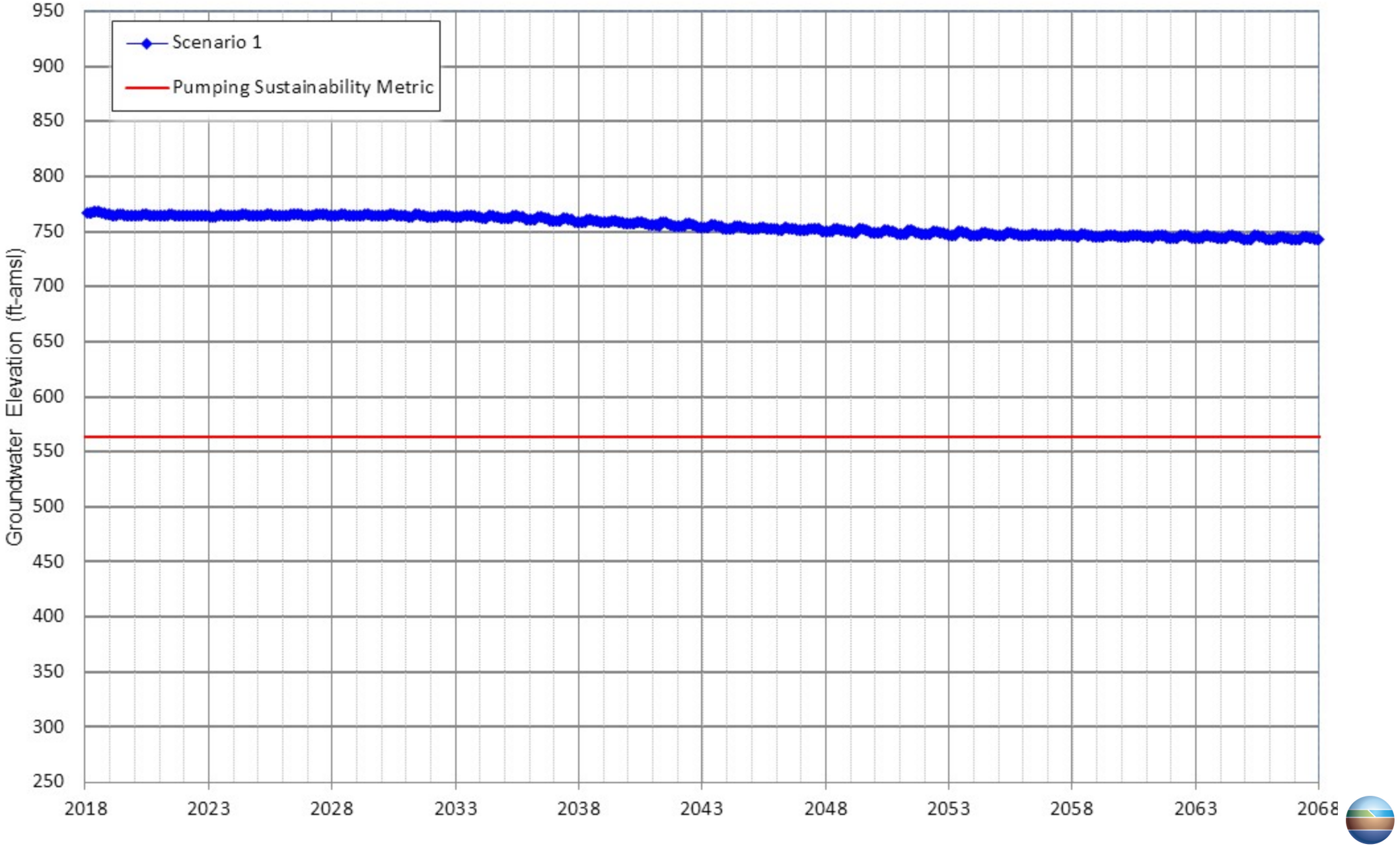

Appendix D-95
Projected Groundwater Elevation for Scenarios 1
MMWC Well 7

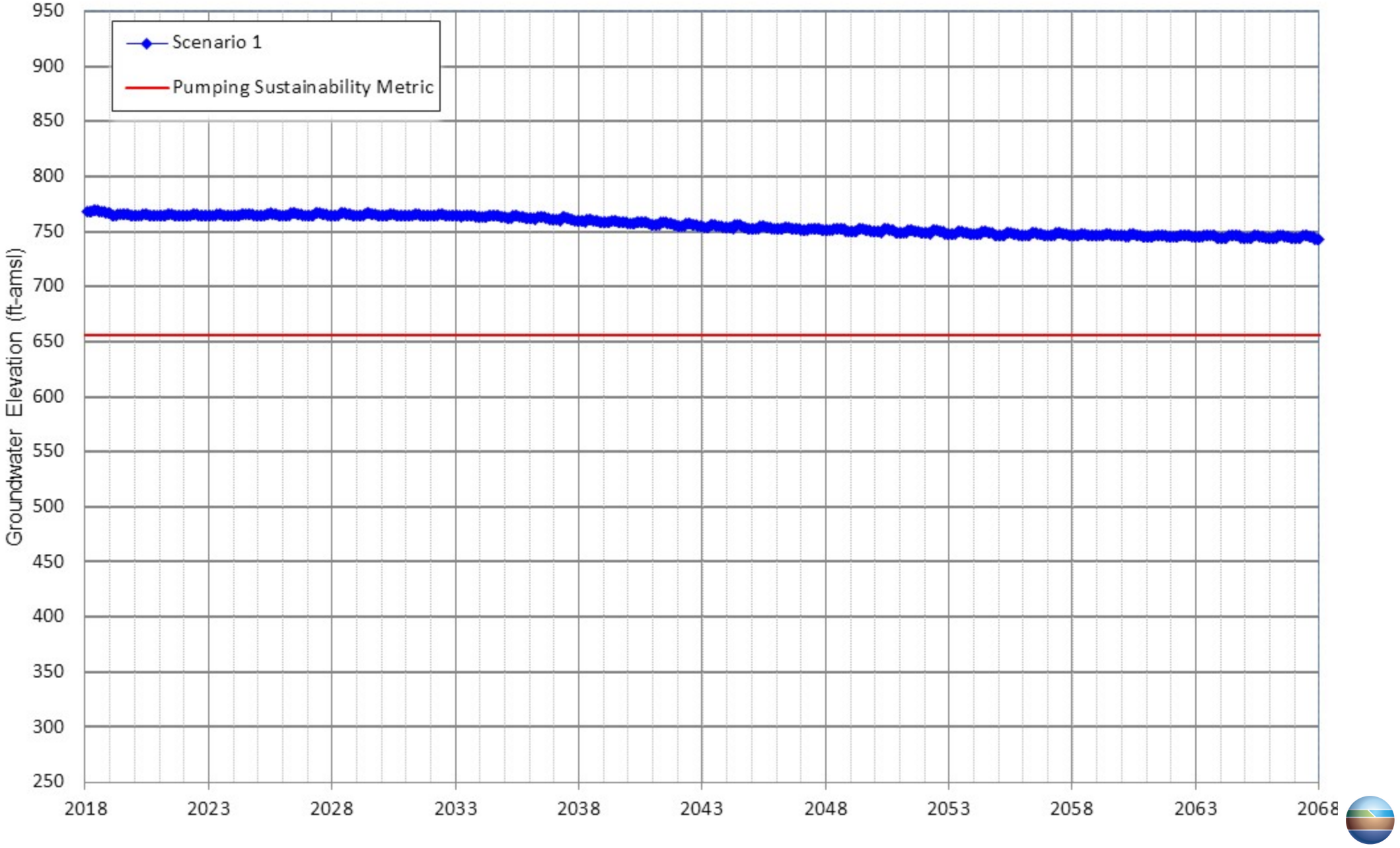

Appendix D-96
Projected Groundwater Elevation for Scenarios 1
MVWD Well 4

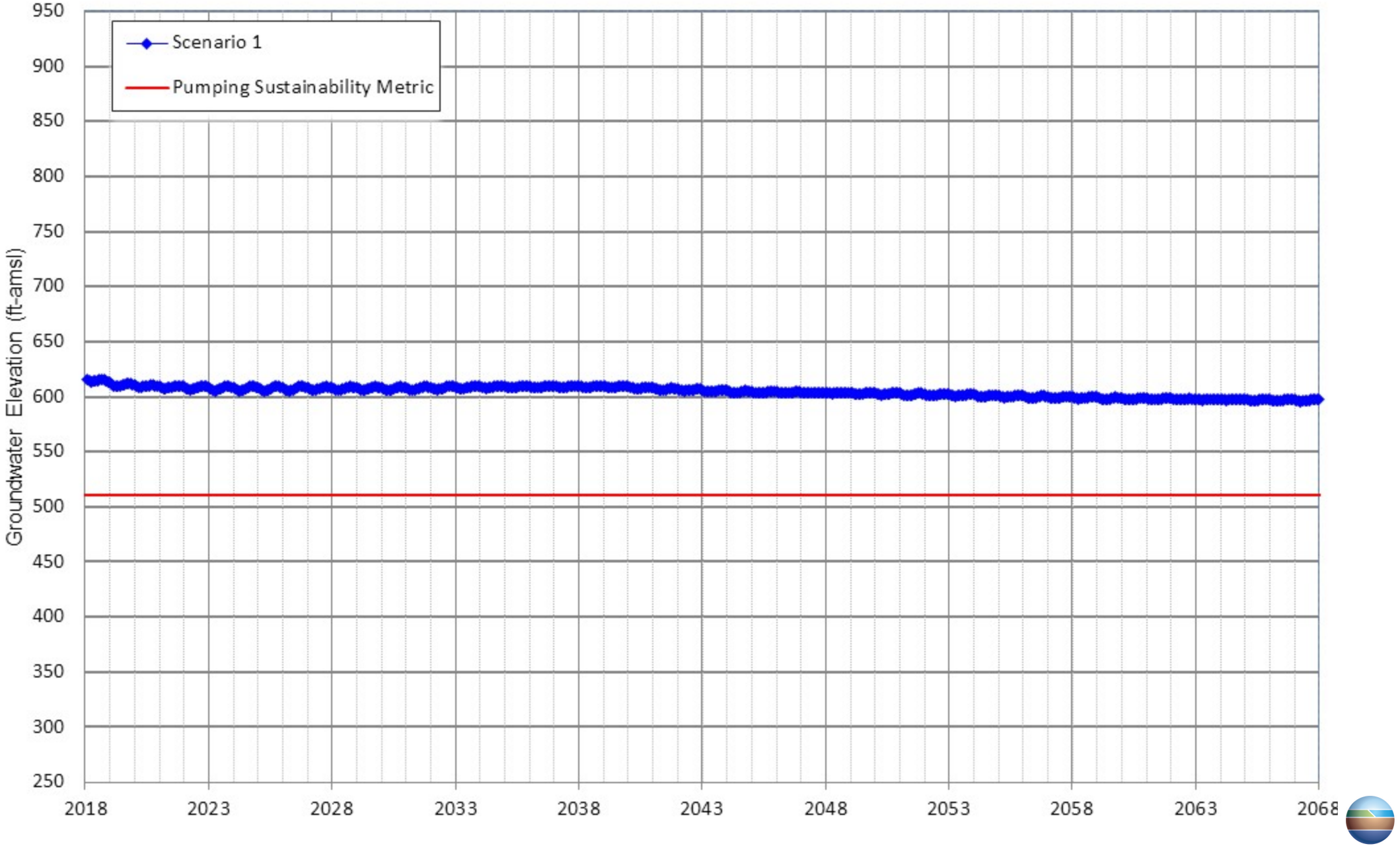

Appendix D-97
Projected Groundwater Elevation for Scenarios 1
MVWD Well 5

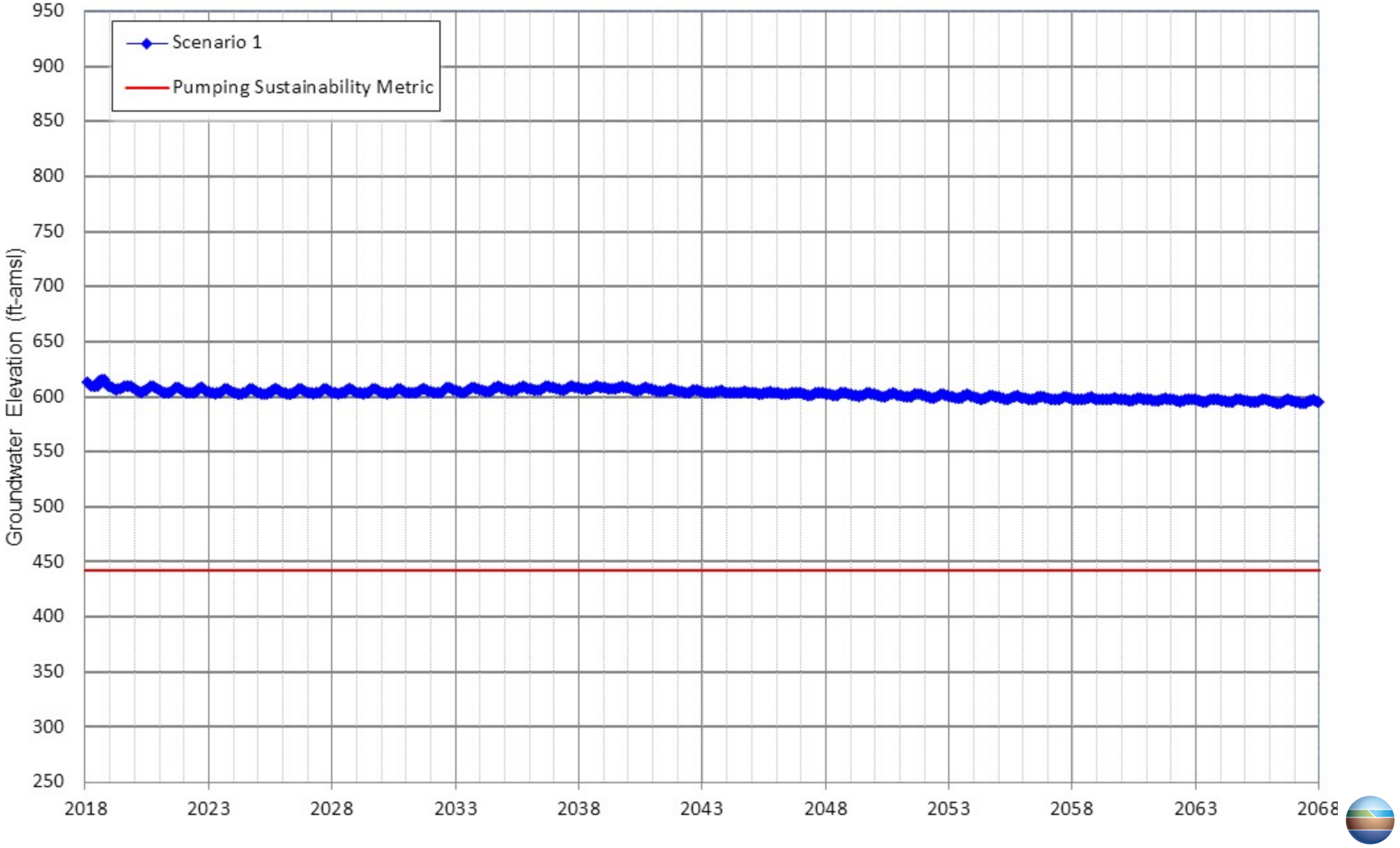

Appendix D-98
Projected Groundwater Elevation for Scenarios 1
MVWD Well 19

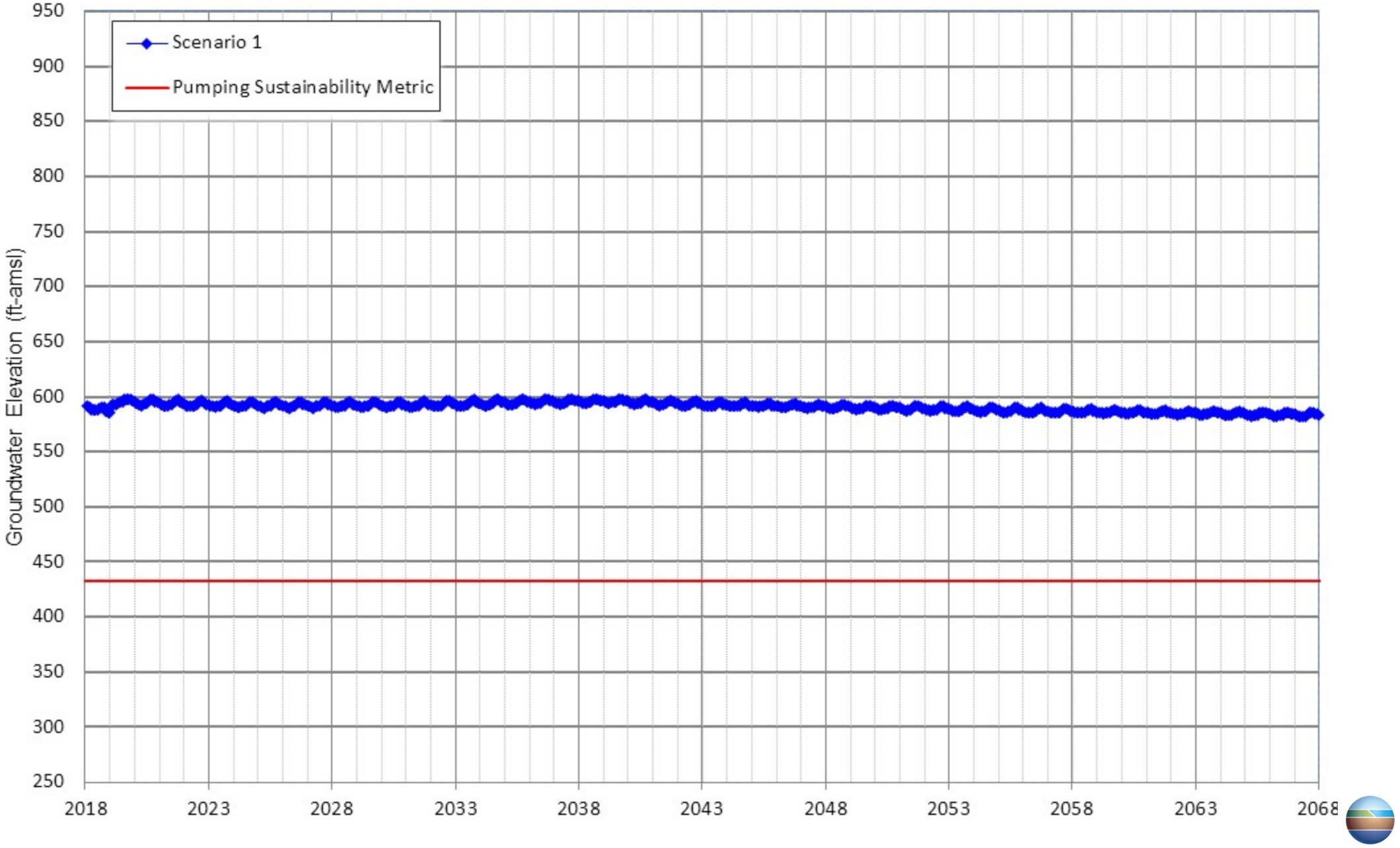

Appendix D-99
Projected Groundwater Elevation for Scenarios 1
MVWD Well 26

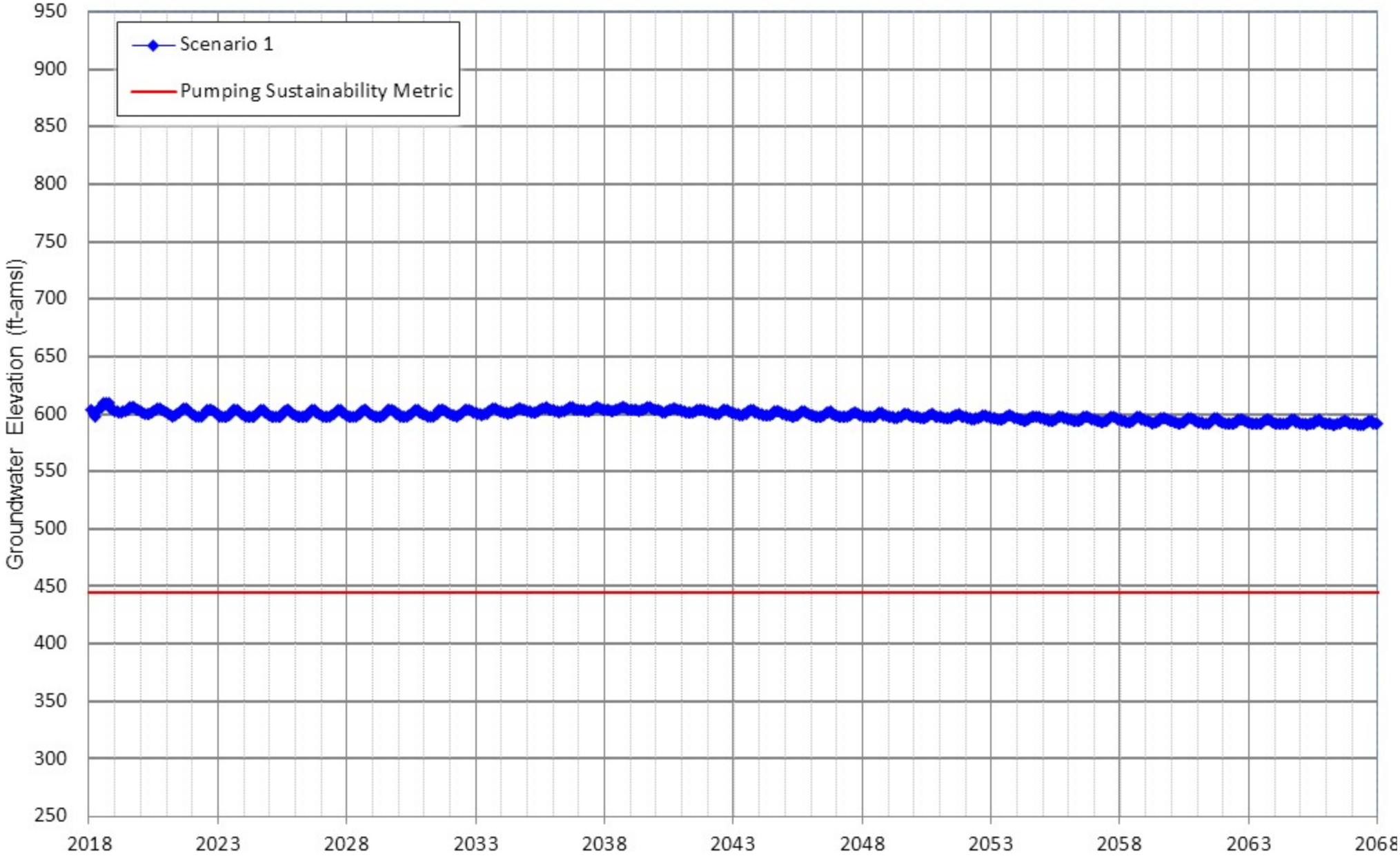

Appendix D-100
Projected Groundwater Elevation for Scenarios 1
MVWD Well 27

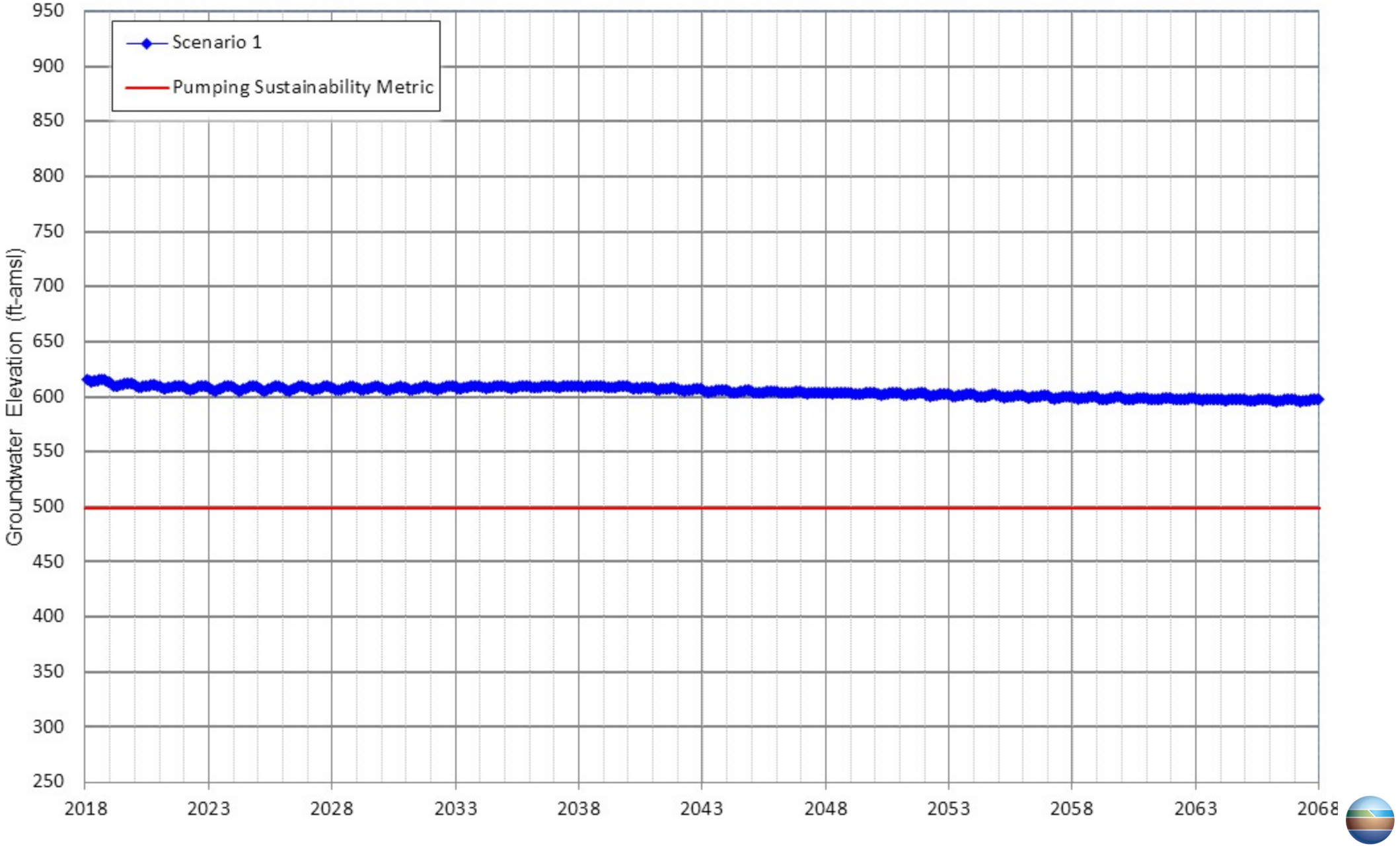

Appendix D-101
Projected Groundwater Elevation for Scenarios 1
MVWD Well 28

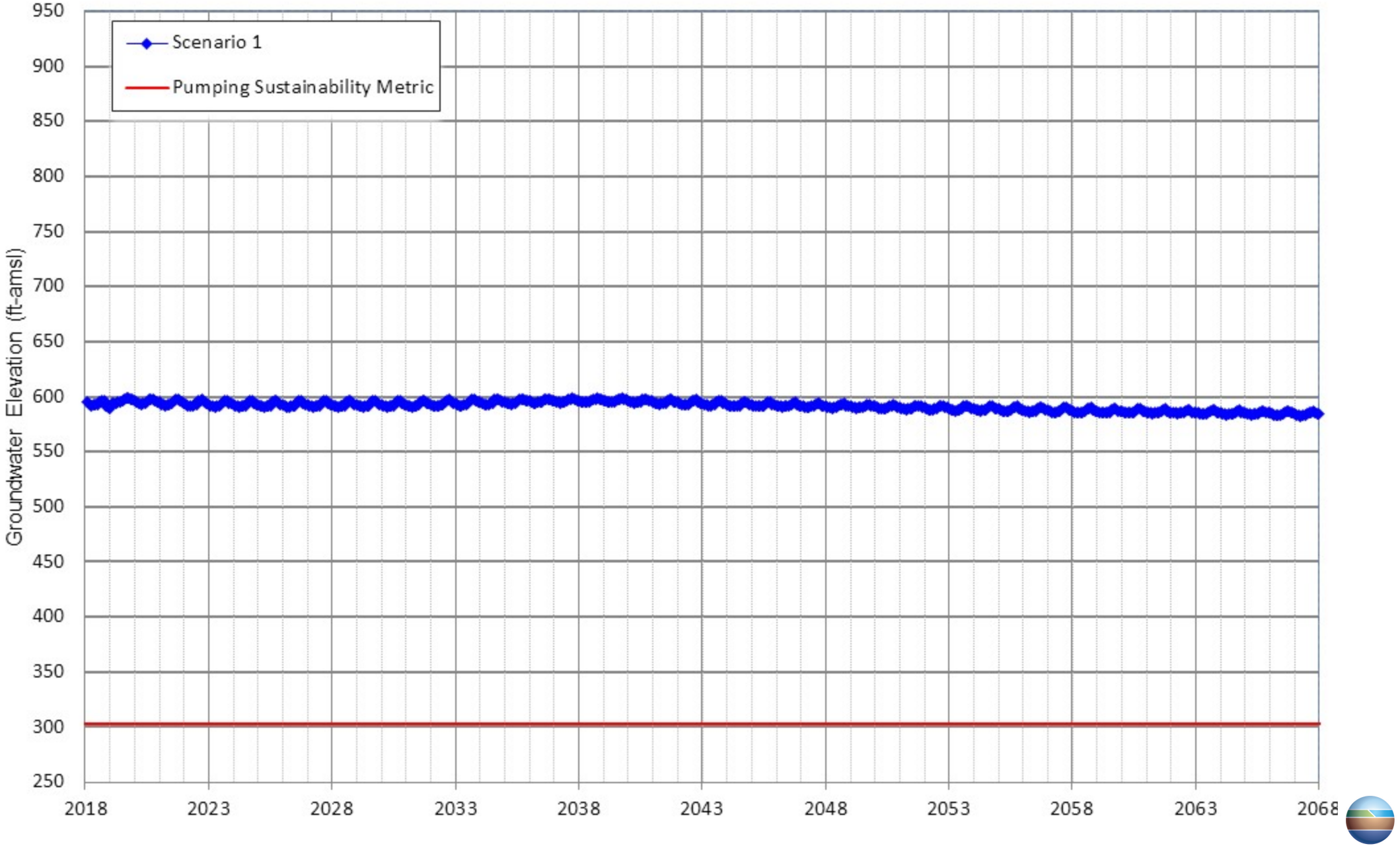

Appendix D-102
Projected Groundwater Elevation for Scenarios 1
MVWD Well 30

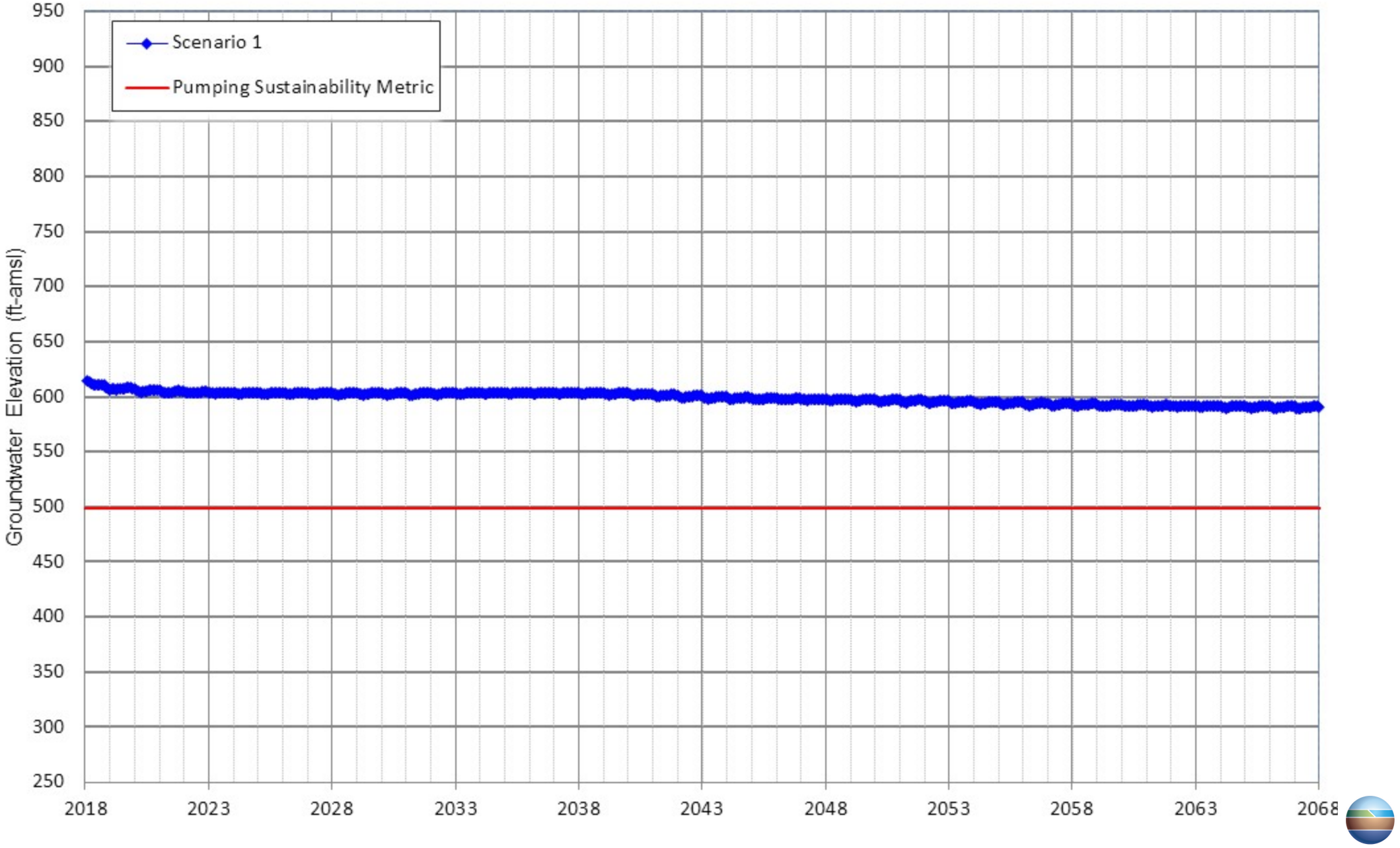

Appendix D-103
Projected Groundwater Elevation for Scenarios 1
MVWD Well 31

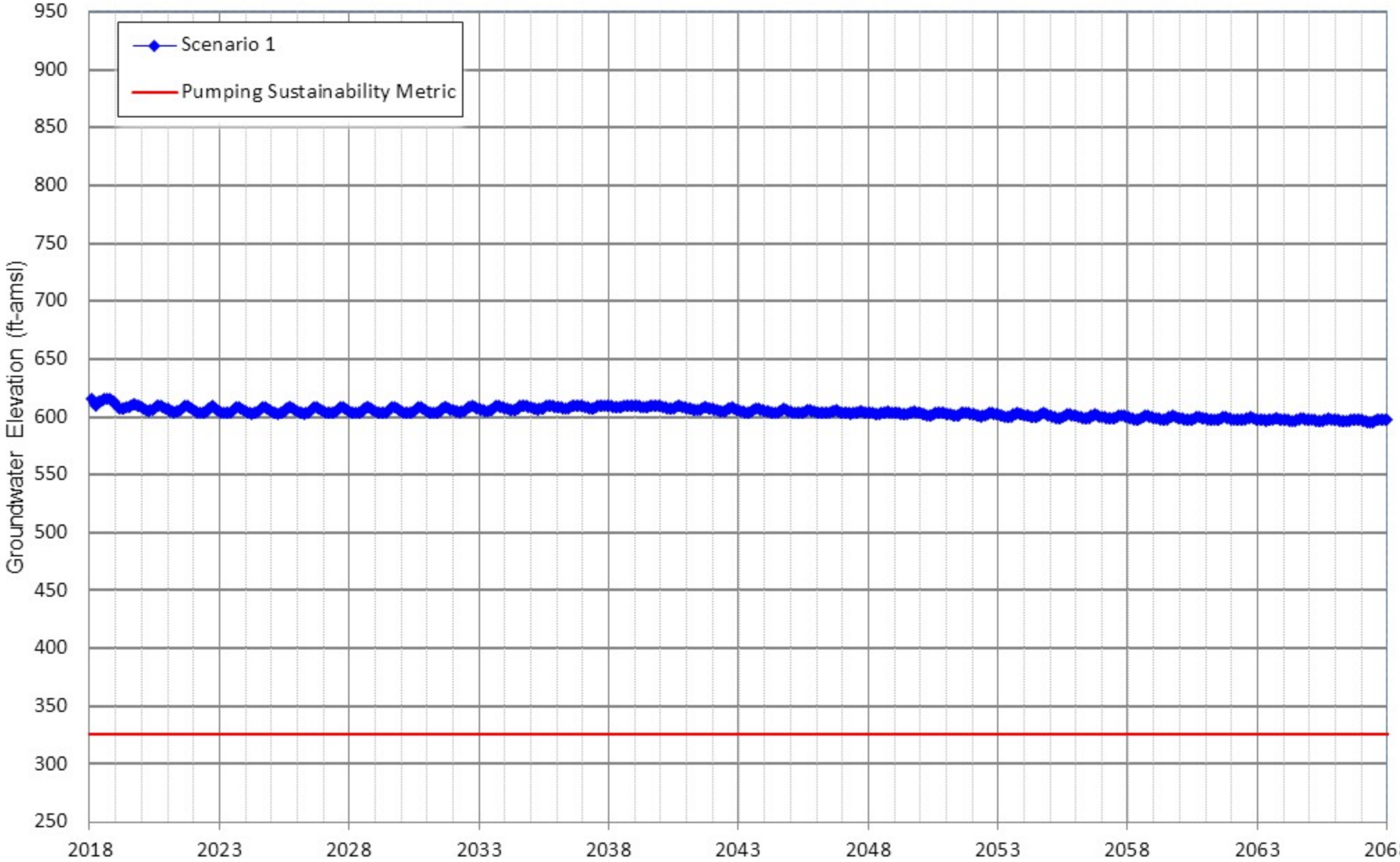

Appendix D-104
Projected Groundwater Elevation for Scenarios 1
MVWD Well 32

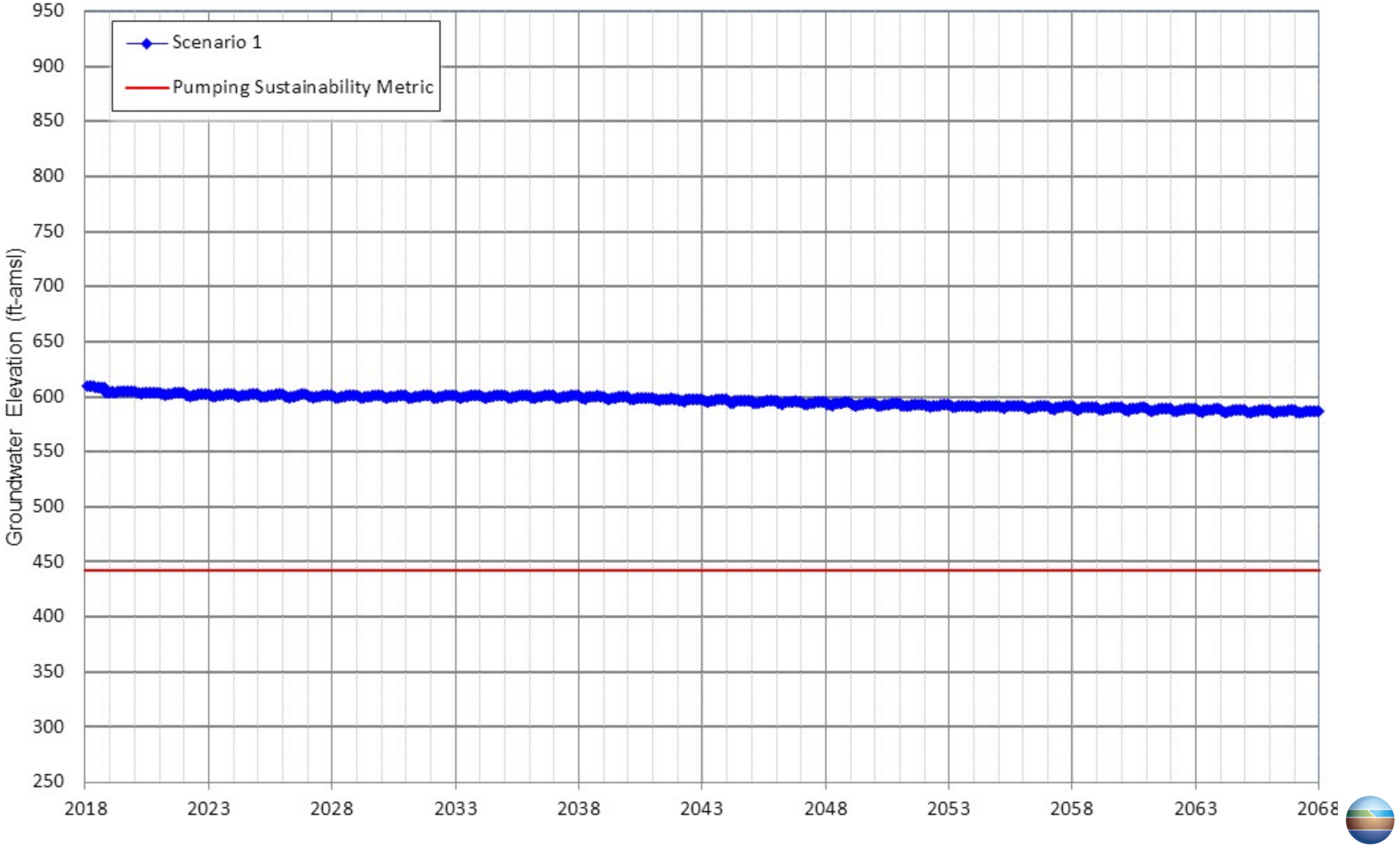

Appendix D-105
Projected Groundwater Elevation for Scenarios 1
MVWD Well 33

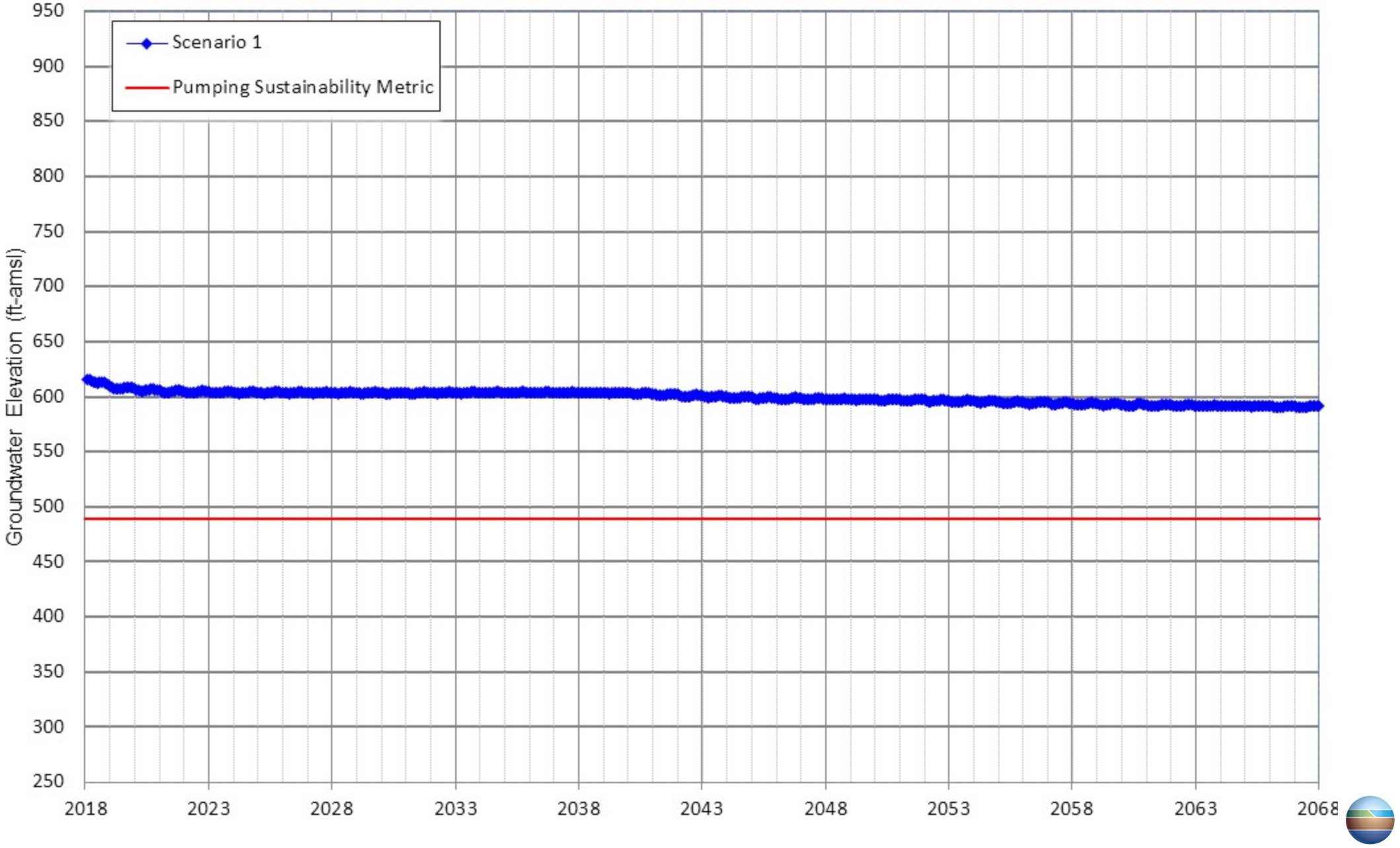

Appendix D-106
Projected Groundwater Elevation for Scenarios 1
MVWD Well 34

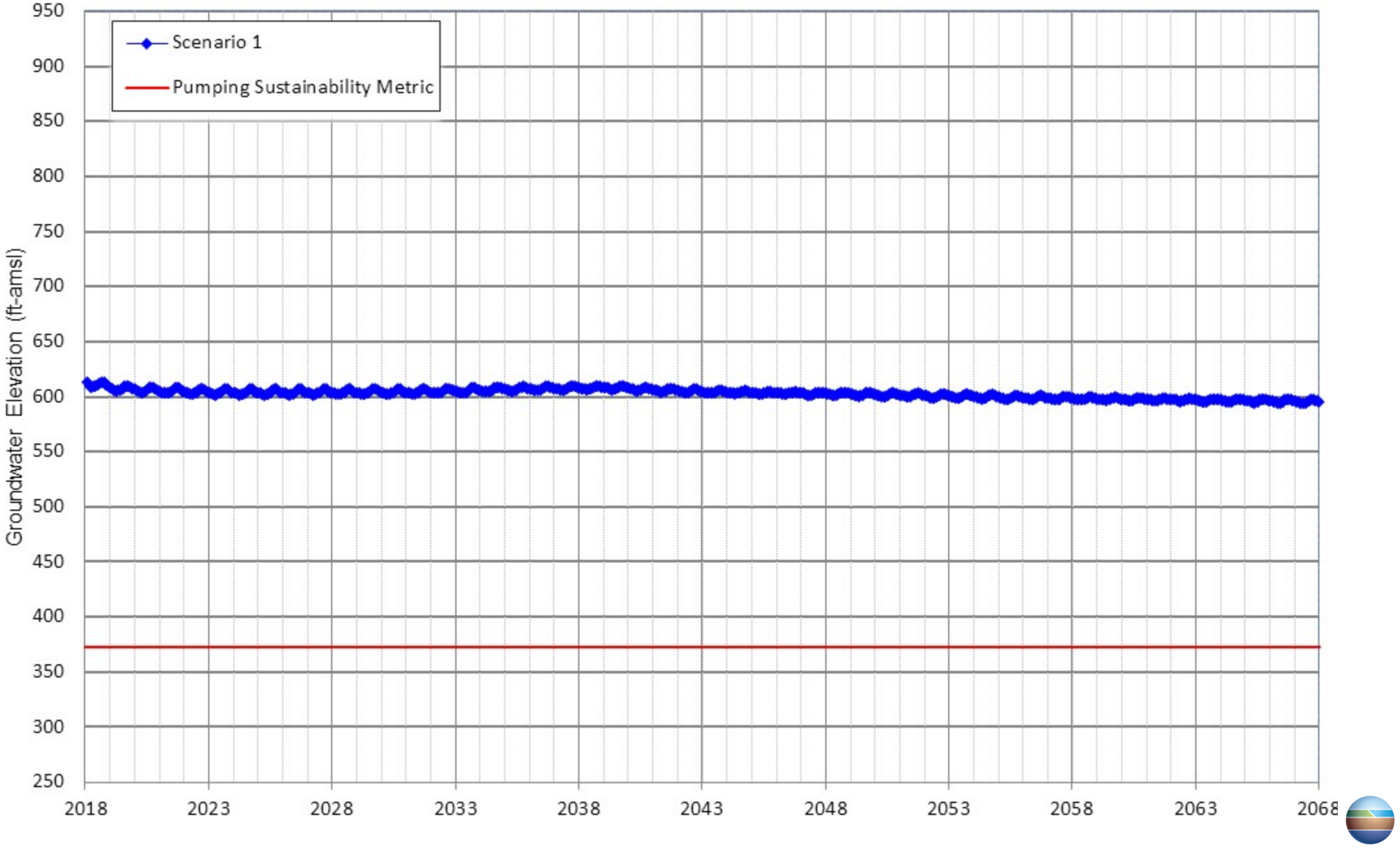

Appendix D-107
Projected Groundwater Elevation for Scenarios 1
City of Ontario Well 24

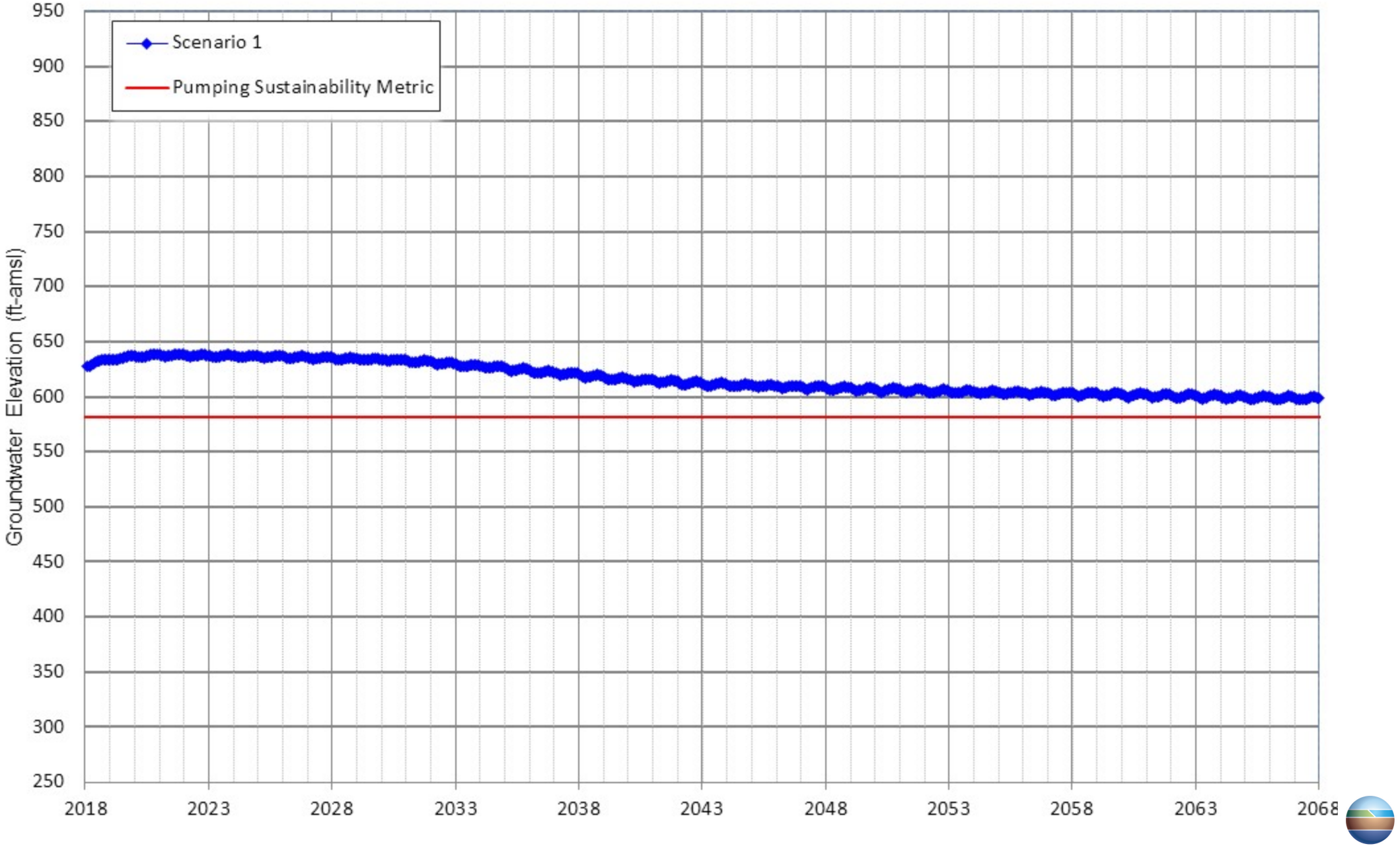

Appendix D-108
Projected Groundwater Elevation for Scenarios 1
City of Ontario Well 25

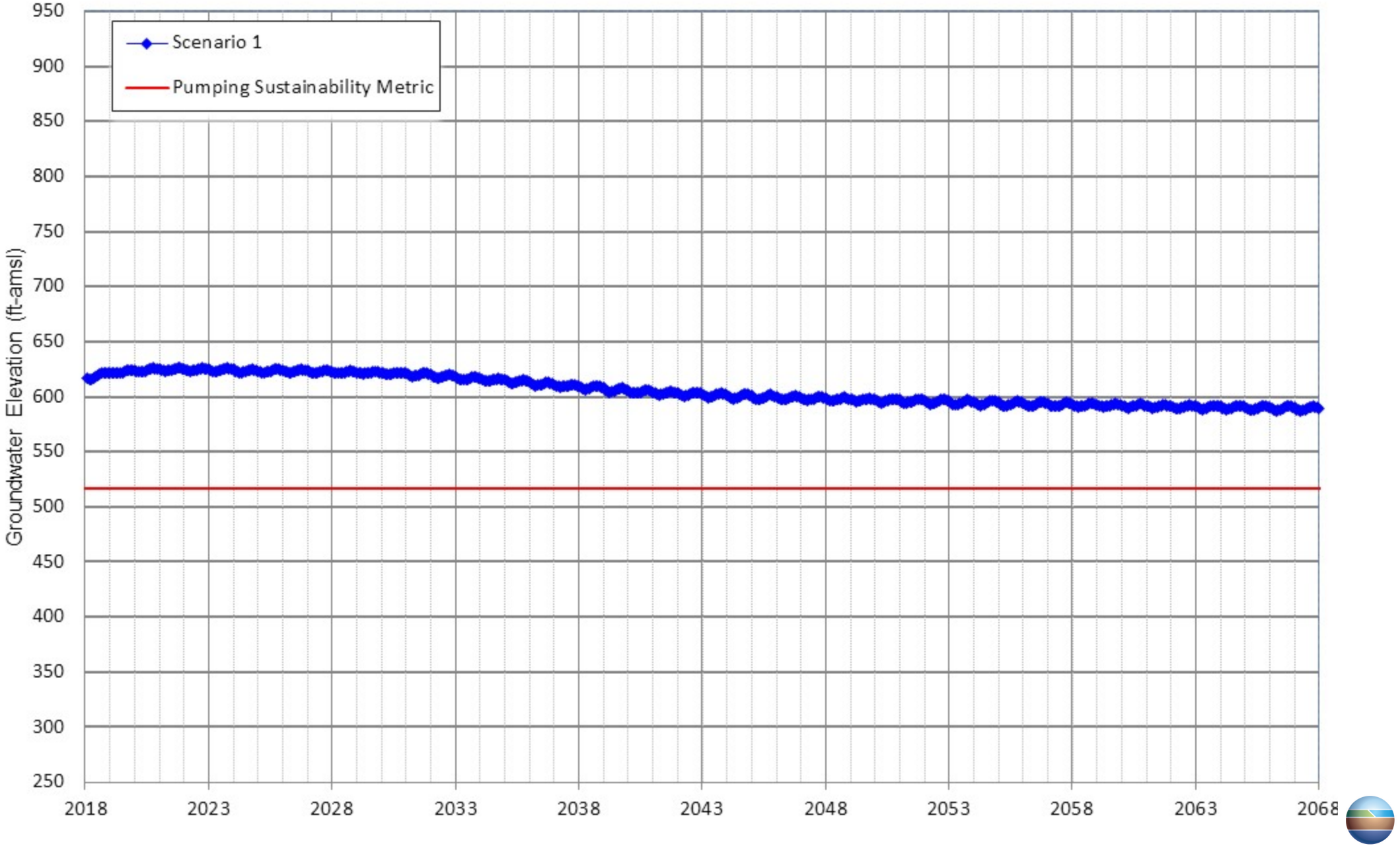

Appendix D-109
Projected Groundwater Elevation for Scenarios 1
City of Ontario Well 29

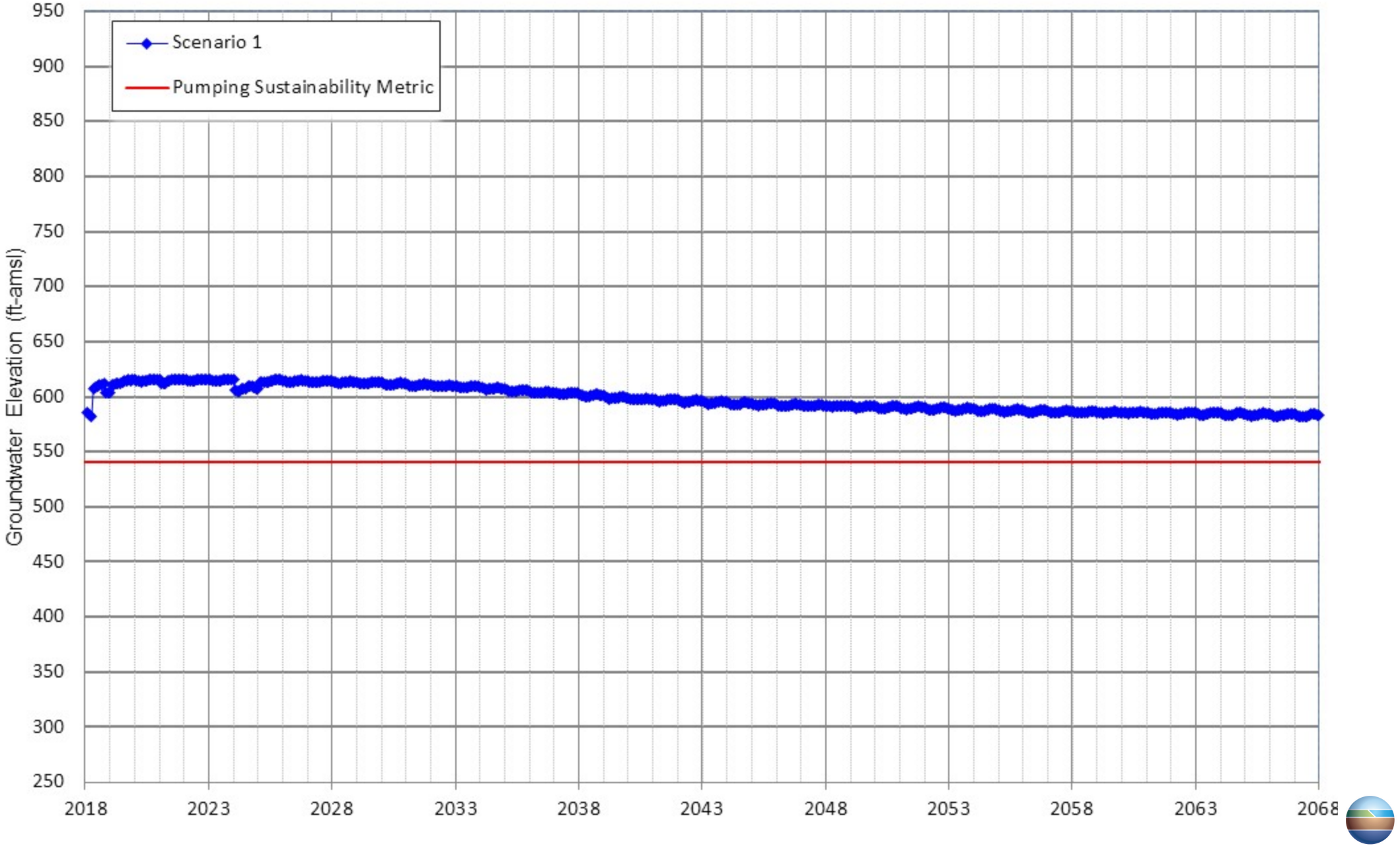

Appendix D-110
Projected Groundwater Elevation for Scenarios 1
City of Ontario Well 30

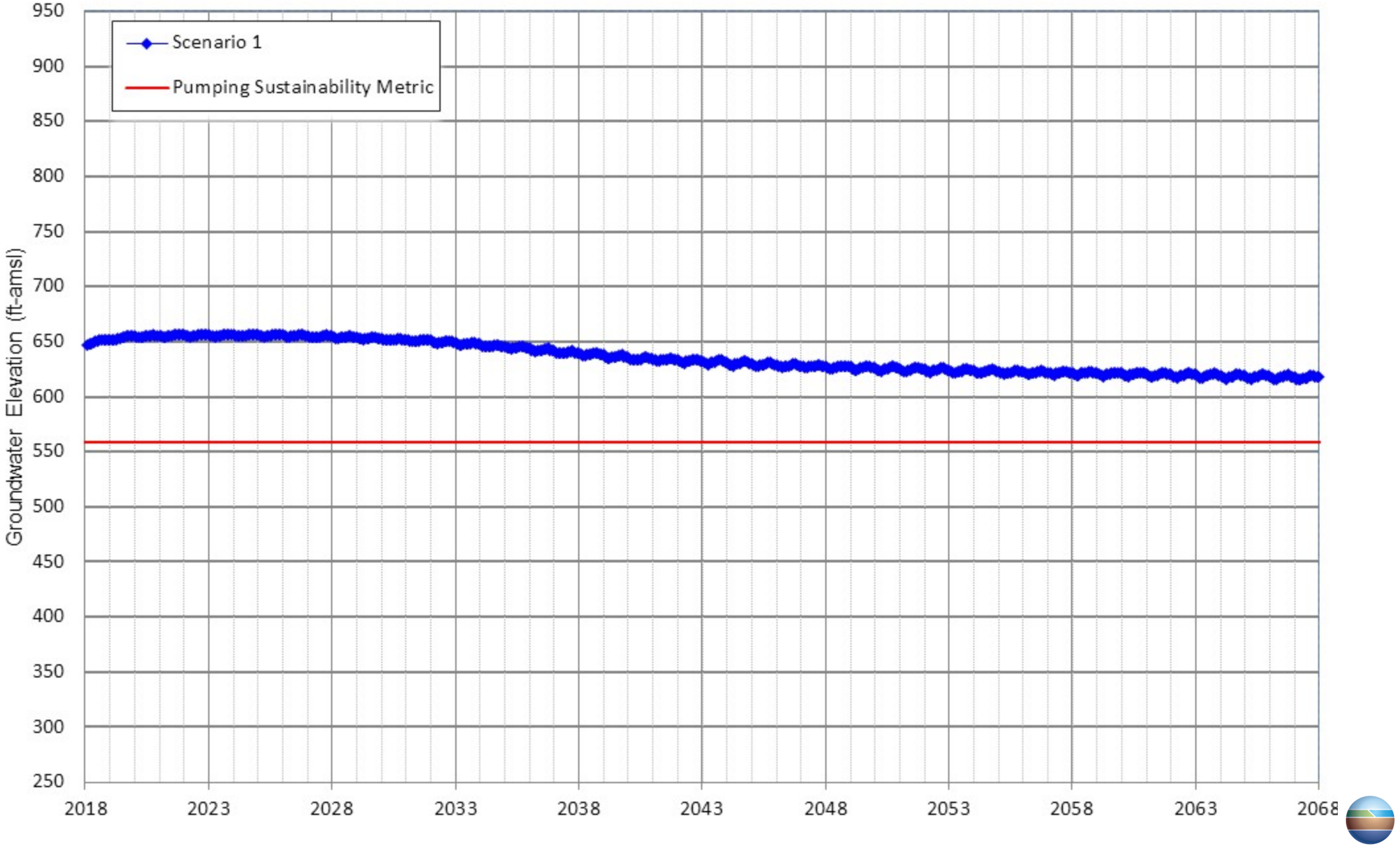

Appendix D-111
Projected Groundwater Elevation for Scenarios 1
City of Ontario Well 31

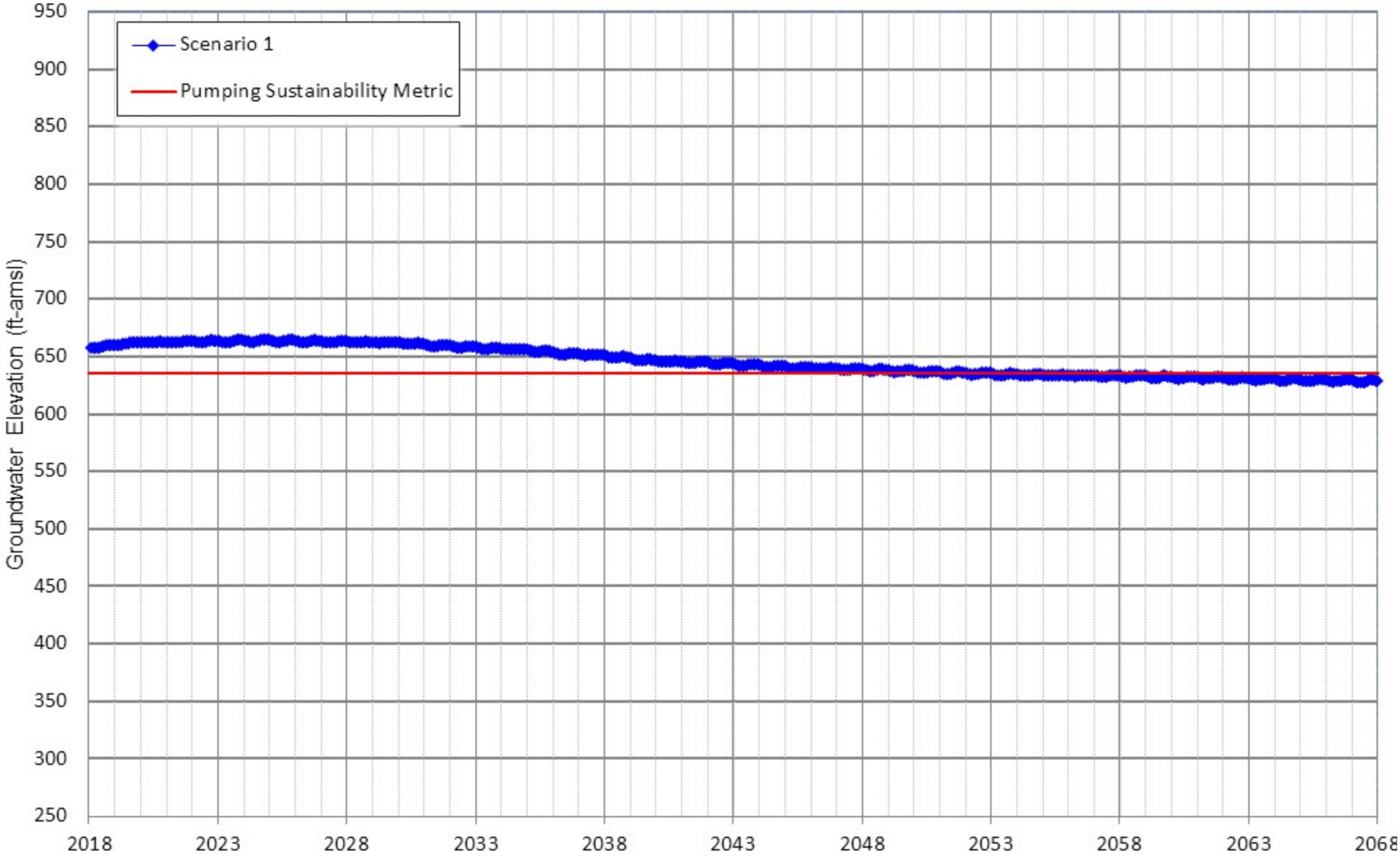

Appendix D-112
Projected Groundwater Elevation for Scenarios 1
City of Ontario Well 34

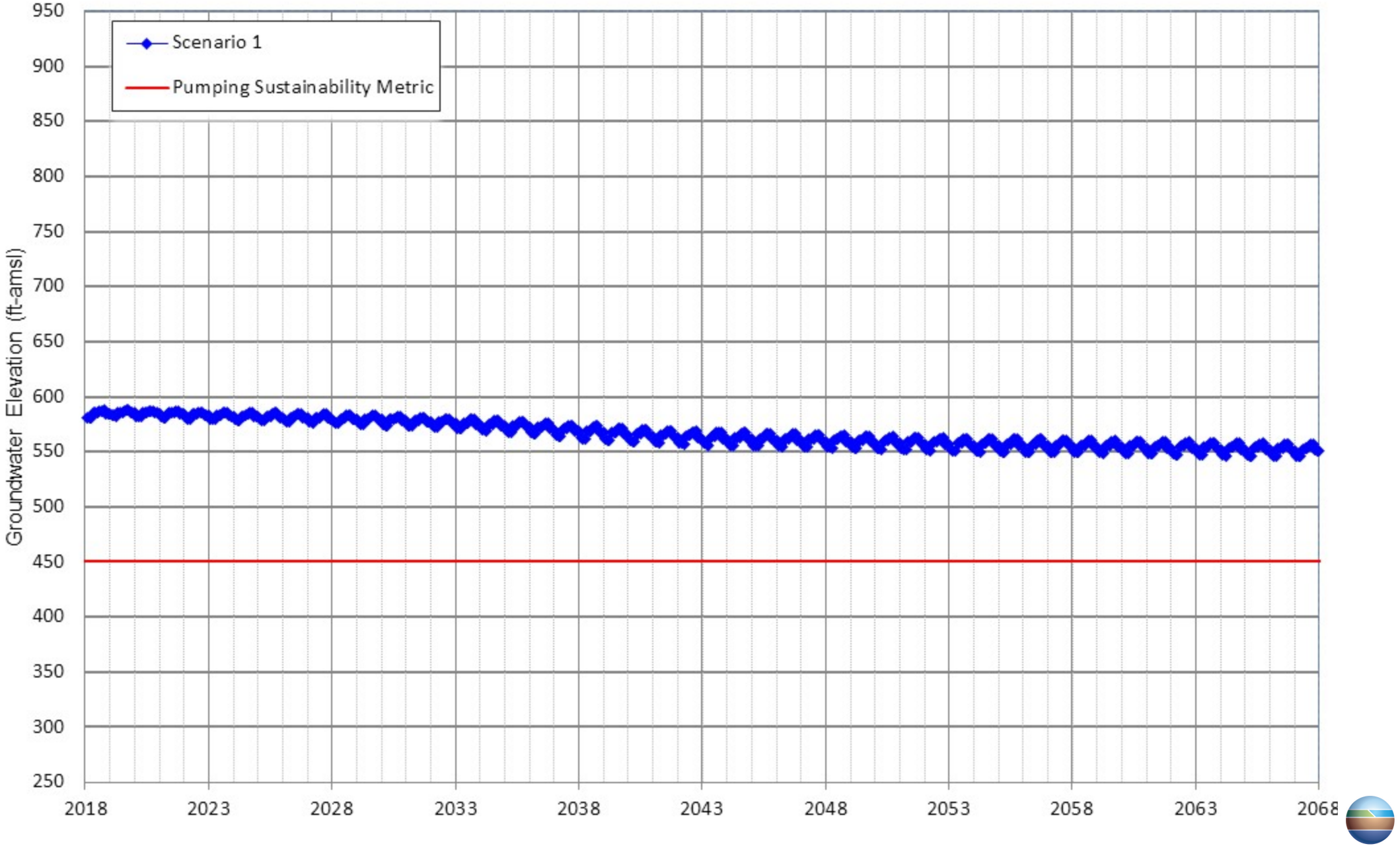

Appendix D-113
Projected Groundwater Elevation for Scenarios 1
City of Ontario Well 35

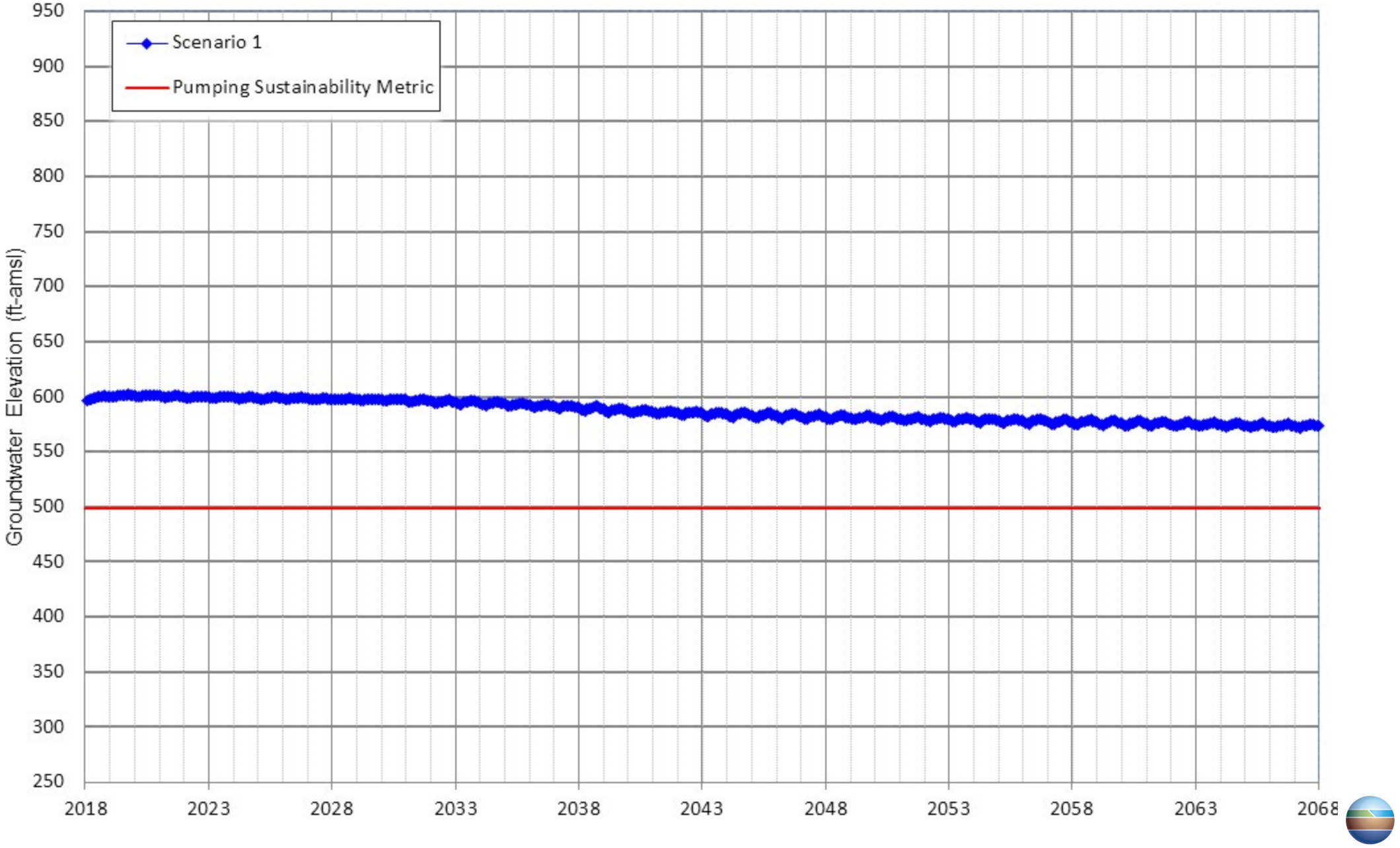

Appendix D-114
Projected Groundwater Elevation for Scenarios 1
City of Ontario Well 36

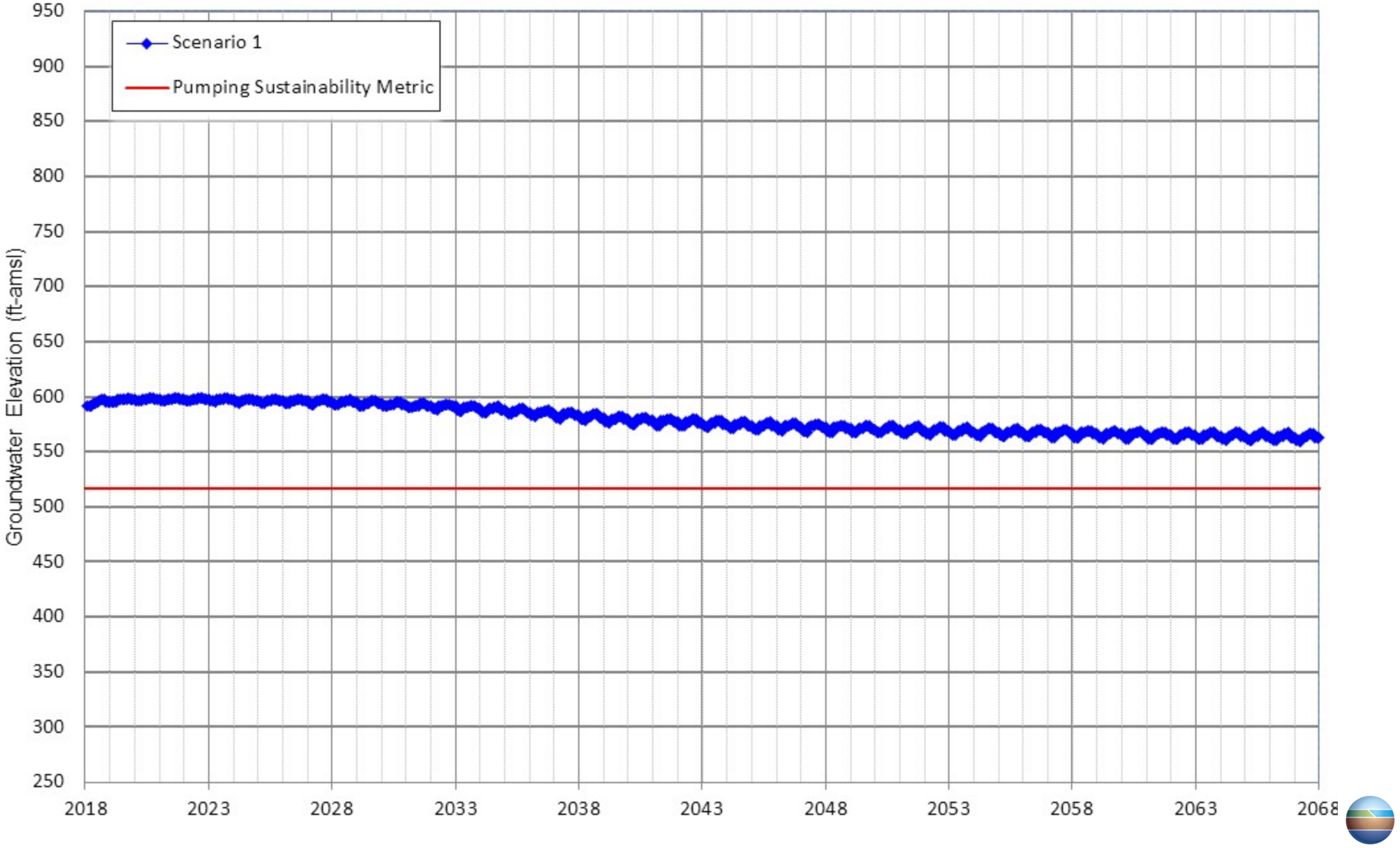

Appendix D-115
Projected Groundwater Elevation for Scenarios 1
City of Ontario Well 37

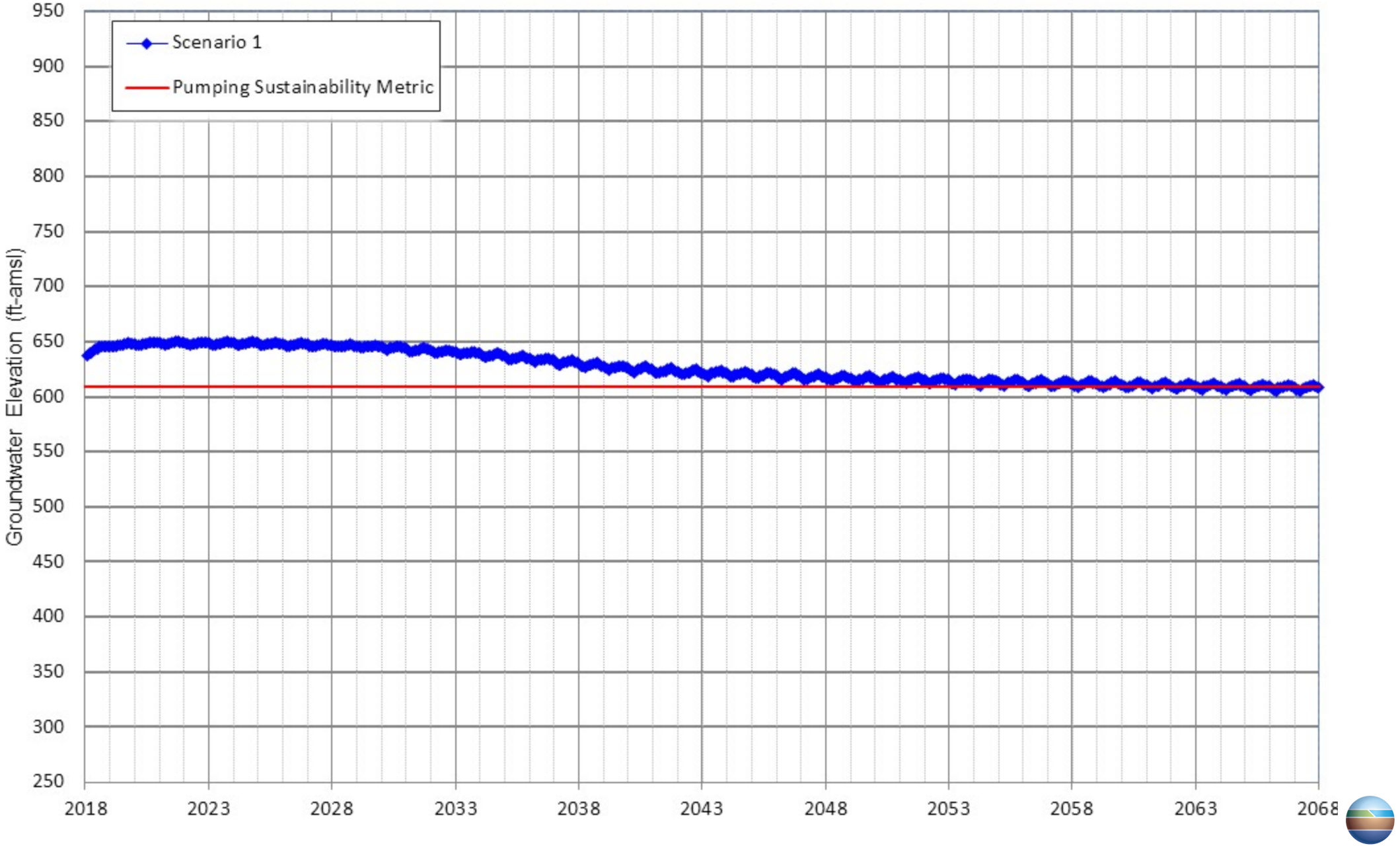

Appendix D-116
Projected Groundwater Elevation for Scenarios 1
City of Ontario Well 38

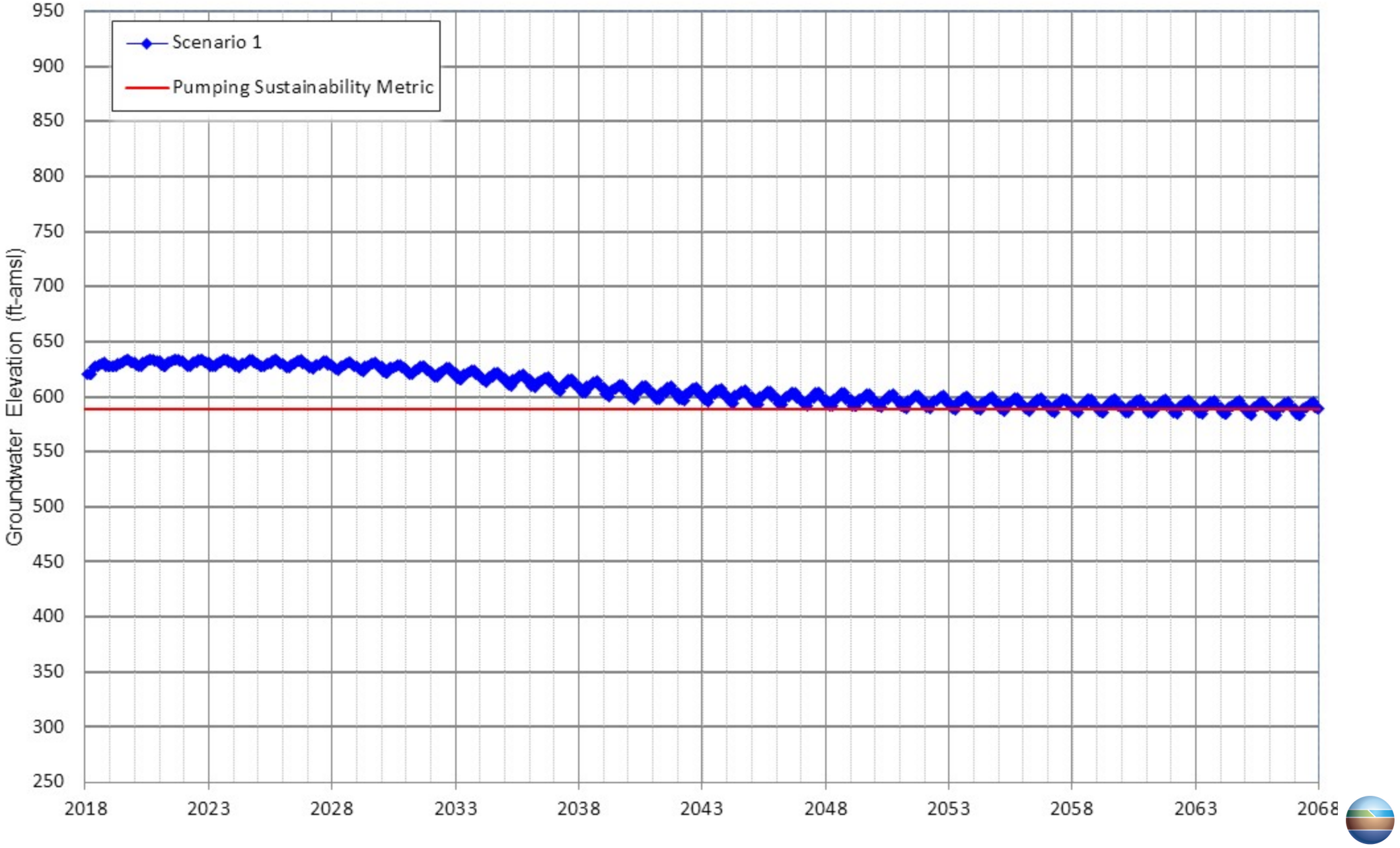

Appendix D-117
Projected Groundwater Elevation for Scenarios 1
City of Ontario Well 39

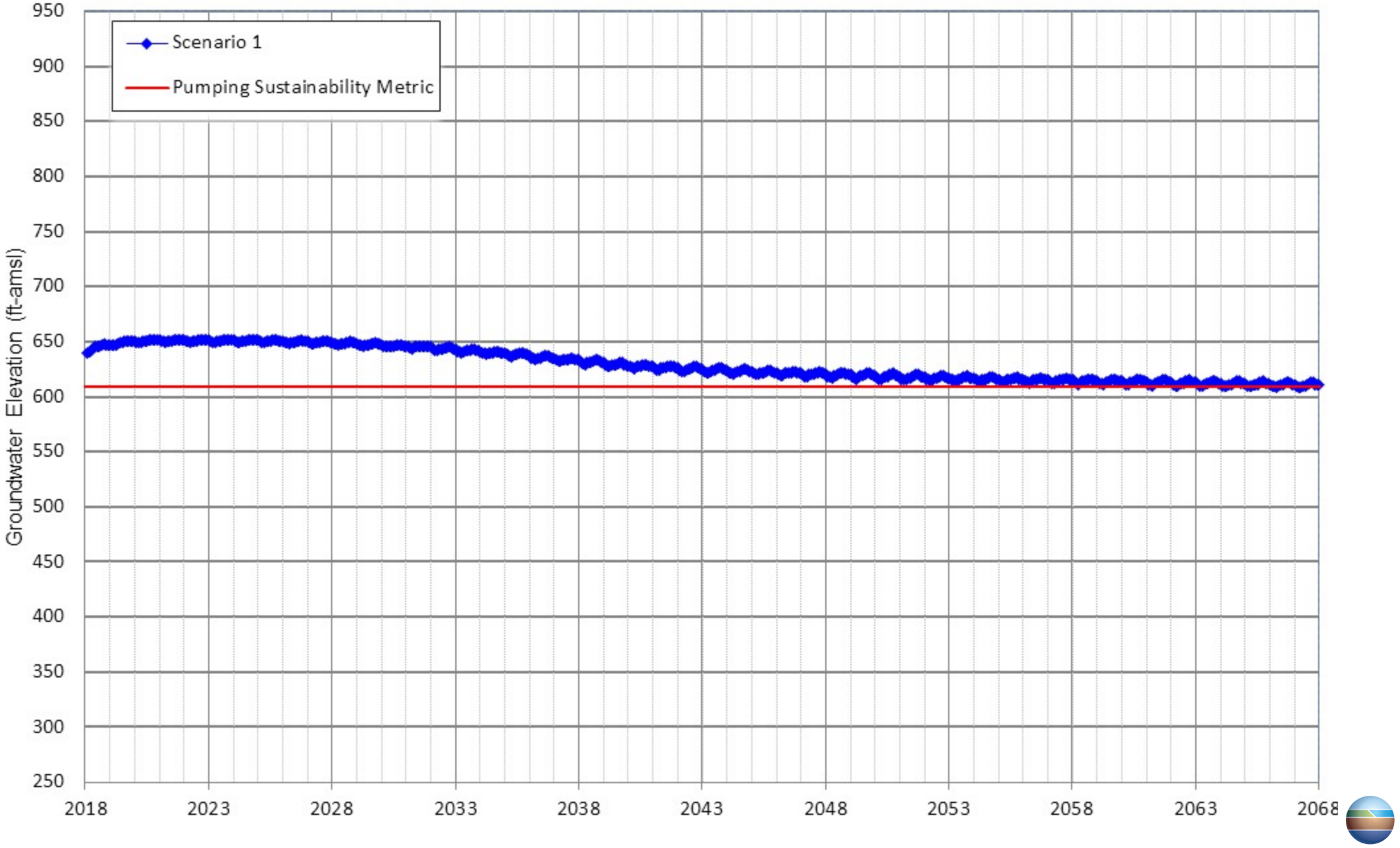

Appendix D-118
Projected Groundwater Elevation for Scenarios 1
City of Ontario Well 40

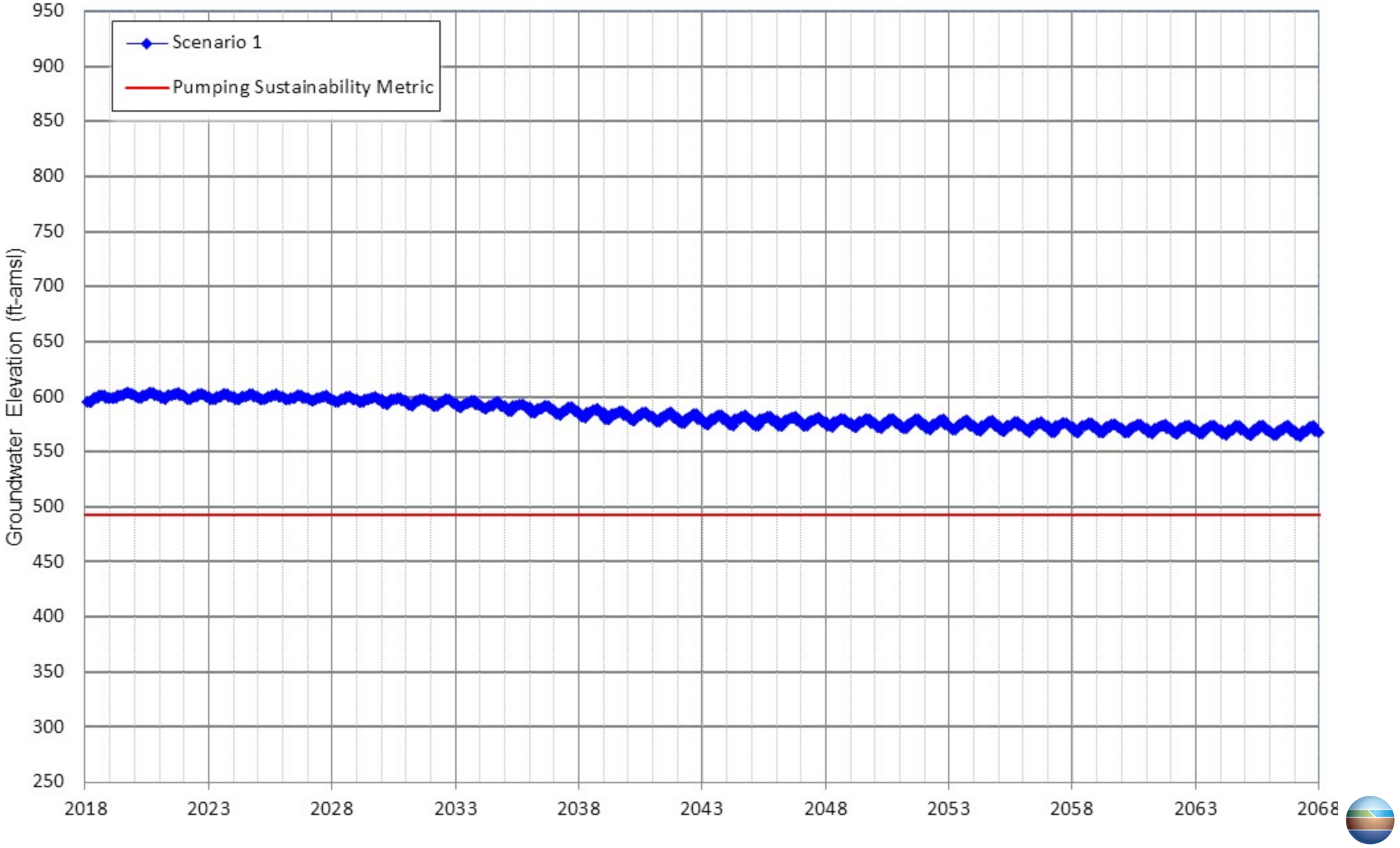

Appendix D-119
Projected Groundwater Elevation for Scenarios 1
City of Ontario Well 41

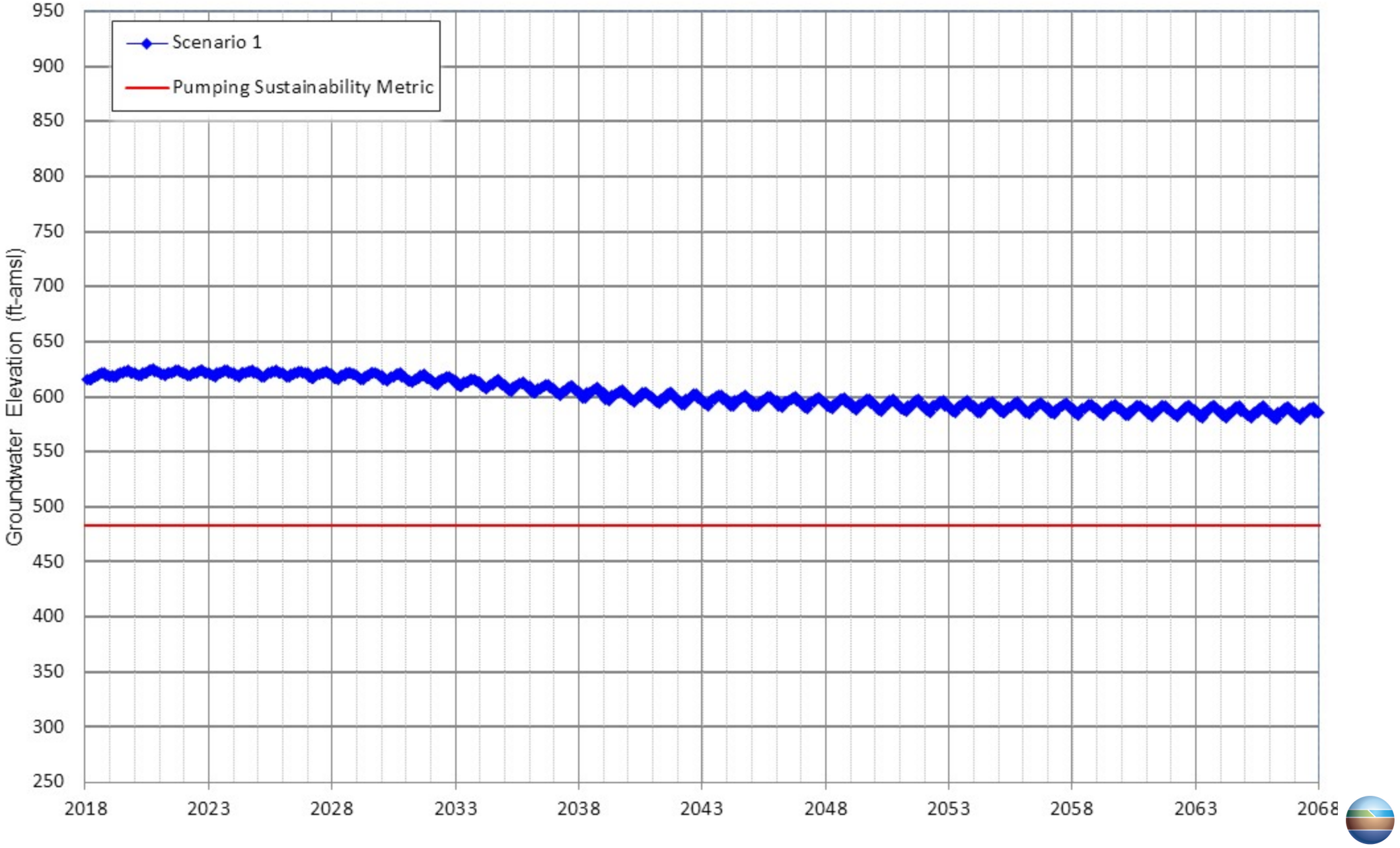

Appendix D-120
Projected Groundwater Elevation for Scenarios 1
City of Ontario Well 42

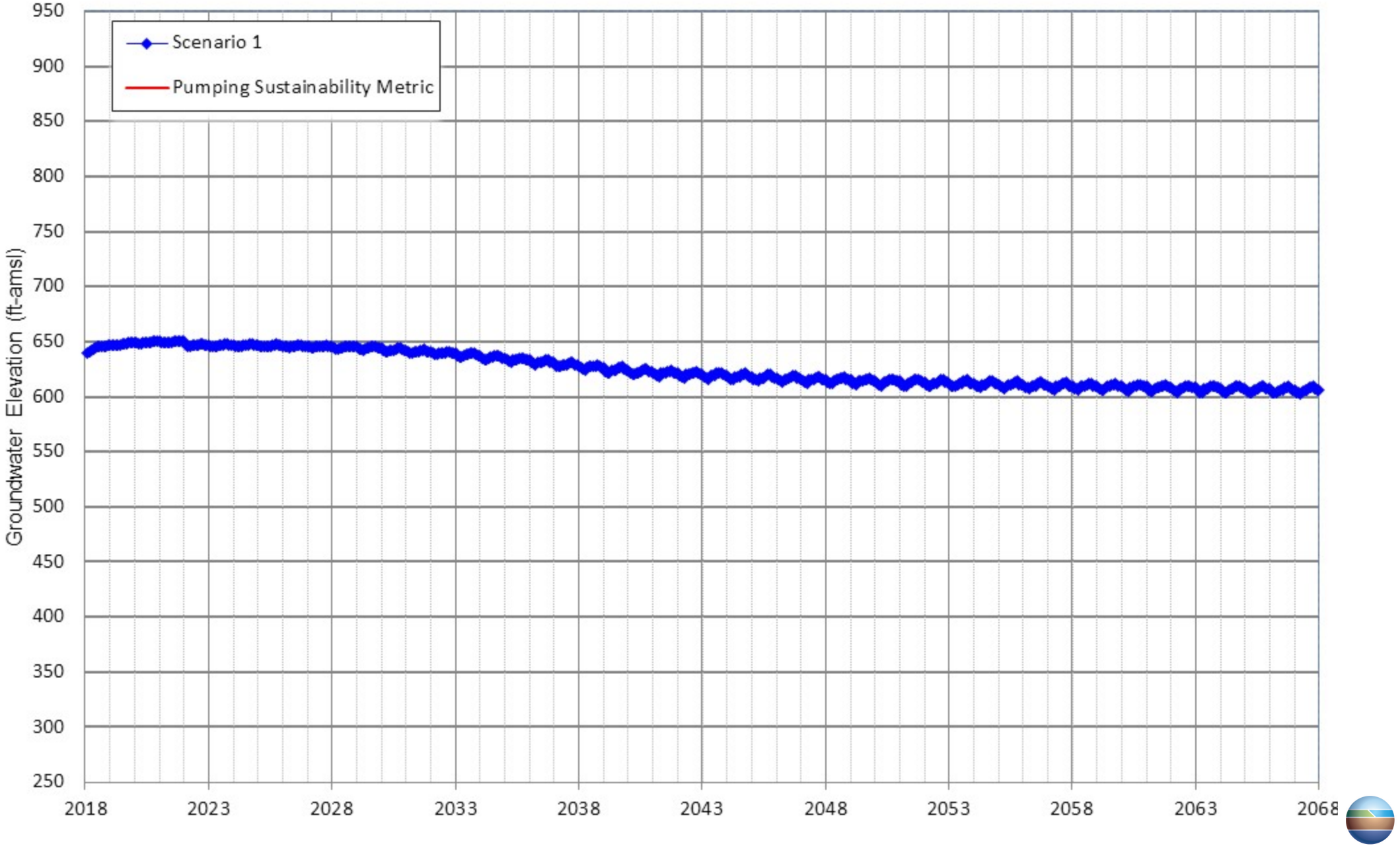

Appendix D-121
Projected Groundwater Elevation for Scenarios 1
City of Ontario Well 43

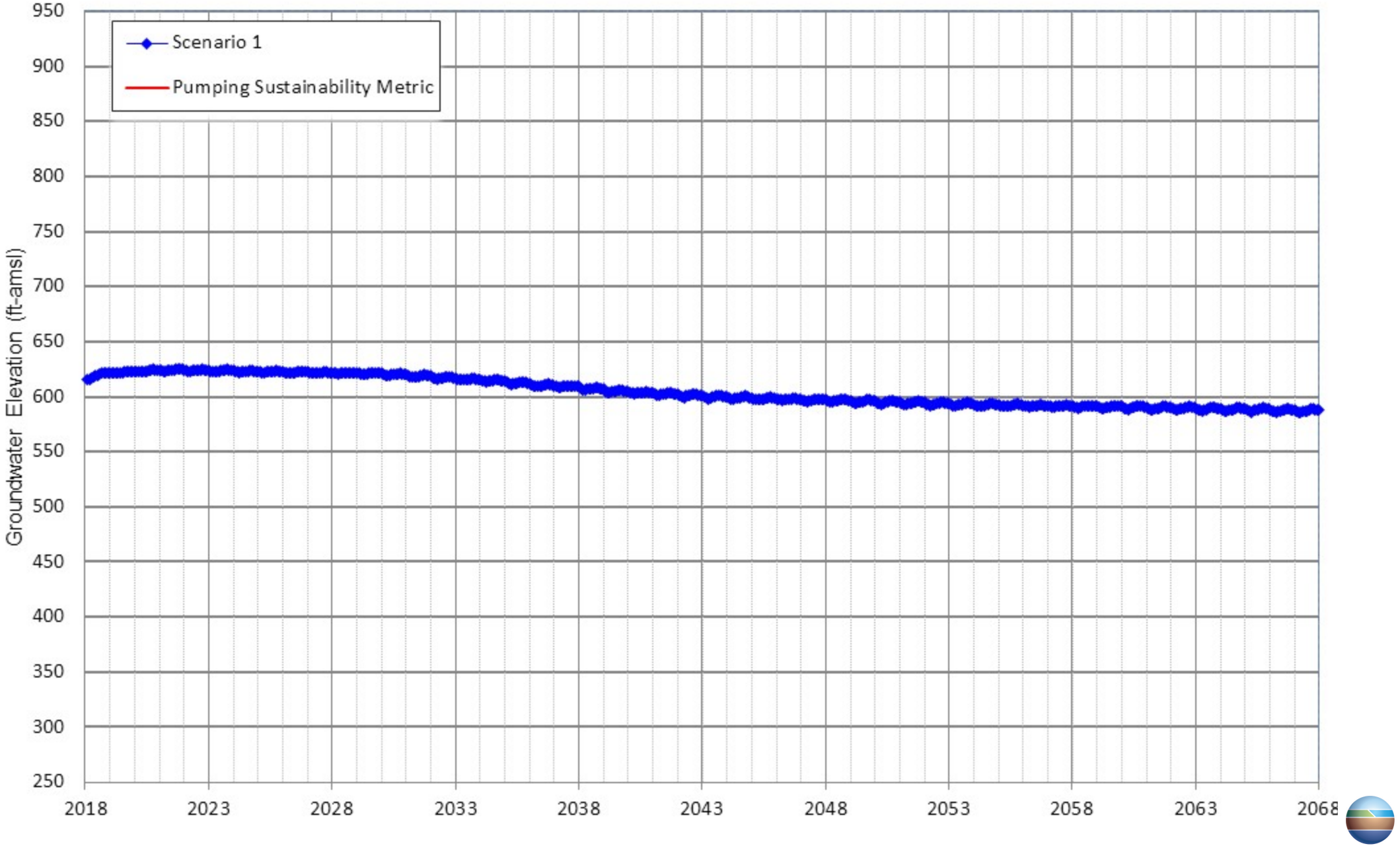

Appendix D-122
Projected Groundwater Elevation for Scenarios 1
City of Ontario Well 44

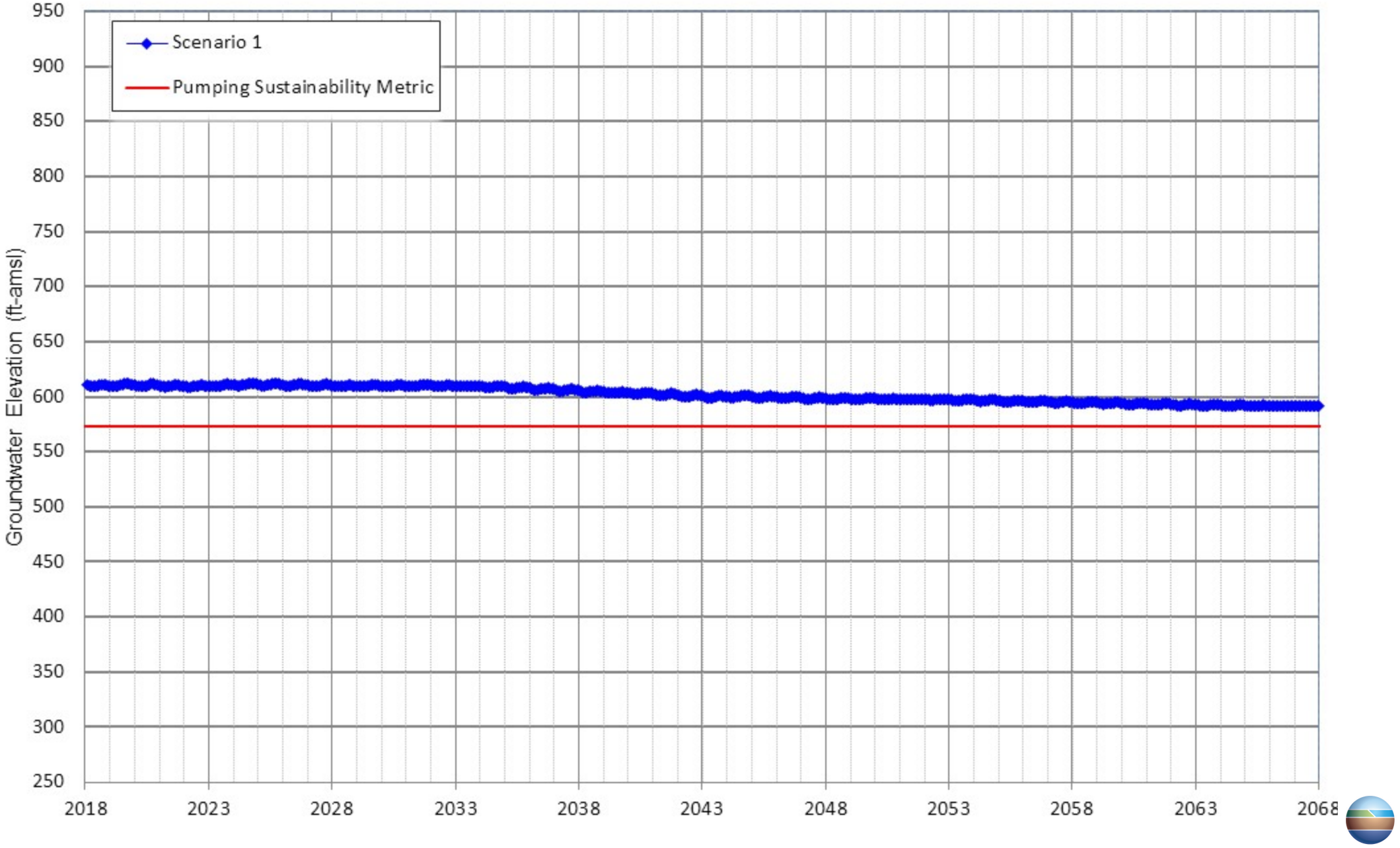

Appendix D-123
Projected Groundwater Elevation for Scenarios 1
City of Ontario Well 45

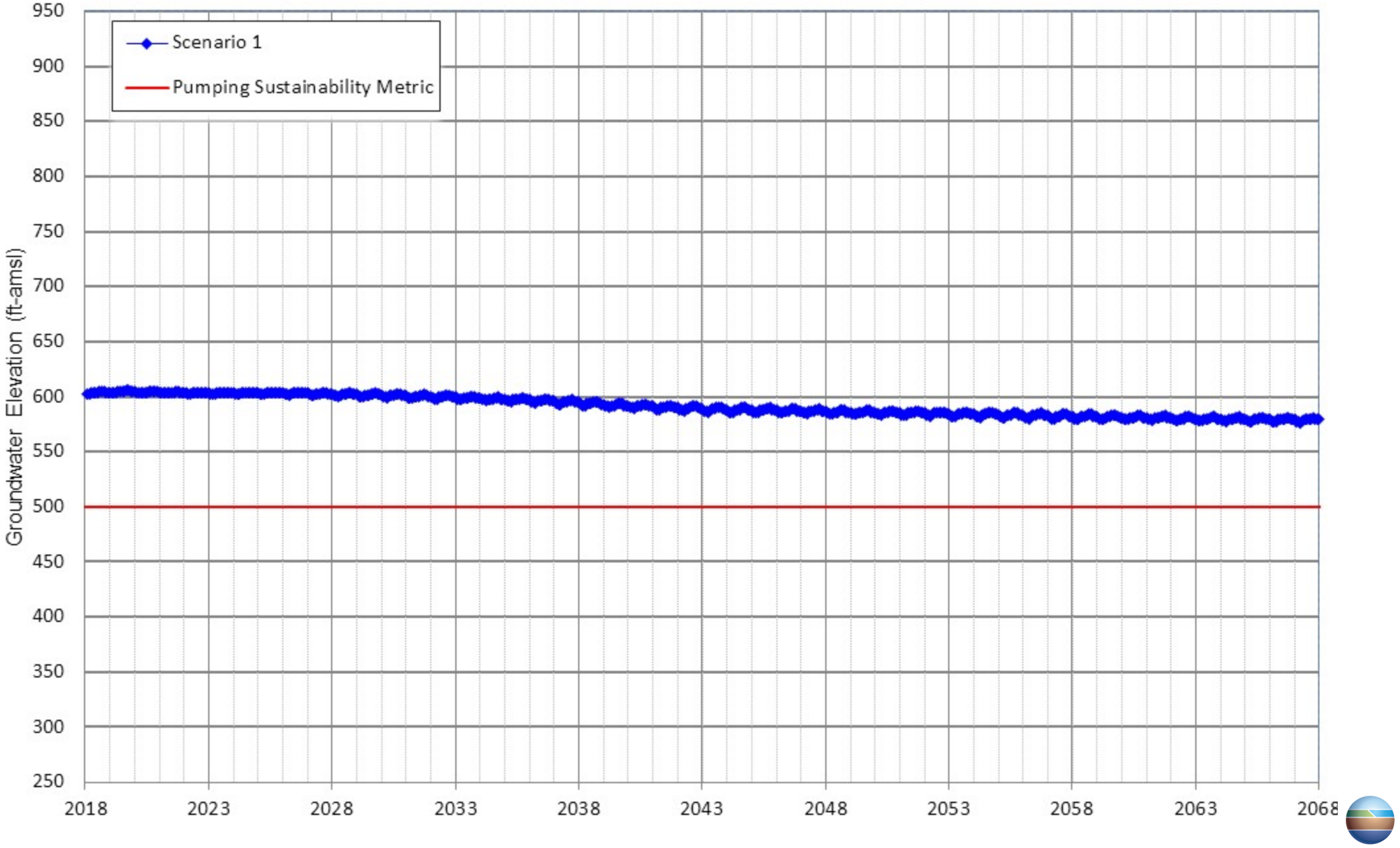

Appendix D-124
Projected Groundwater Elevation for Scenarios 1
City of Ontario Well 46

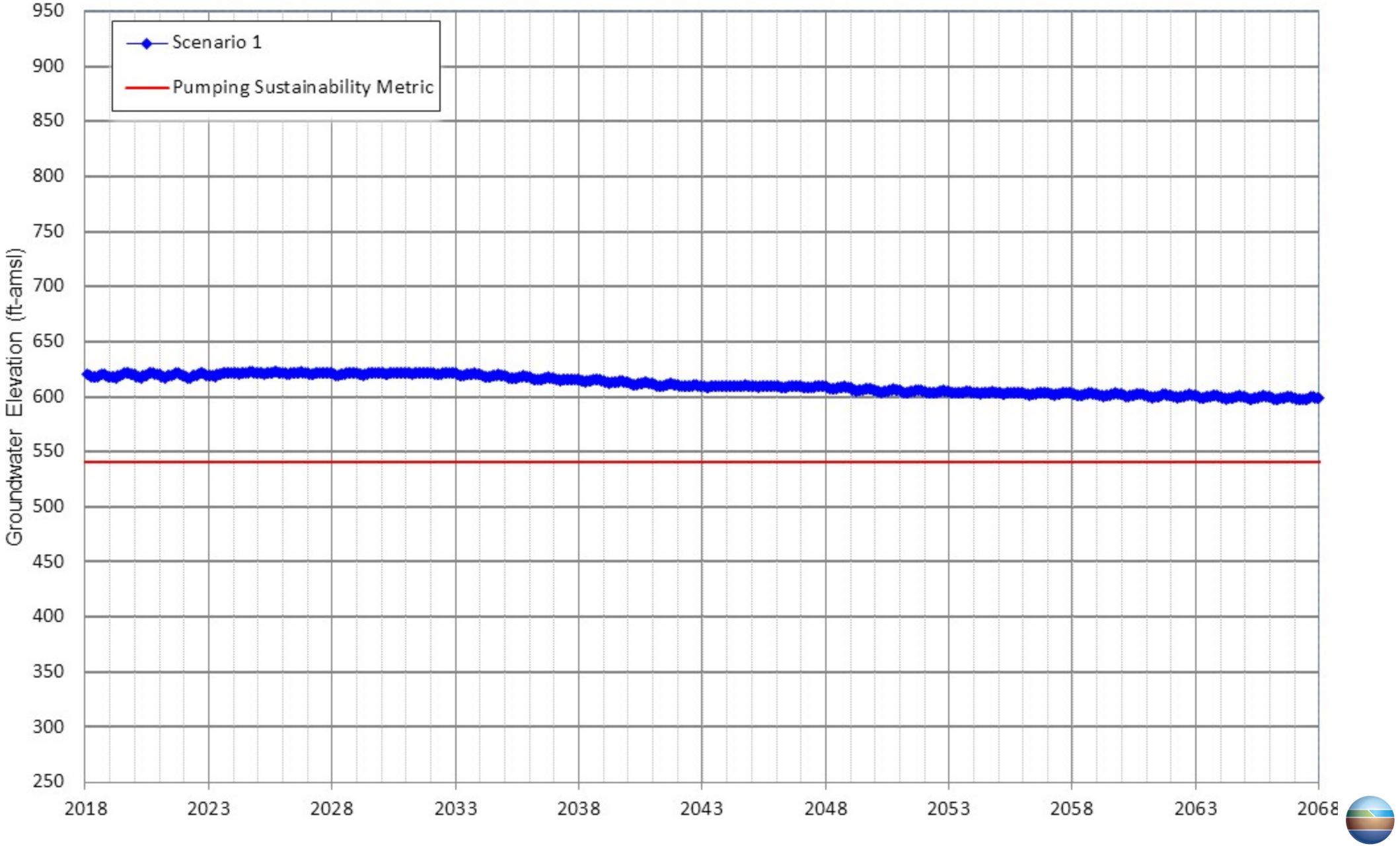

Appendix D-125
Projected Groundwater Elevation for Scenarios 1
City of Ontario Well 47

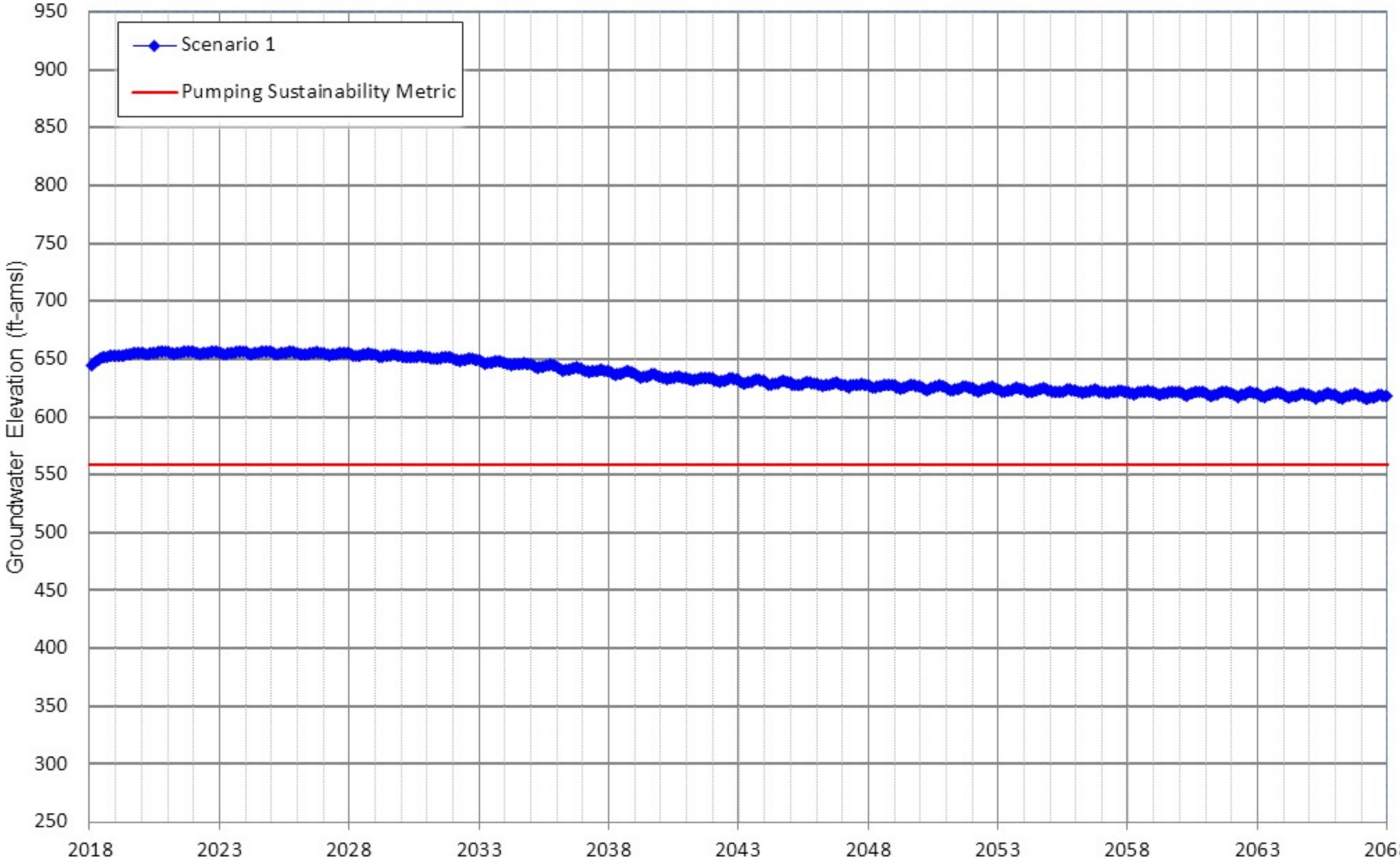

Appendix D-126
Projected Groundwater Elevation for Scenarios 1
City of Ontario Well 48

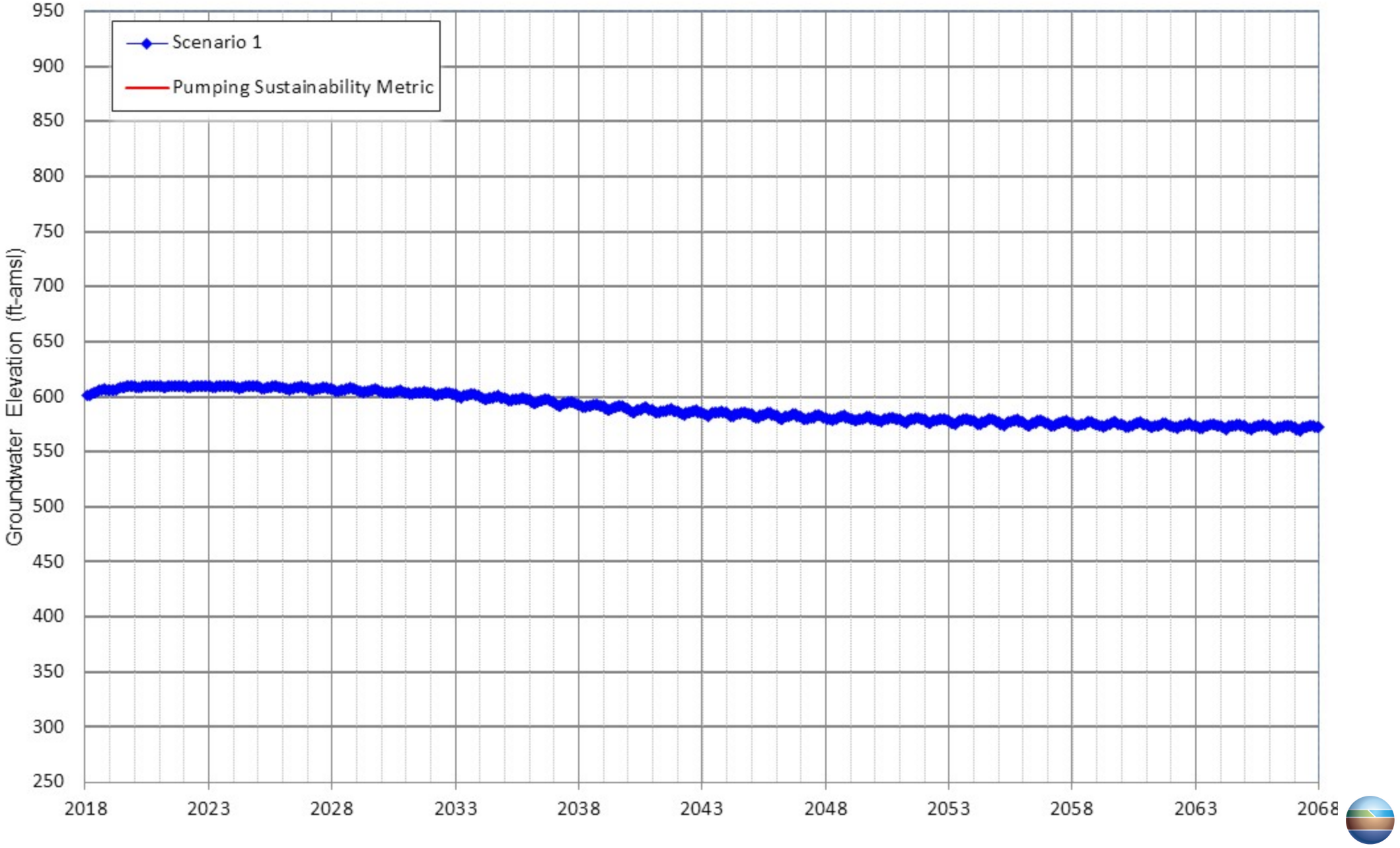

Appendix D-127
Projected Groundwater Elevation for Scenarios 1
City of Ontario Well 49

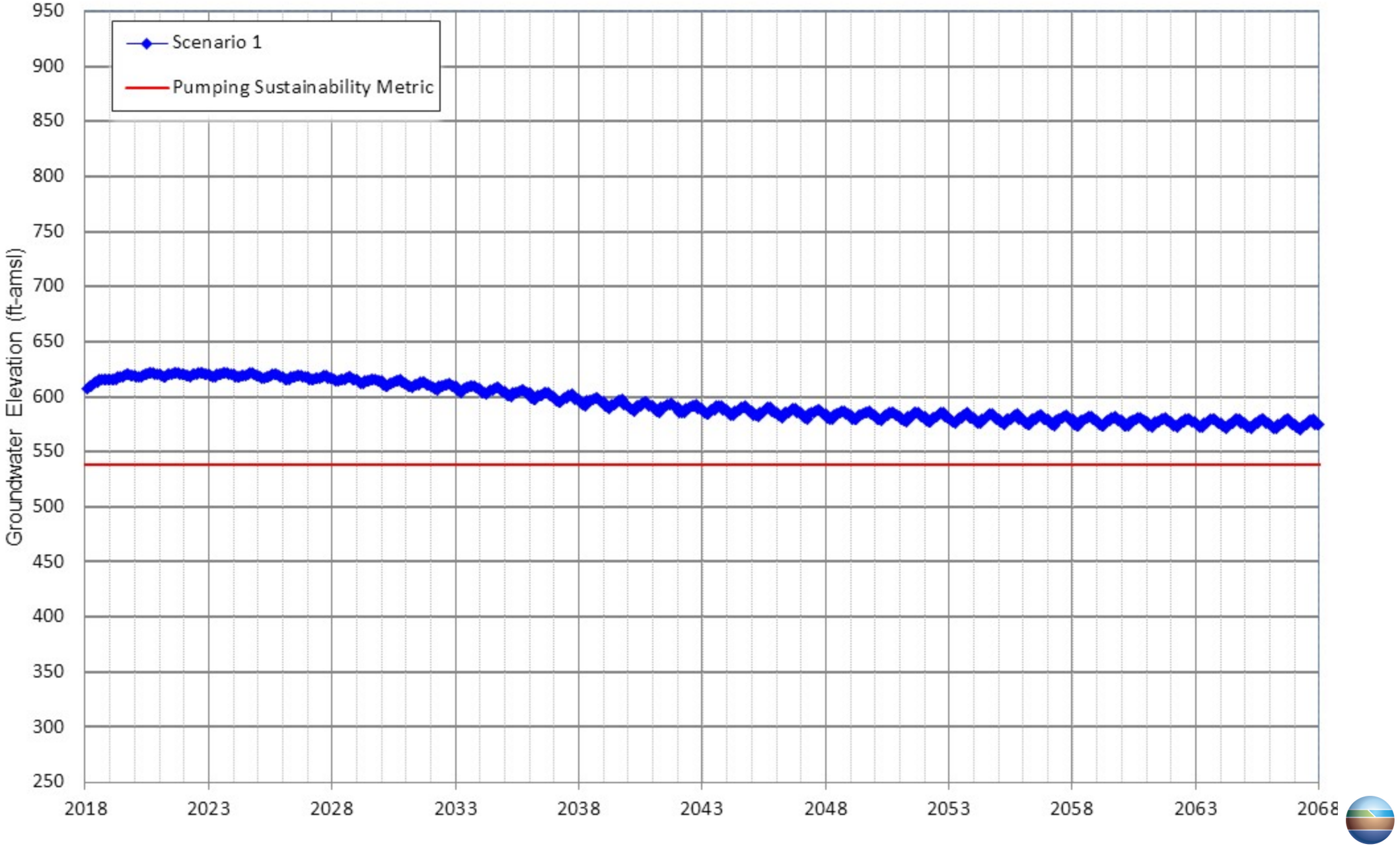

Appendix D-128
Projected Groundwater Elevation for Scenarios 1
City of Ontario Well 50

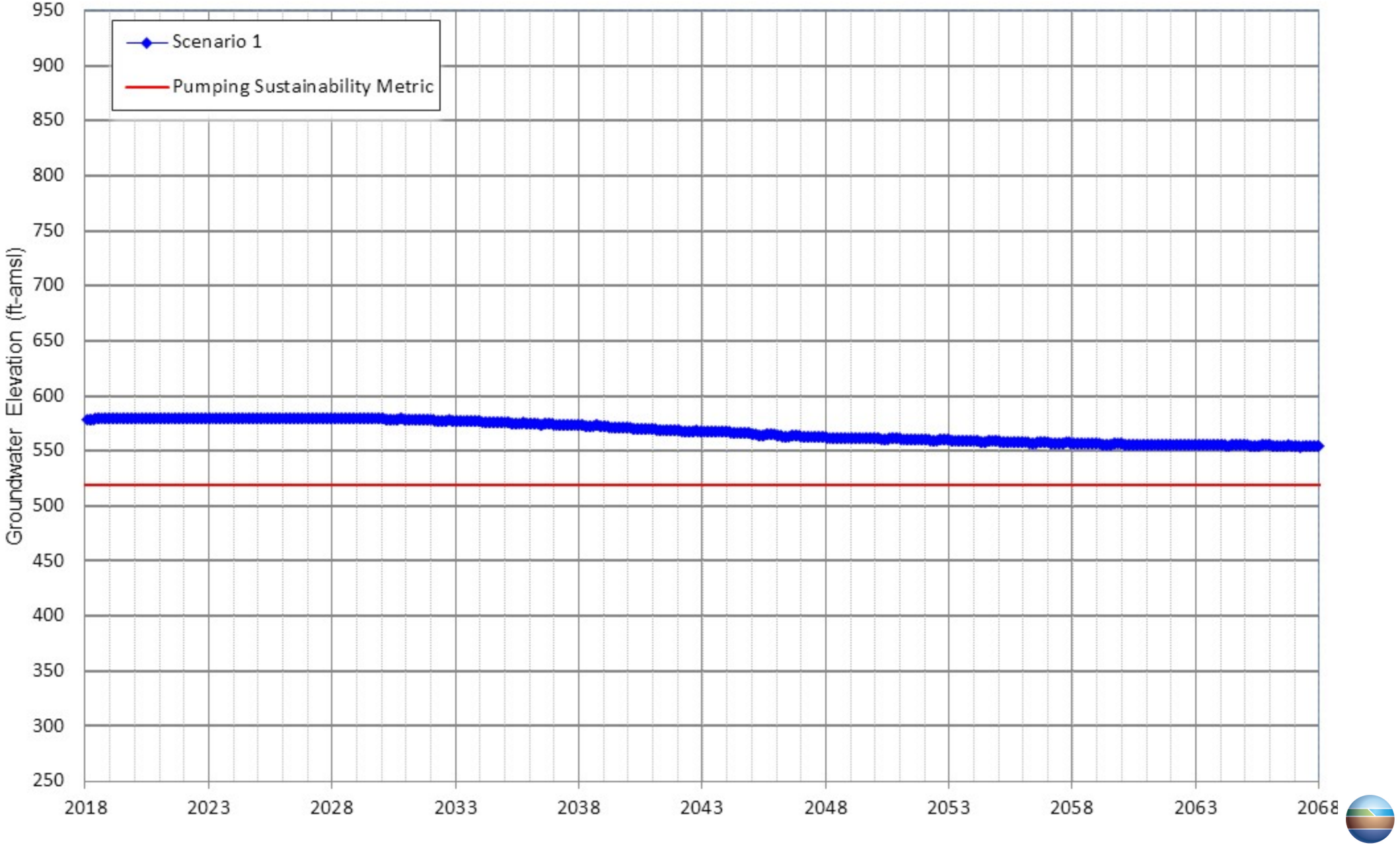

Appendix D-129
Projected Groundwater Elevation for Scenarios 1
City of Ontario Well 51

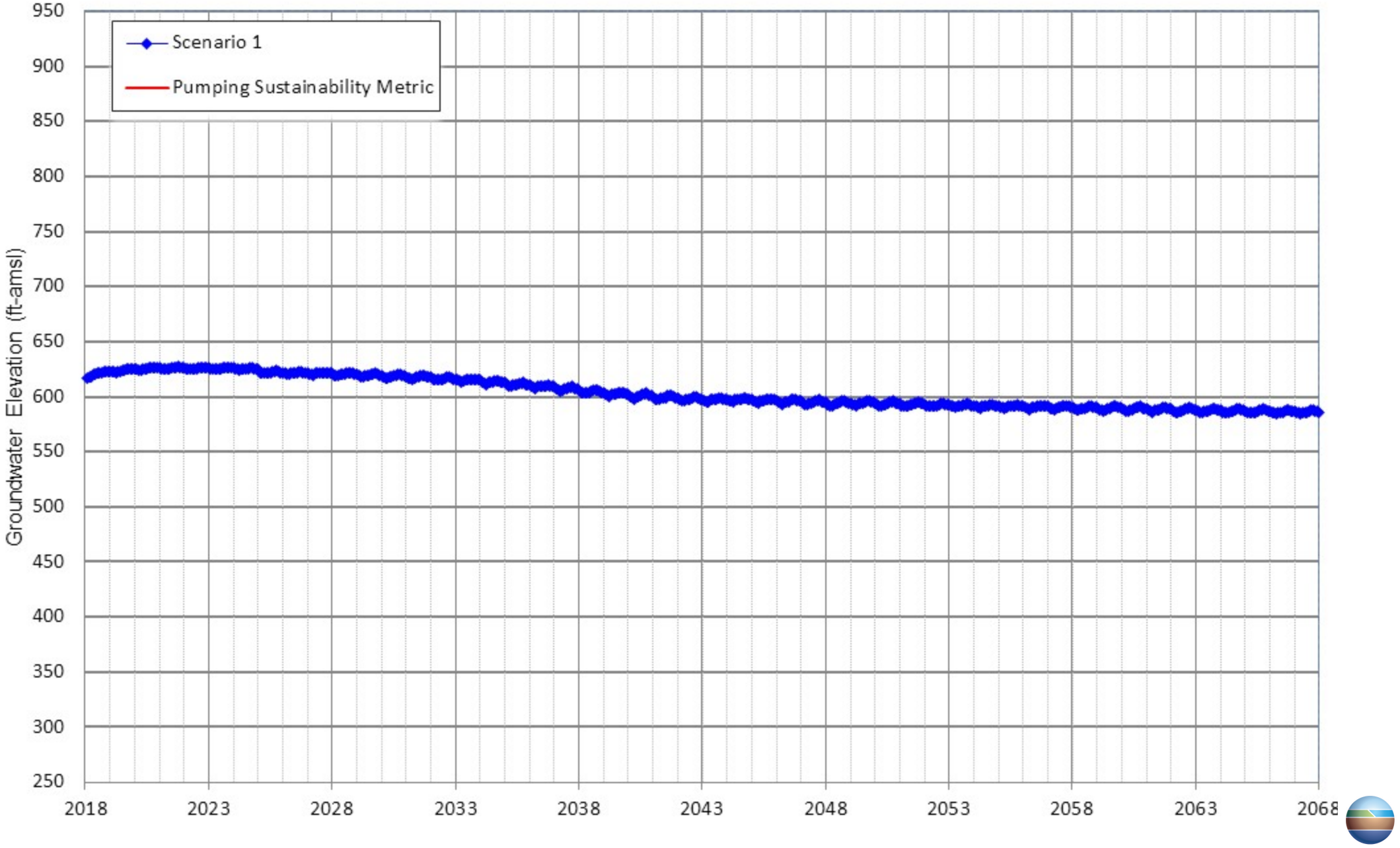

Appendix D-130
Projected Groundwater Elevation for Scenarios 1
City of Ontario Well 52

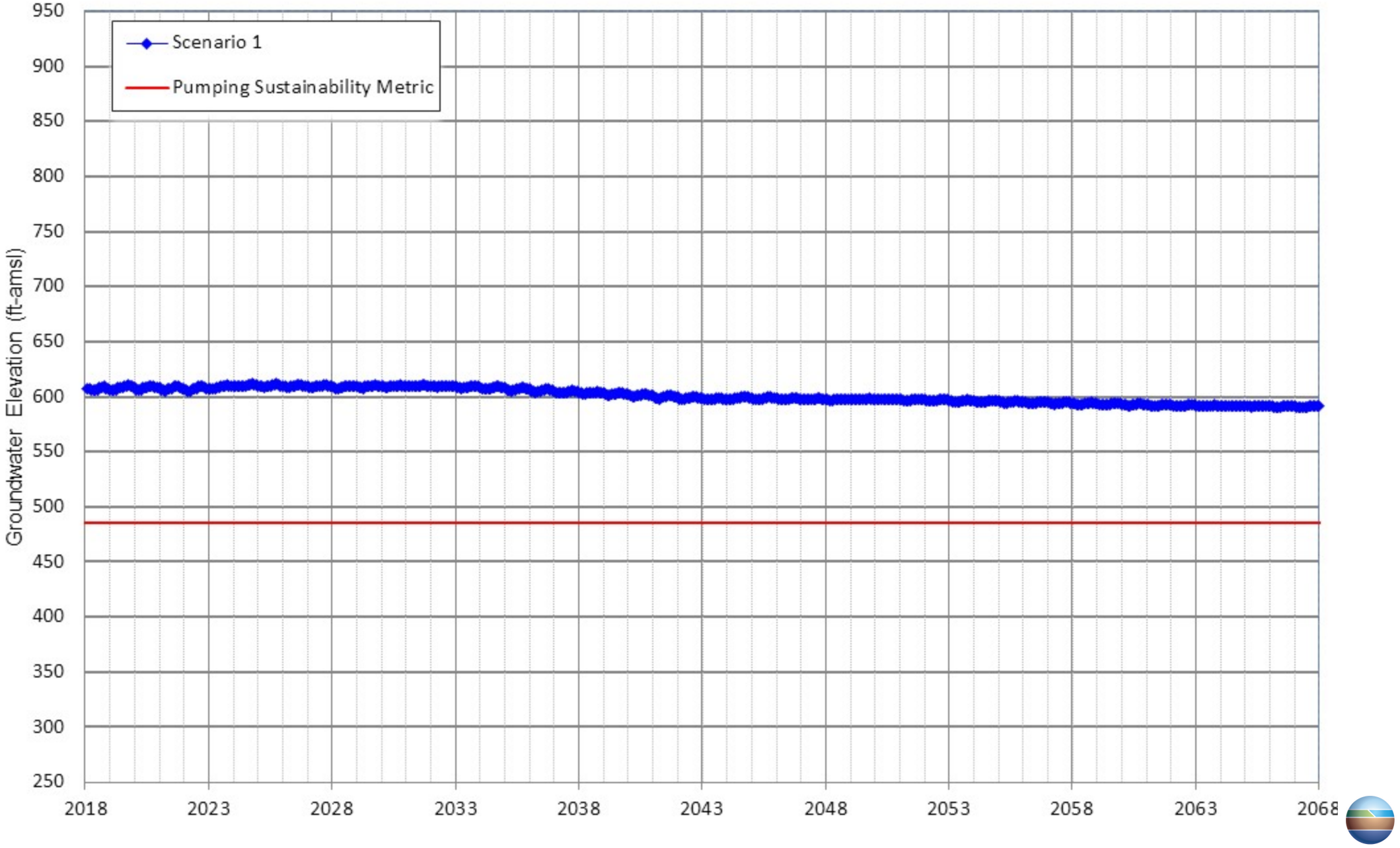

Appendix D-131
Projected Groundwater Elevation for Scenarios 1
City of Ontario Well 100

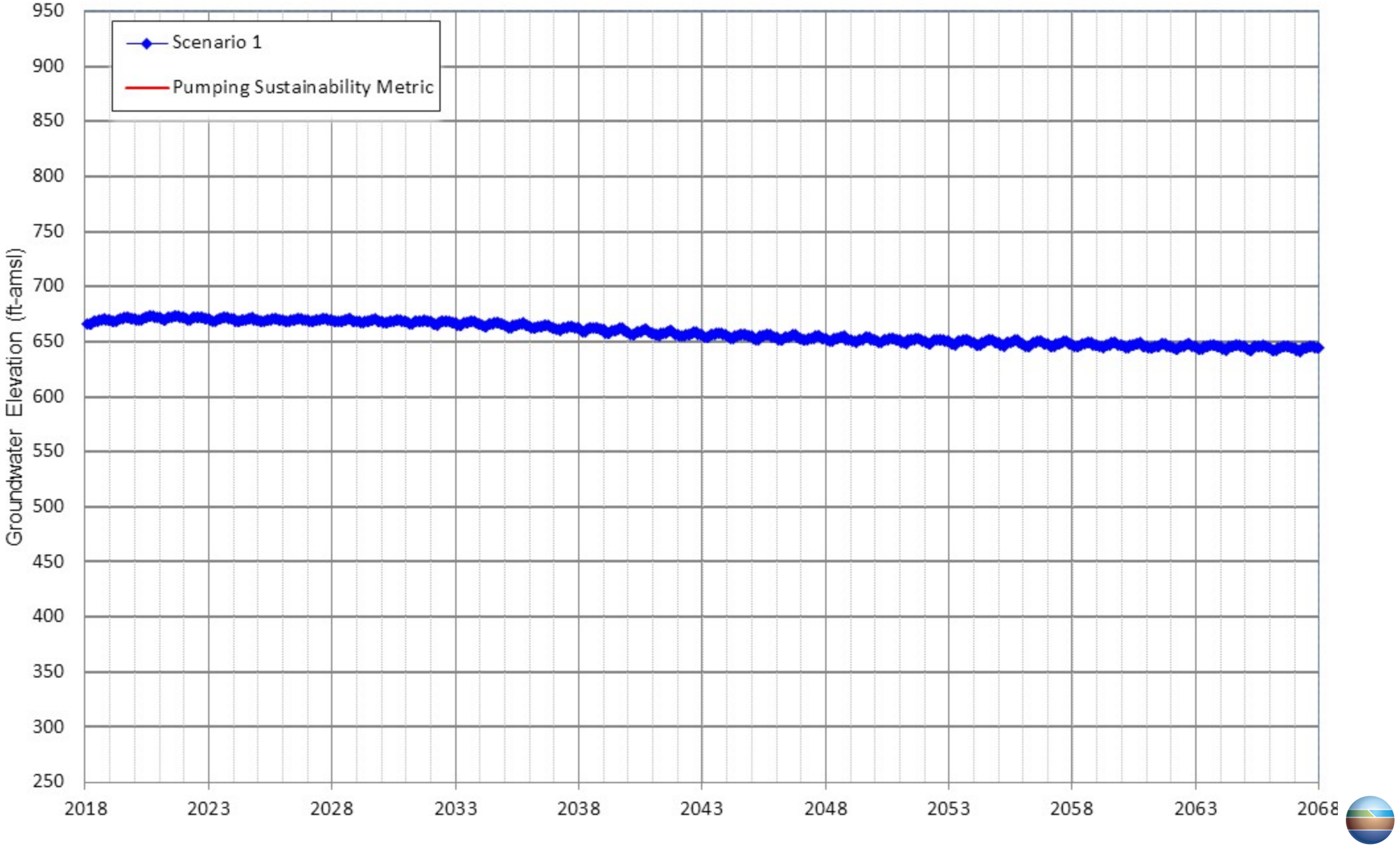

Appendix D-132
Projected Groundwater Elevation for Scenarios 1
City of Ontario Well 101

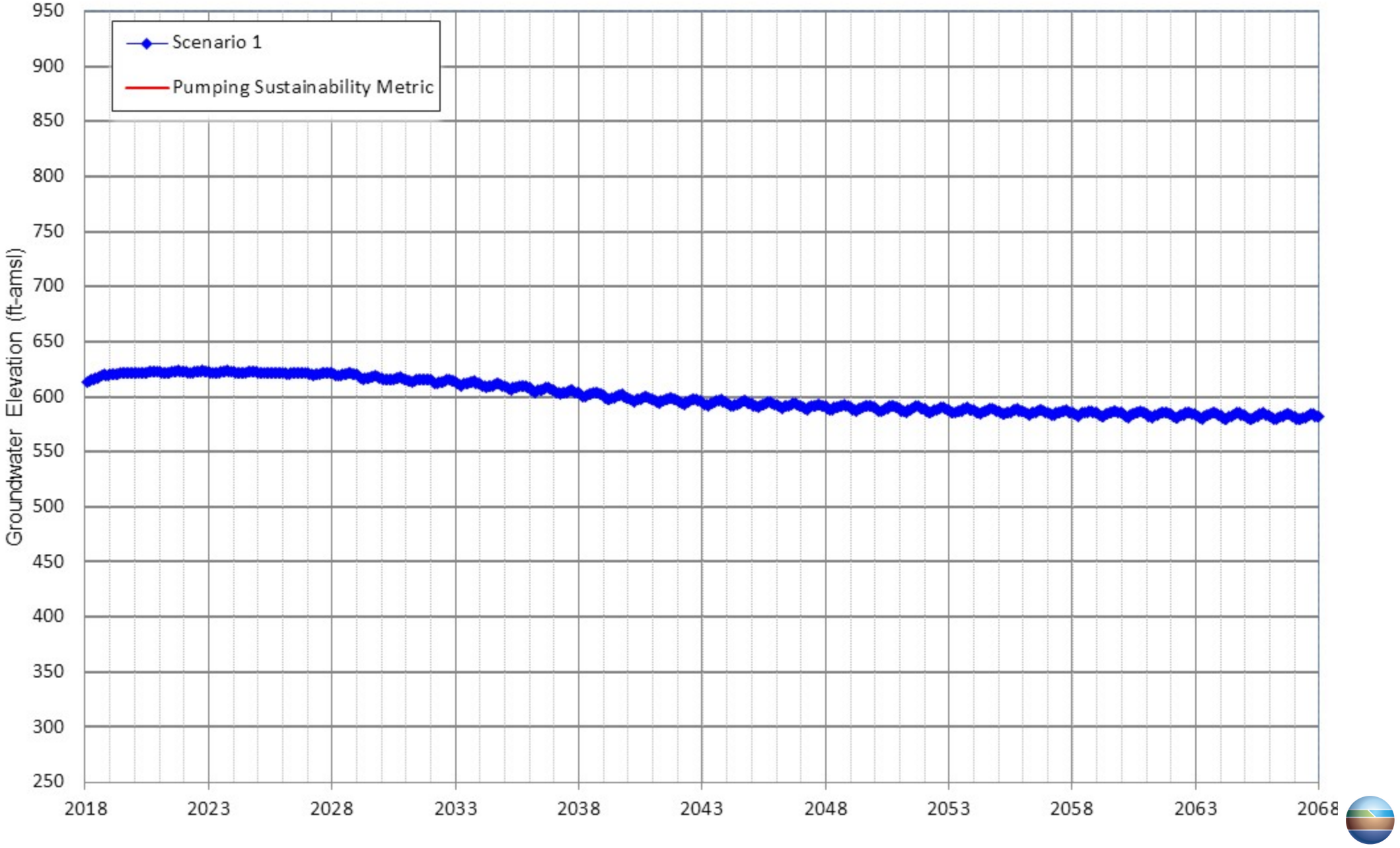

Appendix D-133
Projected Groundwater Elevation for Scenarios 1
City of Ontario Well 103

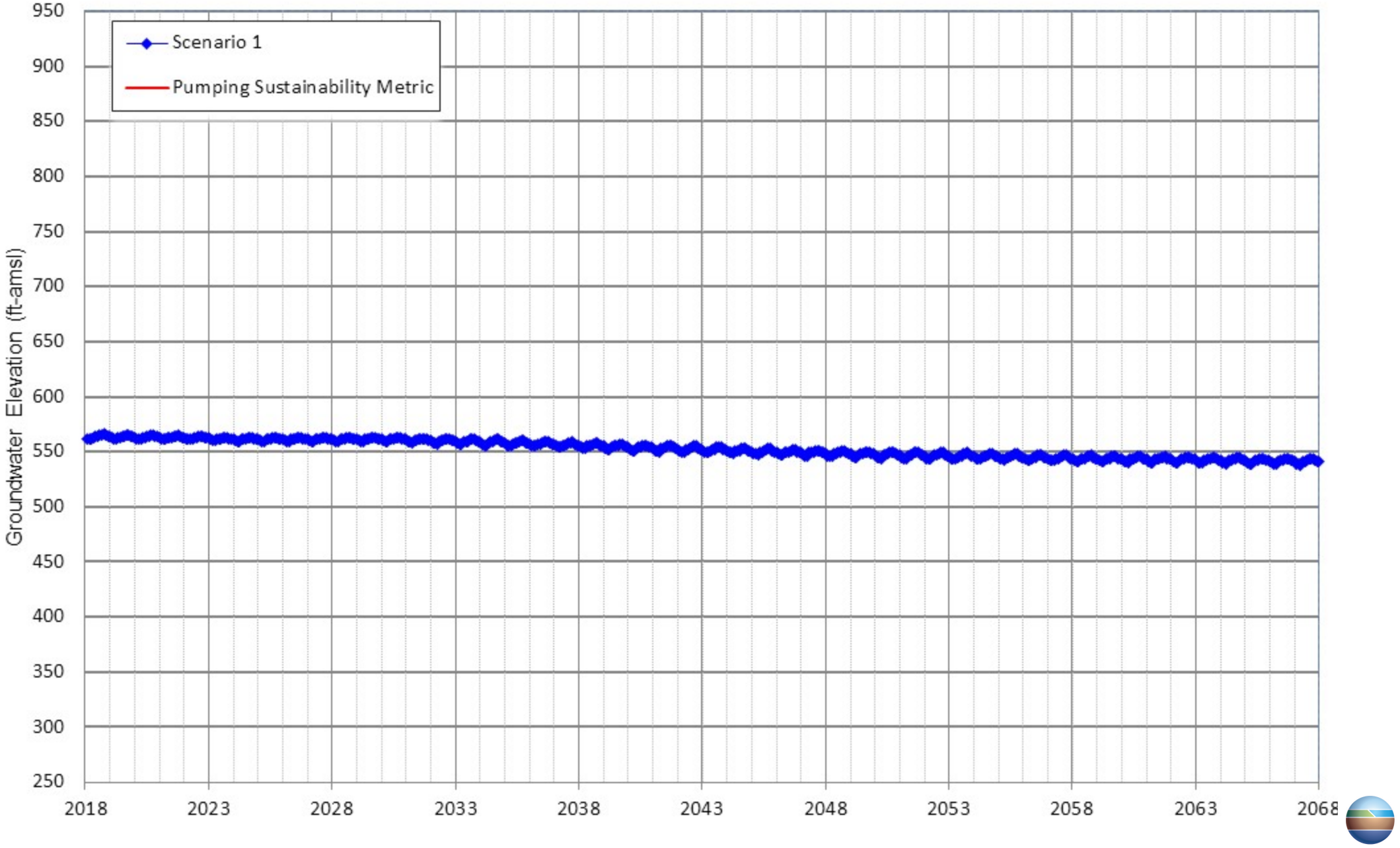

Appendix D-134
Projected Groundwater Elevation for Scenarios 1
City of Ontario Well 104

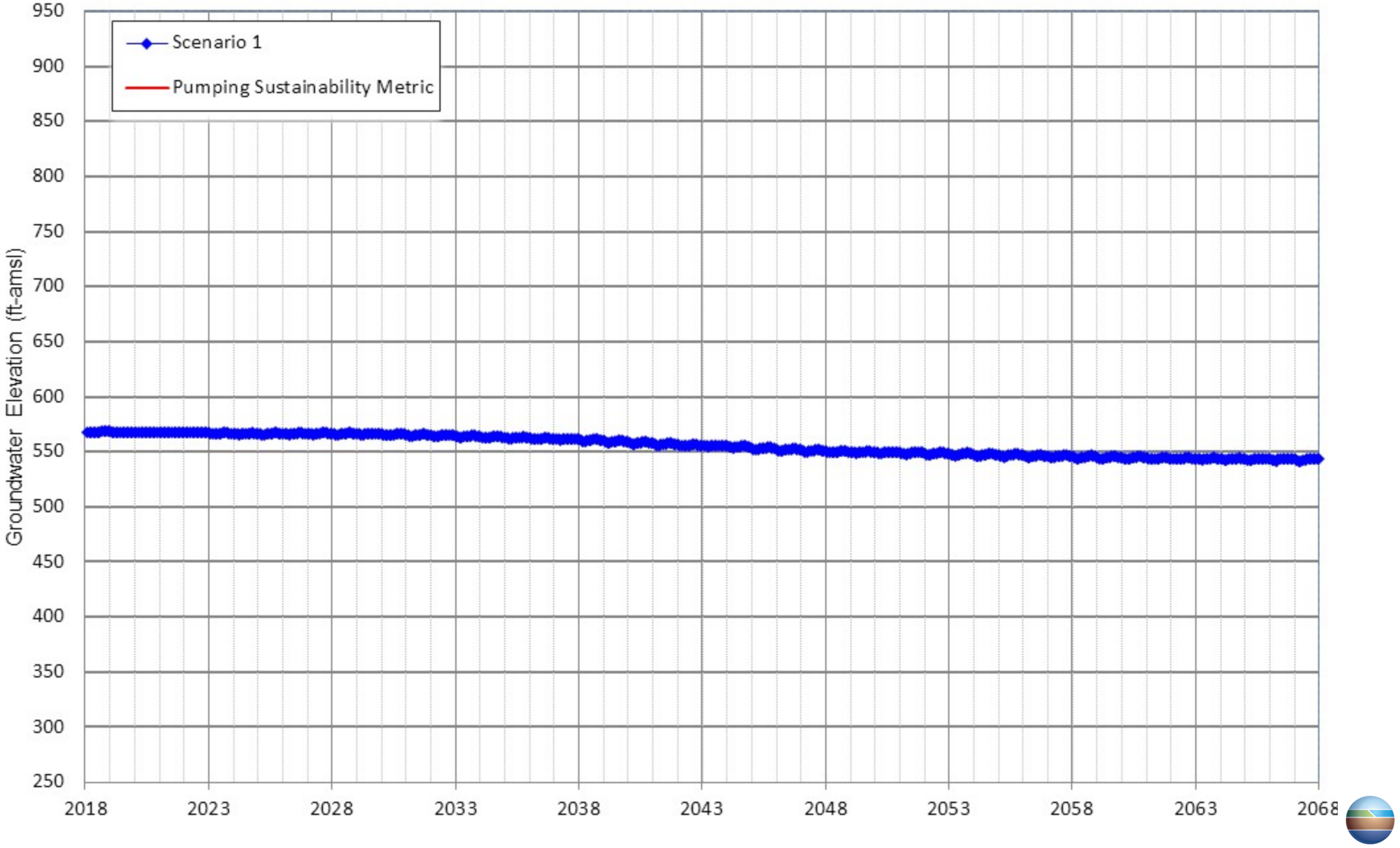

Appendix D-135
Projected Groundwater Elevation for Scenarios 1
City of Ontario Well 105

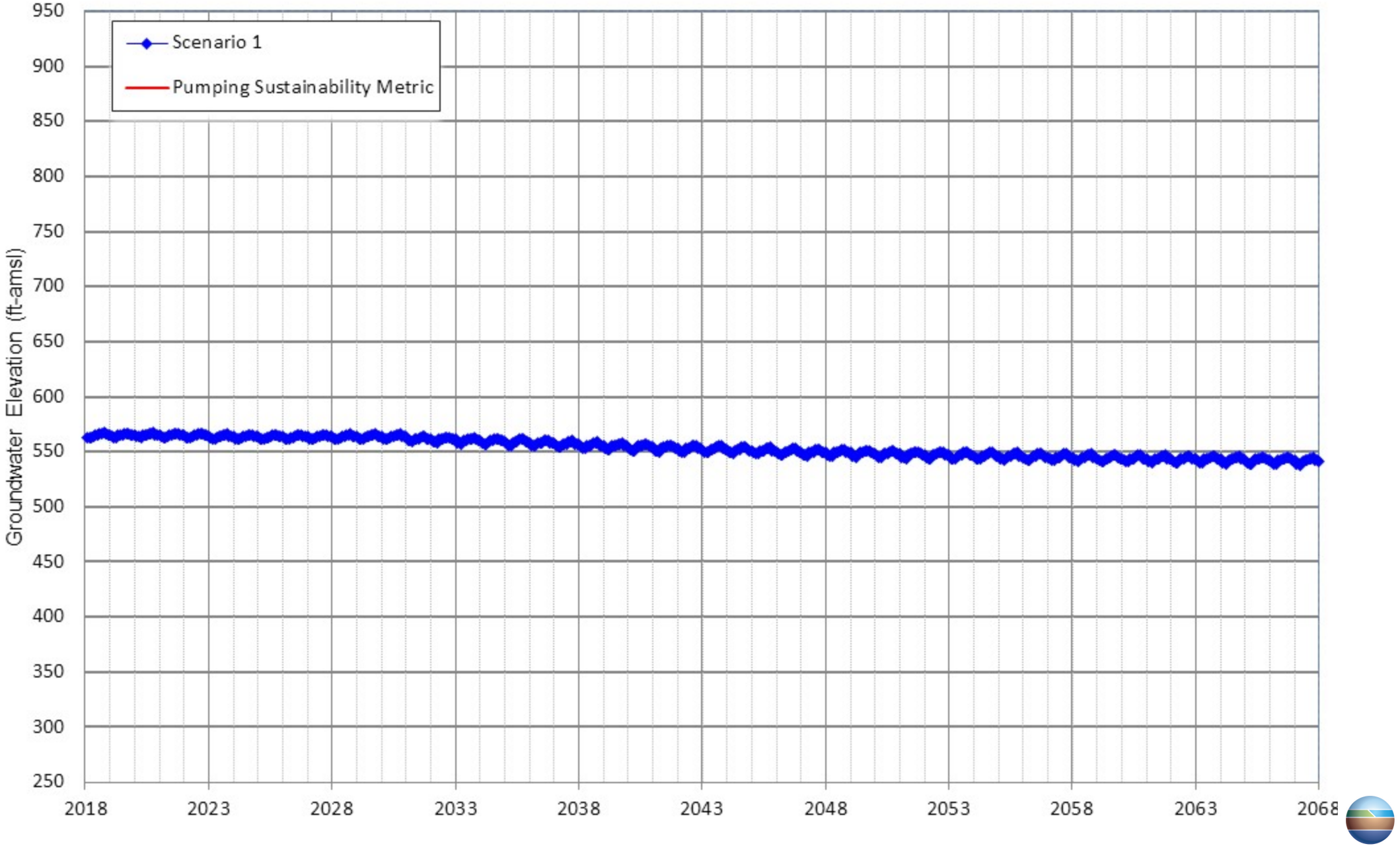

Appendix D-136
Projected Groundwater Elevation for Scenarios 1
City of Ontario Well 106

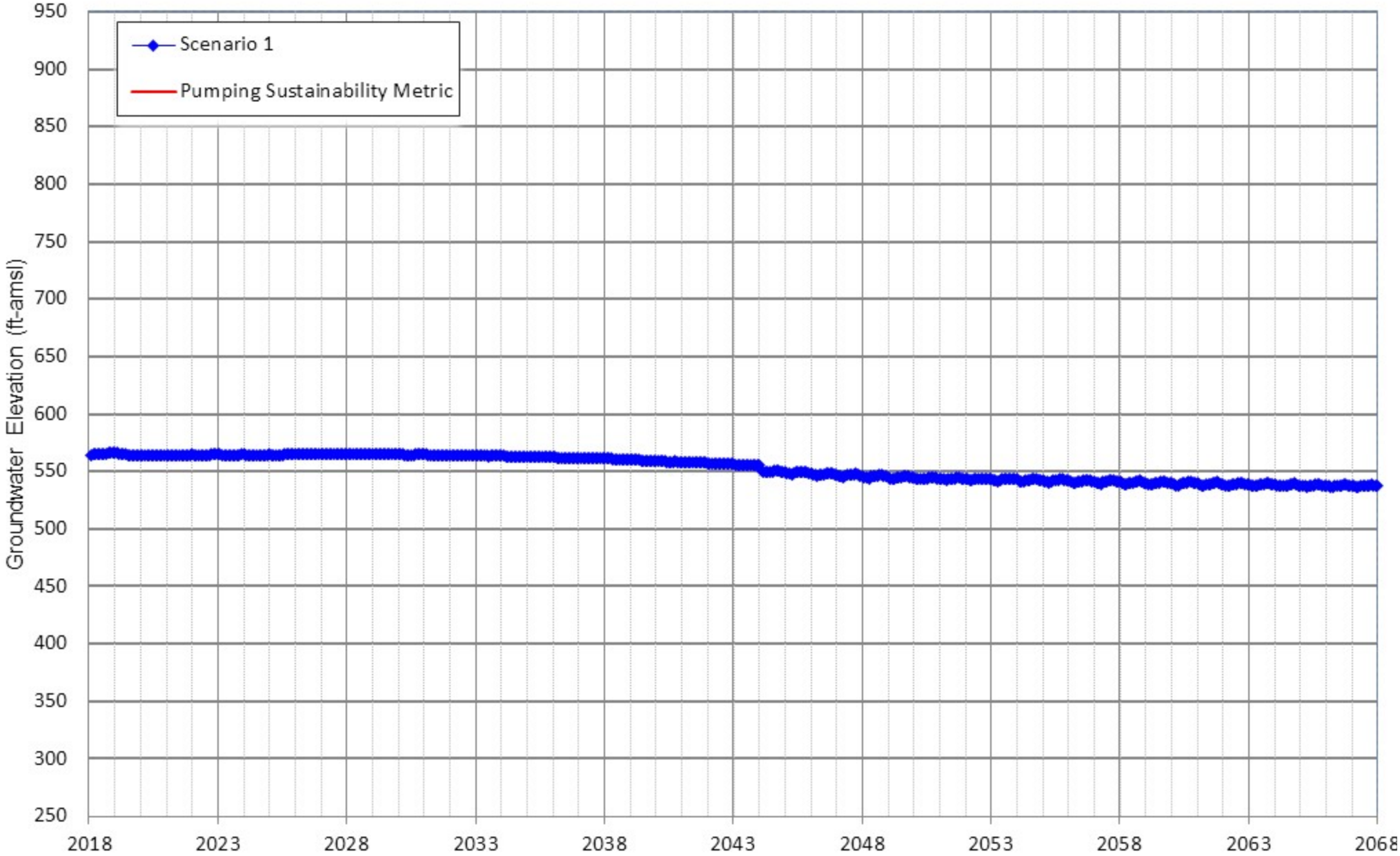

Appendix D-137
Projected Groundwater Elevation for Scenarios 1
City of Ontario Well 109

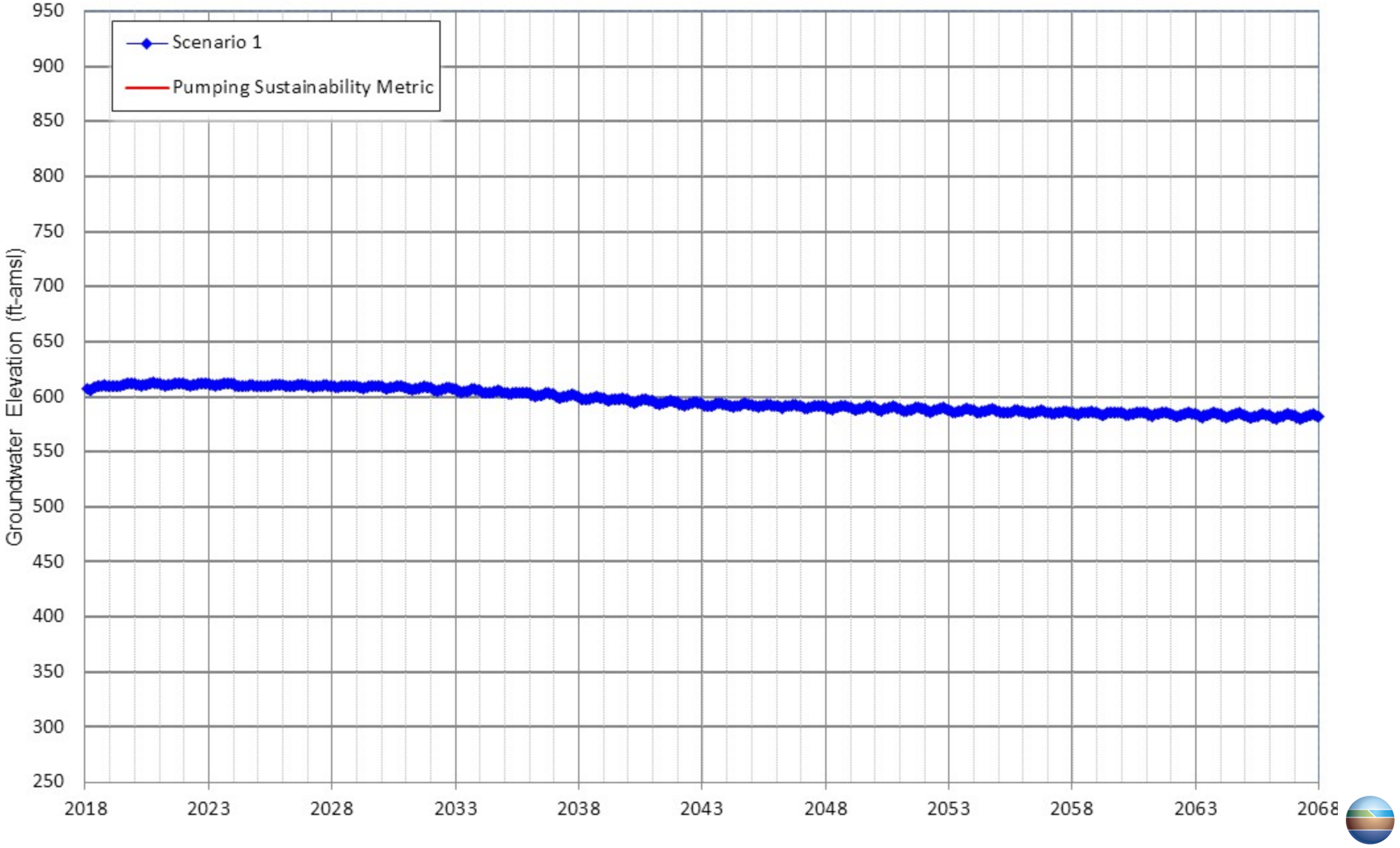

Appendix D-138
Projected Groundwater Elevation for Scenarios 1
City of Ontario Well 111

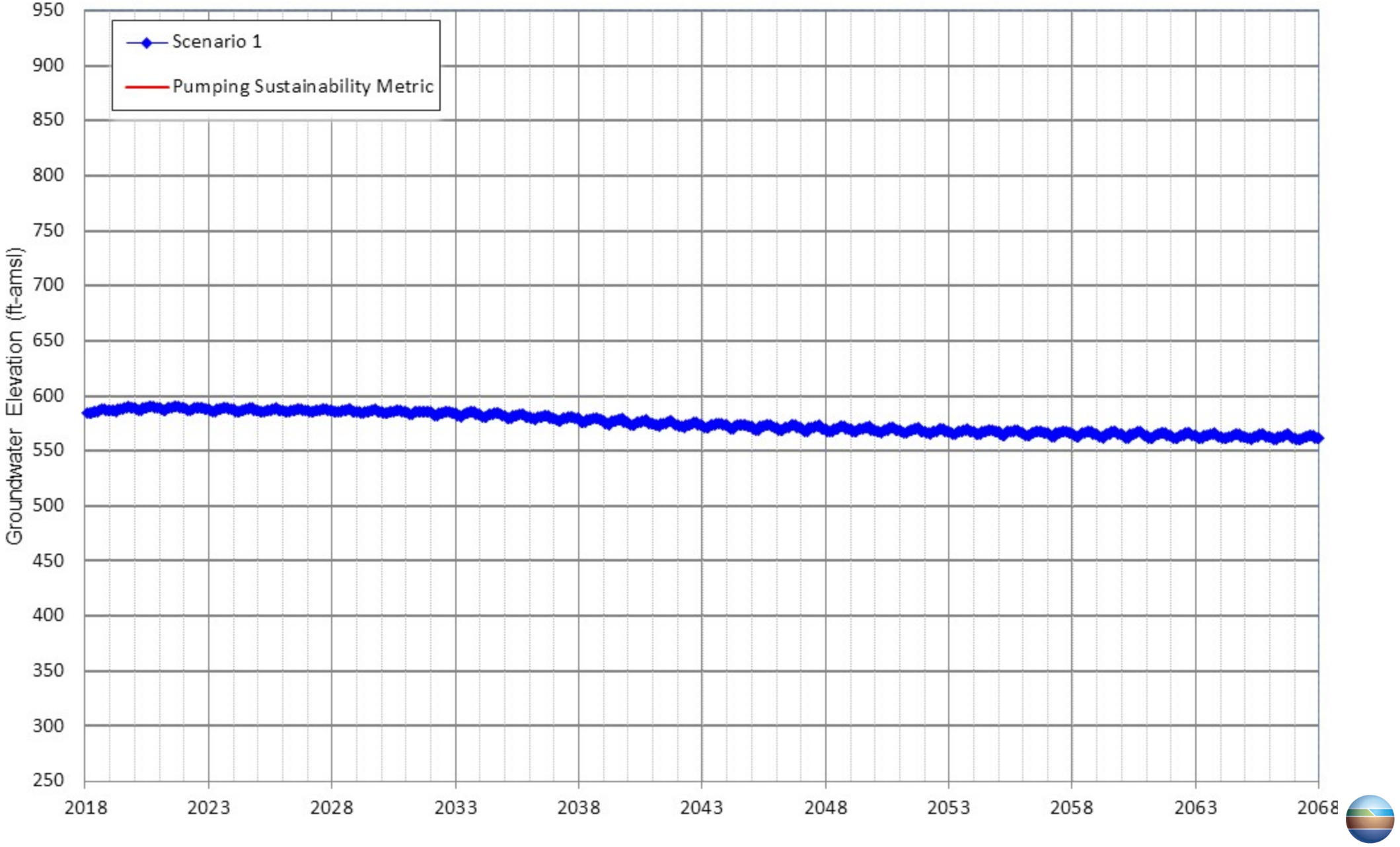

Appendix D-139
Projected Groundwater Elevation for Scenarios 1
City of Ontario Well 119

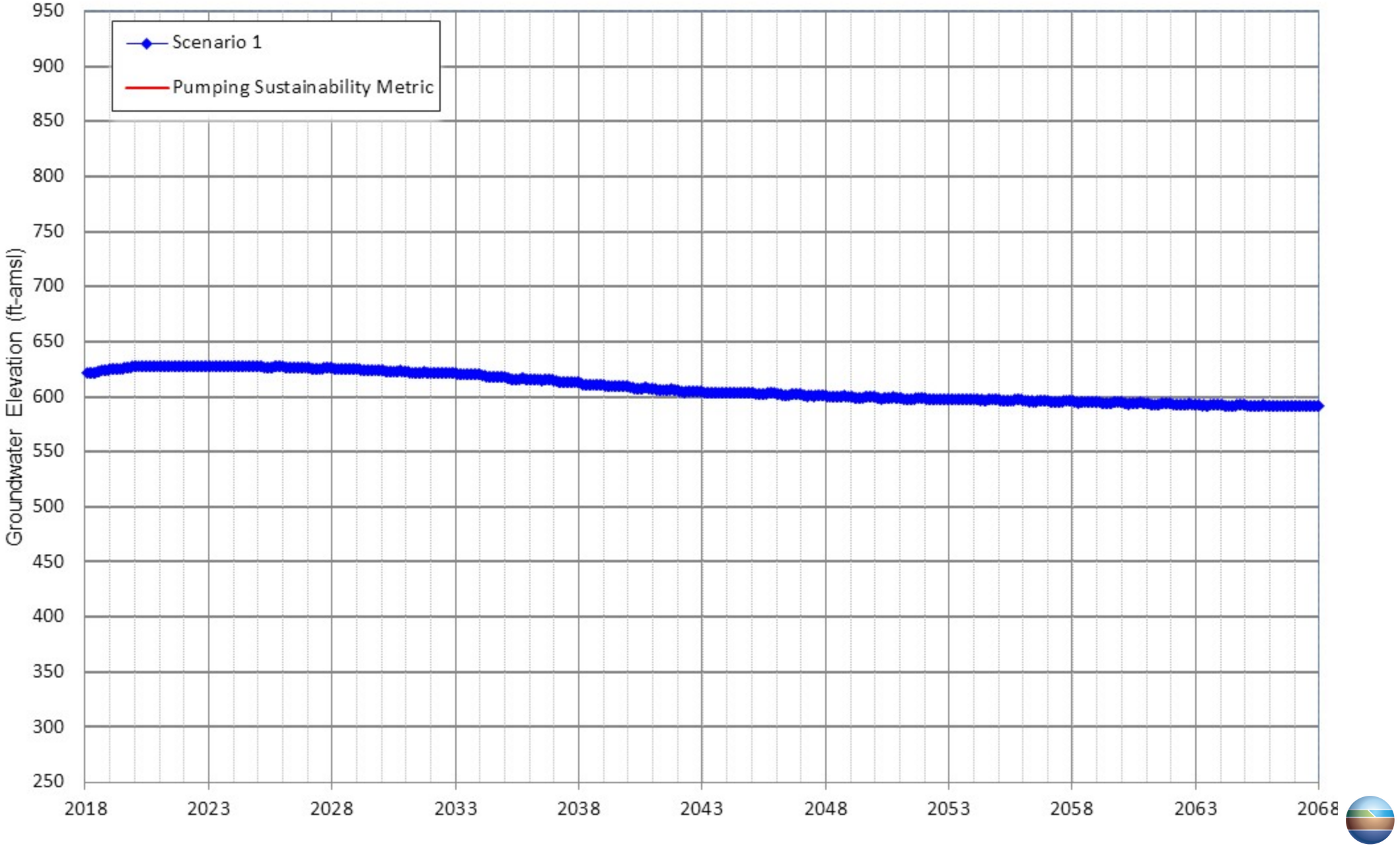

Appendix D-140
Projected Groundwater Elevation for Scenarios 1
City of Ontario Well 115

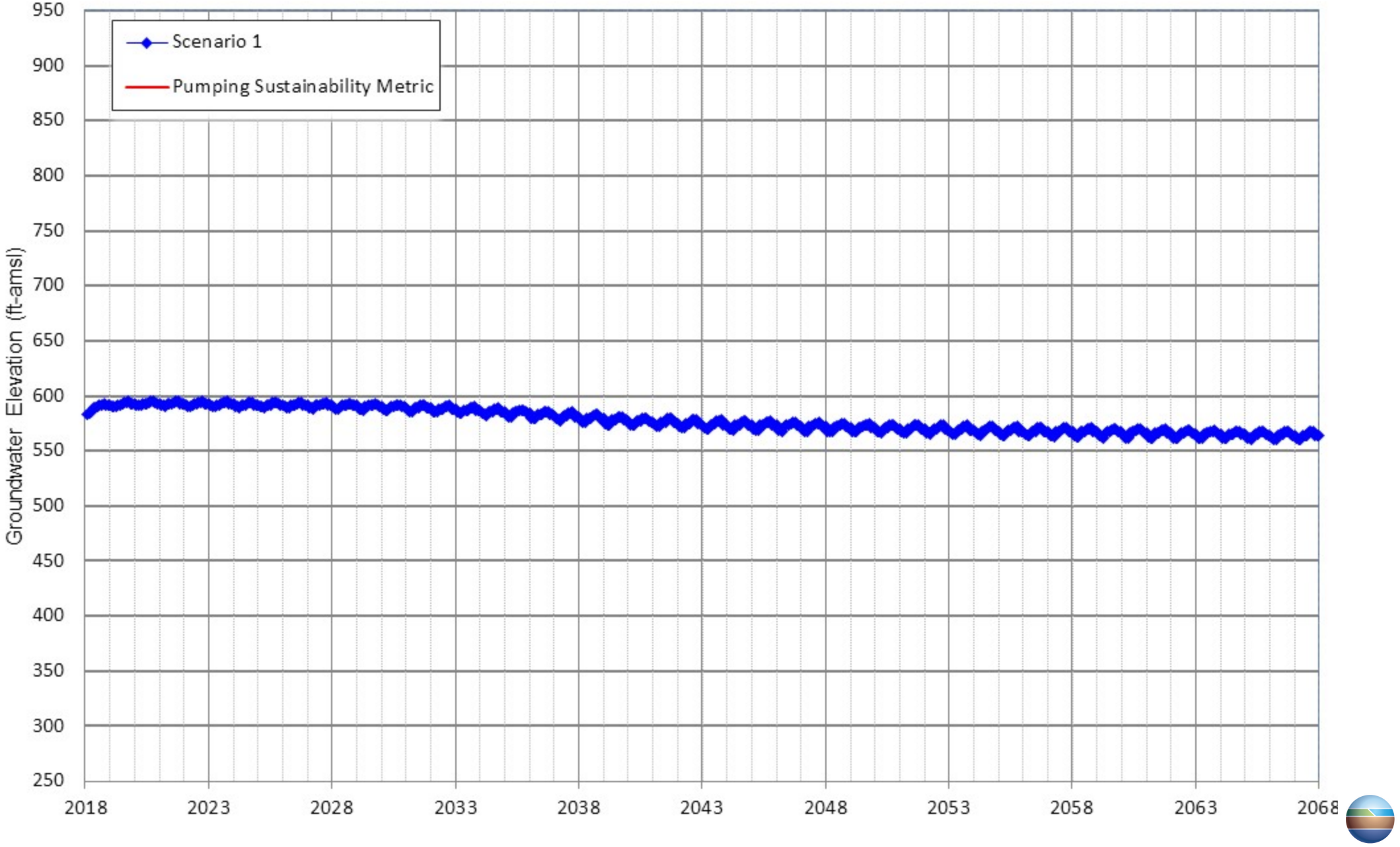

Appendix D-141
Projected Groundwater Elevation for Scenarios 1
City of Ontario Well 120

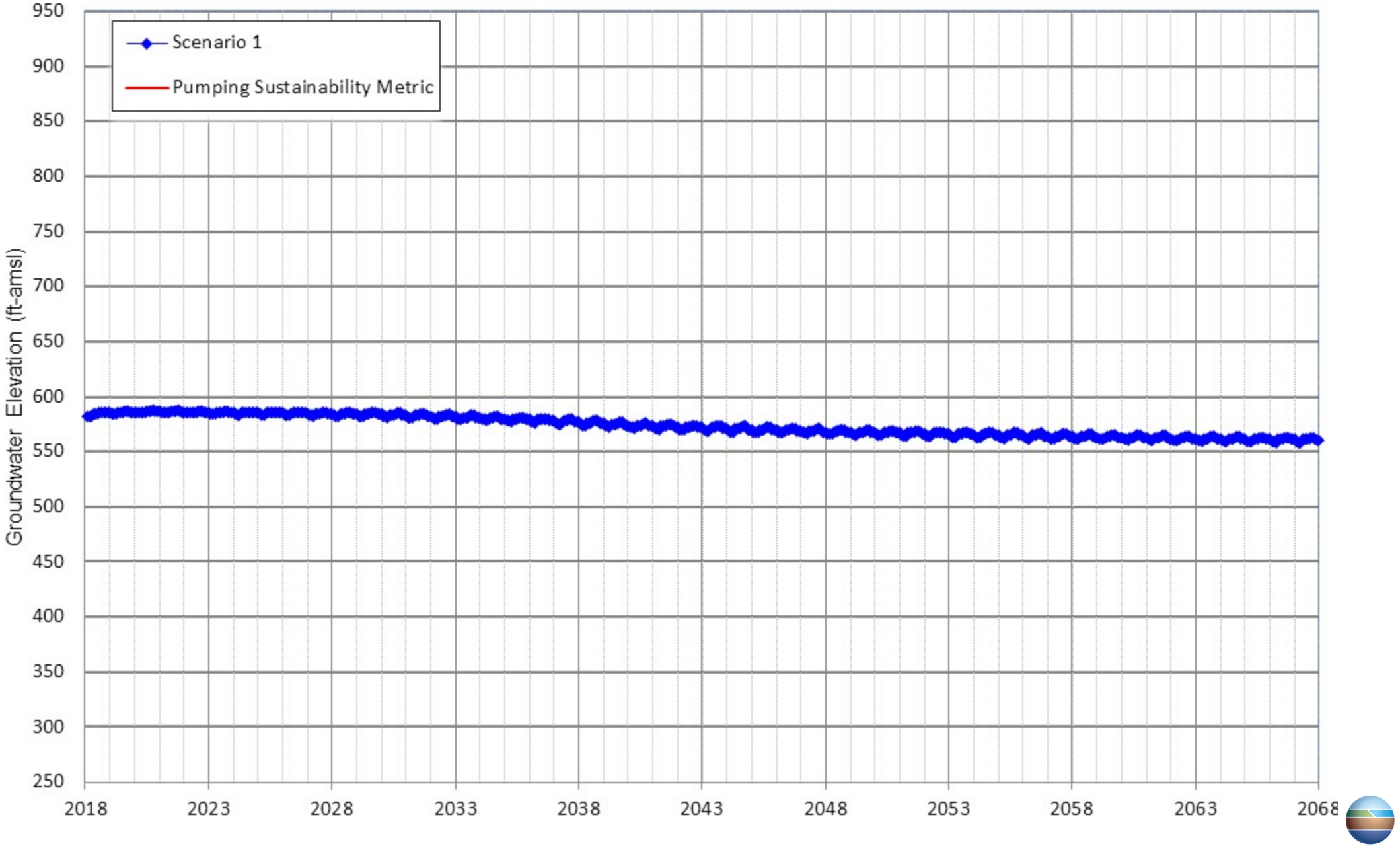

Appendix D-142
Projected Groundwater Elevation for Scenarios 1
City of Ontario Well 126

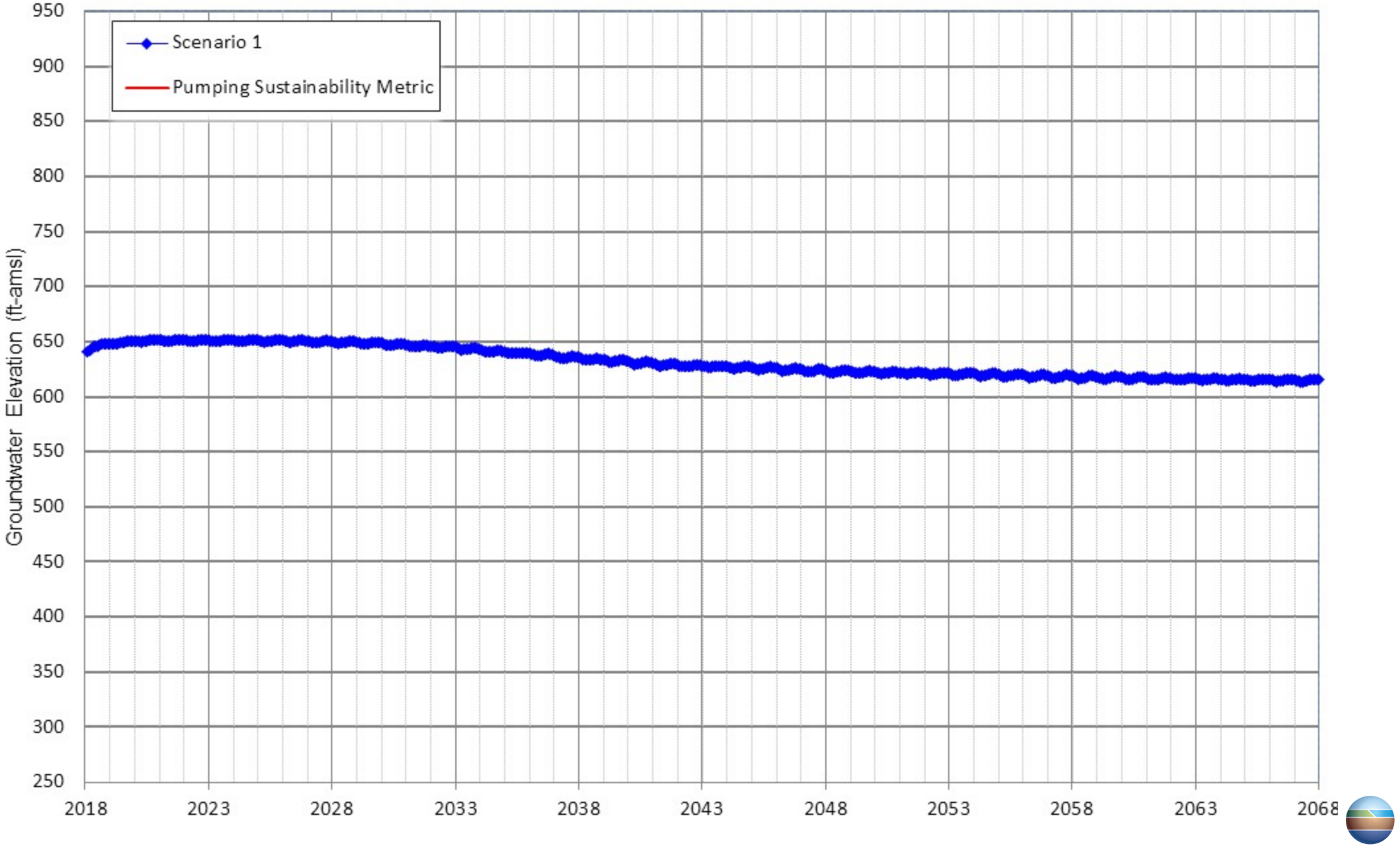

Appendix D-143
Projected Groundwater Elevation for Scenarios 1
City of Ontario Well 134

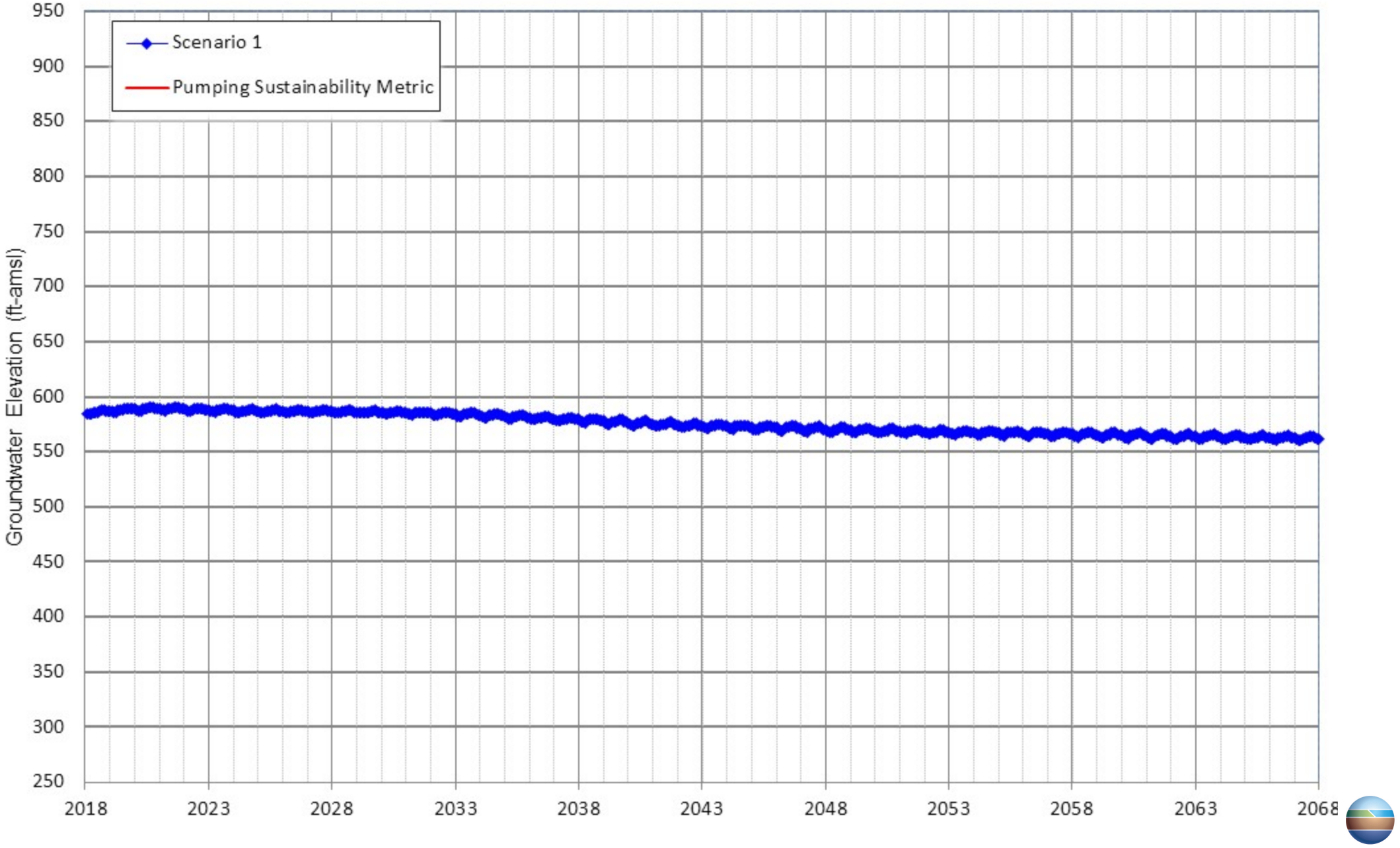

Appendix D-144
Projected Groundwater Elevation for Scenarios 1
City of Ontario Well 136

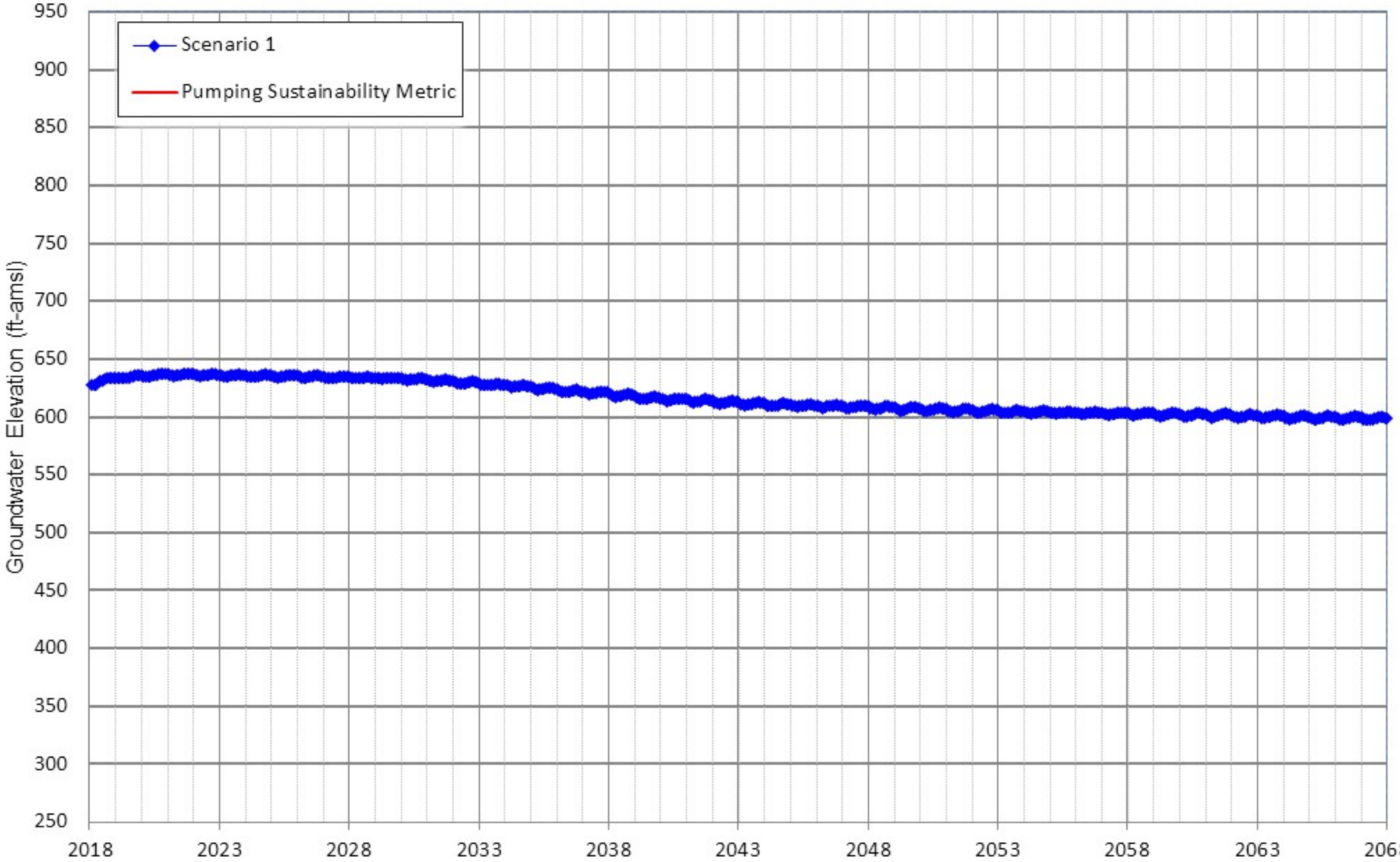

Appendix D-145
Projected Groundwater Elevation for Scenarios 1
City of Ontario Well 138

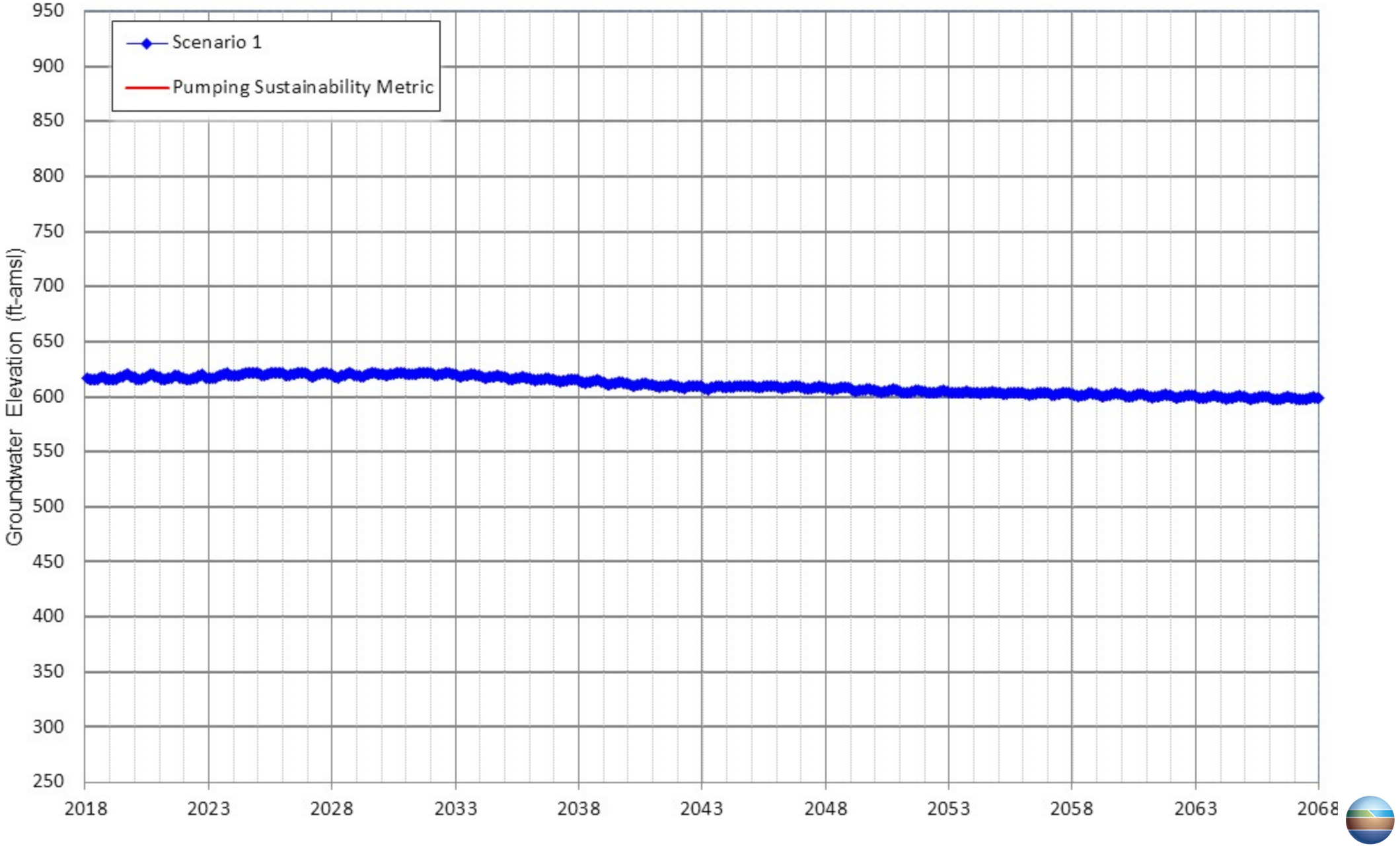

Appendix D-146
Projected Groundwater Elevation for Scenarios 1
City of Pomona Well 2

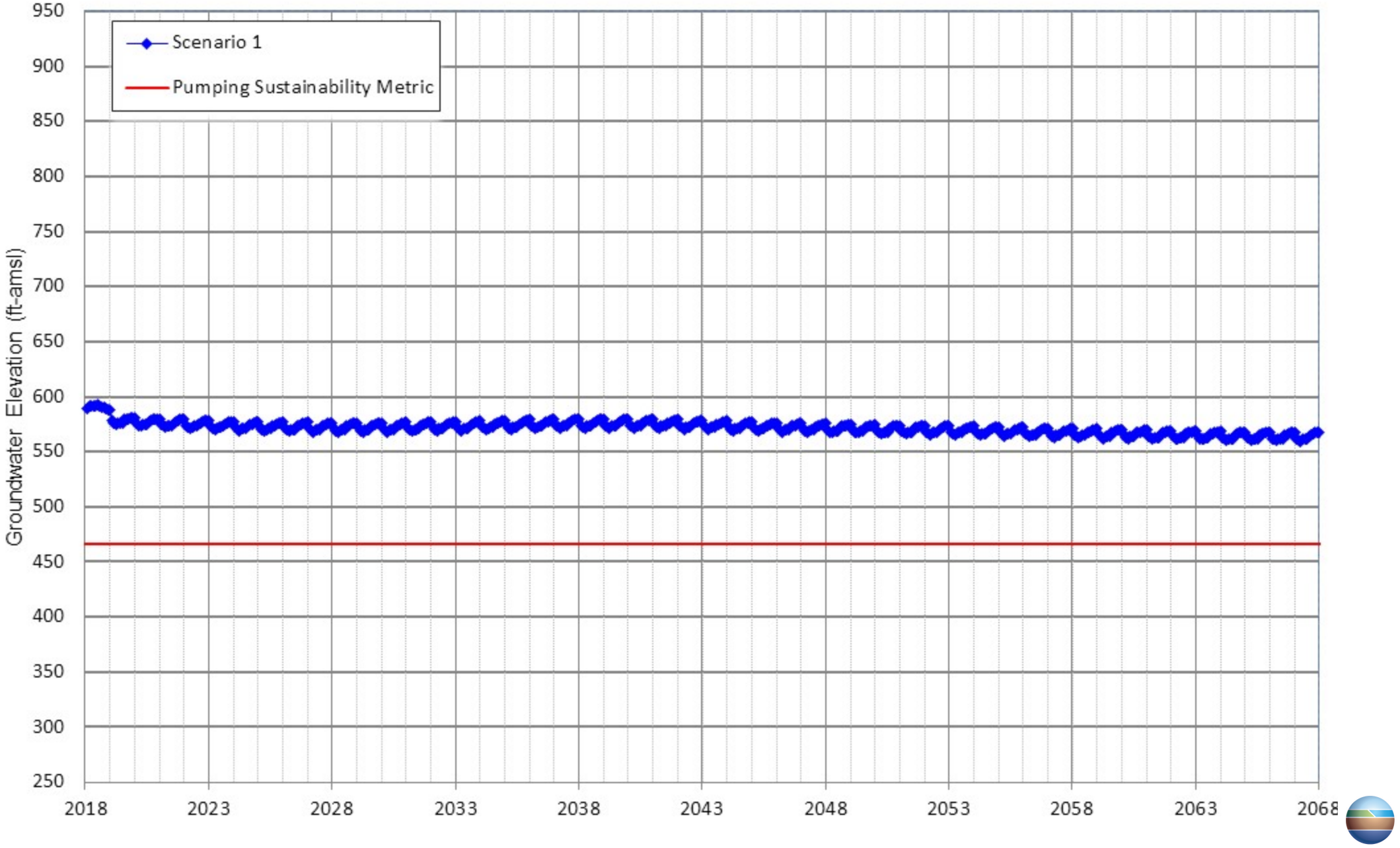

Appendix D-147
Projected Groundwater Elevation for Scenarios 1
City of Pomona Well 5B

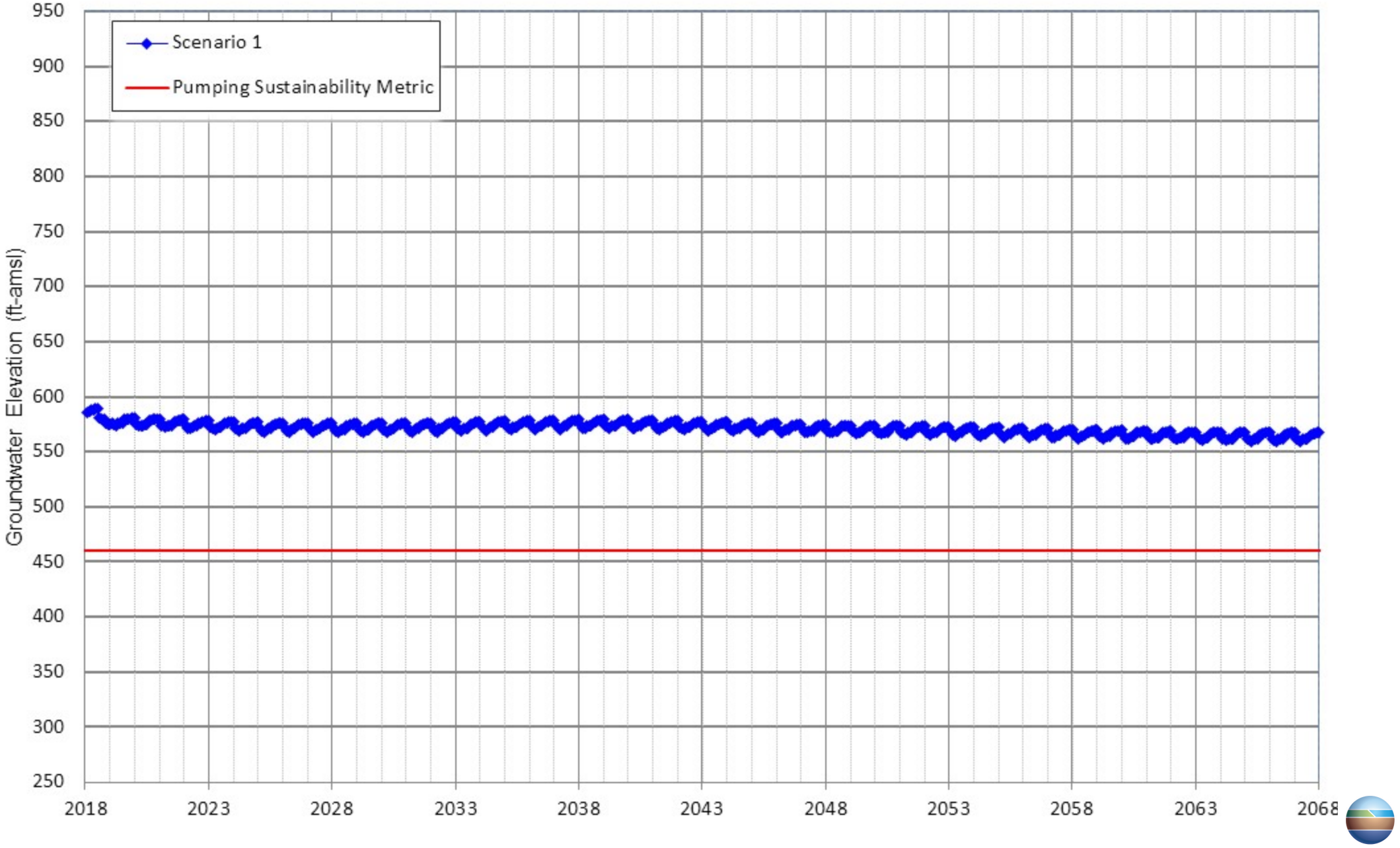

Appendix D-148
Projected Groundwater Elevation for Scenarios 1
City of Pomona Well 6

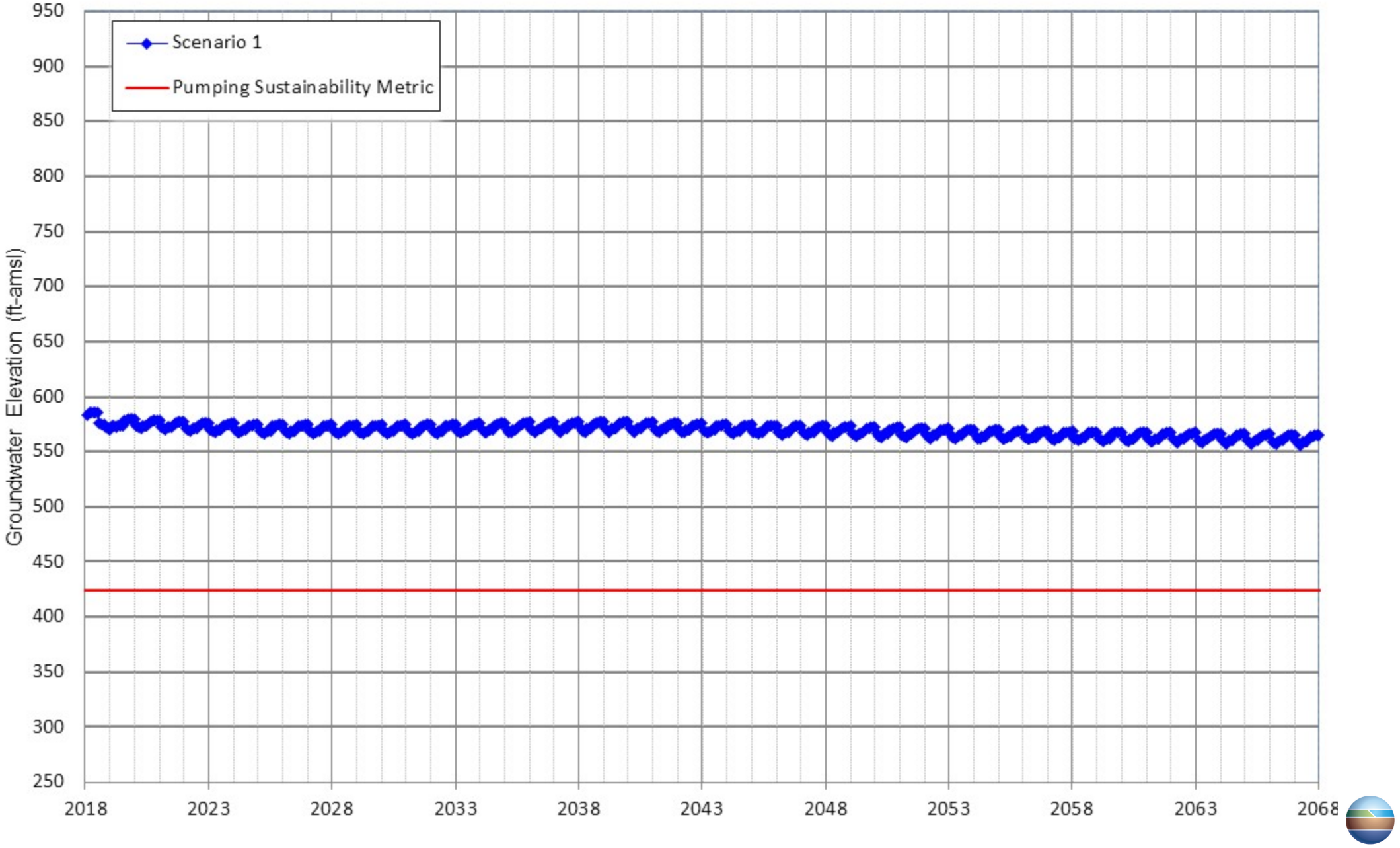

Appendix D-149
Projected Groundwater Elevation for Scenarios 1
City of Pomona Well 10B

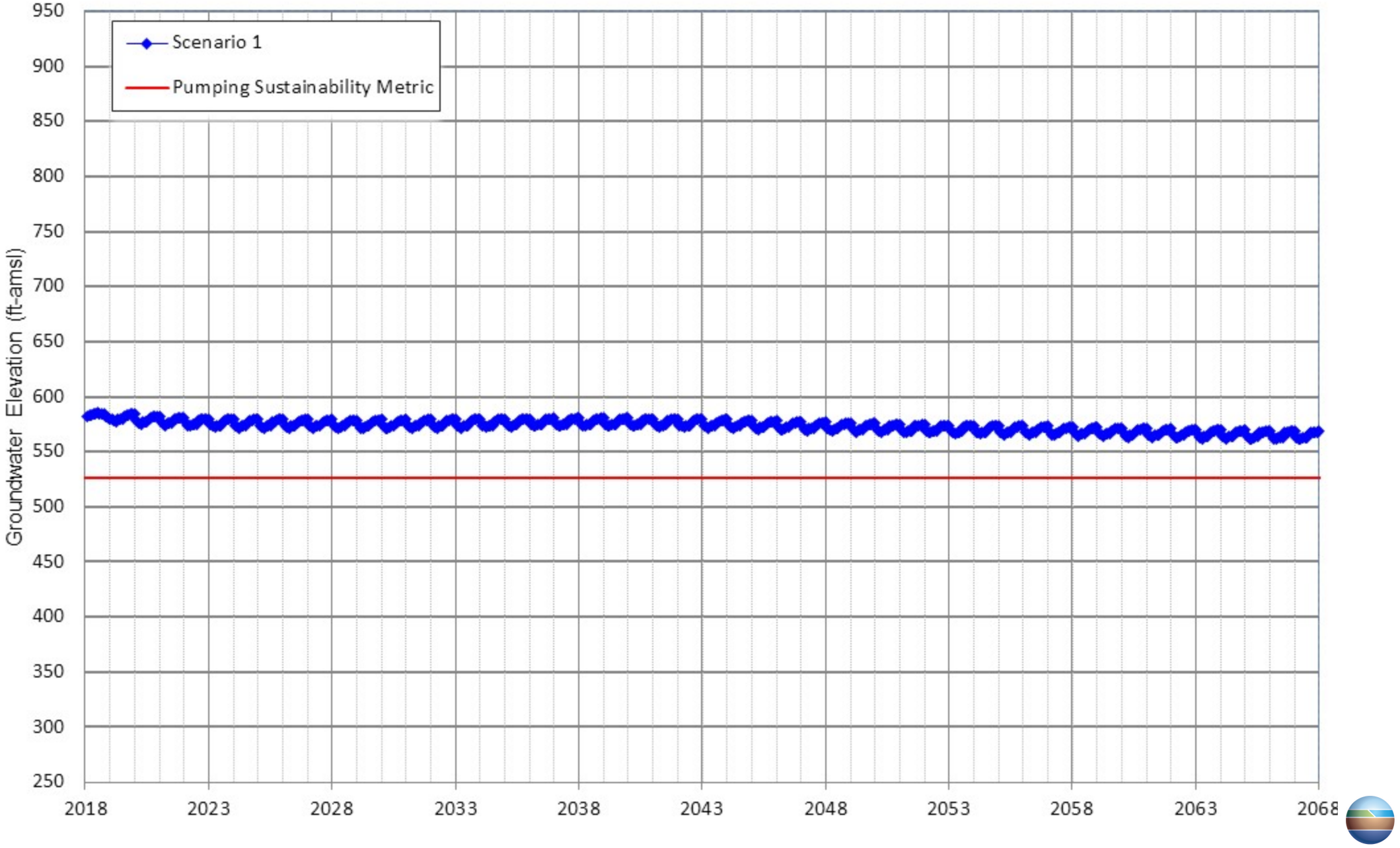

Appendix D-150
Projected Groundwater Elevation for Scenarios 1
City of Pomona Well 15

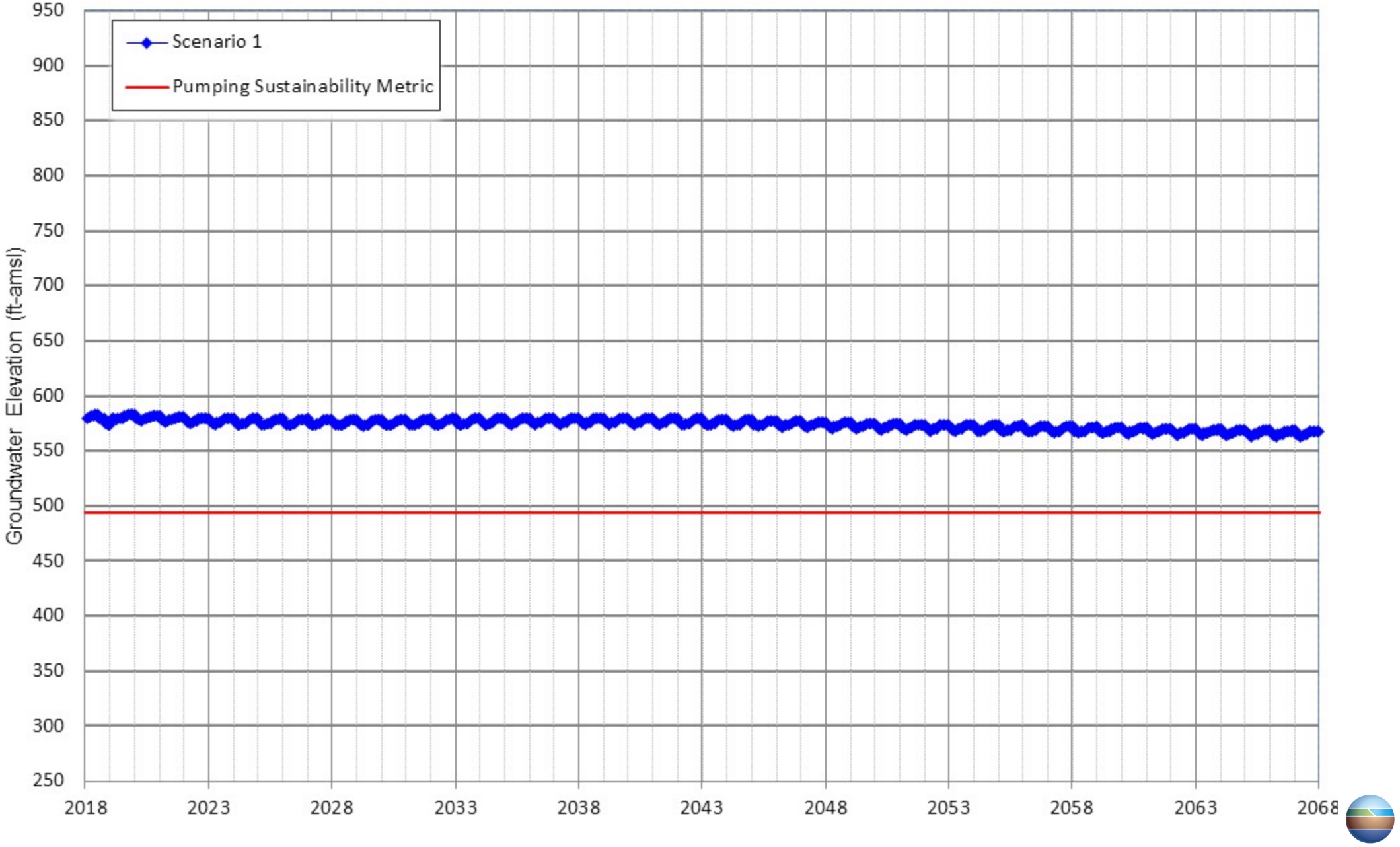

Appendix D-151
Projected Groundwater Elevation for Scenarios 1
City of Pomona Well 16

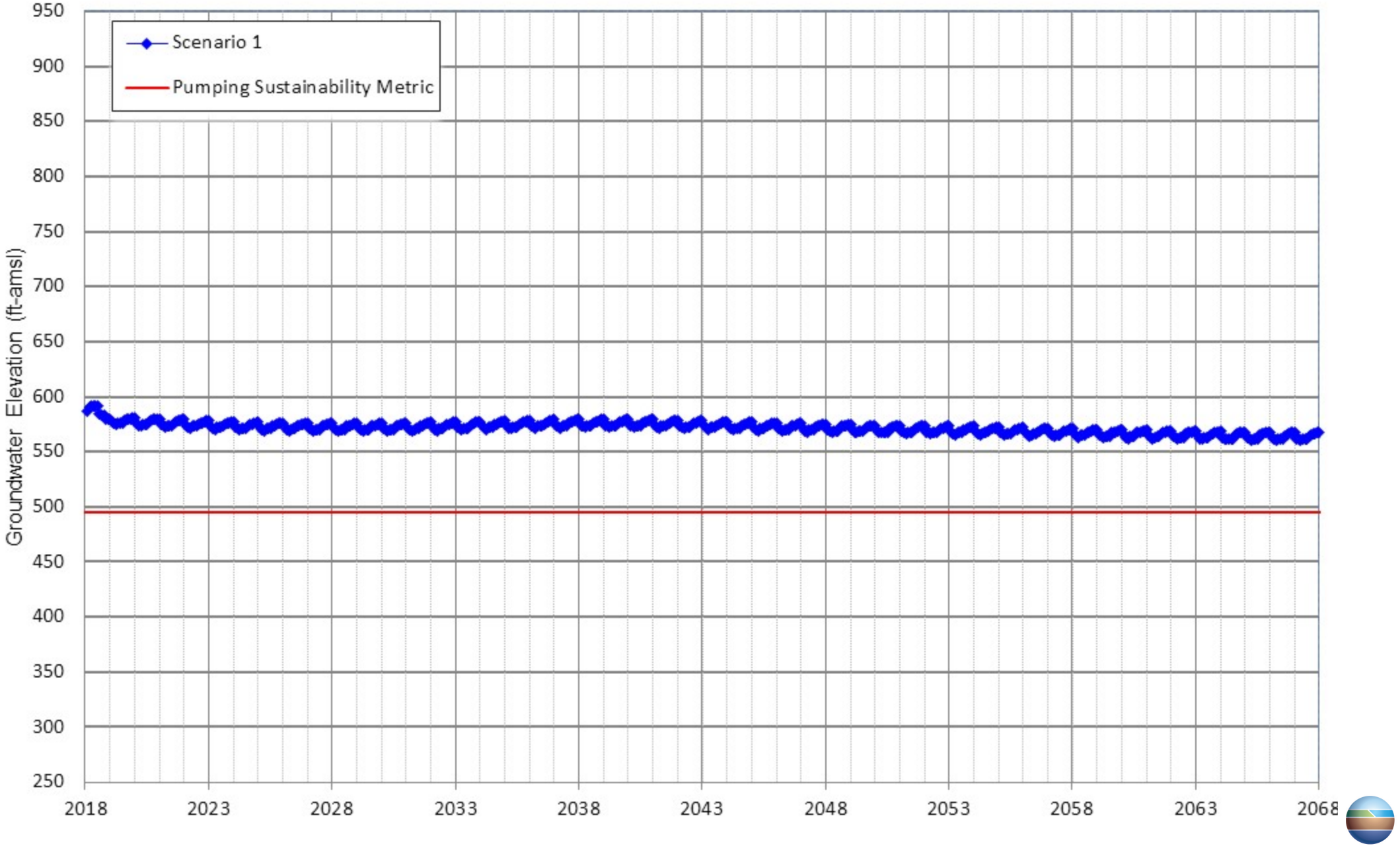

Appendix D-152
Projected Groundwater Elevation for Scenarios 1
City of Pomona Well 17

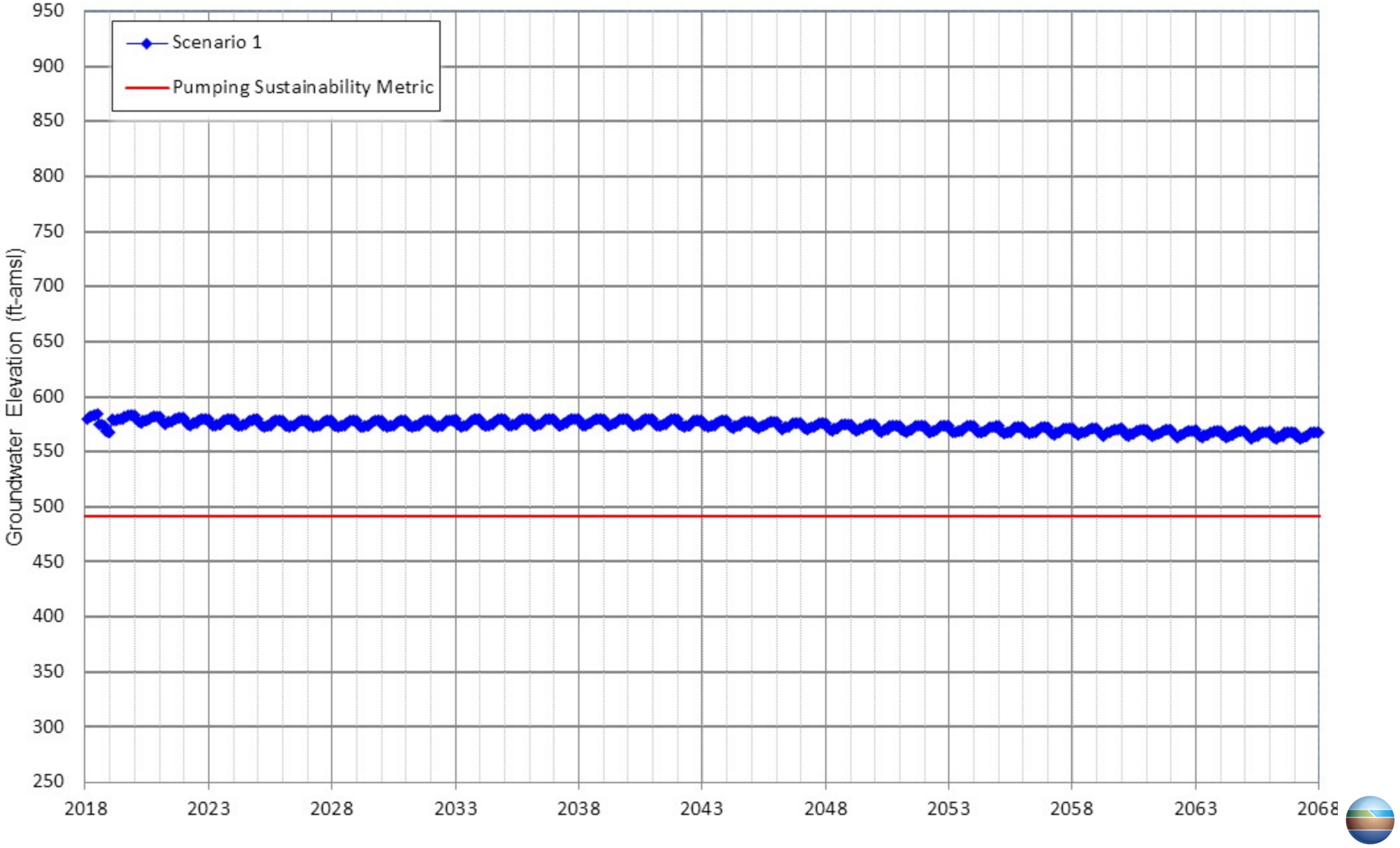

Appendix D-153
Projected Groundwater Elevation for Scenarios 1
City of Pomona Well 21

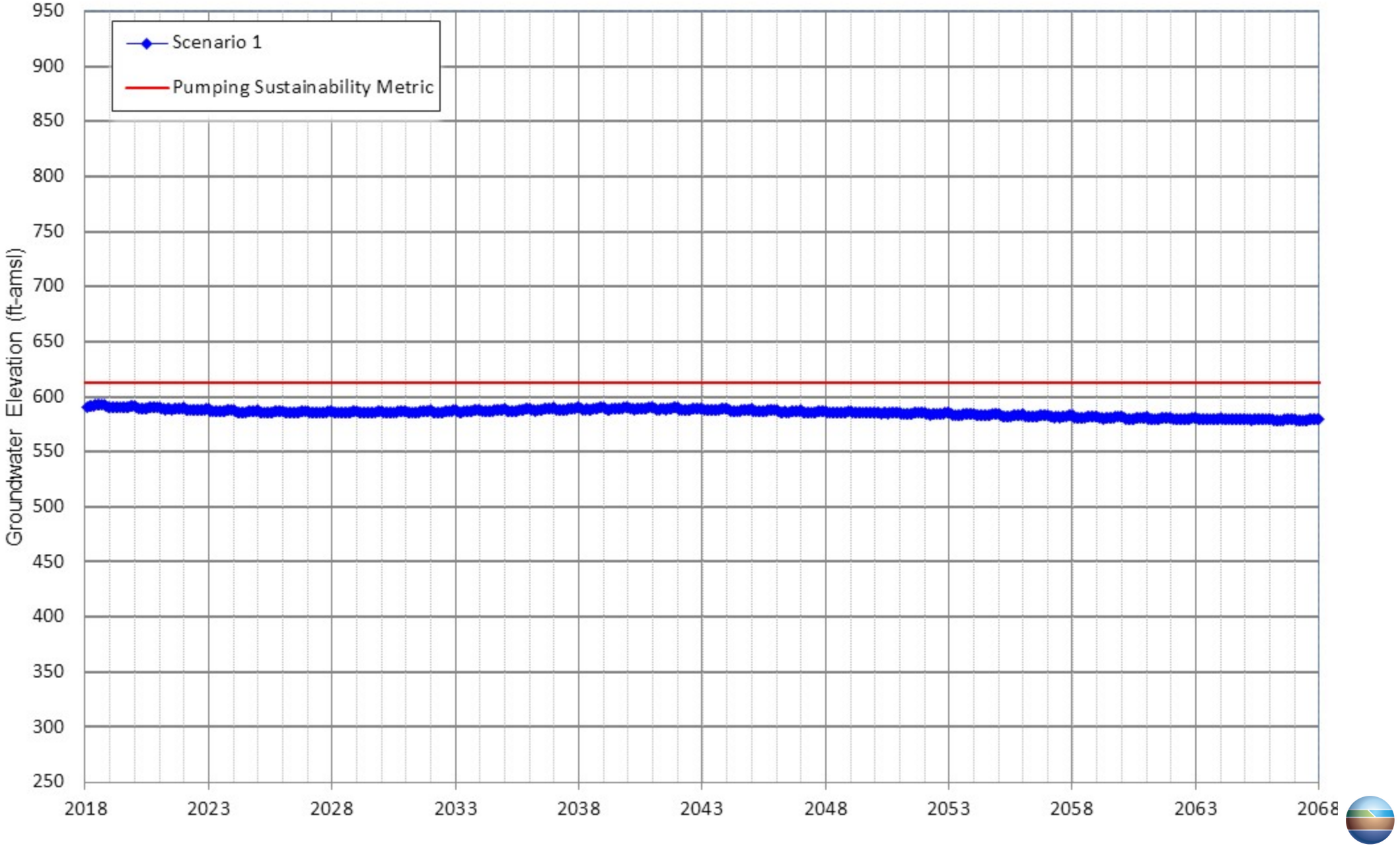

Appendix D-154
Projected Groundwater Elevation for Scenarios 1
City of Pomona Well 23

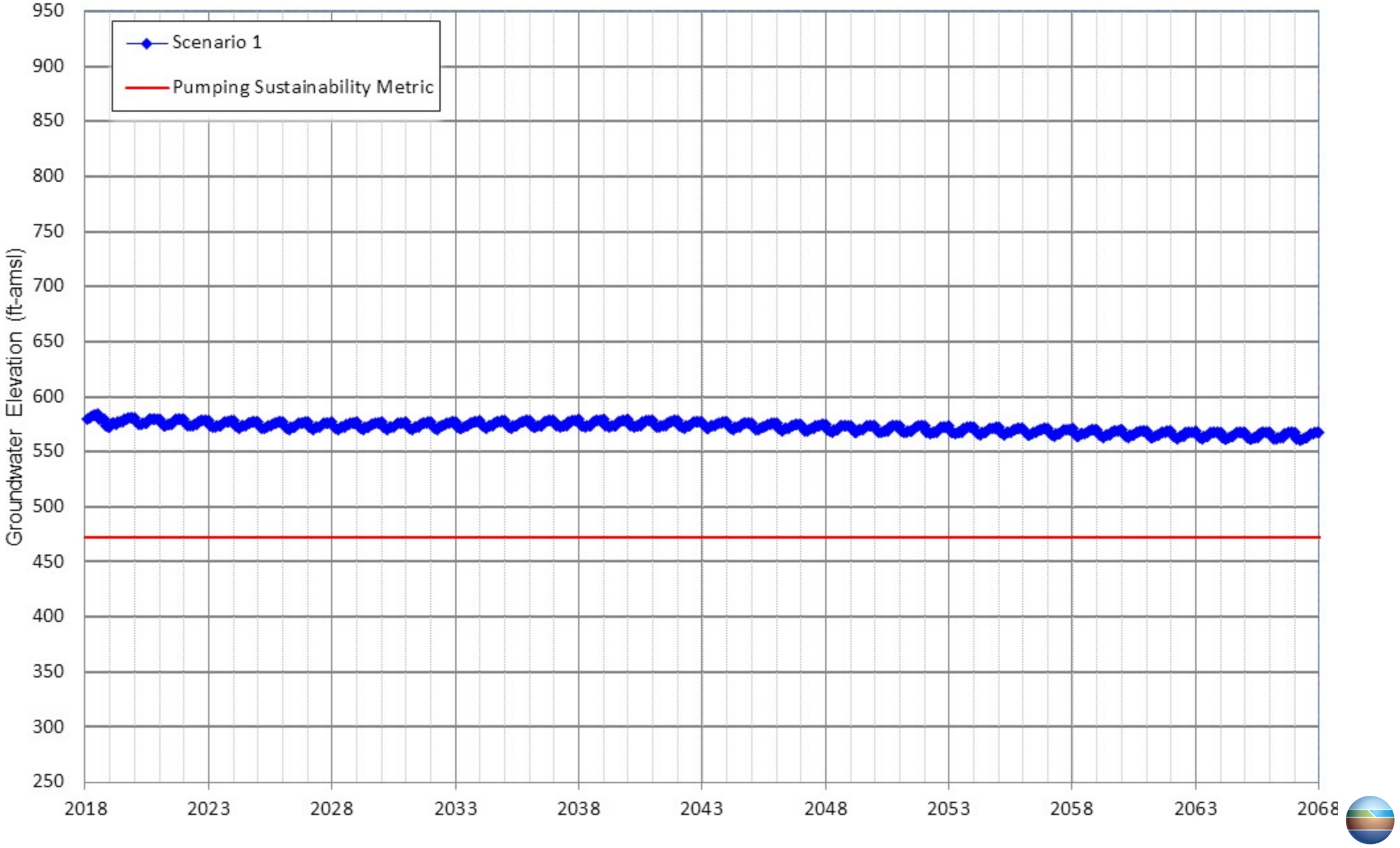

Appendix D-155
Projected Groundwater Elevation for Scenarios 1
City of Pomona Well 25

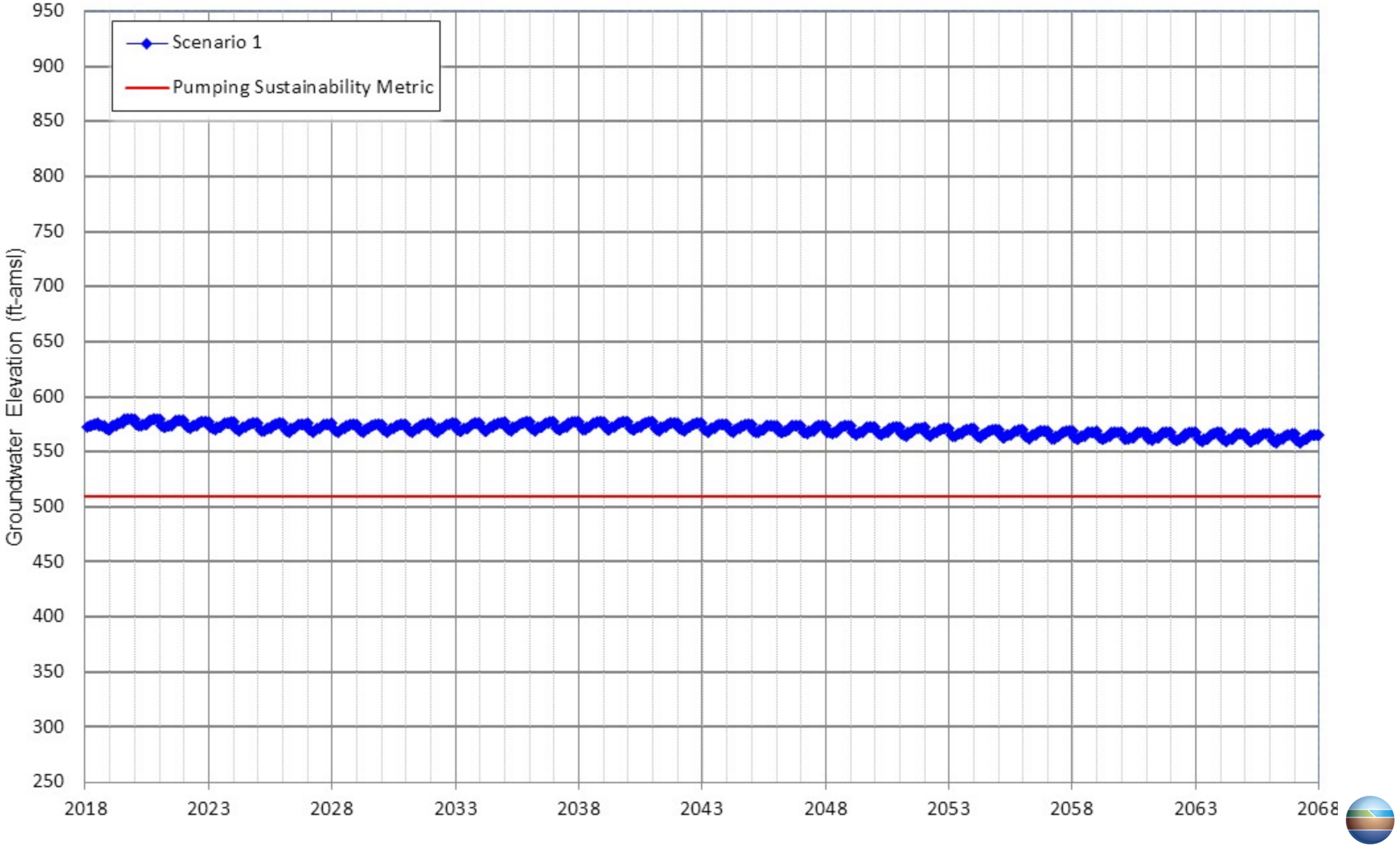

Appendix D-156
Projected Groundwater Elevation for Scenarios 1
City of Pomona Well 26

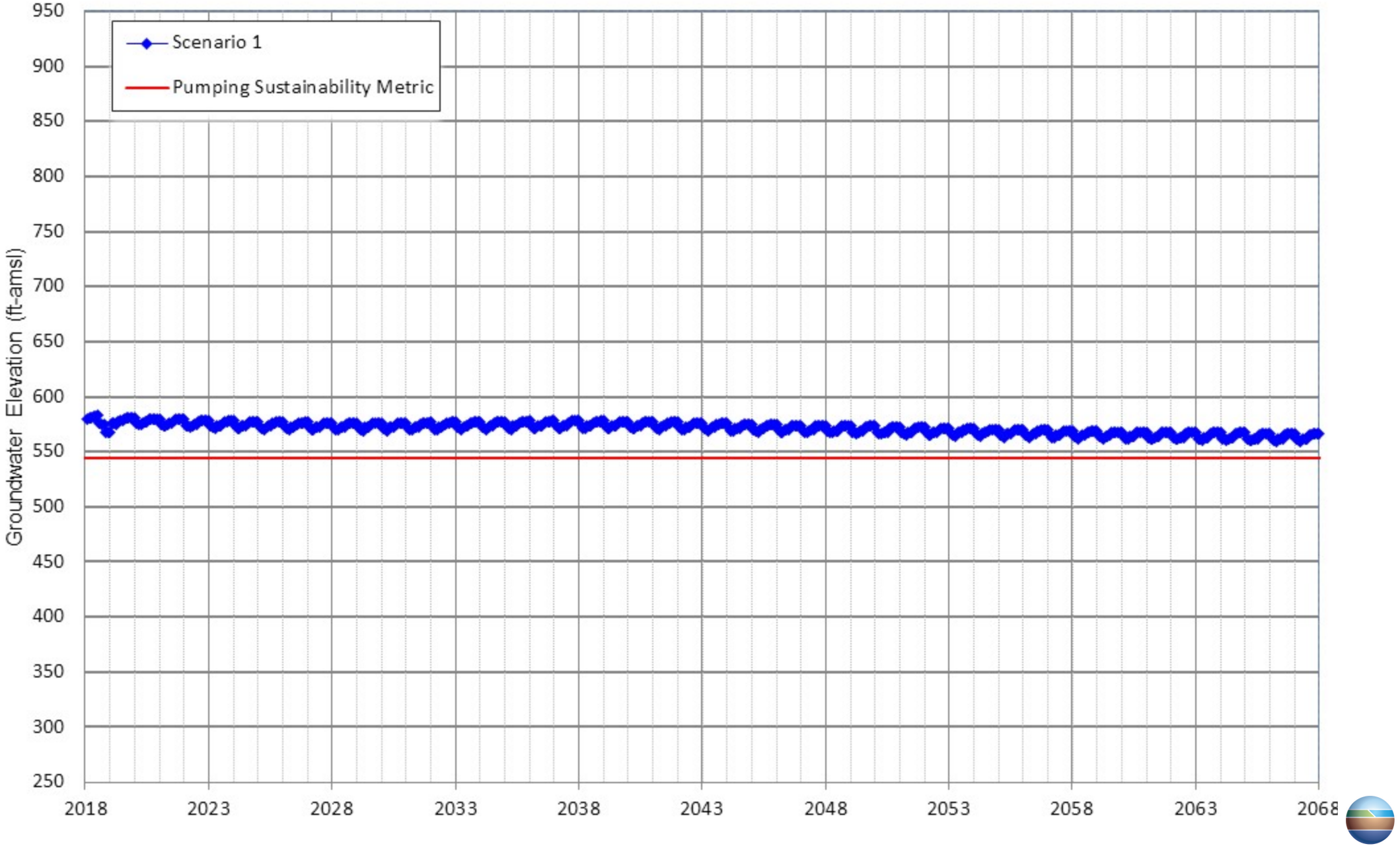

Appendix D-157
Projected Groundwater Elevation for Scenarios 1
City of Pomona Well 27

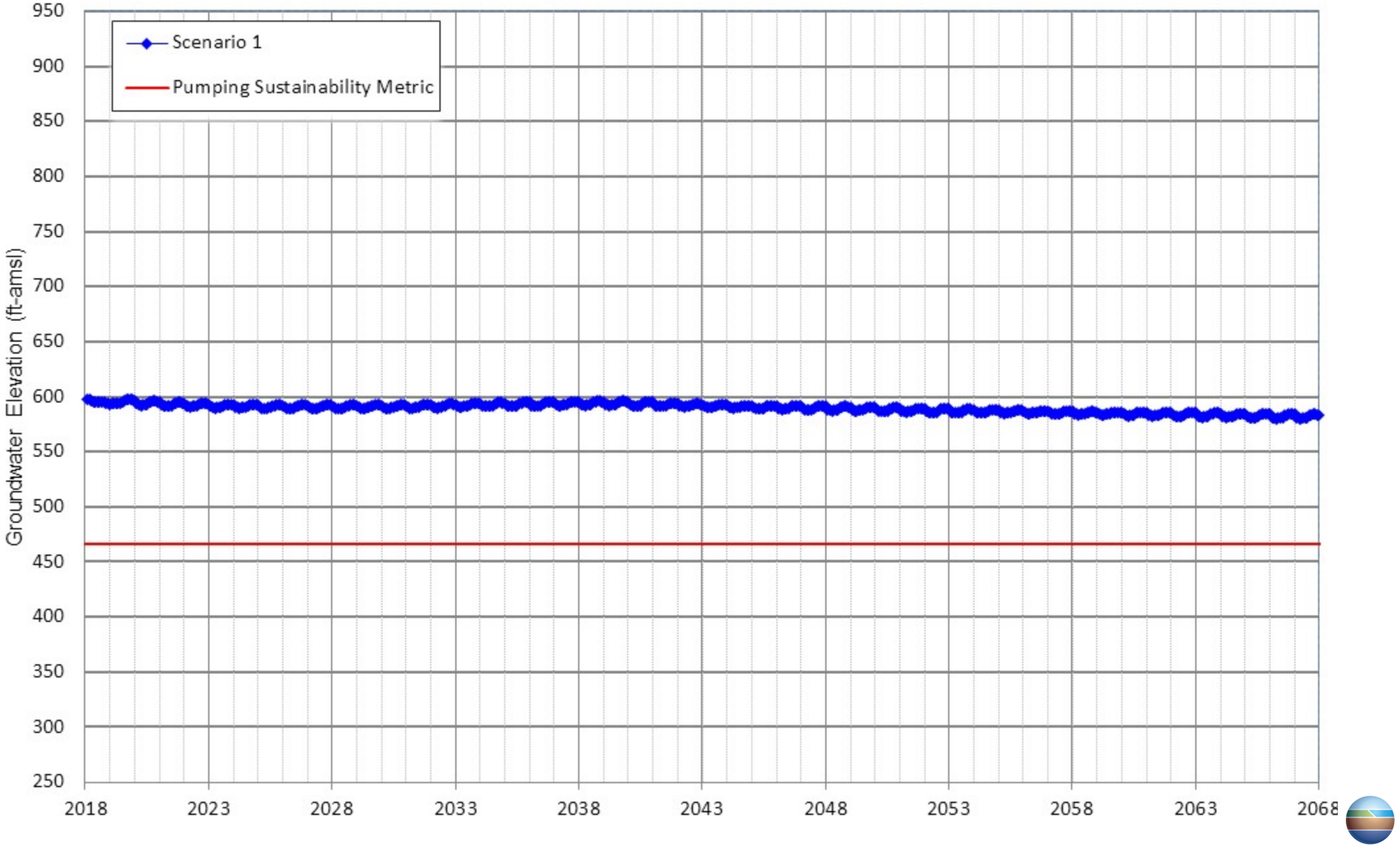

Appendix D-158
Projected Groundwater Elevation for Scenarios 1
City of Pomona Well 29

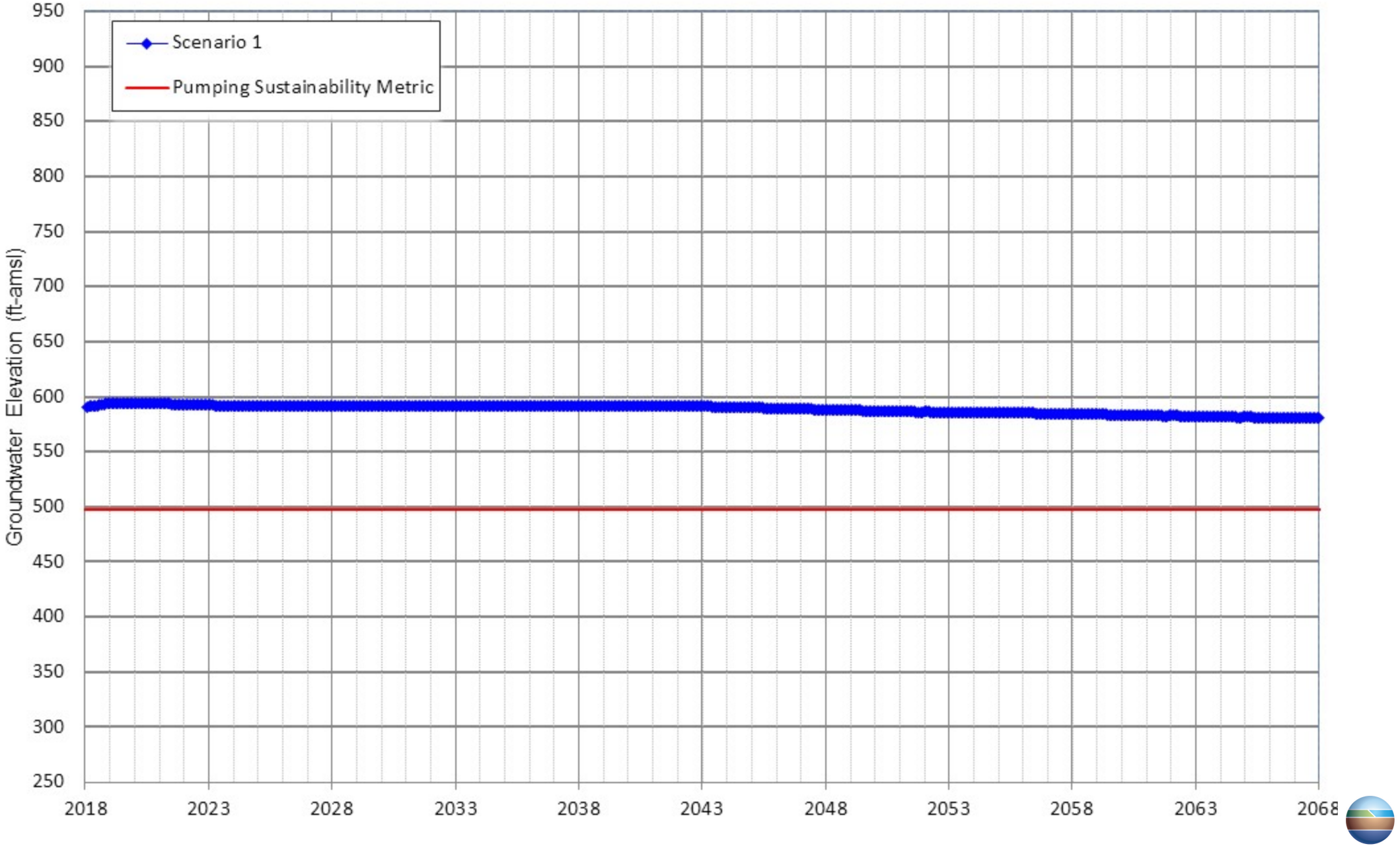

Appendix D-159
Projected Groundwater Elevation for Scenarios 1
City of Pomona Well 34

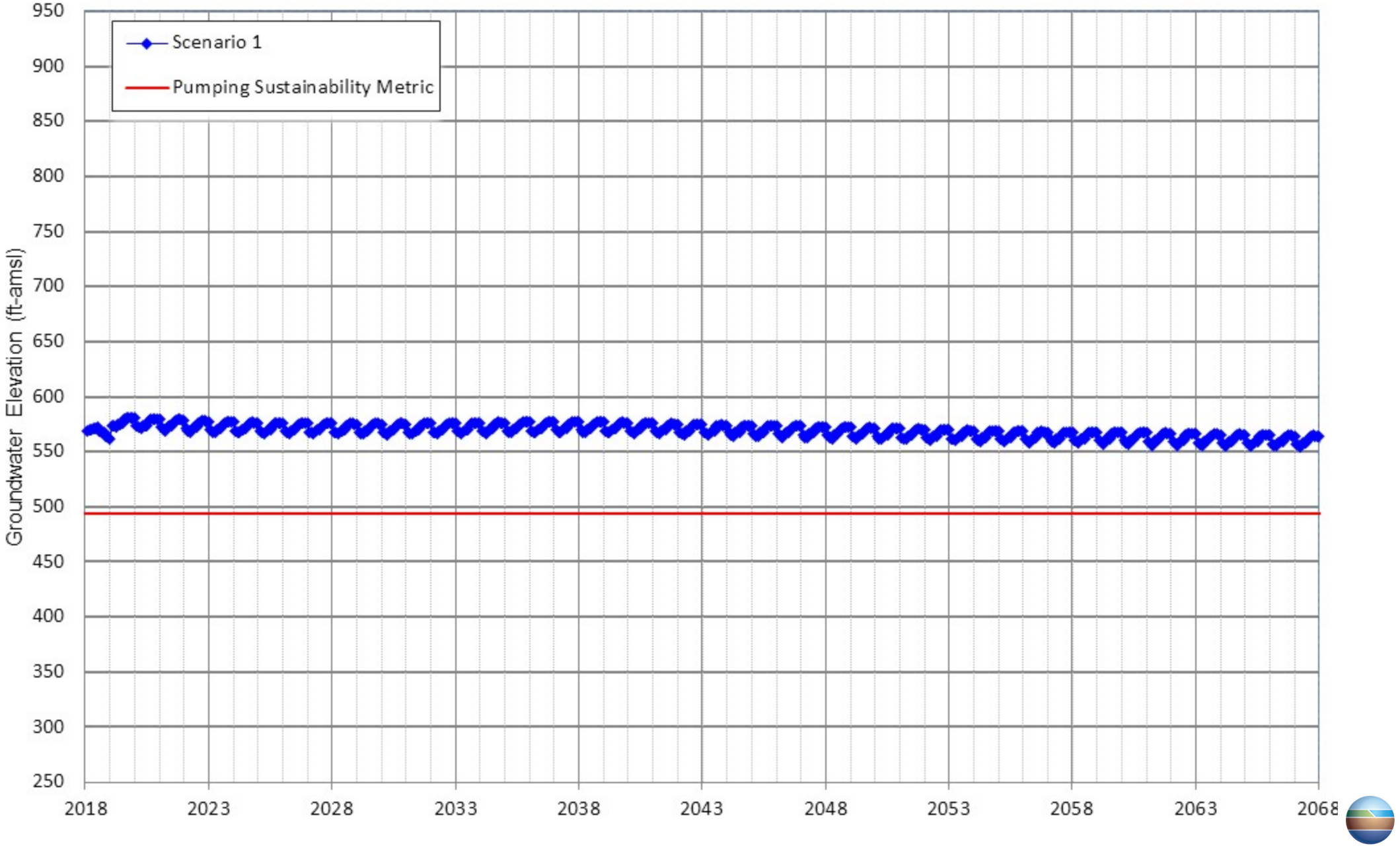

Appendix D-160
Projected Groundwater Elevation for Scenarios 1
City of Pomona Well 35

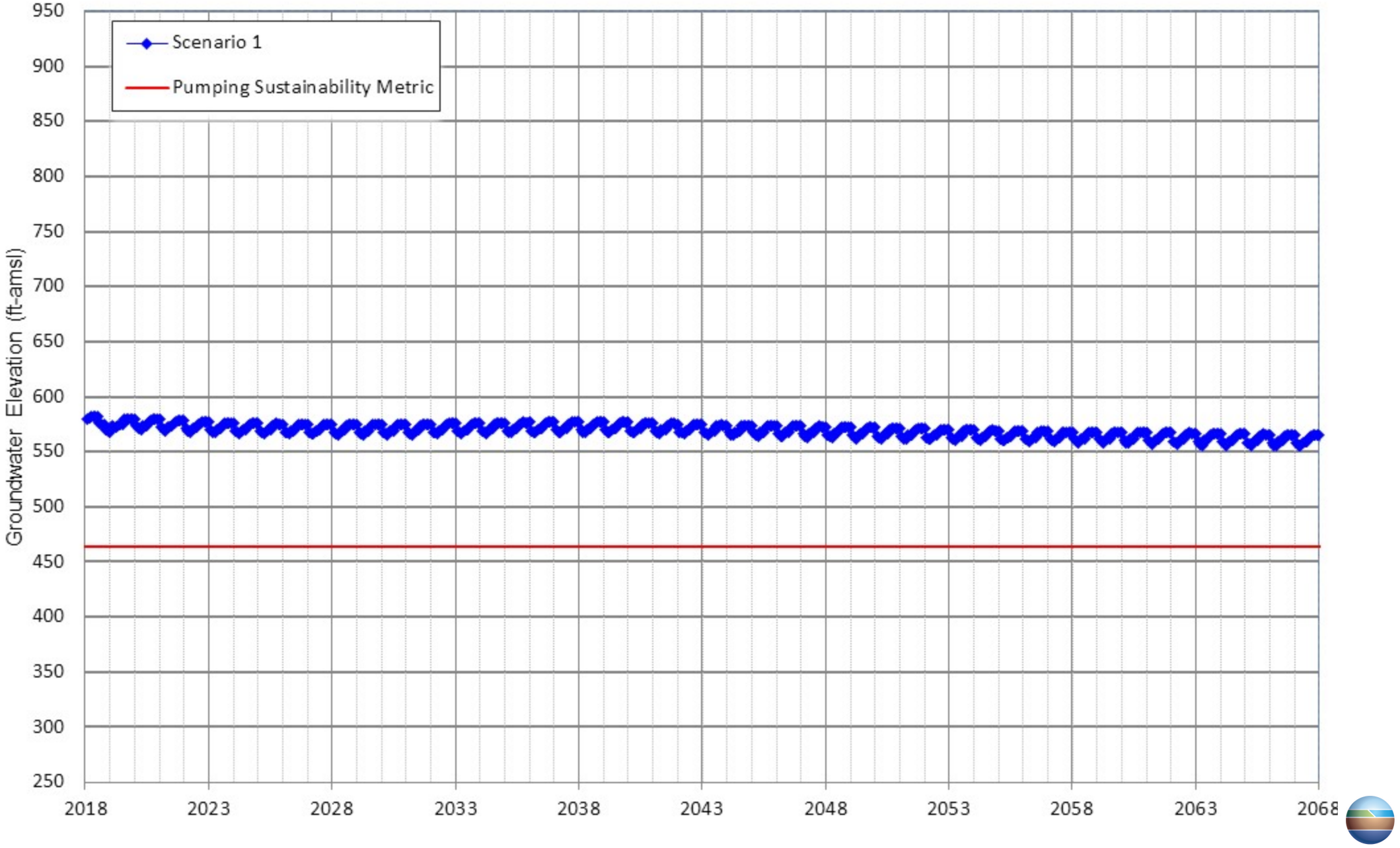

Appendix D-161
Projected Groundwater Elevation for Scenarios 1
City of Pomona Well 36

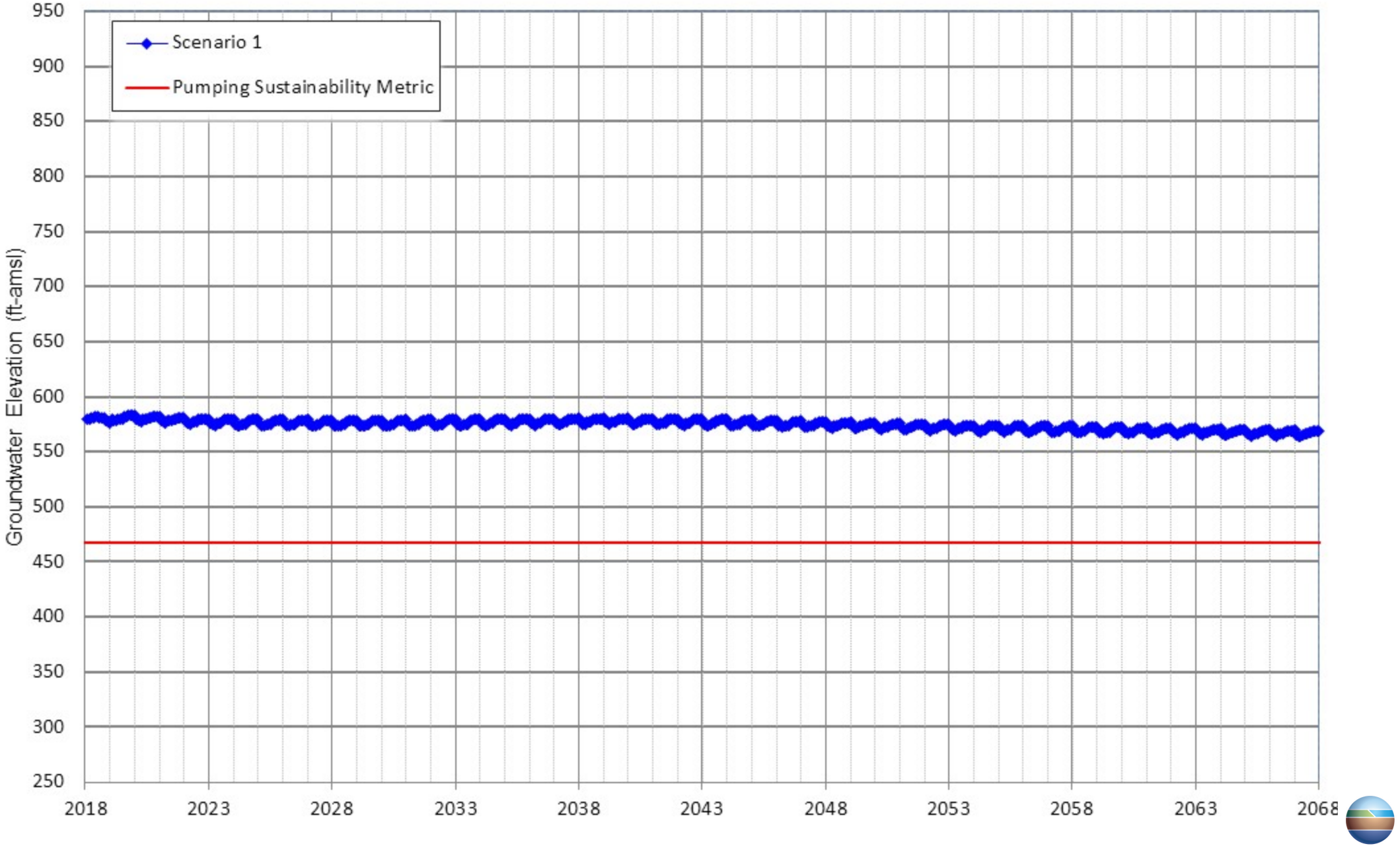

Appendix D-163
Projected Groundwater Elevation for Scenarios 1
City of Upland Well 3

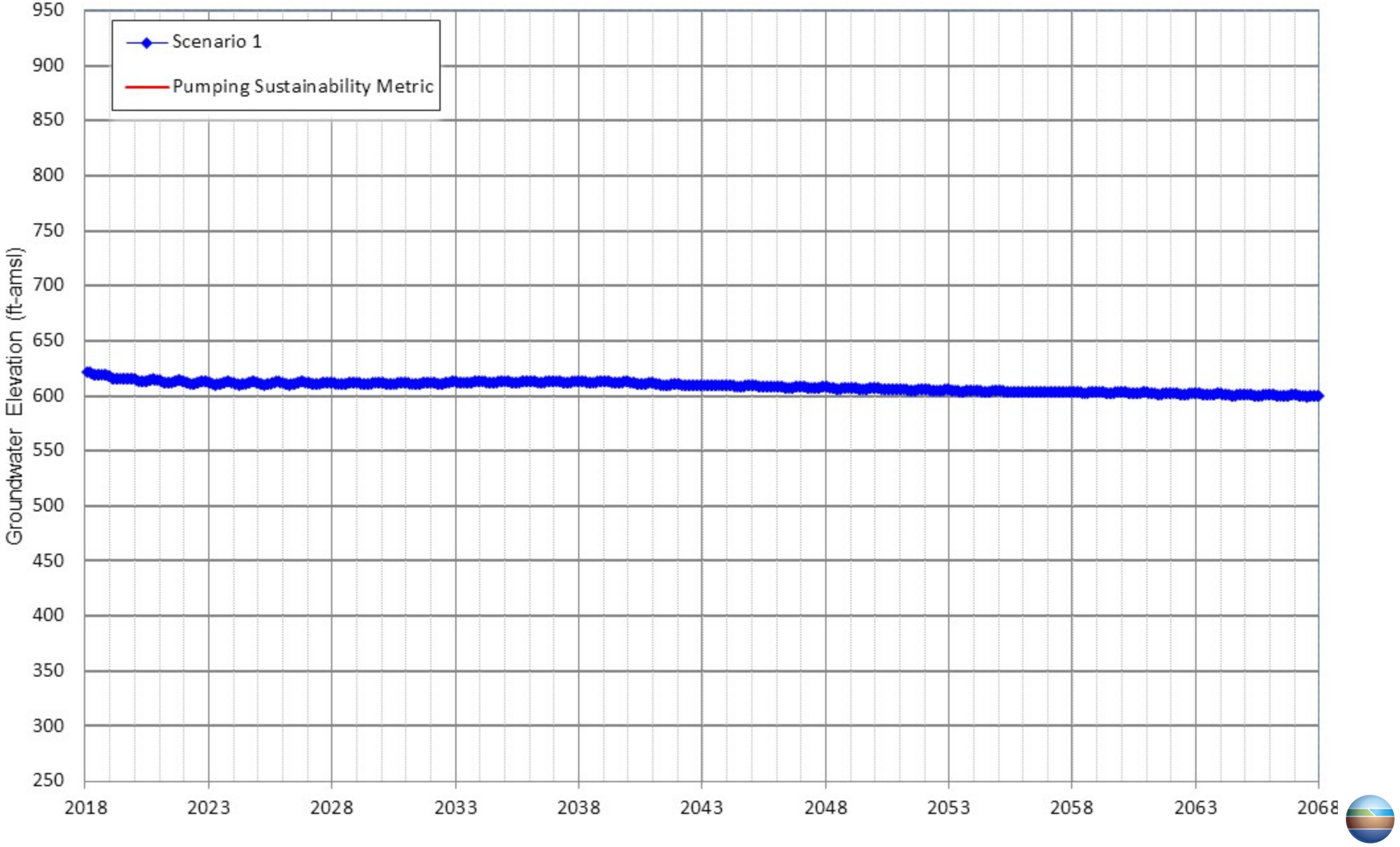

Appendix D-164
Projected Groundwater Elevation for Scenarios 1
City of Upland Well 7A

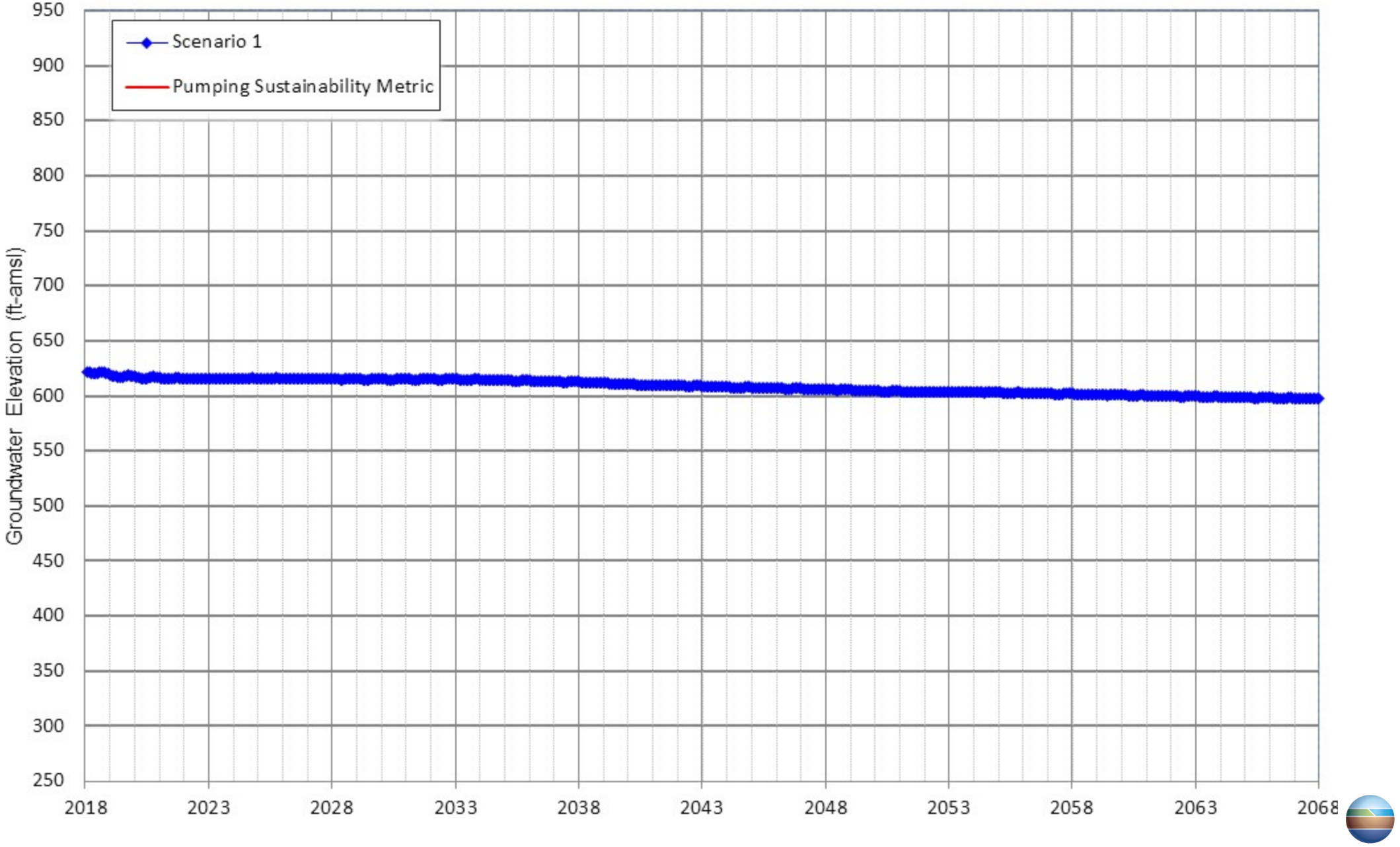

Appendix D-165
Projected Groundwater Elevation for Scenarios 1
City of Upland Well 8

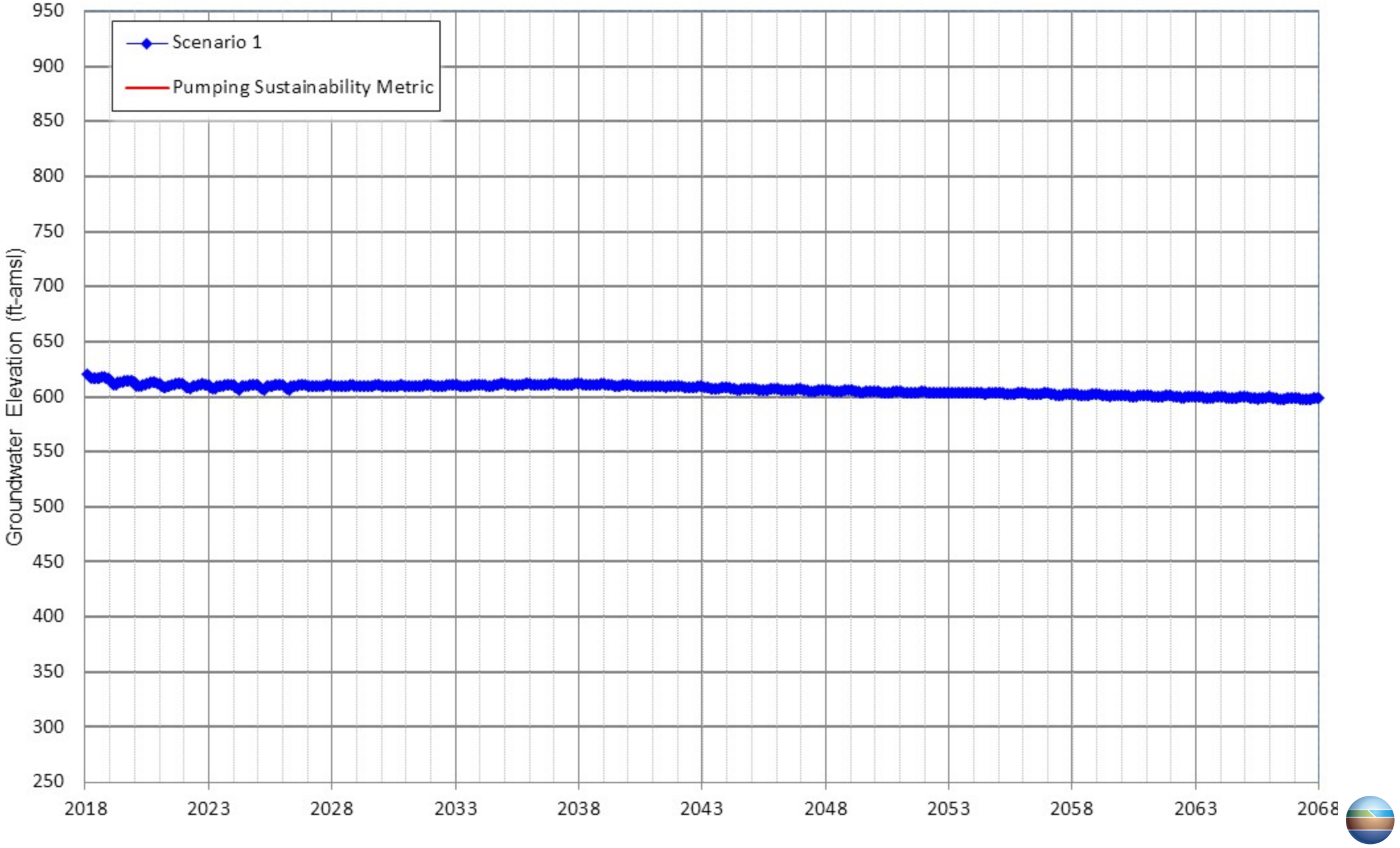

Appendix D-166
Projected Groundwater Elevation for Scenarios 1
City of Upland Well 20

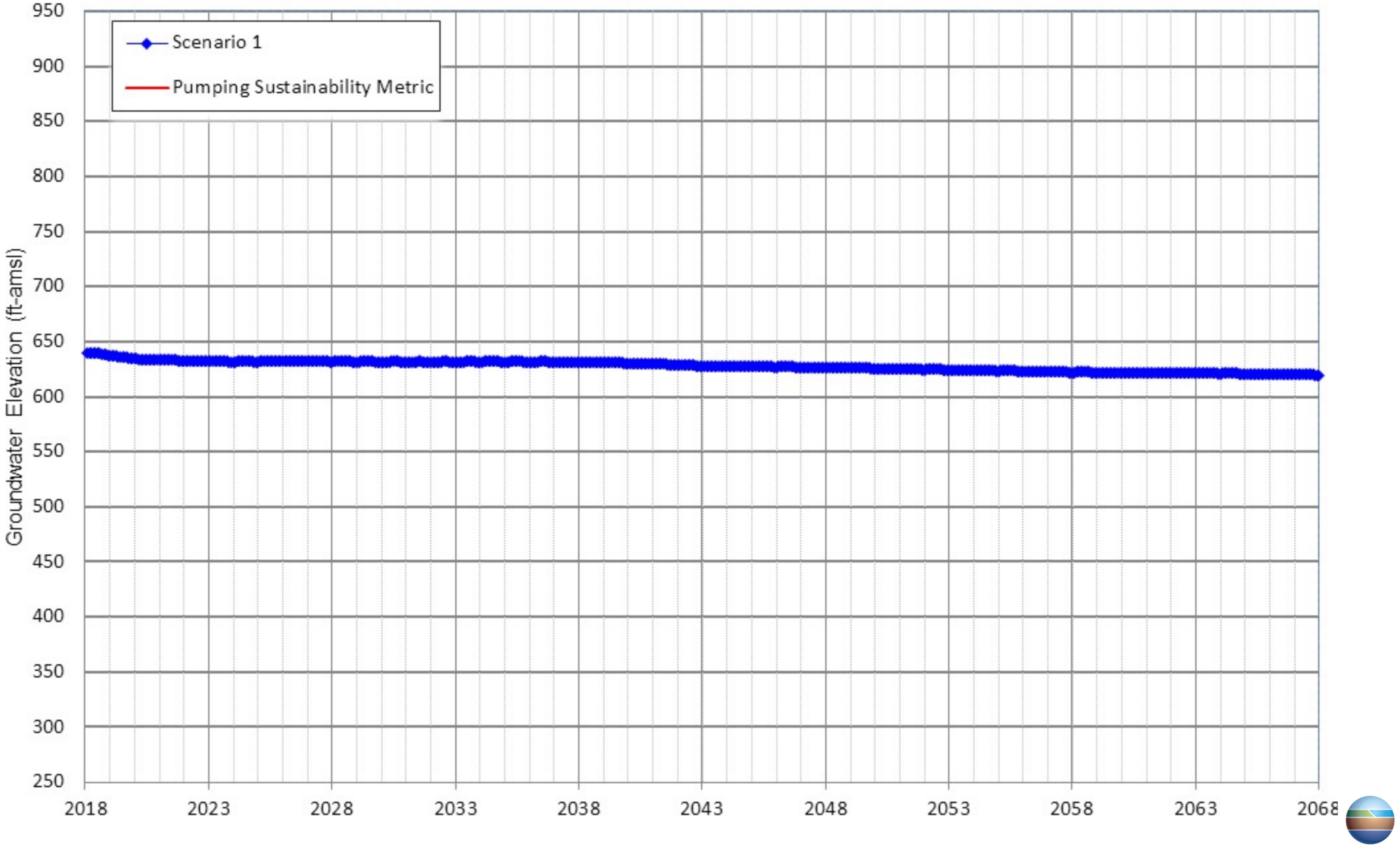

Appendix D-167
Projected Groundwater Elevation for Scenarios 1
City of Upland Well 21A

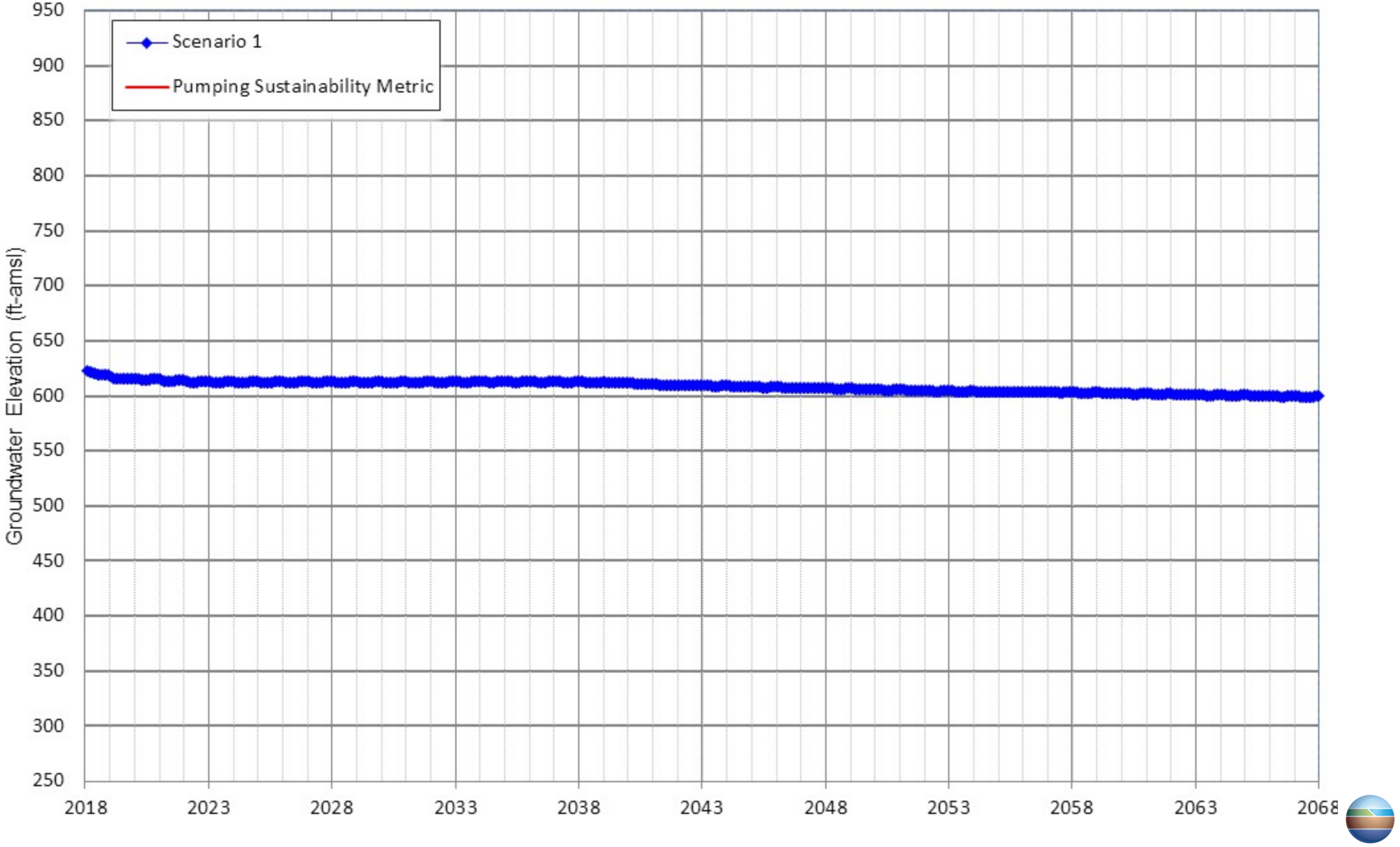

Appendix D-168
Projected Groundwater Elevation for Scenarios 1
CBWM Well AP-PA/7

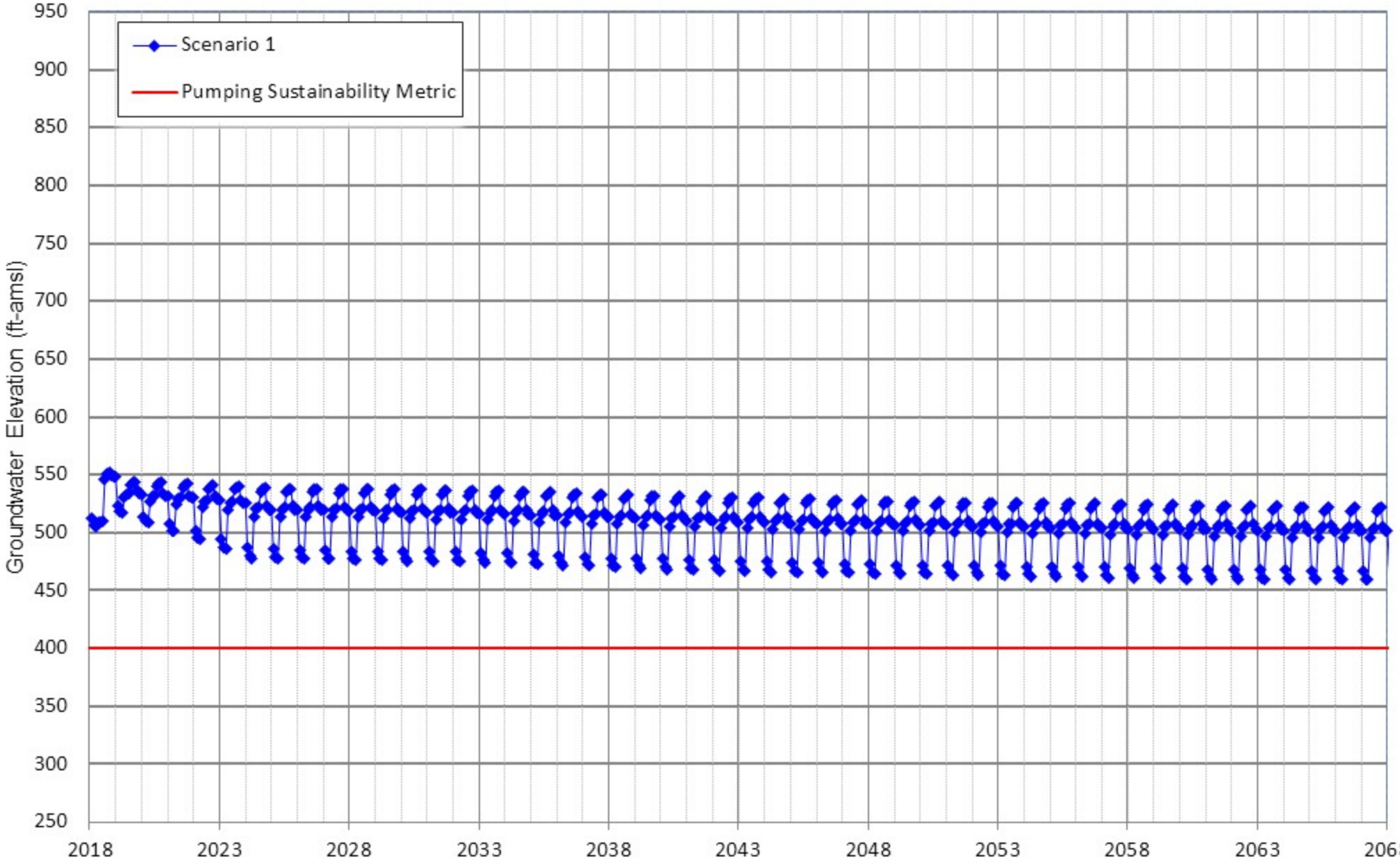

Appendix E

Maps of Calibrated Hydraulic Parameters

Table E-1 Comparison of Horizontal Hydraulic Conductivity Estimates for Aquifer Stress Tests to Initial and Model Calibrated Values (ft/d)

Well Name	Hydraulic Conductivity Value Provided by THA Based on Jacobs Solution	Hydraulic Conductivity Value Estimated by WEI Using Neuman Solution	Hydraulic Conductivity Value Estimated by WEI Using Theis Solution	Model Layers Perforated by Well	Initial Estimate of Hyrdaulic Conductivity from Lithology Model (ft/day)	Initial Parameter Zone Coefficient	Initial Hydraulic Conductivity in Model (ft/day)	Final Parameter Zone Coefficient	Final Hydraulic Conductivity in Model (ft/day)
CH 19		5.8	5.8	1					
				2					
				3	45.77	0.140	6.41	0.110	5.03
				4					
				5					
ONT 40[1]	61.78			1					
				2					
				3	47.11	0.396	18.64	1.259	59.31
				4					
				5	45.86	0.139	6.38	0.211	9.67
ONT 41[1]	35.29			1					
				2					
				3	45.89	0.396	18.16	1.259	57.77
				4					
				5	54.54	0.139	7.58	0.211	11.50
ONT 43	36.14	27.27		1					
				2					
				3	82.28	0.174	14.34	0.617	50.80
				4					
				5	73.70	0.032	2.38	0.021	1.53
ONT 44[2]	53.11			1					
				2					
				3	42.65	0.396	16.88	1.259	53.69
				4					
				5	52.98	0.139	7.36	0.211	11.17
ONT 45	41.74	44.22	55.68	1	87.50	0.475	41.57	0.982	85.90
				2					
				3	43.17	0.174	7.52	0.617	26.65
				4					
				5	43.36	0.032	1.40	0.021	0.90
ONT 46	155.24	21.57	25.27	1	91.65	0.581	53.28	0.801	73.39
				2					
				3	49.44	0.396	19.57	1.259	62.24
				4					
				5	42.30	0.139	5.88	0.211	8.92
ONT 47	67.46		55.13	1					
				2					
				3	85.55	0.396	33.85	1.259	107.69
				4					
				5	87.55	0.139	12.17	0.211	18.46
ONT 49	48.01		41.00	1	62.24	0.475	29.57	0.982	61.10
				2					
				3	94.68	0.174	16.50	0.617	58.45
				4					
				5	61.83	0.032	2.00	0.021	1.28
ONT 50	103.10	70.80		1	43.74	1.530	66.92	1.779	77.83
				2					
				3	118.55	0.347	41.14	0.526	62.35
				4					
				5					
ONT 52	40.14		14.00	1					
				2					
				3	55.24	0.396	21.86	1.259	69.53
				4					
				5	62.13	0.139	8.64	0.211	13.10
JCSD 22	304.80	92.90		1	91.14	1.526	139.08	0.716	65.25
				2					
				3					
				4					
				5					
JCSD 23	289.76	144.82		1	95.90	1.526	146.34	0.716	68.66
				2					
				3					
				4					
				5					
JCSD 25	162.37	157.00		1	84.69	1.526	129.23	0.716	60.64
				2					
				3					
				4					
				5					

Table E-1 Comparison of Horizontal Hydraulic Conductivity Estimates for Aquifer Stress Tests to Initial and Model Calibrated Values (ft/d)

Well Name	Hydraulic Conductivity Value Provided by THA Based on Jacobs Solution	Hydraulic Conductivity Value Estimated by WEI Using Neuman Solution	Hydraulic Conductivity Value Estimated by WEI Using Theis Solution	Model Layers Perforated by Well	Initial Estimate of Hyrdaulic Conductivity from Lithology Model (ft/day)	Initial Parameter Zone Coefficient	Initial Hydraulic Conductivity in Model (ft/day)	Final Parameter Zone Coefficient	Final Hydraulic Conductivity in Model (ft/day)
MMWC 06	62.40		90.48	1					
				2					
				3	41.31	0.396	17.33	1.259	52.00
				4					
				5	46.19	0.160	7.39	0.211	9.74
MVWD 31	15.41		13.53	1					
				2					
				3	43.80	0.396	17.33	1.259	55.14
				4					
				5	38.57	0.160	6.17	0.211	8.13
CDA I-13	120.71	56.00		1	89.97	1.530	137.66	1.779	160.09
				2					
				3					
				4					
				5					
CDA I-14	133.97	70.00		1	84.48	1.200	101.38	1.052	88.86
				2					
				3					
				4					
				5					
CDA I-15	171.49	129.00		1	89.97	1.200	107.97	1.052	94.63
				2					
				3					
				4					
				5					
CDA I-16[1]	16.42	16.55		1	66.06	0.340	22.46	0.249	16.45
				2					
				3					
				4					
				5					
CDA I-17	11.05	12.40		1	43.57	0.340	14.81	0.249	10.85
				2					
				3					
				4					
				5					
CDA I-18	21.01	7.80		1	53.92	0.340	18.33	0.249	13.43
				2					
				3					
				4					
				5					
CDA I-20	10.73	8.16		1	35.89	0.798	28.64	0.249	8.92
				2					
				3					
				4					
				5					
CDA I-21	18.19	15.36		1	53.17	0.798	42.43	0.249	13.21
				2					
				3					
				4					
				5					
CDA II-1	229.60	146.00		1	72.45	1.200	86.94	1.052	76.20
				2					
				3					
				4					
				5					
CDA II-2	399.65	151.09		1	80.98	1.200	97.17	1.052	85.17
				2					
				3					
				4					
				5					
CDA II-3	209.50	118.00		1	88.42	1.200	106.11	1.052	93.01
				2					
				3					
				4					
				5					
CDA II-4	246.31	157.00		1	92.52	1.200	111.02	1.052	97.31
				2					
				3					
				4					
				5					

Table E-1 Comparison of Horizontal Hydraulic Conductivity Estimates for Aquifer Stress Tests to Initial and Model Calibrated Values (ft/d)

Well Name	Hydraulic Conductivity Value Provided by THA Based on Jacobs Solution	Hydraulic Conductivity Value Estimated by WEI Using Neuman Solution	Hydraulic Conductivity Value Estimated by WEI Using Theis Solution	Model Layers Perforated by Well	Initial Estimate of Hyrdaulic Conductivity from Lithology Model (ft/day)	Initial Parameter Zone Coefficient	Initial Hydraulic Conductivity in Model (ft/day)	Final Parameter Zone Coefficient	Final Hydraulic Conductivity in Model (ft/day)
CDA II-6	358.09	136.00		1	85.35	1.200	102.41	1.052	89.77
				2					
				3					
				4					
				5					
CDA II-7	399.29	108.00		1	86.67	1.200	104.01	1.052	91.16
				2					
				3					
				4					
				5					
CDA II-8	406.25	154.00		1	91.18	1.200	109.41	1.052	95.90
				2					
				3					
				4					
				5					
CDA II-9	350.54	118.00		1	90.39	1.200	108.47	1.052	95.08
				2					
				3					
				4					
				5					
CDA II-10	757.13	119.00		1	71.47	1.200	85.77	1.052	75.17
				2					
				3					
				4					
				5					
CDA II-11	525.20	111.00		1	91.18	1.530	139.50	1.779	162.23
				2					
				3	81.55	0.347	28.30	0.526	42.90
				4					
				5					

(1) WEI did not estimate the hydraulic conductivity because the well completion report did not contain the stress test data

(2) WEI did not estimate the hydraulic conductivity because the well completion report did not contain sufficient data to estimate it

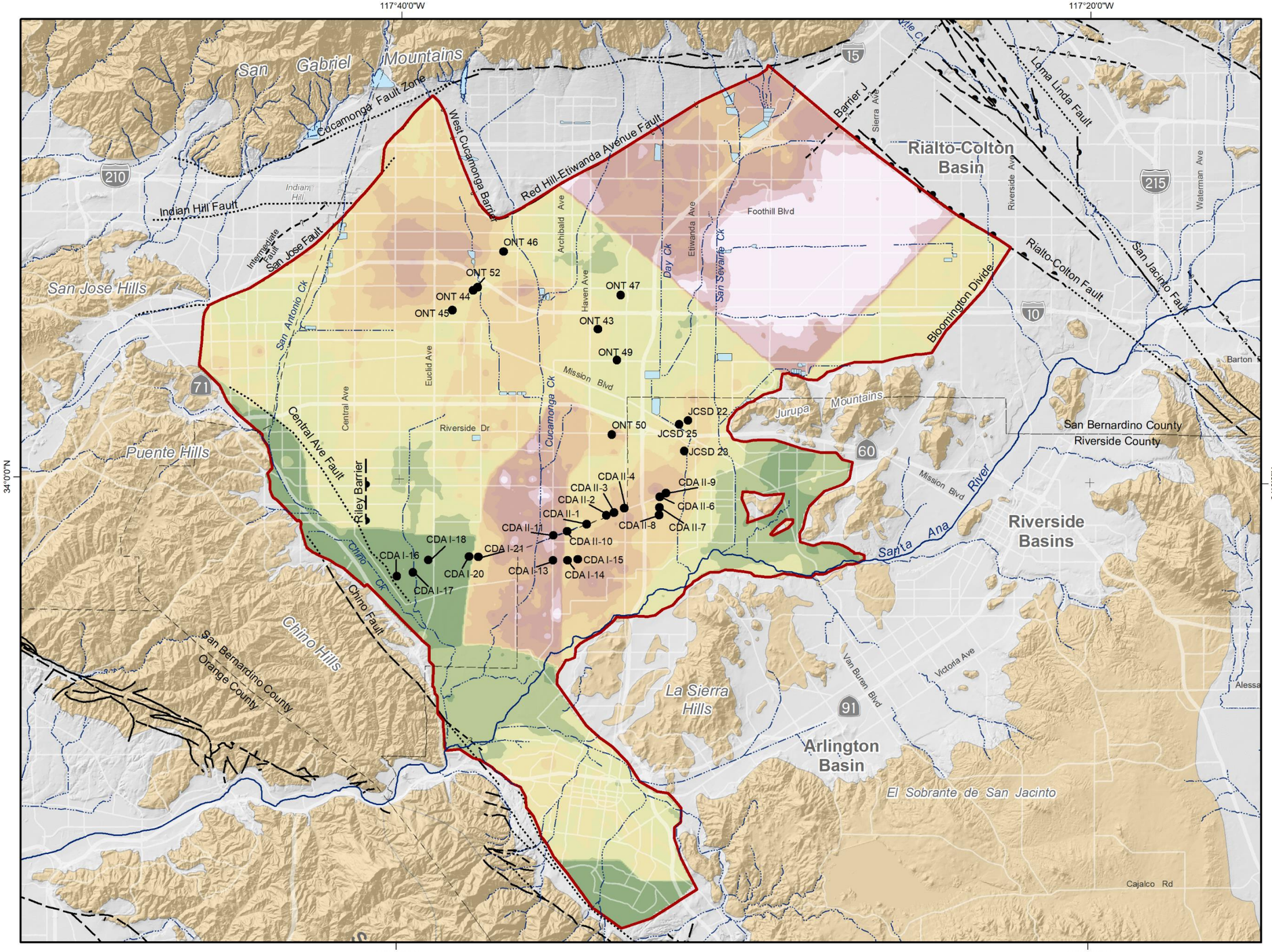

Calibrated Horizontal Hydraulic Conductivity
Layer 1 (ft/day)

- 3 - 21
- 22 - 40
- 41 - 58
- 59 - 76
- 77 - 95
- 96 - 113
- 114 - 132
- 133 - 150
- 151 - 168
- 169 - 187

- Wells Screened in Layer 1 Where Stress Tests Have Been Performed
- Model Domain
- Streams & Flood Control Channels
- Flood Control & Conservation Basins

Geology

Water-Bearing Sediments

- Quaternary Alluvium

Consolidated Bedrock

- Undifferentiated Pre-Tertiary to Early Pleistocene Igneous, Metamorphic, and Sedimentary Rocks

- Fault (solid where accurately located; dashed where approximately located or inferred; dotted where concealed)

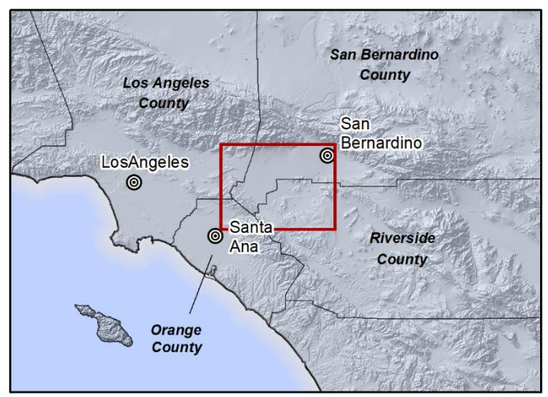

Produced by:

WEI
Wildermuth Environmental, Inc.

Author: LJS
Date: 5/4/2020
Document Name: Figure_E-1_L1Kh

0 1 2 3 4 5 Miles
0 2 4 6 8 KM

Prepared for:

2020 Safe Yield Recalculation

Chino Basin Watermaster
Partners in Basin Management

Calibrated Horizontal Hydraulic Conductivity Layer 1

Figure E-1

117°40'0"W

117°20'0"W

34°0'0"N

Calibrated Horizontal Hydraulic Conductivity
Layer 2 (ft/day)

- 3 - 21
- 22 - 40
- 41 - 58
- 59 - 76
- 77 - 95
- 96 - 113
- 114 - 132
- 133 - 150
- 151 - 168
- 169 - 187

- Model Domain
- Streams & Flood Control Channels
- Flood Control & Conservation Basins

Geology

Water-Bearing Sediments

- Quaternary Alluvium

Consolidated Bedrock

- Undifferentiated Pre-Tertiary to Early Pleistocene Igneous, Metamorphic, and Sedimentary Rocks

- Fault (solid where accurately located; dashed where approximately located or inferred; dotted where concealed)

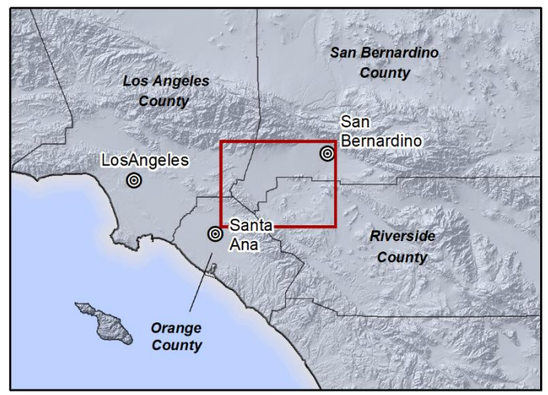

Produced by:

WEI
Wildermuth Environmental, Inc.

Author: LJS
Date: 4/28/2020
Document Name: Figure_E-2_L2Kh

0 1 2 3 4 5 Miles
0 2 4 6 8 KM

Prepared for:

2020 Safe Yield Recalculation

Chino Basin Watermaster — Partners in Basin Management

Calibrated Horizontal Hydraulic Conductivity Layer 2

Figure E-2

117°40'0"W

117°20'0"W

34°0'0"N

San Gabriel Mountains

Cucamonga Fault Zone

West Cucamonga Barrier

Red Hill-Etiwanda Avenue Fault

Barrier J

Lima Linda Fault

Rialto-Colton Basin

Indian Hill

Indian Hill Fault

Intermediate Fault

San Jose Fault

MVWD 31

ONT 46

ONT 52

ONT 41

ONT 44

ONT 45

ONT 40

ONT 47

ONT 43

ONT 49

ONT 50

MMWC 06

Foothill Blvd

Archibald Ave

Haven Ave

Day Ck

Etiwanda Ave

San Sevaine Ck

Riverside Ave

Waterman Ave

Rialto-Colton Fault

San Jacinto Fault

Bloomington Divide

San Jose Hills

San Antonio Ck

Euclid Ave

Central Ave

Mission Blvd

Riverside Dr

Cucamonga Ck

Jurupa Mountains

San Bernardino County

Riverside County

Barton

Puente Hills

Central Ave Fault

Riley Barrier

CH19

Bellegrave Ave

Limonite Ave

Mission Blvd

Santa Ana River

Riverside Basins

CDA I-11

CDA I-20

CDA I-21

CDA I-14

Chino Ck

Chino Fault

Chino Hills

San Bernardino County

Orange County

La Sierra Hills

Van Buren Blvd

Victoria Ave

Arlington Basin

El Sobrante de San Jacinto

Cajalco Rd

Alessa

210

15

215

71

10

60

91

Calibrated Horizontal Hydraulic Conductivity
Layer 3 (ft/day)

- 3 - 21
- 22 - 40
- 41 - 58
- 59 - 76
- 77 - 95
- 96 - 113
- 114 - 132
- 133 - 150
- 151 - 168
- 169 - 187

Wells Screened in Layer 3 Where Stress Tests Have Been Performed

Model Domain

Streams & Flood Control Channels

Flood Control & Conservation Basins

Geology

Water-Bearing Sediments

Quaternary Alluvium

Consolidated Bedrock

Undifferentiated Pre-Tertiary to Early Pleistocene Igneous, Metamorphic, and Sedimentary Rocks

Fault (solid where accurately located; dashed where approximately located or inferred; dotted where concealed)

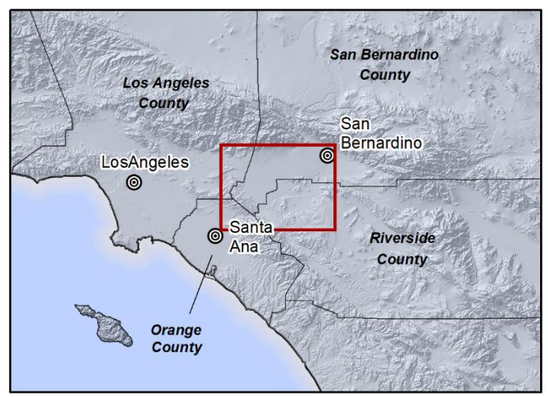

Produced by:

WEI
Wildermuth Environmental, Inc.

Author: LJS
Date: 5/4/2020
Document Name: Figure_E-3_L3Kh

0 1 2 3 4 5 Miles
0 2 4 6 8 KM

Prepared for:

2020 Safe Yield Recalculation

Chino Basin Watermaster
Partners in Basin Management

Calibrated Horizontal Hydraulic Conductivity Layer 3

Figure E-3

Calibrated Horizontal Hydraulic Conductivity
Layer 4 (ft/day)

- 3 - 21
- 22 - 40
- 41 - 58
- 59 - 76
- 77 - 95
- 96 - 113
- 114 - 132
- 133 - 150
- 151 - 168
- 169 - 187

- Model Domain
- Streams & Flood Control Channels
- Flood Control & Conservation Basins

Geology

Water-Bearing Sediments

- Quaternary Alluvium

Consolidated Bedrock

- Undifferentiated Pre-Tertiary to Early Pleistocene Igneous, Metamorphic, and Sedimentary Rocks
- Fault (solid where accurately located; dashed where approximately located or inferred; dotted where concealed)

Produced by:

WEI
WILDERMUTH ENVIRONMENTAL, INC.

Author: LJS
Date: 4/28/2020
Document Name: Figure_E-4_L4Kh

0 1 2 3 4 5 Miles
0 2 4 6 8 KM

Prepared for:

2020 Safe Yield Recalculation

CHINO BASIN WATERMASTER
Partners in Basin Management

Calibrated Horizontal Hydraulic Conductivity Layer 4

Figure E-4

117°40'0"W

117°20'0"W

34°0'0"N

Calibrated Horizontal Hydraulic Conductivity
Layer 5 (ft/day)

- 3 - 21
- 22 - 40
- 41 - 58
- 59 - 76
- 77 - 95
- 96 - 113
- 114 - 132
- 133 - 150
- 151 - 168
- 169 - 187

- Wells Screened in Layer 5 Where Stress Tests Have Been Performed
- Model Domain
- Streams & Flood Control Channels
- Flood Control & Conservation Basins

Geology

Water-Bearing Sediments

- Quaternary Alluvium

Consolidated Bedrock

- Undifferentiated Pre-Tertiary to Early Pleistocene Igneous, Metamorphic, and Sedimentary Rocks
- Fault (solid where accurately located; dashed where approximately located or inferred; dotted where concealed)

Produced by:

WEI
WILDERMUTH ENVIRONMENTAL, INC.

Author: LJS
Date: 5/4/2020
Document Name: Figure_E-5_L5Kh

0 1 2 3 4 5 Miles
0 2 4 6 8 KM

Prepared for:

2020 Safe Yield Recalculation

CHINO BASIN WATERMASTER
Partners in Basin Management

Calibrated Horizontal Hydraulic Conductivity Layer 5

Figure E-5

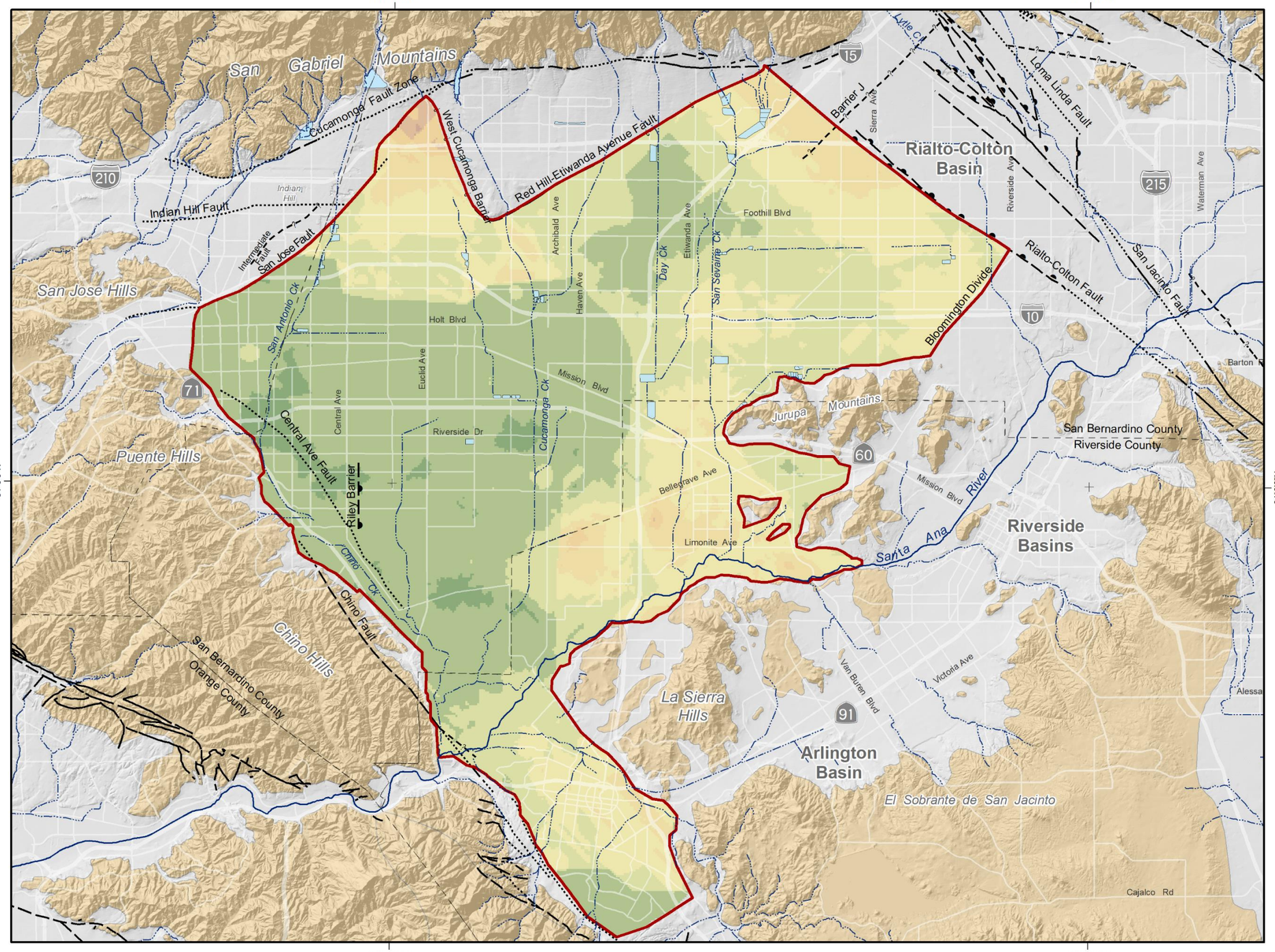

Calibrated Vertical Hydraulic Conductivity
Layer 1
(ft/day)

- < 0.01
- 0.01 - 1
- 1 - 5
- 5 - 10
- 10 - 15
- 15 - 20
- 20 - 25
- 25 - 30
- 30 - 35
- 35 - 40
- 40 - 50

Model Domain

Streams & Flood Control Channels

Flood Control & Conservation Basins

Geology

Water-Bearing Sediments

Quaternary Alluvium

Consolidated Bedrock

Undifferentiated Pre-Tertiary to Early Pleistocene Igneous, Metamorphic, and Sedimentary Rocks

Fault (solid where accurately located; dashed where approximately located or inferred; dotted where concealed)

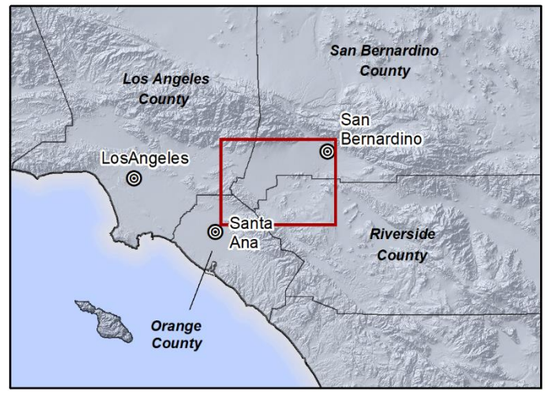

Produced by:

WEI
Wildermuth Environmental, Inc.

Author: LJS
Date: 4/28/2020
Document Name: Figure_E-6_L1Kv

0 1 2 3 4 5 Miles
0 2 4 6 8 KM

Prepared for:

2020 Safe Yield Recalculation

Chino Basin Watermaster
Partners in Basin Management

Calibrated Vertical Hydraulic Conductivity Layer 1

Figure E-6

117°40'0"W

117°20'0"W

34°0'0"N

Calibrated Vertical Hydraulic Conductivity
Layer 2
(ft/day)

- < 0.01
- 0.01 - 1
- 1 - 5
- 5 - 10
- 10 - 15
- 15 - 20
- 20 - 25
- 25 - 30
- 30 - 35
- 35 - 40
- 40 - 50

Model Domain

Streams & Flood Control Channels

Flood Control & Conservation Basins

Geology

Water-Bearing Sediments

Quaternary Alluvium

Consolidated Bedrock

Undifferentiated Pre-Tertiary to Early Pleistocene Igneous, Metamorphic, and Sedimentary Rocks

Fault (solid where accurately located; dashed where approximately located or inferred; dotted where concealed)

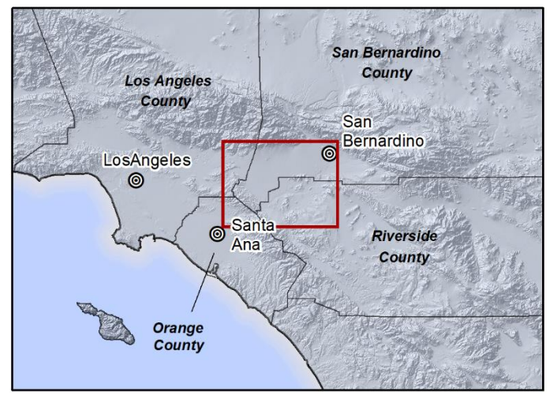

Produced by:

WEI
WILDERMUTH ENVIRONMENTAL, INC.

Author: LJS
Date: 4/28/2020
Document Name: Figure_E-7_L2Kv

0 1 2 3 4 5 Miles

0 2 4 6 8 KM

Prepared for:

2020 Safe Yield Recalculation

CHINO BASIN WATERMASTER
Partners in Basin Management

Calibrated Vertical Hydraulic Conductivity Layer 2

Figure E-7

117°40'0"W

117°20'0"W

34°0'0"N

Calibrated Vertical Hydraulic Conductivity
Layer 3
(ft/day)

- < 0.01
- 0.01 - 1
- 1 - 5
- 5 - 10
- 10 - 15
- 15 - 20
- 20 - 25
- 25 - 30
- 30 - 35
- 35 - 40
- 40 - 50

Model Domain

Streams & Flood Control Channels

Flood Control & Conservation Basins

Geology

Water-Bearing Sediments

Quaternary Alluvium

Consolidated Bedrock

Undifferentiated Pre-Tertiary to Early Pleistocene Igneous, Metamorphic, and Sedimentary Rocks

Fault (solid where accurately located; dashed where approximately located or inferred; dotted where concealed)

Produced by:

WEI
WILDERMUTH ENVIRONMENTAL, INC.

Author: LJS
Date: 4/28/2020
Document Name: Figure_E-8_L3Kv

0 1 2 3 4 5 Miles
0 2 4 6 8 KM

Prepared for:

2020 Safe Yield Recalculation

CHINO BASIN WATERMASTER
Partners in Basin Management

Calibrated Vertical Hydraulic Conductivity Layer 3

Figure E-8

117°40'0"W

117°20'0"W

34°0'0"N

San Gabriel Mountains

Cucamonga Fault Zone

West Cucamonga Barrier

Red Hill-Etiwanda Avenue Fault

Barrier J

Lytle Ck

Loma Linda Fault

Rialto-Colton Basin

Indian Hill

Indian Hill Fault

Intermediate Fault

San Jose Fault

San Jose Hills

San Antonio Ck

Archibald Ave

Day Ck

Etiwanda Ave

San Sevaine Ck

Foothill Blvd

Riverside Ave

Waterman Ave

Rialto-Colton Fault

San Jacinto Fault

Bloomington Divide

Holt Blvd

Haven Ave

Euclid Ave

Central Ave

Mission Blvd

Riverside Dr

Cucamonga Ck

Central Ave Fault

Riley Barrier

Puente Hills

Jurupa Mountains

San Bernardino County

Riverside County

Bellegrave Ave

Limonite Ave

Mission Blvd

Santa Ana River

Riverside Basins

Chino Ck

Chino Fault

Chino Hills

San Bernardino County

Orange County

La Sierra Hills

Van Buren Blvd

Victoria Ave

Arlington Basin

El Sobrante de San Jacinto

Cajalco Rd

Barton

Alessa

Calibrated Vertical Hydraulic Conductivity
Layer 4
(ft/day)

- < 0.01
- 0.01 - 1
- 1 - 5
- 5 - 10
- 10 - 15
- 15 - 20
- 20 - 25
- 25 - 30
- 30 - 35
- 35 - 40
- 40 - 50

Model Domain

Streams & Flood Control Channels

Flood Control & Conservation Basins

Geology

Water-Bearing Sediments

Quaternary Alluvium

Consolidated Bedrock

Undifferentiated Pre-Tertiary to Early Pleistocene Igneous, Metamorphic, and Sedimentary Rocks

Fault (solid where accurately located; dashed where approximately located or inferred; dotted where concealed)

Produced by:

WEI
Wildermuth Environmental, Inc.

Author: LJS
Date: 4/28/2020
Document Name: Figure_E-9_L4Kv

0 1 2 3 4 5 Miles
0 2 4 6 8 KM

Prepared for:

2020 Safe Yield Recalculation

Chino Basin Watermaster
Partners in Basin Management

Calibrated Vertical Hydraulic Conductivity Layer 4

Figure E-9

117°40'0"W

117°20'0"W

34°0'0"N

San Gabriel Mountains

Cucamonga Fault Zone

West Cucamonga Barrier

Red Hill-Etiwanda Avenue Fault

Barrier J

Lytle Ck

Loma Linda Fault

Rialto-Colton Basin

Indian Hill

Indian Hill Fault

Intermediate Fault

San Jose Fault

San Jose Hills

San Antonio Ck

Archibald Ave

Day Ck

Etiwanda Ave

San Sevaine Ck

Foothill Blvd

Riverside Ave

Waterman Ave

Rialto-Colton Fault

San Jacinto Fault

Bloomington Divide

Holt Blvd

Haven Ave

Euclid Ave

Central Ave

Mission Blvd

Riverside Dr

Cucamonga Ck

Central Ave Fault

Riley Barrier

Puente Hills

Jurupa Mountains

San Bernardino County

Riverside County

Bellegrave Ave

Limonite Ave

Mission Blvd

Santa Ana River

Riverside Basins

Chino Ck

Chino Fault

San Bernardino County

Orange County

Chino Hills

La Sierra Hills

Van Buren Blvd

Victoria Ave

Arlington Basin

El Sobrante de San Jacinto

Cajalco Rd

Barton

Alessa

15

210

215

10

71

60

91

117°40'0"W

117°20'0"W

34°0'0"N

Calibrated Vertical Hydraulic Conductivity
Layer 5
(ft/day)

- < 0.01
- 0.01 - 1
- 1 - 5
- 5 - 10
- 10 - 15
- 15 - 20
- 20 - 25
- 25 - 30
- 30 - 35
- 35 - 40
- 40 - 50

Model Domain

Streams & Flood Control Channels

Flood Control & Conservation Basins

Geology

Water-Bearing Sediments

Quaternary Alluvium

Consolidated Bedrock

Undifferentiated Pre-Tertiary to Early Pleistocene Igneous, Metamorphic, and Sedimentary Rocks

Fault (solid where accurately located; dashed where approximately located or inferred; dotted where concealed)

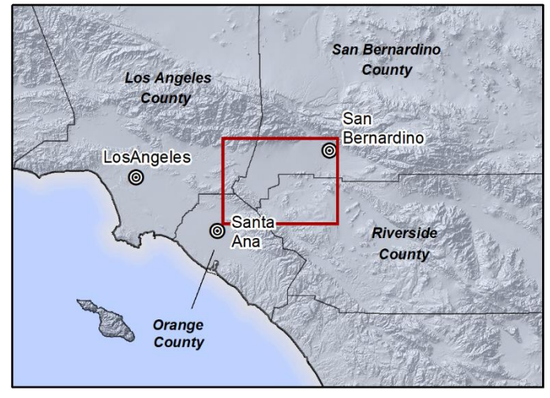

Produced by:

WEI
Wildermuth Environmental, Inc.

Author: LJS
Date: 4/28/2020
Document Name: Figure_E-10_L5Kv

0 1 2 3 4 5 Miles

0 2 4 6 8 KM

Prepared for:

2020 Safe Yield Recalculation

Chino Basin Watermaster
Partners in Basin Management

Calibrated Vertical Hydraulic Conductivity Layer 5

Figure E-10

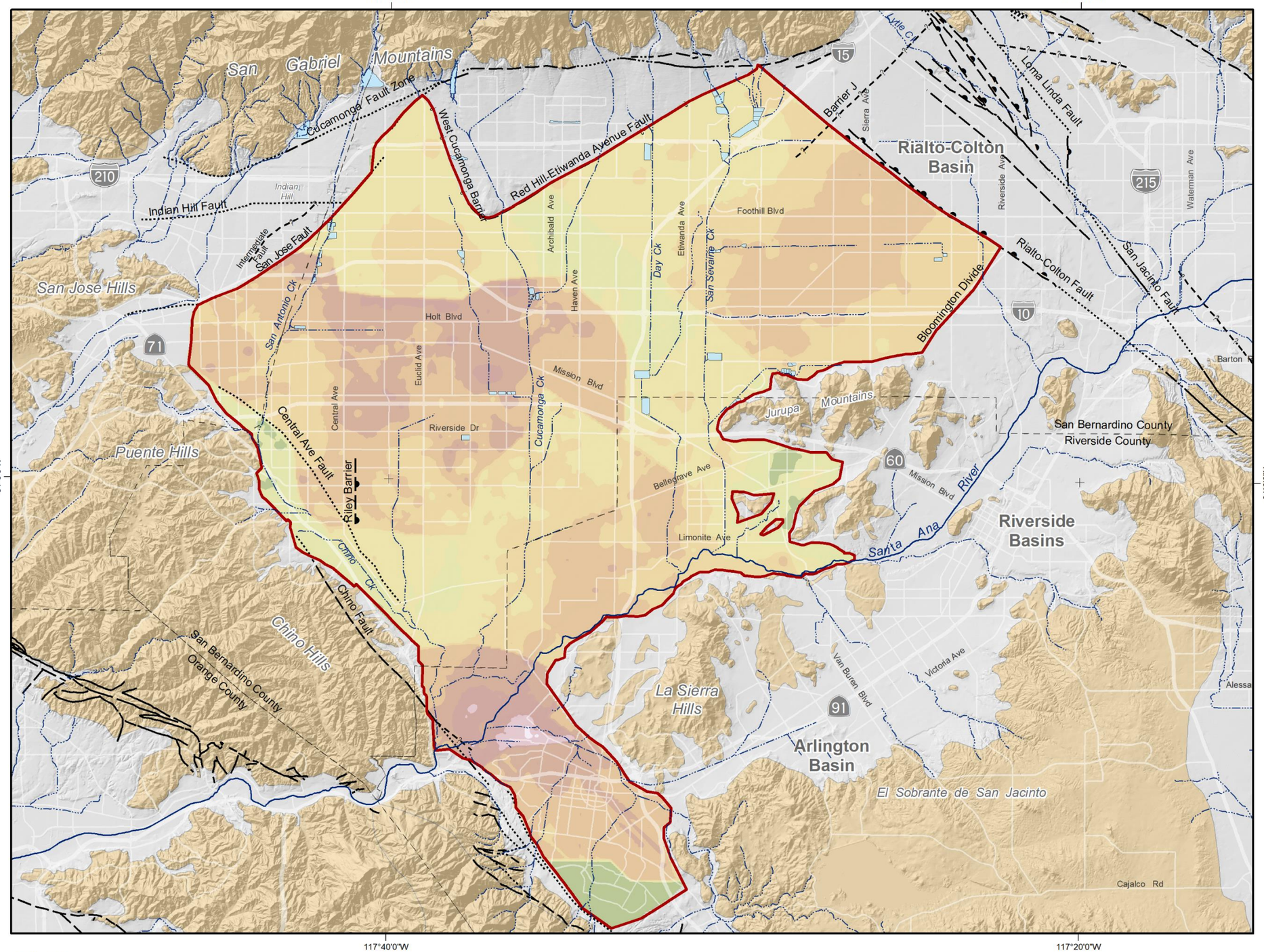

Calibrated Specific Yield
Layer 1

- 0.001 - 0.025
- 0.026 - 0.05
- 0.051 - 0.075
- 0.076 - 0.1
- 0.101 - 0.125
- 0.126 - 0.15
- 0.151 - 0.175
- 0.176 - 0.199
- 0.2 - 0.224
- 0.225 - 0.249

Model Domain

Streams & Flood Control Channels

Flood Control & Conservation Basins

Geology

Water-Bearing Sediments

Quaternary Alluvium

Consolidated Bedrock

Undifferentiated Pre-Tertiary to Early Pleistocene Igneous, Metamorphic, and Sedimentary Rocks

Fault (solid where accurately located; dashed where approximately located or inferred; dotted where concealed)

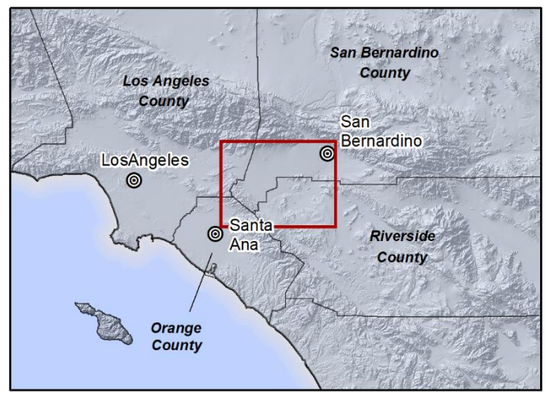

Produced by:

WEI
Wildermuth Environmental, Inc.

Author: LJS
Date: 4/28/2020
Document Name: Figure_E-11_L1Sy

0 1 2 3 4 5 Miles
0 2 4 6 8 KM

Prepared for:

2020 Safe Yield Recalculation

Chino Basin Watermaster
Partners in Basin Management

Calibrated Specific Yield Layer 1

Figure E-11

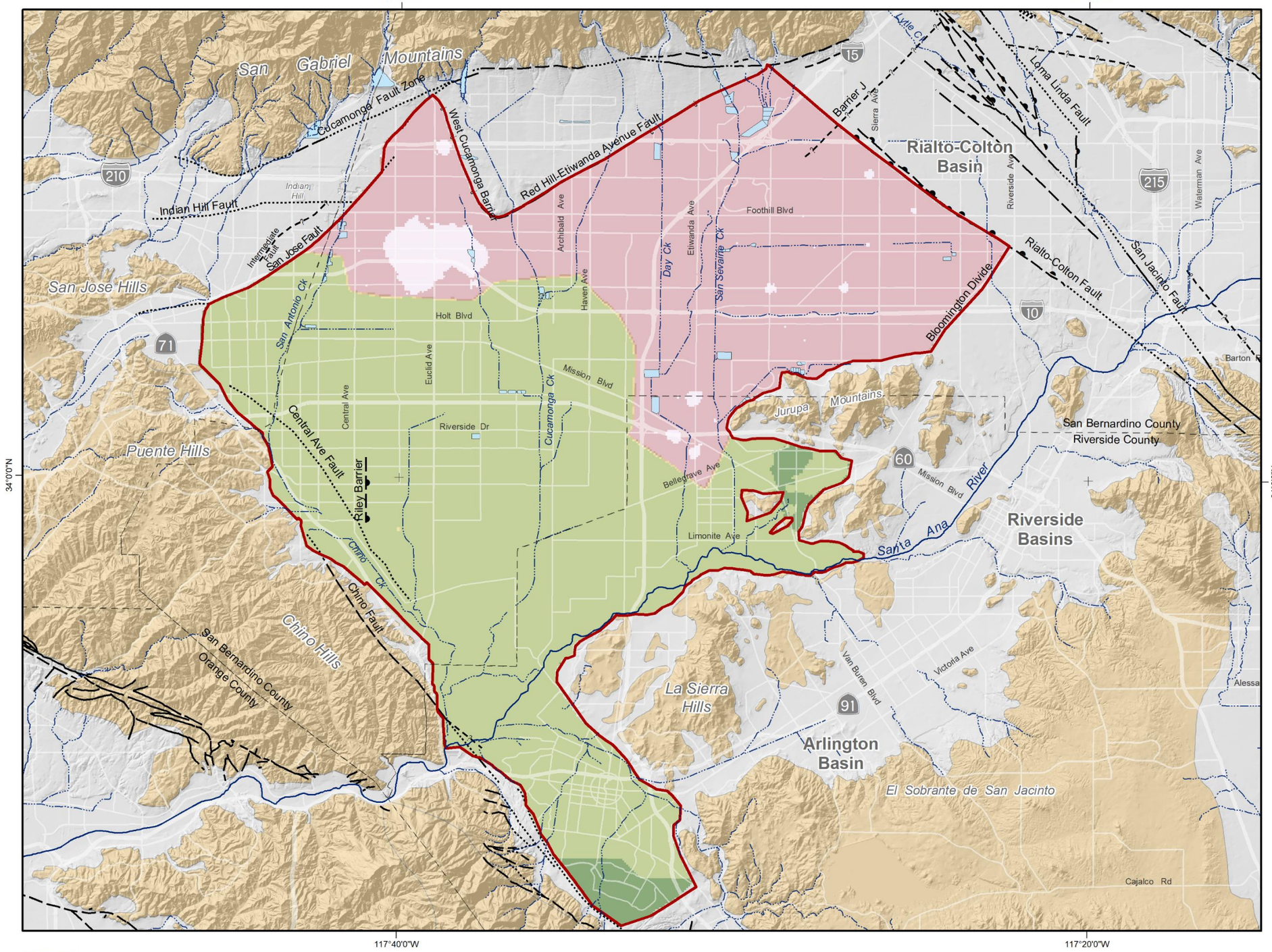

Calibrated Specific Storage
Layer 2 (1/ft)

- 1e-8 - 1e-7
- 1e-7 - 5e-7
- 5e-7 - 1e-6
- 1e-6 - 5e-6
- 5e-6 - 1e-5
- 1e-5 - 5e-5
- 5e-5 - 0.0001
- 0.0001 - 0.0004

Model Domain

Streams & Flood Control Channels

Flood Control & Conservation Basins

Geology

Water-Bearing Sediments

Quaternary Alluvium

Consolidated Bedrock

Undifferentiated Pre-Tertiary to Early Pleistocene Igneous, Metamorphic, and Sedimentary Rocks

Fault (solid where accurately located; dashed where approximately located or inferred; dotted where concealed)

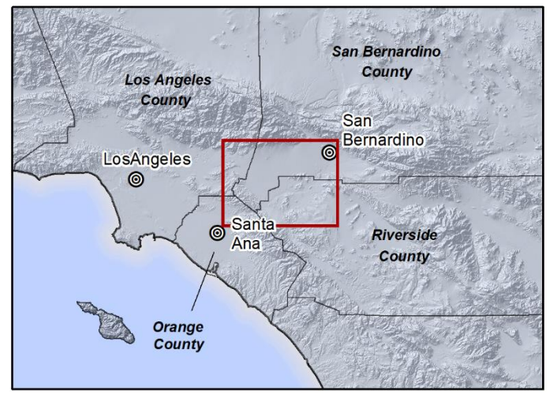

Produced by:

WEI
Wildermuth Environmental, Inc.

Author: LJS
Date: 4/28/2020
Document Name: Figure_E-12_L2Ss

0 1 2 3 4 5 Miles
0 2 4 6 8 KM

Prepared for:

2020 Safe Yield Recalculation

Chino Basin Watermaster
Partners in Basin Management

Calibrated Specific Storage Layer 2

Figure E-12

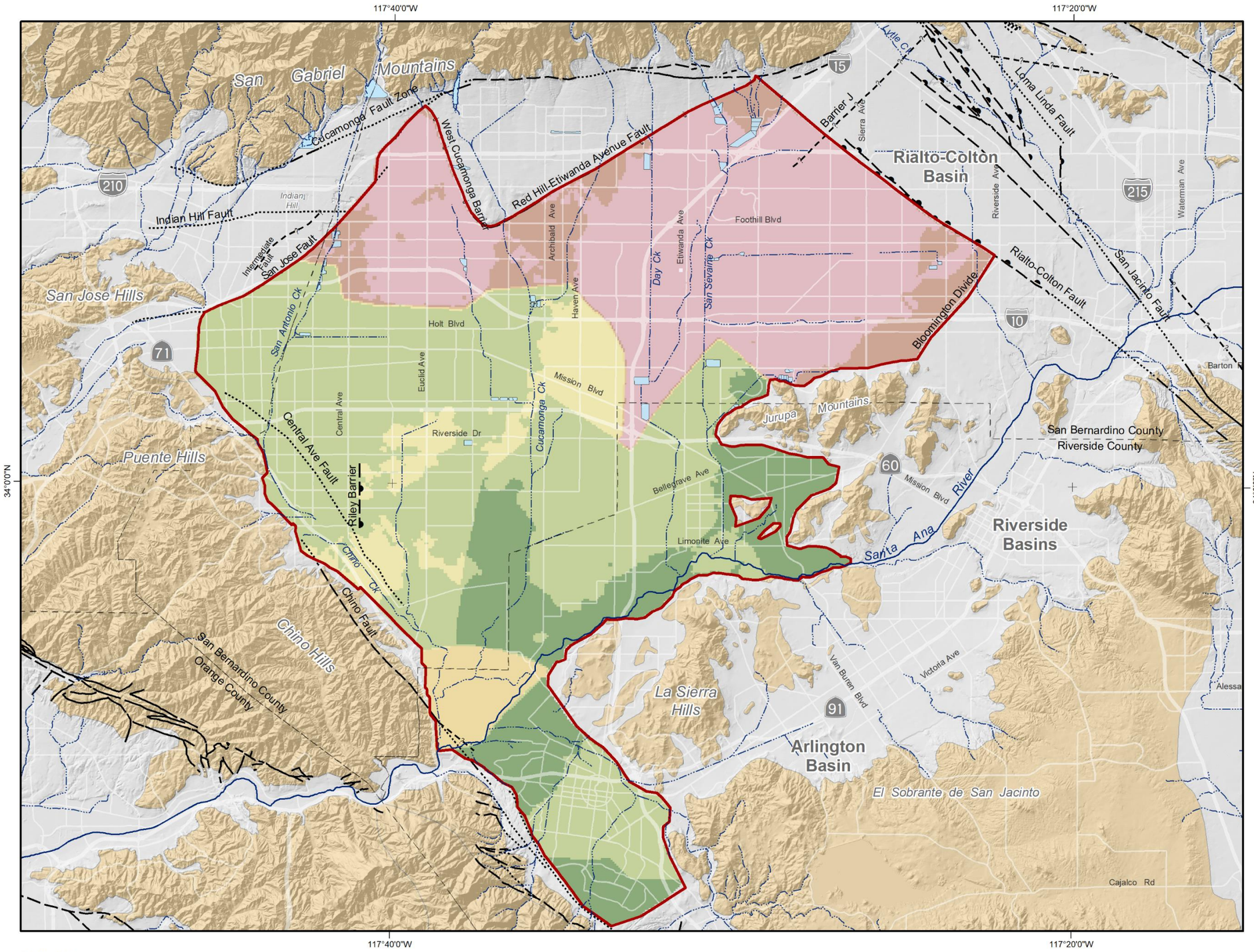

Calibrated Specific Storage
Layer 3 (1/ft)

- 1e-8 - 1e-7
- 1e-7 - 5e-7
- 5e-7 - 1e-6
- 1e-6 - 5e-6
- 5e-6 - 1e-5
- 1e-5 - 5e-5
- 5e-5 - 0.0001
- 0.0001 - 0.0004

Model Domain

Streams & Flood Control Channels

Flood Control & Conservation Basins

Geology

Water-Bearing Sediments

Quaternary Alluvium

Consolidated Bedrock

Undifferentiated Pre-Tertiary to Early Pleistocene Igneous, Metamorphic, and Sedimentary Rocks

Fault (solid where accurately located; dashed where approximately located or inferred; dotted where concealed)

Produced by:

WEI
Wildermuth Environmental, Inc.

Author: LJS
Date: 4/28/2020
Document Name: Figure_E-13_L3Ss

0 1 2 3 4 5 Miles
0 2 4 6 8 KM

Prepared for:

2020 Safe Yield Recalculation

Chino Basin Watermaster
Partners in Basin Management

Calibrated Specific Storage Layer 3

Figure E-13

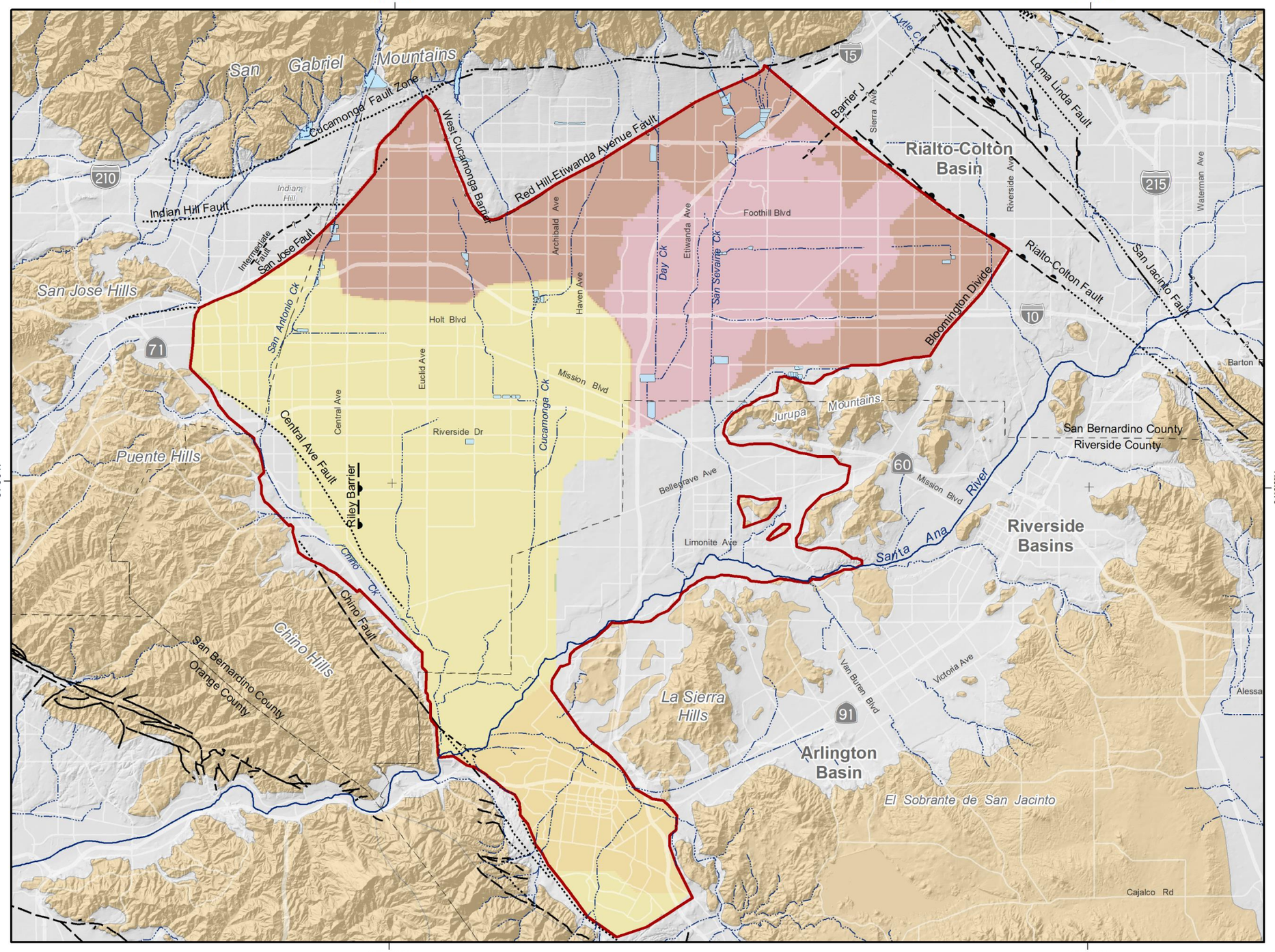

Calibrated Specific Storage
Layer 4 (1/ft)

- 1e-8 - 1e-7
- 1e-7 - 5e-7
- 5e-7 - 1e-6
- 1e-6 - 5e-6
- 5e-6 - 1e-5
- 1e-5 - 5e-5
- 5e-5 - 0.0001
- 0.0001 - 0.0004

- Model Domain
- Streams & Flood Control Channels
- Flood Control & Conservation Basins

Geology

Water-Bearing Sediments

- Quaternary Alluvium

Consolidated Bedrock

- Undifferentiated Pre-Tertiary to Early Pleistocene Igneous, Metamorphic, and Sedimentary Rocks

- Fault (solid where accurately located; dashed where approximately located or inferred; dotted where concealed)

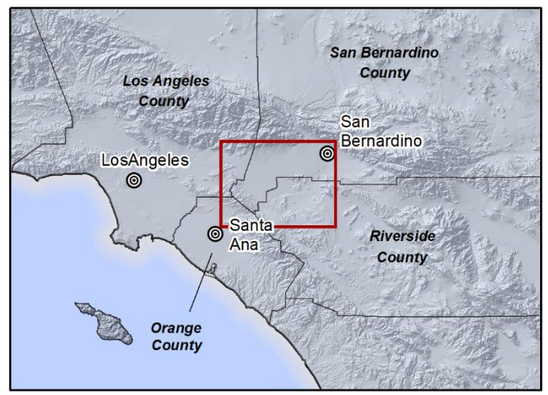

Produced by:

WEI
Wildermuth Environmental, Inc.

Author: LJS
Date: 4/28/2020
Document Name: Figure_E-14_L4Ss

0 1 2 3 4 5 Miles
0 2 4 6 8 KM

Prepared for:

2020 Safe Yield Recalculation

Chino Basin Watermaster
Partners in Basin Management

Calibrated Specific Storage Layer 4

Figure E-14

117°40'0"W

117°20'0"W

34°0'0"N

Calibrated Specific Storage
Layer 5 (1/ft)

- 1e-8 - 1e-7
- 1e-7 - 5e-7
- 5e-7 - 1e-6
- 1e-6 - 5e-6
- 5e-6 - 1e-5
- 1e-5 - 5e-5
- 5e-5 - 0.0001
- 0.0001 - 0.0004

- Model Domain
- Streams & Flood Control Channels
- Flood Control & Conservation Basins

Geology

Water-Bearing Sediments

- Quaternary Alluvium

Consolidated Bedrock

- Undifferentiated Pre-Tertiary to Early Pleistocene Igneous, Metamorphic, and Sedimentary Rocks

- Fault (solid where accurately located; dashed where approximately located or inferred; dotted where concealed)

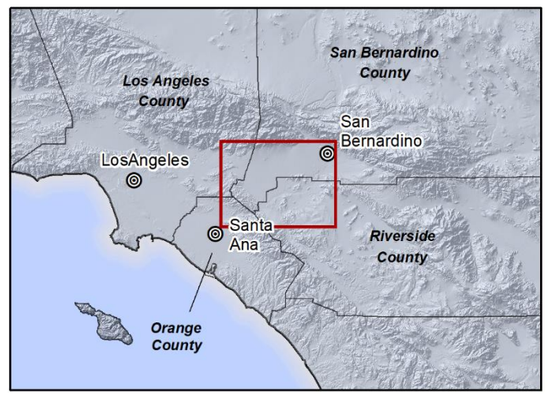

Produced by:

WEI
WILDERMUTH ENVIRONMENTAL, INC.

Author: LJS
Date: 4/28/2020
Document Name: Figure_E-15_L5Ss

0 1 2 3 4 5 Miles
0 2 4 6 8 KM

Prepared for:

2020 Safe Yield Recalculation

CHINO BASIN WATERMASTER
Partners in Basin Management

Calibrated Specific Storage Layer 5

Figure E-15

Appendix F

Response to Questions and Comments

from: Colleague/Peer Review Workshops, Public Workshop, and Stakeholder Review of Draft Final Report and Stakeholder Workshop. And, the Report of the Technical Expert

Appendix F Table of Contents

TECHNICAL MEMORANDUM

January 16, 2020

TO: File 007-019-012.10

FROM: Wenbin Wang, Eric Chiang, Jeff Hwang and Michael Blazevic

RE: Comments and responses for first colleague peer review of the 2020 Safe Yield Recalculation Model

Comment/Question 1: What version of MODFLOW was used for the Salinity management project?

Response: *MODFLOW NWT was used for the simulation of groundwater flow. The main reasons for selecting MODFLOW NWT was its improved numerical stability for drying and rewetting cells, that it supports the Streamflow Routing (SFR2) Package and provides output data that are required by the Streamflow Transport (SFT) Package of MT3D-USGS. MT3D-USGS will be used to simulate transport of TDS and TIN in groundwater and in the streams for future studies.*

Comment/Question 2: What was logic to introduce new confining layers (i.e. layers 2 and 4) in the updated MODFLOW model? What was the reason you want to do that?

Response: *The Chino Basin consists of a shallow unconfined aquifer and deep confined aquifers. Historical flowing artesian conditions were mapped in the early 1900s in the southwest portion of the Chino Basin (Mendenhall, 1905, 1908; Fife et al., 1976), which indicates the existence of confining layers in these areas. Likewise, review of water level time-series, water quality data, and aquifer testing data support confined groundwater conditions in the western portion of Chino Basin.[1] It has also been demonstrated in the Annual Report of the Ground-Level Monitoring Committee that the observed aquifer-system deformation in the Managed Area is a result of groundwater pumping from the deep and confined aquifer-system.[1] Similarly in Northwest MZ-1, available evidence indicates that the most likely mechanism behind the observed subsidence in the Northwest MZ-1 Area is the compaction of fine-grained sediment layers (aquitards) within the aquifer-system.[1]*

New confining layers (Layers 2 and 4) were added to hydrostratigraphic conceptual model to support our improved understanding of the Chino Basin's hydrostratigraphy, to simulate land subsidence across the Chino Basin, and to support the MODFLOW SUB package. The new Chino

[1] http://www.cbwm.org/rep_engineering.htm

Wildermuth Environmental, Inc.
23692 Birtcher
Lake Forest, CA 92630

Basin model that incorporates the MODFLOW SUB package will be used to support the future development of a subsidence management plan.

Comment/Question 3: Next to San Sevaine Creek, we have drilled some monitoring wells for IEUA to about 750 feet deep. Are they included in the cross-section (J-J')? Clay interbeds in the shallow aquifer system (note see well 1223033 in the cross-section J-J' near I-15) do not seem to be captured in the model.

Response: *The cross-sections depict the hydrostratigraphy used for the model based on borehole, geophysical logs, well screen position, water level, water quality, spinner logs, and specific capacity data. The delineation of the layering was based on a holistic analysis of the entire data set. For this reason, the layer boundaries do not always match specific observations at every well on every cross-section but do honor our general understanding of the Chino Basin's depositional environment and hydrostratigraphy.*

Comment/Question 4: Was there specific characteristics of the clay that you are looking for? … moving into Fontana area, you still have the clay. Are you going to keep the clay in the same depth? What do you want to do with it?

Response: *See response to comment/question 3 above.*

Comment/Question 5: How are the pumping tests used to determine the value of hydraulic conductivity in the model? …I would start with pumping test and I would like to see how the hydraulic parameters based on pumping test data match [with texture data]…We have flow meter survey data, that help us understand how much flow are occurring by the depth… as oppose to [use] driller's log…I don't want to build the model based on the lithology data [alone]. I want other data to be considered.

Response: *All available pumping, spinner, and specific capacity test data were collected and reviewed. These test results were used to derive transmissivity values and the pumping allocation across the different model layers and inform the calibration process.*

Comment/Question 6: The hydraulic data are based on lithology and then are used for Kriging. I recommend taking into consideration of the variability of these hydraulic data and use the max/min of those data to constrain calibration.

Response: *During the kriging process and model calibration, reasonable upper and lower bounds for the hydraulic data were used to constrain the calibration results.*

Comment/Question 7: How do you plan to distribute that critical head in the model for the Subsidence package?

Response: *Pre-consolidation pressure is the maximum <u>effective</u> vertical overburden stress that a particular soil sample has sustained in the past. In other words, the pre-consolidation stress is the lowest head in the aquifers and aquitards in the past. As shown in the figures below, the 1978 groundwater levels represent the lowest water levels in the period between 1930 and 1978. The initial pre-consolidation head across Chino Basin will be set to the 1978 water levels. With the groundwater flow simulation, the pre-consolidation heads in aquifers and aquitards are replaced by the new lowest water levels. Calibration of the land subsidence will occur after the Safe Yield process concludes.*

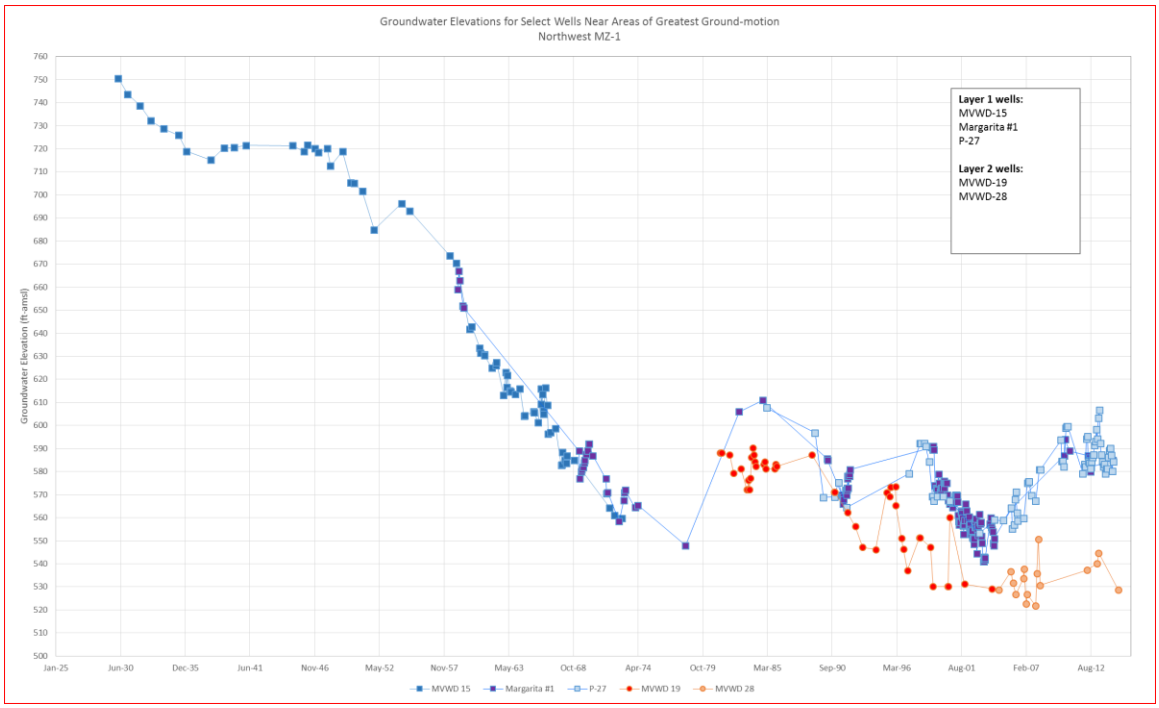

Historical Water Level in Ayala Park

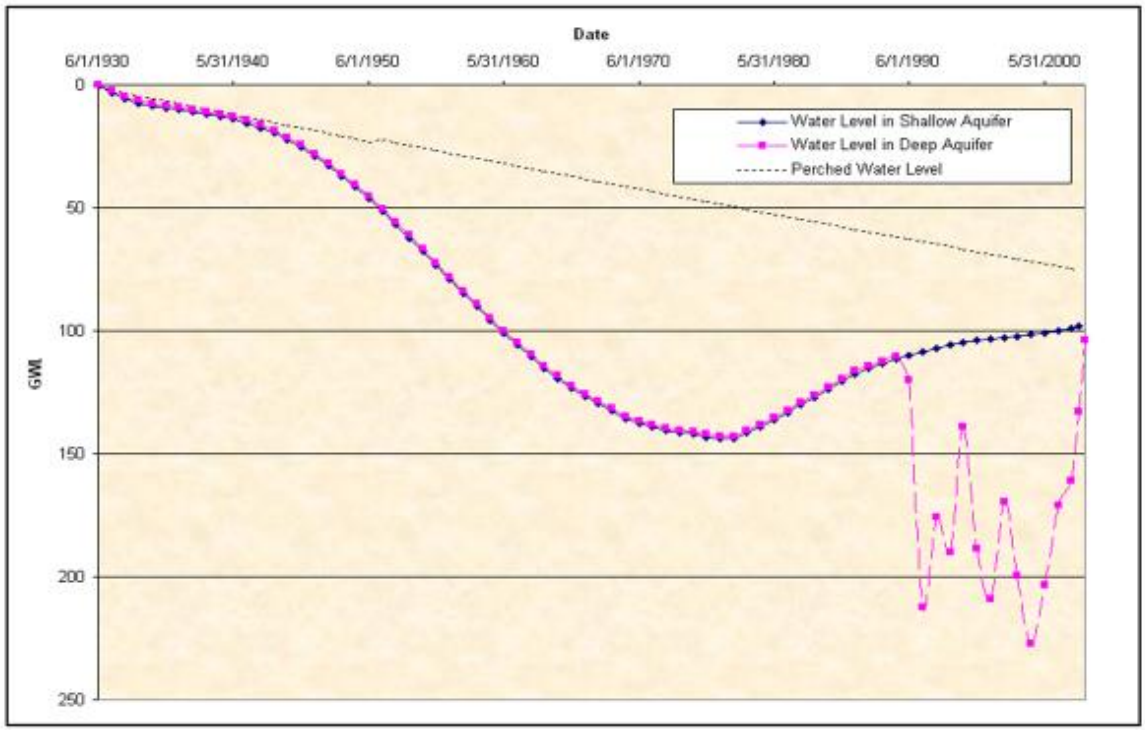

Comment/Question 8: On this [Cucamonga] part of the model did you maintain the layering that you had in the main Chino Basin or do you have different layering? [How] did you meld it up to the current larger [Chino Basin] model?

Response: *Cucamonga and Six Basins are considered to be hydrogeologically separated from the Chino Basin and the hydrostratigraphy (layering) is different than the Chino Basin. The connections to Chino Basin from the Cucamonga and Six Basins are simulated as barriers. The deep aquifers in Cucamonga and Six Basins will be modeled as weakly connected to Chino Basin's deep aquifer-system by using the barrier's hydraulic conductivity parameter. See figure depicting a cross-section of the model below.*

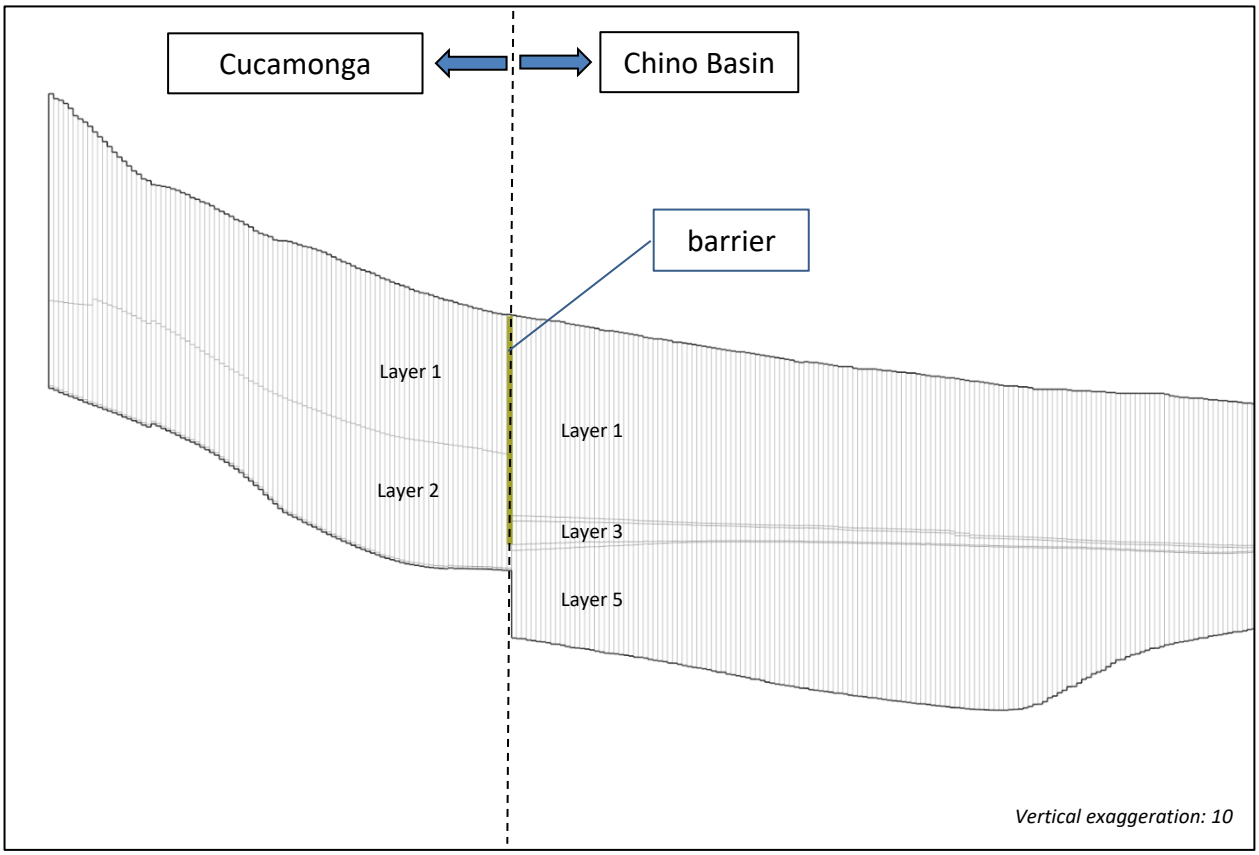

Comment/Question 9: Expressed concerns that on the east [of the Cucamonga basin] there is only one boring.

Response: Comment noted. All available borehole records were reviewed from CVWD's database, WEI's database, and borehole logs requested directly from the DWR.

Comment/Question 10: What is the philosophy in terms of combining those [hydraulic parameters] together that you don't really have data?

Response: *Combining hydraulic parameter zones in areas where borehole data is sparse is based on our understanding of the geology and hydrogeology of the area, using other nearby borehole data, and our best professional judgement.*

Comment/Question 11: Expressed concerns about the sharp boundary of parameter values between zones after calibration.

Response: *Comment noted.*

Comment/Question 12: I want to know what was changed [between the new and the old R4 model].

Response: *The changes include: increasing the number of hydrologic subareas over the Chino Basin; improved resolution in the land use data for historical and projection periods; updates to the spreading basin infiltration rates; revision of the 2013 RMPU projects incorporated into future projections; and extending the precipitation, ET, evaporation record and gaged inflow to model domain through June 2019. More specifically:*

- *The number of land use types changed from 14 to 20. Land use types 15 to 18 were added to simulate the impact of Model Water Efficient Landscape Ordinance (MWELO), required by California Department of Water Resources. Land use types 19 and 20 were added to simulate the impact of recycled water irrigation and dairy wash water application.*
- *Surface water modeling area was expanded to include Chino Basin, Cucamonga Basin, Six Basins, Spadra Basin and Temescal Basin.*
- *Hydrologic subarea (HSA) boundaries were refined to reflect the groundwater basin boundaries. Total number of hydrologic subareas are increased from 180 to 344.*
- *WEI developed the HSPF model for San Gabriel Mountain, and its calculated daily runoff from mountain watersheds were used as boundary inflow to the R4 modeling area.*
- *Calibration period was extended through fiscal year 2018.*

Comment/Question 13: When you refine the land use, do you refine the waste allocation as well?

Response: *Water use, return flows and stormwater runoff are specific to each land use. If the land use is refined or updated then the associated water use return flows and stormwater runoff will be changed.*

Comment/Question 14: What is the source of [Crop Coefficient] data?

Response: *See references below:*

CA DWR, 1974. *Vegetative Water Use in California, 1974,* California Department of Water Resources, Bulletin No. 113-3, April 1975.

Merkel & Associates, Inc, 2007. *Evapotranspiration Analysis of the Prado Basin, Santa Ana River, California*, prepared for Wildermuth Environmental, Inc., November, 2007.

Snyder, R.L., M. Orang, S. Matyac, L. Bali, and S. Eching, *Basin Irrigation Scheduling (BIS),* Regents of the University of California, April, 2007.

Snyder, R.L., M. Orang, S. Matyac, and S. Eching, Crop Coefficients, Regents of University of California, Last Update March 2, 2007

Allen, R.G., L.S. Pereira, E. Raes, and M Smith, *FAO Irrigation and Drainage Paper No. 56, Crop Evapotranspiration (guidelines for computing crop water requirements),* Food and Agriculture Organization of the United Nations, 1998.

UCCE and CADWR, 2000, *A guide to Estimating Irrigation Water Needs of Landscape Plantings in California*, University of California Cooperative Extensions and California Department of Water Resources, August 2000

Comment/Question 15: What is the source of [Irrigation efficiency] data?

Response: *See references below:*

Sandoval-Solis, S, M. Orang, R.L. Snyder, S. Orloff, K.E. Williams, and J.M. Rodriguez, 2013. *Spatial Analysis of Application Efficiencies for the State of California,* prepared for United States Geological Survey and California Institute for Water Resources, University of California Davis.

Salas, W., P. Green, S, Frolking, C. Li, and S. Boles, *Estimating Irrigation Water Use for California Agriculture, 1950s to Present,* PIER Project Report, Prepared for California Energy Commission.

TECHNICAL MEMORANDUM

March 1, 2020

TO: File 007-019-012.10

FROM: Wenbin Wang, Eric Chiang and Mark Wildermuth

RE: Comments and responses for the second colleague peer review of the 2020 Safe Yield Recalculation that occurred on January 27, 2020

There are three Sections to this TM that include comments and questions captured from the attendees of the January 27 colleague/peer review meeting and subsequent correspondence from the Overlying Ag Pool and the City of Chino.

Comments and Questions from the January 27, 2020 Meeting

Many questions were asked at the January 27 Colleague/Peer review meetings and most were answered. Those questions that were not answered fully or where the answer would be revised subsequent to the meeting are included below.

Comment/Question 1: Tom Harder – What calibration points did you use for the HSPF model?

Response: *The HSPF model was calibrated to observed daily discharges on Live Oak Creek, San Antonio Creek, Cucamonga Creek and Day Creek*

Comment/Question 2: Amanda Coker: **–** Do you know the percentage of the agricultural pool pumping that is estimated vs what is metered?

Response: *We refer you to Watermaster to answer that question*

Wildermuth Environmental, Inc.
23692 Birtcher
Lake Forest, CA 92630

Comment/Question 3: Tom Harder – Why is the Santa Ana riverbed classified as "D" which is the most impervious soil type?

Response: *We don't know. This map was prepared by the NRCS decades ago. We use the hydrologic soil group classification for precipitation-based runoff calculation and not for streambed recharge.*

Comment/Question 4: Amanda Coker – Is the MS4 compliance data incorporated in the model?

Response: *No. There is no information available on the performance and maintenance of MS4 facilities that could be used to quantitatively assess the historical contribution to recharge or to project future recharge.*

Comment/Question 5: Attribution unknown – Have you retroactively changed the irrigation efficiency for any land use types that have been retrofitted, for example adding artificial turf, etc.?

Response: *No.*

Comment/Question 6: Tom Harder – How well is the HSPF model calibrated?

Response: *Please see Section 6 in the 2020 Safe Yield Recalculation Report (hereafter Report).*

Comment/Question 7: Eric Fordham – Did you use flux as well as head to calibrate the model? If both, what order did you use?

Response: *This is discussed in some detail in the Report in Sections 5 and 6. In summary, all flux terms, with the exception of three fluxes, are based on precipitation, estimated applied water and measured fluxes (e.g. Santa Ana River and Temescal Wash inflow to the active CVM domain, imported water recharge, recycled water recharge). The exceptions are subsurface inflow from the Rialto Basin (assumed a constant); subsurface inflow from the Riverside Basin through the Bloomington Divide (variable, based on head in the Riverside Basin); and subsurface outflow from the Spadra Basin to the Puente Basin (variable, based on head in the Puente Basin). When used for planning, the subsurface inflow from the Riverside Basin and subsurface*

outflow form the Spadra Basin were assumed to be a constant value and equal to the average flow from the last five years of the calibration period.

Comment/Question 8: Tom Harder – Did you calibrate land subsidence?

Response: *No. 2020 CVM was updated to be able to calibrate it for land subsidence. Calibration for land subsidence will be done in the next fiscal year as part of the land subsidence management work being done by Watermaster*

Comment/Question 9: Attribution unknown – Is climate change applied to the availability of imported water?

Response: *No.*

Comment/Question 10: Tom Harder – Commented that wet years are not increasing the DIPAW, it is only leveling it out. Would the same thing happen if we had a couple really wet years in the near future?

Response: *Because of the decrease in pervious area and historical drainage practices, the contribution of precipitation to DIPAW has diminished over time. The occurrence of a couple of "really wet years" in the future will increase DIPAW but not as much as it would have in 1970s.*

Comment/Question 11: Tom Harder – How did you deal with the drought hangover in SFI?

Response: *To support Watermaster planning efforts from 2015 forward through the 2018 SFI work, we would annually update the previous model one year at a time without calibrating he model. Planning investigations, such as the 2018 SFI, used the model results from the end of the historical modeling for initial conditions. During these efforts there was no specific acknowledgement of a drought hangover.*

Comment/Question 12: Tracy Egoscue – Did you say that you were not confident in the MS4 recharge facility data..

Response: *There is no information available on the performance and maintenance of MS4 facilities that could be used to quantitatively assess the historical contribution to recharge or to project future recharge.*

Comment/Question 13: Tracy Egoscue – Will new recharge facilities counteract the effects of the drought?

Response: *New recharge facilities will increase future recharge and contribute to mitigating the effects of changes in cultural conditions and future drought.*

Comment/Question 14: Eric Fordham – Why doesn't the long term average DIPAW go down due to climate change?

Response: *In our work, we did not include any future outdoor water conservation measures as to do so would be speculative. This means that in the future if ET were to increase and precipitation decrease, that the more water would be used for irrigation and this would increase irrigation returns.*

Comment/Question 15: Katie Gienger – Did you include future standards for outdoor water use set by the state?

Response: *No. The recent legislation (AB 1668 & SB 606), collectively known as "Making Conservation a California Way of Life," to establish new water efficiency standards for purveyors, will result in new water conservation requirements for irrigation water use. Regulations on irrigation will come into effect in 2023 and it is expected that they will significantly reduce irrigation and subsequently irrigation return flows to groundwater.*

Comment/Question 16: Tom Harder – Can we incorporate possible alternative pumping scenarios?

Response: *No, it is not within our scope of work*

Comment/Question 17: Tom Harder – Really wants to optimize pumping to maximize SY. What happens if they change the way they pump and safe yield increases?

Response: *To be determined.*

Comments and Questions from February 3, 2020 Email fby Tracy Egoscue for the Overlying Ag Pool

Comment/Question 1: The Ag Pool is very interested in the "vadose zone drought hangover on DIPAW and the potential implications this may have on Safe Yield. Please explain any potential adjustments or revisions that have been, or may be made to the modeling approach or Safe Yield Reset Methodology to address this issue.

Response: There were no changes in approach or Safe Yield Reset Methodology. The same approach and methodology were used in the 2020 Safe Yield recalculation.

Comment/Question 2: The information presented in the workshop and on workshop presentation slide no. 236 in the PDF (Comparison of DIPAW Discharging Into and Out of the Vadose Zone) does not indicate how much of the decline in DIPAW discharge to the phreatic zone is due to drought and how much is due to gradual change in other persistent factors, such as land use and/or cultural conditions. Please explain this breakdown. The Ag Pool will have more specific comments or questions on this and/or related issues when the additional information becomes available.

Response: It is clear from our analysis that the change in cultural conditions are very significant when comparing the historical time series DIPAW from wet years, that the precipitation part of the DIPAW has significantly decreased. We did not do an investigation to quantitively assess the historical individual contributions of changes in cultural conditions and drought to historical DIPAW.

Comment/Question 3: Finally, please provide a summary of developed yield estimates through the current model calibration as these were not provided during the Safe Yield workshop.

Response: Please refer to Section 6 of the Report.

February 21, 2020 Comments and Questions from City of Chino and Eric Fordham

Comment/Question 1: The greatest amount of subsurface inflow is attributed to the Bloomington Divide (page 66 of PowerPoint presentation). (a) Why does this recharge inflow

show increases since 2005 while inflow from the other boundaries appear to decrease or remain relatively constant? (b) How is the variable head boundary that is assigned to this recharge boundary calibrated? (c) Model parameters in this area of the model appear to be very sensitive and there are fewer calibration targets. How are the model parameters in the Bloomington Divide area constrained?

Response: (a) In the calibration period, the time series of groundwater elevations in the Riverside Basin at or near the Bloomington Divide are used to simulate the groundwater elevation on the model boundary. Groundwater elevations in the Fontana area have historically been declining relative to the groundwater elevations at the Bloomington divide. The groundwater elevation gradient into the Chino Basin has increased causing the increase in subsurface inflow from the Riverside Basin. With the exception of the Rialto Basin subsurface inflow, the subsurface inflows on the active CVM domain are based on precipitation. (b) and (c) The model parameters were calibrated using manual and optimization techniques that included constraints on the model parameters.

Comment/Question 2: Review of the model parameter sensitivity in Table 6-1 indicates some values that do not appear reasonable. For example, the parameters labeled "sylz**" for layer 1, which presumably represents specific yield, range from 0.47 to 1.01. Generally, specific yield is expected to be 0.3 or less. Considering the specific yield in layer I is a very sensitive parameter, more zonation and parameter control may be required. Please explain. Also, "vklzl" is presumably the vertical hydraulic conductivity for zone I of layer 1, which has a value of 32.7 ft/d (units are presumed) compared to "hklzl," which is presumably the horizontal hydraulic conductivity for zone I of layer I with a value of 2.5 ft/d. Generally, the vertical hydraulic conductivity of a zone is less than the horizontal hydraulic conductivity by half to an order of magnitude. The reported values are not consistent with generally accepted alluvial hydrostratigraphy. As these were initial estimates to assess sensitivity, presumably more constraints that are consistent with generally accepted hydrogeologic concepts were imposed during further modeling calibration. Please confirm and provide examples of final model parameter values used in the 2020 model.

Response: The table does not contain actual aquifer parameter values – it contains parameter zone scalers. Please see Section 5 of the Report for a description of the parameter zone scalers.

Comment/Question 3: Deep Infiltration of Precipitation and Applied Water (DIPAW). The chart on page 67 of the PowerPoint Presentation shows DIPAW to Saturated Zone with a difference from 1995 to 2018 of about 50,000 afy total over the time period. This decrease trends at a rate of about 2,200 afy, which is plotted on the attached chart. The 2013 DIPAW model decreases at a trend that is less than the current model, suggesting a decrease from 1996 to 2012 of about 1,500 afy. (a) Considering the surface area in the 2020 R4 model is larger than that of the 2013 model, what are the significant changes in the 2020 model that results in a

greater decrease in DIPAW compared to the 2013 model? (b) Is the 700 afy difference within the error of the modeling estimates? (c) What are the sensitivities to those parameters that are most significant to DIPAW?

Response: (a) The primary difference in the DIPAW estimates is caused by improvements in the data used in compute DIPAW and surface runoff. Improvements in the data that include improved precipitation estimates and land use resolution. (b) We have not prepared a quantitative assessment of modeling error. (c) The sensitivity is self-evident from the differences in DIPAW estimates from the 2013 and 2020 models.

Comment/Question 4: Over the past 5 to 6 years, recharge has been constant or has increased while discharge (presumably mostly pumping) has decreased, although increase in storage has not been observed until the last 3 years (page 73 of PowerPoint presentation). (a) Why is there a lag of 2 years shown (2015 to 2016) considering the recharge is to the phreatic zone? (b) A table that provides the water budget, such as was provided in Table 3-1 of the 2013 CBWM Model Update would be helpful in better understanding the nuances of the 2020 model.

Response: (a) Our reading of the chart that shows recharge, discharge and change in storage to directly show the storage increasing with increased imported water recharge and slightly declining pumping as would be expected. (b) See Section 6 in the report for the historical water budget table.

Comment/Question 5: How were the lag times with respect to DIPAW determined (Figure 3-1; pages 78 and 79 of the PowerPoint presentation). As indicated during the workshops, soil texture and depth to water are considered. However, are these lag times calibrated to measured data, such as rainfall events and subsequent measured increases in groundwater level. This may have been explained but was not clear.

Response. See Section 5 of the Report for the derivation of the lag times.

Comment/Question 6: While we agree in total the model calibration is impressive, we suggest providing map views of calibration targets for key layers that represent the total error in order to better understand if there are any bias's in the model that either underpredicts or overpredicts recharge/discharge in various portions of the basin's management zones.

Response: See Section 6 of the Report for well location maps, scatter plots and residual analyses.

Comment/Question 7: The Safe Yield Recalculation Tech Memo (December 18, 2019) refers to Table C-2 in the 2020 Storage Management Plan as an example of the replenishment calculation methodology. (a) Review of Table C-2 suggests that Safe Yield (column 3) is inversely related to groundwater pumping (column 2) where reduced pumping through 2020 results in an increased Safe Yield from 2021 through 2030 followed by a decrease in Safe Yield through 2040 as a result of increasing pumping from 2021 through 2030, which then results in an increase in Safe Yield for 2041 through 2050. (b) Based on this relationship, the Safe Yield calculation should include scenarios that consider increased future groundwater pumping in order to better test the maximum Safe Yield potential.

Response: (a) In Table C-2 from the 2020 SMP, the Projected Safe Yield increases in the period 2021 through 2030 because the 2013 RMPU come online in 2021 and the increase in stormwater recharge boost the yield. Because pumping is less than pumping rights, storage builds up and suppresses the yield in the subsequent decade. (b) We disagree. The Safe Yield calculation should be based on the best estimate of how the basin will be which includes the best projection of future pumping provided by the Parties. An optimization investigation could be done with the new 2020 CVM to inform the Parties on how to maximize the Safe Yield through managing pumping, recharge and storage.

TECHNICAL MEMORANDUM

April 15, 2020

TO: Peter Kavounas

FROM: Mark Wildermuth, Eric Chiang, Wenbin Wang, Lauren Sather

RE: Review of and responses to questions posed by Thomas Harder in his February 3, 2020 Task Memorandum to you: *2020 Safe Yield Reset – Follow-Up to Technical Review Meeting on January 27, 2020*

Model Calibration – Surface Water Model

Mr. Harder wrote: *Please provide the calibration plots (measured vs. model-generated scatter plots) for the stream gages located north of Cucamonga Basin (one appears to be in Cucamonga Creek and one appears to be in Day Creek).*

WEI response: The scatter plots are attached to this TM as Figures 1 and 2.

Mr. Harder wrote: *Simulated recharge in managed recharge basins in the surface water model is not matching the measured data provided by IEUA. The fit of model-generated to measured data at Ely Basins and RP-3 Basins show a linear regression fit of less than 0.6. As indicated in the technical meeting, the recharge in the basins is estimated based on interpretation of staff gage readings and not direct measurement of inflow to and outflow from the basins, adjusted for evapotranspiration (ET) losses. Thus, WEI is calibrating the basin recharge in the surface water model to estimated data which results in considerable uncertainty. Given the importance of storm water capture/recharge to the estimate of Safe Yield in the Chino Basin, it is recommended to equip these basins with more accurate surface water balance monitoring equipment (e.g. calibrated gages at the inflow/outflow structures and weather stations to measure precipitation and ET) for recharge measurements.*

WEI response: We concur with your recommendation. Watermaster staff is currently in the process of assessing how the IEUA estimates stormwater capture, and it will be making recommendations for improvements in monitoring equipment and computational procedures to improve the accuracy of stormwater recharge estimates.

Model Calibration – Groundwater Model

Mr. Harder wrote: *For the groundwater flow model, please provide maps showing the final calibrated model distribution of:*

- *Specific Yield of Layer 1*
- *Specific storage of Layers 2, 3, 4 and 5*
- *Hydraulic conductivity of Layers 1 through 5*

WEI response: Please see Figures 3 through 12.

Mr. Harder wrote: *On the hydraulic conductivity maps, please plot the hydraulic conductivities derived from pumping tests, as provided by Thomas Harder & Co. following the July 23, 2020 technical meeting.*

WEI response: Per our coordination call on April 13, we prepared Table 1, which compares horizontal hydraulic conductivity (Kh)—developed from stress tests and estimated by WEI and others—to the final calibrated Kh's in the 2020 Chino Valley Model (CVM). Note that for the stress-test based Kh's provided by you:

- For confined aquifers, the stress-test based Kh's and the model-calibrated values are comparable.
- For unconfined aquifers, the stress-test based Kh's are consistently greater than the model-calibrated values.

The stress-test based Kh's, provided by you, for unconfined aquifers are based on the Jacob's solution for confined aquifers. By its formulation, the Jacobs solution for confined aquifers will always estimate greater values of Kh for an unconfined aquifer than solutions developed specifically for unconfined aquifers. The stress-test based Kh for CDA well I-16 was estimated by WEI using Neuman's solution for an unconfined aquifer. The stress-test based Kh for Chino Hills 19 was estimated with the Neuman-Witherspoon solution for a confined aquifer and corroborated using Theis, Hantush-Jacob, modified Hantush, and Moench solutions. Note that the model calibrated Kh's are close to the WEI estimated Kh's for CDA I-16 and Chino Hills 19.

Mr. Harder wrote: *For the hydrographs showing model-generated vs. measured groundwater levels, it is not clear which model layer the model-generated groundwater levels represent. For example, Chino Well 13 is perforated across Layers 1, 2 and 3 of the updated model (Section B-B' from July 23, 2019 technical meeting). MODFLOW will provide a layer-specific hydraulic head value but not a composite layer head value. Please provide the calibration hydrographs with a description of which model layer the model-generated groundwater level represents. If the*

model-generated groundwater level is not specific to a layer, provide a detailed explanation of how you arrived at the model-generated groundwater level shown on the hydrographs.

WEI response: Calibration targets are available generally as measured groundwater levels, and they are not always available as groundwater levels in individual layers. We used a transmissivity-weighting function to calculate the groundwater level value at a calibration well h_{well} as follows:

$$h_{well} = \sum_{i=1}^{n} (h_i \times f_i)\,;\;\; f_i = \frac{T_i}{T_{sum}};\;\; T_{sum} = \sum_{i=1}^{n} T_i$$

Where n is the number of screened layers, h_i is the model-calculated groundwater level in layer i, f_i is the weighting factor of layer i, and T_i is the transmissivity of the screened thickness in layer i.

Mr. Harder wrote: *Please provide a calibration hydrograph for Chino II-2.*

WEI response: Please see Appendix C, Exhibit C-9, in the final 2020 Safe Yield Recalculation Report (page 296 of the report pdf).

Mr. Harder wrote: *For Wells AP-PA7, the model doesn't replicate the groundwater level variation measured in the well. As this is a monitoring well, the variations are not associated with pumping groundwater levels and are therefore most likely indicative of pumping interference from nearby wells. The relatively large residuals were also observed in the later data for CH HIL 07C hydrograph. It is recommended to review the model pumping input and aquifer parameters in this area to make sure they are representative of measured data.*

WEI response: As you recommended, we reviewed the model pumping input and aquifer parameters. Chino Hills pumping is intermittent and large drawdown occurs at these wells. It is very difficult to find representative groundwater levels at these wells to calibrate to when the wells are operated this way. As to the aquifer parameters, next fiscal year, Watermaster will revise the CVM to include land subsidence and that process will include fine-tuning the aquifer parameters in this area and may lead to improved matching of observed and computed groundwater levels. It is our opinion that the occurrence of these residuals at these two wells does not impact the estimate of net recharge and Safe Yield.

Model Planning Scenario

Mr. Harder wrote: *The comparison of deep infiltration of precipitation and applied water (DIPAW) from the meeting raises several questions:*

1. *What assumptions/data changed in the surface water model that resulted in as much as approximately 15,000 acre-ft/yr more groundwater recharge from DIPAW in the current version of the model versus the 2013 version for the time period from approximately 1985 to 2005?*
2. *What assumptions/data changed that resulted in the greater downward trend in DIPAW in the current version of the model relative to the 2013 version?*
3. *In each of questions 1 and 2 above, what is the basis for the changed assumptions in the model?*
4. *How has the overall groundwater budget changed as a result of the changes in DIPAW?*

WEI response: (1) WEI is involved in a parallel effort to assist Watermaster and the IEUA in assessing alternative TDS compliance metrics for recycled water use. In that effort, the watershed was refined to comport more accurately with the groundwater basin boundaries, and land use delineations were updated to more accurately reflect water use and salt loading. Since the prior Safe Yield recalculation, the number hydrologic subareas have substantially increased to more accurately estimate stormwater recharge. These improvements were carried forward into the 2020 CVM. In the 2020 CVM, the method for estimating reference ET (ET_0) across the watershed was improved from past reliance on a relationship between the Pomona CIMIS station ET_0 and Puddingstone reservoir evaporation to a new ET_0 model that is based on empirical relationships of temperature and ET_0 measurements at the Pomona and Riverside CIMIS stations and using these relationships to estimate ET_0 temporally and spatially based on PRISM estimates of monthly temperature across the watershed. In the 2020 CVM, the method for estimating daily precipitation for each hydrologic subarea was improved from past reliance of interpolating daily precipitation at precipitation stations across the watershed using Thiessen polygons to the use of monthly precipitation estimates for each hydrologic subarea based on monthly PRISM estimates and converting the monthly estimates to daily precipitation estimates based on daily precipitation patterns from nearby precipitation stations. As to precipitation, these improvements were made prior to 2002. After 2002, daily precipitation estimates for the hydrologic subareas were based on NEXRAD estimates, as was done in the prior Safe Yield recalculation. The changes in the historical DIPAW estimates are primarily the result of these improvements in the data used in the R4 model.

(2) The primary drivers of the greater downward trend in DIPAW in the current version of the model relative to the 2013 version are the data improvements described in (1) above and the 20 -year drought period that started in 1999—the latter of which is the greatest dry-period in the instrumental record for the region.

(3) The hydrologic delineation of subareas and improvements in land use delineations as well as ET_0 and precipitation estimates were implemented to improve the accuracy of the recharge components in the Safe Yield recalculation; these improvements are consistent with the Court-ordered Safe Yield recalculation methodology.

(4) The changes in DIPAW and some other recharge components computed for the 2020 Safe Yield recalculation for the historical period are larger than those reported in the prior Safe Yield recalculation. Compare Table 6-3 and Figure 6-16 in the 2020 Safe Yield Recalculation report to Table 3-1 in the 2015 Safe Yield Recalculation report.

Mr. Harder wrote: *Please provide the groundwater budget for the updated model for the 1977 to 2018 calibration period (i.e. an updated version of Table 3-1 from the 2013 Safe Yield model report).*

WEI response: See Table 6-3 in the final 2020 Safe Yield Recalculation Report.

Figure 1 Comparison of Simulated Discharge and Measured Discharge for Cucamonga Creek (1949 - 1975)

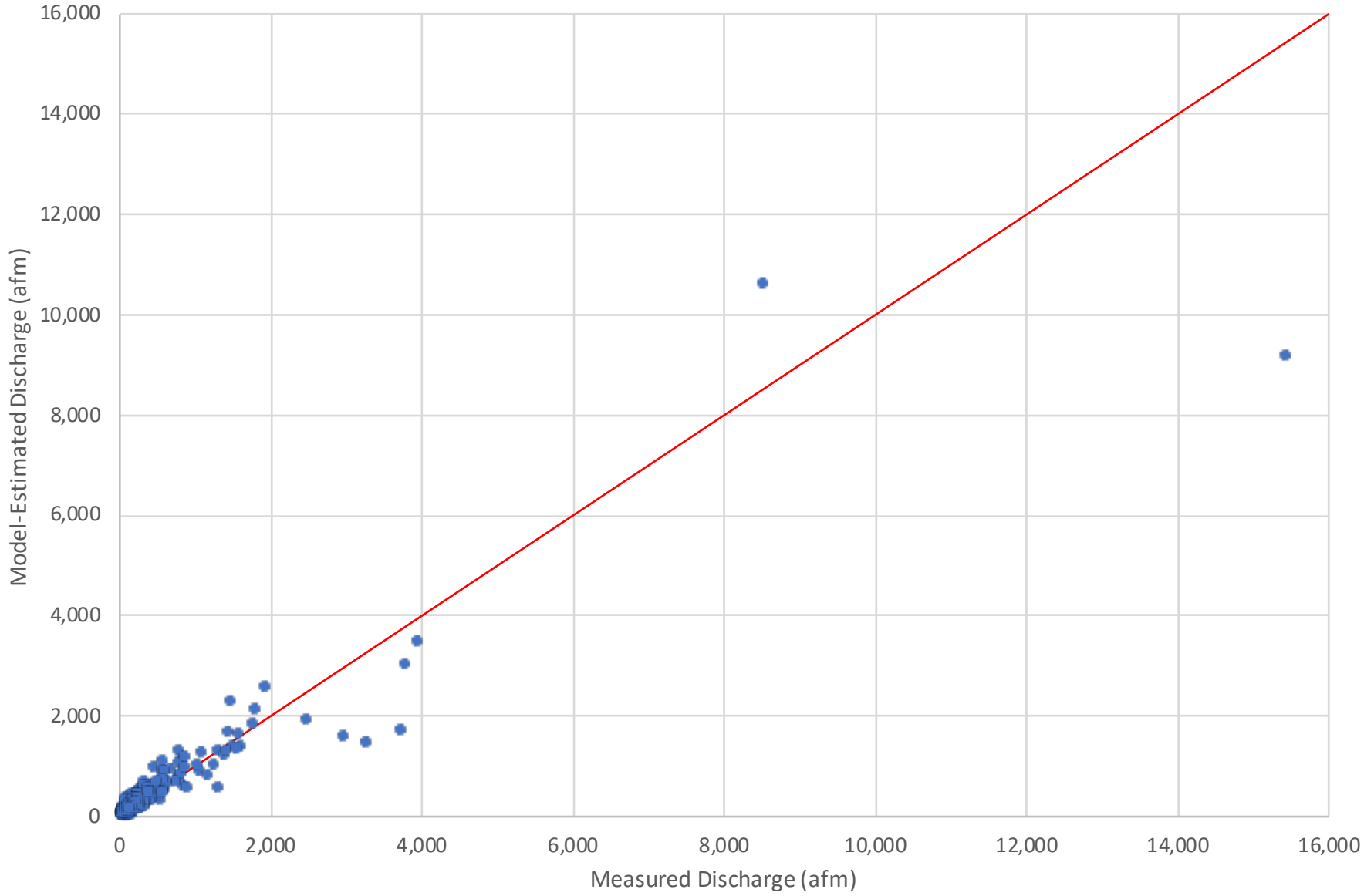

Figure 2 Comparison of Simulated Discharge and Measured Discharge for Day Creek (1950 - 1971)

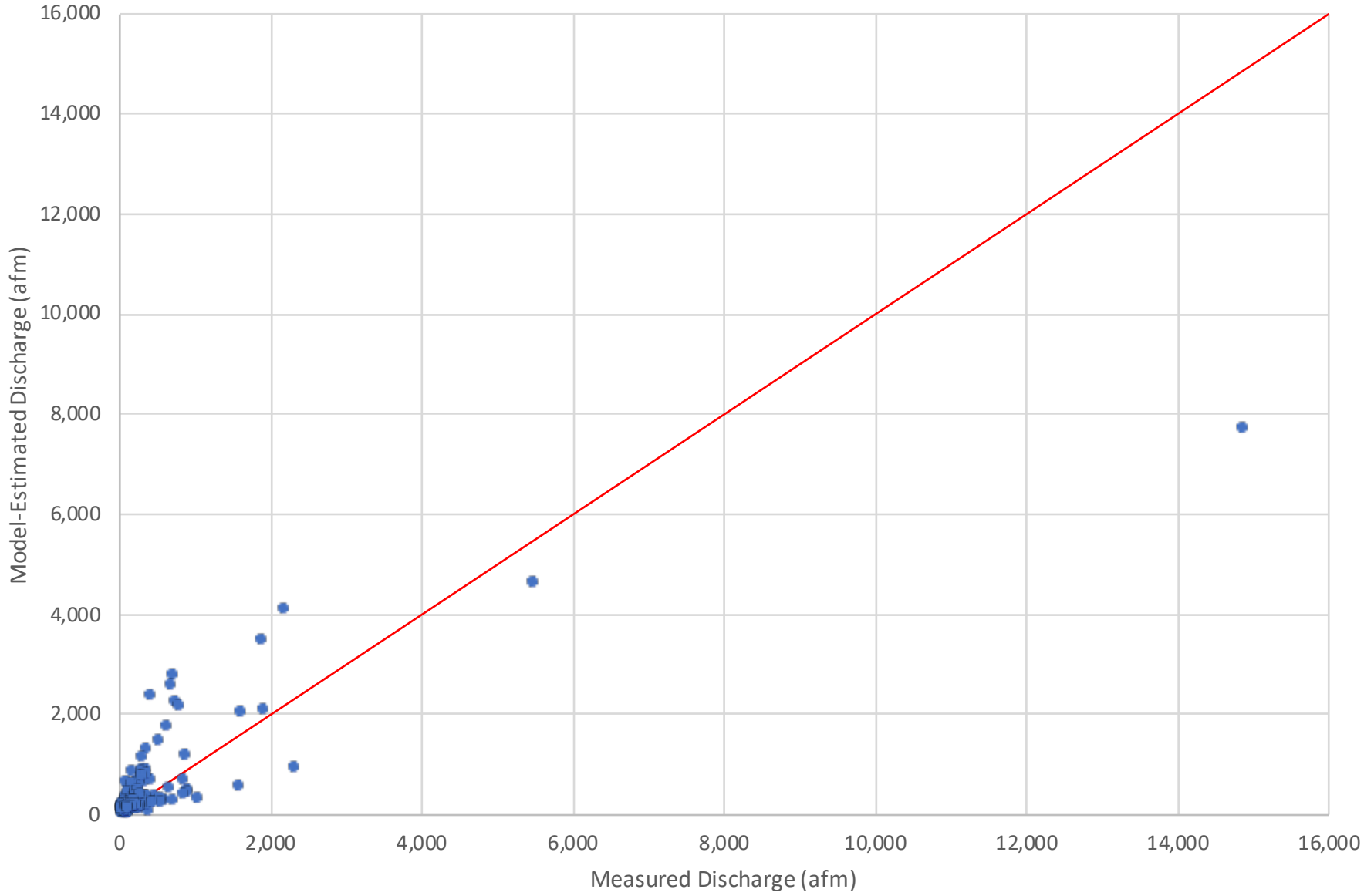

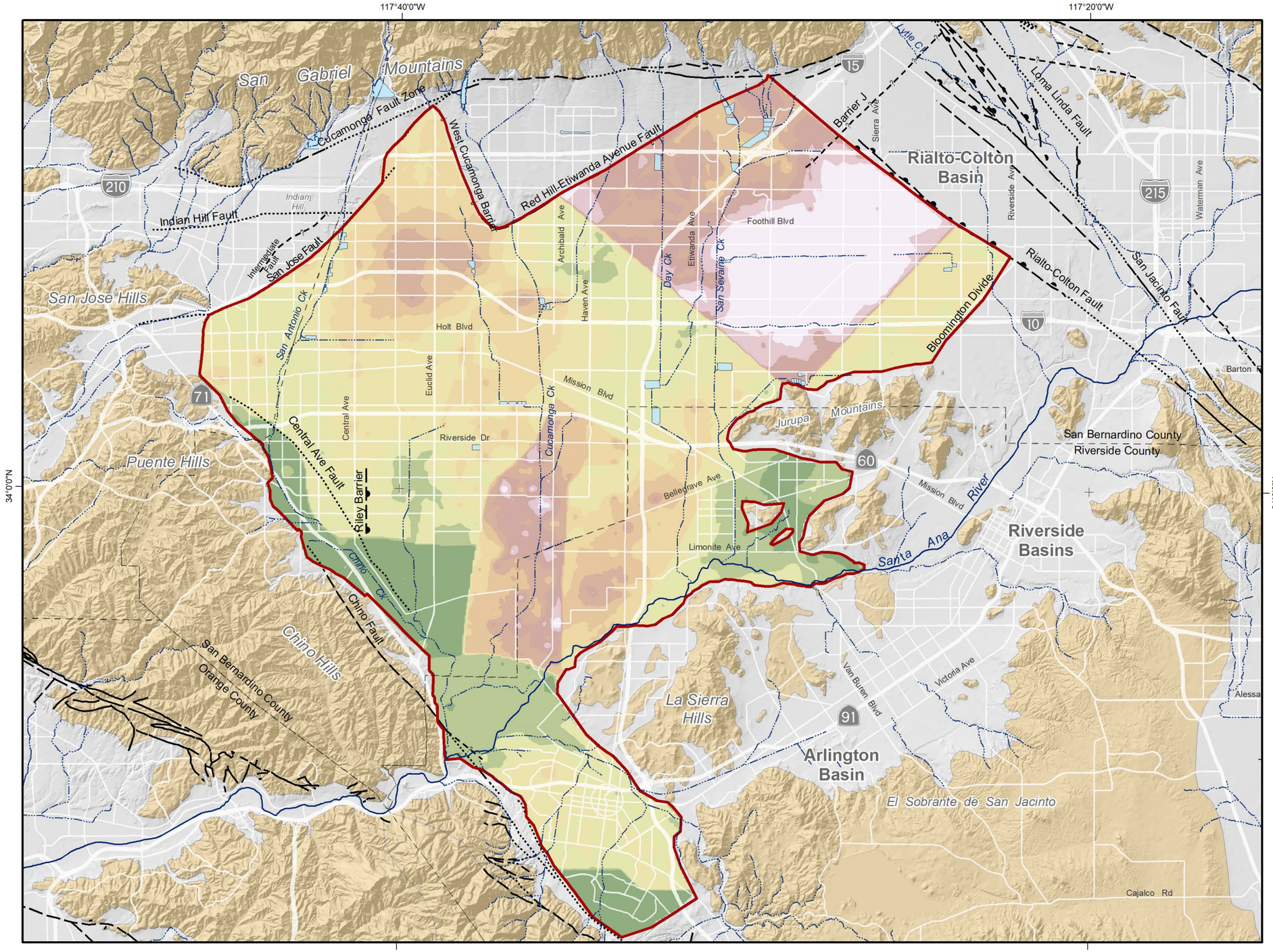

Calibrated Horizontal Hydraulic Conductivity
Layer 1 (ft/day)

- 3 - 21
- 22 - 40
- 41 - 58
- 59 - 76
- 77 - 95
- 96 - 113
- 114 - 132
- 133 - 150
- 151 - 168
- 169 - 187

- Model Domain
- Streams & Flood Control Channels
- Flood Control & Conservation Basins

Geology

Water-Bearing Sediments

- Quaternary Alluvium

Consolidated Bedrock

- Undifferentiated Pre-Tertiary to Early Pleistocene Igneous, Metamorphic, and Sedimentary Rocks

- Fault (solid where accurately located; dashed where approximately located or inferred; dotted where concealed)

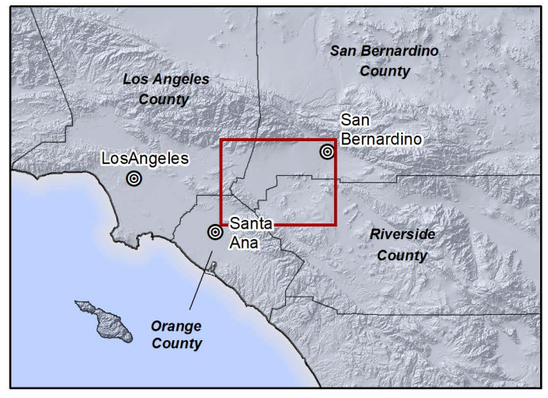

Produced by:

WEI
Wildermuth Environmental, Inc.

Author: LJS
Date: 4/13/2020
Document Name: L1Kh

0 1 2 3 4 5 Miles
0 2 4 6 8 KM

Prepared for:

2020 Safe Yield Recalculation

Chino Basin Watermaster
Partners in Basin Management

Calibrated Horizontal Hydraulic Conductivity Layer 1

Figure 3

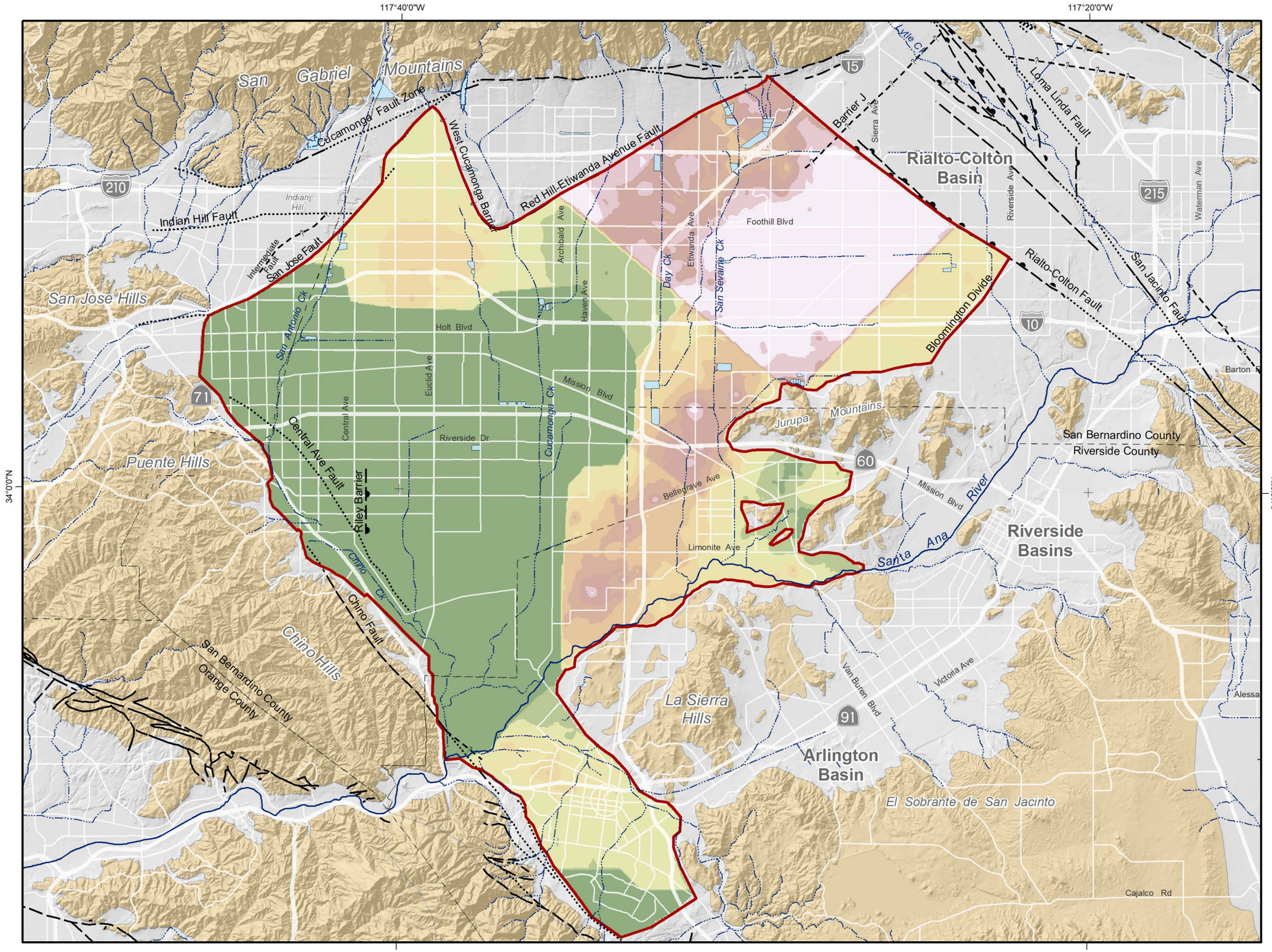

Calibrated Horizontal Hydraulic Conductivity
Layer 2 (ft/day)

- 3 - 21
- 22 - 40
- 41 - 58
- 59 - 76
- 77 - 95
- 96 - 113
- 114 - 132
- 133 - 150
- 151 - 168
- 169 - 187

Model Domain

Streams & Flood Control Channels

Flood Control & Conservation Basins

Geology

Water-Bearing Sediments

Quaternary Alluvium

Consolidated Bedrock

Undifferentiated Pre-Tertiary to Early Pleistocene Igneous, Metamorphic, and Sedimentary Rocks

Fault (solid where accurately located; dashed where approximately located or inferred; dotted where concealed)

Produced by:

WEI
WILDERMUTH ENVIRONMENTAL, INC.

Author: LJS
Date: 4/13/2020
Document Name: L2Kh

0 1 2 3 4 5 Miles
0 2 4 6 8 KM

Prepared for:

2020 Safe Yield Recalculation

CHINO BASIN WATERMASTER
Partners in Basin Management

Calibrated Horizontal Hydraulic Conductivity Layer 2

Figure 4

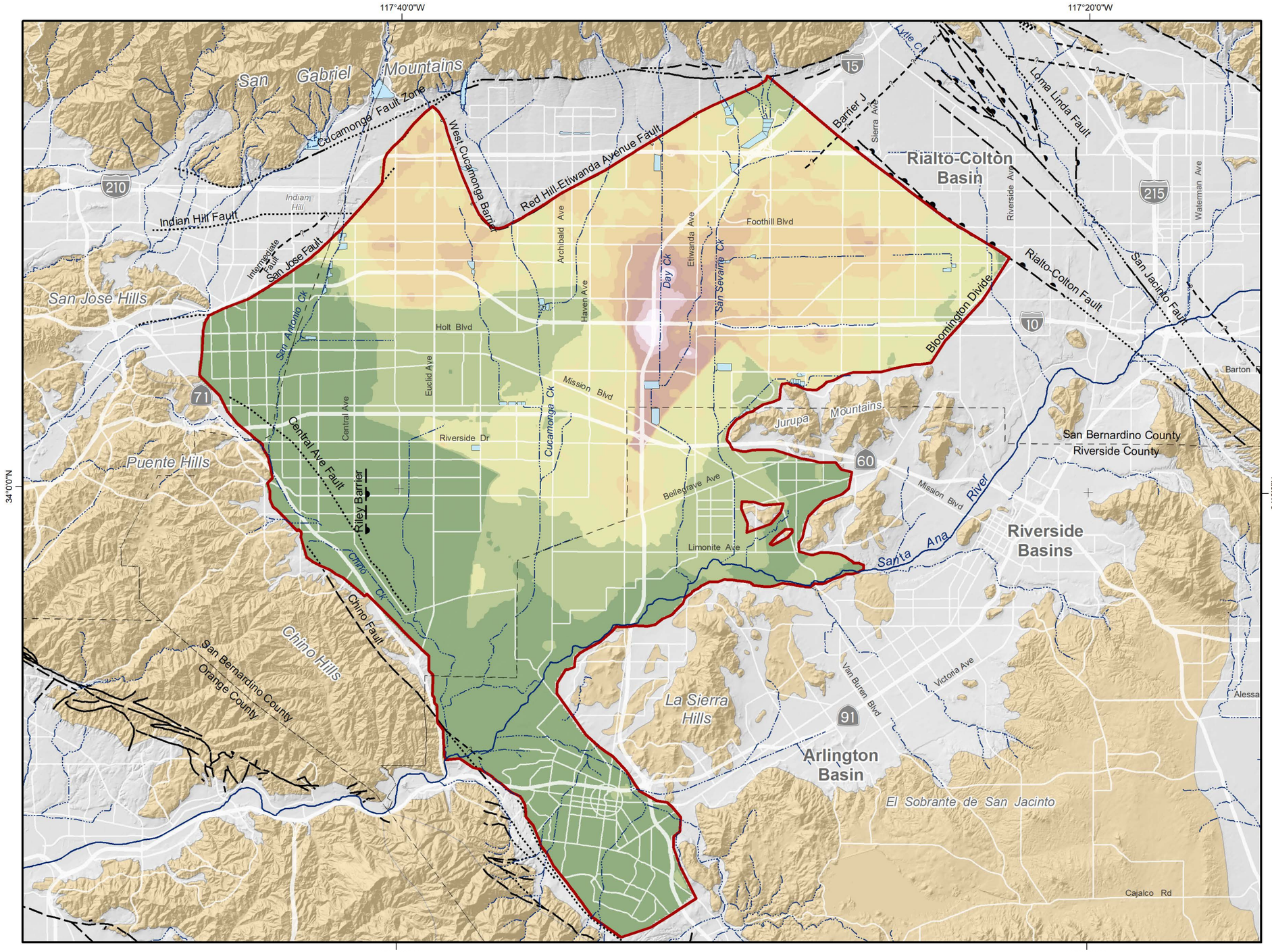

Calibrated Horizontal Hydraulic Conductivity
Layer 3 (ft/day)

- 3 - 21
- 22 - 40
- 41 - 58
- 59 - 76
- 77 - 95
- 96 - 113
- 114 - 132
- 133 - 150
- 151 - 168
- 169 - 187

Model Domain

Streams & Flood Control Channels

Flood Control & Conservation Basins

Geology

Water-Bearing Sediments

Quaternary Alluvium

Consolidated Bedrock

Undifferentiated Pre-Tertiary to Early Pleistocene Igneous, Metamorphic, and Sedimentary Rocks

Fault (solid where accurately located; dashed where approximately located or inferred; dotted where concealed)

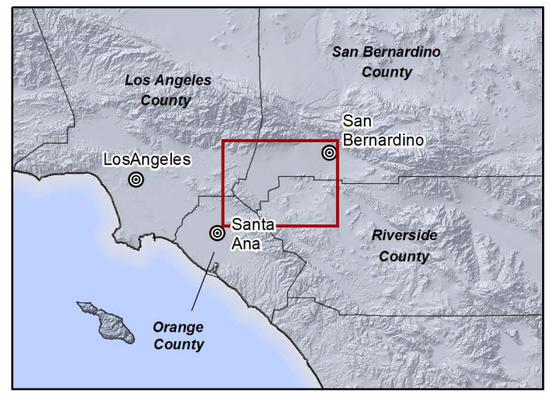

Produced by:

WEI
Wildermuth Environmental, Inc.

Author: LJS
Date: 4/13/2020
Document Name: L3Kh

0 1 2 3 4 5 Miles
0 2 4 6 8 KM

Prepared for:

2020 Safe Yield Recalculation

Chino Basin Watermaster
Partners in Basin Management

Calibrated Horizontal Hydraulic Conductivity Layer 3

Figure 5

117°40'0"W

117°20'0"W

34°0'0"N

Calibrated Horizontal Hydraulic Conductivity
Layer 4 (ft/day)

- 3 - 21
- 22 - 40
- 41 - 58
- 59 - 76
- 77 - 95
- 96 - 113
- 114 - 132
- 133 - 150
- 151 - 168
- 169 - 187

Model Domain

Streams & Flood Control Channels

Flood Control & Conservation Basins

Geology

Water-Bearing Sediments

Quaternary Alluvium

Consolidated Bedrock

Undifferentiated Pre-Tertiary to Early Pleistocene Igneous, Metamorphic, and Sedimentary Rocks

Fault (solid where accurately located; dashed where approximately located or inferred; dotted where concealed)

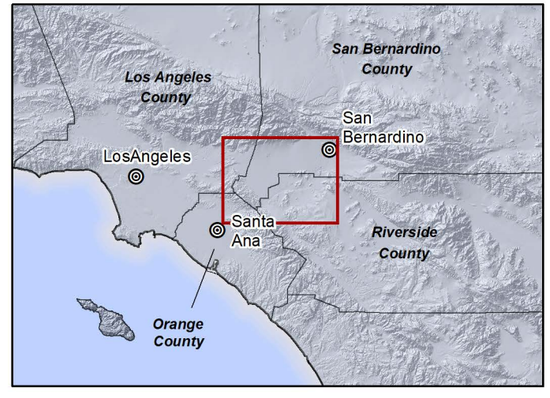

Produced by:

WEI
WILDERMUTH ENVIRONMENTAL, INC.

Author: LJS
Date: 4/13/2020
Document Name: L4Kh

0 1 2 3 4 5 Miles
0 2 4 6 8 KM

Prepared for:

2020 Safe Yield Recalculation

CHINO BASIN WATERMASTER
Partners in Basin Management

Calibrated Horizontal Hydraulic Conductivity Layer 4

Figure 6

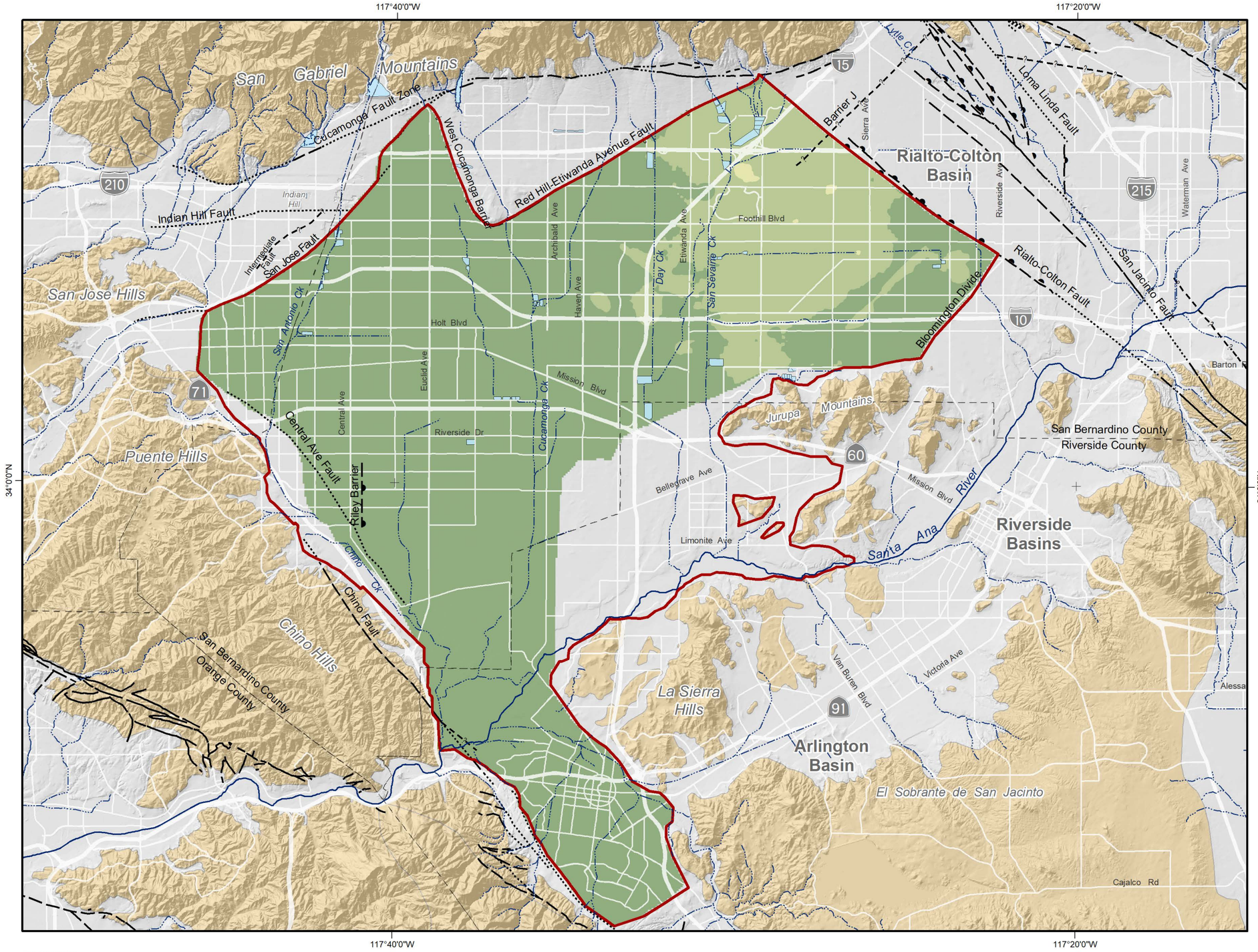

Calibrated Horizontal Hydraulic Conductivity
Layer 5 (ft/day)

- 3 - 21
- 22 - 40
- 41 - 58
- 59 - 76
- 77 - 95
- 96 - 113
- 114 - 132
- 133 - 150
- 151 - 168
- 169 - 187

Model Domain

Streams & Flood Control Channels

Flood Control & Conservation Basins

Geology

Water-Bearing Sediments

Quaternary Alluvium

Consolidated Bedrock

Undifferentiated Pre-Tertiary to Early Pleistocene Igneous, Metamorphic, and Sedimentary Rocks

Fault (solid where accurately located; dashed where approximately located or inferred; dotted where concealed)

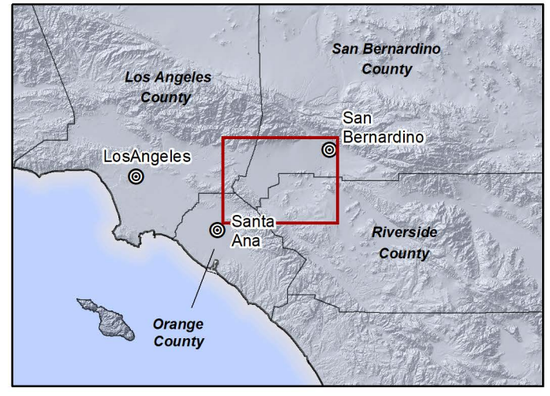

Produced by:

WEI
Wildermuth Environmental, Inc.

Author: LJS
Date: 4/13/2020
Document Name: L5Kh

0 1 2 3 4 5 Miles
0 2 4 6 8 KM

Prepared for:

2020 Safe Yield Recalculation

Chino Basin Watermaster
Partners in Basin Management

Calibrated Horizontal Hydraulic Conductivity Layer 5

Figure 7

117°40'0"W

117°20'0"W

34°0'0"N

San Gabriel Mountains

Cucamonga Fault Zone

West Cucamonga Barrier

Red Hill-Etiwanda Avenue Fault

Barrier J

Lytle Ck

Loma Linda Fault

Rialto-Colton Basin

Riverside Ave

Waterman Ave

Sierra Ave

Indian Hill

Indian Hill Fault

Intermediate Fault

San Jose Fault

San Jose Hills

San Antonio Ck

Archibald Ave

Day Ck

Etiwanda Ave

San Sevaine Ck

Foothill Blvd

Haven Ave

Holt Blvd

Bloomington Divide

Rialto-Colton Fault

San Jacinto Fault

Barton R

Euclid Ave

Central Ave

Mission Blvd

Cucamonga Ck

Riverside Dr

Central Ave Fault

Riley Barrier

Puente Hills

Jurupa Mountains

San Bernardino County

Riverside County

Bellegrave Ave

Limonite Ave

Mission Blvd

Santa Ana River

Riverside Basins

Chino Ck

Chino Fault

San Bernardino County

Orange County

Chino Hills

La Sierra Hills

Van Buren Blvd

Victoria Ave

Arlington Basin

El Sobrante de San Jacinto

Alessa

Cajalco Rd

210

71

15

215

10

60

91

Calibrated Specific Yield
Layer 1

- 0.001 - 0.025
- 0.026 - 0.05
- 0.051 - 0.075
- 0.076 - 0.1
- 0.101 - 0.125
- 0.126 - 0.15
- 0.151 - 0.175
- 0.176 - 0.199
- 0.2 - 0.224
- 0.225 - 0.249

Model Domain

Streams & Flood Control Channels

Flood Control & Conservation Basins

Geology

Water-Bearing Sediments

Quaternary Alluvium

Consolidated Bedrock

Undifferentiated Pre-Tertiary to Early Pleistocene Igneous, Metamorphic, and Sedimentary Rocks

Fault (solid where accurately located; dashed where approximately located or inferred; dotted where concealed)

Produced by:

WEI
Wildermuth Environmental, Inc.

Author: LJS
Date: 4/15/2020
Document Name: Figure_8_L1Sy

0 1 2 3 4 5 Miles

0 2 4 6 8 KM

Prepared for:

2020 Safe Yield Recalculation

Chino Basin Watermaster
Partners in Basin Management

Calibrated Specific Yield Layer 1

Figure 8

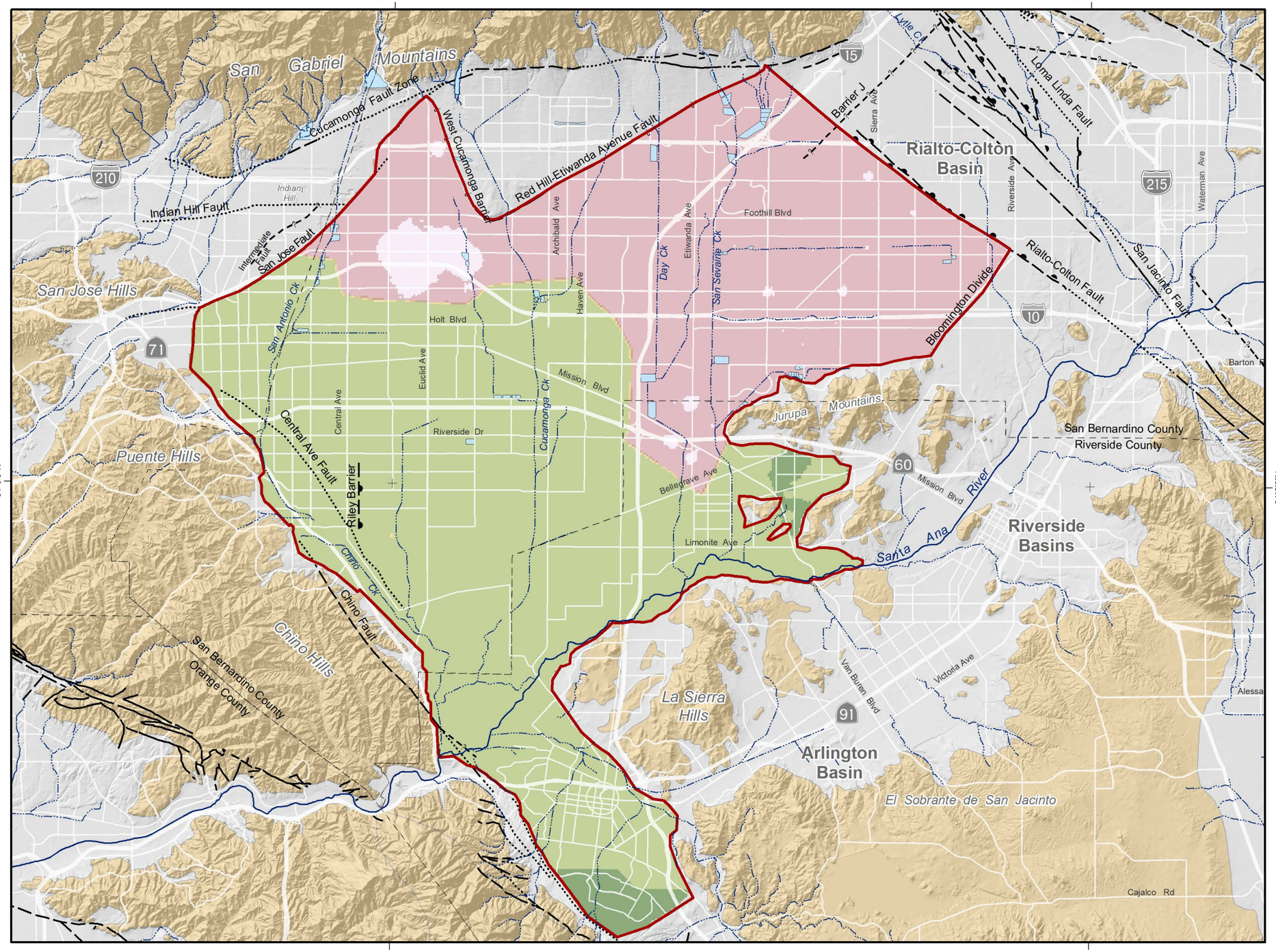

Calibrated Specific Storage
Layer 2

- 1e-8 - 1e-7
- 1e-7 - 5e-7
- 5e-7 - 1e-6
- 1e-6 - 5e-6
- 5e-6 - 1e-5
- 1e-5 - 5e-5
- 5e-5 - 0.0001
- 0.0001 - 0.0004

Model Domain

Streams & Flood Control Channels

Flood Control & Conservation Basins

Geology

Water-Bearing Sediments

Quaternary Alluvium

Consolidated Bedrock

Undifferentiated Pre-Tertiary to Early Pleistocene Igneous, Metamorphic, and Sedimentary Rocks

Fault (solid where accurately located; dashed where approximately located or inferred; dotted where concealed)

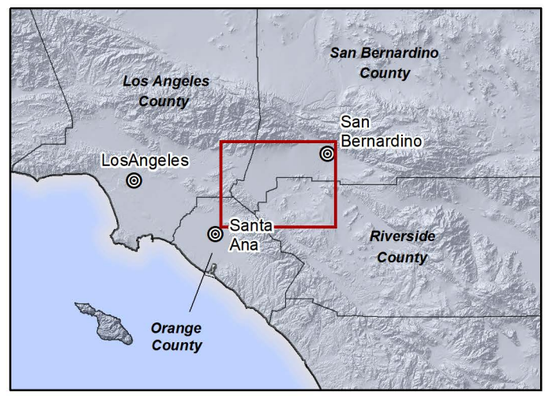

Produced by:

WEI
Wildermuth Environmental, Inc.

Author: LJS
Date: 4/15/2020
Document Name: Figure_9_L2Ss_new_intervals

0 1 2 3 4 5 Miles
0 2 4 6 8 KM

Prepared for:

2020 Safe Yield Recalculation

Chino Basin Watermaster
Partners in Basin Management

Calibrated Specific Storage
Layer 2

Figure 9

117°40'0"W

117°20'0"W

34°0'0"N

San Gabriel Mountains

Cucamonga Fault Zone

West Cucamonga Barrier

Red Hill-Etiwanda Avenue Fault

Barrier J

Lytle Ck

Loma Linda Fault

Rialto-Colton Basin

Indian Hill

Indian Hill Fault

Intermediate Fault

San Jose Fault

San Jose Hills

San Antonio Ck

Archibald Ave

Foothill Blvd

Day Ck

Etiwanda Ave

San Sevaine Ck

Riverside Ave

Waterman Ave

Rialto-Colton Fault

Bloomington Divide

San Jacinto Fault

Holt Blvd

Haven Ave

Euclid Ave

Central Ave

Central Ave Fault

Mission Blvd

Cucamonga Ck

Riverside Dr

Jurupa Mountains

San Bernardino County

Riverside County

Puente Hills

Riley Barrier

Bellegrave Ave

Limonite Ave

Mission Blvd

Santa Ana River

Riverside Basins

Chino Ck

Chino Fault

Chino Hills

San Bernardino County

Orange County

La Sierra Hills

Arlington Basin

El Sobrante de San Jacinto

Van Buren Blvd

Victoria Ave

Cajalco Rd

Alessa

Barton R

71

210

15

215

10

60

91

Calibrated Specific Storage
Layer 3

- 1e-8 - 1e-7
- 1e-7 - 5e-7
- 5e-7 - 1e-6
- 1e-6 - 5e-6
- 5e-6 - 1e-5
- 1e-5 - 5e-5
- 5e-5 - 0.0001
- 0.0001 - 0.0004

Model Domain

Streams & Flood Control Channels

Flood Control & Conservation Basins

Geology

Water-Bearing Sediments

Quaternary Alluvium

Consolidated Bedrock

Undifferentiated Pre-Tertiary to Early Pleistocene Igneous, Metamorphic, and Sedimentary Rocks

Fault (solid where accurately located; dashed where approximately located or inferred; dotted where concealed)

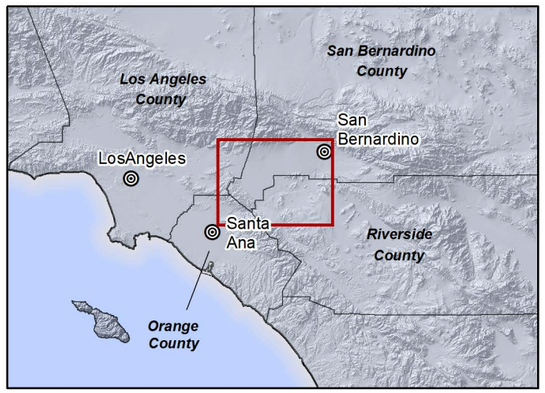

Produced by:

WEI
Wildermuth Environmental, Inc.

Author: LJS
Date: 4/15/2020
Document Name: Figure_10_L3Ss

0 1 2 3 4 5 Miles

0 2 4 6 8 KM

Prepared for:

2020 Safe Yield Recalculation

Chino Basin Watermaster
Partners in Basin Management

Calibrated Specific Storage Layer 3

Figure 10

117°40'0"W

117°20'0"W

34°0'0"N

San Gabriel Mountains

Cucamonga Fault Zone

West Cucamonga Barrier

Red Hill-Etiwanda Avenue Fault

Barrier J

Lytle Ck

Loma Linda Fault

Rialto-Colton Basin

Indian Hill

Indian Hill Fault

Intermediate Fault

San Jose Fault

San Jose Hills

Archibald Ave

Foothill Blvd

Day Ck

Etiwanda Ave

San Sevaine Ck

Riverside Ave

Waterman Ave

Rialto-Colton Fault

San Jacinto Fault

Bloomington Divide

Barton

Holt Blvd

Haven Ave

San Antonio Ck

Euclid Ave

Central Ave

Mission Blvd

Riverside Dr

Cucamonga Ck

Central Ave Fault

Riley Barrier

Jurupa Mountains

San Bernardino County

Riverside County

Bellegrave Ave

Limonite Ave

Mission Blvd

Santa Ana River

Riverside Basins

Puente Hills

Chino Ck

Chino Fault

Chino Hills

San Bernardino County

Orange County

La Sierra Hills

Van Buren Blvd

Victoria Ave

Arlington Basin

El Sobrante de San Jacinto

Cajalco Rd

Alessa

15

210

215

71

10

60

91

Calibrated Specific Storage
Layer 4

- 1e-8 - 1e-7
- 1e-7 - 5e-7
- 5e-7 - 1e-6
- 1e-6 - 5e-6
- 5e-6 - 1e-5
- 1e-5 - 5e-5
- 5e-5 - 0.0001
- 0.0001 - 0.0004

Model Domain

Streams & Flood Control Channels

Flood Control & Conservation Basins

Geology

Water-Bearing Sediments

Quaternary Alluvium

Consolidated Bedrock

Undifferentiated Pre-Tertiary to Early Pleistocene Igneous, Metamorphic, and Sedimentary Rocks

Fault (solid where accurately located; dashed where approximately located or inferred; dotted where concealed)

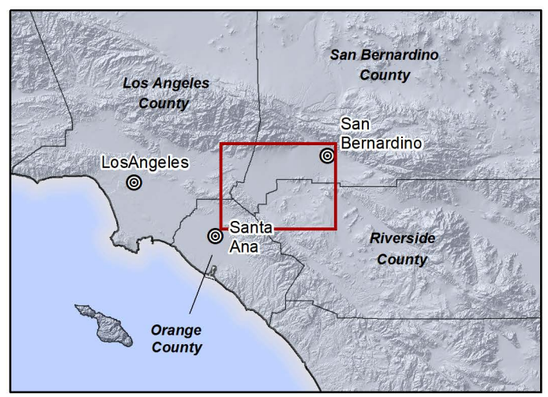

Produced by:

WEI
WILDERMUTH ENVIRONMENTAL, INC.

Author: LJS
Date: 4/15/2020
Document Name: Figure_11_L4Ss

0 1 2 3 4 5 Miles

0 2 4 6 8 KM

Prepared for:

2020 Safe Yield Recalculation

CHINO BASIN WATERMASTER
Partners in Basin Management

Calibrated Specific Storage Layer 4

Figure 11

117°40'0"W

117°20'0"W

34°0'0"N

San Gabriel Mountains

Cucamonga Fault Zone

West Cucamonga Barrier

Red Hill-Etiwanda Avenue Fault

Barrier J

Lytle Ck

Loma Linda Fault

Rialto-Colton Basin

Indian Hill

Indian Hill Fault

Intermediate Fault

San Jose Fault

San Jose Hills

San Antonio Ck

Archibald Ave

Haven Ave

Day Ck

Etiwanda Ave

San Sevaine Ck

Foothill Blvd

Riverside Ave

Waterman Ave

Rialto-Colton Fault

San Jacinto Fault

Bloomington Divide

Holt Blvd

Euclid Ave

Central Ave

Central Ave Fault

Riley Barrier

Mission Blvd

Cucamonga Ck

Riverside Dr

Jurupa Mountains

San Bernardino County

Riverside County

Puente Hills

Bellegrave Ave

Limonite Ave

Mission Blvd

Santa Ana River

Riverside Basins

Chino Ck

Chino Fault

Chino Hills

San Bernardino County

Orange County

La Sierra Hills

Van Buren Blvd

Victoria Ave

Arlington Basin

El Sobrante de San Jacinto

Cajalco Rd

Barton

Alessa

71

210

15

215

10

60

91

117°40'0"W

117°20'0"W

34°0'0"N

Calibrated Specific Storage
Layer 5

- 1e-8 - 1e-7
- 1e-7 - 5e-7
- 5e-7 - 1e-6
- 1e-6 - 5e-6
- 5e-6 - 1e-5
- 1e-5 - 5e-5
- 5e-5 - 0.0001
- 0.0001 - 0.0004

Model Domain

Streams & Flood Control Channels

Flood Control & Conservation Basins

Geology

Water-Bearing Sediments

Quaternary Alluvium

Consolidated Bedrock

Undifferentiated Pre-Tertiary to Early Pleistocene Igneous, Metamorphic, and Sedimentary Rocks

Fault (solid where accurately located; dashed where approximately located or inferred; dotted where concealed)

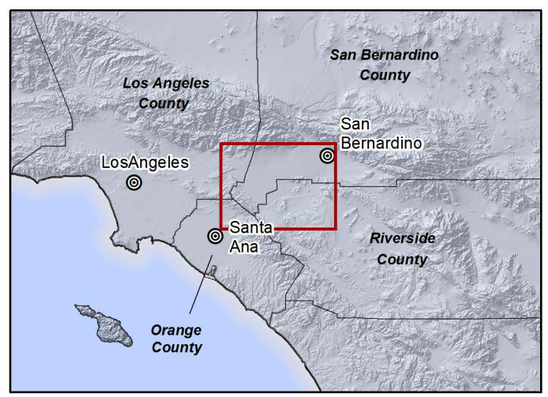

Produced by:

WEI
WILDERMUTH ENVIRONMENTAL, INC.

Author: LJS
Date: 4/15/2020
Document Name: Figure_12_L5Ss

0 1 2 3 4 5 Miles

0 2 4 6 8 KM

Prepared for:

2020 Safe Yield Recalculation

CHINO BASIN WATERMASTER
Partners in Basin Management

Calibrated Specific Storage Layer 5

Figure 12

Table 1 Comparison of Stress Test Derived Hydraulic Conductivities to Initial Hydraulic Conductivity Values Derived from a Lithology Model and Final Calibrated Values (f/d)

Well Name	Stress Test Based Hydraulic Conductivity Value Provided by THA or WEI (ft/day)	Model Layers Perforated by Well[2]	Initial Estimate of Hydraulic Conductivity from Lithology Model (ft/day)	Initial Parameter Zone Coefficient	Initial Hydraulic Conductivity in Model (ft/day)	Final Parameter Zone Coefficient	Final Hydraulic Conductivity in Model (ft/day)
CH19[1]	5.80	1					
		2					
		3	45.77	0.140	6.41	0.110	5.03
		4					
		5					
ONT 40	61.78	1					
		2					
		3	47.11	0.396	18.64	1.259	59.31
		4					
		5	45.86	0.139	6.38	0.211	9.67
ONT 41	35.29	1					
		2					
		3	45.89	0.396	18.16	1.259	57.77
		4					
		5	54.54	0.139	7.58	0.211	11.50
ONT 43	36.14	1					
		2					
		3	82.28	0.174	14.34	0.617	50.80
		4					
		5	73.70	0.032	2.38	0.021	1.53
ONT 44	53.11	1					
		2					
		3	42.65	0.396	16.88	1.259	53.69
		4					
		5	52.98	0.139	7.36	0.211	11.17
ONT 45	41.74	1	87.50	0.475	41.57	0.982	85.90
		2					
		3	43.17	0.174	7.52	0.617	26.65
		4					
		5	43.36	0.032	1.40	0.021	0.90
ONT 46	155.24	1	91.65	0.581	53.28	0.801	73.39
		2					
		3	49.44	0.396	19.57	1.259	62.24
		4					
		5	42.30	0.139	5.88	0.211	8.92
ONT 47	67.46	1					
		2					
		3	85.55	0.396	33.85	1.259	107.69
		4	85.55				
		5	87.55	0.139	12.17	0.211	18.46
ONT 49	48.01	1	62.24				
		2	0.10				
		3	94.68	0.174	16.50	0.617	58.45
		4	0.10				
		5	61.83	0.032	2.00	0.021	1.28
ONT 50	103.10	1	43.74	1.530	66.92	1.779	77.83
		2					
		3	118.55	0.347	41.14	0.526	62.35
		4					
		5					
ONT 52	40.14	1					
		2					
		3	55.24	0.396	21.86	1.259	69.53
		4					
		5	62.13	0.139	8.64	0.211	13.10
JCSD 22	275.13	1	91.14	1.526	139.08	0.716	65.25
		2					
		3					
		4					
		5					

Table 1 Comparison of Stress Test Derived Hydraulic Conductivities to Initial Hydraulic Conductivity Values Derived from a Lithology Model and Final Calibrated Values (f/d)

Well Name	Stress Test Based Hydraulic Conductivity Value Provided by THA or WEI (ft/day)	Model Layers Perforated by Well[2]	Initial Estimate of Hydraulic Conductivity from Lithology Model (ft/day)	Initial Parameter Zone Coefficient	Initial Hydraulic Conductivity in Model (ft/day)	Final Parameter Zone Coefficient	Final Hydraulic Conductivity in Model (ft/day)
JCSD 23	261.65	1	95.90	1.526	146.34	0.716	68.66
		2					
		3					
		4					
		5					
JCSD 25	162.37	1	84.69	1.526	129.23	0.716	60.64
		2					
		3					
		4					
		5					
MMWC 06	62.40	1					
		2					
		3	41.31	0.396	17.33	1.259	52.00
		4					
		5	46.19	0.160	7.39	0.211	9.74
MVWD 31	15.41	1					
		2					
		3	43.80	0.396	17.33	1.259	55.14
		4					
		5	38.57	0.160	6.17	0.211	8.13
CDA I-13	120.71	1	89.97	1.530	137.66	1.779	160.09
		2					
		3					
		4					
		5					
CDA I-14	133.97	1	84.48	1.200	101.38	1.052	88.86
		2					
		3					
		4					
		5					
CDA I-15	171.49	1	89.97	1.200	107.97	1.052	94.63
		2					
		3					
		4					
		5					
CDA I-16[1]	16.42	1	66.06	0.340	22.46	0.249	16.45
		2					
		3					
		4					
		5					
CDA I-17	11.05	1	43.57	0.340	14.81	0.249	10.85
		2					
		3					
		4					
		5					
CDA I-18	21.01	1	53.92	0.340	18.33	0.249	13.43
		2					
		3					
		4					
		5					
CDA I-20	10.73	1	35.89	0.798	28.64	0.249	8.92
		2					
		3					
		4					
		5					
CDA I-21	18.19	1	53.17	0.798	42.43	0.249	13.21
		2					
		3					
		4					
		5					

Table 1 Comparison of Stress Test Derived Hydraulic Conductivities to Initial Hydraulic Conductivity Values Derived from a Lithology Model and Final Calibrated Values (f/d)

Well Name	Stress Test Based Hydraulic Conductivity Value Provided by THA or WEI (ft/day)	Model Layers Perforated by Well[2]	Initial Estimate of Hydraulic Conductivity from Lithology Model (ft/day)	Initial Parameter Zone Coefficient	Initial Hydraulic Conductivity in Model (ft/day)	Final Parameter Zone Coefficient	Final Hydraulic Conductivity in Model (ft/day)
CDA II-1	193.42	1	72.45	1.200	86.94	1.052	76.20
		2					
		3					
		4					
		5					
CDA II-2	399.65	1	80.98	1.200	97.17	1.052	85.17
		2					
		3					
		4					
		5					
CDA II-3	209.50	1	88.42	1.200	106.11	1.052	93.01
		2					
		3					
		4					
		5					
CDA II-4	200.57	1	92.52	1.200	111.02	1.052	97.31
		2					
		3					
		4					
		5					
CDA II-5	225.09	1	85.35	1.200	102.41	1.052	89.77
		2					
		3					
		4					
		5					
CDA II-6	289.10	1	85.35	1.200	102.41	1.052	89.77
		2					
		3					
		4					
		5					
CDA II-7	300.54	1	86.67	1.200	104.01	1.052	91.16
		2					
		3					
		4					
		5					
CDA II-8	288.89	1	91.18	1.200	109.41	1.052	95.90
		2					
		3					
		4					
		5					
CDA II-9	280.43	1	90.39	1.200	108.47	1.052	95.08
		2					
		3					
		4					
		5					
CDA II-10	623.52	1	71.47	1.200	85.77	1.052	75.17
		2					
		3	57.14	0.347	19.83	0.526	30.06
		4					
		5					
CDA II-11	460.56	1	91.18	1.530	139.50	1.779	162.23
		2					
		3	81.55	0.347	28.30	0.526	42.90
		4					
		5					

1 -- Stress test-based Kh estimated by WEI with Neuman formula for unconfined aquifers; all other stress test-based Kh estimated by others with Jacobs formula for confined aquifers

2 -- Layer 1 is unconfined and layers 2 through 5 are confined.

TECHNICAL MEMORANDUM

April 27, 2020

TO: Peter Kavounas

FROM: Mark Wildermuth, Eric Chiang, Wenbin Wang, Lauren Sather

RE: Review of and responses to Richard Rees and Kapo Coulibaly's questions in their April 15, 2020 memo: *Requests for Additional Information on the Proposed April 2, 2020 "2020 Safe Yield Recalculation Final Report" for Chino Basin*

The following responses were prepared to address Rees and Coulibaly's questions and requests for additional information on the 2020 CVM, as posed in their memo. Please contact Mark Wildermuth if you have any questions regarding the responses provided below.

Comment 1

Mr. Rees and M. Coulibaly: *The 2020 Model presents notably different values for deep infiltration plus applied water (hereafter, "DIPAW"), net recharge, and change in storage through the calibration period of the 2020 Model (i.e., 1977 through 2018) than were calculated by the 2013 Model. The cumulative change in storage calculated by the 2013 Model for the period 1977 to 2000 was negative 268,320 AF. The cumulative change in storage calculated by the 2020 Model for this same period is positive 155,628 AF. In other words, the difference between the cumulative change in storage values calculated by the two models for the same period is 423,836 AF. Please provide a detailed explanation for this difference, including at a minimum the information requested in items (a) and (b) below:*

(a) *Provide a plot of the cumulative change in storage since 1977 from Table 3-1, "Water Budget for Chino Basin," from the 2015 Report along with the cumulative change in storage since 1977 from Table 6-3, "Water Budget for the Chino Basin for the Calibration Period," in the 2020 Report*

(b) *Calculate change in storage based on measured groundwater levels and interpreted groundwater contours for 1977 and 2000 and compare the results with the cumulative change in storage values calculated by the 2013 and 2020 Models*

WEI response: WEI is involved in a parallel effort to assist Watermaster and the IEUA in assessing alternative TDS compliance metrics for recycled water use. In that effort, the watershed delineation was refined to comport more accurately with the groundwater basin boundaries, and land use delineations were updated to more accurately reflect water use and

salt loading. Since the prior Safe Yield recalculation, the number of hydrologic subareas has substantially increased to more accurately estimate precipitation/runoff processes and stormwater recharge. These improvements were carried forward into the 2020 CVM. In the 2020 CVM, the method for estimating reference ET (ET_0) across the watershed was improved from past reliance on the relationship between the Pomona CIMIS station ET_0 and Puddingstone reservoir evaporation to a new ET_0 model that is based on the empirical relationships of temperature and ET_0 measurements at the Pomona and Riverside CIMIS stations and using these relationships to estimate ET_0 temporally and spatially based on PRISM estimates of monthly temperature across the watershed. In the 2020 CVM, the method for estimating daily precipitation for each hydrologic subarea was improved from past reliance on interpolating daily precipitation at precipitation stations across the watershed using Thiessen polygons to the use of monthly precipitation estimates for each hydrologic subarea based on monthly PRISM estimates and converting those monthly estimates to daily precipitation estimates based on daily precipitation from nearby precipitation stations. As to precipitation, these improvements were made for the period prior to 2002. After 2002, daily precipitation estimates for the hydrologic subareas are based on NEXRAD estimates. The historical DIPAW estimate changes primarily result from these improvements in the data used in the R4 model.

Subsurface inflows from the Cucamonga and Riverside Basins are greater in the 2020 CVM relative to the 2013 Model: the former occurs because it was integrated directly into the 2020 CVM, and the latter occurs due to changes in the estimated hydraulic conductivity in the northeast domain 2020 CVM. Subsurface inflow from the mountain front areas increased due to the refinements in the R4 data for DIPAW (described above).

Streambed infiltration in the Santa Ana River also increased. This is, in part, due to converting the streamflow package in MODFLOW to SFR2, through the incorporation of updated channel geometry, and calibration.

The improvements incorporated into the 2020 CVM are consistent with the Court-ordered Safe Yield recalculation methodology.

In response to part (a) of this comment, we prepared Figure 1. Figure 1 shows the estimated time history of the cumulative change in storage for 2013 Model and the 2020 CVM. Note that rate of divergence between the 2020 CVM projected cumulative change in storage and the comparable 2013 Model projection is the greatest between 1978 and 1988 and that after 1988 the rate of divergence diminishes and two projections have virtually identical trends. This occurs because the updates to the 2020 CVM affect DIPAW more significantly for agricultural land uses with lower imperviousness. To better demonstrate this, we prepared Figure 1a, which compares the estimated time history of the cumulative change in storage for these models for the 2000 through 2018 period referenced to the year 2000. This corresponds to the period where the OBMP has been implemented and a period with significantly less agricultural land uses. The cumulative change in storage for the 2013 Model after 2011 is based on the

planning projection used to estimate net recharge and Safe Yield. Note that the cumulative change in storage is nearly identical.

In response to part (b), we did not develop the contour maps and compute the storage as requested. Our experience in the Chino Basin has demonstrated that most of the storage change occurs in the northern part of the basin and that the spatial distribution of wells, measurement data, well construction and temporal availability of water level observations can produce at best, very approximate estimates of the change-in-storage.

Using the suggested substitute storage change methodology involves selecting a representative groundwater level at wells for a specific point in time, plotting the groundwater level on a map, creating groundwater level contours and interpolation between the contours to estimate groundwater levels for each cell in the model grid. This would be done for pairs of years that bracket a period of interest (for example, the 1977 to 2000 as suggested). To undertake this effort, the difference in groundwater level for each model cell would be estimated for each pair of years. The calculated storage change would then be equal to the sum of the differences multiplied by the specific yield.

In short, you are suggesting a substitution of groundwater level data for modeling. We do not believe the suggested substitute methodology is appropriate in this instance. Here is why. Our view is that there are challenges in preparing these maps that could easily result in significant error in the estimation of storage change. Examples include: groundwater level measurement error, groundwater level data at a well may not exist at the time of interest (so no groundwater level is used or an estimated groundwater level is used in place of an actual measurement), spatial density of groundwater level measurements (most wells are far apart), spatial coverage (wells do not cover parts of the basin and extrapolation will be required), drawing contours of equal groundwater level (human error) and interpolation schemes introduce estimation errors between perfect point groundwater level estimates (which we don't have access to) and they can amplify errors with imperfect data (which we mostly have).

Using the calibrated model, we made a calculation to determine how much storage change would occur with a basin-wide increase/decrease of one foot based on the specific yield values estimated through calibration. The answer is 18,000 af.

For comparative context, simple errors in data selection, contouring and involved in the groundwater level approach could easily result in ranges of difference between the model-based estimates and the groundwater level estimate in the amount of 50,000 and 100,000 af. Consequently, the suggested effort is both work intensive and not likely to result in a material improvement or better understanding of change in storage.

Comment 2

Mr. Rees and M. Coulibaly: *Provide calculated net recharge as a column in Table 6-3.*

WEI response: See Table 1.

Comment 3

Mr. Rees and M. Coulibaly: *Section 7 does not discuss or compare the previous net recharge projections based on the 2013 Model and the net recharge values now calculated using the 2020 Model to have occurred during that period. (a) Provide a summary of previous estimates of annual net recharge values for the planning period as identified in the 2015 Report and compare these with the calculated values of net recharge based on actual data in the 2020 Report. (b) Were the differences in net recharge due solely to precipitation (c) Were some differences in net recharge attributable to differences between predicted and actual pumping or water imports during the period? (d) Does this comparison point to any ways to improve the forecasts or process for this and future safe yield recalculations?*

WEI response: Section 7 does compare planning projections of average net recharge for the planning period by decade for 2021 through 2050.

(a) Figure 2 shows the projected net recharge for the period 2011 through 2050 for the 2013 Model and the 2020 CVM.

(b) No.

(c) Yes. The pumping projections used in the 2020 Safe Yield recalculation are about 6,000 to 27,000 afy less for 2015 through 2035 compared to the pumping projections from the prior Safe Yield recalculation.

(d) Watermaster is initiating a process to develop improved pumping projections, replenishment projections, and other planning data for use in its planning work, and it has included this process in its fiscal 2020/21 budget.

Comment 4

Mr. Rees and M. Coulibaly: *For the 2020 Model, please provide the following information to help assess calibration:*

(a) A chart of residuals over time for the calibration period for the 2020 Model.

(b) The residual mean, the absolute residual mean, and the root mean square for the Chino Basin, Cucamonga Basin, and Six Basins, for model layers 1, 3, and 5 in each basin.

WEI response: (a) Please see Figure 3 “Residual time history from Chino Basin calibration”; (b) Please see Figure 4 “Layer 1 Residuals” for wells completed only in model layer 1. All other

wells are completed in multiple aquifers, so no maps were prepared. Table 3 contains the requested statistics for all groundwater basins in the 2020 CVM.

Comment 5

Mr. Rees and M. Coulibaly: *Figure 6-11 shows that Cucamonga Basin and Six Basins have all negative residuals, which implies that the 2020 Model over-predicts water levels in these areas. Please provide an explanation of the reason for this spatial bias and any implications for the Chino Basin.*

WEI response: Figure 6-11 shows only residual statistics for the Chino Basin and well locations in the other basins. This figure has been updated to include the mean residual for all of the basins; it is included herein as Figure 5. We acknowledge the appearance of the bias along the boundary of the Six Basins and Chino Basin. The wells in the Six Basins and Chino Basin near the San Jose Fault are perforated across multiple model layers, and the model-estimated groundwater level is influenced by the head in each layer. It is difficult to draw a definitive conclusion from the comparison of mean residual trends across the San Jose Fault. The slight over-prediction in the Six Basins and under-prediction in Chino Basin implied in Figure 5 suggests that subsurface inflow from the Six Basins to the Chino Basin could be higher than would occur if there was less or no bias. That said, the subsurface inflow from the Pomona Basins area of the Six Basins is a relatively small recharge component to the Chino Basin—about 2 percent of annual recharge to the Chino Basin in the projection period—and the effect of the apparent bias on subsurface inflow would be a fraction of that.

Comment 6

Mr. Rees and M. Coulibaly: *Similarly, the western portion of the Chino Basin shows mainly positive residuals (i.e., underprediction) except for the edges. Please provide an explanation for this bias and discuss any implications for the Chino Basin*

WEI response: In general, in this area, the model slightly under-predicts groundwater levels during the calibration period. There is no significant implication for net recharge estimates. The model could overestimate new land subsidence and pumping sustainability challenges in this area.

Comment 7

Mr. Rees and M. Coulibaly: *Please provide (a) maps of the location and values of the hydraulic conductivities and specific yields used for the initial distribution along with the (b) fitted semi-variogram model and (c) for the distribution of final hydraulic parameters (hydraulic conductivity and specific yield) after calibration.*

WEI response: (a) Figures 6 through 9 include location maps and parameter values of the point hydraulic conductivities and point specific yields used for their initial distribution. These maps were prepared at large scale so that their data is readable.

(b) Table 4 contains the parameters for the *Stable* semi-variogram model that was used to rasterize the model parameters. The formula of the stable semi-variogram model is as follows

$$\gamma(h) = b + C_0 \cdot \left(1 - e^{-\frac{h^s}{a}}\right)$$

Where

- b is the nugget of the variogram. This is the value of independent variable at the distance of zero. This is usually attributed to non-spatial variance.
- C_0 is the sill of the variogram, where it flattens out.
- h specifies the lag of separating distances that the dependent variable shall be calculated for.
- s is the smoothness or shape parameter. The smoothness parameter can shape a smooth or rough variogram function. A value of 0.5 will yield the exponential function, while a smoothness of +inf is exactly the Gaussian model. Typically, a value of 10 is close enough to Gaussian shape to simulate its behavior. Low values are "smooth," while larger values are considered to describe a "rough" random field.
- a is the range parameter and is calculated from the effective range r as $a = r/(3^{1/s})$.

(c) Please see Figures 3 through 8 in Watermaster's response to Thomas Harder's February 3, 2020 memo. They can be found here: https://cbwm.syncedtool.com/shares/folder/e83081106c3072/?folder_id=2396

Comment 8

Mr. Rees and M. Coulibaly: *Figure 6-2 indicates that the monthly discharge from Chino Creek at Shaefer Avenue is overestimated by the 2020 Model. Please explain this discrepancy and describe any effect it has on the overall model.*

WEI response: Strictly speaking, the graphic referred to characterizes the HSPF/R4 model calibration to the USGS gage and not the 2020 CVM calibration. The surface water model fits well for monthly discharges less than about 2,500 afm (88 percent of measured values) and overestimates discharges between 2,500 and 5,000 afm (8 percent of measured values). The same models are used to estimate stormwater recharge in the Upland, Montclair, and Brook's Street Basins, and their calibration performance does not indicate that stormwater recharge is overestimated. There is no significant impact from the overestimation of discharges between 2,500 and 5,000 afm on the net recharge and Safe Yield estimates.

Comment 9

Mr. Rees and M. Coulibaly: *Figure 6-7 a-b: the R^2 does not provide a comprehensive measure to assess the goodness of fit for calibration; the statistics requested in comment 4-b should be displayed on these graphs.*

(a) *Figure 6-7a seems to show that the model does not calibrate particularly well to the lower water levels (funnel shape residual distribution), even without the Chino Hills wells. Please explain this discrepancy and describe the effect it has on the overall model.*

(b) *Figure 6-7c, of simulated and predicted water levels in the Six Basins, shows that the model misses groundwater level trends, which are key metrics for assessing model calibration, especially for prediction of future changes. Please explain this mismatch and any effect the quality of calibration in Six Basins may have on predicted underflow to the Chino Basin or other aspects of the overall model.*

WEI response: We have included the requested statistics on Figures 6-7a-b; they are included herein as Figures 10 and 11, respectively, and for all basins in the 2020 CVM, listed in Table 3.

(a) This is not a discrepancy: it's a model artifact caused by the representativeness of available groundwater level measurements, the monthly time-step used in the model, and the complexity of the geology in the vicinity of the Chino and Chino Hills deep wells. Chino Hills' pumping at its deep wells is intermittent, and large drawdown occurs. It is very difficult to find representative groundwater levels at these wells to calibrate to when the wells are operated this way. The same artifacts were present in the 2013 Model calibration and the recently completed *Integrated Santa Ana River Model* developed for the Santa Ana River HCP. The occurrence of residuals at these wells does not impact the estimates of net recharge and Safe Yield.

(b) The Six Basins is geologically complex with many faults that act as barriers and divide the Six Basins into several smaller basins. The Six Basins is highly reactive in wet years, and the Six Basins model's groundwater level prediction in and immediately following these wet years in the northern part of the Six Basins (i.e., the Claremont Basin) is muted compared to measured groundwater levels. Even with these complexities and larger residuals, the Six Basins model calibration achieves an R^2 of 0.95. Review of Figure 5 shows that the bias in the Claremont Basin is the opposite of the bias in the Pomona Basin and suggests that 2020 CVM estimated inflow from the Claremont Basin could be underestimated (the opposite of what is implied for the Pomona Basin area as described above). That said, the subsurface inflow from the Claremont Basin area of the Six Basins is a relatively small recharge component to the Chino Basin—about 1 percent of annual recharge to the Chino Basin in the projection period—and the effect of the apparent bias on subsurface inflow would be a fraction of that.

Comment 10

Mr. Rees and M. Coulibaly: *The DIPAW approach used is the moving average approach, which does not keep track of storage in the vadose zone. Please provide an explanation of how the vadose storage shown on Figure 6- 12a is estimated.*

WEI response: The continuity equation was used to estimate vadose zone storage in parallel with the moving average.

Comment 11

Mr. Rees and M. Coulibaly: *DIPAW is made of natural recharge (rainfall) and applied water (return flow from irrigation). (a) Please provide a time series of these different components. (b) Given the long lag time, it is assumed that DIPAW values in 1978 are impacted by flows and climate as far back as 1948, so data for at least 30 years preceding the calibration period should also be provided.*

WEI response: (a) The R4 model rootzone module does not distinguish which water is discharged from the rootzone, so we cannot furnish these to you as separate components. (b) It was. Vadose zone initiation began in 1943. See Table 2.

Figure 1 Comparison of the Estimate Cumulative Change in Storage for the 2013Model and 2020 CVM

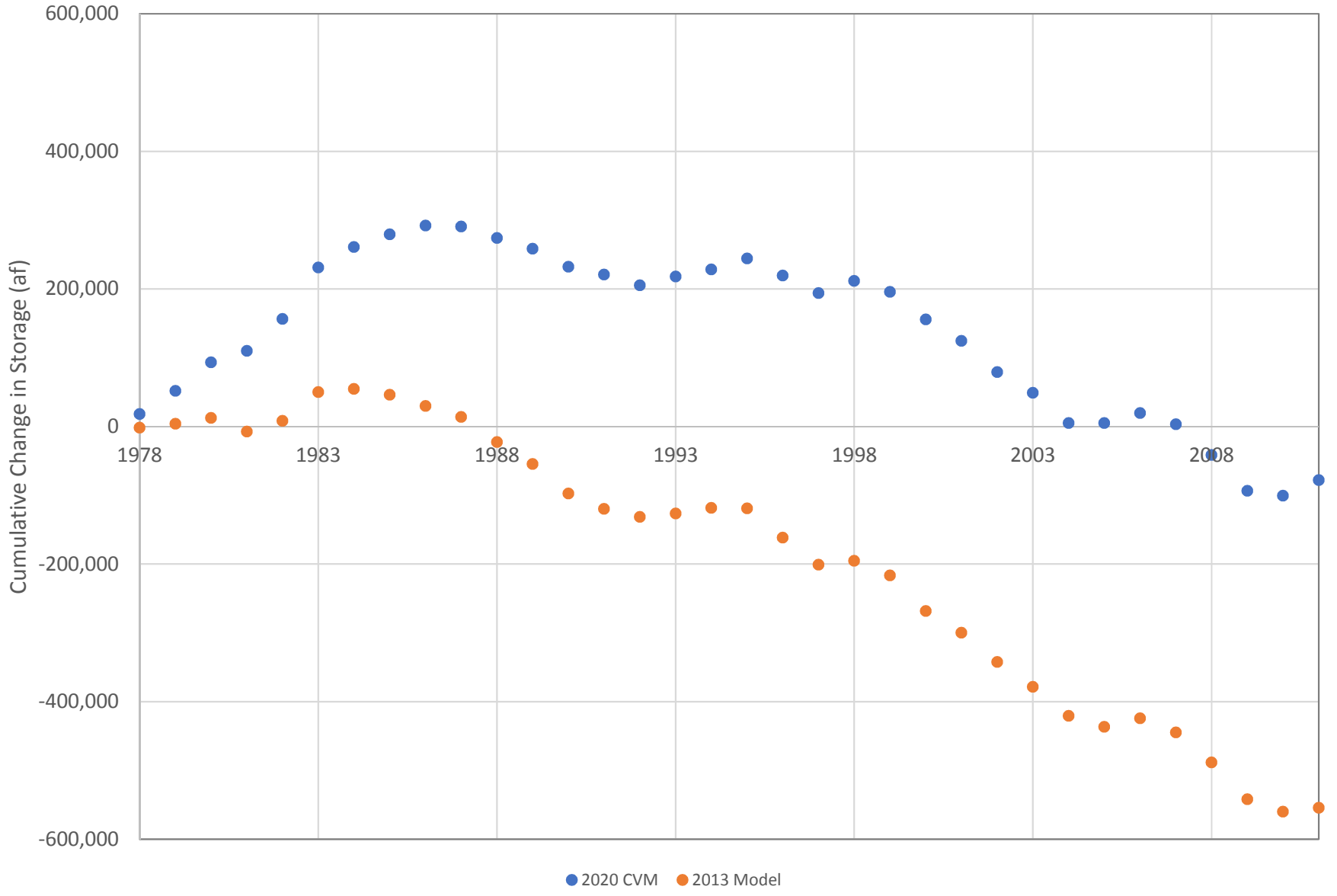

Figure 1a Comparison of the Estimate Cumulative Change in Storage for the 2013 Model and 2020 CVM for the OBMP Period and Referenced to July 1, 2000

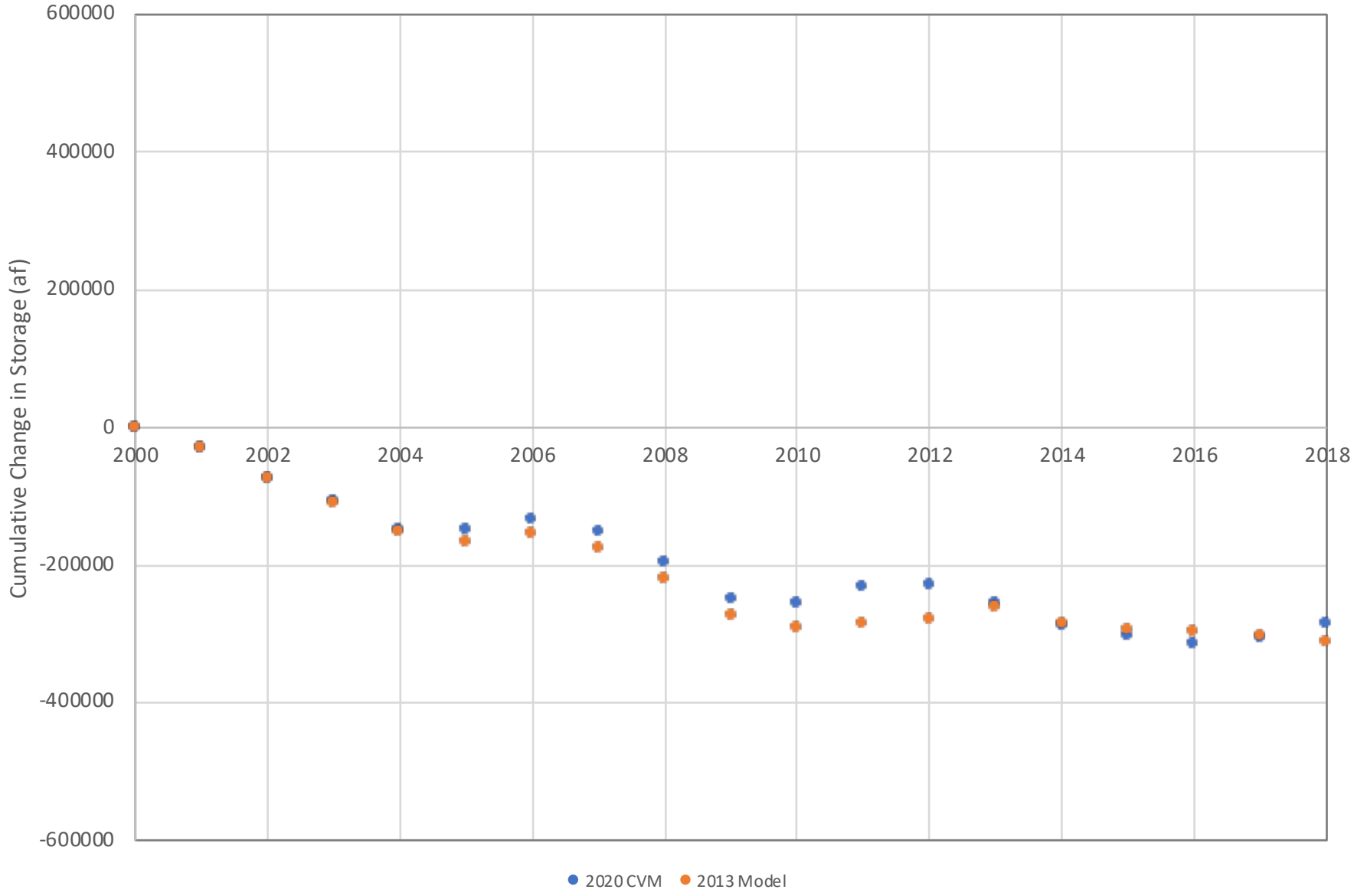

Figure 2 Comparison of the Estimate Net Recharge for the 2013 and 2020 Chino Basin Models for the Period 2011 through 2050

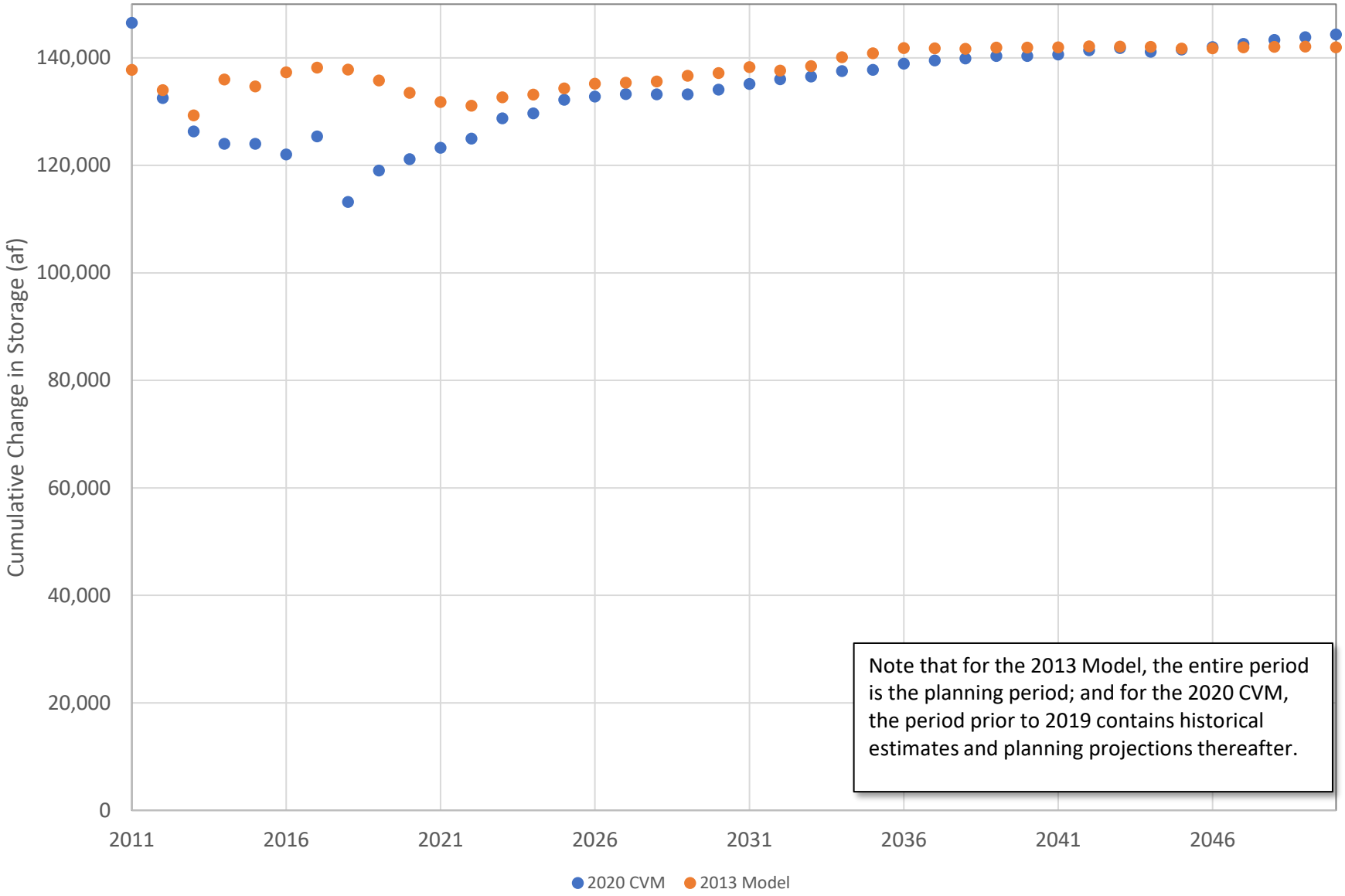

Figure 3. Residual Time Series in Chino Basin

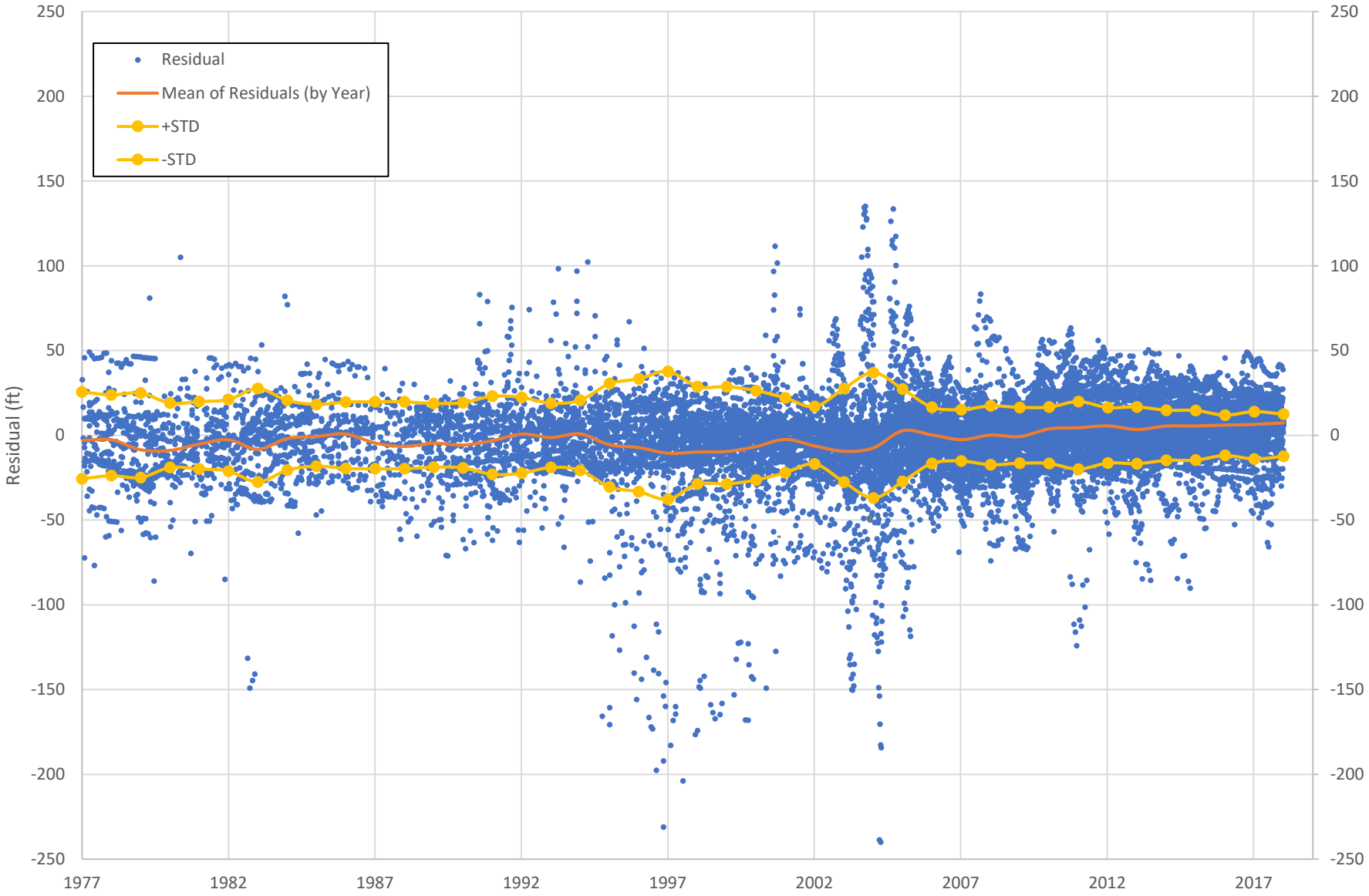

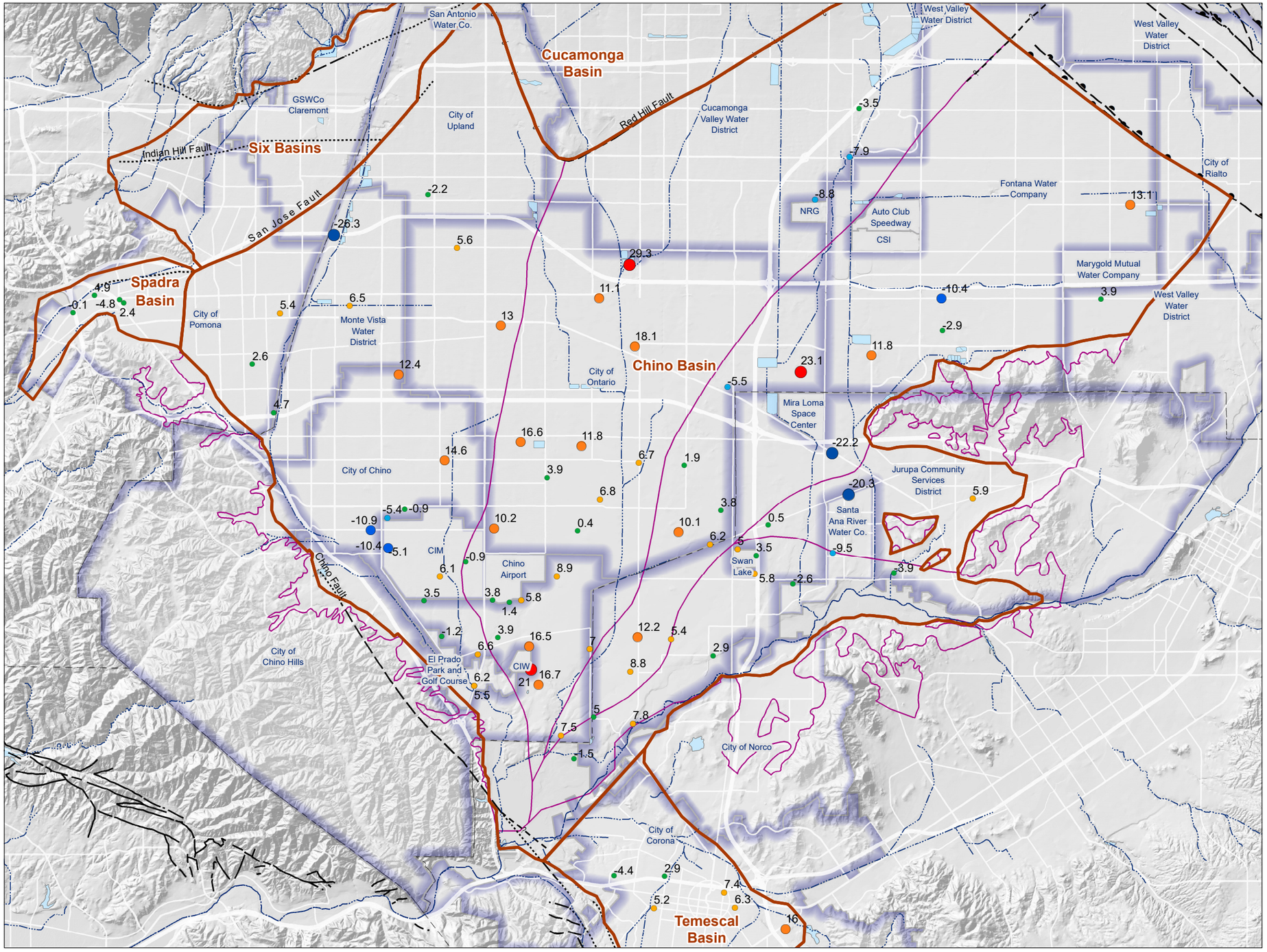

Mean Residual Error

- < -30
- -30 - -20
- -20 - -10
- -10 - -5
- -5 - 5
- 5 - 10
- 10 - 20
- 20 - 30
- >30

Streams & Flood Control Channels

Flood Control & Conservation Basins

Water Service Area

OBMP Management Zones

Faults

- Location Certain
- Location Approximate
- Approximate Location of Groundwater Barrier
- Location Concealed
- Location Uncertain

Prepared by:

WEI
Wildermuth Environmental, Inc.

Author: LS
Date: 4/22/2020
File: Figure_4_Mean_Residuals_L1only_v2.mxd

0 1 2 3 4 5 Miles
0 2 4 6 8 Km

Prepared for:

2020 Safe Yield Recalculation

Chino Basin Watermaster
Partners in Basin Management

Layer 1 Residuals
Chino Basin

Figure 4

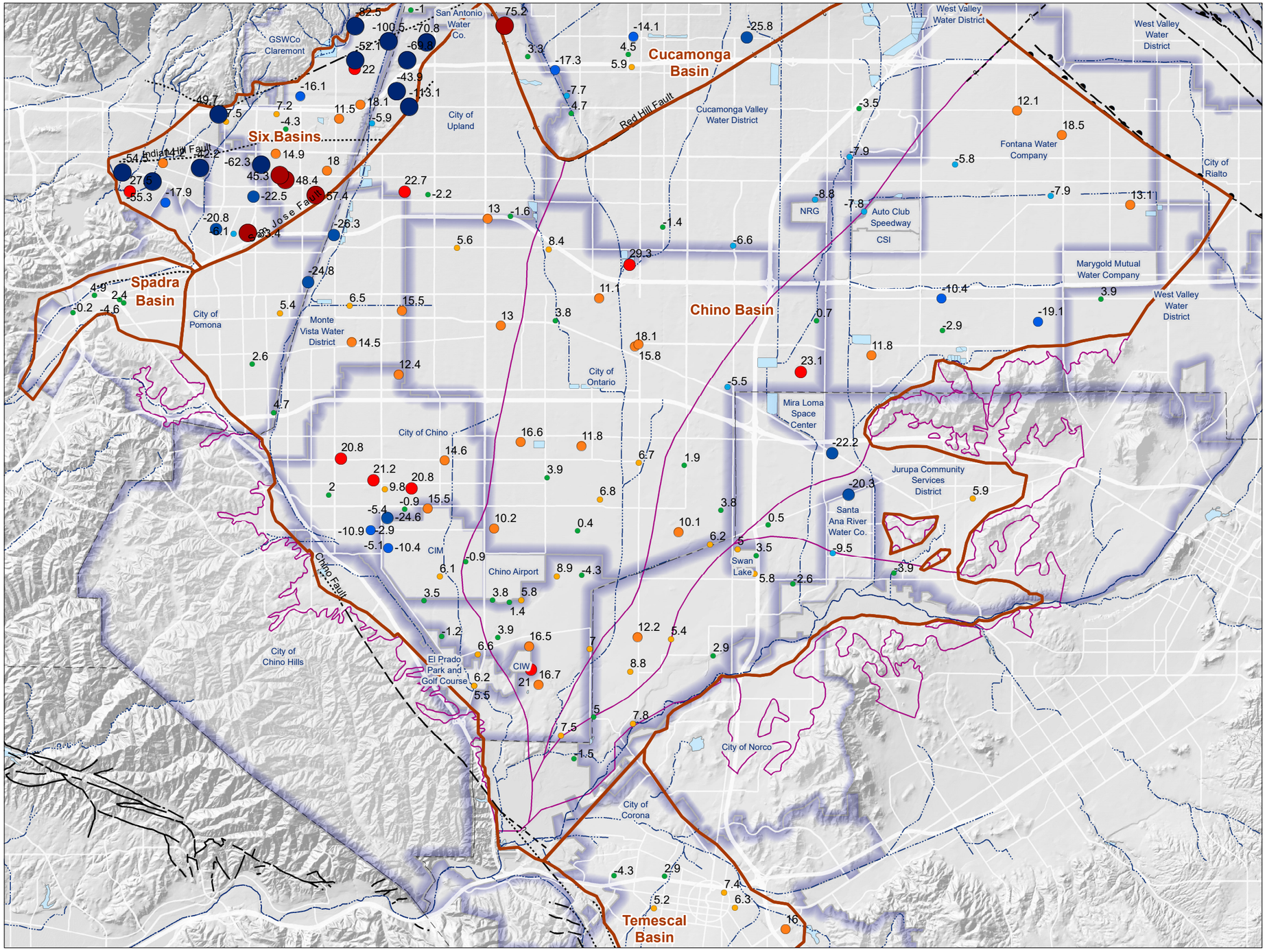

Mean Residual Error

- < -30
- -30 - -20
- -20 - -10
- -10 - -5
- -5 - 5
- 5 - 10
- 10 - 20
- 20 - 30
- >30

Streams & Flood Control Channels

Flood Control & Conservation Basins

Water Service Area

OBMP Management Zones

Faults

- Location Certain
- Location Approximate
- Approximate Location of Groundwater Barrier
- Location Concealed
- Location Uncertain

Prepared by:

WEI
Wildermuth Environmental, Inc.

Author: LS
Date: 4/21/2020
File: Figure 6-11 Mean Residua_Response toRees.mxd

0 1 2 3 4 5 Miles
0 2 4 6 8 Km

Prepared for:

2020 Safe Yield Recalculation

Chino Basin Watermaster — Partners in Basin Management

Mean Residual Error of Calibration Wells -- Updated

Figure 5

117°40'0"W

34°0'0"N

San Gabriel Mountains

Cucamonga Fault Zone

West Cucamonga Barrier

Red Hill-Etiwanda Avenue Fault

Barrier J

Rialto-Colton Basin

Indian Hill Fault

Indian Hill

Intermediate Fault

San Jose Fault

San Jose Hills

San Antonio Ck

Holt Blvd

Haven Ave

Archibald Ave

Etiwanda Ave

Day Ck

San Sevaine Ck

Foothill Blvd

Riverside Ave

Bloomington Divide

Euclid Ave

Central Ave

Central Ave Fault

Riverside Dr

Mission Blvd

Cucamonga Ck

Jurupa Mountains

Puente Hills

Riley Barrier

Chino Ck

Chino Fault

Chino Hills

San Bernardino County

Orange County

Bellegrave Ave

Limonite Ave

Santa Ana River

La Sierra Hills

Van Buren Blvd

Victoria Ave

Arlington Basin

210

71

60

91

117°40'0"W

34°0'0"N

Initial Estimated Horizontal Hydraulic Conductivity

Layer 1 (ft/day)

- 3 - 21
- 22 - 40
- 41 - 58
- 59 - 76
- 77 - 95
- 96 - 113
- 114 - 132
- 133 - 150
- 151 - 168
- 169 - 187

Borehole with Lithologic Data used to Estimate Horizontal Hydraulic Conductivity

Chino Valley Basins Groundwater Flow Model Boundary

Streams & Flood Control Channels

Flood Control & Conservation Basins

Geology

Water-Bearing Sediments

Quaternary Alluvium

Consolidated Bedrock

Undifferentiated Pre-Tertiary to Early Pleistocene Igneous, Metamorphic, and Sedimentary Rocks

Fault (solid where accurately located; dashed where approximately located or inferred; dotted where concealed)

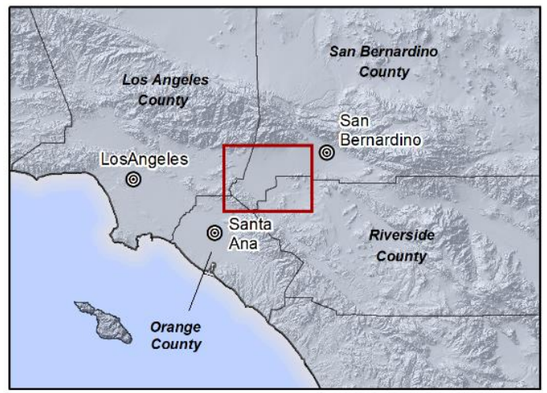

Produced by:

WEI Wildermuth Environmental, Inc.

Author: LJS

Date: 5/8/2020

Document Name: Figure_6-8_Kh_11x17

0 1 2 3 4 5 Miles

0 2 4 6 8 KM

Prepared for:

2020 Safe Yield Recalculation

Chino Basin Watermaster – Partners in Basin Management

Layer 1 Initial and Pre-calibrated Horizontal Hydraulic Conductivity Based on Borehole Lithology and Lithologic Modeling

Figure 6

117°40'0"W

34°0'0"N

San Gabriel Mountains

Cucamonga Fault Zone

West Cucamonga Barrier

Red Hill-Etiwanda Avenue Fault

Barrier J

Rialto-Colton Basin

Indian Hill Fault

Indian Hill

Intermediate Fault

San Jose Fault

San Jose Hills

San Antonio Ck

Holt Blvd

Haven Ave

Archibald Ave

Etiwanda Ave

Day Ck

San Sevaine Ck

Foothill Blvd

Riverside Ave

Bloomington Divide

Euclid Ave

Central Ave

Central Ave Fault

Mission Blvd

Cucamonga Ck

Riverside Dr

Jurupa Mountains

Puente Hills

Riley Barrier

Bellegrave Ave

Limonite Ave

Mission Blvd

Santa Ana River

Chino Ck

Chino Fault

Chino Hills

San Bernardino County

Orange County

La Sierra Hills

Van Buren Blvd

Victoria Ave

Arlington Basin

210

71

60

91

117°40'0"W

34°0'0"N

Initial Estimated Horizontal Hydraulic Conductivity
Layer 3 (ft/day)

- 3 - 22
- 23 - 41
- 42 - 60
- 61 - 79
- 80 - 99
- 100 - 118
- 119 - 137
- 138 - 156
- 157 - 175
- 176 - 195

Borehole with Lithologic Data used to Estimate Horizontal Hydraulic Conductivity

Chino Valley Basins Groundwater Flow Model Boundary

Streams & Flood Control Channels

Flood Control & Conservation Basins

Geology

Water-Bearing Sediments

Quaternary Alluvium

Consolidated Bedrock

Undifferentiated Pre-Tertiary to Early Pleistocene Igneous, Metamorphic, and Sedimentary Rocks

Fault (solid where accurately located; dashed where approximately located or inferred; dotted where concealed)

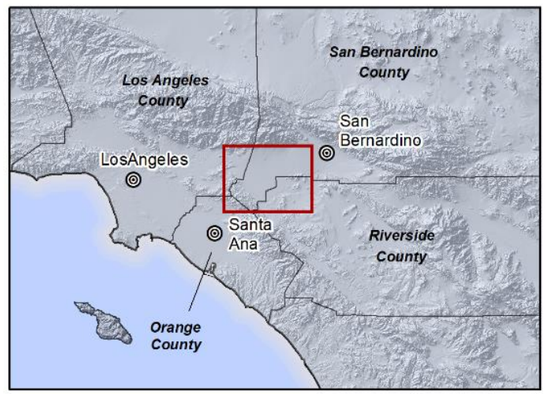

Produced by:

WEI
WILDERMUTH ENVIRONMENTAL, INC.

Author: LJS
Date: 5/8/2020
Document Name: Figure_6-8_Kh_11x17

0 1 2 3 4 5 Miles
0 2 4 6 8 KM

Prepared for:

2020 Safe Yield Recalculation

CHINO BASIN WATERMASTER
Partners in Basin Management

Layer 3 Initial and Pre-calibrated Horizontal Hydraulic Conductivity Based on Borehole Lithology and Lithologic Modeling

Figure 7

117°40'0"W

34°0'0"N

San Gabriel Mountains

Cucamonga Fault Zone

West Cucamonga Barrier

Red Hill-Etiwanda Avenue Fault

Barrier J

Rialto-Colton Basin

Riverside Ave

Sierra Ave

Indian Hill

Indian Hill Fault

Intermediate Fault

San Jose Fault

n Jose Hills

San Antonio Ck

Archibald Ave

Etiwanda Ave

Day Ck

San Sevaine Ck

Haven Ave

Foothill Blvd

Holt Blvd

Euclid Ave

Central Ave

Central Ave Fault

Riverside Dr

Mission Blvd

Cucamonga Ck

Bloomington Divide

Jurupa Mountains

Puente Hills

Riley Barrier

Bellegrave Ave

Limonite Ave

Santa Ana River

Chino Ck

Chino Fault

Chino Hills

San Bernardino County

Orange County

La Sierra Hills

Van Buren Blvd

Victoria Ave

Arlington Basin

210

71

60

91

Initial Estimated Horizontal Hydraulic Conductivity

Layer 5 (ft/day)

- 3 - 24
- 25 - 45
- 46 - 65
- 66 - 86
- 87 - 107
- 108 - 128
- 129 - 149
- 150 - 170
- 171 - 190
- 191 - 211

Borehole with Lithologic Data used to Estimate Horizontal Hydraulic Conductivity

Chino Valley Basins Groundwater Flow Model Boundary

Streams & Flood Control Channels

Flood Control & Conservation Basins

Geology

Water-Bearing Sediments

Quaternary Alluvium

Consolidated Bedrock

Undifferentiated Pre-Tertiary to Early Pleistocene Igneous, Metamorphic, and Sedimentary Rocks

Fault (solid where accurately located; dashed where approximately located or inferred; dotted where concealed)

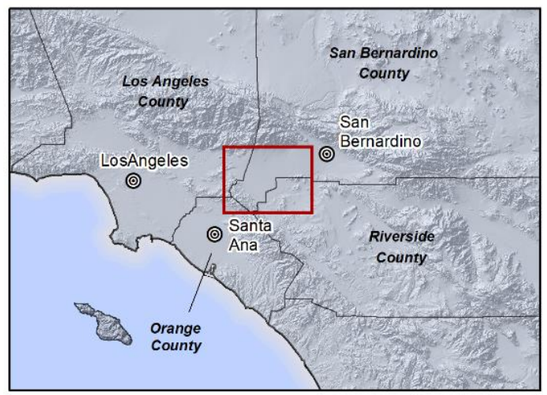

Produced by:

WEI
Wildermuth Environmental, Inc.

Author: LJS
Date: 5/8/2020
Document Name: Figure_6-8_Kh_11x17

0 1 2 3 4 5 Miles

0 2 4 6 8 KM

Prepared for:

2020 Safe Yield Recalculation

Chino Basin Watermaster — Partners in Basin Management

Layer 5 Initial and Pre-calibrated Horizontal Hydraulic Conductivity Based on Borehole Lithology and Lithologic Modeling

Figure 8

117°40'0"W

34°0'0"N

San Gabriel Mountains

Cucamonga Fault Zone

West Cucamonga Barrier

Red Hill-Etiwanda Avenue Fault

Barrier J

Rialto-Colton Basin

Indian Hill Fault

Indian Hill

San Jose Fault

Foothill Blvd

Archibald Ave

Etiwanda Ave

Day Ck

San Sevaine Ck

Riverside Ave

Bloomington Divide

San Jose Hills

San Antonio Ck

Holt Blvd

Haven Ave

Euclid Ave

Mission Blvd

Central Ave Fault

Central Ave

Cucamonga Ck

Riverside Dr

Jurupa Mountains

Puente Hills

Riley Barrier

Bellegrave Ave

Chino Ck

Chino Fault

Chino Hills

San Bernardino County

Orange County

Limonite Ave

Santa Ana River

La Sierra Hills

Van Buren Blvd

Victoria Ave

Arlington Basin

210

71

60

91

117°40'0"W

Initial Estimated Specific Yield
Layer 1

- 0.001 - 0.025
- 0.026 - 0.05
- 0.051 - 0.075
- 0.076 - 0.1
- 0.101 - 0.125
- 0.126 - 0.15
- 0.151 - 0.175
- 0.176 - 0.199
- 0.2 - 0.224
- 0.225 - 0.249

Borehole with Lithologic Data used to Estimate Specific Yield

Chino Valley Basins Groundwater Flow Model Boundary

Streams & Flood Control Channels

Flood Control & Conservation Basins

Geology

Water-Bearing Sediments

Quaternary Alluvium

Consolidated Bedrock

Undifferentiated Pre-Tertiary to Early Pleistocene Igneous, Metamorphic, and Sedimentary Rocks

Fault (solid where accurately located; dashed where approximately located or inferred; dotted where concealed)

Produced by:

WEI
Wildermuth Environmental, Inc.

Author: LJS
Date: 5/8/2020
Document Name: Figure_6-8_Kh_11x17

0 1 2 3 4 5 Miles
0 2 4 6 8 KM

Prepared for:

2020 Safe Yield Recalculation

Chino Basin Watermaster
Partners in Basin Management

Layer 1 Initial and Pre-calibrated Specific Yield Based on Borehole Lithology and Lithologic Modeling

Figure 9

Figure 10
Comparison of Simulated and Measured Water Levels in the Wells of Chino Basin

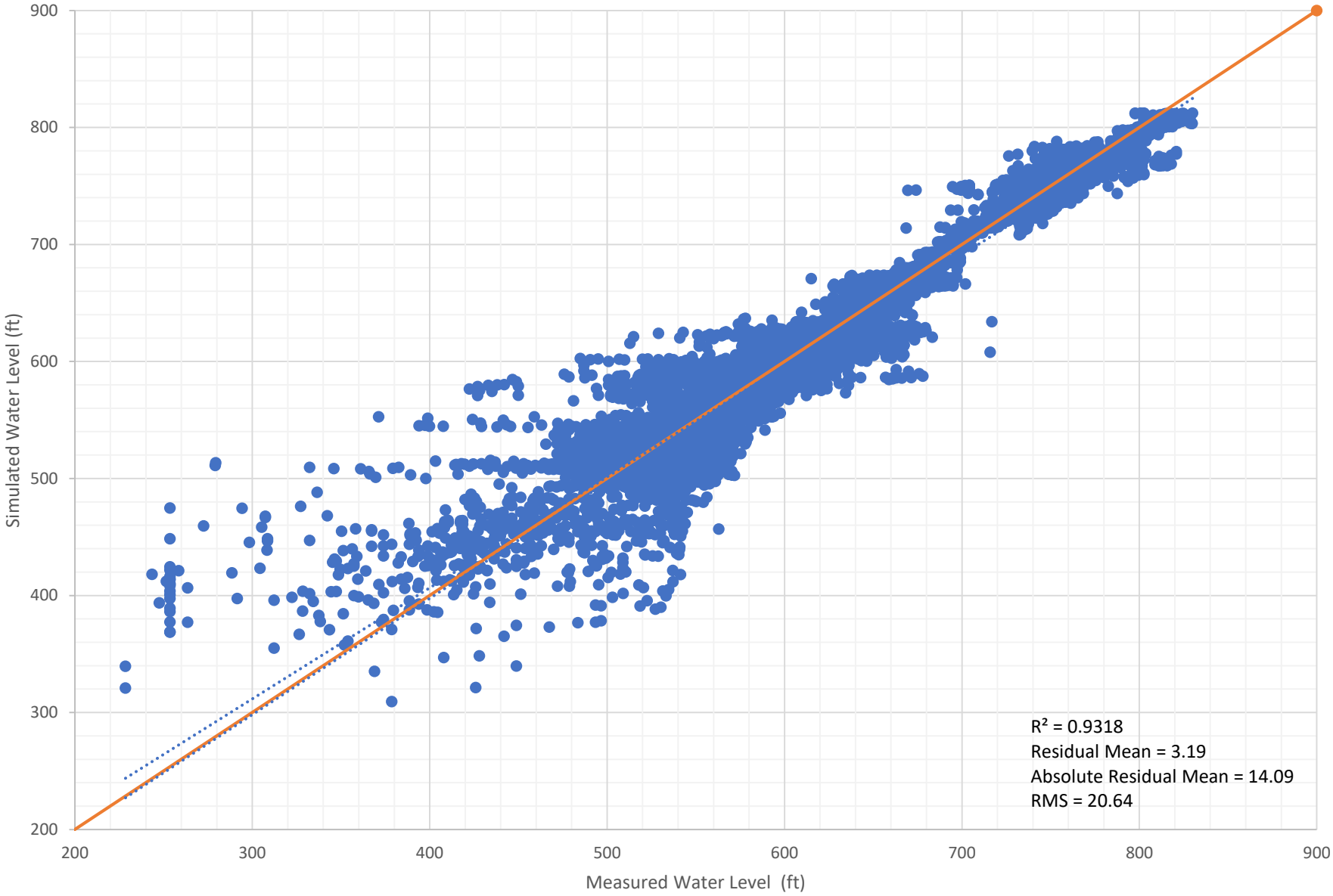

Figure 11
Comparison of Simulated and Measured Water Levels in the Wells of Cucamonga Basin

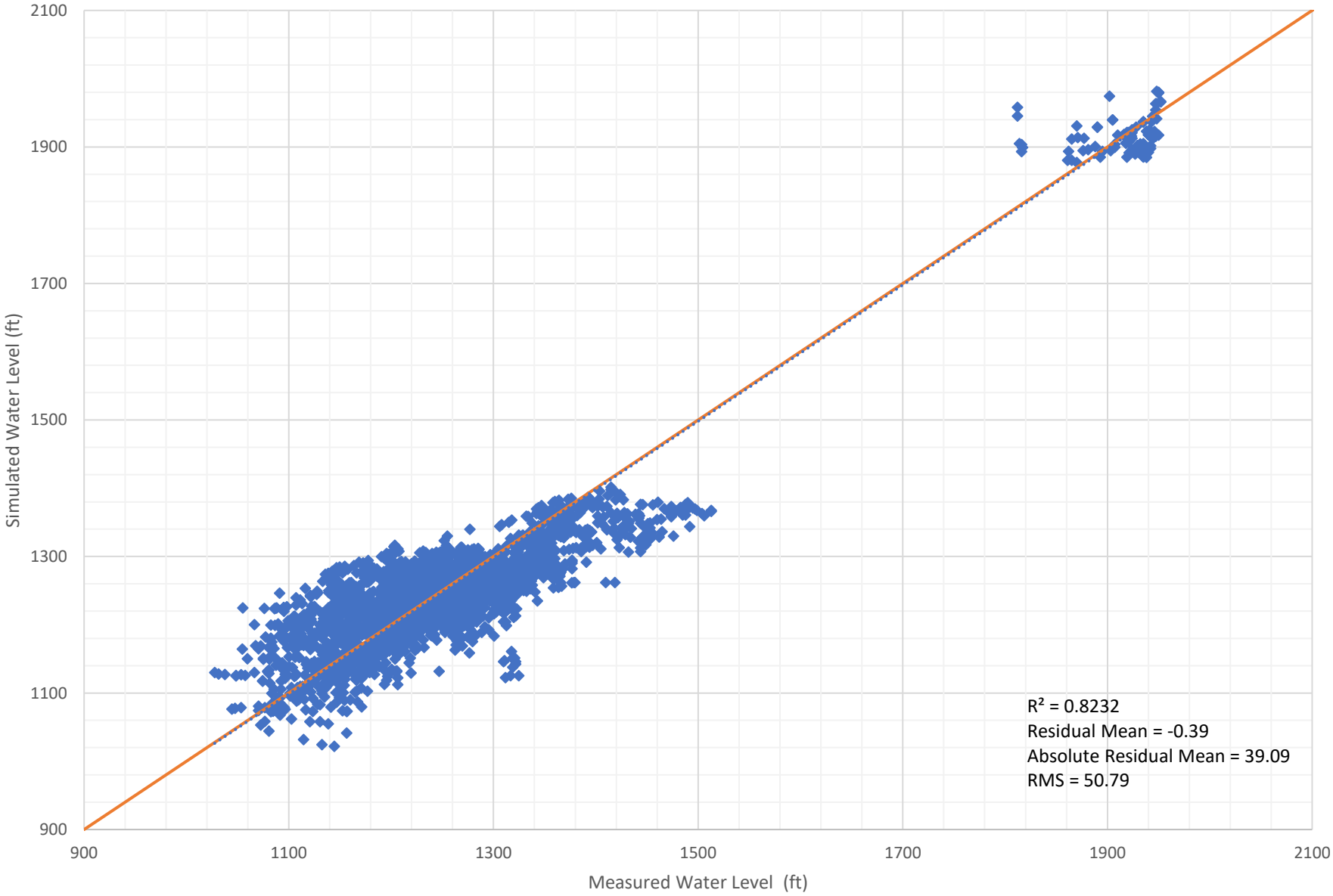

Table 1 Water Budget for the Chino Basin for the Calibration Period (Based on Table 6-3 in Draft Final Report)

Fiscal Year	Recharge														Discharge						Change in Storage		
	Subsurface Inflow							Deep Infiltration of Precipitation and Applied Water	Santa Ana River Streambed Infiltration	Streambed Infiltration from Santa Ana River Tributaries	Managed Aquifer Recharge			Total Recharge	Groundwater Pumping			Riparian Veg ET	Rising Groundwater	Total Discharge	Annual	Cumulative	Net Recharge
	Bloomington Divide	Chino/Puente Hills, Jurupa Hills, and Rialto Basin	Net Temescal Basin	Pomona Basin	Claremont Basin	Cucamonga Basin	Spadra Basin				Storm Water	Recycled Water	Imported Water		CDA Pumping	Overlying Non Ag and Appropriative Pools	Overlying Agricultural Pool						
1978	11,404	8,811	2,502	2,278	2,277	12,032	961	117,423	37,046	24,456	5,183	3,175	6,952	234,499	0	64,771	120,072	16,951	14,495	216,289	18,210	18,210	192,927
1979	11,002	9,659	3,101	2,867	2,574	11,628	576	122,211	33,871	15,620	2,951	3,049	28,347	247,456	0	65,008	118,922	17,257	12,619	213,805	33,651	51,861	186,185
1980	12,497	10,790	3,420	2,922	2,578	11,567	498	126,236	38,002	20,253	4,662	3,232	16,537	253,195	0	69,503	110,885	16,404	14,897	211,689	41,505	93,366	202,125
1981	13,071	10,955	4,216	3,024	2,585	11,537	476	126,479	30,545	7,647	1,219	3,451	20,850	236,055	0	72,927	116,470	17,194	13,035	219,626	16,429	109,795	181,525
1982	13,337	11,289	4,987	2,892	2,470	11,401	480	126,714	33,792	11,112	3,096	3,726	21,641	246,937	0	68,404	101,624	16,868	13,389	200,284	46,652	156,447	191,313
1983	13,316	10,685	5,161	3,008	2,597	11,552	496	132,273	35,436	18,011	6,703	3,873	27,590	270,704	0	67,259	94,508	16,139	17,899	195,805	74,898	231,346	205,202
1984	14,378	9,829	6,112	3,222	2,752	11,871	511	133,497	29,048	8,724	2,472	982	22,400	245,799	0	74,726	107,238	16,642	17,412	216,018	29,782	261,127	188,363
1985	13,577	8,729	6,343	3,085	2,561	11,887	526	128,408	30,446	6,257	2,032	0	20,782	234,631	0	79,626	105,444	16,810	14,364	216,243	18,388	279,515	182,676
1986	12,428	9,439	6,192	3,007	2,456	11,668	549	127,728	33,461	6,062	2,903	0	18,327	234,221	0	83,822	105,254	16,877	15,805	221,757	12,463	291,979	183,212
1987	11,951	8,844	6,493	2,944	2,379	11,309	553	121,909	32,772	2,874	1,789	0	19,938	223,754	0	88,675	104,829	17,090	14,383	224,976	-1,222	290,756	172,344
1988	11,385	7,674	5,839	2,790	2,274	10,771	538	122,069	34,246	2,925	2,641	0	2,485	205,637	0	94,222	95,264	17,187	15,603	222,276	-16,640	274,117	170,361
1989	11,408	7,528	5,339	2,681	2,214	10,364	529	120,836	31,310	1,422	2,393	0	7,332	203,357	0	97,218	89,511	17,407	14,798	218,935	-15,578	258,539	163,820
1990	11,788	7,121	4,579	2,536	2,124	10,448	509	115,495	31,487	433	1,430	0	0	187,950	0	98,914	83,775	17,482	13,942	214,113	-26,163	232,376	156,526
1991	12,630	6,656	4,009	2,421	2,092	10,335	474	113,633	33,477	712	2,198	0	3,634	192,271	0	88,986	83,073	17,525	14,171	203,756	-11,484	220,891	156,941
1992	13,286	7,250	3,737	2,438	2,136	10,393	442	112,979	34,141	1,028	3,598	0	5,568	196,997	0	102,664	77,336	17,736	14,905	212,640	-15,643	205,248	158,788
1993	13,611	8,300	2,863	2,725	2,434	10,588	423	116,794	37,980	2,239	6,619	0	14,224	218,800	0	88,040	83,284	17,404	17,162	205,889	12,910	218,159	170,010
1994	13,637	8,223	3,621	2,994	2,560	10,871	425	117,935	30,748	650	1,486	0	16,448	209,597	0	93,564	72,115	18,155	15,589	199,423	10,174	228,333	159,405
1995	13,478	9,217	2,488	2,899	2,507	10,967	428	119,075	35,361	1,538	4,662	0	10,375	212,995	0	98,173	62,171	17,711	19,136	197,191	15,803	244,136	165,773
1996	13,289	9,146	3,546	3,017	2,560	11,015	455	117,398	29,441	709	2,425	0	82	193,085	0	109,609	71,220	18,429	18,553	217,811	-24,726	219,410	156,021
1997	13,292	9,072	3,290	2,829	2,430	10,883	481	116,836	30,483	1,007	3,305	0	16	193,925	0	112,998	68,968	18,564	18,917	219,448	-25,523	193,887	156,427
1998	13,650	8,754	2,402	2,803	2,417	10,727	503	117,046	33,821	1,637	5,780	0	8,352	207,895	0	104,141	45,302	18,238	22,456	190,138	17,757	211,644	158,848
1999	13,956	8,514	3,516	2,936	2,489	10,756	494	115,042	26,381	519	1,007	0	5,839	191,449	0	118,738	46,730	19,035	22,794	207,298	-15,849	195,795	143,780
2000	14,451	7,890	2,858	2,707	2,341	10,563	508	109,843	27,081	499	1,985	507	997	182,232	523	133,086	46,538	18,938	23,315	222,400	-40,168	155,628	138,476
2001	14,556	7,970	3,132	2,532	2,254	10,223	525	107,823	25,419	598	3,162	500	6,538	185,230	9,470	120,396	41,429	18,717	26,464	216,476	-31,245	124,382	133,011
2002	15,177	7,242	3,565	2,467	2,206	10,028	517	102,792	25,922	230	1,148	505	6,493	178,292	10,173	129,760	38,650	18,472	26,544	223,599	-45,307	79,075	126,279
2003	15,747	6,518	2,932	2,377	2,145	9,868	504	102,305	28,672	859	6,284	185	6,548	184,945	10,322	123,471	36,507	18,157	26,630	215,087	-30,142	48,934	133,425
2004	16,088	6,780	1,994	2,407	2,123	9,860	492	99,010	27,465	536	3,357	49	7,607	177,768	10,480	128,548	36,809	18,069	27,669	221,574	-43,807	5,127	124,374
2005	14,346	7,918	721	2,643	2,336	9,816	481	99,647	30,922	5,917	17,648	158	12,259	204,813	10,595	112,943	34,503	17,178	29,844	205,064	-251	4,876	145,373
2006	14,568	7,648	1,891	3,152	2,571	9,897	467	99,823	30,439	1,806	12,940	1,303	34,567	221,073	19,819	113,553	30,812	17,561	24,576	206,321	14,752	19,627	143,065
2007	15,150	7,607	1,268	2,911	2,413	9,826	412	96,008	29,276	79	4,745	2,993	32,960	205,647	28,529	123,695	29,919	18,276	21,441	221,859	-16,212	3,415	129,978
2008	15,044	7,346	1,173	2,627	2,240	9,842	384	93,275	31,703	1,530	10,205	2,340	0	177,709	30,116	127,696	26,280	18,358	20,003	222,453	-44,744	-41,329	137,008
2009	15,271	7,363	696	2,509	2,178	9,950	414	91,489	33,318	839	7,512	2,684	0	174,220	28,456	137,345	23,386	18,561	18,475	226,223	-52,003	-93,331	134,500
2010	15,584	6,402	562	2,448	2,167	9,809	441	88,512	35,285	1,939	14,273	7,210	5,000	189,632	28,964	108,983	22,038	18,686	18,067	196,739	-7,107	-100,438	140,669
2011	15,960	6,889	557	2,601	2,299	9,891	452	88,763	36,213	3,358	17,052	8,065	9,465	201,564	28,941	94,413	18,042	18,739	18,765	178,901	22,663	-77,775	146,530
2012	15,577	6,971	1,397	2,713	2,317	9,820	441	84,009	34,463	463	9,271	8,634	22,560	198,637	28,230	108,501	22,412	19,282	15,649	194,074	4,563	-73,212	132,511
2013	15,144	6,651	1,516	2,676	2,203	9,748	426	80,130	33,536	243	5,271	10,479	0	168,023	27,380	111,748	24,074	17,348	13,871	194,421	-26,398	-99,610	126,325
2014	15,067	6,355	1,371	2,645	2,144	9,548	440	78,395	34,301	241	4,299	13,593	795	169,195	29,626	118,849	22,131	17,426	13,348	201,380	-32,185	-131,795	124,032
2015	15,230	5,760	1,217	2,547	2,096	8,721	458	75,817	34,907	421	8,001	10,840	0	166,014	30,022	104,317	17,552	17,580	13,585	183,056	-17,042	-148,837	124,009
2016	15,716	5,015	1,057	2,498	2,062	7,809	449	73,547	36,134	476	9,236	13,222	0	167,221	28,191	101,301	16,908	17,824	14,147	178,371	-11,150	-159,988	122,028
2017	15,967	5,587	1,529	2,462	2,056	8,311	423	72,874	35,805	1,920	11,575	13,934	13,150	185,593	28,284	98,960	16,191	17,869	15,261	176,565	9,028	-150,960	125,379
2018	15,711	5,385	2,306	2,510	2,072	8,041	388	69,532	32,664	2,165	4,494	13,212	35,621	194,101	30,088	93,904	16,776	18,147	13,914	172,828	21,272	-129,687	113,206
Statistics for the Calibration Period 1978 through 2018																							
Total	572,725	325,781	125,499	111,751	95,688	426,142	19,947	4,381,613	1,326,822	159,955	223,013	131,900	472,281	8,373,116	418,208	4,133,457	2,484,952	728,293	737,893	8,502,803	-129,687		6,302,749
Percent	6.8%	3.9%	1.5%	1.3%	1.1%	5.1%	0.2%	52.3%	15.8%	1.9%	2.7%	1.6%	5.6%	100.0%	4.9%	48.6%	29.2%	8.6%	8.7%	100.0%			
Average	13,969	7,946	3,061	2,726	2,334	10,394	487	106,869	32,362	3,901	5,439	3,217	11,519	204,222	10,200	100,816	60,609	17,763	17,997	207,385	-3,163		153,726
Median	13,956	7,674	2,932	2,707	2,317	10,393	480	113,633	33,318	1,530	4,299	507	7,607	198,637	0	101,301	46,730	17,711	15,805	212,640	-7,107		156,021
Maximum	16,088	11,289	6,493	3,222	2,752	12,032	961	133,497	38,002	24,456	17,648	13,934	35,621	270,704	30,116	137,345	120,072	19,282	29,844	226,223	74,898	291,979	205,202
Minimum	11,002	5,015	557	2,278	2,056	7,809	384	69,532	25,419	79	1,007	0	0	166,014	0	64,771	16,191	16,139	12,619	172,828	-52,003	-159,988	113,206

Table 2 Estimated DIPAW (Excluding OWDS Discharge) at the Rootzone, Vadose Zone Storage and DIPAW Discharge to Saturated Zone

Year	DIPAW at Rootzone	Starting Storage in Vadose Zone	DIPAW at Saturated Zone	Ending Storage in Vadose Zone	Year	DIPAW at Rootzone	Starting Storage in Vadose Zone	DIPAW at Saturated Zone	Ending Storage in Vadose Zone
1943	174,698	0	12,478	162,219	1997	100,603	635,189	116,836	618,956
1944	175,758	162,219	25,033	312,944	1998	137,454	618,956	117,046	639,364
1945	152,616	312,944	35,934	429,627	1999	59,366	639,364	115,042	583,689
1946	137,864	429,627	45,781	521,710	2000	83,161	583,689	109,843	557,006
1947	147,229	521,710	56,297	612,641	2001	85,900	557,006	107,823	535,083
1948	114,466	612,641	64,474	662,634	2002	53,176	535,083	102,792	485,468
1949	121,177	662,634	73,129	710,682	2003	99,689	485,468	102,305	482,851
1950	141,584	710,682	83,242	769,024	2004	64,903	482,851	99,010	448,744
1951	112,394	769,024	91,270	790,148	2005	150,701	448,744	99,647	499,798
1952	206,211	790,148	106,000	890,359	2006	63,968	499,798	99,823	463,943
1953	114,865	890,359	114,204	891,019	2007	42,753	463,943	96,008	410,688
1954	139,462	891,019	124,166	906,315	2008	65,855	410,688	93,275	383,268
1955	103,718	906,315	131,574	878,459	2009	62,076	383,268	91,489	353,855
1956	108,842	878,459	139,349	847,952	2010	83,642	353,855	88,512	348,986
1957	93,748	847,952	133,567	808,133	2011	91,054	348,986	88,763	351,276
1958	185,939	808,133	134,294	859,778	2012	49,131	351,276	84,009	316,398
1959	77,535	859,778	128,931	808,382	2013	44,350	316,398	80,130	280,618
1960	77,858	808,382	124,645	761,596	2014	48,186	280,618	78,395	250,408
1961	70,085	761,596	119,135	712,546	2015	57,254	250,408	75,817	231,845
1962	126,314	712,546	119,981	718,879	2016	52,447	231,845	73,547	210,745
1963	85,352	718,879	117,422	686,809	2017	85,217	210,745	72,874	223,088
1964	103,894	686,809	114,730	675,973	2018	46,436	223,088	69,532	199,992
1965	117,206	675,973	115,073	678,106	2019	83,347	199,992	68,414	214,925
1966	131,171	678,106	109,714	699,563	2020	83,362	214,925	70,654	227,632
1967	159,379	699,563	112,893	746,049	2021	83,377	227,632	71,823	239,186
1968	103,276	746,049	110,308	739,017	2022	83,393	239,186	73,046	249,533
1969	198,049	739,017	117,046	820,020	2023	83,408	249,533	73,119	259,822
1970	87,581	820,020	115,528	792,073	2024	83,423	259,822	73,798	269,448
1971	95,456	792,073	115,650	771,879	2025	83,439	269,448	76,723	276,163
1972	93,059	771,879	109,015	755,923	2026	83,454	276,163	77,507	282,109
1973	143,559	755,923	113,731	785,751	2027	83,469	282,109	77,962	287,616
1974	109,045	785,751	115,959	778,837	2028	83,485	287,616	77,884	293,217
1975	101,791	778,837	118,224	762,404	2029	83,500	293,217	77,731	298,986
1976	78,738	762,404	114,825	726,316	2030	83,515	298,986	78,662	303,839
1977	98,939	726,316	115,796	709,459	2031	83,508	303,839	79,555	307,792
1978	218,406	709,459	117,423	810,442	2032	83,508	307,792	80,269	311,031
1979	133,701	810,442	122,211	821,932	2033	83,508	311,031	80,565	313,974
1980	184,350	821,932	126,236	880,046	2034	83,507	313,974	81,379	316,102
1981	82,618	880,046	126,479	836,185	2035	83,507	316,102	81,429	318,180
1982	116,757	836,185	126,714	826,228	2036	83,506	318,180	82,433	319,253
1983	187,813	826,228	132,273	881,768	2037	83,506	319,253	82,901	319,858
1984	96,588	881,768	133,497	844,858	2038	83,506	319,858	83,073	320,291
1985	92,519	844,858	128,408	808,970	2039	83,505	320,291	83,366	320,431
1986	111,038	808,970	127,728	792,280	2040	83,505	320,431	83,255	320,681
1987	73,244	792,280	121,909	743,614	2041	83,518	320,681	83,370	320,828
1988	93,633	743,614	122,069	715,179	2042	83,547	320,828	83,850	320,525
1989	84,123	715,179	120,836	678,466	2043	83,576	320,525	84,001	320,100
1990	68,974	678,466	115,495	631,945	2044	83,605	320,100	84,202	319,503
1991	100,255	631,945	113,633	618,567	2045	83,634	319,503	84,303	318,835
1992	115,532	618,567	112,979	621,120	2046	83,663	318,835	84,378	318,120
1993	184,520	621,120	116,794	688,845	2047	83,692	318,120	84,596	317,216
1994	73,134	688,845	117,935	644,044	2048	83,721	317,216	84,923	316,014
1995	138,746	644,044	119,075	663,714	2049	83,750	316,014	85,133	314,632
1996	88,873	663,714	117,398	635,189	2050	83,779	314,632	85,317	313,094

Table 3 Calibration Statistics for Groundwater Basins in the 2020 CVM

Basin	Residual Mean	Absolute Residual Mean	RMSE
Chino Basin	0.061	14.230	21.411
Six Basins	-16.272	49.012	65.849
Cucamonga Basin	-0.394	39.085	50.792

Table 4 Stable Semivariogram Model Parameters used in Chino Basin

Model Layer	Hydraulic Parameters	C0	b	h	r	s
Layer1	Sy	2.31E-03	0	400	4800	0.21934
Layer1	Kh	2.27E+03	0	400	4800	0.24219
Layer1	Kv	3.86E+02	0	400	3000	0.20000
Layer3	Kh	5.34E+03	0	400	4000	0.24922
Layer3	Kv	3.37E+03	0	400	4000	0.25449
Layer5	Kh	5.34E+03	0	400	4000	0.24922
Layer5	Kv	3.37E+03	0	400	4000	0.25449

Response to Questions and Comments on the April 2, 2020 Safe Yield Recalculation Report

April 23, 2020 Letter from Overlying (Agricultural Pool) re Safe Yield Recalculation for Chino Basin Questions

Comment No. 1a. Page 1, first paragraph. Comment reads: "1a: Safe Yield is computed over arbitrary 10-year increments; however, the safe yield calculation should consider a Base Period with a time period whose average precipitation is equal to the long-term precipitation average. If the Safe Yield is not computed over a hydrologic base period but based on court ordered methodology, resulting Safe Yield values could be biased in the results when the precipitation record is recycled in some fashion for the future predictions."

Response. This comment is noted. This comment does not request any information or explanation regarding the 2020 Safe Yield Recalculation Final Report. Nevertheless, the comment reflects a misstatement and an apparent misunderstanding of the Court-ordered methodology. The 10-year period selected is not arbitrary. It was ordered by the Court and informed by the exercise of professional judgment. A long-term hydrology is used with precipitation data being evaluated over a 122-year period and adjusted after considering the veracity and integrity of the data collected. The 10-year forecast takes into account projected conditions that are expected to occur over the ensuing 10 years. While it is possible to extend the period for additional increments of time, longer forecasting entails further speculation. Historical experience in evaluating trends in the Chino Basin suggests that the projections become less reliable as they extend beyond the 10-year horizon. It is considerably easier to adjust to discrepancies between set expectations over a 10-year period than longer periods of time and consequently there is less risk to the parties and to the basin.

Comment No. 1b. Page 1, second paragraph. Comment reads: "1b: A Planning period spanning 62 years (from 1950 through 2011) was used to estimate net recharge and Safe Yield (Section 7.2). But planning simulations only extend for a 32-year period from 2019 through 2050, and Safe Yield is computed for every 10-year period. Why isn't the entire period of 62 years from 2018 through 2070 used for determining Safe Yield?"

Response. The comment offers several assertions as the basis for a foundation for a question that is addressed in the response to Comment 1.a. above. Further, please see the response to the 4/23 Appropriative Pool Response to Comment No. 82.

Comment No. 2. Page 1, third paragraph. Comment reads: "The table "Summary of Net Recharge by Decade in the Calibration Period" indicates that net recharge is about 1.0 million acre-feet from 2011 through 2018. Extrapolating this 8-year record for 10 years gives approximately 1.25 million acre-feet over the 2011 through 2020 period which is approximately 125,000 acre-feet per year. (a) Why is Safe Yield 135,000 acre-feet and not 125,000 acre-feet for the 2011 through 2020 period? (b) Was there or will there be an adjustment in Storage Accounts to account for the difference?"

Response. (a) The Safe Yield value of 135,000 afy was calculated in the prior Safe Yield recalculation and it is based on long-term average recharge. The 125,000 afy hindcast mentioned in the comment is based on actual hydrology that includes the most intense dry-period in the Chino Basin area in the instrumental record (see the April 2, 2020 Safe Yield Recalculation Report, Figure 3-14). (b) The Court-ordered Safe Yield reset methodology does not provide for any retroactive adjustments to Safe Yield or storage accounts. The probability of future hydrology is determined on the basis of the predicted reoccurrence of a multitude of wet, normal and dry years through the historic record. The recent hydrology adds to the lengthy record; it is not a substitute. Over the fullness of time, series of wet, normal and dry years have occurred and are reasonably expected to occur again in the future.

Comment No. 3. Page 1, fourth paragraph. Comment reads: "The Draft Report dated March 23, 2020 included Figures 7-6 and 7-7 which are missing in the final report. These should be included. Also, in these figures, the precipitation used for future conditions is not shown, and that may help to figure out increasing DIPAW trends."

Response. The figures referenced by the commenter and associated text in the March 23rd draft were replaced with other figures and text that more clearly communicate the trends in DIPAW.

Comment No. 4. Page 1, fifth paragraph. Comment reads: "DIPAW increases from 2019 through 2050 in Table 7-2. Total pervious area is decreasing through this period, so it is not clear why DIPAW should increase."

Response. In the 2020 SYR1 planning scenario, DIPAW discharging from the rootzone to the vadose zone is equal to the long-term average DIPAW based on 62 years of daily precipitation, ET and applied water consistent with the cultural condition for each year. The DIPAW in Table 7-2 is the DIPAW discharge from the vadose zone to the saturated zone. In the planning period, the DIPAW discharge to the saturated zone is asymptotically approaching the DIPAW discharge at the rootzone.

Comment No. 5a. Pages 1, sixth paragraph. Comment reads: "5a: Section 7.4 states that "the primary driver for the reduction in net recharge during the 2021 through 2030 period were changes in cultural conditions prior to the planning period and extremely low precipitation that occurred during the 20 years prior to the planning period". However, Figure 7-7 (in Draft Report) showed an increase in net recharge from 2021 through 2030."

Response. The April 2, 2020 Safe Yield Recalculation report also shows an increase in net recharge from 2021 through 2030. There is no inconsistency between the administrative draft report and the April 2, 2020 report and the observed and modeled conditions contained therein.

Comment No. 5b. Page 2, first paragraph. Comment reads: "5b: Also, if the last 20 years of the precipitation record are from drought conditions (2011 through 2020 in the calibration period which would coincide with the 2050 through 2070 of the predictive period) then why were drought conditions not considered in the Safe Yield determination."

Response. Drought conditions were considered. Recall that recharge in the planning period is based on the simulation of 62 years of daily precipitation, ET and applied water consistent with the cultural condition for each year. Prolonged dry periods occur in the 1950 through 2011 period (e.g., 1950 through 1977, 1999 through 2011).

Comment No. 6. Page 2, second paragraph. Comment reads: "Safe Yield was decreasing through the years in the 2007 model but increasing in the 2020 model (up to 2050). What was different between the models to cause that?"

Response. The differences are due to new data, better use of data and other improvements that were incorporated in the update of the 2007 model to the 2013 model and recent update of the 2013 model to the 2020 CVM.

Comment No. 7a. Page 2, fourth paragraph. Comment reads: "The figure below shows the difference between 2020 model and 2013 model values for various inflows. These flow amounts are not consistent between the models. The figure was generated from tables in the 2020 and 2013 Safe Yield update reports. 7a: The largest differences are in DIPAW followed by Subsurface inflow. (i) Why were these differences larger in earlier times and smaller in later times? If the differences are due to more refined precipitation and more refined R4 model infrastructure, then that refinement was considered throughout the time period so a generally constant difference through time would be expected. (ii) Did precipitation decrease through time in one model and not in the other, such that DIPAW and subsurface inflow differences show temporal trends?"

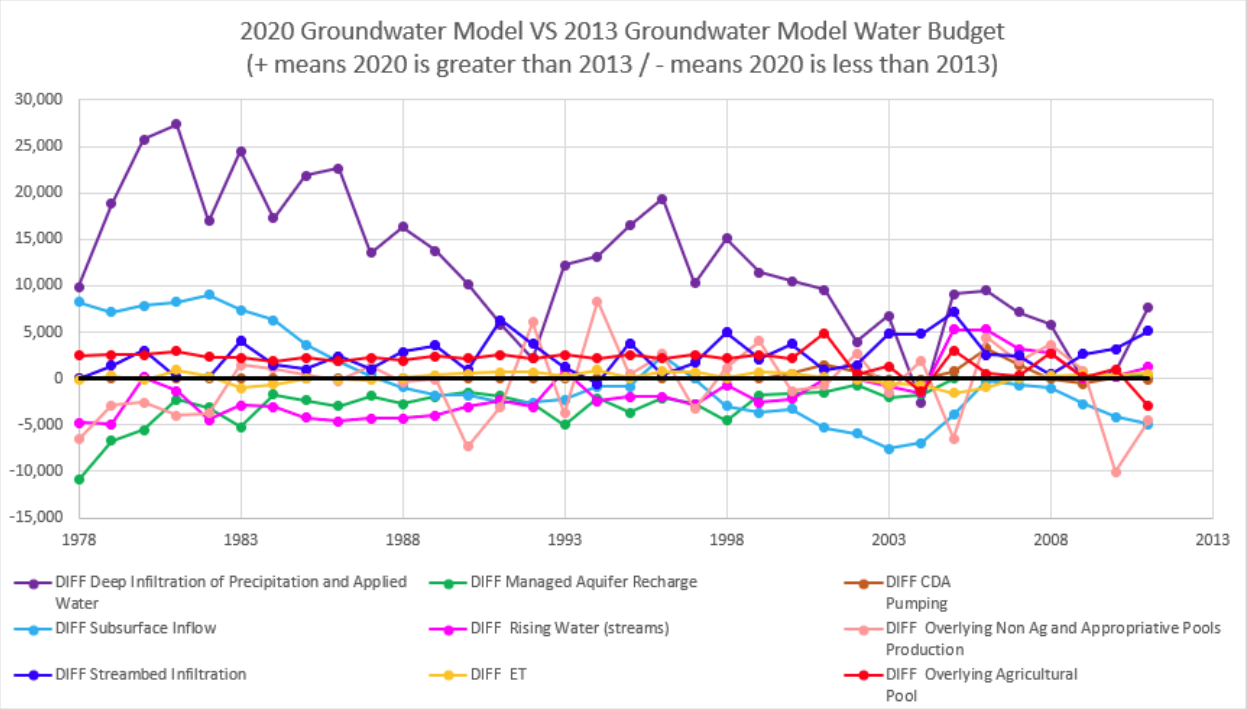

Response. (i) Several improvements were incorporated into the update of the 2013 model to the 2020 CVM and the major improvements include:

- WEI is involved in a parallel effort to assist Watermaster and the IEUA in assessing alternative TDS compliance metrics for recycled water use. In that effort, the watershed delineation was refined to comport more accurately with the groundwater basin boundaries, and land use delineations were updated to more accurately reflect water use and salt loading. In the update of the 2013 model to the 2020 CVM the number of hydrologic subareas has substantially increased to more accurately estimate precipitation/irrigation/runoff processes and stormwater recharge.
- In the update of the 2013 model to the 2020 CVM, the method for estimating reference ET (ET0) across the watershed was improved from past reliance on the relationship between the Pomona CIMIS station ET0 and Puddingstone reservoir evaporation to a new ET0 model that is based on the empirical relationships of temperature and ET0 measurements at the Pomona and Riverside CIMIS stations and using these relationships to estimate ET0 temporally and spatially based on PRISM estimates of monthly temperature across the watershed.
- In the update of the 2013 model to the 2020 CVM, the method for estimating daily precipitation for each hydrologic subarea was improved from past reliance on interpolating daily precipitation at precipitation stations across the watershed using Thiessen polygons to the use of monthly precipitation estimates for each hydrologic subarea based on monthly PRISM estimates and converting those monthly estimates to daily precipitation estimates based on daily precipitation from nearby precipitation stations. As to precipitation, these improvements were made for the period prior to 2002. After 2002, daily precipitation estimates for the hydrologic subareas are based on

NEXRAD estimates. The historical DIPAW estimate changes primarily result from the improvements in the data used in the R4 model described in this and the two prior bulleted items.

- Subsurface inflows from the Cucamonga and Riverside Basins are greater in the 2020 CVM relative to the 2013 model: the former occurs because during the model update process the Cucamonga Basin was integrated directly into the 2020 CVM, and the latter occurs due to changes in the estimated hydraulic conductivity in the northeast domain of the 2020 CVM. Subsurface inflow from the mountain front areas increased due to the refinements in the R4 data for DIPAW (described above).
- In the update of the 2013 model to the 2020 CVM, streambed infiltration in the Santa Ana River also increased. This is, in part, due to converting the streamflow package in MODFLOW to SFR2, through the incorporation of updated channel geometry, and calibration.

(ii) No.

Comment No. 7b. Page 2, fifth paragraph. Comment reads: "7b: Why are there differences in fixed value items such as Managed Aquifer Recharge (MAR), and overlying Non-Agricultural and Appropriative Pools pumping? Was the reporting in earlier years adjusted?"

Response. In the update of the 2013 model to the 2020 CVM, the stormwater recharge prior to the availability of IEUA stormwater recharge estimates is based on R4 simulations with improved data relative to the 2013 model. As to the other MAR estimates, the data used in the in the update of the 2013 model to the 2020 CVM was taken from IEUA and Watermaster records. As to Overlying Non-Agricultural and Appropriative Pools pumping, the data used in the update of the 2013 model to the 2020 CVM was taken from Watermaster records. Some of the pumping assigned to the Overlying Agricultural Pool in the 2013 model was incorrectly assigned to the Overlying Non-Agricultural Pool and this has been corrected.

Comment No. 8. Page 3, first paragraph. Comment reads: "It was explained at the Agricultural Pool March meeting that the new model had more updated and refined inputs and that is why results are different between models, that the differences are not too large each year, that calibration statistics of both models are comparable, and that differences in cumulative storage do not matter since models are being used for future MPI evaluations. However, the cumulative storage impact of the two models is considerably different. The net storage between any two years is the space between the water levels of those two years. If the two models were calibrated to the same data, then something is inconsistent on a model-wide scale. For instance, between 1978 and 1999, the 2020 model shows a cumulative increase in water levels while the 2015 model shows that water levels have declined during that same time period as noted in the figure below. The figure was generated from tables in the 2020 and 2013 Safe Yield update reports."

Response. This comment is noted. First, it includes an incorrect representation. There is one model, not two. The 2013 model was updated to the 2020 CVM to include new data,

improvements in the use of data and further refinements. Second, for the purpose of estimating Safe Yield under the Court-ordered methodology, the model-estimated storage change for the 2013 model and the 2020 CVM for the period 2000-2018 closely track each other.

Comment No. 9. Page 3, second paragraph. Comment reads: "It was mentioned that the 2013 model was used to evaluate the impacts of the storage management plan, but the Safe Yield was estimated using the updated 2020 model. It was mentioned that they should give the same results but that is hard to reconcile until the 2020 model is used to evaluate impacts of storage management since it is a different model and anticipated results may be different."

Response. This comment is noted. The 2020 CVM has been used for purpose of addressing Safe Yield. Its application for other purposes is not before Watermaster. See response to Comment No. 8 above.

Comment No. 10. Page 4, first paragraph. Comment reads: "A total water budget is not provided for any model. A water budget that includes R4/HSPF models, and vadose zone approximations along with the groundwater budgets helps to understand the other annual water budget terms such as precipitation, root zone ET, and how they changed from earlier models."

Response. This comment is noted. The 2020 Safe Yield Recalculation Final Report reflects the application of the Court-ordered methodology. The comment suggests further work to assist in the understanding of the changes related to the model update. Watermaster disagrees that such work is reasonably required to accept the recommendations in the Final Report.

Response to Questions and Comments on the April 2, 2020 Safe Yield Recalculation Report

April 23, 2020 Letter from the Appropriative Pool re Technical Review of the Models and Methodology Used as a Basis for the 2020 Safe Yield Reset

Comment No. 1. Page 2, first paragraph. Comment reads: "The methodology described in WEI (2020) to estimate the Safe Yield of the Chino Basin for the period from 2021 to 2030 generally follows the methodology described in Appendix A to the Safe Yield Reset Agreement. Watermaster Rules and Regulations Section 6.5 specifies "The reset will rely upon long-term hydrology and will include data from 1921 to the date of the reset evaluation." As described in WEI (2020), the 2020 Safe Yield estimation relies on precipitation data for the period 1950 to 2011 and does not include precipitation data extending back to 1921 as was specified in the Rules and Regulations Section 6.5 (d). As such, the methodology used in the 2020 Safe Yield reset does not explicitly comply with the Chino Basin Rules and Regulations."

Response. The methodology used in the 2020 Safe Yield Reset Final Report ("Final Report") follows the methodology in the Court's April 28, 2017 order as carried forward in the Chino Basin Watermaster Rules and Regulations. The court-ordered methodology requires, and the 2020 Safe Yield recalculation used, a long-term historical record of precipitation falling on current and projected future land uses to estimate the long-term average net recharge to the Basin. The Court order states that the Safe Yield reset will rely upon long-term hydrology and will include data from 1921 to the date of the reset evaluation (emphasis added). Watermaster used long-term precipitation data from 1895 to the present to estimate the long-term average precipitation inclusive of the period 1921 to the present. From that analysis we selected the period 1950 through 2011, a sixty-two year period, for the planning period. It represents a balancing between the availability of climate change factors (1915 through 2011) and the need to select a period where the average period-precipitation equals the long-term average precipitation, per standard practice. The long-term average precipitation for 1921 to 2011 period is greater than the long term average precipitation and use of the 1921 to 2011 period would overestimate the long term recharge, net recharge and Safe Yield. Use of the 1921 to 2011 period would not be consistent with the court-ordered methodology

Comment No. 2. Page 2, second paragraph. Comment reads: "The Court-approved methodology to estimate the Safe Yield of the Chino Basin relies on a series of models to simulate the distribution and movement of water at the land surface, within the unsaturated zone, and within the aquifer system. While there is no explicit statement in WEI (2020) or previous Safe Yield Reset documentation that says so, it is assumed that the Watermaster considers these models appropriate to help determine the Safe Yield because they are widely-

accepted, widely-tested, and/or acceptably calibrated to measured data. Indeed, the latest versions of the Chino Basin models are calibrated to an extensive dataset within what would be considered industry standards."

Response: The initial form of the Watermaster model was critically reviewed by the Assistant to the Special Referee in 2007. The Watermaster model has been updated over time to incorporate and reflect new and better data. Watermaster views the model to be reasonable, appropriate and effective. It has engaged and accepted peer review from expert consultants representing parties to the Judgment. In addition, Watermaster engaged the services of Will Halligan in 2020, an independent expert, to evaluate the Final Report. For reasons stated in the Final Report and repeatedly in these Response to Comments, the use of the model in support of the recommendation is reasonable and prudent.

Comment No. 3. Pages 2 to 3. Comment reads: "While the models used to determine the Safe Yield of the Chino Basin can be considered calibrated, there is significant uncertainty in the numerous combinations and distributions of parameters derived to achieve calibration and it is not possible that the calibration is unique. In other words, there are other combinations of parameters, all within plausible ranges, that, if assigned to the model, could result in an acceptable calibration. Each calibrated model would result in a different water budget and estimate of Safe Yield. To be clear, the magnitude of data available for developing and calibrating the Chino Basin models is extensive and it is among the best constrained models with which I have experience. Nonetheless, there is no way to directly measure all the parameters across every square inch of the basin necessary to develop a perfectly complete water budget and achieve a perfectly constrained model. A primary concern I have is that the Chino Valley Model is being presented as "accurate" and the implication is that it is the only correct model. Some model-derived data are being presented to the nearest acre-foot implying a level of accuracy that is not defensible given the uncertainty of the input parameters. In reality, the model presented in the report is one of many plausible hydrogeological conceptualizations of the Chino Basin, each of which would result in a calibrated model."

Response: This comment is noted. Watermaster disagrees with the Comment. The development of the Model was initially subject to critical review and scrutiny by the Assistant to the Special Referee (see Response to Comment No.2 above). The Comment misstates the degree of risk of error associated with uncertainty arising from the use of the Model. The Model has been calibrated. The Watermaster Engineer has a high degree of confidence in the use of the Model for the purpose of estimating Safe Yield as the Court has previously ordered. Watermaster has followed the specific methodology and employed an independent expert to evaluate the propriety of Watermaster's use of the model in this specific instance. Use of the Model is reasonable and prudent.

Comment No. 4. Page 3, second paragraph. Comment reads: "All these parameters, and more, are uncertain and variations in assigned values change the water budget. There is further uncertainty in the assumptions necessary to develop the future water budget that is analyzed with the model to determine the Safe Yield (projected magnitude and location of pumping,

recharge, and hydrology). Depending on how the uncertainty is addressed dictates the model outcome."

Response: This comment is noted. The Comment expresses an objection to the Court ordered methodology. Moreover, Watermaster disagrees that "these parameters and more, are uncertain" as alleged in the Comment detract from or undermine confidence in the application of the fully calibrated Model. (See Responses to Comments 2 and 3 above).

Comment No. 5. Pages 3-4. Comment reads: "This uncertainty is apparent when comparing the water budgets of the previous Safe Yield reset model (WEI, 2015b)5 with the results of the current one (WEI, 2020).6 For example, changes in model assumptions to estimate Deep Infiltration of Precipitation and Applied Water (DIPAW) were revised between the previous model and current one that resulted in significant differences in this recharge over the previous Safe Yield estimation period from 2011 to 2020. The differences in annual DIPAW during this time period were as much as approximately 27,000 acre-ft (see Table 1). Both models were/are acceptably calibrated, but the water budgets are different. In the current model, other assumed model parameters would likely have been changed during calibration to adjust to the new recharge rates and achieve acceptable calibration. The revised DIPAW rates may be more representative than the original. However, they are still estimated and subject to change in the future as more information becomes available, as is the case for all assumed parameters in the model. If the past is any indication of the future, the next model will likely have a different set of DIPAW values, and/or other revised model input values that will likely yield different results. This type of uncertainty is inherent in all surface water and groundwater models."

Response: This comment is noted. See above Responses to Comment Nos 2-4 above. There is one Model, continuously updated to account for new data and best practices. The Model is subject to change on the basis of new data; this is precisely the point. As new and better information is collected, the Model will be regularly and routinely updated and applied in accordance with the Court ordered methodology.

Comment No. 6. Page 4, second paragraph. Comment reads: "Following the above observations, it is my opinion that the most significant omission from the WEI (2020) model analysis and report is an uncertainty analysis. Performance of a predictive uncertainty analysis using publicly-available software is now commonplace in the technical literature and is considered standard practice in groundwater modeling. Uncertainty analysis is also a California Department of Water Resources (CDWR) best management practice for predictive model analysis in support of the Sustainable Groundwater Management Act (SGMA). Such an analysis would consider multiple realizations of the models with ranges of parameter values, each constrained in such a way as to result in acceptable calibration. The estimated Safe Yield from each model realization would be plotted on a cumulative probability chart, which can be used to identify an acceptable range within which to manage the basin. This would provide the basin managers with a sense as to potential variability in the Safe Yield estimate, for use in making decisions."

Response: This comment is noted. See above Responses to Comment Nos 2-5. The Final Report provides a recommendation that is derived from following the Court ordered methodology. The fact that other additional technical work evaluations might be undertaken by Watermaster in connection with making a recommendation for Safe Yield does not detract from the reasonableness and prudency of the recommendation. The application of the Court ordered methodology in this case was subjected to expert comment and independent peer review.

Comment No. 7. Page 5, first paragraph. Comment reads: "In keeping with the estimated nature of the Safe Yield and to be consistent with the language in the Safe Yield Methodology adopted by the Court, I recommend to replace the word "Recalculation" in the title of the report with "Reset" or "Redetermination." The same would apply to other areas of the report where "recalculation" is used."

Response: The process through which the Basin's Safe Yield is estimated and reset is described in various manners throughout the Watermaster guidance documents. Paragraph 15.(a) of the Judgment refers to the Court's retained jurisdiction to undertake a "redetermination" of the Safe Yield. Paragraph 10.(a)(1) of the Appropriative Pool Pooling Plan, Exhibit "H" to the Restated Judgment, refers to a reduction in Safe Yield "by reason of recalculation thereof." The OBMP Implementation Plan, in its discussion of Program Elements 8 and 9, variously refers to the "comput[ation]", "estim[ation]," "re-determination" and "reset" of the Safe Yield. The Court's April 28, 2017 order found that the reset of the Safe Yield to 135,000 afy was a "recalculation" and required Watermaster to conduct a Safe Yield "evaluation and reset process" beginning in 2019. Based on all of these descriptions, it is unclear that the use of one description as opposed to another in WEI's report has any import or effect.

The Court's April 28, 2017 order explains the Safe Yield evaluation and reset process that Watermaster must follow. This includes the Court's adoption of a specified methodology for this process, that includes the methodology in the Reset Technical Memorandum. Step 5 of the Reset Technical Memorandum's methodology includes the qualitative evaluation of groundwater production at the net recharge estimated by the groundwater flow model.

Comment No. 8. Page 5, second paragraph. Comment reads: "Section 1.2 pg. Listing of undesirable results: It should be noted that these undesirable results are listed as examples and that not all are specific to the Chino Basin."

Response. This comment is noted. The language of the Final Report does not imply these results are specific to the Chino Basin and instead reflects the commonly held view of what is an "undesirable result". (See Sustainable Groundwater Management Act – Water Code Section 10721(x).) The fact that not all potential results are present in the Chino Basin does not change the customary use of the phrase "undesirable results".

Comment No. 9. Page 5, third paragraph. Comment reads: "Section 1.2 pg. 1-2, last paragraph: It would be helpful to clarify the relationship between net recharge and Safe Yield prior to this point."

Response. The relationship of net recharge to Safe Yield is developed in text that follows the report text referenced by commenter.

Comment No. 10. Page 5, fourth paragraph. Comment reads: (a) "Section 1.3 pg. 1-4: Is this long-term hydrology analogous to/defined by the base period?"

..."meets other Safe Yield related criteria,..." (b) Are these the criteria you discuss in Sections 1.3.1 through 1.3.5? If so, this isn't clear. If not, what are the criteria, per the title of this section? MPI is not discussed as a criterion as per the court approved methodology and consistent with the title of Section 1.3.

Response. (a) Yes. (b) Text revised to read: "If the period includes representative long-term hydrology and meets other safe yield related criteria *described below*, the net recharge for that period can be assumed to be the safe yield."

Comment No. 11. Page 5, fifth paragraph. Comment reads: "Section 1.3.1 pg. 1-4, 1st paragraph: The base period needs to be defined. What period was used and why was the selected period used. What is its significance with respect to the Chino Basin Safe Yield calculation? How is it applied? The connection is not clear."

Response. This section of the report provides the theoretical foundation for the safe yield concept as commonly used groundwater management. The application of these concepts is presented in Section 7 of the Report.

Comment No. 12. Page 5, sixth paragraph. Comment reads: "Section 1.3.1 pg. 1-4, last paragraph: I'm not sure what you are saying here. (a) If the historical record is not useable, what did you use? (b) Is this only for land use or does it apply to precipitation as well?"

Response. (a) The historical record cannot be used directly to estimate future Safe Yield because the cultural conditions of the past are changing over time and not representative of the future. We updated and calibrated models based on the historical record and applied them with current and projected cultural conditions to estimate future net recharge and Safe Yield. (b) Land use and the associated water management practices.

Comment No. 13. Page 5, seventh paragraph. Comment reads: "Section 1.3.2 Storage pg. 1-4: (a) Need to define what is meant by the term "operational storage space." Presumably "operational storage" is a subset of the total storage space; (b) has the volume and spatial distribution required for "operational storage" been defined?"

Response. (a) Operational storage space is the volume of storage required to regulate variable recharge over time to ensure that the safe yield can be pumped. This definition was added as footnote to the report text. (b) No.

Comment No. 14. Page 5, eighth paragraph. Comment reads: "Section 1.3.3 Basin Area pg. 1-5: More explanation is needed to justify assigning the recharge and discharge terms for the hydrologic boundary to the adjudicated boundary. Are you confident that the net recharge/safe yield calculated for one area and applied to another is representative?"

Response. The area being referred to is located in the northern part of the Chino Basin that lies between the boundary defined by the Judgment and the hydrologic boundary used in the 2020 CVM. The short answer is yes.

Comment No. 15. Page 5, ninth paragraph. Comment reads: "Section 1.3.4 Cultural Conditions, pg. 1-5: There is some confusion as to what constitutes a "cultural condition." I think a definition and examples of such would be helpful up front. For example, are groundwater production patterns, stormwater capture/recharge, storage programs, and basin re-operation considered cultural conditions? Along those lines, are the changes in drainage patterns described in Section 1.3.5 considered cultural conditions?"

Response. The report text has been modified to include a definition of cultural conditions that reads: "Cultural conditions, as used herein, refers to land use and associated soil, crop and water management practices." The text in Section 1.3.5 has been included in Section 1.3.4.

Comment No. 16. Page 6, first paragraph. Comment reads: "Section 1.4 Court Direction to Reset Safe Yield, pg. 1-6, Section 4.4, 2nd Sentence: "The reset will rely upon long-term hydrology and will include data from 1921 to the date of the reset evaluation." The methodology described in Section 7.2, using an average precipitation from 1950 to 2011, appears to contradict what was directed by the Court."

Response. See Response to Comment No. 1.

Comment No. 17. Page 6, second paragraph. Comment reads: "Section 1.5 Court Approved Methodology to Calculate Safe Yield pg. 1-7, No. 5: This is a critical criterion to defining safe yield, which is not mentioned in Section 1.3."

Response. Section 1.3 provides the theoretical foundation for the safe yield concept as commonly used groundwater management. Section 1.5 describes court-ordered methodology that specifies additional requirements to calculate Safe Yield specific to the Chino Basin.

Comment No. 18. Page 6, third paragraph. Comment reads: "Section 1.6 Scope of Work, pg. 1-8 Task 5: This task bullet implies that multiple planning simulations would be conducted. Did this occur?"

Response. We simulated the 2020 SYR1 scenario once. Upon evaluation of basin response to the SYR1 scenario, we concluded there was no MPI or undesirable results. Therefore, pursuant to the Court-ordered methodology, no iterations were required.

Comment No. 19. Page 6, fourth paragraph. Comment reads: "Section 1.7 Scope of the Model Update, pg. 1-8, 2nd paragraph: We need assurance that the outflow reported by Cucamonga and Six Basins is the same as the inflow to Chino. Have the changes you implemented in the Chino Basin model been implemented in the models relied on by the neighboring basins?"

Response. The short answer to the question is "yes". The 2020 Chino Valley Model includes the Chino, Cucamonga, Six, Spadra and Temescal Basins. The model calculates the subsurface discharge among the basins.

Comment No. 20. Page 6, fifth paragraph. Comment reads: "Section 1.8 Scope of the Planning Projection Update, pg. 1-8, 1st paragraph: The last sentence indicates future water supply and demand information was "provided by the Parties and others." Who/what are the "others"?"

Response. Non-Chino Basin Judgment parties in the Six and Temescal Basins.

Comment No. 21. Page 6, sixth paragraph. Comment reads: "Section 2.5 Aquifer Systems pg. 2-13, 2nd paragraph: (a) Have the aquifer and aquitard layers in the Cucamonga and Six Basins areas been revised to match the new Chino Basin conceptualization or vice versa? (b) How do the aquifers line up at the basin boundaries? (c) Are the conceptualizations identified in WEI (2012) and WEI (2017) the latest?"

Responses (a) and (b). The Response to Comment No. 8 in "Appendix E-1 Comments and responses for first colleague peer review of the 2020 Safe Yield Recalculation Model" provided the following answer to questions (a) and (b).

"Cucamonga and Six Basins are considered to be hydrogeologically separated from the Chino Basin and the hydrostratigraphy (layering) is different than the Chino Basin. The connections to Chino Basin from the Cucamonga and Six Basins are simulated as barriers. The deep aquifers in Cucamonga and Six Basins will be modeled as weakly connected to Chino Basin's deep aquifer-system by using the barrier's hydraulic conductivity parameter."

Response (c). The latest Cucamonga Basin conceptualization is included in WEI (2012). The latest published conceptualization for the Six Basins is included in WEI (2017)**.** Six Basins recently updated its conceptualization and the updated conceptualization is included in the 2020 CVM.

Comment No. 22. Page 6, seventh paragraph. Comment reads: "Section 2.6 Aquifer Properties pg. 2-18, Equation and 1st full paragraph: While this relationship may work in a laboratory on a sample with a known grain size distribution and cementation, it has little value in interpreting general descriptions of "sand" and "clay" from driller's logs. Attached is a typical driller's log

from the Chino Basin. What is the source of the equation on the top of pg. 2-18? How was the equation on the top of page 2-18 applied to the information in a driller's log such as the one attached (see Attachment A)? This equation is similar to those published by Hazen (2011) and others. It is noted that, in most cases, it is only applicable to sediments with grain size distributions in the range of 0.1 to 0.3 mm (Fetter, 2001)."

Response: The initial estimates of the aquifer parameters of the 2020 CVM are obtained by analyzing over 1100 lithological (driller's) logs, where the lithological codes are related to hydraulic parameters. The equation of the top of page 2-18 of the draft report is given solely to illustrate the relationship between the soil texture (grain size) and hydraulic conductivity. That equation was developed by M. King Hubbert in his paper The Theory of Ground-water Motion published in 1940. Freeze and Cherry (1979) illustrates how the equation was derived. The Hubbert equation is indeed similar to the Hazen equation $K = C \times (d_{10})^2$ published in 1911, and both equations involve an empirical constant that must be adjusted to include influence of other properties that affect flow.

Comment No. 23. Page 6, eighth paragraph. Comment reads: "Section 2.6 Aquifer Properties pg. 2-18, 2nd paragraph: It is noted that McCuen et al., 1981 addresses soil infiltration, not specific yield."

Response: This comment is noted. This comment does not request any information or explanation regarding the 2020 Safe Yield Recalculation Final Report and is therefore not addressed further.

Comment No. 24. Page 6, ninth paragraph. Comment reads: "Section 2.6.1 Compilation of Existing Well Data pg. 2-18, 1st sentence: See comment above."

Response: This comment is noted. This comment does not request any information or explanation regarding the 2020 Safe Yield Recalculation Final Report and is therefore not addressed further.

Comment No. 25. Page 7, first paragraph. Comment reads: "Section 2.6.2 Classification of Texture and Reference Hydraulic Values for Aquifer Sediments pg. 2-18, 2nd paragraph, 2nd sentence: (a) How have data from these pumping tests been used to constrain the texture analysis? Other than this statement, there is no mention of how pumping test data, which are specifically designed and conducted to address model needs, were used to either determine initial parameter values or constrain calibrated values. Pumping tests have been conducted on all of the Chino Basin Desalter Wells, which provides critical information for constraining aquifer parameters in one of the most vital areas of the basin – where hydraulic control is achieved and maintained. It is my opinion that data obtained from controlled pumping tests are more reliable than grain size analysis for determining hydraulic conductivity and, if interference well measurements can be obtained, storage coefficients."

Response. As to question (a) Please see the discussion in Section 5 on how the initial hydraulic conductivities based on the lithologic model are adjusted to pre-calibration values. We created a new Appendix E that contains, among other things, Table E-1 that compares horizontal hydraulic conductivity estimates from aquifer stress tests estimated by others and by WEI to initial hydraulic conductivity estimates based on the lithologic model, the initial estimates of hydraulic conductivity prior to calibration and final calibrated values.

Comment No. 26. Page 7, second paragraph. Comment reads: "Section 2.6.2 Classification of Texture and Reference Hydraulic Values for Aquifer Sediments pg. 2-19, last paragraph of section: "Using this method, specific yield, horizontal hydraulic conductivity, and vertical hydraulic conductivity values were computed for each layer at each well location." Are the values computed using texture analysis initial values?"

Response. Yes, initial values for K_h, K_v, and S_y for each layer at each well location were computed using hydraulic properties corresponding to the sediment textures. These values are then adjusted to pre-calibration values as discussed in Section 5 and final calibrated values as discussed in Section 6.

Comment No. 27. Page 7, third paragraph. Comment reads: "Section 2.6.4 Specific Yield pg. 2-20: What were the criteria for accepting a driller's log as useful for the analysis? Model estimated specific yields should be compared to values derived from pumping tests to confirm modeling results."

Response. Each well completion report was reviewed and professional judgment was used to determine if the lithologic description was acceptable for inclusion in the textural analysis.

Comment No. 28. Page 7, fourth paragraph. Comment reads: "Section 2.6.5 Specific Yield pg. 2-20: Model estimated hydraulic conductivity or values derived from texture analysis should be compared to values derived from pumping tests to confirm modeling results. It is my understanding that a table of pumping test-derived hydraulic conductivity values will be provided in the final report."

Response. See Response to Comment No. 25.

Comment No. 29. Page 7, fifth paragraph. Comment reads: "Figures 2-10, 2-11, and 2-12. These figures need to be relabeled to make it clear that they are pre-calibrated parameter distributions.

Response. The figure titles have been revised indicating that they are pre-calibrated parameters.

Comment No. 30. Page 7, sixth paragraph. Comment reads: Section 2.6.6 Vertical Hydraulic Conductivity pg. 2-21: It is not clear in this section how you determined vertical hydraulic conductivity."

Response. The vertical hydraulic conductivity for each layer at each well location were calculated based on the equation in Section 2.6.2 (on page 2-19 of the draft report). For each layer, the calculated values were interpolated to all model cells in that layer using the Kriging method.

Comment No. 31. Page 7, sixth paragraph. Comment reads: "Section 2.7 Land Subsidence in the Chino Basin pg. 2-21: Land subsidence is, in part, a function of the storage properties of the aquitards, which you have now included in the model as Layers 2 and 4. This section should include a discussion of why model layers 2 and 4 where included in the 2020 CVM and their relationship to future land subsidence evaluations. Have the inelastic and elastic storage properties that dictate aquitard compaction been incorporated into this model? As it appears that the land subsidence package has not been included in this model, when you calibrate land subsidence, you will need to adjust the elastic/inelastic storage properties during that process. During that process, it may be prudent to adjust the other aquifer parameters in the model to optimize calibration. This will cause changes to the model-predicted water budget."

Response: 2020 CVM was updated to enable it to be calibrated for land subsidence. Calibration for land subsidence will be done in the next fiscal year as part of the land subsidence management work being done by Watermaster. As noted in Appendix B-20, the volume of groundwater discharged from aquitards due to land subsidence within MZ1 is estimated at 181 afy. This quantity is insignificant in the overall water budget of the 2020 CVM.

Comment No. 32. Page 8, first paragraph. Comment reads: "Section 3.1.1.1 Subsurface Inflow from Adjacent Groundwater Basins pg. 3-2, 1st paragraph: Is there no inflow from the Cucamonga Basin and Six Basins?"

Response. This section refers to subsurface inflow into the 2020 CVM domain. The Cucamonga and Six Basins are in the 2020 CVM domain.

Comment No. 33. Page 8, second paragraph. Comment reads: "Section 3.1.1.4 MAR pg. 3-3: This should be spelled out in the title. Also, this is defined as "Managed Artificial Recharge" in some parts of the report and "Managed Aquifer Recharge" in others."

Response. The report text has been updated.

Comment No. 34. Page 8, third paragraph. Comment reads: "Section 3.1.2.1 Groundwater Pumping pg. 3-3: It should be noted that Agricultural pumping after 2004 is metered."

Response. The report text was updated and now reads: "Overlying agricultural groundwater pumping was estimated: by the R4 model for the period 1978 through 2004 and in the planning scenarios and is therefore dependent on the same data as the R4; and with pumping estimates provided by the Chino Basin Watermaster that relies on meters installed at some wells and a water duty method for the other wells."

Comment No. 35. Page 8, fourth paragraph. Comment reads: "Section 3.2.5 Precipitation, 1st full paragraph on pg. 3-6 and Figure 3-13: Is the precipitation data presented in this section and shown on Figure 3-13 spatially averaged over the 2020 CVM or is this data for a specific location? In addition to providing general observations on the range of precipitation over the 2020 CVM for the historic period, as well as the occurrence of dry periods, a statistical evaluation of the distribution of rainfall data showing standard deviation bands about the mean should also be provided. An example of the statistical distribution of rainfall for a 75-year time period for a Riverside County station is provided as an example in the upper left graph of Attachment B. For comparison, the example precipitation data set is evaluated for a 10-year moving average (same time length used for the Safe Yield reset; lower left graph). These data are further evaluated to assess the probability for an average rainfall over a 10-year period exceeding the mean (graphs shown on the right). For the example shown, the probability that any 10-year period may exceed the mean rainfall for the period is 49.5% and may exceed the mean by 50% is about 18%. Using the 16th and 84th percentile distributions (+/-1 standard deviation) of rainfall to estimate DIPAW could provide additional useful information on the possible likely range in groundwater recharge for use in management decisions."

Response. Figure 3-13 shows the spatially-averaged annual precipitation falling on the 2020 CVM watershed. The spatially-averaged annual precipitation was estimated from the gridded monthly precipitation estimates obtained from the PRISM Climate Group and spatially averaged over the 2020 CVM. It appears that this comment is based on a misunderstanding that average precipitation was used to estimate long-term recharge. Average precipitation is not used in the 2020 Safe Yield recalculation, so the remainder of the comment is not addressed.

Comment No. 36. Page 8, fifth paragraph. Comment reads: "Section 3.2.5 Precipitation, last paragraph on pg. 3-6: What was the time period for the daily precipitation data used with the HSPF and R4 models?"

Response. The HSPF models were calibrated for Cucamonga and Day Creeks using the time periods that bracket their available gaged discharge records which were 1949 to 1975 and 1950 to 1971, respectively; and 1950 through 2011 for the planning period. The R4 model was calibrated for surface water discharge with precipitation data from 2005 through 2018. The R4 models used precipitation data from 1943 through 2018 for the calibration period and 1950 through 2011 for the planning period.

Comment No. 37. Page 8, sixth paragraph. Comment reads: "Figure 3-7. It appears that the Cypress Channel is represented as being fully concrete lined. Based on City of Chino staff review of aerial photos, it appears that approximately 3,000 feet of the channel located immediately north of Kimball Avenue (within the CIM property) is unlined and the channel condition along this segment may be characterized as natural soft bottom."

Response: We reviewed similar aerial photos and concur. Figure 3-7 has been updated.

Comment No. 38. Page 8, seventh paragraph. Comment reads: "Section 5.1 Surface Water Models 2nd paragraph, 2nd sentence. This sentence implies you used HSPF to estimate MAR? Is that true?"

Response. The HSPF model is used to estimate surface water discharge from the San Gabriel Mountains streams draining to the Chino Valley area. This discharge becomes a boundary inflow to streams simulated by R4. Local runoff plus these boundary inflows are routed through the stream systems across the Chino Valley, including the routing of surface water through conservation basins where MAR of stormwater occurs.

Comment No. 39. Page 9, first paragraph. Comment reads: "Section 5.2.1 Model Domain and Grid 1st full paragraph on pg. 5-2. As noted on the March 27 technical conference call, these layers don't pinch out but are simulated with the same hydrologic parameters as the overlying layer."

Response: Geologically the confining layers 2 and 4 pinch out near the east of MZ2. Since model layers in a numerical model may not be partially removed (i.e., pinched out), the geologically pinched-out portion of the model layers 2 and 4 are simulated with same hydraulic parameters as the respective overlying layer.

Comment No. 40. Page 9, second paragraph. Comment reads: "Section 5.2.1 Model Domain and Grid 2nd paragraph on pg. 5-2. "The Six Basins consists of three layers and the Cucamonga and Spadra Basins consist of two layers." How is the layering in the adjacent basins reconciled at the Chino Basin boundary with the 5-layer model in the Chino Basin?"

Response. Please see responses (a) and (b) to Comment No. 21.

Comment No. 41. Page 9, third paragraph. Comment reads: "Section 5.2.3 Hydraulic Properties and Zonation 1st full paragraph on pg. 5-3, 2nd sentence. "The calculated parameter value for any model..." Do you mean "cell" instead of "model"? If not, I don't understand this sentence.

Response. It should be "cell" not "model." The report text was updated.

Comment No. 42. Page 9, fourth paragraph. Comment reads: Section 5.2.3 Hydraulic Properties and Zonation (last paragraph, page 5-3 and Table 5-1). Tabulation of the range of aquifer parameters for each zone/layer would be more meaningful than the zone coefficients."

Response: The report text and Table 5-1 have been updated. Table 5-1 now consists of 5-1a that shows the initial parameter estimates and ranges based on the lithology model and 5-1b shows the initial parameter estimates and ranges used to start the calibration. The latter values are based on the formula shown on Section 5.2.3.

Comment No. 43. Page 9, fifth paragraph. Comment reads: "Table 5-2: Add the range of parameter values assigned."

Response: This comment seems to be referring to Table 5-1 as comment is not relevant to Table 5-2. Please see Response to Comment No. 42 above.

Comment No. 44. Page 9, sixth paragraph. Comment reads: "Section 5.2.4.1 Initial Condition In the Vadose Zone (last paragraph, page 5-3 and Figure 5-4): Considering lag time is a key parameter that relates the amount of time it takes for DIPAW to move through the vadose zone, it is recommended to include more control points than the few, widely distributed evaluated boreholes used in the model."

Response: This comment is noted. This comment does not request any information or explanation regarding the 2020 Safe Yield Recalculation Final Report and is therefore not addressed further.

Comment No. 45. Page 9, seventh paragraph. Comment reads: "Section 5.2.4.1 Initial Condition In the Vadose Zone, pg 5-4, 2nd paragraph: The last sentence of the paragraph indicates the linear reservoir approach "was difficult to calibrate and created unrealistic volumes of water stored in the vadose zone." (a) Despite the calibration difficulties, did it calibrate? (b) Were the "unrealistic volumes of stored water" too little or too much? (c) How is the volume of water stored in the vadose zone known to be unrealistic when using the linear reservoir approach?"

Response. (a) We did not attempt full-scale calibration of the 2007 model with the linear reservoir approach due to the initial condition challenge, the difficulty in estimating K and unrealistic amounts of vadose zone storage that resulted in test simulations. (b) Too much. (c) In our 2007 testing the linear reservoir approach, the vadose zone became largely saturated.

Comment No. 46. Page 9, eighth paragraph. Comment reads: "Section 5.2.4.2 Initial Condition in the Saturated Zone, pg. 5-5. How much data was available to constrain the groundwater levels in the Cucamonga and Six Basins? Show control points on Figures 5-5a and 5-5b."

Response. The measured water levels around April – July of 1977 in the 77 wells were used to derive the initial water level in Six Basin, while measured water levels from 14 wells at the same time were used to derive initial water level in Cucamonga Basin. The derived initial water levels were further adjusted based on the groundwater model. Figures 5-5a and 5-5b were updated.

Comment No. 47. Page 9, ninth paragraph. Comment reads: "Section 5.2.5.1 Subsurface Inflow from Mountain Boundaries, pg. 5-5. The surface water inflow from the San Gabriel Mountains, which is the basis for the subsurface inflow, is highly uncertain."

Response: This comment is noted. This comment does not request any information or explanation regarding the 2020 Safe Yield Recalculation Final Report and is therefore not addressed further.

Comment No. 48. Page 9, tenth paragraph. Comment reads: "Section 5.2.5.3 Recharge from San Gabriel Mountain Streams Tributary to the Santa Ana River, 1st paragraph, last sentence. The storm-water capture is estimated so, in this case, you are calibrating the model to estimated data. This introduces uncertainty to the results. More robust measurement of stormwater capture will improve the reliability of the calibration."

Response: This comment is noted. This comment does not request any information or explanation regarding the 2020 Safe Yield Recalculation Final Report and is therefore not addressed further.

Comment No. 49. Page 10, first paragraph. Comment reads: "Section 5.2.5.4 Surface Water and Groundwater Interaction in the Santa Ana River and Its Lower Tributaries, 1st paragraph on pg. 5-7. Is there a reference document that you relied on to characterize the Santa Ana River streambed? If so, please cite."

Response: The report text has been updated to cite USGS Water Supply Paper 1849: Roughness Characteristics of Natural Channels.

Comment No. 50. Page 10, second paragraph. Comment reads: "Section 5.2.6.2 Streamflow-Routing Package (SFR2). (a) What were the streambed hydraulic conductivities used for SFR2? (b) What is the basis for the streambed hydraulic conductivity values? (c) Do the streambed hydraulic conductivities vary from stream segment to stream segment? If so, what is that based on? (d) Were streambed conductivities varied during PEST calibration?"

Response. (a) and (c) The streambed conductivity for the Santa Ana River was calibrated to be 1 f/d and does not vary from segment to segment. The streambed conductivity of segments in Chino Creek ranges between 0.05 and 1 f/d. (b) and (d) The streambed conductivities were initially estimated based on observed soil texture in the streambed along Santa Ana River and tributaries and the final conductivity values were determined during the calibration process based on measured inflows to the Santa Ana River and its tributaries, measured Santa Ana River discharge at Prado dam and groundwater levels.

Comment No. 51. Page 10, third paragraph. Comment reads: "Section 5.2.6.5 Evapotranspiration Segments Package (ETS), 2nd paragraph. What was the extinction depth that you assigned to the ETS package? What was it based on?"

Response. The Extinction depth assigned to the ETS package is 20 ft. Please refer to Appendix B-18 of the draft report for a description of how the amount of water consumed by the riparian vegetation in Prado through evapotranspiration (ET) was estimated as well as how the model calculates the portion of this amount that is derived from groundwater.

Comment No. 52. Page 10, fourth paragraph. Comment reads: "Section 5.2.6.5 Evapotranspiration Segments Package (ETS), 2nd paragraph, last sentence. "When MODFLOW solves for groundwater elevations, the evapotranspiration rate of a model cell is determined by

using the user defined relationship of evapotranspiration rate to the calculated depth." What user defined relationship did you use specific to this model?"

Response. The relationship is shown in Figure B-18-2. Please refer to Appendix B-18 of the draft report for a description of how the amount of water consumed by the riparian vegetation in Prado through evapotranspiration (ET) was estimated as well as how the model calculates the portion of this amount that is derived from groundwater.

Comment No. 53. Page 10, fifth paragraph. Comment reads: "Section 5.2.6.6 Horizontal-Flow Barrier Package (HFB): How did you determine the horizontal hydraulic conductivities assigned to the horizontal flow barriers (i.e. faults)?"

Response. The horizontal hydraulic conductivities of the horizontal flow barriers were initially estimated and then determined through calibration.

Comment No. 54. Page 10, sixth paragraph. Comment reads: "Section 5.2.7.2 Sensitivity Process (SEN) and Observation Process (OBS) (page 5-9): This section should be expanded to include a discussion on how "Observational Sensitivities" were used in the modeling process."

Response. The following paragraph has been added to Section 5.2.7.2: "Prior to executing model calibration, the observation sensitivity values were calculated, and used to guide the selection of calibration wells ensuring that adequate observation sensitivities exist in the selected wells.

Comment No. 55. Page 10, seventh paragraph. Comment reads: "Table 5-1. While I think I understand why you constructed this table the way you did, it is not very meaningful to the average reader. These values are multipliers and not actual values assigned to zones. I'd like to see a table showing the initial parameter estimate and the range of values that the initial estimate was allowed to vary during the PEST calibration."

Response: Please see the Response to Comment No. 42.

Comment No. 56. Page 10, eighth paragraph. Comment reads: "Section 6 – Model Calibration, 1st sentence, pg 6-1): Model calibration does not "validate" the water budget. It results in inflow and outflow values used to "estimate" the water budget."

Response. The report text was updated and now reads: "The purpose of model calibration is to estimate the best set of the model parameters and to use them to estimate the water budget."

Comment No. 57. Page 10, ninth paragraph. Comment reads: "Section 6.2.1 Calibration to Estimated Discharge and Diversion, 1st paragraph, page 6-2: (a) Were the HSPF and R4 models calibrated based on IEUA data for the time period 2005 to 2017? (b) Were the IEUA data rather than model data used explicitly for stormwater MAR in the model? The time range for

measured data and calibrated data used in the model is not clear from the discussion in this section and in Section 5.1."

Response. (a) The R4 model was calibrated based on IEUA data for the time period 2005 to 2017 and USGS discharge data. (b) Yes, and when IEUA recharge estimates were not available, HSPF/R4-based stormwater MAR estimates were used.

Comment No. 58. Page 10, tenth paragraph. Comment reads: "Section 6.2.1 Calibration to Estimated Discharge and Diversions, last paragraph on pg. 6-2: Is the evapotranspiration (ET) referenced in this paragraph the Puddingstone Data? Is the ET data depth-dependent? How did you determine depth-dependent ET?"

Response. Puddingstone Reservoir evaporation data was used to estimate evaporation from water stored in conservation facilities. Evapotranspiration data is not used.

Comment No. 59. Page 11, first paragraph. Comment reads: "Section 6.3.2 Selection of Calibration Data, 3rd paragraph. "To ensure that the water level measurements were distributed evenly over time, and to avoid bias toward high-frequency water level measurements, a subset of water level measurements were selected for calibration purposes and the selected water levels are at least 15-days apart." It seems to me that if you are collecting groundwater levels at high frequency (e.g. multiple times per day or daily), selecting an average groundwater level for the month would be more representative and avoid bias or the possibility of inadvertently selecting an outlier"

Response: This comment is noted. This comment does not request any information or explanation regarding the 2020 Safe Yield Recalculation Final Report and is therefore not addressed further.

Comment No. 60. Page 11, second paragraph. Comment reads: "Section 6.3.3 Sensitivity Analysis and Covariance Matrix, pg. 6-6, 2nd and 3rd paragraphs: Generally, parameters that are correlated either directly or inversely are tied during parameter estimation such that the parameters move together (or inversely) but not independently in order to reduce parameter estimation runs. This section indicates the correlated parameters were "excluded." Does this mean these parameters were fixed and not included in the parameter estimation process? This would be counter to the approach generally used for parameter estimation."

Response: The correlated parameters were not fixed and are included in the parameter estimation process. Correlated parameters were adjusted as a group based on their initial parameter ratios.

Comment No. 61. Page 11, third paragraph. Comment reads: "Section 6.3.4.2 Calibration Results, pg. 6-8, 4th paragraph. "...indicate that the model parameterization and the water budget for the 2020 CVM are accurate: it would not be possible to achieve good calibration in the groundwater basin and the surface water system, as indicated by the high values for the

coefficient of determination and NSE index, if the model parameterization and the water budget were not accurate." The use of the term "accurate" is not appropriate for this model or any other model relying on assumptions and estimates with varying degrees of uncertainty to achieve calibration. Models are simplified representations of a natural system and there are inherent uncertainties in the parameters and necessary simplifications used to describe the system, which is very complex. Given this, models may or may not provide reasonable predictions (e.g. Oreskes et al. 1994, Poeter 2007,10 Doherty et al 2010, and Rubin 2003). The 2020 CVM is no different. A predictive uncertainty analysis is needed to characterize the uncertainty in the water budget and Safe Yield estimated using the 2020 CVM."

Response: See Response to Comment No. 6.

Comment No. 62. Page 11, fourth paragraph. Comment reads: "Pg. 6-7 last paragraph: Presumably meant to read "at deep wells screened in layers 3 and 5 of the so-called ..."."

Response. The report text has been updated.

Comment No. 63. Page 11, fifth paragraph. Comment reads: "Section 6.3.5 Residual Analysis, pg. 6-9, 2nd paragraph. There is no statement in the report that says what this calibration means for estimating Safe Yield."

Response. The report text has been updated. The first sentence of the paragraph now reads: "The Cucamonga, Six, Spadra, and Temescal Basins are included in the 2020 CVM and they contribute subsurface inflow to the Chino Basin. Thus, these basins need to be well calibrated to ensure the reliability of the subsurface inflow estimates to the Chino Basin."

Comment No. 64. Page 12, first paragraph. Comment reads: "Section 6.3.6.1.3.3 MAR, pg 6-12 and Table 6-3: Table 6-3 is for the time period 1978 through 2018, though in Section 5.1 the available data for calibration is 2005 through 2018. Please clarify which data set are used for calibration."

Response. See Response to Comment No. 36.

Comment No. 65. Page 12, second paragraph. Comment reads: "Section 6.3.6.3 Change in Storage. This change in storage should be checked against a change in storage using changes in hydraulic head and specific yield across the model area. We need to know if the changes in storage estimated from the model/spreadsheet are consistent with what is physically happening in the basin."

Response. This is not required because the model is calibrated to match observed groundwater levels.

Computing change in storage from groundwater level measurements requires the creation of groundwater level maps from groundwater levels at well. There are challenges in preparing

these maps that could easily result in significant error in the estimation of storage change. Examples include: groundwater level measurement error, groundwater level data at a well may not exist at the time of interest (so no groundwater level is used or an estimated groundwater level is used in place of an actual measurement), spatial density of groundwater level measurements (most wells are far apart), spatial coverage (wells do not cover parts of the basin and extrapolation will be required), drawing contours of equal groundwater level (human error) and interpolation schemes introduce estimation errors between perfect point groundwater level estimates (which we don't have access to) and they can amplify errors with imperfect data (which we mostly have).

Most of the storage change occurs in the northern part of the basin and that the spatial distribution of wells, measurement data, well construction and temporal availability of water level observations can produce at best, very approximate estimates of the change-in-storage. The process required to estimate change in storage involves: selecting a representative groundwater level at well for a specific point in time, plotting the groundwater level on a map, creating groundwater level contours and interpolation between the contours to estimate groundwater levels for each cell in the model grid. This would be done for pairs of years that bracket a period of interest. To undertake this effort, the difference in groundwater level for each model cell would be estimated for each pair of years. The calculated storage change would then be equal to the sum of the differences multiplied by the specific yield.

Using the calibrated model, we made a calculation to determine how much storage change would occur with a basin-wide increase/decrease of one foot based on the specific yield values estimated through calibration. The answer is 18,000 af. For comparative context, simple errors in data selection, contouring could easily result in ranges of difference between the model-based estimates and the groundwater level estimate in the amount of 50,000 and 100,000 af. Consequently, the suggested effort is both work intensive and not likely to result in a material improvement or better understanding of change in storage. Prior to the next scheduled Safe Yield reset, Watermaster will convene a process to review methods for verifying groundwater storage change estimates.

Comment No. 66. Page 12, third paragraph. Comment reads: “Section 6.3.6.4 Total Basin Storage, table at the top of pg. 6-15. Quantifying the storage in the basin to the nearest acre-ft suggests a level of accuracy that is not realistic. These should be rounded.”

Response: This comment is noted. In our view the rounding is not required. The suggested change in formatting and presentation does not impact the recommendation regarding Safe Yield and is therefore not addressed further.

Comment No. 67. Page 12, fourth paragraph. Comment reads: “Section 6.3.7 Net Recharge, 2nd table on pg. 6-15. Same comment as for Section 6.3.6.4.”

Response: This comment is noted. This comment does not request any information or explanation regarding the 2020 Safe Yield Recalculation Final Report and is therefore not addressed further.

Comment No. 68. Page 12, fifth paragraph. Comment reads: "Table 6-2. Initial and Calibrated Parameter Zone Scalers: The table should include the range of actual values derived for each zone as well as the bounds that PEST was allowed to vary during calibration."

Response. The report text was updated, Table 6-2 was replaced with a new Table 6-2 responsive to the comment that shows the final calibrated parameter estimates. The report text was updated and now reads: "Table 6-2 contains the final calibrated parameter values."

Comment No. 69. Page 12, sixth paragraph. Comment reads: "Table 6-3. Water Budget for the Chino Basin for the Calibration Period: Please identify which data are estimated (modeled) and which are measured."

Response. The water budget tables, Tables 6-3 and 7-2 have been updated to indicate recharge and discharge components that are directly input (I) to the 2020 CVM and components that are 2020 CVM results (R). The report text in Section 6 has been updated to read: "Individual recharge and discharge components with a column heading of "I" were input directly into the 2020 CVM and components with a column heading "R" are computational results produced by the 2020 CVM."

Comment No. 70. Page 12, seventh paragraph. Comment reads: "Section 6 Figures: The horizontal hydraulic conductivity and specific yield parameter distribution maps from the calibrated model, as provided via email from WEI on April 15, 2020 in response to my request for information, should be included in the report (see my comments to these data starting on pg. 10 below). In addition, I'd like to see parameter distribution maps for vertical hydraulic conductivity for each layer of the model provided in the report as well. Further, aquifer parameters derived from pumping tests should be shown on the maps or provided in a table and referenced to a location on the maps. The table of "stress derived hydraulic conductivities" and calibrated model aquifer parameters provided via email on April 15, 2020 will suffice although I'd like the well locations in the table shown on the aquifer parameter maps of horizontal hydraulic conductivity."

Response: Appendix E containing these exhibits will be incorporated into the final report.

Comment No. 71 Page 12, eighth paragraph. Comment reads: "Section 7.2 Long-Term Historical Records Used to Estimate Net Recharge (procedures, pages 7¬2 and 7-3, Table 7-2 and Figures 7-6 and 7-7). The use of the long-term average precipitation and ETo in the HSPF and R4 simulations with DWR change factors should also include application of the 16th and 84th percentile precipitation and ETo values to provide upper and lower bounds for estimated DIPAW. Such a range can be incorporated into an uncertainty analysis as part of an overall assessment of the potential projected range in Safe Yield of the basin."

Response. This comment appears to be based on a misunderstanding of the approach used to estimate long-term average recharge. Long-term average recharge is not based on long term average precipitation.

We selected the years 2018, 2030, 2040, 2070 to estimate the average recharge from 62 years of daily precipitation, applied water and ET specific to the cultural conditions in those years and adjusted for climate change. In each year we use surface water models to estimate the daily response to precipitation, applied water and ET. We calculate recharge on a daily basis. Then we aggregate the daily data to monthly values. There is no expectation of a specific precipitation in the future, just the expected recharge with specific cultural conditions. We use linear interpolation to estimate recharge between the years mentioned above.

Comment No. 72. Page 13, first paragraph. Comment reads: "Section 7.3 Present and Projected Future Cultural Conditions, 1st sentence. It was my understanding that land subsidence will be evaluated with a future version of the model. If that is still the case, this sentence should be modified to reflect that."

Response. The report text was updated to read: "The 2020 CVM was used to project net recharge, groundwater levels and the state of hydraulic control for the 2019 through 2050 period."

Comment No. 73. Page 13, second paragraph. Comment reads: "Section 7.3.1.1 Groundwater Pumping Projections, pg. 7-5, 2nd paragraph. Pumping distribution and magnitude could change the Safe Yield of the basin. Potential changes in pumping patterns should be evaluated to assess how we can optimize the basin and preserve Safe Yield."

Response: This comment is noted. Potential changes in pumping patterns and the impact on Safe Yield is speculative. Forecasted pumping conditions based upon hypotheticals are not suitable for developing a recommendation of Safe Yield. However, it is true that potential changes in pumping patterns may have a beneficial impact on Safe Yield if they are enforceable or otherwise reasonably certain to occur. It is possible that such an evaluation might be undertaken in connection with an update to the OBMP.

Comment No. 74. Page 13, third paragraph. Comment reads: "Section 7.3.1.2 Methodology to Project Replenishment Obligations, pg. 7-7: This description indicates it was assumed that 80% of replenishment would occur via unused pumping rights and stored water. Presumably, the 80% assumption has some influence on the Safe Yield estimate. Knowing (now) that this assumption influences the calculated Safe Yield, the Appropriators may opt to modify their behavior and cause more (or less) replenishment to be satisfied from storage than 80%. This is just one example of how the model should be used as a tool for the development of the Safe Yield recalculation and not the sole predictor of Safe Yield."

Response: This comment is noted. See Response to Comment No. 73. The assumption that 80 percent of replenishment obligation would occur via unused pumping rights and stored water is based on an investigation by Watermaster on the historical use of such water to meet replenishment obligations and thus it is representative of the behavior of the Parties. Changing this assumption for the Safe Yield recalculation is completely speculative. However, actual commitments to changes in pumping and replenishment behavior may have a positive impact on Safe Yield and might be considered in connection with updates to the OBMP.

Comment No. 75. Page 13, fourth paragraph. Comment reads: "Section 7.3.2 Impacts of Drought and Future Water Conservation Vadose Zone Storage Initial Conditions: While this section describes discrete periods of relatively recent drought, what would be the effect of using stored water rather than using replenishment water to augment the calculated net recharge, assuming this would become a temporary adjustment (increase) to the reset SY?"

Response: This comment calls for a speculation that is outside the scope of the 2020 Safe Yield recalculation effort. See Response to Comments No.s 74 and 75.

Comment No. 76. Page 13, fifth paragraph. Comment reads: "Section 7.3.2, last paragraph. All the parameters listed in this paragraph, with the possible exception of the initial groundwater levels, are estimated. These estimated values resulted in the DIPAW recharge term, which is also estimated. This comment is only to emphasize that the use of the term "accurate" in Section 6.3.4.2 is inappropriate and misrepresents the reliability of the model."

Response: See response to Comment No. 3.

Comment No. 77. Page 13, sixth paragraph. Comment reads: "Section 7.3.3 Conservation Related Impacts of Assembly Bill 1668 and Senate Bill 606, pgs 7-9 and 7-10: While the imposed irrigation ETAF will likely result in reduced DIPAW and net recharge and Safe Yield, has the implied irrigation reductions also been accounted for in the planned water demand scenarios? One would think the conservation effort would offset the amount of water used."

Response. No, the water demand and supply plans do not account for legislation as they were developed before the legislation became law.

Comment No. 78. Page 13, seventh paragraph. Comment reads: "Section 7.4.3 Change in Storage, pg. 7-10, 1st paragraph of section: Is the controlled overdraft of the basin accounted for in the methodology to estimate Safe Yield? If so, how?"

Response. The controlled overdraft of 200,000 af pursuant to the original Judgment and some of the Reoperation water authorized by the Peace II Agreement occurred in the period prior to the planning projection and the impact of these controlled overdraft were incorporated directly into the calibration. Reoperation pursuant to the Peace II Agreement has been accounted for in the planning scenario used to estimate net recharge and Safe Yield. See Section 7.3.1.2 and Table 7-3.

Comment No. 79. Page 13, eighth paragraph. Comment reads: "Section 7.4.4 1st Table. For the recharge components, there are two rows that appear to represent Santa Ana River Streambed Infiltration. I believe one of them may represent streambed infiltration from Santa Ana River tributaries(?) Also, the last recharge component for Managed Artificial Recharge appears to be cut off – should be "Recycled and Imported."

Response: The report text was updated to expand the rows to fully show the intended text.

Comment No. 80. Pages 13 to 14. Comment reads: "Section 7.4.4, pg. 7-12, 2nd paragraph and Figure 7-7. The reduction in net recharge for the 2021 to 2030 time period resulting from carryover of the extreme dry period in the 20 years preceding the planning period is a relatively short-term phenomenon and does not represent a long-term hydrological average. The Safe Yield should be estimated by more than just 10 years into the future in order to average out relatively short-term climatic variations, such as the recent dry period."

Response. This comment is noted. Watermaster disagrees. Forecasting conditions for periods in excess of 10 years would depend upon increased speculation and therefore, risk to the Basin and the parties to the Judgment. Watermaster followed the Court Ordered methodology. (See 4/23 Ag Pool Response to Comment No. 1a and 4/29 Workshop Response to Comment No. 2.)

Comment No. 81. Page 14, second paragraph. Comment reads: "Section 7.6 Recommended Safe Yield. In implementing the methodology for estimating Safe Yield described in Section 7.1, did you identify MPI in any of the iterative model runs to determine Safe Yield, as per No. 5 of that section? If so, at what initial Safe Yield did you determine MPI, what was the nature of the MPI, and where did it occur?"

Response. Upon evaluation of basin response to the SYR1 scenario, we concluded there was no MPI or undesirable results. Therefore, pursuant to the Court-ordered methodology, no iterations were required.

Comment No. 82. Page 14, third paragraph. Comment reads: "Section 7.6 Recommended Safe Yield. It appears that the Safe Yield is estimated from the average net recharge of the time period from 2020 to 2030. However, there is nothing in the Court-ordered methodology or Rules and Regulations that require Watermaster to limit the prospective time period over which the net recharge is estimated to the 10-year period over which the Safe Yield will be applied. In fact, it is contrary to relying on a long-term hydrology as a basis for the estimate."

Response. The Court-ordered methodology was the methodology used in the prior Safe Yield recalculation and the ten-year period used to set the Safe Yield is included, albeit implicitly, in that methodology. There is great uncertainty in how the parties will pump and manage storage in the next ten years and that uncertainty is greater beyond ten years. Using the period beyond ten years involve speculation is not prudent given prior experience. For example, the pumping projections used in the 2020 Safe Yield recalculation are about 6,000 to 27,000 afy less for 2015

through 2035 period used in the prior Safe Yield recalculation. Over the last 20 years, the parties have consistently pumped less groundwater than they projected and this has the effect of overestimating net recharge and Safe Yield. This over-estimation increases relative risk to the Basin and the parties to the Judgment and is not therefore reasonable and prudent in this case. (See Response to Comment No. 80, 4/23 Ag Pool Response to Comment No. 1a and 4/29 Workshop Response to Comment No. 2.)

Comment No. 83. Page 14, fourth paragraph. Comment reads: "Appendix B: The appendix includes three WEI memos, one dated 2/6/20 and two others dated 2/11/20.
(a) The 2/6 memo indicates the step 7 density analyses were performed independently by two to three persons and then those results were averaged. What was the variability in the spread of the independent analyses? (b) One of the 2/11 memos describes the assumptions attributable to septic system contributions to groundwater recharge, and indicates the "unit" contributions decrease with time. Most existing septic systems have been in-service for decades, and if true then what explanation(s) are provided to support assumed decreasing contribution to groundwater recharge? It does not seem reasonable to assume their operational efficiencies have changed. (c) The other 2/11 memo discusses groundwater discharged from aquitards due to land subsidence, and indicates such contribution is considered negligible. Please provide what estimated volume would be anticipated and considered negligible."

Response: (a) Between all seven years analyzed, the variability in the spread of the independent analyses averaged 11 percent and ranged from 0 percent to 55 percent. (b) The decreasing trend of septic tank contributions to groundwater recharge reflects effects of water use conservation. The numbers that were used in the model are given in Appendix B-19. (c) The volume of groundwater discharged from aquitards due to land subsidence in the Management Zone 1 (MZ1) of the Chino Valley Watershed was described in Appendix B-20. The volume of groundwater discharged from aquitards due to land subsidence of all active model cells within MZ1 is calculated as 181 afy.

Comment No. 84. Page 14, fifth paragraph. Comment reads: "Appendix D, D-162. The message of the figure is not evident."

Response. Figure D-162 was inadvertently included in Appendix D and it will be deleted from the final report.

Comment No. 85. Pages 14 to 15. Comment reads: "Pg. 2 second to last paragraph and Table 1: WEI has stated that the stress test hydraulic conductivities that I provided for the Chino Basin Desalter wells were based on Jacob's straight-line solution for confined aquifers and that, in so doing, the values are overestimated because the aquifer is unconfined. The application of the Jacob straight line method for estimating aquifer transmissivity and hydraulic conductivity can easily be corrected by plotting and analyzing adjusted drawdown values using the following relationship:

$$s' = s - s^2 / 2h$$

Where:

s' = adjusted drawdown (ft)
s = measured drawdown (ft)
h = aquifer thickness (ft)

For the stress test-derived horizontal hydraulic conductivity at Chino II-2, the value in Table 1 of the WEI response to comments is approximately 400 ft/day. When the correction is applied to the drawdown data, the adjusted hydraulic conductivity for unconfined conditions is approximately 470 ft/day. Both corrected and uncorrected values are significantly higher than the value used in the calibrated model for that location (approximately 85 ft/day). Hydraulic conductivity values derived from pumping tests are higher than model calibrated values at all of the desalter wells. Were the stress test horizontal hydraulic conductivity data summarized in Table 1, or a corrected version, used to constrain aquifer parameterization during calibration? What were the upper and lower bounds assigned to the initial hydraulic conductivity values in PEST? Was the prior information from the stress test data used to constrain the bounds assigned to PEST? Were they allowed to vary as high as the values derived from pumping tests?"

Response. See Response to Comment No. 25

Comment No. 86. Page 15, second paragraph. Comment reads: "Figure 3. There is a significant change in horizontal hydraulic conductivity along straight lines in multiple locations of Layers 1 and 2. These lines correlate to parameter zones described in WEI (2020). It is noted that, from a conceptual perspective, sediments would not be expected to be deposited with linear boundaries as shown on these maps. There is likely a high degree of uncertainty in how these zones are simulated in the model. It is further noted that the horizontal hydraulic conductivities shown for Layer 1 along Bellgrave Avenue and in the vicinity of Mission Boulevard and the 60 Freeway are lower than indicated from pumping test-derived data."

Response. This comment is noted. This comment does not request any information or explanation regarding the 2020 Safe Yield Recalculation Final Report, and is therefore not addressed further.

Comment No. 87. Pages 15 to 16. Comment reads: "Page 3, Equation at the top of page. This relationship applies to horizontal flow of water in an aquifer and is representative if there isn't significant vertical flow of water in the borehole. Are there significant hydraulic head differences between aquifers in the model? If so, what are the magnitude of differences?"

Response. As shown in Table 6-1, most calibration wells were single-layer wells. There are no significant hydraulic head differences at the location of multiple-layer calibration wells.

Comment No. 88. Page 16, second paragraph. Comment reads: "Page 3, last paragraph, last sentence. While the residuals at the Ayalla Park monitoring well may not impact the Safe Yield

estimate significantly, future calibration for land subsidence will involve changes to the aquifer storage properties in this area, which may improve groundwater level calibration but will also change the water budget and could result in changes to the Safe Yield."

Response. We have estimated the amount of water released from storage by compaction of aquitards in the subsiding area of the basin and concluded that the contribution to yield is negligible. Please see Appendix B-20.

Comment No. 89. Page 16, third paragraph. Comment reads: "As mentioned earlier in this letter, the biggest omission in the 2020 Safe Yield Recalculation is a predictive uncertainty analysis. Such an analysis has become an industry standard procedure when using complex models to inform groundwater basin management decisions. The predictive uncertainty analysis would involve developing multiple versions (preferably hundreds) of the Chino Valley Model, each with unique parameter distributions. The unique model distributions can be developed automatically using PEST and its associated utility programs. Parameter bounds would be selected to be within plausible ranges based on available data. The water budgets for realizations with acceptable model calibrations would then be processed to determine the Safe Yield for each realization, resulting in a range of Safe Yield estimates for the basin. I recommend conducting this analysis prior to finalizing the Safe Yield for the next 10 years."

Response: This comment is noted. Watermaster disagrees that the suggested expanded modeling effort is required to develop a reasonable and prudent recommendation for the recalculation of Safe Yield. (See Response to Comment No. 6).

Comment No. 90. Pages 16 to 17. Comment reads: "In addition to the predictive uncertainty analysis and prior to finalizing the Safe Yield, I recommend the following:

- (a) Conduct a check of the change in groundwater storage for the period 2011 to 2018 using the following relationship:

$$Vw = (Sy)(A)(\Delta h)$$

Where:

Vw	=	the volume of groundwater storage change (acre-ft).
Sy	=	specific yield of aquifer sediments (unitless).
A	=	the surface area of the aquifer within the Chino Basin (acres).
Δh	=	the change in hydraulic head (i.e. groundwater level) (feet).

The change in groundwater storage will be specific to the shallow aquifer (Model Layer 1). The areal distribution of specific yield should be the same as that used in the calibrated model used to estimate Safe Yield. Either model-generated or hand-drawn groundwater contours for 2011 and 2018 would be exported to/digitized in GIS software, which can then be used to calculate the change in hydraulic head across the

area. The storage change estimated in this way would then be compared to the change in storage shown in Table 6-3 of the model report WEI (2020).

- (b) Compute the Safe Yield for the 2020 to 2030 time period based on a long-term projected net recharge from at least 2020 to 2050 in order to smooth out short-term hydrologic conditions such as the lingering impacts of recent historic dry conditions.

- Use the above information to inform the AP for redetermining the Safe Yield of the Chino Basin for the 2020 to 2030 time period.

Response:
(a) See Response to Comment No. 65. (b) Please see Response to Comment No. 82.

Response to Questions and Comments on the April 2, 2020 Safe Yield Recalculation Report

April 29, 2020 Questions and Comments from Stakeholders at the April 29th workshop

Comment No 1. From Thomas Harder, regarding slides 10 and 44. "Annual Precipitation, is presented in the slide as the mean precipitation across the basin. Is this based on one or more precipitation stations? How is this chart prepared?"

Response: This chart contains annual times series of spatially averaged precipitation over the CVM watershed. The source of data is the 800-meter gridded monthly precipitation estimates provided by the PRISM Climate Group at the University of Oregon. For each year, the spatially averaged monthly precipitation over the CVM watershed is summed to create an annual CVM watershed estimate.

Comment No 2. From Thomas Harder, regarding slide 24. "If we limit ourselves to the 2020-2030 period for setting SY, it is strongly influenced by near-term drought that just occurred. In the spirt of the method, my opinion is that a longer term average would be appropriate to capture a longer term condition. Just a statement."

Response: This comment is noted as a statement. Watermaster disagrees with the use of a longer period. First, the Court ordered Watermaster to follow the proposed methodology in April 2017. That methodology used a 10-year period for prospective cultural conditions; still relying on long-term hydrology. Second, projections of cultural conditions, inclusive of changes in land use, pumping patterns, applied water, regulatory requirements and conservation practices become less reliable and overly speculative when they are extended beyond 10 years for purposes of calculating Safe Yield. A 20-year period may, under some circumstances, be appropriate in the future. However, the variable conditions in the Basin do not support a 20-year forecast at the present time.

Comment No 3. From Eric Fordham, regarding slides 24 and 26. "Re: ETAF values. Does the chart in slide 24 incorporate the ETAF values shown in slide 26? With respect to DIPAW, were the ETAFs considered to compute it?"

Response: The ETAFs for the historical period were derived from the R4 model. For future projections, the ETAFs listed for the period 2020 through 2070 were used.

Comment No 4. From Justin Scott Coe, regarding slide 26. "What legislation are you referring to that applies to the requirement for legacy urban to comply with reduced irrigation? My understanding of the law it will not apply to legacy urban."

Response: The 2020 Safe Yield Recalculation Final Report references AB 1668 and SB 606, collectively referred to as "Making Conservation a California Way of Life." As described in the Report, the eventual outcome of the State's process to develop residential outdoor water use standards, and the manner in which those standards will be implemented, is too speculative to evaluate at this time how that implementation might affect the Basin's net recharge. Moreover, it is possible that mitigation may limit the adverse impact on the Basin. As described in the Report's recommendation, Watermaster will monitor these developments and consider any impacts on net recharge.

Comment No 5. From Geoff Vanden Heuvel, regarding slide 30. " (a) What are we to conclude from Slide 30? Does this mean that the safe yield has been over allocated by 10,000 afy for the 2011 to 2020 period? (b) There is no mechanism to go back and correct if we have been inaccurate in past estimates. The chart shows we over allocated the Safe Yield by 10,000 afy. Am I reading it wrong? (c) This is not an insignificant amount of water. Had we known then what we know now, would we have set it at 125,000 afy?"

Response: (a) No we are not to conclude Safe Yield was overallocated. Simply put the difference is: one instance is a forecast and the other is a hindcast. One conclusion from Slide 30 is that the historical recharge in the period 2011 through 2018 was less than the long-term average recharge. The Safe Yield for the 2011 through 2020 period was calculated in 2013 based on the expected long-term average recharge that was based on the precipitation record of 1921 through 2011 and then-current and projected cultural conditions. The 1921 through 2011 precipitation period contains wet and dry periods. In 2020, using actual precipitation for the period 2011 through 2018 and extrapolating to 2020, the 10-year net recharge for 2011 through 2020 has been estimated at about 125,000 afy. What needs to be understood is that the period 2011 through 2018 is an extremely dry period that includes the driest five-year period in the last 122 years and contains part of the driest 10-year period in the last 122 years (see Figure 3-14 in April 2, 2020 Safe Yield Recalculation report); the period of 2011 through 2018 is considerably drier than the long-term average. Comparing both estimates is comparing apples (long-term average recharge) to oranges (short-term average recharge from a record-setting dry period). In both the 2013 and 2020 Safe Yield recalculation efforts, the estimated long-term average recharge, in the absence of drought effects, appears to be comparable for the periods 2031 to 2040 and 2041 to 2050. As a result, in the fullness of time, the difference between the long-term average based Safe Yield of 135,000 afy and the historical recharge of 125,000 afy will be offset in future years when wet periods occur. The intent in using a prospective long-term average to set the Safe Yield was to acknowledge that variations in annual recharge caused by wet and dry periods will occur, that the Parties could use the storage space in the basin to buffer recharge variations and benefit from the use a long-term

recharge-based Safe Yield. The primary benefit being a stable planning environment to manage their water portfolio and to invest in facilities

(b) The Court-ordered Safe Yield evaluation and reset methodology does not include any mechanism for retroactive adjustments to allocated Safe Yield nor should it. The prior answer explains the differences in estimated yield between the 2013 prospective estimate and the 2020 calibration estimate. As described above, using the Court-ordered prospective methodology, these differences can be reasonably expected to be off-set by future wet periods consistent with the historical record. That is, projections will still be made in accordance with the long-term hydrology and actual recharge will be evaluated and calibrated by the model in arrears.

(c) Please see prior responses.

Comment No 6. From Sorab Panday, regarding slide 14. "Can you please further explain the approach used to compute the average recharge, explaining more specifically how it is not based on average precipitation?"

Response: We selected the years 2018, 2030, 2040, 2070 to estimate the average recharge from 62 years of daily precipitation, applied water and ET specific to the cultural conditions in those years and adjusted for climate change. In each year we use surface water models to estimate the daily response to precipitation, applied water and ET. We calculate recharge on a daily basis. Then we aggregate the daily data to monthly values. There is no expectation of a specific precipitation in the future, just the expected recharge with specific cultural conditions. We use linear interpolation to estimate recharge between the years mentioned above.

Comment No 7. From Sorab Panday. "How does the SYR-1 scenario relate to the storage framework investigation. When you look at maximum storage value in SFI Table 7-3."

Response: The maximum managed storage value projected in the 2018 Storage Framework Investigation report is estimated to be about 695,000 af and the maximum managed storage value projected in the 2020 Safe Yield Recalculation report is estimated to be about 612,000 af. The latter is less because the assumed Safe Yield is less by 80,000 af through the decade.

Comment No 8. From Sorab Panday. "The basin is expected to operate in different storage bands. Shouldn't the SYR be based on expectation of future storage management programs rather than based on a baseline condition?"

Response: The 2020 SYR1 planning scenario used to recalculate Safe Yield includes the projected storage management activities of the Judgment Parties and the existing Dry-Year Yield program. Storage and Recovery Program proponents will submit applications to Watermaster to operate Storage and Recovery Programs in the Chino Basin. The basin response to each proposed Storage and Recovery Program will be evaluated by Watermaster and all potential adverse impacts and MPI identified by Watermaster must be fully mitigated by the

Storage and Recovery Program proponents pursuant to the Peace Agreement. The impact on Safe Yield due to a proposed Storage and Recovery Program will be evaluated by comparing a baseline scenario that includes the storage management activities of the Judgment Parties (and the DYYP if it is still in operation) to an identical scenario with the proposed Storage and Recovery Program. Reductions in net recharge and Safe Yield projected to be caused by the proposed Storage and Recover Program must be fully mitigated by the Storage and Recovery Program proponent for the program to be approved and implemented.

Comment No 9. From Sorab Panday. "The RMPU states that MS4 projects will be considered in the 2020 Safe Yield reset. Were these projects considered?"

Response: Yes. Watermaster conducts an annual information request of the Appropriative Pool Parties to provide information on the number of MS4 projects in their service areas. Based on the last report (WEI, 2018) 114 MS4 compliance projects were identified that relied on groundwater recharge to comply with the MS4 permit. Of these projects only 36 could be verified to have been constructed and of these only 17 had information that demonstrated that some maintenance had occurred. No MS4 project recharge was included in the Safe Yield recalculation due to the uncertainty of their existence, operations and maintenance. Our engineering assessment based on what is knowable is that recharge from the existing MS4 projects is negligible.

Comment No 10. From Sorab Panday. "When we talk about total aggregate managed storage volume, where is this number computed from? Is it from the old or new model?"

Response: The term "managed storage" as used herein refers to water stored by the Parties and other entities and includes Carryover, Local Storage, and Supplemental Water held in storage accounts by the Parties and Storage and Recovery Programs. Local Storage includes Excess Carryover for the Overlying Non-Agricultural Pool Parties and Excess Carryover and Supplemental Waters for the Appropriative Pool and Overlying Non-Agricultural Pool Parties. Watermaster tracks the various types of water stored by the Parties and others and reports them in its annual reports and assessment package.

Comment No 11. From Sorab Panday. "What are the storage thresholds based on? What do they mean and how do we change them?"

Response: The context of the safe storage threshold originated in 2000 in the OBMP. The value was set at 500,000 af for the purpose of being able to store water safely, without causing material physical injury (MPI) to the Basin or any Party. The CEQA analysis for the OBMP was based on this estimation. Amounts could be stored in excess of the safe storage quantity but were required to mitigate any adverse impacts or MPI as a condition of storing water. This became part of the Court order. Subsequently, a CEQA addendum was done to enable temporarily increase in storage from 500,000 af to 600,000 af, based on a demonstration that 600,000 af would not cause adverse impacts or MPI. Then, the 2018 Storage Framework Investigation identified that 800,000 af could be the new storage limit. However, the rules set

forth in the Peace Agreement and the OBMP Implementation Plan still remain and control the discretion of Watermaster. The 2020 Storage Management Plan was written to suggest a method for making that space available to the Parties for their Local Storage activities and for the Metropolitan Water District in the existing DYY program.

Comment No 12. From Thomas Harder. "Did you iterate multiple times to arrive at the Safe Yield value of 131,000 afy that causes no Material Physical Injury?

Response: Upon evaluation of basin response to the 2020 SYR1 scenario, we concluded there was no MPI or undesirable results. Therefore, pursuant to the Court-ordered methodology, no iterations were required.

Comment No 13. From Rick Rees and Marilyn Levine. Rick Rees: "My April comment memo for the State requested model files. We did not receive these files." Marilyn Levine: "This is a question. We want to understand the response. Will you be releasing the model files that were requested?

Response: No. Watermaster will not be releasing the model files unless instructed to by the Court. Watermaster has a duty to administer the decree and has a responsibility for recalculating Safe Yield as described in the Judgment and in the Court's Order of April 28, 2017. The CVM is Watermaster's proprietary model. As the administrator of the decree, Watermaster has no specific interest in the application of the model, other than for the assistance to the parties to the Judgment and under the direct oversight of the Court. Maintaining the integrity of the model is paramount to its duties. Release of the model could lead to parties and individuals changing inputs into the model that enable advocacy to be injected into the modeling process. As a result, public confidence in the Judgment may be undermined by Watermaster and the Court having to respond to allegations supported by various and potentially iterations of the model and modeling reports.

The Parties are not disadvantaged by not having the model files. The 2020 CVM and findings from its use have been the subject of three peer review workshops where the Parties and their technical experts participated. Watermaster retained an independent expert to review the Watermaster's hydrologist modeling work and that expert found that the model "does meet or exceed generally accepted industry standards" and that "application of the model and the updated safe yield analysis were consistent with prevailing professional standards in addition to being compliant with the Court-approved methodology for estimating net recharge and associated safe yield." Since the publication of the April 2, 2020 Safe Yield Recalculation report, 120 questions/comments were submitted by the Overlying Agricultural and Appropriative Pools and others and they have been responded to. Watermaster and its professional team will continue to work with the Parties to respond to new questions as they arise. Watermaster's assurances regarding transparency and open access to information are buttressed by the Court's oversight pursuant to its continuing jurisdiction over Safe Yield.

Comment No 14. From Rick Rees, Thomas Harder and Sorab Panday. All three requested that groundwater storage change calculations be performed to verify the change in storage estimated in Table 6-3 of the April 2, 2020 Safe Yield Recalculation report.

Response: It has been explained in other Responses to Comments (see response to comment 65 from April 23, 2020 Letter from the Appropriative Pool re: Technical Review of the Models and Methodology Used as a Basis for the 2020 Safe Yield Reset) that verifying model-predicted groundwater storage change calculations through other methods is not effective. Prior to the next scheduled Safe Yield reset, Watermaster will convene a process to review methods for verifying groundwater storage change estimates.

Comment No 15. From Justin Scott Coe. "To re-emphasize a written comment regard the use of the term "recalculation" in the title of the WEI report. We would be more comfortable with a change to the title along the lines of "Safe Yield Reset". Recalculation is not used in the Court Order and there was a reason for that, because the model is a tool use to support the process. The Reset requires use of judgement of information available. Please consider the change."

Response: The process through which the Basin's Safe Yield is estimated and reset is described in various manners throughout the Watermaster guidance documents. Paragraph 15.(a) of the Judgment refers to the Court's retained jurisdiction to undertake a "redetermination" of the Safe Yield. Paragraph 10.(a)(1) of the Appropriative Pool Pooling Plan, Exhibit "H" to the Restated Judgment, refers to a reduction in Safe Yield "by reason of recalculation thereof." The OBMP Implementation Plan, in its discussion of Program Elements 8 and 9, variously refers to the "comput[ation]", "estim[ation]," "re-determination" and "reset" of the Safe Yield. The Court's April 28, 2017 order found that the reset of the Safe Yield to 135,000 afy was a "recalculation" and required Watermaster to conduct a Safe Yield "evaluation and reset process" beginning in 2019. Based on all of these descriptions, it is unclear that the use of one description as opposed to another in WEI's report has any import or effect.

The Court's April 28, 2017 order explains the Safe Yield evaluation and reset process that Watermaster must follow. This includes the Court's adoption of a specified methodology for this process, that includes the methodology in the Reset Technical Memorandum. Step 5 of the Reset Technical Memorandum's methodology includes the qualitative evaluation of groundwater production at the net recharge estimated by the groundwater flow model.

Luhdorff & Scalmanini
Consulting Engineers

April 5, 2020
File No. 20-1-040

Mr. Peter Kavounas, General Manager
Chino Basin Watermaster
9641 San Bernardino Road
Rancho Cucamonga, CA 91730

SUBJECT: REVIEW OF CHINO BASIN UPDATED SAFE YIELD, CHINO BASIN, CALIFORNIA

Dear Mr. Kavounas:

Luhdorff and Scalmanini Consulting Engineers (LSCE) are pleased to provide this letter summarizing LSCE's review of the updated safe yield analysis conducted by Wildermuth and Associates for the Chino Basin. The scope of the review focused on the following three tasks:

1. Does the basin model used to develop the updated safe yield meet or exceed generally accepted industry standards;
2. Were the application of the model and the updated safe yield determination undertaken consistent with the prevailing professional standards?; and
3. Provide recommendations for how to manage the water resources of the basin in the future.

Task 1

The model used to develop the updated safe yield does meet or exceed generally accepted industry standards in my opinion. The model tool is based upon previous versions that were used in the development of safe yield that were vetted by the parties to the Judgement and approved by the Court. Therefore, many elements of the model construction have not changed or have been improved upon based upon additional data collection efforts and corresponding improvements in the conceptual model from which the model tool represents. The Administrative Draft report that was reviewed in this effort did not include the calibrated aquifer parameters for the model. Rather, the Administrative Draft included the degree in which the most sensitive aquifer parameters varied and directing the reader to previous model reports that included the actual aquifer parameter values. Since the approved scope of the LSCE review did not include review of these prior model reports, LSCE was not able to assess how the calibrated model represented the conceptual model aquifer properties. However, there was sufficient information on other aspects of the model and output results (water budget, calibration statistics, etc.) to conclude that the model meets or exceeds those industry standards described by Wildermuth Environmental, Inc. (WEI) in section 6.4.2 and therefore, is more than adequate in developing an updated safe yield estimate.

Task 2

The application of the model and the updated safe yield analysis were consistent with prevailing professional standards in addition to being compliant with the Court-approved methodology for estimating net recharge and associated safe yield. WEI accounted for all known recharge and discharge water budget components in developing the net recharge for the 2021 through 2030 time frame for the updated safe yield analysis and also for the period that extends out to 2050. WEI also described some limitations that could impact the updated safe yield in the form of future State of California water conservation measures. The scope of these water conservation measures are not currently quantifiable at the time of the updated safe yield analysis.

Task 3

Recommendations for managing water resources in the basin moving forward are described below.

- Tracking and verifying the use of imported water supplies from Met and how variations in actual year to year deliveries correlate to projected estimates is recommended to ensure that the updated safe yield projection is based on verifiable data. The increase in projected imported supplies from Met, compared to 2015 levels, is significant during the 2021 through 2030 safe yield period, thereby allowing for a corresponding decrease in groundwater pumping. If the projected amounts of imported water fall short of projections and is offset by increases in groundwater pumping, then the projected safe yield estimate reported in the Administrative Draft report will overestimate of the actual safe yield and potentially result in overdraft.
- The utilization of water (rising groundwater, increased runoff from impervious surfaces to the Santa Ana River, etc.) resulting from changes in cultural conditions in the Basin should be considered for future projects to enhance safe yield or as a source of replenishment water (assuming acceptable water quality). However, with the passage of the Sustainable Groundwater Management Act (SGMA) any capture of "tributary" inflow to the Santa Ana River from such projects would need to consider whether such projects would result in significant and unreasonable impacts to beneficial uses of surface water.
- Uniform monitoring and reporting procedures that are implemented by all parties in the Basin would address some data gaps and reduce uncertainty in future estimates of safe yield and also provide a more complete datasets for the evaluation of the effectiveness of water management programs and accounting of the groundwater resources in the Basin.

If you have any questions, please let us know.

Sincerely,
LUHDORFF & SCALMANINI
CONSULTING ENGINEERS

William L. Halligan

William L. Halligan, P.G.
Senior Principal Hydrogeolgist

LSCE

May 22, 2020 Watermaster Board Special Meeting Roll Call Vote for
Business Item I.A. 2020 Safe Yield Reset

Member	Alternate	Vote
Bowcock, Bob		yes
Curatalo, James, Vice-Chair		yes
Elie, Steve		yes
Galleano, Don		yes
Hofer, Paul		no
Kuhn, Bob, Secretary/Treasurer		yes
Preciado, Victor		yes
Rogers, Peter		yes
Pierson, Jeff, Chair		no
	OUTCOME:	**Passed by Majority**